# Importance of the structural components of *C*-linked glycopeptides to specific-antifreeze activity: from glycopeptides to small molecule inhibitors of ice recrystallization

John Frederick Trant

B.Sc. Biopharmaceutical Sciences (Medicinal Chemistry)-University of Ottawa 2006

Thesis submitted to the
Faculty of Graduate & Postdoctoral Studies
University of Ottawa
In partial fulfillment of the requirements for the
Degree of Doctor of Philosophy in the
Ottawa-Carleton Chemistry Institute

| Candidate | Supervisor |
| --- | --- |
| John Frederick Trant | Professor Robert N. Ben |

© John Frederick Trant, Ottawa, Canada, 2012

*Dedicated to my family, but most of all Dana, my partner in life and love*

*All of old. Nothing else ever. Ever tried. Ever failed. No matter. Try again. Fail again.* ***Fail better.***

- Samuel Beckett (*Westward Ho*)

## Acknowledgements

These efforts would not have been possible without the assistance and support of a great many people who have influenced me over the course of this degree. I owe a large debt of gratitude to Dr. Robert Ben who willingly provided me with my first experience in research organic chemistry and then kindly invited me to pursue graduate studies. His willingness to provide help and support as well as a immense “degree of freedom” for me to pursue my research ideas and projects whether they were good or bad, has taught me more than I can say. His advice and assistance in the preparation of this document is kindly recognized; it would not have been possible without him.

I would also like to thank those who started me down this academic road, notably Dr. Natalie Goto who graciously accepted me into her research laboratory after my 2nd year undergraduate and Dr. Tony Durst, without whose inspired teaching and mentorship I would never have given organic chemistry a second glance. I would also like to thank those who I have taught, mentored, and tutored over the past nine years and who have kept my excitement in chemistry and teaching chemistry alive especially Maureen Robinson and Kathryn Davis.

I would like to reserve a special thank you to the long-suffering graduate students who taught me technique and appreciation for the discipline: Jenny Cheng from the Goto group whose hands off supervision allowed me to learn the best way one can: by making the mistakes; Elizabeth von Moos for introducing me to organic chemistry and allowing me to share her fume-hood and work on a very exciting project; Mat LeMay for teaching me to about methodology and providing the bulk of the effort that led to my first published article; Asim Mohammed for providing me with tons of support during my Honour’s thesis when Mat wasn’t available, and providing me with advice ever since.

I’d really like to thank my labmates—especially the “Ben Lab 6”—for more than I can write here: Jennifer Chaytor, Roger Tam, Pawel Czechura, Elizabeth von Moos, and Tahir Rana. Tahir put up with sharing a bay with me: accepting my “expansionary research technique,” my music and my conversation. Liz was excellent company and we share music taste and a love of running. Pawel for making every day exciting through his friendship, boisterousness, and “judgemental” personality. Pawel also taught me more than I can mention about practical experimental chemistry and how it should and could be done. Jenn for her friendship and our shared coffee and lunch runs: a great colleague and an even better friend. Finally Roger for all of his help with everything: he is the most talented, most modest, and friendliest chemist I have ever had the pleasure to work with. In addition to these six, I would also thank Dr. Mathieu Leclère, a friend and colleague over the entirety of my graduate degree for always

kindly correcting my errors: we might not have always agreed, but there is no one whose opinion I respect more. I'd also like Jackie Tokarew who took Tahir's place as my benchmate provided endless conversation, entertainment, and song.

I'd like to thank my other graduate colleagues for their inspiration, and friendship over the past years, the "Ben Bunnies" Wendy Campbell for all the fulljoying and fun, Ruoying (Gloria) Gong for her attitude and example of courage, and Sandra Ferreira for the atmosphere she brought to the place. My more recent colleagues Anna Balcerzak, Chantelle Capicciotti, and Taz Cheema have all contributed to the environment and have all enhanced the experience in their own way. Thanks go especially to Anna for agreeing to edit this document.

A special thanks goes to the undergraduate students I have had the honour to work with and supervise over this period: Yolanda Jong, Josephine Ta, Bonnie Kwok, Chantelle Capicciotti, Robyn Biggs and Malay Doshi. Working with all of them was a joy, and without these individuals portions of this work may never have been completed.

I would like to thank all the technical assistance I have received over the course of this work: especially Glenn Facey for his masterful command of the mysteries of the NMR machines, and his constant willingness to help with even the most unreasonable demands, Clem Kazakoff for his assistance with ESI and Jacek Spacek for his assistance with MALDI.

I would like to thank my family, my parents who have always supported me and encouraged me to chase my dreams and my limits, my brother for his friendship and light-hearted attitude and my in-laws: the best family one could ever hope to acquire and who have accepted me like a son. My personal family must be acknowledged, our twin cats Zipper and Zest have always taught me the importance of napping and eating regularly and Zipper was instrumental in the supervision of the writing of this thesis and kept me company every day from his basket next to the monitors.

I am deeply honoured to thank my committee, including Drs. Keillor, Boddy, Sundarajan and Wooley for agreeing to read this thesis and provide all of the excellent suggestions that have made it the best possible document. Any remaining errors are only mine alone.

Finally, and most importantly I owe everything accomplished in this thesis and everything not included in it to Dana Ménard, the rock of my life who has always been there when I needed her most, especially when the times were hardest. Without her I could never have completed this degree.

## Abstract

One of the largest problems in current medicine is the availability of organs for transplant. Due to the appropriately strict guidelines for viability, many willing donors are unable to contribute due to the current technological limitations in the storage of organs for any length of time. A possible solution to this problem would involve cryopreservation, and some strategies are currently used to assist in the cryopreservation of biological material. However, current cryopreservatives such as sucrose or DMSO have concerning cytotoxic issues that limit their possible applications.

A major cause of cryoinjury is the uncontrolled recrystallization of inter and intra-cellular ice crystals that occurs during the thawing process leading to mechanical damage and dehydration. The Ben lab has thus been interested in the design of compounds, based on AFGP-8 found in Teleost fish that are capable of inhibiting this process but do not possess other undesirable properties found in the native compounds. These synthetic analogues have been shown to increase cellular viability post-thaw.

The purpose of the studies in this thesis is twofold- to better understand the structural requirement for ice recrystallization inhibition (IRI) and to design and prepare more potent and (possibly simpler) IRI active compounds. These goals were approached from several different angles.

Modifications to the peptide backbone have been shown to affect IRI activity. Therefore, a series of mixed α/β glycopeptides are prepared and analyzed for antifreeze properties. The results of this study imply that it is not the gross conformation of the glycopeptide that is responsible for activity, but rather that intramolecular relationships may orient the different moieties of the glycopeptide in such a way that the molecule disrupts the reorganization of ice.

Modifications to the linker between carbohydrate and peptide have been shown to greatly affect IRI activity. A technique was devised for the incorporation of triazoles into this spacer to investigate the importance of the linker and to greatly simplify the synthesis of a library of glycoconjugates. It was found that the IRI activity of glycopeptides is very sensitive to the distance between carbohydrate and peptide backbone.

Simple sugars have been previously shown to exhibit IRI activity in direct correlation to their hydration index. However, some unnatural disaccharides which are predicted to be among the most potent, had not previously been prepared for analysis. Their preparation and IRI activity are reported and compared to other natural and unnatural disaccharides that have been examined for IRI activity.

The electron density at the anomeric oxygen is an important parameter with respect to intramolecular networks and possibly hydration. Although the intramolecular networks may be involved in determining IRI activity of simple sugars, no study has been carried out to affect these networks directly. A series of substituted galactosides is presented that modify the electronics of the anomeric oxygen, and thus the hydrogen-bond accepting capability of this atom. The results demonstrate that decreasing electron density at this position appears to improve IRI activity in a predictable manner. This suggests that anomeric electron density, and possibly intramolecular networks play a role in IRI activity.

Of all the *C*-linked glycopeptide analogues produced by the Ben group, one compound has repeatedly shown higher than expected activity. To better understand the remarkable IRI activity of this analogue, it was systematically truncated, tripeptide by tripeptide and atom by atom to its constituent building blocks. Although this study shed little light on the root cause of the IRI activity of the glycopeptide, it led to the serendipitous discovery of a series of very highly IRI active analogues that do not contain a peptide backbone. These compounds represent the first non-glycopeptides that can show very significant IRI activity even at very low concentrations.

The final portion of the thesis reports the efforts towards the preparation of a carbasugar analogue of AFGP-8. The target compound was pursued using two different methods, both of which failed to provide the desired derivative. However, several carbasugars were prepared and analyzed for IRI activity. These compounds were found to have similar potency to the native carbohydrates suggesting that the presence or absence of the endocyclic oxygen is unimportant for determining IRI activity.

# Table of Contents

Acknowledgements ..... iii

Abstract ..... v

List of Figures ..... xiii

List of Tables ..... xviii

List of Schemes ..... xix

Note to the reader regarding numbering ..... xxii

List of abbreviations ..... xxiii

Chapter 1 : Properties, structures and functions of biological antifreezes ..... 1

1.1 Applications of cryopreservation ..... 1

1.2 Properties of ice and water ..... 3

1.3 Introduction to biological antifreezes ..... 8

1.3.1 Discovery and evolution of biological antifreezes ..... 8

1.3.2 Antifreeze oligosaccharides ..... 15

1.3.3 Antifreeze proteins ..... 15

1.3.4 Antifreeze glycoproteins ..... 18

1.4 Interactions between ice and biological antifreezes ..... 20

1.5 Thermal hysteresis and dynamic ice shaping ..... 24

1.5.1 Dynamic ice-shaping ..... 25

1.5.2 Mechanism of thermal hysteresis ..... 25

1.5.3 Corollaries and applications of thermal hysteresis ..... 32

1.5.4 Structural domains of AFGPs required for TH activity and early syntheses of AFGP analogues ..... 34

1.6 Ice Recrystallization Inhibition (IRI) ..... 40

1.6.1 Applications of IRI ..... 41

1.6.2 Proposed mechanisms for IRI in AFPs and AFGPs ..... 43

1.6.3 Effects of structural modification on the IRI activity of *O*-linked AFGPs ..... 45

1.6.4 Effects of structural modification on the IRI activity of *C*-linked AFGPs ..... 48

1.6.5 Effects of structural modification on the IRI activity of monosaccharides and disaccharides ..... 52

1.6.6 Effects of hydration on IRI activity and revised proposal for the mechanism of *C*-linked AFGP analogues ..... 57

References ..... 62

Chapter 2 Goals and Objectives ..... 80

2.1 Factors responsible for antifreeze activity in C-linked AFGPs ..... 80

2.1.1 Objective 1: Determination of the effect of β-amino peptides on IRI activity (Chapter 3) ..... 81

2.1.2 Objective 2: Determination of the effect of triazole-containing glycopeptides on IRI activity (Chapter 4) ..... 83

2.2 Understanding IRI activity in carbohydrates: towards small molecule IRI inhibitors ..... 87

2.2.1 *Objective 3*: Determination of the IRI activity of 1-1 and 1-3 galactosyl-galactose derivatives (Chapter 5) ..... 88

2.2.2 *Objective 4*: Determination of the effect on IRI activity of electronic effects of anomeric aromatic substituted galactose derivatives (Chapter 6) ..... 89

2.2.3 *Objective 5*: Determination of the essential requirements for IRI activity in analogue 118 (Chapter 7) ..... 90

2.2.4 Objective 6: Synthesis and IRI analysis of carbasugar analogues of 118 and galactose (Chapter 8) ..... 91

2.3 Summary of research objectives ..... 93

References ..... 94

Chapter 3 : Determination of the effect of β-amino acid peptides on IRI activity in *C*-AFGPs. ..... 98

3.1 Effect of backbone modification on IRI activity ..... 98

3.2 Introduction to peptidomimetics as applied to AFGPs ..... 99

3.2.1 Conformations and secondary structures of β-peptides and mixed α/β peptides ..... 102

3.2 Variation in side chain, peptide backbone, and the introduction of a β-amino acid: precedence for the investigation of β-peptides ..... 104

3.3 Synthesis of mixed α and β glycopeptides ..... 106

3.3.1 Synthesis of the α-glycoconjugate ..... 107

3.3.2 Synthesis of the β-glycoconjugate ..... 109

3.3.3 Solid-phase synthesis of the glycopeptides ..... 113

3.4 Assessing the solution conformation of β-amino acid containing AFGPs ..... 115

3.5 Assessing antifreeze properties of β-amino acid AFGPs ..... 118

3.6 Chapter summary ..... 123

References ..... 124

Chapter 4 : Synthesis and IRI activity of triazole-containing analogues of *C*-AFGP ..... 128

4.1 Introduction to triazoles as amido-mimetics ..... 128

4.2 Introduction to the copper-catalyzed Huisgen-cycloaddition ..... 129

4.3 Previous applications of the CuAAC reaction to solid-phase synthesis..... 132

4.4 Determination of optimized conditions for solid-phase synthesis using a solution-phase model 134

4.4.1 Synthesis of glycosyl building block and preparation of amino acid building block ..... 134

4.4.2 Effect of temperature on the CuAAC reaction..... 136

4.4.3 Effect of copper source on the CuAAC reaction ..... 137

4.4.4 Effect of solvent on the CuAAC reaction..... 138

4.4.5 Effect of water content on the CuAAC reaction ..... 140

4.4.6 Effect of azide equivalents on the CuAAC reaction. ..... 142

4.4.7 Effect of substrate on the CuAAC reaction ..... 143

4.5 Synthesis of first generation triazole-containing *C*-glycopeptides ..... 146

4.5.1 Initial attempts at solid-phase supported CuAAC reactions between alkynyl peptides and azido carbohydrates..... 146

4.5.2 Application of microwaves to the CuAAC reaction between galactosylazides and resin-supported propargyl peptides. ..... 148

4.5.3 Synthesis of azide derivative 430..... 151

4.5.4 Synthesis of 1$^{st}$ generation glycopeptides using the on-bead CuAAC reaction..... 154

4.6 Assessment of the conformation of the first generation triazole-containing analogues using CD 155

4.7 Assessment of antifreeze activity of first-generation triazole-containing analogues ..... 157

4.7.1 TH and dynamic ice shaping ability of the triazole-containing glycopeptides..... 157

4.7.2 IRI activity of the first generation triazole-containing glycopeptides ..... 158

4.8 Comparison of IRI activity of the first generation triazole *C*-AFGPs with amide derivatives and peptoid triazole-containing derivatives ..... 159

4.9 Summary of results for 1$^{st}$ generation triazole-containing analogues..... 162

4.10 Design of 2$^{nd}$ generation triazole-containing analogues ..... 163

4.11 Synthesis of 2$^{nd}$ generation triazole AFGP analogues..... 165

4.11.1 Synthesis of amino acid building blocks ..... 167

4.11.2 Synthesis of glycosyl alkyne building blocks ..... 171

4.11.2.1 Preparation of the Ohira-Bestmann reagent 489..... 171

4.11.2.2 Synthesis of C-propargyl galactoside 453 ..... 172

4.11.2.3 Synthesis of C-butynyl galactoside 454..... 173

4.11.2.4 Synthesis of C-ethynyl galactoside 452 ..... 175

4.11.3 Solid Phase synthesis of peptides ..... 179

4.11.4 On-resin CuAAC synthesis of 2nd generation triazole AFGP analogues ..... 180

4.12 Assessing the conformation of 2nd generation triazole-containing glycopeptides ..... 183

4.13 Assessing the antifreeze activity of 2nd generation triazole-containing glycopeptides ..... 185

4.14 Chapter summary ..... 189

References ..... 191

Chapter 5 : IRI activity of (1,1)- and (1,3)-galactosyl-galactose derivatives and simple *C*-linked galactosides ..... 198

5.1 Disaccharides as small molecule inhibitors of ice recrystallization ..... 198

5.1.1 Early investigations into the antifreeze activity of *O*- and *C*-linked AFGP analogues ..... 198

5.1.2 IRI activity of previously prepared disaccharides ..... 201

5.2 Design and synthesis of a (1,3)-linked galactosyl-galactose derivative ..... 203

5.2.1 Synthesis of (1,3)-linked galactosyl-galactose ..... 204

5.3 Design and IRI analysis of (1,1)-galactosyl-galactose derivatives ..... 210

5.3.1 Synthesis of (1,1)-linked disaccharides ..... 210

5.3.2 Analysis of *C*-linked disaccharides produced via Glaser coupling. ..... 212

5.4 Preparation of monosaccharide derivatives ..... 213

5.4 IRI activity of disaccharides and the monosaccharide derivatives ..... 216

5.5 Chapter Summary ..... 220

References ..... 221

Chapter 6 : An exploration of the effect of anomeric aryl substituents on the IRI activity of pyranoses ..... 224

6.1 Design and synthesis of anomeric-substituted galactose derivatives ..... 225

6.2 IRI activity of anomeric-substituted galactose derivatives: correlation between activity and Hammett coefficient ..... 227

6.3 Chapter Summary ..... 234

References ..... 235

Chapter 7 : *C*-linked AFGPs as a platform for the development of small molecule IRI inhibitors. ..... 237

7.1 Precedent for exploring the activity of simple derivatives of highly active glycopeptide 118 ..... 237

7.1.1 Importance of the number of tripeptide repeats to antifreeze activity ..... 238

7.1.2 The difference in IRI activity between glycopeptides and small molecules ..... 238

7.2 Synthesis and IRI activity of monomer, dimer and trimer of 118 ..... 240
7.2.1 Synthesis of monomer dimer and trimer ..... 240
7.2.2 Antifreeze activity of monomer dimer and trimer compared to tetramer ..... 241
7.3 Synthesis and antifreeze activity of the glycoconjugate building block and its truncated derivatives ..... 242
7.3.1 Synthesis of glycoconjugate building block 228 and its truncated derivatives ..... 242
7.3.1.1 Synthesis of glycoconjugate building blocks 228 and 709 ..... 242
7.3.1.2 Synthesis of alkyl derivatives of 228 ..... 243
7.3.1.3 Synthesis of functionalized derivatives of building block 228 ..... 244
7.3.2 Antifreeze activity of glycoconjugate building block 228 and its derivatives ..... 248
7.4 Synthesis and antifreeze activity of structural analogues of propyl derivative 706 ..... 249
7.5 Synthesis and antifreeze activity of long-chain alkyl analogues of 228 ..... 254
7.6 Synthesis and antifreeze activity of terminal hydroxyl analogues of 228 ..... 260
7.7 Possible rationale for the activity of long-chain alkyl analogues ..... 262
7.8 Chapter Summary ..... 267
References ..... 268
Chapter 8 : Studies towards the synthesis of a carbasugar derivative of 118 and the synthesis of carbasugar derivatives of galactose and glucose ..... 272
8.1 Carbasugars as excellent, configurationally stable, mimics of natural sugars ..... 272
8.2 General synthetic strategies for the preparation of carbasugars ..... 274
8.3 End-stage retrosynthetic analysis of glycopeptide 231 ..... 275
8.4 Synthetic design involving a Sinaÿ rearrangement ..... 276
8.4.1 Synthesis of furyl galactose derivative ..... 278
8.4.1.1 Synthesis of galacto-furyl derivative 817 ..... 278
8.4.1.2 Attempts at elimination ..... 282
8.4.2 Synthesis of thiophenyl derivative 888 ..... 289
8.4.2.1 Synthesis of thiophenyl derivative 889 ..... 290
8.4.2.2 Attempts to introduce the anomeric furan using 834 and 835. ..... 291
8.4.3 Section summary and future possibilities ..... 292
8.5 Synthesis and antifreeze activity of galactose and glucose carbasugar analogues ..... 294
8.5.1 Retrosynthetic analysis of carbasugars. ..... 294

8.5.2 Antifreeze activity of carbasugar derivatives ..... 300
8.6 Chapter summary ..... 302
References ..... 303
Chapter 9 : Conclusions and Future Work ..... 310
Experimental protocols and characterization data ..... 318
General methods and materials for chemical reactions ..... 318
Procedure for circular dichroism ..... 319
Procedure for thermal hysteresis (TH) assay ..... 319
Procedure for ice recrystallization inhibition (IRI) assay ..... 320
General protocol for solid-phase peptide synthesis ..... 321
General protocol for solid-phase glycopeptide synthesis ..... 321
Experimental protocols for Chapter 2 ..... 323
Experimental Protocols for Chapter 3 ..... 343
Experimental Protocols for Chapter 4 ..... 357
Experimental Protocols for Chapter 5 ..... 394
Experimental Protocols for Chapter 6 ..... 410
Experimental Protocols for Chapter 7 ..... 415
Experimental Protocols for Chapter 8 ..... 456
Claims to Original Research ..... 486
Publications (Published and submitted as of submission of thesis) ..... 486
Supplementary Spectral Data ..... 488

# List of Figures

Figure 1.1 Hexagonal prism shape of an $I_h$ ice crystal showing the basal plane, the six prism planes and the main *C*-axis. ..... 4

Figure 1.2 Three dimensional structure of ice showing (A) the chair-like hexagons along the horizontal plane in pink, and (B) the boat-like hexagons along the three vertical planes in mahogany, navy and red (purple bond shared between two boats). The red circles represent the oxygen of a water molecule. ..... 4

Figure 1.3 Diagram showing the relative densities of water molecules in ice (blue) water (red) and the QLL (orange, yellow, and green). Each ball represents the oxygen atom of a water molecule ..... 7

Figure 1.4 Proposed xylopyranose-mannopyranose core of the antifreeze oligosaccharide of *U. ceramboides*..... 15

Figure 1.5 General structure of the Antarctic AFGPs. A galactosyl (blue)-N-acetyl-galactosamine (Green) disaccharide is linked through an α-glycosidic bond to a threonine (red)-alanine-alanine (purple) backbone..... 18

Figure 1.6 Diagram showing the TH effect. Blue line represents cooling without THCs. Red line represents cooling in presence of THCs. Green area represents temperature range protected by colligative properties. Orange region represents temperature range in which the fish are protected by the TH gap of their AFPs..... 23

Figure 1.7. Representation of the causation and results of DIS. THCs bind to the prismatic faces preventing further growth along this axis forcing the deposition of a new layer of ice forming the hexagonal bipyramid. ..... 25

Figure 1.8 Two-dimensional cross-section of the matress model of TH activity. The red balls, representing the THC associate with the ice surface forcing the ice to grow in acurved fasion between THCs. ..... 26

Figure 1.9. Early chemical tests carried out by DeVries and coworkers to determine AFGP structure and structural features required for TH activity. ..... 34

Figure 1.10 Previous syntheses of *O*-linked AFGP-8 analogues. (A) Anderson 1988; (B) Meldal, 1990; (C) Filira 1990; (D) Chen 2001; (E) Nishimura 1996-2001. ..... 36

Figure 1.11. TH activity of polymers of the AFGP core tripeptide at 40 mg/mL produced by Nishimura. .. 37

Figure 1.12. Analogues of AFGP prepared by Nishimura with a variety of different carbohydate functionalities. Presence of absence of TH activity is noted. All analogues expressed at least weak DIS activity. ..... 38

Figure 1.13. *C*-linked AFGP analogues showing weak or no TH activity. ..... 39

igure 1.14. Images of PBS, the positive control for recrystallization (A) and an IRI active compound (B) showing the difference in crystal size. Both images were obtainedat the same magnification. Field of view is approximately 100 μm. ..... 43

Figure 1.15 *O*-linked AFGP-8 analogues initially prepared by Nishimura and co-workers and re-synthesized by V. Bouvet for testing their IRI activity. ..... 46

Figure 1.16 IRI activity of Lysine derivatives generated by Eniade and Ben. All glycopeptides were tested at a carbohydrate concentration of $2.1 \times 10^{-5}$ M; consequently AFGP-8, 114, 115, 116, and 117 were examined at $5.5 \times 10^{-6}$, $2.1 \times 10^{-5}$, $7.0 \times 10^{-6}$, $3.0 \times 10^{-6}$, and $2.0 \times 10^{-6}$ respectively..... 48

Figure 1.17 Strucutral similarity of ornithine-linked glycoconjugate with arginine linked glycoconjugate found in arctic cod. ..... 49

Figure 1.18 Structure and IRI activity of analogues designed to examine the importance of the linker between the peptide and carbohydrate. ..... 49

Figure 1.19 Structures of the glycopolymers prepared by Gibson. Note that molecular masses range up to 107,420 Da ($PMAMGlc_{405}$). ..... 52

Figure 1.20 Simple carbohydrates tested for IRI activity. ..... 55

Figure 1.21 Disaccharides that were analyzed for IRI activity. ..... 55

Figure 1.22 IRI activity of mono- and disaccharides as tested by Tam and co-workers. All sugars tested at 22 mM. ..... 56

Figure 1.23. Hydration model of a solute in water showing the inner hydration layer (navy), the outer hydration layers (medium blue), and the bulk water phase (cyan). Hydration number is a count of the number of water molecules directly associated with the solute (white), while partial molar compressibility measures the compressibility (i.e. density) of the outer hydration sphere. ..... 57

Figure 1.24. (A) Correlation between hydration number and IRI activity from Tam et al. Notice the two parallel linear correlations. When the hydration number is divided by the molar volume to obtain the hydration index (B) a single linear relationship defines all points. ..... 58

Figure 1.25 Lowest-energy intramolecular water-bridged hydrogen bond networks. A) β-D-*O*-phenyl-galactopyranose; B) β-D-*O*-phenyl-glucopyranose; C) α-D-methylgalactopyranoside. ..... 60

Figure 2.1 The three components of the *C*-linked AFGP-8 analogues: carbohydrate, peptide and linker. 80

Figure 2.2 Proposed analogues of 118 incorporating a mixture of α (n, m, or p = 0) and β (n, m, or p =1) amino acids. ..... 82

Figure 2.3 Electronic and structural features of a Z- amide bond and its isostere, the 1,4-triazole ring. ... 84

Figure 2.4 Isomers of 118 designed to probe the importance of different features of the amide bond in the linker. ..... 84

Figure 2.5 Objective of this study. A) Optimization of reaction conditions between propargyl glycine derivative and azido-galactoses. B) Application of conditions from A for the synthesis of first generation triazole analogues containing propargyl glycine. C) Target triazoles containing various azido amino acids and alkynyl sugars—Analogue 217 is a direct triazole analogue of 118. ..... 85

Figure 2.6 Target disaccharides 222, 223, and 224. ..... 88

Figure 2.7 Examples of substituted phenyl galactosides envisioned for this study. ..... 89

Figure 2.8 Initial conceptual plan for the truncation of 118 to determine the features responsible for its IRI activity. ..... 91

Figure 2.9 A) A carbasugar compared to the true carbocyclic carbohydrate inositol; B) two important cyclitol derivatives: cyclophelitol and tamiflu. ..... 92

Figure 2.10 The mutarotation of galactose through the four most populated isomers and their relative abundance. ..... 92

Figure 2.11 A) Carbasugar glycopeptide target and the secondary B) carbasugar monosaccharide targets. ..... 93

Figure 3.1 IRI activity of glycopeptides with modified backbones..... 98

Figure 3.2 Previously prepared compounds with backbone modifications..... 100

Figure 3.3 Comparison between peptoid and mixed peptide as peptidomimetics. ..... 102

Figure 3.4 Possible backbone hydrogen-bond interactions and the resulting secondary structures formed in β peptides. Models are provided to show the relative orientation of side-chains in the three most common helices. Interactions adapted from Wu,[2] and models reproduced from Kritzer..... 103

Figure 3.5 General structure of $\alpha$ amino acids and the five types of mono-substituted (per carbon) β amino acids. ..... 103

Figure 3.6 IRI activity of previously prepared β-amino acid-containing peptides compared with their α-analogues..... 104

Figure 3.7 Mixed α- and β-peptides produced for this study. ..... 106

Figure 3.8 CD spectra of mixed peptides generated in this study, vertical axis is expressed in molar ellipticity..... 116

Figure 3.11 Photograph of the sample holder, containing the small wells, held by a standard set of tweezers to show scale. Photograph replicated from Thapa 2006..... 118

Figure 3.10 Microscopy images of ice crystals from analogue 204 (left) which shows mild dynamic ice shaping, note the nascent faces, and an ice crystal in pure water (right) which is strictly circular..... 118

Figure 3.12 IRI activity of mixed glycopeptides produced in this study. Glycopeptides were analyzed for activity at both 5.5 μM (red bars) and 550 μM (blue bars)..... 121

Figure 3.13 Possible important relationship in analogue 202 and 118..... 122

Figure 4.1 Electronic and structural features of a Z- amide bond and its isostere, a 1,4-triazole ring. .... 128

Figure 4.2 A) Peptoid derivatives prepared by Norgren et al. and B) *O*-linked derivative prepared by Miller et al..... 133

Figure 4.3 Conditions applied to the reaction between 413 and 416 to determine the preferred temperature..... 136

Figure 4.4 Structures of glycosyl azides and their respective glycoconjugates examined in the substrate investigation. ..... 143

Figure 4.5 Resin supported peptides produced for the 1$^{st}$ generation analogues..... 147

Figure 4.6 CD spectrum of glycoconjugates 209-212. All spectra were acquired at 22 ºC in triplicate, with a concentration of 43 μM. CD data has been normalized for concentration and number of chromaphores. ..... 155

Figure 4.7 IRI activity of 1$^{st}$ generation triazole analogues (blue) compared to AFGP-8, PBS and active amide-containing analogue 118 (red). ..... 158

Figure 4.8 1$^{st}$ Generation triazole-containing *C*-AFGP analogues (209-212) and their reversed amide-containing (441-444), peptoid (410) and amide-containing homologues (118, 133-135)..... 159

Figure 4.9 IRI activity of the 2nd generation amide and *C*-serine analogues with various linker lengths. 161

Figure 4.10 Synthetic conditions, products, and yields from the resin-supported CuAAC reaction to generate 2nd generation triazole-containing glycopeptides. ..... 180

Figure 4.11 Isolated Glaser-type byproducts from the CuAAC reaction. 182

Figure 4.12 CD spectra of 2nd generation triazole glycopeptides 213-221. All spectra were acquired in triplicate at 22 ºC at a concentration of 43 μM. CD data has been normalized for concentration and the number of chromaphores. 183

Figure 4.13 Microscopy images of ice crystals from analogue 213, which is circular and similar to the ice crystals seen in distilled water, and analogue 217 with slight, but clearly observable hexagonal ice shaping. 185

Figure 4.14 IRI activity of 2nd generation triazole-containing glycopeptides. Compounds were analyzed at two concentrations, 550 μM (blue) and 5.5 μM (red). 186

Figure 5.1 IRI activity of disaccharide glycopeptides prepared by Czechura. 199

Figure 5.2 Measured partial molar compressibilities of several disaccharides by Galema and Høiland. The disaccharides examined in this text are highlighted in red. A more negative value implies a larger hydration sphere surrounding the solute. 200

Figure 5.3 IRI activity of previously examined disaccharides from the work of Tam and co-workers, S. Ferreira and A. Balcerzak. Galactose containing analogues are in orange, Galactosamine-containing analogues are in blue. 201

Figure 5.4 Target disaccharides. 202

Figure 5.5 Glaser-disaccharides produced in Chapter 4. 203

Figure 5.6 Monosaccharide control compounds analyzed for IRI activity in Figure 5.7. Compounds are categorized by functional group (vertical) and length of anomeric substituent (horizontal). Compound 539 was previously prepared by J. Chaytor. Polyols 538 and 540 were prepared as shown in Scheme 5.12 below. All other compounds were obtained through Zemplén deprotection from the corresponding acetate. 214

Figure 5.7 IRI activity of monosaccharide derivatives in Figure 5.6. All compounds are analyzed at 22 mM. Compounds are categorized by functional group (colour), and spacer length (groups). Spacer length indicates the number of methylene groups between the anomeric carbon of the sugar and the functional group for the azide (red), and alkyne (blue) or a methanol moiety in the case of the alcohols (orange). 217

Figure 5.8 IRI activity of disaccharides prepared in this chapter and their previously examined direct analogues. 218

Figure 6.1 IRI activity of β-aryl galactosides: electron rich, red; phenyl derivative, blue; electron poor, orange; galactose, green. 227

Figure 6.2 Hammett plot showing the relationship between the rate of recrystallization and the electronic effect of the substituents at the anomeric position. 231

Figure 6.3 Proposed hydrogen-bonding network present in galactose. Adapted from Carçabal 2005. 233

Figure 7.1 IRI activity of simple C-linked derivatives of galactose. 239

Figure 7.2 Planned truncation of OGG(gal) to determine the importance of structural feature to antifreeze activity. 239

Figure 7.3 Synthesis of glycopeptides 225-227. 240

Figure 7.4 IRI activity of the glycopeptides: monomer (225, red), dimer (226, blue), trimer (227, orange) and tetramer (118, green) at three concentrations. 241

Figure 7.5 IRI activity of initial analogues of the glycoconjugate building block: carboxylic acid and primary amide (702, 703 blue), alkyl amides (red, 704-708), terminal alcoholic amide (728, orange), charged derivatives (229, 230 and 716, purple) and zwitterionic building blocks (228, 709, green). ..... 248

Figure 7.6 IRI activity of propyl-motif containing analogues: root propyl analogue (706, red), branched analogues (729-732, blue), cyclic analogues (733-734, green) and unsaturated (713, 714, 735-737, orange). ..... 252

Figure 7.7 IRI activity of medium-chain alkyl analogues soluble at 22 mM: benzyl and isoamyl (712, 751, blue) and *n*-alkyls (708, 752-754, red) ..... 255

Figure 7.8 The relationship between IRI activity and the length of the alkyl amide. ..... 255

Figure 7.9 IRI activity of long-chain alkyl derivatives over a range of concentrations. ..... 257

Figure 7.10 Linear relationship between chain length and IRI activity for the long chain alkyl analogues at both 5.5 and 550 μM. ..... 259

Figure 7.11 IRI activity of terminal alcohol derivatives at various concentrations. ..... 261

Figure 7.12 SEM image of analogue 751 at 80,000x magnification showing a fibrous network typical of a gel. ..... 263

Figure 7.13 Cartoon representation of the proposed mechanism for ice recrystallization inhibition. Carbohydrates reside at the quasi-liquid layer (QLL)-bulk water interface. Reproduced from Tam et al. 265

Figure 8.1 The mutarotation of galactose through the four most populated isomers and their relative abundance in water at 31 ºC. ..... 273

Figure 8.2 Target carbasugars. ..... 274

Figure 8.3 IRI activity of galactose (red) and glucose (blue) carbasugar analogues and the inositols tested by C. Capicciotti (orange) compared to glucose and galactose. ..... 300

Figure 8.4 Structures of the inositols tested by C. Capicciotti. ..... 300

# List of Tables

Table 1.1 Physical properties, strucutres, and ice-binding mechanisms of known antifreeze proteins..... 17

Table 3.1 Crude and purified yields of mixed glycopeptides. ..... 114

Table 3.2 Deconvolution of the CD spectra in Figure 3.8 showing the contributions of different secondary structures to the conformation of the glycopeptide. Data was calculated using CD Pro IBASIS 5 and from an average of the values produced from three different deconvolution algorithms. ..... 117

Table 4.1. Effect of copper source on reaction time, conversion, and isolated yield of the CuAAC reaction between 413 and 416..... 137

Table 4.2 Effect of solvent on reaction time, conversion and isolated yield of the CuAAC reaction between 413 and 416. ..... 139

Table 4.3. Swelling volumes of selected solvents. Values indicate the swollen volume of a given mass of Wang resin after excess solvent has been removed. ..... 140

Table 4.4 Effect of water content in the solvent system on the reaction time, conversion and isolated yield of the CuAAC reaction between 413 and 416..... 141

Table 4.5 Effect of water content and equivalents of glycosyl azide on the reaction time, conversion and isolated yield of the CuAAC reaction between 413 and 416..... 142

Table 4.6 Effect of the solvent system on the reaction time, conversion and isolated yield of the CuAAC reaction between 413 and 416 (pink), 417 (white), and 420 (blue). ..... 144

Table 4.7 CD deconvolution data for triazole containing *C*-AFGPs, AFGP-8 and active amide analogue 118. Data was calculated using CD Pro IBASIS 5 and form an average of the values produced from three different deconvolution algorithms. ..... 156

Table 4.8 Nine 2$^{nd}$ generation triazole-containing *C*-AFGP analogues derived from three resin-supported glycopeptides and three galactosyl alkynes..... 164

Table 4.9 Selected conditions for the homologation of aldehyde 435 to alkyne 1407. ..... 177

Table 4.10 Secondary structure of glycopeptides 213-221 derived from the deconvolution of the CD spectra in Figure 4.12. ..... 184

Table 6.1 Synthesis of β-aryl substituted galactose derivatives. ..... 225

Table 6.2 $\sigma_I$ values used for the Hammett plot. Values obtained from Hansch et al. ..... 231

Table 7.1 Synthesis and structure of propyl-motif analogues prepared in this study. Yields are provided for the acetylated and deprotected constructs prepared from commercially available amines. ..... 250

Table 7.2 Synthesis of long-chain alkyl analogues. ..... 254

Table 7.3 Synthesis of long-chain primary alcohol-containing analogues..... 260

Table 8.1 Selected conditions examined to glycosylate 872 and preferentially provide 820. ..... 279

Table 8.2 Selected conditions attempted for the formation of 815 through activation and elimination of the C-6 hydroxyl group. Isolated yields are provided of both activated species (822, 826, or 827) and anhydrosugar 823 at both stages of the sequence when relevant. ..... 284

# List of Schemes

Scheme 3.1 Synthesis of carboxylic acid 315. 107

Scheme 3.2 Synthesis of amino acid 318 and the preparation of glycoconjugate 320. 108

Scheme 3.3 Retrosynthetic options for the synthesis of 320. 109

Scheme 3.4 Synthesis of 321 through Arndt-Eistert homologation of the glycoconjugate. 110

Scheme 3.7 General strategy for the SPPS synthesis of peptides and glycopeptides. 113

Scheme 4.1 Proposed mechanism for the Copper-catalyzed azide alkyne cycloaddition (CuAAC). 130

Scheme 4.2 Proposed mechanism for β-chlorination through the *in situ* production of $PCl_4^+$ as a Lewis acid. 135

Scheme 4.3 Synthetic strategy for the preparation of protected propargyl glycine 414 and glycosyl azides 416, 417 and 420. 135

Scheme 4.4 Initial attempt to carry out CuAAC reaction on solid phase with conventional heating. 147

Scheme 4.5 Microwave-assisted CuAAC synthesis of glycopeptides 428 and 429. 149

Scheme 4.6 Initial attempts to synthesize glycosyl azide 430. 151

Scheme 4.7 Synthesis of methylazido galactose derivative 430. 153

Scheme 4.8 On-resin CuAAC reaction between peptide 426 and glycosyl azides to prepare glycopeptides 209, 210 and 211. 154

Scheme 4.9 Application of the synthetic conditions and glycosyl azide 430 to the synthesis of glycopeptide 212 by Dr. M. Leclère. 156

Scheme 4.10 Retrosynthetic analysis of 2nd generation triazole-containing glycopeptides. 167

Scheme 4.11 Synthesis of azido amino acid 459 from methionine. 168

Scheme 4.12 Initial synthesis of Fmoc-protected azido lysine (461) and ornithine (460) derivatives. 170

Scheme 4.13 Alternative synthesis of Fmoc-protected azido-lysine and ornithine derivatives 460 and 461. 171

Scheme 4.14 Synthesis of the Ohira-Bestmann reagent. Phosphate 489 was prepared according to the protocol of Pietruszka and Witt, and tosyl azide is prepared according to Pollex. 172

Scheme 4.15 Synthesis of galactosyl alkyne 453 using the Bestmann-Ohira reagent (489) 173

Scheme 4.16 Synthesis of butynyl derivative 454 via either direct oxidation of a carbon-boron bond or through one-carbon homologation using a Wittig olefination. 175

Scheme 4.18 Attempted synthesis of glycosyl alkyne 1403 as a model system using alkynyl nucleophiles. 177

Scheme 4.17 Jobron and co-workers' synthesis of alkynyl-glycosides. 177

Scheme 4.19 Key mechanistic steps in the Ohira-Bestmann modification of the Seyferth-Gilbert homologation. ..... 179

Scheme 4.20 Final steps in the synthesis of 452 and 1408. ..... 180

Scheme 5.1 Original approach to 508 relying on the selective protection of galactose derivative 511 ..... 203

Scheme 5.2 Alternative approach to β-D-galactopyranosyl-(1→3)-D-galactopyranose derivative 508 relying on selective ring-opening of an orthoester to provide 514. ..... 204

Scheme 5.3 Synthesis of selectively protected galactose derivative 511. ..... 204

Scheme 5.4 Synthesis of acetate protected glycosyl acceptor 514. ..... 205

Scheme 5.5 Stereoelecteronic rationale for the preferential formation of 514 over its *C*-3 acetate isomer. ..... 207

Scheme 5.6 Synthesis of glycosyl sulfoxide 513. ..... 208

Scheme 5.7 Attempted synthesis of disaccharide 527 using $Tf_2O$ as activator. ..... 208

Scheme 5.8 Synthesis of disaccharide 508 using TfOH as promoter. ..... 209

Scheme 5.9 Proposed retrosynthesis of galacto-trehalose-like disaccharides 223 and 224. ..... 210

Scheme 5.10 Synthesis of *galacto*-trehaloses 223 and 224. ..... 211

Scheme 5.11 Preparation and structure of Glaser-type disaccharides. ..... 213

Scheme 5.12 Synthesis of polyols 538 and 540 for use in the IRI assay. ..... 215

Scheme 7.1 Concomitant deprotection of backbone Fmoc and carbohydrate acetate groups. ..... 243

Scheme 7.2 Synthesis of simple alkyl amide derivatives. Yields for 704-706 are for the two steps from 315. Yields for 707 and 708 are from 710 and 711 respectively. ..... 244

Scheme 7.3 Synthesis of primary amide derivative 703. ..... 244

Scheme 7.4 Synthesis of amino derivatives 229 and 716. ..... 245

Scheme 7.5 Synthesis of carboxylic acid derivative 230 and pentanol derivative 728. ..... 247

Scheme 7.6 Preparation of crotyl derivative 737. ..... 250

Scheme 7.7 Synthesis of enamide analogues 713 and 714. ..... 251

Scheme 7.8 Synthesis of amino alcohols 775 and 779. ..... 261

Scheme 8.1 Target glycopeptide 231, carbasugar analogue of highly IRI active 118, and key intermediate 801. ..... 272

Scheme 8.2 Retrosynthetic analysis of carbasugar glycopeptide 231 to key intermediate 801. ..... 276

Scheme 8.3 Proposed mechanism for the Sinaÿ rearrangement. ..... 276

Scheme 8.4 Initial retrosynthetic analysis of 801 employing the Sinaÿ rearrangement as the key transformation. ..... 277

Scheme 8.5 Synthesis of *C*-linked galactose intermediate 817. ..... 278

Scheme 8.6 Results of the iodination of primary alcohol 817. ..... 283

Scheme 8.7 Attempts to produce 815 through intramolecular strategies. ..... 286

Scheme 8.8 Dehydration of 831 and attempted Sinaÿ rearrangement of 833. ..... 287

Scheme 8.9 Two chair conformations of 822 and 832 showing the number of axial substituents present in each ..... 288

Scheme 8.10 Retrosynthetic analysis of 815 involving a late-stage introduction of the anomeric furyl substituent. ..... 289

Scheme 8.11 Synthesis of sulfide 835 and sulfoxides 834a and 834b. ..... 290

Scheme 8.12 Proposals for the alternate preparations of 801 utilizing the Sinaÿ rearrangement. ..... 293

Scheme 8.13 Synthesis of bicyclic 846 and triacetate 847 from furan and acrylic acid. ..... 295

Scheme 8.15 Synthesis of carbasugars 232, 233, and 234 from lactone 847. ..... 297

Scheme 8.14 Retrosynthetic analysis of carbasugars 232-234 ..... 297

## Note to the reader regarding numbering

To simplify the navigation of the document, each compound has, in the usual fashion, been given a unique numeric identifier. However, the numbers are not continuous. The first (not previously mentioned) compound in each chapter is provided the number **X01** where **X** represents the chapter number. Thus, each number identifies the chapter in which the compound is first encountered. For those chapters with more than 100 compounds, the 99$^{th}$ compound is designated **X99** while the 100$^{th}$ compound is designated **1X00**. It is hoped that this system simplifies the reading experience and helps orient the reader to the document. Experimental and spectral data is likewise reported in numeric order of appearance.

John Trant

## List of abbreviations

| | |
|---|---|
| α | Alpha |
| β | Beta |
| βO | Beta-ornithine (glycosylated) |
| βG | Beta-glycine |
| γ | Gamma |
| δ | Delta |
| Δ | Heat |
| λ | Light |
| σ | Sigma, substituent constant (Hammet relationship) |
| $^{1}H$ | Proton (NMR) |
| $^{13}C$ | Carbon (NMR, carbon-13) |
| ACC | Antarctic circumpolar current |
| AcOH | Acetic acid |
| $Ac_2O$ | Acetic anhydride |
| AFP | Antifreeze protein |
| AFGP(s) | Antifreeze glycoprotein(s) |
| AFGP-8 | Antifreeze glycoprotein fraction 8 |
| Ala | Alanine |
| AllylOH | Allyl alcohol |
| Asn | Asparagine |
| Atm | Atmospheres |
| bd | Broad doublet |
| Bn | Benzyl |
| BOC | *t*-Butoxycarbonyl- |
| $BOC_2O$ | Di-*tert*-butyl dicarbonate |
| bs | Broad singlet |
| Bu | Butyl |
| *(t)*-BuOH | (*tert*)-Butanol |

| | |
|---|---|
| *C*-18 | Octadecyl-bonded silica |
| *C*-AFGP | *C*-Linked antifreeze glycoprotein analogue |
| Calc | Calculated |
| Cat. | Catalytic |
| Cbz | Carboxybenzyl- |
| CD | Circular dichroism |
| $CDCl_3$ | Deuterated chloroform |
| CDI | Carbonyldiimidazole |
| $CD_3OD$ | Deuterated methanol |
| CPG | Controlled-Pore Glass |
| CuAAC | Copper catalyzed (or assisted) alkyne/azide cycloaddition |
| d | Doublet |
| $D_2O$ | Deuterium oxide (deuterated water) |
| dd | Doublet of doublets |
| DCM | Dichloromethane |
| DIPEA | Diisopropylethylamine |
| DIS | Dynamic ice-shaping |
| DMAP | 4-(*N,N*-Dimethyl)-amino pyridine |
| DMF | Dimethylformamide |
| DMSO | Dimethylsulfoxide |
| dt | Doublet of triplets |
| DTBMP | 2,6-di-*tert*-butyl-4-methyl pyridine |
| EI | Electron impact |
| ESI | Electrospray ionization |
| Et | Ethyl |
| $Et_2O$ | Diethyl ether |
| EtOAc | Ethyl acetate |
| EtOH | Ethanol |
| Fmoc | 9-Fluorenylmethyloxycarbonyl |

| | |
|---|---|
| FT-IR | Fourier transform infrared spectroscopy |
| G | Glycine |
| Gal | Galactose |
| GalNHAc | N-acetyl galactosamine |
| GFP | Green fluorescent proteins |
| Glc | Glucose |
| H-bond | Hydrogen bond |
| HBTU | 2-(1H-Benzotriazol-1-yl)-1,1,3,3-tetramethyuronium hexafluorophosphate |
| HCTU | 2-(6-chloro-1H-Benzotriazol-1-yl)-1,1,3,3-tetramethyuronium hexafluorophosphate |
| HMPA | Hexamethylphosphoramide |
| HOBT | *N*-hydroxyl benzotriazole |
| HPLC | High pressure (performance) liquid chromatography |
| hr(s) | Hour(s) |
| IBX | *o*-iodobenzoic acid |
| IDCP | Iodine dicollidine perchlorate |
| Ile | Isoleucine |
| IRI | Ice recrystallization inhibition |
| IRIC | Ice recrystallization inhibition active compound |
| LAH | Lithium aluminum hydride |
| LDL | Low-Density Lipoprotein |
| Leu | Leucine |
| m | Multiplet |
| $M^+$ | Parent molecular ion |
| m/z | (Molecular) mass to charge ratio |
| MALDI-TOF | Matrix assisted laser desorption/ionization-time of flight |
| MD | Molecular dynamics |
| Me | Methyl |

| | |
|---|---|
| MeOD | Deuterated methanol |
| MeOH | Methanol |
| MLGS | Mean largest grain size |
| MGS | Mean grain size |
| min(s) | Minute(s) |
| MS | Molecular sieves |
| MS | Mass spectrometry |
| Ms | Methanesulfonyl |
| Na Asc. | Sodium ascorbate |
| $NEt_3$ | Triethylamine |
| NHAc | *N*-acetyl |
| NIS | *N*-Iodosuccinamide |
| NMM | *N*-methyl morpholine |
| NMP | *N*-Methyl pyrrolidone |
| NMR | Nuclear magnetic resonance |
| O | Ornithine |
| p | Pentuplet |
| PBS | Phosphate-buffered saline, pH = 7.4. |
| PDB | Protein databank |
| Pent | Pentyl |
| Pd/C | Palladium supported on charcoal (10 % dry weight) |
| PDB | Protein Database |
| PG | Protecting group |
| PGALEMA | Poly[(β-D-galactosyloxy)ethyl methacrylate] |
| Phe | Phenylalanine |
| PMAMGlc | Poly(methyl-6-*O*-methacryloyl-α-D-glucopyranoside) |
| PMC | Partial molar compressibility |
| PP II | Polyproline type II |
| ppm | parts per million |

| | |
|---|---|
| PVA | Poly(vinyl alcohol) |
| Pyr | Pyridine |
| q | Quartet |
| qd | Quartet of doublets |
| QLL | Quasi-liquid layer |
| Quant. | Quantitative yield |
| RCM | Ring-closing metathesis |
| RP-HPLC | Reversed-phase (i.e. C-18) high pressure liquid chromatography |
| RP-SPE | Reversed-phase (i.e. C-18) solid phase extraction |
| Rf | Retention factor |
| RT | Room temperature |
| s | Singlet |
| septd | septuplet of doublets |
| Ser | Serine |
| SPE | Solid-phase extraction |
| SPPS | Solid-phase peptide synthesis |
| Su | Succinimyl- |
| $T_R$ | Retention time |
| TBAF | Tetrabutyl ammonium fluoride |
| TBDMS | *tert*-Butyldimethylsilyl |
| TBS | *tert*-Butyldimethylsilyl |
| td | Triplet of doublets |
| TEMPO | 1-oxyl-2,2,6,6-tetramethylpiperidine |
| TES | Triethylsilyl- |
| TFA | Trifluoroacetic acid |
| $TfO_2$ | Trifluoromethanesulfonic anhydride |
| TfOH | Trifluoromethanesulfonic acid |
| TH | Thermal hysteresis |
| THC | Thermal hysteresis (active) component |

| | |
|---|---|
| THF | Tetrahydrofuran |
| Thr | Threonine |
| TIPS | Triisopropylsilyl- |
| TIS | Triisopropylsilane |
| TLC | Thin layer chromatography |
| TMS | Trimethylsilyl- **or** Tetramethylsilane |
| TMSOTf | Trimethylsilyl trifluoromethane sulfonate |
| Ts | Toluenesulfonyl |
| tsept | Triplet of septuplets |
| v/v | Volume/volume |

# Chapter 1 : Properties, structures and functions of biological antifreezes

## 1.1 Applications of cryopreservation

Cryogenics, the preservation of biological material at sub-zero temperatures, is still in its infancy.[16] Initial efforts were directed towards the freezing of whole organisms (including humans) immediately after death in order to preserve them to some future date when they could be "woken-up" and supposedly cured of the medical condition that caused or was about to cause natural death. Unsurprisingly, although somewhat popular and inspiring in a science-fiction manner, the technique most likely results in complete tissue, let alone organismal, death resulting from mechanical cell damage, dehydration and cellular "leakage" due to compromised membranes during the freezing process. Likewise, any tissue that miraculously survives the freezing process would most likely fail to recover from the thawing process, a transition that in many ways can be far more dangerous because, although it is relatively easy to flash-freeze tissue, thawing must occur over a longer period of time and the resulting growth in ice crystals due to recrystallization would be fatal for most cells.[28] There are, however, several companies that, for a modest fee (from anywhere between $ 28,000 to $ 200,000), are willing to freeze a client's body and store it until such a time that the client could be resuscitated and returned to life.[32, 33] However, the veracity of these corporate claims remains, to be charitable, doubtful.

A more important, reasonable and achievable first step in cryogenics would be the temporary storage of organs for transplant. As the oxygen in the blood declines

rapidly following cardiac death, organs degrade very quickly. For example, a heart or lung is only viable for four hours following cardiac death while a liver can be viable up to twelve hours following cardiac death and the comparably robust kidneys can be viable for up to three days. Unfortunately, with current techniques the organs can only be stored at 4 ºC (to prevent ice formation) which does slow the degradation process, but only to a limited degree. This greatly limits the number of organs available for transplant as the number of young healthy individuals dying of brain death in hospital is quite small; these are the ideal donors as the cardiac system can be kept alive just prior to transplant in order to keep the organs viable. This issue has caused considerable consternation in the transplant community and complex policy decisions at the Ontario provincial level are implemented to attempt to somewhat negate the difficulties involved.[35] It would be ideal if there was a way to maintain the viability of organs, especially hearts, past the four-hour mark, in order to greatly expand the pool of potential donors to include those dying suddenly in hospitals or in accidents outside institutions. Being able to freeze the organs and halt all metabolism including any degradation process would allow the organs to be stored indefinitely: the greatest challenge in the transplant field, the need to localize a live but dying donor and recipient in the same place at very short notice, would be overcome. However, to achieve this objective, mechanisms are required that interfere with the formation, expansion, and re-organization of ice crystals and the consequent damage they cause; this goal, in turn, requires a greater understanding of the physics and dynamics of ice and ice-growth.

## 1.2 Properties of ice and water

Ice. The word itself carries considerable cultural significance; it brings to mind a cold, harsh, sharp, dangerous environment. It is no wonder that the last places on the surface of the Earth to be conquered by man were the North Pole, the South Pole and, of special significance for Canadians, the Northwest Passage. But as harsh as ice is at the macro-level, it is at least as great a challenge at the micro-level: ice crystals can cause significant and severe damage to cells and tissues both during the freezing process (due to mechanical cell damage due to ice crystal growth), while frozen (due to osmotic pressures causing desiccation and consequent membrane disruption of the cells), and during the thawing process (due to mechanical cell damage caused by ice-recrystallization). The combination of these effects leads to the inescapable conclusion that ice is toxic to cells. However, as mentioned above, sub-zero storage would be ideal for slowing down metabolism and thus, if the challenges could be overcome, ideal for preserving biological material. A better understanding of ice could allow for the medical community to benefit from, or at least neutralize, its unique properties and allow for the exploitation of cryopreservation.

Although 15 different crystalline forms of ice are known, ice on Earth under natural conditions exists only as hexagonal ice.[36] It has been proposed that a meta-stable form, cubic ice, can be formed in clouds in the troposphere under very specific conditions, but even if true, this ice would never come into contact with the biosphere.[37] However, it could become relevant in the storage of tissues below -80 ºC as hexagonal ice tends to convert to cubic ice at these temperatures. All other forms of crystalline ice

require high pressures to induce formation (above 100 MPa) and can play no significant role in nature on the Earth's surface.

In addition to these crystalline isoforms, amorphous ice is formed by the extremely rapid cooling of liquid water, normally by the condensation of water vapour on a very smooth (no edges for crystallization) surface below -150 ºC: submersion of a sample in liquid helium is insufficient for providing such a cooling rate. This rapid rate of cooling is technically incredibly difficult to obtain even in the laboratory and consequently amorphous ice remains a curiosity on Earth although it is the dominant form in interstellar space and although it might be important for xenobiological considerations some time in the future, it need not be further considered here.[38]

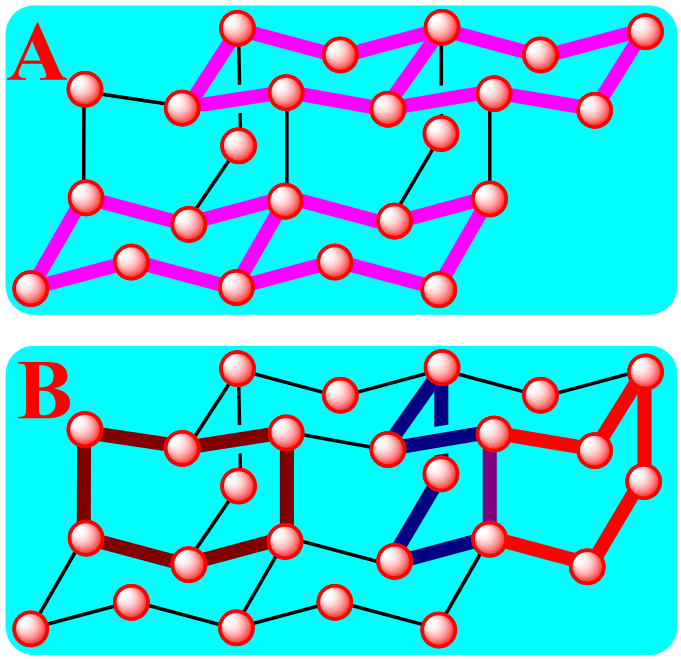



**Figure 1.2 Three dimensional structure of ice showing (A) the chair-like hexagons along the horizontal plane in pink, and (B) the boat-like hexagons along the three vertical planes in mahogany, navy and red (purple bond shared between two boats). The red circles represent the oxygen of a water molecule.**

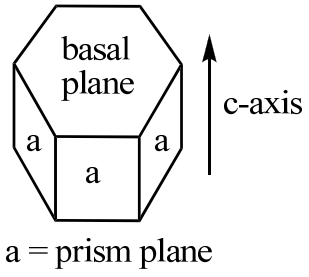



**Figure 1.1 Hexagonal prism shape of an $I_h$ ice crystal showing the basal plane, the six prism planes and the main *C*-axis.**

The only "native" form of ice, hexagonal ice, $I_h$, derives its name from the core repeating subunit, which takes on the structure of interlocking tetrahedral-based

hexagons with an oxygen atom at the location of each carbon and a single hydrogen atom lying directly along the axis between each oxygen atom (Figure 1.2). Although closely resembling the crystal structure of diamond on first glance it differs in a key manner. Unlike diamond (made up of perfect interlocking “chairs”), $I_h$ has two different axes giving the crystals a hexagonal prism shape (Figure 1.1) with a basal plane and six prism planes. The basal plane, perpendicular to the primary axis, the c-axis, is constituted of sheets of water molecules arranged in a chair conformation (Figure 1.2 A). The prism plane, perpendicular to the basal plane, is formed by sheets of water molecules arranged in a “boat” conformation (Figure 1.2 B). It is this formation of these three boats, each at 120 º to one another but all parallel to the c-axis that leads to the hexagonal shape of the ice crystal. This difference in geometries of the two planes is an essential aspect of ice formation: because of the different positions of the water molecules when they add to each face, the rate of expansion of the ice crystal is not the same for the two faces. Under general conditions, it tends to be easier for ice to add to the prism faces of the growing ice crystal and ice crystals tend to expand along the prism face more rapidly than they grow along the basal face (ie. the ice crystal grows outward rather than upward).

The most important aspect of ice crystals for the purposes of this thesis are the surface interactions. The especially interesting question involves what exactly is occurring at the point where ice and water meet. The predominant theory for the past couple of centuries has proposed that there was a direct boundary between ice and water. This was first put forward by Thomson who believed that when two pieces of ice initially come into contact only at a “geometric point,” the “intensity must be great,”

sufficient in fact to melt the ice even at low temperatures. He proposed that this newly formed water immediately refreezes to form an ice bridge.[39] This conveniently explained why ice skates worked, as they could glide on a thin layer of water rather than ice, and was widely adopted as the predominant explanation. However, prior to Thomson putting forward this theory, Faraday observed that "a particle of fluid water…when in contact with ice on two or more sides [has a greater tendency to freeze] above that it had when in contact on one side only." He then proposed that ice and water always co-exist in equilibrium and that ice is most likely coated with a thin layer of water.[40] Some have suggested that in doing so he predicted the existence of a quasi-liquid layer (QLL),[41] although a closer reading makes this seem an anachronistic desire on the part of current researchers rather than a "true interpretation" of the original text. The existence of a QLL was first proposed by Stranski in 1941 with regards to metallic crystals: the solid crystals are coated by a layer that is neither liquid nor part of the crystal when they are below their melting point.[42] The first time the term arises with respect to water is in the work of Fletcher who proposed, in 1968, a theory for the molecular structure of the surface of ice proposing that the QLL layer is the boundary between bulk water and ice.[43] More recently, this layer has been measured through a wide variety of techniques including atomic force microscopy,[44, 45] X-ray diffraction,[46] infrared spectroscopy,[47] proton-backscattering,[48] Raman spectroscopy,[49] quartz-crystal microbalance measurements,[50] photoelectron spectroscopy,[51] optical ellipsometry,[52] molecular simulations,[41, 53] optical reflection,[54] and even mechanical measurements.[55] These results appear to indicate that the thickness lies approximately between 10 and 15 Å at -1 ºC to -10 ºC, although some estimates range as high as 3000 Å,[41] depending on the

exact temperature and crystal face being examined.[56] Colder temperatures result in a smaller QLL (maximum width is obtained right at the freezing point) and the QLL appears to be thicker on the prismatic faces rather than on the basal face. A recent effort from Nada and Furukawa calculated the order parameters,[57] a normalized parameter that indicates the degree of order in a system (in this case the ice lattice is assigned a value of 0, fully ordered, and the bulk water a value of 1, fully disordered), of the different faces of a growing ice crystal.[58] They found that the QLL associated with the basal face has a parameter value of 0.7, while that of the prism face has a value of 0.4. This indicates that the QLL on the prism faces more closely resembles the order of ice (explaining the larger layer on this face) than that of the basal face. Unlike bulk water or ice, it does not have a uniform structure, rather the density of the water molecules slowly increases as one moves away from the ice surface (Figure 1.3) in a sigmoidal relationship.[17] It is still a poorly understood and modeled layer due to the complexities of the different intermolecular potential functions required to describe the differing properties of ice, water, and the varying layers of the QLL; however, it certainly plays a key role in the interaction of any solutes with ice, including those biology has evolved to exploit the geometric shape and surface properties of ice to reduce the potential for cryo-injury.

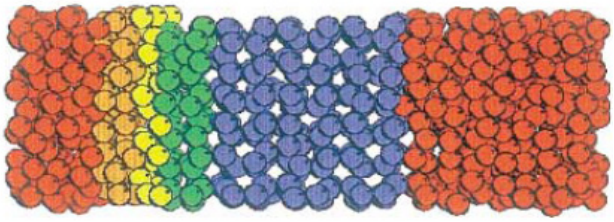


**Figure 1.3 Diagram showing the relative densities of water molecules in ice (blue) water (red) and the QLL (orange, yellow, and green). Each ball represents the oxygen atom of a water molecule. Reproduced from Madura et al.[17]**

## 1.3 Introduction to biological antifreezes

### 1.3.1 Discovery and evolution of biological antifreezes

Nature abhors a vacuum and the subzero polar environments are no exception. A considerable portion of the planet's surface is covered with ice, and a considerable portion of the arctic oceans are well below 0 ºC. Warm-blooded mammals and birds have evolved various forms of insulation such as down, thick coats of fur, and blubber to protect them from the cold; however these techniques are not possible for cold-blooded organisms, such as fish or insects unable, by definition, to regulate their internal temperature. These environments should be uninhabitable as ice would quickly form and cause massive cellular damage in these organisms. However, there exists no climactic niche so obscure that life has not found some means to colonize, whether it be by thermophiles in heat vents,[59] by lithophiles living in sedimentary rock over 3 km under the Earth's surface,[60] or by cryophiles that have evolved mechanisms to protect themselves in the sub-zero environments on the Earth.

Some cold-blooded organisms survive seasonal temperature changes through various mechanisms involving colligative properties to lower the freezing point of their blood serum, or by accepting desiccation and the halt in metabolism that it entails through employing trehalose (which protects cell membranes from disintegration caused by the decrease in cellular volume that occurs with freezing).[61] However, many organisms, through a remarkable example of convergent evolution, have evolved a different mechanism that involves inhibiting the growth of ice crystals and consequently can live and thrive at temperatures below the freezing point without suffering cellular damage or a significant reduction in biological functioning.

The fish inhabiting the Antarctic Ocean such as *Trematomus borchgrevinkii* and *Dissostichus mawsoni* occupy an environment with an ambient temperature of -1.9 ºC. Surprisingly, however, the colligative effects of the solutes in their blood serum should only protect them from freezing down to a temperature of -1.2 ºC. The remaining temperature gap, 0.7 ºC, should result in the formation of ice crystals and a rapid freezing of the whole fish. These fish, however, are clearly not [yet] frozen fish sticks. This led to an investigation into the cause of this remarkable survival trick that was inexplicable through traditional means—although valiant attempts were made in the 1950s by invoking the possibility of the "special" properties of super-cooled water. The work of Scholander and colleagues deserves special mention for the challenges they faced: despite making a trek to Nain in Labrador and waiting for three weeks at the airbase to gain access to the coast to have the honour of cutting a dozen holes through 4-foot ice with hand-tools, they managed to catch only three little fish in two weeks. The largest fish yielded 1 mL of blood serum, the smallest fish yielded 0.05 mL of serum, and the medium-sized fish was eaten by a dog.[62]

The explanation for the fishes' mechanism of survival arose a decade later through a serendipitous collaboration between fish researcher Arthur DeVries and Professor Robert Feeney who was at McMurdo Sound studying penguin albumin.[63] Consequently, the first biological antifreezes were isolated through their collaboration in the late 1960s over several expeditions to the Ross Ice Shelf.[63-65] After extensive degradation studies and chemical modification experiments, DeVries and co-workers were able to determine that the thermal hysteresis active component (THC) was a glycoprotein, creatively named antifreeze glycoprotein (AFGP). In the following decades

additional THCs were identified: interestingly, although characterized first, AFGPs are vastly outnumbered by the antifreeze proteins (AFPs), which fall into six different classes (Type I through VI), that have been more recently isolated from a variety of sources.[1, 2, 23, 34, 66-68]

The evolution of a strategy to survive sub-zero environments is fascinating. The subject has been extensively reviewed and only an overview will be provided here.[69-73] Biological antifreezes are one of the few examples where a change in genotype has a one-to-one correspondence with a significant change in phenotype in eukaryotes: without these genetic antifreezes the fish species would not be able to survive their environment. Every antifreeze has its own evolutionary origin, but they can broadly be broken down into two categories: the Arctic and Antarctic antifreezes. The Arctic antifreezes show a great variety: all 4 types of AFPs are represented as well as an AFGP in a northern cod species. In the Antarctic the dominant antifreeze is the AFGP found in the Notothenioids, a suborder of fish that make up greater than 90 % of the fish biomass in the upper (colder) reaches of the Antarctic ocean.[74, 75] These fish, and their AFGP, appear to have evolved exclusively in the Antarctic and very few examples have been found north of the Antarctic Circumpolar Current (ACC). The ACC is not just a line of demarcation; it has played a key evolutionary role as it is both a thermal and a physical barrier. It is the most powerful current in the world flowing at more than 4 km/hour with a combined flow greater than that of all the Earth's rivers.[76] On the surface this current coincides with the famous *Roaring Forties* and *Furious Fifties* at their eponymous latitudes: powerful circumplanetary winds that while facilitating intercontinental trade in the 18$^{th}$ and 19$^{th}$ centuries had (and still maintain amongst

sailors) a horrible reputation for power and ferocity. These conditions make it difficult for fish to either transition north or south of this near-impenetrable border that separates the warm, tropical waters of the Southern oceans from the frigid Antarctic Ocean. The ACC started to form around 25-20 million years ago as the Drake passage opened up between South America and Antarctica completing the isolation of the latter continent.[76] Most of the fish species south of this border went extinct as the water temperatures dropped 10 to 15 million years ago as the current reached its modern potency depriving the Antarctic of the warmth of more northerly waters.[74, 77] Consequently the one stock which did have a rudimentary antifreeze, the notothenioids, "underwent adaptive radiation and diversification to become the predominant fish taxon in the Antarctic Ocean."[72] The question arises as to how this antifreeze first evolved.

Genetic studies have actually "caught evolution in the act" where a chimeric gene was found that was in transition from coding for a trypsinogen-like protease to coding for an AFGP.[71] The gene contains the information for the same signal (localization) peptide as the AFGP gene does and it also contains the genetic data coding for a TAA sequence, the trimeric repeat found in AFGP, just upstream of the coding intron.[78] It appears that the primordial antifreeze glycoproteins were first encoded due to a typical gene duplication event and a serendipitous doubling of this 3-codon sequence (TAA) followed by a deletion of the remaining exons in the gene. The current gene common to the notothenioids encodes a large number of AFGP proteins of the different lengths in a single exon. Each protein is spaced from its neighbour through a linker (either Leu-Asn-Phe or Leu-Ile-Phe) which is easily cleaved and removed by chymotrypsin to liberate the individual mature antifreeze glycopeptides after post-translational glycosidation.[71, 78]

The only other antifreeze found in the Antarctic is a Type III AFP found in some Antarctic eel-pouts which are closely related to a northern hemisphere eel-pout with a similar Type III AFP. This family has a near global range; in this case migration may have occurred into the Antarctic at a more recent date.[72]

The story in the Arctic is both simpler and more interesting. Unlike the Antarctic which became almost completely physically isolated to provide the evolutionary pressure to produce some form of antifreeze, the fish of the Arctic have much more freedom of migration. Consequently when a region becomes cold due to local effects, only the local fish are affected and most can survive through simple migration to warmer climes. Those that remain or those that re-enter the environment to take advantage of newly-vacant niches have adapted individual solutions to the problems arising from cold-temperature living: hence the variety of northern AFPs and the AFGP of the Northern cod relative to the single solution common in the Antarctic.

Type I antifreezes have no identified genomic precursor. They are evolutionarily unique from the other antifreeze proteins in that they are not only translated in the liver, they are also produced in the skin of the fish,[79] suggesting that, for these fish at least, their role is to protect the fish from contact with sea ice.[80]

The Type II AFPs, found in rainbow smelt, herring and the sea raven originated from *C*-Type lectins. These lectins are specific for binding carbohydrates, and are all known to be calcium dependent. The antifreezes in the herring and smelt likewise require $Ca^{2+}$ for activity and appear to have appropriated the carbohydrate binding site for ice-binding.[81, 82] It is important to note, however, that all three species, and their Type II AFPs, evolved independently of one another; they do not derive from a common

mutation. This convergence appears to indicate that this is a simple and ready solution to the problem.

The Type IV AFPs arose from apolipoproteins,[83] proteins responsible for lipid transport and binding. They have a 4-helix bundle structure similar to apolipoprotein E, responsible in humans for binding LDL and transporting it to the lipoprotein receptors on cell surfaces.[84] These proteins already have an affinity for hydrophobic surfaces, and it has been proposed that the transference of this affinity from lipids to the hydrophobic ice face is not as drastic a modification as it first seems. There is, however, evidence that Type IV AFP is not biologically relevant as the titres are so low.[85]

Type III AFPs have evolved from yet another source.[86] Unlike Type I and Type IV, the Type III antifreeze may only have evolved once as both known sources (wolf-fish and eel-pouts) are closely related species.[87] Unlike other antifreezes, multiple isoforms of Type III AFPs are often found in the same species and higher copy numbers seem to occur in species inhabiting more challenging climes.[88, 89] Furthermore, it has been proposed that multiple isoforms provide slightly different antifreeze mechanisms, and consequently reduce the freezing point to a greater degree than would an equal concentration of a single protein.[86] The original evolutionary source of Type III AFPs is not, however, known at this time.

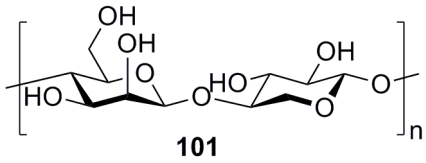
Northern cod AFGPs are remarkably similar to those of the Antarctic species, but appear to have no evolutionary connection: the taxa are unrelated and the species are, and have always been, separated by the vast expanses of the temperate oceans over their evolutionary history.[90] The main differences between the two isoforms being that unlike the Antarctic AFGPs, the northern cod have the occasional threonine residue

replaced by an arginine residue, have a completely different signalling peptide, and also contain different spacers between the genetic copies of the antifreeze glycoprotein.[78] It is, however, remarkable that both families use both a Thr-Ala-Ala repeat as the main structural feature and also exploit a galactopyranosyl-N-acetyl-galactosamine disaccharide core as their carbohydrate moiety. This is one of the truly great examples of convergent evolution.[77]

The most important conclusion to be drawn from these observations is that there is no “best” solution to surviving in the polar oceans. Nature has often co-evolved a substrate and a receptor, for example, and it is often very difficult for a synthetic drug to improve upon the natural ligand. This is not the case for ice-binding. Nature made use of a wide variety of biological material to jury-rig solutions to ice binding in the very recent past (evolutionarily speaking), but none of these solutions are necessarily ideal or even the best solution with the chosen scaffold—the time frames have simply not been long enough for the optimization process to fully run its course. Consequently, it should be kept in mind that designed synthetic alternatives, perhaps based on peptide scaffolds or based on scaffolds unavailable to biotic systems, may provide a better solution to the antifreeze problem than those that have evolved in nature. The design of such compounds, however, is foolhardy without an examination of the solutions that nature has evolved to approach this challenge: antifreeze oligosaccharides, proteins, and glycoproteins.

### 1.3.2 Antifreeze oligosaccharides

As of writing, only one example of the first category has been described. A xylomannan antifreeze, isolated from a freeze tolerant Alaskan beetle (*Upis ceramboides*), was reported by Walters and co-workers in late 2009.[13] As of yet full characterization of the compound has not been provided, but although it appears to contain little or no protein component there is evidence that a fatty acid domain is associated with the proposed xylopyranosyl-mannopyranose core (Figure 1.4). Antifreeze activity of this compound is comparable on a mass per mass basis with the best insect antifreeze proteins (Type V AFPs).




**101**

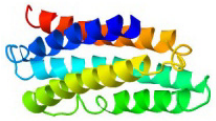
**Figure 1.4 Proposed xylopyranose-mannopyranose core of the antifreeze oligosaccharide of *U. ceramboides*.[13]**

### 1.3.3 Antifreeze proteins

As of the preparation of this thesis, four types of fish antifreeze proteins have been identified, as have two general families of antifreeze proteins found in insects and plants respectively (Table 1). The proteins are classified according to primary amino acid sequence and resulting tertiary structure rather than due to any evolutionary taxonomy as shall be seen below. The antifreeze proteins encompass the widest diversity of structures of the known antifreezes, and are also comprised of the most active antifreezes seen to date: the hyperactive AFPs present in insects, some of which are able to prevent freezing down to -20 ºC. Furthermore, although in general they are proposed to act through an ice-binding and freezing-point depression mechanism (thermal hysteresis or TH), this does not appear to be the case for the Type VI proteins found in plants as they show only very mild interactions with ice; rather, they appear to

be designed to limit cellular damage due to the ice recrystallization (IRI) that occurs during the cold winter months.[91, 92] The functional flexibility of proteins is remarkable and the real commonality between all types of AFPs is that they have at least one face that is potentially capable of interacting with ice and preventing its growth.

**Table 1.1 Physical properties, strucutres, and ice-binding mechanisms of known antifreeze proteins[19, 20]**

| | AFP I[1, 93] | AFP II[2, 81] | AFP III[23, 89, 94] | AFP IV[24, 83] | AFP V[29, 68, 95] | AFP VI[34, 91, 96-99] |
|---|---|---|---|---|---|---|
| **Source species** | European plaice (*Pleuronectes platessa*) Winter flounder (*Pseudopleuronectes americanus*) Short-horned sculpins (*Myoxocephalus scorpius*) | Rainbow smelt (*Osmerus mordax*) Atlantic herring (*Clupea harentus harengus*) Sea raven (*Hemitripherus americanus)* | Eel Pouts (Zoarcidae) Wolffish (Anarhichadidae) | Long-horn sculpin (*Myoxocephalus octodecimspinosis)* | Yellow mealworm beetle (*Telebrio molitor*) | Perennial ryegrass (*Lolium perennae*) |
| **Molecular Mass (kDa)** | 3-5 | 14-24 | 7 | 12.3 | 8-10[95, 100, 101] | 14.5-34[102] |
| **Structural Features** | Single α-helix | Globular (*C*-Type lectin fold) with disulfide bonds | Globular, β-sandwich fold with flat external surfaces | Anti-parallel 4-helix bundle | Rigid parallel β-helix | β-roll: Parallel β-sheets |
| **Tertiary Structure** |  |  |  |  |  |  |
| **Amino acid bias** | >60 % alanine | 8 % cysteine | None | 17 % glutamine | Cysteine rich (disulfide bridges essential for activity) | Threonine, valine and serine important on ice binding face |
| **Heterogeneity amongst class** | Different lengths of helix, some have repeats, some without | $Ca^{2+}$ dependent, $Ca^{2+}$ independent (calcium domain removed) | Multiple isoforms Heterogeneous dimers | Only one known example | Repeats of conserved 12 amino acid loops xTCTxSxxCxxA | Semi-conserved seven-amino acid repeat XXNXVXG |
| **Ice binding surface properties** | Can bind through hydrophobic TAN face, or hydrophilic TAA face. | Planar surface of $Ca^{2+}$ binding loop/hydrophilic residues of carbohydrate binding domain | Polar groups presented from the mostly hydrophobic planar surfaces | Uncharacterized | β-sheet surface | One plane (a-side) of barrel |
| **Primary antifreeze activity** | TH and IRI | TH | TH | TH | TH | IRI, no TH |

**Depictions of protein structures obtained from the protein databank. AFP Type I: PDB accession code 1WFA;[1] AFP Type II: PDB accession code 2AFP;[2-4] AFP Type III: PDB accession code 1MSI;[9, 23] AFP Type IV (modeled on human apolipoprotein III): PDB accession code 1AEP;[24, 25] AFP Type V: PDB accession code 1L1I;[29] AFP Type VI: PDB accession code 1I3B.[34]**

### 1.3.4 Antifreeze glycoproteins

Antifreeze glycoproteins (AFGPs) have, as mentioned above, evolved separately in the Arctic and Antarctic, and in both cases these molecules have converged on a single solution. As mentioned, all the glycopeptides share a common structure shown in Figure 1.5. The main scaffold is a threonine-alanine-alanine tripeptide core that is linked by the β-*O* of the threonine residue to a D-galactopyranosyl-β-(1→3)-*N*-acetylgalactosamine through an α glycosidic linkage. The only natural variance to this form are the occasional substitution of a proline residue for an alanine residue in the lower molecular weight glycopeptides,[103] and the sometime replacement of threonine with arginine in the northern cod. Traditionally they have been divided into 8 "fractions" (although a greater number of isoforms are known now, this nomenclature is still used and arises from a function of the initial isolation procedure) differing mainly by the number of repeats.[104] The largest molecules, with a molecular weight of around 32 kDa, or 50 repeats are known as AFGP-fraction 1 (or AFGP-1) while the smallest, at 2.7 kDa, or 4 repeats are known as AFGP-8.[103] Although the low molecular weight AFGPs are more prevalent numerically than their higher massed brethren, it has been demonstrated that antifreeze activity increases as the number of repeats increases.[5, 105] Unlike the AFPs, the AFGPs have resisted attempts to characterize their solution-phase

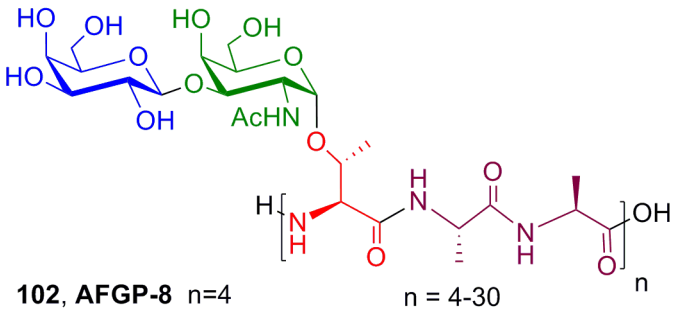



**Figure 1.5 General structure of the Antarctic AFGPs. A galactosyl (blue)-N-acetyl-galactosamine (Green) disaccharide is linked through an α-glycosidic bond to a threonine (red)-alanine-alanine (purple) backbone.**

tertiary structure and the spatial relationship between the sugar and the backbone. Several different structural models have been presented, many of which appear to be mutually exclusive.[106] Using FT-IR, Drewes and Rowlen proposed that γ-turns play a key role in the secondary structure.[107] Polyproline Type II (PP II) helices were initially proposed by Bush and Feeney using NMR[108, 109] and circular dichroism studies.[110] Quasi-electric light scattering studies on the other hand suggested an extended coil conformation: a slightly more rigid form than a random coil.[111] According to Franks and Morris, the NMR spectra and CD measurements, along with the abrogation of antifreeze activity by the introduction of charged groups, all point to a structured but unique and tight secondary structure—interestingly they interpret their CD spectra of AFGP as being the horizontal reflection of that typical of a β-sheet believing that the magnitude of the spectral peaks is too great for that observed for random coils.[112] Another interpretation of the CD spectra by Raymond, Radding and DeVries at various temperatures shows that the CD spectrum does not degrade with increasing temperature as would be expected from a PP II helix or other ordered form, and is thus most likely a random coil.[113] These results from DeVries have been supported more recently by work from the Ben lab showing that AFGP-8 adopts mainly a random coil structure in solution.[114] More recent NMR studies support this hypothesis, including natural abundance $^{13}C$ studies examining relaxation times that have strongly suggested that there is no preferred conformation, and that the peptide simply adopts a random coil with possible temporary and localized secondary structure.[115-117] The frequency of the appearance of these temporary secondary structures, especially β-turns and the more rigid extended coils, increases as the temperature drops, and Tsvetkova and co-

workers propose that it is precisely the availability of the different conformations that leads to the antifreeze activity of the AFGPs.[118] All studies, however, agree that α-helices are not present in the secondary structure of AFGPs.[27, 103, 119] Despite this intense debate, the fervent wishes and plaintive calls of many authors for an X-ray crystal structure (repeated in many of the above reports) seem in vain; the relevance of a crystal structure for a flexible peptide that changes its conformation at different temperatures and in the presence of ice is questionable. Since a defined structure may not exist, searching for it using any technique may not be a fruitful enterprise: it has been suggested that the lack of any defined structure, and their inherent structural flexibility, is essential for the antifreeze activity of these compounds.[109] Unlike the highly organized and rigid AFPs, AFGPs most likely adopt random-coil conformations that are capable of temporarily organizing into localized ordered-structures or becoming any of a variety of ordered structures upon binding to an ice surface as the situation requires.[120] In doing so, they demonstrate the unique physical properties of biological antifreezes: thermal hysteresis (TH) and ice recrystallization inhibition (IRI).

## 1.4 Interactions between ice and biological antifreezes

Before discussing the details of the TH and IRI properties it is important to briefly examine the proposed mechanisms for the ice-protein interaction. One can envision the interaction as one between a receptor and a ligand where the receptor is the antifreeze, and the ligand is the surface of the ice lattice. The interaction here is special only in that the ligand is much larger than the receptor, and is in very large excess.[15] It is proposed that there is a similar overall binding mechanism for all the AFPs despite the large divergence in backbone and surface properties and difference in the precise details of

the interaction. There are various arguments discussing the relative importance of enthalpic terms (such as hydrogen-bonding between the ice lattice and the protein) and the entropic terms.

On the enthalpic side of the equation, the key observation is that most of the AFPs have a repetitive structure including threonines and serines regularly interspersed on mainly hydrophobic surfaces. It has been proposed that these distances correspond to the pattern of water in the ice lattice. The planar nature of the surface also appears important as all the proteins contain at least one planar face. Surprisingly, although regular spacing of hydrophilic groups intuitively seems important to ice binding, it does not appear to be essential; point mutations of threonine to valine have much smaller effects on antifreeze activity than mutations of threonine to serine.[121-123] This observation makes sense: H-bonds between a peptide and ice are considerably weaker than those between peptide and water due to the reduced flexibility of the two surfaces to arrange spatially relative to each other.[67, 124] Consequently, it has been suggested that these alcoholic residues cannot play a key role as water should satisfy the hydrogen-bonding desires of AFPs to a much greater degree than ice:[125] if this was the key interaction, the AFPs would be located in the bulk water rather than on the ice surface. The current argument is that the density of the surface interaction, the regular undulations and balance of polarity of the protein façade fitting into the ice-lattice face (rather than hydrogen-bonding) leads to high levels of binding due to the favourable van der Waals interactions.[67, 126, 127]

On the entropic side of the equation, one would expect that an increase in rigidity would improve ice-binding (i.e. antifreeze activity improves as the degree of helicity

improves for Type I AFPs)[128] as would a restriction in side chain mobility.[129] This would theoretically arise from the smaller decrease in the entropy term expected when an already organized molecule binds to the ice lattice rather than that expected for the binding of a less restricted compound. Although, as mentioned above, AFGP most likely adopts a random coil conformation, it has been suggested that the sugar adopts an organized conformation relative to the peptide backbone, possibly due to a hydrogen bond between the amide of the *N*-acetyl group on the carbohydrate and the peptide backbone.[130, 131] Cogent arguments can also be made that it is entropic factors, akin to protein hydrophobic collapse, that drive the ice-binding of the protein to the ice surface. Isolated, both the ice and the protein must be fully solvated: water is organized around both of these solutes. Consequently, when the hydrophobic surface of the protein (requiring considerable solvation) comes into contact with the polar but irregular (with regard to spacing of the hydrogen bonds relative to bulk water) surface of the ice, the ordered water required to solvate both of these surfaces is released for a considerable net gain in entropy, possibly providing the driving force behind the ice-protein interaction. This interaction would be more sensitive to steric modifications of the ice binding face than to the substitution of hydrophilic with isosteric but hydrophobic residues.[132] This has been supported through several experimental mutagenesis studies with AFP Type I,[123, 124] AFP Type VI[97], and AFP Type III.[121, 132] Consequently, the larger the volume of water displaced, the larger the surface of the ice that is blocked, the larger the entropic gain. From this hypothesis, one would expect that simply fusing other proteins to the AFP should result in an improvement in activity as the larger protein would release a correspondingly higher number of water molecules

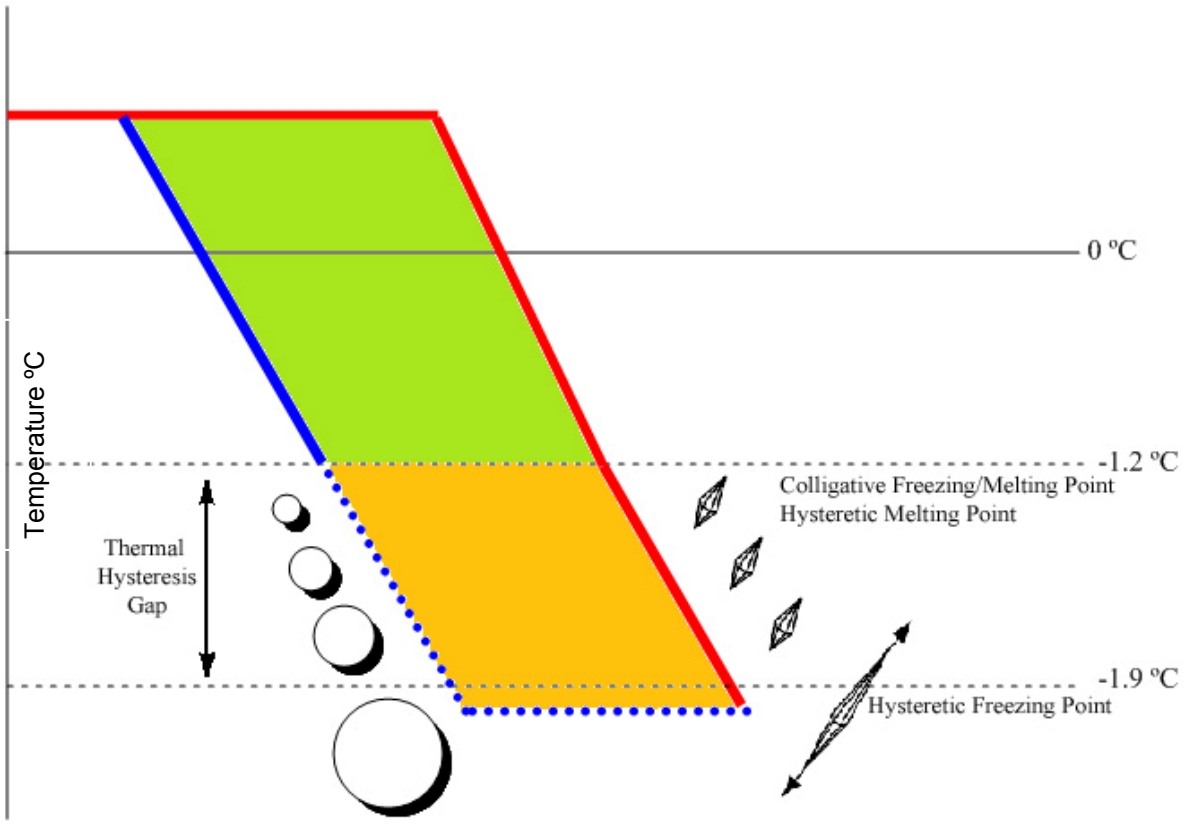



**Figure 1.6 Diagram showing the TH effect. Blue line represents cooling without THCs. Red line represents cooling in presence of THCs. Green area represents temperature range protected by colligative properties. Orange region represents temperature range in which the fish are protected by the TH gap of their AFPs. Figure adapted from Jia and Davies.[15]**

upon binding. This can be seen in the work of Wu and co-workers when they added antibodies to a solution of Type V antifreeze protein[133] or when fusion proteins were created between AFPs and a maltose binding protein (a protein with a similar fold, but no independent antifreeze activity)[134] or GFPs.[135] Furthermore, it appears that at least some Type V antifreezes recruit additional proteins to attain their notable "hyperactive" state *in vivo*, and it is suggested that these proteins simply increase the volume of the AFP rather than act in any ice-binding capacity.[136, 137]

All these mechanisms of binding lead directly to the first, and traditionally more investigated, property of biological antifreezes: thermal hysteresis.

## 1.5 Thermal hysteresis and dynamic ice shaping

Thermal hysteresis, in the context of biological antifreezes, is the selective depression of the freezing point of a solution without a concomitant decrease in the melting point (Figure 1.6). In a solution of pure water, ice and water are at equilibrium at 0 ºC: below this temperature, the equilibrium favours the incorporation of water into the ice lattice, and above this temperature, the equilibrium favours the melting of the ice crystals. If a solute is added, the freezing temperature and the melting temperature are both decreased by an equal amount due to a concentration-dependent colligative effect that is independent of the nature of the solute (Figure 1.6). In the diagram presented, the solutes are sufficient to prevent freezing down to -1.2 ºC (green area). If the temperature drops below this point, the solution will rapidly freeze; however, if a low concentration of antifreeze is added to such a solution, the macroscopic melting point remains unchanged, at -1.2 ºC, but the macroscopic freezing point decreases, in this case to -1.9 ºC. This gap created between the melting and freezing points is known as the thermal hysteretic gap. This non-colligative phenomenon is believed to be caused by the interaction of antifreeze molecules with the surface of the ice lattice in a manner that inhibits ice growth beyond a certain size while simultaneously shaping the ice in distinct geometries. In this temperature range (orange area) ice crystals do not grow, so that the fish are protected from the harmful effects of ice. Several mechanisms have been proposed for explaining the manifestation of this phenomenon and its related corollary, dynamic ice-shaping.

### 1.5.1 Dynamic ice-shaping

Dynamic ice shaping refers to the moulding of the shape of an ice crystal in the presence of THCs. THCs often show a preference for a particular facet of an ice crystal, especially the prismatic face. Consequently, they tend to adsorb to this facet preventing further ice crystal growth along this axis. Therefore, ice crystal growth must continue on the basal face instead. However, as a new layer of ice is formed, additional antifreeze molecules bind to the prism face of this new layer as well. This process inevitably results in the formation of hexagonal bipyramidal crystal structure (Figure 1.7). Upon formation of the apical layer, no more ice can be added to the crystal and growth is halted as long as the crystal remains in the TH gap. The confusing term “dynamic” refers to the iterative (but static) blocking of prismatic faces rather than any ongoing equilibrium process that continues throughout the entire TH gap temperature range. The crystals form very quickly initially, but become static according to the traditional mechanistic model for explaining thermal hysteresis.

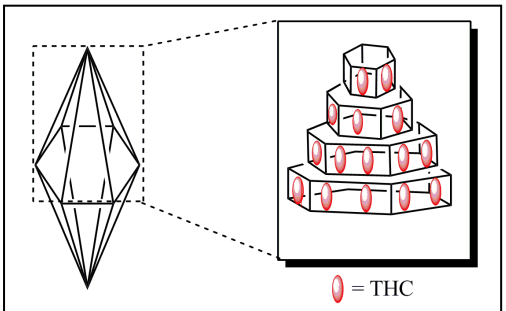



**Figure 1.7. Representation of the causation and results of DIS. THCs bind to the prismatic faces preventing further growth along this axis forcing the deposition of a new layer of ice forming the hexagonal bipyramid. Figure adapted from Jia and Davies.[15]**

### 1.5.2 Mechanism of thermal hysteresis

Thermal hysteresis has been extensively reviewed and only a brief overview will be provided here.[15, 19, 98, 106, 138-142] Thermal hysteresis and dynamic ice shaping arise from the manner in which the molecules bind to ice. There are two conflicting hypotheses for the binding. The first and historically predominant is known as the

absorption-inhibition model.[143] It stipulates that the antifreeze molecules bind tightly and irreversibly to the ice surface, and was initially supported due to AFGP-induced changes in interfacial energies between water and ice suggesting strong binding in the opinion of Feeney and co-workers.[144]

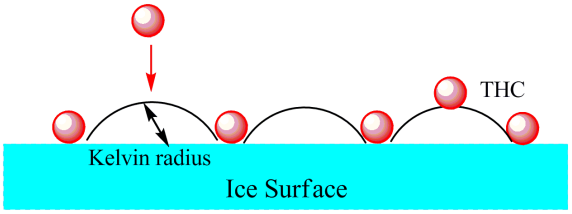



**Figure 1.8 Two-dimensional cross-section of the matress model of TH activity. The red balls, representing the THC associate with the ice surface forcing the ice to grow in acurved fasion between THCs. Adapted from Wilson et al.[5]**

To explain how binding could cause the TH effect, a “mattress button” model has been proposed where, like the buttons on a mattress, the antifreezes bind tightly to a layer of ice.[145-147] In between these “buttons” the ice can grow and curve outwards, but this curvature is limited by the presence of the adjacent button (Figure 1.8). As shown in Figure 1.8, this model implies that the THCs bind irreversibly to the nascent ice crystal (preferentially on the prism faces as later studies have shown),[5] and force the crystal to continue to grow with a high degree of curvature. At this point the crystals, at the macroscopic level, will not appear to continue to grow as all growth will occur in small arcs between absorbed antifreeze molecules; however, the Thomson-Gibbs equation states that the localized temperature required to add additional water molecule decreases (known as “undercooling”) as the radius of curvature of the crystal surface increases. This is due to the fact that surface molecules are inherently less stable than internal molecules: a higher radius of curvature implies a higher surface area: volume ratio, and hence a higher overall degree of enthalpic instability on the surface. At temperatures within the TH gap, this theoretical under-cooling point is below the ambient temperature, and so the expansion of the radius of curvature (the Kelvin radius)

is arrested before the arcs become semicircles; consequently, ice growth is completely halted, one can think of it as a very localized decrease in the freezing point. However, as the temperature falls to the hysteretic freezing point, the curvatures of the arcs approach true semicircles, and consequently become tangent to their neighbours at the hysteretic freezing point. At this point they then simply over-freeze any absorbed antifreezes. Once this has occurred, the crystals expand extremely rapidly as the removal of these curved arcs returns the freezing point to the colligatively determined value. This implies that the solution is super-cooled and consequently it is extremely favourable for additional water molecules to add to the ice lattice and the crystal will tend to grow in an uncontrolled fashion.

It is a very attractive and simple model, invoking traditional physical explanations such as the Kelvin effect and the formation and breaching of the critical-temperature radius at the hysteretic freezing point to explain the abrupt transition from controlled stasis within the TH gap to uncontrolled growth below this gap. It is also considerably easier to comprehend than other proposed models.[148, 149] To summarize: the irreversible binding of antifreeze molecules to the ice surface leads to a halt in macroscopic growth until conditions change drastically enough that the molecules are “over-frozen” causing immediate rapid ice-growth. If the binding of these molecules were reversible, the crystal should undergo considerable reorganization within this gap as the antifreeze molecules would dynamically absorb and dissociate from the crystal. Likewise, employing this model, only irreversible binding is consistent with the sudden transition at the hysteretic freezing point. If binding were reversible, adjacent Kelvin radii should be able to fuse upon dissociation of the antifreeze from the ice surface. This

would blur the transition point considerably as vastly different sized radii would undergo uncontrolled growth at different temperatures.[19]

Irreversible binding implies that the only kinetic parameter involved in the process is the rate of absorption. Crystal morphology is developed immediately upon cooling due to dynamic ice shaping in a concentration dependent manner (absorption would be dependent on the solution concentration of antifreezes). Consequently, as absorbed molecules cannot dissociate under this model, once the crystal forms, TH measurements should be independent of the cooling rate, as the only parameter that would matter would be the average critical Kelvin radius. This average Kelvin radius would have been determined when the THCs first bound. Consequently, it should be irrelevant how fast the sample is cooled: the radius will not be affected by this parameter, and consequently, neither should the TH gap. Unfortunately, TH measurements are not independent of the cooling rate. It has been shown that cooling at 0.20 ºC/min (instead of 0.01 ºC/min) can result in a failure to observe the magnitude of the TH gap by as much as 50 %.[150] The authors suggest that this is due to the additional binding of THCs to the convex face as cooling continues, which should occur more readily at slow cooling rates than faster cooling rates. This is not a very convincing argument as the near immediate formation of the bipyramidal crystal appears to indicate that the rate of absorption of the THCs can compete with the rate of ice-lattice formation itself. It stretches credulity that a small increase in cooling rate (not temperature) would so massively decrease the binding affinity of the THC to the ice surface as is required by this model. The lack of a plausible explanation has led to increasing criticism of this hypothesis over the past decade.[19, 148]

Further evidence against irreversible binding include measurements that show that the number of THCs incorporated into the ice lattice below the TH gap is lower than the number of THCs that are determined to be on the surface of the ice crystals in the TH gap (in an irreversible model, all bound THCs in the TH gap should be included in the ice crystal that results following cooling below the TH gap: THCs frozen into the lattice should be equal to the number located on the surface).[143, 151] Furthermore, mutant AFPs have been produced that lack a sudden burst point and consequently show a slow but residual ice growth in their TH gap.[132, 152] Other researchers have demonstrated that the kinetic studies modelling the behaviour of ice crystals in the presence of THCs indicate an equilibrium process rather than an irreversible event.[153-155]

A final fatal criticism of the absorption-inhibition model is that if binding were irreversible, antifreezes would not diffuse away from the ice lattice surface. However, this event has been observed through observation of an ice crystal constrained to grow in only one direction.[156-158] AFGPs, tagged with fluorescein isothiocyanate were localized to the surface of a single ice crystal of length $L_0$ in the TH gap. With controlled cooling below the TH gap, the crystal was allowed to grow unidirectionally to length $L_1$. Growth was halted by returning the temperature of the crystal to the TH gap and the newly established interface was examined by fluorescence microscopy. The same relative fluorescence was observed on the surface of the ice crystal as before, and there was no incorporation of any fluorescence in the ice crystal. If binding were irreversible, the fluorescence should be expected to have been incorporated at $L_0$, now located inside the ice crystal. It was not. It was all still located at the new water/ice interface at

$L_1$. At much faster rates of freezing, the ice appeared to integrate the antifreeze, but upon closer examination the antifreeze appeared only to inhabit seams in the ice and was not actually incorporated into the lattice itself.

These observations could, however, be explained if the binding of the antifreeze was an equilibrium rather than an irreversible process.[19, 120, 151, 154-156] The evidence provided above strongly suggests that TH is an equilibrium process rather than an irreversible process. The energy of binding to ice for a Type I AFP has been calculated to be 4.1 kcal/mol.[125] This is certainly not an insurmountable barrier, being approximately equal to the energy of rotation around the $C_2$-$C_3$ bond of butane (3.8 kcal/mol) and would not suggest irreversible binding (previous estimates on the order of hundreds of kcal/mol did not thoroughly account for the hydration energies of the AFP and the ice surface prior to the binding event, consequently they over-estimated entropic benefit).[159]

The adherence to the irreversible model is, as Brown puts it, due to a “lack of mechanistic ideas” and creativity amongst researchers.[19] The observation that there is a $10^4$-$10^7$ excess (normally on the higher end of this scale) of water relative to THC makes many uncomfortable with the idea of a reversible process, “as even a transient desorption of [THCs] would allow water molecules to join the lattice.”[135] However, the existence of the QLL layer should give cause for pause and hope. The antifreeze molecules could prefer to localize in or at the QLL layer over bulk water and so, not only would the localized concentration be considerably higher than when considering the bulk water as a whole, but the molecules of antifreeze would be maintained in close physical proximity to the ice lattice.

Two mechanisms have been proposed to incorporate all of the above observations. Wilson proposed that TH could be explained through an anisotropic interfacial effect: the fact that ice in pure water forms discs, is due to the fact that crystals will grow in order that the lowest energy face has the largest surface area.[149] As discussed above, the conformation of the ice lattice makes the basal face the lowest energy face, ensuring that ice will grow on the prism faces preferentially. However, if the prism faces are partially blocked by solute, the crystals would be forced to grow from the basal face. But, this blocking would also localize a higher concentration of solutes on the prism face which would in turn lower the freezing point of the prism face relative to the basal face. According to Wilson, this would make it less favourable for ice crystal growth to occur, in effect depressing the freezing point. A second theory relies on negative line excess, relying on the avoidance of molecules to add to the edge of a crystal due to the destabilizing interactions.[148]

As an addendum to this controversy, a very recent report from the Davies group presented a crystal structure of an AFP isolated from an Antarctic bacterium, the largest AFP ever yet isolated (1.5 MDa) that contains a $Ca^{2+}$ dependent β-helix.[160] During the acquisition of this structure at 100 K, they observed water molecules organized on the putative ice-binding face. They propose that these anchored water molecules mediate the interaction between the AFP and the ice interface to create a very tight junction, possibly explaining the “hyper-active” activity of this antifreeze. They propose that this confirms that water does not need to dissociate from the peptide prior to ice-binding as it can remain bound to actually improve the interaction between the peptide and ice. As the ice binding face of this peptide is made up of 19 β-sheet repeats (the largest ice-

binding interface yet reported) the sheer number of interactions might make binding, in the case of this antifreeze, functionally irreversible. This evidence of the mechanistic importance of these bound water molecules is strong for this antifreeze, and it would be interesting to see if such tightly bound water could be found associated with the other AFPs to generalize this mechanism. No mechanistic studies, unfortunately, have been carried out with this antifreeze to date.

A truly general mechanism, if it exists, remains to be determined although many researchers imply that the QLL may segregate the antifreezes near the surface. They propose (implicitly) that the interaction with the ice surface is reversible, but that the two phases are not bulk water and ice as rightly rejected by the pioneers, but rather the ice surface and the QLL.[161] This neatly sidesteps a lot of the concerns outlined regarding both the irreversible and reversible models although there is no direct experimental support for this model as of yet.

### 1.5.3 Corollaries and applications of thermal hysteresis

Regardless of the correct theoretical mechanistic model for thermal hysteresis, there are some definite effects at the macroscale level. For the Teleost fish, TH is the key property. Halting ice crystal growth and keeping nucleated ice crystals small and harmless is incredibly useful and protects the cellular membranes from being mechanically damaged. As sea water cannot fall below -1.9 ºC, they cannot suffer from the unfortunate side effect of TH that occurs when the temperature falls below the non-colligative freezing point: spiculation. This is the formation of needles due to uncontrolled freezing along the c-axis when the antifreezes are not longer able to halt the formation of ice. Sharp ice needles are quite dangerous to cell membranes and can

cause significant damage. This “negative” TH effect can be harnessed in cryosurgery where the desired outcome is tissue damage. For example, cold temperatures can be used to kill tissue, but not all of it dies, hence the need for repeated treatments of warts with liquid nitrogen. Rubinsky and co-workers showed that adding a small amount of AFPs as a cryoadjuvant can assist in killing liver cells.[162] The application of AFPs in cryosurgery was recently reviewed and they have also been used in the treatment of prostate cancer.[163]

The other major applications involve agriculture and aquaculture. Transgenic crop species expressing THCs are of great interest to the agribusiness community for frost tolerance purposes.[164, 165] A transgenic tomato plant expressing Type I AFP was created, as was a tobacco variant, but unfortunately in neither case did AFP expression improve the freeze tolerance of the plant.[166, 167] However, this research is still in its infancy, and may show better results in the future. A second application is the creation of transgenic salmon. Salmon is the most important aquacultured fish but one large problem is that temperatures in the North Atlantic can fall below the colligative freezing point of salmon blood serum. In the wild, the salmon simply migrate to avoid freezing, but in captivity this is not an option leading to a restriction in the geographic locations appropriate for salmon farming. Efforts are currently underway to improve the antifreeze protein titres in transgenic salmon to provide the appropriate cold resistance required on Canada’s East coast.[168, 169] However, none of these applications are yet fully realized and consequently there is continuing effort towards identifying the structural features of the antifreezes that are required for TH activity.

## 1.5.4 Structural domains of AFGPs required for TH activity and early syntheses of AFGP analogues

As thermal hysteresis has traditionally been the most studied property of biological antifreezes, considerable effort has been expended to determine the essential

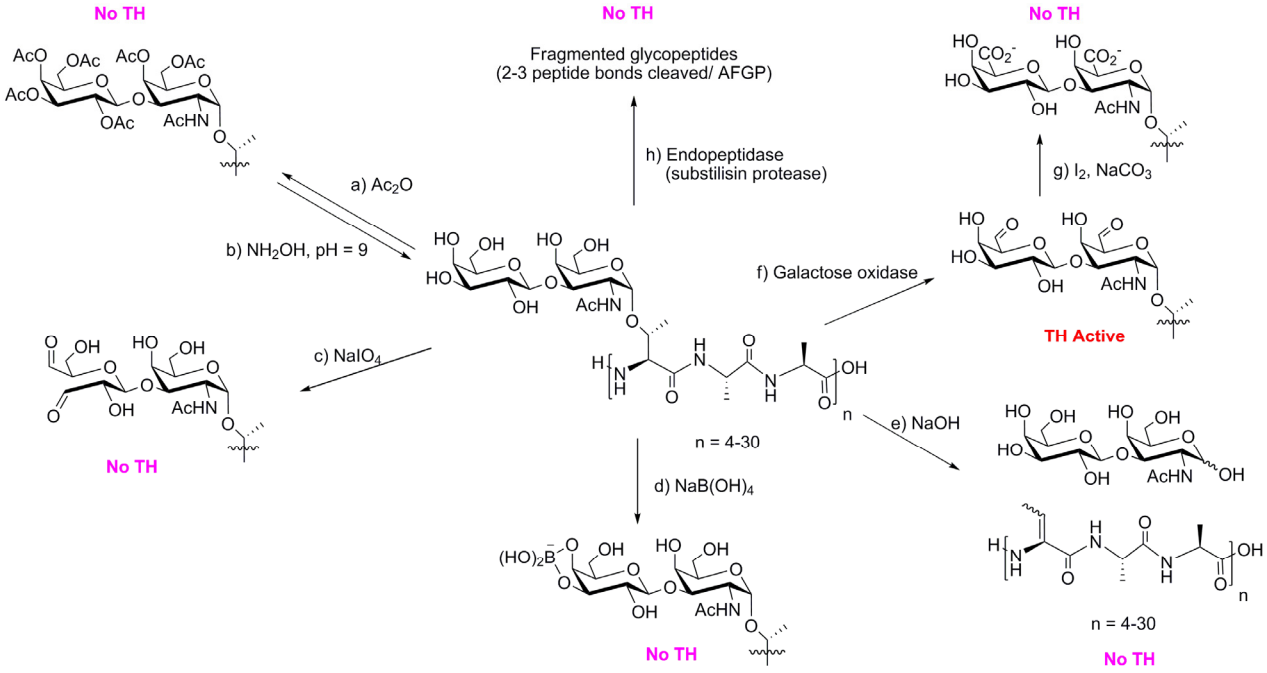



**Figure 1.9. Early chemical tests carried out by DeVries and coworkers to determine AFGP structure and structural features required for TH activity. Adapted from Tam,[14] Komatsu and co-workers,[22] Vandenheede and co-workers[26], and Ahmed and co-workers.[30]**

structural features. Seminal early research by the Feeney, DeVries and co-workers involved the chemical modification of isolated AFGPs (Figure 1.9).[22] They found that partial acetylation of the sugar residue destroyed TH activity (Figure 1.9a), but the activity could be restored following saponification of the acetate groups (Figure 1.9b). Both oxidative degradation of the terminal galactose (Figure 1.9c), and alkali-mediated beta elimination of the carbohydrate (Figure 1.9e) resulted in a complete loss of TH activity. Finally, even limited protease digestion (only one or two amide bonds cleaved per glycoprotein) resulted in the destruction of activity at the tested concentrations

(Figure 1.9h). These results indicate that the terminal galactose is important (degradation results in the loss of activity), and that the presence of both peptide and carbohydrate moieties is important for TH activity, as both acetylation (negating the ability of the sugar to donate hydrogen bonds) and cleavage of the carbohydrate results in a complete loss of activity. Finally, the research provided the first evidence that activity is very sensitive to glycopeptide length as even a few cleaved bonds is enough to destroy activity. A second study by the Feeney group was carried out to examine the relative importance of the different hydroxyl groups of the disaccharide.[26] They found that oxidation of the *C*-6 oxygen to an aldehyde did not damage TH activity (Figure 1.9f); however, further oxidation to the carboxylic acid (present as a carboxylate at physiological and TH assay pH) resulted in a complete elimination of TH activity (Figure 1.9g). This study indicates that although the *C*-6 OH itself is not essential for TH activity, the presence of a charge on the sugar is detrimental. A third study was carried out to examine the importance of the hydroxyl groups on the terminal galactose residue.[30] Sodium borate was added to a solution of AFGP and this led to TH inactivation (Figure 1.9d). It is proposed that it bound to the *C*-3 and *C*-4 hydroxyl groups of the terminal galactose (this was elegantly demonstrated by showing that the addition of the borate solution to the aldehyde derivative, lacking a *C*-6 OH, shown in Figure 1.9 also abrogated activity).

In the late 1980s and early 1990s several successful syntheses of AFGP and simple analogues were carried out but the synthesized compounds were not examined for antifreeze activity. The glycosylated tripeptide core, **103**, was first prepared using solution phase techniques by Anderson in 1988 (Figure 1.10 A). The disaccharide was

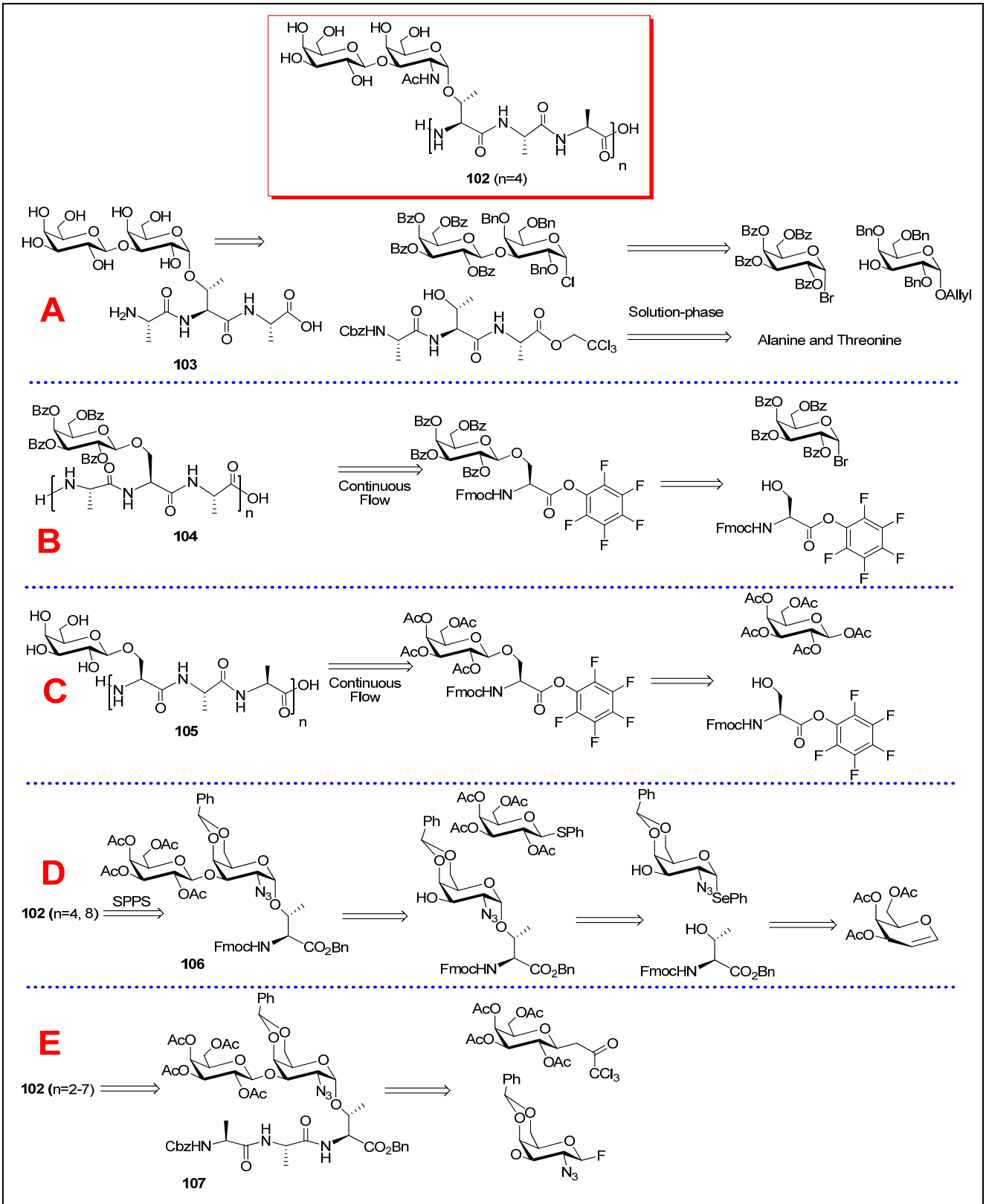



**Figure 1.10 Previous syntheses of *O*-linked AFGP-8 analogues. (A) Anderson 1988;[7] (B) Meldal, 1990;[21] (C) Filira 1990;[27] (D) Chen 2001;[31] (E) Nishimura 1996-2001.[90,162-164]**

added to the short peptide after the latter had already been prepared.[7] Meldal used the

simple repeating structure of the AFGPs as a test system for his pentafluorophenyl ester protecting group and prepared protected galactose derivatives **104** (Figure 1.10 B) using a continuous-flow procedure.[21] Using a nearly identical synthetic sequence and taking advantage of Meldal's chemistry, the dimer, trimer, tetramer and heptamers (**105**) of this core sequence were synthesized by Filira and coworkers in 1990 (Figure 1.10 C).[27] A streamlined preparation of a true synthetic AFGP-8, **102** was reported by Chen and co-workers in 2001 by applying solid phase peptide synthesis (SPPS) to glycoconjugate **106** (Figure 1.10 D).[31] Using an inverse sequence, they coupled the reducing-end sugar to the threonine residue before forming the disaccharide through activation of a thiophenyl group. However, the most important synthesis for current purposes is the first synthesis of a synthetic AFGP-8, **102**, and its homologues reported by the Nishimura group in 1996 with further preparations reported in the following five years (Figure 1.10E).[10, 105, 170, 171] It is these analogues which have provided the second series of key studies, carried out in collaboration with Fletcher, to examine the relationship between the structural features of AFGP analogues and TH activity.[10] They first synthetically prepared AFGP derivatives of varying lengths and determined that only two repeats of the core trimer was sufficient for TH activity to be expressed at 40 mg/mL. They found a positive, non-linear relationship between chain length and TH activity (Figure 1.11) where the activity becomes asymptotic with 5 or more repeats. Interestingly, although the monomer showed no TH activity at any of the

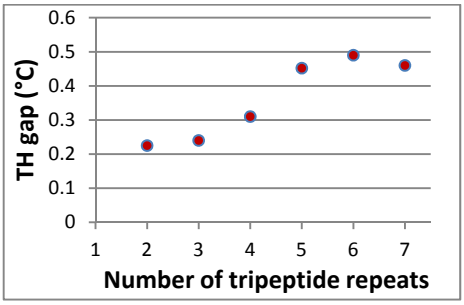



**Figure 1.11. TH activity of polymers of the AFGP core tripeptide at 40 mg/mL produced by Nishimura.[163]**

tested concentrations, it did show dynamic ice shaping, suggesting that it was interacting, if only weakly, with the ice surface. They then examined a series of analogues and determined that the antifreeze activity is very sensitive to subtle changes in carbohydrate structure (Figure 1.12).

The first modification was the aglycon derivative (not shown) which failed to show any TH or DIS, consistent with the observations of Komatsu, DeVries and Feeney. Similarly, the removal of the methyl group of the threonine (substitution with serine, not shown) also resulted in the loss of TH activity, although some residual dynamic ice shaping (DIS) was still observable.

Replacement of the GalNHAc derivative with a second galactose residue (**108**) led to the loss of TH activity although, again the hexagonal crystals resulting from DIS were observed as was the case when the α-linkage to the threonine was replaced with a β linkage (**109**). Removing the terminal galactose entirely, leaving only a galactose monosaccharide (**110**) decreased, but did not eliminate, TH activity as did the seemingly large change involved in substituting a *N*-acetyl lactosamine derivative (**111**) as both the connectivity and orientation of the *C*-4 hydroxyl group have changed relative to N-acetyl galactosamine. Galactose and lactose derivatives (**112** and **113**)

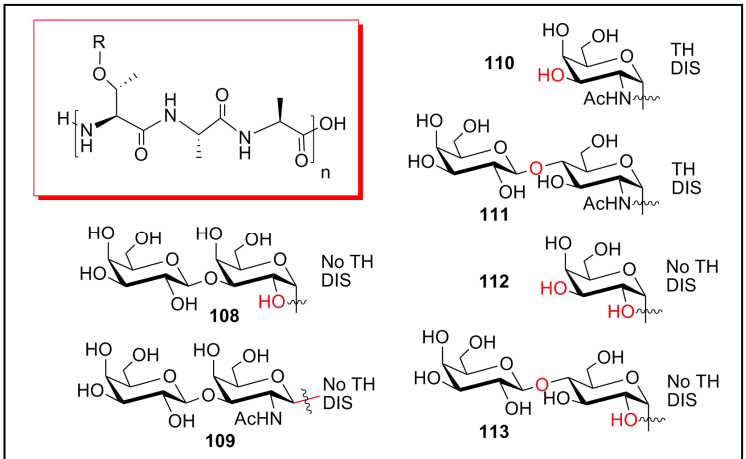
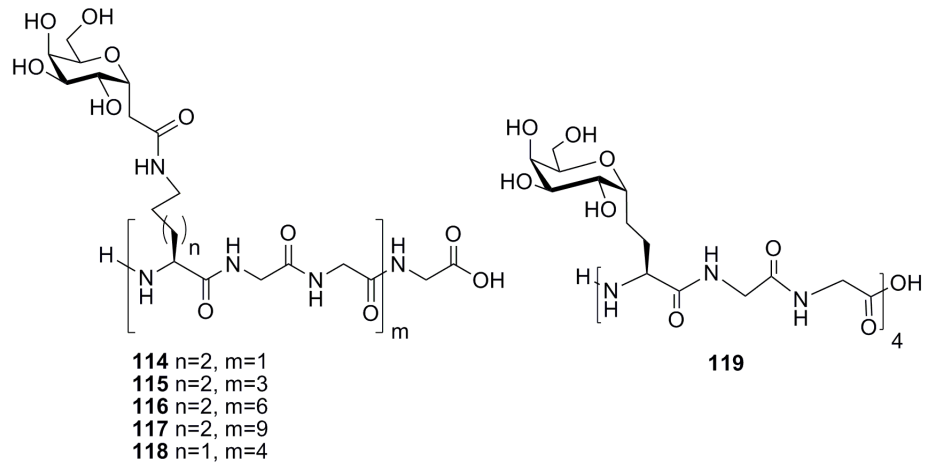



**Figure 1.12. Analogues of AFGP prepared by Nishimura with a variety of different carbohydate functionalities. Presence of absence of TH activity is noted. All analogues expressed at least weak DIS activity.[10]**

showed no TH but both expressed residual DIS activity. When combined with an NMR-based molecular modelling investigation into the solution conformation of the glycoproteins, Nishimura concluded that the ability of the glycoproteins to be able to access key conformations is essential to their activity. This could explain the lack of activity of the serine analogue as the methyl groups have been suggested to be essential for preventing an alpha-helix conformation. Similarly, the elimination of the N-acetyl group appears to be fatal for activity in these analogues, possibly because it plays an essential role in properly orienting the carbohydrate with respect to the backbone through an intramolecular hydrogen bond,[130] or through a water bridge.[172] Interestingly, this was the first time that it was shown that the disaccharide was not necessary for TH activity as **110** retains some TH activity.

More recent efforts from the Ben group have shown that in *C*-linked derivatives of AFGP-8, the TH gap is almost completely eliminated; only in two analogues was a very small gap detected: lysine derivatives **116** and **117** both show a TH gap of 0.06 ºC (Figure 1.13).[11] The shorter peptides, monomer **114** and dimer **115** do not show any TH activity. Ornithine derivative **118**, on the other hand, only shows weak dynamic ice-shaping with no discernable TH gap.[3]




**114** n=2, m=1
**115** n=2, m=3
**116** n=2, m=6
**117** n=2, m=9
**118** n=1, m=4

**119**

**Figure 1.13. *C*-linked AFGP analogues showing weak or no TH activity.[11]**

Similarly, a *C*-serine derivative of AFGP (**119**) failed to show any TH or DIS activity.[9] However, these last two analogues (**118** and **119**) do show remarkably good ice recrystallization inhibition (IRI) activity.

TH activity consequently appears to be very sensitive to structural modification: perturbation from the native system by removing the methyl group of the threonine residue or by removing the N-acetyl galactosamine residue appear to almost completely eliminate the effect. The *C*-linked analogues from the Ben group are of particular interest as they dispense with the TH activity and all of its harmful side effects but retain potent IRI behaviour.

## 1.6 Ice Recrystallization Inhibition (IRI)

Ice recrystallization is the growth of large ice crystals at the expense of small ice crystals in a solution of water maintained just below its colligative freezing point. This occurs as a result of Ostwald ripening, which is defined as the "dissolution of small crystals or sol particles and the redeposition of the dissolved species on the surfaces of larger crystals or sol particles."[173] This occurs because small particles have a higher surface area to volume ratio than a larger particle. As such, they have higher Gibbs energy, meaning they are less stable, and consequently have a higher solubility in the bulk solvent. This thermodynamic process would eventually result (at $t = \infty$) in the formation of a single crystal as the molecules would have minimum energy under those circumstances.

Some compounds are known to inhibit this process by slowing it down. These compounds, known as ice recrystallization inhibition active compounds (IRICs), have almost always been the same compounds implicated in TH activity. Until quite recently

in fact, it was thought that the two phenomena, TH and IRI, were different manifestations of the same physical process described above. However, with the discovery first of plant Type V AFPs that showed potent IRI activity but no TH activity,[66] and second of *C*-linked AFGP analogues with similar properties,[11] this assumption has been revisited.

### 1.6.1 Applications of IRI

Ice recrystallization inhibitors have many potential applications including in the food sector, horticulture, and, most importantly of all, cryopreservation and have been excellently reviewed recently by Venketesh and Dayananda.[101] IRICs are already seeing service in the food industry where several ice-cream manufacturers are including AFPs in their product to reduce the recrystallization that inevitably occurs in the premium quality ice creams upon standing. This can drastically increase their shelf-life and consumer satisfaction.[174] They can also be used in preventing recrystallization in frozen foods; a serious issue that leads to a destruction in texture in frozen produce (strawberries, tomatoes and raspberries for instance). Furthermore IRICs can be used to improve the quality of frozen meat where the reorganization of ice crystals causes damage to the muscle tissue and results in an inferior quality of meat. Payne has carried out several studies that show that treating muscle tissue with solutions of antifreeze protein reduce ice recrystallization,[175] and that injection of lambs prior to slaughter can improve the quality of the frozen meat through a reduction in ice crystal size.[176] Yeh and coworkers demonstrated that a transgenic AFP produced by a food-grade corn micro-organism (*Lactococcus lactis*) can be used to similarly preserve meat

and dough (the dough was “accepted” by consumers to the same degree as fresh dough rather than the less “accepted” dough frozen without antifreeze).[177]

In horticulture an IRI based strategy has also been envisaged. Transgenic plants with plant AFPs could survive freezing over the winter as it has been proposed that it is not TH, but IRI that is the dominant mechanism for the Type V antifreezes. This makes perfect sense when considering the environment. Preventing ice growth is not a viable strategy in grasses such as lolium as soil surface temperatures can fall below -30 ºC; however if the crystals do not grow once formed, small crystals would not damage the cells to as great a degree as larger ice crystals. This could expand the northern range of many crops that cannot survive the harsher winters of Northern Europe and North America.[164, 167]

In cryopreservation, possibly the most important and exciting application, antifreeze proteins show various degrees of promise.[101, 178-181] Ice recrystallization is a harmful process that occurs during the thawing of frozen tissue and leads to cellular death and consequently its inhibition should be beneficial to survival. TH, however, is very harmful in the freezing process as the inevitable formation of spicules will puncture cell membranes and lead to cellular and hence organ death. Consequently, IRI activity is a very desirable property for cryopreservation while TH is not.[182, 183] AFPs have been applied to cryopreservation and have shown mixed results. In some studies AFPs appear to provide improvements to the survival of tissue after freezing,[164, 184-187] namely with spermatozoa,[188-190] pancreatic islets,[191] livers,[192, 193] ovaries (including in the production of a line of transgenic mice expressing AFP III),[194, 195] and complete hearts.[196, 197] Contrastingly, in other studies a decrease in viability post-freezing is

observed in cultures treated with antifreeze relative to the untreated control.[179, 182, 183, 198-201] Several hypotheses have been forwarded proposing that these molecules play a vital role in the protection of the integrity of membranes during the freezing process,[187, 197] or even their ability to promote ice crystal growth around the cell membrane, presumably providing a degree of protection.[202] The negative outcomes are often noted at higher concentrations and may be due to cytotoxic or TH effects;[180, 201, 203, 204] IRI effects on the other hand are positively correlated with the survival of cryo-preserved cells.[205] Consequently, the design of IRI active compounds lacking TH activity could provide better solutions to the problems involved in cryopreservation.

### 1.6.2 Proposed mechanisms for IRI in AFPs and AFGPs

Unlike thermal hysteresis, there have been very few mechanistic suggestions for the IRI effect. This is partially because that until recently it was believed that the phenomena were directly related and mechanistically identical.[206] However, in recent years with evidence showing the independence of the two properties, the attention of the Ben lab has become focused on providing some preliminary mechanistic suggestions other than relying on the same one used to explain thermal hysteresis above. It is important to note that despite the recent evidence regarding the independence of the two phenomena, and the lack of correlation between the two activities, there still exists a tendency to conflate the two

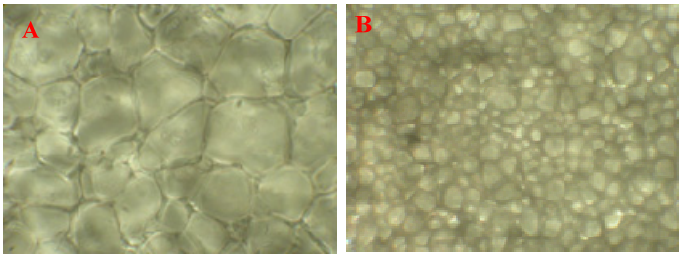



**Figure 1.14. Images of PBS, the positive control for recrystallization (A) and an IRI active compound (B) showing the difference in crystal size. Both images were obtainedat the same magnification. Field of view is approximately 100 μm.**

properties and ascribe the mechanism described above to both.[207] The suggestion from the Ben lab has been that, at least in the case of the *C*-linked AFGPs, there is a strong correlation between hydration (the number of water molecules associated with the solute) and the antifreeze activity of the molecule.[3, 12] It appears that solutes that fit poorly into, and consequently disrupt and increasingly disorder, bulk water, show higher IRI activity than those that fit better into this phase. Solutes that would fit better into the natural order of bulk water would not disrupt the transfer to the QLL relative to water itself, but those that force disorder in water would increase the entropic cost of transference to the more highly ordered QLL, and would thus slow down this process. Galactose is a very highly hydrated solute; it fits very poorly into water, and shows considerably improved IRI activity relative to talose, a sugar that has a much better fit in water.[12, 208] The Ben lab has previously proposed that such solutes might interfere and affect the kinetics of the equilibrium between the QLL and bulk water, thus slowing desorption and absorption of the water molecules due to Ostwald ripening. These hypotheses have been constructed using evidence obtained from a quantitative analysis of IRI activity.

IRI has been measured in several different ways,[209, 210] but the most accepted method is the “splat” cooling assay as devised by Knight,[211, 212] and improved by Horwath and co-workers.[213] In this splat cooling assay, a 10 µL aliquot of antifreeze solution at the appropriate concentration prepared in a standard saline solution (used to eliminate non-specific IRI interactions), was dropped two metres onto an aluminum plate maintained at -78 ºC. The sample is then transferred, on a glass cover slip, to a Peltier unit that allows for controlled electrical cooling, and allowed to anneal for 30

minutes at -6.4 ºC. The full solution nucleates and freezes into small crystals immediately upon dropping—an advantage of this technique is that it is independent of the nucleation event (unlike the competing capillary method)[209]--and the crystals reorganize over the subsequent annealing period and are then photographed and analyzed for size.

A solution containing large crystals, approaching the size of those in the stock solution (Figure 1.14A), is said to have poor to no IRI activity while solutions containing smaller crystals, crystals that have not reorganized to the same degree, has better IRI activity (Figure 1.14B). The IRI activity of any family of compounds has been found to be very sensitive to even slight structural changes and a variety of *O*- and *C*-linked glycoconjugates have been prepared to further examine this relationship.

### 1.6.3 Effects of structural modification on the IRI activity of *O*-linked AFGPs

Compared to the extensive structural studies carried out on TH activity, relatively little comparable effort has been expended on the IRI activity of *O*-linked AFGP analogues. Budke and co-workers demonstrated that the monosaccharide *O*-linked *N*-acetyl galactosamine analogue **109** (Figure 1.12 C), previously prepared by Nishimura, shows IRI activity.[214] Other than this study, the remaining efforts in this field have been generally provided by the Ben lab. A series of Nishimura's monosaccharide analogues prepared by V. Bouvet, a member of the Ben lab, during his doctoral research are outlined in Figure 1.15.[6]

A note should be made about the presentation of this data. All data is presented as a ratio of the ice crystal area (mean grain size) of the tested analyte at the stated

concentration to the ice crystal size in the PBS control (measured on the same day). First generation measurements used more primitive software to determine the size of the ice grains and the details of the technique are provided in the experimental appendix to this document. For this reason, some of the IRI ratios in Chapter 1 are calculated using the largest crystals present in the sample. Later studies, including all the studies presented in this thesis used a more advanced technique to measure crystal size and calculate the IRI ratios based on the average crystal size in a sample. A small bar represents a compound showing significant IRI activity while a large bar represents a compound showing little IRI activity. The error bars, in all cases, represent the standard error of the mean.

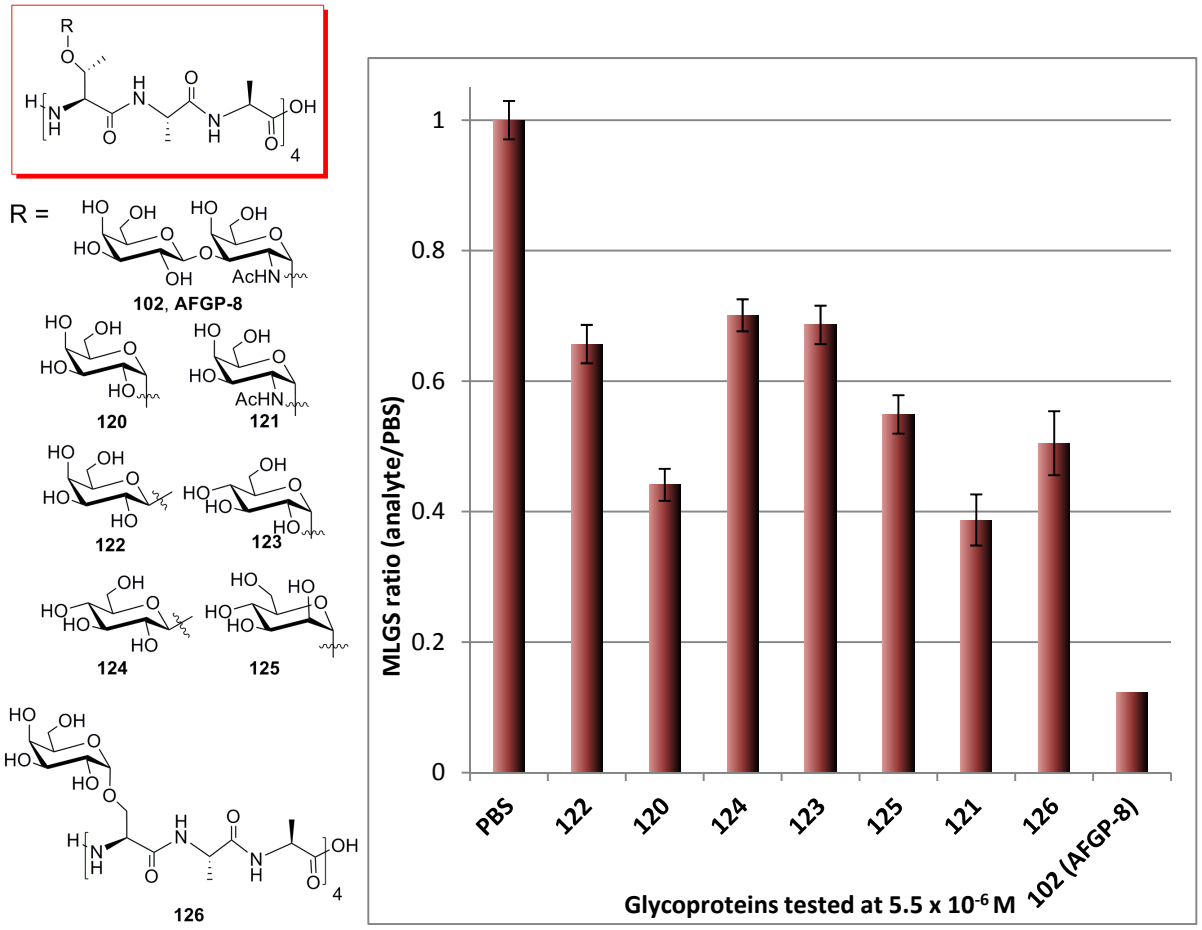



**Figure 1.15 *O*-linked AFGP-8 analogues initially prepared by Nishimura and co-workers and re-synthesized by V. Bouvet for testing their IRI activity.[6]**

All analogues showed moderate activity relative to the highly active AFGP-8. The most active analogue was the N-acetyl-galactosamine derivative **121** followed closely by galactose derivative **120**. Mannose derivative **125** produced ice crystals 55 % the size of PBS, which is considerably better than that seen in both α- and β- glucose (**123** and **124**) and the β-galactose (**122**) derivatives. It is interesting to note that the substitution of the threonine residue with a serine resulted in a significant decrease in IRI activity (**126**). These findings are very important as they illustrate certain structural features that prove essential for potent IRICs. It appears that the stereochemistry of the carbohydrate is important to IRI activity; namely the presence of an axial hydroxyl group at *C*-4, and to a lesser degree *C*-2, is beneficial as is an α anomeric linkage. Both of these features are found in the native system. These IRI results parallel the TH results found by Nishimura and indicate that many of the same structural features are responsible for these activities,[10] but that potent IRI can occur in analogues that have no TH activity. A related study was recently carried out by W. Campbell in which the oxygen of the serine side-chain was replaced with a sulphur atom.[215] Four analogues were prepared based on two backbones, (thioserine-glycine-glycine or thioserine-alanine-alanine repeats) and two sugars, *N*-acetyl galactosamine or galactose. All four compounds showed little to no IRI activity (not shown). This demonstrates how sensitive IRI activity is to even the smallest structural substitutions such as replacing oxygen with sulphur.

Despite the initial promise of these results, it is known that the *O*-linked AFGP analogues, and AFGP itself, are unstable to biotic conditions[216] and, by helping to induce apoptosis in mammalian cells, are cytotoxic.[204] Consequently the attention of the

Ben lab has turned towards the more stable *C*-linked derivatives; therefore much more is known about the structure-function relationships in the *C*-linked derivatives.

### 1.6.4 Effects of structural modification on the IRI activity of *C*-linked AFGPs

*C*-linked analogues are attractive for a variety of reasons. The *O*-linkage in the native system can be quite labile under acidic or basic conditions and is sensitive to galactosidase enzymes and consequently unstable under biotic conditions.[216-218] The *C*-linked analogues, however, do not suffer from these drawbacks and would have relatively long life-times relative to the *O*-linked analogues. The first *C*-linked AFGP analogue (*C*-AFGP) was prepared by Eniade and co-workers in our group.[11] A lysine-based derivative of the native system was prepared (Figure 1.13, **114**, **115**, **116**, **117**) with various numbers of tripeptide repeats (1, 3, 6 and 9 respectively). These compounds were targeted because the lysine-derived amide connection resembles the Arginine found in the arctic cod species (Figure 1.17). These compounds, discussed above in relation to TH activity, were found to exhibit some moderate IRI

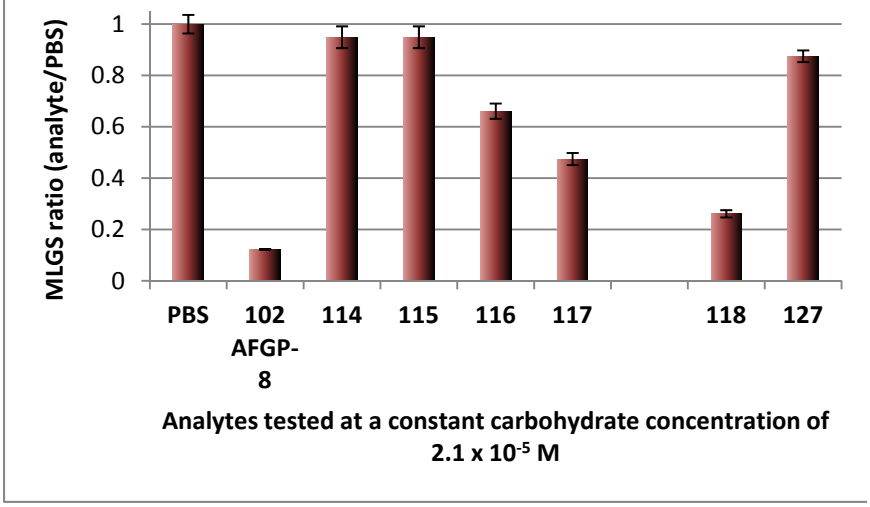



**Figure 1.16 IRI activity of Lysine derivatives generated by Eniade and Ben. All glycopeptides were tested at a carbohydrate concentration of 2.1 x $10^{-5}$ M; consequently AFGP-8, 114, 115, 116, and 117 were examined at 5.5 x $10^{-6}$, 2.1 x $10^{-5}$, 7.0 x $10^{-6}$, 3.0x$10^{-6}$, and 2.0 x $10^{-6}$ respectively.[11]**

activity (Figure 1.16): monomer **114** and trimer **115** showed no discernable activity at 2.2 x $10^{-5}$ M (carbohydrate concentration), however hexamer **116** and nonamer **117** showed increasingly better activity consistent with the positive correlation between peptide length and IRI activity found by Feeney. The activity of these analogues was, however, quite modest: analogue **117** remained considerably weaker at inhibiting ice recrystallization than AFGP-8.

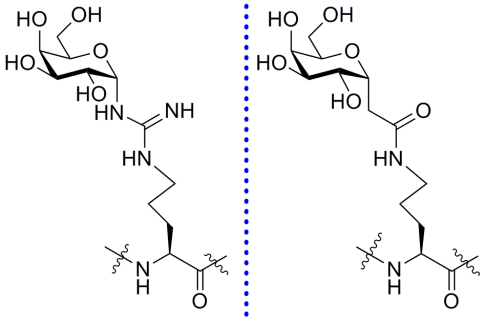


**Figure 1.17 Strucutral similarity of ornithine-linked glycoconjugate with arginine linked glycoconjugate found in arctic cod.**

To further examine the features responsible for IRI activity, a second generation of analogues was envisaged which better matched the native system. A fourmer of the lysine system, **127**, was produced along with a tetramer of the ornithine

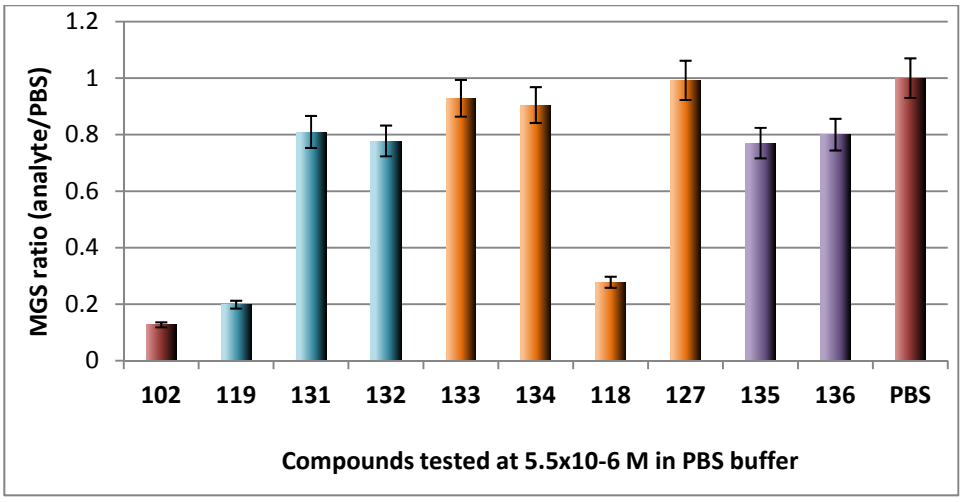



**Figure 1.18 Structure and IRI activity of analogues designed to examine the importance of the linker between the peptide and carbohydrate.[9]**

system, **118**. The lysine tetramer, **127**, showed activity comparable to the trimer **115**. However, replacing the lysine residue with ornithine, **118**, an isometric mimic of arginine (Figure 1.17), resulted in a considerable improvement in activity.[3, 219] Compound **118** is nearly as potent as the native system, but was found to possess no TH activity. This result is critical and the remarkable activity of this compound has spurred on further efforts in the design of *C*-linked AFGP analogues. From these promising results, it appears that ornithine provides much better activity than lysine. Various attempts to modify the backbone further were made, and these studies are further discussed in Chapter 3, but none of the other analogues approached the activity of **118**.

A second series of studies investigated the importance of the carbohydrate component and found that the galactose residue was superior to all other tested carbohydrates; furthermore it was noted that a correlation existed between the hydration of the carbohydrate and the IRI activity of the molecule. The more the carbohydrate disrupted water, by requiring a higher level of hydration, the better the IRI activity. The details of this study are provided in Chapter 5.

A third series of second generation analogues were prepared by Suhai Liu and Roger Tam examining the importance of the length of the linker between the carbohydrate and the peptide backbone (Figure 1.18).[4, 9, 14, 220] The results were extraordinary. As can be seen, *C*-serine analogue **119**, isometric with AFGP-8 (**102**) approaches the native system in IRI activity; however, increasing the chain length by one or two methylene groups (**131** or **132**) results in a near complete loss of IRI activity. A similar dependence on length is seen with the amide family of analogues prepared by Tam. The previously mentioned active analogue, **118**, loses its activity if the chain

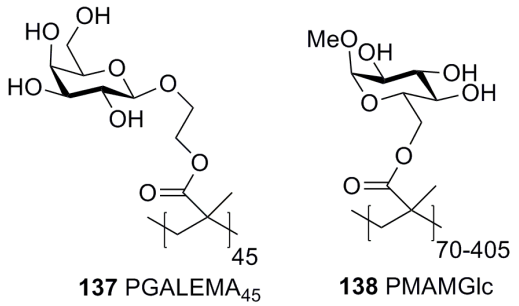
length extends by a methylene to lysine (**127**), or is decreased by 1 or 2 units (**133** and **134** respectively).

This shows how important the linker length is to activity: it appears to be a more important factor than either the nature of the peptide or the nature of the carbohydrate. However, even if the linker is maintained at the same length, Tam observed that activity was significantly decreased if the amide bond was moved closer to the peptide backbone (**135** and **136**). It appears the amide functionality is located in a “sweet” spot in **118,** and is an important feature for eliciting the remarkable activity of analogue **118**. It would be interesting if the relationship between length and relative position of the functionality in the linker could be further examined to provide additional support to describe the generality of this effect or whether this is simply a special feature of these two families of analogues. These studies are further discussed and elaborated upon in Chapter 4.

In summary, a considerable amount of evidence has been developed regarding the structural features of *C*-linked AFGP analogues responsible for IRI activity. The nature of the peptide component is very important and it was found that glycine backbones in general provided more active compounds than those containing alanines or prolines. Similarly, glycosylated ornithine, a direct mimic of the arginine found in nature, provided more active compounds than glycosylated lysine. Interestingly, the introduction of β-amino acids appeared to have a positive effect with regard to the lysine analogues, but not with the ornithine analogues. It is a question whether this discrepancy is due to the increased rigidity and changes in conformation or due to a disruption in intramolecular interactions. The carbohydrate also appears to be an

essential component for IRI activity and the most active compounds all include a galactose residue. Substitution of an N-acetyl galactosamine or galactose-containing disaccharide for the galactose residue results in a more moderate decrease in IRI activity compared to the more extensive loss upon substitution with glucose, mannose or talose. It appears that galactose has a privileged role in antifreeze activity. Finally, the linker between these two components is at least as important as they are themselves; deviating from the ideal length appears to result in a significant decrease in antifreeze activity. However, each of these glycoconjugates required significant synthetic effort. The observation that IRI activity in these compounds varied based on identity of the carbohydrate moiety, in addition to the observation that free carbohydrates alone appear to produce a non-colligative antifreeze effect, has opened the door to the possibility that smaller, simpler molecules could find use as biological antifreezes.

### 1.6.5 Effects of structural modification on the IRI activity of monosaccharides and disaccharides




**137** PGALEMA$_{45}$ **138** PMAMGlc

**Figure 1.19 Structures of the glycopolymers prepared by Gibson.[8] Note that molecular masses range up to 107,420 Da (PMAMGlc$_{405}$).**

Despite the progress made in terms of understanding the features required for IRI activity, the Ben lab has also examined the possibility of using non-glycopeptides as IRI active compounds. These molecules have the distinct advantage of being easier to prepare (not requiring SPPS), easier to characterize, and easier to modify. No reports had been produced on the IRI activity of small

molecules prior to our study, although several fully synthetic polymers have been shown to inhibit ice recrystallization and have been reviewed more recently.[8, 221] A couple of notable examples are worth mentioning explicitly. In the seminal publication in the field, Knight, Wen and Laursen showed that polyvinyl alcohol is a strong inhibitor of ice recrystallization, and the higher the molecular weight, the stronger the inhibition; this effect was also seen with polyhydroxyproline.[212] This trend is analogous to that found with the native system. However other polymers, such as poly-aspartic acid, poly-asparagine and poly-vinylpyrrolidone do not show any specific IRI activity.

A second study of particular interest is that of Gibson and coworkers on the synthesis and IRI activity of glycopolymers (Figure 1.19).[8] The study confirmed the moderate IRI activity of high molecular weight polyvinyl alcohol (9000-115500 Daltons) at relatively high concentrations. Galactose (**137**) and glucose (**138**) derivatives of various molecular weights were examined (Figure 1.19), and showed only moderate IRI activity; however, as the IRI activity of the glycopeptides is very sensitive to even small structural changes, it is possible that further small modifications to their backbone or linker may lead to significantly more active analogues, possibly with much lower molecular weights.

Efforts from the Ben lab on small molecule ice recrystallization inhibitors (SMIRIs) have involved the native mono- and disaccharides.[12] Interest arose from two observations. The first was that mentioned above: the IRI activity of antifreeze glycopeptides correlated with the hydration of the saccharide moiety in that activity improved as the hydration of the carbohydrate increased. In other words, as the solutes became more solvated, organizing a larger hydration shell, activity improved.[3] The

second interesting observation was made by Mastai and co-workers.[222] They carried out an extensive study of mono-, di- and oligosaccharides and observed that compounds containing OH-OH distances between 4.2 and 4.5 Å depressed the freezing point of water to a greater degree than expected from colligative effects alone. This distance matches the inter-molecular distances found on the basal face of hexagonal ice suggesting the possibility of direct ice binding. Carbohydrates without this distance did not, for the most part, show any freezing point depression.

Carbohydrates have long been known to help protect proteins from cryo-damage during freezing, most likely due to the restructuring of water around the protein itself.[223-225] In a series of studies,[226, 227] Furuki showed that a wide variety of disaccharides have differential but significant impacts on the glass-transition temperatures and the amounts of unfrozen water when present at high weight percentages and these two properties appear to be strongly correlated with the stereochemistry of the hydroxyl groups at *C*-2 and *C*-4 rather than simply with the number of equatorial hydroxyl groups as first supposed. Carbohydrates with an equatorial *C*-2 hydroxyl and an axial *C*-4 hydroxyl such as galactose (interestingly gulose, the *C*-3 epimer of galactose and the only other sugar to meet these criteria has never been examined for antifreeze activity) appear to be much better at increasing the number of unfrozen water molecules than those with an equatorial *C*-4 and either an axial or equatorial OH at *C*-2 (such as glucose and mannose). Consequently, it appeared that simple monosaccharides might show specific antifreeze activity although no TH gap had ever been measured nor had they been examined for IRI activity (an exception would be a study by Uchida and co-workers

demonstrating that trehalose has a significant impact on the recrystallization of ice crystals, but the effect was not quantified).[228]

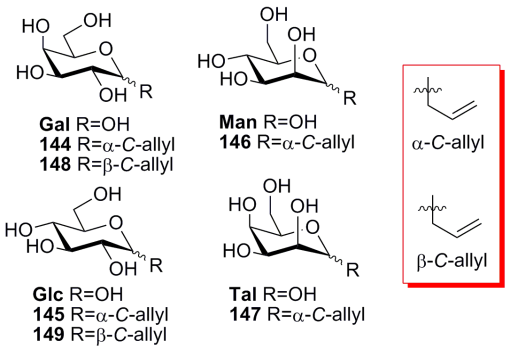



**Figure 1.20 Simple carbohydrates tested for IRI activity.[12]**

To study the relationship between hydration and IRI activity a series of mono and disaccharides were obtained. Commercially available galactose (Gal), glucose (Glc), mannose (Man) and talose (Tal) as well as their synthetic α-*C*-allyl derivatives (**144**-**147**) were prepared (Figure 1.20). The α-*C*-allyl compounds were examined as they fixed the anomeric centre in the same orientation as that found in the previously tested *C*-linked AFGP analogues. β-*C*-allyl derivatives of galactose (**148**) and glucose (**149**) were also prepared to see if the decrease in activity noticed in β-linked AFGP analogues (both *O*- and *C*-linked) was mirrored in the carbohydrate system. With respect to the disaccharides, commercially available melibiose (**139**), lactose (**140**), trehalose (**141**), maltose (**142**) and sucrose (**143**) were obtained (Figure 1.21). All of the above carbohydrates were tested for IRI activity (Figure 1.22).

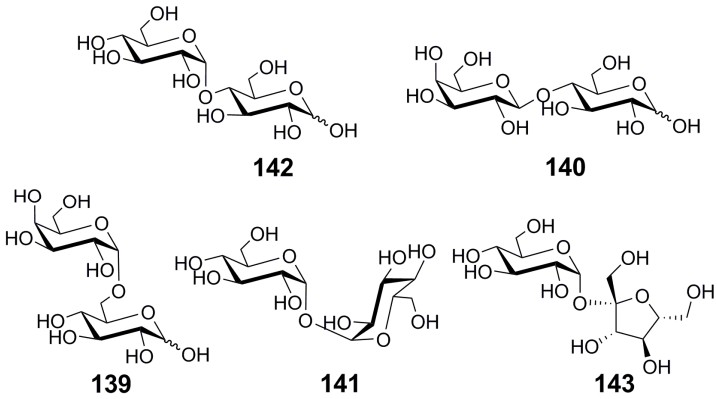



**Figure 1.21 Disaccharides that were analyzed for IRI activity.[12]**

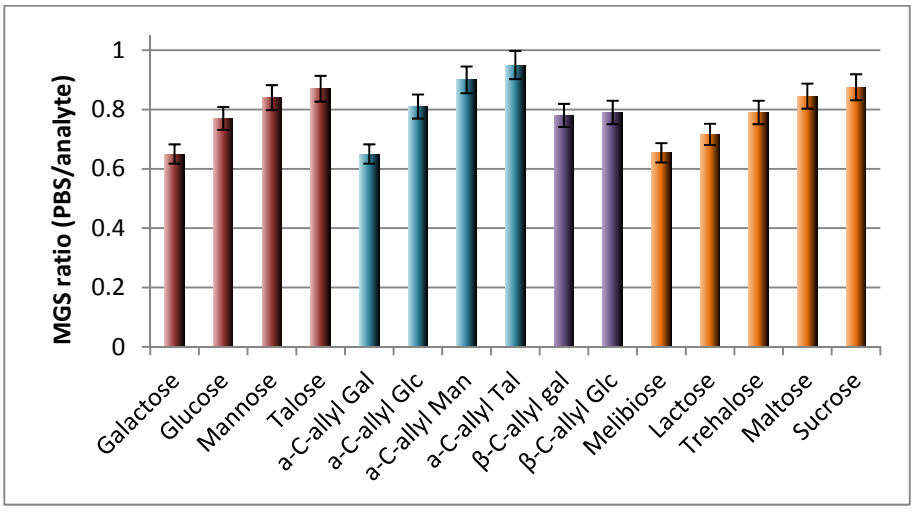



**Figure 1.22 IRI activity of mono- and disaccharides as tested by Tam and co-workers. All sugars tested at 22 mM.[12]**

Several trends are immediately visible. The first is that activity is similar for both the reducing sugars and their α-*C*-allyl derivatives, and that galactose is the most active residue, talose the least active, and glucose and mannose possess intermediate activity. Consistent with the previous research,[10] the β-*C*-linked analogue of galactose shows decreased antifreeze activity and the differential between glucose and galactose disappears. The disaccharides also show considerable variation, and surprisingly, unlike what one would expect considering its preferred role in nature,[61] trehalose (**141**) is not the most active inhibitor. Interestingly, the two galactose-containing disaccharides show the best activity (**139**, **140**), followed by trehalose and the least active were the glucose-based maltose (**142**) and sucrose (**143**), the latter of which has seen significant use in cryopreservation at high concentrations. These results are further discussed in Chapter 5 and 6.

The working hypothesis for this effort, based on the earlier observations, was that increasing the hydration of the sugars should increase the IRI activity. This appears to be the case with both the mono and disaccharides, but, according to this hypothesis the disaccharides should all have considerably better activity than found in the study. This

led Tam and co-workers to propose a modification to the hypothesis to explain these experimental findings and possibly lead to the rational design of molecules with better IRI activity.[12]

### 1.6.6 Effects of hydration on IRI activity and revised proposal for the mechanism of *C*-linked AFGP analogues

Measuring hydration is not a simple procedure, but through a combination of methods including ultrasonic and density experiments,[229] kinetic experiments,[230, 231] and molecular dynamic simulations,[232] Galema and Engberts derived a series of parameters to describe the hydration of carbohydrates and suggested that the hydration of carbohydrates is determined by their stereochemistry.[208, 231] As mentioned above, it appears that carbohydrates can be divided into three categories, those with *C*-4 OH axial and *C*-2 OH axial groups fit very well into the water lattice and require little hydration compared to those with *C*-4 OH equatorial (regardless of the orientation of *C*-

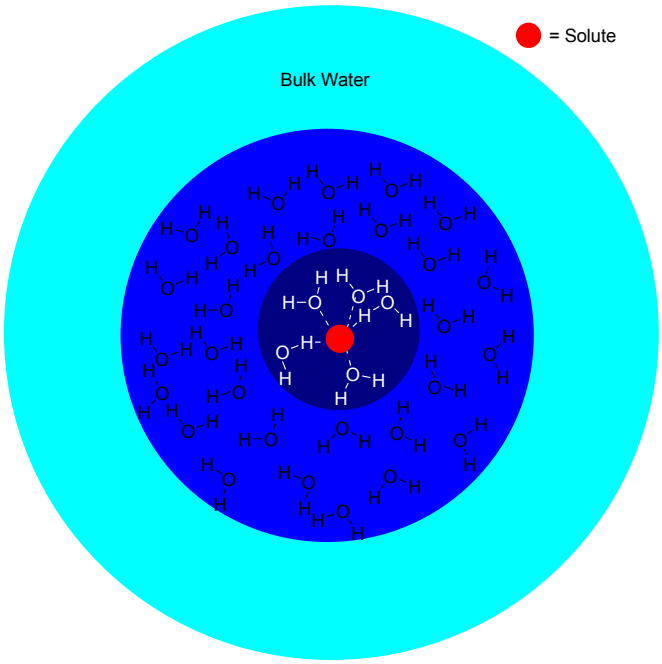



**Figure 1.23. Hydration model of a solute in water showing the inner hydration layer (navy), the outer hydration layers (medium blue), and the bulk water phase (cyan). Hydration number is a count of the number of water molecules directly associated with the solute (white), while partial molar compressibility measures the compressibility (i.e. density) of the outer hydration sphere.**

2) and especially those with *C*-4 axial and *C*-2 equatorial which show very poor fit into the thee-dimensional structure of water and as such require a greater degree of

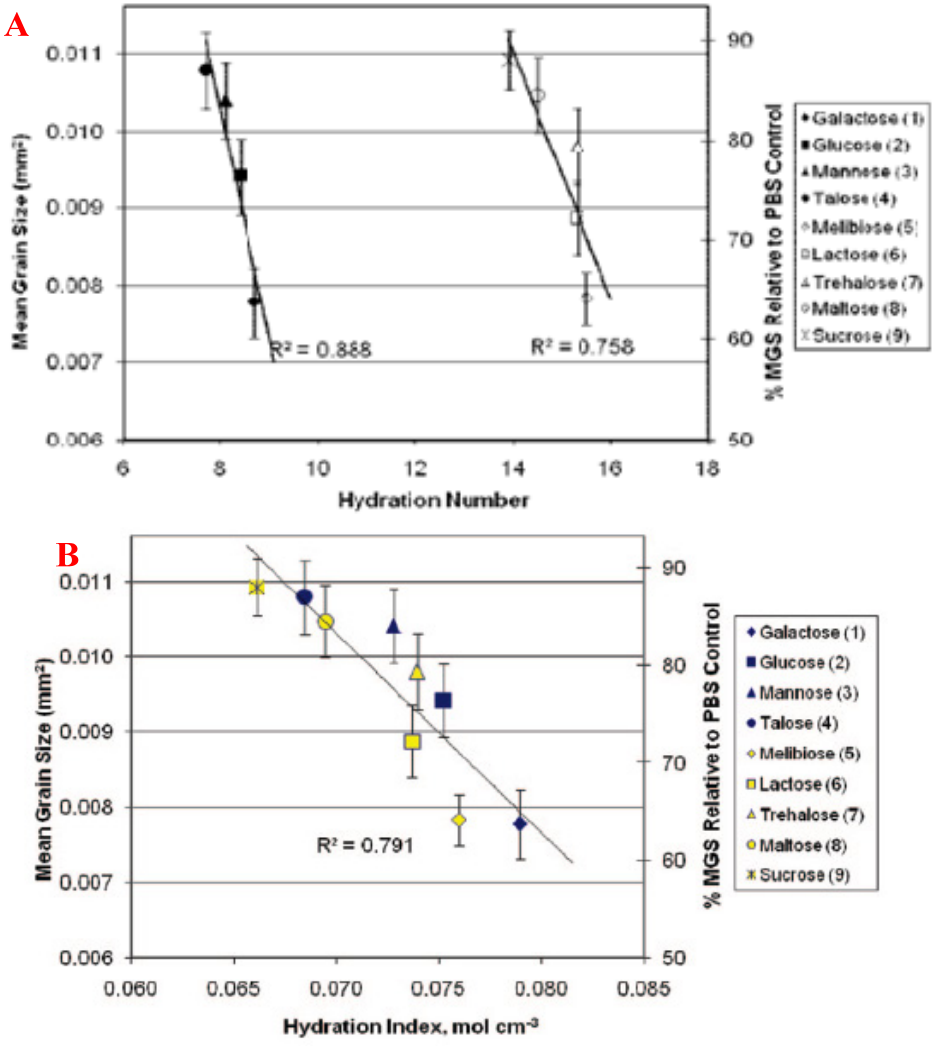



**Figure 1.24. (A) Correlation between hydration number and IRI activity from Tam et al.[12] Notice the two parallel linear correlations. When the hydration number is divided by the molar volume to obtain the hydration index (B) a single linear relationship defines all points.**

hydration. The most relevant of the parameters determined by Galema and Engberts were the “hydration number” and “partial molar compressibility” (PMC). The first of these is the measurement of the minimum number of water molecules directly associated with the carbohydrate in an “inner sphere” of hydration (Figure 1.23, Navy). The more water molecules located in this sphere, the more water molecules are required in outer

spheres to mask the solute and integrate it into the bulk water. It makes an excellent approximation for the overall hydration of the carbohydrate. The second parameter (PMC) is a measurement of the density of the hydration shell of the water around a particular solute. For example, in the presence of ions, very large partial molar compressibilities are observed (~-40 x $10^{-4}$ $cm^3$ $mol^{-1}$ $bar^{-1}$). Bulk water has a PMC of 8.17 x $10^{-4}$ $cm^3$ $mol^{-1}$ $bar^{-1}$. This large difference indicates that the water around the ion is very organized and hence very dense: it is very difficult to compress it any further with an increase in pressure. Bulk water on the other hand has considerable room for compression as it is much more locally dilute. Carbohydrates tend to be intermediate between these values.[229] The hydration sphere of a solute and the relevance of the parameters is graphically described in Figure 1.23.

Tam and coworkers determined that although both parameters showed a good correlation with the IRI of the tested monosaccharides, only hydration number provided a linear correlation with the disaccharides (Figure 1.24A).[12] However, when they divided the hydration number by the molar volume of the compounds, defined as the hydration index, they obtained a single linear correlation (Figure 1.24B). The hydration index is thus a measurement of the density of closely bound molecules within the first hydration sphere. Upon reflection it makes intuitive sense that this parameter would be important. The more densely packed the molecules in this sphere, the more perturbed this first hydration sphere is relative to bulk water, and hence it requires a larger outer hydration sphere to integrate the solvent into the solution as a whole. Denser primary hydration shells should consequently lead to a greater disruption of water than a less dense shell. This differential density may provide a mechanism for the localization of the solute at

the QLL interface as has been proposed; the higher density of water molecules in a packed hydration sphere would more closely approximate the density of the QLL than the bulk water phase.[12, 228] The presence of these molecules at the interface provides them with the opportunity to interfere with the addition and subtraction of water molecules from the ice-lattice, possibly stabilizing the crystal and slowing down ice-recrystallization

A second, related set of data is that provided by Simons and coworkers from Oxford.[233, 234] Through a series of resolved UV resonant two-photon ionization mass spectrometry/spectroscopy experiments, Simons and coworkers examined the conformation of a several mono- and disaccharides to determine the directionality of an intramolecular hydrogen bonding network both with and without the presence of water. They determined that the anhydrous molecules adopt considerably different conformations (in the gas phase) than their monohydrated counterparts (Figure 1.25).[18] Several interesting observations arise from their extensive studies: in the case of glucopyranosides (Figure 1.25B) and mannopyranosides (not shown) the first water molecule inserts between *O*-3 and *O*-6 to complete a circum-molecular network; alternatively, and less favourably, insertion can occur between *O*-6 and *O*-5 (the endocyclic oxygen) resulting in two separate networks

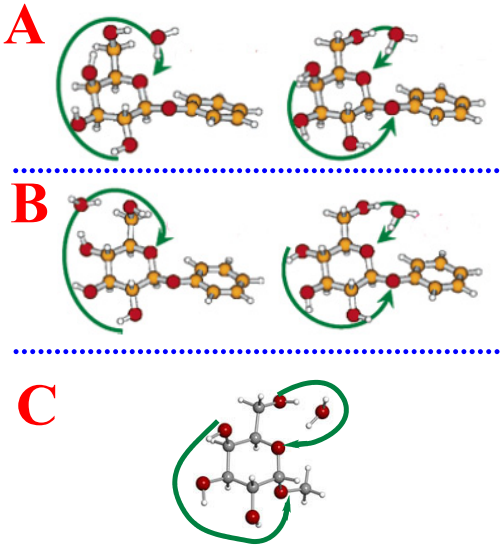



**Figure 1.25 Lowest-energy intramolecular water-bridged hydrogen bond networks. A) β-D-*O*-phenyl-galactopyranose; B) β-D-*O*-phenyl-glucopyranose; C) α-D-methylgalactopyranoside.[18]**

within the same molecule: a higher energy conformation. On the other hand, in the case of either α or β galactopyranosides (Figure 1.25A), the first water molecule prefers to insert between *O*-6 and *O*-5 as the axial stereochemistry of *O*-4 allows this hydroxyl group to interact with *O*-6 directly,[18, 235] while in the other two monosaccharides, the equatorial stereochemistry at *C*-4 prohibits this interaction due to distance constraints. This shows a particular molecular difference between galactose and the other common monosaccharides. It is important to note that this is not only seen in phenyl-substituted derivatives, as the network is identical even in α-methoxy substituted galactose derivatives (Figure 1.25C) Furthermore, it is interesting to note that Simons suggests that these networks, both their directionality and the position of the water molecules, have an influence on the global hydration shell of the carbohydrates.[234] Consequently a disruption of these networks through substitution of the hydrogen for another substituent (such as a methyl group, or another saccharide moiety) would have a significant impact on the hydration of the molecule as a whole; not only is one removing a hydrogen bond donor and (depending on the steric implications of the substitution) acceptor, that interact with the surrounding hydration shell, one is also disrupting the conformation of the other hydroxyl groups. Consequently, it appears that the least disruptive position for substitution would be the anomeric position as the other positions would imperil the network and the special ability of galactose to bridge the *O*-4/*O*-6 gap due to its stereochemistry. Along with the hydration index theory of Tam and co-workers, this can help explain some of the structure-IRI relationships found in galactose derivatives and will be further explored in Chapters 5, 6 and 8.

Hydration provides a very attractive theory for explaining the differentials in activity found in previous analogues, but all such hypotheses are merely that and require more experimental evidence to determine the exact location of solutes at the ice-water interface and the influence of hydration, on IRI activity. More compounds are consequently required to examine the factors responsible for IRI activity. The efforts described in the following chapters are directed towards a better understanding of the IRI implications of structural modifications to both glycopeptides and carbohydrates in order to both better understand the phenomenon and to attempt to produce synthetically simple but highly IRI active compounds for the myriad of applications that await.

## References

1. Sicheri, F.; Yang, D. S. C., *Nature* **1995,** *375* (6530), 427-431.

2. Gronwald, W.; Loewen, M. L. C.; Lix, B.; Daugulis, A. J.; Sönnichsen, F. D.; Davies, P. L.; Sykes, B. D., *Biochemistry* **1998,** *37* (14), 4712-4721.

3. Czechura, P.; Tam, R. Y.; Dimitrijevic, E.; Murphy, A. V.; Ben, R. N., *J. Am. Chem. Soc.* **2008,** *130* (10), 2928-2929.

4. Tam, R. Y.; Rowley, C. N.; Petrov, I.; Zhang, T.; Afagh, N. A.; Woo, T. K.; Ben, R. N., *J. Am. Chem. Soc.* **2009,** *131* (43), 15745-15753.

5. Wilson, P. W.; Beaglehole, D.; Devries, A. L., *Biophys. J.* **1993,** *64* (6), 1878-1884.

6. Bouvet, V. R. Novel AFGP8 Analogues: Synthesis and Biological Evaluation of Potent Recrystallization Inhibitors. PhD. Thesis, University of Ottawa, Ottawa, 2006.

7. Anisuzzaman, A. K. M.; Anderson, L.; Navia, J. L., *Carb. Res.* **1988,** *174*, 265-278.

8. Gibson, M. I.; Barker, C. A.; Spain, S. G.; Albertin, L.; Cameron, N. R., *Biomacromol.* **2008,** *10* (2), 328-333.

9. Liu, S.; Ben, R. N., *Org. Lett.* **2005,** *7* (12), 2385-2388.

10. Tachibana, Y.; Fletcher, G. L.; Fujitani, N.; Tsuda, S.; Monde, K.; Nishimura, S.-I., *Angew. Chem. Intl. Ed.* **2004,** *43*, 856-862.

11. Eniade, A.; Purushotham, M.; Ben, R. N.; Wang, J. B.; Horwath, K., *Cell. Biochem. Biophys.* **2003,** *38*, 115-124.

12. Tam, R. Y.; Ferreira, S. S.; Czechura, P.; Chaytor, J. L.; Ben, R. N., *J. Am. Chem. Soc.* **2008,** *130* (51), 17494-17501.

13. Walters, K. R.; Serianni, A. S.; Sformo, T.; Barnes, B. M.; Duman, J. G., *Proc. Natl. Acad. Sci. U. S. A.* **2009,** *106* (48), 20210-20215.

14. Tam, R. Y. Studies into the structural features of *C*-linked antifreeze glycoprotein analogues responsible for ice-recrystallization inhibition activity. PhD. Thesis, University of Ottawa, Ottawa, 2010.

15. Jia, Z.; Davies, P. L., *Trends Biochem. Sci.* **2002,** *27* (2), 101-106.

16. Baudot, A.; Boutron, P., *Rev. Gériatrie.* **2006,** *31* (9), 717-730.

17. Madura, J. D.; Baran, K.; Wierzbicki, A., *J. Mol. Recog.* **2000,** *13* (2), 101-113.

18. Carcabal, P.; Jockusch, R. A.; Huenig, I.; Snoek, L. C.; Kroemer, R. T.; Davis, B. G.; Gamblin, D. P.; Compagnon, I.; Oomens, J.; Simons, J. P., *J. Am. Chem. Soc.* **2005,** *127* (32), 11414-11425.

19. Brown, D. J.; Sönnichesen, F. D., *Mol. Aspects Fish Mar. Biol.* **2002,** *1* (Fish Antifreeze Proteins), 109-138.

20. Davies, P. L.; Sykes, B. D., *Curr. Opin. Struc. Biol.* **1997,** *7* (6), 828-834.

21. Meldal, M.; Jensen, K. J., *Chem. Commun.* **1990,** (6), 483-485.

22. Komatsu, S. K.; Devries, A. L.; Feeney, R. E., *J. Biol. Chem.* **1970,** *245* (11), 2909-2913.

23. Jia, Z.; Deluca, C. I.; Chao, H.; Davies, P. L., *Nature* **1996,** *384* (6606), 285-288.

24. Zhao, Z.; Deng, G.; Lui, Q.; Laursen, R. A., *Biochim. Biophys. Acta - Prot. Struct. Mol. Enzymol.* **1998,** *1382* (2), 177-180.

25. Breiter, D. R.; Kanost, M. R.; Benning, M. M.; Wesenberg, G.; Law, J. H.; Wells, M. A.; Rayment, I.; Holden, H. M., *Biochem.* **1991,** *30* (3), 603-608.

26. Vandenheede, J. R.; Ahmed, A. I.; Feeney, R. E., *J. Biol. Chem.* **1972,** *247* (24), 7885-7889.

27. Filira, F.; Biondi, L.; Scolaro, B.; Foffani, M. T.; Mammi, S.; Peggion, E.; Rocchi, R., *Int. J. Biol. Macromol.* **1990,** *12* (1), 41-49.

28. Pegg, D. E., *Cryobiology* **2010,** *60* (3, Supplement 1), S36-S44.

29. Daley, M. E.; Spyracopoulos, L.; Jia, Z.; Davies, P. L.; Sykes, B. D., *Biochem.* **2002,** *41* (17), 5515-5525.

30. Ahmed, A. I.; Yeh, Y.; Osuga, Y. Y.; Feeney, R. E., *J. Biol. Chem.* **1976,** *251* (10), 3033-3036.

31. Tseng, P.-H.; Jiaang, W.-T.; Chang, M.-Y.; Chen, S.-T., *Chem. – Eur. J.* **2001,** *7* (3), 585-590.

32. Best, B. The Cryonics Institute. www.cryonics.org (accessed 19/05).

33. More, M. Alcor life extension foundation. www.Alcor.org.

34. Kuiper, M. J.; Davies, P. L.; Walker, V. K., *Biophys. J.* **2001,** *81* (6), 3560-3565.

35. *Organ and tissue donation and transplantation*; Office of the Auditor General of Ontario: Toronto, 2010; pp 240-271.

36. Malenkov, G., *J. Phys.-Condens. Mat.* **2009,** *21* (28), 283101.

37. Murray, B. J.; Knopf, D. A.; Bertram, A. K., *Nature* **2005,** *434* (7030), 202-205.

38. Mayer, E.; Pletzer, R., *Nature* **1986,** *319* (6051), 298-301.

39. Thomson, J., *P. Roy. Soc. Lond.* **1860,** *11*, 198-204.

40. Faraday, M., *Philos. Mag.* **1859,** *17* (113), 162 - 169.

41. Ryzhkin, I.; Petrenko, V., *J. Exper. Theor. Phys.* **2009,** *108* (1), 68-71.

42. Stranski, I. N., *Naturwissenschaften* **1941,** *29* (49), 743-743.

43. Fletcher, N. H., *Philos. Mag.* **1968,** *18* (156), 1287 - 1300.

44. Döppenschmidt, A.; Butt, H.-J., *Langmuir* **2000,** *16* (16), 6709-6714.

45. Pittenger, B.; Fain, S. C.; Cochran, M. J.; Donev, J. M. K.; Robertson, B. E.; Szuchmacher, A.; Overney, R. M., *Phys. Rev. B.* **2001,** *63* (13), 134102.

46. Dosch, H.; Lied, A.; Bilgram, J. H., *Surf. Sci.* **1996,** *366* (1), 43-50.

47. Sadtchenko, V.; Ewing, G. E., *J. Chem. Phys.* **2002,** *116* (11), 4686-4697.

48. Golecki, I.; Jaccard, C., *J. Phys. C.* **1978,** *11* (20), 4229.

49. Kahan, T. F.; Reid, J. P.; Donaldson, D. J., *J. Phys. Chem. A.* **2007,** *111* (43), 11006-11012.

50. Kaverin, A.; Tsionsky, V.; Zagidulin, D.; Daikhin, L.; Alengoz, E.; Gileadi, E., *J. Phys. Chem. B.* **2004,** *108* (26), 8759-8762.

51. Bluhm, H.; Ogletree, D. F.; Fadley, C. S.; Hussain, Z.; Salmeron, M., *J. Phys.-Condens. Mat.* **2002,** *14* (8), L227.

52. Beaglehole, D.; Nason, D., *Surf. Sci.* **1980,** *96* (1-3), 357-363.

53. Benatov, L.; Wettlaufer, J. S., *Phys. Rev. E.* **2004,** *70* (6 1), 061606-1-061606-7.

54. Elbaum, M.; Lipson, S. G.; Dash, J. G., *J. Cryst. Gr.* **1993,** *129* (3-4), 491-505.

55. Gilpin, R. R., *J. Colloid and Interf. Sci.* **1980,** *77* (2), 435-448.

56. Karim, O. A.; Haymet, A. D. J., *J. Chem. Phys.* **1988,** *89* (11), 6889.

57. Nada, H.; Furukawa, Y., *J. Cryst. Gr.* **2005,** *283* (1-2), 242-256.

58. Clarke, J. B.; Hastie, J. W.; Kihlborg, L. H. E.; Metselaar, R.; Thackeray, M. M., *Pure Appl. Chem.* **1994,** *66* (3), 577-594.

59. Averhoff, B.; Mueller, V., *Res. Microbiol.* **2011,** *161* (6), 506-514.

60. Karavaiko, G. I.; Dubinina, G. A.; Kondrat'eva, T. F., *Microbiol.* **2006,** *75* (5), 512-545.

61. Crowe, J. H.; Crowe, L. M.; Chapman, D., *Science* **1984,** *223* (4637), 701-703.

62. Scholander, P. F.; Van Dam, L.; Kanwisher, J. W.; Hammel, H. T.; Gordon, M. S., *J. Cell. Comp. Physiol.* **1957,** *49* (1), 5-24.

63. Feeney, R. A.; Osuga, D. T., Early research on proteins from the Antarctic: Antifreeze glycoproteins. In *Fish Antifreeze Proteins*, Ewart, K. V.; Hew, C. L., Eds. World Scientific Publishing Co.: Singapore, 2002; pp 1-16.

64. Devries, A. L.; Komatsu, S. K.; Feeney, R. E., *J. Biol. Chem.* **1970,** *245*, 2901-2908.

65. Devries, A. L.; Wohlschlag, D. E., *Science* **1969,** *163* (3871), 1073-1075.

66. Sidebottom, C.; Buckley, S.; Pudney, P.; Twigg, S.; Jarman, C.; Holt, C.; Telford, J.; Mcarthur, A.; Worrall, D.; Hubbard, R.; Lillford, P., *Nature* **2000,** *406* (6793), 256-256.

67. Sönnichsen, F. D.; Deluca, C. I.; Davies, P. L.; Sykes, B. D., *Struct.* **1996,** *4* (11), 1325-1337.

68. Tomchaney, A. P.; Morris, J. P.; Kang, S. H.; Duman, J. G., *Biochemistry* **1982,** *21* (4), 716-721.

69. Li, Z.; Lin, Q.; Low, W.-K.; Miao, M.; Hew, C. L., *Ocean Polar Res.* **2003,** *25* (4), 607-615.

70. Cheng, C.-H. C., *Curr. Opin. Genet. Dev.* **1998,** *8* (6), 715-720.

71. Cheng, C.-H. C., Origin and mechanism of evolution of antifreeze glycoproteins in polar fishes. In *Evolution of the Antarctic Ichthyofauna*, Prisco, G. D.; Pisano, E.; Clarke, A., Eds. Springer-Verlag: Italia, 1998; pp 311-328.

72. Cheng, C. C. M.; Devries, A. L., *Mol. Aspects Fish Mar. Biol.* **2002,** *1* (Fish Antifreeze Proteins), 83-107.

73. Ewart, K. V.; Lin, Q.; Hew, C. L., *Cell. Mol. Life Sci.* **1999,** *55* (2), 271-283.

74. Raymond, J. A., *Can. J. Zoo.* **1993,** *71* (9), 1849-1854.

75. Bargelloni, L.; Ritchie, P. A.; Patarnello, T.; Battaglia, B.; Lambert, D. M.; Meyer, A., *Mol. Biol. Evol.* **1994,** *11* (6), 854-863.

76. Barker, P. F.; Thomas, E., *Earth-Sci. Rev.* **2004,** *66*, 143-162.

77. Doolittle, R. F., *Trends Biochem. Sci.* **1994,** *19* (1), 15-18.

78. O'grady, S. M.; Schrag, J. D.; Raymond, J. A.; Devries, A. L., *J. Exper. Zool.* **1982,** *224* (2), 177-185.

79. Gong, Z.; Ewart, K. V.; Hu, Z.; Fletcher, G. L.; Hew, C. L., *J. Biol. Chem.* **1996,** *271* (8), 4106-4112.

80. Patel, S. N.; Graether, S. P., *Biochem. Cell Biol.* **2010,** *88* (2), 223-229.

81. Ewart, K. V.; Fletcher, G. L., *Mol. Mar. Biol. Biotech.* **1993,** *2* (1), 20-7.

82. Drickamer, K., *Curr. Opin. Struc. Biol.* **1999,** *9* (5), 585-590.

83. Deng, G.; Andrews, D. W.; Laursen, R. A., *FEBS Lett.* **1997,** *402* (1), 17-20.

84. Wilson, C.; Wardell, M. R.; Weisgraber, K. H.; Mahley, R. W.; Agard, D. A., *Science* **1991,** *252* (5014), 1817-1822.

85. Gauthier, S. Y.; Scotter, A. J.; Lin, F.-H.; Baardsnes, J.; Fletcher, G. L.; Davies, P. L., *Cryobiology* **2008,** *57* (3), 292-296.

86. Kelley, J. L.; Aagaard, J. E.; Maccoss, M. J.; Swanson, W. J., *J. Mol. Evol.* **2010,** *71* (2), 111-118.

87. Nelson, J. S., *Fishes of the world*. 3rd ed.; Wiley: New York, 1994; p 600.

88. Hew, C. L.; Wang, N. C.; Joshi, S.; Fletcher, G. L.; Scott, G. K.; Hayes, P. H.; Buettner, B.; Davies, P. L., *J. Biol. Chem.* **1988,** *263* (24), 12049-12055.

89. Schrag, J. D.; Cheng, C.-H. C.; Panico, M.; Morris, H. R.; Deries, A. L., *Biochim. Biophys. Acta - Prot. Struct. Mol. Enzymol.* **1987,** *915* (3), 357-370.

90. Howes, G. J., *J. Biogeogr.* **1991,** *18* (6), 595-622.

91. Lauersen, K. J.; Brown, A.; Middleton, A.; Davies, P. L.; Walker, V. K., *Cryobiology* **2011,** *62* (3), 194-201.

92. Atıcı, Ö.; Nalbantoğlu, B., *Phytochem.* **2003,** *64* (7), 1187-1196.

93. Baardsnes, J.; Kondejewski, L. H.; Hodges, R. S.; Chao, H.; Kay, C.; Davies, P. L., *FEBS Lett.* **1999,** *463* (1-2), 87-91.

94. Hew, C. L.; Slaughter, D.; Joshi, S. B.; Fletcher, G. L.; Ananthanarayanan, V. S., *J. Comp. Physiol. B.* **1984,** *155* (1), 81-88.

95. Liou, Y.-C.; Tocilj, A.; Davies, P. L.; Jia, Z., *Nature* **2000,** *406* (6793), 322-324.

96. Kumble, K. D.; Demmer, J.; Fish, S.; Hall, C.; Corrales, S.; Death, A.; Elton, C.; Prestidge, R.; Luxmanan, S.; Marshall, C. J.; Wharton, D. A., *Cryobiology* **2008,** *57* (3), 263-268.

97. Middleton, A. J.; Brown, A. M.; Davies, P. L.; Walker, V. K., *FEBS Lett.* **2009,** *583* (4), 815-819.

98. Urrutia, M. E.; Duman, J. G.; Knight, C. A., *Biochim. Biophys. Acta - Prot. Struct. Mol. Enzymol.* **1992,** *1121* (1-2), 199-206.

99. Pudney, P. D. A.; Buckley, S. L.; Sidebottom, C. M.; Twigg, S. N.; Sevilla, M. P.; Holt, C. B.; Roper, D.; Telford, J. H.; Mcarthur, A. J.; Lillford, P. J., *Arch. Biochem. Biophys.* **2003,** *410* (2), 238-245.

100. Tyshenko, M. G.; Doucet, D.; Davies, P. L.; Walker, V. K., *Nat. Biotech.* **1997,** *15* (9), 887-890.

101. Venketesh, S.; Dayananda, C., *Crit. Rev. Biotech.* **2008,** *28* (1), 57-82.

102. Moffatt, B.; Ewart, V.; Eastman, A., *Physiol. Plantarum* **2006,** *126* (1), 5-16.

103. Devries, A. L.; Komatsu, S. K.; Feeney, R. E., *J. Biol. Chem.* **1970,** *245* (11), 2901-2908.

104. Devries, A. L.; Vandenheede, J.; Feeney, R. E., *J. Biol. Chem.* **1971,** *246* (2), 305-308.

105. Tachibana, Y.; Matsubara, N.; Nakajima, F.; Tsuda, T.; Tsuda, S.; Monde, K.; Nishimura, S.-I., *Tetrahedron* **2002,** *58* (51), 10213-10224.

106. Yeh, Y.; Feeney, R. E., *Chem. Rev.* **1996,** *96* (2), 601-618.

107. Drewes, J. A.; Rowlen, K. L., *Biophys. J.* **1993,** *65*, 985-991.

108. Bush, C. A.; Feeney, R. E., *Int. J. Pep. Prot. Res.* **1986,** *28* (4), 386-397.

109. Bush, C. A.; Ralapati, S.; Matson, G. M.; Yamasaki, R. B.; Osuga, D. T.; Yeh, Y.; Feeney, R. E., *Arch. Biochem. Biophys.* **1984,** *232* (2), 624-631.

110. Bush, C. A.; Feeney, R. E.; Osuga, D. T.; Ralapati, S.; Yeh, Y. I. N., *Int. J. Pep. Prot. Res.* **1981,** *17* (1), 125-129.

111. Ahmed, A. I.; Feeney, R. E.; Osuga, D. T.; Yeh, Y., *J. Biol. Chem.* **1975,** *250* (9), 3344-3347.

112. Franks, F.; Morris, E. R., *Biochim. Biophys. Acta.* **1978,** *540* (2), 346-356.

113. Raymond, J. A.; Radding, W.; Devries, A. L., *Biopolym.* **1977,** *16* (11), 2575-2578.

114. Bouvet, V. R.; Lorello, G. R.; Ben, R. N., *Biomacromol.* **2005,** *7* (2), 565-571.

115. Lane, A. N.; Hays, L. M.; Tsvetkova, N.; Feeney, R. E.; Crowe, L. M.; Crowe, J. H., *Biophys. J.* **2000,** *78* (6), 3195-3207.

116. Lane, A. N.; Hays, L. M.; Crowe, L. M.; Crowe, J. H.; Feeney, R. E., *Protein Sci.* **1998,** *7* (7), 1555-1563.

117. Berman, E.; Allerhand, A.; Devries, A. L., *J. Biol. Chem.* **1980,** *255* (10), 4407-4410.

118. Tsvetkova, N. M.; Phillips, B. L.; Krishnan, V. V.; Feeney, R. E.; Fink, W. H.; Crowe, J. H.; Risbud, S. H.; Tablin, F.; Yeh, Y., *Biophys. J.* **2002,** *82* (1, Pt. 1), 464-473.

119. Rao, B. N. N.; Bush, C. A., *Biopolym.* **1987,** *26* (8), 1227-1244.

120. Krishnan, V. V.; Yeh, Y. In *Structure and functional dynamics of antifreeze glycoproteins*, Nova Science Publishers, Inc.: 2011; pp 105-140.

121. Haymet, A. D. J.; Ward, L. G.; Harding, M. M.; Knight, C. A., *FEBS Lett.* **1998,** *430* (3), 301-306.

122. Chao, H.; Houston, M. E.; Hodges, R. S.; Kay, C. M.; Sykes, B. D.; Loewen, M. C.; Davies, P. L.; Sönnichsen, F. D., *Biochemistry* **1997,** *36* (48), 14652-14660.

123. Zhang, W.; Laursen, R. A., *J. Biol. Chem.* **1998,** *273* (52), 34806-34812.

124. Haymet, A. D. J.; Ward, L. G.; Harding, M. M., *J. Am. Chem. Soc.* **1999,** *121* (5), 941-948.

125. Jorov, A.; Zhorov, B. S.; Yang, D. S. C., *Protein Sci.* **2004,** *13* (6), 1524-1537.

126. Wen, D.; Laursen, R. A., *J. Biol. Chem.* **1993,** *268* (22), 16401-16405.

127. Wen, D.; Laursen, R. A., *J. Biol. Chem.* **1992,** *267* (20), 14102-14108.

128. Wen, D.; Laursen, R. A., *J. Biol. Chem.* **1993,** *268* (22), 16396-16400.

129. Patel, S. N.; Graether, S. P., *Protein Sci.* **2010,** *19* (12), 2356-2365.

130. Mimura, Y.; Yamamoto, Y.; Inoue, Y.; Chûjô, R., *Int. J. Biol. Macromol.* **1992,** *14* (5), 242-248.

131. Mimura, Y.; Inoue, Y.; Maeji, N. J.; Chûjô, R., *Int. J. Pep. Prot. Res.* **1989,** *34* (5), 363-368.

132. Haymet, A. D. J.; Ward, L. G.; Harding, M. M., *FEBS Lett.* **2001,** *491* (3), 285-288.

133. Wu, D. W.; Duman, J. G.; Xu, L., *Biochim. Biophys. Acta - Prot. Struct. Mol. Enzymol.* **1991,** *1076* (3), 416-420.

134. Deluca, C. I.; Comley, R.; Davies, P. L., *Biophys. J.* **1998,** *74* (3), 1502-1508.

135. Pertaya, N.; Marshall, C. B.; Diprinzio, C. L.; Wilen, L.; Thomson, E. S.; Wettlaufer, J. S.; Davies, P. L.; Braslavsky, I., *Biophys. J.* **2007,** *92* (10), 3663-3673.

136. Wu, D. W.; Duman, J. G., *J. Comp. Physiol. B.* **1991,** *161* (3), 279-283.

137. Wang, L.; Duman, J. G., *Biochemistry* **2005,** *44* (30), 10305-10312.

138. Kristiansen, E.; Zachariassen, K. E., *Cryobiology* **2005,** *51* (3), 262-280.

139. Barrett, J., *Int. J. Biochem.Cell B.* **2001,** *33* (2), 105-117.

140. Schneppenheim, R.; Theede, H., *Polar Biol.* **1982,** *1* (2), 115-123.

141. Knight, C. A.; Driggers, E.; Devries, A. L., *Biophys. J.* **1993,** *64* (1), 252-259.

142. Knight, C. A.; De Vries, A. L.; Oolman, L. D., *Nature* **1984,** *308* (5956), 295-296.

143. Raymond, J. A.; Devries, A. L., *Proc. Natl. Acad. Sci. U. S. A.* **1977,** *74* (6), 2589-2593.

144. Kerr, W. L.; Feeney, R. E.; Osuga, D. T.; Reid, D. S., *Cryo-Lett.* **1986,** *6*, 371-378.

145. Knight, C. A.; Cheng, C. C.; Devries, A. L., *Biophys. J.* **1991,** *59* (2), 409-418.

146. Wen, D.; Laursen, R. A., *Biophys. J.* **1992,** *63* (6), 1659-1662.

147. Wilson, P. W., *Cryo-Lett.* **1993,** *14*, 31-36.

148. Hall, D. G.; Lips, A., *Langmuir* **1999,** *15* (6), 1905-1912.

149. Wilson, P. W., *Cryobiology* **1994,** *31* (4), 406-412.

150. Takamichi, M.; Nishimiya, Y.; Miura, A.; Tsuda, S., *FEBS J.* **2007,** *274* (24), 6469-6476.

151. Li, L. F.; Liang, X. X.; Li, Q. Z., *Chem. Phys. Lett.* **2009,** *472* (1-3), 124-127.

152. Deluca, C. I.; Chao, H.; Sönnichsen, F. D.; Sykes, B. D.; Davies, P. L., *Biophys. J.* **1996,** *71* (5), 2346-2355.

153. Burcham, T. S.; Osuga, D. T.; Yeh, Y.; Feeney, R. E., *J. Biol. Chem.* **1986,** *261* (14), 6390-6397.

154. Li, Q.; Luo, L., *Chem. Phys. Lett.* **1993,** *216* (3-6), 453-457.

155. Li, Q.; Luo, L., *Chem. Phys. Lett.* **2000,** *320* (3-4), 335-338.

156. Zepeda, S.; Nakaya, H.; Uda, Y.; Yokoyama, E.; Furukawa, Y., Diffusion, incorporation, and segregation of antifreeze glycoproteins at the ice/solution interface. In *Physics and Chemistry of Ice* Kuhs, W. F., Ed. Royal Society of Chemistry: London, 2007; pp 669-675.

157. Zepeda, S.; Uda, Y.; Furukawa, Y., *Nippon Kessho Seicho Gak.* **2008,** *35* (3), 151-160.

158. Zepeda, S.; Yokoyama, E.; Uda, Y.; Katagiri, C.; Furukawa, Y., *Cryst. Growth Des.* **2008,** *8* (10), 3666-3672.

159. Cheng, A.; Merz Jr, K. M., *Biophys. J.* **1997,** *73* (6), 2851-2873.

160. Garnham, C. P.; Campbell, R. L.; Davies, P. L., *Proc. Natl. Acad. Sci. U. S. A.* **2011,** *108* (18), 7363-7367.

161. Yeh, Y.; Krishnan, K.; Fink, W. H.; Duan, Y. In *The quasi-liquid layer involvement in antifreeze function*, American Chemical Society: 2007; pp COMP-013.

162. Koushafar, H.; Pham, L.; Lee, C.; Rubinsky, B., *J. Surg. Oncol.* **1997,** *66* (2), 114-121.

163. Goel, R.; Anderson, K.; Slaton, J.; Schmidlin, F.; Vercellotti, G.; Belcher, J.; Bischof, J. C., *J. Biomech. Eng.* **2009,** *131* (7), 074003-11.

164. Breton, G.; Danyluk, J.; Ouellet, F.; Sarhan, F., *Biotechnol. Annu. Rev.* **2000,** *6*, 59-101.

165. Fletcher, G. L.; Goddard, S. V.; Wu, Y., *CHEMTECH.* **1999,** *29* (6), 17-28.

166. Hightower, R.; Baden, C.; Penzes, E.; Lund, P.; Dunsmuir, P., *Plant Mol. Biol.* **1991,** *17* (5), 1013-1021.

167. Lemaux, P. G., *Annu. Rev. Plant Biol.* **2008,** *59* (1), 771-812.

168. Low, W.-K.; Hew, C. L.; Shears, M. A.; Fletcher, G. L.; Davies, P. L., *Mol. Aspects Fish Mar. Biol.* **2002,** *1* (Fish Antifreeze Proteins), 213-227.

169. Zbikowska, H. M., *Transgen. Res.* **2003,** *12* (4), 379-389.

170. Tsuda, T.; Nishimura, S.-I., *Chem. Commun.* **1996,** (24), 2779-2780.

171. Hachisu, M.; Hinou, H.; Takamichi, M.; Tsuda, S.; Koshida, S.; Nishimura, S.-I., *Chem. Commun.* **2009**, 1641-1643.

172. Corzana, F.; Busto, J. H.; Jiménez-Osés, G.; García De Luis, M.; Asensio, J. L.; Jiménez-Barbero, J.; Peregrina, J. M.; Avenoza, A., *J. Am. Chem. Soc.* **2007,** *129* (30), 9458-9467.

173. Iupac, Ostwald ripening. In *Gold Book*, 2nd ed.; Mcnaught, A. D.; Wilkinson, A., Eds. Blackwell Scientific: Oxford, 2006.

174. Regand, A.; Goff, H. D., *J. Dairy Sci.* **2006,** *89* (1), 49-57.

175. Payne, S. R.; Sandford, D.; Harris, A.; Young, O. A., *Meat Sci.* **1994,** *37* (3), 429-438.

176. Payne, S. R.; Young, O. A., *Meat Sci.* **1995,** *41* (2), 147-155.

177. Yeh, C.-M.; Kao, B.-Y.; Peng, H.-J., *J. Agric. Food Chem.* **2009,** *57* (14), 6216-6223.

178. Fuller, B. J., *Cryo-Lett.* **2004,** *25* (6), 375-388.

179. Rubinsky, B., *Heart Fail. Rev.* **2003,** *8* (3), 277-284.

180. Makarevich, A. V.; Kubovicova, E.; Popelkova, M.; Fabian, D.; Cikos, S.; Pivko, J.; Chrenek, P., *Zygote* **2010,** *18* (2), 145-153.

181. Palasz, A. T.; Mapletoft, R. J., *Biotechnol. Adv.* **1996,** *14* (2), 127-149.

182. Wang, J.-H., *Cryobiology* **2000,** *41* (1), 1-9.

183. Mazur, P., *Science* **1970,** *168* (3934), 939-949.

184. Hirano, Y.; Nishimiya, Y.; Matsumoto, S.; Matsushita, M.; Todo, S.; Miura, A.; Komatsu, Y.; Tsuda, S., *Cryobiology* **2008,** *57* (1), 46-51.

185. Amir, G.; Horowitz, L.; Rubinsky, B.; Yousif, B. S.; Lavee, J.; Smolinsky, A. K., *Cryobiology* **2004,** *48* (3), 273-282.

186. Martinez-Paramo, S.; Barbosa, V.; Perez-Cerezales, S.; Robles, V.; Herraez, M. P., *Cryobiology* **2009,** *58* (2), 128-133.

187. Rubinsky, B.; Arav, A.; Devries, A. L., *Cryobiology* **1992,** *29* (1), 69-79.

188. Payne, S. R.; Oliver, J. E.; Upreti, G. C., *Cryobiology* **1994,** *31* (2), 180-184.

189. Upreti, G. C.; Payne, S. R.; Duganzich, D. M.; Oliver, J. E.; Smith, J. F., *Anim. Reprod. Sci.* **1996,** *41* (1), 27-36.

190. Prathalingam, N. S.; Holt, W. V.; Revell, S. G.; Mirczuk, S.; Fleck, R. A.; Watson, P. F., *Theriogenology* **2006,** *66* (8), 1894-1900.

191. Matsumoto, S.; Matsusita, M.; Morita, T.; Kamachi, H.; Tsukiyama, S.; Furukawa, Y.; Koshida, S.; Tachibana, Y.; Nishimura, S.-I.; Todo, S., *Cryobiology* **2006,** *52* (1), 90-98.

192. Rubinsky, B.; Arav, A.; Hong, J. S.; Lee, C. Y., *Biochem. Biophys. Res. Commun.* **1994,** *200* (2), 732-41.

193. Soltys, K. A.; Batta, A. K.; Koneru, B., *J. Surg. Res.* **2001,** *96* (1), 30-34.

194. Bagis, H.; Akkoc, T.; Tas, A.; Aktoprakligil, D., *Mol. Reprod. Dev.* **2008,** *75* (4), 608-613.

195. Bagis, H.; Aktoprakligil, D.; Mercan, H. O.; Yurdusev, N.; Turgut, G.; Sekmen, S.; Arat, S.; Cetin, S., *Mol. Reprod. Dev.* **2006,** *73* (11), 1404-1411.

196. Amir, G.; Rubinsky, B.; Horowitz, L.; Miller, L.; Leor, J.; Kassif, Y.; Mishaly, D.; Smolinsky, A. K.; Lavee, J., *Ann. Thorac. Surg.* **2004,** *77* (5), 1648-55.

197. Amir, G.; Rubinsky, B.; Kassif, Y.; Horowitz, L.; Smolinsky, A. K.; Lavee, J., *Eur. J. Cardiothorac. Surg.* **2003,** *24* (2), 292-297.

198. Wang, T.; Zhu, Q.; Yang, X.; Layne, J. R.; Devries, A. L., *Cryobiology* **1994,** *31* (2), 185-192.

199. Mazur, P., *Am. J. Physiol. Cell Physiol.* **1984,** *247* (3), C125-C142.

200. Carpenter, J. F.; Hansen, T. N., *Proc. Natl. Acad. Sci. U. S. A.* **1992,** *89* (19), 8953-7.

201. Chao, H.; Davies, P. L.; Carpenter, J. F., *J. Exp. Biol.* **1996,** *199* (9), 2071-2076.

202. Fan, W.; Ma, X.; Liu, T.; Cui, Z., *Shengwu Yixue Gongchengxue Zazhi.* **2005,** *22* (3, Suppl.), 81-82.

203. Hansen, T. N.; Smith, K. M.; Brockbank, K. G. M., *Transplant. Proc.* **1993,** *25* (6), 3182-4.

204. Liu, S.; Wang, W.; Von Moos, E.; Jackman, J.; Mealing, G.; Monette, R.; Ben, R. N., *Biomacromol.* **2007,** *8* (5), 1456-1462.

205. Wu, L. K.; Tokarew, J. M.; Chaytor, J. L.; Von Moos, E.; Li, Y.; Palii, C.; Ben, R. N.; Allan, D. S., *Carb. Res.* **2011,** *346* (1), 86-93.

206. Knight, C. A., *Nature* **2000,** *406* (6793), 249-251.

207. Yu, S. O.; Brown, A.; Middleton, A. J.; Tomczak, M. M.; Walker, V. K.; Davies, P. L., *Cryobiology* **2010,** *61* (3), 327-334.

208. Galema, S. A.; Engberts, J. B. F. N.; Hoeiland, H.; Foerland, G. M., *J. Phys. Chem.* **1993,** *97* (26), 6885-6889.

209. Tomczak, M. G.; Marshall, C. B.; Gilbert, J. A.; Davies, P. L., *Biochem. Biophys. Res. Commun.* **2003,** *311*, 1041-1046.

210. Norgren, A. S.; Budke, C.; Majer, Z.; Heggemann, C.; Koop, T.; Sewald, N., *Synthesis* **2009**, 488-494.

211. Knight, C. A.; Hallett, J.; Devries, A. L., *Cryobiology* **1988,** *25* (1), 55-60.

212. Knight, C. A.; Wen, D.; Laursen, R. A., *Cryobiology* **1995,** *32* (1), 23-34.

213. Horwath, K.; Easton, C. M.; Poggioli, G. J.; Myers, K.; Schnorr, I. L., *Eur. J. Entomol.* **1996,** *93*, 419-433.

214. Budke, C.; Heggemann, C.; Koch, M.; Sewald, N.; Koop, T., *J. Phys. Chem. B.* **2009,** *113* (9), 2865-2873.

215. Campbell, W. Novel Sulphur-linked AFGP analogues: synthesis and evaluation of antifreeze activity. MSc. Thesis, University of Ottawa, Ottawa, 2010.

216. Specker, D.; Wittmann, V., Synthesis and application of glycopeptide and glycoprotein mimics. In *Glycopeptides and glycoproteins: synthesis, structure and applications*, Wittmann, V., Ed. Springer-Verlag: Berlin and Heidelberg, 2007; Vol. 267, pp 65-107.

217. Schweizer, F., *Angew. Chem., Int. Ed.* **2002,** *41* (2), 230-253.

218. Dondoni, A.; Marra, A., *Chem. Rev.* **2000,** *100* (12), 4395-4422.

219. Murphy, A. V. Preparation of structurally diverse C-linked antifreeze glycoprotein analogues and assessment for antifreeze protein-specific activity. PhD. Thesis, State University of New York, Binghampton, 2004.

220. Liu, S. Novel *C*-linked antifreeze glycoprotein analogues as potent recrystallization inhibitors: preparation, assessment and *in vitro* studies. PhD. Thesis, University of Ottawa, Ottawa, 2006.

221. Gibson, M. I., *Polym. Chem.* **2010,** *1* (8), 1141-1152.

222. Baruch, E.; Belostotskii, A. M.; Mastai, Y., *J. Mol. Struct.* **2008,** *874* (1-3), 170-177.

223. Arakawa, T.; Timasheff, S. N., *Biochemistry* **1982,** *21* (25), 6536-6544.

224. Carpenter, J. F.; Crowe, J. H., *Cryobiology* **1988,** *25* (3), 244-255.

225. Whittam, J. H.; Rosano, H. L., *Cryobiology* **1973,** *10* (3), 240-243.

226. Furuki, T., *Carb. Res.* **1999,** *323* (1-4), 185-191.

227. Furuki, T., *Carb. Res.* **2002,** *337* (5), 441-450.

228. Uchida, T.; Nagayama, M.; Shibayama, T.; Gohara, K., *J. Cryst. Gr.* **2007,** *299* (1), 125-135.

229. Galema, S. A.; Hoeiland, H., *J. Phys. Chem.* **1991,** *95* (13), 5321-5326.

230. Galema, S. A.; Blandamer, M. J.; Engberts, J. B. F. N., *J. Org. Chem.* **1992,** *57* (7), 1995-2001.

231. Galema, S. A.; Blandamer, M. J.; Engberts, J. B. F. N., *J. Am. Chem. Soc.* **1990,** *112* (26), 9665-9666.

232. Galema, S. A.; Howard, E.; Engberts, J. B. F. N.; Grigera, J. R., *Carb. Res.* **1994,** *265* (2), 215-225.

233. Simons, J. P.; Jockusch, R. A.; Carcabal, P.; Huenig, I.; Kroemer, R. T.; Macleod, N. A.; Snoek, L. C., *Int. Rev. Phys. Chem.* **2005,** *24* (3-4), 489-531.

234. Simons, J. P.; Davis, B. G.; Cocinero, E. J.; Gamblin, D. P.; Stanca-Kaposta, E. C., *Tet. Assym.* **2009,** *20* (6-8), 718-722.

235. Cocinero, E. J.; Stanca-Kaposta, E. C.; Scanlan, E. M.; Gamblin, D. P.; Davis, B. G.; Simons, J. P., *Chem. Eur. J.* **2008,** *14* (29), 8947-8955.

# Chapter 2 Goals and Objectives

## 2.1 Factors responsible for antifreeze activity in C-linked AFGPs

For the purposes of structure-activity relationship studies, the key *C*-linked AFGP analogue **118**, is divided into three parts: carbohydrate head, peptide backbone, and the linker that connects the two (Figure 2.1). As described in the introduction, the carbohydrate moiety has been the focus of much structure-function work, and it has been found that galactose provides the best IRI activity. In terms of structural modifications to the peptide backbone, alanine and proline have both been introduced and the peptide backbone itself has also been replaced with various non-biotic polymeric systems.[1, 2] In almost all these studies, replacing glycine with any other residue resulted in a decrease in IRI activity. The only noted exception to this trend was when β-lysine residues were utilized: these compounds showed better activity than their α-lysine analogues.

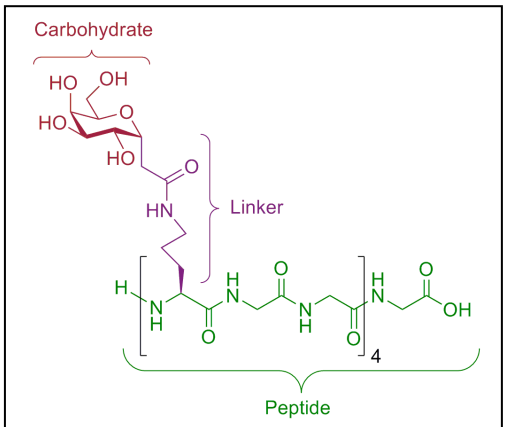



**Figure 2.1 The three components of the *C*-linked AFGP-8 analogues: carbohydrate, peptide and linker.**

The third structural component of the *C*-AFGP is the linker. At first glance it may appear less important than either of the other two components; it is simply the tether that holds the two other portions together; however, studies by Tam[3] and Liu[4] have shown that either extending or shortening the linker has far more drastic implications for activity than modifications of either the saccharide or peptide moieties.

With these observations in mind, the first set of objectives of this thesis is twofold: firstly to explore the relationship between β-amino acid substitution and IRI and TH activity; and secondly to investigate linker alternatives, hopefully not only to elucidate the importance of this domain, but also to possibly provide easier access to glycopeptide analogues.

### 2.1.1 Objective 1: Determination of the effect of β-amino peptides on IRI activity (Chapter 3)

As mentioned previously, incorporation of β-lysine for the lysine residue resulted in improved activity. This is consistent with theories describing the importance of ordered secondary and tertiary structure for antifreeze activity.[5] Mixed α/β and β peptides are known to adopt a more structured and rigid motif than their purely α counterpart as the β-peptide can induce a certain degree of conformational restriction. [6] As illustrated in the introduction, it has been proposed that the rigid, organized structures of AFPs lead to improved binding to the ice, and hence higher IRI activity.

Another great advantage of incorporating β amino acids into peptides is that even one or two residues introduced into a normal peptide can significantly reduce susceptibility to proteases further extending the biological half-life of these molecules relative to the native system.[7, 8] Most efforts in this field have focused on the synthesis of pure β-peptides, especially with regard to studying the structural features (primary sequence and otherwise) that determine specific conformations.[9-19] Some recent efforts, however, have been directed towards their integration into α-peptides as this can drastically increase the structural library available to chemists and biologists.[6, 20] Unfortunately, the conformations adopted by such peptides have not been studied in

great detail and are only poorly understood. However, the initial studies suggest that they are a mixture of those found in the natural peptide and those found in the β-peptides.

Following the preliminary studies in the Ben lab it was found that in the case of lysine the substitution of β-residues was beneficial to IRI activity, but when ornithine was replaced with a β-ornithine, a decrease in IRI activity was observed. It is uncertain as to whether this differential response is due to either increased rigidity or conformational change, or whether it is due to the disruption of an intramolecular interaction between the backbone and either the sugar or the amide on the side chain. This question could not be answered with the available data.[21]

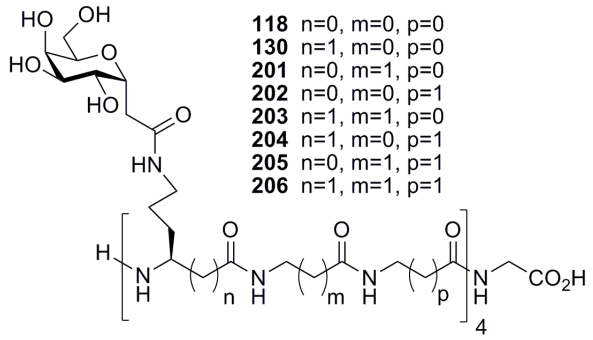



**Figure 2.2 Proposed analogues of 118 incorporating a mixture of α (n, m, or p = 0) and β (n, m, or p =1) amino acids.**

To examine these possibilities, a series of analogues are envisioned that would encompass the full range of possible substitution patterns in the trimeric repeat (Figure 2.2). If increased rigidity imparted by the β-amino acid incorporation resulted in a decrease in IRI activity, then “mono-β” compounds **130**, **201**, and **202** should all give rise to similar levels of activity. Similarly, this activity would be expected to further decrease for analogues **203**, **204** and **205** that contain two β-residues, and should reach a nadir at the true β-peptide, analogue **206**; however, if the decrease in activity observed for analogue **130** relative to **118** was due to a disruption of a specific, important intramolecular interaction, one would not expect to find this pattern.

This second hypothesis is possible as it has been proposed by Tam and coworkers that there may be a water-mediated interaction between the amide N-H of the linker and the backbone carbonyl. This interaction is similar to that found in other analogues AFGP-8 by the contributions of Corzana and Mimura.[3, 22, 23] Although the two groups identify different key interactions, both propose that either water pockets or direct hydrogen bonds involving the amide of the native carbohydrate play a role in its interaction with the peptide backbone and that the conformation thus accessed may be responsible for antifreeze activity.

If the disruption of some such interaction is responsible for the observed changes in IRI activity upon β-substitution, then the IRI activity of certain analogues should be expected to be less affected by substitution than others as key interactions would not necessarily be disrupted: in short, the location of the substitution should be more important than the degree of substitution.

Either way, this study should provide some insight into the differential response of the lysine and ornithine analogues to β-substitution.

### 2.1.2 Objective 2: Determination of the effect of triazole-containing glycopeptides on IRI activity (Chapter 4)

The second part of the *C*-glycopeptide that requires further investigation is the linker. The sensitivity of IRI activity to linker length is truly extraordinary compared to the relative resilience of IRI activity when either the peptide or the carbohydrate is modified. However, the importance of the amide bond in the linker for activity is unclear. Although, as mentioned above, it is suggested that this functional group may play a key role in orienting the carbohydrate with respect to the backbone, there is no firm evidence

supporting this hypothesis. Consequently several analogues were envisioned to examine the different aspects of the amide bond and their relative importance in eliciting the remarkable IRI activity of **118** (Figure 2.3).

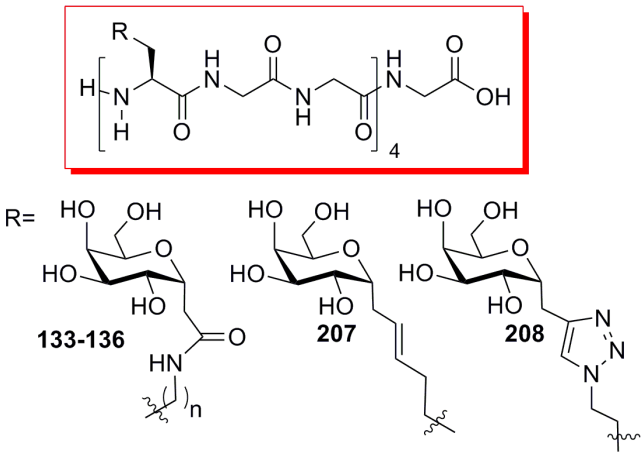



**Figure 2.4 Isomers of 118 designed to probe the importance of different features of the amide bond in the linker.**

The first analogues that were synthesized "shifted" the relative position of the amide bond as already described in the introduction (**133-136**). A second series, comprising analogue **207**, involved synthesizing a glycopeptide in which the amide bond was replaced with an *E* olefin. This analogue would retain the rigidity of the amide, but would remove both any hydrogen-bond capability and any dipole moment. This analogue was targeted by Tahir Rana and although significant progress was made, syntheses of the analogue was not completed.[24] The third set of analogues (such as **208**) is the subject of this objective. These compounds incorporate a 1,4-substituted 1,2,3-triazole moiety, an isostere of the amide bond with much weaker hydrogen bonding capability but with a similar dipole moment and degree of inflexibility (Figure 2.3).[25]

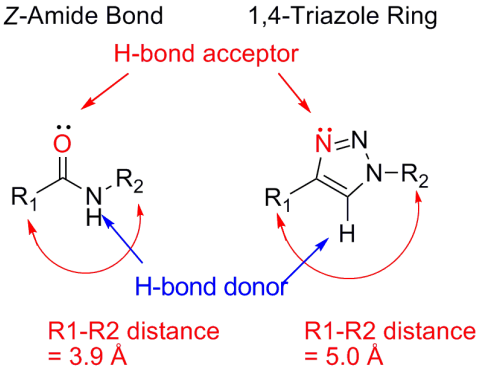



**Figure 2.3 Electronic and structural features of a Z- amide bond and its isostere, the 1,4-triazole ring.**

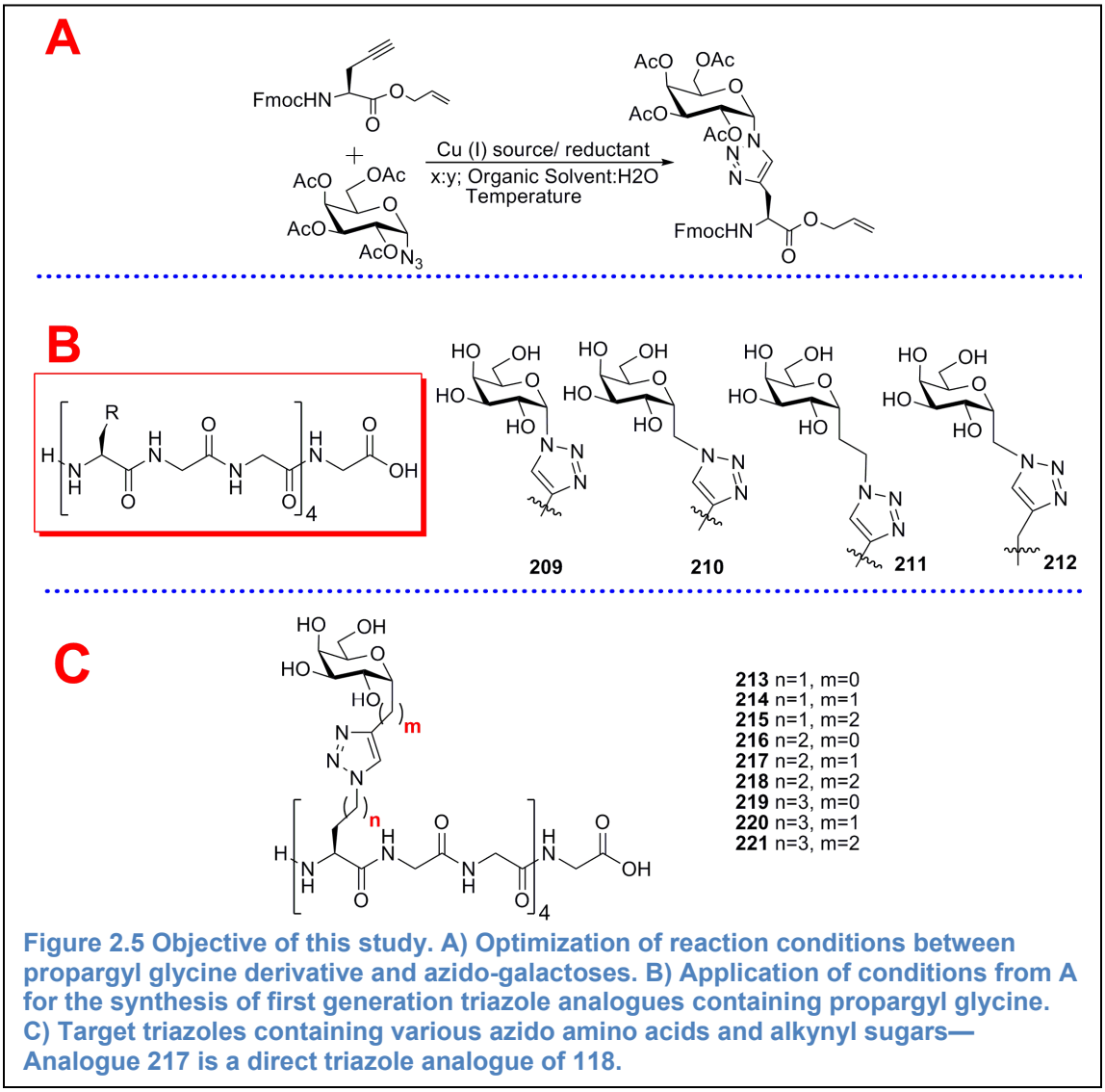



**Figure 2.5 Objective of this study. A) Optimization of reaction conditions between propargyl glycine derivative and azido-galactoses. B) Application of conditions from A for the synthesis of first generation triazole analogues containing propargyl glycine. C) Target triazoles containing various azido amino acids and alkynyl sugars—Analogue 217 is a direct triazole analogue of 118.**

The key advantage of the triazole analogue is that it can be accessed using the copper-catalyzed [3 + 2] Huisgen cycloaddition between an azide and an alkyne.[26, 27] This reaction, commonly referred to as the CuAAC (Copper-assisted Azide-Alkyne Cycloaddition) or (commonly, but incorrectly)[28] as the "Click" reaction, is a powerful and highly efficient method to link an alkyne and an azide together. Yields are greater than 98% for most simple, unhindered alkynes and azides.[29] However, yields and purities for solid-supported methodologies, even those involving a single ligation, let alone 2 or more simultaneously, have often been much more modest.[26, 30-34] Consequently, a

thorough systematic study will be carried out to examine the effects of solvent, temperature and catalyst source on a model system. The goal of this study is to determine optimal reaction conditions for the substrate that are amenable to solid-phase synthesis.

The power of this technique is that rather than synthesizing glycoconjugate building blocks for solid-phase synthesis, the peptides could be built first and glycosylated after the completion of SPPS. This is desirable as, compared to procedures involving only amino acids, SPPS involving more complicated glycoconjugate building-blocks generally result in lower yields and decreased purity of the cleaved products. This is mainly due to a decreased number of equivalents of reagents used in the synthesis. Although convergent syntheses have been used before by our group to approach the synthesis of *C*-linked AFGP analogues using traditional peptide coupling as the glycosidation strategy,[35] the approach was not deemed competitive with the more traditional linear glycoconjugate synthesis and was not re-visited. A CuAAC strategy however should allow for a simple post-synthetic glycosylation of the peptide.

This study therefore, is envisioned to be divided into three components: an investigation into the conditions optimal for the CuAAC reaction between the desired substrates (Figure 2.5 A), carried out in collaboration with Chantelle Capicciotti (an honours student at the time); a proof-of-concept stage with the production of simple triazole-containing *C*-linked AFGP analogues based on a (commercially available) propargyl glycine system (**209**-**212**, Figure 2.5 B); and a final, most important stage, where a systematic series of direct analogues of *C*-linked AFGP **118** would be

investigated to truly determine the IRI relevance of both the amide bond and the linker length between the carbohydrate and peptide components of AFGPs (**213**-**221**, Figure 2.5 C).

## 2.2 Understanding IRI activity in carbohydrates: towards small molecule IRI inhibitors

Despite the unmatched activity of glycopeptides, they are rather difficult to prepare and alternatives have recently been sought. Since the initial efforts from the Ben lab describing the IRI activity of various mono- and disaccharides outlined in the introduction,[36] attention has been directed towards the synthesis and preparation of various small molecule galactose analogues, including methoxy-galactose derivatives,[37] amino-substituted galactose derivatives,[38] and N-acetyl galactosamine containing disaccharides,[39, 40] to determine the importance and role of the various hydroxyl groups and their stereochemistry to the potency of ice recrystallization inhibition. These studies have demonstrated the importance of the galactose residue and that the substitution or capping of the non-reducing hydroxyl groups results in an attenuation of activity. Several families of key compounds have not however been previously examined. These include some particularly interesting disaccharides, various substituted anomeric phenyl derivatives, and carbasugar derivatives of galactose. The preparation and synthesis of these compounds will provide a better understanding of IRI activity in small molecules. Finally, there is the essential question regarding the minimum requirements for the antifreeze activity of analogue **118**. From previous efforts, it is clear that there is a direct correlation between both TH and IRI activity and number of tandem repeats of the

trimeric core, but questions remain as to the role that the individual components of the trimer and glycoconjugate building block play in the activity of the analogue as a whole: analogue **118** is approximately 50,000 times more active than galactose itself on a mole/mole basis. A better understanding of the role of the different domains of this analogue could lead to the design and preparation of small, simpler IRI active compounds, possibly even removing the need for a peptide backbone altogether.

### 2.2.1 *Objective 3*: Determination of the IRI activity of 1-1 and 1-3 galactosyl-galactose derivatives (Chapter 5)

A small family of disaccharides containing N-acetyl galactosamine (GalNHAc) or galactose residues as the reducing sugar have been recently prepared and analyzed for activity.[39, 40] However three analogues of specific interest have not been synthetically prepared for analysis. These analogues are the β-D-galactopyranosyl-(1→3)-D-galactopyranose (**222**), the all-galactose derivative of the T-antigen disaccharide found in AFGPs; and the all-galactose trehalose-like analogues α-D-galactopyranosyl-(1→1)-α-D-galactopyranose (**223**) and β-D-galactopyranosyl-(1→1)-α-D-galactopyranose (**224**) (Figure 2.6), sugars without a free reducing hydroxyl group. These trehalose analogues are interesting for two reasons. The first is that, in nature, trehalose plays an essential role in the cryopreservation of amphibians; these animals produce very large amounts of trehalose prior to freezing and are able to protect their cellular membranes from cryo-injury over the winter; consequently, trehalose has a

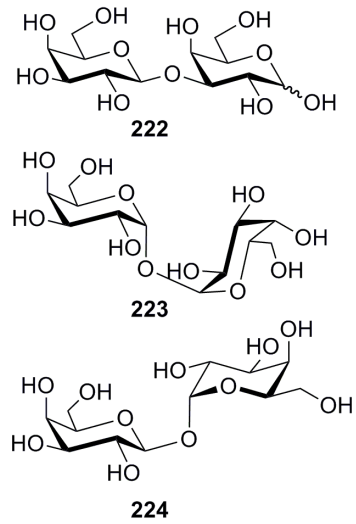
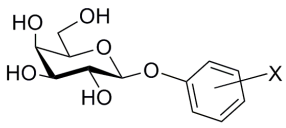



**Figure 2.6 Target disaccharides 222, 223, and 224.**

privileged role in nature as a cryopreservative.[41] On a more mechanistic basis, these galacto-trehaloses are of interest as studies by Chaytor and Ben have shown that the IRI activity of galactose is negatively impacted by methylation (and substitution in general) at the 2,3,4, and, to a lesser degree, the 6 position.[37] However, IRI activity is minimally disrupted by substitutions at the anomeric position; in fact, in many cases, IRI activity remains potent despite significant modifications to the anomeric position (described below). Hence creating a disaccharide with two galactose residues (the most active monosaccharide) through dimerization at the least sensitive position should provide an analogue with interesting and potent IRI activity.

### 2.2.2 *Objective 4*: Determination of the effect on IRI activity of electronic effects of anomeric aromatic substituted galactose derivatives (Chapter 6)




**X** = F, $NO_2$, OMe, OH, Me, H etc.

**Figure 2.7 Examples of substituted phenyl galactosides envisioned for this study.**

The Simons group postulates that an important factor in determining the hydration of monosaccharide residues is the nature of the intramolecular network of hydrogen bonds.[42, 43] Interestingly, many of their studies were carried out with phenyl blocking units at the anomeric position of the monosaccharides, and it appears that these groups do influence the directionality of the network. However, these gas-phase studies were carried out in vacuum with only one or two water molecules per sugar, conditions radically different from those found for a fully solvated carbohydrate; consequently, their relevance to an aqueous solution remains in doubt. However differential electronics on the aryl ring should radically change the electron density around the anomeric oxygen: increased in the presence of electron donating

substituents and decreased in the presence of electron poor phenyl derivatives. Modifying the electronics of the anomeric oxygen may influence the hydrogen bonding network (if it exists in aqueous solution) and may in turn affect the IRI activity of the molecule as a whole. To investigate this possibility a series of mono- (para substituted so as to maximize electronic influences on the anomeric oxygen but minimize steric considerations), di- (3,5-disubstituted) and tri- (3,4,5-trisubstituted) derivatives were designed (Figure 2.7). The synthesis and testing were then carried out in collaboration with undergraduate student, Malay Doshi.

### 2.2.3 *Objective 5*: Determination of the essential requirements for IRI activity in analogue 118 (Chapter 7)

With the results of the above studies in conjunction with previous research, considerable data regarding the IRI activity of various mono- and disaccharides and their simple derivatives is being obtained. Although galactose appears to be the most active sugar and compound yet tested, it is still orders of magnitude less active than AFGP-8 and *C*-linked analogue **118**.[36] Consequently, a molecule intermediate in complexity between a simple carbohydrate and a full glycopeptide is sought that could bridge the IRI activity gap between these two very different classes of compounds. As a starting point, a series of analogues outlined in Figure 2.8 are envisioned whereby one trimeric unit at a time, **118** would be pared back through the trimer (**227**) and dimer (**226**) to the monomer (**225**). The monomer would be further reduced to the simple zwitterionic glycoconjugate (**228)**. This in turn would be reduced to the mono-functional amine, **229**, or carboxylic acid, **230** (both functionalities would be charged at both physiological and IRI assay pH). Further truncation, one carbon at a time, would lead

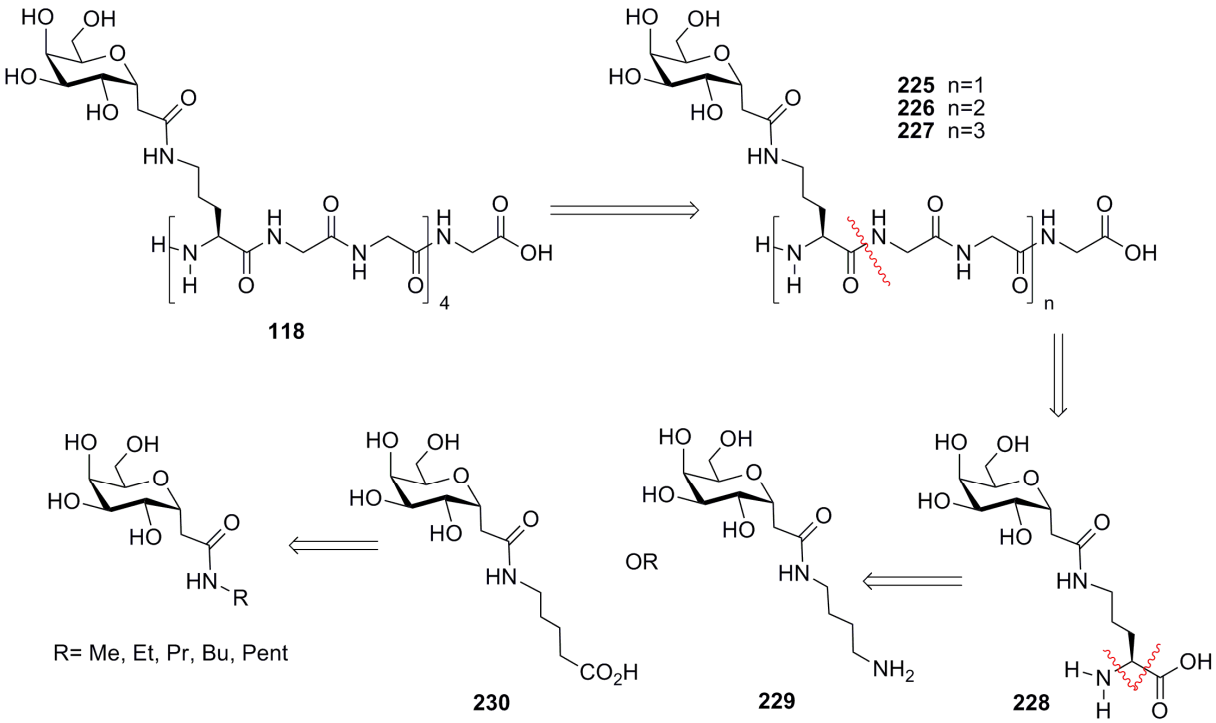



**Figure 2.8 Initial conceptual plan for the truncation of 118 to determine the features responsible for its IRI activity.**

eventually to the 1º amide, isosteric with the previously examined carboxylic acid.[37] This initial scan would possibly give insights as to which further structural modifications could be made to produce analogues with improved IRI activity, hopefully bridging the activity gap, while retaining a simple carbohydrate based structure. The initial stages of this research were carried out in collaboration with Robyn Biggs (an honours student at the time).

### 2.2.4 Objective 6: Synthesis and IRI analysis of carbasugar analogues of 118 and galactose (Chapter 8)

The final objective of this thesis is the preparation of carbasugar analogues of galactose for IRI testing. Carbasugars, or cylclitols, are produced in nature as glycosidase inhibitors as the lack of an endocyclic oxygen removes the labile acetal linkage at the anomeric position. They are not true carbohydrates, as they lack the

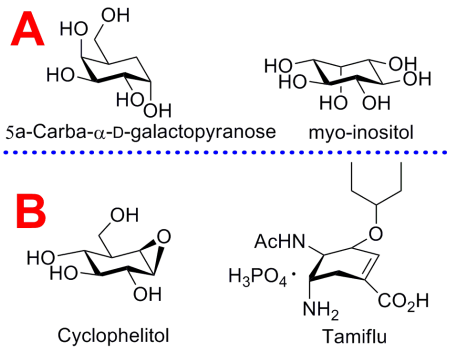



**Figure 2.9 A) A carbasugar compared to the true carbocyclic carbohydrate inositol; B) two important cyclitol derivatives: cyclophelitol and tamiflu.**

appropriate stoichiometry of $C_n(H_2O)_n$ to be "hydrates of carbon," and as such are functionally different from inositols which are true carbohydrates (Figure 2.9 A). However, unlike inositols, carbasugars more closely resemble the pyranose and furanose forms of natural monosaccharides as they contain the *C*-6 methanol moiety. Consequently, although many enzymes, especially glycosidases, recognize these compounds, they cannot degrade them and these enzymes are even often irreversibly inhibited by various "suicide" mechanisms such as epoxides (cyclophelitol) or reversibly inhibited and occupied by transition-state mimics of oxocarbenium ions (such as Tamiflu, Figure 2.9 B).[44] Because of this excellent mimicry of carbohydrates, cyclitols are of considerable interest in the community and their synthesis and applications have been extensively reviewed.[44-47]

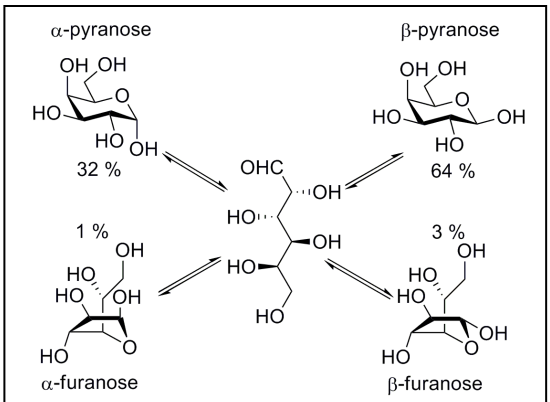



**Figure 2.10 The mutarotation of galactose through the four most populated isomers and their relative abundance.**

In relation to hydration, and thus IRI activity, the actual importance of the ring-oxygen is unexplored, although previous efforts from the Ben lab, and those of other researchers, indicate that the anomeric stereochemistry does play a role in determining IRI activity. The natural sugars are, of course, free to undergo mutarotation and exist, in four different forms (Figure 2.10). The carbasugar analogues, however, allow access to

anomerically pure α and β analogues of the natural sugars with the minimum of structural changes as only the endocyclic oxygen is removed. Furthermore, the literature on carbasugars demonstrates that the endocyclic oxygen plays little role in biological recognition (implying a limited relevance to intramolecular interactions) and the carbasugars adopt nearly identical conformations, to the native monosaccharides, in solution.[45, 48] Likewise, to the best of the author's knowledge, no study has investigated the hydration of carbasugars (there is not even MD simulation evidence for the impact the methylene for endocyclic oxygen substitution will have on the hydration of the sugar as a whole). However, its removal may cause a large change in hydration and possible decrease in activity. However the directionality of this change, if any, is impossible to predict. Consequently these compounds are of considerable interest as conformationally and chemically stable analogues of galactose.

The primary goal of this project is to synthesize a *C*-linked AFGP analogue incorporating a carbasugar moiety, **231**, and a secondary goal is to produce carbasugar analogues of galactose (**232** and **233**) and glucose (**234**) for testing and analysis and comparison with the previously examined carbohydrates (Figure 2.11).

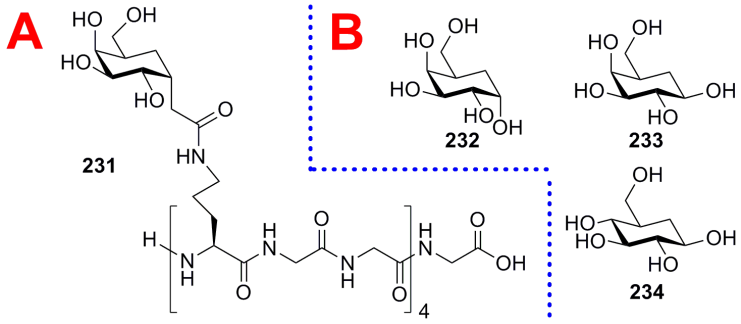



**Figure 2.11 A) Carbasugar glycopeptide target and the secondary B) carbasugar monosaccharide targets.**

## 2.3 Summary of research objectives

The objectives can be divided into two families and then individual sub-objectives:

i) Design and synthesis of a family of β-amino acid containing compounds to determine the importance of backbone structure to IRI activity.

ii) Design both reaction conditions and substrates and preparation of triazole-linked-*C*-AFGP analogues to determine the importance of the linker functionalities to IRI activity.

iii) Design, synthesis and IRI testing of three disaccharides to investigate the correlation between substitution regiochemistry and IRI activity of dimeric galactose derivatives.

iv) Synthesis of variously functionalized β-aryl-anomeric substituted galactosides to determine the effect of electron density at the anomeric oxygen on the IRI activity of galactose derivatives.

v) Systematic truncation of IRI active *C*-linked AFGP analogue **118** to determine the key structural features required for IRI activity and to investigate the possibility of small molecule inhibitors of ice recrystallization.

vi) Design, synthesis and preparation of carbasugar derivatives of **118** and galactose to determine the role of the endocyclic oxygen to IRI activity.

## References

1. Gibson, M. I., *Polym. Chem.* **2010,** *1* (8), 1141-1152.

2. Liu, S. Novel *C*-linked antifreeze glycoprotein analogues as potent recrystallization inhibitors: preparation, assessment and *in vitro* studies. PhD. Thesis. University of Ottawa, Ottawa, 2006.

3. Tam, R. Y.; Rowley, C. N.; Petrov, I.; Zhang, T.; Afagh, N. A.; Woo, T. K.; Ben, R. N., *J. Am. Chem. Soc.* **2009,** *131* (43), 15745-15753.

4. Liu, S.; Ben, R. N., *Org. Lett.* **2005,** *7* (12), 2385-2388.

5. Daley, M. E.; Spyracopoulos, L.; Jia, Z.; Davies, P. L.; Sykes, B. D., *Biochemistry* **2002,** *41* (17), 5515-5525.

6. Horne, W. S.; Gellman, S. H., *Acc. Chem. Res.* **2008,** *41* (10), 1399-1408.

7. Steer, D. L.; Lew, R. A.; Perlmutter, P.; Smith, A. I.; Aguilar, M.-I., *Curr. Med. Chem.* **2002,** *9* (8), 811.

8. Hanson, H. T.; Smith, E. L., *J. Biol. Chem.* **1948,** *175* (2), 833-848.

9. Cheng, R. P.; Gellman, S. H.; DeGrado, W. F., *Chem. Rev.* **2001,** *101* (10), 3219-3232.

10. DeGrado, W. F.; Schneider, J. P.; Hamuro, Y., *J. Pept. Res.* **1999,** *54* (3), 206-217.

11. Gademann, K.; Hintermann, T.; Schreiber, J. V., *Curr. Med. Chem.* **1999,** *6* (10), 905-925.

12. Gellman, S. H., *Acc. Chem. Res.* **1998,** *31* (4), 173-180.

13. Gellman, S. H., *sp2.* **2002,** *1* (5), 30-31.

14. Gelman, M. A.; Gellman, S. H. In *Using constrained β-amino acid residues to control β-peptide shape and function*, John Wiley & Sons, Inc.: 2005; pp 527-591.

15. Koert, U., *Angew. Chem., Int. Ed.* **1997,** *36* (17), 1836-1837.

16. Kritzer, J. A.; Stephens, O. M.; Guarracino, D. A.; Reznik, S. K.; Schepartz, A., *Bioorg. Med. Chem.* **2004,** *13* (1), 11-16.

17. Martinek, T. A.; Fueloep, F., *Eur. J. Biochem.* **2003,** *270* (18), 3657-3666.

18. Seebach, D.; Matthews, J. L., *Chem. Commun.* **1997,** (21), 2015-2022.

19. Wu, Y.-D.; Han, W.; Wang, D.-P.; Gao, Y.; Zhao, Y.-L., *Acc. Chem. Res.* **2008,** *41* (10), 1418-1427.

20. North, M., *J. Pept. Sci.* **2000,** *6* (7), 301-313.

21. Thapa, I. *C*-Linked AFGP analogues containing beta-amino acids: preparation, assessment and *in vitro* studies. MSc. Thesis. University of Ottawa, Ottawa, 2006.

22. Corzana, F.; Busto, J. H.; Jiménez-Osés, G.; García de Luis, M.; Asensio, J. L.; Jiménez-Barbero, J.; Peregrina, J. M.; Avenoza, A., *J. Am. Chem. Soc.* **2007,** *129* (30), 9458-9467.

23. Mimura, Y.; Yamamoto, Y.; Inoue, Y.; Chûjô, R., *Int. J. Biol. Macromol.* **1992,** *14* (5), 242-248.

24. Rana, T. Synthesis of a *C*-linked antifreeze glycoprotein building block containing an internal olefin. MSc. Thesis. University of Ottawa, Ottawa, 2009.
25. Brik, A.; Alexandratos, J.; Lin, Y. C.; Elder, J. H.; Olson, A. J.; Wlodawer, A.; Goodsell, D. S.; Wong, C. H., *ChemBioChem* **2005,** *6*, 1167-1169.
26. Tornöe, C. W.; Christensen, C.; Meldal, M., *J. Org. Chem.* **2002,** *67* (9), 3057-3064.
27. Rostovtsev, V. V.; Green, L. G.; Fokin, V. V.; Sharpless, K. B., *Angew. Chem. Intl. Ed.* **2002,** *41*, 2596-2599.
28. Sharpless, K. B.; Finn, M. G.; Kolb, H. C., *Angew. Chem. Intl. Ed.* **2001,** *40*, 2004-2021.
29. Bock, V. D.; Hiemstra, H.; van Maarseveen, J. H., *Eur. J. Org. Chem.* **2006,** *6*, 51-68.
30. Bera, S.; Zhanel, G. G.; Schweizer, F., *Bioorg. Med. Chem. Lett.* **2010,** *20* (10), 3031-3035.
31. Ingale, S.; Dawson, P. E., *Org. Lett.* **2011,** *13*, 2822-2825.
32. Jølck, R. I.; Berg, R. H.; Andresen, T. L., *Bioconjugate Chem.* **2010,** *21*, 807-810.
33. Kutterer, K. K.; Barnes, M. L.; Arya, P., *J. Comb. Chem.* **1999,** *1*, 28-31.
34. Pourceau, G.; Meyer, A.; Vasseur, J.-J.; Morvan, F., *J. Org. Chem.* **2009,** *74*, 1218-1222.
35. Eniade, A.; Ben, R. N., *Biomacromol.* **2001,** *2*, 557-561.
36. Tam, R. Y.; Ferreira, S. S.; Czechura, P.; Chaytor, J. L.; Ben, R. N., *J. Am. Chem. Soc.* **2008,** *130* (51), 17494-17501.
37. Chaytor, J. L. Examining the role of carbohydrate hydration and structure in preventing ice-recrystallization. PhD. Thesis. University of Ottawa, Ottawa, 2010.
38. Tokarew, J. Investigating the relationship between structure, ice recrystallization inhibition activit and cryopreservation ability of various galactopyranose derivatives. MSc. Thesis. University of Ottawa, Ottawa, 2011.
39. Ferreira, S. S. Improving the rational design of antifreeze glycoproteins through identification of the parameters that influence ice recrystallization inhibition. MSc. Thesis. University of Ottawa, Ottawa, 2009.
40. Balcerzak, A.; Ben, Robert N., Unpublished Results. 2011.

41. Crowe, J. H.; Crowe, L. M.; Chapman, D., *Science* **1984,** *223* (4637), 701-703.

42. Simons, J. P.; Jockusch, R. A.; Carcabal, P.; Huenig, I.; Kroemer, R. T.; Macleod, N. A.; Snoek, L. C., *Int. Rev. Phys. Chem.* **2005,** *24* (3-4), 489-531.

43. Carcabal, P.; Jockusch, R. A.; Huenig, I.; Snoek, L. C.; Kroemer, R. T.; Davis, B. G.; Gamblin, D. P.; Compagnon, I.; Oomens, J.; Simons, J. P., *J. Am. Chem. Soc.* **2005,** *127* (32), 11414-11425.

44. Kobayashi, Y., Carbasugars: Synthesis and functions. In *Glycoscience*, Fraser-Reid, B. O.; Tatsuta, K.; Thiem, J., Eds. Springer-Verlag: Berlin and Heidelberg, 2008; Vol. 3, pp 1913-1997.

45. Arjona, O.; Gómez, A. M.; López, J. C.; Plumet, J., *Chem. Rev.* **2007,** *107*, 1919-2036.

46. Wardrop, D. J.; Waidyarachchi, S. L., *Nat. Prod. Rep.* **2010,** *27*, 1431-1468.

47. Duchek, J.; Adams, D. R.; Hudlicky, T., *Chem. Rev.* **2011,** *111*, ASAP.

48. Bock, K.; Fernandez Bolanos Guzman, J.; Ogawa, S., *Carb. Res.* **1988,** *174*, 354-359.

# Chapter 3 : Determination of the effect of β-amino acid peptides on IRI activity in *C*-AFGPs.

The first goal of this thesis is to explore the importance of the peptide backbone to antifreeze activity. Besides previous efforts from the Ben lab that have examined the substitution of proline for alanine or glycine, very little research has been carried out regarding the possibilities of structural change to the backbone of the peptide to influence the IRI activity of the construct as a whole.

## 3.1 Effect of backbone modification on IRI activity

One of the first SAR studies carried out by the Ben group was an investigation into the ideal peptide backbone to elicit IRI activity. The native system and most of the analogues previously prepared by other research groups included alanine in the backbone in place of the glycines used by the Ben lab. The original reason for the choice of glycine was to minimize the risk of racemization during synthesis. However, the relative activity of alanine versus glycine

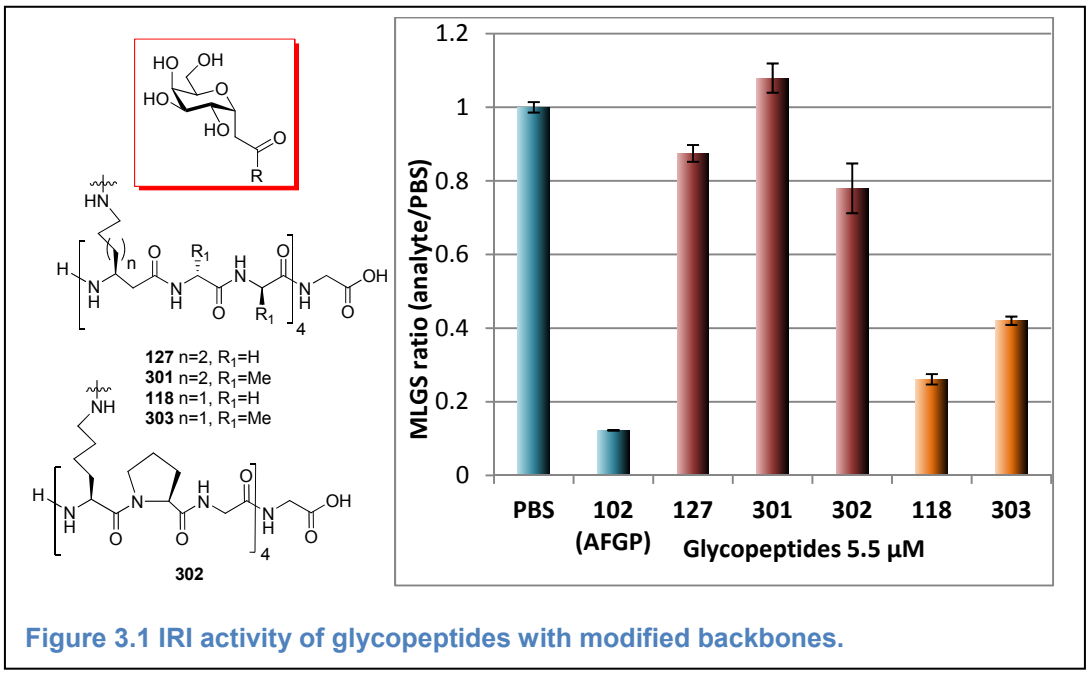



**Figure 3.1 IRI activity of glycopeptides with modified backbones.**

needed to be addressed and as such, ornithine (Figure 3.1, orange) and lysine (Figure 3.1, red) analogues were prepared containing polypeptide backbones with alanines and even prolines, as in the Northern Cod AFGP-8, to determine their impact on the IRI activity (Figure 3.1). Surprisingly, replacing the glycines of **127** with alanines, as in the native system resulted in a decrease in antifreeze activity, **301**.[3] Likewise, in an attempt to improve rigidity and to provide a direct analogue to some of the systems found in nature, lysine residues in the backbone were replaced with proline in analogue **302**. However, this did not result in any improvement in IRI activity.[5] Replacing the lysine residue with ornithine resulted in a considerable improvement in activity with either glycine (**118**) or alanine-derived (**303**) backbones.[5, 6] However, the glycine peptide outperforms alanine in this system as well. From this limited set of results, the sum total of the peptide modifications made in the *C*-linked series, a few tentative conclusions can be reached. Modification of the glycine backbone is not tolerated by these analogues as substitution with either alanine or proline resulted in a decrease in antifreeze activity. Whether this is due to induced rigidity or some other effect could not be determined with the available data. However, there are alternatives to the use of native amino acids in glycopeptides.

## 3.2 Introduction to peptidomimetics as applied to AFGPs

In addition to the “natural” peptides described above, some research from the Ben laboratory has been directed towards the application of peptidomimetics to this problem. Results from these studies demonstrated that incorporating Freidinger lactams (**304**)[7] or glycosylated succinamide-derived polymers (**305**)[8] as the backbone structure failed to provide significant antifreeze activity at 5.5 μM (Figure 3.2). The former

compound was prepared through traditional SPPS from the glycoconjugate and appropriate amino acids, and the latter compound was prepared through the application of ROMP to alkene **306** using the 1st generation Grubbs catalyst. Other attempts to integrate non-peptide structures based on poly(methacrolyl) or poly(ethylmethacrylate) scaffolds by the Gibson group showed only very moderate IRI activity at relatively high concentrations as described above (1.6.4).[9] One of the few other examples of peptidomimetics applied to IRI activity are the peptoid analogues prepared by the Sewald group, but these compounds have not shown significant IRI activity (see Chapter 4 below). They contain a triazole in the linker between the carbohydrate and the backbone and hence the lack of activity may be due to the introduction of this triazole linkage rather than the peptoid itself.[10] Finally, several small cyclic glycopeptides based on AFGP-8 have been prepared by the Nishimura group. These compounds, despite the drastic conformational change induced by cyclization rather than a linear structure, were nonetheless capable of inducing dynamic ice shaping and considerable thermal hysteresis.[11]

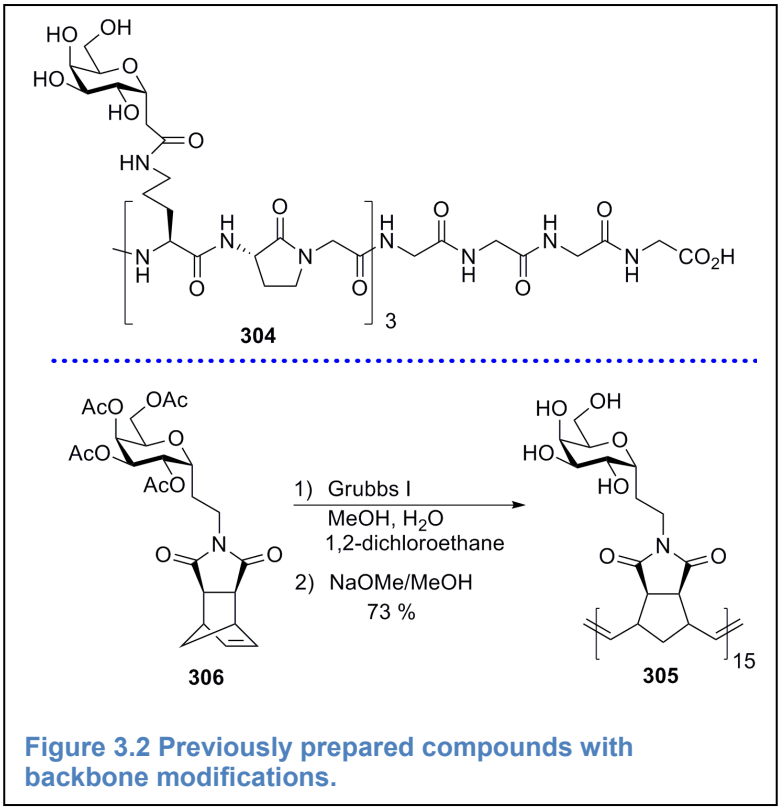



**Figure 3.2 Previously prepared compounds with backbone modifications.**

However, except for the last example above, all compounds appear to have been prepared mainly in order to take advantage of powerful oligomerization or ligation chemistries (ROMP in the case of the succinamide chemistry, classical polymerization in the case of the Gibson analogues), or to demonstrate the power of new chemical techniques (CuAAC chemistry in the case of the Sewald group),[10] rather than to act as systematically modified analogues of previous compounds, to determine the structural foundations of the IRI phenomenon. Perhaps it is then unsurprising that these compounds fail to exhibit IRI activity. The data arising from the cyclic glycopeptides of Hichisu on the other hand seems to indicate that the lively debate as to the natural solution-phase conformation of the linear natural AFGP may be irrelevant: even when in a cyclic form (certainly different from any conformation that the linear glycopeptide can adopt), the trimeric repeat is able to generate ice-shaping and recrystallization inhibition effects. Thus the overall conformation of AFGP may play little role in the interaction between the peptide and the ice, rather the important conformation may be defined in terms of the position and orientation of the peptide backbone relative to the sugar. This interaction may possibly be mediated through a hydrogen bond or water bridge involving the amide bond on the backbone. The ability to affect IRI activity through modifications to the carbohydrate has been shown by the Ben group in a recent publication.[6] Likewise IRI activity has been shown to be sensitive to modifications of the linker as further described below in Chapter 4,[12, 13] or even to modification of the backbone itself through the careful design of peptidomimetics to relocate the amide bond on the backbone. A peptoid derivative that has eliminated the hydrogen bond-donating ability of the amide of ornithine derivative (**118**) may be of interest, but the

ideal structural candidates for this investigation are mixed glycopeptides containing both α and β amino acids. Unlike the peptoids, these compounds would be expected to retain the hydrogen bond-capability of the native system, and likewise would avoid introducing the complicating factor of having the sidechains on the nitrogen atom (as in a peptoid) as opposed to the α-carbon (mixed peptide) (Figure 3.3). Consequently any deviations in IRI activity would be due to the introduction of the additional methylene β-residue rather than the removal of the amide bond. Therefore, if the analogues with a single β-residue substitution differ markedly in activity from the native system, it would strongly suggest that the change was due to the interruption of the carbohydrate-peptide interaction rather than due to some other effect. To further consider this possibility, it is important to have a familiarity with the secondary structures of β and mixed peptides.

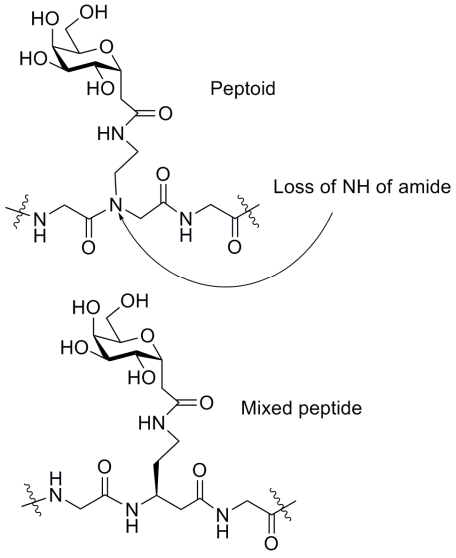



**Figure 3.3 Comparison between peptoid and mixed peptide as peptidomimetics.**

## 3.2.1 Conformations and secondary structures of β-peptides and mixed α/β peptides

Unlike (mono-substituted) α-amino acids that can be simply L or D, β-amino acids can fall into five enantiomeric pairs (one of which is degenerative, Figure 3.5). The simplest is the achiral unsubstituted homoglycine (β-*h*Gly), the polymer of which adopts a 12-helix in solution (Figure 3.4). The next level of complexity comprises the mono-substituted residues. The $\beta^2$-amino acid, mono-substituted adjacent to the carboxylic

acid, is a reasonably difficult residue to access and as such is considerably less studied than the $\beta^3$-amino acids which are readily accessible through the homologation of their

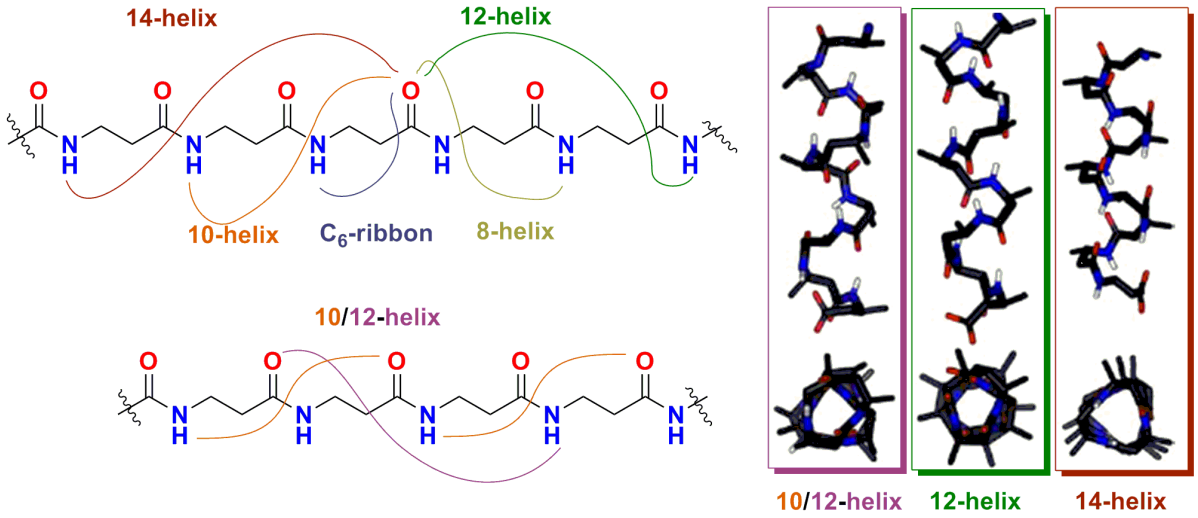



**Figure 3.4 Possible backbone hydrogen-bond interactions and the resulting secondary structures formed in β peptides. Models are provided to show the relative orientation of side-chains in the three most common helices. Interactions adapted from Wu,[2] and models reproduced from Kritzer.[4]**

α-amino acid counterparts. Polymers of both $\beta^2$ and $\beta^3$-residues tend to adopt the stable 14-helix; however, incorporating a considerable number of β-homoglycines tends to change the conformation into a 10/12 helix, a complicated di-helix where both ($i$+ *1* and $i$+ 2) interactions exist. β-amino acids can also be substituted at both the 2 and the 3 positions simultaneously. Polymers of $\beta^{2,3}$ amino acids tend to generally form 10/12 helices, and although specific constrained substituents can favour the 10- or 8-helix as well as the $C_6$ ribbon, these three conformations are rare enough to be unimportant for the present

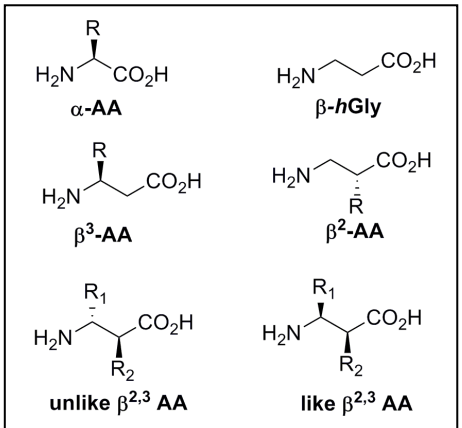



**Figure 3.5 General structure of α amino acids and the five types of mono-substituted (per carbon) β amino acids.**

purposes.

This predictable, but wide variety of available conformations is based mainly on the regiochemistry of substitution rather than (for the most part)[14] identity of the side-chain functionalities and is a definite benefit for designing “foldamers” with β- rather than α-amino acids.[4, 15, 16]

## 3.2 Variation in side chain, peptide backbone, and the introduction of a β-amino acid: precedence for the investigation of β-peptides

Thus, the incorporation of multiple β-amino acid residues can lead to a change in

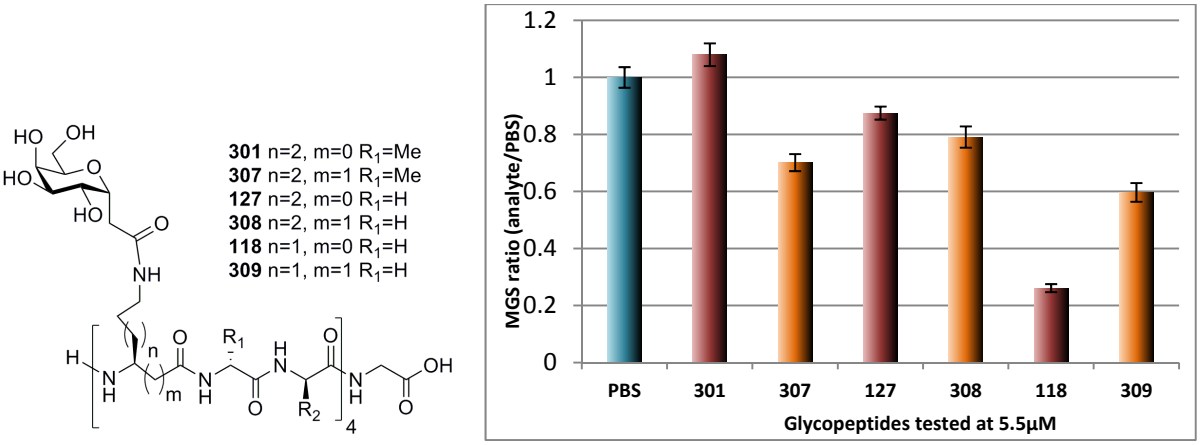



**Figure 3.6 IRI activity of previously prepared β-amino acid-containing peptides compared with their α-analogues.**

conformation of the peptide. An initial investigation into the use of β-amino acids in IRI active glycopeptides was carried out by Indira Thapa in her master’s thesis.[1] As described above in the introduction, the results of this study were rather contradictory. Three analogues containing β residues were prepared (Figure 3.6, orange). The first with β-lysines integrated into an alanine backbone (**307**), the second with the same residue inserted into a glycine backbone (**308**) and the third containing a β-ornithine

residue in a glycine backbone (**309**). These three analogues were then compared to their respective α-amino acid counterparts previously prepared by Eniade and Murphy (**301**, **127**, **118**, Figure 3.6, red).[17, 6] As can be seen, the incorporation of the β-lysine residue was very beneficial for alanine-based glycopeptide **301**, and also for glycine-containing **127** as both **307** and **308** exhibit improvement in activity compared to the α-amino acid glycopeptides. However, in the case of the ornithine analogue **118**, this improvement in activity was not observed. Rather, **309** is significantly less active than its α-containing compound. Although **301**, **127** and **118** all have very different IRI activities, all three β-amino acid containing compounds, (**307**-**309**) share similar levels of ice recrystallization inhibition.

The reason for the disparity in the behaviour between the two sets of analogues, lysine and ornithine, was not further explored at the time, but two hypotheses can be proposed. In the first, the introduction of the β-amino acid residue initiates a change in solution-conformation of the ornithine glycopeptide such that it is less able to interact with the QLL or the ice surface. In the case of the lysine analogue, on the other hand, any supposed conformational change is beneficial to IRI activity. The second possibility invokes the importance of an intramolecular interaction, either through a water bridge or the formation of a hydrophobic pocket between the backbone and the carbohydrate and is very sensitive to structural considerations. The unique spatial relationships available to **118** have been proposed to be responsible for the potent activity of this analogue.[18] Such a relationship would, presumably not exist for either **127** or **301**, consequently the lysine analogues would not be expected to respond in the same way to this substitution.

If the interaction between the carbohydrate and peptide in **118** exists and can be disrupted, possibly through simply shifting the position of the amide bond on the backbone (by introducing a β-residue) then one would expect activity to be affected only in cases where the introduction of a β-amino acid residue interferes with a water-bridge, hydrophobic pocket or other intramolecular interaction; however, at this point it is impossible to determine which of these relationships is active. However, if a change in the conformation of the glycopeptide due to the number of β-residues is responsible for deviation in IRI activity, then activity should only vary as a result of the degree of substitution. To investigate these two possibilities, a series of analogues was envisioned as described above in Chapter 2 (**200**-**206**, Figure 3.7). Compound **200** was re-synthesized for the current study as the initial compound was no longer available and the author was unconvinced of the purity of the previously prepared sample. Hyperactive analogue **118** was not re-prepared for the current study, and the original data point provided by A. Murphy outlined in the introduction was used for comparison purposes.

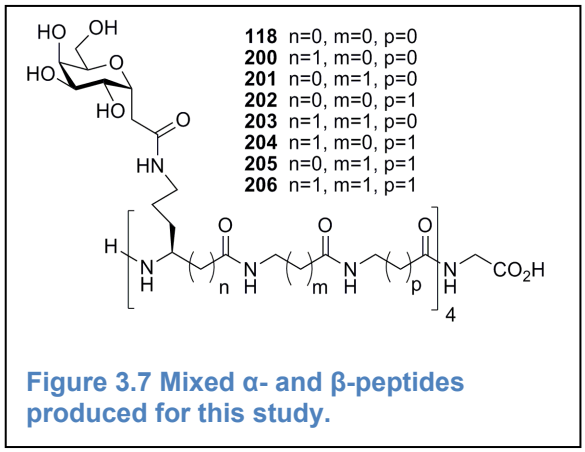


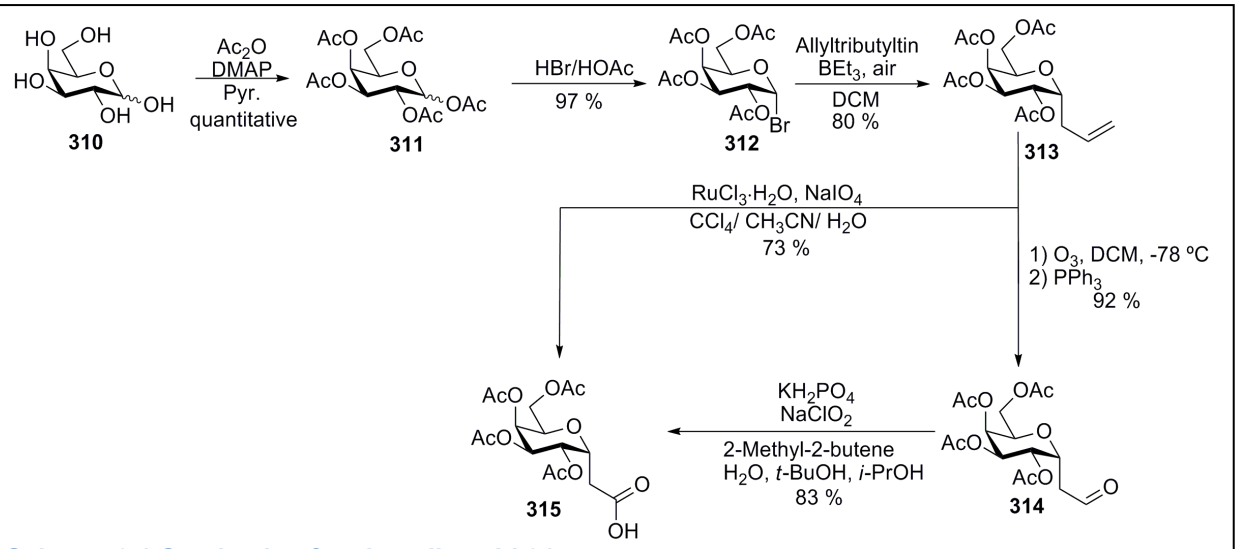

**Figure 3.7 Mixed α- and β-peptides produced for this study.**

The methodology previously used for the preparation of **200** was considered lengthy, and consequently a new strategy was applied to the synthesis of the β-amino acid and its related glycoconjugate required for the synthesis of the glycopeptide.

## 3.3 Synthesis of mixed α and β glycopeptides

### 3.3.1 Synthesis of the α-glycoconjugate

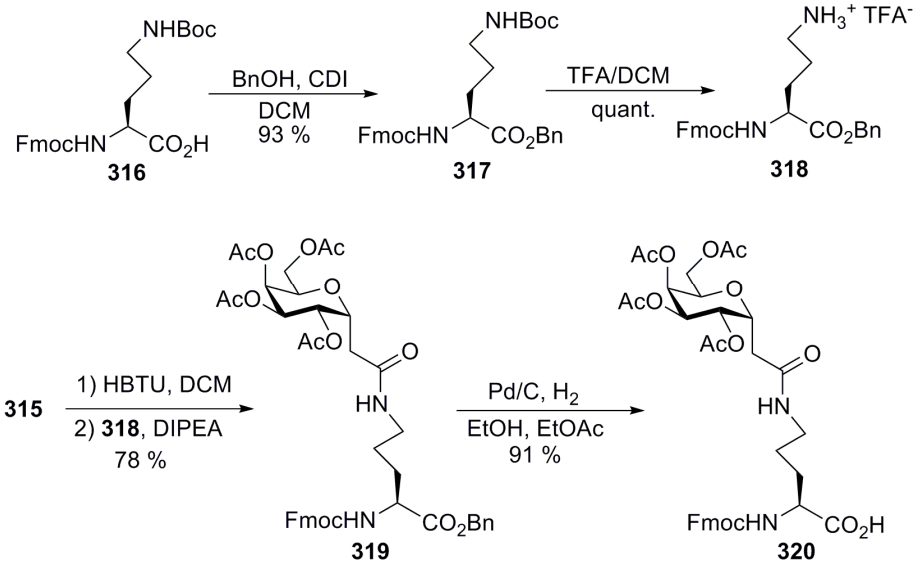
The α glycoconjugate was prepared in a manner similar to that previously described in syntheses from the Ben laboratory (Scheme 3.1).[6] D-Galactose, **310**, was




**Scheme 3.1 Synthesis of carboxylic acid 315.**

acetylated in the usual fashion to provide the mixture of anomers **311** in quantitative yield. Either this mixture, or commercially available β-D-galactose pentacetate (depending on availability), was treated with 33 % HBr in acetic acid to provide, following precipitation, α-bromide **312** in excellent near-quantitative yields. Over the course of the research, several different strategies were used to carry out the *C*-allylation to generate **313**, including photo-mediated radical chemistry using *bis*(tributyltin) in the presence of light as radical initiator and allylphenylsulfone as the allyl source,[19] and ionic allylation using allyltrimethylsilane as nucleophile and boron trifluoride as the Lewis acid activator of an anomeric acetate group.[20] Both strategies had serious weaknesses. The first involves a very complicated set-up and the reaction was not amenable to scale-up. Furthermore, the yields, even in identical reactions set up in parallel, tend to vary markedly and the reagents for this reaction, especially the

allylphenylsulfone, are quite expensive. The second strategy was far simpler involving more easily obtained reagents, but unfortunately it always produced a mixture of anomers that required a purification sequence including acetate removal followed by re-crystallization of the desired anomer, and the reprotection of this compound to obtain the desired product. This lengthy sequence, although very functional, could be improved by a shorter route. Consequently, the conditions identified in Scheme 3.1, recently developed by M. Leclère, were applied and could consistently provide **313** in high yield and, when the addition of air was slowed, often without the need to resort to chromatography as all starting material is consumed.[21-24] The allyl sugar **313** could then be converted to carboxylic acid **315** in one of two manners. The method originally used in the Ben lab involved a two stage process whereby the olefin was oxidatively cleaved to aldehyde **314** under standard conditions in good yields. This aldehyde could then be derivatized to a number of useful compounds, but simply using a classic Pinnick-Lindgren oxidation to elaborate the molecule to the desired oxidation state generally provide **315** in good yields (83 %).[6, 25, 26] The second method involves the direct oxidation of the allyl



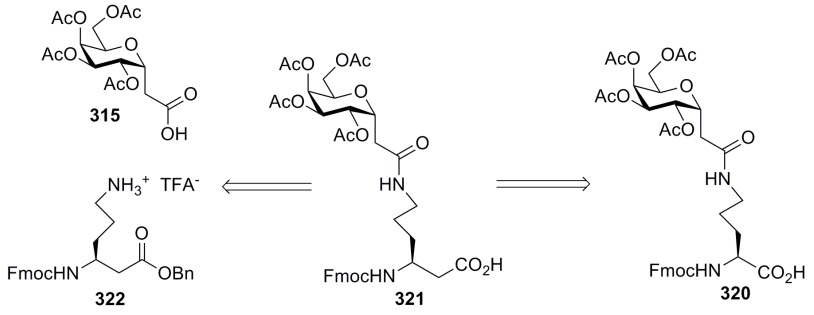

**Scheme 3.2 Synthesis of amino acid 318 and the preparation of glycoconjugate 320.**

group using ruthenium (III) catalysis and periodate as the oxidant.[6] This approach generally functions well in providing **315** in acceptable yields (73 %). Over the course of this work, this compound was prepared multiple times in both manners.

The required amino acid component is readily accessible from commercially available protected ornithine derivative **316** (Scheme 3.2). Esterification was accomplished using CDI as activator to provide benzyl ester **317** in the manner previously described.[6, 12] The δ amino group was selectively deprotected using standard conditions to obtain the TFA salt, **318**, in quantitative yield.[27] Then, using conditions previously applied by both P. Czechura and A. Murphy, carboxylic acid **315** was coupled with free amine **318** in the presence of HBTU and excess DIPEA to provide protected glycoconjugate **319** in 78 % yield. Finally, the carboxyl terminus was unmasked to provide **320**, the building block required for solid phase peptide synthesis in 91 % yield. This sequence provides the α building block previously prepared and required for analogues **201**, **202** and **205;** furthermore, it also acts as the starting point for the original synthesis of the β analogue.

## 3.3.2 Synthesis of the β-glycoconjugate

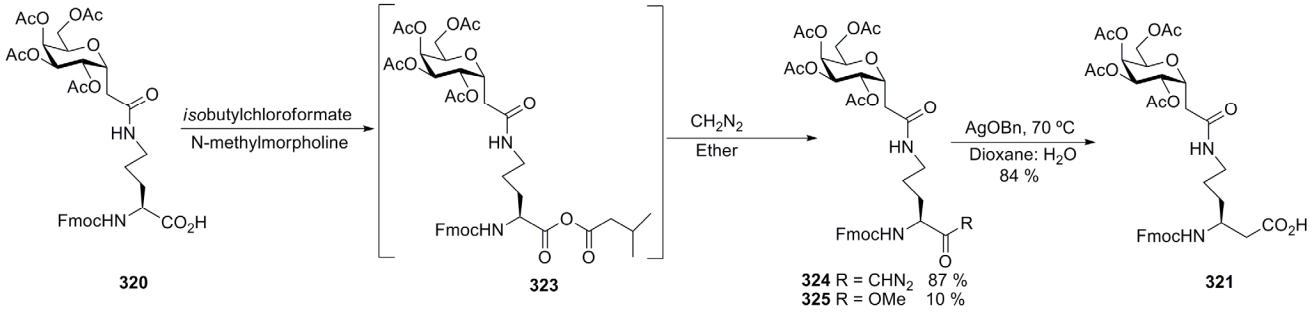
There are two simple strategies to obtain the β analogue **321**, both relying on the Arndt-Eistert homologation (Scheme 3.3).[28, 29] In the first approach (right), the homologation can be carried out after glycoconjugate **320** is




**Scheme 3.3 Retrosynthetic options for the synthesis of 320.**

synthesized to provide **321**. In the second approach, the homologation would be carried out prior to coupling, so as to minimize the number of transformations required on the united glycoconjugate. Thus, residue **322** would be coupled to **315** to provide **321** directly (following appropriate deprotection). The first route was the one followed by Mrs. Thapa in her research,[1] and was used for the initial production of **321** in this current study. The second route was eventually chosen for the current synthesis as it simplifies the approach.

The first approach, post-coupling homologation, is described in Scheme 3.4.



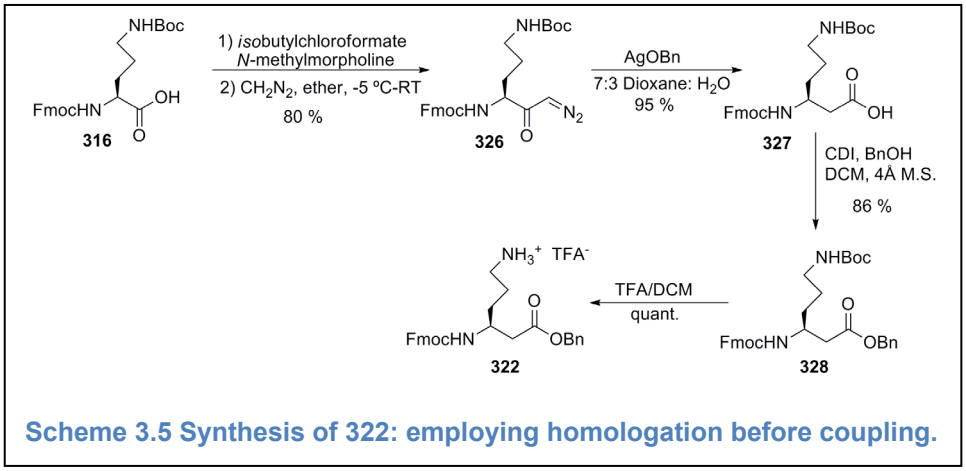

**Scheme 3.4 Synthesis of 321 through Arndt-Eistert homologation of the glycoconjugate.**

Building block **320** must be converted to an activated species; in this case the mixed anhydride formed by *iso*-butylchloroformate was selected (**323**). Without isolation this reactive compound is immediately treated with freshly prepared diazomethane. The desired reaction takes place smoothly to generate diazo compound **324** in 87 % yield, which can be isolated on silica gel and stored indefinitely without decomposition with no special precautions. Unfortunately, due to the techniques used in the preparation of the diazomethane, trace hydroxide may be present and either base-catalyzed hydrolysis of mixed anhydride **3283** or unreacted carboxylic acid **320** reacts under these conditions to provide the methyl ester as minor product **325** in approximately 10 % yield; this value

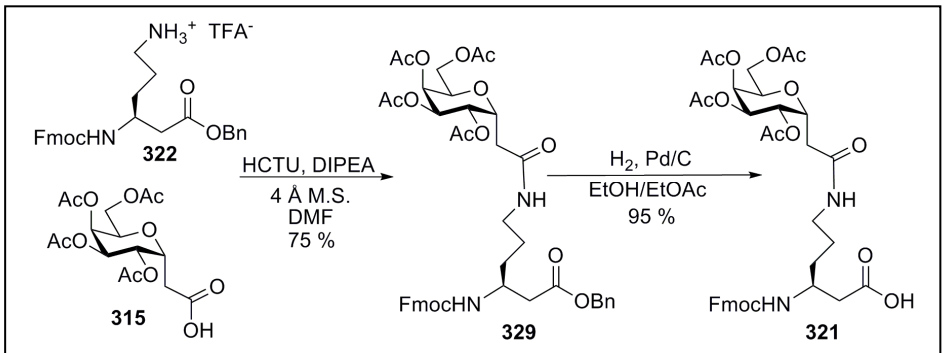
varied trial by trial, although the factors responsible for the variation were not ascertained.

The synthesis of **321** was completed through the Wolff rearrangement, where silver benzoate was added to accelerate the reaction, using a mixture of water and dioxane as solvent. These conditions cleanly provided **321** in 84 % yield from **324** or 73 % overall yield from α-homologue **320**.

This sequence worked well, but recoveries and yields may be limited by the complexity of the glycoconjugate. It was felt that the homologation sequence might proceed more smoothly if it were carried out on the amino acid component alone as described in Scheme 3.6. Once again, commercially available **316** acts as the feedstock, and is converted to diazo derivative **326** in 80 % yield over the two steps. This is comparable to the conversions observed for the glycoconjugate




**Scheme 3.5 Synthesis of 322: employing homologation before coupling.**



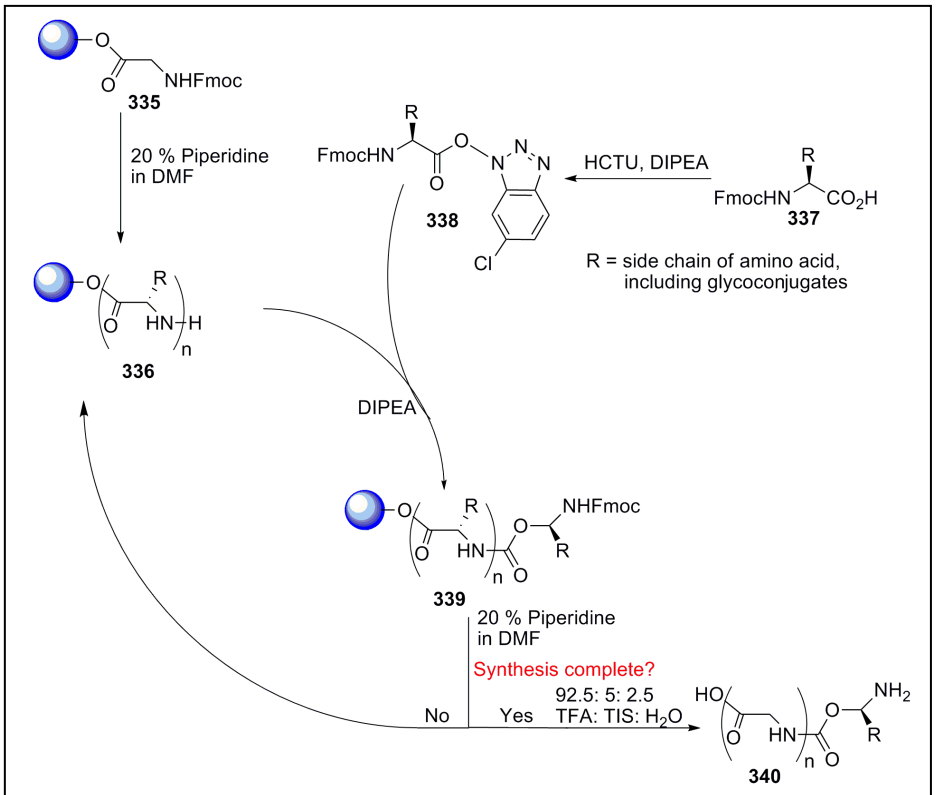

**Scheme 3.6 Coupling of 322 and 315 and completion of the synthesis of 321.**

homologation sequence. Wolff rearrangement progressed more smoothly for this compound however, providing β-amino acid **327** in 95 % yield. Attempts were made to use benzyl alcohol in place of water in the Wolff rearrangement, removing the requirement for the benzylation of the newly formed acid, but the excess benzyl alcohol was difficult to remove and complicated the recovery of the product to such an extent that attempting to shorten the sequence in this manner did not prove fruitful. Allyl alcohol, on the other hand, was successfully used to transform diazo **326** into the allyl protected derivative of **328**, **337**, in 82 % yield. Consequently **327** was then benzylated normally with CDI to provide **328** in 86 % yield which in turn was deprotected to yield the TFA salt **322** in quantitative yield.

The final step in this sequence was the coupling and deprotection of the benzyl ester. Amino acid **322** and carboxylic acid **315** were coupled in a similar fashion to that used previously with the exception that HCTU was used in place of HBTU and DMF in place of DCM. This reaction produced **329** in 75 % yield following purification. Hydrogenolysis under standard conditions supplied **321** in 95 % yield completing the synthesis of the required building blocks for solid phase synthesis. The yield of this process is nearly identical (47.6 % yield from **316**), to the alternative employing post-coupling homologation (48.1 % yield), although the purifications of the glycoconjugates was simpler with the newer protocol as they involved fewer steps and impurities at the latter stages.

### 3.3.3 Solid-phase synthesis of the glycopeptides

Solid phase peptide synthesis (SPPS) was generally accomplished using standard protocols as described in Chan.[30] These protocols are the same used in latter chapters and will be briefly discussed here. The strategy of the sequence is illustrated in Scheme 3.7. Commercially available Wang resin preloaded with Fmoc-glycine, **330**, is first swollen in an appropriate solvent and then deprotected using 20 % piperidine in DMF to produce the deprotected amine **331**. This primary amine is then treated with an activated ester such as **333**, generated from **332** through treatment with an activating agent such as HCTU (shown) to generate a dipeptide (n=1) such as **334**. The Fmoc group on the newly introduced residue is removed with piperidine. If the synthesis is incomplete, the cycle is repeated until the desired sequence has been generated. When the sequence is complete, the peptide is cleaved from the bead using a "cleavage cocktail." Different preparations are used for sequences incorporating different residues, but in this case a standard solution was




**Scheme 3.7 General strategy for the SPPS synthesis of peptides and glycopeptides.**

applied consisting of strong acid, TFA, an acid scavenger such as triisopropylsilane (TIS) and water. At this point the peptide, **335**, can be purified or if it is a glycopeptide, the protecting groups on the carbohydrate (if not acid labile) can be removed prior to purification.

In this study eight glycopeptides and one control peptide were prepared. The peptides are given in Figure 3.7 and the yields in Table 3.1. The crude yields, determined following cleavage, deacetylation, and de-salting using SPE cartridges and lyophilization are all quite high (Table 3.1). In fact even with a simple peptide synthesized on this batch of Wang resin, yields rarely exceed 95 %, as there is always a certain amount of unreacted glycine recovered following bead cleavage. Nevertheless, all peptides remained contaminated with truncated sequences, unreacted glycine, and various amounts of more hydrophobic impurities. Thus, they were all subjected to HPLC purification. Despite precautions such as flushing the column extensively between runs, the mass recoveries from the process were disappointing to say the least. Considerably higher yields were obtained for **202** and **206**, the last two peptides prepared, through using multiple injections of approximately 10 mg of material on an analytical column rather than two injections (50 mg) onto a semi-preparatory column. Finally, **336**, the aglycon of **206** was prepared as a control to determine the impact of the carbohydrate to conformation of the β-peptide. This was felt to be necessary as the impact of the

**Table 3.1 Crude and purified yields of mixed glycopeptides.**

| compound | sequence | crude yield (%) | purified yield (%)[a] |
|---|---|---|---|
| **200** | βO-G-G | 90 | 5 |
| **201** | O-βG-G | 91 | 8 |
| **202** | O-G-βG | 95 | 28 |
| **203** | βO-βG-G | 91 | 7 |
| **204** | βO-G-βG | 90 | 18 |
| **205** | O-βG-βG | 85 | 3 |
| **206** | βO-βG-βG | 97 | 32 |
| **336** | βO-βG-βG (aglycon) | ------- | 14 |

[a] Purified yields determined from mass of pure lyophilized fractions recovered from HPLC.

glycosylation was difficult to predict. Carbohydrates without C-2 acetamides are known to have little impact on the backbone conformation of α-peptides relative to the aglycon,[31-33] while those with C-2 acetamides have a considerably greater influence on conformation.[34, 35] However the effect of glycosylation on the potentially more structured conformations of β-peptides is unexplored to the best of the author's knowledge. Consequently, aglycon peptide **336** was prepared to control for any conformational changes that were due to the presence of the carbohydrates on the β-peptide rather than a conformational change due to the backbone substitutions themselves. If peptide **336** adopted a considerably different conformation compared to the glycopeptides, this could indicate that the carbohydrates were influencing the conformation of the peptide backbone considerably. Consequently, this compound was produced prior to the synthesis of the glycopeptides using a different experimental protocol and no crude yield was determined for this product at that time.

Despite the poor isolated yields, all syntheses provided sufficient purified material for characterization and analysis of conformation and activity, both of which are described below.

## 3.4 Assessing the solution conformation of β-amino acid containing AFGPs

Caution must be taken in interpreting the CD spectra of β-peptides. Little research has been done into the CD-spectra of these compounds, and even less into the CD spectra of mixed peptides. Nevertheless, it is still a very useful tool for examining relative changes in conformation. Figure 3.8 shows the CD spectra of the newly generated peptides. Surprisingly, all peptides share a similar secondary structure

independent of the percentage of β-amino acid content in their backbone. This common curve is qualitatively different from those seen for **118** or **102** (AFGP-8) and also from aglycon **336**. The mixed-peptides do not qualitatively resemble any common secondary structure motif. The maximum at 217 nm is consistent with a polyproline type II helix, but the spectra lack the far more distinctive minimum at 196 nm. The spectra are,

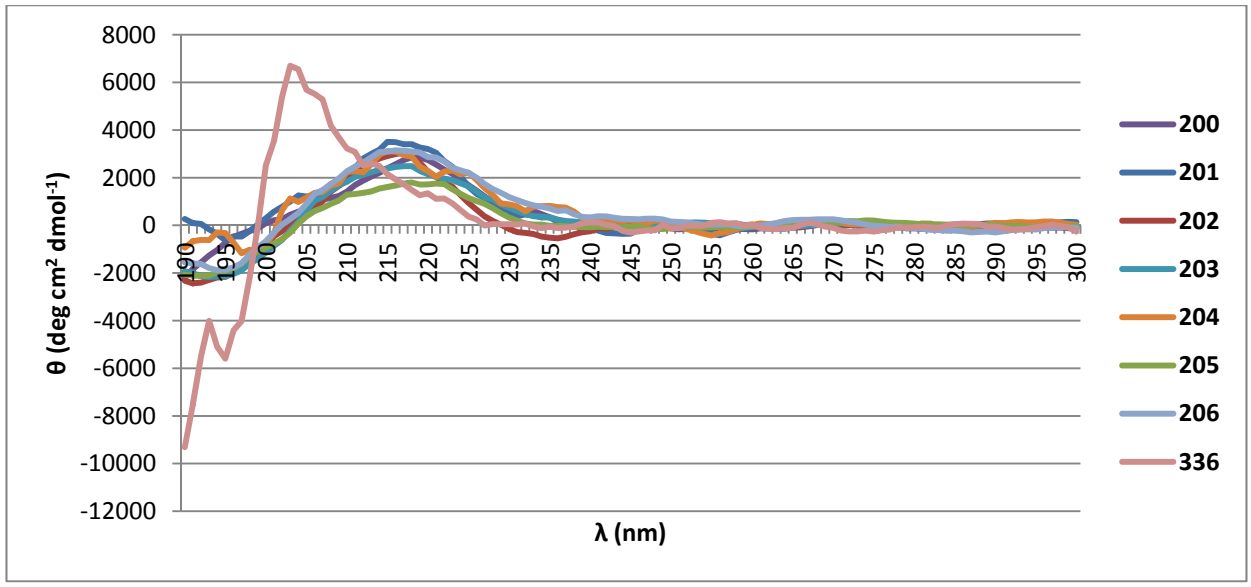



**Figure 3.8 CD spectra of mixed peptides generated in this study, vertical axis is expressed in molar ellipticity.**

however, broadly similar to that expected for a random coil.

The local maximum at 217 nm is consistent with a 14-helix,[36] but, again, the strong negative band at 196 nm is missing and the amplitude of the spectrum is much less than would be expected. The spectrum of peptide **336** on the other hand, appears to be similar to the 12-helix conformation;[36, 37] surprising in that this helix is generally seen only in systems incorporating a five-membered ring in the backbone.[37, 38] However, Raguse and co-workers generated a similar peptide containing trimeric repeats of (βLys-βLeu-βLeu) and obtained a similar spectrum, though with higher

amplitude, and assigned it a 12-helix conformation.[36] This might be a factor common amongst some peptides containing a charged amino group every three residues.

Deconvolution of these spectra, however, shows that in terms of the secondary structures commonly found in α-peptides, the glycopeptides (**200**-**206**) and peptide **336** have remarkably similar conformations (Table 3.2). A note needs to be made about the technique used for deconvolution. There is no library of β-peptides available to use as the basis of a deconvolution algorithm: in most cases in fact, the CD spectrum of the "pure" secondary structure is not available. This is true of the 12-helix, β-peptide random coil, and 10/12 helix amongst others. However, as the majority of the peptides are not pure β-peptides, even if such a library were available, its utility would be no more valid than that formed by the α-peptides used above. The deconvoluted data in Table 3.2 is provided only for comparative future purposes, and should not be interpreted further.

**Table 3.2 Deconvolution of the CD spectra in Figure 3.8 showing the contributions of different secondary structures to the conformation of the glycopeptide. Data was calculated using CD Pro IBASIS 5 and from an average of the values produced from three different deconvolution algorithms.**

| peptide | α-helix | β-sheet | β-turn | polyproline type II helix | random coil |
|---|---|---|---|---|---|
| **308** | -0.055 | 0.116 | 0.071 | 0.113 | 0.71 |
| **118** | 0.159 | -0.017 | 0.157 | 0.197 | 0.544 |
| **200** | 0.012 | 0.323 | 0.119 | 0.151 | 0.395 |
| **201** | 0.012 | 0.35 | 0.124 | 0.164 | 0.35 |
| **202** | 0.055 | 0.342 | 0.135 | 0.165 | 0.303 |
| **203** | 0.006 | 0.338 | 0.114 | 0.159 | 0.383 |
| **204** | 0.006 | 0.338 | 0.114 | 0.159 | 0.383 |
| **205** | 0.008 | 0.326 | 0.115 | 0.155 | 0.397 |
| **206** | 0.009 | 0.343 | 0.122 | 0.163 | 0.363 |
| **336** | 0.001 | 0.337 | 0.105 | 0.126 | 0.448 |

The β-Lysine containing analogue produced by I. Thapa, **308**, is included for comparison as is IRI active all-α-peptide **118**. The amplitude of the curve suggests a random coil, however, it is impossible to rule out other possible structures. Regardless, all the ornithine-based peptides incorporating β-amino acids appear to adopt a very

similar conformation, and consequently, conformation will not, in itself explain differences in IRI activity between these compounds.

## 3.5 Assessing antifreeze properties of β-amino acid AFGPs

All glycopeptides were then examined for antifreeze activity. As described in the introduction, antifreeze activity can be sub-divided into two phenomena, thermal hysteresis (TH) and ice recrystallization inhibition (IRI). These two phenomena are measured and examined separately.

TH activity is evaluated using nanolitre osmometry. This involves the suspension of a small drop (nanolitre scale) of solution (10 mg/mL of analyte in doubly distilled water) into small wells in a sample holder loaded with paraffin oil (Figure 3.11). The sample holder is then placed on an electric cryostage specially adapted to use with a light microscope and flash frozen at -40 ºC. The sample is then carefully melted until only a single crystal of ice remains in the aqueous solution. The melting point can then determined for the sample. The temperature is then slowly decreased at a rate of 10 milliOsmols (mOsmols) (0.0186 ºC) per 15 seconds. This unit is a measurement of number of moles of

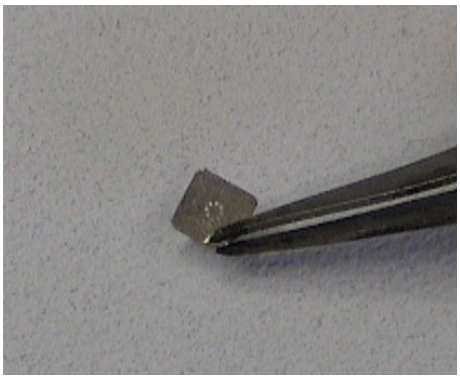


**Figure 3.11 Photograph of the sample holder, containing the small wells, held by a standard set of tweezers to show scale. Photograph replicated from Thapa 2006.[1]**

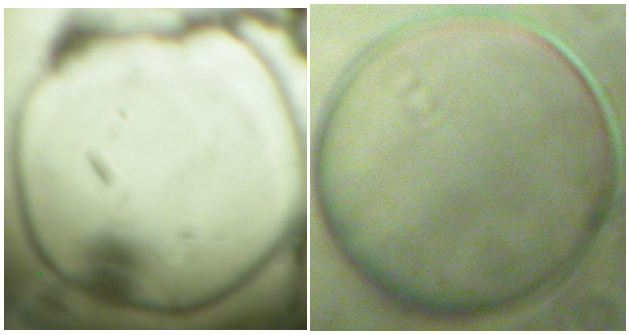


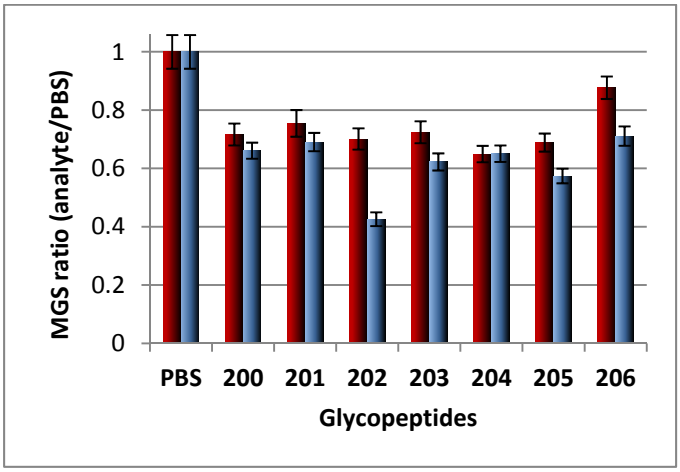
**Figure 3.10 Microscopy images of ice crystals from analogue 204 (left) which shows mild dynamic ice shaping, note the nascent faces, and an ice crystal in pure water (right) which is strictly circular.**

compound that contribute to the solution's osmotic pressure. This unit is consequently simply an analogue of temperature with regards to phase transitions: as one increases the concentration of solutes in a solution, one decreases the colligative melting point. Due to the small value of the unit (in terms of temperature) it is a convenient unit for the measurement of small temperature gaps. The thermal hysteresis gap can be readily determined as it is defined as the temperature range over which no ice crystal growth is detected. This measurement is repeated at least three times to accurately delineate the magnitude of the TH gap, if any.

A weaker manifestation of the TH gap is dynamic ice shaping, or the ability of the analyte to cause the ice crystal to deviate from a circular shape to a hexagon. This effect can sometimes be observed even in cases where no TH gap is discernable (Figure 3.10). The glycopeptides examined above were all tested for TH activity. All compounds failed to show any measurable TH gap: the melting and freezing point were identical. This is consistent with the previous observations made for *C*-linked AFGP analogues.[6, 12, 13] The first synthetic preparation of **308** and **200** by I. Thapa both showed measurable TH gaps of approximately -0.10 ºC and both compounds appeared to express strong dynamic ice shaping. This was not, however, present in the freshly prepared analogues. None of the compounds exhibited either dynamic ice shaping or any TH gap, except compound **204** which showed only a very slight deviation from circular with no accompanying TH gap (Figure 3.10). The new data is more consistent with the current understanding of the TH behaviour of Ornithine analogues than I. Thapa's observations: no such TH gaps have been observed in any previously prepared Ornithine-based analogue. The original sample was possibly contaminated with small

amounts of a TH-active compound. None of the other *C*-linked amide analogues of this length have ever shown TH activity.

Finally, the new glycopeptides were examined for IRI activity. This is done through the “splat-cooling” assay developed by Knight.[39, 40] This assay is thoroughly discussed in the introduction above (1.6.1). The study was carried out on the glycopeptides at two different concentrations, 5.5 μM, and 550 μM (red and blue respectively in Figure 3.12). The lower concentration (5.5 μM) is the standard value used to determine the IRI activity of glycopeptides in the Ben lab. The higher concentration of 550 μM was included as it became clear upon data analysis that it was difficult to determine the presence of any true variability in the data at the lower concentration. At 5.5 μM, all compounds save **206** have nearly identical IRI activities: **204** is slightly better, **201** is slightly poorer. β-peptide, **206** on the other hand is considerably less active than the all the other compounds. It is interesting to note that the new batch of TH-inactive **200** has identical IRI activity to the TH-active batch previously analysed by I. Thapa.[1] All analogues possess considerably less IRI activity than **118**, indicating that any modification to the peptide whatsoever is quite harmful to IRI activity. However there are differences within this series that deserve greater attention.




| compound | sequence |
|---|---|
| 200 | βO-G-G |
| 201 | O-βG-G |
| 202 | O-G-βG |
| 203 | βO-βG-G |
| 204 | βO-G-βG |
| 205 | O-βG-βG |
| 206 | βO-βG-βG |

**Figure 3.12 IRI activity of mixed glycopeptides produced in this study. Glycopeptides were analyzed for activity at both 5.5 μM (red bars) and 550 μM (blue bars).**

At the higher concentration, however, a starker difference is apparent. Glycopeptide **202** is considerably more potent than the other compounds. On first examination this is perplexing, but this discrepancy can possibly be explained. The structural difference between **202** and all other analogues is that **202** does not change the distance between the amide on the backbone (and the carbohydrate in general) and the (*i*+1) position. All other compounds do change this distance, extending it by one or more methylene groups. Nor is simply maintaining an α-amino acid at the glyconjugate position (ornithine) sufficient to maintain activity because of the two other analogues satisfying this condition, **201** is among the poorest inhibitors while **205** is only slightly better (although it is the second most potent inhibitor after **202**). The same logic holds regarding maintaining the α-glycine at the ($i$+1) residue: the two other analogues containing this amino acid (**200** and **204**) exhibit only average activity. The difference in IRI activity cannot be ascribed to the percentage of β-substitution: the other two analogues with only a single β-amino acid, **200** and **201** are not significantly more active than those with two β-amino acids; this result is consistent with the CD analysis as the spectra indicate that all analogues exhibit a similar secondary structure regardless of the ratio of α to β amino acids in the backbone. Furthermore, even with drastic changes to the conformation of the peptide (not supported by the deconvolution data), the work

of Hachisu on preparing cyclic analogues of AFGP-8 and finding them to be highly TH active seems to indicate that the gross conformation is not necessarily important to determining antifreeze activity.[11] Most importantly though, any introduction of a β-peptide does significantly decrease IRI activity relative to analogue **118**. Consequently, although the current data suggest that this indicated distance may be important, it appears that any deviation from **118** is harmful to IRI activity.

Consequently it appears that it is not the change in conformation that is responsible for the decreased IRI activity of the other β-amino acid containing analogues relative to **202** as increasing this variable through increasing the degree of β-substitution does not seem to have any noticeable effect. A possible explanation lies in the invocation of an intramolecular interaction. Figure 3.13 shows the structures of **202** and **118**, and the possible key structural distance between the NH of the linker and the carbonyl of the ($i$+1) residue. The nature of this interaction cannot be identified at this stage, but may include a water bridge, the formation of a hydrophobic pocket or even another explanation entirely. Any hypothesis would be pure speculation. However, this interaction is only intact in analogue **202**. As was mentioned in the introduction and will be thoroughly investigated in the next chapter, it appears that a correlation may exist between IRI activity and both the spatial

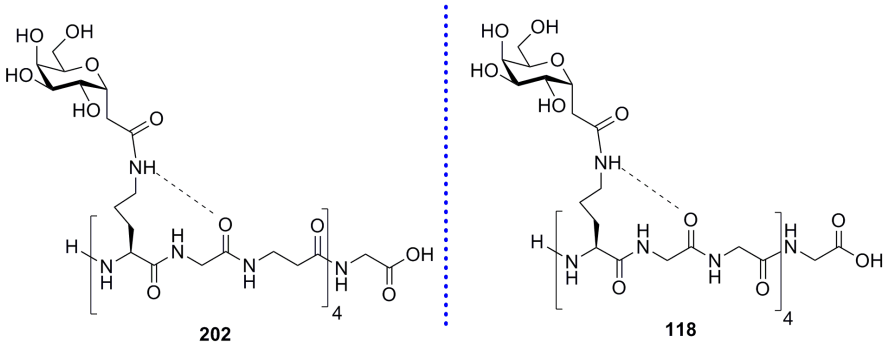



Figure 3.13 Possible important relationship in analogue 202 and 118.

relationship of the carbohydrate and the backbone and the nature of the tether linking the two moieties. The specific values of these parameters may explain the remarkable activity of **118** as it consistently performs better than would be suggested by the trends apparent in studies involving analogues of this compound.[5, 6, 13, 17, 41, 42]

Thus, although **202** is by no means even close in activity to **118**, it is considerably more active than the other mixed peptides, suggesting that maintaining a certain spacing between the amide bond of ($i$+1) and the linker/carbohydrate (the spacing between the linker/carbohydrate and ($i$-1) NH or ($i$-2) carbonyl does not appear to be important) has ramifications for IRI activity. This implies that the conformation of concern is not that of the glycopeptide as a whole, but that of the carbohydrate relative to the backbone.

## 3.6 Chapter summary

This study was initiated to explore the influence on IRI activity of modifying the peptide backbone with β-amino acids. This was inspired by the observation of I. Thapa that the introduction of β-amino acids was beneficial for the activity of lysine-containing residues but was greatly detrimental to the IRI activity of ornithine-containing residues. I. Thapa also observed that these analogues were TH active. However the reason for these changes in activity were not clear and could be due either to conformational change imposed by the introduction of the β-residues or could be ascribed to the disruption of some intramolecular interaction. To this end the complete series of mixed α/β peptides were prepared and examined for antifreeze activity. All compounds exhibited the same solution conformation, but the CD spectrum is different from that exhibited by **118**, although the deconvolution data suggests that the conformations are

quite similar. Unfortunately, the TH measurements of I. Thapa on **200** were not reproducible and no compound showed any TH activity. The original observation may have been due to the presence of a small amount of TH-active impurity and was generally inconsistent with all other recorded data. The IRI assay demonstrated that the newly prepared mixed peptide compounds were universally much less potent than α-peptide **118**. However, at 550 μM, analogue **202** containing Orn-Gly-βGly as the tripeptide repeat was considerably more active than any other peptide. Only **202** has the same relationship between the glycosylated side-chain of the ornithine residue and the amide bond of the (*i*+1) glycine residue as **118**. This result suggests that this spatial relationship may be important for IRI activity.

## References

1. Thapa, I. *C*-Linked AFGP analogues containing β-amino acids: preparation, assessment and *in vitro* studies. MSc. Thesis. University of Ottawa, Ottawa, 2006.
2. Wu, Y.-D.; Han, W.; Wang, D.-P.; Gao, Y.; Zhao, Y.-L., *Acc. Chem. Res.* **2008,** *41* (10), 1418-1427.
3. Bouvet, V. R. Novel AFGP8 Analogues: Synthesis and Biological Evaluation of Potent Recrystallization Inhibitors. PhD. Thesis. University of Ottawa, Ottawa, 2006.
4. Kritzer, J. A.; Stephens, O. M.; Guarracino, D. A.; Reznik, S. K.; Schepartz, A., *Bioorg. Med. Chem.* **2004,** *13* (1), 11-16.
5. Murphy, A. V. Preparation of structurally diverse C-linked antifreeze glycoprotein analogues and assessment for antifreeze protein-specific activity. PhD. Thesis, State University of New York, Binghampton, 2004.
6. Czechura, P.; Tam, R. Y.; Dimitrijevic, E.; Murphy, A. V.; Ben, R. N., *J. Am. Chem. Soc.* **2008,** *130* (10), 2928-2929.
7. Kontes, F. Synthesis of a conformationally constrained antifreeze glycoprotein analogue. BSc. Thesis, University of Ottawa, Ottawa, 2006.

8. Liu, S. Novel *C*-linked antifreeze glycoprotein analogues as potent recrystallization inhibitors: preparation, assessment and *in vitro* studies. PhD. Thesis, University of Ottawa, Ottawa, 2006.

9. Gibson, M. I.; Barker, C. A.; Spain, S. G.; Albertin, L.; Cameron, N. R., *Biomacromol.* **2008,** *10* (2), 328-333.

10. Norgren, A. S.; Budke, C.; Majer, Z.; Heggemann, C.; Koop, T.; Sewald, N., *Synthesis* **2009**, 488-494.

11. Hachisu, M.; Hinou, H.; Takamichi, M.; Tsuda, S.; Koshida, S.; Nishimura, S.-I., *Chem. Commun.* **2009,** (13), 1641-1643.

12. Liu, S.; Ben, R. N., *Org. Lett.* **2005,** *7* (12), 2385-2388.

13. Tam, R. Y.; Rowley, C. N.; Petrov, I.; Zhang, T.; Afagh, N. A.; Woo, T. K.; Ben, R. N., *J. Am. Chem. Soc.* **2009,** *131* (43), 15745-15753.

14. Martinek, T. A.; Fueloep, F., *Eur. J. Biochem.* **2003,** *270* (18), 3657-3666.

15. Gellman, S. H., *Acc. Chem. Res.* **1998,** *31* (4), 173-180.

16. Gellman, S. H., *sp2.* **2002,** *1* (5), 30-31.

17. Eniade, A.; Purushotham, M.; Ben, R. N.; Wang, J. B.; Horwath, K., *Cell. Biochem. Biophys.* **2003,** *38*, 115-124.

18. Tam, R. Y.; Rowley, C. N.; Petrov, I.; Zhang, T.; Afagh, N. A.; Woo, T. K.; Ben, R. N., *J. Am. Chem. Soc.* **2009,** *131*, 15745-15753.

19. Pontén, F.; Magnusson, G., *J. Org. Chem.* **1996,** *61* (21), 7463-7466.

20. Mari, S.; Cañada, F. J.; Jiménez-Barbero, J.; Bernardi, A.; Marcou, G.; Motto, I.; Velter, I.; Nicotra, F.; La Ferla, B., *Eur. J. Org. Chem.* **2006,** *2006* (13), 2925-2933.

21. Leclère, M.; Kwok, B. K.; Wu, L. K.; Allan, D. S.; Ben, R. N., *Bioconj. Chem.* **2011**, null-null.

22. Guindon, Y.; Jung, G.; Guérin, B.; Ogilvie, W. W., *Synlett.* **1998,** *1998* (03), 213,220.

23. Guindon, Y.; Lavallée, J. F.; Boisvert, L.; Chabot, C.; Delorme, D.; Yoakim, C.; Hall, D.; Lemieux, R.; Simoneau, B., *Tet. Lett.* **1991,** *32* (1), 27-30.

24. Ollivier, C.; Renaud, P., *Chem. Rev.* **2001,** *101* (11), 3415-3434.

25. Lindgren, B. O.; Nilsson, T., *Acta. Chem. Scand.* **1973,** *27*, 888-890.

26. Bal, B. S.; Childers, W. E.; Pinnick, H. W., *Tetrahedron* **1981,** *37* (11), 2091-2096.

27. Ben, R. N.; Eniade, A.; Hauer, L., *Org. Lett.* **1999,** *1* (11), 1759-1762.

28. Matthews, J. L.; Braun, C.; Guibourdenche, C.; Overhand, M.; Seebach, D., Preparation of entiopure β-amino acids from α-amino acids using the Arndt-Eistert homologation. In *Enantioselective synthesis of β-amino acids*, 2nd ed.; Juaristi, E.; Soloshonok, V. A., Eds. Wiley: Hoboken, NJ, 1997.

29. Arndt, F.; Eistert, B., *Ber. Deut. Chem. Ges.* **1935,** *68* (1), 200-208.

30. Chan, W. C.; White, P. D., Basic procedures. In *Fmoc Solid Phase Peptide Synthesis: A Practical Approach*, Chan, W. C.; White, P. D., Eds. Oxford Univesity Press: Oxford, 2000; pp 41-76.

31. Tachibana, Y.; Fletcher, G. L.; Fujitani, N.; Tsuda, S.; Monde, K.; Nishimura, S.-I., *Angew. Chem. Intl. Ed.* **2004,** *43*, 856-862.

32. Meyer, B.; Möller, H., Conformation of glycopeptides and glycoproteins. In *Glycopeptides and glycoproteins: synthesis, structure and applications*, Wittmann, V., Ed. Springer-Verlag: Berlin and Heidelberg, 2007; Vol. 267, pp 187-251.

33. Coltart, D. M.; Royyuru, A. K.; Williams, L. J.; Glunz, P. W.; Sames, D.; Kuduk, S. D.; Schwarz, J. B.; Chen, X.-T.; Danishefsky, S. J.; Live, D. H., *J. Am. Chem. Soc.* **2002,** *124* (33), 9833-9844.

34. O'Connor, S. E.; Imperiali, B., *J. Am. Chem. Soc.* **1997,** *119* (9), 2295-2296.

35. O'Connor, S. E.; Imperiali, B., *Chem. Biol.* **1998,** *5* (8), 427-437.

36. Raguse, T. L.; Lai, J. R.; Gellman, S. H., *Helv. Chem. Acta* **2002,** *85*, 4154-4164.

37. Park, J.-S.; Lee, H.-S.; Lai, J. R.; Kim, B. M.; Gellman, S. H., *J. Am. Chem. Soc.* **2003,** *125* (28), 8539-8545.

38. Seebach, D.; Matthews, J. L., *Chem. Commun.* **1997,** (21), 2015-2022.

39. Knight, C. A.; Wen, D.; Laursen, R. A., *Cryobiology* **1995,** *32* (1), 23-34.

40. Knight, C. A.; Hallett, J.; DeVries, A. L., *Cryobiology* **1988,** *25* (1), 55-60.

41. Capicciotti, C. J.; Trant, J. F.; Leclère, M.; Ben, R. N., *Bioconj. Chem.* **2011,** *22* (4), 605-616.

42. Czechura, P. Elucidating the relationship between hydration and ice recrystallization inhibition with *C*-linked antifreeze glycoproteins. PhD. Thesis. University of Ottawa, Ottawa, 2009.

# Chapter 4 : Synthesis and IRI activity of triazole-containing analogues of *C*-AFGP

## 4.1 Introduction to triazoles as amido-mimetics

Of all of the components of the *C*-AFGP analogues, the linker is the least explored. One would expect that modifications to the linker would have a smaller impact than those to either the carbohydrate moiety or the peptide backbone. However, the previous studies by Liu and Tam have shown that this is not the case and that in fact, IRI activity is very sensitive to the nature of the linker.[10, 11] Despite these efforts however, the importance of the amide bond, both its presence and its relative position in the linker, remains unclear. As mentioned above, triazoles are known to be excellent isosteres of the amide bond as they approximate the length and rigidity of the functionality while maintaining hydrogen-bond accepting capability, and, according to some sources, a limited hydrogen bond-donating ability, while simultaneously being very easy to prepare (Figure 4.1).[12-19]

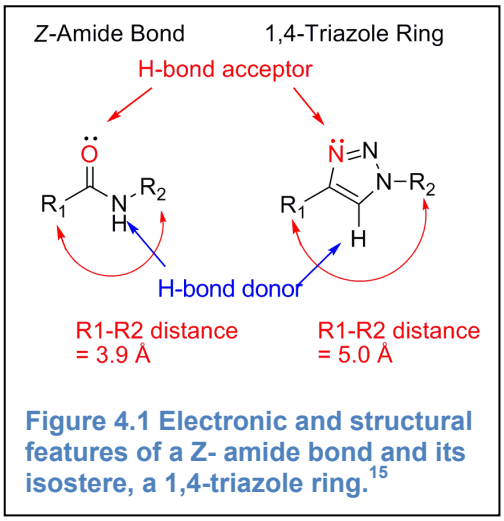
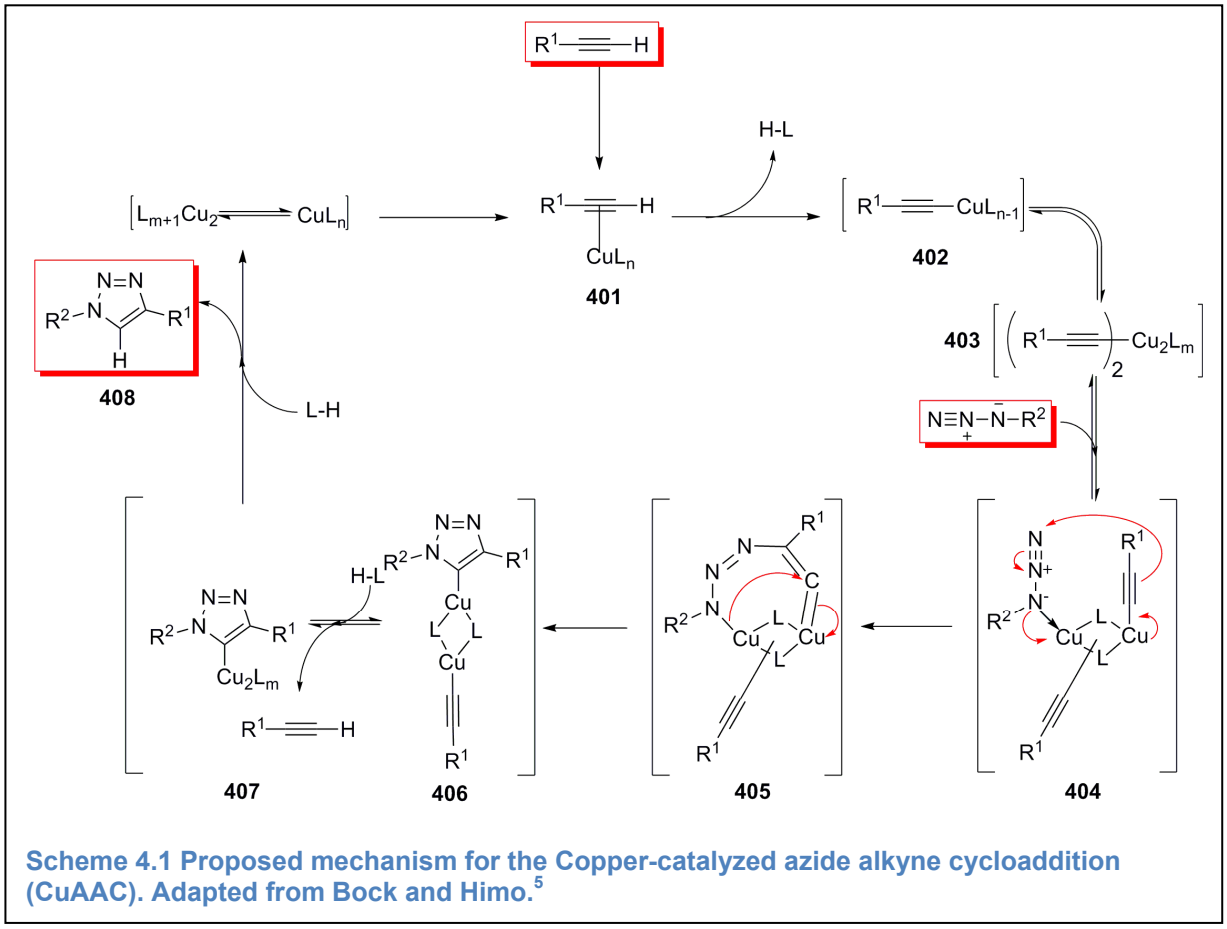



**Figure 4.1 Electronic and structural features of a Z- amide bond and its isostere, a 1,4-triazole ring.[15]**

Therefore, it is not surprising that they have found widespread usage in synthetic chemistry. This in turn makes them excellent tools to investigate the linker in *C*-AFGP analogues

## 4.2 Introduction to the copper-catalyzed Huisgen-cycloaddition

1,2,3-Triazoles (referred to as triazoles for the rest of this document) have long been prepared using the Huisgen cycloaddition reaction between an alkyne and an azide.[20, 21] Traditionally, however, this reaction was of little use to synthetic chemists as the extended reaction times and high temperatures made it unsuitable for many applications.[21] Furthermore, under such energetic conditions, regioselectivity was difficult to control and reactions resulted in a mixture of the 1,4- and 1,5- substituted triazoles. This challenge was independently overcome by the groups of Meldal at the Carlsberg Institute in Denmark and Sharpless at the Scripps Institute. Both observed that the addition of small amounts of copper (I) salt lead to a drastic increase in the rate of reaction. Meldal used PEGA-based resins functionalized with propargylic acid and found that the reaction progressed very well in the presence of diisopropyl ethylamine as solvent and CuI as the copper source.[22] Sharpless observed that in aqueous mixtures of water and *tert*-butanol, the presence of copper (II) salts and an *in situ* reductant such as sodium ascorbate allowed for the formation of a wide variety of 1,4-substituted triazoles.[23] These two sets of conditions: organic solvent with amine base and copper (I) salts; or aqueous/organic solvent mixture with copper (II) salts and sodium ascorbate have been the two sets of conditions exploited in the literature. Further investigations have been carried out into the mechanism of the transformation by the Sharpless group,[24] and later by the van Maarseveen group.[5]




**Scheme 4.1 Proposed mechanism for the Copper-catalyzed azide alkyne cycloaddition (CuAAC). Adapted from Bock and Himo.[5]**

Both investigations found that the mechanism involves a complicated higher order copper complex (Scheme 4.1). The expected initial association of the copper salt with the alkyne (**401**) is followed by deprotonation to generate copper (I) acetylide **402**. The order of the reaction was found to lie intermediate between 1 and 2 with respect to the alkyne and it appears that, in some cases at least, the acetylide complexes dimerize (**403**). The second copper of this dimeric metallocyclic dimer can then associate with the inner nitrogen of the azide functionality (**404**). Ring-closing accompanied by a formal oxidative addition leads to the strained putative bicyclic intermediate **405**, which is then (formally) reductively eliminated to copper-associated-triazole **406**. Reprotonation releases the second unreacted alkyne (if present) to generate **407**, and a second

reprotonation liberates the triazole product (**408**) leaving a copper dimer that can dissociate to re-enter the catalytic cycle.

The presence of amine salts was found to stabilize the Cu (I) salts and prevent their oxidation to Cu (II) and thus their removal from the cycle. Since these initial reports, this chemistry, essentially a powerful ligating technique, has been exploited in a wide variety of chemical fields including polymers, *in vitro* and *in vivo* labelling of biological processes, medicinal chemistry, and combinatorial chemistry amongst others.[25-27] Almost all the applications rely on the two reaction condition strategies outlined above (with the notable exception of the copper-free reaction pioneered by Bertozzi involving the use of strained cyclooctynes as a high-energy coupling partner for the azides-appropriate for systems in which copper may be toxic).[28]

Unfortunately, neither of these conditions perfectly met the current requirements of the presented work; namely, solid-supported (Wang resin) triazole synthesis without the presence of amine bases. Unfortunately, both water and *t*-butanol are the worst possible solvents for swelling of Wang resin.[4] Similarly, organic bases should be avoided as their presence could lead to the formation of unwanted by-products through a Glaser-type mechanism. Finally, to the best of the author's knowledge, no comprehensive, systematic examination of reaction conditions has been reported in the literature. If a comment on conditions accompanies a contribution, it is normally of the nature that the reaction functions well in most solvents or required some form of thermal activation; however, as even small differences in yields could greatly simplify or complicate purification protocols with respect to triazole-containing glycoconjugates, it

was important to investigate whether subtle differences existed between various organic solvents before the reactions were attempted on solid-phase.

## 4.3 Previous applications of the CuAAC reaction to solid-phase synthesis

The possibilities for this reaction to complement solid-phase technology were recognized immediately - Meldal's seminal publication described the potential directly.[22] Since that time the CuAAC reaction has been applied in solid-phase strategies to prepare peptides, oligonucleotides, lipopeptides and glycoconjugates.[29-36] The advantage of this chemistry is that it is very high yielding and is not substrate specific; consequently it can encompass a wide variety of both structural features (1º, 2º or 3º azides and alkynes can all be successful, although increased steric effects do result in decreased yields for 3º substrates), and functional groups. Add to this the fact that in many cases the un-reacted solution-phase reagent may be recoverable by simple extraction or crystallization unencumbered by impurities and the reaction appears to be perfectly designed for solid-phase applications.

When this project was initiated, there had been no reported syntheses of defined multivalent glycopeptides reported, but as the initial manuscript was in preparation several reports were published showing the potential of the CuAAC reaction in the synthesis of AFGP and mucin-like glycopeptides (Figure 4.2). These efforts have been mostly directed towards investigating the technology for its suitability for the preparation of glycopeptides rather than for investigating antifreeze activity. The AFGPs are rare amongst glycopeptides for their repetitive and short structure and multivalency with

simple carbohydrate moieties. The contribution from the Sewald group involved the on-resin ligation of azido sugars with poly-acetylenic peptoids using excess CuI and sodium ascorbate in anhydrous DMF and DIPEA (Scheme 4.3 A) to produce glycopeptoids **409**-**411**. The IRI activity of these compounds is discussed below.[3] The Brimble group has prepared several different glycopeptides using CuAAC techniques. In their first report, they coupled an O-propargyl GalNHAc with an azido-serine derivative in solution-phase using 10-20 mol % $CuSO_4$ and 25-50 mol % sodium ascorbate at 80 ºC under microwave heating (**412**, Scheme 4.3 B).[8] More recently they also used a similar technique to prepare mucin-like glycoconjugates using tris(carboxyethyl)phosphine in place of sodium ascorbate as reductant with both reagents in five-fold excess over the substrate. Brimble's compounds have not been examined for IRI activity.[37]

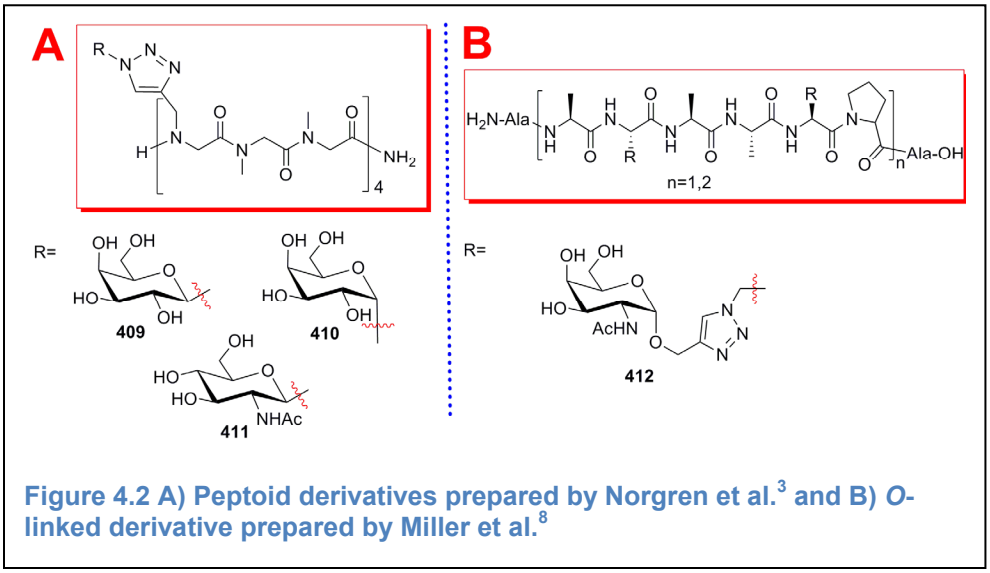



**Figure 4.2 A) Peptoid derivatives prepared by Norgren et al.[3] and B) *O*-linked derivative prepared by Miller et al.[8]**

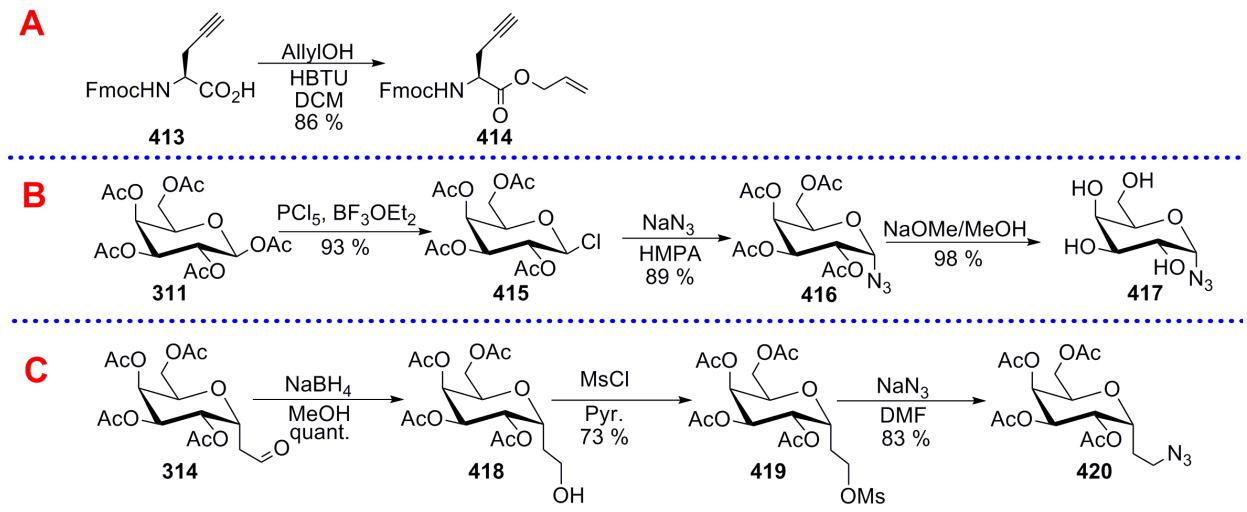
However, although these reports provide conditions for solid-phase synthesis of glycopeptides, they were not available when the current study began, and consequently the current study was initiated by examining which solvents were appropriate for our model system in solution phase. The following results (sections 4.4-4.7) have been reported in a recent publication.[38]

## 4.4 Determination of optimized conditions for solid-phase synthesis using a solution-phase model

To determine the optimal conditions for the solid-phase application, we investigated several different parameters. We determined that the ideal order to examine these parameters would be to first investigate the temperature of reaction, followed by the copper source, and finally the solvent system. The optimal conditions could then be tested against different substrates to determine their generality and suitability for the preparation of a variety of different glycoconjugates. The initial substrates envisioned for this study included azido-α-D-galactopyranose (**417**), its acetylated derivative (**416**) and 2-ethylazido-(2,3,4,6-tetra-*O*-acetyl-α-D-galactopyranose) (**420**) as the azido sugars and a protected derivative of the commercially available propargylglycine (Scheme 4.3).

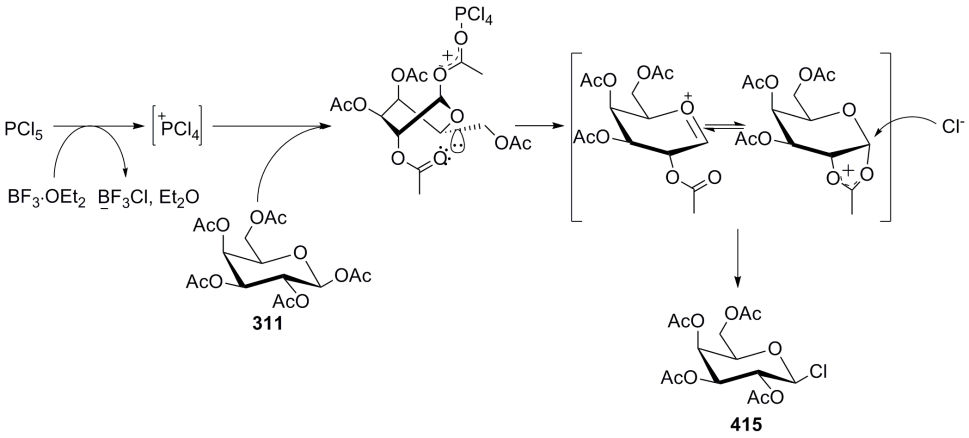
### 4.4.1 Synthesis of glycosyl building block and preparation of amino acid building block

Propargylglycine is the alkynyl amino acid found in nature. It is produced by some species of mushrooms as a defensive toxin (by mimicking cysteine and methionine intermediates they can inhibit hepatic synthesis in potential predators).[39-41] It is also a commercially available compound and was consequently selected as the alkynyl coupling partner for this study. Commercially available Fmoc-protected propargyl glycine (**413**, Chem-Impex) was protected with an allyl group (**414**) under standard conditions and purified prior to use in 86 % yield (Scheme 4.2A).




**Scheme 4.3 Synthetic strategy for the preparation of protected propargyl glycine 414 and glycosyl azides 416, 417 and 420.**

The glycosyl coupling partners were also readily accessible. Known azido galactose **416**[42] was prepared through a rather unusual activation of the acetate group of **311** with $BF_3{\cdot}OEt_2$ and phosphorus pentachloride (Scheme 4.3).[6] This leads to the formation of an oxocarbenium ion which would be stabilized by the *C*-2 acetate through anchiomeric assistance. This functionality would then be displaced by the chloride to provide the β anomer, **415**, exclusively. The chlorinated product was crystallized, in greater than 90 % yield and purity, and was




**Scheme 4.2 Proposed mechanism for β-chlorination through the *in situ* production of $PCl_4^+$ as a Lewis acid. Mechanism is adapted from Ibatullin and co-workers.[6]**

immediately treated with sodium azide in HMPA as solvent for a direct $S_N2$-like displacement at the anomeric centre to provide anomeric azide **416** in 89 % yield.

Additionally, the deprotected variant, **417**, was accessed through a standard Zemplén deacetylation from **416**.[43] Ethyl azido compound **420** was accessed starting with aldehyde **314**, which was reduced to the alcohol (**418**) using sodium borohydride in methanol in quantitative yield. The free alcohol was immediately mesylated to provide sulfonic ester **419** in 73 % yield, and this primary leaving group was in turn displaced by sodium azide to afford the ethyl azido derivative **420** in 83 % yield following recrystallization. With these simple building blocks in hand, the initial optimization studies could be undertaken. The following studies were carried out in collaboration with Chantelle Capicciotti, an honours student at the time.

### 4.4.2 Effect of temperature on the CuAAC reaction

The first variable examined was reaction temperature. The goal of this exercise was to determine a high enough temperature that allowed the reaction to take place in a reasonable period of time, less than the 16 or 24 hours reported often in the literature, but not so high that the rate of the reaction would be so rapid that subtle differences (in conversions and yields, and approximate reaction times)

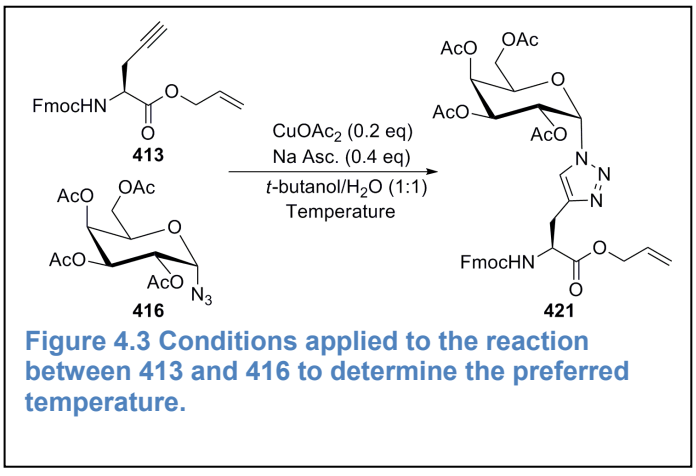



**Figure 4.3 Conditions applied to the reaction between 413 and 416 to determine the preferred temperature.**

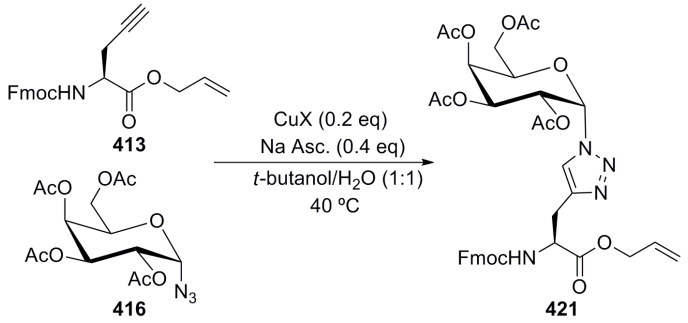
between sets of conditions could not be determined. To accomplish this goal, model substrates (**413** and **416**) were treated under standard Sharpless conditions over a small range of temperatures, 30, 40, 50 and 70 ºC (Figure 4.3).

At the two higher temperatures, it appeared that the Cu (I) catalyst reverted to an inactive Cu (II) state rapidly, prior to the completion of the reaction, making them unsuitable for the reaction under these conditions (presumably a more exhaustive exclusion of oxygen would have prevented this outcome). At 30 ºC, the reaction was not complete, even after 8 hours of reaction time. At 40 ºC, the reaction was complete, with quantitative conversion after 8 hours (no starting material was detectable by either TLC or NMR). As such, 40 ºC was selected as the preferred temperature to carry out the remaining scans as the reaction completed in a reasonable period of time, but not so rapidly that differences in conditions could not be noted.

### 4.4.3 Effect of copper source on the CuAAC reaction

The second parameter investigated was the preferred source of catalyst for the reaction. The standard Sharpless conditions make use of Cu (II), whereas Cu (I) is often used in the presence of organic solvents. As mentioned

**Table 4.1. Effect of copper source on reaction time, conversion, and isolated yield of the CuAAC reaction between 413 and 416.**




| entry | catalyst | reaction time (hrs) | yield (%) | conversion (%) |
|---|---|---|---|---|
| i | $Cu(OAc)_2$ | 5 | 65 | 81 |
| ii | CuI | 4 | 0 | 0 |
| iii | $CuSO_4$ | 4 | 63 | 66 |

above, it is Cu (I) that is the active catalyst for this reaction. In oxidative conditions, copper tends to readily return to the $2^+$ oxidation state, and hence the efforts to exclude excess oxygen from the reaction (and the possible issue with the higher temperatures mentioned above).

With both cupric acetate and sulphate, the reaction progressed well (Table 4.1, entries i and ii). Upon addition of the sodium ascorbate, the reaction immediately changes colour from a deep royal blue to a deep yellow indicating the reduction of the copper salt. CuI on the other hand resulted in no reaction (entry iii): the salts had difficulty dissolving into the reaction mixture and no conversion was observed. Sodium ascorbate was present in the same amount as for the cupric reactions, and as such it does not appear to be a problem of catalyst stability, but rather of catalyst solubility.

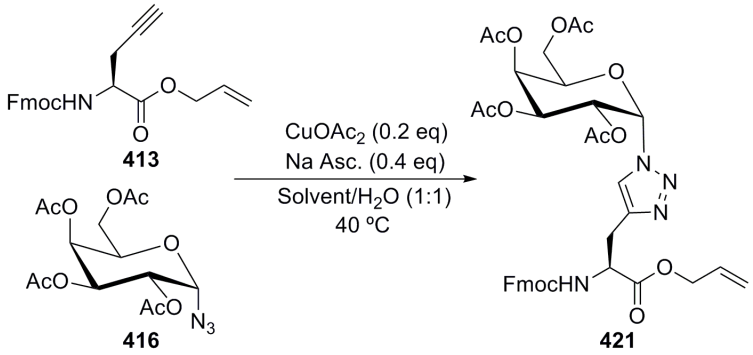
Both cupric sources provided very similar results. As there was a ready supply of anhydrous copper (II) acetate, it was arbitrarily chosen as the catalyst source for the further studies.

### 4.4.4 Effect of solvent on the CuAAC reaction

Unlike many other reactions, the CuAAC reaction appears to be rather insensitive to solvent changes. Most early reports state that the reactions progress extremely well in a wide variety of solvents including THF, DMF, DIPEA, $NEt_3$, toluene, acetonitrile, dichloromethane and water/*t*-BuOH.[22, 23] These solvents span a large range of polarities and include both protic and aprotic solvents. In an attempt to determine whether there was in fact no real difference between the various solvents (and to obtain a solvent system compatible with Wang resin), a series of conditions were examined for the reaction between **413** and **416** as outlined below. The reactions were followed by

TLC, and were quenched when either they were deemed complete by TLC analysis or after 5 hours, whichever occurred first. *tert*-Butanol, the standard solvent for these catalyst conditions, is actually a rather poor system as the reaction had not yet reached completion after 5 hours (Table 4.2, entry i). Following quenching, the reaction was found to have reached 81 % conversion and a yield of 65 % of **421** was obtained. Acetone provided much better results with near quantitative conversion after only 15 minutes, but the isolated yield was poor at only 55 % (entry ii). DMF showed excellent yield, at 96 % but the reaction required 4 hours (entry iii), while combining DMF and acetone in a 1:1 mixture provided a quantitative conversion and 82 % isolated yield of **421** after only 30 minutes (entry iv). To complement this excellent result, other aprotic polar solvents were tested including NMP which provided 88 % yield in quantitative conversion after 3 hours (entry v); dioxane which provided similar results but after only 1 hour (entry vi), and THF which provided a quantitative conversion and a 87 % yield of **421** after only 30 minutes of reaction time (entry vii). The results from this study clearly show that not all solvents are equal: it

**Table 4.2 Effect of solvent on reaction time, conversion and isolated yield of the CuAAC reaction between 413 and 416.**




| entry | co-solvent | reaction time (hrs) | yield (%) | conversion (%) |
|---|---|---|---|---|
| i | *t*-BuOH | 5 | 65 | 81 |
| ii | Acetone | 0.25 | 55 | 97 |
| iii | DMF | 4 | 96 | 78 |
| iv | DMF/Acetone | 0.5 | 82 | >98 |
| v | NMP | 3 | 88 | >98 |
| vi | Dioxane | 1 | 89 | 95 |
| vii | THF | 0.5 | 87 | >98 |

appears that the excellent yields provided by THF, DMF, dioxane and NMP point to a general preference for polar aprotic solvents. The truly startling result though is that *tert*-butanol, the standard solvent used with this catalytic system, is the only solvent that does not recommend itself in any way: the reaction is quite sluggish in this solvent and the yields and conversions remain only moderate even after extended reaction times; the solvent was probably initially chosen by the Sharpless group due to their previous use of this system for other catalytic transformations such as the Sharpless dihydroxylation.[44] With the results of the solvent study in hand, attention turned to an optimization of the conditions for solid-phase applications.

### 4.4.5 Effect of water content on the CuAAC reaction

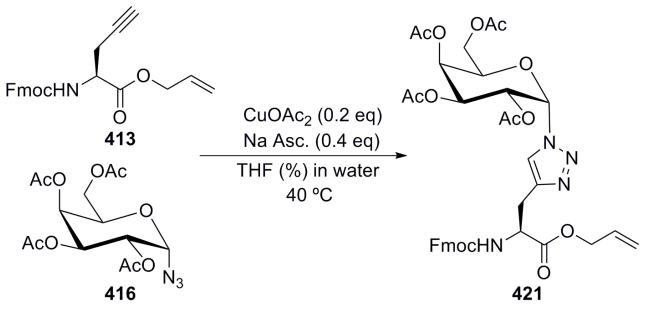
The solvent scan was important, but as the goal was to adapt these conditions for solid-phase synthesis, the solvent system had to be compatible with polystyrene Wang resin beads. Swelling is essential for a successful synthesis, and is a very important parameter in all SPPS work. This requirement is largely responsible for the extensive use of DMF and NMP as solvents in SPPS as they are both excellent at swelling the polystyrene bead and at solubilizing the growing peptide chains (DCM, although an excellent swelling solvent for the bead themselves, is not as good at solvating the growing peptide chains and hence can cause complications in longer syntheses).[45, 46] Fortunately all the polar aprotic solvents listed above are excellent swelling solvents and this ability has been quantified by Santini and Griffiths (Table

**Table 4.3. Swelling volumes of selected solvents. Values indicate the swollen volume of a given mass of Wang resin after excess solvent has been removed.[4]**

| solvent | swelling volume (mL/g) |
|---|---|
| NMP | 6.4 |
| THF | 6.0 |
| DMF | 5.2 |
| Dioxane | 5.6 |
| Water | 1.6 |
| t-Butanol | 1.6 |
| THF/$H_2O$ (1:1) | 2.8 |
| DMF/$H_2O$ (1:1) | 2.0 |

4.3).[4] As can be seen, all the organic solvents swell the beads to between 5.6 and 6.4 mL, while water and *t*-butanol (along with methanol and heptanes) have the distinction of being the poorest swelling solvents tested and provide only 1.6 mL/g of swollen bead. For comparison, the dry resin has a volume of 1.0 mL/g. Even 1:1 mixtures of water with THF or DMF provide poor swelling results with a volume only half that of the organic solvent alone. Consequently, it is necessary to decrease the volume of water by a significant amount. To carry out this study, THF, the solvent with the best general results from the solvent scan above, was used as solvent, and while keeping the concentration constant, the proportion of organic solvent to water was varied (Table 4.4). As the 1:1 mixture of organic and aqueous solvents is well documented and generally used, the expectation was that there would be a decrease in reaction efficiency as the values deviated from this equi-volume standard, but, surprisingly, the reaction became more facile as the volume of water was decreased. As noted previously, THF was an efficient solvent providing 88 % conversion after only 15 minutes when mixed 1:1 with water (entry i). When THF content was increased to 75 %, quantitative conversion and yields were obtained after only 45 minutes (entry ii), and at 80 % THF, the same results were obtained after only

**Table 4.4 Effect of water content in the solvent system on the reaction time, conversion and isolated yield of the CuAAC reaction between 413 and 416**



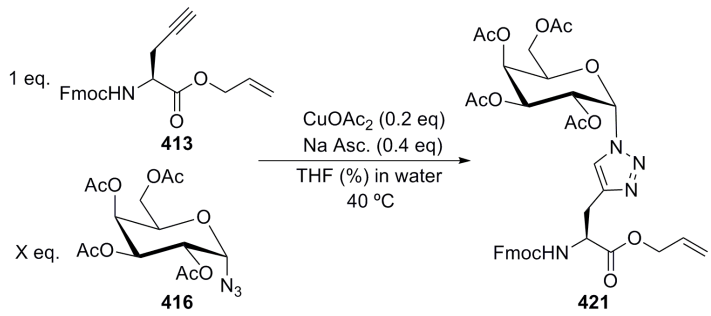

| entry | THF content (%) | reaction time (min) | yield (%) | conversion (%) |
|---|---|---|---|---|
| i | 50 | 30 | 87 | >98 |
| ii | 75 | 45 | >98 | >98 |
| iii | 80 | 15 | >98 | >98 |
| iv | 90 | 30 | 81 | >98 |

15 minutes (entry iii). At 90 % THF content, the yield decreased slightly and reaction times lengthened showing that although increased organic content is very beneficial for the reaction, this trend does have a limit (entry iv). Although 80% organic solvent should theoretically provide good swelling properties, it is of interest to increase the proportion of organic solvent even further; to accomplish this the number of equivalents of azide was increased.

### 4.4.6 Effect of azide equivalents on the CuAAC reaction.

Although the increase in THF content appears to improve reaction efficiency, above 80 % content, the isolated yields decreased. To restore the near quantitative yields, the reactions were repeated with an excess of the azide reagent. These conditions approximate those planned for the solid-phase application: the use of excess reagents is not seen as problematic or inefficient as, following the reaction, the unreacted azide should be recoverable from the reaction solution as it should be the only organic-soluble component present. Consequently, following the precedents of solid-phase peptide synthesis (SPPS), 5 equivalents of azide was deemed an appropriate amount (Table 4.5).[47] As the reaction was already optimized at 80 % THF in water, no change in the

**Table 4.5 Effect of water content and equivalents of glycosyl azide on the reaction time, conversion and isolated yield of the CuAAC reaction between 413 and 416.**




| entry | THF content (%) | azide (eq.) | reaction time (min) | yield (%) | conversion (%) |
|---|---|---|---|---|---|
| i | 80 | 1 | 15 | >98 | >98 |
| ii | 80 | 5 | 15 | >98 | >98 |
| iii | 90 | 1 | 30 | 81 | >98 |
| iv | 90 | 5 | 15 | 92 | >98 |

results was expected due to the increase in azide concentration, and the quantitative conversions and yield were maintained under the new forcing conditions (entry ii). With 90 % THF content, the reaction yield improved to 92 % yield after only 15 minutes (entry iv) when five equivalents of azide were used. This was a marked improvement over the previous results. With the excellent reactivity recovered, the conditions appeared to be optimized for this substrate. The next step was to test whether the conditions could be generalized to other glycosyl azides.

### 4.4.7 Effect of substrate on the CuAAC reaction

Two other readily accessible substrates were of considerable interest at this time, the fully deprotected analogue of azido-galactose (**417**), and the α-ethylazido derivative of galactose (**420,** Figure 4.4). The synthesis of both compounds is outlined above in Scheme 4.3. The first compound is interesting because, if the CuAAC reaction can be carried out efficiently in the presence of a fully deprotected sugar, this would alleviate the need for a deprotection step after the formation of the glycopeptide. Eliminating chemical steps on such a complicated molecule is, obviously, beneficial. The second compound was of interest as the

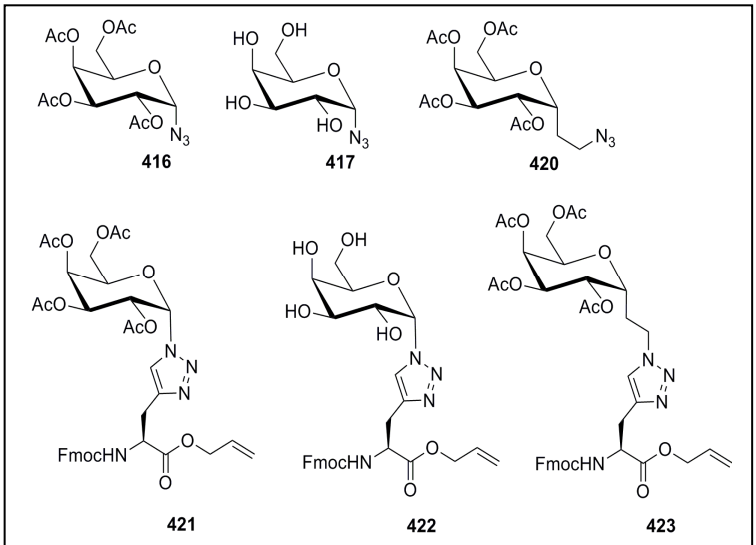
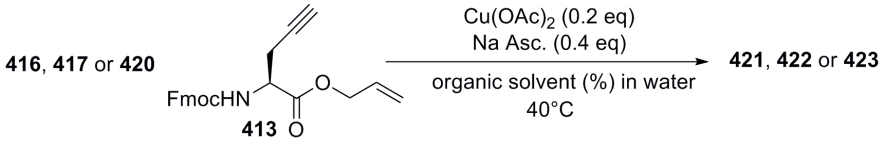



**Figure 4.4 Structures of glycosyl azides and their respective glycoconjugates examined in the substrate investigation.**

glycoconjugate formed from it and propargylglycine would have the same linker length as the highly active *C*-linked AFGP analogue **118**. The resulting glycopeptide would thus be directly analogous, as far as linker length is concerned, with **118** and would act as an initial probe into the importance of the amide bond to IRI activity. The first set of experiments carried out was to determine whether the solvent preferences of the model substrate were mirrored in the two new substrates. This was not a given as the fully deprotected sugar should be considered to have fairly different solubility properties compared with the other two substrates. These studies are outlined in Table 4.6. In short, the conditions are general. Even in the presence of two equivalents of deprotected azido sugar **417**, the CuAAC reaction is still hindered (to an even greater degree than for the acetate-protected sugar) in the presence of *t*-butanol (entry ii). It is clear that this is not an appropriate reaction system for these substrates. In NMP, dioxane and DMF (all solvents that worked very well for

**Table 4.6 Effect of the solvent system on the reaction time, conversion and isolated yield of the CuAAC reaction between 413 and 416 (pink), 417 (white), and 420 (blue).**




| entry | co-solvent | organic solvent (%) | glycosyl azide | product | reaction time (hrs) | conversion % (yield %) |
|---|---|---|---|---|---|---|
| i | tBuOH | 50 | **416** | **421** | 5 | 81 (65) |
| ii | tBuOH[a] | 50 | **417** | **422** | 6 | 52 (41) |
| iii | NMP | 50 | **416** | **421** | 3 | >98 (88) |
| iv | NMP | 50 | **417** | **422** | 6 | 93 (52) |
| v | NMP | 50 | **420** | **423** | 0.5 | >98 (85) |
| vi | Dioxane | 50 | **416** | **421** | 1 | 95 (89) |
| vii | Dioxane | 50 | **417** | **422** | 6 | 14 (7) |
| viii | Dioxane | 50 | **420** | **423** | 0.5 | >98 (72) |
| ix | DMF | 50 | **416** | **421** | 4 | 96 (76) |
| x | DMF | 50 | **417** | **422** | 6 | 22 (5) |
| xi | DMF | 50 | **420** | **423** | 0.25 | 78 (72) |
| xii | THF | 50 | **416** | **421** | 0.5 | >98 (87) |
| xiii | THF | 50 | **417** | **422** | 4 | >98 (93) |
| xiv | THF | 50 | **420** | **423** | 0.5 | >98 (93) |
| xv | THF | 80 | **417** | **422** | 2 | 95 (>98) |
| xvi | THF[b] | 90 | **417** | **422** | 4 | 82 (95) |

[a]The ratio of azide to alkyne was 2:1.
[b] The ratio of azide to akyne was 5:1.

the protected species), the deprotected compound showed very poor conversion and yields of glycoconjugate **420** (entries iv, vii, and x)**.** It is also interesting to note that in all these cases reactions were allowed to run to a maximum of 6 hours, which in some cases is several-fold longer than the time allotted for its protected counterpart **416**. These results seemed to indicate that the deprotected sugar, although reactive, was not suitable for solid-phase synthesis as the yields were too poor. However in THF, a conversion of greater than 98 % and a yield of 93 % were observed, although the reaction was slower by a factor of eight relative to the protected analogue (entry xiii). These results seem to indicate that the paucity of use of deprotected sugars for CuAAC chemistry applications in the literature is not an oversight on the part of researchers, but rather a direct result of their poor reactivity compared with their protected counterparts.

The less sterically hindered analogue **418** shows very similar reactivity compared with the initial model compound **413**, as would be predicted. Conversions and yields tend to be comparable across all solvents, with THF, once again, appearing to be the optimal solvent. As the primary azide **418** is slightly less sterically hindered than **413**, the reaction times tend to be lower, by a factor of 2-4, showing that the reaction is a little simpler with this substrate.

The solvent conditions appear general: most polar aprotic solvents perform well with the protected derivatives (better with the less hindered azide), less so with the fully deprotected derivative; *tert*-butanol, the traditional solvent is not appropriate for the CuAAC reaction between propargyl glycine and glycosyl azides raising questions as to its appropriateness for other substrate systems, and THF appears to provide the best results for all three substrates.

The final experiments carried out were to determine whether increasing the proportion of THF in the solvent system would have a similar effect on the conversion of **417** to **421** as it did on the reaction of **416** to **420**. With 80 % THF in water, under standard conditions (entry xv), **421** was obtained in 95 % yield with quantitative conversion after only 2 hours of reaction, by far the best result observed for this substrate. When the proportion of THF was increased to 90 %, however, the yield decreased to 82 % even when the reaction was carried out in the presence of five equivalents of **417** (entry xvi), consistent with the previous results observed for **416**.

Although these results implied a considerable improvement for the deprotected sugar, the protected compound provided consistently better results in a more predictable way and so it was **416** that we used in the initial attempts towards on-resin CuAAC reactions.

## 4.5 Synthesis of first generation triazole-containing *C*-glycopeptides

### 4.5.1 Initial attempts at solid-phase supported CuAAC reactions between alkynyl peptides and azido carbohydrates

For the initial syntheses, three peptides were prepared (Figure 4.5). Tetra-peptide **424** (AFGPrg) was selected as it would provide a reasonable space for the propargyl group such that it would suffer no steric effects due to the proximity of the polymer-resin's backbone. The phenylalanine residue was incorporated to provide a UV-active tag to simplify HPLC purification. A second short peptide (GGGPrg, **425**) was prepared to act as a monovalent mimic for the full Tetrameric peptide (**426**). All the

peptides were synthesized through standard Fmoc-solid phase synthesis techniques (see Chapter 3).[47] Small amounts of each peptide were cleaved from the resin to determine the yield of the synthesis and to ensure that the desired peptides were in fact formed. All three peptides were successfully synthesized in 78, 91, and 70 % yields respectively following purification by HPLC (peptides **425** and **426**) or preparative TLC (**424**). The first attempts to carry out the CuAAC reaction were made with peptide **425** and azide **416** under the optimized conditions found above (Scheme 4.4). Although these conditions led to excellent yields in solution phase with very similar substrates, they failed to lead to the formation of desired resin-supported glycoconjugate **427** after 24 hours. The reaction mixture was transferred to a sealed tube, and then heated to 80 ºC, (additional sodium ascorbate solution was added as necessary to regenerate the catalyst) but no product was identified after even 96 hours of reaction. Possible explanations were that even the small amount of water present was interfering with the appropriate swelling of the beads or that the catalyst was not able to associate with the resin bound alkyne. Although little research had been carried out at the time into solid

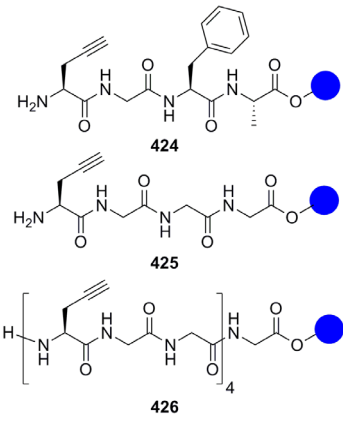
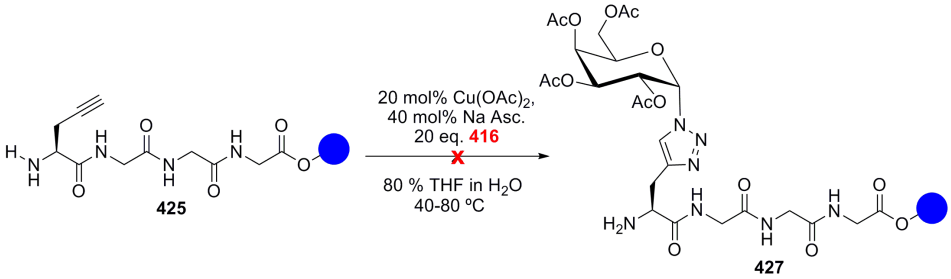



**Figure 4.5 Resin supported peptides produced for the 1st generation analogues.**




**Scheme 4.4 Initial attempt to carry out CuAAC reaction on solid phase with conventional heating.**

phase applications with this Cu (II) catalyst system (as opposed to the considerable efforts made with respect to the Meldal Cu(I)/amine base system), there were several interesting recent reports in the literature involving the application of microwave heating to the Cu (II) catalytic system.[29, 48, 49] As conventional heating had failed, this new synthetic strategy was adopted.

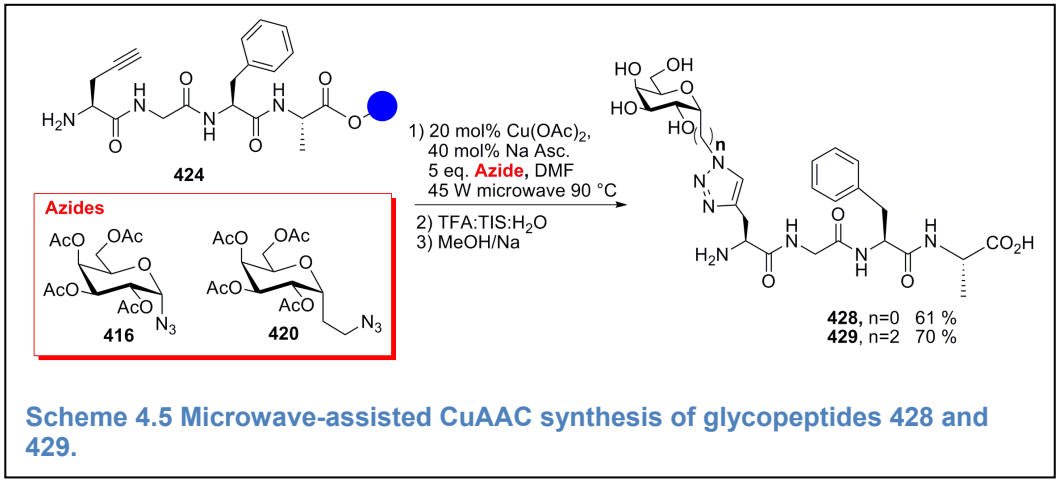
### 4.5.2 Application of microwaves to the CuAAC reaction between galactosylazides and resin-supported propargyl peptides.

In a report by Bouillon and co-workers, microwave heating at 60 ºC was used to accelerate the reaction between a galactosyl azide and a controlled-pore-glass resin-supported oligonucleotide in a 1:1 mixture of water and methanol as solvent.[29] The presence of water, so carefully excised as much as possible from the above optimized conditions, is only possible because of their choice of resin, controlled pore glass (CPG). The advantage of using CPG resins, common in oligonucleotide synthesis, but mostly unused in peptide synthesis, is that no swelling is required or even possible, consequently no ill effects are suffered as a result of the inclusion of 50 % water in the reaction mixture. No comment was made regarding the choice of microwave irradiation (as opposed to conventional heating) as a form of thermal activation in the article and there is a lively debate as to whether microwave heating differs qualitatively from equivalent conventional heating.[50]

As conventional heating failed to provide any trace of product in the reaction between **425** and **416**, showing only the untransformed peptide as the solid-supported result of the reaction (as examined by ESI-MS), microwave heating was attempted. Three reactions were attempted in parallel containing 9:1 THF: water, 9:1 DMF: water,

and 9:1 NMP: water using the optimized conditions described above with resin-supported peptide **425** and azide **416**. All three reactions were heated to 90 ºC with microwave heating at 300 W (this resulted in the microwaves being generated only about 5 % of the time as this was all the power required to maintain the temperature at 90 ºC), the reactions were filtered and beads were washed extensively with DMF, water and isopropanol.[51] The peptides were cleaved off the beads and the crude products were examined using MALDI mass spectrometry. Unfortunately no product was detected.

At this point the possibility that even a small amount of water could interfere with appropriate bead-swelling was revisited as the beads that had been removed from the reaction mixture appeared smaller to the naked eye than those that swelled in organic solvent alone. For this reason, a fourth microwave reaction was prepared with the optimized conditions; however, the solvent system was changed to anhydrous DMF, a solvent that has performed exceedingly well in solid-phase applications. The other modification was that resin-supported peptide **424** was substituted for peptide **425** as the larger mass and UV-active phenylalanine residue would facilitate the detection of product by HPLC and mass spectrometry. After the 2



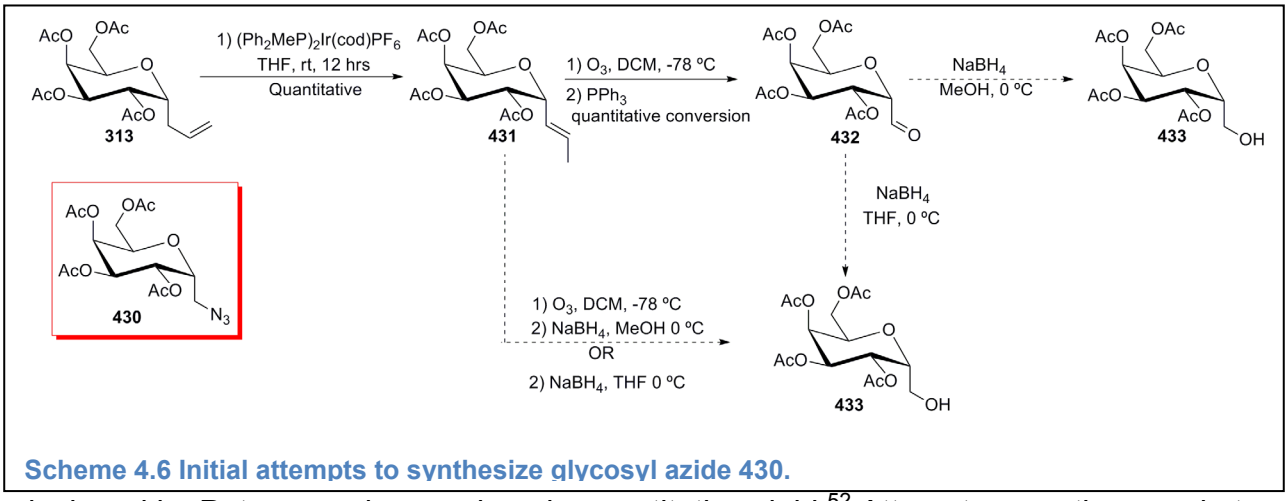

**Scheme 4.5 Microwave-assisted CuAAC synthesis of glycopeptides 428 and 429.**

hour reaction time, under these conditions, some **428** (albeit accompanied by considerable amounts of **424**) was finally observed by MALDI.

The next step was based on the observation that the beads, post-cleavage, appeared black rather than the deep orange expected from previous experience. Believing that this might be a function of too much microwave power and a possible polymerization of the beads or the peptides, the reaction was repeated exactly as before except that the reaction time was shortened to 1.5 hours and the power of the microwave was reduced to 45 Watts, or 15 % of that used previously. This power value, determined by trial and error, ensured that the microwave heating was nearly continuously applied to maintain the temperature of the reaction solvent at 90 ºC. This time the crude MALDI showed only the desired product **428**: there was no trace of the propargyl glycine starting material (Scheme 4.5). Following Zemplén deprotection and reverse-phase HPLC (reversed-phase HPLC) purification, the desired glycopeptide was obtained in 61 % yield (based on peptide loading). With this excellent result, the same resin supported peptide was treated under identical conditions with the ethyl-azido derivative **420** to provide the appropriate glycopeptide **429** in 70 % yield following deprotection and reversed-phase HPLC purification (Scheme 4.5). With these results in hand, attention turned towards the synthesis of the final glycosyl azide required for the synthesis of the tetrameric glycopeptides.

### 4.5.3 Synthesis of azide derivative 430

To complete the study, a third glycosyl azide, **430**, was designed and synthesized according to the process outlined below in Scheme 4.6 . The *C*-allyl galactose derivative **313**, was isomerized to the internal olefin **431** using the conditions




Scheme 4.6 Initial attempts to synthesize glycosyl azide 430.

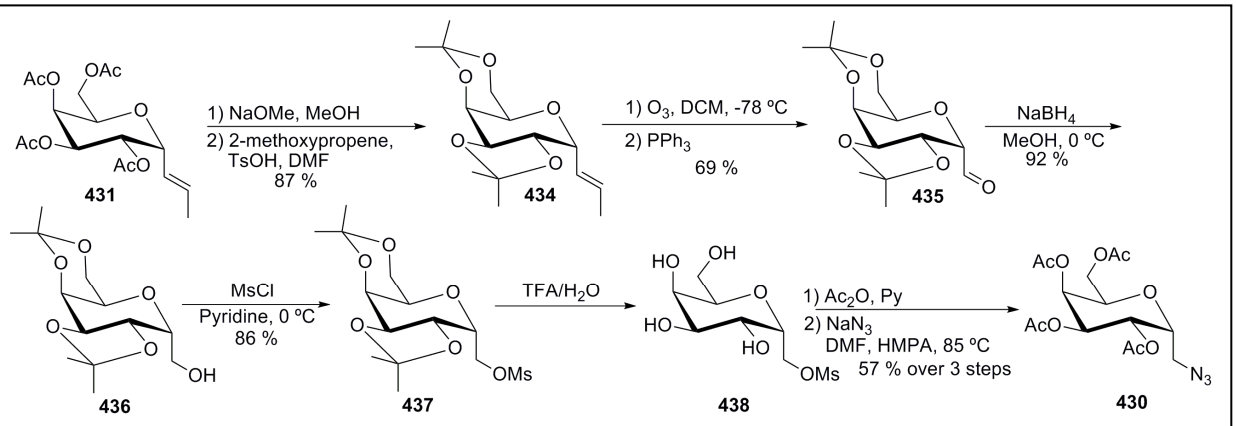
designed by Patnam and co-workers in quantitative yield.[52] Attempts were then made to oxidatively cleave the olefin to generate aldehyde **432**. Although this did succeed and the aldehyde was obtained, the presence of the acetyl protecting groups made the compound anomerically unstable and it would readily epimerize to the β anomer in the presence of silica gel (either through an acidic-catalyzed mechanism in the un-treated form, or presumably a base-catalyzed mechanism if the silica was pre-neutralized with triethylamine and the column executed with 0.1 % triethylamine in the eluting solvent). If the compound was left unpurified by chromatography (the bulk of the excess triphenylphosphine could be removed through trituration with hexanes, and the bulk of the triphenylphosphine oxide could be removed through precipitation from diethyl ether) attempts to reduce the material using sodium borohydride in methanol failed to produce the desired product (**431**) cleanly. A mixture of at least four compounds was present,

including at least the two major compounds that had become anomerized to the β-configuration; most likely the mixture was complicated by acetate migration under the weakly basic conditions. Attempting to carry out the reaction in THF as solvent is known to be much slower than in protic solvents, but it was hoped that this solvent would help suppress acetate migration through the elimination of the possibility of the formation of catalytic methoxide. However, even under these conditions the reaction produced a complex mixture of compounds.

These attempts having failed, direct reduction of the ozonide without treatment with triphenylphosphine was attempted. Following the initial oxidation of the olefin, the ozone was removed by saturating the solution with nitrogen. The solvent was then diluted by a factor of two by the addition of either methanol or THF. Sodium borohydride was then added portion-wise to provide a reductive work-up and an *in situ* reduction of **432** to **433**. In the case of methanol, the reaction resulted in a complex and inseparable mixture of products. In the presence of THF, the major product appeared to be the β-anomer, showing that even under aprotic conditions the compound was not configurationally stable. With the failure of this route to **433**, an alternative approach needed to be explored.

To avoid these two complications, the 2-propenyl derivative **431** could be reprotected with isopropylidenes rather than the problematic acetate groups (Scheme 4.7). Thus, Zemplén deacetylation followed by isopropylidene protection under kinetic conditions (using 2-methoxypropene) led to the formation of di-isopropylidene protected **434** in 87 % yield over the two steps. Ozonolysis followed by reductive work-up with triphenylphosphine provided crude product that could be purified by flash

chromatography to provide aldehyde **435** in 69 % yield. None of the β-anomer was



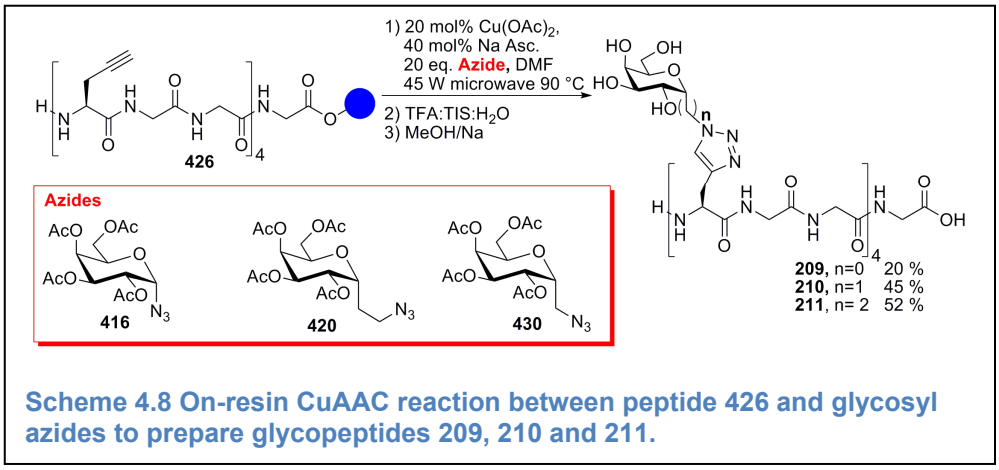

**Scheme 4.7 Synthesis of methylazido galactose derivative 430.**

detected, clearly implicating the electron withdrawing properties of the acetate protecting group for the failure of the earlier synthetic sequence. It is important to note that although **435** is anomerically stable, the isopropylidene groups on it and the following compounds are extremely labile in the presence of acidic silica. Consequently all silica required pre-treatment with triethylamine to avoid the loss of the bulk of the material during the purification stages. Reduction of **435** with sodium borohydride under standard conditions cleanly reduced the aldehyde to alcohol **436**, again with complete retention of anomeric configuration, in 92 % yield. Treatment with methanesulfonylchloride in pyridine provided sulfonic ester **437** in 86 % yield following chromatography. Attempts to substitute an azido functionality for the mesylate failed at this stage: a mixture of starting materials and partially deprotected sugars were all that were recovered from treatment of this compound with sodium azide at 80 ºC for up to 24 hours. This is possibly due to steric effects of the isopropylidenes interfering with the approach vectors for the azide nucleophiles. Due to their lability under acidic conditions

(including column chromatography), isopropylidenes were not considered a preferred system for protecting the hydroxyl groups during the upcoming CuAAC reactions; acetates are far preferable for this application. Consequently, the protected mesylate was treated with a 4:1 mixture of TFA: water, quenched with triethylamine, and following concentration, to provide crude sugar **438** in 60-68 % yield. This compound was then reprotected in the normal fashion before being directly treated with sodium azide in DMF with HMPA as co-solvent: HMPA selectively solvates cations, destabilizing their associated anions and consequently is known to accelerate $S_N2$ reactions. Unlike in the case of isopropylidene groups, the reaction proceeds smoothly with azide groups present resulting in formation of desired azide **430** in 57 % yield over three steps from the isopropylidene protected mesylate following recrystallization from diethyl ether and hexanes. This sequence provided the final sugar required for the synthesis of the desired glycopeptides.

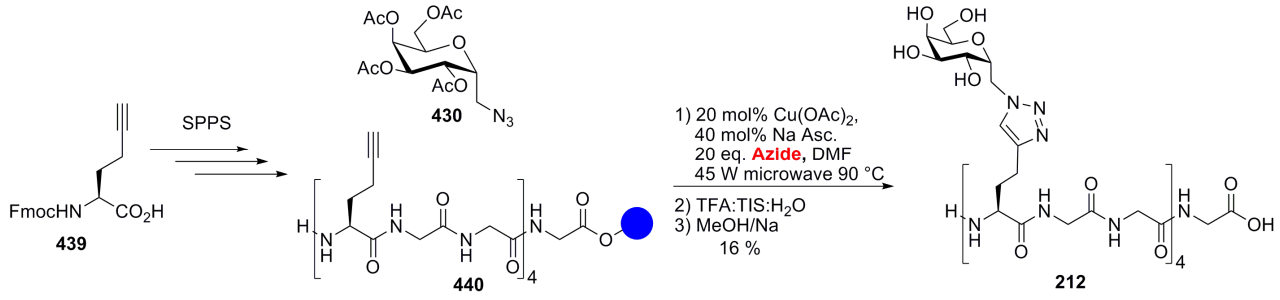
### 4.5.4 Synthesis of 1st generation glycopeptides using the on-bead CuAAC reaction

With all three glycosyl azides available, resin-supported peptide **426** was subjected to the conditions described above with the three azido carbohydrates. The syntheses progressed very cleanly, as




**Scheme 4.8 On-resin CuAAC reaction between peptide 426 and glycosyl azides to prepare glycopeptides 209, 210 and 211.**

expected, and all three glycopeptides (**209**, **210**, and **211**) were purified using reversed-phase HPLC, providing the peptides in 20, 54, and 45% respectively. These three glycopeptides, along with a fourth produced by Dr. Mathieu Leclère (**212** from peptide **440** and protected amino acid **439**, Scheme 4.9), were examined by CD spectrometry, and then tested for TH activity using nanolitre osmometry and IRI activity using the splat-cooling assay.




**Scheme 4.9 Application of the synthetic conditions and glycosyl azide 430 to the synthesis of glycopeptide 212 by Dr. M. Leclère.**

## 4.6 Assessment of the conformation of the first generation triazole-containing analogues using CD

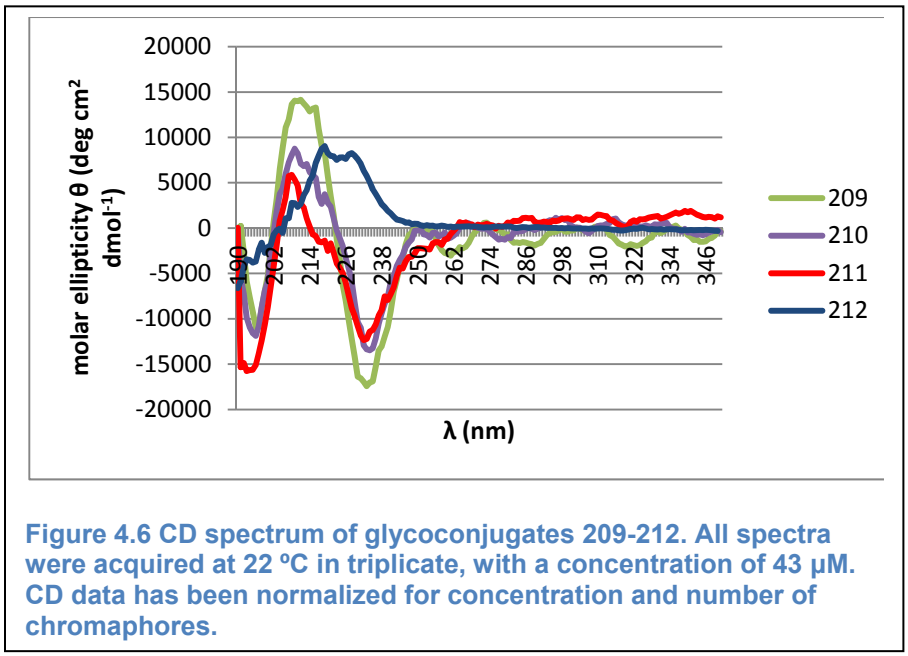



**Figure 4.6 CD spectrum of glycoconjugates 209-212. All spectra were acquired at 22 ºC in triplicate, with a concentration of 43 µM. CD data has been normalized for concentration and number of chromaphores.**

The solution conformations of the above glycoconjugates were analyzed using CD spectrometry. All samples were prepared at 43 µM in micropore-filtered distilled water, and all data was collected on a JASCO 810 spectrometer. The spectra for the analogues are presented in Figure 4.6. All three glycopeptides based on the propargyl glycine backbone share similar spectra with local minima at 235 nm and 198 nm, and a local maximum at 209 nm. The local minima at 235 nm is not consistent with the spectrum of any common

secondary structure, while the local maximum at 209 nm is consistent with random coil and β-turn structures, while the final minimum at 198 nm is similar to that found in random coils and polyproline type II helices.[53] The compound based on the butynyl glycine backbone has a considerably different spectrum, with the only distinctive feature being a very broad positive band between 205 and 245 nm. This feature is found in random coiled structures.[54-57] However, the deconvolution of these spectra, performed using CD Pro (and the included algorithms SELCON3, CONTINLL and CDSSTR)[55, 58] suggests that all four glycopeptides adopt a similar secondary structure. They are mostly random coil with the possibility of localized β-sheet conformations and smaller contributions from β-turns and polyproline type II helices. Like most previous data, the amount of α-helix is negligible.[11, 59-62] This is consistent with the previous reports that α-helices are not an important structure in AFGPs.[63, 64] Of course, caution must be taken when interpreting these CD spectra results as very little research has been carried out into the CD spectra of triazole containing peptides,[35] let alone glycopeptides, so the effect that triazoles may have by interacting with the amide backbones is currently unknown. However, as far as can be seen, the gross conformation of the triazole-containing *C*-AFGPs does not, to any great extent, deviate from that of highly IRI active

**Table 4.7 CD deconvolution data for triazole containing *C*-AFGPs, AFGP-8 and active amide analogue 118. Data was calculated using CD Pro IBASIS 5 and form an average of the values produced from three different deconvolution algorithms.**

| glycopeptide | α Helix | β sheet | β Turn | PP II helix | Random Coil |
|---|---|---|---|---|---|
| **209** | 0.011 | 0.2975 | 0.1435 | 0.1225 | 0.4275 |
| **210** | 0.022 | 0.2505 | 0.1445 | 0.1125 | 0.469 |
| **211** | 0.0135 | 0.2855 | 0.1345 | 0.107 | 0.4555 |
| **212** | 0 | 0.358 | 0.093 | 0.193 | 0.356 |
| **102 (AFGP-8)** | 0.146 | 0.189 | 0.152 | 0.122 | 0.432 |
| **118** | 0.162 | 0.175 | 0.071 | 0.055 | 0.573 |

**118** or even AFGP-8 itself and is not in itself responsible for any difference in antifreeze activities.

## 4.7 Assessment of antifreeze activity of first-generation triazole-containing analogues

### 4.7.1 TH and dynamic ice shaping ability of the triazole-containing glycopeptides

As described above, the previous generations of *C*-linked antifreeze analogues have not expressed measurable TH activity,[10, 11, 60] with the exception of two lysine derivatives with small TH gaps (approximately 0.6 ºC at 10 mg/mL).[65] Some have, however, shown dynamic ice shaping. Analogue **118** for example, produced hexagonal crystals, implying some interaction with the ice lattice.[66]

The protocol for the TH measurement is identical to that described in Chapter 3 above, with the solution being examined at 10 mg/mL using nanolitre osmometry.[67] Freezing points were depressed relative to pure water solutions, consistent with previous measurements from our laboratory, but there was no selective freezing point depression observed. Furthermore, no dynamic ice shaping was seen in any of the analogues: ice crystals adopted their natural spherical shape, consistent with solutions without THCs. These effects were expected and the lack of TH activity is consistent with the data seen for other *C*-linked analogues.

### 4.7.2 IRI activity of the first generation triazole-containing glycopeptides

The compounds were then screened for IRI activity using the splat cooling assay in the manner described above in Chapter 3.[68-70] As discussed in the introduction, the special property of the *C*-linked AFGPs is their capacity for IRI activity independent of TH activity. As per the previous results from Dr. Tam and Dr. Liu,[10, 11] the hypothesis was that deviation from the "ideal" chain length would result in a decrease in IRI activity. The insertion of the triazole for the amide would also be expected to have an impact if either the orientation or hydrogen-bond capability of the amide is important. If the importance of the amide bond is simply its ability to increase the rigidity of the linker, then the activity of analogues (**211** and **212**) would be expected to be similar to that of **118**.

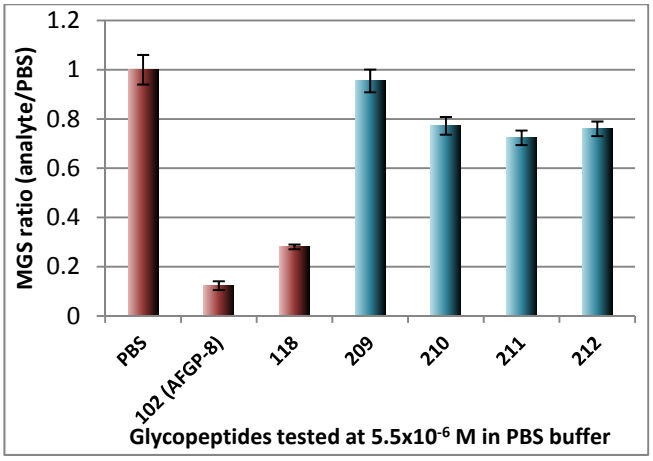



**Figure 4.7 IRI activity of 1st generation triazole analogues (blue) compared to AFGP-8, PBS and active amide-containing analogue 118 (red).**

As can be seen in Figure 4.7, the newly generated analogues do not have IRI activity comparable with that of amide analogue **118**. However, it is interesting to note that activity improves slightly as the chain length grows longer, from 4 atoms in the peptide/carbohydrate linker of analogue **209**, to 5 atoms in the linker of **210**, and then to 6 atoms in the linker of **210,** to 6 atoms in the linker of **211** and **212**. However, this activity is weak relative to that of either analogue **118** or **102** (AFGP-8), indicating that inversed-triazole substitution with these linker lengths was detrimental to IRI activity.

## 4.8 Comparison of IRI activity of the first generation triazole *C*-AFGPs with amide derivatives and peptoid triazole-containing derivatives

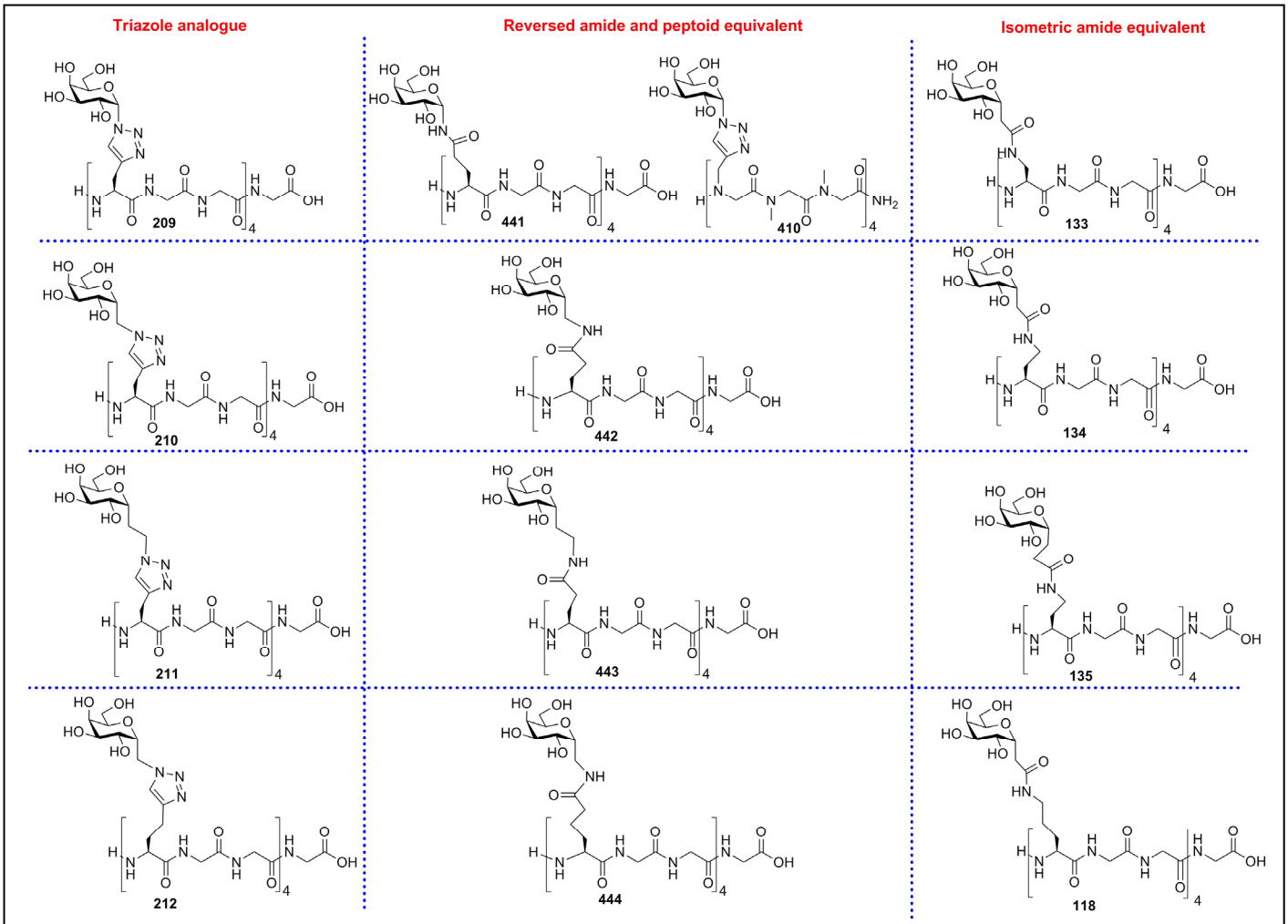



**Figure 4.8 1st Generation triazole-containing *C*-AFGP analogues (209-212) and their reversed amide-containing (441-444), peptoid (410) and amide-containing homologues (118, 133-135).**

Taking a closer look at the structural relationship of these analogues can help explain this trend in activity. These results can be compared to the previously prepared analogues (**118**, **133-135**, Figure 4.8)[11, 60, 62] and can also be compared to the triazole-containing glycopeptides generated by the Brimble and Sewald groups (Figure 4.8).[3, 8]

The analogues produced by the Brimble group were not examined for IRI activity, while the report from the Sewald group includes a quantitative examination of the IRI activity of their compounds using a variant of the capillary method. The size of the ice crystals in the presence of the peptides, 1 mM in 40 % aqueous sucrose, was compared to those in a control solution (40 % sucrose) and a solution of $PVA_{5800}$. The ice crystals in the presence of their peptoid antifreezes did not differ from the size of the ice crystals in their positive (for ice recrystallization) control, demonstrating that these compounds showed no IRI activity (no dynamic ice shaping was observed either).[3] These glycopeptoids from the Sewald group were tested at a much higher concentration (1 mM) than the triazole-containing glycopeptides produced in this study (5.5 μM), so there is scant possibility that the peptoid analogues, when further diluted by a factor of 20 (to bring them in line with the glycopeptides in this study), would express any activity. Fortunately, analogue **209**, with the anomeric triazole group is a direct mimic of one of these peptoid compounds (**410**). The glycopeptoids showed no discernable IRI activity (although the ice crystals in the sample are slightly smaller than those in the PBS control, the difference is well within the error range of the two values). Similarly, the amide containing equivalent of this compound, **133,** (Figure 4.9) also shows very poor activity.

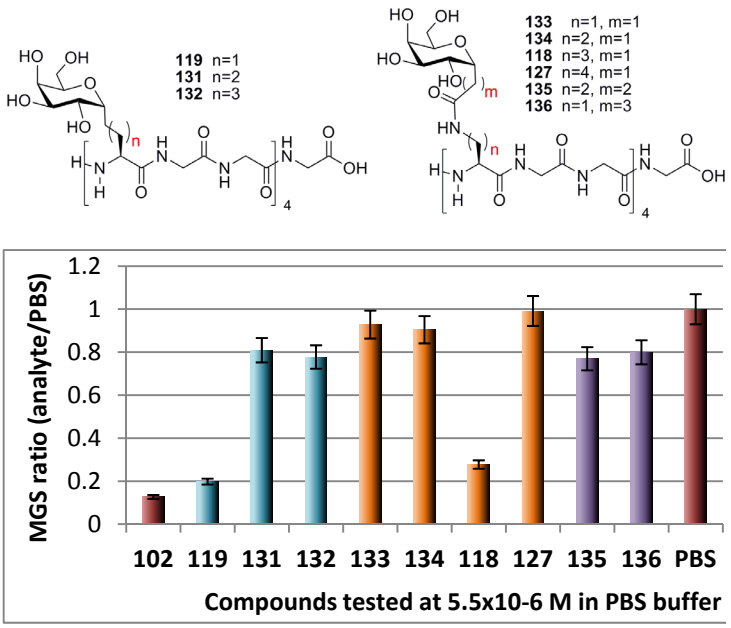



**Figure 4.9 IRI activity of the 2nd generation amide and *C*-serine analogues with various linker lengths.**

The activity of analogues (**210**, **211**, and **212**) improves as the chain length becomes longer. It is notable that analogue **210**, is more active than the amide analogue of the same chain length (**134**), whereas analogue **211** and **212** are considerably less active than their isometric companion, the very active amide analogue, **118**. However, the activity of **211** and **212** is similar and even slightly better than that of **135** or **136**. These two analogues have the same linker length as both **211** and **212**, and also **118**, but their amide bond has been shifted one or two atoms closer to the peptide (Figure 4.8, Figure 4.9). This seems to indicate that it is not only the presence of an amide in the side-chain that is important, but also its exact position relative to the backbone and the carbohydrate linker, and that simply having a linking functionality at this position is insufficient; however, the direct analogues of the newly synthesized compounds would include a reversed-amide bond (**441**-**444**). Unfortunately, to this point, none of the reversed amide bond analogues have been synthesized, although the perbenzylated derivative of **444**, the direct reversed-amide analogue of **118**, has been prepared, but attempts to deprotect the glycoconjugate failed. Consequently no comparison can be made with these analogues.

It is important to note that in the case of these first generation analogues, the dipole moment of the triazole is inverted relative to the amide bonds of previous *C*-linked AFGP analogues (Figure 4.8). Consequently, the inversion of the functionality may be responsible for differences in activity between the triazole containing analogues and the amide analogue **118**. Regardless, the length of the linker appears to be a good predictor for IRI activity: the triazole analogues appear to all have similar IRI activity as their isometric amide counterparts. The only exception to this rule, as always, is amide analogue **118** whose activity is much better than predicted by chain length alone.

## 4.9 Summary of results for 1st generation triazole-containing analogues

This first part of the study has provided several useful results, and has recently been published.[38] Firstly, a systematic optimization study was performed showing that not only is the *t*-butanol/water system not necessarily the ideal solvent system for the CuAAC reaction, but it was in fact the poorest solvent system tested; likewise, rather than a 50: 50 mixture of aqueous and organic solvent that have traditionally been used to carry out the reaction, an 80:20 mixture appears to work better; a full substrate scan with a variety of different azides and alkynes would possibly show the generality of these conditions for a wider variety of compounds. Secondly, a rapid and easy approach to glycoconjugates through the development of an on-resin CuAAC protocol was provided. This approach greatly streamlines the synthetic process as the SPPS can be carried out with simple amino acids, and each resin-bound peptide can be used for several different glycoconjugate syntheses. This strategy should be compared to the

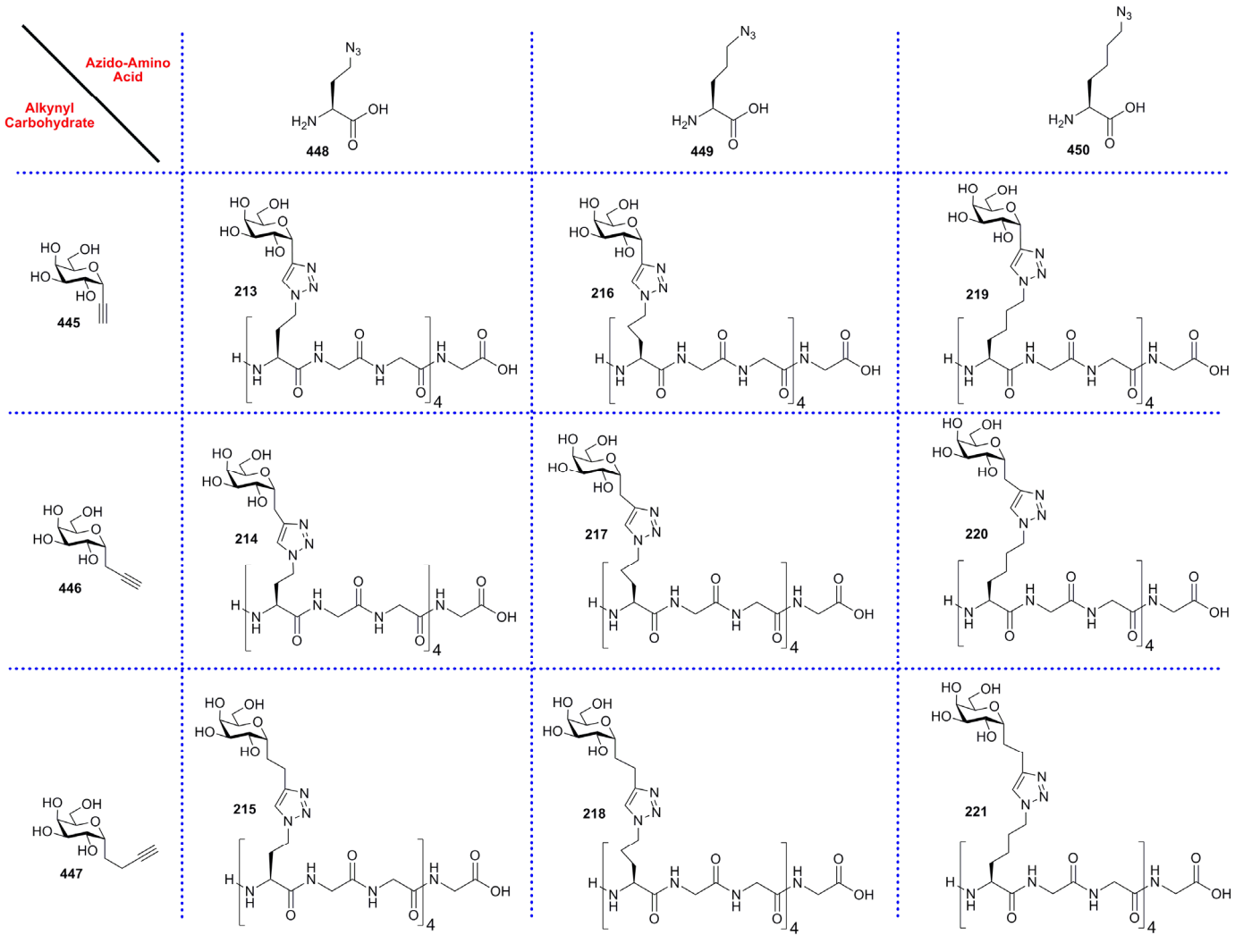
original glycoconjugate strategy where each glycoconjugate building block must be prepared separately. Finally, the prepared glycoconjugates were analyzed for IRI activity. Consistent with the previous reports,[10, 11] linker length is closely correlated with IRI activity: as the chain length is shortened relative to an ideal length, IRI activity rapidly decreases. However, triazole-containing analogues **211** and **212**, although approximately isometric with highly IRI active analogue **118**, are much less active. In the case of analogue **211**, a direct analogue of amide analogue **135**, the loss of IRI activity may be due to the shifting of the position of the linker (as both triazole-linked **211** and amide-linked **135** have similar IRI activities), but analogue **212** is an exact analogue (except for the reversed dipole moment of the triazole relative to the natural amide **118**, Figure 4.8) of highly IRI active glycopeptide **118**. The question thus arises as to whether it is the lack of a hydrogen bond donor or whether it is the inverted nature of the triazole that leads to the decreased activity of these triazole analogues relative to **118**. To explore these questions, a 2$^{nd}$ generation of triazole analogues was envisioned in which the triazole functionality is oriented with the same directionality (thus reversed relative to those in **209**-**212**) as the amide bond in **118**.

## 4.10 Design of 2$^{nd}$ generation triazole-containing analogues

The second generation analogues, unlike the 1$^{st}$ generation which were more of a proof-of-concept study, are designed to specifically imitate and mimic highly-active IRI analogue **118**. As such, the only modification is the replacement of the amide bond with a triazole while maintaining the same directionality of the dipole moment. Consequently, this requires the azido functionality to be present on the amino acid, and the alkyne

functionality to be present on the carbohydrate coupling partner. As the resin-supported CuAAC protocol developed previously was so robust and appropriate to divergent syntheses, this scaffold also makes an excellent tool for examining questions regarding the importance of the length of linker and the importance of the position of the triazole functionality relative to the peptide and carbohydrate moieties. Consequently nine triazole-containing glycopeptides were envisioned (**213**-**221**) as described in Chapter 2, through the conceptual combination of 3 glycosyl alkynes (**445**-**447**) and

**Table 4.8 Nine 2nd generation triazole-containing *C*-AFGP analogues derived from three resin-supported glycopeptides and three galactosyl alkynes.**

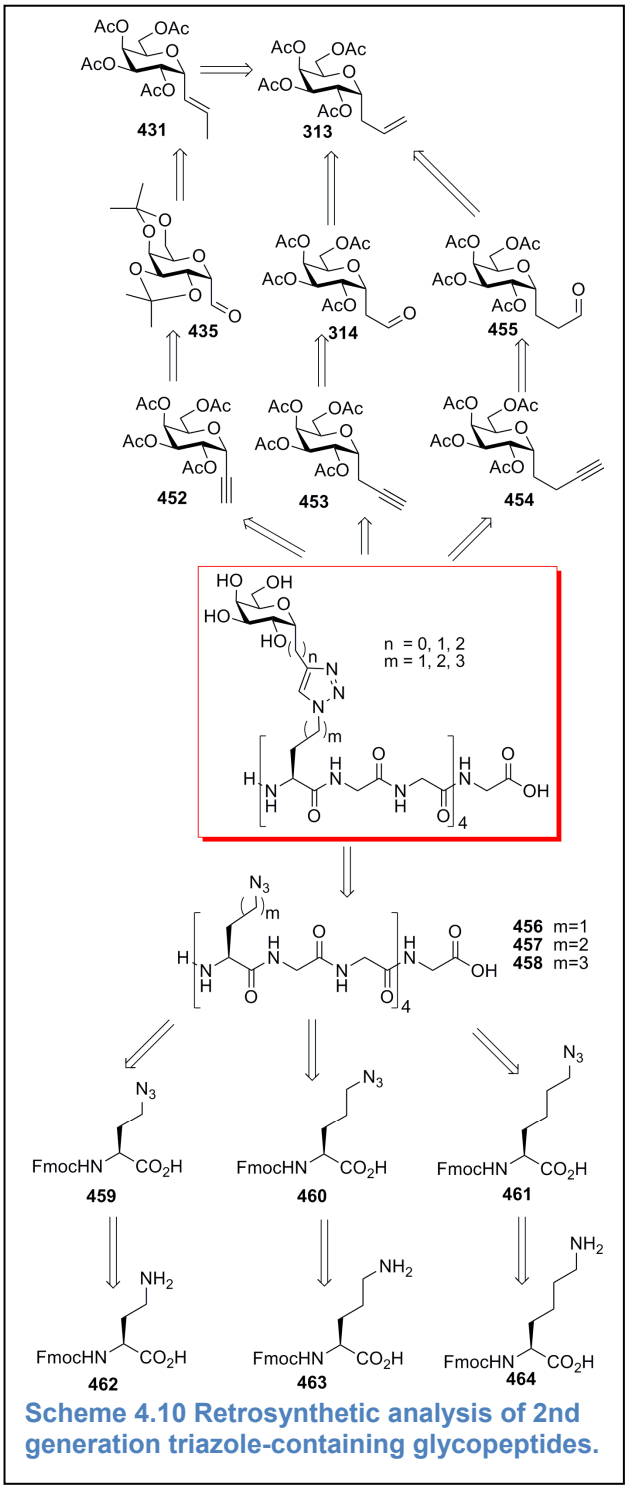


three azido-peptides (**448**-**450**, Table 4.8). All nine analogues could arise from three resin-supported peptides and three alkynyl *C*-galactosides. Rather than constructing nine separate glycoconjugates and carrying out nine separate solid-phase syntheses, these analogues can be accessed from only three solid phase syntheses; furthermore, no glycoconjugates need to be synthesized and purified prior to the SPPS steps. This provides for a much more rapid and simple process for the preparation of these compounds. Likewise, as simple SPPS can provide tridecamers (the required length in this case) in very high yield, it was felt that this approach, rather than the lower yielding syntheses involving glycoconjugates, may provide peptides in high enough purity that no HPLC purification would be necessary. As the purification step is the most detrimental to the final isolated yield, avoiding it would not only imply a high conversion in all reactions, a laudable goal on its own account, but should also allow for a considerably higher isolated yield. However, to achieve this goal, both the azido-peptides and the alkynyl carbohydrates needed to be prepared.

## 4.11 Synthesis of 2nd generation triazole AFGP analogues

One of the objectives of this research was to streamline the synthesis of glycopeptides and consequently, methodologies were sought that could make use of general reaction conditions or common starting materials to simplify the preparation of the desired targets: rather than designing all glycoconjugates *de novo*, divergent methodologies are preferable. Consequently, the retrosynthesis was planned as shown in Scheme 4.10. This strategy envisions a common pathway for the preparation of the Fmoc-protected azido amino acids for SPPS (**459**-**461**). In the case of the glycosyl

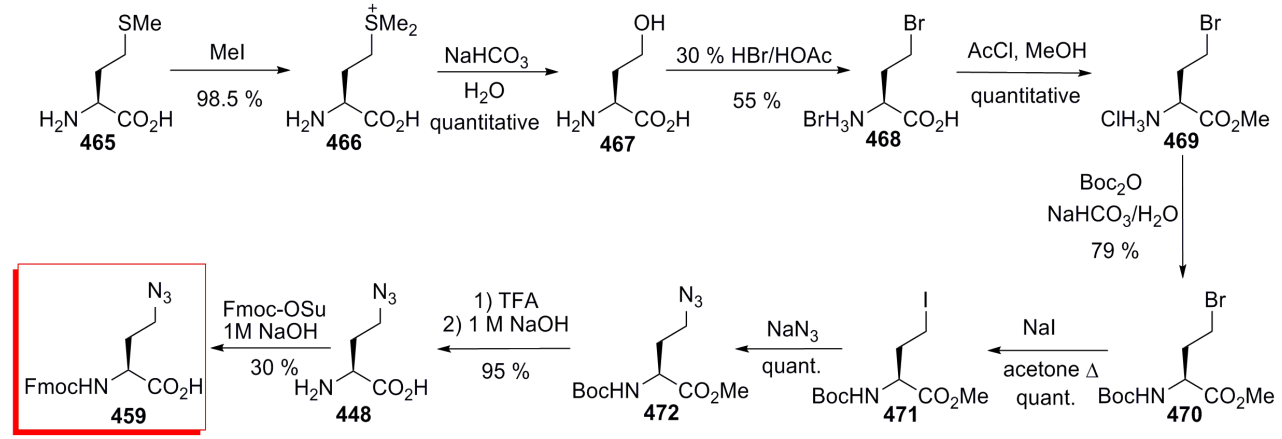
alkynes (**452**-**454**), all three compounds can be synthesized *via* the Ohira-Bestmann reagent from their respective aldehydes, **435**, **314**, and **455**. Aldehyde **435** could be prepared as described above in Scheme 4.7. Aldehyde **314** has been commonly prepared in our lab, as seen in Chapter 3, and is an intermediate in the synthesis of **118** and related glycopeptides. Finally aldehyde **455**, first synthesized by a former colleague, Dr. Suhai Liu, towards the synthesis of *C*-serine derivatives such as **119**, can be derived from a selective oxidation of **313**. Therefore, all three sugars can be derived from *C*-allyl-galactose derivative **313** allowing for an efficient divergent synthesis with a common key step of an oxidative homologation of the aldehydes to their respective alkynes. However, before exploring the synthesis of the sugars, attention was first turned to the preparation of the peptides and their amino-acid precursors.




**Scheme 4.10 Retrosynthetic analysis of 2nd generation triazole-containing glycopeptides.**

### 4.11.1 Synthesis of amino acid building blocks

Although all three azido-amino acids can be derived from their respective amine side chain roots, this strategy is only efficient for lysine derivative **460** and ornithine derivative **461**. In both of these cases, the root amino acid is readily available. The third amino acid, (*S*)-2,4-diamino-butyric acid, is not naturally found in nature and is not



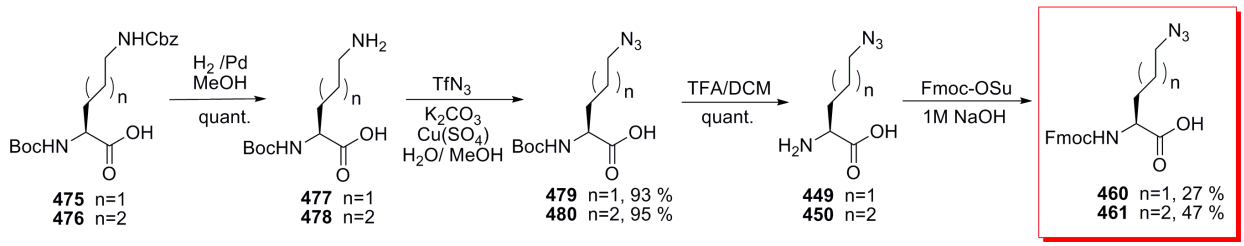

**Scheme 4.11 Synthesis of azido amino acid 459 from methionine.**

commercially available at a reasonable price. Consequently, this amino acid was synthesized from methionine according to modified published protocols as shown in Scheme 4.11 .[71-74] Methionine was *S*-methylated to methyl sulfonium salt **466** using 3 equivalents of methyl iodide at 40 ºC. Recrystallization from ethanol and water provided the salt in near quantitative (98.5 %) yield after two crops. The sulfonium was selectively hydrolyzed in a refluxing solution of sodium bicarbonate. This step required careful attention in order to maintain the pH between 5 and 2 to ensure that the solution remained sufficiently basic to allow for the reaction to take place, but sufficiently acidic to maintain the selectivity. L-Homoserine, **467**, was isolated in quantitative yield following lyophilization of the precipitate recovered through recrystallization of the crude

reaction mixture from water, ethanol and acetone. The terminal hydroxyl group was converted to a bromide through an acid catalyzed bromination in a sealed tube at 110 ºC. The product, bromide **468**, was recovered following diethyl-ether assisted precipitation from the reaction mixture in 55 % yield. Further crops of crystals were contaminated with starting material and although recovered, were not repurified due to time constraints. According to the report of Le Chevalier Isaad and coworkers,[73] brominated salt **468** should be methylated through treatment with HCl in methanol (1:3) in two hours at ambient temperature. However, this protocol failed to provide the desired ester **469** even at elevated temperatures (40-50 ºC). Consequently, the compound was esterified using acetyl chloride in methanol at 0 ºC to ambient temperature, in 30 minutes to provide chloride salt **469** in quantitative yield following concentration. This compound was protected with a Boc group and for the first time in the sequence, this intermediate, carbamate **470**, was purified through chromatography to provide the desired compound as a thick oil in 79 % yield. A Finkelstein reaction provided iodide derivative **471** in quantitative yield that was then in turn subjected to sodium azide to allow access to the desired azido derivative **472** in quantitative yield. Deprotection of both the amino and carboxyl protecting groups proceeded smoothly under standard conditions to generate the desired deprotected azido-amino acid **448** in 95 % yield. Unfortunately, the Fmoc protection, required for SPPS, was more complicated than expected and the product, **474**, was contaminated with Fmoc-OSu, and a minor unidentified amino-acid impurity. The reaction conversion was near quantitative, but due to extensive purification through crystallization, silica chromatography and finally HPLC, the desired pure Fmoc amino acid was only isolated

in 30 % yield. Due to time constraints, the reaction was not optimized, although this transformation should result in a considerably higher recovery of pure product. Regardless, purified **459** was obtained in a sufficient scale for the requirements of the planned SPPS.

As briefly mentioned above, the preparation of the ornithine and lysine derivatives was considerably more straightforward. Both amino acids are commercially available with a series of different substitution patterns for the protecting groups. The

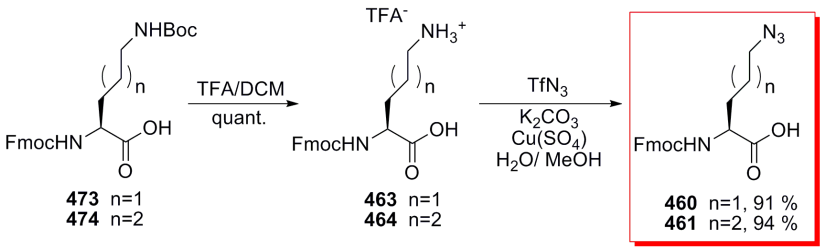



**Scheme 4.12 Initial synthesis of Fmoc-protected azido lysine (461) and ornithine (460) derivatives.**

more inexpensive Boc/Cbz derivatives (**475** and **476**) were first used for the synthesis of the desired Fmoc-protected azido derivatives as shown in Scheme 4.12. This synthesis is carried out in the manner described by Le Chevalier Isaad and co-workers except that a larger excess of triflic azide (prepared according to Nyffeler)[75] was employed in the azido-transfer reaction to ensure complete conversion.[73] Hydrogenolysis of commercially available Cbz derivatives **475** and **476** under standard conditions at ambient temperature and pressure produced the deprotected derivatives **477** and **478** in quantitative yield. These compounds were then treated with freshly prepared triflic azide (2.4-2.7 eq.) in the copper-catalyzed azido-transfer reaction to provide the Boc-protected azide derivative of lysine, **480**, and ornithine, **479**, in 95 and 93 % yields respectively. The compounds were deemed sufficiently pure and required no further

purification at this stage. To prepare these compounds for SPPS, the Boc group was removed under standard conditions (and in quantitative yield) to provide the azido amino acids **449** and **450**. Again, however, the Fmoc protection was more complex than expected and extensive purification was required (including recrystallization, dry vacuum chromatography and finally, reversed-phase HPLC) to provide **483** and **484** in a sufficiently pure form (27 and 47 % respectively), without contamination from Fmoc-OSu or a minor amino acid impurity, so that they can be used for SPPS. Unfortunately, the approximately 1 g of material recovered was insufficient for the scale of the SPPS synthesis desired, and consequently, rather than expend more material, or time, on an inefficient process, an alternative was sought.

Fmoc/Boc protected derivatives **473** and **474** are common precursors for glycopeptide syntheses. Although moderately more expensive than **475** and **476**, it was felt that removing the inefficient Fmoc-protection step from the synthesis might result in not only a more efficient process in terms of conversions and preparative time, but because of these savings, the synthesis might also be more cost-effective as well. Consequently, as seen in Scheme 4.13, commercially available **473** and **474** were deprotected under standard conditions to provide Fmoc-protected derivatives **463** and **464** in quantitative yield. These TFA salts were then treated with triflic azide, under the conditions described above except excess



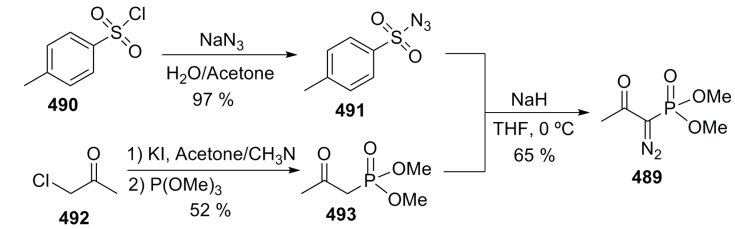

**Scheme 4.13 Alternative synthesis of Fmoc-protected azido-lysine and ornithine derivatives 460 and 461.**

potassium carbonate was added to compensate for the protonated side-chains. Following flash chromatography the two derivatives, **460**, and **461** were isolated in 91 and 94 % respectively, providing 1.52 and 1.60 g of material respectively, more than sufficient for the SPPS requirements, and in considerably higher yields than expected. All three amino acids were then available in sufficient scale for the desired studies; consequently attention turned towards the synthesis of the glycosyl alkynes.

## 4.11.2 Synthesis of glycosyl alkyne building blocks

### *4.11.2.1 Preparation of the Ohira-Bestmann reagent 489*

The key step in the synthesis of all three glycosyl alkynes is the modified Seyferth-Gilbert homologation using the Ohira-Bestmann reagent (**489**).[76] The reagent is commercially available, but sources are limited and costs are not negligible.[77] Consequently, the compound was synthesized *de novo* (Scheme 4.14). *para*-Toluenesulfonyl chloride, **490**, was treated with sodium azide to create sulfonyl azide **491** in near quantitative yield (97 %). This azide is surprisingly stable, but should, under no circumstances, be heated above 120 ºC. Simultaneously, chloroacetone, **492**, was treated with potassium iodide for a Finkelstein reaction in acetone/acetonitrile. The iodide intermediate was treated *in situ* with trimethylphosphite to afford the desired phosphonate **493** in moderate (52 %) yield. The phosphonate was deprotonated with sodium hydride and

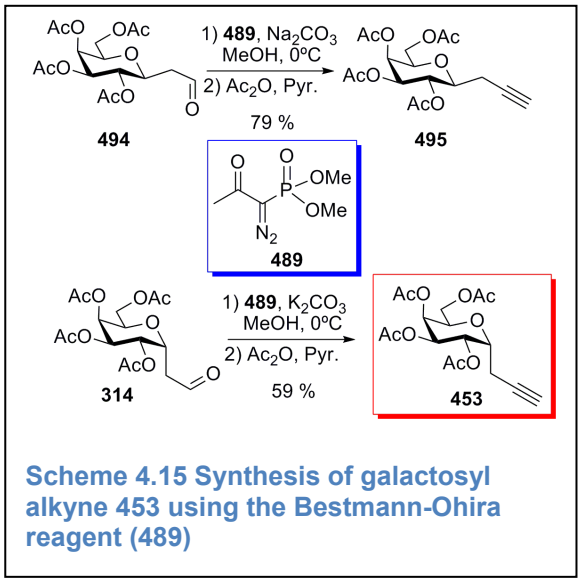



**Scheme 4.14 Synthesis of the Ohira-Bestmann reagent. Phosphate 489 was prepared according to the protocol of Pietruszka and Witt,[1] and tosyl azide is prepared according to Pollex.[9]**

the anion was quenched with the tosyl azide to generate the Bestmann-Ohira reagent **489** in 65 % yield following distillation under reduced pressure. This procedure rapidly provided 9.2 g of the desired reagent.

### *4.11.2.2 Synthesis of C-propargyl galactoside 453*

The first glycosyl alkyne to be attempted was the most easily accessible: propargyl galactose **453**. This compound should be obtainable following homologation of aldehyde **314**, whose synthesis is described in Chapter 3. A similar compound (**495**) had been prepared by René Roy's group in their synthesis of galectin inhibitors.[78] However, their synthetic protocol was not repeatable, and resulted in a complex mixture of products in very low yield in the desired transformation of **314** to **453**. The only structural difference between the two aldehydes is that the one employed by Giguère and co-workers was β-oriented, while the aldehyde in the current case is of an α-configuration. From close inspection of their experimental protocol, two concerns arose. In place of potassium carbonate, they employed sodium carbonate. This is not in and of itself of great concern; however the less reactive sodium salt could account for some of the variability between the successes of the two protocols and is rarely used in the Ohira-Bestmann system. Of more concern was the fact that following the reaction and the removal of the methanol, they partitioned the crude alkyne between water and ether,




**Scheme 4.15 Synthesis of galactosyl alkyne 453 using the Bestmann-Ohira reagent (489)**

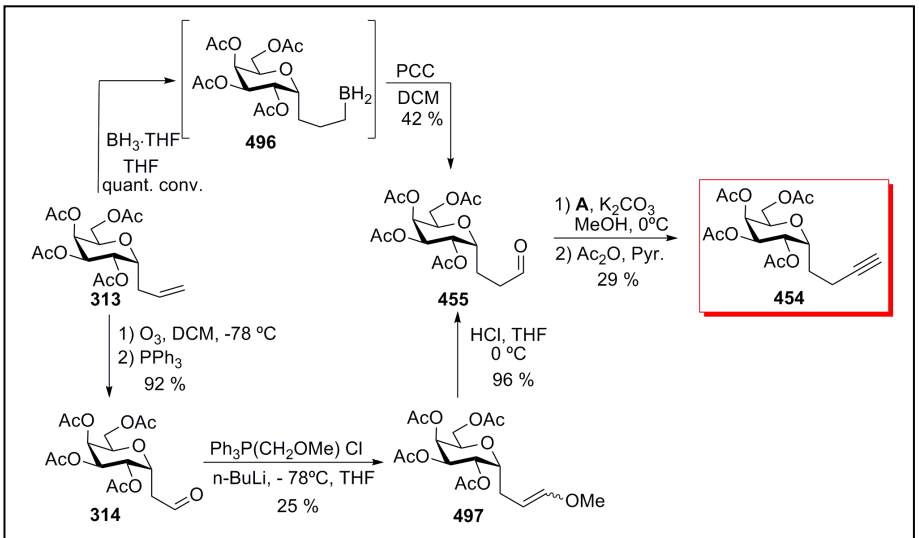
and went on to acetylate the ether fraction; however, when the same protocol was attempted using **314**, the acetate groups had, unsurprisingly, been cleaved by the catalytic sodium methoxide generated under the reaction conditions. Consequently, the vast majority of the carbohydrate product was located in the aqueous fraction: acetylation of the organic fraction led mainly to the formation of various uncharacterized phosphonate derivatives. In fact, an organic wash was a relatively simple way of removing many by-products of the reaction leaving the aqueous phase enriched in alkynyl carbohydrate.

Consequently, some modifications were made to the protocol after several trial reactions. Potassium carbonate was employed in place of sodium carbonate, DOWEX resin was used to neutralize the reaction and remove the potassium salts prior to concentration, and the crude alkyne was washed with ethyl acetate to remove the majority of the phosphonate derivatives prior to re-acetylation. These conditions resulted in the recovery of the desired alkyne **453** in 59 % yield. Attempts to increase the yield by using additional excess Ohira-Bestmann reagent did not result in success: lower purities and lower yields were the result. Likewise, caesium carbonate, often used as an additive to improve the reactivity of more unreactive aldehydes did not result in an improvement in yield.[79] Still, this protocol did provide sufficient material in an acceptable yield for the required CuAAC reactions.

#### *4.11.2.3 Synthesis of C-butynyl galactoside 454*

With the first alkynyl sugar in hand, the preparation of the butenyl derivative **454** was carried out. The required aldehyde, **455** had previously been synthesized by S.

Liu.[10] In this sequence (Scheme 4.16), allyl galactoside **313** was hydroborated using the borane-THF complex. Following quenching of excess reagent with water, and removal of solvent and excess water through co-evaporation with toluene, the borate intermediate **496** was oxidized directly using a large excess of PCC in anhydrous DCM to provide aldehyde **455** in a moderate 42 % overall yield following column chromatography. The aldehyde had also been prepared by R. Tam through a simple one carbon Wittig olefination as seen in Scheme 4.16.[62] Aldehyde **314**, easily accessible from *C*-allyl galactoside **313**, was treated with (methoxymethyl) triphenylphosphonium chloride premixed with *n*-butyl lithium to produce **497** as a diastereomeric mixture. The resulting yields from this process were capricious though, varying widely from trial to trial (18-58 %). The resulting diastereomeric mixture of enol ethers could readily be decomposed to the required aldehyde in near quantitative yields. However, due to the inconsistency of this reaction, the more reliable protocol involving a direct oxidation was preferable as the overall yield was more constant. Furthermore, the olefination was highly sensitive to opportunistic water, as expected, and great care and time had to be




**Scheme 4.16 Synthesis of butynyl derivative 454 via either direct oxidation of a carbon-boron bond or through one-carbon homologation using a Wittig olefination.**

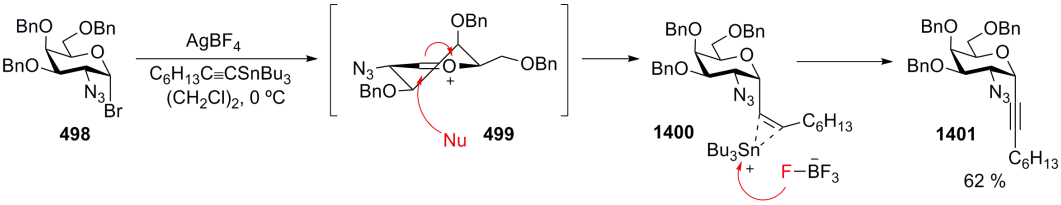
taken to ensure the complete dryness of all reagents. Additionally, the direct oxidation protocol is considerably simpler in that it involved two fewer flash chromatography steps.

With the required aldehyde finally in hand, the Ohira-Bestmann protocol used for **314** was applied to aldehyde **455**. Unfortunately, the yields were consistently even more disappointing than in the previous case providing the desired alkyne in only 29 % yield; however, through several trials sufficient material was generated to allow for the SPPS reactions to proceed.

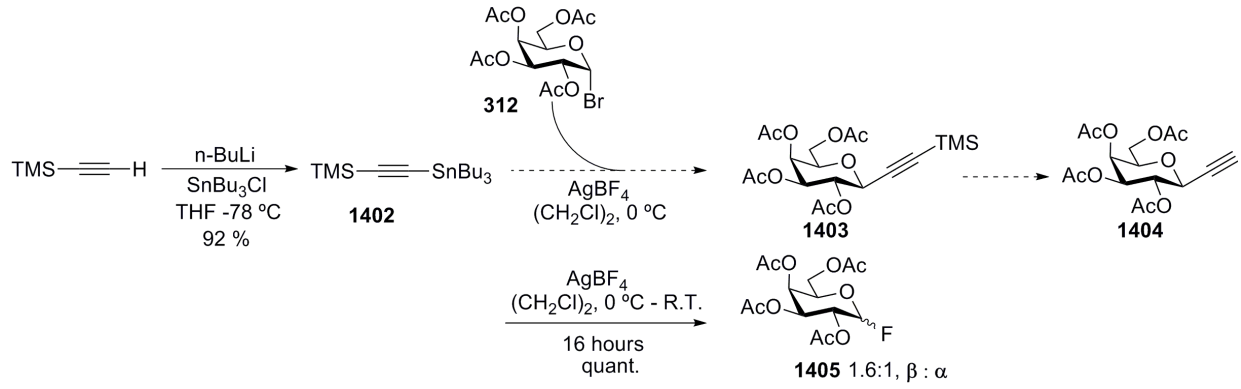
#### *4.11.2.4 Synthesis of C-ethynyl galactoside 452*

The final alkynyl monosaccharide to be attacked is the most difficult. Besides the lengthy deprotection and re-protection strategy that needs to be employed to allow for the success of the ozonolysis, the immediate concern was the epimerizable anomeric proton $\alpha$ to the aldehyde. The Ohira-Bestmann homologation is carried out under much milder conditions than similar homologations such as the Seyferth-Gilbert homologation, which employs alkyl lithiums or potassium *tert*-butoxide,[80] or the Corey-Fuchs reaction which makes use of *n*-butyl lithium.[81] These reactions lead to decomposition in much simpler systems (structurally) than aldehyde **435**, and the conditions would certainly be more challenging than the Bestmann-Ohira approach. As noted above however (Scheme 4.6), the configurational stability of the aldehyde is severely compromised even under the mildest of basic conditions; consequently, to avoid complications, an approach was attempted that would involve an ionic coupling of an ethynyl substituent to the anomeric position.

In 1994, Jobron and co-workers reported the syntheses of several *C*-galatoacetylenes through the direct displacement of anomeric halides with 1-tributylstannylalkynes, such as the synthesis of **1401** from **498** (Scheme 4.17). They propose the existence of an anomeric fluoride intermediate that is in equilibrium with the oxocarbenium ion (**498**); this intermediate resolves itself by nucleophilic attack through a chair-like transition state to generate, following destannylation of intermediate **1400**, the desired anomeric alkyne **1401** (62 % yield in this case). On the basis of this study, an attempt was made to carry out a similar reaction on a readily available model system, **312** (Scheme 4.18). Trimethylsilylacetylene was treated with *n*-butyl lithium at -78 ºC and quenched with tributylstannylchloride according to the protocol of Logue and Teng to provide **1402** in 92 % yield.[82] The protected acetylene was then used in a reaction with the acetylated bromosugar **312**. This donor was expected to be less reactive than the benzyl derivative



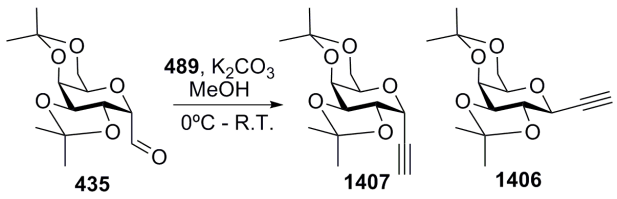

**Scheme 4.18 Jobron and co-workers' synthesis of alkynyl-glycosides.**[7]




**Scheme 4.17 Attempted synthesis of glycosyl alkyne 1403 as a model system using alkynyl nucleophiles.**

used by Jobron as it is disarmed compared to bromosugar **498**; consequently it was expected the reaction might not proceed as well or need longer reaction times. The β-product, **1403**, was expected due to anchiomeric assistance from the *C*-2 *O*-acetyl group, which could, theoretically, then be desilylated to give the β-alkenyl derivative **1404**. If this process worked, the α-derivative should theoretically be accessible through taking advantage of solvent and the anomeric effects present in a perbenzylated bromosugar. However, even after extended reaction times and higher temperatures, an anomeric mixture of fluoro-sugars (**1405**) was isolated in near quantitative yield following chromatography; an unfortunate result that led to the abandonment of this approach. It is hard to determine whether it is the alkyne reagent or the acetate protections that are responsible for the failure of this transformation, and the synthesis of the appropriate benzyl-protected sugar was lengthy enough that attention returned to a homologation strategy first. However, with the appropriate glycosyl donor or a more suitable alkyne reagent (if the electropositive silicon blocking group renders the alkyne insufficiently nucleophilic) this strategy would most likely afford the desired compound. Jobron notes, however, that the unsubstituted derivative was completely unreactive under their conditions.

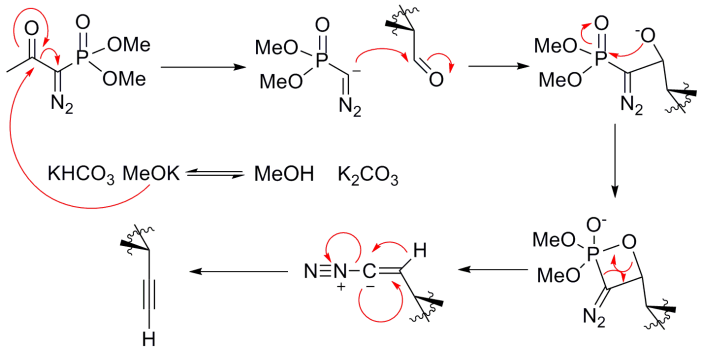
**Table 4.9 Selected conditions for the homologation of aldehyde 435 to alkyne 1407.**




| entry | eq. 489 | eq. base | Time (hrs) | Yield 1407 (%) | Yield 1406 (%) | Comments |
|---|---|---|---|---|---|---|
| i | 1.4 | 2 | 16 | 7 % | 38 % | Normal addition |
| ii | 1.4 | 1.7 | 16 | 28 % | 16 % | Premix base and **489** |
| iii | 1.3 | 1.3 | 3 | 43 % | 3 % | Premix base and **489** |

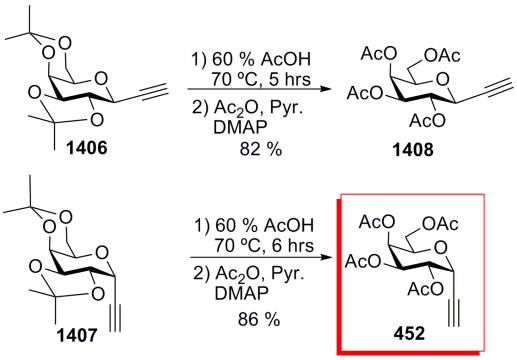
Returning to the homologation approach, the previously synthesized aldehyde **435** (Scheme 4.7) was treated under the conditions described above.

Unfortunately this resulted in recovery, as feared, of the β-alkynyl galactoside **1406** as the major product in 38 % yield with only a 7 % yield of the desired α-anomer, **1407** (Table 4.9, entry i). Most sources indicate that at least two equivalents of base are required for the successful transformation of aldehyde into the desired alkyne using **489**.[2, 76] It is also conventional in the Bestmann-Ohira protocol to premix the aldehyde and base in dry methanol and add the phosphonate last. However, it was considered that there is no true mechanistic reason for this order according to the currently proscribed mechanism (Scheme 4.19), and that the sequence of addition was most likely chosen simply because the reaction between the base and the phosphonate would only start when all three (four if one considers the methanol) molecules are present together. Thus, an experiment was carried out in which 1.4 equivalents of phosphonate **489** was dissolved in anhydrous methanol and cooled to 0 ºC. To this was added 1.7 equivalents of potassium carbonate, and the solution was allowed to stir for thirty minutes, only at which point was the aldehyde added. Following the reaction and column purification, the overall yield of the two anomers was nearly identical to the previous trial, but the desired α-anomer **1407** was now formed preferentially as the major product (Table 4.9 entry ii). Several different modifications to the reaction time and the number of




**Scheme 4.19 Key mechanistic steps in the Ohira-Bestmann modification of the Seyferth-Gilbert homologation. Adapted from Kürti and Czakó.[2]**

equivalents of base and phosphonate were performed, and the reaction was found to work reasonably well when 1.3 equivalents of base were premixed with 1.3 equivalents of **489** prior to the addition of the aldehyde. The reaction was quenched three hours later, and following chromatography the desired alkyne **1407** was isolated in 43 % yield while only a very small amount of the β-anomer was formed (3 %, Table 4.9 entry iii). With this synthetic tactic in hand, sufficient isopropylidene-protected alkynyl-sugar was generated for SPPS purposes. The isopropylidenes of **1407** were then removed using 60 % acetic acid at 70 ºC, and the fully deprotected sugars were acetylated under standard conditions and purified through flash chromatography to provide the α-anomer **452** in 86 % yield, and the β-anomer (**1408**, from the minor fraction) in 82 % yield (Scheme 4.20), providing the final building block required for the on-bead CuAAC reaction.




**Scheme 4.20 Final steps in the synthesis of 452 and 1408.**

## 4.11.3 Solid Phase synthesis of peptides

Solid phase synthesis of the three tetra-azido peptides proceeded very smoothly. All three peptides were prepared starting with 200 mg of Wang resin pre-loaded with Fmoc-glycine. Following a standard double-coupling synthesis, carried out according to Scheme 3.7, small amounts of peptide (10 mg of bead, 0.004 mmol) were cleaved and purified using reversed-phase solid-phase extraction (RP-SPE) cartridges, and

characterized to demonstrate the success of the solid-phase synthesis: the only peptide products recovered were the desired azido peptides.

## 4.11.4 On-resin CuAAC synthesis of 2nd generation triazole AFGP analogues

With the peptides and alkynes in hand, the resin-supported glycopeptide synthesis was undertaken. Using the conditions optimized in the previous study (with the caveat that the azides were now on solid support while the alkynes were in solution), the different permutations of peptide and carbohydrate were prepared one by one (Figure 4.10). The first glycopeptides generated, **215**, **217** and **219** were all cleaved from the solid-support under standard conditions, and after the removal of volatiles under a constant air flow at ambient temperature, were subjected to Zemplén deacetylation. The crude

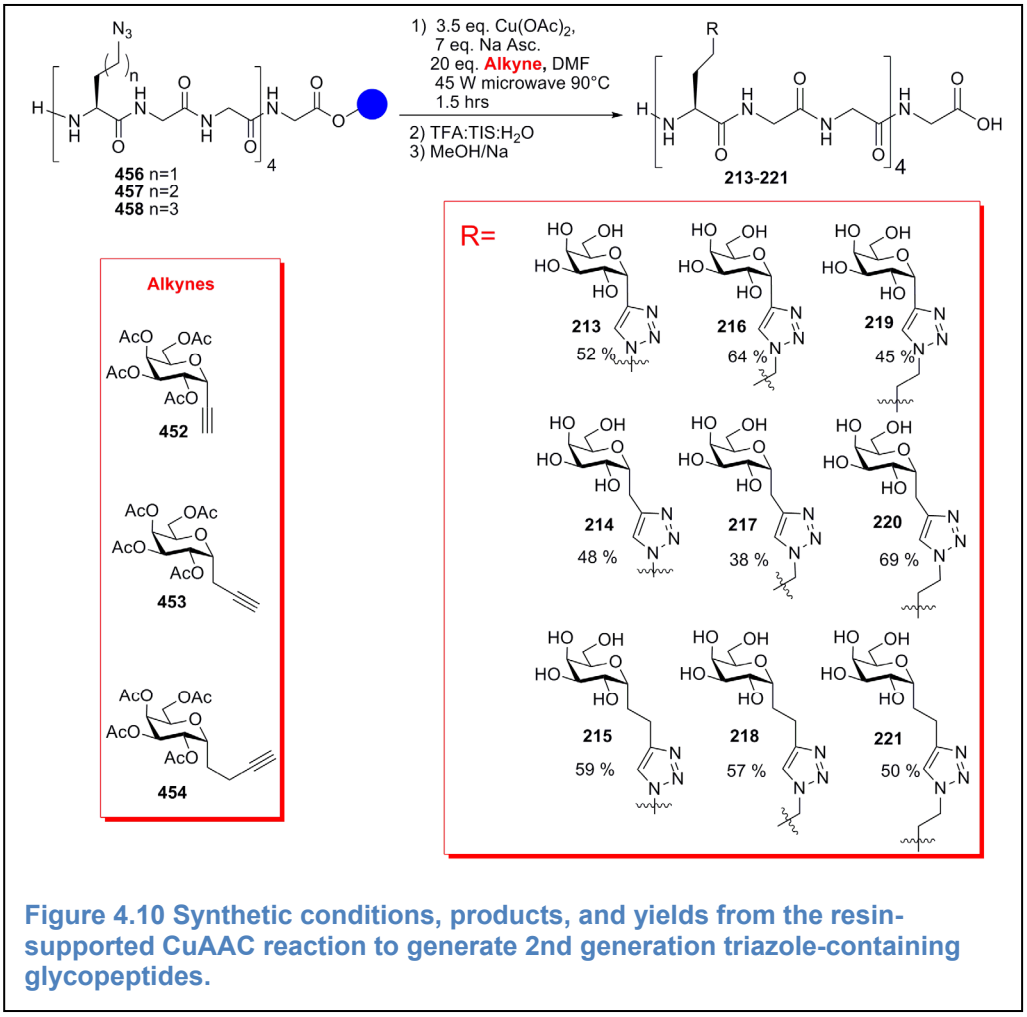



**Figure 4.10 Synthetic conditions, products, and yields from the resin-supported CuAAC reaction to generate 2nd generation triazole-containing glycopeptides.**

glycopeptides were examined by NMR and found to be contaminated only by trace glycine, as expected, and several aromatic and highly hydrophobic impurities, most likely derived from the resin. They were then purified by RP-HPLC to generate the desired compounds in only trace yield. Conversion had not been the issue as no unreacted azido peptides were evident in the NMR or MALDI spectra; similarly, deprotection had likewise not been an issue as the compounds were cleanly converted to the desired deprotected glycoconjugate with no remaining acetate protecting groups observable by NMR (in all three cases, the peak due to sodium acetate was clearly visible in the spectra). The sole complication had been the dilution and loss of compound on the HPLC instrument. However, the near purity of the compounds inspired an alternative methodology for removing the contaminants.

The three glycopeptides were resynthesized, removed from the bead, and concentrated under the same protocol as above. This time, the crude acetylated peptides were passed through *C*-18 solid-phase extraction (RP-SPE) cartridges to remove salts and some hydrophobic impurities. The fractions containing the desired glycopeptides were deprotected using 0.1 M sodium methoxide in methanol with minimal water, as required, to maintain the solubility of the peptides. Following neutralization, the glycopeptides were again loaded onto an RP-SPE cartridge, and the separated from the remaining hydrophobic impurities to provide the pure compounds after lyophilization. The yields for the three glycoconjugates were 59 %, 38 %, and 45 % respectively. Using this greatly simplified protocol, possible because of the high purity of both the SPPS and the quantitative conversion of the CuAAC reaction, the remaining six glycopeptides were rapidly synthesized in their respective yields as indicated in

Figure 4.10. These compounds were ready for conformational and antifreeze activity analysis.

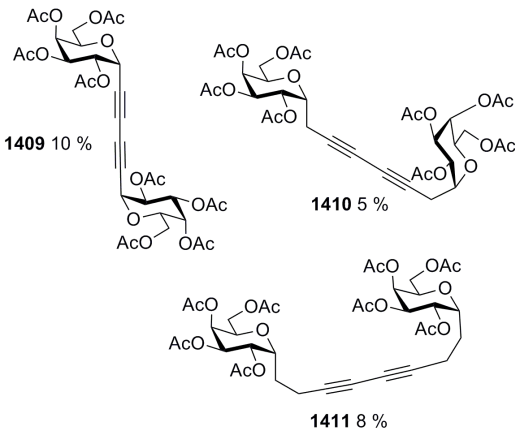



**Figure 4.11 Isolated Glaser-type byproducts from the CuAAC reaction.**

One of the benefits of the CuAAC solid-phase reaction is that following the reaction, the unreacted sugars can be recovered. In the 1st generation analogues described above, the unreacted azido sugars were recovered analytically pure after a simple extraction. In the case of the 2nd generation analogues described here, following the extraction of the recovered reaction mixture, a second compound other than the unreacted starting material was observed by TLC in all reactions. Following column chromatography to isolate the unknown product and recover unreacted starting material, the byproduct was identified as the Glaser-coupled product (**1409**-**1411**, Figure 4.11). Copper salts are well precedented for their tendency to catalyze these dimerization reactions; however, they normally require the addition of amine bases or a large excess of oxygen to carry out the transformation.[83] This is one reason why attempts were made to avoid the use of bases in these reactions to suppress this possible side-reaction; likewise, all vessels were purged with argon, and the solvents were saturated with argon prior to sealing the vessels for the microwave reaction. The mechanism is complicated but variable and involves higher-order copper complexes. It also appears to be highly dependent on the exact conditions present in the reaction mixture. In this example the reaction is being carried out under reducing conditions with the presence of the sodium ascorbate and

the only bases present are the enol of ascorbate, the acetate from the copper source, or the free terminal amine of the resin-bound peptides. The exact mechanism for this transformation remains, currently, unknown. Although the yields of the byproducts **1409**-**1411** are not high, they provided sufficient material for the properties of these compounds to be explored further and they will be discussed in greater detail below in Chapter 6 along with other disaccharides.

## 4.12 Assessing the conformation of 2nd generation triazole-containing glycopeptides

The conformations of the analogues were examined using CD spectroscopy in a manner identical to that described above. The spectra are presented in Figure 4.12 and the deconvoluted data is presented in Table 4.10. As can be seen immediately from the spectrum, all nine analogues adopt a very similar distribution of secondary structures. The CD spectrum has a very weak local maximum at approximately 250 nm, a slightly more prominent

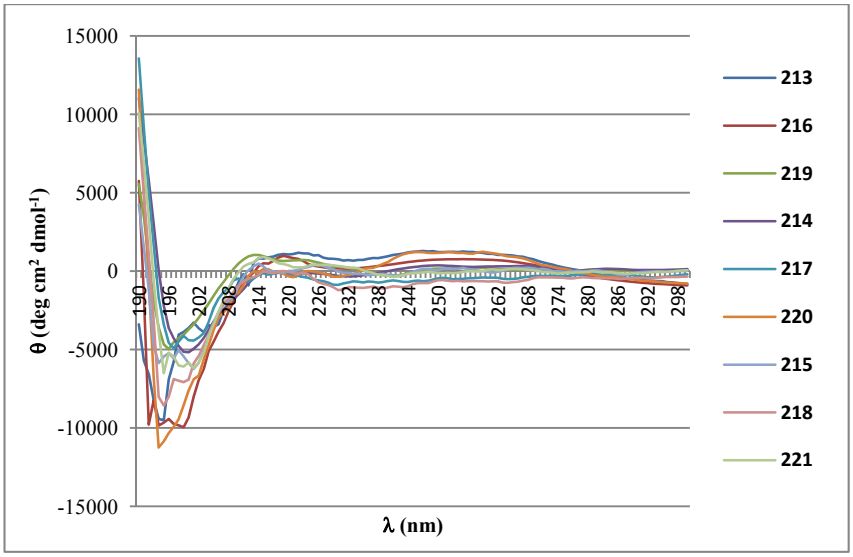



**Figure 4.12 CD spectra of 2nd generation triazole glycopeptides 213-221. All spectra were acquired in triplicate at 22 ºC at a concentration of 43 µM. CD data has been normalized for concentration and the number of chromaphores.**

maximum at around 216 nm, and a much more prominent local minimum at approximately 196 nm. These spectra are nearly identical to that seen for AFGP-8, and adopt a shape that almost resembles a vertical reflection of a β-sheet. This was an observation and conclusion drawn by Franks and Morris with respect to AFGP-8 who stated that this must be a previously uncharacterized secondary structure.[84] Similarly, the local maxima and minima values correlate well with those found in PP II helices, although the amplitude is lower than one would expect. Consequently, it is not surprising that the curve shape and amplitude values most closely match those expected from a random coil. The wide variety of contributing structures, dominated by the random coil, seen in the CD conformational analysis is most likely responsible for the confusion that permeates discussions regarding the "true" secondary structure of these antifreeze glycopeptides. The deconvolution data, however, are less ambivalent and appear to indicate that these compounds primarily adopt a random coil, with possible localized β-sheets and PP II structures as mentioned above. Once again, however, according to the deconvolution, α-helices do not appear to play any part in the secondary structure.

The most important observation to be made at this point is that, compared to the inverted triazoles of the 1st generation analogues that presented unusual CD

**Table 4.10 Secondary structure of glycopeptides 213-221 derived from the deconvolution of the CD spectra in Figure 4.12.**

| | α-Helix | β-Sheet | β-Turn | Poly proline Type II | Random coil |
|---|---|---|---|---|---|
| **213** | 0.006 | 0.320 | 0.098 | 0.136 | 0.440 |
| **214** | 0.009 | 0.314 | 0.111 | 0.125 | 0.442 |
| **216** | 0.010 | 0.312 | 0.113 | 0.128 | 0.437 |
| **215** | 0.012 | 0.316 | 0.121 | 0.120 | 0.430 |
| **217** | 0.040 | 0.289 | 0.129 | 0.112 | 0.430 |
| **219** | 0.008 | 0.321 | 0.116 | 0.124 | 0.430 |
| **218** | 0.008 | 0.313 | 0.112 | 0.127 | 0.440 |
| **220** | 0.008 | 0.320 | 0.104 | 0.123 | 0.445 |
| **221** | 0.006 | 0.321 | 0.096 | 0.124 | 0.453 |

spectra (compared to those previously obtained for *O* and *C*-linked AFGP analogues), the 2nd generation triazole-containing analogues all adopt similar conformations independent of the length of the linker (varying between five and nine atoms in **213** and **221** respectively) or the position of the triazole relative to either the peptide backbone or the carbohydrate. Consequently, the unusual spectra observed for the 1st generation analogues (Figure 4.6, Table 4.7) are a function not of the triazole itself but rather perhaps of the reversed dipole moment of this linker. This implies that the orientation of the functional group in the linker may have an important role to play in the subtle conformational differences observed through CD spectroscopy.

## 4.13 Assessing the antifreeze activity of 2nd generation triazole-containing glycopeptides

All nine analogues were examined for dynamic ice shaping and thermal hysteretic activity using the nanolitre osmometry as described above. None of the compounds showed any discernable thermal hysteretic gap. However, one compound, **217**, did show weak dynamic ice shaping, with the ice crystal adopting a hexagonal shape when at the colligative freezing point (Figure 4.13). All other analogues, such as **213**, produced only round ice crystals indicating little or no significant interaction with the ice lattice. This lack of any TH activity is still consistent with previous results showing that *C*-linked

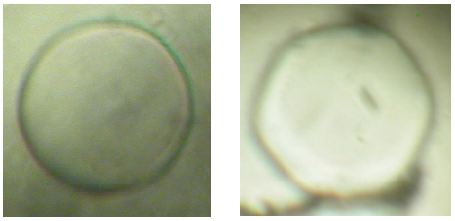


**Figure 4.13 Microscopy images of ice crystals from analogue 213, which is circular and similar to the ice crystals seen in distilled water, and analogue 217 with slight, but clearly observable hexagonal ice shaping.**

AFGP analogues interact little, if at all, with the ice-lattice. The compounds were then screened for IRI activity using the “splat” cooling assay.

Due to concerns that subtle differences in IRI activity may be undetectable at low concentrations, the analogues were screened at two different concentrations using the splat-cooling assay developed by Knight and co-workers.[68] The first concentration, 5.5 μM is the standard used thus far. The second concentration, 550 μM, is one-hundred-fold more concentrated. Both concentrations have been found to be ideal in discriminating subtle differences in IRI activity in glycoconjugates.[10, 11, 60, 65] The data is presented in Figure 4.14 where the compounds are ordered in terms of linker length. A few observations can be drawn from the data.

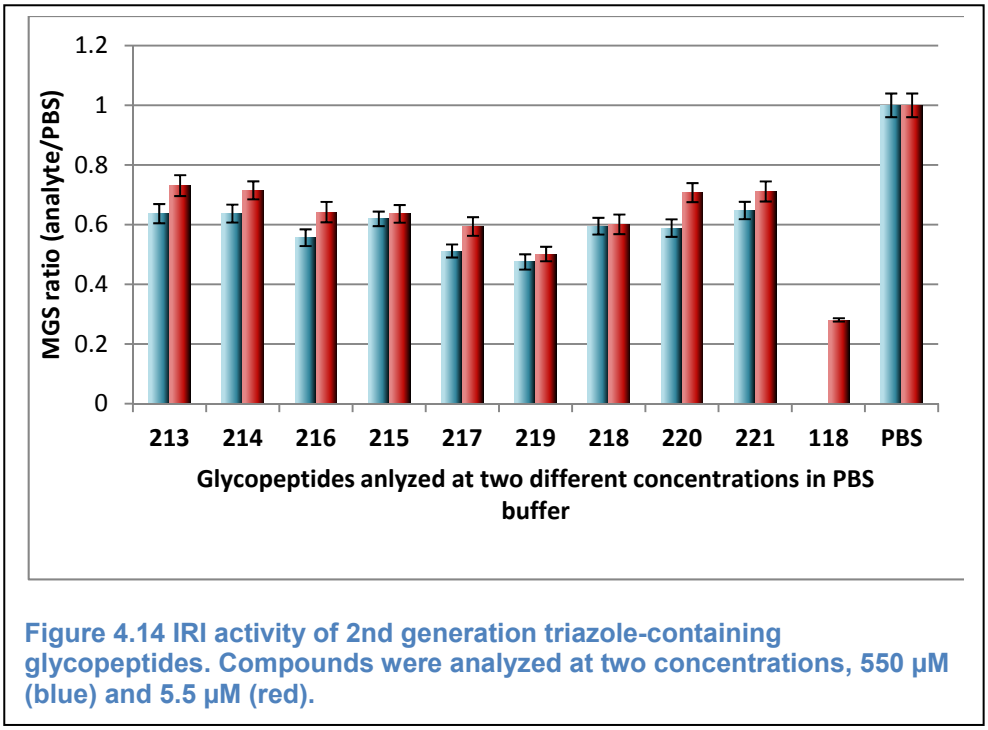



**Figure 4.14 IRI activity of 2nd generation triazole-containing glycopeptides. Compounds were analyzed at two concentrations, 550 μM (blue) and 5.5 μM (red).**

Firstly, all analogues are considerably less active than **118** although they are very competitive, and more active, than most other *C*-linked glycopeptides that have been prepared earlier in the Ben lab. With respect to the comparison between the 2nd generation analogues, it appears that there is an ideal chain length for optimal IRI activity. The most active analogues lie in the middle of the range with compounds

containing seven atoms in the linker, especially **219**. IRI activity appears to decrease as the length of the peptide-carbohydrate linker is either lengthened or shortened from this central value. This finding supports the previous results obtained from the amide analogues discussed above where deviation from the ideal 6-atom length in **118** led to a decrease in activity.[11] Three of the most active triazole analogues have a similar "6-atom" linker (in the case of the triazole glycopeptides, this linker is in fact 7 atoms long, but the three atoms of the triazole are only slightly longer than the two atoms of an amide bond). The highly active *C*-linked glycopeptide **118** is analogous to **217**. The most active analogue, at both concentrations, is the isometric **219**. The amide analogue of this compound has not yet been prepared but may show excellent activity. It is very interesting to note that this, the most active IRI analogue, is also the only one to show weak dynamic ice shaping. It is also suggested that analogues containing amino-butyric acid derivatives (**213**, **214**, **215**) are slightly less active at both concentrations than their respective isometric ornithine or lysine analogues, perhaps indicating a preference for locating the rigid triazole a greater distance from the peptide backbone. Furthermore, despite a hundred-fold increase in concentration, the IRI activity of the analogues does not increase immensely between 5.5 and 550 μM. This lack of change in activity over a broad concentration range has been observed previously for *C* and *O*-linked AFGP analogues, and is possibly a result of a saturation of binding sites: in the frozen sample 5.5 μM provides sufficient interruption of the recrystallization process such that even a large increase in the number of additional molecules does not appreciably enhance the inhibition properties of the solution. From these results it appears that although the relative position of the triazole is important, the overall length of the spacer appears to

be much more significant for predicting IRI activity. Needless to say, the introduction of a triazole for an amide is not a beneficial substitution as, again, all analogues are less active than **118**.

These results suggest that the strong IRI activity of **118** is not entirely due to an interaction of some type between the amide of the linker and the backbone, but that the length itself is privileged and plays a key role as the proposed interaction is most likely not available to the triazole analogues. The CD data does not support a different secondary conformation for the more active analogues, as all analogues adopt a similar structure, nor does it imply that the amide analogues adopt a unique conformation compared to the triazole-compounds: the side-chain hydrogen bond donor/acceptor is not responsible for secondary conformation. Rather it is more probable that the active analogues may assist in orienting the carbohydrate in a specific manner relative to the peptide.[11] Comparing the second generation analogues to their first generation counterparts (Figure 4.7), it appears that even the least active of the new analogues (**213**, **220**, and **221** with activities of 73, 71, and 71 % respectively) are at least as active as the most active reversed triazole compounds (**211** and **212**, 72 and 76 % respectively). This startling result suggests that the orientation of the linking group is incredibly important as simply reversing it leads to a great difference in activity.

A second possible explanation can be proposed to explain the difference in activity between the two generations of analogues (that will be revisited in Chapter 5 below), is that the difference in activity between the two generations of analogues may be due to the nature of the linking group connecting the carbohydrate to the triazole.

None of the newly synthesized analogues approach the activity of **118**, but all of these triazole analogues appear to be more IRI active than the inactive *C*-linked antifreeze analogues (**127**, **131**-**136**), suggesting perhaps that an improper positioning of the sugar with an inappropriately located amide might not only be sub-optimal, but might in fact be detrimental to IRI activity as the activity is improved in these cases when the amide bond is replaced entirely with a triazole. Finally, these results provide strong support to the hypothesis that the length of the linker is strongly correlated with IRI activity.

## 4.14 Chapter summary

This chapter encompassed three goals. The first was the development of solution-phase conditions for the CuAAC reaction that would be applicable to solid phase technology. In the process of investigating conditions it was found that the traditional solvent system of *tert*-butanol: water (1:1) was not an appropriate system for the solution-phase reaction, and much better results were obtained with a variety of different organic solvents, especially THF, and yields were significantly improved by deviating from the equi-volume solvent system to one containing 80 % organic solvent.

The second objective was to apply these conditions to the on-resin solid phase synthesis of several proof-of-concept reversed-triazole-containing *C*-AFGPs. The optimized conditions failed to result in the formation of the desired compounds, but a similar anhydrous methodology accompanied by microwave heating led to the desired glycoconjugates. It is interesting to note that conventional heating, at a similar temperature for a considerably longer time, failed to procure the glycopeptides, as did

microwave heating methodologies where microwave irradiation was very sporadic; only with the near constant application of lower-powered microwaves were the desired compounds obtained. The compounds were found to have mutually similar secondary structures but unprecedented CD spectra (within the scope of AFGP analogues), but deconvolution and the low amplitude of the curves suggests that they adopt a random coil (although alternative non-traditional secondary structure are possible). None of the analogues showed TH activity and IRI activity was correlated with linker length: the longer the linker (the more it approached the “ideal” of **118**), the better the activity.

With the success of this synthetic strategy, a series of nine triazole glycoconjugates with the same dipole orientation as the previously prepared active amide analogues were generated. A new isolation protocol avoided the use of HPLC in the purification of the glycopeptides. CD analysis showed that the compounds all adopt a conformation similar to that of previously prepared amide-containing *C*-AFGPs and AFGP-8 itself; this demonstrates that the presence of the triazole does not impact secondary conformation. None of the compounds showed TH activity, although one compound, **217**, showed dynamic ice shaping activity (In effect, a sub-threshold manifestation of TH). All compounds showed moderate to fair IRI activity and even the least active were more active than the best first generation triazole-*C*-AFGP analogues (and by extension, amide-containing *C*-AFGPs deviating from the ideal 6-atom length). This comparison indicates that the orientation of the linker plays some important role in IRI activity; furthermore, these results suggest that the amide bond is not in and of itself responsible for IRI activity, but that in one particular analogue, **118**, it may play a key part in orienting the sugar relative to the peptide in a way that is unavailable to its

triazole analogue.[11] Finally, and most importantly, these results support the growing body of evidence that implicates the linker length as a definitive parameter in determining IRI activity.

## References


1. Pietruszka, J.; Witt, A., *Synthesis* **2006,** (24), 4266-4268.
2. Kürti, L.; Czakó, B., Seyferth-Gilbert Homologation. In *Strategic application of named reactions in organic synthesis*, Elsevier: Burlington, MA, 2005.
3. Norgren, A. S.; Budke, C.; Majer, Z.; Heggemann, C.; Koop, T.; Sewald, N., *Synthesis* **2009**, 488-494.
4. Santini, R.; Griffith, M. C.; Qi, M., *Tetrahedron Lett.* **1998,** *39*, 8951-8954.
5. Bock, V. D.; Hiemstra, H.; van Maarseveen, J. H., *Eur. J. Org. Chem.* **2006,** *6*, 51-68.
6. Ibatullin, F. M.; Selivanov, S. I., *Tetrahedron Lett.* **2002,** *43*, 9577-9580.
7. Jobron, L.; Leteux, C.; Veyrières, A.; Beau, J.-M., *J. Carb. Chem.* **1994,** *13* (3), 507-512.
8. Miller, N.; Williams, G. M.; Brimble, M. A., *Org. Lett.* **2009,** *11*, 2409-2412.
9. Pollex, A.; Hiersemann, M., *Org. Lett.* **2005,** *7* (25), 5705-5708.
10. Liu, S.; Ben, R. N., *Org. Lett.* **2005,** *7* (12), 2385-2388.
11. Tam, R. Y.; Rowley, C. N.; Petrov, I.; Zhang, T.; Afagh, N. A.; Woo, T. K.; Ben, R. N., *J. Am. Chem. Soc.* **2009,** *131*, 15745-15753.
12. Pedersen, D. S.; Abell, A., *Eur. J. Org. Chem.* **2011**, 2399-2411.
13. Angell, Y. L.; Burgess, K., *Chem. Soc. Rev.* **2007,** *36* (10), 1674-1689.
14. Horne, W. S.; Yadav, M. K.; Stout, C. D.; Ghadiri, M. R., *J. Am. Chem. Soc.* **2004,** *126* (47), 15366-15367.
15. Wang, Q.; Chittaboina, S.; Barnhill, H. N., *Lett. Org. Chem.* **2005,** *2*, 293-301.
16. Palmer, M. H.; Findlay, R. H.; Gaskell, A. J., *J. Chem. Soc. Perk. Trans. 2.* **1974,** (4), 420-428.

17. Liu, Y.; Zhang, L.; Wan, J.; Li, Y.; Xu, Y.; Pan, Y., *Tetrahedron* **2008,** *64*, 10728-10734.

18. Zhao, Z.; Yuan, W.; Gu, S.; Ren, T.; Ren, J., *Huaxue Jinzhan* **2010,** *22*, 417-426.

19. Moses, J. E.; Moorhouse, A. D., *Chem. Soc. Rev.* **2007,** *36*, 1249-1262.

20. Huisgen, R., *P. Chem. Soc.* **1961**, 357-396.

21. Huisgen, R., Historical note, general principle and mechanistic criteria. In *1,3-dipolar cycloaddition chemistry*, Padwa, A., Ed. Wiley: New York, 1984; Vol. 1, pp 1-176.

22. Tornöe, C. W.; Christensen, C.; Meldal, M., *J. Org. Chem.* **2002,** *67* (9), 3057-3064.

23. Rostovtsev, V. V.; Green, L. G.; Fokin, V. V.; Sharpless, K. B., *Angew. Chem. Intl. Ed.* **2002,** *41*, 2596-2599.

24. Himo, F.; Lovell, T.; Hilgraf, R.; Rostovtsev, V. V.; Noodleman, L.; Sharpless, K. B.; Fokin, V. V., *J. Am. Chem. Soc.* **2004,** *127* (1), 210-216.

25. Aragão-Leoneti, V.; Campo, V. L.; Gomes, A. S.; Field, R. A.; Carvalho, I., *Tetrahedron* **2010,** *66* (49), 9475-9492.

26. Schilling, C.; Jung, N.; Bräse, S., Common Synthons for Click Chemistry in Biotechnology. In *Click Chemistry for Biotechnology and Materials Science*, John Wiley & Sons, Ltd: 2009; pp 9-28.

27. van Dijk, M.; Rijkers, D. T. S.; Liskamp, R. M. J.; van Nostrum, C. F.; Hennink, W. E., *Bioconjugate Chem.* **2009,** *20*, 2001-2016.

28. Baskin, J. M.; Bertozzi, C. R., Copper-Free Click Chemistry. In *Click Chemistry for Biotechnology and Materials Science*, John Wiley & Sons, Ltd: 2009; pp 29-51.

29. Bouillon, C.; Meyer, A.; Vidal, S.; Jochum, A.; Chevolot, Y.; Cloaree, J. P.; Praly, J. P.; Vasseur, J. J.; Morvan, F., *J. Org. Chem.* **2006,** *71*, 4700-4702.

30. Santoyo-Gonzalez, F.; Hernandez-Mateo, F., *Top. Heterocycl. Chem.* **2007,** *7*, 133-177.

31. Franc, G.; Kakkar, A. K., *Chem. Soc. Rev.* **2010,** *39*, 1536-1544.

32. Pourceau, G.; Meyer, A.; Vasseur, J.-J.; Morvan, F., *J. Org. Chem.* **2008,** *73*, 6014-6017.

33. Ortega-Muñoz, M.; Lopez-Jaramillo, J.; Hernandez-Mateo, F.; Santoyo-Gonzalez, F., *Adv. Synth. Catal.* **2006,** *348*, 2410-2420.

34. Pourceau, G.; Meyer, A.; Vasseur, J.-J.; Morvan, F., *J. Org. Chem.* **2009,** *74*, 1218-1222.

35. Ingale, S.; Dawson, P. E., *Org. Lett.* **2011,** *13*, 2822-2825.

36. Jølck, R. I.; Berg, R. H.; Andresen, T. L., *Bioconjugate Chem.* **2010,** *21*, 807-810.

37. Lee, D. J.; Harris, P. W. R.; Brimble, M. A., *Org. Biomol. Chem.* **2011,** *9*, 1621-1626.

38. Capicciotti, C. J.; Trant, J. F.; Leclère, M.; Ben, R. N., *Bioconjugate Chem.* **2011,** *22* (4), 605-616.

39. Ohta, J.; Ubuka, T.; Kodama, H.; Sugahara, K.; Nagamine, N., *Biochim. Biophys. Acta.* **1997,** *1334* (2-3), 240-246.

40. Marcotte, P.; Walsh, C., *Biochemistry* **1978,** *17* (26), 5613-5619.

41. Konno, R.; Ikeda, M.; Yamaguchi, K.; Ueda, Y.; Niwa, A., *Arch. Toxicol.* **2000,** *74* (8), 473-479.

42. Szilágyi, L.; Györgydeák, Z. A., *Carb. Res.* **1985,** *143*, 21.

43. Wang, Z., Zemplén Deacetylation. In *Comprehensive Organic Name Reactions and Reagents*, John Wiley & Sons, Inc.: 2010.

44. Wang, Z., Sharpless Dihydroxylation. In *Comprehensive Organic Name Reactions and Reagents*, John Wiley & Sons, Inc.: 2010.

45. Sarin, V. K.; Kent, S. B. H.; Merrifield, R. B., *J. Am. Chem. Soc.* **1980,** *102* (17), 5463-5470.

46. Merrifield, R. B., *J. Am. Chem. Soc.* **1963,** *85*, 2149-2154.

47. Chan, W. C.; White, P. D., Basic procedures. In *Fmoc Solid Phase Peptide Synthesis: A Practical Approach*, Chan, W. C.; White, P. D., Eds. Oxford Univesity Press: Oxford, 2000; pp 41-76.

48. Appukkuttan, P.; Dehaen, W.; Fokin, V. V.; Van der Eycken, E., *Org. Lett.* **2004,** *6* (23), 4223-4225.

49. Bougrin, K.; Soufiaoui, M.; Bashiardes, G., Microwaves in cycloadditions. In *Microwaves in organic synthesis*, Loupy, A., Ed. Wiley-VCH: Weinheim, 2006; Vol. 2, pp 524-578.

50. Perreux, L.; Loupy, A., Nonthermal effects of microwaves in organic synthesis. In *Microwaves in organic synthesis*, Loupy, A., Ed. Wiley-VCH: Weinheim, 2006; Vol. 1, pp 134-212.

51. The unreacted azido sugars were recovered from the reaction mixture. Following reaction, the solution was filtered, and the filtrate was diluted with ethyl acetate and water and the phases were separated. The aqueous phase was extracted twice more with ehtyl acetate and the combined organic phases were washed with 10 % HCl, saturated sodium bicarbonate and brine successively. Following drying and concentration, the unreacted azide would be recovered cleanly from the organic phase. No purification was required.

52. Patnam, R.; Juárez-Ruiz, J. M.; Roy, R., *Org. Lett.* **2006,** *8*, 2691-2694.

53. Greenfield, N. J.; Fasman, G. D., *Biochemistry* **1969,** *8* (10), 4108-4116.

54. Towell, J. F. I.; Manning, M. C., Chapter 6 Analysis of protein structure by circular dichroism spectroscopy. In *Techniques and Instrumentation in Analytical Chemistry*, Purdie, N.; Brittain, H. G., Eds. Elsevier: 1994; Vol. Volume 14, pp 175-205.

55. Sreerama, N.; Woody, R. W., *J. Mol. Biol.* **1994,** *242* (4), 497-507.

56. Sreerama, N.; Venyaminov, S. Y.; Woody, R. W., *Anal. Biochem.* **2000,** *287* (2), 243-251.

57. Chen, Y.-H.; Yang, J. T.; Martinez, H. M., *Biochem.* **1972,** *11* (22), 4120-4131.

58. Sreerama, N.; Woody, R. W., *Anal. Biochem.* **2000,** *287* (2), 252-260.

59. Thapa, I. *C*-Linked AFGP analogues containing β–amino acids: preparation, assessment and *in vitro* studies. MSc. Thesis, University of Ottawa, Ottawa, 2006.

60. Czechura, P.; Tam, R. Y.; Dimitrijevic, E.; Murphy, A. V.; Ben, R. N., *J. Am. Chem. Soc.* **2008,** *130* (10), 2928-2929.

61. Czechura, P. Elucidating the relationship between hydration and ice recrystallization inhibition with *C*-linked antifreeze glycoproteins. PhD. Thesis, University of Ottawa, Ottawa, 2009.

62. Tam, R. Y. Studies into the structural features of *C*-linked antifreeze glycoprotein analogues responsible for ice-recrystallization inhibition activity. PhD. Thesis, University of Ottawa, Ottawa, 2010.

63. DeVries, A. L.; Komatsu, S. K.; Feeney, R. E., *J. Biol. Chem.* **1970,** *245* (11), 2901-2908.

64. Rao, B. N. N.; Bush, C. A., *Biopolymers* **1987,** *26* (8), 1227-1244.

65. Eniade, A.; Purushotham, M.; Ben, R. N.; Wang, J. B.; Horwath, K., *Cell. Biochem. Biophys.* **2003,** *38*, 115-124.

66. Murphy, A. V. Preparation of structurally diverse C-linked antifreeze glycoprotein analogues and assessment for antifreeze protein-specific activity. PhD. Thesis, State University of New York, Binghampton, 2004.

67. Chakrabartty, A.; Hew, C. L., *Eur. J. Biochem.* **1991,** *202*, 1057-1063.

68. Knight, C. A.; Hallet, J.; DeVries, A. L., *Cryobiology* **1988,** *25*, 55-60.

69. Knight, C. A.; Wen, D.; Laursen, R. A., *Cryobiology* **1995,** *32* (1), 23-34.

70. Jackman, J.; Noestheden, M.; Moffat, D.; Pezacki, J. P.; Findlay, S.; Ben, R. N., *Biochem. Biophys. Res. Commun.* **2007,** *354*, 340-344.

71. Boyle, P. H.; Davis, A. P.; Dempsey, K. J.; Hosken, G. D., *Tet. Assym.* **1995,** *6* (11), 2819-2828.

72. Xiao, Y.; Lee, K.; Liu, P., *Org. Lett.* **2008,** *10* (24), 5521-5524.

73. Le Chevalier Isaad, A.; Barbetti, F.; Rovero, P.; D'Ursi, A. M.; Chelli, M.; Chorev, M.; Papini, A. M., *Eur. J. Org. Chem.* **2008,** *2008* (31), 5308-5314.

74. McLaughlin, M.; Mohareb, R. M.; Rapoport, H., *J. Org. Chem.* **2003,** *68* (1), 50-54.

75. Nyffeler, P. T.; Liang, C.-H.; Koeller, K. M.; Wong, C.-H., *J. Am. Chem. Soc.* **2002,** *124*, 10773-10778.

76. Müller, S.; Liepold, B.; Roth, G. J.; Bestmann, H. J., *Synlett* **1996,** *1996* (6), 521-522.

77. TCI-UK http://www.tci-uk.co.uk/catalog/D3546.html (accessed July 5th).

78. Giguère, D.; Patnam, R.; Bellefleur, M.-A.; St-Pierre, C.; Sato, S.; Roy, R., *Chem. Commun.* **2006**, 2379-2381.

79. Bondarenko, L.; Dix, I.; Hinrichs, H.; Hopf, H., *Synthesis* **2004,** *2004*, 2751,2759.

80. Gilbert, J. C.; Weerasooriya, U., *J. Org. Chem.* **1979,** *44* (26), 4997-4998.

81. Corey, E. J.; Fuchs, P. L., *Tetrahedron Lett.* **1972,** *13* (36), 3769-3772.

82. Logue, M. W.; Teng, K., *J. Org. Chem.* **1982,** *47* (13), 2549-2553.

83. Siemsen, P.; Livingston, R. C.; Diederich, F., *Angew. Chem. Int. Ed.* **2000,** *39* (15), 2632-2657.

84. Franks, F.; Morris, E. R., *Biochim. Biophys. Acta.* **1978,** *540* (2), 346-356.

# Chapter 5 : IRI activity of (1,1)- and (1,3)-galactosyl-galactose derivatives and simple *C*-linked galactosides

One of the ultimate goals of the Ben research program has been to discover small molecule alternatives to the glycopeptides that exhibit potent ice recrystallization (IRI) activity. While the *C*-linked glycopeptides are potent inhibitors of ice recrystallization, the synthesis of these molecules is lengthy and not always amenable to scale-up or preparation of large quantities of compound. Consequently, it would be preferable if antifreeze activity comparable to that expressed by the glycopeptides could be found in a small molecule analogue. Carbohydrates have been shown to exhibit IRI activity, and are used extensively as cryopreservatives in a variety of applications (both in nature and in technology) as described above. For this reason, they provide a natural starting point in the search for simple IRI-active, non-toxic compounds. Two strategies to achieve this goal are investigated in this chapter: the rational design, synthesis and analysis of several key disaccharides, and an investigation into the relationship between IRI activity and the length and nature of the substituent in *C*-linked galactosides.

## 5.1 Disaccharides as small molecule inhibitors of ice recrystallization

### 5.1.1 Early investigations into the antifreeze activity of *O*- and *C*-linked AFGP analogues

The Ben laboratory has done some SAR work on *O*-linked glycoconjugates over the past few years. A former student, P. Czechura, synthesized a series of disaccharides containing glycopeptides and analyzed them for IRI activity (Figure 5.1).[1] Combining these data points with the monosaccharides tested by V. Bouvet (Figure 1.15), several tentative conclusions could be reached regarding the structural features responsible for potent IRI activity. The most important parameter for IRI activity does not appear to necessarily be the presence of an N-acetyl group at *C*-2; the presence of a terminal galactose unit appears more important. This is evidenced by the most active compounds, melibiose (**501**) where the terminal galactose is linked through the *C*-6 of the glucose residue, and the (1,3)-linked Gal-GalNHAc derivative **503.** The other two tested derivatives are less active. However, a direct comparison between the importance of a galactosamine residue compared to a galactose residue to IRI activity is impossible with the current data as there exists no "matched set" of analogues where one contains a galactose and the other a galactosamine.

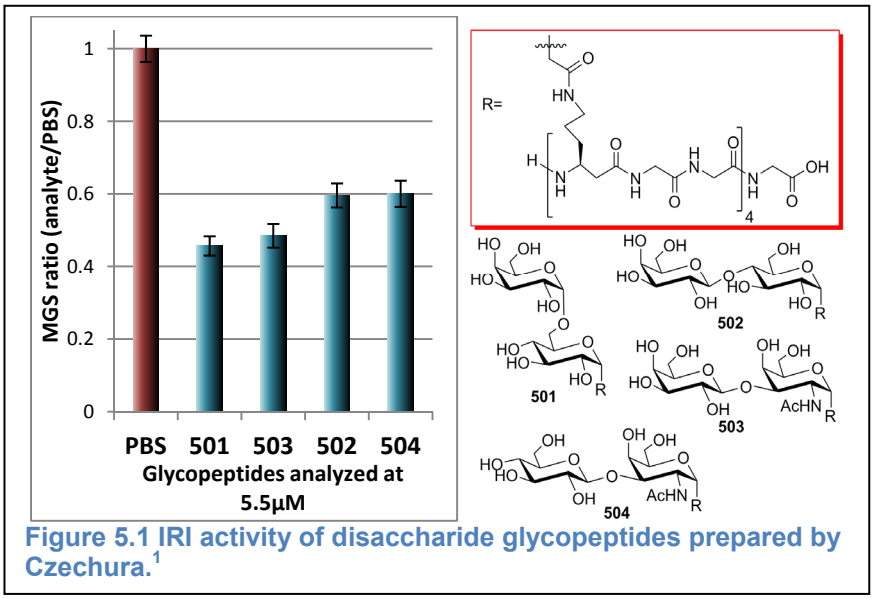



**Figure 5.1 IRI activity of disaccharide glycopeptides prepared by Czechura.[1]**

Interestingly, the relative positions of the data points for **501** and **502** are also consistent with the relative partial molar compressibilities (a measurement of hydration) as calculated by Galema and Høiland

(Figure 5.2), as would be predicted if increased hydration leads to improved IRI activity.[2] Unfortunately, these two disaccharides are the only tested disaccharides that have known partial molar compressibilities. Besides highly IRI active amide-linked **118** and *C*-serine derivative **119**, analogues **501** and **503** are amongst the most active identified to date.

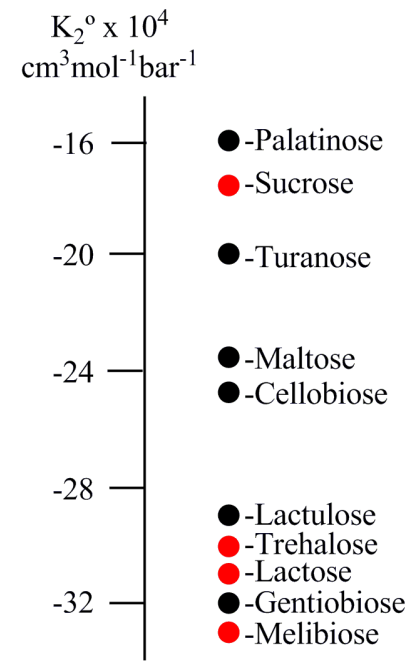



**Figure 5.2 Measured partial molar compressibilities of several disaccharides by Galema and Høiland. The disaccharides examined in this text are highlighted in red. A more negative value implies a larger hydration sphere surrounding the solute.[2]**

Interestingly, analogue **504**, the least active in this series, is the only glycoconjugate synthesized that lacks a terminal galactose, although it does contain a galactose-based residue (GalNHAc) anchoring it to the peptide. This appears to be insufficient to obtain high levels of IRI activity indicating the importance of a terminal galactose to IRI activity. This observation, coupled with the apparent relationship between hydration and IRI activity in monosaccharide *C*-linked AFGP derivatives,[4] led to the investigation of the possibility of using disaccharides as IRI inhibitors.

### 5.1.2 IRI activity of previously prepared disaccharides

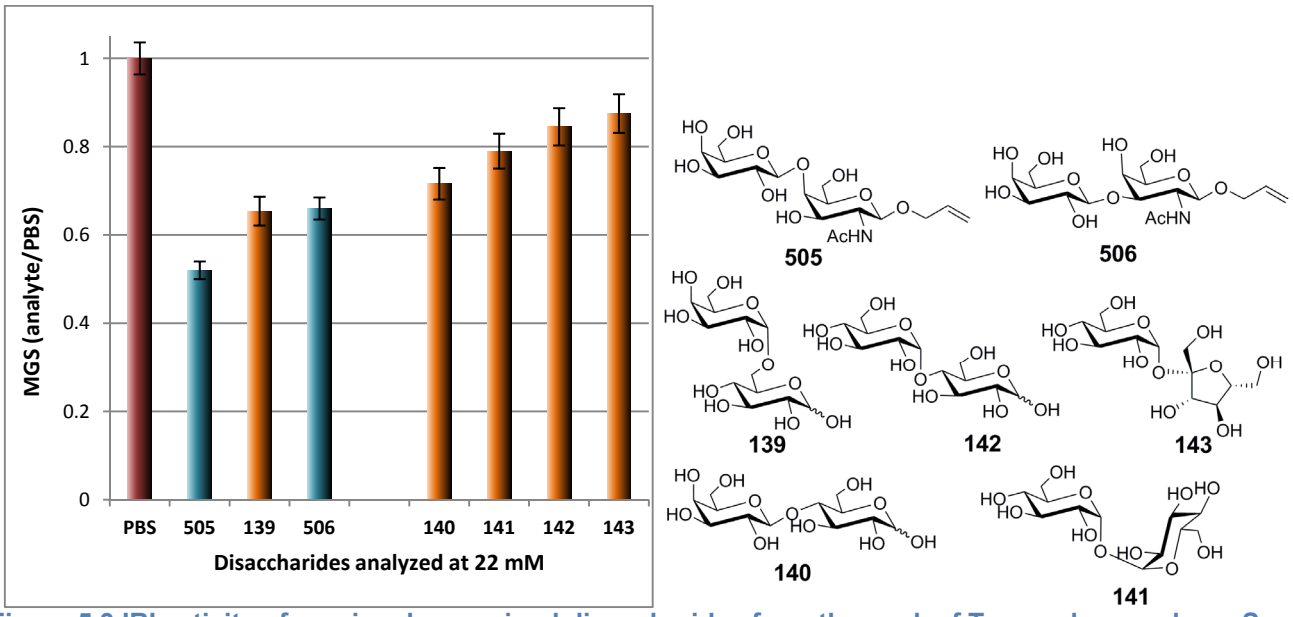



**Figure 5.3 IRI activity of previously examined disaccharides from the work of Tam and co-workers, S. Ferreira and A. Balcerzak.[3,6,7] Galactose containing analogues are in orange, Galactosamine-containing analogues are in blue.**

An initial report describing the correlation of disaccharide IRI activity with hydration parameters involved the examination of several commercially available disaccharides (**139**-**143**).[3] These compounds, along with some N-acetyl derivatives with β-O-allyl groups at the anomeric position produced by S. Ferreira (**505**-**506**),[5, 6] are the only disaccharides that have currently been tested, and their IRI activity is presented in Figure 5.3. A couple of observations can be made about this data. In general, as with the glycopeptides, the most important parameter is a terminal galactose moiety.[7] Of the eight disaccharides examined, all five of the best inhibitors have this feature while the three poorest do not. In general, the presence of the N-acetyl galactosamine residue results in more potent IRI activity than when either a glucose or fructose is the reducing sugar. However the relative merits of the GalNHAc compared to galactose cannot be determined as there are no "matched sets" where both the galactose and N-acetyl galactosamine derivatives are present. The activity of the carbohydrates not containing

a GalNHAc has been correlated to their hydration number (the order of which is mirrored by the partial molar compressibilities shown above in Figure 5.2).[3] Interestingly, of all the analogues that do not include a terminal galactose residue, the most active compound is trehalose (**141**), the (1,1) dimer of glucose.

There are several analogues that should be prepared to better understand the structure-activity relationship of disaccharide IRI activities, but due to limited time, three were specifically chosen for their importance. The first is β-D-galactopyranosyl-(1→3)-D-galactopyranose (**222**). This compound is the direct analogue of the (1,3)-β-Gal-GalNHAc residue found in native AFGP (**506**). The synthesis of this compound would provide the first analogue available for direct comparison between the N-acetyl galactosamine containing derivatives and those lacking this residue to determine what effect the *C*-2 acetamide group has on IRI activity. As the Gal-NHAc containing-residues were prepared with β-O-allyl groups at the anomeric position, the actual target of this study is not **222**, but rather **508**, as this will allow for direct comparison.

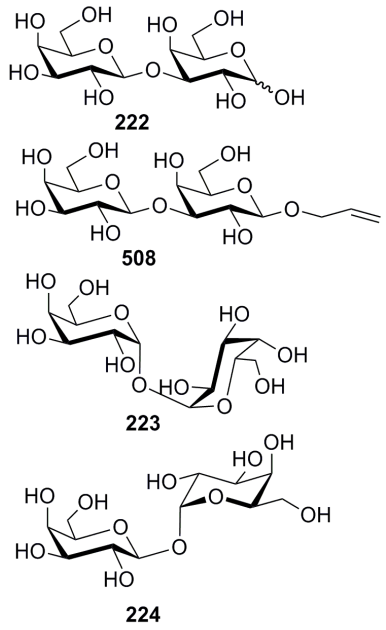


Figure 5.4 Target disaccharides.

The other two analogues chosen are the (1,1)-dimers of galactose (**223** and **224**). As the (1,1)-dimer of glucose, trehalose (a natural cryoprotectant),[8, 9] shows considerably better activity than its configurational isomer melibiose, the same might be true of galactose. Consequently, the observed trends indicate that these compounds may show considerable promise. It has also been noted in both

glycopeptides and simple *C*-linked monosaccharides, that α-linked carbohydrates tend to demonstrate improved IRI activity compared to their β-counterparts. Thus, through the direct comparison of an (α-α)-linked sugar, **223**, with an (α-β)-linked sugar, **224**, it would be possible to see if this trend is extended to disaccharides. For this reason, both of these sugars are also identified as priority targets.

Finally, three other (1,1)-linked disaccharides, namely those produced in Chapter 4 (**1409**-**1411**, Figure 5.5), provide interesting homologues of **223** as the di-alkynyl spacer changes the intra-molecular interactions between the two residues of the disaccharide, and hence the hydration of the compound. The deprotected derivatives of **1409**-**1411** would therefore provide a series for investigating the relationship between the length of a rigid intra-saccharidic linker and IRI activity in (1,1)-linked galactosyl galactose molecules.

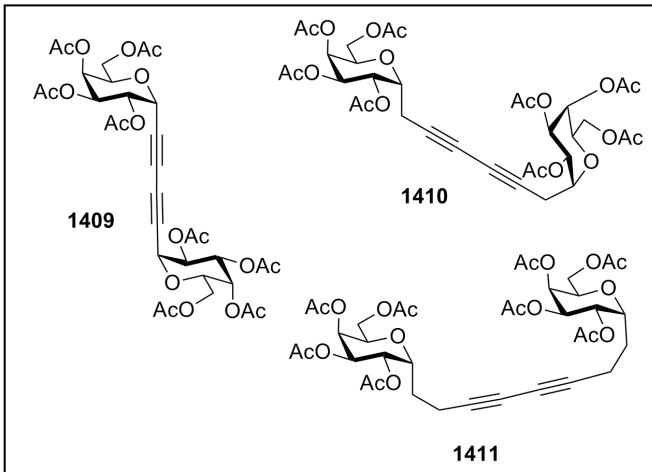
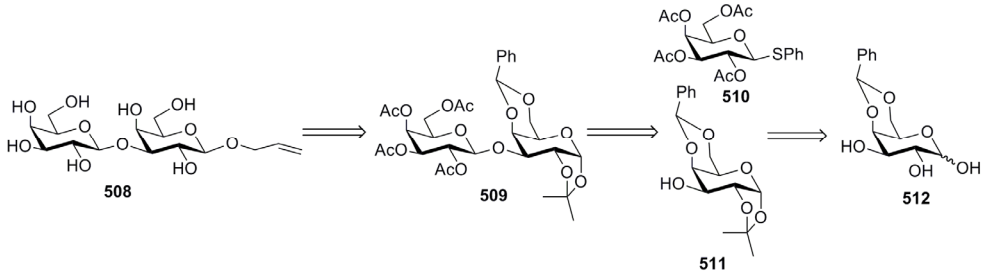



**Figure 5.5 Glaser-disaccharides produced in Chapter 4.**

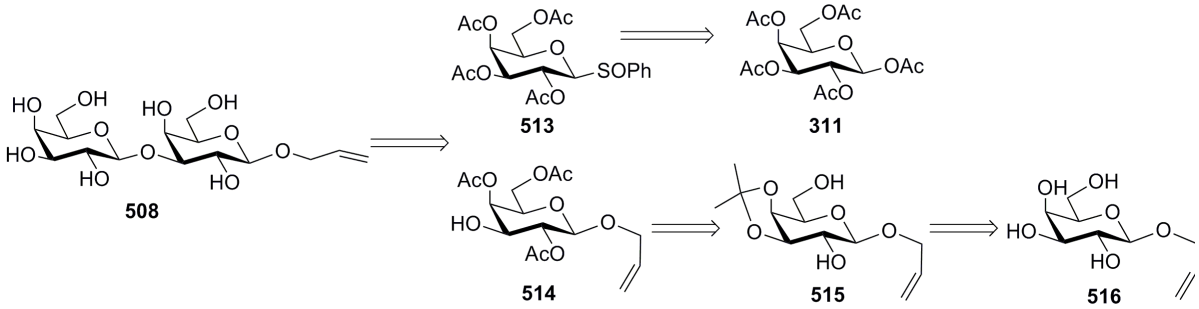
## 5.2 Design and synthesis of a (1,3)-linked galactosyl-galactose derivative

Scheme 5.1 describes the initially attempted approach to **508**.




**Scheme 5.1 Original approach to 508 relying on the selective protection of galactose derivative 511.**

The disaccharide could be formed by the glycosylation of β-thiophenyl galactoside **510** with selectively protected **511** (Scheme 5.1).[11] An alternative approach to **508** incorporates the selective opening of an orthoester to access the desired glycosyl

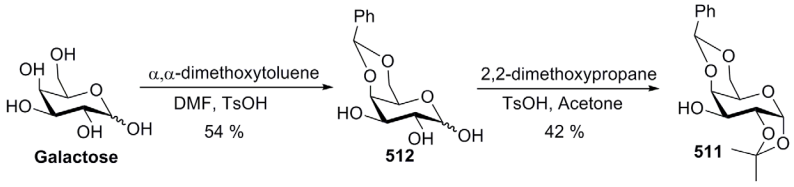



**Scheme 5.2 Alternative approach to β-D-galactopyranosyl-(1→3)-D-galactopyranose derivative 508 relying on selective ring-opening of an orthoester to provide 514.**

acceptor **514** (Scheme 5.2) using the strategy developed by Lemieux.[10] In both cases the glycosyl donor was envisaged to arise from a thioglycoside: an orthogonally activated functional group appropriate for glycosidic couplings, yet at the same time very stable to a variety of reaction conditions. Peracetylation of the donor would likewise ensure the production of the β-anomer in the glycosidation.

## 5.2.1 Synthesis of (1,3)-linked galactosyl-galactose

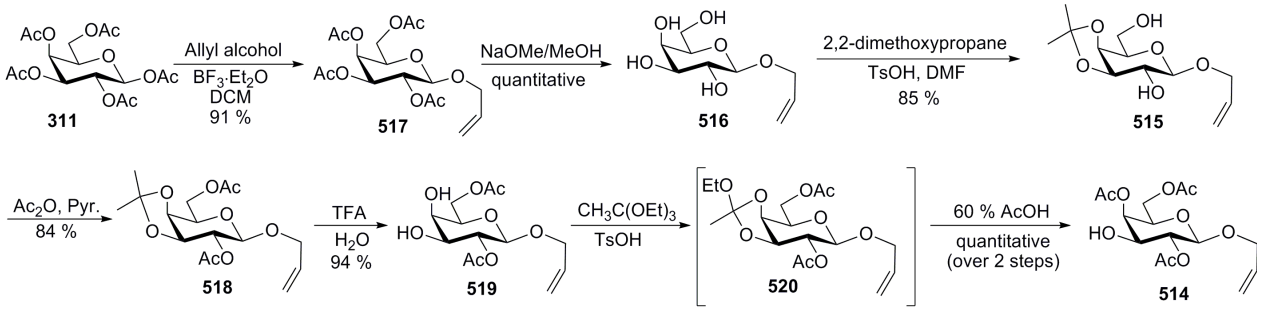
Using the initial approach, galactose was protected as the 4,6-benzylidene under acid-catalyzed thermodynamic conditions to provide protected derivative **512** in 54 % yield after recrystallization (Scheme 5.3). This benzylidene derivative was then further protected using the conditions described by Busse to provide the diacetonide derivative **511** in 42 % yield.[11] Coupling, as envisioned in Scheme 5.1, was then attempted with the desired




**Scheme 5.3 Synthesis of selectively protected galactose derivative 511.**

glycosyl donor (**510**) which was synthesized from β-D-galactose pentacetate under normal conditions in quantitative yield (shown below, Scheme 5.6). The reaction was attempted using recrystallized NIS as activator. The resulting reaction mixtures, however, comprised inseparable mixtures of products. Chromatography of these crude reaction mixtures provided fractions which in turn showed complex mixtures of saccharides with various numbers of acetates, isopropylidenes and benzylidenes. Significant protecting group rearrangement was taking place under the reaction conditions, including ring-opening and ring-closing of the isoproylidene group of **508**.[1] Several attempts at the coupling were made and all failed to produce identifiable product. This result was disappointing but the lability of acetal protecting groups is a common challenge faced in carbohydrate chemistry.

Due to the difficulties arising with the first approach, it was felt that synthesizing the disaccharide would be simpler using a more resilient acetate-protected derivative similar to that used by the Lemieux and Kochetkov groups.[10, 12] The benefits of this route would be the incorporation of the desired O-allyl group prior to glycoside coupling, and in the final step, all protecting groups could be removed simultaneously using Zemplén conditions rather than requiring two separate sets of conditions.[13] Beginning



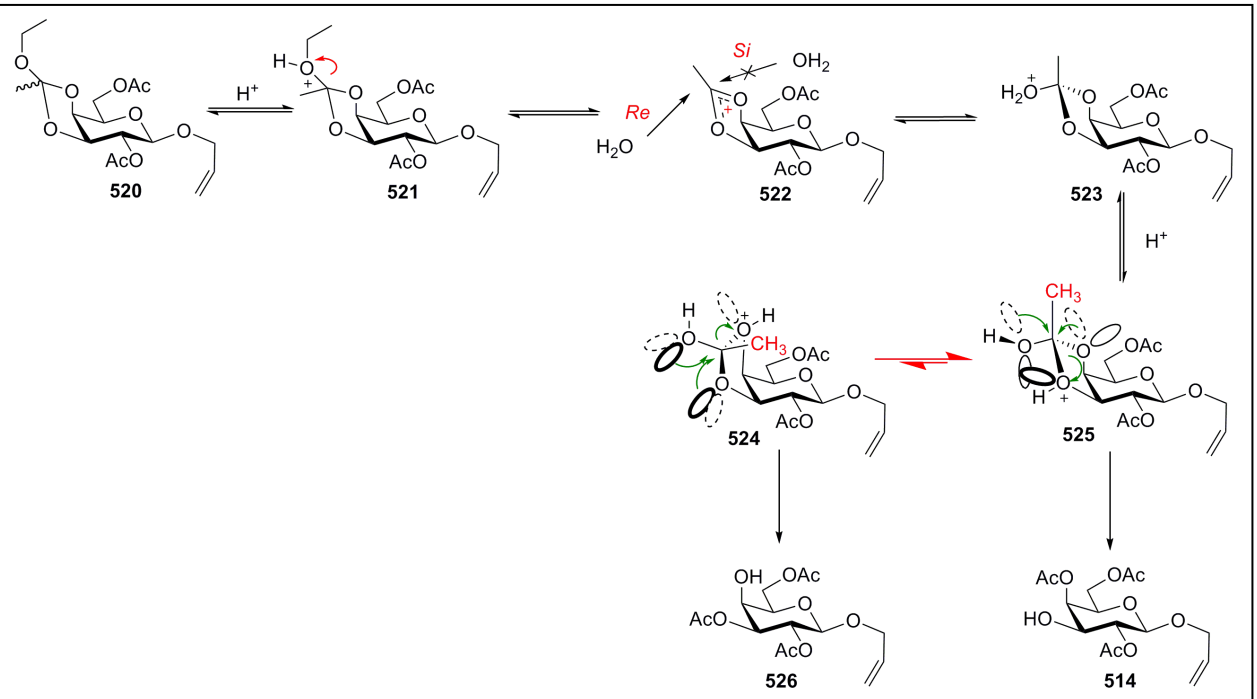

**Scheme 5.4 Synthesis of acetate protected glycosyl acceptor 514.**

with galactose pentacetate (**311**), the sugar is selectively allylated at the β-position

through activation of the anomeric acetate using $BF_3$ as a Lewis acid providing **517** in excellent yield (91 %). The allylated sugar was deprotected under standard conditions using sodium methoxide to provide a quantitative yield of **516**, which was in turn derivatized to the favoured 3,4-isopropylidene **515** under thermodynamic conditions (85 % yield). The remaining hydroxyl groups were acetylated under standard conditions to provide fully protected residue **518** in 84 % yield. Removal of the isopropylidene group under the conditions outlined by Christensen led cleanly to diol **519**, recovered in 94 % yield.[14] This derivative was then subjected to the key transformation, transesterification using triethyl orthoacetate, to produce the diastereomeric mixture of orthoactates (**520**) followed by a regioselective ring opening under acidic conditions to cleanly provide the equatorial hydroxyl derivative **514** in quantitative yield.

This reaction was first described by King and Allbutt in 1970.[15, 16] They observed that when a dioxolenium ring was fused to a cyclohexane, the orthoester functionality tended to open to provide the axial-protected product. However, the exact mechanism of this transformation was better rationalized using stereoelectronic theory (Scheme 5.5).[17] The diastereomeric mixture, **520**, is reversibly protonated under the reaction conditions to **521** and can expel ethanol to generate a planar dioxolenium ion, **522**. Theoretically, the ion could be attacked in either a *Si* or *Re* manner, but the *Si* approach would be severely inhibited by the presence of the pyranose ring, whereas the *Re* face is completely unhindered. Consequently, the addition of water is very stereoselective providing **523** as the only product. Proton transfer could result in one of two isomers, **524** or **525**. These two compounds should be able to equilibrate, but two factors favour

**525**. The first is the increased basicity of the equatorial hydroxyl group relative to the

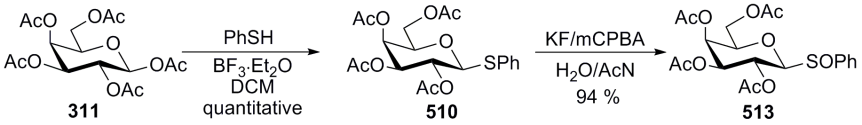



**Scheme 5.5 Stereoelecteronic rationale for the preferential formation of 514 over its *C*-3 acetate isomer. Modified from Deslongchamps.[16]**

axial hydroxyl group,[17] and the second is the dramatically unfavourable steric interaction between the methyl group of the tetrahedral intermediate and the *C*-2 hydrogen, at the very least. These are the two conformations that are most likely to result in ring opening, as they are the only two in which two oxygen orbitals lie parallel with the anti-bonding orbital of the requisite cleavable bond (green arrows). Consequently, as the population of **524** is expected to be small due to its considerably higher energy relative to **525**, the major product isolated from the reaction would be expected to be the one in which the axial hydroxyl group becomes acetylated. This produces **514**, with an equatorial group free for further functionalization, rather than its isomer, **526**, which would arise from the fragmentation of **524**.

In the current case, the reaction is incredibly selective providing **514** in a quantitative yield with no need for further purification. This compound is considerably

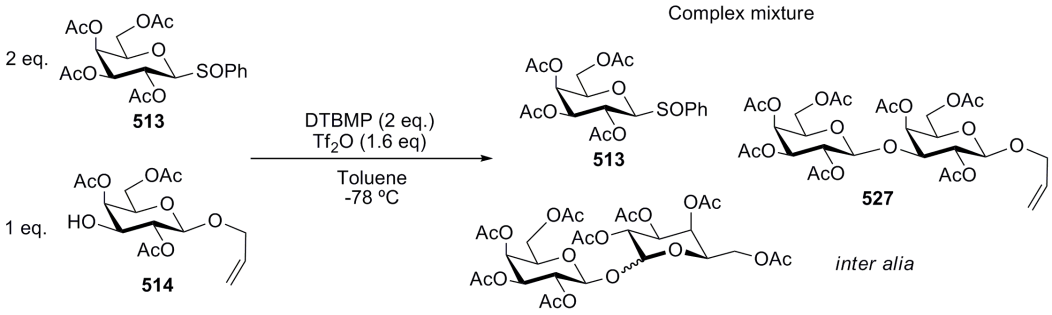
more chemically stable to Lewis acidic conditions than the diacetonide **511**, making it more appropriate for use in glycosidic couplings.




**Scheme 5.6 Synthesis of glycosyl sulfoxide 513.**

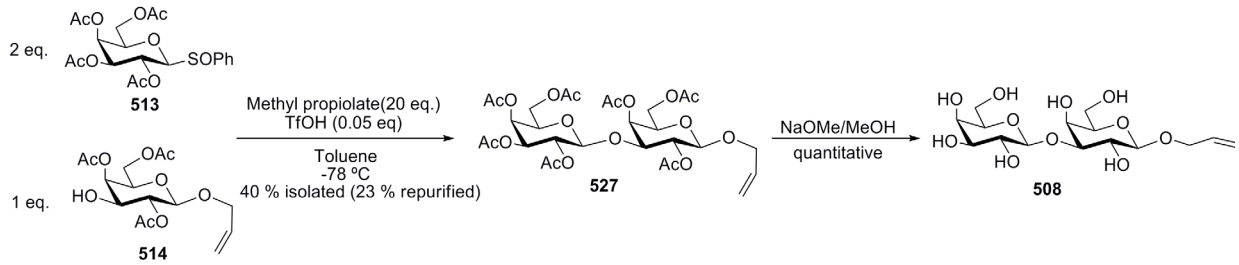
Due to concerns about possible the low(er)-reactivity of thiophenyl derivative **510**, and because glycosyl acceptor **514** would be expected to be less nucleophilic than **511** due to the presence of electron withdrawing acetate groups, sulfoxide derivative **513** was selected as an appropriate glycosyl donor. The product was readily accessible from thiophenyl derivative **510** through a mild and selective oxidation using KF and mCPBA,[18] that gives rise to a 1:1 mixture of the two sulfoxide diastereomers. This reaction presumably produces KOF·AcN as the active oxidation species, a more selective oxidant than mCPBA. This is a very efficient process with no over-oxidation products observed, a drawback common amongst other sulfoxidation reactions attempted.[19, 20]

With this compound in hand, the coupling between sulfoxide **513** and glycosyl acceptor **514** was attempted. There are two common activators for glycosyl sulfoxides. The first uses 1.5-2 equivalents of triflic anhydride in the presence of 2,6-di-*tert*-butyl-4-methyl pyridine (DTBMP), the second




**Scheme 5.7 Attempted synthesis of disaccharide 527 using $Tf_2O$ as activator.**

uses catalytic triflic acid in the presence of a large excess of methyl propiolate.[21, 22] The exact mechanism of the glycosidation is still under debate and appears to be highly substrate dependent.[23] From previous reports, a disarmed donor such as **513** most likely progresses through a $S_N2$-like displacement of either the anchiomeric group or either an $\alpha$-triflate or sulfenate.[24] Yields for these transformations are normally moderate resulting from the high potential for the activators to instigate side-reactions and the high sensitivity of the reaction to adventitious water. Initial attempts using triflic anhydride[25] resulted in very complex mixtures of products in all cases (Scheme 5.7). Major components of this mixture included unreacted sulfoxide **513**, (1,1)-galactose dimers (mixture of anomers), and many different disaccharides, including,

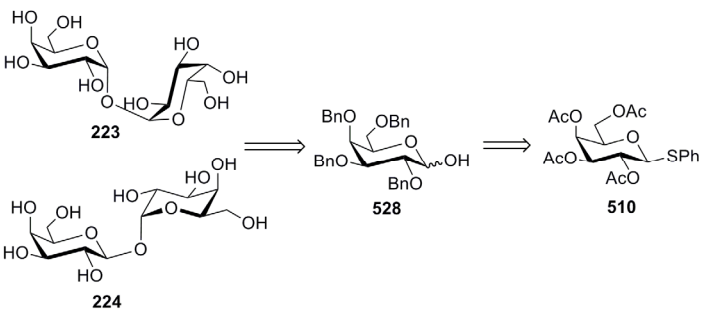



**Scheme 5.8 Synthesis of disaccharide 508 using TfOH as promoter.**

retrospectively, the desired compound, **527**. However, with approximately 15 compounds present, this approach was not deemed a viable strategy to access the desired disaccharide. The large amount of unreacted sulfoxide present after the quench suggested that a more potent promoter was required, and so the reaction was attempted with triflic acid in the presence of methyl propiolate (Scheme 5.8).[26] Starting materials **513** and **514** were combined with freshly activated molecular sieves and dried *in vacuo* in the presence of phosphorous pentoxide. DCM and the acid scavenger methyl propiolate were then added under argon followed by triflic acid at -78 ºC.

Following the reaction, flash chromatography provided a fraction highly enriched with the desired disaccharide, **527**, with a variety of minor contaminants in approximately 40 % yield. This fraction was further purified by preparative TLC to provide **527** in 23 % isolated yield. No further attempts were made to optimize the yield or purity profile of the reaction. The synthesis was then completed through global deprotection of the disaccharide under standard conditions to provide the desired allyl-protected derivative **508** in quantitative yield ready for IRI analysis.

## 5.3 Design and IRI analysis of (1,1)-galactosyl-galactose derivatives



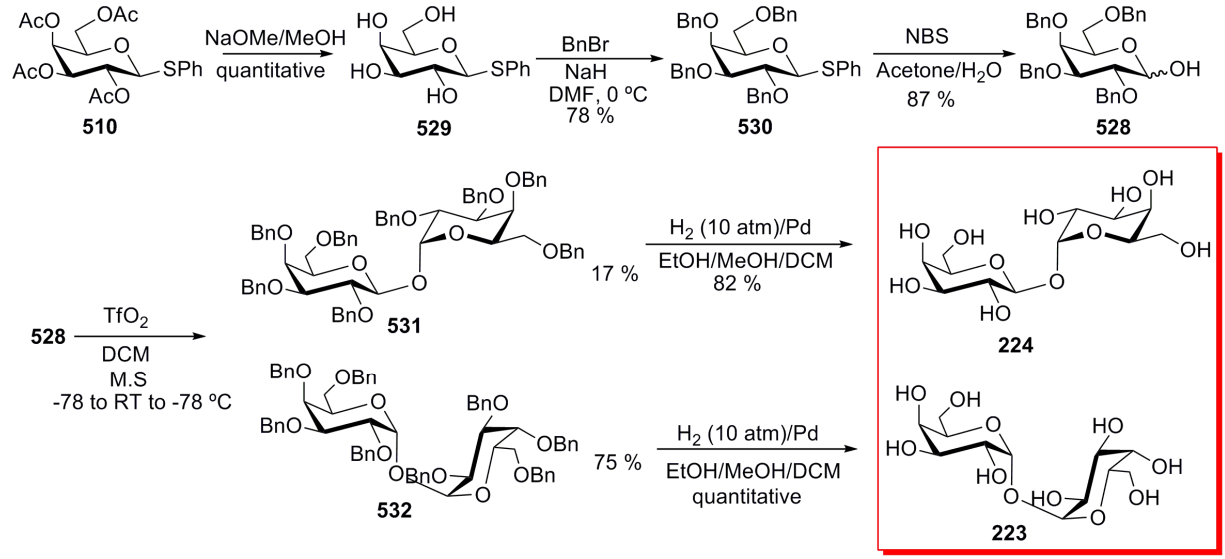

**Scheme 5.9 Proposed retrosynthesis of galacto-trehalose-like disaccharides 223 and 224.**

Compared to the preparation of the (1,3)-linked disaccharide, the synthesis of (1,1)-linked derivatives are simple and the α-analogue has previously been prepared by Pavia.[27] The (α,α)-(**223**) and (α,β)-(**224**) analogues can be readily accessed from the benzyl-protected reducing sugar **528** via a dimerization reaction followed by deprotection (Scheme 5.9). This derivative can be obtained in turn from **510** using well established synthetic protocols involving protecting group exchange followed by desulfurization of the anomeric position.

### 5.3.1 Synthesis of (1,1)-linked disaccharides

The synthesis begins with the preparation of reducing sugar **528** from thiophenyl derivative **510**. Removal of the acetate groups of **510** proceeds very smoothly to provide

deprotected derivative **529** in quantitative yield. This deprotected derivative was benzylated under standard conditions,[28] providing benzyl protected galactoside **530** in 78 % yield after recrystallization from methanol. Desulfurization was accomplished using NBS in the presence of acetone and water to generate the reducing-sugar benzyl derivative **528** in 87 % yield. With **528** extensively dried to remove all traces of water, the dimerization reaction was carried out on **528** using triflic anhydride.[29] It was found that when following the Pavia protocol exactly, the disaccharide appeared to form under the reaction conditions, but was not isolated following workup: only starting material was recovered. It was speculated that this may be due to hydrolysis of the glycosidic bond by triflic acid. Consequently, prior to quenching the reaction with water at – 78 ºC, any triflic acid was neutralized through the addition of excess triethylamine. Following standard aqueous work-up and flash chromatography of the crude reaction mixture, the




**Scheme 5.10 Synthesis of *galacto*-trehaloses 223 and 224.**

two desired disaccharides were isolated in excellent combined yields (75 % for the (α,α) isomer **532** and 17 % for the (α,β) isomer **531**). Interestingly, the ratio of compounds (4.4: 1) differs markedly from that found by Pavia and co-workers (1.6: 1) using the

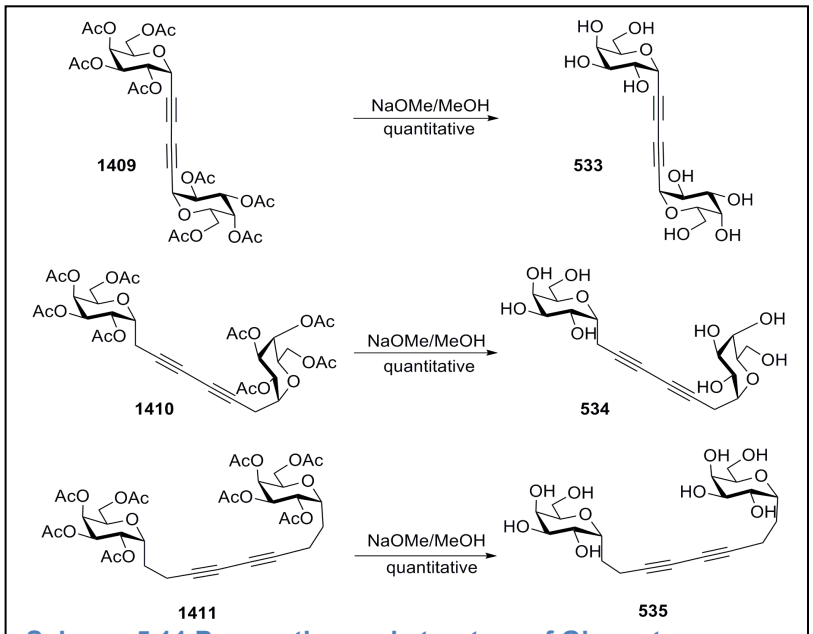
same protocol. The only difference was that the Pavia reaction was carried out at -70 ºC, while a colder -78 ºC was used for the current protocol.

Attempts to de-benzylate both **531** and **532** under atmospheric conditions all failed, including the use of $Pd(OH)_2$, acetic acid as solvent, elevated temperatures and a combination of all three. All reduction conditions returned the starting material unchanged. Consequently high-pressure hydrogenolysis was prescribed as carried out by Pavia; however, initial attempts to deprotect the galactosides also failed under high pressures using ethanol as solvent, the system suggested in the earlier publication. Following reaction, the solution was (clearly) cloudy indicating that solubility might be to blame for the failure. Consequently, a suitable solvent system employing a small amount of more non-polar DCM was employed to fully solubilize the sugars and under these conditions, both compounds were converted in 18 hours to the desired deprotected sugars under 10 atmospheres of hydrogen. Following filtration through a celite pad, the α,α isomer (**223**) was obtained in quantitative yield following lyophilization, while the α,β isomer (**224**) appeared to have become contaminated with some hydrophobic material. Preparative TLC purification provided the disaccharide in 82 % yield following lyophilization. Both compounds were consequently ready for IRI analysis.

### 5.3.2 Analysis of *C*-linked disaccharides produced via Glaser coupling.

The final disaccharides to be prepared are the deprotected derivatives of the Glaser-type compounds generated during the preparation of triazole-containing glycopeptides in Chapter 4. As mentioned, their isolation was surprising as the Glaser coupling normally requires an amine base to be present,[30] and the only basic species

present in solution are sodium ascorbate, released acetate from copper (II) acetate and the free terminal amines of the glycopeptides. Regardless of the mechanism of formation, small amounts of three Glaser disaccharides were isolated from the reaction mixtures, and were immediately recognized as an interesting set of compounds. Their deprotected counterparts are, in effect, (1,1)-linked disaccharides with varying linker lengths between the sugars. The rigidity of the linker makes direct interaction between the two sugars impossible for **533**, and still limits any such interaction in the cases of **534** and **535**. The differences in IRI activity between these compounds and the "natural" (1,1)-linked sugars such as **224** and **223** may be instructive. Consequently all three Glaser-coupled derivatives were deprotected under standard conditions to provide the free sugars in quantitative yields in all cases, ready for IRI analysis.




**Scheme 5.11 Preparation and structure of Glaser-type disaccharides.**

## 5.4 Preparation of monosaccharide derivatives

Another series of analogues of interest for the preparation of small molecule IRI active compounds are *C*-linked α-anomerically substituted galactosides (Figure 5.6). Consequently, to determine whether the nature of the anomeric substituent plays a important role in determining IRI activity, several monosaccharide derivatives were also

tested for IRI activity. These analogues are of general interest as they help to provide further data on the effect of the nature of the anomeric substituent on the IRI activity of galactose derivatives. Our lab has previously produced several *C*-linked analogues with various functional groups at their terminus, reviewed in Chapter 3.[3, 31] These new analogues extend this study into two new functional groups (alkyne and azide) and also allow for an investigation into the relationship between spacer length and IRI activity for alkyne, azide and alcohol series. Consequently, three sets of compounds were examined: the alkyne containing monomers (**445**-**447**), their azide substituted analogues (**417, 536** and **537**), and the hydroxylated analogues of these derivatives (**538**-**540**, Figure 5.6). The alkyne compounds are of particular interest at this point as, due to the unusual nature of the linker between the Glaser disaccharides, any difference in IRI activity could be ascribed to the nature of the linker rather than to the interaction of the carbohydrates. Each series contains three compounds with different carbon spacer lengths ranging from 0 to 2 methylene groups (Figure 5.6). In the case of the alkynes and azides, the length parameter indicates the

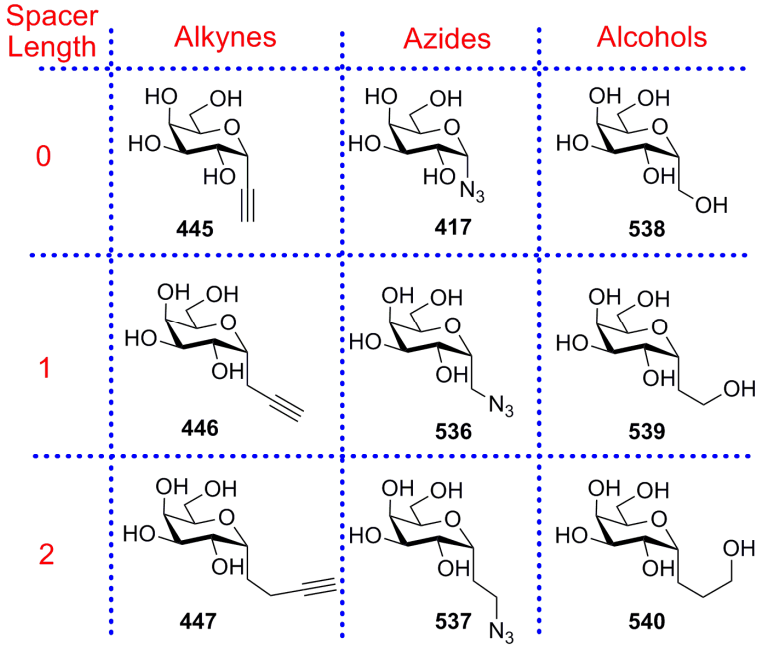
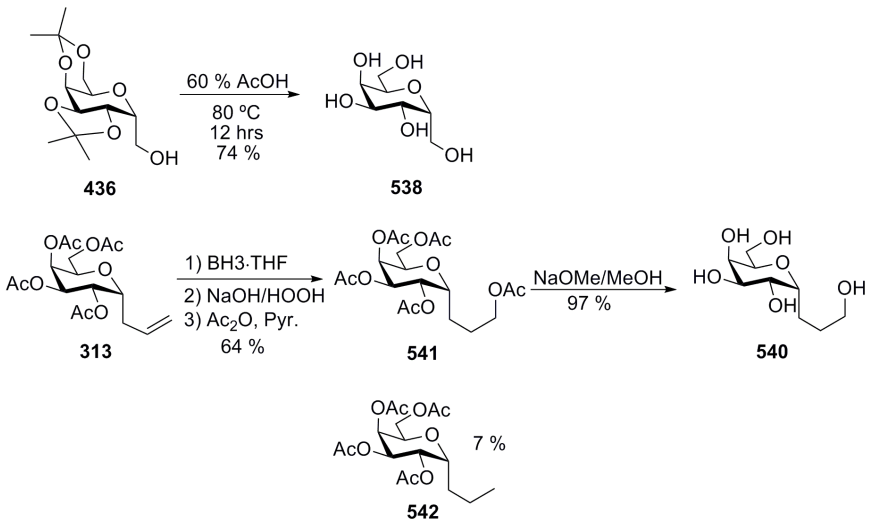



**Figure 5.6 Monosaccharide control compounds analyzed for IRI activity in Figure 5.7. Compounds are categorized by functional group (vertical) and length of anomeric substituent (horizontal). Compound 539 was previously prepared by J. Chaytor. Polyols 538 and 540 were prepared as shown in Scheme 5.12 below. All other compounds were obtained through Zemplén deprotection from the corresponding acetate.**

number of methylene spacers between the anomeric carbon and the functional group. In the case of the alcohol series, the parameter indicates the number of methylene groups between the anomeric carbon and a *C*-linked methanol group. The overall length of each substituent is equal in each category (3 atoms of the substituent in the case of the (0) group, 4 in the case of the (1) group, and 5 in the case of the (2) group).

All the azide and alkyne derivatives were readily available as their acetylated counterparts played key roles in the syntheses of the various glycopeptides already described in Chapter 4. The alcohols had to be prepared separately. Their synthesis will be briefly described here.

*C*-galactoside **539** had previously been prepared and tested by J. Chaytor,[31] leaving only **538** and **540** to be prepared. Both compounds were readily accessed from synthetic intermediates used in the preparation of sugars **445** and **447** respectively (Scheme 5.12).




**Scheme 5.12 Synthesis of polyols 538 and 540 for use in the IRI assay.**

Derivative **538** could be readily prepared from **436**. Simple acetolysis at 80 ºC provided the desired glycoside following preaparative TLC in 74 % yield. *C*-propanol derivative **540** required a little more extensive effort. *C*-allyl galactose derivative **313** was treated with borane as described in the synthesis of **447** (Chapter 4), but rather

than a direct over-oxidation of the boron-carbon bond to provide the aldehyde, the intermediate was treated under more traditional deboration conditions (hydrogen peroxide and sodium hydroxide), and the crude product was immediately reacetylated to provide the acetylated anti-Markovnikov product **541** in 64 % yield after standard work-up and flash chromatography. Interestingly, the only other compound present in the organic phase was identified as the fully hydrogenated **542** in 7 % yield. The formation of this compound is extremely surprising: the boron bond is cleaved under very oxidizing conditions, and so a reduction product is not expected. The formation of this compound may merit further study. Regardless, the acetylated **541** was deprotected under standard conditions in quantitative conversion, but unfortunately had to be purified through extraction as plasticizer was observed in the initial NMR of **540**. This process lowered the isolated yield to a still very respectable 97 %. With all compounds in hand, the IRI analysis of the disaccharides and these monosaccharides was ready to be carried out.

## 5.4 IRI activity of disaccharides and the monosaccharide derivatives

The compounds produced above were then analyzed for IRI activity using the splat cooling assay. The monosaccharides have been arranged in order of increasing spacer length (brackets) between the functional group and the carbohydrate (Figure 5.7). The colours in the figure represent the different series of compounds: azides are in red, alkynes in blue and alcohols in orange. In the azide family, activity increases moderately as the linker becomes longer (**536** and **537** compared to shorter **417**). However, this trend is clearly not present for either the alkyne or alcohol series: in both

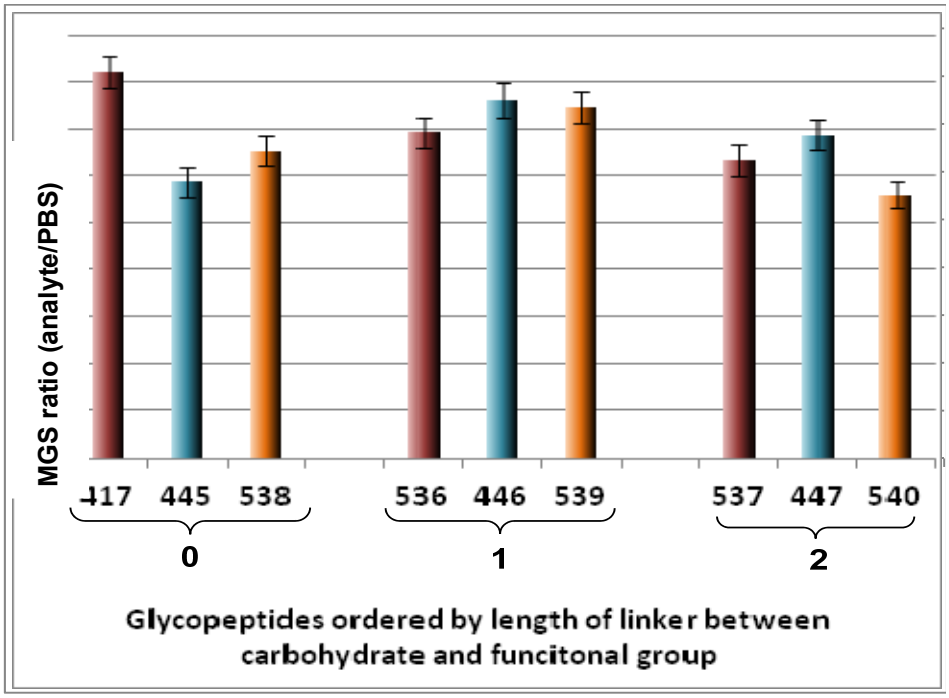



**Figure 5.7 IRI activity of monosaccharide derivatives in Figure 5.6. All compounds are analyzed at 22 mM. Compounds are categorized by functional group (colour), and spacer length (groups). Spacer length indicates the number of methylene groups between the anomeric carbon of the sugar and the functional group for the azide (red), and alkyne (blue) or a methanol moiety in the case of the alcohols (orange).**

cases linker lengths of 0 and 2 methylene groups (**445**, **447**, **538**, **540**) show moderately improved activity relative to those with a single methylene spacer (**446** and **539**). Clearly, the length of the alkynyl linker would not predict a trend in IRI activity for the Glaser coupled-disaccharides based on these results. However, all compounds show only modest IRI activity, and besides the anomeric azide **417**, the differences within and between any series are not large. It appears that the length and nature of the anomeric substituents of *C*-galactosides are not defining parameters for determining IRI activity.

With these monosaccharides examined, the Glaser-type, and “natural” disaccharides were likewise examined for IRI activity (Figure 5.7). The (1,3)-derivatives are in orange, the (1,1)-derivatives in blue and the Glaser-derived disaccharides are in red. Within each series interesting results arise. The first result is the direct comparison of previously tested (1,3)-linked galactosyl-N-acetyl galactosamine **507** compared to the (1,3)-linked galactosyl-galactose **508**, the first time a GalNHAc-containing disaccharide

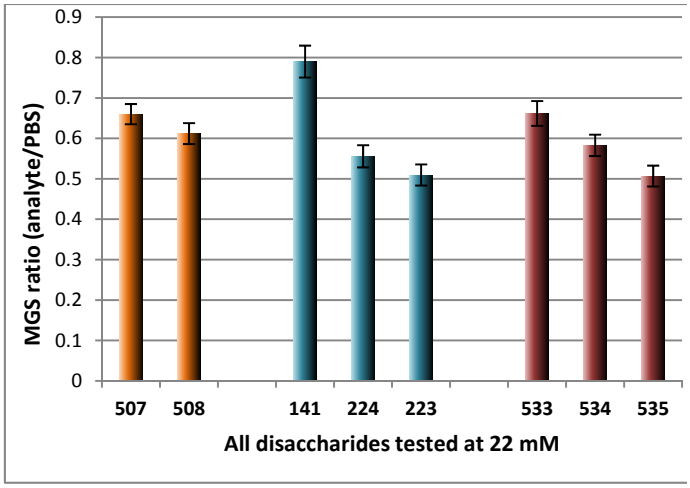



**Figure 5.8 IRI activity of disaccharides prepared in this chapter and their previously examined direct analogues.**

and its galactose analogue have been directly compared. The work of Nishimura showed that when these two sugars are both linked to a peptide backbone, the analogue containing **507** (the native AFGP disaccharide) shows TH activity while that containing **508** does not.[32] However, these results show that when present as simple disaccharides, both compounds show comparable activity in the splat cooling assay (when both have a β-*O*-allyl group blocking the anomeric position on the reducing sugar). The higher-level of antifreeze activity (TH) for the acetamide derivative compared with the galactose-containing disaccharide observed by Nishimura in the case of a glycoconjugate is most likely due to the participation of the N-acetyl group in some form of intramolecular interaction with the peptide rather than due to the inherent nature of the group itself. Clearly, in the case of isolated disaccharides, the presence or absence of an N-acetyl group plays little role in determining IRI activity. It would be interesting to see if this is a general trend or simply specific to this particular regioisomeric pair. To properly address this question, the other regioisomers of **508** would need to be prepared.

In the case of the (1,1)-linked disaccharides, both **223** and **224** show considerably better activity than their glucose analogue, trehalose, **141**. In fact (α,α)-isomer **223** shows the best IRI activity of any disaccharide tested to date (although it is only slightly more active than melibiose, **505**), as was hypothesized above. In fact, if

anything, it is rather surprising that (α,α) analogue **223** is not even more potent than its (α,β) analogue **224**. The importance of an α-linkage, rather than a β-linkage for antifreeze activity is well precedented.[4, 7, 31-33] This is true for (peptide-linked) disaccharides as well. However, in the case of most analyzed disaccharides, the intra-saccharidic linkage is often β and no clear trend in IRI activity is apparent when comparing disaccharides linked α with those with a β-intra saccharidic bond. Consequently, perhaps anomeric configuration is only important at the peptide-bound residue, consistent with the small difference in IRI activity observed between **223** and **224**.

The trehalose-like compounds (**223** and **224**) both show remarkable activity and are two of the more potent disaccharides tested to date. Anomeric substitution has previously been shown to have the smallest detrimental effect to IRI activity in monosaccharide derivatives.[31] This result is consistent with the proposals of Simons suggesting that substitution at the anomeric position purportedly has the least impact on the hydration network of carbohydrates. The relevance of Simons' observations on the intramolecular hydrogen-bonding networks in carbohydrates in the gas phase to those in aqueous solution is questionable. However, tentatively, substitution at the anomeric position would be expected to have the smallest impact to the hydration of the sugar, and consequently, if relevant to the aqueous system, one would expect the best IRI activity from compounds of this type. Analogues **223** and **224** appear to suggest that this relationship may be present in disaccharides as well.

Finally a very interesting trend is observed in the Glaser coupled derivatives (**533**-**535**). As the length of the linker between the disaccharides becomes longer, the

IRI activity of the compounds appears to improve. The carbohydrate components of the disaccharide remains unchanged, only the length of the linker gets bigger. It would be interesting to examine longer Glaser-coupled disaccharides to determine whether this trend continues and to propose a hypothesis for this trend in activity. Nevertheless, these are all (1,1)-linked disaccharides and like the trehalose analogues examined above, the activity of these compounds, especially **535**, are amongst the most potent of the disaccharide analogues tested to date. This is further evidence regarding the privileged nature of the (1,1) glycosidic linkage. All analogues are at least as potent ( in terms of IRI activity) as galactose, and **534** and **535** are more active than galactose, demonstrating that there is a possibility for developing non-peptide based inhibitors of ice recrystallization.

## 5.5 Chapter Summary

In this study, three key “natural” disaccharides were chosen as synthetic targets to explore the importance of the N-acetyl galactosamine motif to IRI activity and to examine the effect that a (1,1) substitution pattern would have on IRI activity. Similarly, the three Glaser-type disaccharides prepared in Chapter 4 formed an interesting series of analogues that allowed for an investigation into the importance of the length of the intra-saccharidic linker to IRI activity. To control for explanations that could arise regarding the nature of local interactions due to the anomeric substituent of the monomer, nine control monosaccharides were synthesized and tested.

The results of these studies indicated that a (1,3)-linked disaccharide without a *C*-2 N-acetyl domain showed better activity than the N-acetyl galactosamine derivative. Similarly, the two all-galactose trehalose derivatives were significantly more potent, in

terms of IRI activity, than trehalose and were both more potent than other galactose-containing disaccharides tested to date, both with and without an N-acetyl moiety. This is significant as it corroborates the studies by Simons,[34, 35] and Engberts and Galema,[2, 36] that show that (1,1)-linked sugars are (or should be) more highly hydrated than their regioisomers, and that this hydration expresses itself directly in terms of improved IRI activity.

The studies on monosaccharides showed that in the case of azide-containing analogues, the number of methylene groups is positively correlated with IRI activity. However, in the case of alkyne or alcohol–containing derivatives, there is no obvious correlation between length and activity in such short-chain analogues.

However, the IRI activity of these analogues shows that there is a possibility for the generation of simple, non-peptide based IRI inhibitors. The special success of the (1,1)-linked disaccharides is consistent with Simons' theory of a putative intramolecular hydrogen bonding network being important to hydration, and consequently IRI activity, in bulk solvent. This relationship cannot be dismissed and clearly deserves further study.

## References

1. Czechura, P. Elucidating the relationship between hydration and ice recrystallization inhibition with *C*-linked antifreeze glycoproteins. PhD. Thesis, University of Ottawa, Ottawa, 2009.

2. Galema, S. A.; Hoeiland, H., *J. Phys. Chem.* **1991,** *95* (13), 5321-5326.

3. Tam, R. Y.; Ferreira, S. S.; Czechura, P.; Chaytor, J. L.; Ben, R. N., *J. Am. Chem. Soc.* **2008,** *130* (51), 17494-17501.

4. Czechura, P.; Tam, R. Y.; Dimitrijevic, E.; Murphy, A. V.; Ben, R. N., *J. Am. Chem. Soc.* **2008,** *130* (10), 2928-2929.

5. Ferreira, S. S. Improving the rational design of antifreeze glycoproteins through identification of the parameters that influence ice recrystallization inhibition. University of Ottawa, Ottawa, 2010.
6. Balcerzak, A.; Ben, R. N., Unpublished work. 2011.
7. Bouvet, V. R. Novel AFGP8 Analogues: Synthesis and Biological Evaluation of Potent Recrystallization Inhibitors. PhD. Thesis, University of Ottawa, Ottawa, 2006.
8. Leslie, S. B.; Israeli, E.; Lighthart, B.; Crowe, J. H.; Crowe, L. M., *App. Env. Microbiol.* **1995,** *61* (10), 3592-3597.
9. Crowe, J. H.; Crowe, L. M.; Chapman, D., *Science* **1984,** *223* (4637), 701-703.
10. Lemieux, R. U.; Driguez, H., *J. Am. Chem. Soc.* **1975,** *97* (14), 4069-4075.
11. Busse, H.; Hakoda, M.; Stanley, M.; Streicher, H., *J. Carb. Chem.* **2007,** *26* (3), 159-194.
12. Chernyak, A. Y.; Levinsky, A. B.; Dmitriev, B. A.; Kochetkov, N. K., *Carb. Res.* **1984,** *128*, 269-282.
13. Wang, Z., Zemplén Deacetylation. In *Comprehensive Organic Name Reactions and Reagents*, John Wiley & Sons, Inc.: 2010.
14. E. Christensen, J.; Goodman, L., *Carb. Res.* **1968,** *7* (4), 510-512.
15. King, J. F.; Allbutt, A. D., *Can. J. Chem.* **1969,** *47* (9), 1445-1459.
16. King, J. F.; Allbutt, A. D., *Can. J. Chem.* **1970,** *48* (11), 1754-1769.
17. Deslongchamps, P., *Stereoelectronic effects in organic chemistry*. 1st ed.; Pergamon: Oxford, 1983; p 375.
18. Agnihotri, G.; Misra, A. K., *Tetrahedron Lett.* **2005,** *46* (47), 8113-8116.
19. Chen, M.-Y.; Patkar, L. N.; Chen, H.-T.; Lin, C.-C., *Carb. Res.* **2003,** *338* (12), 1327-1332.
20. Chen, M.-Y.; Patkar, L. N.; Lin, C.-C., *J. Org. Chem.* **2004,** *69* (8), 2884-2887.
21. Kürti, L.; Czakó, B., Kahne glycosidation. In *Strategic application of named reactions in organic synthesis*, Elsevier: Burlington, MA, 2005.
22. Aversa, M. C.; Barattucci, A.; Bonaccorsi, P., *Tetrahedron* **2008,** *64* (33), 7659-7683.
23. Crich, D.; Sun, S., *J. Am. Chem. Soc.* **1997,** *119* (46), 11217-11223.

24. Gildersleeve, J.; Pascal, R. A.; Kahne, D., *J. Am. Chem. Soc.* **1998,** *120* (24), 5961-5969.
25. Kahne, D.; Walker, S.; Cheng, Y.; Van Engen, D., *J. Am. Chem. Soc.* **1989,** *111* (17), 6881-6882.
26. Raghavan, S.; Kahne, D., *J. Am. Chem. Soc.* **1993,** *115* (4), 1580-1581.
27. Pavia, A. A.; Rocheville, J.-M.; Ung, S. N., *Carb. Res.* **1980,** *79*, 79-89.
28. Czernecki, S.; Georgoulis, C.; Provelenghiou, C., *Tetrahedron Lett.* **1976,** *17* (39), 3535-3536.
29. The dimerization reaction was also attempted using the acetate protected derivative. The reaction conditions led to a very compex mixture of products, including both monosaccharides and disaccharides (by mass spectrometry) most likely due to acid-catalyzed migration of acetate groups. This unfortunate outcome is most likely realted to the difficulties encountered in the sysnthesis of the earlier disaccaride.
30. Siemsen, P.; Livingston, R. C.; Diederich, F., *Angew. Chem. Intl. Ed.* **2000,** *39* (15), 2632-2657.
31. Chaytor, J. L. Examining the role of carbohydrate hydration and structure in preventing ice-recrystallization. PhD. Thesis, University of Ottawa, Ottawa, 2010.
32. Tachibana, Y.; Fletcher, G. L.; Fujitani, N.; Tsuda, S.; Monde, K.; Nishimura, S.-I., *Angew. Chem. Intl. Ed.* **2004,** *43*, 856-862.
33. von Moos, E. Investigating the importance of hydrophobicity and hydration of carbohydrates and antifreeze glycoprotein analogues to ice recrystallization inhibition activity and cryopreservation. PhD. Thesis, University of Ottawa, Ottawa, 2011.
34. Simons, J. P.; Davis, B. G.; Cocinero, E. J.; Gamblin, D. P.; Stanca-Kaposta, E. C., *Tetrahedron: Assym.* **2009,** *20* (6-8), 718-722.
35. Simons, J. P.; Jockusch, R. A.; Carcabal, P.; Huenig, I.; Kroemer, R. T.; Macleod, N. A.; Snoek, L. C., *Int. Rev. Phys. Chem.* **2005,** *24* (3-4), 489-531.
36. Galema, S. A.; Howard, E.; Engberts, J. B. F. N.; Grigera, J. R., *Carb. Res.* **1994,** *265* (2), 215-225.

# Chapter 6 : An exploration of the effect of anomeric aryl substituents on the IRI activity of pyranoses

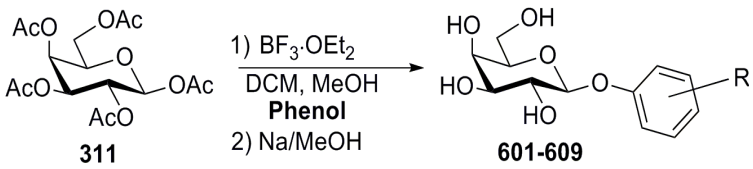
The results described in Chapter 5 above, and the efforts of previous research from the Ben group, suggest that substitution at the anomeric position is better tolerated (and in fact can be beneficial) in terms of maintaining IRI activity, than substitution at other positions.[3, 4] This is supported by the fact that the 1,1-substituted trehalose has been shown to both have better IRI activity and be better hydrated, than the other regioisomers.[5, 6] Similarly, monosaccharide derivatives substituted at the anomeric position, with methoxy groups for example, show considerably better IRI activity than those with substituents at other positions.[3, 4] The anomeric position appears to be privileged as a locus for substitution with respect to IRI activity. It is possible that changes to the electronics of the anomeric oxygen may have an influence on IRI activity. Therefore a series of analogues, substituted at the anomeric position with variously functionalized *O*-aryl groups, were considered interesting targets for the investigation of the role that the electronics of the anomeric oxygen may have on IRI activity. If the electronics of the anomeric oxygen are important to IRI activity, it would suggest that the electronics of this atom affect the hydration of the carbohydrate as a whole rather than any purely local effect. This is because the removal of the anomeric oxygen altogether appears to have no effect on IRI activity, consequently mild changes to its electronics would not be expected to influence IRI activity if the removal of the oxygen completely does not influence IRI activity.[3, 4]

Therefore, in an attempt to investigate the importance of this parameter to IRI activity, a series of anomeric aryl-substituted galactose residues were designed. Their synthesis was, for the most part, carried out by Malay Doshi under the supervision of the author as an honour's thesis.

## 6.1 Design and synthesis of anomeric-substituted galactose derivatives

To fully investigate the electronic effect of anomeric substitutions, compounds with *para*-substituted groups were felt to be the most desirable initially as the functional group would not, itself, interact with the hydrogen-bonding network of the sugar. To cover a wide range of possible electronics, strong electron withdrawing groups, such as 4-Fluoro, 4-(trifluoromethyl)- and 4-nitrophenols were selected. In terms of strong electron donating groups, the 4-methoxyphenol was desirable as was the slightly electron-rich 4-methylphenyl and the "neutral" phenyl derivatives. All compounds were synthesized according to the same procedure, using commercially available β-D-galactose pentacetate (**311**) as the glycosyl donor and $BF_3{\cdot}OEt_2$ as the Lewis acid activator (Table 6.1).[7] Following standard work-up, the crude products were deacetylated and purified through recrystallization of the deprotected β-galactosides. This worked well for all compounds

**Table 6.1 Synthesis of β-aryl substituted galactose derivatives.**




311 601-609

| entry | phenol reagent | product | yield |
|---|---|---|---|
| i | phenol | **601** | 41 % |
| ii | 4-methoxyphenol | **602** | 82 % |
| iii | 4-methylphenol | **603** | 48 % |
| iv | 4-fluorophenol | **604** | 75 % |
| v | 4-(trifluoromethyl)phenol | **605** | 19 % |
| vi | 4-nitrophenol | **606** | 19 % |
| vii | 3,5-difluorophenol | **607** | 22 % |
| viii | 3,5-dimethylphenol | **608** | 29 % |
| ix | 3,4,5-trifluorophenol | **609** | 20 % |

except for the two most electron deficient, and hence least nucleophilic, phenols (**605** and **606**, entries v and vi). No attempt was made to optimize the yields or change the conditions for these substrates. Once the initial IRI results were obtained with the mono-substituted derivatives, the di-substituted methyl- and fluorophenyl (entries vii, and viii) were prepared as was the tri-substituted fluoro derivative.

Interestingly, in the case of the trifluorinated compound (**609**), a mixture of the $\alpha$ and β anomers was obtained (1:3.3) following purification as an inseparable anomeric mixture, and was tested as such. Likewise, in the case of the *para*-nitro compound (**606**), some of the $\alpha$-anomer was also obtained, but could be readily removed through recrystallization (contributing to the low yield in this case); similarly some of the α-product was also observed in the preparation of mono-fluorinated **604**, but was easily separated at the acetate stage. That this occurred in three of the more electron deficient phenols is most likely not coincidental as their low reactivity can lead to the formation of the α-anomer through the oxocarbenium intermediate. In the case of an electron poor-substituent, the kinetic anomeric effect should be amplified as the transition state leading to the α-anomer would be stabilized through the lower lying σ* orbital of nascent anomeric bond. This would decrease the energy difference between the α and β-forming transition states, and would be expected to decrease selectivity in the glycosidation reaction.

With all compounds in hand (Table 6.1), the analogues were examined for IRI activity using the “splat”-cooling assay in the manner described above.[8, 9]

## 6.2 IRI activity of anomeric-substituted galactose derivatives: correlation between activity and Hammett coefficient

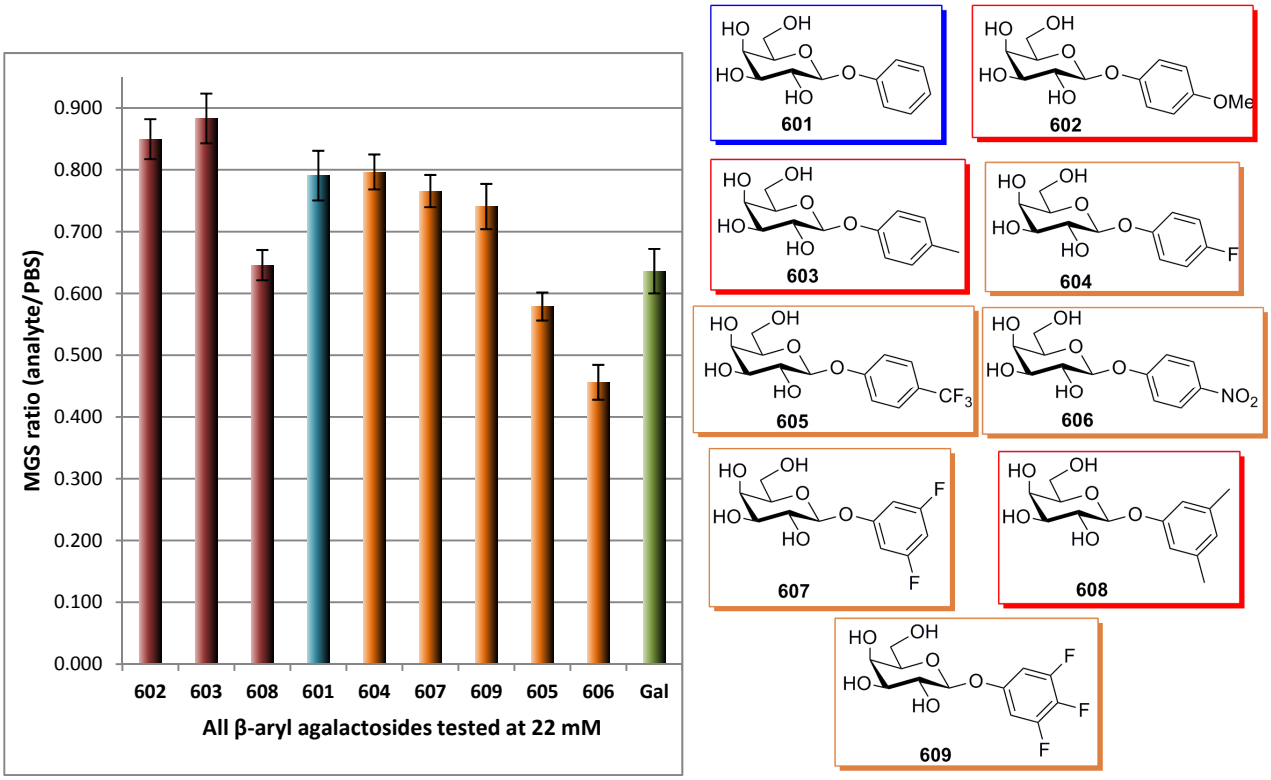



**Figure 6.1 IRI activity of β-aryl galactosides: electron rich, red; phenyl derivative, blue; electron poor, orange; galactose, green.**

The IRI data is provided in Figure 6.1 arranged in order of decreasing electron density at the anomeric oxygen. The analogues with higher electron density at the anomeric oxygen than phenyl derivative **601** are presented in red, those with lower electron density than **601** are presented in orange, the "neutral" phenyl group is presented in blue, and galactose itself is in green. As a reminder, the ice crystals in galactose itself are 65 % the size of those in PBS (similar to **608**).

Amongst the electron rich substituents, no clear trend is discernable. Although methoxy-derivative **602** is considerably more electron-rich than methyl or dimethyl derivatives **603** and **608** respectively, it exhibits activity similar to **603**. The surprisingly

strong activity of **608** is most likely unrelated to any electronic factor, and may be due, rather, to increased hydrophobicity relative to **603**. Consequently, with respect to electron rich phenyl rings, the electronic component appears to have no correlation to IRI activity.

The story is considerably different with respect to electron-poor substrates. The electronically neutral phenyl derivative **601** shows quite poor activity (MGS ratio of 0.79 to PBS), very similar to the slightly electron deficient mono-fluorinated analogue and to previously prepared β-allyl galactosides indicating that the introduction of a phenyl group does not significantly affect IRI activity compared to allyl groups, as seen in the introduction (Figure 1.22). The interactions between and effects of the functionalities on the aryl groups and the hydration shell are not known, and cannot, currently, be measured. However, as electron density is reduced at the anomeric oxygen, IRI activity does as well. However, keeping this caveat in mind, the trend is still remarkable as the comparably hydrophobic trifluoromethyl-substituted derivative **605** and hydrophilic 4-nitro derivative, **606**, show activity corresponding to their electron density rather than due to the presence or absence of inducible dipoles.

Changing the electron density of the anomeric oxygen (or indeed any oxygen) could alter the hydration of the molecule as a whole. Interestingly, however, the substitution of a *C*-allyl group for a *O*-allyl group at the anomeric position does not result in any change in IRI activity.[4] If this oxygen was truly involved in hydration, its removal and replacement with an electronically very different methylene group would be noted in the IRI activity. It is also well precedented that C-glycosides adopt very similar conformations and structure to O-glycosides in solution indicating that the anomeric

oxygen does not play an important role in the interactions between the glycoside and the bulk water.[10, 11] Consequently the hydration shell does not appear to be significantly affected by interactions with the anomeric oxygen itself. Thus, it is quite possible that in the case of electron poor substrates, it is in fact the electronics of the aryl ring, and its effect on the electronics at the anomeric oxygen, that are defining the IRI activity. Fortunately, there is a method to examine this relationship, the Hammett relationship, although it is only valid for di-substituted aryl rings.[1, 12]

The Hammett relationship is the empirical observation that there is a relationship between equilibrium constants and reaction rates. In practical terms, this has been extensively applied to reactions involving an aryl group near the reaction site; changing the electronics on the aryl group (and thus the ionization (equilibrium) constant for the respective benzoic acid derivative) affects the reaction rate in a predictable manner.[1, 13] Consequently any kinetic process can be examined through the Hammett relationship to determine the influence of the electronics of the aryl group on the reaction rate. Although IRI is not a reaction *per se*, it is a kinetic measurement, and the measurement of the ice crystal area is akin to an initial velocity of ice recrystallization. The size of the ice crystals after 30 minutes of annealing is dependent on the rate of Ostwald ripening. The slower the ice recrystallization process, the smaller the crystals. Consequently, the ice crystal area is a kinetic measurement, and as such can be correlated to the Hammett coefficients (σ) through the Hammett relationship.

$$\rho\sigma_x = \log K_x - \log K_H$$

$$\rho\sigma_x = \log k_x - \log k_H$$

**Equation 6.1 Hammett equations**

The σ value is defined by the Hammett equation (Equation 6.1). The σ parameter for a substituent (meta or para) is equivalent to the difference in the logarithms of the

equilibrium (ionization) constants between the substituted benzoic acid ($K_x$) and benzoic acid itself ($K_H$).[13, 14] In the case of the ionization constant for benzoic acid derivatives, the standard model for this relationship, the slope of the resulting linear relationship is 1. However, in the case of any other reaction, the slope may differ and hence a proportionality constant, the reaction constant ρ, is included. Normally, the Hammett plot can help determine the mechanism of a reaction occurring adjacent, or close to, an aryl substituent as the formation of partial or full charges should be either greatly accelerated, or inhibited, by the electronic nature of the substituent. If the electronic influence of the aryl substituents affects the reaction rate this is apparent through a linear relationship between the logarithm of the ratio of reaction rates (substituted aryl/phenyl) and a parameter, σ (the substituent constant), that represents the combined field and inductive effects of a substituent. There are several different coefficients available depending on the exact nature of the interaction between the aryl group and the reactive centre and whether or not the substituents of the aryl group either participate directly in the stabilization of the transition state through resonance or simply through field or inductive effects. It has been a contention of the “English school” of physical chemistry that electronic influences of substituents are made up of these two effects, field/inductive and resonance, and that they are generally independent of each other.[1] Consequently, a substituent may influence a reaction through either or both of these effects. Fortunately, in regards to the substituents on aryl groups, the two effects can be quantified separately and their influence is defined in terms of a σ value. As mentioned, the σ value has then been successfully subdivided into its resonance ($\sigma_R$) and inductive/field ($\sigma_I$) components, the sum of which is the Hammett σ value. As

mentioned, the plots can be made from either ratios of equilibrium constants or of reaction rates. In the case of IRI rate is measured, and it is this form of the equation that is used.

In this case, as there is no possibility of resonance stabilization of the hydration shell by the aryl substituent (in fact the statement fails to make any sense as they are not linked through chemical bonds), any kinetic influence of the aryl group would simply be through induction and field effects on the electronics of the intramolecular hydrogen-bonding network.[1, 15] Consequently, the $\sigma_I$ coefficient was selected rather than $\sigma_R$.[1] These values are presented in Table 6.2. In Figure 6.1 above there appears to be no correlation between electron density at the anomeric oxygen (influenced by the aryl substituent) and IRI activity. However with the logarithm of the ratio of reaction rates, which are directly proportional to the reaction rate constants as the concentrations are the same (measured by the relative mean grain area of a cross section of the ice crystals in the presence of

**Table 6.2 $\sigma_I$ values used for the Hammett plot. Values obtained from Hansch et al.[1]**

| Compound | Substituent | $\sigma_I$ (para) |
|---|---|---|
| **601** | H | 0 |
| **602** | OMe | -0.27 |
| **603** | Me | -0.17 |
| **604** | F | 0.06 |
| **605** | $CF_3$ | 0.54 |
| **606** | $NO_2$ | 0.78 |

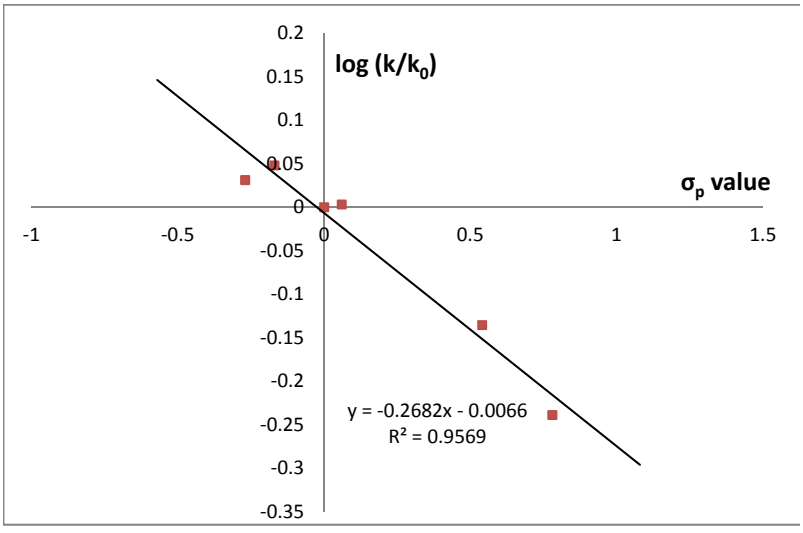



**Figure 6.2 Hammett plot showing the relationship between the rate of recrystallization and the electronic effect of the substituents at the anomeric position.**

**602**-**606** to those in the phenyl derivative, **601**) a Hammett plot can be generated. The correlation is unmistakable (Figure 6.2). There is a clear linear relationship ($R^2$ = 0.96), and the negative slope implies that recrystallization of ice is accelerated by the presence of EDGs, and inhibited by the presence of EWGs. Although a slope of -0.27 is not large, it is on the order of that seen for the disassociation of arylacetic (0.54) or arylpropanoic acids (0.24).[15] Both of these effects, creating actual charges three or four atoms away from the aryl ring, would be expected to be considerably larger than effects seen from modifications to the hydrogen-bonding network. That they are on the magnitude as the observed effect implies that the electronics at the anomeric oxygen may have considerable impact on the IRI activity of an analogue. This quantitative Hammett relationship supports the qualitative relationship seen in Figure 6.2, and suggests that electron density at the anomeric position is a clear predictor of IRI activity. As the anomeric oxygen itself seems unimportant for IRI activity, and considering that substitution at any other position in the ring (with methyl groups, for example) leads to a significant reduction in IRI activity,[4] it is possible that an intramolecular network could be least partially responsible for determining the hydration of a carbohydrate. It would be interesting to corroborate this data with additional substituents at both the para and meta position, as although the relationship seems to be consistent, there are fewer data points than are ideal to confirm this relationship. However, the analogues chosen for further studies must be picked carefully to avoid excellent hydrogen-bond donors and acceptors that could interact with water independent of the carbohydrates network creating a considerable confound. In the case of a Hammett plot, there is an assumption that the ratio of the entropy and enthalpy terms remain relatively constant over a

temperature range, and reflects the relationship of these terms found in the case of the ionization constant of benzoic acid derivatives. It is quite possible that the entropic term is more important in the current case, and consequently, this observed relationship may not be valid over a temperature range. A further caveat is that the Hammett relationship is defined for the reaction occurring in pure water at 25 ºC, not at -6.4 ºC. Although this difference in temperature is small, it may none the less affect the σ values of the substituents slightly differently, imparting some degree of further uncertainty into the relationship.

One possible explanation to correlate intramolecular hydrogen-bonding networks to anomeric oxygen electron-density is provided by the work of Simons.[2, 16, 17] Briefly, the Simons group examined the location and orientation of a single water molecule added to β-substituted phenyl glycosides (in the gas phase). From this information they deduced the directionality and the participants in an intramolecular hydrogen-bonding network. In the case of galactose, two conformations were of very similar energies (Δ(ΔG)=0.3 kJ/mol, Figure 6.3).[2, 17] In both cases the initial water molecule inserts between the *C*-6 hydroxyl and the *C*-5 (endocyclic oxygen) "hydroxyl" groups. In the first galactose conformation (Figure 6.3 **A**), there exists a single network invoking all of the galactoside's oxygens except that at the anomeric position. In the second conformation (Figure 6.3**B**, 0.3 kJ/mol higher in energy than **A**) all of the oxygens are involved, but to include the anomeric oxygen in this network requires a division of the network into two. One would expect that changes to the

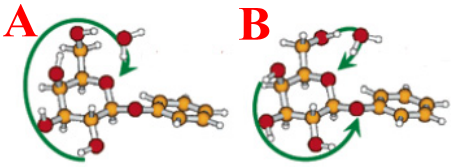



**Figure 6.3 Proposed hydrogen-bonding network present in galactose. Adapted from Carçabal 2005.[2]**

electron density at the anomeric position might have an effect on disrupting the relative populations of these two networks due to the small energy difference present in the electronically neutral phenyl derivative; however, although Simons proposes that this H-bonding network plays a role in the hydration of the sugars, he does not suggest which, if either, of these two networks, (Figure 6.3 A or B) increases or decreases the hydration of the sugar. Furthermore, the networks proposed by Simons were only validated for mono, di and tri-hydrated carbohydrates. Consequently, the direct applicability of these networks to the aqueous phase carbohydrates is uncertain, however, they may provide the foundation to the networks found in aqueous solution and several authors have postulated the importance of intramolecular hydrogen bond-networks (carbohydrate co-operativity) to the solvation of carbohydrates in water.[18, 19] As the anomeric oxygen acts as a hydrogen-bond acceptor in network **B**, it is reasonable to expect that as the electron-density at the anomeric oxygen decreases (leading to a decreased propensity to act as a hydrogen bond acceptor), the population of this network relative to **A** would decrease. An intramolecular hydrogen-bonding network might thus be the mechanism through which modifications of the electronics of the oxygen atom may influence IRI activity.

## 6.3 Chapter Summary

In this chapter the preparation and IRI analysis of a series of galactose residues β-substituted with aryl derivatives was described. These compounds show IRI activity that can be predicted using the Hammet relationship, demonstrating that IRI activity, in the case of *p*-substituted aryl analogues of galactose, is possibly dependent on the electron density of the anomeric oxygen of the carbohydrate. Electron poor anomeric

oxygens appear to lead to improved IRI activity. Although definite improvements in IRI activity were determined in this study, they are not improvements by an order of magnitude. To find improved small molecule inhibitors of IRI, attention returned to the highly active glycopeptide **118**, to determine what features could help explain its remarkable activity and if it could be used as a starting point for the development of highly active small molecule inhibitors.

## References


1. Hansch, C.; Leo, A.; Taft, R. W., *Chem. Rev.* **1991,** *91* (2), 165-195.
2. Carcabal, P.; Jockusch, R. A.; Huenig, I.; Snoek, L. C.; Kroemer, R. T.; Davis, B. G.; Gamblin, D. P.; Compagnon, I.; Oomens, J.; Simons, J. P., *J. Am. Chem. Soc.* **2005,** *127* (32), 11414-11425.
3. Tam, R. Y.; Ferreira, S. S.; Czechura, P.; Chaytor, J. L.; Ben, R. N., *J. Am. Chem. Soc.* **2008,** *130* (51), 17494-17501.
4. Chaytor, J. L. Examining the role of carbohydrate hydration and structure in preventing ice-recrystallization. PhD. Thesis, University of Ottawa, Ottawa, 2010.
5. Galema, S. A.; Howard, E.; Engberts, J. B. F. N.; Grigera, J. R., *Carb. Res.* **1994,** *265* (2), 215-225.
6. Galema, S. A.; Hoeiland, H., *J. Phys. Chem.* **1991,** *95* (13), 5321-5326.
7. Janczuk, A. J.; Zhang, W.; Andreana, P. R.; Warrick, J.; Wang, P. G., *Carb. Res.* **2002,** *337* (14), 1247-1259.
8. Knight, C. A.; Hallet, J.; DeVries, A. L., *Cryobiology* **1988,** *25*, 55-60.
9. Jackman, J.; Noestheden, M.; Moffat, D.; Pezacki, J. P.; Findlay, S.; Ben, R. N., *Biochem. Biophys. Res. Commun.* **2007,** *354*, 340-344.
10. Vauzeilles, B.; Urban, D.; Doisneau, G.; Beau, J.-M., *C*-glycosyl analogs of oligosaccharides. In *Glycoscience*, 2nd ed.; Fraser-Reid, B.; Tatsuta, K.; Thiem, J., Eds. Springer-Verlag: Berlin, 2008; Vol. 3, pp 2021-2077.
11. Goekjian, P. G.; Wu, T. C.; Kishi, Y., *J. Org. Chem.* **1991,** *56* (22), 6412-6422.

12. IUPAC, Hammet equation (Hammett relation). In *Compendium of Chemical Terminology*, 2nd ed.; McNaught, A. D.; Wilkinson, A., Eds. Blackwell: Oxford, 1997.

13. Hammett, L. P. *J. Am. Chem. Soc.* **1937,** *59* (1), 96-103.

14. Hammett, L. P. *Chem. Rev.* **1935,** *17* (1), 125-136.

15. Carey, F. A.; Sundberg, R. J., *Advanced Organic Chemistry*. 4th ed.; Kluwer Academic: New York, 2000; Vol. 1.

16. Simons, J. P.; Davis, B. G.; Cocinero, E. J.; Gamblin, D. P.; Stanca-Kaposta, E. C., *Tetrahedron Assym.* **2009,** *20* (6-8), 718-722.

17. Simons, J. P.; Jockusch, R. A.; Carcabal, P.; Huenig, I.; Kroemer, R. T.; Macleod, N. A.; Snoek, L. C., *Int. Rev. Phys. Chem.* **2005,** *24* (3-4), 489-531.

18. Dashnau, J. L.; Sharp, K. A.; Vanderkooi, J. M., *J. Phys. Chem. B* **2005,** *109* (50), 24152-24159.

19. López de la Paz, M.; Ellis, G.; Pérez, M.; Perkins, J.; Jiménez-Barbero, J.; Vicent, C., *Eur. J. Org. Chem.* **2002,** *2002* (5), 840-855.

# Chapter 7 : *C*-linked AFGPs as a platform for the development of small molecule IRI inhibitors.

## 7.1 Precedent for exploring the activity of simple derivatives of highly active glycopeptide 118

Despite the progress in improving IRI activity with anomerically-substituted derivatives, and various disaccharides, the IRI potency of small molecules is still orders of magnitude weaker than that of the glycopeptides such as analogue **118**. The full reasons for the potency of this analogue are not yet understood at this time. To further investigate the remarkable activity of this compound, a systematic evaluation of the IRI activity of its constituent parts could prove valuable. Furthermore, as these components are synthetically simpler than the glycopeptide itself, they offer the benefit of increased ease of access and consequently simplify the generation of a library of analogues. As such, they also show better promise for eventual clinical applications if activity can be sufficiently improved. To date, Wu and co-workers have shown that monosaccharides as small molecule inhibitors of ice recrystallization are able to enhance cryopreservation outcomes and this ability is directly correlated to their IRI activity.[3] However, 220 mM of disaccharide is required to show clinically significant effects: at this concentration, the sugars are slightly cytotoxic.[3] Consequently, if more potent inhibitors can be found, the concentrations can be lowered and the toxicity effects possibly avoided. Similarly, as **118** shows such uniquely potent activity, it makes a logical starting point for developing

small molecule inhibitors. The goal of this study would thus be twofold, to better understand the activity of **118**, and to develop a small-molecule inhibitor of IRI activity.

### 7.1.1 Importance of the number of tripeptide repeats to antifreeze activity

In terms of antifreeze activity of glycopeptide derivatives, the number of repeats of the core trimer is an important parameter defining their antifreeze activity. Nishimura and Fletcher studied the relationship between TH and the number of trimeric repeats of the peptide. They showed that TH activity improved as the number of repeats increased, and that two repeats was sufficient to express some level of TH activity as mentioned in the introduction.[4] Similarly, in a *C*-linked system, both IRI and TH activity appeared to be dependent on the number of repeats: as the peptide chain became longer, activity improved.[5] However, despite these precedents, the effect of the number of repeats in the case of analogue **118** has not been investigated. It is unknown whether four repeats are necessary to obtain the excellent IRI activity, or if this activity is reachable using a shorter, and therefore simpler, molecule.

### 7.1.2 The difference in IRI activity between glycopeptides and small molecules

There is a large (approximately 10,000-fold difference) between the activity of analogue **118** and that of galactose.[1, 2] This difference in IRI activity between the glycopeptides and small molecules might be decreased through using a compound intermediate in complexity between these two structural extremes. Earlier studies carried out by Chaytor and Ben provided the IRI activity of some simple *C*-linked derivatives of galactose including *C*-allyl (**144**), *C*-ethanol (**539**), *C*-propyl (**701**), and *C*-

ethanoic acid (**702**). These analogues have activity comparable with galactose itself (Figure 7.1).[2, 6] However, the activity difference between these analogues and the glycopeptide itself is several orders of magnitude. Consequently, it was determined that a systematic scan of the full

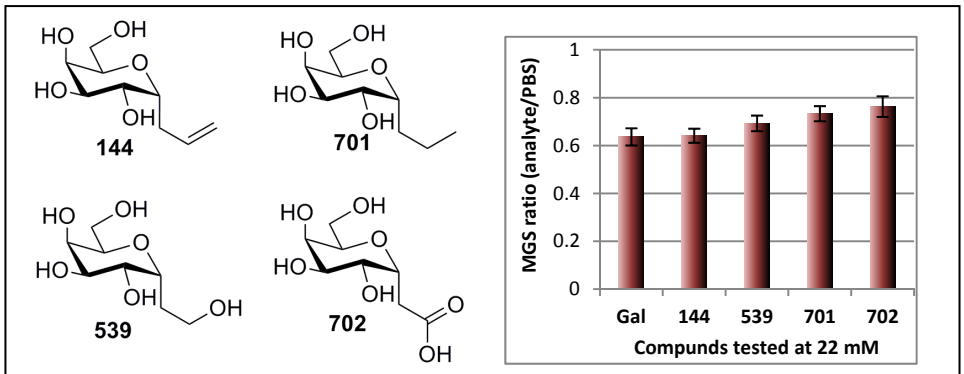



**Figure 7.1 IRI activity of simple C-linked derivatives of galactose.**

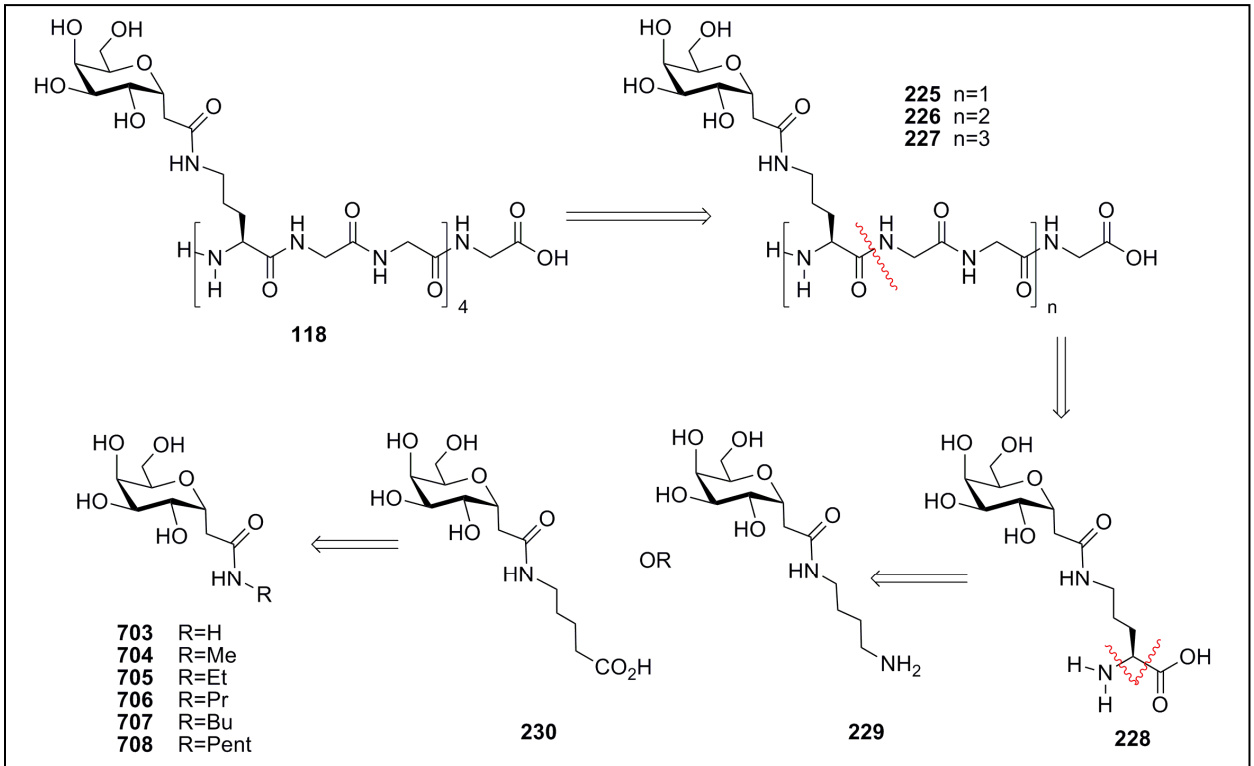



**Figure 7.2 Planned truncation of OGG(gal) to determine the importance of structural feature to antifreeze activity.**

range of compounds obtained by truncating glycopeptide **118**, would be beneficial (Figure 7.2).

This systematic truncation would initially involve the synthesis of the monomer (**225**), dimer (**226**) and trimer (**227**) of **118** using standard SPPS techniques as used in the preparation of tetramer **118** itself, and in the analogues previously generated above (Chapters 3 and 4).[1, 7] The next step would involve the preparation of fully deprotected zwitterionic building blocks **228** (and its β-amino acid analogue, **709**, to provide a second data point), and the synthesis of amine and carboxylic acid derivatives **229** and **230.** Finally this initial phase of the study would be completed by the analysis of simpler alkyl amide derivatives of galactose, from primary amide **703** through pentyl amide **708**, thereby completing the analysis of the structural space between previously prepared tetramer **118** and carboxylic acid **702**.

## 7.2 Synthesis and IRI activity of monomer, dimer and trimer of 118

### 7.2.1 Synthesis of monomer dimer and trimer

Using the previously prepared glycoconjugate building block **320**, acetylated glycopeptides were prepared using standard SPPS techniques (Figure 7.3).[1, 7] Following Zemplen deacetylation,[8] the dimer and trimer were then purified through reversed-phase HPLC to provide glycopeptides

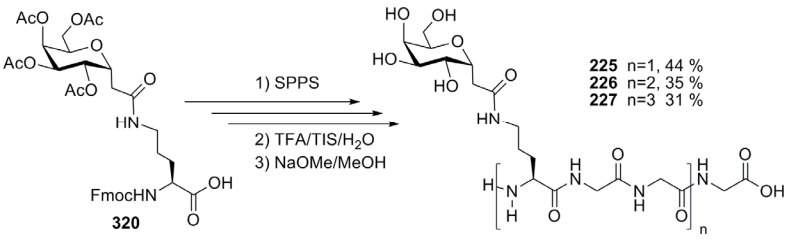



**Figure 7.3 Synthesis of glycopeptides 225-227.**

**226** and **227** as white powders in 35 and 31 % yields respectively (based on peptide loading of the Wang resin). The monomer was too polar and could not be separated from the inorganic salts through either reversed-phase HPLC or SPE. Consequently, the monomer was purified by preparative TLC (60 % methanol in water) to provide glycopeptide **225** in 44 % yield. The glycopeptides were then ready to be examined for IRI activity.

### 7.2.2 Antifreeze activity of monomer dimer and trimer compared to tetramer

IRI activity was tested at three different concentrations: 22 mM, the same concentration used for small molecule analytes such as mono- and disaccharides; 550 μM to provide an intermediate measurement; and 5.5 μM, the same concentration used to test previously generated glycopeptides such as **118** (Figure 7.4). Glycopeptide **118** had been examined in a previous study,[1] from where the plotted data point has been obtained, but was not re-synthesized for this analysis and consequently was not available for IRI analysis at the higher concentrations. At 22 mM all three compounds show remarkable activity with trimer **227** being particularly potent. At 550 μM however, much of the activity has been lost, and although **227** remains more potent than **225** and **226**, the

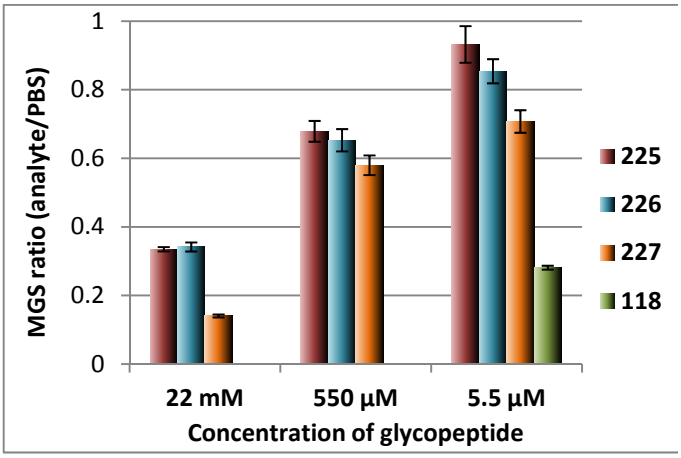



**Figure 7.4 IRI activity of the glycopeptides: monomer (225, red), dimer (226, blue), trimer (227, orange) and tetramer (118, green) at three concentrations.[1]**

effect is not pronounced. At 5.5 μM, the monomer **225** and dimer **226** no longer express significant IRI activity. Trimer **227**, however retains much of the activity observed at the 100-fold higher concentration, but compared to tetramer **118**, the compound is comparably inactive.

These results are somewhat surprising since in previous glycopeptide series, there had not been such a significant difference in the IRI activity of the trimer and the tetramer.[5, 9, 10] This indicates that analogue **118** behaves differently with regards to the relationship between IRI activity and the number of repeats. It appears that the tetramer is considerably more active than the trimer than would be predicted by the activity seen in other glycopeptide series.

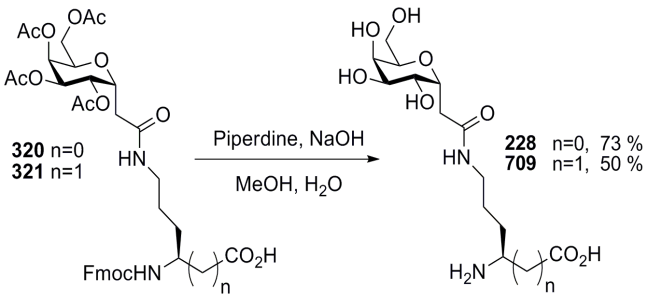
Although the truncated glycopepties are considerably less active than **118** itself, they are still synthetically more complicated than simple derivatives of carbohydrates. Furthermore, at 22 mM, they are still considerably more active than the carbohydrate derivatives synthesized to date. Consequently, in an effort to retain the IRI activity, but create synthetically simpler targets, the monomer **225** was then truncated further to glycoconjugate building block **228** and its constituents.

## 7.3 Synthesis and antifreeze activity of the glycoconjugate building block and its truncated derivatives

### 7.3.1 Synthesis of glycoconjugate building block 228 and its truncated derivatives

#### *7.3.1.1 Synthesis of glycoconjugate building blocks 228 and 709*

In the course of the preparation and IRI analysis of the deprotected building block **320**, it was felt that a second data point would better validate the impact that the zwitterionic nature of the compound had on IRI activity. Consequently, deprotected derivative **709**, derived from β-amino acid building block **321** (first prepared for the generation of mixed α and β peptides) was also prepared. These compounds were accessed from their Fmoc and acetate protected precursors used for SPPS (Scheme 7.1). Initial attempts at deprotection using a variety of conditions including aqueous base to carry out both deprotections simultaneously; or only piperidine prior to isolation of the free amine before solvolysis with basic methanol,[11] failed to provide the desired product cleanly. Instead a complicated mixture of compounds, including N-acetylated derivatives, was recovered. However, when the building block was dissolved in a solution of methanol and water to which was added piperidine followed ten minutes later by sodium hydroxide, acetate migration was suppressed and desired glycoconjugates **228** and its β-amino acid analogue **709** could be purified through simple extraction and recrystallization as the major components in 73 and 50 % respectively.

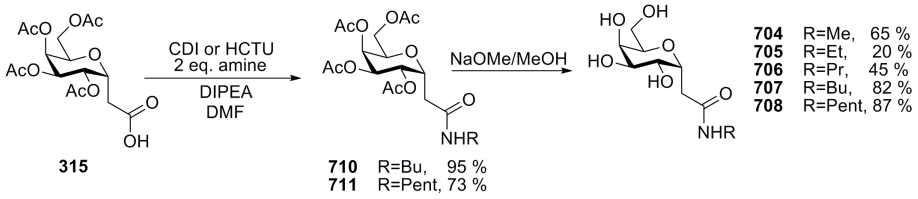



**Scheme 7.1 Concomitant deprotection of backbone Fmoc and carbohydrate acetate groups.**

### *7.3.1.2 Synthesis of alkyl derivatives of 228*

The simple amides could be similarly obtained in a relatively straightforward manner. Alkyl derivatives **704**-**708** (**704-707** were prepared by R. Biggs during her

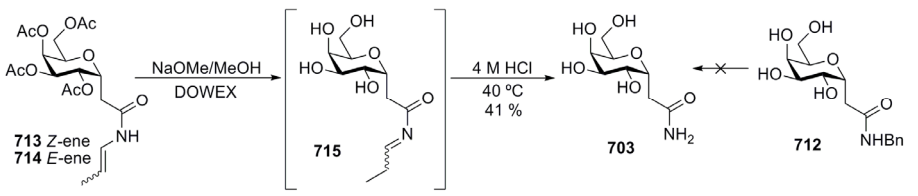
Honour's project) were obtained by coupling the appropriate alkyl amine to previously synthesized galactose carboxylic acid derivative **315** (Scheme 7.2) using standard peptide coupling conditions.[1] The methyl, ethyl and propyl derivatives were suitably pure after aqueous work-up at the acetate stage that they were directly subjected to deacetylation under standard conditions. Although the yield for methyl analogue **704** was acceptable at 65 % over two steps, the isolated yields of ethyl analogue **705** and propyl analogue **706** were more disappointing. Although these methods produced sufficient material for IRI analysis, all future analogues were purified at the acetate stage prior to deprotection. This resulted in considerably improved yields, as peracetylated butyl and pentyl analogues **710** and **711** were isolated in 95 % and 73 % yields respectively, which were then deprotected and repurified in 82 and 87 % yields to provide **707** and **708** respectively. This strategy clearly provided higher overall yields, and was generally preferred to the crude-reaction protocol.




**Scheme 7.2 Synthesis of simple alkyl amide derivatives. Yields for 704-706 are for the two steps from 315. Yields for 707 and 708 are from 710 and 711 respectively.**

### *7.3.1.3 Synthesis of functionalized derivatives of building block 228*

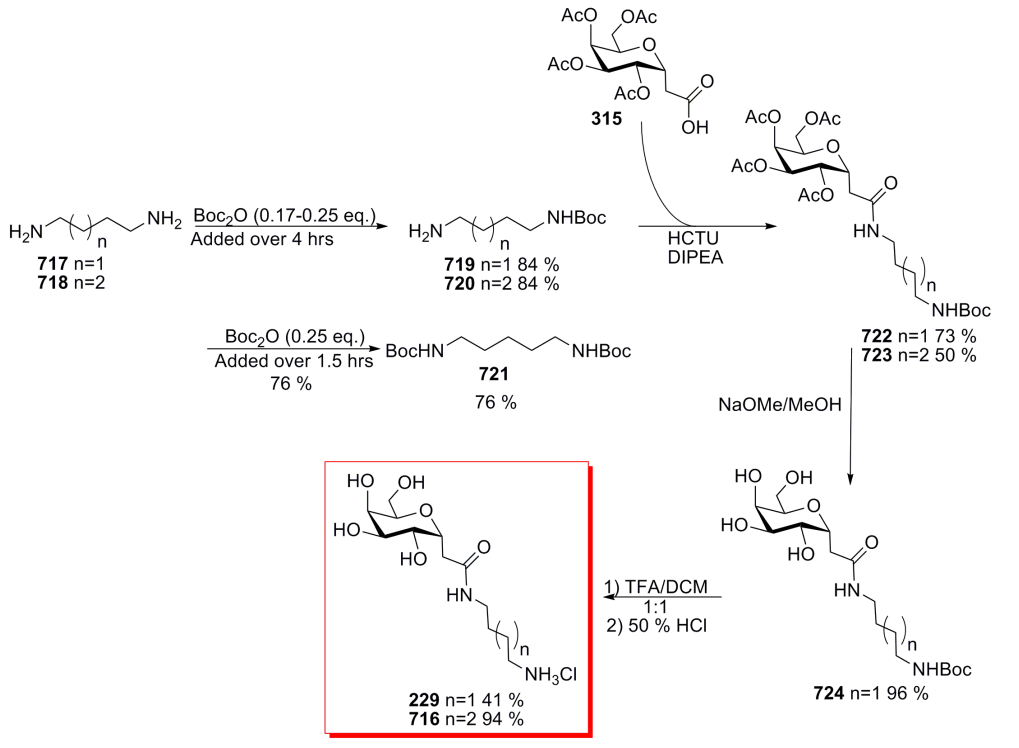
Primary amide derivative **703** was first attempted from benzyl amide **712** using hydrogenolysis under high pressure (15 atm).




**Scheme 7.3 Synthesis of primary amide derivative 703.**

This failed to remove any benzyl groups and the starting material was recovered quantitatively. It has been noted previously that in some cases it may be impossible to remove amide benzyl groups by hydrogenolysis.[12] Rather than attempt single electron reductions (using Li or K metal in liquid ammonia) an alternative substrate, a mixture of **713** and **714**, whose syntheses are discussed below (Scheme 7.6), was used instead. The peracetylated derivatives were deprotected under standard conditions, and were treated with DOWEX 50-X resin in the usual manner which tautomerized the enamines to the imine (**715**) *in situ*. The imine derivative was then hydrolyzed under acidic conditions to provide the primary amide derivative **703** in 41 % yield (Scheme 7.3).

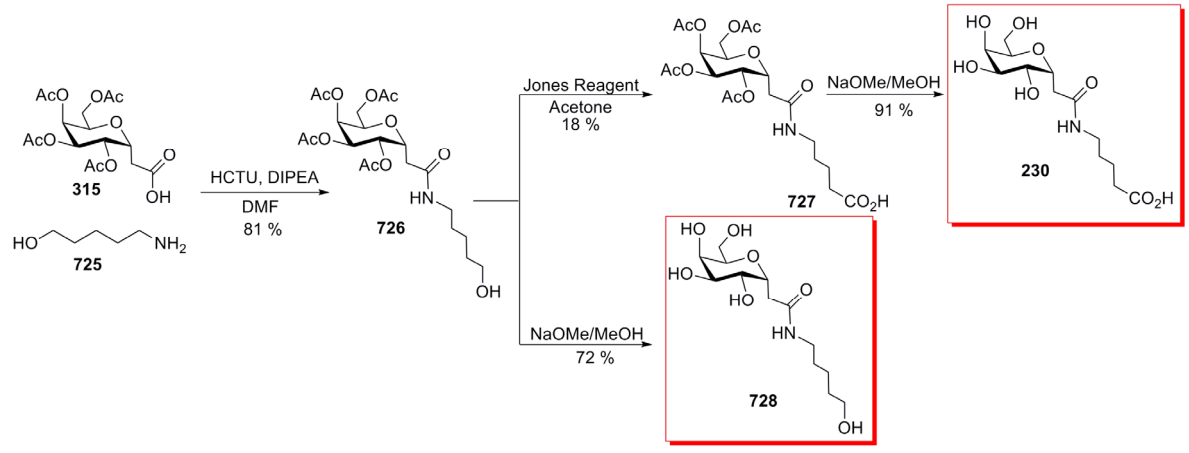
It was felt that the IRI activity of the amine derivative may be of particular interest, and consequently, in addition to the previously mentioned butyl amine derivative **229**, pentyl amine derivative **716** was also targeted. The compounds were prepared as described in Scheme 7.4. Butyl derivative




**Scheme 7.4 Synthesis of amino derivatives 229 and 716.**

**721** was prepared first, and putrescine, **717**, was selectively protected as the mono-carbamate (**719**) with Boc anhydride in 84 % yield according to the protocol of West.[13] However, when the same protocol was applied to cadaverine, **718** (albeit with a faster rate of addition), surprisingly dicarbamate **721** was isolated as the major product. However, with a slowing of the rate of addition back to a period of 4 hours, and a decrease in the ratio of anhydride to amine, the mono-carbamate **720** was isolated successfully as the major product in 84 % yield. These mono-protected diamines were then coupled to carboxylic acid **315** in the usual manner to produce butyl derivative **722** in 73 % yield, and pentyl derivative **723** in 50 % yield. The butyl derivative was first deacetylated to provide the carbamate protected **724** in 96 % yield before the Boc group was removed, under standard conditions, and the resulting TFA salt was exchanged for the HCl salt to provide butylamine derivative **229** as the hydrochloride following lyophilization in 41 % yield. This process was not very efficient and consequently, the pentyl amino analogue **723** was treated slightly differently. The deacetylation was carried out as before, but rather than isolating the deprotected sugar, the compound was immediately treated with TFA, followed by ether. The precipitate was collected, the TFA salt replaced by the HCl salt, and aminopentyl derivative **716** was isolated in a greatly improved 94 % yield. Both methods provided sufficient material for characterization and IRI analysis, and consequently neither sequence was further optimized.

The final analogue to be prepared was carboxylic acid derivative **230** according




**Scheme 7.5 Synthesis of carboxylic acid derivative 230 and pentanol derivative 728.**

to the method described in Scheme 7.5. 5-Aminopentanol, **725**, was coupled with carboxylic acid **315** to provide primary alcohol **726** in 81 % yield. Some of this material was deacetylated to obtain polyol **728** in 72 % yield following purification. Although not directly related to the initial plan of study, the hydroxyl group is of considerable interest as it maintains hydrogen bonding capability of the amine and carboxylic acid, but, unlike those derivatives, would not be charged under the assay conditions (pH = 7.4) and consequently acts as a functional intermediate between the charged species and the hydrophobic alkyl derivatives described above.

Returning to the preparation of **230**, several strategies were attempted to oxidize the alcohol to the corresponding acid. IBX,[14] and TEMPO-mediated oxidation,[15] both failed to provide significant yields of the desired compound and resulted in an inseparable mixture of compounds. Jones reagent, however, had been used in the oxidation of a similar terminal alcohol to a carboxylic appended to a per-acetylated carbohydrate by Dondoni.[16] Using the same conditions provided **727** as the major

component amongst a large number of minor impurities in 18 % yield. This compound was then deprotected in turn to provide carboxylic acid derivative **230** in 91 % yield. With all the desired analogues prepared, attention turned towards an analysis of their IRI activity.

### 7.3.2 Antifreeze activity of glycoconjugate building block 228 and its derivatives

This initial study provided some promising results (Figure 7.5). The simple charged compounds, primary amide **703** and carboxylic acid **702**, have the same IRI activity. However, as the first methylene groups are added, activity decreases. The methyl, ethyl, and butyl derivatives, **704, 705**, and **707**, are all very poor inhibitors of IRI. Propyl derivative **706** is more active than its homologues, either longer (**707**) or shorter (**704**, **705**). As the chain lengthens, though, activity generally appears to improve and when the alkyl chain is extended to five carbons (**708**) activity is comparable to galactose.

In contrast, the introduction of an ionizable functional group appears to decrease IRI activity relative to the alkyl chain of similar length (compare pentyl analogue **708** with acid **230** or amine **716**). It does not appear to matter greatly whether a positive or negative charge is present. However,

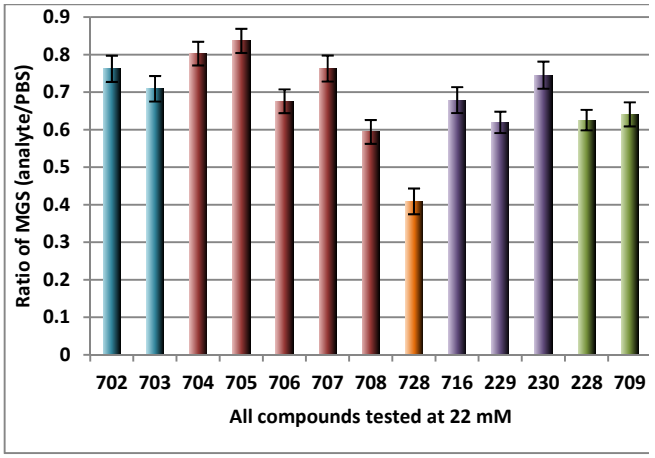


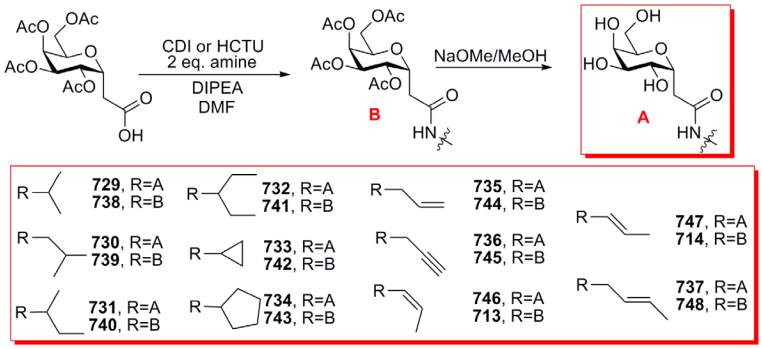

**Figure 7.5 IRI activity of initial analogues of the glycoconjugate building block: carboxylic acid and primary amide (702, 703 blue), alkyl amides (red, 704-708), terminal alcoholic amide (728, orange), charged derivatives (229, 230 and 716, purple) and zwitterionic building blocks (228, 709, green).**

length, or possibly conformation determined by length, may be more important: surprisingly, butylamine derivative **229** is considerably more active than butyl derivative **707** and is even slightly more active than longer pentylamine derivative **716** whereas the same is certainly not true with respect to the relationship between pentylamine derivative **716** and pentyl derivative **708**. Glycosylated amino acids **228** and **709** have similar moderate IRI activity comparable to galactose (with an MGS ratio of 0.65). This is consistent with recent results showing that glycoconjugate building blocks show only very mild increased recrystallization inhibition activity relative to the free sugars themselves.[17, 18] Most intriguingly of all, perhaps, is pentanol derivative **728**, which shows significantly improved activity relative to either the pentyl derivative or the corresponding carboxylic acid. Besides this data point, this study has failed to produce any molecules with enhanced IRI activity, and certainly nothing capable of bridging the activity difference between small molecules and glycopeptides. This set of results, however, does raise three interesting questions. The first regards the origin of the unusual activity of the propyl derivative (**706**); the second is whether IRI activity continues to improve as the alkyl chain becomes longer; and the third is whether the observation that the introduction of a terminal alcohol improving activity relative to the alkyl chain is a general correlation or is simply specific to this case. Each of these questions is examined in turn below.

## 7.4 Synthesis and antifreeze activity of structural analogues of propyl derivative 706

Propyl derivative **706** clearly has better activity than would be expected based on its length (Figure 7.5). To further study this effect, a series of analogues containing a propyl motif were synthesized and examined for IRI activity. Analogues **729-736** were synthesized in two steps using their respective commercially available amines in the usual fashion (Table 7.1). Yields for the couplings tended to be good to excellent.

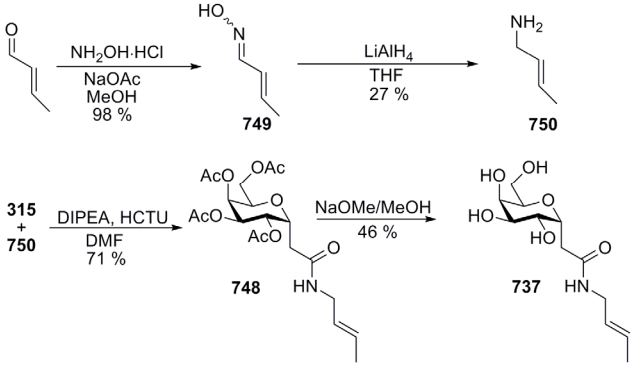
**Table 7.1 Synthesis and structure of propyl-motif analogues prepared in this study. Yields are provided for the acetylated and deprotected constructs prepared from commercially available amines.**




| compound (acetylated, B) | yield (%) | compound (deprotected, A) | yield (%) |
|---|---|---|---|
| **738** | 89 | **729** | 95 |
| **739** | 90 | **730** | 93 |
| **740** | 86 | **731** | 84 |
| **741** | 92 | **732** | 86 |
| **742** | 82 | **733** | 84 |
| **743** | 76 | **734** | 93 |
| **744** | 81 | **735** | 71 |
| **745** | 81 | **736** | 81 |

The root amines of the 1-propenylamine diastereomeric derivatives **713** and **714** as well as the crotylamine derivative **737** were not available commercially, and were consequently prepared synthetically using two very different strategies.

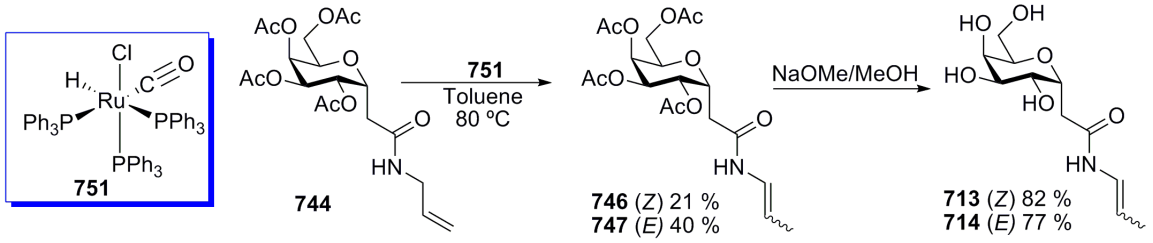
Crotylamine was prepared through a condensation/reduction strategy (Scheme 7.6). Freshly distilled crotonaldehyde (>95 % *trans*), was treated with hydroxylamine hydrochloride in the presence of sodium




**Scheme 7.6 Preparation of crotyl derivative 737.**

acetate as base. This provided the crotylhydroxylamine **749** in near quantitative yield. The reduction proved considerably more challenging than expected. The published preparation of **750** dates from 1951 and was carried out on a very large scale.[19, 20] The reaction progressed sluggishly in diethyl ether, generally considered a superior solvent for LAH reductions,[21] however it functioned sufficiently well in THF to provide the crotylamine, **750**, in 27 % yield (more material was collected in impure fractions and discarded) after reactive extraction and two successive fractional distillations.[19] Coupling then proceeded under standard conditions to provide acetylated glycoconjugate **748** in 71 % yield which was then deprotected under standard conditions and re-purified to obtain deprotected analogue (*trans* only) **737** in 46 % yield.

The propenyl derivatives **713** and **714** had to be prepared in a very different manner as the theoretical amine precursor, an enamine, would be unstable. However, when this functional group is integrated into an amide, the stability of the compound is greatly increased, although it remains sensitive to acid (this sensitivity was exploited in the synthesis of **703** above). Consequently, their synthesis was envisioned to arise from




**Scheme 7.7 Synthesis of enamide analogues 713 and 714.**

an isomerization of the olefin in allyl derivative **744** (Scheme 7.7). Initial attempts to carry out the reaction with several iridium catalysts failed to provide any conversion,[22] and consequently, although not a common transformation, ruthenium catalyst **751** was

used to catalyze the isomerization of the allyl group.[23] The crude NMR showed a 1:7:15 ratio of allyl to *Z*-1-propene to *E*-1-propene. Removal of unreacted starting material was trivial, but separation of the two isomers was considerably more challenging and could most reproducibly be done through preparatory TLC using multiple elutions to provide the *E* and *Z* isomers **746** and **747** in 21 and 40 % respectively. Following purification, they were each deprotected separately and the inorganic salts were removed without acidification to obtain the desired enamides **713** and **714** in 82 and 77 % yields. With the synthesis of all the propyl analogues completed, the "splat" cooling IRI assay was carried out.

The data is presented in Figure 7.6 and has been colour-coded. The root propyl derivative **706** itself is in red, the saturated, branched-linear analogues are in blue, the cyclic analogues in green and the unsaturated analogues in orange.

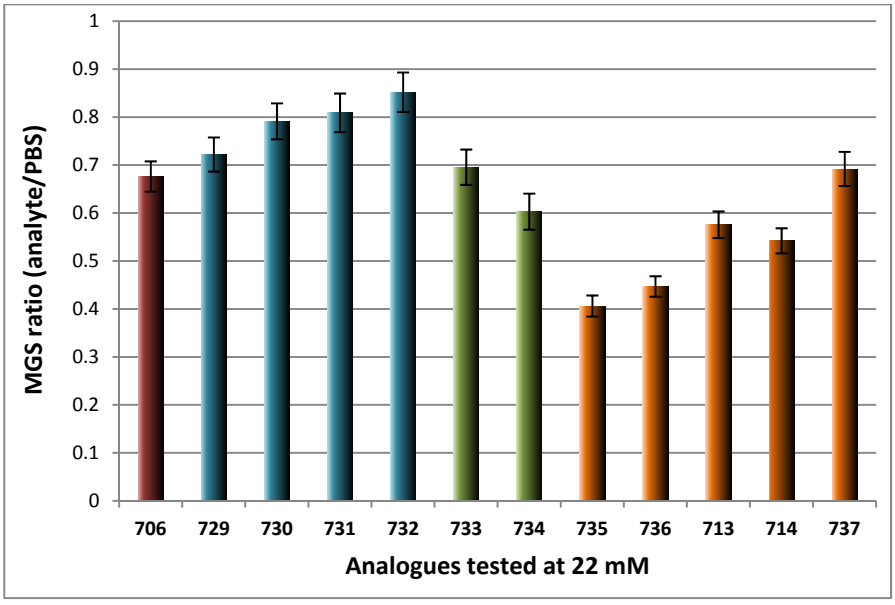



**Figure 7.6 IRI activity of propyl-motif containing analogues: root propyl analogue (706, red), branched analogues (729-732, blue), cyclic analogues (733-734, green) and unsaturated (713, 714, 735-737, orange).**

*Iso*-propyl derivative **729** showed weaker IRI activity than propyl derivative **706** and the activity continued to decline as the local steric volume (especially near the amide

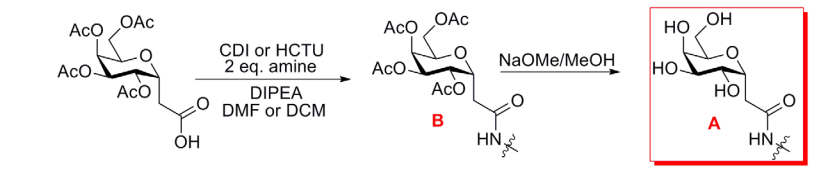
functionality) increased through the *iso*-butyl (**730**) and *sec*-butyl (**731**) derivatives,[24] and activity was nearly completely abrogated for 1-ethylpropyl derivative **732**. Cyclopropane derivative **733** had activity similar to **729**. These two alkyl groups would have quite similar volumes. A more drastic effect was seen in the case of cyclopentane **734**, the cyclic analogue of **732**, where through decreasing the hydrophobic volume, IRI activity was not only recovered but in fact was slightly better than that of the root propyl analogue. This data seems to indicate that not only is the propyl length privileged, but it does not tolerate methyl substitution and that activity is not improved through increasing steric bulk. Increased steric volume near the amide group clearly seems contraindicated for improved IR activity. It was however possible that slightly smaller and lower-volume substituents than propyl might be able to improve activity. The bond angles of allyl analogue **735** and, especially, propargyl analogue **736**, differ considerably from the propyl analogue, and might adopt a different position relative to the sugar, and the decreased steric bulk from the removal of the hydrogens certainly decreases molecular volume. These analogues showed good activity with MGS ratios of 0.41 and 0.45 respectively (relative to PBS), considerably better than that of the propyl analogue itself. Interestingly, the two enamides, **713** and **714**, although more potent than propyl derivative, are less active than the allyl derivative. The activity seems to be mostly independent of the stereochemistry at the olefin with the *trans* and *cis*-oriented diastereomers showing the same activity. This result appears to indicate that the beneficial effect of introducing unsaturations is slightly lost when the olefin is located internally rather than being positioned at the end of the chain. The results for crotyl analogue **737**, which is considerably less active than the other unsaturated analogues,

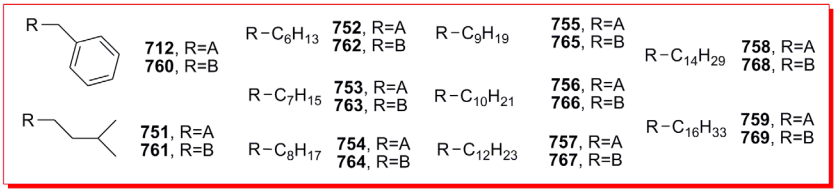
appear to suggest that the effect is specific to the 3-carbon length chain. In all, this study appears to indicate that the propyl-length chain does indeed appear to constitute a preferred structure for IRI activity relative to the ethyl and butyl lengths, and activity is improved with the incorporation of smaller unsaturated substituents rather than larger branched alkyl groups.

## 7.5 Synthesis and antifreeze activity of long-chain alkyl analogues of 228

The second nascent trend that merited further investigation was the apparent increase in activity as the chain length became longer. To examine this correlation, the series of medium length alkyl chain derivatives were synthesized **751**-**755** with chain lengths up to nine carbons long (Table 7.2). All analogues were prepared directly from the commercial amines without any prior purification of the reagents. An added complication was the lower volatility of the higher molecular weight amines.

**Table 7.2 Synthesis of long-chain alkyl analogues.**




| amine | compound (acetylated) | yield (%) | compound (deprotected) | yield (%) |
|---|---|---|---|---|
| benzylamine | **760** | 83 | **712** | 95 |
| *iso*-amylamine | **761** | 80 | **751** | 80 |
| hexylamine | **762** | 65 | **752** | 78 |
| heptylamine | **763** | 83 | **753** | 78 |
| octylamine | **764** | 43 | **754** | 70 |
| nonylamine | **765** | 85 | **755** | 72 |
| decylamine | **766** | 73 | **756** | 68 |
| dodecylamine | **767** | 55 | **757** | 81 |
| tetradecylamine | **768** | 68 | **758** | 56 |
| hexadecylamine | **769** | 72 | **759** | 71 |

Purification of the acetate protected derivatives consequently involved more careful removal of excess amine reagent, and in some cases, trace residual amine was not finally removed until the recrystallization of the final products. It was also found that DMF did not necessarily provide the best solvent for the coupling of these reagents, and DCM was used for most of the higher molecular weight amines as it was found to be better able to solubilize the long hydrophobic reagents. *Iso*-amylamine derivative **751** was included to act as a branched analogue of pentyl derivative **708**, to determine if the relationship between sterics and IRI activity seen for the propyl analogues were general. Benzyl derivative **712** was prepared to investigate the possible effect of the introduction of a phenyl ring. The assay was then applied to the synthesized compounds.

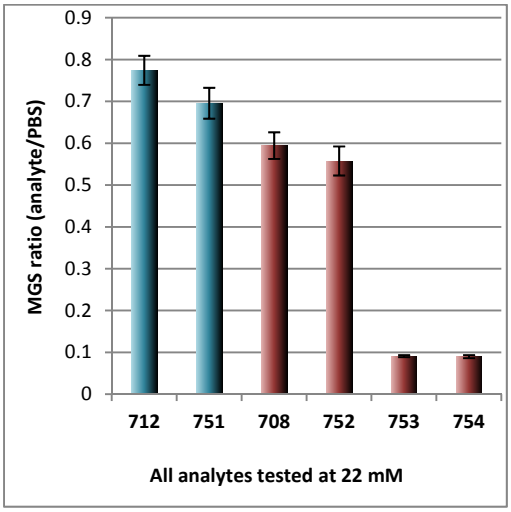



**Figure 7.7 IRI activity of medium-chain alkyl analogues soluble at 22 mM: benzyl and isoamyl (712, 751, blue) and *n*-alkyls (708, 752-754, red)**

The IRI analysis, however, was complicated by the limited solubility of octyl derivative **754** in PBS buffer at 22 mM (buffer solution had to be warmed to 40 ºC), and nonyl derivative **755** was not soluble at this concentration.

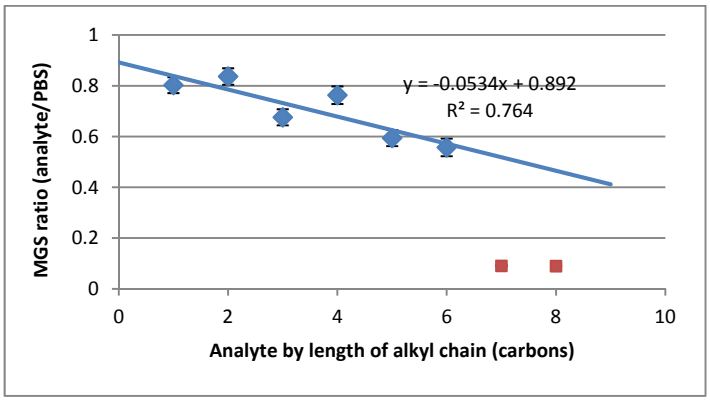



**Figure 7.8 The relationship between IRI activity and the length of the alkyl amide.**

Nevertheless, the activity of the soluble analogues was assessed and is provided in Figure 7.7.

Some startling and exciting results arise from this figure. Starting with benzyl analogue **712**, it is apparent that the benzyl group has only very poor IRI activity. This is somewhat unexpected as the unsaturated analogues had shown improved activity, yet it may indicate that it was the geometries of the unsaturated propyl analogues that led to their activity rather than any interactions directly related to π electron density. The branched *iso*-amyl analogue **751** is less active than its *n*-pentyl isomer **708**, as expected, consistent with the results seen in the propyl analogues: increasing steric volume rather than chain length appears to be detrimental to activity. However, **751** is as active as butyl derivative **707**. This activity was not seen with the propyl derivatives; consequently, the steric-bulk effect may be more pronounced for the propyl derivatives than for the other chain lengths.

This scan also found that hexyl derivative **752** is approximately as active as the pentyl derivative continuing the trend that longer chains improve IRI activity. The truly startling results arise from analogues **753** and **754**. Their activity is not simply an incremental improvement on the hexyl analogue, it is a large jump in activity that does not fit the trend (Figure 7.8). Previously (from the methyl through the hexyl analogue), the IRI actiivty improved by around 5 % for every extra methylene group added. However, with the addition of a single methylene group, the MGS ratio falls from 0.56 to 0.09, a drastic change. Octyl analogue **754** has similarly potent activity. Such a break in activity appears to portend a change in mechanism for the IRI phenomenon; the same factors that were gradually increasing IRI activity appear to have been supplanted by a

much more powerful determinant. However, the reason for this large increase in activity was not apparent and consequently to further explore this effect, the longer chain analogues (**756**-**759)** in Table 7.2 above were prepared and readied for IRI analysis. Again, in the synthesis of these compounds (all obtained from their respective commercially available amines) DCM was chosen as solvent, and reaction times were

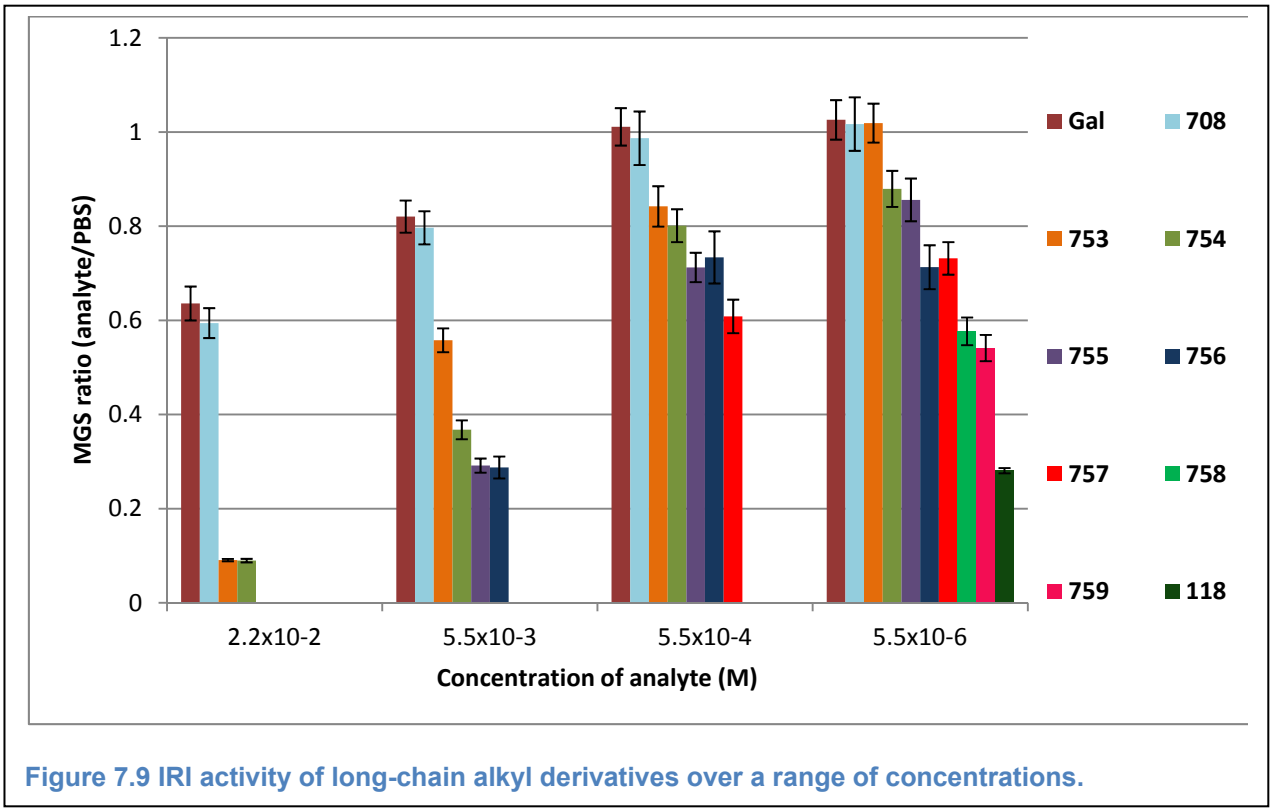



**Figure 7.9 IRI activity of long-chain alkyl derivatives over a range of concentrations.**

trebled for the longest two substrates due to low reactivity of the amines.

Because of the relative insolubility of these compounds in aqueous solutions, a concentration scan was performed at 22 mM, 5.5 mM, 550 μM and 5.5 μM. These values were chosen as they allowed for the maximum range of concentrations to investigate the relationship between relative IRI activity and concentration and span the range from that at which small molecules have been previously tested (22 mM) down to

that at which glycopeptides have been examined (5.5 μM) (Figure 7.9). The lowest concentration (5.5 μM) was also appropriate because all analogues were soluble at this level. All analogues were tested at their maximum soluble concentration, and again at all lower concentrations. This treatment was provided for the heptyl analogue and all the analogues with a longer alkyl chain (**753-759**) as well as pentyl analogue **708** and galactose as controls. Glycopeptide **118** has also been included for comparison at the lowest concentration.

The long chain alkyl analogues clearly have unprecedented IRI activity for small molecules. Activity does tend to improve as the chain length gets longer, but once again, in a new linear fashion (Figure 7.10). The nonyl (**755**) and decyl (**756**) analogues are first soluble at 5.5 mM and show remarkable activity (29% of PBS). A ten-fold dilution to 550 μM curtails much of the activity, although these analogues are broadly equivalent to galactose at 22 mM (40 times more concentrated). Surprisingly, much of the activity is retained even with a 100 fold decrease in concentration to 5.5 μM. Dodecyl analogue **757**, first soluble at 550 μM, is more active at this concentration than galactose, the best monosaccharide, is at 22 mM. Likewise, tetradecyl analogue (**758**, soluble at 55 μM) and hexadecyl homologue (**759**, first soluble at 5.5 μM) remain more active than their shorter counterparts at this concentration. Remarkably, these two analogues remain as active at 5.5 μM as galactose is at 22 mM. These analogues are consequently around 4000 times better inhibitors of ice recrystallization than galactose. This means that the difference in IRI activity between glycopeptides and galactose has narrowed greatly: from a 10,000-fold difference to a 2 or 3-fold difference.

The hexadecyl analogue can only be dissolved at 5.5 μM at 40 ºC, and begins to visibly precipitate after 4 hours; consequently, it is likely that the practical limit for this effect has been reached, and any longer analogues would have to be diluted further.

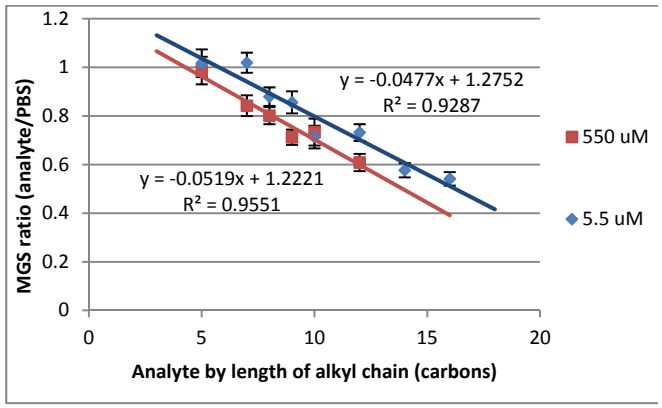



**Figure 7.10 Linear relationship between chain length and IRI activity for the long chain alkyl analogues at both 5.5 and 550 μM.**

It is interesting to note that the trend for improved activity as chain length increases is maintained at all concentrations and it is notable that although activity decreases as the solutions become ever more dilute, the series of molecules as a whole does not appear to lose activity at low concentrations as they do not trend towards complete inactivity at the same rate that galactose or pentyl analogue (**708**) do. This can be seen in Figure 7.10: the slopes of the linear relationship between the analogues at 550 μM and 5.5 μM are very similar: it does not become appreciably less negative. This indicates that the relative IRI activity between these compounds is largely independent of concentration at these dilutions.

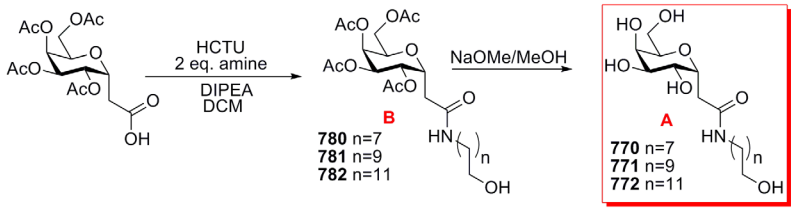
It is also interesting to note the relative potency of the very active glycopeptide analogue **118**. The new analogues show only double the MGS of the ice crystals produced in the presence of this analogue at the same concentration. These new compounds are considerably more active than most of the glycopeptides described in previous chapters. Their activity is nothing short of remarkable for a small molecule. Although these compounds show incredible activity, in the initial study, the pentanol

derivative **728** showed considerably better activity than the pentyl (**708**) or even hexyl (**752**) derivatives. Consequently, a series of analogues was designed to see if this trend was general and if even more potent analogues could be prepared by adding a terminal hydroxyl group.

## 7.6 Synthesis and antifreeze activity of terminal hydroxyl analogues of 228

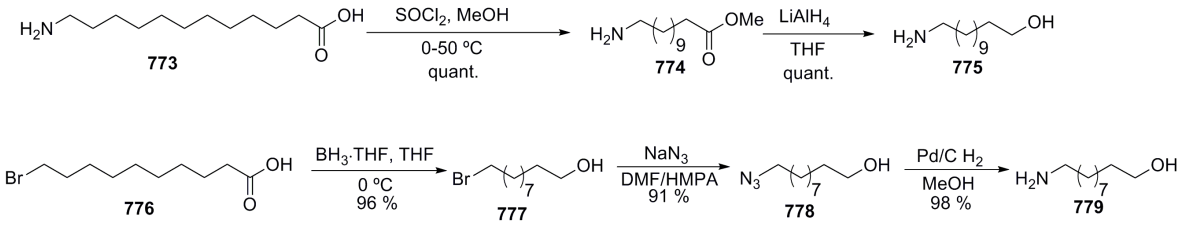
To carry out this analysis, three compounds were chosen: octanol derivative **770**, decanol derivative **771** and dodecanol derivative **772** (Table 7.3). One of the amines, 8-aminooctanol, is readily commercially available; however the other two are either prohibitively expensive or unavailable commercially. Consequently they were synthesized according to Scheme 7.8. Direct reduction of **773** to **775** using borane failed to achieve the desired transformation, presumably due to solubility issues of **773** in THF. Consequently a two step reduction was used instead as suggested by Usuki [25] with thionyl chloride assisted methylation proceeding in quantitative yield to provide ester **774**. A standard LAH reduction resulted in the isolation of amino alcohol **775** in quantitative yield. This proved to be a very efficient process.

**Table 7.3 Synthesis of long-chain primary alcohol-containing analogues**




| amine | compound (acetylated) | yield (%) | compound (deprotected) | yield (%) |
|---|---|---|---|---|
| 8-aminooctanol | **780** | 83 | **770** | 92 |
| 10-aminodecanol | **781** | 81 | **771** | 84 |
| 12-aminododecanol | **782** | 72 | **772** | 93 |

Amino-decanol derivative **779** was synthesized from 10-bromodecanoic acid (**776**) using a similar strategy starting with a standard borane reduction to provide the primary alcohol **777** in 96 % yield. Sodium azide was then used to displace the primary




**Scheme 7.8 Synthesis of amino alcohols 775 and 779.**

bromide and provide azido-derivative **778** in 91 % yield and hydrogenolysis cleanly provided amino alcohol **779** in near quantitative yield. Both amino alcohols were prepared without resort to chromatography.

With the amino alcohols in hand, the couplings proceeded smoothly under standard conditions (again, DCM was preferred due to solubility concerns) to provide acetylated derivatives **770**-**772** as did the deacetylations under Zemplén conditions (Table 7.3).[8] Following this synthesis, IRI analysis was again carried out over a range of concentrations to determine whether they behaved similarly to the long-chain alkyl compounds described

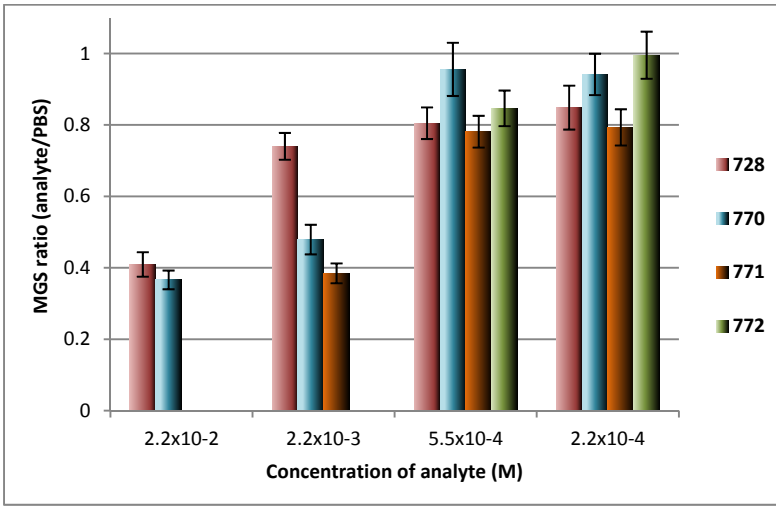



**Figure 7.11 IRI activity of terminal alcohol derivatives at various concentrations.**

above. The data is presented in Figure 7.11. Again, only the pentanol and octanol derivatives **728** and **770** are soluble at 22 mM. Decanol derivative **771** was soluble at 2.2 mM, and dodecanol derivative **772** became soluble at 550 μM. The IRI behaviour of these compounds is considerably different compared to that of the alkyl analogues. At higher concentrations this is not immediately apparent as again there appears a good correlation between chain length and IRI activity at 22 and 2.2 mM, although the activity at both concentrations is considerably less than that observed for the alkyl analogues. However, below this point all the analogues, regardless of chain length, appear to lose the majority of their activity very rapidly. Because of their poor activity at 220 μM, no analysis was done at lower concentrations. Activity is certainly not maintained as the concentration falls in the manner seen in the alkyl analogues (Figure 7.9). Furthermore, the relationship between IRI activity and chain length, at the lower concentrations, resembles a horizontal line, not the negatively sloped line previously observed for the alkyl analogues or even these same alcohols at higher concentrations (Figure 7.8, Figure 7.10). Consequently, it appears that the higher IRI activity of pentanol derivative **732** compared with its alkyl analogues (pentyl derivative **708** and hexyl (same length if including the hydroxyl group) **752**) is not generalizable, at least not in the case of longer chain analogues.

## 7.7 Possible rationale for the activity of long-chain alkyl analogues

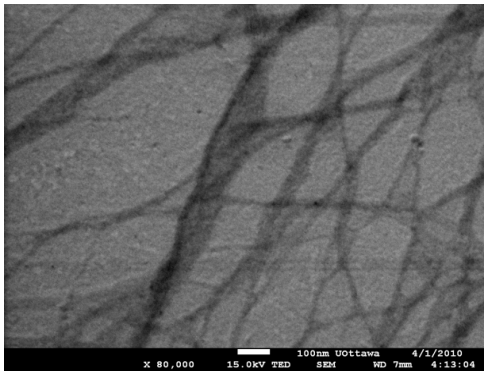



**Figure 7.12 SEM image of analogue 751 at 80,000x magnification showing a fibrous network typical of a gel.**

The combination of the results from highly active alkyl analogues and the less active terminal hydroxyl compounds were possibly explained by the following serendipitous finding: upon standing for a day, a solution of nonyl analogue **752** appeared to form a gel. To investigate this effect, the pentyl, hexyl, heptyl, octyl, and nonyl analogues were examined for gelation behaviour in pure water. It was found that the gel points (minimum concentration of compound required for gelation) were 5.9 mM for the nonyl analogue **755**, 36 mM for the octyl analogue **754**, and 98 mM for the heptyl analogue **753**.[26] SEM images were then acquired of a reduced solution of the octyl analogue **754** showing a fibrous network typical of an intramolecular network (Figure 7.12). The hexyl (**752**) and pentyl (**708**) analogues did not form an observable gel at either ambient temperature or 4 ºC at any concentration.[27] The fact that the hexyl analogue does not appear to form a gel while the heptyl analogue does may provide an explanation for the drastic increase in activity observed by the addition of the single methylene group that differentiates the two. This result would also explain why pentanol derivative **728** shows improved activity compared to pentyl derivative **708**, while the other long chain alcohol compounds show lower activity than their alkyl counterparts: if the mechanism for IRI activity has changed for alkyl compounds with chain lengths longer than 6 carbons due to the formation of intermolecular networks, it would not

follow that the terminal alcohol derivatives would undergo the same improvement in IRI activity as they do not appear to form gels at any temperature or concentration.

Why should a gel (or gel-like intermolecular interactions) assist in better IRI activity? Activity is not slightly increased in the presence of the hydrogelator, it is drastically increased. This is, however, not an unprecedented effect. A somewhat similar phenomenon was identified by Highgate, Knight and Probert regarding ice recrystallization inhibition in the presence of hydrophilic polymers.[28] In that case, they concluded that the polymers inhibit “the normal freezing process” or recrystallization. They proposed that this could be due to the water molecules being temporarily “bound” (or absorbed) to sites in the molecular lattice of the polymers. Water so absorbed would not be available to form ice crystals, and consequently these constructs result in IRI activity. This property has received some focus in surface chemistry where attempts have been made to integrate a hydrophilic surface into paints in order to reduce the formation of frost (essentially a macro-effect of recrystallization), and they function well, considerably reducing the onset and thickness of frost on these compounds.[29-31] However this effect is lost in such compounds over many freeze/thaw cycles. This has been shown to be due to the breakdown and damage to the hydrophilic polymer caused by ice-formation.[32] In the case of a gel formed from an intermolecular network, such as the hydrogels observed with the long chain alkyl analogues here, this would not be observed as the network is not dependent on a rigid polymeric construct; rather it is formed by a flexible intramolecular network suggesting that activity would be retained through many freeze-thaw cycles (unfortunately the “splat” assay technique employed to measure IRI activity in this study is not amenable to freeze-thaw cycle analysis).

Previous explanations involving the importance of hydration proposed the following mechanism for IRI activity (Figure 7.13).[2] In a flash-frozen sample with many independent nucleation events, ice crystals meet each other at a grain boundary. These boundaries consist of three phases, the ice lattice, the QLL layer and a thin layer of bulk water. Water may dissociate from the ice and transfer to the quasi-liquid layer, or QLL, a zone of intermediate organization between bulk water and the ice crystal. Carbohydrate IRI inhibitors are proposed to be localized to this position as their lack of TH activity makes it unlikely that they interact directly with the ice surface and carbohydrates have never been identified as being present in the QLL; furthermore, in the one study examining the localization of a carbohydrate in ice, Uchida and co-workers proposed that trehalose is localized at the bulk water-QLL interface.[33] Water in the QLL may then enter the bulk water, transfer via another QLL and merge with the neighbouring ice-crystal. As mentioned in the introduction, large ice crystals will grow at the expense of smaller ice crystals due to Ostwald ripening, and so this system is constantly in flux until such a point that at $t_\infty$ the sample has collapsed to a single ice crystal. A solute, such as a carbohydrate, lying in the bulk water phase would disrupt the surrounding bulk water. This increases the energy associated with the passage of water into the QLL from the bulk water. This change in energy slows the process of ice recrystallization down and should result in a

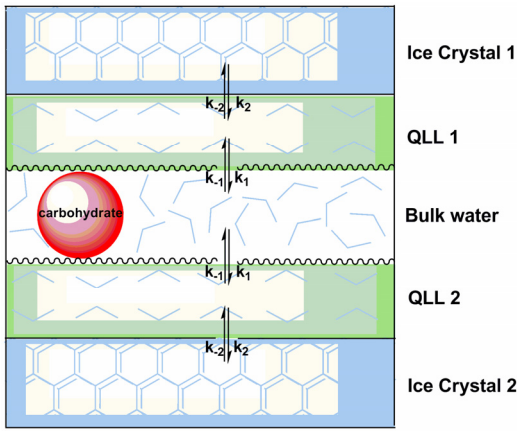



**Figure 7.13 Cartoon representation of the proposed mechanism for ice recrystallization inhibition. Carbohydrates reside at the quasi-liquid layer (QLL)-bulk water interface. Reproduced from Tam et al.[2]**

better inhibitor of recrystallization (Figure 7.13). Another way of looking at the same process is that the water associated with the carbohydrate must dissociate from the carbohydrate's hydration shell to reorganize with bulk water before transferring to an adjacent QLL. A gel network formed from a good IRI inhibitor would have a similar but stronger impact. Water would be sequestered in a gel layer (as proposed by Highgate), presumably located within the bulk water between adjacent ice crystals slowing down the process by which it can transfer from one ice crystal to the adjacent crystal. The formation of a form of network in the presence of heptyl analogue **750** rather than simply having a solute present with a large hydration shell, such as hexyl **749**, would be a possible explanation for the drastic difference in activity between the two analogues. It should be noted that more recent efforts from the Ben lab have demonstrated that not all gels are capable of slowing IRI, it appears that a core IRI-active structure is still required, and its removal can lead to inactive compounds. Similarly, the formation of micelles has not been found to be related to IRI activity. The reason for this behaviour is unknown at this time. In this case the core structure is galactose, although hydrogelators based on non-carbohydrate scaffolds have also recently shown promise.[34]

Further notes of interest regarding this possibility is that at the concentrations currently used in cryopreservation, common additives, such as sucrose and trehalose, most certainly form highly viscous solutions that may function through a somewhat similar mechanism in addition to the other known mechanisms of activity ascribed to these cryo-preservatives.

It is also interesting to note that the long chain alkyl group imitates the long hydrophobic backbone of the peptide component in **118**. Although the glycopeptides have not shown any gelator activity, this structural similarity is intriguing. Further studies are currently being undertaken to fully elucidate the importance of intra-molecular networks to IRI activity.

## 7.8 Chapter Summary

The initial goal of the project was to investigate the importance of different structural moieties of glycopeptide **118** for its IRI activity. It is clear that activity decreases rapidly as the number of repeats of the tripeptide unit falls below four (Figure 7.4). The glycoconjugate building block also only expresses moderate activity relative to the previously characterized activity of galactose. Similarly, the charged carboxylate or ammonium derivatives also showed limited IRI activity (Figure 7.5). Furthermore, shorter alkyl derivatives, rather than increasing the activity of the analogues relative to galactose, actually caused a decrease in activity. These results were not promising in the search for a compound able to bridge the concentration/activity gap between galactose and the glycopeptides such as **118**. However, propyl analogues showed improved activity relative to either their butyl or ethyl neighbours and this activity could be modulated by either increasing steric volume (decreases IRI activity) or decreasing the volume through introducing unsaturations (which increase IRI activity, in some cases significantly). However the truly impressive result is that long-chain alkyl compounds show remarkable IRI activity even at very low concentrations. This is possibly due to the formation of intramolecular networks as deduced by the tendency of

the solutions to form gels upon extended standing. Notably, mono-glycosylated tetra- and hexadecyl derivatives **758** and **759** have better activity than glycopeptide trimer **227** at 5.5 μM; likewise their activity at this concentration is better than all but a select few glycopeptides previously prepared in the Ben lab (see introduction and chapters 3 and 4). It is highly interesting to note that they attain this feat while being only a fraction the size of a glycopeptide. For example, the molecular weight of **188** is 1803 Daltons, while the heaviest analogue here, **759**, has a molecular weight of only 446 Daltons. That is a not insignificant difference. Furthermore, this implies that at 5.5 μM, with the compound able to inhibit the growth of ice crystals such that they are only 54 % the size of those in PBS, 1 mg of the compound is diluted into approximately 400 mL of solution. This is considerably more impressive when one considers the molecular target of this compound is not a few (thousand or million) receptors on a cell, but rather the combined surfaces of all the growing ice crystals.

Consequently, the efforts described above have demonstrated that it is not only possible to develop small molecule IRI active compounds, but also that they can compete on the same order of magnitude as the highly active glycopeptides (and are more active than the vast majority of antifreeze glycopeptides previously produced by the Ben group despite being far smaller). These presented compounds provide excellent lead targets for the development of future generations of small molecule inhibitors of ice recrystallization.

## References

1. Czechura, P.; Tam, R. Y.; Dimitrijevic, E.; Murphy, A. V.; Ben, R. N., *J. Am. Chem. Soc.* **2008,** *130* (10), 2928-2929.

2. Tam, R. Y.; Ferreira, S. S.; Czechura, P.; Chaytor, J. L.; Ben, R. N., *J. Am. Chem. Soc.* **2008,** *130* (51), 17494-17501.

3. Wu, L. K.; Tokarew, J. M.; Chaytor, J. L.; von Moos, E.; Li, Y.; Palii, C.; Ben, R. N.; Allan, D. S., *Carb. Res.* **2011,** *346* (1), 86-93.

4. Tachibana, Y.; Fletcher, G. L.; Fujitani, N.; Tsuda, S.; Monde, K.; Nishimura, S.-I., *Angew. Chem. Intl. Ed.* **2004,** *43*, 856-862.

5. Eniade, A.; Purushotham, M.; Ben, R. N.; Wang, J. B.; Horwath, K., *Cell. Biochem. Biophys.* **2003,** *38*, 115-124.

6. Chaytor, J. L. Examining the role of carbohydrate hydration and structure in preventing ice-recrystallization. PhD. Thesis, University of Ottawa, Ottawa, 2010.

7. Chan, W. C.; White, P. D., Basic procedures. In *Fmoc Solid Phase Peptide Synthesis: A Practical Approach*, Chan, W. C.; White, P. D., Eds. Oxford Univesity Press: Oxford, 2000; pp 41-76.

8. Wang, Z., Zemplén Deacetylation. In *Comprehensive Organic Name Reactions and Reagents*, John Wiley & Sons, Inc.: 2010.

9. Murphy, A. V. Preparation of structurally diverse C-linked antifreeze glycoprotein analogues and assessment for antifreeze protein-specific activity. PhD. Thesis, State University of New York, Binghampton, 2004.

10. Bouvet, V. R. Novel AFGP8 Analogues: Synthesis and Biological Evaluation of Potent Recrystallization Inhibitors. PhD. Thesis, University of Ottawa, Ottawa, 2006.

11. Vuljanic, T.; Bergquist, K.-E.; Clausen, H.; Roy, S.; Kihlberg, J., *Tetrahedron.* **1996,** *52* (23), 7983-8000.

12. Wuts, P. G. M.; Greene, T. W., Protection for the amino group. In *Greene's protective groups in organic synthesis*, 4th ed.; Wiley: Hobocken, NJ, 2007; p 904.

13. West, C. W.; Estiarte, M. A.; Rich, D. H., *Org. Lett.* **2001,** *3* (8), 1205-1208.

14. Thottumkara, A. P.; Bowsher, M. S.; Vinod, T. K., *Org. Lett.* **2005,** *7* (14), 2933-2936.

15. Zhao, M.; Li, J.; Mano, E.; Song, Z.; Tschaen, D. M.; Grabowski, E. J. J.; Reider, P. J., *J. Org. Chem.* **1999,** *64* (7), 2564-2566.

16. Dondoni, A.; Mariotti, G.; Marra, A.; Massi, A., *Synthesis.* **2001,** *2001* (14), 2129,2137.

17. Chaytor, J. L.; Ben, R. N., *Bioorg. Med. Chem. Lett.* **2010,** *20* (17), 5251-5254.

18. Von Moos, E. Investigating the importance of hydrophobicity and hydration of carbohydrates and antifreeze glycoprotein analogues to ice recrystallization inhibition activity and cryopreservation. University of Ottawa, Ottawa, 2011.

19. Curtin, D. Y.; Gerber, S. M., *J. Am. Chem. Soc.* **1952,** *74* (16), 4052-4056.

20. Nystrom, R. F.; Brown, W. G., *J. Am. Chem. Soc.* **1947,** *69* (5), 1197-1199.

21. Pirrung, M. C., *The synthetic organic chemist's companion*. Wiley: Hoboken, NJ, 2007; p 198.

22. Patnam, R.; Juárez-Ruiz, J. M.; Roy, R., *Org. Lett.* **2006,** *8*, 2691-2694.

23. Krompiec, S.; Pigulla, M.; Krompiec, M.; Baj, S.; Mrowiec-Bialon, J.; Kasperczyk, J., *Tetrahedron Lett.* **2004,** *45* (27), 5257-5261.

24. Meyer, A. Y., *Struct. Chem.* **1990,** *1* (2), 265-279.

25. Usuki, Y.; Matsumoto, K.; Inoue, T.; Yoshioka, K.; Iio, H.; Tanaka, T., *Bioorg. Med. Chem. Lett.* **2006,** *16* (6), 1553-1556.

26. Alemán, J.; Chadwick, A. V.; He, J.; Hess, M.; Hoie, K.; Jones, R. G.; Kratochvil, P.; Meisel, I.; Mita, I.; Moad, G.; Penczek, S.; Stepto, R. F. T., *Pure Appl. Chem.* **2007,** *79* (10), 1801-1829.

27. Rather, the compound precipitates out before any gel is formed.

28. Highgate, D.; Knight, C.; Probert, S. D., *App. Ener.* **1989,** *34* (4), 243-259.

29. Gou, Y. J.; Zhong, X. H.; Liu, Z. L., *App. Materials Res.* **2011,** *287-290*, 410-414.

30. Liu, Z.; Wang, H.; Zhang, X.; Meng, S.; Ma, C., *Int. J. Refrig.* **2006,** *29* (2), 229-236.

31. Liu, Z.; Wang, H.; Zhang, X.; Meng, S.; Ma, C., *Int. J. Refrig.* **2006,** *29* (2), 237-242.

32. Okoroafor, E. U.; Newborough, M.; Highgate, D., *J. Phys. D.* **1998,** *31* (21), 3130-3138.

33. Uchida, T.; Nagayama, M.; Shibayama, T.; Gohara, K., *J. Cryst. Grow.* **2007,** *299* (1), 125-135.

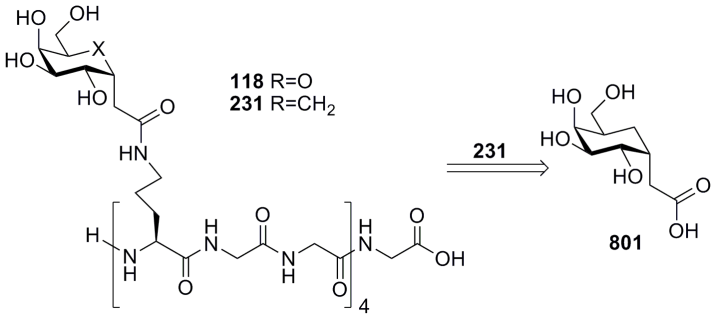
34. Balcerzak, A.; Ben, R. N., Unpublished work. 2011.

# Chapter 8 : Studies towards the synthesis of a carbasugar derivative of 118 and the synthesis of carbasugar derivatives of galactose and glucose

Carbasugar is the name given to the cyclitols that mimic the structure of true sugars; specifically they contain the same five contiguous stereocentres, the endocyclic ring oxygen of the furanose or pyranose ring is replaced with a methylene group and, although rare, are found in nature, and are increasingly important in medicinal chemistry as is evidenced by the carbasugar-derivative Tamiflu.[3-9] Their lack of an anomeric oxygen makes them intriguing targets for IRI SAR studies.

## 8.1 Carbasugars as excellent, configurationally stable, mimics of natural sugars

The actual role of the ring oxygen has never been explored in the hydration or IRI literature and consequently the IRI effect of substituting a methylene group for the oxygen is unpredictable. This substitution would increase the hydrophobic nature of the molecule; however it would also affect, even if only moderately, the intramolecular hydrogen-bond network.[10-12] Unlike the inositols, carbasugars maintain the presence of the *C*-6 methanol moiety, and act as much better mimics of the natural sugars, and




**Scheme 8.1 Target glycopeptide 231, carbasugar analogue of highly IRI active 118, and key intermediate 801.**

consequently appear to be the rational choice for an SAR study. To this end, **231**, the carbasugar derivative of **118**, was chosen as the glycopeptide target. This implies that carboxylic acid derivative **801** is the key intermediate for the synthesis of this desired compound (Scheme 8.1).

A second key question that carbasugars can address relates to the IRI activity of the simple carbohydrates. D-galactose in solution is not a single compound, but is in fact made up of six different molecules in equilibrium (Figure 8.1): 64 % of the molecule exists as the β-pyranose form (**802**), 29 % exists as the α-pyranose form (**803**), 4 % exists as the β-furanose (**804**), and 3 % as the α-furanose (**805**).[13] Trace amounts also exist as the open chain intermediate (**806**) and its hydrate (not shown). It is well established that α-linked glycosides maintain considerably better IRI activity than their respective β-anomers.[15-18] Consequently, the question arises as to whether the IRI activity of α-galactose differs from β-galactose. This query cannot be answered using the carbohydrate itself, for there is no method to isolate the individual anomers and maintain their anomeric configuration for IRI analysis.[19] Techniques involving the addition of an anomeric methoxy group, which has been used to isolate each anomer,[20] only provides a partial answer to this question as changing the anomeric hydroxyl for a

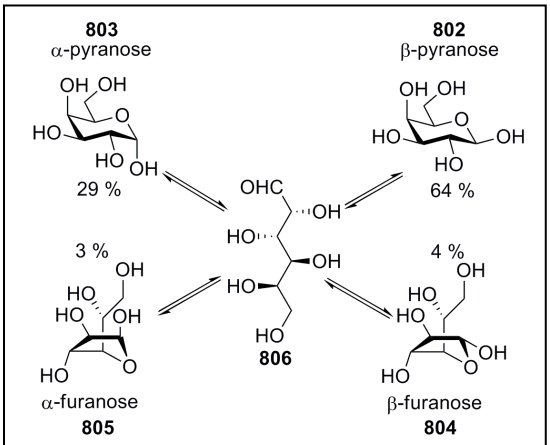



**Figure 8.1 The mutarotation of galactose through the four most populated isomers and their relative abundance in water at 31 °C.[13, 14]**

methyl ether is, in fact, a rather drastic structural intervention, especially in regards to hydrogen-bonding considerations.[15]

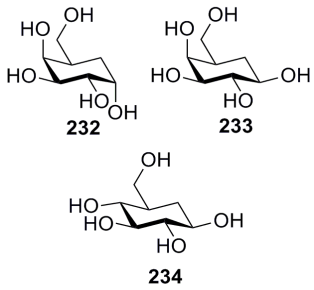



**Figure 8.2 Target carbasugars.**

The replacement of the oxygen with a methylene allows access to configurationally stable forms of each anomer allowing for the IRI activity to be assessed separately. Although certainly not identical to the native sugar, these compounds provide a "best analogue" with the minimal structural modification possible to examine this question. To carry out this study, three analogues were targeted as mentioned in Chapter 2 (Figure 8.2), 5a-carba-α-galactopyranose (**232**), 5a-carba-β-galactopyranose (**233**) and 5a-carba-β-glucopyranose (**234**). The first two are the carbasugar derivatives of galactose. Glucose derivative **234** can be used as a control to determine if any trend in the change to IRI activity is generalizable across the series of carbasugars, or simply specific to galactose. However, the challenge of preparing the carba-glycopeptide was addressed first.

## 8.2 General synthetic strategies for the preparation of carbasugars

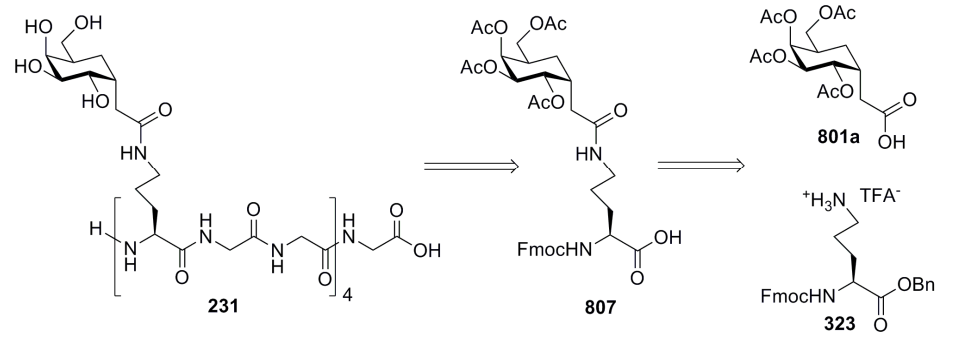
"Replacing the oxygen atom of the sugar ring with carbon is easy on paper, but it is more difficult to carry out this transformation and form five- and six-membered carbon rings in the flask" Sinaÿ notes in his review on the subject.[2] There are several traditional approaches to the synthesis of carbasugars and they have been extensively reviewed.[9, 21-25] Carbasugar synthesis is quite difficult: in effect the chemist is attempting to prepare a cyclohexane ring with five contiguous stereocentres, and four contiguous hydroxyl

groups. This is quite the challenge. Seeing as an ideal synthesis would seek to produce only a single enantiomer of the final compound simply complicates the problem further. In the synthesis of **231**, this challenge is exacerbated in that one of the hydroxyl groups (at *C*-1) must be replaced with an α-carbon linkage. Although not seemingly that onerous on first inspection, this requirement played a key role in the selection of the preferred synthetic routes.

Several strategies have been developed over the past 40 years to prepare carbasugars, with the pioneering work being carried out by the McCasland group in the late 1960s who employed a strategy involving the functionalization of 1,3,5,7-cyclooctatetraene and later the exploitation of 7-oxanorbornene derivatives.[26-28] The four most common approaches are as follows: ring-closing metathesis (RCM); [22, 29, 30] chemo-enzymatic desymmetrization and elaboration of benzene derivatives; [31-35] ring opening of 7-oxanorbornene derivatives; [23, 27, 36, 37] and Ferrier Type II rearrangements, especially the Sinaÿ modification.[1, 2, 14, 38-41] The latter two approaches were deemed the most appropriate for the current requirements and synthetic approaches towards **801** were carried out using these strategies, although as only limited success was achieved with the 7-oxabornene approach, only the efforts towards the Sinaÿ approach are described below.

## 8.3 End-stage retrosynthetic analysis of glycopeptide 231.

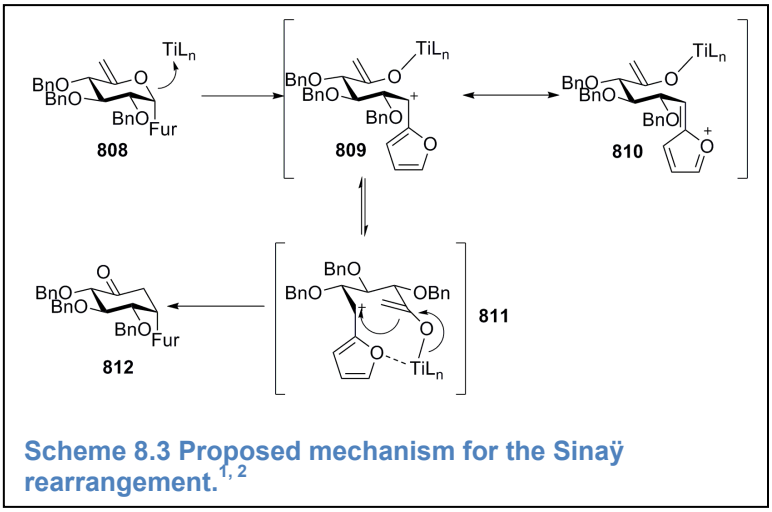
Regardless of the technique employed to prepare the carbasugar, the same retrosynthetic strategy was envisioned for the completion of the glycopeptide synthesis (Scheme 8.2). Glycopeptide **231** would be prepared from glycoconjugate **807** and Fmoc-protected glycine using standard SPPS techniques described in Chapter 3. The




Scheme 8.2 Retrosynthetic analysis of carbasugar glycopeptide 231 to key intermediate 801.

glycoconjugate would be synthesized through the coupling of previously described TFA salt **323** and key intermediate **801a**, the acetylated derivative of **801**. None of these steps are expected to involve any complications. The difficulty in this synthesis would be in the production of **801**.

## 8.4 Synthetic design involving a Sinaÿ rearrangement

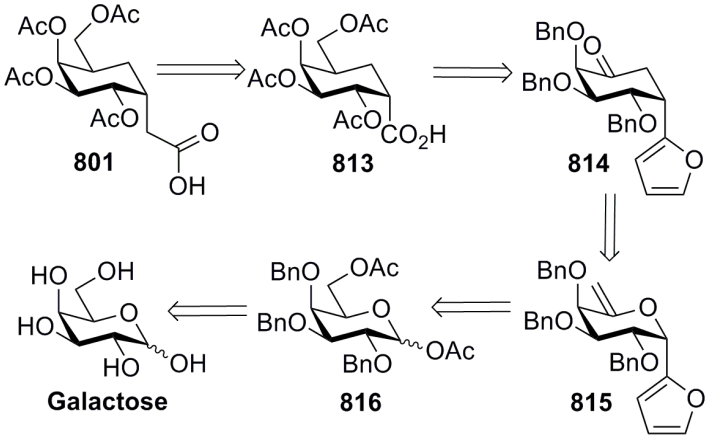



Scheme 8.3 Proposed mechanism for the Sinaÿ rearrangement.[1, 2]

The initial retrosynthetic analysis of **801** envisioned the titanium-mediated Sinaÿ-rearrangement as the key transformation (Scheme 8.3). In this reaction, the Titanium co-ordinates to the endocyclic oxygen (**808**) allowing for bond cleavage to form the anomeric carbocation (**809**). The charge is stabilized by the anomeric substituent (in this case furan, **810**) and following rotation of the *C*-4, *C*-5 bond (which allows the titanium to chelate the furan oxygen, **811**), ring closing occurs with the retention of α-stereochemistry providing

cyclohexanone derivative **812**. This approach is applied to the retrosynthetic analysis of **801** (Scheme 8.4).

Key intermediate **801** should be accessible through the homologation of **813** using the Arndt-Eistert reaction.[42] This carboxylic acid should be obtainable from **814** through a short sequence of transformations. Methenylation (a one-carbon Wittig,[43] Tebbe methenylation,[44] or Petasis methenylation[45]) of the ketone would install *C*-6, hydroboration using a large bulky boron reagent (such as 9-BBN) would ensure addition from the less crowded bottom face, and ozonolysis would oxidatively cleave the furan to the required carboxylic acid moiety along with possible concomitant deprotection of the benzyl groups. Intermediate **814** would be accessible through the Sinaÿ rearrangement of **815**. A similar substrate an α-methoxy galactoside has been employed in this reaction as has the glucose derivative of **815**. Therefore **815** should be convertible to **814**. The 5-ene-6-deoxy derivative **815** should be obtainable from **816** through glycosylation using furan followed by a functional group transformation of the *C*-6 acetoxy group to the desired olefin. Finally, di-acetate **816** has been prepared from galactose over 3 steps, allowing easy access to this intermediate from a very inexpensive starting material.[46]

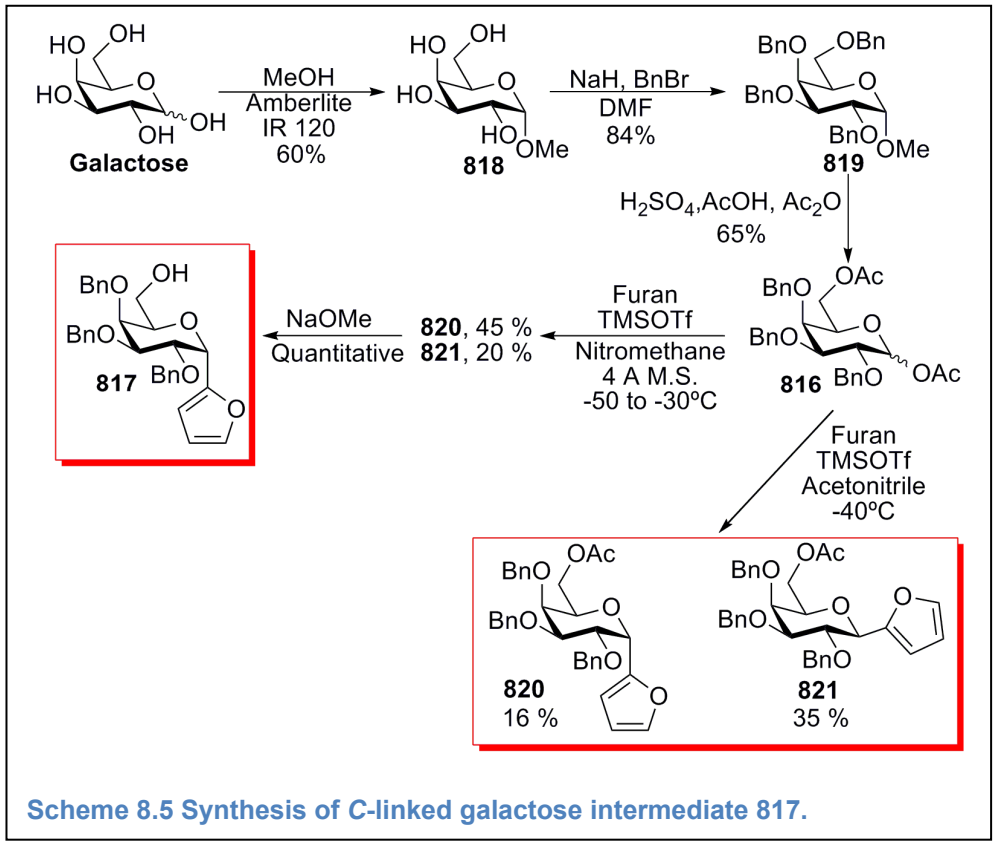



**Scheme 8.4 Initial retrosynthetic analysis of 801 employing the Sinaÿ rearrangement as the key transformation.**

## 8.4.1 Synthesis of furyl galactose derivative

### *8.4.1.1 Synthesis of galacto-furyl derivative 817*

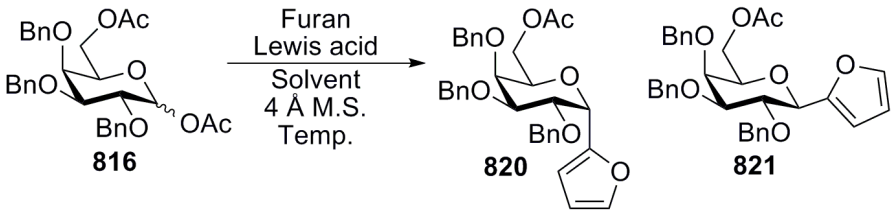
The synthesis of key intermediate **817** was accomplished as shown in Scheme 8.5. Galactose was treated with Amberlite resin in methanol under reflux for 72 hours. Following chromatography to remove unreacted starting material and the furanose forms, methyl-α-D-galactopyranose, **818**, was crystallized from 2-propanol in 60 % yield as per Moradai and co-workers.[47, 48] Perbenzylation proceeded smoothly to provide **819** in 84 % yield according to the protocol of Fletcher and co-authors.[49] Due to the difference in reactivity between the 1º benzyl group at *C*-6 and the 2º benzyls at the other positions, treatment of **819** in the presence of sulfuric acid, acetic acid and acetic anhydride led to the preparation of **816** as an anomeric mixture in 65 % yield.[46]. Using acetonitrile as solvent, and in the presence of 3 equivalents of furan, and 1.2 equivalents of TMSOTf at -40 to -20 ºC, the Sinaÿ group obtained a 71 % yield of the glucose isomer of **820**




**Scheme 8.5 Synthesis of *C*-linked galactose intermediate 817.**

from the glucose isomer of **816**.[38] When identical conditions were applied to **816**, the reaction was far less efficient. The α-anomer **820** was obtained in only 16 % yield, while the β-anomer, **821**, was produced in 35 % yield. The reaction was repeated and a very

**Table 8.1 Selected conditions examined to glycosylate 872 and preferentially provide 820.**




| entry | temperature (ºC) | solvent | Lewis acid | yield 820 (%) | yield 821 (%) | recovered 816 (%) |
|---|---|---|---|---|---|---|
| i | -40 | Acetonitrile | TMSOTf | 16 | 35 | 5 |
| ii | -40 | $Et_2O$ | TMSOTf | 15 | 0 | 50 |
| iii | -40 | DCM | TMSOTf | 43 | 6 | 7 |
| iv | -40 | $Et_2O$ | $BF_3{\cdot}OEt_2$ | 10 | 4 | 46 |
| v | -40 | DCM | $BF_3{\cdot}OEt_2$ | 32 | 5 | 9 |
| vi | -78 | $Et_2O$ | $BF_3{\cdot}OEt_2$ | 0 | 0 | 75 |
| vii | -78 | DCM | $BF_3{\cdot}OEt_2$ | 6 | 21 | 3 |
| viii | -20 | $Et_2O$ | $BF_3{\cdot}OEt_2$ | 6 | 9 | 42 |
| ix | -20 | DCM | $BF_3{\cdot}OEt_2$ | 25 | 15 | <3 |
| x | 23 | $Et_2O$ | $BF_3{\cdot}OEt_2$ | 0 | 0 | <3 |
| xi | 23 | DCM | $BF_3{\cdot}OEt_2$ | <3 | <3 | 0 |
| xii | -40 | Furan | TMSOTf | 42 | 40 | 0 |
| xiii | -40 | Furan | $BF_3{\cdot}OEt_2$ | 31 | 35 | 0 |
| xiv | -40 | DCM | TMSOTf/ $BF_3{\cdot}OEt_2$ | 7 | 22 | 0 |
| xv | -50 | Acetonitrile | TMSOTf | 30 | 9 | <3 |
| xvi | -50 | Nitromethane | $BF_3{\cdot}OEt_2$ | 32 | 5 | <3 |
| xvii | -50 to -30 | Nitromethane | TMSOTf | 45 | 20 | <3 |

similar result was obtained. Clearly, this yield was not sufficient to provide **820** (a relatively early intermediate in the preparation of key carboxylic acid **801**) in synthetically useful amounts. Consequently, an attempt was made to improve the yield of this reaction.

A couple of factors were considered important, including solvent, temperature and Lewis Acid. The choice of solvent appeared unusual as acetonitrile is known as a participating solvent and generally would be expected to provide β-products in

glycosidations.[50, 51] Attempting other solvents might further improve yields of the α product.

To optimize this reaction, a number of experiments were carried out and a selected series of conditions and their results is supplied in Table 8.1. Reactions were quenched after 12 hours and the amount of **820**, **821** and unreacted **816** was quantified from the purified fractions following chromatography. In addition to these isolated compounds, TLC of the crude reactions often showed significant amounts of decomposed products. The NMR spectra of these streaks were incredibly complicated containing a multitude of carbohydrate-based compounds; none of these minor impurities was ever successfully isolated or characterized.

The initial reaction was carried out under the Sinaÿ conditions as mentioned above (entry i). This produced the β-anomer as the major product and resulted in considerable decomposition. Consequently, non-participating DCM and diethyl ether were used.

At -40 ºC, diethyl ether provides a 15 % yield of α-anomer **820**, with no observable formation of **821** (entry ii). However the conversion was extremely poor even after 12 hours at room temperature with 50 % of the starting material recovered. DCM at the same temperature provided a reproducible 43 % yield of the desired anomer (entry iii). However, when the reaction was scaled up to synthetically useful quantities (500 mg), this efficiency was not sustained and yields fell to ~23 %.

$BF_3{\cdot}OEt_2$ can also be used as a Lewis acid activator of anomeric acetate groups, and a temperature scan using this reagent was carried out with both DCM and diethyl ether. At -78 ºC, both solvents were sluggish with the diethyl ether reaction returning no

yield of either product, only starting material (entry vii), and the DCM reaction providing only a 6 % yield of **820** along with a 21 % yield of **821** (entry viii). At -40 ºC, ether provided a 10 % yield of **820**, but the plurality of the material was recovered unreacted (entry iv). At the same temperature DCM provided the desired product in 32 % yield with only trace amount of the β and starting materials present (entry v).

As the temperature rose, the rate of decomposition increased rapidly. At -20 ºC, the ether reaction, still recovering 42 % of the material as **816**, with only 6 % being transformed to **820** (entry viii); DCM fared only slightly better with 25 % yield of **820** and the majority of the remaining material being lost to decomposition (entry ix). At room temperature, the vast majority of the material decomposed with only trace amounts of the three products being observed in either solvent system (entries x and xi).

The conclusion from this study was that diethyl ether, although supposed to assist in the selective formation of the α-anomer, failed to provide good conversions or yields at any temperature as the reactions were slow and tended to lead to decomposition. DCM on the other hand was relatively effective around -40 ºC; the conversions were too poor at -78º, and decomposition became a significant issue at all temperatures above -40 ºC. Other non-participating solvents were examined at -40 ºC (results not shown) including toluene, benzene, chloroform and carbon tetrachloride, but none performed better than DCM. Conducting the reaction using furan as solvent was also attempted. Using TMSOTf, the neat reaction yielded an excellent combined yield (82 %) of **820** and **821**, but unfortunately in nearly equimolar amounts. $BF_3{\cdot}OEt_2$ provided a similar result with reduced yields. It appeared that TMSOTf was indeed a better Lewis acid for the transformation than the boron reagent.

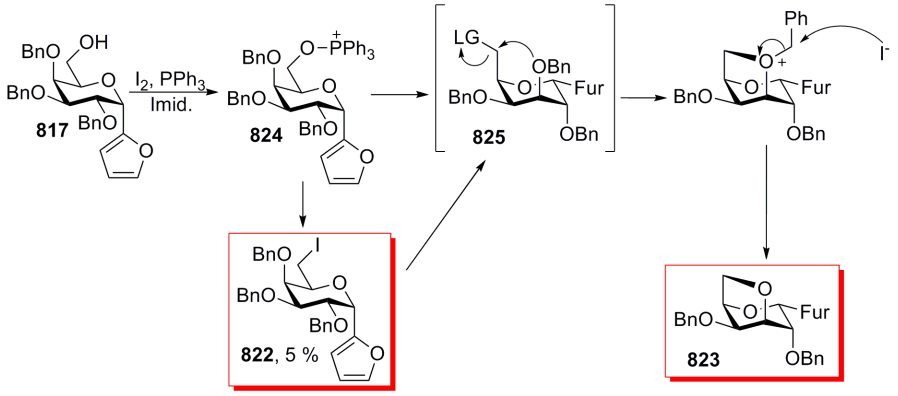
TMSOTf is the stronger Lewis acid,[52] and in an attempt to improve yields by strengthening it still further, the Lewis acid was changed to $BF_2OTf$.[53] Applying this catalyst to the optimized conditions (DCM, -40 ºC) provided much poorer yields of **820** and much poorer α-selectivity (but complete conversion of starting material) than either Lewis acid alone (entry xiv).A final attempt was made to improve the reaction by returning to acetonitrile and nitromethane. Nitromethane is of interest as it has been known to offer highly selective formation of α-anomers under glycosylation conditions in the presence of TMSOTf.[50, 54, 55] As shown in , at -50 ºC using TMSOTf as catalyst in acetonitrile, 30 % yield of **820** was obtained against only 9 % yield of **821** (entry xv). Nitromethane on the other hand provided surprisingly strong results: with $BF_3{\cdot}OEt_2$ as catalyst, 32 % of **820** was obtained (entry xvi), and using TMSOTf as catalyst provided the best yield of **820** seen to date (45 %, with an additional 20 % yield of the β-anomer). Nitromethane is believed to interact with the β-face of the oxocarbenium ion in a manner similar to diethyl ether. The discrepancy between ether and nitromethane is possibly due to the greater polarity and polarizability of the latter: allowing it to better stabilize the oxocarbenium and possibly decrease the propensity towards decomposition.[56]

The final step to access *C*-6 alcohol **817** is a simple Zemplén deacetylation that proceeded in the usual fashion to provide a quantitative yield of the desired compound. With this alcohol in hand, attention could be turned to the preparation of 6-deoxy-5-ene derivative **815**, the substrate for the key Sinaÿ rearrangement.

#### *8.4.1.2 Attempts at elimination*

When **817** was treated with iodine and triphenylphosphine in the presence of imidazole to accomplish a Garegg iodination,[57, 58] two spots were present on the TLC.

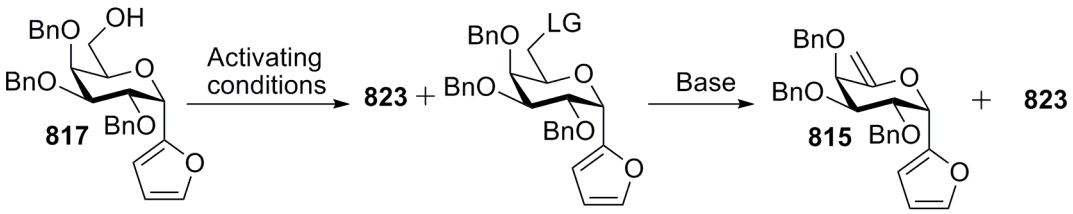
Surprisingly, following purification, the standard Garegg's iodination product (**822**) was not the major component of the mixture: it was obtained in only 5 % yield. The major product, obtained in 78 % yield, was identified (through mass spectrometry and NMR analysis) as the 3,6-anyhydro derivative of galactose (**823**). Examination of the literature showed that such bicycles had been encountered a few times before in the preparation of very similar compounds with α-methoxy or benzyloxy substituents.[59-61] It appears that α-furyl derivatives react in an identical fashion. A proposed mechanism is provided in Scheme 8.6. The alcohol is activated as expected to triphenylphosphonium **824**. This compound is either attacked by iodine to provide **822** or it undergoes the transformation implied by conformer **825**. This involves a ring flip to the $^{1}C_{4}$ chair and an intramolecular attack from the perfectly positioned axial *C*-3 benzyl group. Of course, this same reaction can occur on the iodine product rather than the phosphorous intermediate, thereby consuming the desired product. Following the attack, any present nucleophile, in this case the iodide or even possibly the triphenylphosphine, would be able to debenzylate the newly-generated bicycle and provide the anhydrosugar **823**.




**Scheme 8.6 Results of the iodination of primary alcohol 817.**

An attempt was made to determine conditions that would either generate enol ether **815** *in situ* from a spontaneous $E_2$ elimination, or conditions that would provide an activated alcohol that could be hopefully subjected to traditional $E_2$ reagents to provide **815** in two steps while avoiding the formation of anhydrosugar **823**. The efforts in these directions are described in Table 8.2. As mentioned, iodination failed to provide the desired compound (entry i), as did triflation at either 0 or 60 ºC (entries ii and iii) or

**Table 8.2 Selected conditions attempted for the formation of 815 through activation and elimination of the C-6 hydroxyl group. Isolated yields are provided of both activated species (822, 826, or 827) and anhydrosugar 823 at both stages of the sequence when relevant.**



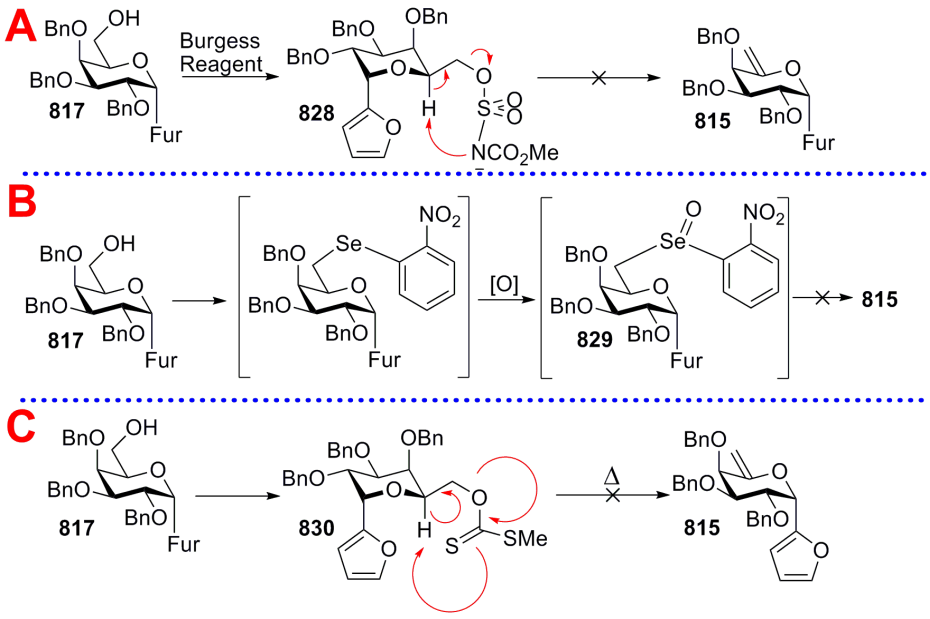

| entry | activating conditions | yield (%) and identity of activated species | yield (%) of 823 | elimination conditions | yield (%) of 823 | yield 815 (%) |
|---|---|---|---|---|---|---|
| i | $I_2$, $PPh_3$, Imidazole | 5 (**822**, LG = I) | 78 | ---------- | ---------- | ---------- |
| ii | $Tf_2O$, DBU, Pyr 0° | 0 | 60 | ---------- | ---------- | ---------- |
| iii | $Tf_2O$, DBU - 60° | 0 | 75 | ---------- | ---------- | ---------- |
| iv | $CBr_4$, $PPh_3$, $K_2CO_3$ | 10 | 56 | ---------- | ---------- | ---------- |
| v | TsCl, Pyr 0° | 53 (**826**, LG = Ts) | 20 | ---------- | ---------- | ---------- |
| vi | MsCl, Pyr 0° | 68 (**827**, LG = Ms) | <5 | NaH, DMF 0° | 70 | 0 |
| vii | MsCl, Pyr 0° | 68 (**827**, LG = Ms) | <5 | NaH, DMF 50° | 56 | 0 |
| viii | MsCl, Pyr 0° | 68 (**827**, LG = Ms) | <5 | LDA | 53 | 0 |
| ix | MsCl, Pyr 0° | 68 (**827**, LG = Ms) | <5 | K$^t$OBu | 46 | 0 |
| x | MsCl, Pyr 0° | 68 (**827**, LG = Ms) | <5 | Hunig's Base | * | 0 |
| xi | MsCl, Pyr 0° | 68 (**827**, LG = Ms) | <5 | 2,4,6-Collidine | * | 0 |
| xii | Burgess Reagent | ---------- | --------- | ---------- | 38 | 0 |
| xiii | $H_3PO_4$ 100°C | ---------- | --------- | ---------- | 42 | 0 |
| xiv | HOAc 100°C | ---------- | --------- | ---------- | 60 | 0 |

*The product was detected as the major product, but not isolated.

bromination using the Appel reaction (entry iv).[62-64] All of these conditions provided the anyhydrosugar as the major product. Better yields were obtained with the less reactive sulfonic esters: both tosyl (entry v, 53 %) and mesyl (68 %, entry vi) provided the desired activated derivatives **826** and **827** respectively. As the yield of the mesylate was moderately higher, it was used for many additional reactions.

Having overcome the difficulty of installing the leaving group and isolating the compound without it undergoing an intramolecular cyclization, it appeared that simply carefully choosing an appropriate base for the reaction with mesylate **827** would readily lead to the formation of **815**. However, non-nucleophilic sodium hydride failed to provide **815** at either 0 ºC (entry vi) or at 50 ºC (entry vii); rather the anhydrosugar was again obtained in reasonable yields. The same result was obtained when strong bulky bases such as LDA or *t*-BuOK were applied to **827** (entries viii and ix). Believing that the strong bases might be assisting the intramolecular nucleophilic attack, Hunig's base and 2,4,6-collidine were used with the same result (entries x and xi). Intermolecular deprotonation did not appear to be a productive means of accessing the desired compound as it did not seem to be able to compete with the intramolecular reaction. Consequently, rather than pursuing the fruitless intermolecular approach, an intramolecular deprotonation methodology was thought to afford the best possibility for the successful synthesis of desired compound: it should be able to compete kinetically with the intramolecular nucleophilic attack of the *C*-3 benzyl group (which can only occur in the higher energy chair conformation).

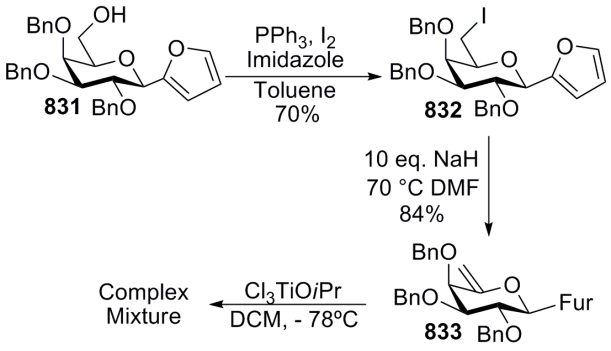
Alcohol **817** was then treated under Burgess' conditions. This reagent has been extensively used for the dehydration of alcohols (and direct displacement of alcohols) through an intramolecular mechanism via sulfamate derivative **828** (Scheme 8.7A).[65-67] Generally, the Burgess reagent functions well with only secondary and tertiary alcohols. Primary alcohols generally lead to the preparation of the corresponding carbamate. However, the author felt that any reaction, even this inter-conversion, may prove inspiring. Frustratingly, these conditions led to neither the carbamate nor **815**. The anhydro sugar was isolated instead. Two other similar reactions were also attempted. The Grieco elimination (Scheme 8.7B) involves the displacement of the primary alcohol using a selenium nucleophile and tributylphosphine as hydroxyl activator.[68, 69] Oxidation of the selenide using hydrogen peroxide to form **829** is theoretically followed by a *syn* elimination utilizing the selenoxide oxygen as the basic atom. Although these reaction conditions did not produce the anhydro sugar, they also failed to produce any detectible **815**. A large number of unidentified compounds were observed following work-up. A final attempt was made utilizing the Chugaev




**Scheme 8.7 Attempts to produce 815 through intramolecular strategies.**

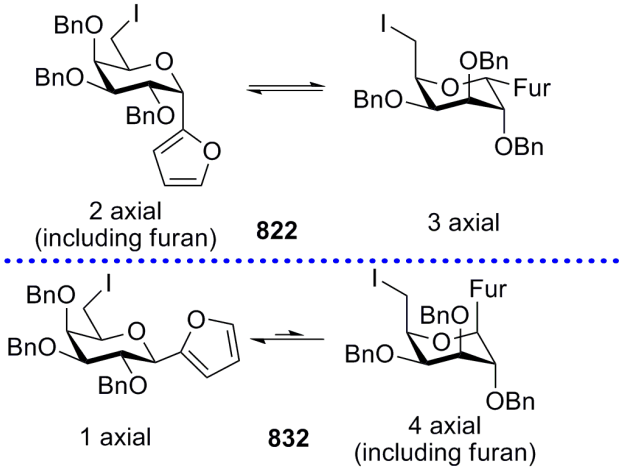
elimination. This reaction is a two-step process involving the preparation of a (usually methyl) xanthate from an alcohol followed by thermal decomposition, or pyrolysis via a *cis*-elimination (Scheme 8.7C).[70] Temperatures are normally on the order of 100 to 200 ºC.

This strategy was consequently attempted on **817**. The anion formed by the treatment of the alcohol with sodium hydride and carbon disulfide was quenched with methyl iodide. The intermediate was isolated by extraction, providing xanthate intermediate **830** in 32 % yield. This compound was then immediately dissolved in toluene and heated to reflux (BP = 111 ºC). After 28 hours, the starting material remained untouched. Toluene was then removed and replaced with *p*-cymene (BP = 177 ºC). After 44 hours the starting material remained untouched. The reaction was then diluted with diphenyl ether (BP = 258 ºC) and the reaction was heated to reflux. The starting material began to be consumed within the hour, but there was no discernable product detected by TLC; however, material began to appear at the baseline. Consequently, it appeared that at temperatures sufficient to initiate the desired reaction, the product (an enol ether) was not stable and began to decompose as soon as it was formed: no carbohydrate-like compounds were identified in the decomposed product mixture. In many cases the furan had also (apparently) reacted and/or decomposed under the high temperatures.




**Scheme 8.8 Dehydration of 831 and attempted Sinaÿ rearrangement of 833.**

The problems with the α-furan should be contrasted with the results obtained from reactions with the β-anomer, **821**, and its *C*-6 deprotected derivative **831** (Scheme 8.8). Unlike for the α-anomer, the first set of conditions attempted, the Garegg iodination, proceeded smoothly to provide iodide **832** in 70 % yield. Elimination with NaH was slow at low temperatures, but proceeded rapidly and cleanly at 70 ºC to provide **833** in 84 % yield. Both yields are unoptimized and no special precautions were taken to maximize the purified yields; therefore, the conversions are probably higher. However, as expected (and noted by Sollogoub),[1] the titanium-mediated Sinaÿ reaction was not effective at producing the desired rearrangement and simply resulted in a reproducible complex mixture of products. Theoretically, the aluminum-mediated reductive rearrangement system could have been used, but this would still have resulted in the formation of the β-product, not the desired isomer.



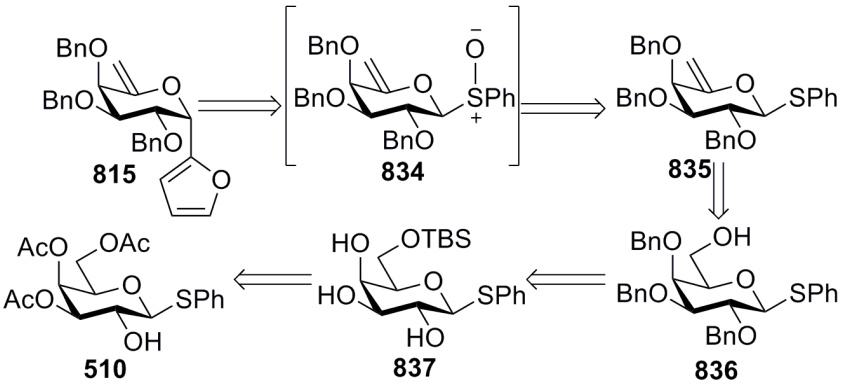

**Scheme 8.9 Two chair conformations of 822 and 832 showing the number of axial substituents present in each.**

The failure to synthesize enol ether **815** through any of the above strategies forced the reluctant abandonment of this route. The problem appears to be that the energy differences between the two chairs of the α-anomer **822** are too small, allowing ready access to the conformation that allows for the intramolecular substitution (Scheme 8.9). The energy differences for β-anomer **832** would be expected to be much greater explaining the success with this compound. A possible solution was envisioned:

if the enol ether could not be installed in the presence of the furyl group, then perhaps the enol ether could be installed first and the furyl group added later.

## 8.4.2 Synthesis of thiophenyl derivative 888

This inverse introduction of functionality relied upon the use of a thiophenyl blocking group. This group, or the sulfoxide derivative, can be activated under relatively mild conditions such as triflic anhydride, catalytic triflic acid, or electrophilic halogen. There is a high probability that either the thiophenyl group in **835**, or failing that, the sulfoxide in **834**, would be more reactive under these conditions than the putative enol ether functionality.



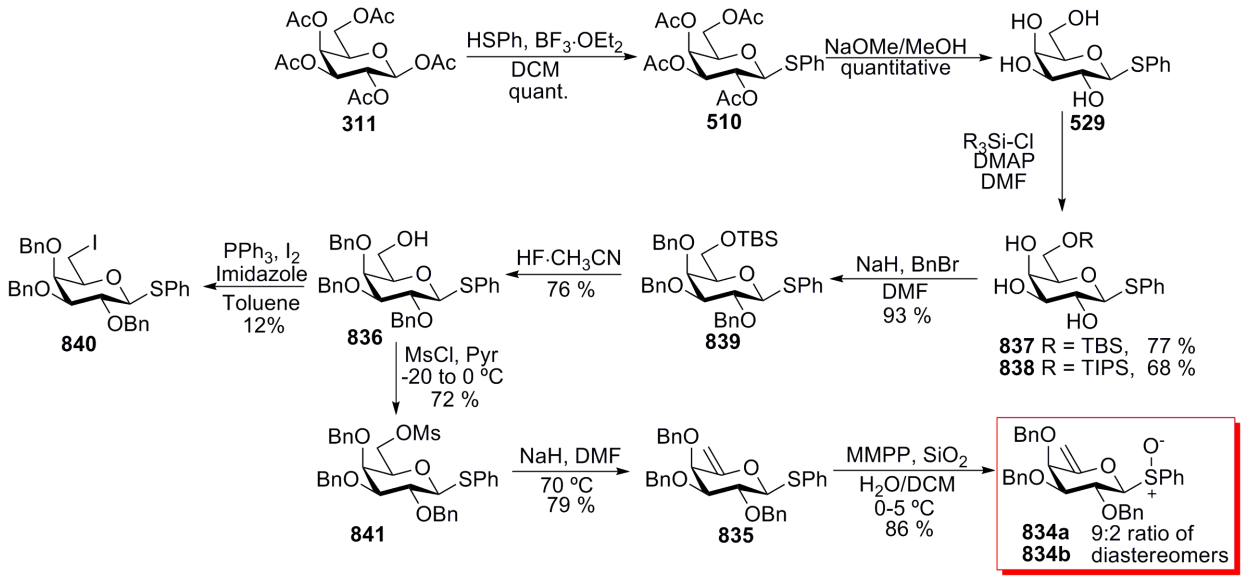

**Scheme 8.10 Retrosynthetic analysis of 815 involving a late-stage introduction of the anomeric furyl substituent.**

The proposed retrosynthesis is provided in Scheme 8.10. Target **815** should be accessible through *C*-glycosylation of either sulfoxide **834** or sulfide **835**. Both are considerably more reactive, and thus more appropriate, anomeric leaving groups than the *ad hoc* acetate used previously. Enol ether **835** could be prepared from activation and elimination of the primary alcohol in **836**. Without the axial *C*-1 group, the formation of the anhydro sugar should not be a concern. This compound can in turn be accessed through a protection/deprotection strategy involving TBS-protected glycosyl sulfide **837**

as a key intermediate. The thiophenyl group could be introduced through the synthesis of **510**, whose synthesis was discussed earlier in this document.

### *8.4.2.1 Synthesis of thiophenyl derivative 889*

The synthesis began with the thiophenylation of **311** under standard conditions (Scheme 8.11). The acetate groups on **510** are then removed to provide **529** in




**Scheme 8.11 Synthesis of sulfide 835 and sulfoxides 834a and 834b.**

quantitative yield, as shown earlier. Several different conditions and protecting groups were examined for the *C*-6 position including trityl (45 % yield) and triisopylsilyl (**838**, 68 % yield), but the best results were obtained with the *t*-butyldimethylsilyl protecting group (TBS). Under normal conditions, TBS-protected **837** was provided in 77 % yield. Standard benzylation of **837** went very smoothly with this substrate providing the differentially protected **839** in 93 % yield. A series of different deprotection strategies involving TBAF were attempted, but the isolated yields were all unsatisfactory for a simple deprotection. Consequently, hydrogen fluoride acetonitrile complex was applied to **839** for the desilylation to provide primary alcohol **836** in 76 % yield. Initial attempts at

activating the hydroxyl group resulted in failure. At 0 ºC, both mesylation and tosylation provided the product in only poor yield. Garegg iodination, unsurprisingly, activated the sulfur rather than the oxygen leading to a free reducing sugar and only a 12 % yield of desired iodide **840**. However, revisiting the mesylation, the reaction proceeded much more smoothly at -20 ºC, providing **841** in 72 % yield. Sodium hydride-assisted elimination did not occur at either 0 ºC or ambient temperature; however, at 70 ºC the elimination proceeded well. Following purification, enol ether **835** was isolated in an excellent yield of 79 % (considering the difficulties in accessing the furyl analogue above). To access the sulfoxide, selective oxidation of the thioether derivative was accomplished using magnesium monoperoxyphthalate (MMPP) in the presence of wet silica and DCM.[71] These conditions left the enol ether completely untouched, and allowed for the preparation of the diastereomeric sulfoxides, **834a** and **834b**, without over-oxidation to the sulfone, in 86 % yield in a 9:2 ratio of diastereomers.

#### *8.4.2.2 Attempts to introduce the anomeric furan using 834 and 835.*

The final step required was anticipated to be problematic. Conditions needed to be developed that would activate the anomeric leaving group without affecting the enol ether, itself an excellent nucleophile. Unsurprisingly, halogen activation of the thioether failed to provide the desired product: electrophilic attack appeared to occur at the olefin instead. Thus, NBS, NIS, and IDCP (iodine dicollidine perchlorate) all failed to provide the desired furan derivative from the thio-ether derivative **835**. These three activators comprise the “work-horses” of thioglycoside chemistry, although many specialty reagents have been developed along with the traditional techniques that incorporate mercury and other heavy metals.[72]

Oxidation to the sulfoxide, **834**, provided a greater chance for success as the activating agents, including $TfO_2$, and catalytic triflic acid in the presence of excess nitrogenous base (such as DTBMP), should be more orthogonal to the enol ether. However, even with these - supposedly more selective - conditions with a (much) more reactive glycosyl donor, the reactions still resulted in decomposition, presumably due to activation of the enol ether.

With this negative result, and due to time constraints, no further approaches to access **815** or an analogue were pursued.

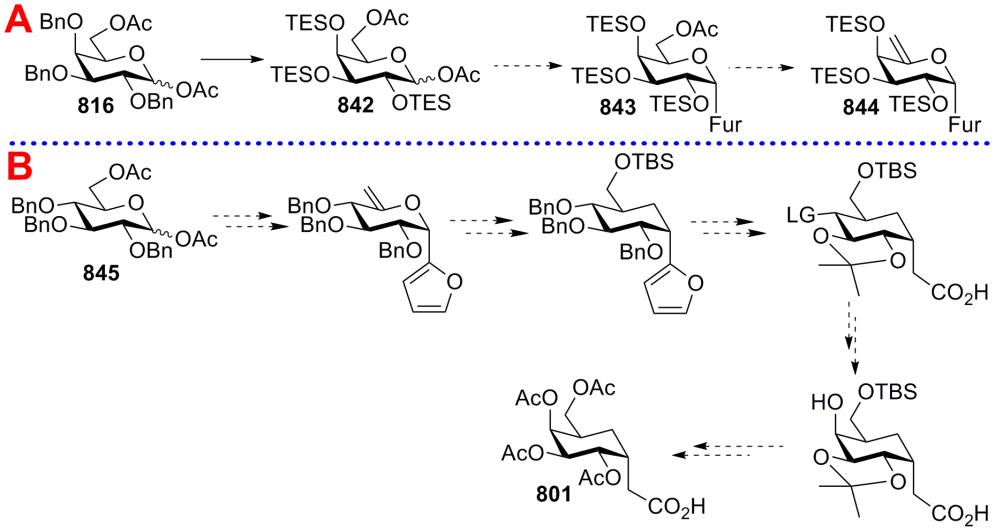
### 8.4.3 Section summary and future possibilities

In the above section, two approaches towards synthesizing key intermediate **815**, substrate for the Sinaÿ rearrangement, are provided. Unfortunately, the cross-reactivity of protecting groups and functional groups prevented the successful attainment of the desired compound. In the first approach, a *C*-furyl group was successfully installed onto a galactose scaffold in acceptable yield after considerable effort; however, the equilibrium and relative reactivities of the chair forms of the α-anomer favoured the intramolecular nucleophilic attack of the *C*-3 benzyl group over all the conditions attempted to elicit an $E_2$ sequence. The β-anomer, on the other hand, successfully and smoothly underwent elimination to provide **833**, the β-anomer of **815**, in good yields on the first attempt. Unfortunately the titanium-catalyzed Sinaÿ rearrangement is not compatible with anomeric β-substitution.

The problem was possibly due to the ratio of axial to equatorial substituents (Scheme 8.9). Consequently, rather than installing the furyl group first, a strategy was devised to introduce the enol ether functionality first, using a thiophenyl group as a

latent activator at the anomeric position as it is stable to a wide variety of conditions and can be readily converted into an activated leaving group for glycosylation. The synthesis progressed well, but glycosylation failed as the enol ether functionality was more readily activated than the anomeric thiophenyl group.

The Sinaÿ approach is still a valid technique for accessing the desired substrate as two other approaches were designed and initiated (although, due to time constraints, were not completed). In the first (Scheme 8.12A), the perbenzylated diacetate derivative **816** was deprotected using either $BCl_3$ or $H_2$/Pd and then persilylated to generate **842** which was isolated as the α-anomer (almost exclusively). Initial attempts at introducing the furan at the anomeric position of this sugar failed, possibly due to the steric bulk of the TES group at *C*-2; however, there remain many other alternative glycosylation conditions that can be employed. Once the group is introduced, however, the resulting protection system (**843**), should allow the elimination to proceed more smoothly. The silyl protecting groups will decrease the electron density of their covalently linked oxygens, and hence may be able to influence the mechanistic balance between elimination and




**Scheme 8.12 Proposals for the alternate preparations of 801 utilizing the Sinaÿ rearrangement.**

substitution sufficiently as to lead to the generation of the desired compound, **844**.

The second approach, beginning with **845** (Scheme 8.12B) envisions carrying out the Sinaÿ rearrangement with the glucose derivative, and then, post cyclization, employing a strategy to invert the stereochemistry at *C*-4 to eventually produce **801**. A variation on this strategy will be seen the next portion of this chapter. This approach makes use of well established derivatives for the key chemical steps and should be a relatively problem-free (if inelegant) route towards the desired target. Compound **845** was prepared, but the synthesis was not pursued due to time constraints.

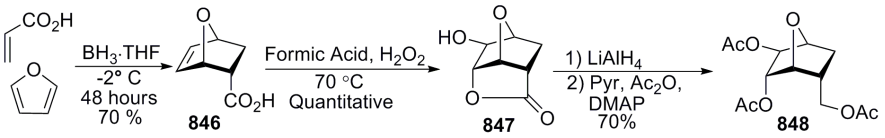
## 8.5 Synthesis and antifreeze activity of galactose and glucose carbasugar analogues

The 7-oxobornene ring-opening approach (not shown), like the Sinaÿ approach, also failed to provide the desired glycoconjugate building block; however, the chemistry was readily amenable to the production of the carbasugar analogues of galactose and glucose.

### 8.5.1 Retrosynthetic analysis of carbasugars.

Fortunately, the carbasugars are more readily accessed. In fact, the α-galactose, **232**, and β-glucose, **234**, carbasugars can be readily generated from intermediates from the 7-oxobornene approach towards the glycoconjugate. Furthermore, the Ogawa group was interested in preparing β-O-alkyl galactosides and their synthesis can be easily manipulated towards the preparation of a simple β-galactose carbasugar **233** (Scheme 8.14).[73] Bicyclic **846** acts as the key intermediate and is synthesized from furan an acrylic acid as shown in Scheme 8.13.

Bicycle **846** has become a somewhat common intermediate in organic synthesis.[74]




**Scheme 8.13 Synthesis of bicyclic 846 and triacetate 847 from furan and acrylic acid.**

However the traditional protocols to prepare **846** described in these earlier publications were quite slow, requiring 75 days,[75] 9 days,[76] or a high pressure system.[77] A new process was patented in 2003 that used simple Lewis acid catalysis to synthesize the desired cycloadduct.[78] It was reported that borane catalysis led to the successful formation of product at 2 ºC in 63 % yield with the *endo* cycloadduct **846**/*ent*-**846** crystallizing out of the furan reaction mixture.

When the procedure given in the patent was repeated (granted, on slightly smaller scale), the yield was not reproducible, nor was the exclusive presence of the *endo*-product in the crystals. Temperature control was maintained using a large electrically cooled cryobath set to 2 ºC. After many attempts over a range of conditions (not shown), it was found that -2 ºC reliably resulted in a 70 % yield of the pure *endo* compound in the crystals that form in the reaction mixture. Temperatures much below this point (-5 ºC) result in little to no formation of crystalline product (although product is formed in solution and can be recovered following concentration, extraction, and recrystallization). Temperatures above this point result in an increase in the level of *exo*-impurities present in the crystal and reduce the yield, presumably due to the greater solubility of the product in the reaction medium at higher temperatures.

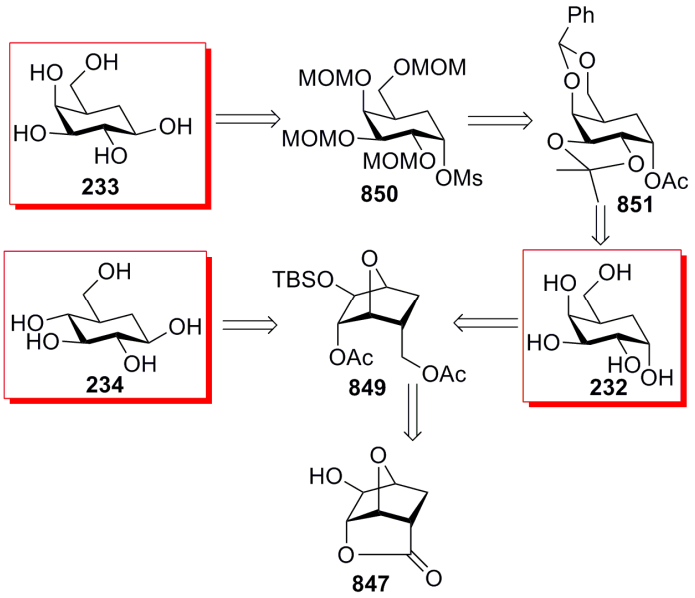
In addition to the 70 % yield recovered directly, an additional 12 % yield can be recovered from chromatography of the remaining product in the mother liquor; however,

this was rarely considered worth the effort due to the relatively large scale (3 x 16 mL of acrylic acid and 60 mL of furan) that was generally used for the reaction. The carboxylic acid product could be enantioenriched through fractional crystallization of the diastereomeric phenylethylamine salts from ethanol, and although this approach was pursued in the glycoconjugate synthesis, racemic **846** was used in the carbasugar synthesis.

Carboxylic acid **846** was then transformed to lactone **847** through an oxidative cyclization protocol in a solution made up of formic acid and 33 % hydrogen peroxide carried out at elevated temperatures. This reaction is not amenable to scale-up and has an unfortunate tendency to develop an uncontrollable exotherm if it is carried out on more than 30 g of starting material. In the case of such an event occurring, no product **847** and little starting material **846** is detected in the residue recovered from the explosion. Presumably the internal energy rises to a significant enough level that **847** undergoes a retro-Diels-Alder to regenerate furan and acrylic acid: the presence of the latter can be readily detected by its distinctive odour. However, on smaller scale the reaction proceeds extremely well providing the desired product in quantitative yield. A simple LAH reduction of the lactone followed by acetylation under standard conditions prepares **848** in 70 % isolated yield.

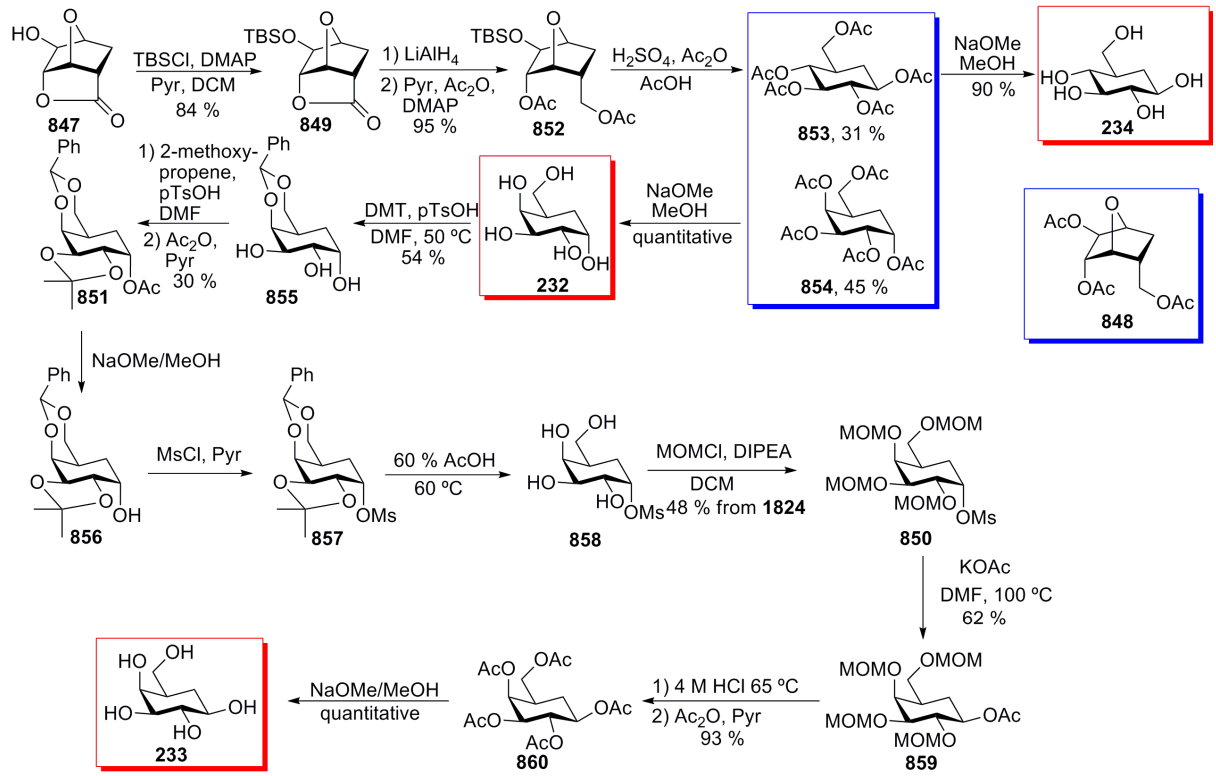
The retrosynthesis of the carbasugars employs bicyclic lactone **847** as the key starting material which is converted to the mono-TBS derivative (**849**) of triacetate **848**. The introduction of the large TBS group is an attempt to bias ring opening from the front face, which would lead to the galactose series. Likewise, depending on the regioselectivity of the ring-opening nucleophilic attack, both **234** (attack from the back

face of **849**) and **232** (attack from the front face of **849**) arise from this common intermediate. β-galactose carbasugar **233** should be obtainable from mesylate **850** through a direct displacement. Mesylate **850** has previously been prepared from differentially protected **851**, which in turn arises from the α-carbasugar **232**.[73] With this plan in hand, the synthesis was undertaken (Scheme 8.15).




**Scheme 8.15 Retrosynthetic analysis of carbasugars 232-234.**

The synthesis began with TBS protection of lactone **847**. The reason for this step




**Scheme 8.14 Synthesis of carbasugars 232, 233, and 234 from lactone 847.**

was that when Ogawa used the triacetate derivative of **849**, **848**, as the substrate for the ring opening sequence, the galactose and glucose isomers (**854** and **853** respectively) were obtained in equal amounts. This is clearly not what is desired in this case. The glucose isomer would only be required to undergo one further transformation, a deprotection, while the galactose isomer requires a much more lengthy process to generate **233**. Consequently, it is desirable to bias the formation of galactose carbasugar **854** over its glucose counterpart **853**. Although the TBS group cannot be expected to survive the harsh acidic ring-opening conditions, it was hoped that it might remain bound long enough to bias the reaction a little bit more in favour of the galactose product. Consequently, TBS protected lactone **849** was produced in 84 % yield. The reduction/acetylation sequence was carried out in the same fashion as described above, providing **852** in an excellent 95 % yield. The fragmentation of **852** was accomplished using concentrated sulphuric acid dissolved in a solution of acetic anhydride and acetic acid. To afford conversion, the reaction was heated to 85 ºC in a sealed tube for 48 hours (Some **848** was present in the reaction mixture after 24 hours although approximately 80 % of **852** had been converted to products **853** and **854**. TBs protected **852**, however, was no longer present, showing that the TBS group had been completely removed, as expected, but that the bicycle had not all been consumed). This reaction, after purification, provided a 45 % yield of the galactose derivative **854** and a 31 % yield of glucose derivative **853**. This yield for the galactose derivative is slightly higher than that reported by Ogawa (41 %), while the yield for the glucose derivative is considerably lower than that reported by Ogawa (42 %).[73] This result appears to indicate that although the TBS group does not survive long under the reaction

conditions, it appears to slightly bias the reaction against attack from the back face that produces the glucose analogue. Another bulky protecting group that is very acid stable could have been employed, but this may have necessitated an additional deprotection step, an unnecessary complication.

To complete the synthesis of 5a-carba-β-glucopyranose, **234**, pentacetate **853** was deprotected under the standard Zemplén condition to provide the desired compound in 90 % yield following recrystallization. The 5a-carba-α-galactopyranose, **232**, was produced from **854** in quantitative yield in an identical manner. A portion was set aside for IRI analysis and further characterization, while the bulk of the material was protected with a 4,6-benzylidene using α,α-dimethoxytoluene with acid catalysis to produce triol **855** in 54 % yield. This compound was further elaborated using 2-methoxypropene to provide the kinetic trans-acetonide. The anomeric position was acetylated in the usual fashion to simplify purification, and following chromatography, the fully protected derivative **851** was obtained in 30 % yield. The acetate group on **851** was then removed to provide anomeric alcohol **856** and the free hydroxyl group was immediately refunctionalized as the mesylate, **857**. Acidolysis provided deprotected carbasugar **858** that was reprotected as the methoxymethylether analogue **850** in the manner of Ogawa.[73] This sequence, from **851** to **850** was accomplished in 48 % overall yield. The synthesis of **233** was completed through the key inversion of the stereochemistry at *C*-1, by using potassium acetate, as nucleophile, at 100 ºC. Following purification, β-galactose derivative **859** was recovered in 62 % yield. Methoxymethylether deprotection was accomplished under acidic conditions (the anomeric acetate was likewise removed at this time) and the carbasugar was

reprotected as the acetate (to simplify purification), allowing access to **860** in 93 % yield. The final Zemplén deprotection proceeded in quantitative yield to provide 5a-carba-β-galactopyranose (**233**).

With the three desired carbasugars in hand, **232-234**, the final IRI analysis was conducted.

## 8.5.2 Antifreeze activity of carbasugar derivatives

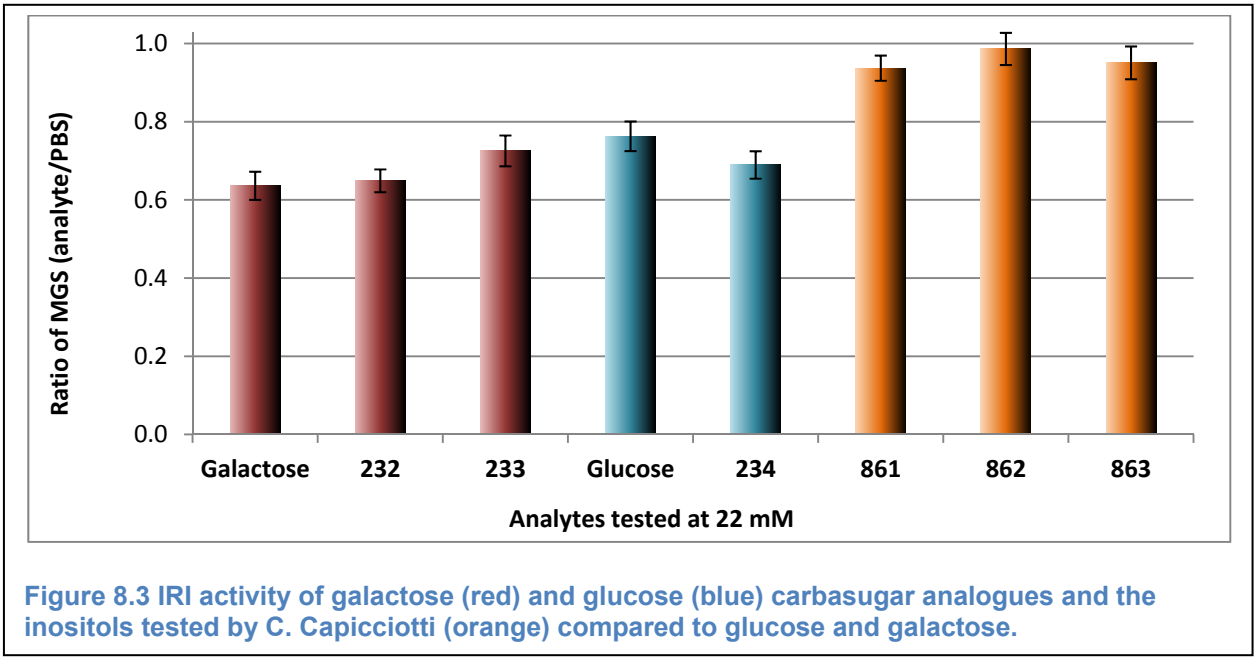



**Figure 8.3 IRI activity of galactose (red) and glucose (blue) carbasugar analogues and the inositols tested by C. Capicciotti (orange) compared to glucose and galactose.**

The "splat cooling" assay was carried out to provide the data presented in Figure 8.3. The carbasugars are also compared with the inositols tested by C. Capicciotti (Figure 8.4).[79]

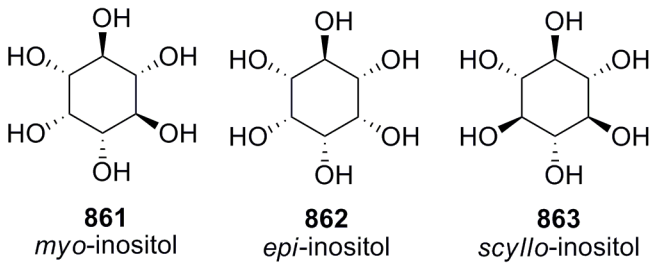



**Figure 8.4 Structures of the inositols tested by C. Capicciotti.**

The contrast between the carbasugars and inositols is stark. The inositols, lacking the *C*-6 hydroxyl group, show no IRI activity. The

carbasugars on the other hand, simply lacking the ring oxygen, show activity comparable to the native sugars. Furthermore, the α-derivative of galactose (**232**) shows better activity than the β-anomer (**233**), and the activity is identical to the native sugar. The β-glucose analogue **234** shows nearly identical activity to the native glucose. It appears that the replacement of the ring *O* with *C* has little, if any, effect on IRI activity. To the best of the author's knowledge, no efforts have been made towards exploring the hydration of carbasugars.

It is possible that the intramolecular hydrogen-bonding network of Simons could explain this discrepancy between carbasugars and inositols as the carbasugars would have networks that closely resemble those in the native sugars. The water molecules in the case of glucose would still insert preferentially between the hydroxyls of *C*-4 and *C*-6 as described above (Chapters 5 and 6), a pattern unavailable to the inositols; the presence of the *exo*-cyclic methanol moiety is important to the hydration of the molecule as a whole.[12] Computational studies involving the hydration shell of monosaccharides from the Momany group also support the contention that the endocyclic oxygen is of little importance to hydration as it does not appear to significantly interact with the hydration shell.[10, 80, 81] From these results it appears that the ring oxygen plays little role in hydration. If this atom was critical, then its removal would have been expected to be reflected by a change in IRI activity.

The interesting observation that the α-analogue shows better activity than the β-analogue suggests that this anomeric relationship is general. It is not only true for *O*- and *C*-linked glycopeptides and alkyl derivatives, but also for the simple anomeric hydroxyls. Consequently, the synthesis and IRI analysis of these carbasugars appears

to suggest that the replacement of the endocyclic oxygen of pyranoses with a methylene does not significantly affect IRI activity.

## 8.6 Chapter summary

This chapter describes the two failed approaches towards the production of a *C*-linked carbasugar. The first was planned to involve the Sinaÿ rearrangement as the key transformation, however, the desired substrate for this reaction was not successfully produced through any of several approaches, nor was it obtained through an approach incorporating the opening and functionalization of 7-oxonorbornene.

However, carbasugar analogues of α and β galactose and β-glucose were prepared using similar, mostly established, chemistry and were found to exhibit IRI activity comparable to the native sugars with the α-galactose analogue outperforming its β-anomer. Furthermore, inositols, cyclitols with the ring-oxygen removed but lacking the *C*-6 carbon, show no IRI activity, regardless of the stereochemistry of their hydroxyl groups.

The carbasugar results suggest that the ring oxygen of glycopyranoses plays little role in determining IRI activity through interactions with the hydration network as replacing it with a methylene group does not affect IRI activity. These results are consistent with the findings of Simons and Momany regarding the relative unimportance of the endocyclic oxygen to the hydration of the sugar as a whole (compared with the other oxygens in the sugar). This work demonstrates that carbasugar analogues can act as equally effective IRI inhibitors as their true carbohydrate counterparts. This is in stark contrast to the inositols which show no IRI activity: consequently, it appears that the *C*-6 position is very important to the IRI activity of carbohydrates.

## References

1. Sollogoub, M.; Mallet, J.-M.; Sinaÿ, P., *Tetrahedron Lett.* **1998,** *39* (21), 3471-3472.

2. Dalko, P. I.; Sinaÿ, P., *Angew. Chem. Intl. Ed.* **1999,** *38* (6), 773-777.

3. Kobayashi, Y., Carbasugars: Synthesis and functions. In *Glycoscience*, Fraser-Reid, B. O.; Tatsuta, K.; Thiem, J., Eds. Springer-Verlag: Berlin and Heidelberg, 2008; Vol. 3, pp 1913-1997.

4. Ferrero, M.; Gotor, V., *Chem. Rev.* **2000,** *100* (12), 4319-4348.

5. Zhu, X.-F., *Nucleos. Nucleot. Nuc.* **2000,** *19* (3), 651-690.

6. Miller, T. W.; Arison, B. H.; Albers-Schonberg, G., *Biotech. Bioeng.* **1973,** *15* (6), 1075-1080.

7. Atsumi, S.; Umezawa, K.; Iinuma, H.; Naganawa, H.; Nakamura, H.; Iitaka, Y.; Takeuchi, T., *J. Antibiot.* **1989,** *43* (1), 49-53.

8. Nobuji, Y.; Noriko, C.; Takashi, M.; Shigeru, U.; Kenzon, A.; Michaki, I. 06306000, 1994.

9. Arjona, O.; Gómez, A. M.; López, J. C.; Plumet, J., *Chem. Rev.* **2007,** *107* (5), 1919-2036.

10. Momany, F. A.; Appell, M.; Willett, J. L.; Bosma, W. B., *Carb. Res.* **2005,** *340* (9), 1638-1655.

11. Simons, J. P.; Jockusch, R. A.; Carcabal, P.; Huenig, I.; Kroemer, R. T.; Macleod, N. A.; Snoek, L. C., *Int. Rev. Phys. Chem.* **2005,** *24* (3-4), 489-531.

12. Carcabal, P.; Jockusch, R. A.; Huenig, I.; Snoek, L. C.; Kroemer, R. T.; Davis, B. G.; Gamblin, D. P.; Compagnon, I.; Oomens, J.; Simons, J. P., *J. Am. Chem. Soc.* **2005,** *127* (32), 11414-11425.

13. Angyal, S. J.; Pickles, V. A., *Aus. J. Chem.* **1972,** *25* (8), 1695-1710.

14. Kürti, L.; Czakó, B., Ferrier reaction/rearrangement. In *Strategic application of named reactions in organic synthesis*, Elsevier: Burlington, MA, 2005.

15. Chaytor, J. L. Examining the role of carbohydrate hydration and structure in preventing ice-recrystallization. PhD. Thesis, University of Ottawa, Ottawa, 2010.

16. Tam, R. Y.; Ferreira, S. S.; Czechura, P.; Chaytor, J. L.; Ben, R. N., *J. Am. Chem. Soc.* **2008,** *130* (51), 17494-17501.

17. Tachibana, Y.; Fletcher, G. L.; Fujitani, N.; Tsuda, S.; Monde, K.; Nishimura, S.-I., *Angew. Chem. Intl. Ed.* **2004,** *43*, 856-862.

18. Bouvet, V. R. Novel AFGP8 Analogues: Synthesis and Biological Evaluation of Potent Recrystallization Inhibitors. PhD. Thesis, University of Ottawa, Ottawa, 2006.

19. The anomers can be selectively crystallized from solution, but as soon as they return to aqueous solution, for IRI analysis, equilibration begins, making it impossible to determine the IRI activity of a “pure” anomer.

20. α-methoxy-galactose had an IRI index of 0.84, while β-methoxy galactose had an IRI index of 0.98, both of which are considerably less active than galactose with an IRI index of 0.65.

21. Cumpstey, I., *Carb. Res.* **2009,** *344* (17), 2285-2310.

22. Plumet, J.; Gomez, A. M.; Lopez, J. C., *Mini-Rev. Org. Chem.* **2007,** *4* (3), 201-216.

23. Ogawa, S., *Trends Glycosci. Glycotech.* **2004,** *16* (87), 33-53.

24. Rassu, G.; Auzzas, L.; Pinna, L.; Battistini, L.; Curti, L., Advances in chemical synthesis of carbasugars and analogues. In *Studies in Natural Products Chemistry*, Atta ur, R., Ed. Elsevier: 2003; Vol. Volume 29, Part 10, pp 449-520.

25. Vogel, P., *Curr. Org. Chem.* **2000,** *4* (5), 455.

26. McCasland, G. E.; Furuta, S.; Durham, L. J., *J. Org. Chem.* **1966,** *31* (5), 1516-1521.

27. McCasland, G. E.; Furuta, S.; Durham, L. J., *J. Org. Chem.* **1968,** *33* (7), 2835-2841.

28. McCasland, G. E.; Furuta, S.; Durham, L. J., *J. Org. Chem.* **1968,** *33* (7), 2841-2844.

29. Ghosh, S.; Bhaumik, T.; Sarkar, N.; Nayek, A., *J. Org. Chem.* **2006,** *71* (26), 9687-9694.

30. Grondal, C.; Enders, D., *Synlett* **2006,** *2006* (20), 3507,3509.

31. Duchek, J.; Adams, D. R.; Hudlicky, T., *Chem. Rev.* **2011,** *111* (7), 4223-4258.

32. Carless, H. A. J.; Busia, K.; Oak, O. Z., *Synlett* **1993,** *1993* (09), 672,674.

33. Werner, L.; Machara, A.; Hudlicky, T., *Adv. Syn. Cat.* **2010,** *352* (1), 195-200.

34. Hudlicky, T.; Price, J. D.; Rulin, F.; Tsunoda, T., *J. Am. Chem. Soc.* **1990,** *112* (25), 9439-9440.

35. Gonzalez, D.; Martinot, T.; Hudlicky, T., *Tetrahedron Lett.* **1999,** *40* (16), 3077-3080.

36. Ogawa, S.; Iwasawa, Y.; Nose, T.; Suami, T.; Ohba, S.; Ito, M.; Saito, Y., *J. Chem. Soc. Perk. Trans. 1* **1985**, 903-906.

37. Ogawa, S.; Maruyama, A.; Odagiri, T.; Yuasa, H.; Hashimoto, H., *Eur. J. Org. Chem* **2001,** (5), 967-974.

38. Sollogoub, M.; Pearce, A. J.; Hérault, A.; Sinaÿ, P., *Tetrahedron: Assym.* **2000,** *11* (1), 283-294.

39. Das, S. K.; Mallet, J.-M.; Sinaÿ, P., *Angew. Chem. Intl. Ed.* **1997,** *36* (5), 493-496.

40. Ferrier, R. J.; Middleton, S., *Chem. Rev.* **1993,** *93* (8), 2779-2831.

41. Sinaÿ, P., *Pur Appl. Chem.* **1998,** *70* (8), 1495-1499.

42. Matthews, J. L.; Braun, C.; Guibourdenche, C.; Overhand, M.; Seebach, D., Preparation of entiopure β-amino acids from α-amino acids using the Arndt-Eistert homologation. In *Enantioselective synthesis of β-amino acids*, 2nd ed.; Juaristi, E.; Soloshonok, V. A., Eds. Wiley: Hoboken, NJ, 1997.

43. Maryanoff, B. E.; Reitz, A. B., *Chem. Rev.* **1989,** *89* (4), 863-927.

44. Brown-Wensley, K. A.; Buchwald, S. L.; Cannizzo, L.; Clawson, L.; Ho, S.; Meinhardt, D.; Stille, J. R.; Straus, D.; Grubbs, R. H., *Pur Appl. Chem.* **1983,** *55* (11), 1733-1744.

45. Petasis, N. A.; Bzowej, E. I., *J. Am. Chem. Soc.* **1990,** *112* (17), 6392-6394.

46. Madaj, J.; Jankowska, M.; Wisniewski, A., *Carb. Res.* **2004,** *339* (7), 1293-1300.

47. Moradei, O.; du Mortier, C.; Cirelli, A. F.; Thiem, J., *J. Carb. Chem.* **1995,** *14* (4-5), 525-532.

48. Mowery, D. F., *J. Org. Chem.* **1961,** *26* (9), 3484-3486.

49. Fletcher, S.; Jorgensen, M. R.; Miller, A. D., *Org. Lett.* **2004,** *6* (23), 4245-4248.

50. Demchenko, A. V., General aspects of the glycosidic bond formation. In *Handbook of chemical glycosylation*, Demchenko, A. V., Ed. Wiley: Weinheim, 2008; pp 1-27.

51. Eby, R.; Schuerch, C., *Carb. Res.* **1974,** *34* (1), 79-90.

52. Li, Z.-J.; Huang, H.-Q.; Cai, M.-S., *J. Carb. Chem.* **1996,** *15* (4), 501-506.

53. Myers, E. L.; Butts, C. P.; Aggarwal, V. K., *Chem. Commun.* **2006,** (42), 4434-4436.

54. Kadokawa, J.-i.; Nagaoka, T.; Ebana, J.; Tagaya, H.; Chiba, K., *Carb. Res.* **2000,** *327* (3), 341-344.

55. Girgis, N. S.; Michael, M. A.; Smee, D. F.; Alaghamandan, H. A.; Robins, R. K.; Cottam, H. B., *J. Med. Chem.* **1990,** *33* (10), 2750-2755.

56. Carlson, R.; Lundstedt, T.; Albano, C., *Acta. Chem. Scand. B.* **1985,** *39*, 79-91.

57. Garegg, P. J.; Samuelsson, B., *J. Chem. Soc. Chem. Commun.* **1979,** (22), 978-980.

58. Garegg, P. J.; Samuelsson, B., *J. Chem. Soc. Perk. Trans. 1* **1980**, 2866-2869.

59. Brimacombe, J. S.; Ching, O. A., *J. Chem. Soc. C* **1968**, 1642-1646.

60. Yoshimura, J.; Asano, K.; Umemura, K.; Horito, S.; Hashimoto, H., *Carb. Res.* **1983,** *121*, 187-204.

61. Lipták, A.; Balla, E.; Jánossy, L.; Sajtos, F.; Szilágyi, L., *Tetrahedron Lett.* **2004,** *45* (4), 839-842.

62. Appel, R., *Angew. Chem. Intl. Ed.* **1975,** *14* (12), 801-811.

63. Crofts, P. C.; Downie, I. M., *J. Chem. Soc.* **1963**, 2559-2560.

64. Lee, J. B.; Nolan, T. J., *Can. J. Chem.* **1966,** *44* (11), 1331-1334.

65. Santra, S., *Synlett* **2009,** *2009* (02), 328,329.

66. Nicolaou, K. C.; Snyder, S. A.; Longbottom, D. A.; Nalbandian, A. Z.; Huang, X., *Chem.– Eur. J.* **2004,** *10* (22), 5581-5606.

67. Atkins, G. M.; Burgess, E. M., *J. Am. Chem. Soc.* **1968,** *90* (17), 4744-4745.

68. Kadota, I.; Abe, T.; Uni, M.; Takamura, H.; Yamamoto, Y., *Tetrahedron Lett.* **2008,** *49* (22), 3643-3647.

69. Grieco, P. A.; Gilman, S.; Nishizawa, M., *J. Org. Chem.* **1976,** *41* (8), 1485-1486.

70. DePuy, C. H.; King, R. W., *Chem. Rev.* **1960,** *60* (5), 431-457.

71. Chen, M.-Y.; Patkar, L. N.; Lin, C.-C., *J. Org. Chem.* **2004,** *69*, 2884-2887.

72. Zhong, W.; Boons, G.-J., Glycoside synthesis from 1-sulfur/selenium-substituted derivatives. In *Handbook of chemical glycosylation*, Demchenko, A. V., Ed. Wiley: Weinheim, 2008; pp 261-303.

73. Ogawa, S.; Aoyama, H.; Sato, T., *Carb. Res.* **2002,** *337* (21-23), 1979-1992.

74. A SciFinder search (Aug 16 2011) returns 30 references.

75. Suami, T.; Ogawa, S.; Nakamoto, K.; Kasahara, I., *Carb. Res.* **1977,** *58* (1), 240-244.

76. Moore, J. A.; Partain, E. M., *J. Org. Chem.* **1983,** *48* (7), 1105-1106.

77. Kotsuki, H.; Nishizawa, H.; Ochi, M.; Matsuoka, K., *Bull. Chem. Soc. Jpn.* **1982,** *55* (2), 496-499.

78. Tomoya, K.; Katsuji, U.; Smimizu, K.; Shiro, T. Process for preparation of 7-oxobicyclo[2.2.1]hept-5-ene-2caboxylic acid derivatives. 2003.

79. Capicciotti, C.; Ben, R. N., IRI activity of inositols. In *Unpublished data*, 2010.

80. Momany, F. A.; Appell, M.; Willett, J. L.; Schnupf, U.; Bosma, W. B., *Carb. Res.* **2006,** *341* (4), 525-537.

81. Appell, M.; Willett, J. L.; Momany, F. A., *Carb. Res.* **2005,** *340* (3), 459-468.

# Chapter 9 : Conclusions and Future Work

The overall objectives of this work were to 1) investigate the structural features of compounds that are necessary, beneficial, or detrimental to IRI activity and to 2) use this information to attempt to generate more potent IRI active analogues, hopefully with synthetically simpler preparations than used for the previous glycopeptide benchmark compounds.

These goals were addressed in various manners over the previous six chapters. The study involved investigating the importance of the backbone structure, conformation and intramolecular spatial relationships of glycopeptides in determining the remarkable IRI activity of analogue **118**. Mixed α and β glycopeptides were identified as a promising probe for examining these relationships. An initial effort had been made by I. Thapa to substitute a β-amino acid into the peptide backbone of **118**, but this had resulted in a large decrease in activity. However, the incorporation of a β-amino acid into the backbone of a Lysine analogue resulted in a significant improvement in activity. To determine whether the observed effect with the β-analogue of **118** was simply an outlier, or whether it resulted from a change in conformation or from a change in the relative arrangement of the different portions of the glycopeptide, a series of mixed α and β peptides were prepared and analyzed for IRI activity. It was found that modification of the backbone - in any way - from the pure α-peptide was greatly detrimental to IRI activity. However, one analogue retained significant activity, albeit at a higher concentration than required for **118**. This analogue, **202** was identical to **118** except that it incorporated β-glycine residue at the ($i$+2) position in each of the repeats. The other

two analogues incorporating a single β-residue do not show similar activity indicating that the degree of β-substitution is not the determining factor for IRI activity. Rather, like fully α-analogue **118**, this analogue is the only one that leaves certain intramolecular distances unchanged. All other analogues modify this distance to a greater or lesser degree. This result, indicating the importance of intramolecular relationships, is consistent with previous evidence that appears to indicate that the carbohydrate of active analogue **118** is capable of a specific orientation with respect to the backbone. This interaction may possibly be mediated by some form of intramolecular interaction.

Future efforts relating to this project should involve analogues where the linker between the carbohydrate and peptide is modified in conjunction with the introduction of β-amino acids into the backbone to maintain a constant distance between peptide amide, and linker amide, bonds. This could provide evidence as to whether a related relationship is primarily responsible for the remarkable IRI activity of analogue **118**, and perhaps some insight into the specific nature of the interaction itself.

In the second study, the application of CuAAC chemistry to the synthesis of *C*-linked glycopeptides was explored. Preliminary solution-phase experiments indicated that the originally-reported conditions of Sharpless for the CuAAC reaction, equivolumetric amounts of *t*-butanol and water, were in fact the poorest conditions tested. Optimal conversions and isolated yields were obtained from using solutions of approximately 80% THF in water. To adapt the conditions to solid-phase synthesis, microwave heating had to be employed, as ligation between azido-galactosides and resin-supported alkynyl peptides was not detected under conventional thermal conditions. Four ‘proof of concept’ analogues were produced using this technology with

various lengths of linker between peptide and carbohydrate. The shortest analogue (**209**) showed no IRI activity while the three longer analogues (**210**-**212**) showed only very moderate IRI activity. This result could be due to the substitution as not only had the hydrogen-bond donating properties of the amide bond been removed in these analogues, but the dipole moment of the linkage functionality had also been reversed relative to the previously generated analogues. To address this second possibility, a second series of analogues was prepared using the newly developed CuAAC protocol. The power of this chemistry was clearly demonstrated as nine different glycopeptides were prepared from only three different solid-phase syntheses. The SPPS and glycoconjugation steps were complete and clean enough that no HPLC purification was required, increasing the final isolated yields. The IRI activity of these compounds, although much lower than for **118**, was still correlated to the length of the linker: the more the length deviated from that of analogue **118**, the lower the activity. This result strongly suggests that analogue **118** does possess a privileged structure that can possibly adopt a special conformation, resulting in its uniquely (amongst the amide series) potent IRI activity. A further conclusion from this study is that replacement of the amide with a triazole, although resulting in a decrease in IRI activity, does not abrogate it completely. Similarly, the exact location of the triazole in the linker was not an important parameter when compared with the length of the linker, although all analogues produced here with the dipole moment of the triazole oriented in the same manner as the amide in **118** showed better activity than the four inverted compounds generated earlier. These observations suggest that the length of the linker in **118** is

important parameter for determining IRI activity, as is the orientation of the dipole moment within the linking functionality.

This study demonstrates that although post-synthetic glycosylation is a powerful and facile technique for *C*-AFGP analogue construction, the resulting compounds show insufficient activity to be pursued further. Future work regarding triazole introduction into *C*-AFGPs could involve studies investigating the effect of their substitution for the amides in the peptide backbone of synthetic AFGP analogues.

The next four studies attempted to investigate the structural features of the carbohydrate moiety that lead to IRI activity and to use this information to design and synthesize analogues exhibiting improved IRI activity.

The initial studies into small molecule IRI active compounds employed simple mono- and disaccharides. From this study certain trends became apparent: galactose and N-acetyl galactosamine-containing disaccharides showed the best IRI activity; substitution at the 1 or 6 position was preferred over substitutions at the 2, 3 or 4 positions; and α-linkages were generally preferred over their β-anomers. As such, several artificial disaccharides were desirable targets including the α,α and α,β 1,1-linked galactose disaccharides (**223** and **224**) and the 1,3-linked galactosyl-galactose disaccharide (**222**). The latter was of special interest as a series of GalNHAc derivatives have been prepared and have shown good IRI activity (including the 1,3- derivative) but none of the corresponding all-galactose analogues had been synthesized, making it impossible to determine whether the activity of the GalNHAc analogues is due to the incorporation of the galactosamine residue or whether it is simply a result of the *C*-4 hydroxyl stereochemistry. The 1,1-linked galactose disaccharides showed better activity

than that displayed by any previous disaccharide, consistent with the hypothesis regarding the importance of intramolecular hydrogen-bonding. The α-α analogue was also more potent than the α,β-linked analogue, showing that the trend of improved IRI activity of α-linked analogues can be extended to disaccharides. Similarly, the 1,3-linked disaccharide had comparable activity with the previously prepared GalNHAc derivative suggesting that the galactosamine residue, found in native AFGP and essential to antifreeze activity, might not, in an isolated system, be important. Future work on this project should focus on the generation of the other galactose-galactose dimers to determine whether the comparable activity of galactose and N-acetyl galactosamine compounds is specific to this one case, or if it is a generalizable condition for antifreeze disaccharides. This study also investigated the potency of a series of α-substituted *C*-glycosides with short functionalized chains. Activity was similar for all compounds regardless of chain length or functional group. Finally, a series of galactosyl-galactose disaccharides linked with rigid carbon chains were examined for IRI activity. The IRI potency of these compounds improved as the length of the carbon chain, and hence molecular volume, increased.

The second study in this series delved more deeply into the question of the importance of intramolecular hydrogen-bond networks by adjusting the electron density at the anomeric oxygen through the introduction of differentially functionalized aromatic rings. It was found that a Hammett relationship existed between IRI activity and electron density at the anomeric oxygen. As electron density decreased, IRI activity increased. A possible explanation for this effect might involve the weakening of the hydrogen-bond accepting ability of this oxygen. This effect would have ramifications to a potential

intramolecular network that could in turn affect the overall hydration and IRI activity of the molecule as a whole.

The penultimate study involved the systematic evaluation of the constituent pieces of analogue **118** for their individual contributions to IRI activity. It was found that shortening the polymer to even three repeats abrogated a good deal of the IRI activity of the analogue. Activity continued to decrease as the peptide was shortened through the dimer and monomer, reaching its nadir at the level of the glycoconjugate. As the linker between the carbohydrate and peptide was systematically truncated, activity generally continued to decrease, but three interesting results were observed. Firstly, the presence of a terminal alcohol seemed to offer a large increase to IRI activity compared to a simple alkyl group; secondly, the propyl amide analogue offered better activity than was expected; and thirdly, as the *n*-alkyl chain became longer, IRI activity improved. All three observations were further investigated and it was found that small unsaturated groups (such as allyl and propargyl) showed excellent IRI activity. As the chain increased in length, IRI activity increased in a linear fashion, however, it increased dramatically at a certain point, when chain length rose from *n*-hexyl to *n*-heptyl. This increase in activity was associated with the ability of the longer chained analogues to form hydrogels. At the longest lengths investigated (16 carbons), these compounds were comparable in IRI activity - and even surpassed - many of the glycopeptides investigated previously. In contrast, the presence of a terminal hydroxyl functionality, while leading to improved activity in shorter analogues, appears to not form hydrogels, preventing these compounds from being as active as their alkyl analogues when the chain becomes longer than six carbons. This study is very significant as it shows that

small molecule IRI active compounds are not only possible but can be designed to compete with the glycopeptides in activity. Further work is currently being carried out by several members of the Ben group investigating alkyl glycosides, dialkyl amino acids, alkylated polyols and other hydrogel-forming compounds for IRI activity. Such compounds may lead to a synthetically trivial, non-cytotoxic cryopreservative: the eventual goal of the research program.

The final study presented here is the syntheses of carbasugar-containing antifreezes. Two separate approaches towards a *C*-linked carbasugar derivative of **118** failed; one through the inability to successfully generate the required substrate for the key reaction, the other through the failure to introduce an anomeric *C*-nucleophile. Consequently, no glycopeptide was prepared for analysis. However, three carbasugars were prepared (**232-234**), analyzed for IRI activity and compared to previously-tested commercially-available inositols. The results demonstrate that the removal of the endocyclic oxygen is not harmful to IRI activity as the carbasugars had activity similar to their native sugars. However, they were all far more active than the inositols indicating that the specific stereochemical and resulting spatial relationship of the peripheral hydroxyl groups (especially *C*-6) plays the commanding role in determining IRI activity of carbohydrates. Again, the α-galactose carbasugar was more potent than its β-analogue and the β-glucose carbasugar. Future work could produce further carbasugars to: evaluate the generality of this relationship, complete the synthesis of the desired *C*-linked carbasugar glycopeptide, and further modify the endocyclic atom. This final endeavor is currently being pursued by M. Doshi who is replacing the endocyclic oxygen with a nitrogen.

The efforts from this thesis resulted in the preparation of analogues of **118** that investigated the key interactions responsible for its IRI activity. These results can, and are being used, to direct and simplify the future syntheses of IRI active compounds. This discovery has provided small molecule inhibitors active to the same order of magnitude as glycoconjugate **118** - and more than 4000 times more potent than the previous best small molecule (galactose). Glycopeptides such as **118**, although highly active, are simply not commercially viable for any purpose except life-saving medical applications simply due to the cost. Small molecules on the other hand, are far more accessible, much easier to produce, and far cheaper to access than the glycopeptides. Consequently, the discovery of these highly active compounds gives rise to the promise that industrial, commercial, and - most importantly - medical applications may soon be realized.

# Experimental protocols and characterization data

## General methods and materials for chemical reactions

All anhydrous reactions were performed in flame-dried glassware under a positive pressure of dry argon. Air- or moisture-sensitive reagents and anhydrous solvents were transferred with dry syringes or cannulae. All flash chromatography was performed with E. Merck silica gel 60 (230-400 mesh). All solution-phase reactions were monitored using analytical thin layer chromatography (TLC) with 0.2 mm precoated silica gel aluminum plates 60 F254 (E. Merck). Components were visualized by illumination with a short-wavelength (254 nm) ultraviolet light and/or staining (ceric ammonium molybdate, potassium permanganate, ninhydrin, vanillin or orcinol stain solution). Dry-vacuum chromatography was carried out according to the protocol outlined by Pedersen and Rosenbohm.[1] All solvents used for anhydrous reactions were distilled. Tetrahydrofuran (THF) was freshly distilled from a solution preserved with sodium and benzophenone under nitrogen. Dichloromethane (DCM), triethylamine, toluene and diisopropylethylamine (DIPEA) were distilled over calcium hydride. *N*,*N*-Dimethylformamide (DMF) was stored over activated 4 Å molecular sieves under argon. Following work-up, standard procedure was to dry organic phases with anhyrouds magnesium sulfate, filter the solution through a glass-wool plug, and concentrate the filtrate under reduced pressure. $^{1}$H (300, 400 or 500 MHz) and $^{13}$C NMR (75, 101 or 126 MHz) spectra were recorded at ambient temperature, unless otherwise indicated, on a Bruker Avance 300, Bruker Avance 400, Bruker Avance 500, or Varian Inova 500 spectrometer. Deuterated chloroform ($CDCl_3$), methanol ($CD_3OD$ or MeOD), water ($D_2O$), dimethyl sulfoxide (DMSO-d6), or acetone ($(CD_3)_2CO$) were used as NMR solvents. Chemical shifts are reported in ppm downfield from trimethylsilane (TMS) or the solvent residual peak as an internal standard. Splitting patterns are designated as follows: s, singlet; d, doublet; t, triplet; q, quartet; p, quintet; sext, sextet; sept, septuplet; m, multiplet; and br, broad. Low resolution mass spectrometry (LRMS) was performed on a Micromass Quatro-LC Electrospray spectrometer with a pump rate of 20 μL/min using electrospray ionization (ESI), a Voyager DE-Pro matrix-assisted laser desorption/ionization-time-of-flight (MALDI-TOF) (Applied Biosystem, Foster City, CA) mass

spectrometer operated in the reflectron/positive ion mode with DHB in 20% EtOH/$H_2O$ as the MALDI matrix, or a Bruker Microflex MALDI-TOF mass spectrometer with DHB in 20% acetonitrile/$H_2O$ as the MALDI matrix. Analytical and preparatory scale RP-HPLC were carried out with Varian Polaris C-18 columns on a Varian Prostar HPLC system equipped with a variable wavelength detector (ProStar 330 PDA). Desalting was accomplished using C18 solid-phase extraction (RP-SPE) cartridges (Discovery, Supelco) using 40% acetonitrile in water for elution of glycopeptides. All yields are unoptimized.

## Procedure for circular dichroism

Circular dichroism (CD) spectra of the glycopolymers were obtained using a Jasco model J-810 automatic recorder spectropolarimeter interfaced with a Dell computer. All of the measurements were performed in quartz cells with 1.0 cm path length. Spectra were obtained with a 1.0 nm bandwidth, a time constant of 2 s, and a scan speed of 50 nm/min. Each spectrum was the result of four superimposed scans to improve the signal-to-noise ratio, and baseline corrections were made against each sample. All of the spectra were recorded between 190 and 300 nm, and all of the CD experiments were performed in doubly distilled $H_2O$ at pH 7.4. Data obtained from CD spectroscopy were converted into per residue ellipticities (deg $cm^2$ $dmol^{-1}$). Glycopeptide secondary structures were estimated using the deconvolution software using molar ellipticities CD Pro.[2] The data from each spectrum were analyzed using three different deconvolution programs: SELCON3, CDSSTR, and CONTINLL. Of these three programs, SELCON3 and CONTINLL gave the most consistent results. IBASIS 5 was used as the set of reference proteins as in previous studies; it contains 37 proteins with α-helix, β-structure, polyproline II, and unordered conformations with optimal wavelengths of 185-240 nm.[3]

## Procedure for thermal hysteresis (TH) assay

Nanoliter osmometry was performed using a Clifton nanoliter osmometer (Clifton Technical Physics, Hartford, NY), as described by Chakrabartty and Hew.[4] All of the measurements were performed in deionized distilled water. Ice crystal morphology was observed through a Leitz compound microscope equipped with an Olympus 20x (infinity-corrected) objective, a Leitz Periplan 32x photo eyepiece, and a Hitachi KPM2U CCD camera connected to

a Toshiba MV13K1 TV/VCR system. Still images were captured directly using a Nikon CoolPix digital camera.

## Procedure for ice recrystallization inhibition (IRI) assay

Sample analysis for IRI activity was performed using the "splat cooling" method as previously described.[5] In this method, the analyte was dissolved in phosphate buffered saline (PBS) solution and a 10 μL droplet of this solution was dropped from a micropipette through a 2m-high plastic tube (10 cm in diameter) onto a block of polished aluminum pre-cooled to approximately -80 °C. Upon contact, the droplet froze instantly to form a wafer approximately 1 cm in diameter and 20 μm thick which was then carefully removed from the surface of the block and transferred to a cryostage held at -6.4 °C for annealing. After a period of 30 min, the wafer was photographed between crossed polarizing filters using a digital camera (Nikon CoolPix 5000) fitted to the microscope. A total of three images were taken from each wafer. During flash freezing, small ice crystals spontaneously nucleated from the super-cooled solution. During the annealing period recrystallization occurred, resulting in a dramatic increase in ice crystal size. A quantitative measure of the difference in the mean grain size of two compounds X and Y reflects the difference in the dynamics and hence energies of the recrystallization process. Image analysis of the ice wafers was performed using a novel domain recognition software (DRS) program.[6] Employing a Microsoft Windows Graphical User Interface, this software allows a user to visually demarcate and store the vertices of the ice crystals (domains) in a digital micrograph to calculate the corresponding areas. All data was plotted and analyzed using Microsoft Excel. IRI activity is reported as a ratio of the mean grain size (MGS) of ice crystals in the presence of the solute divided by the mean grain size (MGS) of ice crystals in a control solution of phosphate buffered saline (PBS) analyzed on the same day to correct for environmental conditions. This ratio is referred to as the IRI index of a compound. Small indices (ratios) indicate high levels of ice recrystallization inhibition.

## General protocol for solid-phase peptide synthesis

The syntheses of the peptides were carried out using an Advanced Chem Tech APEX 396 automated peptide synthesizer (40 wells), equipped with a dual arm system and argon atmosphere controlled from an IBM PC using *Advanced Chem Tech* version 1.6 software. Preloaded Fmoc-Gly-Wang or Fmoc-Ala-Wang resins were swollen in DMF for 1 hour followed by filtration, and then were subjected to 20% piperidine in DMF twice successively for 30 mins. Peptide couplings were carried out according to standard protocols for Fmoc solid phase synthesis using HCTU as coupling agent.[7] All residues were coupled using 5 equivalents of amino acid per functionalized position on the resin with 1 hour reaction times. All couplings were carried out as double couplings. Following the coupling of each residue deprotection of the Fmoc moiety was accomplished by treatment with 20% piperidine in DMF twice successively for 30 mins. Before and after each coupling, the beads were shaken 4 times with 4 mL of DMF followed by filtration. Following the synthesis the beads were washed extensively with DMF (6 times 4 mL), MeOH (6 times 4 mL), DCM (6 times 4 mL), hexanes (6 times 4 mL), and finally by ethanol (3 times 6 mL) and then removed from the synthesizer and stored in a desiccator under vacuum in the presence of $P_2O_5$ until required. A small amount cleaved from the resin using 92.5: 5: 2.5 (v/v/v) TFA: triisopropylsilane: water. The peptide was purified using RP-HPLC (ramp from 0% to 18% acetonitrile in water over 5 mins followed by isocratic flow for 25 mins) unless otherwise stated using a flow rate of 12 mL/minute on a Polaris C-18 semi-preparative column.

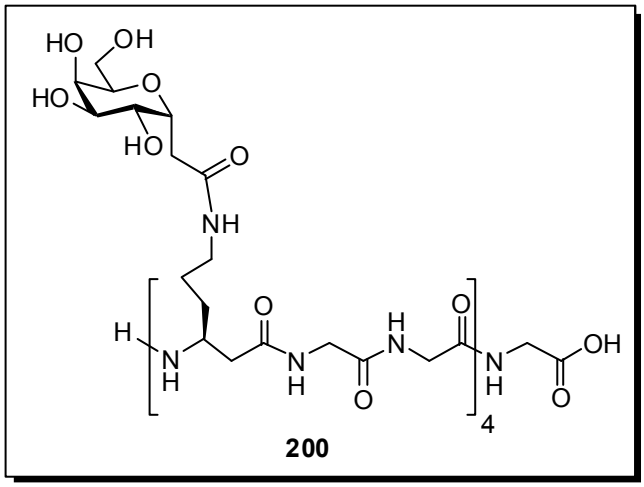
## General protocol for solid-phase glycopeptide synthesis

The syntheses of the peptides were carried out using an Advanced Chem Tech APEX 396 automated peptide synthesizer (40 wells), equipped with a dual arm system and argon atmosphere controlled from an IBM PC using *Advanced Chem Tech* version 1.6 software. Preloaded Fmoc-Gly-Wang or Fmoc-Ala-Wang resins were swollen in DMF for 1 hour followed by filtration, and then were subjected to 20% piperidine in DMF twice successively for 30 mins. Peptide couplings were carried out according to standard protocols for Fmoc solid phase synthesis using HCTU as coupling agent.[7] All glycine and β-glycine residues were coupled using 5 equivalents of amino acid per functionalized position on the resin with 1 hour reaction times.

All glycoconjugates were coupled using 1.5 equivalents of amino acid per functionalized position on the resin with 24 hour reaction times. All couplings were carried out as double couplings. Following the coupling of each residue deprotection of the Fmoc moiety was accomplished by treatment with 20% piperidine in DMF twice successively for 30 mins. Before and after each coupling, the beads were shaken 4 times with 4 mL of DMF followed by filtration. Following the synthesis the beads were washed extensively with DMF (6 times 4 mL), MeOH (6 times 4 mL), DCM (6 times 4 mL), hexanes (6 times 4 mL), and finally by ethanol (3 times 6 mL) and then removed from the synthesizer and stored in a desiccator under vacuum in the presence of $P_2O_5$ until required. Glycopeptides were cleaved from the Wang resin using 92.5: 5: 2.5 (v/v/v) TFA: triisopropylsilane: water. Volatiles were removed under a continuous air-flow. The residue was triturated with hexanes and diethyl ether successively to remove hydrophobic impurities. The remaining residue was re-dissolved in 0.1 M sodium methoxide in methanol and stirred for 3 to 6 hours before being neutralized with trifluoroacetic acid. Solvent was removed, the residue resuspended in doubly distilled water and passed through a SPE cartridge (0 % to 70 % acetonitrile in water; the 0 % fraction was discarded, the other eluants were combined) and lyophilized before the crude mass was determined. The lyophilized peptide was purified using RP-HPLC (isocratic at 1.5 % acetonitrile in water, then a ramp to 25% acetonitrile in water over 35 mins followed by isocratic flow at 75 % acetonitrile in water for 10 mins) using a flow rate of 12 mL/minute on a Polaris C-18 semi-preparative column.

## Experimental protocols for Chapter 2

**{[(S)-Nε-[2-(α-D-galactopyranosyl)ethan-1-amido]-β,ε-diaminohexyric-2-amido]-glycinamido-glycinamido}$_4$-glycine (200)**

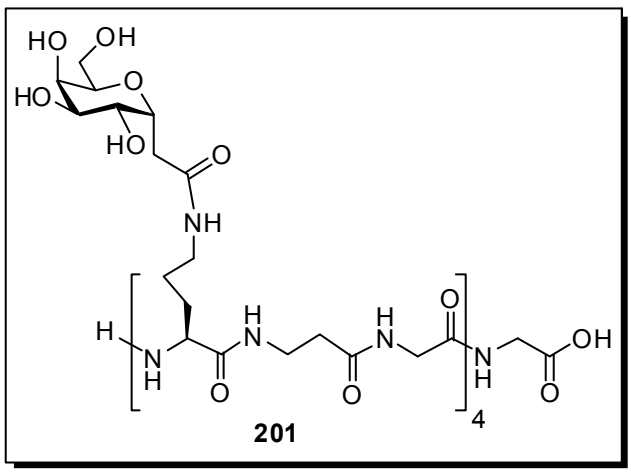


**200**

Glycopeptide **200** was produced using building block **321** according to "General protocol for solid-phase glycopeptide synthesis" with 100 mg of resin (0.061 mmol). Following lyophilization, but prior to purification, 102 mg of brown solid was recovered in 90 % yield (based on peptide conversion). After HPLC purification, 5.5 mg of pure white amorphous powder was obtained in 5 % yield (based on peptide loading).

**$^1$H NMR** (400 MHz, $D_2O$) $\delta_{ppm}$ 4.47 (4H, ddd, J = 10.5, 6.3, 4.4 Hz), 4.24-4.15 (4H, m), 4.01 (4H, dd, J = 9.9, 6.0 Hz), 3.98-3.85 (20H, m), 3.80 (4H, ddd, J = 6.1, 5.8, 1.4 Hz), 3.77-3.65 (14H, m), 3.22 (2H, t, J = 6.6, 6.6 Hz), 3.17 (6H, t, J = 5.4, 5.4 Hz), 2.75 (1H, dd, J = 16.4, 4.7 Hz), 2.70-2.40 (15H, m), 1.73-1.39 (16H, m); **$^{13}$C NMR** (126 MHz, $D_2O$) $\delta_{ppm}$ 176.4, 174.1, 173.6, 173.4, 172.0, 171.9, 171.8, 171.0, 170.7, 170.61, 170.57, 72.9, 72.5, 72.4, 69.6, 68.7, 67.5, 60.83, 60.76, 48.4, 47.1, 43.1, 42.6, 42.41, 42.38, 42.32, 42.28, 41.0, 38.9, 38.7, 32.3, 30.98, 30.96, 24.9, 24.4. **MALDI-TOF** calcd for $C_{74}H_{125}H_{17}O_{38}$ $[M + H]^+$: 1860.85; $[M + Na]^+$: 1882.83. Found 1860.9, 1882.8.

**{[(S)-Nδ-[2-(α-D-galactopyranosyl)ethan-1-amido]-α,δ-diaminopentyric-1-amido]-β-glycinamido-glycinamido}$_4$-glycine (201)**

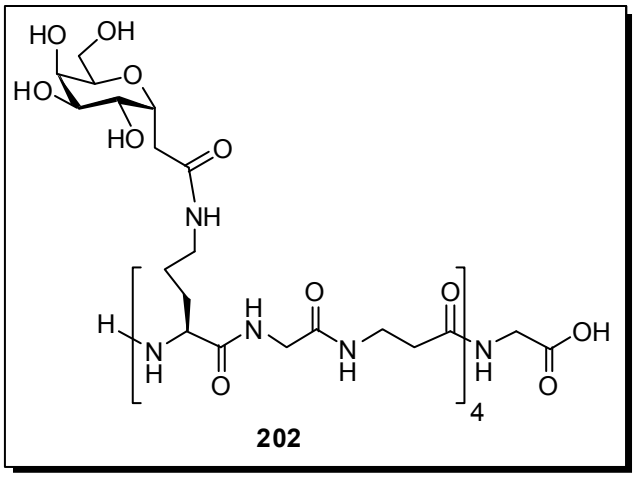


**201**

Glycopeptide **201** was produced using building block **320** according to "General protocol for solid-phase glycopeptide synthesis" with 100 mg of resin (0.061 mmol). Following lyophilization, but prior to purification, 103 mg of brown gel was

recovered in 91 % yield (based on peptide conversion). After HPLC purification, 9.1 mg of pure white amorphous powder was obtained in 8 % yield (based on peptide loading).
**$^1$H NMR** (400 MHz, $D_2O$) $\delta_{ppm}$ 4.36 (4H, ddd, $J$ = 10.4, 5.3, 4.7 Hz), 4.11 (4H, dd, $J$ = 8.3, 5.8 Hz), 3.90 (4H, dd, $J$ = 9.9, 6.1 Hz), 3.69 (4H, t, $J$ = 6.0, 6.0 Hz), 3.93-3.53 (32H, m), 3.08 (8H, t, $J$ = 6.5, 6.5 Hz), 2.54 (4H, dd, $J$ = 14.8, 10.6 Hz), 2.46 (4H, dd, $J$ = 15.4, 4.4 Hz), 2.45-2.33 (8H, m), 1.72-1.32 (16H, m); **$^{13}$C NMR** (126 MHz, $D_2O$) $\delta_{ppm}$ 176.5, 174.6, 174.5, 173.8, 173.7, 173.6, 171.42, 171.40, 171.2, 73.0, 72.5, 69.9, 68.8, 67.6, 60.9, 54.3, 53.7, 43.2, 42.6, 42.4, 38.8, 35.8, 35.1, 35.0, 32.4, 28.44, 28.41, 24.9. **MALDI-TOF** calcd for $C_{74}H_{125}H_{17}O_{38}$ $[M + H]^+$: 1860.85; $[M + Na]^+$: 1882.83; $[M + K]^+$: 1898.80. Found 1860.9, 1882.9, 1898.8.

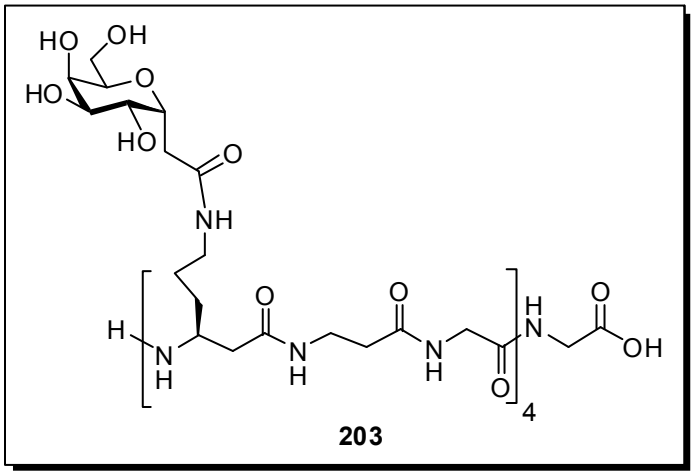
**{[(S)-Nδ-[2-(α-D-galactopyranosyl)ethan-1-amido]-α,δ-diaminopentyric-1-amido]-glycinamido-β-glycinamido}$_4$-glycine (202)**



**202**

Glycopeptide **202** was produced using building block **320** according to "General protocol for solid-phase glycopeptide synthesis" with 100 mg of resin (0.061 mmol). Following lyophilization, but prior to purification, 108 mg of yellow solid was recovered in 95 % yield (based on peptide conversion). After HPLC purification, 32 mg of pure white amorphous powder was obtained in 28 % yield (based on peptide loading).
**$^1$H NMR** (400 MHz, $D_2O$) $\delta_{ppm}$ 4.47 (4H, ddd, $J$ = 10.2, 5.9, 4.6 Hz), 4.29-4.22 (4H, m), 4.01 (4H, dd, $J$ = 9.9, 6.1 Hz), 4.09-3.84 (12H, m), 3.81 (4H, dd, $J$ = 6.0, 6.0 Hz), 3.76-3.65 (14H, m), 3.51-3.43 (8H, m), 3.24 (4H, dd, $J$ = 10.6, 6.9 Hz), 3.21 (4H, d, $J$ = 6.8 Hz), 2.66 (4H, dd, $J$ = 14.9, 10.6 Hz), 2.57 (4H, dd, $J$ = 15.1, 4.6 Hz), 2.61-2.46 (8H, m), 1.96-1.48 (16H, m); **$^{13}$C NMR** (126 MHz, $D_2O$) $\delta_{ppm}$ 176.4, 174.4, 173.6, 173.4, 173.23, 173.19, 171.1, 170.7, 73.0, 72.9, 72.4 69.6, 68.7, 67.5, 60.9, 60.8, 48.5, 47.2, 4.4, 42.4, 41.09, 41.07, 39.02, 38.98, 35.7, 34.94, 34.90, 32.3, 31.0, 25.0, 24.4. **MALDI-TOF** calcd for $C_{74}H_{125}H_{17}O_{38}$ $[M + H]^+$: 1860.85; $[M + Na]^+$: 1882.83; $[M + K]^+$: 1898.80. Found 1860.9, 1882.8, 1898.8.

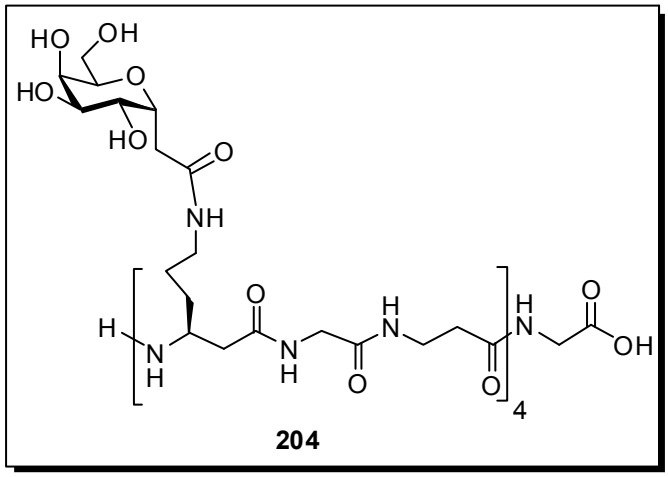
**{[(S)-Nε-[2-(α-D-galactopyranosyl)ethan-1-amido]-β,ε-diaminohexyric-2-amido]-β-glycinamido-glycinamido}$_4$-glycine (203)**



**203**

Glycopeptide **203** was produced using building block **321** according to "General protocol for solid-phase glycopeptide synthesis" with 100 mg of resin (0.061 mmol). Following lyophilization, but prior to purification, 106 mg of brown gel was recovered in 91 % yield (based on peptide conversion). After HPLC purification, 8.1 mg of pure white amorphous powder was obtained in 7 % yield (based on peptide loading). **$^1$H NMR** (400 MHz, $D_2O$) $\delta_{ppm}$ 4.46 (4H, ddd, $J$ = 10.5, 6.0, 4.6 Hz), 4.20-4.10 (4H, m), 4.01 (4H, dd, $J$ = 9.9, 6.1 Hz), 3.97 (4H, dd, $J$ = 2.9, 1.1 Hz), 3.94 (4H, s), 3.80 (4H, t, $J$ = 6.0 Hz), 3.73 (4H, dd, $J$ = 9.9, 3.3 Hz), 3.90-3.62 (16H, m), 3.50-3.37 (10H, m), 3.23-3.13 (8H, m), 2.65 (4H, dd, $J$ = 14.7, 10.8 Hz), 2.56 (4H, dd, $J$ = 15.1, 4.4 Hz), 2.60-2.27 (16H, m), 1.67-1.40 (16H, m); ); **$^{13}$C NMR** (126 MHz, $D_2O$) $\delta_{ppm}$ 176.4, 174.5, 174.3, 173.6, 173.4, 173.21, 173.17, 171.1, 170.63, 170.58, 72.9, 72.5, 72.4, 69.5, 68.7, 67.5, 60.83, 60.75, 48.4, 47.2, 43.1, 42.4, 41.1, 41.0, 38.9, 38.7, 35.6, 34.9, 34.9, 32.3, 31.0, 25.0, 24.3. **MALDI-TOF** calcd for $C_{78}H_{133}H_{17}O_{38}$ $[M + H]^+$: 1916.9. Found 1917.0.

**{[(S)-Nε-[2-(α-D-galactopyranosyl)ethan-1-amido]-β,ε-diaminohexyric-2-amido]-glycinamido-β-glycinamido}$_4$-glycine (204)**



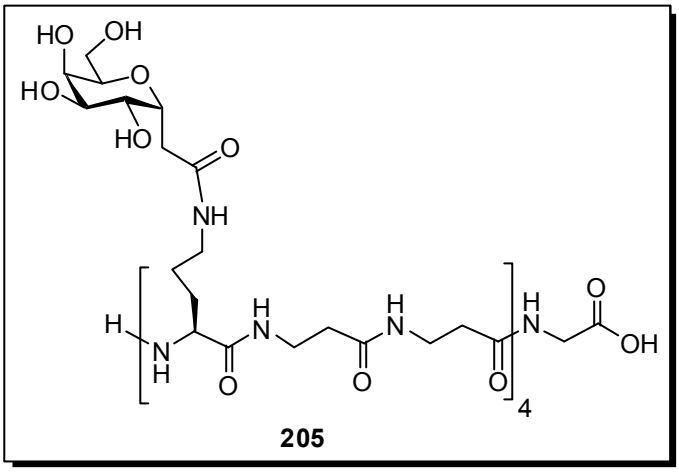
**204**

Glycopeptide **204** was produced using building block **321** according to "General protocol for solid-phase glycopeptide synthesis" with 100 mg of resin (0.061 mmol). Following lyophilization, but prior to purification, 105 mg of brown gel was recovered in 90 % yield (based on peptide

conversion). After HPLC purification, 21 mg of pure white amorphous powder was obtained in 18 % yield (based on peptide loading).

**$^1$H NMR** (400 MHz, $D_2O$) $\delta_{ppm}$ 4.47 (4H, ddd, $J$ = 10.4, 5.7, 4.4 Hz), 4.22-4.09 (4H, m), 4.01 (4H, dd, $J$ = 9.9, 6.0 Hz), 3.99-3.77 (20H, m), 3.73 (4H, dd, $J$ = 9.9, 3.3 Hz), 3.70-3.65 (8H, m), 3.52-3.38 (8H, m), 3.18 (8H, t, $J$ = 5.5 Hz), 2.66 (4H, dd, $J$ = 14.8, 10.9 Hz), 2.56 (4H, dd, $J$ = 15.4, 4.6 Hz), 2.56-2.35 (16H, m), 1.66-1.36 (16 H, m); **$^{13}$C NMR** (126 MHz, $D_2O$) $\delta_{ppm}$ 176.6, 173.8, 173.6, 173.4, 173.2, 171.1, 171.0, 72.9, 72.5, 72.4, 69.5, 68.7, 67.5, 60.8, 60.7, 48.4, 46.9, 43.2, 42.4, 40.9, 39.0, 38.7, 35.9, 35.8, 35.3, 35.2, 35.0, 32.3, 30.9, 25.0, 24.3. **MALDI-TOF** calcd for $C_{78}H_{133}H_{17}O_{38}$ $[M + H]^+$: 1916.9. Found 1916.9.

**{[(S)-Nδ-[2-(α-D-galactopyranosyl)ethan-1-amido]-α,δ-diaminopentyric-1-amido]-β-glycinamido-β-glycinamido}$_4$-glycine (205)**

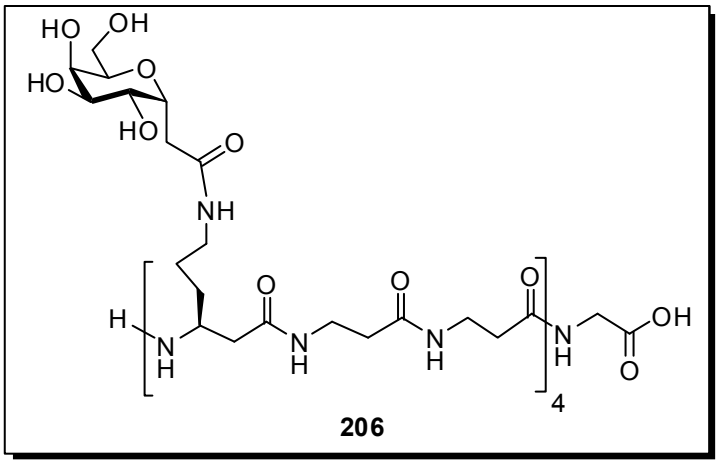


**205**

Glycopeptide **205** was produced using building block **320** according to "General protocol for solid-phase glycopeptide synthesis" with 100 mg of resin (0.061 mmol). Following lyophilization, but prior to purification, 102 mg of brown solid was recovered in 85 % yield (based on peptide conversion). After HPLC purification, 3.6 mg of pure white amorphous powder was obtained in 3 % yield (based on peptide loading).

**$^1$H NMR** (400 MHz, $D_2O$) $\delta_{ppm}$ 4.45 (4H, ddd, $J$ = 9.6, 5.8, 3.7 Hz), 4.15 (4H, t, $J$ = 6.6, 6.6 Hz), 3.99 (4H, dd, $J$ = 9.8, 6.0 Hz), 3.95 (4H, d, $J$ = 2.5 Hz), 3.79 (4H, t, $J$ = 5.8, 5.8 Hz), 3.71 (8H, dd, $J$ = 9.4, 3.0 Hz), 3.67-3.64 (8H, m), 3.46-3.35 (24H, m), 3.18 (8H, t, $J$ = 6.6, 6.6 Hz), 2.70-2.32 (24H, m), 1.82-1.31 (16H, m); **$^{13}$C NMR** (126 MHz, $D_2O$) $\delta_{ppm}$ 176.6, 173.8, 173.6, 173.4, 173.2, 171.1, 171.0, 72.9, 72.5, 72.4, 69.5, 68.8, 67.5, 60.8, 60.7, 48.4, 46.9, 43.2, 42.4, 41.0, 39.0, 38.7, 35.9, 35.8, 35.3, 35.2, 35.0, 32.3, 30.9, 25.0, 24.3. **MALDI-TOF** calcd for $C_{78}H_{133}H_{17}O_{38}$ $[M + H]^+$: 1916.9. Found 1916.9.

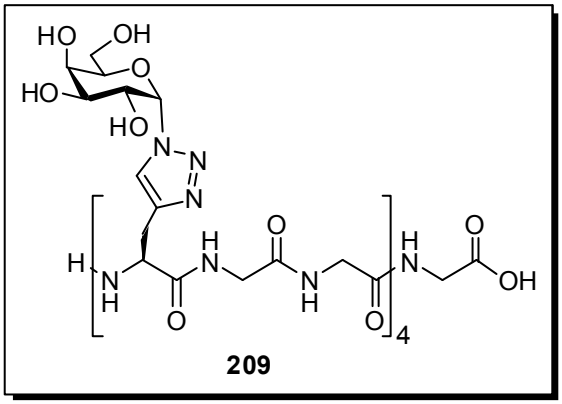
**{[(S)-Nε-[2-(α-D-galactopyranosyl)ethan-1-amido]-β,ε-diaminohexyric-2-amido]-β-glycinamido-β-glycinamido}$_4$-glycine (206)**



**206**

Glycopeptide **206** was produced using building block **321** according to "General protocol for solid-phase glycopeptide synthesis" with 100 mg of resin (0.061 mmol). Following lyophilization, but prior to purification, 120 mg of brown gel was recovered in 97 % yield (based on peptide conversion). After HPLC purification, 40 mg of pure white amorphous powder was obtained in 32 % yield (based on peptide loading). **$^1$H NMR** (400 MHz, $D_2O$) $\delta_{ppm}$ 4.46 (4H, ddd, $J$ = 10.4, 5.7, 4.6 Hz), 4.16-4.07 (4H, m), 4.00 (4H, dd, $J$ = 9.9, 6.0 Hz), 3.98-3.93 (8H, m), 3.80 (4H, t, $J$ = 6.1 Hz), 3.72 (4H, dd, $J$ = 9.9, 3.3 Hz), 3.67 (8H, d, $J$ = 6.0 Hz), 3.47-3.29 (20H, m), 3.16 (8H, t, $J$ = 5.3, 5.3 Hz), 2.64 (4H, dd, $J$ = 14.8, 10.8 Hz), 2.55 (4H, dd, $J$ = 15.1, 4.3 Hz), 2.51 (4H, t, $J$ = 6.4 Hz), 2.45-2.24 (24H, m), 1.63-1.35 (16H, m); **$^{13}$C NMR** (126 MHz, $D_2O$) $\delta_{ppm}$ 174.3, 173.7, 173.63, 17.58, 173.4, 173.13, 173.11, 173.07, 72.9, 72.5, 72.4, 68.6, 68.7, 67.5, 60.8, 60.75, 48.5, 47.0, 41.30, 41.56, 41.2, 39.0, 38.6, 36.4, 36.3, 35.9, 35.9, 35.8, 35.7, 35.3, 35.2, 35.0, 34.8, 32.3, 30.9, 29.2, 25.0, 24.9, 24.3. **MALDI-TOF** calcd for $C_{82}H_{141}H_{17}O_{38}$ $[M + H]^+$: 1972.97. Found 1973.0.

**{[(*S*)-3-[4-(α-D-galactopyranosyl)-2,3,4-triazol-1-yl]-α-aminopropyric-2-amido]-glycinamido-glycinamido}$_4$-glycine (209)**



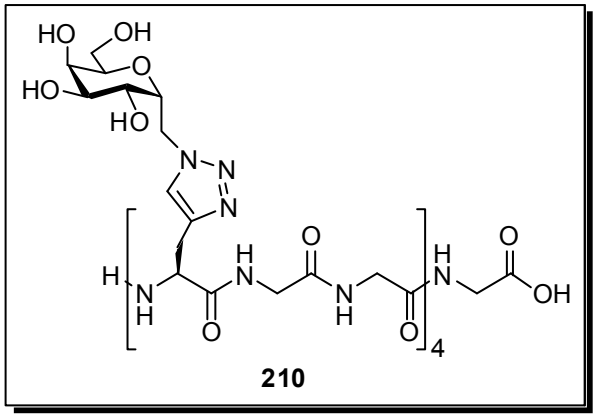
**209**

Resin-supported **426** (60 mg 0.026 mmol) was treated as per the general procedure described above with **416** (190 mg, 0.51 mmol), cupric acetate (3.8 mg, 0.020 mmol), and sodium ascorbate (8.2 mg, 0.041 mmol). Reversed-phase HPLC (1 % acetonitrile in water for 12 mins

followed by a linear gradient from 1 % acetonitrile in water to 10 % acetonitrile in water over 28 mins followed by a linear gradient from 10 % acetonitrile in water to 98 % acetonitrile in water over 40 mins) yielded 9 mg of **209** as a white powder (20 % based on resin loading).

**$^1$H NMR** (500 MHz, $D_2O$): $\delta_{ppm}$ 7.83 (4H, s), 6.12 (4H, d, $J$ = 5.9 Hz), 4.33 (4H, d $J$ = 10.1 Hz), 4.17 (4H, dd, $J$ = 10.0, 6.3 Hz), 3.93 (5H, m), 3.86-3.71 (17H, m), 3.60-3.47 (12H, m), 3.18-2.98 (12 H, m); **$^{13}$C NMR** (126 MHz, $D_2O$): $\delta_{ppm}$ 173.2, 173.0, 172.0, 171.9, 171.83, 171.76, 171.3, 171.28, 171.22, 171.1, 148.8, 125.3, 85.2, 74.8, 69.3, 68.7, 67.0, 61.1, 53.2, 53.16, 53.14, 46.57, 42.59, 42.2, 27.1, 26.9, 26.8, 26.7, 26.65, 26.59, 25.1, 23.7. **MALDI-TOF MS** *m/z* calcd for $C_{62}H_{93}N_{25}O_{34}$ $[M + Na + H]^{2+}$: 877.814. Found: 877.8. **HPLC $T_R$** = 28.5 min.

**{[(*S*)-3-[4-(α-D-galactopyranosylmethyl)-2,3,4-triazol-1-yl]-α-aminopropyric-2-amido]-glycinamido-glycinamido}$_4$-glycine (210)**

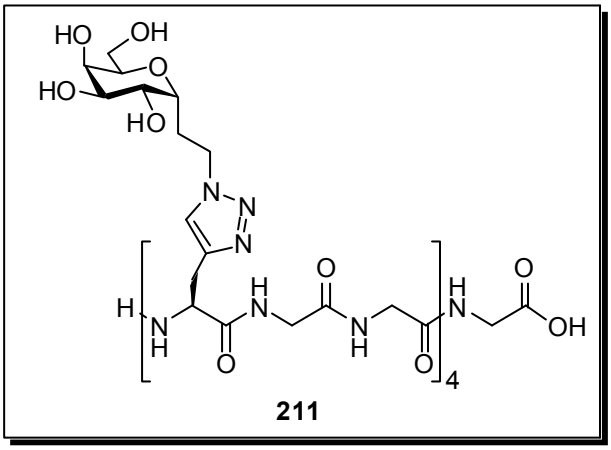


**210**

Resin-supported **426** (70 mg 0.030 mmol) was treated as per the general procedure described above with **430** (94 mg, 0.24 mmol), cupric acetate (6.5 mg, 0.036 mmol), and sodium ascorbate (13 mg, 0.072 mmol). Reversed-phase HPLC (1 % acetonitrile in water for 12 mins followed by a linear gradient from 1 % acetonitrile in water to 10 % acetonitrile in water over 28 mins followed by a linear gradient from 10 % acetonitrile in water to 98 % acetonitrile in water over 40 mins) yielded 25 mg of **210** as a white powder (45 % based on resin loading).

**$^1$H NMR** (500 MHz, $D_2O$): $\delta_{ppm}$ 7.73 (4H, s), 4.53 (4H, m), 4.24 (4H, s), 3.93 (5H, m), 3.88-3.63 (28H, m), 3.59-3.56 (5H, m), 3.54-3.38 (12H, m), 3.13-2.97 (8H, m); **$^{13}$C NMR** (126 MHz, $D_2O$): $\delta_{ppm}$ 171.4, 171.3, 171.2, 171.1, 171.1, 171.0, 170.9, 129.8, 122.6, 74.7, 74.6, 74.5, 72.5, 69.5, 69.4, 69.2, 68.7, 68.6, 68.4, 67.1, 60.8, 45.74, 45.70, 45.6, 42.6, 42.4, 42.3, 42.2, 27.2, 27.13, 27.09, 27.02. **MALDI-TOF MS** *m/z* calcd for $C_{66}H_{101}N_{25}O_{34}$ $[M + H]^+$: 1788.69. Found: 1788.6. **HPLC $T_R$** = 24.6 min.

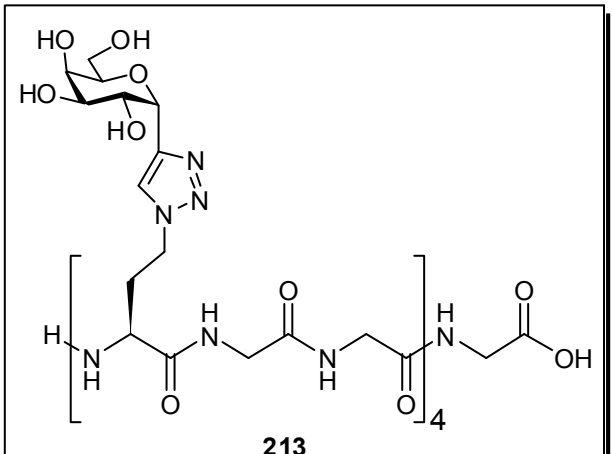
**{[(*S*)-3-[4-(α-D-galactopyranosylethyl)-2,3,4-triazol-1-yl]-α-aminopropyric-2-amido]-glycinamido-glycinamido}$_4$-glycine (211)**



**211**

Resin-supported **426 (**40 mg 0.017 mmol) was treated as per the general procedure described above with **420** (136 mg, 0.34 mmol), cupric acetate (2.5 mg, 0.0136 mmol), and sodium ascorbate (5.5 mg, 0.0275 mmol). Reversed-phase HPLC (2 % acetonitrile in water for 9 mins followed by a linear gradient from 2 % acetonitrile in water to 40 % acetonitrile in water over 30 mins) yielded 17 mg of **211** as a white powder (54 % based on resin loading). **$^1$H NMR** (500 MHz, $D_2O$): $\delta_{ppm}$ 7.84 (1H, s), 7.76 (3H, s), 4.62-4.51 (4H, m), 4.40-4.32 (9H, m), 4.26 (1H, t, $J$ = 6.40 Hz), 3.92-3.70 (24 H, m), 3.63 (12H, dd, $J$ = 10.1, 3.0 Hz), 3.58-3.53 (8H, m), 3.25 (2H, d, $J$ = 6.2 Hz), 3.21-2.96 (6H, m), 2.24-2.10 (4H, m), 1.95-2.10 (4H, m); **$^{13}$C NMR** (126 MHz, $D_2O$): $\delta_{ppm}$ 173.0, 172.0, 171.87, 171.80, 171.69, 171.42, 171.4, 171.36, 171.32, 171.19, 169.8, 169.3, 126.2, 126.1, 72.2, 72.1, 72.0, 69.6, 68.8, 67.7, 65.8, 61.0, 54.4, 53.8, 53.3, 52.7, 47.0, 46.95, 46.91, 42.6, 42.6, 42.3, 42.2, 27.9, 27.2, 27.0, 26.9, 26.8, 26.6, 24.6, 22.2. **MALDI-TOF MS** calcd. for $C_{70}H_{109}N_{25}O_{34}$ $[M]^+$: 1843.76. Found: 1843.8. **HPLC** $\mathbf{T_R}$ = 35.1 min.

**{[(*S*)-4-[(α-D-galactopyranosyl)-1,2,3-triazol-1-yl]-α-aminobutyric-2-amido]-glycinamido-glycinamido}$_4$-glycine (213)**



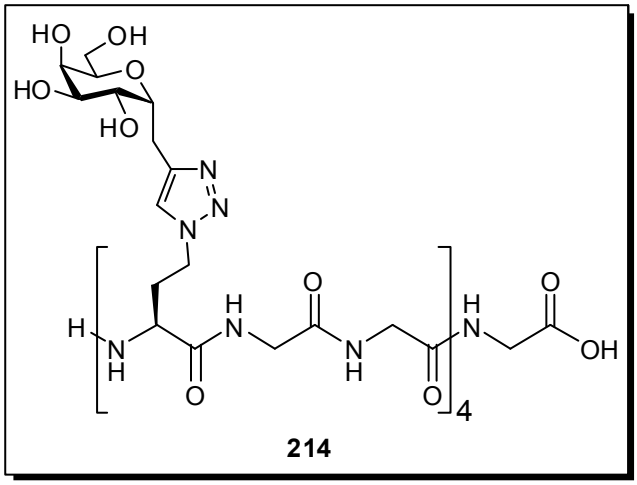
**213**

Glycopeptide **213** was prepared under the standard conditions above. Resin-supported peptide **456** (75 mg, 0.028 mmol) was treated with glycosyl azide **452** (200 mg, 0.57 mmol) in the presence of copper (II) acetate (20 mg, 0.10 mmol) and sodium ascorbate (40 mg, 0.20 mmol). Following cleavage from the bead, RP-SPE,

Zemplen deprotection, and RP-SPE, 26 mg of the title compound, **213**, was recovered as a white solid (52 % yield based on peptide loading).

**$^1$H NMR** (500 MHz, $D_2O$) $\delta_{ppm}$ 8.09 (4H, s), 5.32 (4H, bs), 4.52 (8H, bs), 4.37-4.17 (4H, m), 4.16-3.81 (30H, m), 3.80-3.60 (12H, m), 2.66-2.42 (4H, m), 2.40-2.21 (4H, m); **$^{13}$C NMR** (126 MHz, $D_2O$, with line broadening, 3 Hz, exponential) $\delta_{ppm}$ 174.4, 173.3, 172.2, 171.9, 171.7, 142.5, 126.4, 73.6, 70.3, 70.0, 68.9, 67.6, 61.0, 50.6, 46.6, 42.5, 42.3, 30.7. **MALDI-TOF MS** calcd. for $C_{66}H_{101}N_{25}O_{34}$ $[M + H]^+$: 1788.70; $[M + K]^+$: 1826.65. Found: 1788.73, 1826.65.

**{[(*S*)-4-[(α-D-galactopyranosylmethyl)-1,2,3-triazol-1-yl]-α-aminobutyric-2-amido]-glycinamido-glycinamido}$_4$-glycine (214)**

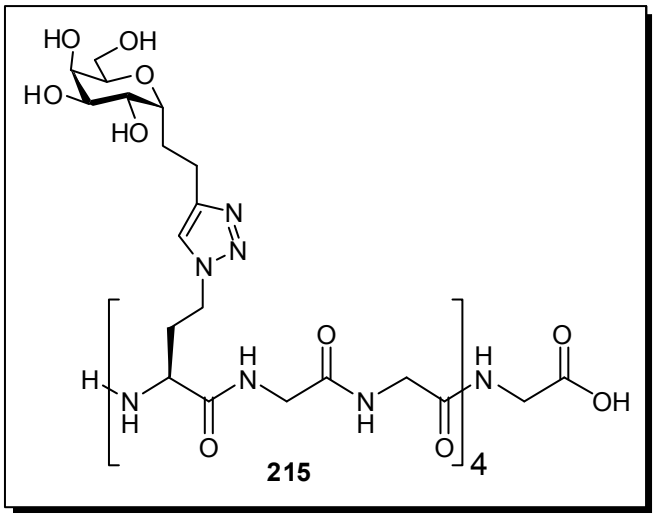


**214**

Glycopeptide **214** was prepared under the standard conditions above. Resin-supported peptide **456** (75 mg, 0.028 mmol) was treated with glycosyl azide **453** (200 mg, 0.54 mmol) in the presence of copper (II) acetate (20 mg, 0.10 mmol) and sodium ascorbate (40 mg, 0.20 mmol). Following cleavage from the bead, RP-SPE, Zemplen deprotection, and RP-SPE, 25 mg of the title compound, **214**, was recovered as a white solid (48 % yield based on peptide loading).

**$^1$H NMR** (500 MHz, $D_2O$) $\delta_{ppm}$ 7.90 (4H, bs), 4.50 (8H, bs), 4.30 (8H, bs), 4.07 (4H, *pseudo*-dd, $J$ = 9.3, 5.8 Hz), 4.03-3.81 (30H, m), 3.70-3.61 (8H, m), 3.14 (4H, *pseudo*-d, $J$ = 10.5 Hz), 3.05 (4H, *pseudo*-d, $J$ = 12.8 Hz), 2.57-2.44 (4H, m), 2.35-2.25 (4H, m); **$^{13}$C NMR** (126 MHz, $D_2O$, with line-broadening, 2Hz, exponential) $\delta_{ppm}$ 173.2, 172.1, 171.9, 171.6, 171.1, 170.9, 143.8, 125.2, 75.0, 73.9, 71.9, 68.5, 68.9, 68.0, 62.6, 60.9, 50.9, 46.7, 42.5, 31.0, 30.8, 20.7. **MALDI-TOF MS** calcd. for $C_{70}H_{109}N_{25}O_{34}$ $[M + K]^+$: 1882.71. Found: 1882.62.

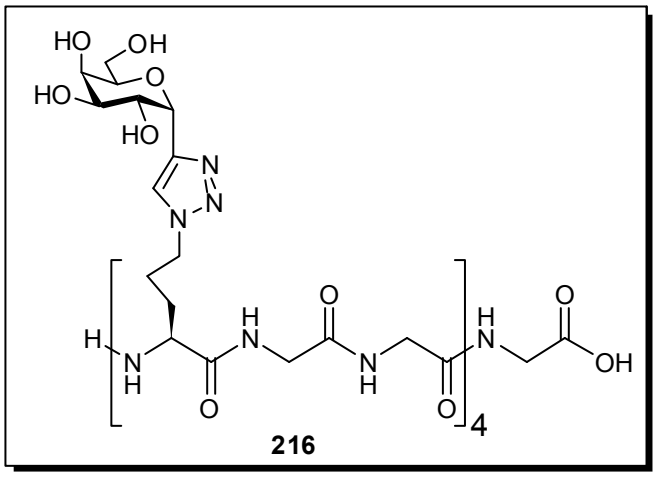
**{[(*S*)-4-[(α-D-galactopyranosylethyl)-1,2,3-triazol-1-yl]-α-aminobutyric-2-amido]-glycinamido-glycinamido}$_4$-glycine (215)**



215

Glycopeptide **215** was prepared under the standard conditions above. Resin-supported peptide **456** (75 mg, 0.028 mmol) was treated with glycosyl azide **454** (150 mg, 0.39 mmol) in the presence of copper (II) acetate (10 mg, 0.05 mmol) and sodium ascorbate (20 mg, 0.10 mmol). Following cleavage from the bead, RP-SPE, Zemplen deprotection, and RP-SPE, 31.5 mg of the title compound, **215**, was recovered as a white solid (59 % yield based on peptide loading). **$^1$H NMR** (500 MHz, *$D_2O$*) $\delta_{ppm}$ 7.80 (4H, bs), 4.60-4.38 (8H, m), 4.31-4.22 (4H, m), 4.09-3.84 (30H, m), 3.80 (8H, *pseudo*-d, *J* = 6.3 Hz), 3.71 (8H, *pseudo*-d, *J* = 5.6 Hz), 2.93-2.78 (4H, m), 2.77-2.66 (4H, m), 2.58-2.43 (4H, m), 2.37-2.23 (4H, m), 2.13-1.98 (4H, m), 1.97-1.84 (4H, m); **$^{13}$C NMR** (126 MHz, *$D_2O$*) $\delta_{ppm}$ 173.2, 171.95, 171.86, 171.68, 171.65, 171.63, 171.5, 169.1, 144.1, 125.8, 74.37, 74.35, 71.7, 69.7, 69.0, 68.1, 61.1, 50.9, 48.4, 46.6, 42.6, 42.5, 42.2, 30.7, 23.5, 20.6. **MALDI-TOF MS** calcd. for $C_{74}H_{117}N_{25}O_{34}$ $[M + H]^+$: 1900.82. Found: 1900.8.

**{[(*S*)-5-[(α-D-galactopyranosyl)-1,2,3-triazol-1-yl]-α-aminopentyric-2-amido]-glycinamido-glycinamido}$_4$-glycine (216)**

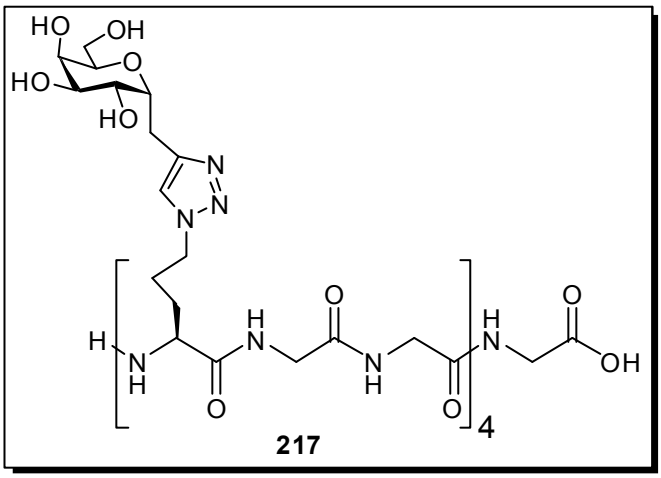


216

Glycopeptide **216** was prepared under the standard conditions above. Resin-supported peptide **457** (75 mg, 0.028 mmol) was treated with glycosyl azide **452** (200 mg, 0.57 mmol) in the presence of copper (II) acetate (20 mg, 0.10 mmol) and sodium ascorbate (40 mg, 0.20 mmol). Following cleavage from the bead, RP-SPE, Zemplen deprotection, and RP-SPE, 33 mg of the title compound, **216**, was recovered as a white solid (64 % yield based on peptide loading).

**$^1$H NMR** (500 MHz, *$D_2O$*) $\delta_{ppm}$ 8.21 (4H, s), 5.33 (4H, bs), 4.48 (8H, bs), 4.34 (4H, *pseudo*-dd, *J* = 13.2, 7.5 Hz), 4.13-3.84 (30H, m), 3.78-3.65 (12H, m), 2.06-1.91 (8H, m), 1.89-1.77 (4H, m), 1.77-1.67 (4H, m); **$^{13}$C NMR** (126 MHz, *$D_2O$*) $\delta_{ppm}$ 174.1, 172.0, 171.9, 171.8, 171.6, 171.5, 171.3, 142.5, 126.2, 73.7, 70.2, 70.1, 68.9, 67.7, 61.0, 53.2, 49.8, 48.8, 4.5,42.4, 42.3, 42.2, 27.6, 25.7. **MALDI-TOF MS** calcd. for $C_{70}H_{109}N_{25}O_{34}$ $[M + Na]^+$: 1866.74. Found: 1866.77.

**{[(*S*)-5-[(α-D-galactopyranosylmethyl)-1,2,3-triazol-1-yl]-α-aminopentyric-2-amido]-glycinamido-glycinamido}$_4$-glycine (217)**

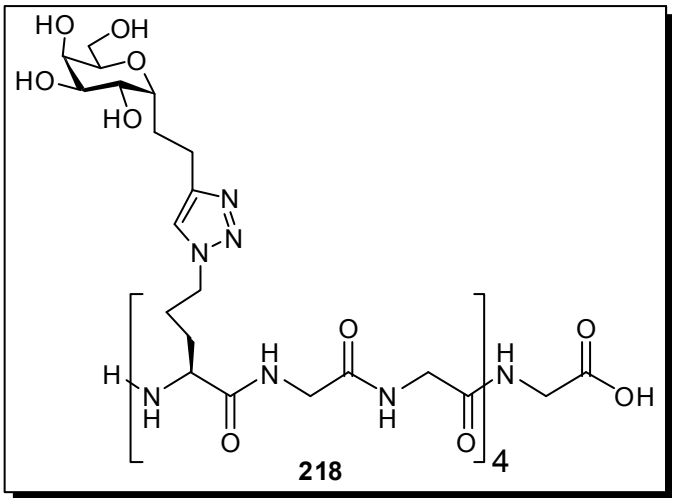


**217**

Glycopeptide **217** was prepared under the standard conditions above. Resin-supported peptide **457** (75 mg, 0.028 mmol) was treated with glycosyl azide **453** (200 mg, 0.54 mmol) in the presence of copper (II) acetate (20 mg, 0.10 mmol) and sodium ascorbate (40 mg, 0.20 mmol). Following cleavage from the bead, RP-SPE, Zemplen deprotection, and RP-SPE, 20 mg of the title compound, **217**, was recovered as a white solid (38 % yield based on peptide loading).

**$^1$H NMR** (500 MHz, *$D_2O$*) $\delta_{ppm}$ 7.95 (4H, bs), 4.52-4.37 (8H, m), 4.37-4.26 (8H, m), 4.12-3.73 (34H, m), 3.70-3.60 (8H, m), 3.23-2.96 (8H, m), 2.03-1.88 (8H, m), 1.88-1.76 (4H, m), 1.74-1.66 (4H, m); **$^{13}$C NMR** (126 MHz, *$D_2O$*) $\delta_{ppm}$ 174.0, 171.9, 171.7, 171.6, 170.9, 143.5, 125.2, 74.9, 71.9, 69.5, 68.9, 68.0, 60.9, 53.3, 53.2, 49.5, 48.8, 42.5, 42.3, 27.7, 27.6, 27.5, 25.8. **MALDI-TOF MS** calcd. for $C_{74}H_{117}N_{25}O_{34}$ $[M + Na]^+$: 1922.81. Found: 1922.71.

**{[(*S*)-5-[(α-D-galactopyranosylethyl)-1,2,3-triazol-1-yl]-α-aminopentyric-2-amido]-glycinamido-glycinamido}$_4$-glycine (218)**

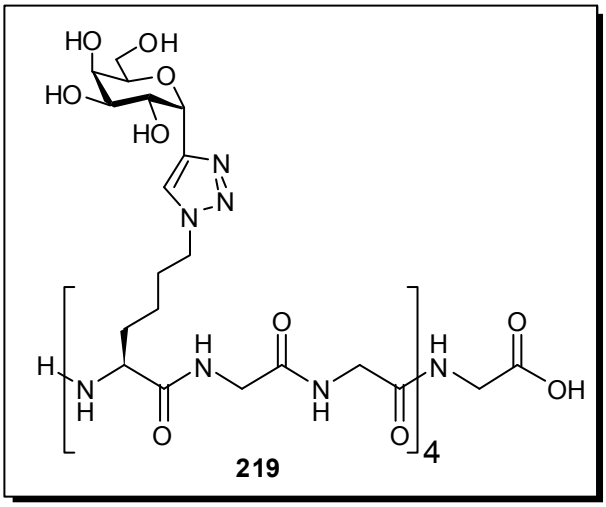


**218**

Glycopeptide **218** was prepared under the standard conditions above. Resin-supported peptide **457** (75 mg, 0.028 mmol) was treated with glycosyl azide **454** (200 mg, 0.52 mmol) in the presence of copper (II) acetate (20 mg, 0.10 mmol) and sodium ascorbate (40 mg, 0.20 mmol). Following cleavage from the bead, RP-SPE, Zemplen deprotection, and RP-SPE, 31 mg of the title compound, **218**, was recovered as a white solid (57 % yield based on peptide loading).

**$^1$H NMR** (500 MHz, $D_2O$) $\delta_{ppm}$ 7.80 (4H, bs), 4.46-4.36 (8H, m), 4.35-4.26 (4H, m), 4.09-3.86 (28H, m), 3.84-3.74 (10H, m), 3.70 (8H, *pseudo*-d, $J$ = 5.8 Hz), 2.89-2.77 (4H, m), 2.76-2.66 (4H, m), 2.15-2.01 (4H, m), 2.02-1.85 (12H, m), 1.85-1.75 (4H, m), 1.75-1.63 (4H, m); **$^{13}$C NMR** (126 MHz, $D_2O$) $\delta_{ppm}$ 174.0, 171.9, 171.8, 171.6, 144.4, 125.9, 74.3, 71.7, 69.7, 69.0, 68.1, 61.0, 53.3, 49.7, 42.5, 42.4, 42.2, 27.6, 27.6, 25.7, 23.4, 20.7. **MALDI-TOF MS** calcd. for $C_{78}H_{125}N_{25}O_{34}$ $[M + Na]^+$: 1956.90. Found: 1956.77.

**{[(*S*)-6-[(α-D-galactopyranosyl)-1,2,3-triazol-1-yl]-α-aminohexyric-2-amido]-glycinamido-glycinamido}$_4$-glycine (219)**

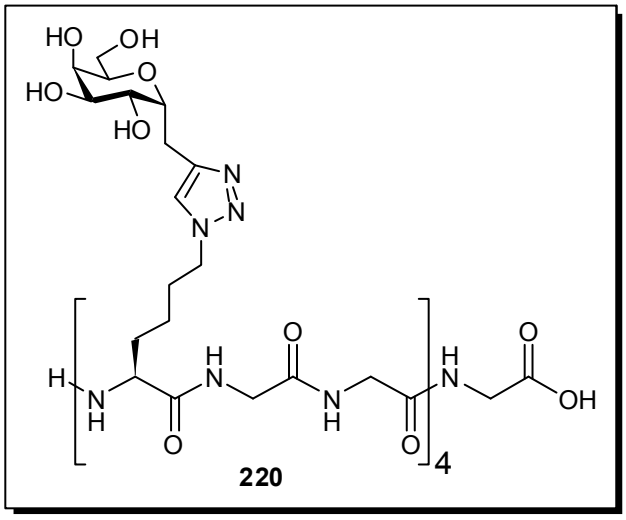


**219**

Glycopeptide **219** was prepared under the standard conditions above. Resin-supported peptide **458** (75 mg, 0.028 mmol) was treated with glycosyl azide **452** (190 mg, 0.53 mmol) in the presence of copper (II) acetate (20 mg, 0.10 mmol) and sodium ascorbate (40 mg, 0.20 mmol). Following cleavage from the bead, RP-SPE, Zemplen deprotection, and RP-SPE, 24 mg

of the title compound, **219**, was recovered as a white solid (45 % yield based on peptide loading). **$^1$H NMR** (500 MHz, $D_2O$) $\delta_{ppm}$ 8.11 (4H, s), 5.34 (4H, *pseudo*-d, $J$ = 6.4 Hz), 4.43 (8H, bs), 4.30 (4H, *pseudo*-dd, $J$ = 12.5, 6.9 Hz), 4.25 (4H, *pseudo*-dd, $J$ = 9.8, 6.6 Hz), 4.11 (4H, *pseudo*-dd, $J$ = 9.7, 2.8 Hz), 4.04 (4H, *pseudo*-d, $J$ = 2.2 Hz), 4.01-3.88 (18H, m), 3.80-3.66 (12H, m), 1.99-1.65 (16H, m), 1.43-1.24 (8H, m); **$^{13}$C NMR** (126 MHz, $D_2O$) $\delta_{ppm}$ 174.6, 171.96, 171.95, 171.87, 171.86, 171.8, 171.5, 142.8, 125.8, 73.7, 70.3, 70.1, 68.9, 67.6, 61.0, 53.7, 50.0, 42.50, 42.47, 42.3, 42.2, 30.0, 29.9, 28.7, 21.9. **MALDI-TOF MS** calcd. for $C_{74}H_{117}N_{25}O_{34}$ $[M + Na]^+$: 1922.81. Found: 1922.71.

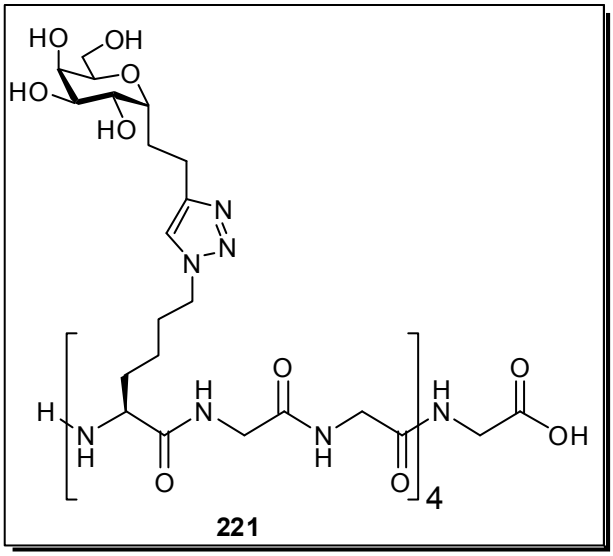
**{[(*S*)-6-[(α-D-galactopyranosylmethyl)-1,2,3-triazol-1-yl]-α-aminohexyric-2-amido]-glycinamido-glycinamido}$_4$-glycine (220)**



**220**

Glycopeptide **220** was prepared under the standard conditions above. Resin-supported peptide **458** (75 mg, 0.028 mmol) was treated with glycosyl azide **453** (200 mg, 0.54 mmol) in the presence of copper (II) acetate (20 mg, 0.10 mmol) and sodium ascorbate (40 mg, 0.20 mmol). Following cleavage from the bead, RP-SPE, Zemplen deprotection, and RP-SPE, 38 mg of the title compound, **220**, was recovered as a white solid (69 % yield based on peptide loading). **$^1$H NMR** (500 MHz, $D_2O$) $\delta_{ppm}$ 7.92 (4H, s), 4.38 (8H, bs), 4.29 (8H, bs), 4.07 (4H, *pseudo*-dd, $J$ = 9.4, 5.9 Hz), 4.02 (4H, s), 4.01-3.81 (26 H, m), 3.72-3.58 (8H, m), 3.13 (4H, *pseudo*-d, $J$ = 10.1 Hz), 3.05 (4H, d, $J$ = 13.2 Hz), 1.97-1.65 (16H, m), 1.41-1.21 (8H, m); **$^{13}$C NMR** (126 MHz, $D_2O$, line braodening, 2 Hz, exponential) $\delta_{ppm}$ 174.6, 171.9, 171.8, 171.5, 171.3, 171.0, 143.2, 125.8, 75.0, 71.9, 70.9, 70.5, 69.5, 68.9, 68.0, 62.6, 61.2, 60.9, 53.6, 53.3, 49.9, 42.5, 42.3, 30.0, 28.7, 21.9, 20.7. **MALDI-TOF MS** calcd. for $C_{78}H_{125}N_{25}O_{34}$ $[M + Na]^+$: 1956.90. Found: 1956.77.

**{[(*S*)-6-[(α-D-galactopyranosylethyl)-1,2,3-triazol-1-yl]-α-aminohexyric-2-amido]-glycinamido-glycinamido}$_4$-glycine (221)**

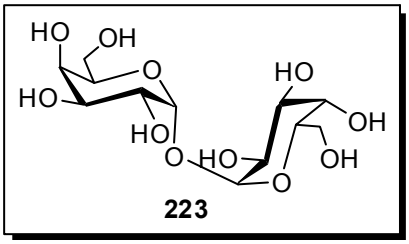


**221**

Glycopeptide **221** was prepared under the standard conditions above. Resin-supported peptide **458** (75 mg, 0.028 mmol) was treated with glycosyl azide **454** (150 mg, 0.39 mmol) in the presence of copper (II) acetate (10 mg, 0.05 mmol) and sodium ascorbate (20 mg, 0.10 mmol). Following cleavage from the bead, RP-SPE, Zemplen deprotection, and RP-SPE, 28 mg of the title compound, **221**, was recovered as a white solid (50 % yield based on peptide loading).

**$^1$H NMR** (500 MHz, *$D_2O$*) $\delta_{ppm}$ 7.82 (4H, bs), 4.46-4.33 (8H, m), 4.33-4.23 (4H, m), 4.10-3.86 (30H, m), 3.79 (8H, *pseudo*-d, *J* = 5.4 Hz), 3.70 (8H, *pseudo*-d, *J* = 5.7 Hz), 2.91-2.79 (4H, m), 2.78-2.67 (4H, m), 2.16-1.99 (4H, m), 1.98-1.79 (16H, m), 1.78-1.68 (4H, m), 1.41-1.21 (8H, m); **$^{13}$C NMR** (126 MHz, *$D_2O$* line braodening, 2 Hz, exponential) $\delta_{ppm}$ 174.5, 171.84, 171.77, 171.6, 171.4, 144.8, 125.3, 74.3, 71.7, 69.7, 69.0, 68.2, 61.0, 53.6, 49.9, 42.5, 42.3, 30.0, 28.7, 23.5, 21.9, 20.8. **MALDI-TOF MS** calcd. for $C_{82}H_{133}N_{25}O_{34}$ $[M + Na]^+$: 2034.94. Found: 2034.77.

**α-D-galactopyranosyl-α-D-galactopyranoside (223)**



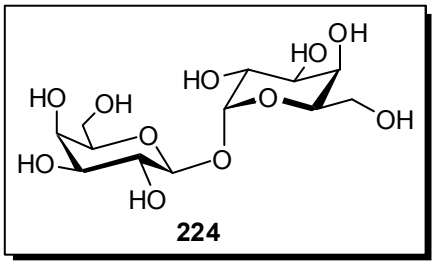
**223**

Benzyl protected disaccharide **532** (80 mg, 0.075 mmol) was dissolved in 18 mL of solvent (10:2:1 ethanol: methanol: DCM) in a bomb flask compatible with a high pressure system. Pd on carbon (80 mg) was added, and the flask was sealed, purged twice with hydrogen, and filled to 10 atmospheres of pressure with hydrogen gas. The reaction was stirred for 24 hours, depressurized, and filtered through a celite pad washed with water. Solvent was removed and the solution was lyophilized to provide 25 mg of deprotected

disaccharide **223** as a white powder in quantitative yield. Spectral data is consistent with the partial data provided by Pavia.[8]

**$^1$H NMR** (500 MHz, $D_2O$) $\delta_{ppm}$ 5.19 (2H, d, $J$ = 3.9 Hz), 4.03 (2H, dd, $J$ = 6.9, 5.5 Hz), 3.98-3.95 (4H, m), 3.86 (2H, ddd, $J$ = 11.4, 4.0, 1.1 Hz), 3.72 (2H, dd, $J$ = 11.8, 7.4 Hz), 3.69 (2H, dd, $J$ = 11.8, 5.0 Hz); **$^{13}$C NMR** (101 MHz, $D_2O$) $\delta_{ppm}$ 93.2, 93.2, 71.3, 71.3, 69.3, 69.3, 69.0, 69.0, 68.0, 68.0, 61.2, 61.2. **ESI-MS** $m/z$ calcd for $C_{12}H_{22}O_{11}$ $[M + Na]^+$: 365.11; $[M + K]^+$: 381.08. Found 365.25, 381.24.

**β-D-galactopyranosyl-α-D-galactopyranoside (224)**

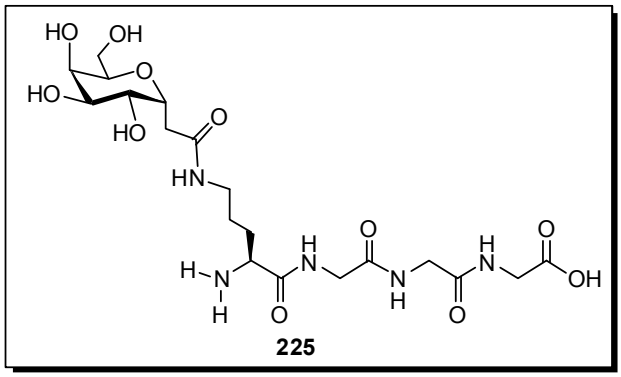


**224**

Benzyl protected disaccharide **531** (20 mg, 0.019 mmol) was dissolved in 10 mL of solvent (10:2:1 ethanol: methanol: DCM) in a bomb flask compatible with a high pressure system. Palladium on carbon (30 mg) was added, and the flask was sealed, purged twice with hydrogen, and filled to 10 atmospheres of pressure with hydrogen gas. The reaction was stirred for 24 hours, depressurized, and filtered through a celite pad washed with water. Solvent was removed and the solution was lyophilized to provide the deprotected disaccharide. The crude product was portioned between water and chloroform. The aqueous layer was extracted three times with chloroform, followed by hexanes and finally DCM prior to being lyophilized a second time to provide 5.2 mg of deprotected disaccharide **224** as a white powder in 82 % yield.

**$^1$H NMR** (500 MHz, $D_2O$, water supression @ 4.79 ppm) $\delta_{ppm}$ 5.22 (1H, d, $J$ = 3.8 Hz), 4.54 (1H, d, $J$ = 7.5 Hz), 4.19 (1H, dd, $J$ = 6.2, 6.2 Hz), 3.96 (1H, d, $J$ = 2.9 Hz), 3.88 (1H, dd, $J$ = 10.3, 3.1 Hz), 3.89 (1H, d, $J$ = 2.9 Hz), 3.81 (1H, dd, $J$ = 10.4, 3.8 Hz), 3.75-3.58 (7H, m); **$^{13}$C NMR** (126 MHz, $D_2O$) $\delta_{ppm}$ 103.3, 100.2, 75.4, 72.4, 71.7, 70.8, 69.28, 69.26, 68.4, 68.4, 61.2, 61.1. **ESI-MS** $m/z$ calcd for $C_{12}H_{22}O_{11}$ $[M + Na]^+$: 365.11. Found 365.33.

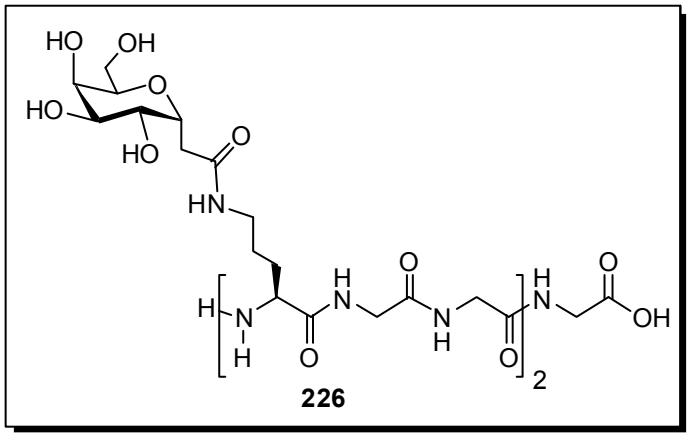
**[(S)-*N*δ-[2`-(α-D-galactopyranosyl)-ethan-1`-amido]-α,γ-diaminopentyric-1-amido]-glycinamido-glycinamido-glycine (225)**



**225**

Peptide **225** was prepared using 200 mg of Wang resin according to standard Fmoc protocols (0.122 mmol scale) using building block **320**.[7] The compound was cleaved off the bead and purified through preparatory TLC (60% methanol in water). The product was eluted off the silica using pure water and was filtered through a sub-micron filter and lyophilized to yield 27 mg (0.053 mmol) of monomer **225** as a white powder in 44 % yield. **$^1$H NMR** (500 MHz, $D_2O$) $\delta_{ppm}$ 7.21 (NH, bs) 4.53 (1H, ddd , $J$ = 10.6, 5.8, 4.2 Hz), 4.18-3.99 (6H, m), 3.92-3.81 (3H, m), 3.79 (1H, dd, $J$ = 10.0, 3.1 Hz), 3.73 (2H, d, $J$ = 5.8 Hz), 3.29 (2H, t, $J$ = 6.4 Hz), 2.72 (1H, dd, $J$ = 15.1, 10.8 Hz), 2.63 (1H, dd, $J$ = 15.0, 4.2 Hz), 2.02-1.89 (2H, m), 1.71-1.61 (2H, m); **$^{13}$C NMR** (126 MHz, $D_2O$) $\delta_{ppm}$ 181.2, 173.7, 171.6, 171.1, 169.5, 73.1, 72.5, 69.5, 68.9, 67.5, 61.0, 53.0, 43.3, 42.5, 42.4, 38.5, 32.3, 28.1, 23.2. **ESI-MS** *m*/*z* calcd for $C_{19}H_{33}N_5O_{11}$ $[M + H]^+$: 508.23; $[M + Na]^+$: 530.21. Found 508.24, 530.22.

**{[(S)-*N*δ-[2`-(α-D-galactopyranosyl)-ethan-1`-amido]-α,γ-diaminopentyric-1-amido]-glycinamido-glycinamido}$_2$-glycine (226)**



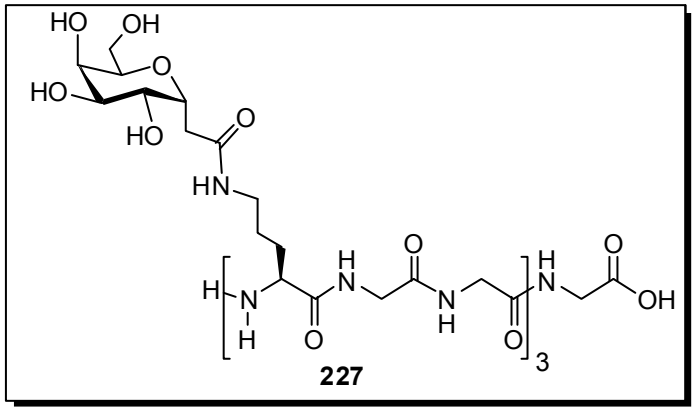
**226**

Peptide **226** was prepared using 100 mg of Wang resin according to standard Fmoc protocols (0.061 mmol scale) using building block **320**.[7] The peptide was cleaved off the bead as described above and purified through RP-HPLC under the conditions described above. The bulk of the acetonitrile was removed, and the remaining solvent was removed through lyophilization to yield 20 mg (0.021 mmol) of the dimer as a white powder in 35 % yield.

**$^1$H NMR** (500 MHz, $D_2O$) $\delta_{ppm}$ 4.45 (2H, dt, $J$ = 10.2, 5.0 Hz), 4.32 (1H, ddd, $J$ = 9.1, 5.2, 5.4 Hz), 4.05-3.83 (12H, m), 3.81-3.77 (3H, m), 3.75-3.69 (4H, m), 3.68-3.59 (4H, m), 3.20 (4H, dd, $J$ = 13.6, 6.8 Hz), 2.64 (2H, dd, $J$ = 14.9, 10.8 Hz), 2.56 (2H, dd, $J$ = 14.7, 5.5 Hz), 1.89-1.64 (4H, m), 1.63-1.49 (4H, m); **$^{13}$C NMR** (126 MHz, $D_2O$) $\delta_{ppm}$ 179.8, 173.6, 173.51, 173.49, 171.8, 171.6, 171.5, 171.3, 171.0, 72.9, 72.9, 72.5, 72.4, 69.5, 69.5, 68.7, 68.7, 67.4, 67.4, 60.83, 60.78, 53.6, 53.2, 43.2, 43.1, 42.5, 42.3, 42.2, 38.65, 38.60, 32.3, 32.3, 28.3, 28.0, 24.7, 24.1. **ESI-MS** *m*/*z* calcd for $C_{36}H_{61}N_9O_{20}$ $[M + H]^+$: 940.41; $[M + K]^+$: 978.37. Found: 940.64, 978.59.

**{[(S)-*N*δ-[2`-(α-D-galactopyranosyl)-ethan-1`-amido]-α,γ-diaminopentyric-1-amido]-glycinamido-glycinamido}$_3$-glycine (227)**

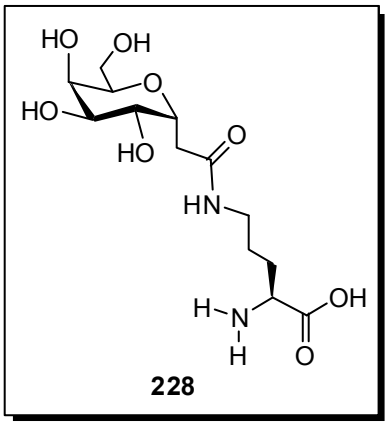
Peptide X was prepared using 100 mg of Wang resin according to standard Fmoc protocols (0.061 mmol).[7] The peptide was cleaved off the bead as described above and purified through RP-HPLC under the conditions described above. The bulk of the acetonitrile was removed, and the remaining solvent was removed through lyophilization to yield 26 mg (0.019 mmol) of the dimer as a white powder in 31 % yield.



**227**

**$^1$H NMR** (500 MHz, $D_2O$) $\delta_{ppm}$ 4.45 (3H, ddd, $J$ = 10.7, 5.2, 5.2 Hz), 4.35-4.27 (2H, m), 4.04-3.89 (18H, m), 3.79 (3H, t, $J$ = 6.0 Hz), 3.76-3.68 (6H, m), 3.67-3.62 (6H, m), 3.23-3.16 (6H, m), 2.63 (3H, dd, $J$ = 14.8, 10.8 Hz), 2.55 (3H, dd, $J$ = 15.0, 4.4 Hz), 1.90-1.78 (3H, m), 1.77-1.66 (3H, m), 1.65-1.43 (6H, m); **$^{13}$C NMR** (126 MHz, $D_2O$) $\delta_{ppm}$ 181.0, 173.7, 173.6, 171.9, 171.5, 171.4, 171.3, 171.1, 72.9, 72.6, 72.5, 69.6, 68.7, 67.5, 60.9, 60.8, 53.7, 52.9, 42.9, 42.5, 42.4, 42.3, 38.7, 38.5, 32.4, 28.0, 24.8, 23.9. **ESI-MS** *m*/*z* calcd for $C_{19}H_{33}N_5O_{11}$ $[M + H]^+$: 508.50; $[M + K]^+$: 530.48. Found: 508.24, 530.22.

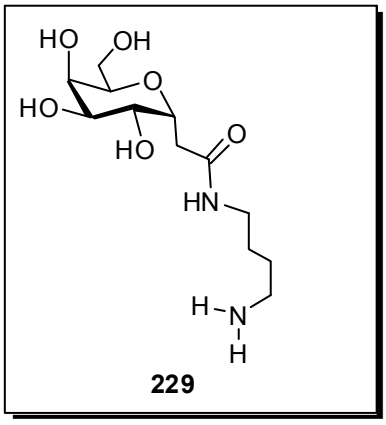
***N*-[(4*S*)-4-amino-4-carboxybutyl)-2-(α-D-galactopyranosyl)ethylamide (228)**



**228**

Acetlyated building block **320** (100.2 mg, 0.138 mmol), prepared according to previously published protocols,[9] was dissolved in 3 mL of methanol, 1 mL of water, and 2 mL of diethyl ether with stirring. Piperidine (1 mL, 10.1 mmol) was added and the mixture was allowed to stir for 20 minutes. At this point, 6N NaOH (1 mL) was added and the reaction mixture was allowed to stir for an addition 5 hours. The two phases were separated and the aqueous phase was washed twice with diethyl ether. The aqueous layer was concentrated and redissolved in minimum TFA. Ether was added until te solution became cloudy and the solution was allowed to stand at 4 ºC for 12 hours. The precipitate was collected by filtration, redissolved in water and lyophilized to yield 34 mg of the title compound as a white powder (73 % yield).
**$^1$H NMR** (400 MHz, *$D_2O$*) $\delta_{ppm}$ 4.49 (1H, ddd, *J* = 10.5, 5.9, 4.8 Hz), 4.02 (1H, dd, *J* = 9.9, 6.0 Hz), 3.98 (1H, dd, *J* = 3.2, 1.5 Hz), 3.82 (1H, ddd, *J* = 6.3, 5.0, 1.0 Hz), 3.77-3.72 (2H, m), 3.70 (1H, d, *J* = 6.7 Hz), 3.69 (1H, d, *J* = 5.3 Hz), 3.25 (2H, t, *J* = 6.8 Hz), 2.67 (1H, dd, *J* = 14.9, 10.6 Hz), 2.59 (1H, dd, *J* = 15.0, 4.5 Hz), 1.95-1.79 (2H, m), 1.70-1.50 (2H, m); **$^{13}$C NMR** (101 MHz, *$D_2O$*) $\delta_{ppm}$ 181.5, 174.6, 73.0, 72.6, 69.6, 68.8, 67.6, 60.9, 54.4, 28.8, 32.4, 27.8, 24.3.
**ESI-MS** *m*/*z* calcd for $C_{13}H_{24}N_2O_8$ $[M + H]^+$: 337.16; $[M + Na]^+$: 359.14; $[M + K]^+$: 375.12. Found: 337.18, 359.18, 375.20.

**N-(4-aminobutyl)-2-(α-D-galactopyranosyl)ethylamide (hydrochloride) (229)**



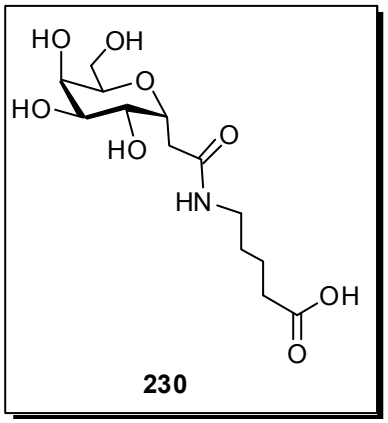
**229**

N-[(4-*tert*-butoxycarbonylamino)butyl]-2-(α-D-galactopyranosyl)ethylamide, **724**, (90 mg, 0.230 mmol) was dissolved in 2 mL of TFA to which 2 mL of DCM was added. The reaction was stirred for 3 hours at ambient temperature and concentrated under a flow of air and was reduced to a brown residue. This residue was triturated four times with diethyl ether and formed a yellow paste. NMR analysis showed complete removal of the Boc protecting group. The paste was resuspended in 50 % HCl

and stirred for 10 minutes. The reaction mixture was concentrated under reduced pressure, resuspended in water and lyophilized to provide 31 mg (0.0945 mmol) of the title salt as an off-white solid in 41 % yield.

**$^1$H NMR** (400 MHz, *$D_2O$*) $\delta_{ppm}$ 4.44 (1H, ddd, *J* = 10.5, 5.8, 4.5 Hz), 3.98 (1H, dd, *J* = 9.9, 6.1 Hz), 3.93 (1H, dd, *J* = 3.3, 1.5 Hz), 3.78 (1H, dt, *J* = 6.1, 1.4 Hz), 3.70 (1H, dd, *J* = 9.9, 3.3 Hz), 3.65 (1H, d, *J* = 6.2 Hz), 3.64 (1H, d, *J* = 5.9 Hz), 3.19 (2H, bt, *J* = 6.8 Hz), 2.95 (2H, bt, *J* = 7.4 Hz), 2.63 (1H, dd, *J* = 15.0, 10.6 Hz), 2.54 (1H, dd, *J* = 15.0, 4.4 Hz), 1.77-1.58 (2H, m), 1.58-1.48 (2H, m); **$^{13}$C NMR** (101 MHz, *$D_2O$*) $\delta_{ppm}$ 172.5, 71.8, 71.4, 68.5, 67.6, 64.9, 59.7, 37.9, 37.5, 31.2, 34.3, 23.0. **ESI-MS** *m/z* calcd for $C_{12}H_{24}N_2O_6$ $[M + H]^+$: 293.17. Found: 293.16.

**_N_-(4-carboxybutyl)-2-(α-D-galactopyranosyl)ethylamide (230)**

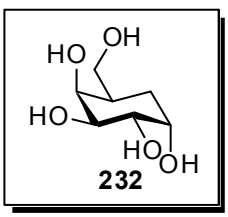


**230**

Carboxylic acid **727** (20 mg, 0.041 mmol) was dissolved in 5 mL of 0.1 M NaOMe in methanol and stirred for 12 hours. The reaction was quenched with 10 % HCl and the reaction mixture was concentrated under reduced pressure and purified using preperatory TLC (3:1:1:1, ethyl acetate: methanol: water: acetonitrile). The eluted product was redissolved in water and and lyophilized providing 12 mg (0.037 mmol) of the title compound as white powder (91 % yield).

**$^1$H NMR** (500 MHz, *$D_2O$*) $\delta_{ppm}$ 4.44 (1H, ddd, *J* = 10.6, 5.9, 4.3 Hz), 3.98 (1H, dd, *J* = 9.9, 6.1 Hz), 3.95 (1H, dd, *J* = 3.3, 1.4 Hz), 3.78 (1H, dt, *J* = 6.1, 1.3 Hz), 3.71 (1H, dd, *J* = 9.9, 3.3 Hz), 3.64 (1H, d, *J* = 6.7 Hz), 3.64 (1H, d, *J* = 5.4 Hz), 3.20-3.14 (2H, m), 2.63 (1H, dd, *J* = 14.9, 10.9 Hz), 2.54 (1H, dd, *J* = 15.0, 4.1 Hz), 2.26 (2H, t, *J* = 7.2 Hz), 1.60-1.51 (2H, m), 1.52-1.44 (2H, m); **$^{13}$C NMR** (75 MHz, *$H_2O$*) $\delta_{ppm}$ 183.3, 173.4, 72.9, 72.4, 69.6, 68.7, 67.5, 60.7, 39.2, 36.9, 32.3, 28.1, 23.1. **ESI-MS** *m/z* calcd for $C_{13}H_{23}N_1O_8$ $[M + H]^+$: 322.15; $[M + Na]^+$: 344.13. Found: 322.22, 344.19. **Rf** = 0.58 (3:1:1:1, ethyl acetate: water: methanol: acetonitrile).

**5a-Carba-α-galactopyranose (232)**



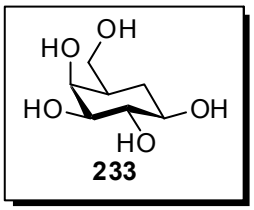
**232**

Racemic acetylated derivative **854** (5.4 g, 13.9 mmol) was dissolved in 50 mL of 0.1 M sodium methoxide in methanol. The reaction mixture was

allowed to stir for seventy-two hours and was neutralized with 5 % HCl to pH 3. Solvent was removed under reduced pressure and the product dried *in vacuo* to provide 2.5 g of the carbasugar in quantitative yield as a white powder. Spectral data is consistent with published data.[10]

**$^1$H NMR** (400 MHz, $D_2O$) $\delta_{ppm}$ 4.09 (2H, bd, $J$ = 7.6 Hz), 3.73-3.69 (2H, m), 3.64 (1H, dd, $J$ = 10.9, 7.9 Hz), 3.50 (1H, dd, $J$ = 11.0, 6.4 Hz), 2.07-1.94 (1H, m), 1.66 (1H, td, $J$ = 14.1, 3.7 Hz), 1.54 (1H, dt, $J$ = 13.7, 2.3 Hz); **$^{13}$C NMR** (101 MHz, $D_2O$) $\delta_{ppm}$ 71.1, 70.9, 69.9, 68.9, 62.4, 36.1, 27.5. **ESI-MS** *m*/*z* calcd for $C_7H_{14}O_5$ $[M + Na]^+$: 201.07. Found: 201.19.

**5a-carba-β-galactopyranose (233)**

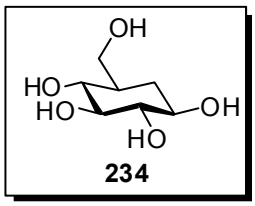


**233**

Racemic acetylated carbasugar **860** (25 mg, 0.064 mmol) was dissolved in 4 mL of 0.1 M sodium methoxide in methanol. The reaction mixture was allowed to stir for four hours and was neutralized with DOWEX 50WX8 (50-100 mesh) ion exchange resin, stirred for 5 minutes and filtered. Solvent was removed under reduced pressure and the product was then dried *in vacuo* to provide 11 mg of carbasugar **233** in quantitative yield as a white powder. Spectral data is consistent with published data.[10]

**$^1$H NMR** (500 MHz, $D_2O$) $\delta_{ppm}$ 3.99 (1H, dd, $J$ = 2.6, 2.6 Hz), 3.61 (1H, dd, $J$ = 10.9, 7.6 Hz), 3.53-3.46 (3H, m), 3.39 (1H, dd, $J$ = 9.4, 3.1 Hz), 1.78-1.69 (2H, m), 1.33 (1H, ddd, $J$ = 13.0, 13.0, 12.8 Hz); **$^{13}$C NMR** (126 MHz, $D_2O$) $\delta_{ppm}$ 74.7, 74.0, 71.7, 69.3, 62.1, 38.3, 28.7. **ESI-MS** *m*/*z* calcd for $C_7H_{14}O_5$ $[M + Na]^+$: 201.07; $[M + NH_4]^+$: 196.12; $[2M + Na]^+$: 379.16. Found 201.12, 196.15, 379.22.

**5a-Carba-β-glucopyranose (234)**



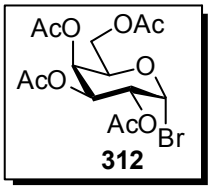
**234**

5a-carba-(1,2,3,4,6-penta-*O*-acetyl)-β-glucopyranose (**853**) (400 mg, 1.03 mmol) was dissolved in 15 mL of 0.1 M sodium methoxide in methanol. The reaction mixture was allowed to stir for four hours and was neutralized with 10 % HCl to pH < 7. Solvent was removed under reduced pressure, and the product was recrystallized from methanol to yield 165 mg of the title compound in 90 % yield. Spectral data is consistent with the literature.[10]

**$^{1}$H NMR** (400 MHz, *$D_2O$*) $\delta_{ppm}$ 3.74 (1H, dd, *J* = 11.2, 3.6 Hz), 3.62 (1H, dd, *J* = 11.2, 6.1 Hz), 3.55 (1H, ddd, *J* = 11.5, 8.8, 4.8 Hz), 3.32-3.18 (3H, m), 1.98 (1H, ddd, *J* = 13.0, 4.6, 3.7 Hz), 1.67-1.55 (1H, m), 1.25 (1H, ddd, *J* = 12.8, 12.8, 12.8 Hz); **$^{13}$C NMR** (101 MHz, *$D_2O$*) $\delta_{ppm}$ 76.9, 76.7, 72.5, 71.0, 62.1, 40.0, 31.6. **ESI-MS** *m*/*z* calcd for $C_7H_{14}O_5$ $[M + Na]^+$: 201.07. Found: 201.12.

# Experimental Protocols for Chapter 3

### 2,3,4,6-Tetra-*O*-acetyl-α-D-galactopyranosylbromide (312)

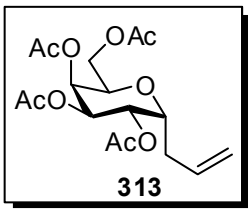


312

Into a flame-dried round bottomed flask under an argon atmosphere at 0ºC was added galactose pentacetate (**311**) (8.00 g, 20.5 mmol). 60 mL of 33% HBr in acetic acid was added portionwise under vigorous stirring over 10 minutes. The reaction was stirred for 1 hour and diluted with water (150 mL) and dichloromethane (150 mL) and the phases were separated. The organic layer was then successively washed with water (150mL x 2), saturated sodium bicarbonate (100 mL) and brine (100 mL). The organic phase was dried and co-evaporated with toluene (2x 15 mL). The residue was then dissolved in boiling diethyl ether followed by a slow addition of hexanes to the point that the solution became cloudy. The flask was then left to stand at 4 ºC for 2 hours. The title compound was recovered following filtration through a sintered glass frit and drying *in vacuo* (8.02 g, 97%). The compound decomposes readily at room temperature or under atmospheric conditions over 48 hours but can be stored indefinitely under argon at -20 ºC. Spectrum is consistent with published data.[11]

**$^{1}$H NMR** (400 MHz, *$CDCl_3$*) $\delta_{ppm}$ 6.70 (1H, d, *J* = 4.0 Hz), 5.52 (1H, dd, *J* = 3.3, 1.3 Hz), 5.41 (1H, dd, *J* = 10.7, 3.3 Hz), 5.05 (1H, dd, *J* = 10.7, 4.0 Hz), 4.49 (1H, dt, *J* = 6.7, 6.5, 0.5 Hz), 4.19 (1H, dd, *J* = 11.4, 6.3 Hz), 4.11 (1H, dd, *J* = 11.4, 6.8 Hz), 2.15 (3H, s), 2.12 (3H, s), 2.06 (3H, s), 2.02 (3H, s); **$^{13}$C NMR** (101 MHz, *$CDCl_3$*) $\delta_{ppm}$ 170.3, 170.0, 169.8, 169.7, 88.1, 71.0, 68.0, 67.7, 66.9, 60.8, 20.7, 20.7, 20.55, 20.53. **Rf**= 0.26 (9:1, toluene: ethyl acetate)

### 3-(2,3,4,6-Tetra-*O*-acetyl-α-D-galactopyranosyl)-prop-1-ene (313)



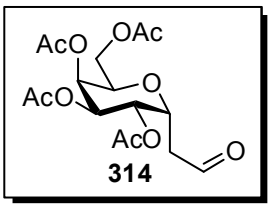
313

Bromosugar **312** (7.00 g, 17.0 mmol) was added to a round-bottomed flask equipped with a magnetic stir-bar and dissolved in 18 mL ACS grade dichloromethane. The flask is sealed with a septum equipped with an outlet to a bubbler. 15.4 mL of allyl tributyl tin was added followed by slow addition of 2 mL of 1.0 M triethylborane. Air was then slowly bubbled into the reaction mixture using a syringe pump (180 mL/10 hours). After 10 hours, NMR analysis showed the reaction had progressed to completion (>99% conversion), and the reaction

mixture was diluted with 40 mL of acetonitrile and 40 mL of petroleum ether and the phases were separated. The acetonitrile phase was washed thrice further with petroleum ether and then concentrated to give a colourless clear gel that solidified upon extended standing to yield the title compound as a white solid (5.10 g, 80%). If necessary, residual bromosugar can be removed through column chromatography (6:3:1 toluene: petroleum ether: ethyl acetate). Spectra are consistent with published data.[12]

**$^1$H NMR** (400 MHz, *$CDCl_3$*) $\delta_{ppm}$ 5.75 (1H, tdd, *J* = 10.1, 7.1, 6.5 Hz), 5.42 (1H, dd, *J* = 3.0, 2.5 Hz), 5.27 (1H, dd, *J* = 9.3, 5.0 Hz), 5.21 (1H, dd, *J* = 9.3, 3.3 Hz), 5.13 (1H, ddd, *J* = 17.2, 3.1, 1.4 Hz), 5.11 (1H, ddd, *J* = 10.6, 2.7, 1.3 Hz), 4.30 (1H, dt, *J* = 9.8, 4.8 Hz), 4.20 (1H, dd, *J* = 12.7, 8.9 Hz), 4.12-4.05 (2H, m), 2.52-2.41 (1H, m), 2.33-2.22 (1H, m), 2.12 (3H, s), 2.07 (3H, s), 2.04 (3H, s), 2.03 (3H, s); **$^{13}$C NMR** (101 MHz, *$CDCl_3$*) $\delta_{ppm}$ 170.6, 170.1, 169.9, 169.8, 133.3, 117.7, 71.4, 68.3, 68.3, 67.9, 67.6, 61.4, 30.9, 20.8, 20.78, 20.72, 20.72, 20.66. Rf= 0.25 (9: 1 toluene: ethyl acetate). **ESI-MS** *m/z* calcd for $C_{17}H_{24}O_9$ $[M + H]^+$: 373.15; $[M+Na]^+$: 395.13; $[M+K]^+$: 411.11. Found 373.19, 395.17, 411.16. **Rf** = 0.25 (3:1 hexanes: ethyl acetate)

**2-(2,3,4,6-Tetra-*O*-acetyl-α-D-galactopyranosyl)-ethanal (314)**



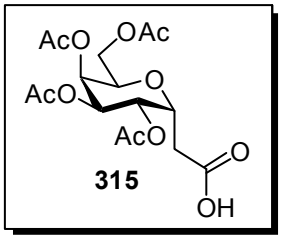
**314**

Allyl Sugar **313** (5.50 g, 14.8 mmol) was dissolved in DCM and cooled to -78 ºC. An oxygen/ozone gas mixture was bubbled through the solution until a deep royal blue colour persisted. argon was then bubbled through the solution until the solution turned clear. Triphenylphosphine (10.0 g, 38.1 mmol) was then added to quench the ozonide, and the reaction mixture stirred uncovered at room temperature for 18h. The solvent was removed under reduced pressure, and the residue dissolved in ether and allowed to stand for 1 hour. The solid triphenylphosphine oxide was removed by filtration, and the filtrate was concentrated and purified by flash chromatography (9: 1 hexanes: ethyl acetate to remove triphenylphosphine, product eluted 1: 1 Hexanes: ethyl acetate), concentrated and dried *in vacuo* to obtain the title compound as a colourless syrup (5.1 g, 92%). Spectral data is consistent with that in the literature.[9]

**$^1$H NMR** (400 MHz, *$CDCl_3$*) $\delta_{ppm}$ 9.76-9.71 (1H, dd, *J* = 2.5, 1.4 Hz), 5.43 (1H, t, *J* = 3.1 Hz), 5.29 (1H, dd, *J* = 8.5, 4.8 Hz), 5.18 (1H, dd, *J* = 8.5, 3.3 Hz), 4.87 (1H, ddd, *J* = 7.9, 5.7, 4.9 Hz), 4.33 (1H, ddd, *J* = 9.7, 6.7, 4.6 Hz), 4.16-4.07 (2H, m), 2.78-2.65 (2H, m), 2.12 (3H, s),

2.07 (3H, s), 2.06 (6H, s); **$^{13}$C NMR** (101 MHz, *CDCl$_3$*) $\delta_{ppm}$ 198.5, 170.5, 169.8, 169.6, 169.5, 69.3, 67.6, 67.5, 66.8, 66.5, 60.7, 41.5, 20.43, 20.41, 20.38, 20.36. **Rf**= 0.3 (4:1, toluene: ethyl acetate).

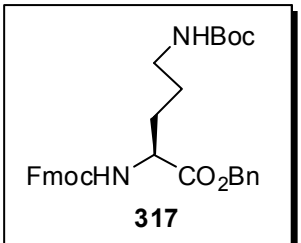
**2-(2,3,4,6-Tetra-*O*-acetyl-α-D-galactopyranosyl)-ethanoic acid (315)**



**315**

Allyl sugar **314** (6.01 g, 16.1 mmol) was suspended in a mixture of water (60 mL), acetonitrile (40 mL) and DCM (40 mL) with vigorous stirring. Sodium periodate (20 g, 97 mmol) was added as was ruthenium trichloride (67 mg, 0.32 mmol) and the mixture was stirred for 1 hour. The reaction was deemed complete by TLC analysis, and the solution was filtered through a celite pad, acidified with 10% HCl, diluted with ethyl acetate, and the organic phase was extracted. This phase was then washed with brine, dried and concnetrated, and further dried *in vacuo* in the presence of phosphorous pentoxide to yield 4.62 g of the title compound as white crystals (73 % yield). The compound was then stored in a dessicator until needed.[a] Spectral data is consistent with that in the literature.[9]
**$^{1}$H NMR** (400 MHz, *CDCl$_3$*) $\delta_{ppm}$ 5.43 (1H, t, *J* = 2.9 Hz), 5.33 (1H, dd, *J* = 8.9, 5.0 Hz), 5.17 (1H, dd, *J* = 8.9, 3.3 Hz), 4.70 (1H, td, *J* = 9.0, 5.3 Hz), 4.24 (1H, dd, *J* = 10.1, 6.4 Hz), 4.18-4.08 (2H, m), 2.72 (1H, dd, *J* = 15.6, 8.8 Hz), 2.63 (1H, dd, *J* = 15.6, 5.6 Hz), 2.12 (3H, s), 2.07 (3H, s), 2.04 (6H, s); **$^{13}$C NMR** (101 MHz, *CDCl$_3$*) $\delta_{ppm}$ 175.0, 170.7, 170.0, 169.9, 169.6, 69.2, 68.8, 67.8, 67.5, 67.1, 61.1, 33.0, 20.6, 20.5, 20.5, 20.5. **ESI-MS** *m/z* calcd for $C_{16}H_{22}O_{11}$ $[M+H]^+$: 391.12; $[M+NH_4]^+$: 408.15; $[M+Na]^+$: 413.11. Found: 391.17, 408.17, 413.14.

**(*S*)-benzyl 1-(9H-fluoren-9-yl)-12,12-dimethyl-3,10-dioxo-2,11-dioxa-4,9-diazatridecane-5-carboxylate (Fmoc-Orn(Boc)-OBn) (317)**



**317**

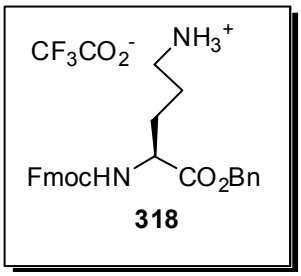
Commercially available *N*-(*S*)-[(9H-fluoren-9-ylmethoxy)carbonyl]ornithine (**316**) (2.5 g, 5.5 mmol) was dissolved

[a] Hydroscopic compound that readily forms a gel when exposed to air for several minutes.

in anhydrous DCM (45 mL) under an argon atmosphere. Carbonyl diimidazole (CDI, 0.98 g, 5.9 mmol) was added and the reaction mixture was allowed to stir for 40 minutes. Benzyl alcohol (0.62 mL, 5.5 mmol) was then added and the reaction was continued for an additional 12 hours. The mixture was then diluted with DCM, and the organic phases were washed with saturated ammonium carbonate and brine successively. The organic phase was dried and concentrated in the usual manner. The crude product was then further purified through flash chromatography (50: 1 DCM: methanol) to provide 2.8 g of benzyl protected **317** as a thick clear oil (93 %). Spectral data is in accordance with the literature.[13]

**$^1$H NMR** (400 MHz, *$CDCl_3$*) $\delta_{ppm}$ 7.77 (2H, *pseudo*-d, *J* = 7.5 Hz), 7.60 (2H, *pseudo*-d, *J* = 7.3 Hz), 7.43-7.28 (9H, m), 5.44 (1H, d, *J* = 8.2 Hz), 5.21 (1H, d, *J* = 12.3 Hz), 5.17 (1H, d, *J* = 12.3 Hz) 4.40 (2H, d, *J* = 7.1 Hz), 4.54-4.36 (2H, m), 4.21 (1H, t, *J* = 7.0 Hz), 3.15-3.06 (2H, m), 1.94-1.83 (1H, m), 1.74-1.65 (1H, m), 1.51-1.49 (2H, m) 1.44 (9H, s). **Rf** = 0.86 (2:1 ethyl acetate: hexanes).

**Benzyl-*N*-(*S*)-[(9H-fluoren-9-ylmethoxy)carbonyl]ornithine · TFA (Fmoc-Orn(TFA)-OBn) (318)**

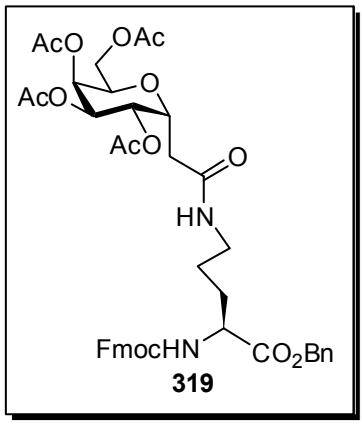


**318**

Boc-protected derivative **317** (2.5 g, 4.6 mmol) was dissolved in DCM (12.5 mL) to which was added TFA (12.5 mL). The reaction was stirred for 4 hours and then concentrated to dryness. The resulting salt was repeatedly co-evaporated with toluene and then dried *in vacuo* to provide 2.5 g of the product as white powder in quantitative yield.

**$^1$H NMR** (400 MHz, *MeOD*) $\delta_{ppm}$ 7.71 (2H, *pseudo*-d, *J* = 7.6 Hz), 7.56 (2H, *pseudo*-d, *J* = 7.1 Hz), 7.43-7.28 (9H, m), 5.12 (2H, bs), 4.39 (1H, dd, *J* = 10.2, 7.0 Hz), 4.32-4.23 (2H, m), 4.15 (1H, t, *J* = 6.7 Hz), 2.90-2.78 (2H, m), 1.91-1.78 (1H, m), 1.76-1.59 (3H, m); **$^{13}$C NMR (HCl salt)** (101 MHz, *MeOD*) $\delta_{ppm}$ 181.5, 153.31, 153.26, 150.3, 145.4, 138.0, 137.6, 137.3, 137.2, 16.6, 134.72, 134.67, 129.7, 75.6, 75.3, 63.1, 56.2, 47.9, 37.0, 33.4. **ESI-MS** *m/z* calcd for $C_{27}H_{29}N_2O_4^+$ $[M]^+$: 445.5. Found 445.5.

***N*-[(4*S*)-4-[*N*-(9H-fluoren-9-ylmethoxy)carbonyl]amino-5-benzyloxy-5-oxopentyl]-2-(2,3,4,6-tetra-*O*-acetyl-α-D-galactopyranosyl)ethylamide (319)**

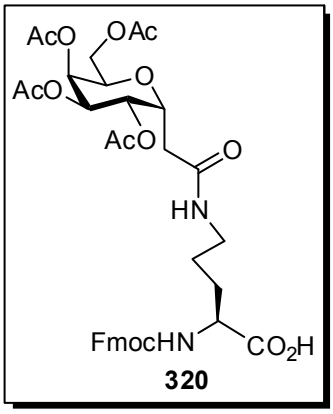


**319**

Carboxylic acid **315** (620 mg, 1.6 mmol) was dissolved in anhydrous DCM in the presence of freshly activated powdered 4 Å molecular sieves. HBTU (703 mg, 1.8 mmol) was added immediately and the reaction was allowed to stir at ambient temperature for 1 hour. At this point TFA salt **318** (1.04 g, 1.91 mmol) and DIPEA (700 μL, 7.28 mmol) were added and the reaction was stirred for an additional 16 hours. The reaction mixture was diluted with DCM, filtered through a celite pad and the organic phase was washed with 10 % HCl, saturated sodium bicarbonate and brine sequentially. The combined organics were dried in the usual fashion and following removal of solvent, the crude product was purified through flash chromatography (1:1 to 3:1 ethyl acetate to hexanes) to provide 1.01 g of protected glycoconjugate **319** as a white amorphous solid in 78 % yield. Spectral data is consistent with the literature.[9]

**$^1$H NMR** (400 MHz, *$CDCl_3$*) $\delta_{ppm}$ 7.76 (2H, *pseudo*-d, *J* = 7.6 Hz), 7.59 (2H, *pseudo*-d, *J* = 7.0 Hz), 7.43-7.27 (9H, m), 6.15 (1H, t, *J* = 5.4 Hz), 5.56 (1H, d, *J* = 8.0 Hz), 5.40 (1H, t, *J* = 3.0 Hz), 5.26 (1H, dd, *J* = 8.3, 4.6 Hz), 5.18 (2H, d, *J* = 3.7 Hz), 5.15 (1H, dd, *J* = 8.3, 3.3 Hz), 4.65 (1H, ddd, *J* = 8.9, 4.2, 4.2 Hz), 4.46-4.34 (3H, m), 4.30-4.18 (2H, m), 4.16-4.09 (2H, m), 3.26 (2H, dd, *J* = 12.3, 6.3 Hz), 2.51 (1H, dd, *J* = 15.3, 9.5 Hz), 2.38 (1H, dd, *J* = 15.5, 4.2 Hz), 2.11 (3H, s), 2.05 (3H, s), 2.04 (3H, s), 2.00 (3H, s), 1.95-1.83 (1H, m), 1.76-1.65 (1H, m), 1.63-1.47 (2H, m); **$^{13}$C NMR** (101 MHz, *$CDCl_3$*) $\delta_{ppm}$ 172.0, 170.6, 169.9, 169.8, 169.6, 169.2, 156.1, 143.9, 143.7, 141.3, 135.2, 128.7, 128.6, 125.4, 127.7, 127.1, 125.1, 120.0, 69.5, 68.8, 68.0, 67.8, 67.0, 66.9, 61.1, 53.6, 47.2, 38.9, 34.6, 30.1, 25.4, 20.73(x3), 20.66. **ESI-MS** *m*/*z* calcd for $C_{43}H_{48}N_2O_{14}$ $[M + Na]^+$: 839.3. Found 839.4. **Rf** = 0.38 (10:1, DCM: MeOH).

***N*-[(4*S*)-4-[*N*-(9H-fluoren-9-ylmethoxy)carbonyl]amino-4-carboxybutyl]-2-(2,3,4,6-tetra-*O*-acetyl-α-D-galactopyranosyl)ethylamide (320)**

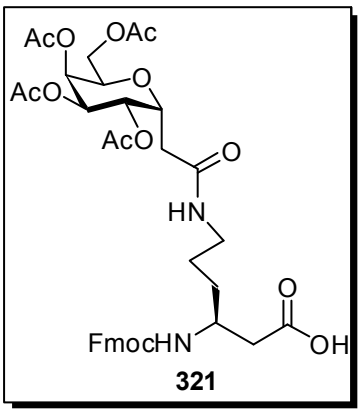


**320**

Glycoconjugate **319** (2.1 g, 2.6 mmol) was dissolved in 100 mL of a 1:1 mixture of ethanol and ethyl acetate. The solution was degassed with nitrogen, and Palladium on carbon (210 mg, 10 % w/w) was added. Hydrogen gas was bubbled through the solution for 1 hour, and the reaction was then maintained under a hydrogen atmosphere with stirring for an additional 12 hours. The solution was diluted with ethyl acetate and filtered through a celite pad. Following concentration, the crude product was purified through flash chromatography (10: 1 DCM: methanol) to provide 1.72 g of **320** as a white powder in 91 % yield. Spectral information is consistent with published data.[9]

**$^1$H NMR** (400 MHz, *$(CD_3)_2CO$*) $\delta_{ppm}$ 7.84 (2H, *pseudo*-d, *J* = 7.4 Hz), 7.70 (2H, dd, *J* = 6.8, 5.9 Hz), 7.39 (2H, *pseudo*-dd = 7.4, 7.4 Hz), 7.31 (2H, ddd, *J* = 7.5, 7.5, 1.0 Hz), 5.36 (1H, dd, *J* = 3.0, 2.6 Hz), 5.25 (1H, dd, *J* = 9.7, 5.2 Hz), 5.19 (1H, dd, *J* = 9.7, 3.3 Hz), 4.71 (1H, ddd, *J* = 9.1, 5.4, 5.4 Hz), 4.34 (1H, dd, *J* = 10.2, 7.4 Hz), 4.29-4.16 (4H, m), 4.10 (2H, d, *J* = 6.4 Hz), 3.28-3.20 (2H, m), 2.70 (1H, dd, *J* = 14.8, 8.9 Hz), 2.54 (1H, dd, *J* = 14.8, 5.4 Hz), 2.08 (3H, s), 2.00 (3H, s), 1.95 (6H, s), 1.93-1.84 (1H, m), 1.79-1.56 (3H, m); **$^{13}$C NMR** (101 MHz, *$(CD_3)_2CO$*) $\delta_{ppm}$ 171.9, 171.44, 171.39, 171.38, 171.38, 155.9, 143.1, 141.9, 129.5, 129.0, 17.20, 127.16, 121.8, 71.8, 70.6, 69.7, 69.5, 69.5, 68.2, 63.1, 55.6, 49.0, 40.5, 35.6, 30.9, 27.9, 21.7 (x3), 21.5. **ESI-MS** *m*/*z* calcd for $C_{36}H_{42}N_2O_{14}$ $[M + H]^+$: 727.27; $[M + Na]^+$: 749.22. Found 727.36, 749.31. **Rf** = 0.23 (9:1, DCM: MeOH).

**_N_-[(4_S_)-4-[_N_-(9H-fluoren-9-ylmethoxy)carbonyl]amino-5-carboxypentyl]-2-(2,3,4,6-tetra-_O_-acetyl-α-D-galactopyranosyl)ethylamide (Fmoc-βOrn-(GalOAc$_4$)-OH) (321)**



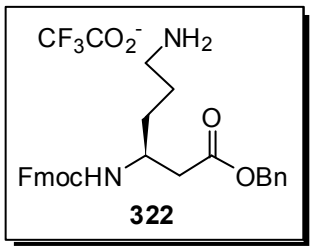
**321**

Method A: Diazo glycoconjugate **324** (216 mg, 0.288 mmol) was dissolved in a solution of water (7 mL) in dioxane (14 mL) along with catalytic silver benzoate (5 mg, 0.022 mmol) in a flask equipped with a water-cooled condenser. The reaction was heated to 72 ºC for 5 hours. The reaction was cooled to ambient temperature,

diluted with ethyl acetate, and passed through a celite pad. The reaction was then washed with 10 % HCl and brine successively before being dried and concentrated in the usual fashion to provide 178 mg of **321** as a white powder in 84 % yield.[a]

Method B: Benzyl ester **329** (1.312 g, 1.58 mmol) was dissolved in 25 mL of a 1:1 (v/v) mixture of ethanol and ethyl acetate. Nitrogen gas was bubbled through the solvent for 15 minutes before charcoal supported palladium (140 mg) was added. Hydrogen gas was then bubbled through the solution for 1.5 hours, and the reaction was stirred under a hydrogen atmosphere for an additional 16 hours before being filtered through a celite pad. The filtrate was concentrated and purified by flash chromatography (15:1 to 9:1 DCM: methanol) to provide 199 mg of building block **321** in 94 % yield.

**$^1$H NMR** (400 MHz, *$(CD_3)_2CO$* ) $\delta_{ppm}$ 7.84 (2H, *pseudo*- , *J* = 7.5 Hz), 7.67 (2H, *pseudo*-dd, *J* = 7.1, 3.4 Hz), 7.39 (2H, *pseudo*-dd, *J* = 7.4, 7.4 Hz), 7.31 (2H, *pseudo*-dd, *J* = 7.5, 7.5 Hz), 5.36 (1H, dd, *J* = 3.0, 2.5 Hz), 5.25 (1H, dd, *J* = 9.7, 5.2 Hz), 5.19 (1H, dd, *J* = 9.7, 3.3 Hz), 4.71 (1H, td, *J* = 8.7, 5.4 Hz), 4.31 (1H, d, *J* = 7.6 Hz), 4.31 (1H, d, *J* = 6.2 Hz), 4.26 (1H, dt, *J* = 6.3, 6.3, 2.2 Hz), 4.20 (1H, dd, *J* = 7.0, 7.0 Hz), 4.10 (2H, d, *J* = 6.4 Hz), 4.02-3.93 (1H, m), 3.26 (2H, dd, *J* = 12.1, 6.1 Hz), 2.69 (1H, dd, *J* = 14.9, 8.9 Hz), 2.53 (1H, dd, *J* = 14.9, 5.5 Hz), 2.50 (1H, dd, *J* = 10.8, 6.7 Hz), 2.08 (3H, s), 2.00 (3H, s), 1.95 (3H, s), 1.95 (3H, s), 1.69-1.46 (4H, m); **$^{13}$C NMR** (101 MHz, *$(CD_3)_2CO$*) $\delta_{ppm}$ 174.9, 172.2, 172.1, 171.9, 1715, 171.4, 158.3, 145.4, 145.3, 142.6, 128.8, 128.2, 126.3, 126.2, 121.0, 71.2, 70.1, 69.3, 69.0, 68.9, 67.6, 62.5, 49.4, 48.5, 40.8, 40.3, 35.0, 33.2, 27.0, 20.75,20.69, 20.66, 20.56. **ESI-MS** *m/z* calcd for $C_{37}H_{44}N_2O_{14}$ $[M + Na]^+$: 763.27. Found 763.4. **Rf** = 0.31 (9:1 DCM: methanol).



**322**

**(S)-benzyl 3-(((9H-fluoren-9-yl)methoxy)carbonylamino)-6-amino hexanoate· Trifluoroacetic acid (Fmoc-βOrn(TFA)-OBn) (322)**

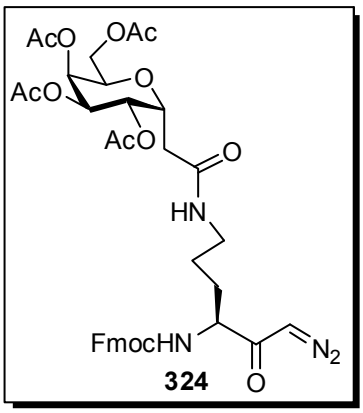
Boc-protected derivative **328** (3.00 g, 5.37 mmol) was dissolved in DCM (6 mL) and TFA (6 mL). The reaction was stirred at ambient temperature for 2 hours, then the solvent was removed under reduced pressure and the resulting residue was precipitated from ethanol and

[a] If necessary, the compound could be further purified by flash chromatography (20:1 to 9:1 DCM: methanol).

diethyl ether to provide 3.06 g of the TFA salt of **322** as a white powder (after drying *in vacuo*) in quantitative yield. Characterized as the HCl salt.[a]

**$^1$H NMR** (400 MHz, *$(CD_3)_2CO$* ) $\delta_{ppm}$ 7.86 (2H, *pseudo*-d, *J* = 7.5 Hz), 7.70 (2H, *pseudo*-d, *J* = 7.5 Hz), 7.43-7.28 (9H, m), 5.11 (2H, s), 4.30 (1H, d, *J* = 7.8 Hz), 4.30 (1H, d, *J* = 6.7 Hz), 4.20 (1H, t, *J* = 7.2, 7.2 Hz), 4.06 (1H, m), 3.78 (1H, ddd, *J* = 13.3, 6.7, 6.7 Hz), 3.70 (1H, ddd, *J* = 14.0, 7.1, 7.1 Hz), 2.65 (1H, dd, *J* = 15.2, 7.2 Hz), 2.59 (1H, dd, *J* = 15.3, 6.4 Hz), 1.98-1.91 (1H, m), 1.83-1.74 (1H, m), 1.74-1.67 (2H, m); **$^{13}$C NMR** (101 MHz, *DMSO-d6*) $\delta_{ppm}$ 170.5, 155.6, 143.8, 143.7, 140.6, 13.9, 128.3, 127.9, 127.8, 127.5, 127.0, 125.1, 125.0, 120.1, 65.5, 65.2, 47.4, 46.6, 39.2, 38.5, 31.1, 23.6. **ESI-MS** *m*/*z* calcd for $C_{28}H_{30}N_2O_4$ $[2M + H]^+$: 917.45. Found 917.4.

**_N_-[(4_S_)-4-[_N_-(9H-fluoren-9-ylmethoxy)carbonyl]amino-6-diazo-5-ketohexyl]-2-(2,3,4,6-tetra-_O_-acetyl-α-D-galactopyranosyl)ethylamide (Fmoc-Orn(GalOAc$_4$)-CHN$_2$) (324)**



**324**

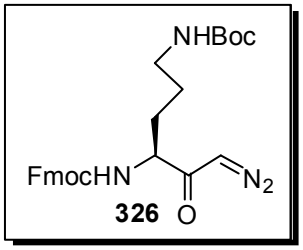
Diazomethane was prepared according to a modified version of the protocol by F. Arndt.[14] A 50 % potassium hydroxide was prepared by dissolving 20 g of KOH in 20 mL of water in an ice bath. The solution was transferred to a flame-polished, unscratched Erlenmeyer flask to which was added 120 mL of diethyl ether. The solution was cooled to 0 ºC, and 12.4 g of *N*-methyl-*N*-nitrosourea was added portion-wise with hand agitation only for stirring (WARNING: Diazomethane is highly toxic as is N-methyl-N-nitrosourea, and the former is also known to be highly explosive when isolated. It should never come into contact with sharp edges, all glassware and pipettes should be polished to remove scratches or sharp edges). Agitation was continued until the solid had fully dissolved, forming a biphasic solution with the yellow ethereal phase containing the diazomethane. In a second new Erlenmeyer flask was place 5 g of KOH pellets and a minimum amount of ether was added to

[a] Line broadening was found to be a serious concern with the resolution of the TFA salt spectra. HCl salt was produced by stirring a small sample of **322** in 4 M HCl for 2 hours before concnetrating to dryness.

cover the pellets. The ethereal phase was decanted into the second Erlenmeyer flask and any remaining organic phase was transferred through pipetting using a flame-polished pipette. The flask containing the organic phase was sealed with parafil and stored at 4 ºC for at least 4 hours prior to use. The aqueous phase was allowed to evaporate slowly over 42 hours, and was diluted and discarded.

Building block **320** (501 mg, 0.689 mmol) was dissolved in anhydrous THF (30 mL) under argon and the reaction was cooled to -20 ºC. Isobutyl chloroformate (105 µL, 110 mg, 0.805 mmol) and *N*-methylmorpholine (91 µL, 84 mg, 0.805 mmol) were added and the reaction was stirred for 1 hour. The reaction was then warmed to -15 ºC, and diazomethane was added dropwise until a deep yellow colour persisted, whereupon the reaction was allowed to warm to ambient temperature and allowed to stir for 2 hours. At this point excess diazaomethane was removed by bubbling nitrogen gas through the solvent until the solution became colourless and the quench was finished through the dropwise addition of 5 % acetic acid. Following quench, the reaction was diluted with water and ethyl acetate and the two phases were partitioned. The aqueous phase was extracted twice with ethyl acetate and the combined organics were washed with 10 % HCl, saturated sodium bicarbonate and brine successively followed by drying and concentration in the usual fashion to provide 568 mg of crude product as thick yellow paste. The crude product was purified through flash chromatography to provide 5.72 g of **324** in 80 % yield. **$^{1}$H NMR** (400 MHz, *$CDCl_3$*) $\delta_{ppm}$ 7.76 (2H, *pseudo*-d, *J* = 7.5 Hz), 7.60 (2H, *pseudo*-dd, *J* = 6.4, 6.4 Hz), 7.40 (2H, *pseudo*-dd, *J* = 7.3, 7.3 Hz), 7.31 (2H, ddd, *J* = 7.4, 7.4, 1.0 Hz), 6.26 (1H, t, *J* = 5.5 Hz), 5.73 (1H, d, *J* = 8.1 Hz), 5.46-5.42 (1H, m), 5.41 (1H, t, *J* = 3.1, 3.1 Hz), 5.25 (1H, dd, *J* = 8.3, 4.5 Hz), 5.15 (1H, dd, *J* = 8.4, 3.3 Hz), 4.66 (1H, ddd, *J* = 9.2, 4.3, 4.3 Hz), 4.49 (1H, dd, *J* = 10.4, 7.0 Hz), 4.40 (1H, dd, *J* = 10.6, 6.8 Hz), 4.30 (1H, dd, *J* = 9.9, 5.3 Hz), 4.32-4.24 (1H, m), 4.20 (1H, t, *J* = 6.6, 6.6 Hz), 4.18-4.10 (2H, m), 3.29 (2H, m), 2.55 (1H, dd, *J* = 15.4, 9.6 Hz), 2.40 (1H, dd, *J* = 15.5, 4.1 Hz), 2.11 (3H, s), 2.06 (3H, s), 2.04 (3H, s), 2.01 (3H, s), 1.90-1.78 (1H, m), 1.62-1.50 (3H, m); **$^{13}$C NMR** (101 MHz, *$CDCl_3$*) $\delta_{ppm}$ 193.5, 170.7, 170.0, 169.8, 169.7, 169.5, 156.2, 143.7, 141.4, 127.8, 127.12, 127.09, 125.1, 125.0, 120.0, 69.6, 68.8, 68.1, 67.8, 66.9, 66.8, 61.1, 47.3, 38.9, 34.6, 31.0, 29.9, 25.6, 20.8 (x3), 20.7. **ESI-MS** *m*/*z* calcd for $C_{37}H_{42}N_4O_{13}$ $[M + K]^+$: 789.24. Found 789.36. **Rf** = 0.77 (10:1 DCM: methanol).

**(S)-tert-butyl 4-[(9H-fluoren-9-ylmethoxy)carbonyl]amino-6-diazohexylcarbamate (Fmoc-Orn(Boc)-$CHN_2$) (326)**



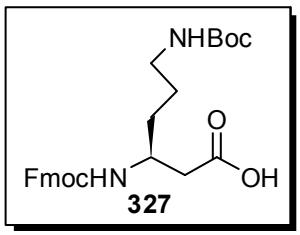
**326**

Diazomethane was produced according to protocol described for **324** above.

Fmoc-protected derivative **316** (7.00 g, 15.4 mmol) was dissolved in anhydrous THF (45 mL) under argon and the reaction was cooled to -20 ºC. Isobutyl chloroformate (2.4 mL, 2.53 g, 18.5 mmol) and *N*-methylmorpholine (2.0 mL, 1.87 g, 18.5 mmol) were added and the reaction was stirred for 35 minutes. The reaction was then warmed to -5 ºC, and diazomethane was added dropwise until a deep yellow colour persisted, whereupon the reaction was allowed to warm to ambient temperature and allowed to stir for 2 hours. At this point excess diazaomethane was removed by bubbling nitrogen gas through the solvent until the solution became colourless when the quench was finished through the dropwise addition of 5 % acetic acid. Following quench, the reaction was diluted with water and ethyl acetate and the two phases were partitioned. The aqueous phase was extracted twice with ethyl acetate and the combined organics were washed with 10 % HCl, saturated sodium bicarbonate and brine successively followed by drying and concentration in the usual fashion to provide 7.11 g of crude product as thick yellow paste. The crude product was purified through dry vacuum chromatography (100 % hexanes to 65 % hexanes in ethyl acetate in 3 % increments, elution at 70 % hexanes) to provide 5.72 g of **326** in 80 % yield. Spectral data is consistent with the literature.[15]

**$^1$H NMR** (400 MHz, *$CDCl_3$*) $\delta_{ppm}$ 7.76 (2H, *pseudo*-d, *J* = 7.5 Hz), 7.60 (2H, *pseudo*-dd, *J* = 7.1, 3.3 Hz), 7.40 (2H, *pseudo*-dd, *J* = 7.5, 7.5 Hz), 7.31 (2H, ddd, *J* = 7.4, 7.4, 1.0 Hz), 5.64 (1H, d, *J* = 6.7 Hz), 5.43 (1H, bs), 4.66-4.57 (1H, m), 4.50-4.36 (2H, m), 4.43 (1H, dd, *J* = 10.0, 7.0 Hz), 4.32-4.23 (1H, m), 4.20 (1H, t, *J* = 6.6 Hz), 3.25-3.07 (2H, m), 1.90-1.79 (1H, m), 1.60-1.47 (3H, m), 1.44 (9H, s); **$^{13}$C NMR** (101 MHz, *$CDCl_3$*) $\delta_{ppm}$ 193.4, 156.2, 156.1, 143.79, 143.77, 141.4, 127.7, 127.1, 125.15, 125.08, 120.0, 79.4, 66.8, 57.4, 66.8, 57.4, 47.3, 39.8, 29.6, 28.4, 26.3. **ESI-MS** *m/z* calcd for $C_{26}H_{30}N_4O_5$ $[M + Na]^+$: 501.21; $[M + K]^+$: 517.18. Found 501.13, 517.10.

**(S)-3-(((9H-fluoren-9-yl)methoxy)carbonylamino)-6-(tert-butoxycarbonylamino) hexanoate (Fmoc-β-Orn(Boc)-OH)**

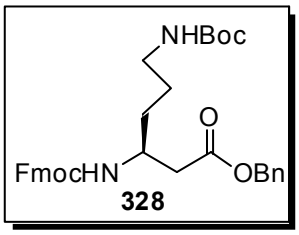


**327**

Diazo derivative **326** (5.71 g, 12.2 mmol) was dissolved in a solution of water (29.4 mL) in dioxane (130.3 mL) and silver benzoate (100 mg, 0.44 mmol) was added. The reaction was fitted with an air-cooled condenser and heated to 70 ºC for 6 hours. Upon cooling, the solution was passed through a celite pad prior to being diluted with ethyl acetate and washed with 10 % HCl. The acidic aqueous phase was extracted twice with ethyl acetate and the combined organic phases were then washed with brine before being dried and concentrated in the usual fashion to provide 5.43 g of amino acid **327** in 95 % yield.[a] Spectral data is conistent with literature.[15]

**$^1$H NMR** (400 MHz, *$(CD_3)_2CO$* ) $\delta_{ppm}$ 7.85 (2H, *pseudo*-d, *J* = 7.5 Hz), 7.69 (2H, *pseudo*-dd, *J* = 7.4, 1.7 Hz), 7.40 (2H, *pseudo*- dd, *J* = 7.4, 7.4 Hz), 7.32 (2H, ddd, *J* = 7.5, 7.5, 0.7 Hz), 6.46 (1H, d, *J* = 8.5 Hz), 5.94 (1H, bs), 4.32 (1H, d, *J* = 7.8 Hz), 4.32 (1H, d, *J* = 6.2 Hz), 4.22 (1H, t, *J* = 7.0 Hz), 4.05-3.93 (1H, m), 3.12-3.05 (2H, m), 2.58 (1H, dd, *J* = 15.5, 6.6 Hz), 2.51 (1H, dd, *J* = 15.6, 6.5 Hz), 1.69-1.48 (4H, m), 1.39 (9H, s); **$^{13}$C NMR** (101 MHz, *MeOD*) $\delta_{ppm}$ 175.0, 158.6, 158.4, 145.5, 145.3, 142.7, 142.6, 128.8, 128.2, 126.3, 126.2, 120.9, 79.9, 67.6, 49.9, 45.6, 41.1, 40.9, 33.0, 28.8, 27.7. **ESI-MS** *m/z* calcd for $C_{26}H_{32}N_2O_6$ $[M + Na]^+$: 491.21. Found 491.4. **Rf** = 0.23 (9:1 DCM: methanol).

**(S)-benzyl 3-(((9H-fluoren-9-yl)methoxy)carbonylamino)-6-(tert-butoxycarbonylamino) hexanoate (Fmoc-Orn(Boc)-OBn) (328)**



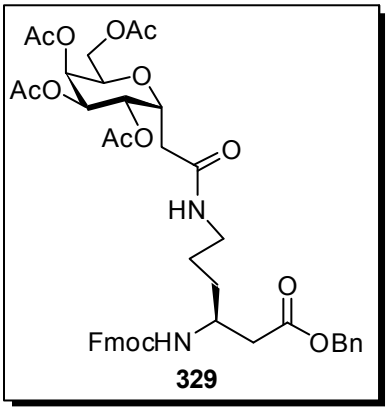
**328**

Carboxylic acid **327** (5.00 g, 10.7 mmol) and CDI (1.9 g, 11.8 mmol) were dissolved in anhydrous DCM (100 mL) under argon in the presence of freshly activated 4 Å powdered molecular sieves and stirred at ambient temperature for 40 minutes. Benzyl alcohol (1.3 g, 11.8 mmol) was added to the activated ester, and the solution was allowed to stir for an additional 12 hours. The

[a] In some trials the reaction did require further purification, in which case flash chromatography was used (9:1 to 8:2 DCM: methanol).

reaction was then diluted with ethyl acetate, filtered through celite, and washed successively with twice 10 % HCl, saturated sodium bicarbonate and brine then dried and concentrated in the usual manner. The crude product was immediately purified by flash chromatography (9:1 to 8:2 petroleum ether to ethyl acetate) to provide 5.133 g of **328** as a thick oil in 86 % yield.
**$^1$H NMR** (400 MHz, *CDCl$_3$*) $\delta_{ppm}$ 7.76 (2H, *pseudo*-d, *J* = 7.5 Hz), 7.58 (2H, *pseudo*-d, *J* = 7.4 Hz), 7.43-7.28 (9H, m), 5.28 (1H, d, *J* = 8.9 Hz), 5.12 (2H, s), 4.53 (1H, bs), 4.38 (2H, m), 4.19 (1H, t, *J* = 6.9 Hz), 4.03-3.95 (1H, m), 3.16-3.04 (2H, m), 2.59 (2H, t, *J* = 4.3, 4.3 Hz), 1.55-1.46 (3H, m), 1.46-1.38 (1H, m), 1.44 (9H, s); **$^{13}$C NMR** (101 MHz, *DMSO-d6*) $\delta_{ppm}$ 170.2, 155.5, 154.1, 143.7, 140.6, 128.8, 128.3, 128.3, 127.8, 127.8, 127.5, 127.2, 126.9, 125.1, 121.3, 120.0, 119.9, 79.5, 65.4, 65.1, 46.7, 44.7 42.7, 34.4, 31.5, 28.2, 26.1. **ESI-MS** *m*/*z* calcd for $C_{33}H_{38}N_2O_6$ $[M + Na]^+$: 581.26; $[M + K]^+$: 597.23. Found 581.4, 597.4.

**_N_-[(4_S_)-4-[_N_-(9H-fluoren-9-ylmethoxy)carbonyl]amino-5-benzyloxy-6-oxohexyl]-2-(2,3,4,6-tetra-_O_-acetyl-α-D-galactopyranosyl)ethylamide Fmoc-βOrn(GalOAc$_4$)-OBn (329)**.

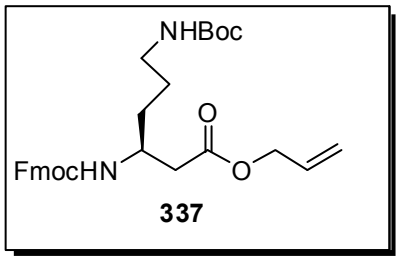


**329**

Protocol is a modified version of that published by Czechura et al.[9] Carboxylic acid **315** (1.00 g, 2.56 mmol) along with HCTU (1.16 g, 2.82 mmol) were added to a flask charged with argon and freshly activated powdered 4 Å molecular sieves. DCM (7.9 mL) was added to the flask and the reaction mixture was stirred for 20 minutes before amino acid **322** (1.90 g, 3.41 mmol) was added followed immediately by DIPEA (1.36 mL, 7.68 mmol) and the reaction was sealed under an argon atmosphere and allowed to stir for an additional 16 hours. The reaction was diluted with DCM, and was immediately filtered through a celite pad. The filtrate was washed with 10 % HCl, saturated sodium bicarbonate, and brine successively. The organic phase was then dried and concentrated in the usual fashion. The crude product was then purified through flash chromatography (15:1 to 8:1 DCM: methanol) to provide 1.60 g of **329** as a white solid in 75 % yield.
**$^1$H NMR** (400 MHz, *CDCl$_3$*) $\delta_{ppm}$ 7.77 (2H, *pseudo*-d, *J* = 7.5 Hz), 7.58 (2H, *pseudo*-d, *J* = 7.4 Hz), 7.47-7.28 (5H, m), 7.40 (2H, *pseudo*-dd, *J* = 7.5, 7.5 Hz), 7.33-7.26 (2H, *pseudo*-dd, *J* =

7.5, 7.5 Hz), 6.16 (1H, t, *J* = Hz), 5.40 (1H, t, *J* = 3.2, 3.2 Hz), 5.36 (1H, d, *J* = 9.1 Hz), 5.26 (1H, dd, *J* = 8.4, 4.6 Hz), 5.15 (1H, dd, *J* = 8.3, 3.3 Hz), 5.13 (2H, bs), 4.66 (1H, td, *J* = 9.5, 4.4, 4.4 Hz), 4.40 (1H, d, *J* = 7.6 Hz), 4.39 (1H, d, *J* = 5.6 Hz), 4.28 (1H, dd, *J* = 13.7, 9.7 Hz), 4.20 (1H, t, *J* = 6.8, 6.8 Hz), 4.16-4.09 (2H, m), 4.06-3.94 (1H, m), 3.31-3.21 (2H, m), 2.59 (1H, t, *J* = 4.7, 4.7 Hz), 2.52 (1H, dd, *J* = 15.7, 9.2 Hz), 2.39 (1H, dd, *J* = 15.4, 4.4 Hz), 2.11 (3H, s), 2.05 (3H, s), 2.04 (3H, s), 2.01 (3H, s), 1.62-1.47 (4H, m); **$^{13}$C NMR** (101 MHz, *$CDCl_3$*) $\delta_{ppm}$ 171.6, 171.0, 170.1, 170.0, 169.9, 169.6, 156.3, 143.9, 143.8, 141.3, 135.5, 132.2, 132.06, 131.99, 128.7, 128.5, 128.3, 127.7, 127.1, 125.1, 120.0, 69.7, 68.6, 68.1, 67.8, 66.9, 66.7, 61.0, 47.6, 47.2, 39.3, 38.9, 34.7, 31.6, 25.8, 20.8, 20.75, 20.74, 20.69. **ESI-MS** *m*/*z* calcd for $C_{44}H_{50}N_2O_{14}$ $[M + Na]^+$: 853.32. Found 853.54. **Rf** = 0.41 (9:1 DCM: methanol).

**(S)-allyl 3-(((9H-fluoren-9-yl)methoxy)carbonylamino)-6-(tert-butoxycarbonylamino) hexanoate (Fmoc-Orn(Boc)-OAllyl) (337)**



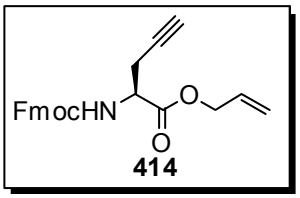
**337**

Diazo amino acid **326** (4.53 g, 9.76 mmol) was dissolved in dioxane (97 mL) and allyl alcohol (30 mL). Catalytic silver benzoate (100 mg, 0.44 mmol) was added and the reaction was fitted with a water-cooled condenser and maintained under argon before being heated to 70 ºC. The reaction was allowed to progress for 8 hours, and then cooled to room temperature and filtered through a celite pad before the reaction was concentrated to dryness. The crude product was purified by dry vacuum column chromatography (100 to 45 % hexanes in ethyl acetate with 5 % increments) to provide 3.95 g allylated β-amino acid **337** in 82 % yield.
**$^{1}$H NMR** (400 MHz, *$CDCl_3$*) $\delta_{ppm}$ 7.77 (2H, *pseudo*-d, *J* = 7.6 Hz), 7.59 (2H, *pseudo*-d, *J* = 7.5 Hz), 7.40 (2H, *pseudo*-dd, *J* = 7.4, 7.4 Hz), 7.32 (2H, *pseudo*-dd, *J* = 7.4, 7.4 Hz), 5.90 (1H, m), 5.32 (1H, dd, *J* = 17.0, 1.0 Hz), 5.24 (1H, dd, *J* = 10.4, 1.0 Hz), 4.59 (2H, d, *J* = 5.7 Hz), 4.63-4.53 (1H, m), 4.44-4.35 (2H, m), 4.22 (1H, m), 4.03-3.95 (1H, m), 3.21-3.07 (2H, m), 2.61 (1H, dd, *J* = 16.3, 5.1 Hz), 2.56 (1H, dd, *J* = 16.3, 5.6 Hz), 1.64-1.47 (4H, m), 1.44 (9H, s); **$^{13}$C NMR** (101 MHz, *$CDCl_3$*) $\delta_{ppm}$ 171.2, 156.0, 155.9, 143.9, 141.4, 131.8, 127.7, 127.1, 125.12, 125.09, 120.0, 118.8, 66.6, 65.4, 48.0, 47.3, 40.1, 39.1, 31.6, 28.4, 26.9. **ESI-MS** *m*/*z* calcd for

$C_{29}H_{36}N_2O_6$ $[M + Na]^+$: 531.25; $[M + K]^+$: 547.22. Found 531.13, 547.13. **Rf** = 0.45 (6.5:3.5, hexanes: ethyl acetate)

## Experimental Protocols for Chapter 4

### N-[[(9H-fluoren-9-ylmethoxy)carbonyl]amino]-L-propargylglycine allyl ester (414)

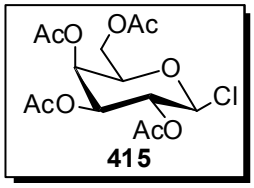


414

In a flame dried round bottom flask with 4Å molecular sieves Fmoc-L-Propargylglycine (338.35 mg, 1.01 mmol) was dissolved in anhydrous DCM (7 mL) under argon atmosphere. HBTU (460 mg, 1.2 mmol) was added and the mixture was stirred for 20 mins. Allyl alcohol (347 μL, 5.1 mmol) was added, followed by a dropwise addition of DIPEA (355.5 μL, 2.04 mmol). The reaction was stirred at room temperature for 16 hrs. Once TLC (9:1 DCM: MeOH) showed complete consumption of starting material, the reaction was diluted with DCM, filtered through a celite pad, and washed with 10% HCl, $NaHCO_3$ and brine successively. The final product was purified by dry vacuum chromatography (DVC) (hexanes/ethyl acetate) to yield 326 mg of a white powder (86% yield). Spectral data is consistent with the literature.[16]

**$^1$H NMR** (400 MHz, *$CDCl_3$*): $\delta_{ppm}$ 7.77 (d, 2H, *J* = 7.52 Hz), 7.61 (d, 2H *J* = 7.43 Hz), 7.40 (t, 2H, *J* = 7.45 Hz), 7.32 (ddd, 2H, *J* = 7.45, 4.29, 1.11 Hz), 5.92 (ddd, 1H, *J* = 16.40, 10.83, 5.57 Hz), 5.66 (d, 1H, *J* = 8.11 Hz), 5.36 (dd, 1H, *J* = 17.19, 0.83 Hz), 5.28 (dd, 1H, *J* = 10.44, 0.89 Hz), 4.70 (dd, 2H, *J* = 2.70, 1.25 Hz), 4.61-4.54 (m, 1H), 4.40 (d, 2H, *J* = 7.22 Hz), 4.25 (t, 1H, *J* = 7.19 Hz), 2.82 (dd, 2H, *J* = 4.45, 2.55 Hz), 2.08 (t, 1H, *J* = 2.37 Hz); **$^{13}$C NMR** (101 MHz, *$CDCl_3$*) $\delta_{ppm}$ 170.0, 155.6, 143.8, 143.7, 141.3, 131.3, 127.7, 127.1, 125.1, 120.0, 119.0, 72.0, 67.3, 66.4, 52.4, 47.1, 22.8. **ESI-MS** *m/z* calcd for $C_{23}H_{21}NO_4$ $[M + H]^+$: 376.15. Found: 376.14.

### 2,3,4,6-Tetra-*O*-acetyl-β-D-galactopyranosyl chloride (415)



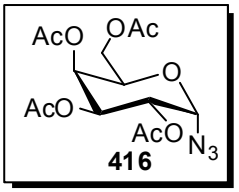
415

Prepared accodring to the protocol of Ibatullin.[17] Galactose pentacetate (100 mg, 0.26 mmol) was dissolved in acetonitrile (1 mL) in a flame-dried round-bottomed flask under argon. Phosphorous pentachloride (65 mg, 0.312 mmol) was added and the reaction was stirred at ambient temperature for 5 minutes. The reaction was then diluted with toluene (1 mL) and DCM (2 mL) and ice water. Following partition and separation, the organic phase was washed successively with ice-cold saturated sodium bicarbonate and water, before being dried and concnetrated in the usual fashion. The residue was co-evaporated twice with toluene and triturated twice with

hexanes to provide 86 mg of β-chloride **415** as a pure white solid in 93 % yield. Spectral data is conistent with the literature.[17]

**$^1$H NMR** (400 MHz, *CDCl$_3$*): $\delta_{ppm}$ 5.44 (1H, dd, *J* = 3.4, 1.0 Hz), 5.39 (1H, dd, *J* = 10.2, 8.9 Hz), 5.25 (1H, d, *J* = 8.8 Hz), 5.01 (1H, dd, *J* = 10.2, 3.4 Hz), 4.17 (2H, d, *J* = 6.5 Hz), 4.01 (1H, ddd, *J* = 6.8, 6.5, 1.2 Hz), 2.18 (3H, s), 2.10 (3H, s), 2.06 (3H, s), 1.99 (3H, s); **$^{13}$C NMR** (400 MHz, *CDCl$_3$*) $\delta_{ppm}$ 170.3, 170.1, 169.9, 169.1, 88.1, 74.4, 70.8, 70.6, 66.7, 61.2, 20.6, 20.6, 20.5, 20.4. **ESI-MS** *m/z* calcd for $C_{14}H_{19}ClO_9$ $[M]^+$: 366.07. Found: 366.15.

**2,3,4,6-Tetra-*O*-acetyl-α-D-galactopyranosyl azide (416)**

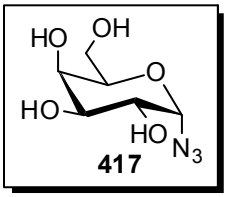


**416**

2,3,4,6-tetra-*O*-acetyl-β-D-galactopyranosyl chloride (**415**) (4.68 g, 12.8 mmol) was dissolved in 15 mL of HMPA. Sodium azide (2.5 g, 38.4 mmol) was added and the reaction was stirred vigorously for 16 hrs at ambient temperature. The mixture was poured into an ice-water mixture and the solid was collected by filtration and washed with water. The product was then recrystallized from ether and petroleum ether to yield 4.32 g of white crystals (89% yield). Characterization data is consistent with that reported previously in the literature.[18]

**$^1$H NMR** (400 MHz, *CDCl$_3$*) $\delta_{ppm}$ 5.67 (d, 1H, *J* = 3.9 Hz), 5.46 (dd, 1H *J* = 2.9, 1.2 Hz), 5.25 (dd, 1H, *J* = 10.8, 3.0 Hz), 5.20 (dd, 1H, *J* = 10.8, 3.9 Hz), 4.37 (dd, 1H, *J* = 6.5, 6.5 Hz), 4.12 (dd, 2H, *J* = 6.5, 4.4 Hz), 2.15 (s, 3H), 2.11 (s, 3H), 2.06 (s, 3H), 2.00 (s, 3H); **$^{13}$C NMR** (101 MHz, *CDCl$_3$*) $\delta_{ppm}$ 170.4, 170.1, 170.0, 169.8, 86.7, 68.6, 67.6, 67.4, 67.2, 61.5, 20.67, 20.64, 20.60, 20.5. **ESI-MS** *m/z* calcd for $C_{14}H_{19}N_3O_9$ $[M + H]^+$: 374.12. Found: 374.09.

**α-D-galactopyranosyl azide (417)**

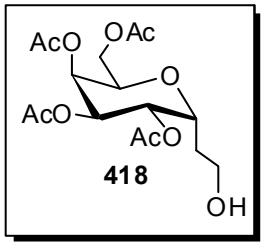


**417**

2,3,4,6-Tetra-O-acetyl-α-D-galactopyranosyl azide, **416** (500 mg, 1.34 mmol), was dissolved in 10 mL of a 0.1 M solution of sodium methoxide in methanol. The reaction was stirred for 1.5 hrs at room temperature whereupon DOWEX 50WX8 (50-100 mesh) ion exchange resin was added until the pH of the solution was neutral. The solution was filtered and concentrated to dryness. The final product was purified by DVC (100% ethyl acetate to 85% ethyl acetate/15% methanol in 3% intervals) to yield 271 mg of white powder (98% yield). Characterization data is consistent with that reported previously in the literature.[19]

**1H NMR** (400 MHz, $D_2O$) $\delta_{ppm}$ 5.41 (d, 1H, J = 4.5 Hz), 3.9 (dd, 1H, J = 5.9, 5.9 Hz), 3.83 (d, 1H, J = 2.9 Hz), 3.78 (dd, 1H, J = 10.2, 4.5 Hz), 3.70-3.54 (m, 3H); **$^{13}$C NMR** (101 MHz, $D_2O$) $\delta_{ppm}$ 89.4, 73.1, 69.2, 69.0, 67.6, 61.2. **ESI-MS** m/z calcd for $C_6H_{11}N_3O_5$ $[M + H]^+$: 206.08. Found: 206.07.

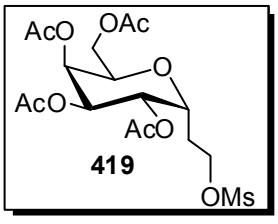
**2-(2,3,4,6-Tetra-*O*-acetyl-α-D-galactopyranosyl)ethanol (418)**




2-(2,3,4,6-tetra-O-acetyl-α-D-galactopyranosyl) acetaldehyde (**314**) (2.5 g, 6.7 mmol) was added to a round bottom flask charged with argon and cooled to 0 °C. 70 mL of MeOH was then added followed by sodium borohydride (983 mg, 26 mmol) and the reaction was stirred for 40 mins when TLC (1:1 hexanes: ethyl acetate) analysis showed consumption of starting material. The reaction was then quenched with 4 mL of acetic acid and the solvent was removed *in vacuo*. Following evaporation, the product was dissolved in ethyl acetate and washed successively with 10% HCl, sodium bicarbonate and brine to yield 2.60 g of crude oil (quantitative conversion). The product was sufficiently pure to use directly in the next transformation. Spectral data matches that in literature.[20]

**$^1$H NMR** (400 MHz, $CDCl_3$) $\delta_{ppm}$ 5.38 (1H, dd, $J$ = 3.5, 3.0 Hz), 5.17 (1H, dd, $J$ = 12.2, 3.4 Hz), 5.15 (1H, dd, $J$ = 12.1, 3.4 Hz), 4.47 (1H, dd, $J$ = 11.7, 8.7 Hz), 4.39 (1H, td, $J$ = 11.3, 3.2 Hz), 4.14 (1H, td, $J$ = 8.5, 3.8, 3.8 Hz), 3.99 (1H, dd, $J$ = 11.8, 3.9 Hz), 3.70 (2H, t, $J$ = 4.7 Hz), 2.43 (1H, bs), 2.07 (3H, s), 2.06 (3H, s), 2.04 (3H, s), 2.02 (3H, s), 1.93-1.80 (1H, m), 1.66-1.57 (1H, m). **ESI-MS** m/z calcd for $C_{16}H_{24}O_{10}$ $[M + Na]^+$: 399.13. Found: 399.15.

**1-*O*-Methanesulfonyl-2-(2,3,4,6-tetra-*O*-acetyl-α-D-galactopyranosyl)ethanol (419)**

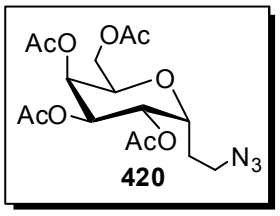



A round bottom flask was cooled to 0 °C in an ice bath. Crude 2-(2,3,4,6-tetra-O-acetyl-α-D- galactopyranosyl)ethanol, **418**, (2.6 g, 6.7 mmol) and methanesulfonylchloride (2.1 mL, 26.8 mmol) were then added to the flask and dissolved in 33 mL of pyridine (0.2 M). The reaction was stirred at 0 °C for 1.5 hrs. Once complete, the reaction was diluted with ethyl acetate and was washed successively with saturated aqueous copper (II) acetate, 10% HCl, saturated sodium bicarbonate and brine. The organic layer was then dried with magnesium

sulfate and the solvent removed *in vacuo* to yield a slightly brown solid. This crude product (2.2 g) was used directly without any further purification (73 % yield).

**$^1$H NMR** (400 MHz, *$CDCl_3$*) $\delta_{ppm}$ 5.42 (1H, t, *J* = 3.1, 3.1 Hz), 5.27 (1H, dd, *J* = 8.7, 4.8 Hz), 5.18 (1H, dd, *J* = 8.7, 3.3 Hz), 4.42-4.26 (4H, m), 4.12-4.06 (2H, m), 3.04 (3H, s), 2.13 (3H, s), 2.10 (3H, s), 2.08 (3H, s), 2.05 (3H, s), 2.01-1.91 (1H, m), 1.35-1.23 (2H, m), 0.88 (2H, dd, *J* = 7.1, 7.1 Hz). **ESI-MS** *m/z* calcd for $C_{17}H_{26}O_{12}S$ $[M + H]^+$: 455.12. Found 455.34.

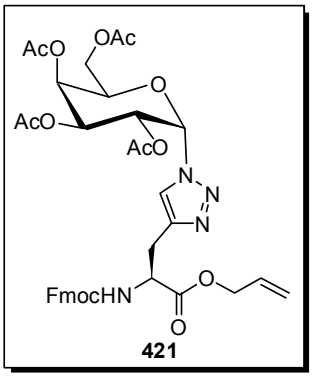
**1-Azido-2-(2,3,4,6-tetra-*O*-acetyl-α-D-galactopyranosyl)ethane (420)**



**420**

Crude **419** (2.2 g, 4.8 mmol) was dissolved in 20 mL of DMF under argon. Sodium azide (760 mg, 11.7 mmol) was added and the reaction was stirred vigorously at room temperature overnight. The mixture was then poured into an ice-water mixture and the solid was filtered out and washed with water. Flash chromatography (7:3 ethyl acetate: hexane) followed by recrystallization from ether and hexanes yielded 1.6 g (60 % over three steps) of **420** as a pure white powder. Characterization data is consistent with that reported previously in the literature.[20] **$^1$H NMR** (400 MHz, *$CDCl_3$*) $\delta_{ppm}$ 5.42 (dd, 1H, *J* = 3.1, 3.1 Hz), 5.25 (dd, 1H, *J* = 8.7, 4.7 Hz), 5.18 (dd, 1H, *J* = 8.7, 3.3 Hz), 4.34-4.32 (m, 2H), 4.09 (ddd, 2H, *J* = 7.8, 5.9, 3.4 Hz), 3.43-3.41 (m, 2H), 2.12 (s, 3H), 2.10 (s, 3H), 2.07 (s, 3H), 2.05 (s, 3H), 1.99-1.87 (m, 1H), 1.75-1.65 (m, 1H); **$^{13}$C NMR** (100 MHz, *$CDCl_3$*) $\delta_{ppm}$ 170.6, 170.0, 169.8, 169.7, 69.0, 68.9, 68.2, 67.9, 67.2, 61.2, 47.7, 26.0, 20.8, 20.8, 20.7; **ESI-MS** *m/z* calcd for $C_{16}H_{23}N_3O_9$ $[M + H]^+$: 402.15. Found 402.13.

**(2*S*)-1-allyl-2-[[(9*H*-Fluoren-9-ylmethoxy)carbonyl]amino]-3-(4-(2,3,4,6-tetra-*O*-acetyl-α-D-galactopyranosyl)-2,3,4-triazol-1-yl)-propanoate (421)**

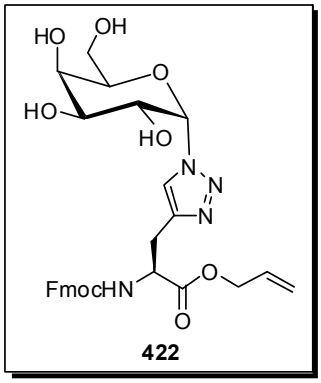


**421**

Compounds **414** (10 mg, 0.027 mmol) and **416** (10 mg, 0.027 mmol) were dissolved in 200 µL of the organic solvent and 150 µL of water in a 3 mL culture tube. A 0.2 M cupric acetate solution (25 µL, 0.005 mmol) was then added and the reaction was sealed with a septum. The tube was flushed with argon for 10 minutes, and then placed in a 40 °C oil bath. A 0.4 M sodium

ascorbate solution (25 μL, 0.01 mmol) was added and the reaction was stirred until completion (for a maximum of 6 hrs). Once deemed complete, the reaction was diluted with ethyl acetate, cooled to room temperature and washed with water and brine. Solvent was removed *in vacuo* and the crude product was purified by preparative TLC (6:4, ethyl acetate: hexanes). **$^1$H NMR** (400 MHz, *$CDCl_3$*): $\delta_{ppm}$ 7.76 (d, 2H, *J* = 7.5 Hz), 7.61 (t, 2H, *J* = 7.3 Hz), 7.40 (ddd, 2H, *J* = 7.4, 7.4, 3.3 Hz), 7.37-7.29 (m, 3H), 6.38 (d, 1H, *J* = 6.1 Hz), 6.16 (dd, 1H, *J* = 10.7, 3.3 Hz), 5.97-5.86 (m, 1H), 5.85 (d, 1H, *J* = 8.2 Hz), 5.65 (d, 1H, *J* = 3.1 Hz), 5.46 (dd, 1H, *J* = 10.8, 6.0 Hz), 5.35 (d, 1H, *J* = 17.1 Hz), 5.27 (d, 1H, *J*= 10.4 Hz) 4.73 (ddd, 1H, *J* = 8.2, 5.2, 5.2 Hz), 4.64 (d, 2H, *J* = 5.6 Hz), 4.60 (dd, 1H, *J* = 6.4, 6.4 Hz), 4.39 (d, 2H, *J* = 7.1 Hz), 4.24 (dd, 1H, *J* = 7.0, 7.0 Hz), 4.10 (dd, 1H, *J* = 11.3, 6.6 Hz), 4.00 (dd, 1H, *J* = 11.3, 6.5 Hz), 3.32 (d, 2H, *J* = 5.1 Hz), 2.19 (s, 3H), 2.01 (s, 3H), 1.95 (s, 3H), 1.88 (s, 3H); **$^{13}$C NMR** (100 MHz, *$CDCl_3$*) $\delta_{ppm}$ 170.6, 170.6, 170.3, 170.0, 169.4, 155.9, 143.8, 143.7, 142.0, 141.3, 141.2, 131.4, 127.8, 127.1, 127.1, 125.1, 124.5, 120.0, 119.2, 81.7, 70.5, 67.7, 67.5, 67.2, 67.2, 66.2, 61.2, 53.4, 47.1, 28.0, 20.61, 20.61, 20.6, 20.3; **ESI-MS** *m/z* calcd for $C_{37}H_{40}N_4O_{13}$ $[M + H]^+$: 749.27. Found: 749.22.

**(2S)-1-Allyl-2-[[(9H-fluoren-9-ylmethoxy)carbonyl]amino]-3-(4-(α-D-galactopyranosyl)-2,3,4-triazol-1-yl)-propanoate (422).** Compounds **414** (10 mg, 0.027 mmol) and **417** (5.5 mg, 0.027 mmol) were dissolved in 200 μL of the organic solvent and 150 μL of water in 3 mL culture tubes. A 0.2 M cupric acetate solution (25 μL, 0.005 mmol) was then added and the reaction was sealed with a septum. The tube was flushed with argon for ten mins, then placed in a 40 °C oil bath. A 0.4 M Sodium Ascorbate solution (25 μL, 0.01 mmol) was added and the reaction was stirred until completion (for a maximum of 6 hrs). Once deemed complete, the reaction was diluted with water and immediately frozen in liquid nitrogen and lyophilized to dryness. The reaction was then either resuspended in methanol and filtered through a sub-micron filter and purified by preparative TLC (12:1:1:1 ethyl acetate: water: acetonitrile: methanol) to provide **422** for analysis. **$^1$H NMR** (400 MHz, *MeOD*): $\delta_{ppm}$ 7.87 (s, 1H), 7.79 (d, 2H, *J* = 7.5 Hz), 7.65 (dd, 2H, *J* = 7.3, 2.6 Hz), 7.39 (t, 2H, *J* = 7.5 Hz), 7.31 (t, 2H, *J* = 7.5 Hz), 6.15 (d, 1H, *J* = 5.7 Hz), 5.92 (ddd, 1H, *J* = 16.2, 11.0, 5.7 Hz), 5.32 (dd, 1H, *J* = 17.1, 1.2 Hz), 5.21 (dd, 1H, *J* = 10.5, 1.3 Hz), 4.63 (d, 2H, *J* = 5.5 Hz), 4.56 (dd, 1H, *J* = 7.9, 5.1 Hz), 4.43 (dd, 1H, *J* = 9.9,

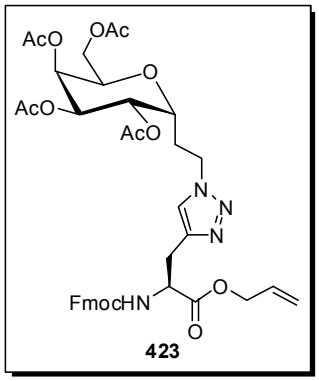


**422**

3.3 Hz), 4.35 (dd, 1H, *J* = 10.4, 7.2 Hz), 4.29 (dd, 2H, *J* = 9.9, 6.2 Hz), 4.20 (dd, 1H, *J* = 6.84, 6.84 Hz), 4.05 (d, 1H, *J* = 2.5 Hz), 4.03 (dd, 1H, *J* = 11.7, 5.7 Hz), 3.67 (d, 2H, *J* = 6.1 Hz), 3.32-3.25 (m, 3H), 3.17 (dd, 1H, *J* = 14.8, 8.1 Hz); **$^{13}$C NMR** (100 MHz, *MeOD*): $\delta_{ppm}$ 172.5, 158.4, 145.3, 142.6, 133.3, 128.8, 128.2, 126.3, 126.3, 121.1, 121.0, 119.0, 87.3, 76.6, 71.3, 70.5, 69.1, 68.2, 67.1, 62.5, 55.4, 48.4, 28.6. **ESI-MS** *m/z* calcd for $C_{29}H_{32}N_4O_9$ $[M + H]^+$: 581.22. Found: 581.25.

**(2*S*)-1-allyl-2-[[(9*H*-Fluoren-9-ylmethoxy)carbonyl]amino]-3-(4-(2,3,4,6-tetra-*O*-acetyl-α-D-galactopyranosylethyl)-2,3,4-triazol-1-yl)-propanoate (423).**

Compounds **414** (11 mg, 0.027 mmol) and **15** (11 mg, 0.027 mmol) were treated as in the preparation of **420** and the reaction was stirred (for a maximum of 4 hrs). Once deemed complete, the reaction was diluted with ethyl acetate and cooled to room temperature and washed with water and brine. Solvent was removed *in vacuo* and the crude product was purified by preparative TLC (7:3, ethyl acetate: hexanes) to provide **423**.

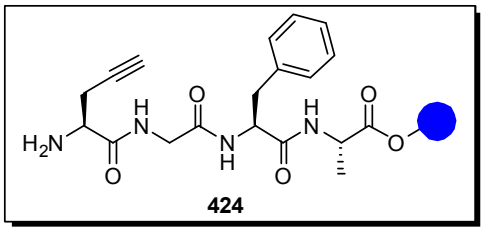


**423**

**$^1$H NMR** (400 MHz, *$CDCl_3$*): $\delta_{ppm}$ 7.76 (d, 2H, *J* = 7.5 Hz), 7.59 (t, 2H, *J* = 7.4 Hz), 7.40 (t, 2H, *J* = 7.4 Hz), 7.37 (s, 1H), 7.31 (t, 2H, *J* = 7.5, 7.5 Hz), 5.94 (d, 1H, *J* = 8.9 Hz), 5.89 (m, 1H), 5.41 (t, 1H, *J* = 2.8, 2.8 Hz), 5.32 (d, 1H, *J* = 17.1 Hz), 5.25 (dd, 1H, *J* = 10.4, 1.1 Hz), 5.20 (d, 1H, *J* = 4.5 Hz), 5.17 (dd, 1H, *J* = 8.7, 3.1 Hz), 4.73 (dd, 1H, *J* = 13.3, 5.4 Hz), 4.66 (d, 2H, *J* = 5.7 Hz), 4.46 (ddd, 1H, *J* = 12.9, 7.9, 4.8 Hz), 4.41-4.27 (m, 4H), 4.23 (dd, 1H, *J* = 7.2, 7.2 Hz), 4.19-4.13 (m, 1H), 4.11-4.02 (m, 2H), 3.31 (d, 2H, *J* = 4.9 Hz), 2.31-2.17 (m, 1H), 2.10 (s, 3H), 2.07 (s, 6H), 2.03 (s, 3H); **$^{13}$C NMR** (100 MHz, *$CDCl_3$*): $\delta_{ppm}$ 170.8, 170.6, 169.9, 169.7, 169.7, 156.0, 143.8, 143.8, 142.7, 141.2, 141.2, 131.6, 127.7, 127.1, 125.2, 125.2, 122.8, 120.0, 118.7, 77.5, 77.2, 76.9, 69.2, 68.6, 68.0, 67.7, 67.1, 66.1, 61.1, 53.5, 47.1, 46.4, 28.1, 27.1, 20.77, 20.74, 20.71, 20.63. **ESI-MS** *m/z* calcd for $C_{39}H_{44}N_4O_{13}$ $[M + H]^+$: 777.298. Found 777.21.

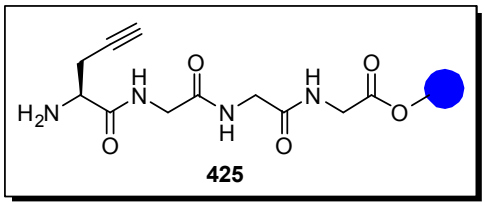
**[(*S*)-1-Aminopent-4-yl-yric-1-amido]-glycinamido-phenylalaninamido-alaninamido-Wang (424)**

Peptide **424** was prepared using 115 mg of Wang resin according to the "general protocol for solid-phase peptide synthesis". 18 mg of resin was cleaved directly and purified by reversed-phase HPLC to yield 3.0 mg of **424** as a white powder in 78% yield (based on resin loading). Characterization is provided for the cleaved peptide. **$^1$H NMR** (400 MHz, *$D_2O$*): $\delta_{ppm}$ 7.40-7.15 (m, 5H), 4.60 (dd, 1H, *J* = 8.2, 6.6 Hz), 4.30 (q, 1H, *J* = 7.3 Hz), 4.19 (t, 1H, *J* = 6.1 Hz), 3.91 (q, 2H, *J* = 16.9 Hz), 3.11 (dd, 1H, *J* = 13.9, 6.5 Hz), 2.96 (dd, 1H, *J* = 13.9, 8.3 Hz), 2.84 (td, 2H, *J* = 3.3, 2.9 Hz), 2.52 (t, 1H, *J* = 2.7 Hz), 1.33 (d, 3H, *J* = 7.3 Hz); **$^{13}$C NMR** (126 MHz, *$D_2O$*): $\delta_{ppm}$ 176.7, 173.2, 171.0, 169.3, 136.8, 129.9, 129.4, 127.8, 83.2, 75.1, 55.4, 52.0, 49.3, 42.87, 42.86, 37.9, 21.7**. ESI-MS** *m/z* calcd for $C_{19}H_{24}N_4O_5$ $[M + H]^+$: 389.182. Found: 389.19**. HPLC $T_R$** = 17.8 min.



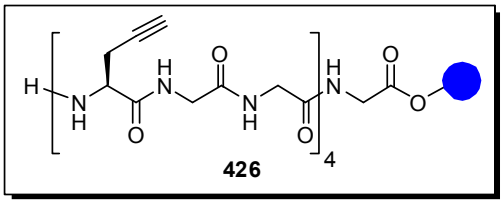

**[(*S*)-1-Aminopent-4-yl-yric-1-amido]-glycinamido-glycinamido-glycinamido-Wang (425)**

Peptide **425** was prepared using 100 mg of Wang resin according to the "general protocol for solid-phase peptide synthesis". 5 mg of resin was directly cleaved and the crude peptide was purified through preparatory TLC (70% methanol in water) to yield 0.8 mg of **425** as a white powder (91% based on resin loading). Characterization is provided for the cleaved peptide.
**$^1$H NMR** (400 MHz, *$D_2O$*): $\delta_{ppm}$ 3.94-3.78 (m, 5H), 3.59 (d, 2H, *J* = 1.35 Hz), 2.64 (d, 2H, *J* = 3.23 Hz, 2H), 2.36 (t, 1H, *J* = 2.21); **$^{13}$C NMR** (101 MHz, *$D_2O$*): $\delta_{ppm}$ 171.4, 171.32, 171.31, 168.9, 76.2, 74.4, 51.4, 42.6, 42.4, 42.3, 21.0. **ESI-MS** *m/z* calcd for $C_{11}H_{16}N_4O_5$ $[M + H]^+$: 285.12. Found: 285.07. **Rf** = 0.73(70% methanol in water).




**{[(*S*)-1-Aminopent-4-yl-yric-1-amido]-glycinamido-glycinamido}$_4$-glycinamido-Wang (426)**

Peptide **426** was prepared using 115 mg of Wang resin according to the "general protocol for solid-phase peptide synthesis." 10 mg of resin was cleaved directly and purified by reversed-phase HPLC to yield



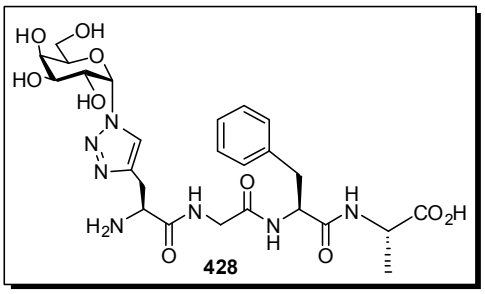
1.8 mg of **426** as a white powder in 70% yield (based on resin loading). Characterization is provided for the cleaved peptide.

**$^1$H NMR** (400 MHz, $D_2O$): $\delta_{ppm}$ 4.58 (m, 3H), 4.29 (t, 1H, $J$ = 5.9 Hz), 4.19-3.79 (m, 18H), 2.93 (dd, 2H, $J$ = 5.9, 2.8 Hz), 2.76 (bd, 6H, $J$ = 6.1 Hz), 2.60 (t, 1H, $J$ = 2.5 Hz), 2.46 (t, 3H, $J$ = 2.4 Hz); **$^{13}$C NMR** (126 MHz, $D_2O$): $\delta_{ppm}$ 172.7, 171.8, 171.5, 171.3, 168.8, 79.2, 76.2, 74.3, 72.2, 52.4, 52.3, 51.3, 42.5, 42.4, 42.2, 20.8. **ESI-MS** *m/z* calcd for $C_{38}H_{49}N_{13}O_{14}$ $[M + H]^+$: 912.36. Found 912.34. **HPLC $T_R$** = 19.2 min.

**General protocol for the solid phase-supported microwave CuAAC reaction.** A CEM Mars X Microwave System with 300 W maximum power and quartz reaction vessels was used for these reactions. The resin supported peptide was initially stirred in DMF for 30 mins under argon. Five equivalents of azide per mol of alkyne and 0.2 equivalents of cupric acetate per mol of alkyne were added and the solution was degassed under argon. 0.4 Equivalents of sodium ascorbate per mol of alkyne was then added and the stirbar was removed. The flask was sealed under argon and placed in the microwave and run under the following conditions: a 2 minute ramp to 90 °C then held at 15 % power for 1.5 hrs. The solvent was then drained,[a] and the beads were washed extensively with 1:1 water: isopropanol followed by DMF (4 x 4 mL), MeOH (4 x 4 mL), DCM (4 x 4 mL), and finally hexanes (4 x 4 mL). The beads were then stirred in 4 mL of 92.5:5:2.5 (TFA: triisopropylsilane: water) cleavage cocktail to remove the product off the resin. Solvent was evaporated at ambient temperature. The residue was triturated with ether (4 x 5 mL) then dissolved in a solution of 0.01 M sodium methoxide in methanol with a drop of water and stirred for 1.5 hrs at room temperature. TFA was added to adjust the pH of the solution to 6. The mixture was evaporated to dryness, desalted, and resuspended in water and purified by RP-HPLC.

[a] Unreacted **9** was recovered from the reaction solution by diluting with 20 mL of water, extracting this using 3 x 10 mL ether, and washing the combined organic layers successively with 15 mL of 10% HCl, 15 mL of saturated $NaHCO_3$, and brine. The organic layer was dried with magnesium sulfate, filtered and concentrated in vacuo to yield 19 mg of off-white **9** indistinguishable from the synthetic material by NMR (70% mass recovery).

**{[(*S*)-3-[4-(α-D-galactopyranosyl)-2,3,4-triazol-1-yl]-α-aminopropyric-2-amido]-glycinamido-phenylalaninamido-alanine (428)**

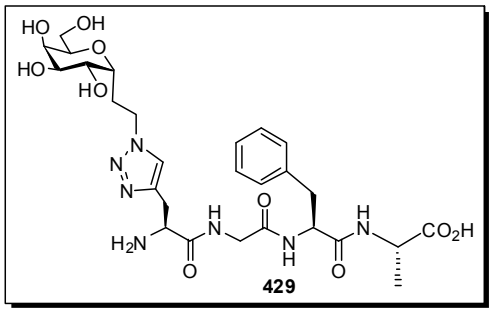


428

Resin-supported **425 (**80 mg, 0.046 mmol) was treated as per the general procedure for microwave CuAAC reactions described above with azide **416** (85.2 mg, 0.23 mmol), cupric acetate (1.7mg, 0.0093 mmol), and sodium ascorbate (3.4 mg, 0.017 mmol). Reversed-phase HPLC (1% acetonitrile in water for 12 mins followed by a linear gradient from 1% acetonitrile in water to 10% acetonitrile in water over 28 mins followed by a linear gradient from 10% acetonitrile in water to 98% acetonitrile in water over 40 mins) yielded 16.7 mg of **428** as a white powder (61% based on resin-loading).

**$^1$H NMR** (500 MHz, $D_2O$): $\delta_{ppm}$ 8.01 (s, 1H), 7.38-7.15 (m, 5H), 6.26 (s, 1H), 4.69-4.56 (m, 1H), 4.51-4.42 (m, 1H), 4.35-4.15 (m, 2H), 4.13-3.96 (m, 3H), 3.89-3.75 (m, 2H), 3.70-3.56 (m, 2H), 3.33-3.09 (m, 3H), 3.04-2.95 (m, 1H), 1.33-1.18 (m, 3H); **$^{13}$C NMR** (126 MHz, $D_2O$): $\delta_{ppm}$ 179.4, 171.8, 170.9, 170.7, 136.6, 129.1, 128.6, 1267.0, 74.9, 69.2, 68.7, 66.8, 61.1, 54.8, 54.2, 46.5, 42.4, 36.7, 17.5**. ESI-MS** *m/z* calcd for $C_{25}H_{35}N_7O_{10}$ $[M + H]^+$: 594.25. Found: 594.42. **HPLC $T_R$** = 33 min.

**{[(*S*)-3-[4-(α-D-galactopyranosylethyl)-2,3,4-triazol-1-yl]-α-aminopropyric-2-amido]-glycinamido-phenylalaninamido-alanine (429)**



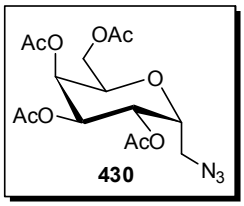
429

Resin-supported **425 (**24 mg, 0.0137 mmol) was treated as per the general procedure for microwave CuAAC reactions described above with azide **420** (27.5 mg, 0.0685 mmol), cupric acetate (0.5mg, 0.0028 mmol), and sodium ascorbate (1 mg, 0.0051 mmol). Reversed-phase HPLC purification (2 % acetonitrile in water for 9 mins followed by a linear gradient from 2% acetonitrile in water to 40 % acetonitrile in water over 30 mins) yielded 6 mg of **429** as a white powder (70 % based on resin-loading).

**$^1$H NMR** (500 MHz, $D_2O$): $\delta_{ppm}$ 7.76 (s, 1H), 7.27-7.09 (m, 5H), 4.37 (dd, 2H, $J$ = 14.0, 6.3 Hz), 4.18 (t, 1H, $J$ = 6.3 Hz), 4.02 (dd, 1H, $J$ = 14.3, 7.0 Hz), 3.76-3.85 (m, 3H), 3.74 (d, 1H, $J$ = 1.6

Hz), 3.66-3.58 (m, 2H), 3.55 (d, 2H, *J* = 5.8 Hz), 3.18 (d, 1H, *J* = 6.3), 3.07 (dd, 1H, *J* = 13.9, 5.4 Hz), 2.87 (dd, 1H, *J* = 13.9, 9.3 Hz), 2.30-1.99 (m, 2H), 1.19 (d, 3H, *J* = 7.2 Hz); **$^{13}$C NMR** (126 MHz, *$D_2O$*): $\delta_{ppm}$ 171.9, 170.4, 169.0, 162.8, 136.4, 129.2, 128.6, 127.0, 72.1, 69.5, 68.7, 67.6, 60.9, 54.8, 52.6, 47.0, 42.2, 36.9, 26.6, 24.6, 17.2. **ESI-MS** *m/z* calcd for $C_{27}H_{38}N_7O_{10}$ $[M + H]^+$: 622.28. Found: 622.15. **HPLC $T_R$** = 25.4 min.

**(2,3,4,6-Tetra-*O*-acetyl-α-D-galactopyranosyl)methyl azide (430)**

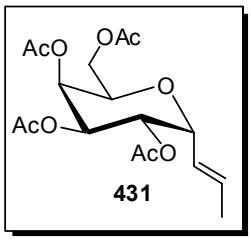


**430**

Crude mesylate **438** (490 mg, 1.8 mmol) was dissolved in pyridine (5 mL) and acetic anhydride (5 mL) and stirred for 4 hours until TLC and NMR analysis showed completion of the reaction;[21] Solvent was removed *in vacuo*, the flask was flushed with argon, and the residue was redissolved in DMF (1.5 mL). HMPA (500 μL) and sodium azide (400 mg, 6.1 mmol) were added and the reaction was heated to 85 ºC for 12 hours after which TLC showed completion of the reaction (6:4 hexanes: ethyl acetate). The solution was diluted with DCM, and washed sequentially with 10% HCl, saturated $NaHCO_3$, and brine. The organic layer was dried with magnesium sulfate, filtered, and concentrated. The final product was purified by DVC (100% hexanes to 100% ethyl acetate in 5% intervals) to yield 457 mg of residue that was recrystallized from diethyl ether/hexanes to yield 373 mg of **430** as a white crystalline solid (57% yield over 3 steps from **437**). Spectral data is consistent with previously published data.[22]

**$^1$H NMR** (400 MHz, *$CDCl_3$*) $\delta_{ppm}$ 5.44 (dd, 1H, *J* = 3.3, 3.3 Hz), 5.27 (dd, 1H, *J* = 8.4, 4.6 Hz), 5.22 (dd, 1H, *J* = 8.4, 3.2 Hz), 4.39 (m, 2H), 4.25 (ddd, 1H, *J* = 8.0, 4.5, 3.4 Hz), 4.11 (dd, 1H, *J* = 11.7, 4.7 Hz), 3.63 (dd, 1H, *J* = 13.5, 8.8 Hz), 3.24 (dd, 1H, *J* = 13.5, 3.7 Hz), 2.12 (s, 3H), 2.11 (s, 3H), 2.07 (s, 3H), 2.06 (s, 3H); **$^{13}$C NMR** (100 MHz, *$CDCl_3$*): $\delta_{ppm}$ 170.7, 169.8, 169.6, 169.5, 70.8, 69.8, 67.7, 67.5, 66.9, 60.7, 48.3, 20.67, 20.66, 20.59. **ESI-MS** *m/z* calcd for $C_{15}H_{21}N_3O_9$ $[M + K]^+$: 426.09. Found: 426.12.

***E*-1-[(2,3,4,6)-Tetra-*O*-acetyl-α-D-galactopyranosyl]-prop-1-ene (431)**



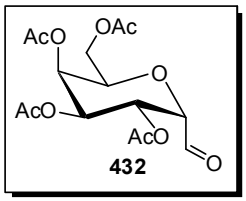
**431**

According to the procedure of Patman,[23] (1,5-Cyclooctadiene)-bis-(methyldiphenylphosphine) Iridium (I) hexafluorophosphate (150 mg, 0.177 mmol) was suspended in 5 mL of THF under nitrogen with vigorous stirring.

The flask was flushed repeatedly with Hydrogen until the suspension dissolved to give a yellow solution. The solution was then flushed with argon for 10 minutes and cannulated into a flask containing **313** (2.31 g, 6.2 mmol) dissolved in THF. The reaction was stirred for 12 hours until complete conversion was observed by NMR. The solution was then concentrated under reduced pressure to yield 2.6 g of crude **431**, in quantitative conversion, as a yellow gel that was used without further purification. Spectral data is consistent with the literature.[24]

**$^1$H NMR** (400 MHz, *CDCl$_3$*) $\delta_{ppm}$ 5.90 (1H, dqd, *J* = 13.0, 6.5, 1.3 Hz), 5.65 (1H, dddd, *J* = 15.4, 6.2, 3.2, 1.6 Hz), 5.41 (1H, dd, *J* = 3.2, 1.5 Hz), 5.28 (1H, dd, *J* = 10.6, 5.8 Hz), 5.17 (1H, dd, *J* = 10.5, 3.3 Hz), 4.75 (1H, p, *J* = -Hz), 4.16 (1H, ddd, *J* = 12.9, 6.6, 1.1 Hz), 4.12-4.07 (2H, m), 2.15 (3H, s), 2.05 (6H, s), 2.01 (3H, s), 1.79 (3H, ddd, *J* = 6.3, 1.4, 1.4 Hz); **$^{13}$C NMR** (101 MHz, *CDCl$_3$*) $\delta_{ppm}$ 170.3, 170.1, 170.0, 169.7, 133.1, 122.5, 73.0, 68.2, 68.0, 67.8, 61.7, 20.7, 20.6, 20.6, 20.5, 18.1. **ESI-MS** *m*/*z* calcd for $C_{17}H_{24}O_9$ $[M + Na]^+$: 395.13. Found 395.17.

**(2,3,4,6-Tetra-*O*-acetyl-α-D-galactopyranosyl)methanal (432)**



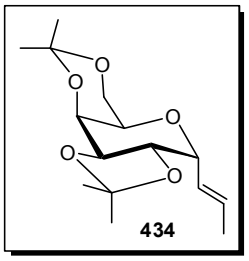
**432**

Propene derivative **431** (201 mg, 0.537 mmol) was dissolved in anhydrous DCM, and cooled to – 78 ºC. An oxygen/ozone gas mixture was bubbled through the solution until a deep royal blue colour persisted. Argon was then bubbled through the solution until the solution turned clear. Triphenylphosphine (400 mg, 1.52 mmol) was then added to quench the ozonide, and the reaction mixture stirred uncovered at room temperature for 18h. The solvent was removed under reduced pressure, and NMR showed complete conversion of olefin to aldehyde. The residue dissolved in ether and allowed to stand for 1 hour. The solid triphenylphosphine oxide was removed by filtration. This process was repeated twice. The residue was then triturated with hexanes twice and this material was then used for any reaction.To obtain a purer sample, the material was triturated with hexanes twice more to remove triphenylphosphine, and the ether precipitation was then repeated twice more. This process provided 13 mg of pure **432** in 6.7 % yield.

**$^1$H NMR** (400 MHz, *CDCl$_3$*) $\delta_{ppm}$ 9.77 (1H, s), 5.52 (1H, dd, *J* = 9.2, 5.9 Hz), 5.46 (1H, t, *J* = 2.9, 2.9 Hz), 5.17 (1H, dd, *J* = 9.2, 3.2 Hz), 4.73 (1H, d, *J* = 5.8 Hz), 4.41 (1H, ddd, *J* = 7.5, 5.0, 2.6 Hz), 4.37-4.28 (1H, d, J = 12.8, 6.2 Hz), 4.12 (1H, dd, *J* = 11.5, 4.7 Hz), 2.13 (3H, s), 2.11

(3H, s), 2.07 (3H, s), 2.04 (3H, s); **$^{13}$C NMR** (101 MHz, *$CDCl_3$*) $\delta_{ppm}$ 198.1, 170.5, 169.8, 169.6, 169.4, 75.6, 71.5, 68.2, 67.2, 67.1, 60.8, 20.64, 20.56, 20.56, 20.51. Attempts to obtain a mass spectrum failed in all cases.

***E*-1-[(2,3;4,6)-di-*O*-isopropylidene-α-D-galactopyranosyl]-prop-1-ene (434)**




The crude product was dissolved in 20 mL of a 0.1 M solution of sodium methoxide in methanol. The reaction was stirred for 1.5 hrs at room temperature whereupon DOWEX 50WX8 (50-100 mesh) ion exchange resin was added until the pH of the solution was neutral. The solution was filtered and concentrated to dryness to yield 1.3 g of crude *E*-1-[α-D-galactopyranosyl]-prop-1-ene as a white solid in quantitative conversion which was used without any further purification.

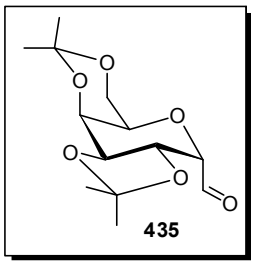
**$^{1}$H NMR** (400 MHz, *$D_2O$*) $\delta_{ppm}$ 5.96 (1H, ddd, *J* = 15.3, 6.3, 0.7 Hz), 5.85 (1H, dddd, *J* = 15.5, 8.4, 2.8, 1.3 Hz), 4.45 (1H, dd, *J* = 7.8, 6.6 Hz), 4.00-3.95 (2H, m), 3.92 (1H, ddd, *J* = 6.6, 5.5, 1.0 Hz), 3.78 (1H, dd, *J* = 10.3, 3.3 Hz), 3.68 (1H, d, *J* = 5.3 Hz), 3.68 (1H, d, *J* = 6.7 Hz), 1.76 (3H, ddd, *J* = 6.3, 1.4, 0.7 Hz); **$^{13}$C NMR** (101 MHz, *$D_2O$*) $\delta_{ppm}$ 135.5,122.7, 77.0, 72.3, 70.1, 69.4, 68.0, 61.3, 17.5. **ESI-MS** *m/z* calcd for $C_9H_{16}O_5$ $[M + Na]^+$: 227.15; $[M + K]^+$: 243.06. Found 227.15, 243.12.

The crude solid (1.3 g, 6.37 mmol) was dissolved in dry DMF under argon with stirring. Para-toluenesulfonic acid monohydrate (100 mg, 0.525 mmol) was added followed by a dropwise addition of 2-methoxypropene (2.9 mL, 30 mmol). The reaction mixture was stirred for forty minutes until deemed complete by TLC analysis (9:1 ethyl acetate: methanol) when 500 μL of triethylamine was added and the solution was concentrated to dryness. Purification by flash chromatography (8:2 hexanes: ethyl acetate) yielded 1.53 g of the title compound (87% yield over 3 steps).

**$^{1}$H NMR** (500 MHz, *$CDCl_3$*): $\delta_{ppm}$ 5.88 (dqd, 1H, *J* = 15.8, 6.4, 1.6 Hz), 5.60 (ddq, 1H, *J* = 15.8, 5.2, 1.6), 4.86 (t, 1H, *J* = 5.3 Hz), 4.45 (bs, 1H), 4.27 (dd, 1H, *J* = 9.9, 5.6 Hz), 4.09 (dd, 1H, *J* = 12.9, 2.1 Hz), 3.90 (dd, 1H, *J* = 12.9, 1.4 Hz), 3.67 (dd, 1H, *J* = 9.9, 2.9 Hz), 3.38 (dd, 1H, *J* = 3.2, 1.7 Hz), 1.74 (ddd, 3H, *J* = 6.5, 1.6, 1.6 Hz), 1.47 (s, 3H), 1.46 (s, 3H), 1.44 (s, 3H), 1.41 (s,

3H); **$^{13}$C NMR** (101 MHz, *$CDCl_3$*): $\delta_{ppm}$ 131.3, 123.3, 110.0, 98.5, 75.2, 74.4, 70.9, 67.7, 63.5, 63.5, 29.3, 26.7, 26.5, 18.5, 18.3. **ESI-MS** *m/z* calcd for $C_{15}H_{24}O_5$ $[M + H]^+$: 285.17; $[M + NH_4]^+$: 302.20; $[M + Na]^+$: 307.15; $[M + K]^+$: 323.13. Found 285.23, 307.20, 323.20.

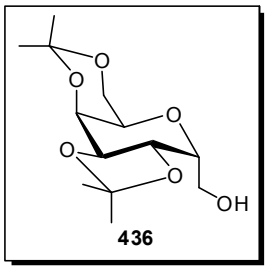
**[(2,3;4,6)-di-*O*-isopropylidene-α-D-galactopyranosyl]methanal (435)**




Olefin **434** (600 mg, 2.20 mmol) was dissolved in dichloromethane (16 mL) and cooled to -78 ºC. Ozone in oxygen was bubbled through the solution until a deep blue colour persisted. The reaction was then purged with nitrogen until the solution became clear. Triphenylphosphine (1.5 g, 5.5 mmol) was then added all at once, and the reaction was allowed to warm to ambient temperature with stirring for 12 hours. The solution was concentrated and resuspended in diethyl ether. Following filtration, the filtrate was concentrated and the residue can be purified by column chromatography (on silica neutralized with triethylamine), (8:2, hexanes: ethyl acetate) to yield 412 mg (1.53 mmol) of the title product as a slightly yellow oil in 69 % yield.

**$^1$H NMR** (300 MHz, *$CDCl_3$*) $\delta_{ppm}$ 9.95 (1H, s), 5.02 (1H, d, *J* = 6.6 Hz), 4.59-4.51 (2H, m), 4.14 (1H, dd, *J* = 13.2, 2.0 Hz), 4.07 (1H, dd, *J* = 13.2, 1.4 Hz) 3.92 (1H, dd, *J* = 3.3, 1.8 Hz), 3.60 (1H, dd, *J* = 10.0, 2.7 Hz), 1.60 (3H, s), 1.55 (3H, s), 1.54 (3H, s), 1.50 (3H, s); **$^{13}$C NMR** (101 MHz, *$CDCl_3$*) $\delta_{ppm}$ 200.8, 111.1, 98.6, 79.2, 76.1, 69.7, 67.4, 66.6, 63.1, 29.2, 26.4, 26.3, 18.4. **Rf** = 0.52 (1:1, hexanes: ethyl acetate). Attempts to obtain a mass spectrum failed in all cases.

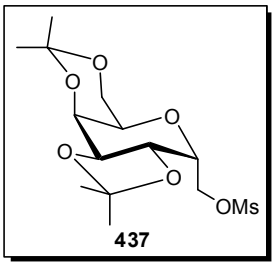
**(2,3;4,6-di-*O*-isopropylidene-α-D-galactopyranosyl)methanol (436)**




Aldehyde **435** (412 mg, 1.53 mmol) was immediately dissolved in methanol (10 mL) and cooled to 0 ºC. Sodium borohydride (340 mg, 9.0 mmol) was added portionwise and the reaction was stirred for 2 hrs. The reaction mixture was filtered through celite and concentrated under reduced pressure. The residue was redissolved in ethyl acetate and washed sequentially with saturated sodium bicarbonate and brine, then dried with magnesium sulfate, filtered and concentrated *in vacuo*. Flash chromatography (6:4 ethyl acetate: hexanes) yielded 386 mg of alcohol **436** as a clear oil (92 % yield).

**$^1$H NMR** (400 MHz, *CDCl$_3$*): $\delta_{ppm}$ 4.55 (td, 1H, *J* = 7.9, 5.9 Hz), 4.52-4.50 (m, 1H), 4.38 (dd, 1H, *J* = 10.1, 6.0 Hz), 4.12 (dd, 1H, *J* = 13.1, 2.2 Hz), 3.95 (dd, 1H, *J* = 13.0, 1.5 Hz), 3.93-3.85 (m, 2H), 3.81 (dd, 1H, *J* = 10.1, 2.9 Hz), 3.40 (dd, 1H, *J* = 3.2, 1.6 Hz), 1.50 (s, 3H), 1.49 (s, 3H), 1.48 (s, 3H), 1.44 (s, 3H); **$^{13}$C NMR** (101 MHz, *CDCl$_3$*): $\delta_{ppm}$ 110.3, 98.6, 75.5, 74.2, 70.3, 67.3, 64.5, 63.3, 58.7, 29.2, 26.6, 18.4; **ESI-MS** *m/z* calcd for $C_{13}H_{22}O_6$ $[M + Na]^+$: 297.13. Found: 297.17.

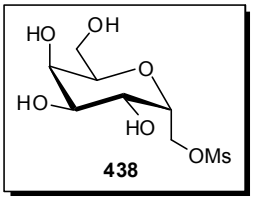
**(2,3;4,6-di-*O*-isopropylidene-α-D-galactopyranosyl)methyl methanesulfonate (437)**



**437**

Alcohol **436** (600 mg, 2.2 mmol) was dissolved in pyridine (12.5 mL) and cooled to 0 ºC. Methanesulfonyl chloride (620 µL, 8 mmol) was added dropwise and the mixture was stirred for 5 hours at 0 ºC until determined complete by TLC (8:2 ethyl acetate:hexanes). The reaction was diluted with DCM (50 mL) and washed twice with 10 % HCl (50 mL) and $NaHCO_3$ then dried with magnesium sulfate, filtered, and concentrated to yield 662 mg of the title compound (86 %) as a clear colourless oil. **$^1$H NMR** (400 MHz, *CDCl$_3$*) $\delta_{ppm}$ 4.70-4.61 (m, 2H), 4.51-4.48 (m, 1H), 4.35 (d, 1H, *J* = 10.0 Hz), 4.34 (dd, 1H, *J* = 15.7, 5.5 Hz), 4.13 (dd, 1H, *J* = 13.2, 2.1 Hz), 3.90 (dd, 1H, *J* = 13.2, 1.4 Hz), 3.61 (dd, 1H, *J* = 10.2, 2.8 Hz), 3.53 (dd, 1H, *J* = 3.1, 1.8 Hz), 3.09 (s, 3H), 1.48 (s, 3H), 1.46 (s, 3H), 1.45 (s, 3H), 1.40 (s, 3H); **$^{13}$C NMR** (101 MHz, *CDCl$_3$*) $\delta_{ppm}$ 110.8, 98.7, 74.5, 74.3, 69.2, 67.1, 64.7, 64.3, 63.2, 38.6, 29.2, 26.6, 26.5, 18.4. **ESI-MS** *m/z* calcd for $C_{14}H_{24}O_8S$ $[M + H]^+$: 353.12. Found: 353.16.

**(α-D-galactopyranosyl)methyl methanesulfonate (438)**

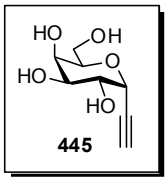


**438**

Mesylate **437** (660 mg, 1.8 mmol) was dissolved in TFA (4 mL) and $H_2O$ (1 mL) at room temperature. The reaction was stirred for 10 minutes and pyridine (10 mL) was added and solvent was removed *in vacuo* to provide 489 mg of deprotected derivative **438** in quantitative yield. **$^1$H NMR** (400 MHz, *CDCl$_3$*) $\delta_{ppm}$ 4.48 (1H, dd, *J* = 10.9, 3.3 Hz), 4.45-4.42 (2H, m), 4.38-4.33 (1H, m), 4.33 (1H, dd, *J* = 10.9, 8.1 Hz), 4.26 (1H, d, *J* = 11.0 Hz), 4.18 (1H, ddd, *J* = 8.1, 3.1, 3.1 Hz), 4.11-4.04 (2H, m), 3.24 (3H, s); **$^{13}$C NMR** (101 MHz, *CDCl$_3$*) $\delta_{ppm}$ 80.7, 77.9, 69.99,

69.96, 69.8, 68.8, 68.2, 36.5. **ESI-MS** *m/z* calcd for $C_8H_{16}O_8S$ $[M + Na]^+$: 295.05. Found: 295.06.

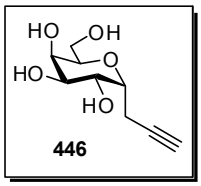
**(α-D-galactopyranosyl)ethyne (445)**




[(2,3,4,6)-tetra-*O*-acetyl-α-D-galactopyranosyl]ethyne **452** (10 mg, 0.028 mmol) was dissolved in 0.1 M sodium methoxide in methanol (4 mL) and stirred for 3 hours at ambient temperature. The reaction was then neutralized with DOWEX 50WX8 (50-100 mesh) ion exchange resin to pH=6, filtered and concentrated. The crude foam was resuspended in HPLC-grade water and lyophilized to yield 5.3 mg of the product as a white powder (quantitative yield).

**$^1$H NMR** (400 MHz, $D_2O$) $\delta_{ppm}$ 4.85 (1H, dd, *J* = 5.7, 2.3 Hz), 4.13 (1H, ddd, *J* = 6.5, 5.6, 0.8 Hz), 3.96 (1H, dd, *J* = 3.2, 1.0 Hz), 3.90 (1H, dd, *J* = 10.2, 5.7 Hz), 3.85 (1H, dd, *J* = 10.2, 3.2 Hz), 3.72 (1H, d, *J* = 5.7 Hz), 3.72 (1H, d, *J* = 6.3 Hz), 2.97 (1H, d, *J* = 2.3 Hz); **$^{13}$C NMR** (101 MHz, $D_2O$) $\delta_{ppm}$ 78.5, 77.6, 74.2, 70.5, 69.0, 68.2, 66.8, 61.2. **ESI-MS** *m/z* calcd for $C_8H_{12}O_5$ $[M + NH_4]^+$: 206.21. Found: 206.21.

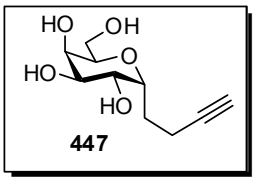
**3-(α-D-galactopyranosyl)-propyne (446)**




3-(2,3,4,6-tetra-*O*-acetyl-α-D-galactopyranosyl)-propyne (**453**) (8.1 mg, 0.022 mmol) was dissolved in 4 mL of 0.1 M NaOMe in methanol and stirred for 5 hours. DOWEX 50WX8 (50-100 mesh) ion exchange resin was added until the pH was neutral, and the solution was filtered and concentrated. The residue was further purified by preperatory TLC (20 % methanol in ethyl acetate) to yield 4 mg of the product as a white powder following lyophilizaton (quantiative yield).

**$^1$H NMR** (400 MHz, $D_2O$) $\delta_{ppm}$ 4.21 (1H, ddd, *J* = 10.4, 5.3, 5.3 Hz), 4.01 (1H, dd, *J* = 9.7, 5.8 Hz), 3.97 (1H, dd, *J* = 3.2, 1.5 Hz), 3.83 (1H, ddd, *J* =7.3, 4.6, 1.6 Hz), 3.80-3.66 (3H, m), 2.64 (1H, ddd, *J* = 17.6, 10.3, 2.6 Hz), 2.56 (1H, ddd, *J* = 17.7, 4.8, 2.7), 2.37 (1H, t, *J* = 2.6 Hz); **$^{13}$C NMR** (101 MHz, $D_2O$) $\delta_{ppm}$ 81.5, 73.6, 72.4, 70.9, 69.4, 68.7, 67.9, 60.8, 15.7. **ESI-MS** *m/z* calcd for $C_9H_{14}O_5$ $[M + Na]^+$: 225.07. Found: 225.12. **Rf** = 0.54 (20 % methanol in ethyl acetate).

**4-(α-D-galactopyranosyl)-1-butyne (447)**

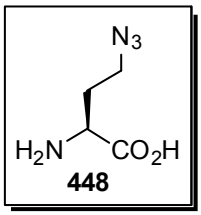


**447**

Protected 4-(2,3,4,6-tetra-*O*-acetyl-α-D-galactosyl)-1-butyne **454** (10 mg, 0.026 mmol) was dissolved in 5 mL of 0.1 M NaOMe in methanol. The reaction was allowed to stir for four hours at which point DOWEX 50WX8 (50-100 mesh) ion exchange resin was added and stirring continued for an additional 5 minutes when pH = 6. The reaction mixture was filtered through a sintered glass frit, and the filtrate was concentrated to dryness then redissolved in HPLC grade water. Lyophilization yielded 5.3 mg of the title compound as a white powder (0.025 mmol) in 94 % yield.

**$^1$H NMR** (500 MHz, $D_2O$) $\delta_{ppm}$ 4.19 (1H, ddd, $J$ = 11.7, 6.0, 3.5 Hz), 4.01 (1H, dd, $J$ = 10.0, 6.0 Hz), 3.97 (1H, dd, $J$ = 3.5, 0.7 Hz), 3.78 (1H, dd, $J$ = 10.0, 3.4 Hz), 3.77-3.67 (3H, m), 2.37 (1H, t, $J$ = Hz), 2.41-2.33 (1H, m), 2.27 (1H, dddd, $J$ = 9.0, 9.0, 7.0, 2.5 Hz), 1.96 (1H, m), 1.84-1.76 (1H, m); **$^{13}$C NMR** (126 MHz, $D_2O$) $\delta_{ppm}$ 84.7, 74.1, 71.7, 69.7, 69.6, 69.0, 68.1, 61.0, 22.6, 13.9. **ESI-MS** *m/z* calcd for $C_{10}H_{16}O_5$ $[M + Na]^+$: 239.22. Found: 239.22.

**(*S*)-2-amino-4-azidobutanoic acid (448)**

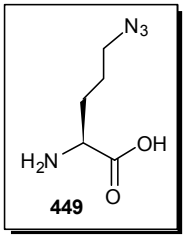


**448**

Prepared according to a published protocol.[25] Methyl ester derivative **472** (12.2 g, 47.3 mmol) was dissolved in TFA (80 mL) and stirred for 30 minutes. The TFA was removed under reduced pressure at ambient temperature. The residue was resuspended in 45 mL of 1 M NaOH and stirred for 8 hours and treated with DOWEX 50WX8 (50-100 mesh) ion exchange resin, washed extensively with water, and lyophilized to yield 6.5 g of azido amino acid **448** as a white solid in 95 % yield. Spectral data is consistent with the literature.[26]

**$^1$H NMR** (300 MHz, $D_2O$) $\delta_{ppm}$ 3.80 (1H, dd, $J$ = 6.9, 5.5 Hz), 3.57 (2H, dt, $J$ = 6.6, 1.2 Hz), 2.23-1.99 (2H, m); **$^{13}$C NMR** (75 MHz, $D_2O$) $\delta_{ppm}$ 163.1, 53.2, 47.9, 29.9. **ESI-MS** *m/z* calcd for $C_4H_8N_4O_2$ $[M + Na]^+$: 167.05. Found: 167.08.

**(*S*)-2-amino-5-azidopentanoic acid (449)**



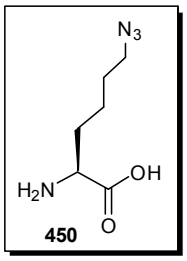
**449**

Azido-ornithine derivative **479** (2.0 g, 7.75 mmol) was dissolved in TFA (25 mL) and DCM (25 mL) and stirred for 3 hours. The solvent was removed under reduced pressure to provide 2.1 g of **449** as a white powder in quantitative

yield. Spectral data is consistent with the literature.[27]

**$^1$H NMR** (500 MHz, *$CDCl_3$*) 4.06 (1H, t, *J* = 6.2Hz), 3.35 (2H, t, *J* = 6.5, 6.5 Hz), 2.06-1.89 (2H, m), 1.77-1.57 (2H, m); **$^{13}$C NMR** (126 MHz, *$CDCl_3$* $\delta_{ppm}$ 173.6, 54.0, 51.5, 28.4, 25.1. **ESI-MS** *m/z* calcd for $C_5H_{10}N_4O_2$ $[M + H]^+$: 159.09. Found 159.11.

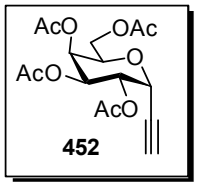
**(*S*)-2-amino-6-azidohexanoic acid trifluoroacetate (450)**




Azido-lysine derivative **480** (3.15 g, 12.2 mmol) was dissolved in TFA (40 mL) and DCM (40 mL) and stirred for 3 hours. The solvent was removed under reduced pressure to provide 3.5 g of the title salt as a white powder in quantitative yield. Spectral data is consistent with the literature.[27]

**$^1$H NMR** (500 MHz, *$CDCl_3$*) $\delta_{ppm}$ 4.03 (1H, t, *J* = 6.2 Hz), 3.29 (2H, t, *J* = 6.7 Hz), 2.02-1.83 (2H, m), 1.64-1.33 (4H, m); **$^{13}$C NMR** (75 MHz, *$CDCl_3$*) $\delta_{ppm}$ 171.7, 52.3, 50.1, 28.8, 27.0, 21.0. **ESI-MS** *m/z* calcd for $C_6H_{12}N_4O_2$ $[M + H]^+$: 173.10. Found: 173.14.

**[(2,3,4,6)-tetra-*O*-acetyl-α-D-galactopyranosyl]ethyne (452)**

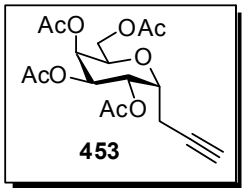



[(2,3;4,6)-di-*O*-isopropylidene-α-D-galactopyranosyl]ethyne, **1407** (253 mg, 0.93 mmol) was dissolved in 11 mL 60 % acetic acid and heated to 75 º C and stirred for six hours. The reaction was cooled to room temperature and the solvent removed. The residue was then co-evaporated three times with toluene and resuspended in 8 mL of pyridine to which was added 8 mL of acetic anhydride and 1 crystal of DMAP. The reaction mixture was allowed to stir for 14 hours when solvent was removed under reduced pressure and the residue co-evaported twice with toluene. The crude product was then purified through flash chromatography (20 % ethyl acetate in hexanes) to yield 286 mg (0.80 mmol) of **452** as an amorphous white solid in 86 % yield.

**$^1$H NMR** (400 MHz, *$CDCl_3$*) $\delta_{ppm}$ 5.32 (1H, dd, *J* = 3.3, 1.0 Hz), 5.20 (1H, dd, *J* = 10.7, 3.4 Hz), 5.03 (1H, dd, *J* = 10.7, 5.8 Hz), 4.94 (1H, dd, *J* = 5.8, 1.9 Hz), 4.28 (1H, dt, *J* = 6.5, 0.9 Hz), 4.00 (1H, dd, *J* = 11.3, 6.4 Hz), 3.94 (1H, dd, *J* = 11.3, 6.7 Hz), 2.57 (1H, d, *J* = 2.3 Hz), 2.01 (3H, s), 1.96-1.95 (3H, m), 1.92 (3H, s), 1.87 (3H, s); **$^{13}$C NMR** (101 MHz, *$CDCl_3$*) $\delta_{ppm}$ 170.3, 170.0, 169.9, 169.8, 78.2, 76.5, 69.5, 68.5, 7.6, 66.6, 65.7, 61.5, 20.7, 20.58, 20.53, 20.51. **ESI-**

**MS** *m/z* calcd for $C_{16}H_{21}O_9$ $[M + H]^+$: 357.12; $[M + NH_4]^+$: 374.14; $[M + Na]^+$: 379.10. Found: 357.18, 374.21, 379.16.

**3-(2,3,4,6-Tetra-*O*-acetyl-α-D-galactopyranosyl)-propyne (453)**

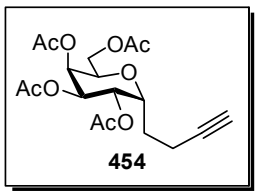


**453**

Aldehyde **314** (640 mg, 1.78 mmol)[9] was dissolved in 26 mL of methanol and cooled to 0 º C. Potassium carbonate (500 mg, 3.62 mmol) and the Bestmann Ohira reagent (394 mg, 2.04 mmol) were added and the ice bath was removed and the reaction was allowed to continue stirring for an additional 15 hours. DOWEX 50WX8 (50-100 mesh) ion exchange resin was added until the pH was neutral. The reaction was filtered through a sintered glass frit and the filtrate was concentrated to dryness. The crude oil was resuspended in water and was extracted twice with ethyl acetate and the organic washings were discarded. The aqueous phase was concentrated to yield 730 mg of a yellow oil which was used without further purification. 500 mg of this residue was redissolved in pyridine (10 mL) and acetic anhydride (10 mL) to which was added a crystal of DMAP. The reaction mixture was allowed to stir for 16 hours after which the solvent was removed under reduced pressure and coevaporated twice with toluene. The crude product was purified by flash chromatography (32 % ethyl acetate in hexanes) to yield 270 mg (0.72 mmol) of the desired product, **453** as a clear, thick oil in 59 % yield.

**$^1$H NMR** (400 MHz, *$CDCl_3$*) $\delta_{ppm}$ 5.39 (1H, t, *J* = 3.0 Hz), 5.28 (1H, dd, *J* = 8.6, 4.6 Hz), 5.22 (1H, dd, *J* = 8.6, 3.2 Hz), 4.39 (1H, ddd, *J* = 8.0, 6.5, 4.7 Hz), 4.31 (1H, dd, *J* = 10.6, 6.7 Hz), 4.17-4.05 (2H, m), 2.57 (1H, ddd, *J* = 17.1, 8.0, 2.7 Hz), 2.49 (1H, ddd, *J* = 17.2, 6.5, 2.7 Hz), 2.13 ( 1 H, s), 2.10 (3H, s), 2.07 (3H, s), 2.04 (3H, s), 2.03 (3H, s); **$^{13}$C NMR** (101 MHz, *$CDCl_3$*) $\delta_{ppm}$ 170.5, 169.9, 169.63, 169.6, 79.0, 70.6, 69.9, 69.2, 67.8, 67.4, 67.0, 60.9, 20.6, 20.6, 20.5, 18.0. **ESI-MS** *m/z* calcd for $C_{17}H_{22}O_9$ $[M + NH_4]^+$: 388.16; $[M + Na]^+$: 393.12. Found: 388.27, 393.24.

**4-(2,3,4,6-Tetra-*O*-acetyl-α-D-galactopyranosyl)-1-butyne (454)**



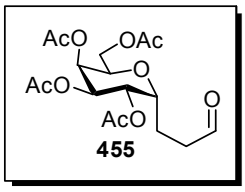
**454**

Aldehyde **455** (776 mg, 1.98 mmol) was dissolved in 30 mL of methanol with vigorous stirring and cooled to 0 ºC. Potassium carbonate (560 mg, 4.05 mmol) was added all at once and allowed to stir for 10 minutes followed by the addition of the Bestmann-Ohira reagent (**489**, 500 mg, 2.60 mol) and the

removal of the ice bath. The reaction was allowed to stir for three hours. Following filtration through a sintered glass frit, the solution was concentrated and resuspended in water and diethyl ether. The phases were separated and the aqueous phase was washed three times with ether. The organic phases were discarded and the aqueous phase was concentrated to dryness and redissolved in 5 mL of pyridine. Acetic anhydride (5 mL) was added as was a single crystal of DMAP. The mixture was allowed to stir for 16 hours under ambient conditions. Solvent was removed under reduced pressure and the residue was twice co-evaporated with 10 mL of toluene. The crude product was then purified through flash chromatography (7: 3 hexanes: ethyl acetate) to yield 220 mg (0.57 mmol) of alkynyl sugar **454** in 29 % yield.

**$^1$H NMR** (400 MHz, *CDCl$_3$*) $\delta_{ppm}$ 5.40 (1H, dd, *J* = 3.1, 2.6 Hz), 5.28 (1H, dd, *J* = 9.1, 5.1 Hz), 5.17 (1H, dd, *J* = 9.2, 3.3 Hz), 4.32 (1H, ddd, *J* = 11.3, 4.9, 3.8 Hz), 4.25 (1H, dd, *J* = 9.6, 4.0 Hz), 4.10-4.02 (2H, m), 2.38-2.18 (2H, m), 2.12 (3H, s), 2.08 (3H, s), 2.05 (3H, s), 2.02 (3H, s), 1.98 (1H, t, *J* = 2.6, 2.6 Hz), 1.96-1.85 (1H, m), 1.74-1.61 (1H, m); **$^{13}$C NMR** (101 MHz, *CDCl$_3$*) $\delta_{ppm}$ 170.3, 169.9, 169.7, 169.6, 82.7, 70.5, 69.1, 68.2, 68.1, 67.8, 67.3, 61.2, 24.9, 20.6, 20.52, 20.52, 20.46, 14.4. **ESI-MS** *m/z* calcd for $C_{10}H_{16}O_5$ $[M + NH_4]^+$: 402.41. Found: 402.33.

**3-(2,3,4,6-tetra-*O*-acetyl-α-D-galactopyranosyl)-propanal (455)**



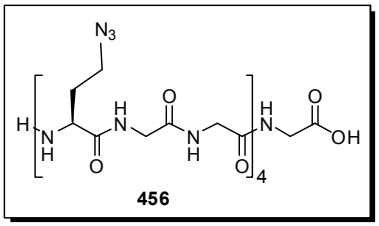
**455**

Allyl-(2,3,4,6-tetra-*O*-acetyl)-α-D-galactopyranoside, **313**, (2.00 g, 5.4 mmol) was disolved in anhydrous THF (41 mL) under an argon atmosphere and cooled to 0 ºC. $BH_3$·THF (17 mL, 17 mmol, 1.0 M) was added dropwise and the reaction was stirred for 65 minutes at 0 ºC before the ice bath was removed and the reaction was allowed to warm to ambient temperature and stirred for an additional 90 minutes. 930 µL (52 mmol) of water was added and the reaction mixture was concentrated to dryness under reduced pressure and then further dried *in vacuo* in the presence of phosphorous pentoxide for 1 hour. The white foam was resuspended in freshly distilled DCM (163 mL) under argon to which was added 12.0 g (56 mmol) of pyridinium chlorochromate portionwise and the solution was allowed to stir at ambient temperature for 14 hours. The reaction mixture was then filtered through a celite pad, and approximately 80 % of the solvent was removed under reduced pressure. The remaining solution was directly purified by flash column chromatography (1: 1

hexanes: ethyl acetate) to yield 860 mg (2.22 mmol) of **455** as a clear gel in 42 % yield over the two steps. Spectral data is consistent with the literature.[28]

**$^1$H NMR** (500 MHz, *$CDCl_3$*) $\delta_{ppm}$ 9.80 (1H, d, *J* = 2.1 Hz), 5.40 (1H, t, *J* = 2.8 Hz), 5.25 (1H, dd, *J* = 9.2, 4.7 Hz), 5.22 (1H, dd, *J* = 9.2, 3.1 Hz), 4.26 (1H, dd, *J* = 10.7, 7.1 Hz), 4.21 (1H, ddd, *J* = 11.6, 4.4, 3.4 Hz), 4.15-4.02 (2H, m), 2.68-2.54 (2H, m), 2.13 (3H, s), 2.11 (3H, s), 2.07 (3H, s), 2.07-2.00 (1H, m) 2.03 (3H, s), 1.86-1.77 (1H, m); **$^{13}$C NMR** (101 MHz, *$D_2O$*) $\delta_{ppm}$ 200.9, 170.3, 169.7, 169.6, 169.5, 71.0, 69.1, 68.0, 67.4, 66.9, 60.9, 39.4, 20.4, 20.34, 20.28, 20.22, 18.3. **ESI-MS** *m/z* calcd for $C_{17}H_{24}O_{10}$ $[M + Na]^+$: 411.13. Found: 411.18.

**{[(*S*)-2-amino-4-azidobutyric-1-amido]-glycinamido-glycinamido]$_4$-glycine (456)**

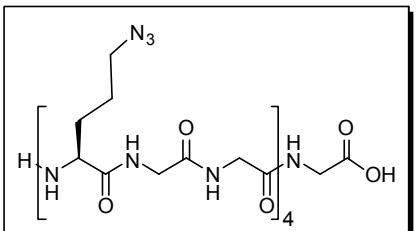


**456**

Prepared according to the "general protocol for solid-phase peptide synthesis" using 200 mg (0.122 mmol) of pre-loaded Fmoc-Gly-Wang resin in two wells and building block **459**. Following final deprotection and wash, 273 mg of bead was recovered from the wells (theoretical yield, 290 mg). A small portion (15 mg) was cleaved using standard cleavage cocktail, while the balance was stored dry under vacuum until required. Following SPE and lyophilization of the filtrate from the cleavage reaction, 5.4 mg of peptide **456** was recovered as a white powder (83 % yield based on original peptide loading).

**$^1$H NMR** (500 MHz, *$D_2O$/MeOD*) $\delta_{ppm}$ 4.60-4.45 (3H, m), 4.07-3.93 (17H, m), 3.84-3.81 (4H, m), 3.54-3.36 (8H, m), 2.21-1.91 (8H, m); **$^{13}$C NMR** (126 MHz, *$D_2O$*) $\delta_{ppm}$ 176.9,175.0, 175.0, 174.9, 172.98, 172.95, 172.80, 172.77, 172.73, 172.67, 52.54, 52.47, 52.44, 52.2, 47.8, 43.6, 43.54, 45.45, 43.39, 31.0, 30.94, 30.90. **ESI-MS** *m/z* calcd for $C_{34}H_{53}N_{25}O_{14}$ $[M + H]^+$: 1036.43; $[M + K]^+$: 1074.38. Found: 1036.81, 1074.78.

**{[(*S*)-2-amino-5-azidopentyric-1-amido]-glycinamido-glycinamido]$_4$-glycine (457)**



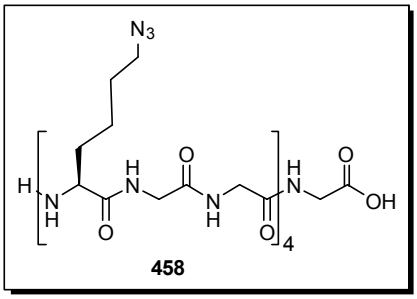
**457**

Prepared according to the "general protocol for solid-phase peptide synthesis" using 200 mg (0.122 mmol) of pre-loaded Fmoc-Gly-Wang resin in two wells and building block **460**.

Following final deprotection and wash, 283 mg of bead was recovered from the wells (theoretical yield, 299 mg). A small portion (15 mg) was cleaved using standard cleavage cocktail, while the balance was stored dry under vacuum until required. Following SPE and lyophilization of the filtrate from the cleavage reaction, 5.7 mg of peptide **457** was recovered as a white powder (94 % yield based on original peptide loading).

**$^1$H NMR** (500 MHz, *$D_2O$/MeOD*) $\delta_{ppm}$ 4.40-4.26 (4H, m), 4.01-3.87 (18H, m), 3.73 (3H, bs), 1.95-1.44 (24H, m); **$^{13}$C NMR** (126 MHz, *$D_2O$*) $\delta_{ppm}$ 179.9, 171.8, 171.7, 171.5, 53.6, 50.6, 50.5, 42.6, 42.5, 42.4, 28.1, 27.6, 24.4. **ESI-MS** *m/z* calcd for $C_{38}H_{61}N_{25}O_{14}$ $[M + H]^+$: 1092.49; $[M + K]^+$: 1130.44. Found: 1092.84, 1130.80.

**{[(*S*)-2-amino-6-azidohexyric-1-amido]-glycinamido-glycinamido]$_4$-glycine (458)**



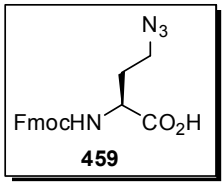
**458**

Prepared according to the "general protocol for solid-phase peptide synthesis" using 200 mg (0.122 mmol) of pre-loaded Fmoc-Gly-Wang resin in two wells using building block **461**. Following final deprotection and wash, 275 mg of bead was recovered from the wells (theoretical yield, 305 mg). A small portion (15 mg) was cleaved using standard cleavage cocktail, while the balance was stored dry under vacuum until required. Following SPE and lyophilization of the filtrate from the cleavage reaction, 5.8 mg of peptide **458** was recovered as a white powder (84 % yield based on original peptide loading).

**$^1$H NMR** (500 MHz, *$D_2O$/MeOD*) $\delta_{ppm}$ 4.41-4.27 (4H, m), 4.05-3.91 (18H, m), 3.80-3.75 (3H, m), 1.96-1.25 (32H, m); **$^{13}$C NMR** (126 MHz, *$D_2O$*) $\delta_{ppm}$ 182.8, 182.1, 180.6, 180.2, 53.8, 50.8, 42.5, 42.43, 42.36, 30.3, 30.2, 29.9, 27.5, 22.3, 21.2. **ESI-MS** *m/z* calcd for $C_{42}H_{69}N_{25}O_{14}$ $[M + H]^+$: 1148.55. Found: 1148.82.

**[(*S*)-2-[(9H-fluoren-9-ylmethoxy)carbonyl]amino-4-azido-butanoic acid (Fmoc-Abu($N_3$)-OH) (459)**

Prepared according to the published protocol.[25] A solution of (2,5-dioxo-1-pyrrolidinyl)(9*H*-fluoren-9-ylmethyl) carbonate (Fmoc-OSu, 7.00 g, 20.7 mmol) in dioxane (70 mL) was cannulated into a flask containing azide

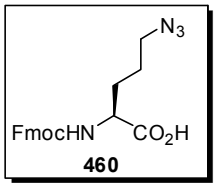


**459**

derivative **448** (3.5 g, 24 mmol) dissolved in dioxane (70 mL). 1 M NaOH was added dropwise until pH = 8. The reaction was then stirred for an additional 2.5 hours at ambient temperature. Water (70 mL) was added and the reaction was acidified with 10 % HCl to pH = 3. The reaction was transferred to a separatory funnel and extracted three times with DCM. The combined organics were then dried, filtered and concentrated. The crude product was then purified through dry vacuum chromatography. The mixed fractions were then repurified though HPLC to yield 2.62 g of **459** (7.20 mmol) as a clear oil that solidifies upon standing in 30 % yield. Spectra is consistent with the literature.[25]

**$^{1}$H NMR** (300 MHz, *CDCl$_3$*) $\delta_{ppm}$ 7.77 (2H, d, *J* = 7.4 Hz), 7.59 (2H, d, *J* = 7.2 Hz), 7.41 (2H, t, *J* = 7.4, 7.4 Hz), 7.32 (2H, dt, *J* = 7.4, 1.1 Hz), 5.44 (1H, bd, *J* = 7.9 Hz), 4.64-4.38 (3H, m), 4.22 (1H, t, *J* = 6.4 Hz), 3.43 (2H, t, *J* = 6.3 Hz), 2.29-2.13 (1H, m), 2.06-1.92 (1H, m); **$^{13}$C NMR** (101 MHz, *CDCl$_3$*) $\delta_{ppm}$ 175.3, 156.4, 143.4, 143.2, 141.1, 127.6, 127.4, 126.9, 124.8, 124.5, 119.9, 67.1, 51.5, 47.4, 46.8, 30.9. **ESI-MS** *m*/*z* calcd for $C_{19}H_{18}N_4O_4$ $[M + Na]^+$: 389.12; $[M + K]^+$: 405.09. Found 389.13, 405.10.

**[(*S*)-2-[(9H-fluoren-9-ylmethoxy)carbonyl]amino-5-azido-pentanoic acid (Fmoc-Orn($N_3$)-OH) (460)**



**460**

**Method A**:. A solution of (2,5-dioxo-1-pyrrolidinyl)(9*H*-fluoren-9-ylmethyl) carbonate (Fmoc- OSu, 5.5 g, 16.25 mmol) in dioxane (38 mL) was cannulated into a flask containing azide derivative **449** (3.80 g, 10.7 mmol) dissolved in dioxane (70 mL). 1 M NaOH was added dropwise until pH = 8. The reaction was then stirred for an additional 2.5 hours at ambient temperature. Water (42 mL) was added and the reaction was acidified with 10 % HCl to pH = 3. The reaction was transferred to a separatory funnel and extracted three times with DCM. The combined organics were then dried, filtered and concentrated. The crude product was then purified through dry vacuum chromatography. The mixed fractions were then repurified though HPLC to yield 1.08 g of product (2.84 mmol) as a clear oil that solidifies upon standing in 27 % yield. Spectrum matches published data.[25]

**Method B**: Protocol is a modification of a previously published procedure.[25]

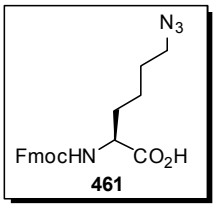
Trifluoromethylsulfonic azide was prepared according to the established protocol.[29] Sodium azide (6.7 g, 103 mmol) was suspended in a mixture of water (17 mL) and dichloromethane (28 mL) and the solution was cooled to 0 º C. Trifluoromethylsulfonic

anhydride (3.5 mL, 21 mmol) was added dropwise with stirring and the ice bath was removed and the reaction allowed to stir for 2 hours. The reaction mixture was then transferred to a separatory funnel and the phases were separated. The aqueous phase was extracted twice with dichloromethane (12 mL) and the combined organic phases were washed with sodium bicarbonate. This solution of triflic azide in dichloromethane was then used directly below.

Fmoc-protected ornithine derivative (**463**, 2.0 g, 4.4 mmol) was dissolved in a mixture of water (26 mL) and methanol (54 mL) and cooled to 0 ºC. Potassium carbonate (2.4 g, 17.6 mmol) was added followed by copper (II) sulfate pentahydrate (20 mg, 0.080 mmol). The prepared solution of triflic azide was then added dropwise via dropping funnel over 1 hour and the reaction was allowed to stir for an additional 16 hours. 10 % HCl was added until pH= 6 (the solution changed colour from blue to bright yellow at this pH) and the two phases were separated. The aqueous phase was extracted three more times with dichloromethane and the combined organic phases were washed with brine, dried, filtered and concentrated. The crude product was then purified by flash chromatography (1 % methanol in dichloromethane) to yield 1.52 g (4.00 mmol) of the azido derivative **460** as a clear oil (91 % yield). Spectrum matches published data.[25] Minor rotamer in [ ] where applicable.

**$^1$H NMR** (300 MHz, *$CDCl_3$*) $\delta_{ppm}$ 9.87 (1H, bs), 7.75 (2H, d, *J* = 7.4 Hz), 7.59 (2H, *pseudo*-d, *J* = 6.6 Hz), 7.40 (2H, t, *J* = 7.4 Hz), 7.31 (2H, t, *J* = 7.4, 7.4 Hz), 5.65 (1H, d, *J* = 8.1 Hz) [6.66 (1H, d, *J* = 6.9 Hz)], 4.67-3.89 (3H, m), 4.20 (1H, t, *J* = 6.3 Hz), 3.28 (1H, t, *J* = 5.5 Hz) [3.14 ( 1 H, t, *J* = 5.9 Hz)], 2.05-1.27 (4H, m); **$^{13}$C NMR** (75 MHz, *$CDCl_3$*) $\delta_{ppm}$ 176.4, 156.1, 143.7, 143.5, 141.3, 127.7, 127.0, 124.9, 120.0, 67.1, 53.2, 50.7, 47.1, 29.5, 24.7. **ESI-MS** *m/z* calcd for $C_{21}H_{22}N_4O_4$ $[M + K]^+$: 419.11. Found: 419.11.

**[(*S*)-2-[(9H-fluoren-9-ylmethoxy)carbonyl]amino-6-azido-hexanoic acid (Fmoc-Lys($N_3$)-OH) (461)**



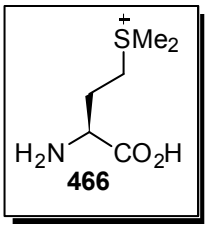
**461**

**Method A**: Amino acid **461** was prepared as described for **460** above using Fmoc-OSu (2.2 g, 6.5 mmol) in dioxane (38 mL) applied to azide derivative **450** (2g, 5.5 mmol) dissolved in dioxane (28 mL). Following HPLC purification yielded 1.02 g of **461** as a clear oil that solidifies upon standing in 47 % yield.

**Method B**: Amino acid **461** was prepared as described above for **460** using Fmoc-protected lysine derivative (**464**, 2.0 g, 4.3 mmol) with potassium carbonate (2.4 g, 17.6 mmol), and

copper (II) sulfate pentahydrate (20 mg, 0.080 mmol). The crude product was then purified by flash chromatography (1 % methanol in dichloromethane) to yield 1.6 g (4.05 mmol) of the azido derivative as a clear oil (94 % yield). Spectral data is consistent with the literature.[25]
**$^1$H NMR** (300 MHz, *$CDCl_3$*) $\delta_{ppm}$ 7.77 (2H, d, *J* = 7.5 Hz), 7.59 (2H, *pseudo*-d, *J* = 7.2 Hz), 7.40 (2H, t, *J* = 7.4 Hz), 7.31 (2H, t, *J* = 7.4 Hz), 5.31 (1H, bd, *J* = 8.1 Hz), 4.62-4.34 (3H, m), 4.22 (1H, t, *J* = 6.8 Hz), 3.28 (2H, *pseudo*-t, *J* = 6.4 Hz), 2.02-1.86 (1H, m), 1.80-1.17 (5H, m); **$^{13}$C NMR** (75 MHz, *$CDCl_3$*) $\delta_{ppm}$ 175.9, 156.3, 143.6, 143.4, 141.1, 127.6, 126.9, 124.9, 124.5, 119.9, 67.1, 53.4,50.8, 46.9, 31.5, 28.1, 22.3. **ESI-MS** *m/z* calcd for $C_{21}H_{22}N_4O_4$ $[M + K]^+$: 433.12. Found: 433.13.

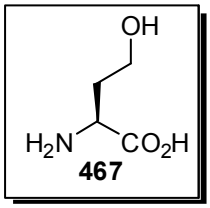
**(*S*)-(3-Amino-3-carboxypropyl)dimethylsulfonium iodide (466)**



**466**

Compound **466** was prepared according to the published protocol but with modifications.[30] To a solution of methionine **455** (20.0 g, 134 mmol) suspended in water (132 mL), methyl iodide (49.0 g, 21.6 mL, 348 mmol) was added dropwise. The flask was fitted with an air-cooled condenser and the reaction was warmed to 40 ºC and allowed to stir for 20 hours. The water and excess methyl iodide was removed under reduced pressure to leave a white solid. This solid was redissolved in 48 mL of water. Ethanol (215 mL) was added and the reaction was allowed to stand at 0 ºC for 3 hours. The resulting precipitate was collected by filtration and washed with *iso*-propanol and dried *in vacuo* to provide 35.01 g of the sulfonium iodide as white crystals in 90.0 % yield. A further 3.42 g of white crystals were obtained in a second recrystallization to provide a combined yield of 38.44 g of product **466** in 98.5 % yield. Spectral data is consistent with the literature.[31]
**$^1$H NMR** (400 MHz, *$D_2O$*) $\delta_{ppm}$ 3.89 (1H, t, *J* = 6.4 Hz), 3.53 (1H, ddd, *J* = 18.1, 14.7, 8.5 Hz), 3.46 (1H, ddd, *J* = 16.1, 14.9, 8.6 Hz), 2.97 (6H, s), 2.45-2.32 (2H, m); **$^{13}$C NMR** (101 MHz, *$D_2O$*) $\delta_{ppm}$ 172.5, 52.8, 39.5, 25.1, 24.80, 24.75. **ESI-MS** *m/z* calcd for $C_6H_{14}N_1O_2S$ $[M]^+$: 164.24. Found 164.17.

**Homoserine (467)**



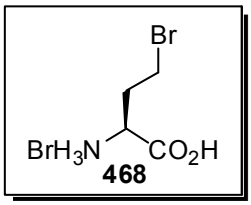
**467**

Compound was prepared according to the published protocol but with modifications.[30] Two of the following reactions were set up in parallel. Iodide

**466** (17.2 g, 59.1 mmol) was added to a three-necked round-bottomed flask charged with water (56 mL). Sodium bicarbonate (5.0 g, 59.5 mmol) was dissolved in 80 mL of water and transferred to a dropping funnel which was fitted to the round bottomed flask. A second neck was equipped with a water-cooled condenser and the third neck was sealed with a glass stopper. The reaction was heated to reflux using a heating mantle and the bicarbonate solution was added portionwise (approximately every 15 minutes) to maintain a pH between 5 and 2.[a] This addition took 6 hours. Following the completion of this addition, the reaction was maintained at reflux for an additional 12 hours before being cooled to ambient temperature when the two parallel reactions were combined. The solvent was removed under reduced pressure to provide a thick oil and redissolved in water (15 mL) and diluted with ethanol (30 mL) and acetone (450 mL). Upon standing for 1 hour, the precipitate was collected and redissolved in water and lyophilized to provide 15.1 g of the product, **467**, as a white solid in a quantitative yield. Spectrum is consistent with the literature.[32]

**$^1$H NMR** (400 MHz, *$D_2O$*) $\delta_{ppm}$ 3.84-3.73 (3H, m), 2.13 (1H, m), 2.00 (1H, m); **$^{13}$C NMR** (101 MHz, *$D_2O$*) $\delta_{ppm}$ 58.6, 53.4, 48.9, 32.3. **EI-MS** *m*/*z* calcd for $C_4H_9N_1O_3$ $[M - H_2O]^+$: 101.10. Found 101.1.

**[(S)-2-Amino-4-bromobutanoic acid] hydrogen bromide (468)**



**468**

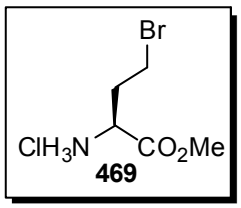
Prepared according to the published protocol.[33] Homoserine (**467** 1.50 g, 12.6 mmol) was added to a sealed tube with 15 mL of HBr in acetic acid (30 %). The tube was sealed and heated to 110 ºC for 5 hours. The reaction was cooled to 0 ºC in an ice bath and 15 mL of diethyl ether was added. Yellow crystals formed quickly and were collected by filtration and dried *in vacuo* to yield 1.8 g of the hydrobromide salt **468** in 55 % yield. Spectral data is consistent with literature.[33]

**$^1$H NMR** (300 MHz, *$D_2O$*) $\delta_{ppm}$ 4.23 (1H, t, *J* = 6.7 Hz), 3.84-3.48 (2H, m), 2.57 (1H, ddd, *J* = 15.2, 13.2, 6.5 Hz), 2.40 (1H, ddd, *J* = 15.2, 13.2, 7.0 Hz); **$^{13}$C NMR** (75 MHz, *$D_2O$*) $\delta_{ppm}$ 207.3,

[a] The pH was conveniently monitored by inserting pH test strips into the reaction solution and monitoring the colour changes

51.7, 32.8, 28.0. **ESI-MS** *m/z* calcd for $C_4H_8\ BrNO_2$ $[M + Na]^+$: 205.01, 207.01. Found: 205.18, 207.21.

**[(S)-methyl 2-Amino-4-bromobutanoate] hydrogen chloride (469)**

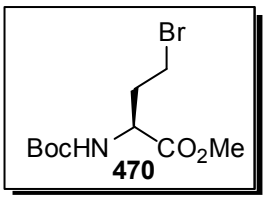


**469**

Prepared according to a published protocol.[34] Acetyl chloride (48 g, 43.2 mL, 612 mmol) was added dropwise to methanol (480 mL) cooled to 0 ºC. The ice bath was removed and this mixture was stirred for 30 minutes. Hydrobromide salt **468** (16 g, 61.3 mmol) was then added and the reaction was stirred for a further 16 hours. Solvent was removed under reduced pressure to yield a thick brown oil that was further dried *in vacuo* to produce 14.2 g of **469** as a brown solid (quantitative yield). Spectral data is consistent with literature.[34]

**$^1$H NMR** (300 MHz, $D_2O$) $\delta_{ppm}$ 4.46 (1H, t, $J$ = 6.6 Hz), 3.95 (3H, s), 3.73 (2H, t, $J$ = 6.4 Hz), 2.70 (1H, ddd, $J$ = 15.0, 6.4, 6.0 Hz), 2.53 (1H, ddd, $J$ = 15.1, 6.6, 6.4 Hz); **$^{13}$C NMR** (75 MHz, $D_2O$) $\delta_{ppm}$ 172.4, 56.7, 54.1, 35.2, 30.8. **ESI-MS** *m/z* calcd for $C_5H_{10}\ BrNO_2$ $[M + H]^+$: 196.00, 198.00. Found: 196.04, 198.04.

**(*S*)-methyl 2-[*tert*-butoxycarbonyl]amino-4-bromobutanoate (470)**



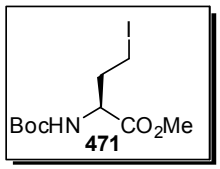
**470**

Prepared according to a published protocol.[34] Bromide **469** (14.2 g, 61.2 mmol) was dissolved in dioxane (144 mL) and cooled to 0 ºC. Di-*tert*-butyl dicarbonate was then added. A solution of $NaHCO_3$ (24.2 g, 288 mmol) in water (144 mL) was added dropwise through a dropping funnel and the reaction stirred at 0 ºC for 20 hours. The reaction was then diluted with water (288 mL) and extracted with dichloromethane (3 x 300 mL). The combined organic extractions were dried, filtered and cocnetrated under reduced pressure to provide 22.3 g of a deep orange oil. This crude product was purified by dry-vacuum chromatography (100 % hexanes to 50 % ethyl acetate in hexanes in 5 % steps) to provide 14.2 g of **470** as a clear, thick oil (79 % yield). Proton NMR matches published data.[25]

**$^1$H NMR** (400 MHz, $CDCl_3$) $\delta_{ppm}$ 5.10 (1H, bs), 4.43 (1H, dd, $J$ = 12.9, 7.2 Hz), 3.77 (3H, s), 3.43 (2H, t, $J$ = 7.1 Hz), 2.41 (1H, td, $J$ = 12.7, 7.0 Hz), 2.20 (1H, dt, $J$ = 14.4, 7.3 Hz), 1.45 (9H, s); **$^{13}$C NMR** (101 MHz, $CDCl_3$) $\delta_{ppm}$ 172.17, 146.6, 80.1, 67.0, 52.5, 35.7, 28.2, 27.3. **ESI-**

MS *m/z* calcd for $C_{10}H_{18}NO_4$ $[M + H]^+$: 296.04, 298.04; $[M + Na]^+$: 318.03, 320.03. Found 318.09, 320.08.

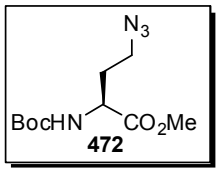
**(*S*)-methyl 2-[*tert*-butoxycarbonyl]amino-4-iodobutanoate (471)**




Prepared according to a published protocol.[34] Bromide aminobutanoic acid derivative **470** (680 mg, 2.3 mmol) was dissolved in acetone (23 mL) in a flask equipped with a water-cooled condenser. Sodium iodide (690 mg, 4.6 mmol) was added and the solution heated to reflux for 3 hours. The reaction was cooled, filtered through a celite pad, and concentrated to provide 1.3 g of crude product. The material was resuspended in DCM, filtered through a 20 μM nylon filter and concentrated to yield 812 mg of **471** as a thick yellow oil in quantitative yield. Spectrum matches previously published data.[34]

**$^1$H NMR** (500 MHz, *CDCl$_3$*) $\delta_{ppm}$ 5.20 (1H, d, *J* = 7.8 Hz), 4.30 (1H, dd, *J* = 12.8, 8.5 Hz), 3.71 (3H, s), 3.14 (2H, t, *J* = 7.5 Hz), 2.42-2.29 (1H, m), 2.19-2.05 (1H, m), 1.40 (9H, s). **ESI-MS** *m/z* calcd for $C_{10}H_{18}NO_4I$ $[M + H]^+$: 344.04; $[M + Na]^+$: 366.02; $[M + K]^+$: 381.99. Found 344.28, 366.14, 382.31.

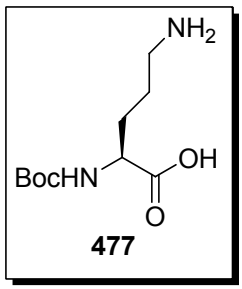
**(*S*)-methyl 2-[*tert*-butoxycarbonyl]amino-4-azidobutanoate (472)**




Iodide derivative **471** (16.5 g, 48 mmol) was dissolved in DMF (140 mL) to which was added sodium azide (9.4 g, 143 mmol) and the reaction was then heated to 90 ºC for 16 hours. The reaction was then filtered through a celite pad, and the filtrate was concentrated. The crude product was partitioned between brine and ethyl acetate and the following extraction, the organic phase was dried, filtered and concentrated to yield 12.3 g of azido derivative **472** in quantitative yield. Spectral data is consistent with the literature.[25]

**$^1$H NMR** (300 MHz, *CDCl$_3$*) $\delta_{ppm}$ 5.32 (1H, d, *J* = 7.0 Hz), 4.32 (1H, dd, *J* = 12.5, 7.5 Hz), 3.69 (3H, s), 3.34 (2H, t, *J* = 6.6 Hz), 2.11-1.95 (1H, m), 1.85 (1H, dt, *J* = 14.0, 13.9, 6.8 Hz), 1.37 (9H, s); **$^{13}$C NMR** (101 MHz, *CDCl$_3$*) $\delta_{ppm}$ 172.4, 155.2, 80.2, 52.5, 51.2, 47.7, 31.8, 28.2. **ESI-MS** *m/z* calcd for $C_{10}H_{18}N_4O_4$ $[M + Na]^+$: 281.12; $[M + K]^+$: 297.09. Found: 281.19, 297.16.

**(*S*)-2-{[(1,1-dimethylethoxy)carbonyl]amino}-5-amino-pentanoic acid (477)**

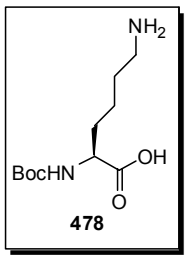


**477**

Boc-Orn(Cbz)-OH (3.15 g, 8.60 mmol) was dissolved in 100 mL of methanol with stirring and purged with nitrogen. Palladium supported on carbon (10 % dry weight, 315 mg) was added and the flask was then purged with hydrogen and fitted with a hydrogen balloon. The reaction was allowed to stir for 14 hours and was then diluted with water (80 mL) and filtered through a celite pad and washed with water. Removal of the solvent under reduced pressure yielded 2.00 g of the product as white precipitate (quantitative yield). Spectrum matches published values.[35]

Some signals are doubled: hindered rotation around C-N bond. **$^1$H NMR** (300 MHz, *$D_2O$*) $\delta_{ppm}$ 3.89 (1H, bs), 3.00 (2H, t, J = 7.1 Hz), 1.86-1.59 (4H, m), 1.42 (9H, s); **$^{13}$C NMR** (126 MHz, *$D_2O$*) $\delta_{ppm}$ 179.2, 157.7, 81.0, 55.3, 38.9, 28.7, 27.5, 23.3. **ESI-MS** *m/z* calcd for $C_{10}H_{20}N_2O_4$ [M + H]$^+$: 233.15. Found: 233.30.

**(*S*)-2-{[(1,1-dimethylethoxy)carbonyl]amino}-6-amino-hexanoic acid (478)**



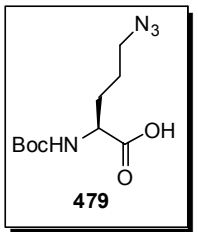
**478**

Boc-Lys(Cbz)-OH (2.00 g, 5.26 mmol) was dissolved in 30 mL of methanol with stirring and purged with nitrogen. Palladium supported on carbon (10 % dry weight, 200 mg) was added and the flask was then purged with hydrogen and fitted with a hydrogen balloon. The reaction was allowed to stir for 14 hours and was then diluted with water (40 mL) and filtered through a celite pad and washed with water. Removal of the solvent under reduced pressure yielded 1.3 g of the product as white precipitate (quantitative yield). Spectral data matches published values.[36]

**$^1$H NMR** (300 MHz, *$D_2O$*) $\delta_{ppm}$ 3.90 (1H, dd, *J* = 7.8, 4.9 Hz), 2.99 (2H, t, *J* = 7.5, 7.5 Hz), 1.84-1.57 (1H, m), 1.49-1.32 (1H, m), 1.42 (1H, s). **ESI-MS** *m/z* calcd for $C_{11}H_{22}N_2O_4$ [M + H]$^+$: 247.31; [M + Na]$^+$: 269.29. Found 247.30, 269.32.

**(*S*)-2-{[(1,1-dimethylethoxy)carbonyl]amino}-5-azido-pentanoic acid (479)**

Protocol is a modification of a previously published procedure.[25] Trifluoromethanesulfuric azide was prepared according to the established protocol described above in the preparation of **460**[29] using sodium azide (6.7



**479**

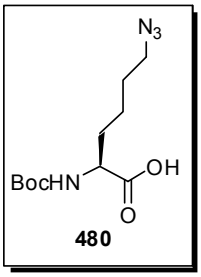
g, 103 mmol), water (17 mL), dichloromethane (28 mL) and trifluoromethanesulfuric anhydride (3.5 mL, 21 mmol).

Boc-protected ornithine derivative (**477**, 2.0 g, 8.62 mmol) was dissolved in a mixture of water (26 mL) and methanol (54 mL) and cooled to 0 ºC. Potassium carbonate (1.7 g, 12.2 mmol) was added followed by copper (II) sulfate pentahydrate (20 mg, 0.080 mmol). The prepared solution of triflic azide was then added dropwise via dropping funnel over 1 hour and the reaction was allowed to stir for an additional 16 hours. 10 % HCl was added until pH= 6 (the solution changed colour from blue to bright yellow at this pH) and the two phases were separated. The aqueous phase was extracted three more times with dichloromethane and the combined organic phases were washed with brine, dried, filtered and concentrated to yield 2.06 g of the azido derivative as a clear oil without further purification (93 % yield). Spectrum matches published data.[25]

(minor rotamer in brackets)

**$^{1}$H NMR** (400 MHz, *$CDCl_3$*) (50 ºC) $\delta_{ppm}$ 6.72 (1H, bs), 5.14 (1H, d, *J* = 7.4 Hz), 4.33 (4.18) (1H, bs), 3.32 (2H, t, *J* = 5.3 Hz), 2.02-1.89 (1H, m), 1.85-1.61 (3H, m), 1.44 ( 9H, s); **$^{13}$C NMR** (126 MHz, *$CDCl_3$*) (55 ºC) $\delta_{ppm}$ 177.4, 155.6, 80.5, 52.8, 50.8, 29.7, 28.2, 24.8. **ESI-MS** *m*/*z* calcd for $C_{10}H_{18}N_4O_4$ $[M + Na]^+$: 281.26; $[M + K]^+$: 297.23. Found 281.27, 297.25.

**6-azido-2*S*-{[(1,1-dimethylethoxy)carbonyl]amino}hexanoic acid (480)**



**480**

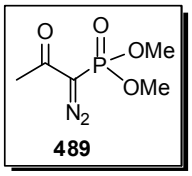
Protocol is a modification of a previously published procedure.[25] Trifluoromethanesulfuric azide was prepared according to the established protocol described above in the preparation of **460**[29] using sodium azide (3.5 g, 54 mmol), water (9 mL), dichloromethane (15 mL) and trifluoromethanesulfuric anhydride (1.8 mL, 11 mmol).

Boc-protected lysine derivative (**478**, 1.00 g, 4.06 mmol) was dissolved in a mixture of water (13 mL) and methanol (27 mL) and cooled to 0 ºC. Potassium carbonate (840 mg, 6.1 mmol) was added followed by copper (II) sulfate pentahydrate (10 mg, 0.040 mmol). The prepared solution of triflic azide was then added dropwise via dropping funnel over 1 hour and the reaction was allowed to stir for an additional 16 hours. 10 % HCl was added until pH= 6 (the solution changed colour from blue to bright yellow at this pH) and the two phases were separated. The aqueous phase was extracted three more times with dichloromethane and the

combined organic phases were washed with brine, dried, filtered and concentrated to yield 1.05 g of azido derivative **480** as a clear oil without further purification (95 % yield). Minor rotamer in parentheses. Spectral data is consistent with the literature.[25]

**$^1$H NMR** (400 MHz, *$CDCl_3$*) (55 ºC) $\delta_{ppm}$ 5.11 (1H, bs), 4.29 (1H, bs), 3.30 (2H, t, *J* = 6.6 Hz), 1.91 (1H, m), 1.73 (1H, m), 1.69-1.60 (2H, m), 1.57-1.48 (2H, m), 1.47 (9H, s); **$^{13}$C NMR** (101 MHz, *$CDCl_3$*) (22 ºC) $\delta_{ppm}$ 176.72 (176.65), 155.6 (156.9), 80.3 (81.9), 53.0 (54.3), 51.0 (51.0), 31.7 (31.6), 28.2 (28.2), 28.1 (28.1), 22.36 (22.43). **ESI-MS** *m/z* calcd for $C_{11}H_{20}N_4O_4$ $[M + Na]^+$: 295.29; $[M + K]^+$: 311.26. Found: 295.29, 311.27.

**Dimethyl-1-diazo-2-oxopropylphosphonate (Bestmann-Ohira reagent) (489)**

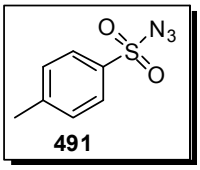


**489**

Sodium hydride (2.1 g, 87 mmol) was suspended in 160 mL of THF and cooled to 0 ºC under an argon atmosphere. Dimethyl-2-oxopropylphosphonate, **493**, (12.2 g, 10.2 mL, 73.6 mmol) was also dissolved in 150 mL of anhydrous THF and was cannulated into the sodium hydride suspension and the solution was stirred for 1 hr at 0 ºC. Toluenesulfonyl azide, **491**, (16 g, 81 mmol) was dissolved in THF (50 mL) and was then cannulated into the reaction mixture and stirred for an additional hour at 0 ºC. The reaction was warmed to ambient temperature and water was added dropwise (5 mL). The reaction mixture was then filtered through a celite pad, rinsed with diethyl ether, and the filtrate was concentrated to dryness to provide the crude product as an orange oil that was then purified by flash chromatography (1 L of silica, compound eluted by 1: 1 ethyl acetate: hexanes (2 L) to 7: 3 ethyl acetate: hexanes (2 L)) to provide 9.2 g of the desired reagent as a thick yellow oil (65 %). Spectral data matches previously published data.[a, 37]

**$^1$H NMR** (400 MHz, *$CDCl_3$*) $\delta_{ppm}$ 3.85 ( 1 H, d, *J* = 11.9 Hz), 2.28 ( 1 H, s); **$^{13}$C NMR** (126 MHz, *$CDCl_3$*) $\delta_{ppm}$ 189.88 (d, *J* = 13.10 Hz), 53.58 (d, *J* = 5.57 Hz), 29.6, 27.1. **ESI-MS** *m/z* calcd for $C_5H_9N_2O_4P$ $[M + H]^+$: 193.04. Found: 193.09.

**Toluenesulfonyl azide (491)**



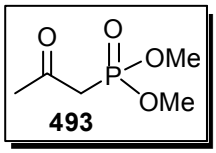
**491**

[a] $^{13}$C spectrum disagrees on chemical shift of (*C*$N_2$) relative to the published spectrum. Proton spectrum and mass spectrum are consistent, however.

Compound prepared in a modified procedure from Pollex.[38] Sodium azide (2.73 g, 420 mmol) was dissolved in 120 mL of water and 60 mL of acetone with stirring and cooled to 0 ºC. Toluenesulfonyl chloride (8.00, 420 mmol) was dissolved in 60 mL of acetone and added dropwise through a dropping funnel to the sodium azide over 30 minutes. The reaction was then allowed to stir for an additional 2 hours, and the acetone was removed under reduced pressure at 30 ºC. WARNING: Toluenesulfonyl azide is a known explosive and should be handled with care and explodes when heated above 120 ºC. The remaining solution was extracted three times with ether (300 mL), and the combined organic layers were dried with anhydrous $MgSO_4$, filtered and concentrated. The resulting white solid was dried *in vacuo* in the presence of phosphorous pentoxide to yield 8.05 g of tosyl azide **491** as a white powder (97 % yield). Spectroscopic data matches published values.[39]

**$^1$H NMR** (400 MHz, *$CDCl_3$*) $\delta_{ppm}$ 7.81 (2H, d, *J* = 8.4 Hz), 7.39 (2H, d, *J* = 8.6 Hz), 2.46 (3H, s); **$^{13}$C NMR** (101 MHz, *$D_2O$*) $\delta_{ppm}$ 146.2, 135.3, 130.1, 127.3, 21.6. **ESI-MS** *m/z* calcd for $C_7H_7N_3O_2S$ $[2M + K]^+$: 433.02. Found: 433.11.

**Dimethyl-2-oxopropylphosphonate (493)**

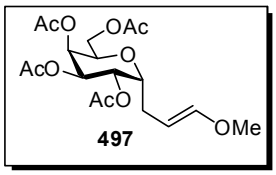


**493**

Potassium iodide (27.0 g, 162 mmol) was suspended in a solution of acetone (33 mL) and acetonitrile (41.3 mL) under an argon atmosphere. Freshly distilled chloroacetone (15.0 g, 13.0 mL, 162 mmol) was added dropwise and stirred for 1 hour. Trimethyl phosphite (20.0 g, 19.1 mL, 162 mmol) was then added portionwise and the reaction mixture was stirred for a further 12 hours. The reaction mixture was then warmed to 50 ºC for three hours before being filtered through a celite pad. The filtrate was concentrated to remove volatiles and the residue was distilled under high vacuum (0.6 mbar) with the use of a heating mantle (84 V) to obtain 14 g (84.3 mmol) of the title compound in the fraction condensing at 85-86 ºC (52 % yield). Spectral data matches published data.[37]

**$^1$H NMR** (300 MHz, *$CDCl_3$*) $\delta_{ppm}$ 3.70 (6H, d, *J* = 11.2 Hz), 3.02 (2H, d, *J* = 22.8 Hz), 2.23 (3H, s); **$^{13}$C NMR** (126 MHz, *$CDCl_3$*) $\delta_{ppm}$ 199.1 (d, *J* = 5.9 Hz), 52.0 (d, *J* = 6.5 Hz), 40.7 (d, *J* = 127.7 Hz), 30.3. **ESI-MS** *m/z* calcd for $C_5H_{11}O_4P$ $[M + H]^+$: 167.05; $[M + K]^+$: 205.00. Found: 167.07, 205.03.

**(E)-3-(2,3,4,6-Tetra-*O*-acetyl-α-D-galactopyran-1-yl)-1-methoxyprop-1-ene (497)**

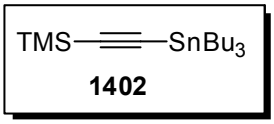


**497**

Anhydrous (Methoxymethyl)triphenylphosphonium chloride (1.88 g, 5.5 mmol) was dissolved in anhydrous THF (20 mL) and cooled, with stirring, to -78ºC. *n*-butyl lithium (880 µL, 2.5 M in THF, 2.2 mmol) was added dropwise. Aldehyde **314** (821 mg, 2.2 mmol) was dissolved in anhydrous THF (10 mL) and was cannulated into the reaction mixture. The reaction was stirred for 90 minutes at -78 ºC before being warmed to ambient temperature and stirred for an additional 8 hours. The reaction was then returned to -78 ºC, and quenched with saturated ammonium chloride solution and immediately warmed to ambient temperature. The reaction mixture was then diluted with diethyl ether and the reaction mixture was then washed three times with water, once with brine, and then dried and concentrated in the usual manner. The crude product was then purified through flash column chromatography (8:1 toluene: acetone) to provide 221 mg of the product as a white solid in 25 % yield. Spectrum matches previously reported data.[40]

**$^{1}$H NMR** (500 MHz, *CDCl$_3$*) $\delta_{ppm}$ 6.35 (1H, d, *J* = 12.5 Hz), 5.41 (1H, t, *J* = 2.6, 2.6 Hz), 5.26 (1H, dd, *J* = 8.4, 4.7 Hz), 5.21 (1H, dd, *J* = 9.1, 3.1 Hz), 4.64 (1H, td, *J* = 12.5, 7.6, 7.6 Hz), 4.26 (1H, dd, *J* = 12.3, 9.3 Hz), 4.16 (1H, td, *J* = 8.9, 4.9, 4.9 Hz), 4.10-4.05 (2H, m), 3.52 (3H, s), 2.37-2.27 (1H, m), 2.17-2.12 (1H, m), 2.12 (3H, s), 2.08 (3H, s), 2.05 (3H, s), 2.03 (3H, s); **$^{13}$C NMR** (126 MHz, *CDCl$_3$*) $\delta_{ppm}$ 170.6, 170.1, 169.9, 169.8, 149.0, 97.1, 72.1, 68.4, 68.4, 67.9, 67.6, 61.5, 59.6, 55.8, 25.1, 20.79, 20.74, 20.67, 20.67.

**1-Trimethylsilyl-2-tributylstannylethyne (1402)**



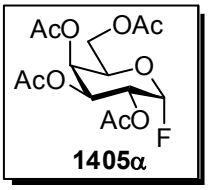
**1402**

This compound was prepared according to a modified protocol of that of Logue and Teng.[41] TMS-acetylene (2 g, 20.36 mmol) was dissolved in anhydrous THF (200 mL) and cooled to -78 ºC. Butyl-lithium (7.72 mL, 19.3 mmol) was added and the reaction was stirred for 30 minutes at which point the anion was quenched with tributylstannyl chloride (7.3 g, 22.4 mmol) and allowed to warm and stir at ambient temperature for 16 hours. The reaction was quenched with saturated ammonium chloride and concentrated under reduced pressure. The liquid residue was partitioned

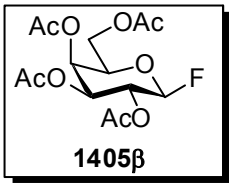
between water and ether, and the aqueous phase was extracted twice with ether, and the combined organic phases were then washed twice with water, dried, and filtered through a celite pad to provide 7.26 g of the product as a clear liquid in 92 % yield. Spectral data is consistent with the literature.[42]

**$^1$H NMR** (400 MHz, *$CDCl_3$*) $\delta_{ppm}$ 1.55 (6H, m), 1.33 (6H, m), 0.98 (6H, m), 0.89 (12H, t, *J* = 7.3 Hz), 0.15 (9H, s); **$^{13}$C NMR** (101 MHz, *$CDCl_3$*) $\delta_{ppm}$ 118.8, 113.1, 28.8, 26.9, 13.6, 11.1, 0.2. **EI-MS** *m*/*z* calcd for $C_{17}H_{36}SiSn$ $[M - CH_3]^+$: 373.14; $[M - C_4H_9]^+$: 331.09. Found 373.15, 331.09.

**2,3,4,6-Tetra-*O*-acetyl-α-D-galactopyranosyl fluoride (1405α)** and **2,3,4,6-Tetra-*O*-acetyl-β-D-galactopyranosyl fluoride (1405β).**



**1405α**



**1405β**

Reaction was carried out according to a modified procedure of that of Jobron.[43] In a flask containing freshly activated 4 Å molecular sieves under argon, acetylene **1402** (1.40 g, 3.65 mmol) and bromosugar **312** (300 mg, 0.73 mmol) were dissolved in DCM (4 mL). The reaction was cooled to 0 ºC and silver tetrafluoroborate (284 mg, 1.46 mmol) was added all at once and the reaction was allowed to stir at ambient temperature for 2 hours when complete consumption of starting materal was observed. The reaction was then quenched with triethylamine and diluted with DCM then filtered through a celite pad. The filtrate was concnetrated and purified by flash column chromatogrpahy (9:1 to 1:1 hexanes to ethyl acetate). The first fraction provided alkyl tin derivatives, the second fraction provided 100 mg of **1405α**, and the third fraction provided 160 mg of **1405β**. Spectra match published values.[44, 45]

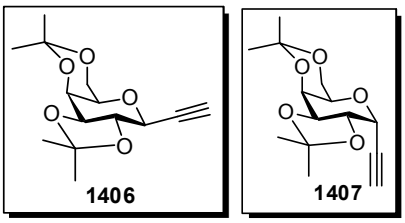
Characterization data for **1405α**

**$^1$H NMR** (500 MHz, *$CDCl_3$*) $\delta_{ppm}$ 5.81 (1H, dd, *J* = 53.3, 2.7 Hz), 5.53 (1H, dd, *J* = 3.1, 1.0 Hz), 5.36 (1H, dd, *J* = 10.9, 3.3 Hz), 5.19 (1H, ddd, *J* = 23.8, 10.9, 2.7 Hz), 4.41 (1H, t, *J* = 6.6, 6.6 Hz), 4.16 (1H, dd, *J* = 11.4, 6.3 Hz), 4.12 (1H, dd, *J* = 11.4, 6.8 Hz), 2.16 (3H, s), 2.13 (3H, s), 2.07 (3H, s), 2.01 (3H, s).

Characterization data for **1405β**

**$^1$H NMR** (500 MHz, *CDCl$_3$*) $\delta_{ppm}$ 5.40 (1H, dd, *J* = 3.0, 1.0 Hz), 5.40 (1H, dd, *J* = 42.2, 3.4 Hz), 5.34-5.33 (1H, m), 5.07 (1H, dd, *J* = 10.8, 3.5 Hz), 4.42 (1H, t, *J* = 6.7, 6.7 Hz), 4.09 (1H, dd, *J* = 6.6, 1.4 Hz), 4.04 (1H, dd, *J* = 6.7, 1.9 Hz), 2.09 (3H, s), 2.04 (3H, s), 2.00 (3H, s), 1.94 (3H, s).

**[(2,3;4,6)-di-*O*-isopropylidene-β-D-galactopyranosyl]ethyne (1406) and [(2,3;4,6)-di-*O*-isopropylidene-α-D-galactopyranosyl]ethyne (1407)**




Bestmann-Ohira reagent **493** (670 mg, 3.5 mmol) was dissolved in 40 mL of methanol and cooled to 0 ºC to which was added potassium carbonate (485 mg, 3.5 mmol) and the mixture was allowed to stir for 30 minutes. [(2,3;4,6)-di-*O*-isopropylidene-α-D-galactopyranosyl]methanal (**435**) (727 mg, 2.67 mmol), dissolved in anhydrous methanol (4 mL), was then added dropwise and the reaction allowed to stir for three hours. The reaction was filtered through a sintered glass frit and neutralised with Amberlite 150 resin. Following filtration and concentration, the residue was purified by flash chromatography (8: 2 hexanes ethyl acetate to 7: 3 hexanes ethyl acetate). The first fraction contained the α-epimer (**1407**) (298 mg, 1.11 mmol, 42 % yield) as a clear oil that solidifies upon extended standing, the second fraction contained the β-epimer (**1406**) (22 mg, 0.082 mmol, 3.2 % yield) as white needles. Alternatively, the material could be used directly in the next step with no purification.

Characterization for the α-epimer (**1407**)

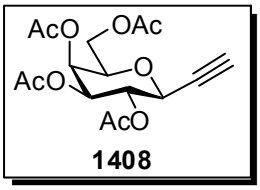
**$^1$H NMR** (400 MHz, *CDCl$_3$*) $\delta_{ppm}$ 5.12 (1H, dd, *J* = 5.2, 2.2 Hz), 4.52 (1H, m), 4.18 (1H, dd, *J* = 9.7, 5.1 Hz), 4.16 (1H, dd, *J* = 13.1, 2.2 Hz), 4.00 (1H, dd, *J* = 9.6, 2.9 Hz), 3.95 (1H, dd, *J* = 13.1, 1.5 Hz), 3.59 (1H, dd, *J* = 3.2, 1.7 Hz), 2.60 (1H, d, *J* = 2.2 Hz), 1.50 (6H, s), 1.47 (3H, s), 1.46 (3H, s); **$^{13}$C NMR** (101 MHz, *CDCl$_3$*) $\delta_{ppm}$ 110.7, 98.6, 77.7, 75.3, 69.8, 67.3, 67.2, 65.0, 63.1, 29.2, 26.62, 26.58, 18.4. **ESI-MS** *m/z* calcd for $C_{14}H_{20}O_5$ $[M + H]^+$: 269.14; $[M + K]^+$: 307.09. Found 269.17, 307.11. **Rf** = 0.72 (6.5:3.5, hexanes: ethyl acetate).

Characterization for the β-epimer (**1406**)

**$^1$H NMR** (300 MHz, *CDCl$_3$*) $\delta_{ppm}$ 4.45 (1H, dd, *J* = 2.7, 1.0 Hz), 4.21 (1H, dd, *J* = 9.5, 2.1 Hz), 4.09 (1H, dd, *J* = 13.6, 2.3 Hz), 4.01 (1H, t, *J* = 9.4, 9.4 Hz), 3.98 (1H, dd, *J* = 13.1, 1.5 Hz),

3.47 (1H, dd, *J* = 9.2, 2.8 Hz), 3.29 (1H, dd, *J* = 3.2, 1.7 Hz), 2.62 (1H, d, *J* = 2.1 Hz), 1.50 (3H, s), 1.46 (3H, s), 1.44 (6H, s); **$^{13}$C NMR** (101 MHz, *CDCl$_3$*) $\delta_{ppm}$ 111.0, 98.6, 79.4, 79.1, 75.3, 72., 69.5, 69.1, 66.7, 62.9, 29.0, 26.5, 26.4, 18.5. **ESI-MS** *m/z* calcd for $C_{14}H_{20}O_5$ $[M + H]^+$: 269.14; $[M + K]^+$: 307.09. Found 269.19, 307.11. **Rf** = 0.54 (6.5:3.5, hexanes: ethyl acetate).

**[(2,3,4,6)-Tetra-*O*-acetyl-β-D-galactopyranosyl]ethyne (1408)**

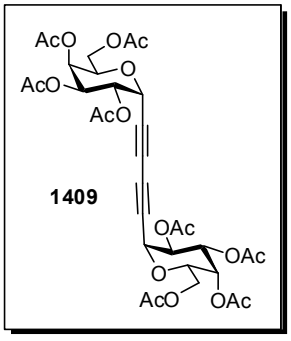


**1408**

Alkyne **1406** (52 mg, 0.19 mmol) was dissolved in 4 mL 60 % acetic acid and heated to 75 º C and stirred for five hours. The reaction was cooled to room temperature and the solvent removed. The residue was then co-evaporated three times with toluene and resuspended in 3 mL of pyridine to which was added 3 mL of acetic anhydride and 1 crystal of DMAP. The reaction mixture was allowed to stir for 14 hours when solvent was removed under reduced pressure and the residue co-evaported twice with toluene. The crude product was then purified through flash chromatography (35 % ethyl acetate in hexanes) to yield 55 mg (0.15 mmol) of β-alkyne (**1408**) as an amorphous white solid in 82 % yield.

**$^1$H NMR** (400 MHz, *CDCl$_3$*) $\delta_{ppm}$ 5.40 ( 1 H, d, *J* = 18.5 Hz), 5.01 ( 1 H, dd, *J* = 10.2, 3.3 Hz), 4.21 ( 1 H, dd, *J* = 9.9, 2.1 Hz), 4.13 ( 1 H, d, *J* = 6.5 Hz), 3.94 ( 1 H, dt, *J* = 6.6, 6.3, 0.7 Hz), 2.57 ( 1 H, d, *J* = 2.1 Hz), 2.17 ( 1 H, s), 2.09 ( 1 H, s), 2.06 ( 1 H, s), 1.99 ( 1 H, s), 5.41 ( 1 H, d, *J* = 10.4 Hz); **$^{13}$C NMR** (101 MHz, *CDCl$_3$*) $\delta_{ppm}$ 170.2, 170.0, 169.9, 169.2, 77.8, 75.1, 74.4, 71.2, 68.6, 68.1, 67.1, 61.4, 20.52, 20.51, 20.48, 20.41. **ESI-MS** *m/z* calcd for $C_{16}H_{21}O_9$ $[M + H]^+$: 357.12; $[M + Na]^+$: 379.10. Found: 357.15, 379.16.

**1, 4-bis[(2,3,4,6)-tetra-*O*-acetyl-α-D-galactopyranosyl]-1,3-butadiyne (1409)**



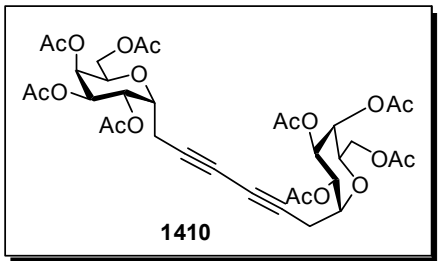
**1409**

In the reaction to produce **219**, **1409** was obtained from the organic washes and following flash chromatography (1: 1, hexane ethyl acetate) providing 42 mg of **1409** as a clear gel in 10 % yield along with 105 mg of unreacted starting material, **452**, as a white solid (50% recovered).

**$^1$H NMR** (400 MHz, *CDCl$_3$*) $\delta_{ppm}$ 5.47 (2H, dd, *J* = 3.2, 1.1 Hz), 5.28 (2H, dd, *J* = 10.0, 3.2 Hz), 5.18 (2H, dd, *J* = 10.0, 5.9 Hz), 5.15 (2H, d, *J* = 5.8 Hz), 4.36 (2H, dt, *J* = 6.6, 0.8 Hz), 4.13 (2H, dd, *J* = 11.4, 6.9 Hz), 4.07

(2H, dd, *J* = 11.3, 6.5 Hz), 2.12 (12H, s), 2.04 (6H, s), 1.99 (6H, s); **$^{13}$C NMR** (101 MHz, *CDCl$_3$*) $\delta_{ppm}$ 170.3, 170.04, 170.03, 169.9, 73.4, 72.6, 70.2, 68.6, 67.4, 66.6, 66.5, 61.2, 20.8, 20.65, 20.57, 20.53. **ESI-MS** *m/z* calcd for $C_{32}H_{38}O_{18}$ $[M + NH_4]^+$: 728.24; $[M + Na]^+$: 733.20. Found 728.32, 733.28.

**1, 6-bis[(2,3,4,6)-tetra-*O*-acetyl-α-D-galactopyranosyl]-2,5-hexadiyne (1410)**

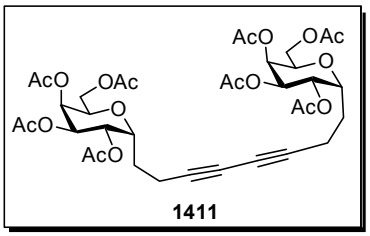


1410

In the reaction to produce **217**, **1410** was obtained from the organic washes and following flash chromatography (1:1, hexane ethyl acetate) providing 20 mg of **1410** as a clear gel in 5 % yield along with 121 mg of unreacted starting material, **453**, as a white solid (55 % recovered).

**$^1$H NMR** (400 MHz, *CDCl$_3$*) $\delta_{ppm}$ 5.38 (2H, t, *J* = 3.0 Hz), 5.25 (2H, dd, *J* = 8.8, 4.8 Hz), 5.18 (2H, dd, *J* = 8.8, 3.3 Hz), 4.37 (2H, m), 4.28 (2H, dd, *J* = 12.8, 9.1 Hz), 4.10-4.03 (4H, m), 2.59 (2H, m), 2.09 (6H, s), 2.07 (6H, s), 2.06 (6H, s), 2.02 (6H, s); **$^{13}$C NMR** (101 MHz, *CDCl$_3$*) $\delta_{ppm}$ 170.6, 169.9, 169.7, 169.7, 72.7, 69.9, 69.2, 67.7, 67.4, 67.2, 67.0, 60.9, 20.69, 20.69, 20.65, 20.59, 19.0. **ESI-MS** *m/z* calcd for $C_{34}H_{42}O_{18}$ $[M + NH_4]^+$: 756.27; $[M + Na]^+$: 761.23. Found 756.39, 761.31.

**1, 8-bis[(2,3,4,6)-tetra-*O*-acetyl-α-D-galactopyranosyl]-2,7-octadiyne (1411)**



1411

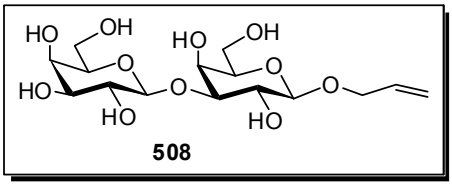
In the reaction to produce **215**, **1411** was obtained from the organic washes and following flash chromatography (1:1, hexane ethyl acetate) providing 38 mg (0.050 mmol) of **1411** as a clear gel in 8 % yield along with 115 mg of unreacted starting material (**454**) as a white solid (50 % recovered).

**$^1$H NMR** (400 MHz, *CDCl$_3$*) $\delta_{ppm}$ 5.38 (2H, dd, *J* = 3.1, 2.5 Hz), 5.26 (2H, dd, *J* = 9.3, 5.1 Hz), 5.14 (2H, dd, *J* = 9.3, 3.3 Hz), 4.29-4.23 (2H, m), 4.22 (2H, dd, *J* = 10.9, 6.8 Hz), 4.12-3.98 (4H, m), 2.44-2.21 (4H, m), 2.10 (6H, s), 2.06 (6H, s), 2.03 (6H, s), 2.00 (6H, s), 1.97-1.84 (2H, m), 1.73-1.61 (2H, m); **$^{13}$C NMR** (101 MHz, *CDCl$_3$*) $\delta_{ppm}$ 170.5, 170.0, 169.8, 169.7, 76.1, 70.8,

68.3, 68.0, 67.9, 67.4, 65.8, 61.3, 24.9, 20.72, 20.66, 20.65, 20.59, 15.3. **ESI-MS** *m*/*z* calcd for $C_{36}H_{46}O_{18}$ $[M + NH_4]^+$: 784.30; $[M + Na]^+$: 789.26. Found 784.41, 789.35.

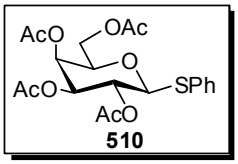
# Experimental Protocols for Chapter 5

### 3-*O*-(β-D-galactopyranosyl)-allyl-β-D-galactopyranose (508)




Acetylated disaccharide **527** (12 mg, 0.018 mmol) was dissolved in 0.1 M sodium methoxide in methanol (2 mL). The reaction was stirred for 4 hours, and neutralized with Dowex-50X resin ion exchange resin until the pH <7. The reaction was filtered, concentrated, redissolved in water and lyophilized to provide 6 mg of the title compound in 88 % yield. Spectral data is conisstent with the partial listing in the literature.[46] **$^1$H NMR** (500 MHz, $D_2O$) $\delta_{ppm}$ 5.94 (1H, dddd, *J* = 17.0, 10.4, 6.5, 5.6 Hz), 5.34 (1H, ddd, *J* = 17.3, 3.1, 1.5 Hz), 5.24 (1H, ddd, *J* = 10.4, 2.7, 1.1 Hz), 4.56 (1H, d, *J* = 7.6 Hz), 4.46 (1H, d, *J* = 8.0 Hz), 4.36 (1H, dddd, *J* = 12.6, 5.5, 1.4, 1.2 Hz), 4.19 (1H, dddd, *J* = 12.6, 6.4, 1.2, 1.2 Hz), 4.15 (1H, dd, *J* = 3.4, 0.6 Hz), 3.87 (1H, dd, *J* = 3.3, 0.7 Hz), 3.78-3.60 (8H, m), 3.56 (1H, dd, *J* = 9.9, 7.6 Hz), 3.54 (1H, d, *J* = 10.7 Hz); **$^{13}$C NMR** (126 MHz, $D_2O$) $\delta_{ppm}$ 133.1, 117.7, 104.3, 101.2, 82.3, 74.9, 74.7, 72.4, 70.9, 70.4, 69.7, 68.4, 68.3, 60.84, 60.78. **ESI-MS** *m*/*z* calcd for $C_{15}H_{26}O_{11}$ $[M + Na]^+$: 405.35. Found 405.43.

### *S*-(2,3,4,6-tetra-*O*-acetyl-β-D-galactopyranosyl)thiophenol (510)

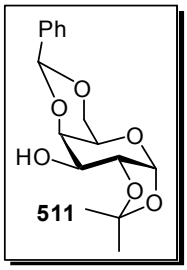



Galactose pentacetate (10.0 g, 25.6 mmol) was dissolved in anhydrous DCM under argon. The flask was cooled to 0 ºC and thiophenol (7.35 mL, 72 mmol) was added. $BF_3{\cdot}OEt_2$ (9.01 mL, 72 mmol) was then added dropwise, the ice bath was removed, and stirring was continued for an additional 12 hours whereupon the reaction was diluted with DCM. The reaction mixture was washed three times with 2 M sodium hydroxide, followed three times with water. The organic phase was dried and concentrated in the usual fashion and purified through flash chromatography (4: 1 hexanes: ethyl acetate to 1: 1 hexanes: ethyl acetate) to provide 11.3 g of the product as a white solid in quantitative yield. Spectral data matches published information.[47]

**$^1$H NMR** (400 MHz, $CDCl_3$) $\delta_{ppm}$ 7.54-7.49 (2H, m), 7.34-7.29 (3H, m), 5.42 (1H, dd, *J* = 3.3, 0.9 Hz), 5.24 (1H, dd, *J* = 10.0, 10.0 Hz), 5.05 (1H, dd, *J* = 9.9, 3.3 Hz), 4.72 (1H, d, *J* = 10.0

Hz), 4.19 (1H, dd, *J* = 11.3, 7.0 Hz), 4.12 (1H, dd, *J* = 6.7, 4.7 Hz), 3.94 (1H, ddd, *J* = 7.0, 6.2, 0.9 Hz), 2.12 (3H, s), 2.10 (3H, s), 2.04 (3H, s), 1.97 (3H, s); **$^{13}$C NMR** (101 MHz, *CDCl$_3$*) $\delta_{ppm}$ 170.3, 170.1, 170.0, 169.4, 132.5, 132.4, 128.8, 128.1, 86.6, 74.4, 72.0, 67.2, 67.2, 61.6, 20.8, 20.63, 20.60, 20.55. **ESI-MS** *m*/*z* calcd for $C_{20}H_{24}O_9S$ $[M + Na]^+$: 463.10. Found 463.19. **Rf** = 0.32 (1:1 hexanes: ethyl acetate).

**4,6-*O*-Benzylidene-1,2-*O*-isopropylidene-α-D-galactopyranose (511)**




Prepared according to a modified protocol of that developed by Busse.[48] Benzylidene **512** (1.8 g, 6.6 mmol) was dissolved in dry acetone (90 mL) along with 2,2-dimethoxypropane (1.03 mL, 8.3 mmol) and *p*-toluenesulfonic acid monohydrate (32 mg, 0.17 mmol) and the solution was stirred at ambient temperature for 4 hours under an argon flow. The reaction was quenched with 1 mL of triethylamine and solvent was removed. The crude product was purified by flash chromatography (2:1 toluene:ethyl acetate) to provide 850 mg of diacetonide **511** in 42 % yield as a clear thick gel. Chromatography also provided 650 mg of **511a** in 34 % yield. The characterization of **511** is consistent with published data.[48]

Characterization data for **511**:

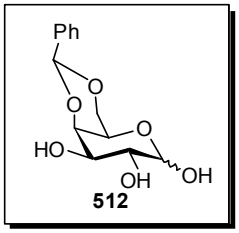
**$^1$H NMR** (400 MHz, *CDCl$_3$*) $\delta_{ppm}$ 7.50-7.44 (2H, m), 7.41-7.36 (3H, m), 5.86 (1H, d, *J* = 4.3 Hz), 5.56 (1H, bs), 4.38 (1H, dd, *J* = 12.7, 1.4 Hz), 4.31 (1H, dd, *J* = 4.1, 2.4 Hz), 4.17 (1H, dd, *J* = 5.4, 4.3 Hz), 4.11 (1H, dd, *J* = 12.8, 2.2 Hz), 4.04 (1H, ddd, *J* = 6.9, 5.2, 5.2 Hz), 3.85 (1H, dd, *J* = 3.7, 2.2 Hz), 1.55 (3H, s), 1.40 (3H, s); **$^{13}$C NMR** (101 MHz, *CDCl$_3$*) $\delta_{ppm}$ 137.4, 129.3, 128.4, 126.2, 109.5, 100.9, 98.2, 77.6, 73.7, 70.6, 70.5, 64.4, 27.9, 26.6. **ESI-MS** *m*/*z* calcd for $C_{16}H_{20}O_6$ $[M + NH_4]^+$: 326.16; $[M + K]^+$: 347.09. Found 326.38, 347.21. **Rf** =0.12 (8:2 diethyl ether: hexanes).

Characterization data for **511a**:

**$^1$H NMR** (400 MHz, *CDCl$_3$*) $\delta_{ppm}$ 7.56-7.34 (5H, m), 5.75 (1H, s), 5.68 (1H, d, *J* = 5.1 Hz), 4.67 (1H, dd, *J* = 8.2, 2.4 Hz), 4.47 (1H, dd, *J* = 5.0, 2.4 Hz), 4.35 (1H, dd, *J* = 8.2, 1.8 Hz), 3.99 (1H, dd, *J* = 5.9, 4.5 Hz), 3.93 (1H, dd, *J* = 11.4, 7.1 Hz), 3.80 (1H, dd, *J* = 11.4, 4.3 Hz), 1.58 (3H, m), 1.36 (3H, s); **$^{13}$C NMR** (101 MHz, *CDCl$_3$*) $\delta_{ppm}$ 138.2, 130.0, 128.5, 127.2, 105.0,

103.9, 96.3, 72.0, 71.9, 70.1, 68.2, 62.2, 26.0, 25.0. **ESI-MS** *m/z* calcd for $C_{16}H_{20}O_6$ $[M + NH_4]^+$: 326.16; $[M + K]^+$: 347.09. Found 326.37, 347.20. **Rf** =0.14 (8:2 diethyl ether: hexanes)

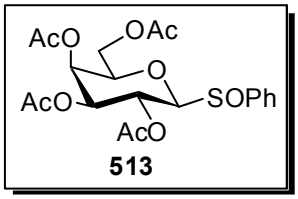
**4,6-*O*-benzylidene-D-galactose (512)**



**512**

D-Galactose (5g, 28 mmol), α,α-dimethoxytoluene (4.20 mL, 4.22 g, 28 mmol), and *p*-toluenesulfonic acid monohydrate (50 mg, 0.27 mmol) were dissolved in DMF (100 mL). The reaction was allowed to stir for 16 hours, at which point 1 mL of triethylamine was added. The bulk of the solvent was removed under reduced pressure until under 10 mL remained. DCM was added and the product precipitated out. The crude product was purified by dry vacuum chromatography [6:1 ethyl acetate: (1:1:1 methanol: water: acetonitrile)] to provide 4.03 g of the benzylidene derivative as a mixture of anomers in 54 % yield following the removal of solvent. **$^1$H NMR** (400 MHz, *$CDCl_3$*) $\delta_{ppm}$ 7.59-7.42 (10H, m), 5.72 (2H, bs), 5.35 (1H, α-anomer, d, *J* = 3.6 Hz), 4.68 (1H, β-anomer, d, *J* = 7.9 Hz), 4.39 (1H, dd, *J* = 3.5, 0.8 Hz), 4.33 (1H, dd, *J* = 3.7, 0.8 Hz), 4.25 (1H, dd, *J* = 12.9, 1.7 Hz), 4.21 (1H, dd, *J* = 2.6, 1.8 Hz), 4.15 (1H, dd, *J* = 12.8, 1.6 Hz), 4.06-3.89 (3H, m), 3.84-3.60 (4H, m); **$^{13}$C NMR** (101 MHz, *$CDCl_3$/MeOD*) $\delta_{ppm}$ 137.93, 129.24, 128.31, 126.48, 101.43, 93.4, 76.7, 69.8, 69.4, 69.0, (137.86, 129.28, 128.29, 126.53, 101.49, 97.2, 76.1, 72.7, 72.4, 66.8, 62.7). **ESI-MS** *m/z* calcd for $C_{13}H_{16}O_6$ $[M + Na]^+$: 291.09. Found 291.10. **Rf** = 0.43 (4:1:1:1, ethyl acetate: water: methanol: acetonitrile)

**2,3,4,6-tetra-*O*-acetyl-phenylsulfinyl-β-D-galactopyranose**



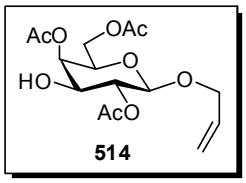
**513**

Potassium fluoride dihydrate (424 mg, 4.5 mmol) was dissolved in a mixture of acetonitrile (7.7 mL) and water (1.5 ml). The solution was cooled to 0 ºC, and mCPBA (777 mg, 4.5 mmol) was added; stirring was continued for 30 minutes. Thiophenyl derivative **510** (1.0 g, 2.3 mmol) was then added all at once and the reaction was stirred an additional 5 minutes before being quenched with 4 mL of saturated aqueous $FeSO_4$. The reaction mixture was then extracted twice with DCM, and the combined organic phases were washed with saturated sodium bicarbonate and brine prior to being dried and filtered in the usual manner. Purification by flash chromatography (1:1 hexanes: ethyl acetate) to furnish, after removal of solvent, 986 mg

of the sulfoxide as a white solid in a mixture of diastereomers (1:1 diastereomeric ratio, epimeric at the sulfur, 94 % yield). Spectral data is consistent with the literature.[49]

**$^1$H NMR** (400 MHz, *CDCl$_3$*) $\delta_{ppm}$ 7.76-7.72 (2H, m), 7.70-7.66 (2H, m), 7.57-7.50 (6H, m), 5.52 (2H, m), 5.38-5.33 (2H, m), 5.13-5.04 (2H, m), 4.38 (1H, d, *J* = 9.9 Hz), 4.27 (1H, d, *J* = 9.8 Hz), 4.09-3.83 (6H, m), 2.09 (3H, s), 2.07 (3H, s), 2.03-2.01 (3H, m), 1.98 (3H, s), 1.98 (9H, s), 1.93 (3H, s); **$^{13}$C NMR** (101 MHz, *CDCl$_3$*) $\delta_{ppm}$ **major diastereomer:** 170.0, 169.8, 169.7, 169.4, 139.2, 131.4, 128.5, 125.7, 92.2, 74.8, 71.8, 71.3, 66.6, 64.8, 60.9, 20.56, 20.42, 20.37, 20.25; **minor diastereomer**: 169.94, 169.9, 169.4, 168.8, 138.7, 131.3, 128.6, 125.7, 90.0, 75.1, 71.8, 66.7, 64.4, 61.1, 20.54, 20.37, 20.34, 20.34. **ESI-MS** *m/z* calcd for $C_{20}H_{24}O_{10}S$ $[M + H]^+$: 457.12; $[M + Na]^+$: 479.10. Found 457.14, 479.11.

**2,4,6-tri-*O*-acetyl-allyl-β-D-galactopyranose (514)**



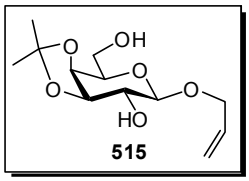
**514**

Compound prepared according to a modified protocol of Chernyak.[50] Diacetate **519** (1.30 g, 4.40 mmol) was dissolved in acetonitrile (34 mL) in a flame-dried round-bottomed flask under argon. *p*-Toluenesulfonic acid monohydrate (48 mg, 0.24 mmol) and triethyl orthoacetate (16.1 mL, 87.8 mmol) were added and the reaction was stirred at ambient temperature for 2 hours. The reaction was then quenched with triethylamine (2.4 ml) and evaporated to dryness. The crude orthoester was immediately treated with 60 % acetic acid (20 mL) and stirred for 75 minutes before being concentrated. The resulting paste was redissolved in minimal ether and the product precipitated upon standing the addition of hexanes to provide 1.51 g of the title compound in quantitative yield. No further purification was required. Spectral data is consistent with the (partial listing) in the literature.[50]

**$^1$H NMR** (400 MHz, *CDCl$_3$*) $\delta_{ppm}$ 5.87 (1H, dddd, *J* = 17.2, 10.5, 6.1, 4.9 Hz), 5.33 (1H, dd, *J* = 3.6, 1.0 Hz), 5.29 (1H, ddd, *J* = 17.2, 3.3, 1.6 Hz), 5.21 (1H, ddd, *J* = 10.4, 2.9, 1.4 Hz), 5.00 (1H, dd, *J* = 10.0, 7.9 Hz), 4.48 (1H, d, *J* = 7.9 Hz), 4.35 (1H, dddd, *J* = 13.2, 4.9, 1.6, 1.6 Hz), 4.18 (1H, dd, *J* = 11.4, 6.5 Hz), 4.14 (1H, dd, *J* = 11.4, 6.6 Hz), 4.11 (1H, dddd, *J* = 13.3, 6.0, 1.2, 1.2 Hz), 3.87-3.81 (2H, m), 2.51 (1H, d, *J* = 6.4 Hz), 2.18 (3H, s), 2.13 (3H, s), 2.06 (3H, s); **$^{13}$C NMR** (101 MHz, *CDCl$_3$*) $\delta_{ppm}$ 171.2, 170.9, 170.5, 133.5, 117.5, 99.7, 72.7, 71.4, 70.9, 70.0,

69.7, 61.9, 20.9, 20.8, 20.7. **ESI-MS** *m/z* calcd for $C_{15}H_{22}O_9$ $[M + Na]^+$: 369.12. Found 369.16. Rf = 0.56 (2:1 ethyl acetate: hexanes).

**3,4-*O*-isopropylidene-allyl-β-D-galactopyranose (515)**

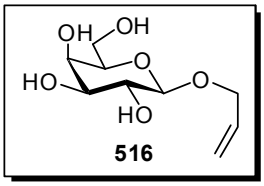


**515**

Allyl-β-D-galactopyranose, **516** (2.7 g, 12.3 mmol), was dissolved in anhydrous DMF (15 mL) along with 2,2-dimethoxypropane (1.8 mL, 15 mmol) and *p*-toluenesulfonic acid monohydrate (50 mg, 0.26 mmol). The flask was sealed under argon and warmed to 60 ºC for 2 hours with stirring. Following cooling, the reaction was neutralized with approximately 500 µL of triethylamine, diluted with ethyl acetate, and washed twice with saturated sodium bicarbonate. Following the extraction, the reaction was dried, filtered, concentrated first under reduced pressure and then *in vacuo* to remove residual DMF. The crude product was purified by flash chromatography (1: 1 to 7: 3 ethyl acetate: hexanes, 1% triethylamine) to provide 2.70 g of the desired compound in 85 % yield as a white solid. Spectral data is consistent with the (partial listing) in the literature.[50]

**$^1$H NMR** (400 MHz, *$CDCl_3$*) $\delta_{ppm}$ 5.94 (1H, dddd, *J* = 16.9, 10.4, 6.3, 5.5 Hz), 5.32 (1H, ddd, *J* = 17.2, 3.1, 1.5, Hz), 5.23 (1H, ddd, *J* = 10.4, 2.6, 1.2 Hz), 4.39 (1H, dddd, *J* = 12.6, 5.4, 1.4, 1.4 Hz), 4.26 (1H, d, *J* = 8.3 Hz), 4.18-4.08 (3H, m), 4.00 (1H, dd, *J* = 13.1, 8.6 Hz), 3.88-3.82 (2H, m), 3.59 (1H, dd, *J* = 8.2, 7.4 Hz), 1.53 (3H, s), 1.35 (3H, s); **$^{13}$C NMR** (101 MHz, *$CDCl_3$*) $\delta_{ppm}$ 133.6, 118.2, 110.5,101.2, 78.9, 73.9, 73.6, 73.5, 70.3, 62.4, 28.1, 26.3. **ESI-MS** *m/z* calcd for $C_{12}H_{20}O_6$ $[M + Na]^+$: 283.12; $[M + K]^+$: 299.09. Found 283.21, 299.19. **Rf** = 0.28 (7:3, ethyl acetate: hexanes).

**Allyl-β-D-galactopyranose (516)**

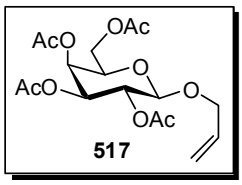


**516**

Allylated derivative **517** (5.40 g, 13.9 mmol) was dissolved in 0.1 M sodium methoxide in methanol (20 mL). The reaction was allowed to stir for 6 hours, when, deemed complete by TLC, Amberlite 150 ion-exchange resin was added to lower the pH to neutral. The resin was removed by filtration, and the solvent was removed under reduced pressure. The product was precipitated through the addition of diethyl ether and dried *in vacuo* to provide 3.07 g of the deprotected sugar in quantitative yield. Spectral data is consistent with published data.[51]

**$^1$H NMR** (500 MHz, *$D_2O$*) $\delta_{ppm}$ 5.99 (1H, dddd, *J* = 17.3, 10.4, 6.4, 5.6 Hz), 5.39 (1H, dddd, *J* = 17.3, 1.6, 1.6, 1.6 Hz), 5.29 (1H, dddd, *J* = 10.4, 1.6, 1.1, 1.1 Hz), 4.44 (1H, d, *J* = 7.9 Hz), 4.40 (1H, dddd, *J* = 12.6, 5.5, 1.5, 1.5 Hz), 4.23 (1H, dddd, *J* = 12.7, 6.4, 1.2, 1.2 Hz), 3.92 (1H, dd, *J* = 3.5, 0.8 Hz), 3.79 (1H, dd, *J* = 11.7, 7.8 Hz), 3.75 (1H, dd, *J* = 11.7, 4.4 Hz), 3.68 (1H, ddd, *J* = 7.8, 4.4, 1.0 Hz), 3.64 (1H, dd, *J* = 9.9, 3.5 Hz), 3.53 (1H, dd, *J* = 9.9, 7.9 Hz); **$^{13}$C NMR** (126 MHz, *$D_2O$*) $\delta_{ppm}$ 133.3, 118.6, 101.7, 75.1, 72.7, 70.7, 70.5, 68.6, 60.9. **ESI-MS** *m/z* calcd for $C_8H_{14}O_6$ $[M + NH_4]^+$: 224.11; $[3M + Na]^+$: 641.23. Found 224.19, 641.31.

**2,3,4,6-Tetra-*O*-acetyl-allyl-β-D-galactopyranose (517)**

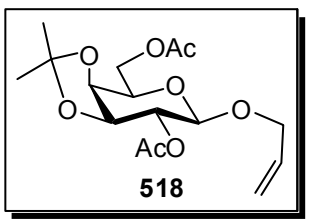


**517**

β-D-Galactose pentacetate **311** (6.00 g, 15.3 mmol) was dissolved in 60 mL of anhydrous DCM in the presence of powdered activated 4 Å molecular sieves. The reaction mixture was cooled to 0 ºC, at which point allyl alcohol (1.4 mL, 19.6 mmol) and $BF_3{\cdot}OEt_2$ (3.0 mL, 25 mmol) were added and the reaction was allowed to warm to ambient temperature and stir for 12 hours. The reaction was quenched with water (1 mL), diluted with ethyl acetate, and filtered through a celite pad. The filtrate was washed with 10 % HCl, saturated sodium bicarbonate, and brine successively, before being dried and concentrated. The crude product was purified by flash chromatography to (7: 3 hexanes: ethyl acetate) to yield 5.4 g of the desired product in 91 % yield. Spectral data is consistent with the literature.[51]

**$^1$H NMR** (400 MHz, *$CDCl_3$*) $\delta_{ppm}$ 5.85 (1H, dddd, *J* = 17.1, 10.5, 6.1, 4.9 Hz), 5.39 (1H, dd, *J* = 3.4, 1.0 Hz), 5.29 (1H, m), 5.27-5.17 (2H, m), 5.02 (1H, dd, *J* = 10.4, 3.4 Hz), 4.52 (1, d, *J* = 8.0 Hz), 4.35 (1, m), 4.22-4.06 (3H, m), 3.89 (1H, ddd, *J* = 6.7, 6.7, 1.1 Hz), 2.15 (3H, s), 2.06 (3H, s), 2.05 (3H, s), 1.98 (3H, s); **$^{13}$C NMR** (101 MHz, *$CDCl_3$*) $\delta_{ppm}$ 170.4, 170.3, 170.2, 169.4, 133.3, 117.6, 100.1, 70.9, 70.6, 70.0, 68.8, 67.0, 61.3, 20.8, 20.7, 20.7, 20.6. **ESI-MS** *m/z* calcd for $C_{36}H_{38}O_7$ $[M + NH_4]^+$: 406.17; $[M + Na]^+$: 411.13; $[M + K]^+$: 427.10. Found 406.22, 411.17, 427.16. **Rf** = 0.46 (1:1, hexanes: ethyl acetate).

**2,6-Di-*O*-acetyl-3,4-*O*-isopropylidene-allyl-β-D-galactopyranose (518)**

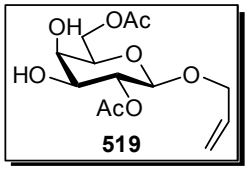


**518**

Isopropylidene protected derivative **515** (2.32 g, 8.9 mmol) was dissolved in pyridine (16 mL) and cooled to 0 ºC. Acetic anhydride (16

mL), and a crystal of DMAP were added and the reaction was stirred for 1 hour. Saturated sodium bicarbonate (1 mL) was added and the voaltiles were removed under reduced pressure. The crude product was then portioned between DCM and 10 % HCl, and the organic phase was washed successively with saturated sodium bicarbonate and brine. Following drying and the removal of solvent, the organic-soluble crude product was purified by flash chromatography (8:2 hexanes: ethyl acetate, 1 % triethylamine) to provide 2.58 g of the title compound as a white solid in 84 % yield. Spectral data is consistent with the (partial listing) in the literature.[50]
**$^1$H NMR** (400 MHz, *$CDCl_3$*) $\delta_{ppm}$ 5.86 (1H, dddd, *J* = 16.7, 10.6, 6.1, 4.9 Hz), 5.26 (1H, ddd, *J* = 17.2, 3.1, 1.6 Hz), 5.18 (1H, ddd, *J* = 10.6, 2.8, 1.3 Hz), 5.01 (1H, dd, *J* = 8.1, 6.8 Hz), 4.40-4.35 (3H, m), 4.32 (1H, dddd, *J* = 13.3, 4.8, 1.5, 1.5 Hz), 4.20-4.14 (2H, m), 4.09 (1H, dddd, *J* = 13.3, 6.1, 1.3, 1.3 Hz), 3.97 (1H, ddd, *J* = 6.2, 6.0, 1.9 Hz), 2.10 (3H, s), 1.56 (3H, s), 1.34 (3H, s); **$^{13}$C NMR** (101 MHz, *$CDCl_3$*) $\delta_{ppm}$ 1708, 169.6, 133.6, 117.3, 110.8, 99.0, 77.0, 73.5, 72.7, 70.8, 69.5, 63.4, 27.6, 26.3, 21.0, 20.8. ESI-MS *m/z* calcd for $C_{16}H_{24}O_8$ $[M + Na]^+$: 367.14. Found 367.16. **Rf** = 0.74 (7:3 ethyl acetate: hexanes).

**2,6-Di-*O*-acetyl-allyl-β-D-galactopyranose (519)**



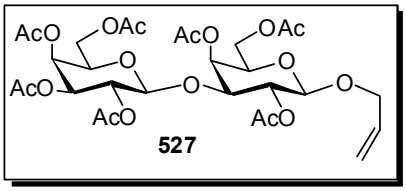
**519**

Fully protected galactose derivative **518** (3.17 g, 9.21 mmol) was dissolved in a solution of 20 mL of TFA and 5 mL of water pre-cooled to 0 ºC. The reaction was stirred for 25 minutes and pyridine was added portionwise until the pH >6. The reaction was diluted with 5 mL water, and much of the solvent was removed under reduced pressure until about 10 mL remained. This layer was extracted thrice with ethyl acetate. The combined organics were then washed with 10 % HCl and three times with saturated sodium bicarbonate before being dried with anhydrous magnesium sulphate, filtered and concentrated under reduced pressure to provide 2.7 g of the diacetate as a white solid in 94 % yield. No further purification was required. Spectral data is consistent with the (partial listing) in the literature.[50]

**$^1$H NMR** (400 MHz, *$CDCl_3$*) $\delta_{ppm}$ 5.94-5.81 (1H, m), 5.29 (1H, ddd, *J* = 17.2, 3.2, 1.7 Hz), 5.20 (1H, ddd, *J* = 10.6, 2.7, 1.5 Hz), 4.96 (1H, dd, *J* = 9.5, 8.1 Hz), 4.44 (1H, d, *J* = 7.9 Hz), 4.40 (1H, dd, *J* = 11.7, 6.6 Hz), 4.34 (1H, ddd, *J* = 13.2, 4.8, 1.8, 1.0 Hz), 4.29 (1H, dd, *J* = 11.5, 6.5

Hz), 4.12 (1H, dddd, *J* = 13.3, 6.0, 1.2, 1.2 Hz), 3.90 (1H, d, *J* = 3.5 Hz), 3.70-3.64 (2H, m), 2.14 (3H, m), 2.10 (3H, s); **$^{13}$C NMR** (101 MHz, *$CDCl_3$*) $\delta_{ppm}$ 171.7, 171.1, 133.6, 117.4, 99.6, 73.5, 72.7, 71.9, 69.8, 68.7, 62.5, 21.0, 20.9**. ESI-MS** *m/z* calcd for $C_{13}H_{20}O_8$ $[M + Na]^+$: 327.11. Found 327.12. **Rf** = 0.30 (2:1 ethyl acetate: hexanes).

**3-*O*-(2,3,4,6-tetra-*O*-acetyl-β-D-galactopyranosyl)-2,4,6-tri-*O*-acetyl-allyl-β-D-galactopyranose (527)**



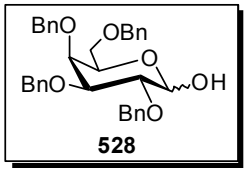
**527**

Sulfoxide **513** (256 mg, 0.56 mmol), and glycosyl acceptor **514** (154 mg, 0.300 mmol) were added to a flame dried round-bottomed flask containing freshly activated 4 Å powdered molecular sieves and the flask was then dried under vacuum in the presence of phosphorous pentoxide on a pig for 16 hours. To this flask was then added anhydrous DCM (8 mL) and methyl propiolate (500 µL, 11.2 mmol) and the reaction was allowed to stir under argon for 2.5 hours prior to being cooled to -78 ºC. One drop of trifluoromethylsulfonic acid was added and the reaction was stirred for four hours at -78ºC before being allowed to warm to ambient temperature and stirred for an additional 16 hours. The reaction was then quenched by injecting 1 mL of saturated sodium bicarbonate and was portioned between DCM and 10 % HCl. The organic layer was then washed with saturated sodium bicarbonate and brine before being dired and concentrated in the usual manner. The crude product was purified by flash chromatography (1:1 hexanes ethyl acetate) to provide 95 mg of crude product in the fraction with Rf = 0.30 (1:1 hexanes ethyl acetate) (approximately 75 % pure). This fraction was further purified by preparatory TLC (6: 4 hexanes ethyl acetate, six consecutive elutions) to provide 45 mg of the title compound in 23 % isolated yield as a white amorphous solid.

**$^1$H NMR** (400 MHz, *$CDCl_3$*) $\delta_{ppm}$ 5.84 (1H, dddd, *J* = 16.6, 10.9, 6.0, 4.8 Hz), 5.38 (1H, dd, *J* = 3.5, 0.7 Hz), 5.34 (1H, dd, *J* = 3.4, 1.0 Hz), 5.25 (1H, ddd, *J* = 17.4, 3.3, 1.7 Hz), 5.22 (1H, dd, *J* = 10.1, 8.1 Hz), 5.19 (1H, dddd, *J* = 10.6, 1.4, 1.4, 1.4 Hz), 5.08 (1H, dd, *J* = 10.6, 7.9 Hz), 4.93 (1H, dd, *J* = 10.5, 3.5 Hz), 4.56 (1H, d, *J* = 7.9 Hz), 4.41 (1H, d, *J* = 8.1 Hz), 4.32 (1H, dddd, *J* = 13.4, 4.8, 1.6, 1.6 Hz), 4.19 (1H, dd, *J* = 11.2, 6.0 Hz), 4.15 (1H, dd, *J* = 11.6, 5.8 Hz), 4.14-4.04 (3H, m), 3.87-3.82 (2H, m), 3.81 (1H, ddd, *J* = 6.8, 5.8, 0.9 Hz), 2.16 (3H, s), 2.12 (3H, s), 2.09 (3H, s), 2.07 (3H, s), 2.05 (3H, s), 2.02 (3H, s), 1.96 (3H, s); **$^{13}$C NMR** (101 MHz, *$CDCl_3$*)

$\delta_{ppm}$ 170.6, 170.41, 170.36, 170.2, 170.0, 169.2, 168.9, 13.4, 117.4, 101.1, 99.8, 75.7, 71.3, 70.9, 70.7, 70.6, 69.7, 68.9, 68.5, 66.7, 62.1, 60.9, 20.9, 20.8, 20.7, 20.7, 20.6, 20.53, 20.51. **ESI-MS** *m*/*z* calcd for $C_{29}H_{40}O_{18}$ $[M + Na]^+$: 699.21. Found 699.34.

**(2,3,4,6-tetra-*O*-benzyl)-D-galactose (528)**

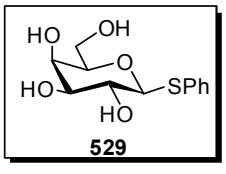


**528**

Thiophenyl derivative **530** (770 mg, 1.22 mmol) was dissolved in a mixture of acetone (5.4 mL) and water (600 μL) with stirring. *N*-bromosuccinamide was added (630 mg, 4.26 mmol) and the reaction was stirred for 10 minutes. Solid sodium bicarbonate was added (1.95 g, 23.18 mmol), and the reaction was concentrated. The solution was diluted with water and ethyl acetate, and the organic phase was further extracted with saturated sodium bicarbonate, water and brine. Following standard drying and concentration, the reaction was purified by flash chromatography (7:3 to 6:4 hexanes: ethyl acetate) to provide 572 mg of the title compound as an amorphous white solid in 87 % yield following drying *in vacuo*.The ratio of α:β is approximately 1.7:1. Spectral data is consistent with the literature.[52]

**$^1$H NMR** (400 MHz, *$CDCl_3$*) $\delta_{ppm}$ 7.34-7.12 (40H, m), 5.20 (1H, d, *J* = 3.5 Hz), 4.89-4.83 (2H, m), 4.76-4.60 (7H, m), 4.58-4.48 (3H, m), 4.43-4.28 (4H, m), 4.13-4.07 (2H, m), 3.99-3.93 (2H, m), 3.90-3.84 (3H, m), 3.81-3.77 (1H, m), 3.74-3.66 (1H, m), 3.56-3.33 (6H, m); **$^{13}$C NMR** (101 MHz, *$CDCl_3$*) $\delta_{ppm}$ 138.6, 138.4, 138.2, 137.7, 91.7, 78.6, 76.5, 74.7, 74.5, 73.33, 73.27, 72.8, 69.3, 69.0; 138.6, 138.4, 138.3, 137.6, 128.31, 128.28, 128.25, 128.18, 128.17, 128.13, 128.11, 128.04, 127.89, 127.88, 127.85, 127.71, 127.65, 127.61, 127.51, 127.50, 127.44, 127.39, 97.7, 82.1, 80.6, 75.0, 74.4, 73.5, 73.39, 73.36, 69.3, 68.8. **ESI-MS** *m*/*z* calcd for $C_{34}H_{36}O_6$ $[M + NH_4]^+$: 558.28; $[M + K]^+$: 579.21. Found 558.47, 579.40.

***S*-(β-D-galactopyranosyl)thiophenol (529)**



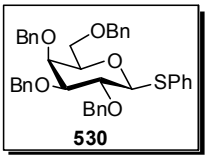
**529**

Thiophenyl derivative **510** (11.3 g, 25.6 mmol) was dissolved in 125 mL of 0.1 M sodium methoxide in methanol and the reaction was stirred at room temperature for 12 hours. Amberlite IR 120 resin was added and stirred an additional 10 minutes. The beads were removed by filtration and

solvent was removed under reduced pressure to provide 6.98 g of the deprotected sugar as a white solid in quantitative yield. Spectral data matches published data.[47]

**$^1$H NMR** (400 MHz, *MeOD*) $\delta_{ppm}$ 7.57-7.52 (2H, m), 7.32-7.25 (2H, m), 7.25-7.20 (1H, m), 4.58 (1H, d, *J* = 9.7 Hz), 3.89 (1H, dd, *J* = 3.3, 0.8 Hz), 3.76 (1H, dd, *J* = 11.4, 6.9 Hz), 3.70 (1H, dd, *J* = 11.4, 5.3 Hz), 3.60 (1H, dd, *J* = 9.5, 9.5 Hz), 3.56 (1H, ddd, *J* = 6.6, 3.5, 0.8 Hz), 3.49 (1H, dd, *J* = 9.2, 3.3 Hz). **ESI-MS** *m*/*z* calcd for $C_{12}H_{16}O_5S$ $[M + Na]^+$: 295.06. Found 295.10.

**_S_-(2,3,4,6-tetra-_O_-benzyl-β-D-galactopyranosyl)thiophenol (530)**

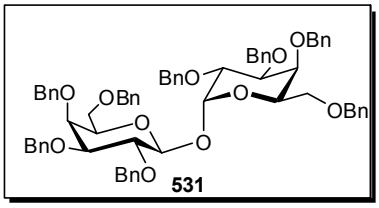


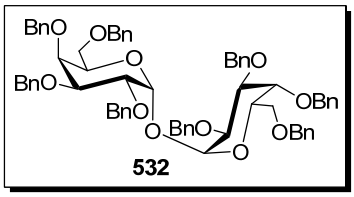
**530**

Deprotected carbohydrate **529** (6.98 g, 25.7 mmol) was dissolved in anhydrous DMF (30 mL) and cooled to 0 ºC. This mixture was cannulated into a suspension of sodium hydride (3.70 g, 154 mmol) in anhydrous DMF (40 mL) under argon at 0 ºC. Following the completion of addition, the reaction was stirred for 20 minutes before benzyl bromide (18.2 mL, 26.2 g, 154 mmol) was added dropwise. The ice bath was removed and the reaction was stirred for 12 additional hours. At this point the reaction was diluted with water and ethyl acetate and the two phases were separated. The organic phase was washed twice with water and one with brine. The organic phase was dried and concentrated in the normal fashion and the crude product was re-dissolved minimum boiling methanol. The crystals were collected, washed with ice-cold methanol, and dried *in vacuo* to provide 12.59 g of the product as a white solid in 78 % yield. Spectral data matches published data.[53]

**$^1$H NMR** (400 MHz, *$CDCl_3$*) $\delta_{ppm}$ 7.56-7.44 (2H, m), 7.33-7.16 (20H, m), 7.13-7.07 (3H, m), 4.89 (1H, d, *J* = 11.5 Hz), 4.71 (1H, d, *J* = 10.2 Hz), 4.67 (1H, d, *J* = 11.9 Hz), 4.66 (1H, d, *J* = 9.4 Hz), 4.63 (1H, d, *J* = 11.8 Hz), 4.57 (1H, dd, *J* = 9.7, 0.9 Hz), 4.53 (1H, d, *J* = 11.6 Hz), 4.40 (1H, d, *J* = 11.7 Hz), 4.34 (1H, d, *J* = 11.6 Hz), 3.91 (1H, d, *J* = 2.5 Hz), 3.86 (1H, dd, *J* = 9.4, 9.4 Hz), 3.60-3.50 (4H, m); **$^{13}$C NMR** (101 MHz, *$CDCl_3$*) $\delta_{ppm}$ 138.7, 138.29, 138.22, 137.8, 134.1, 131.5, 128.8, 128.4, 128.3, 128.2, 127.9, 127.80, 127.78, 127.71, 127.66, 127.54, 127.44, 127., 87.7, 84.2, 77.3, 77.2, 75.6, 74.4, 73.56, 73.54, 72.7, 68.7. **ESI-MS** *m*/*z* calcd for $C_{40}H_{40}O_5S$ $[M + NH_4]^+$: 650.3; $[M + Na]^+$: 655.3. Found 650.5, 655.5.

**2,3,4,6-tetra-*O*-benzyl- β-D-galactopyranosyl 2,3,4,6-tetra-*O*-benzyl-α-D-galactopyranoside (531)** and **2,3,4,6-tetra-*O*-benzyl-α-D-galactopyranosyl 2,3,4,6-tetra-*O*-benzyl-α-D-galactopyranoside (532)**




Compounds were prepared according to modified protocol of Pavia and co-workers.[8] Benzyl protected galactose derivative **528** (300 mg, 0.55 mmol) was dissolved in anhydrous DCM (3.4 mL) under an argon atmosphere. This solution was then cannulated into a flask containing freshly activated 4 Å molecular sieves and the solution was stirred for 20 minutes under argon. The flask was cooled to -78 ºC and trifluoromethylsulfonic anhydride (143 μL, 0.825 mmol) was added dropwise. The reaction was allowed to stir for 5 minutes, and then warmed to ambient temperature for an additional 30 minutes. The flask was then returned to -78 ºC and 1 mL of triethylamine was added, followed by 3 mL of saturated sodium bicarbonate. The quench was allowed to warm to ambient temperature before being filtered through a celite pad along with DCM. The filtrate was washed with water, saturated sodium bicarbonate and brine prior to being dried and concentrated in the usual manner. The crude product was purified by flash chromatography (98:2, toluene: acetone) to provide 220 mg of α,α-isomer **532** as a thick clear oil in 75 % yield, and 50 mg of α,β-isomer **531** as a thick clear oil in 17 % yield. Spectra for **532** is consistent with the literature.[8]

Characterization date for **531**:

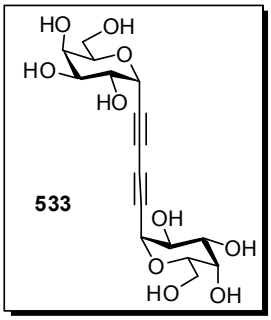
**$^1$H NMR** (400 MHz, *$CDCl_3$*) $\delta_{ppm}$ 7.43-7.10 (40H, m), 5.21 (1H, d, *J* = 3.1 Hz), 5.03 (1H, d, *J* = 11.5 Hz), 4.91 (1H, d, *J* = 11.6 Hz), 4.91 (1H, d, *J* = 11.4 Hz), 4.82-4.65 (7H, m), 4.60 (1H, d, *J* = 11.6 Hz), 4.55 (1H, d, *J* = 7.8 Hz), 4.54 (1H, d, *J* = 11.4 Hz), 4.45-4.26 (5H, m), 4.08 (1H, dd, *J* = 10.1, 2.5 Hz), 4.04 (1H, dd, *J* = 10.1, 3.0 Hz), 4.01 (1H, dd, *J* = 2.3, 1.3 Hz), 3.93 (1H, dd, *J* = 11.3, 2.9 Hz), 3.86 (1H, ddd, *J* = 9.8, 7.7, 5.1 Hz), 3.59-3.39 (6H, m); **$^{13}$C NMR** (101 MHz, *$CDCl_3$*) $\delta_{ppm}$ 139.0, 138.9, 138.8, 138.7, 138.5, 138.4, 138.3, 137.9, 128.7, 128.4, 128.36, 128.27, 128.20, 128.16, 128.13, 128.10, 128.03, 127.88, 127.74, 127.69, 127.62, 127.57, 12.53, 127.50, 127.46, 127.43, 127.33, 127.28, 127.08, 103.7, 99.8, 82.3, 78.93, 78.89, 75.9, 75.0, 74.8, 74.6,

74.0, 73.5, 73.4, 73.3, 73.23, 73.16, 73.0, 72.6, 69.7, 68.5, 68.2. **ESI-MS** *m/z* calcd for $C_{68}H_{70}O_{11}$ $[M + NH_4]^+$: 1080.53; $[M + K]^+$: 1101.45. Found 1080.87, 1101.81.

Characterization data for **532**:

**$^1$H NMR** (400 MHz, *$CDCl_3$*) $\delta_{ppm}$ 7.40-7.17 (40H, m), 5.30 (2H, d, *J* = 3.4 Hz), 4.91 (2H, d, *J* = 11.4 Hz), 4.79 (2H, d, *J* = 11.7 Hz), 4.75 (2H, d, *J* = 12.1 Hz), 4.73 (2H, d, *J* = 11.8 Hz), 4.65 (2H, d, *J* = 12.1 Hz), 4.55 (2H, d, *J* = 11.4 Hz), 4.38 (2H, d, *J* = 11.7 Hz), 4.35 (2H, dd, *J* = 7.0, 7.0 Hz), 4.30 (2H, d, *J* = 11.8 Hz), 4.10 (2H, dd, *J* = 9.9, 3.5 Hz), 4.03 (2H, dd, *J* = 10.0, 2.7 Hz), 4.02-3.99 (2H, m), 3.53 (2H, dd, *J* = 9.0, 7.3 Hz), 3.48 (2H, dd, *J* = 9.1, 6.2 Hz); **$^{13}$C NMR** (101 MHz, *$CDCl_3$*) $\delta_{ppm}$ 138.8, 138.8, 138.64, 138.64, 138.55, 138.55 138.0, 138.0, 128.19, 128.19, 128.17, 128.17, 128.08, 128.08, 128.05, 128.05, 128.02, 128.02, 127.6, 127.6, 127.4, 127.4, 127.3, 127.3, 127.2, 127.2, 93.5, 93.5, 78.6, 78.6, 75.9, 75.9, 74.9, 74.9, 74.7, 74.7, 73.3, 73.3, 72.6, 72.6, 72.6, 72.6, 69.6, 69.6, 68.9, 68.9. **ESI-MS** *m/z* calcd for $C_{68}H_{70}O_{11}$ $[M + NH_4]^+$: 1080.53; $[M + K]^+$: 1101.45. Found 1080.86, 1101.80.

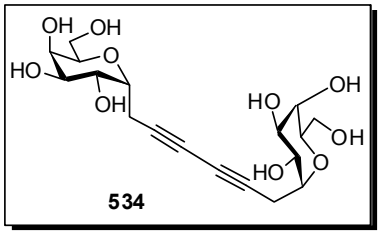
**1, 4-bis(α-D-galactopyranosyl)-1,3-butadiyne (533)**




A 0.1 M solution of sodium methoxide in methanol (5 mL) was added to 40 mg of Glaser disaccharide **1409** and the reaction was stirred for 16 hours at ambient temperature. DOWEX 50WX8 (50-100 mesh) ion exchange resin was added until the pH of the solution was neutral. The reaction mixture was filtered and the filtrate was concentrated, resuspended in water and lyophilized to provide 20 mg of the product as a white powder in quantitative yield. **$^1$H NMR** (400 MHz, *$D_2O$*) $\delta_{ppm}$ 4.95 (2H, d, *J* = 6.0 Hz), 4.09 (2H, ddd, *J* = 6.4, 5.8, 0.8 Hz), 3.97 (2H, dd, *J* = 3.3, 0.7 Hz), 3.92 (2H, dd, *J* = 10.3, 6.0 Hz), 3.82 (2H, dd, *J* = 10.2, 3.3 Hz), 3.72 (4H, d, *J* = 6.0 Hz); **$^{13}$C NMR** (101 MHz, *$D_2O$*) $\delta_{ppm}$ 74.8, 74.5, 722, 70.7, 68.9, 68.9, 67.1 61.2.[a] **ESI-MS** *m/z* calcd for $C_{16}H_{22}O_{10}$ $[M + NH_4]^+$: 392.15; $[M + Na]^+$: 397.11. Found 392.20, 397.13.

[a] All $^{13}$C peaks are duplicated due to the symmetircal nature of the compound.

**1,6-bis[α-D-galactopyranosyl]-2,5-hexadiyne (534)**

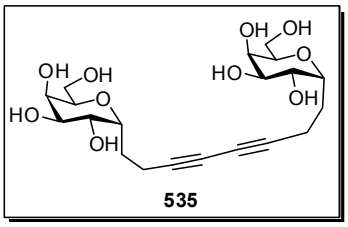


**534**

A 0.1 M solution of sodium methoxide in methanol (3 mL) was added to 20 mg (0.027 mmol) of Glaser-type disaccharide **1410** and the reaction was stirred for 16 hours at ambient temperature. DOWEX 50WX8 (50-100 mesh) ion exchange resin was added until the pH of the solution was neutral. The reaction mixture was filtered and the filtrate was concentrated, resuspended in water and lyophilized to provide 11 mg of the product as a white powder in quantitative yield.

**$^{1}$H NMR** (400 MHz, *$D_2O$*) $\delta_{ppm}$ 4.22 (2H, td, *J* = 10.0, 5.3 Hz), 4.00 (2H, dd, *J* = 9.7, 5.8 Hz), 3.96 (2H, dd, *J* = 3.2, 1.3 Hz), 3.83-3.65 (8H, m), 2.76 (2H, dd, *J* = 17.6, 10.0 Hz), 2.66 (2H, dd, *J* = 17.7, 4.8 Hz); **$^{13}$C NMR** (101 MHz, *$D_2O$*)[a] $\delta_{ppm}$ 78.7, 73.5, 72.4, 69.3, 68.7, 67.8, 66.4, 60.8, 16.7. **ESI-MS** *m/z* calcd for $C_{18}H_{26}O_{10}$ $[M + H]^+$: 403.16; $[M + Na]^+$: 425.14. Found 403.19, 425.16.

**1,8-bis(α-D-galactopyranosyl)-2,7-octadiyne (535)**



**535**

A 0.1 M solution of sodium methoxide in methanol (5 mL) was added to 38 mg (0.050 mmol) of Glaser disaccharide **1411** and the reaction was stirred for 16 hours at ambient temperature. DOWEX 50WX8 (50-100 mesh) ion exchange resin was added until the pH of the solution was neutral. The reaction mixture was filtered and the filtrate was concentrated, resuspended in water and lyophilized to provide 21 mg of the product as a white powder in quantitative yield.

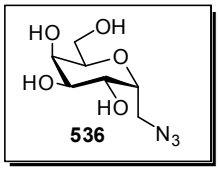
**$^{1}$H NMR** (400 MHz, *$D_2O$*) $\delta_{ppm}$ 4.14 (2H, ddd, *J* = 11.6, 5.9, 3.4 Hz), 3.99 (2H, dd, *J* = 10.1, 6.0 Hz), 3.95 (2H, d, *J* = 3.3 Hz), 3.78-3.65 (8H, m), 2.47-2.28 (4H, m), 2.00-1.89 (2H, m), 1.84-1.73 (2H, m); **$^{13}$C NMR** (101 MHz, *$D_2O$*)[b] $\delta_{ppm}$ 77.6, 74.4, 71.7, 69.7, 69.0, 68.0, 65.1, 60.9, 22.4, 14.8. **ESI-MS** *m/z* calcd for $C_{20}H_{30}O_{10}$ $[M + Na]^+$: 453.17. Found 453.19.

---

[a] All $^{13}$C peaks are duplicated due to the symmetircal nature of the compound

[b] All $^{13}$C peaks are duplicated due to the symmetircal nature of the compound

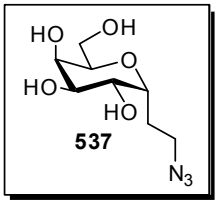
**(α-D-galactopyranosyl)methylazide (536)**




To a 0.1 M solution of NaOMe in methanol was added methylazide galactose derivative **430** (21 mg, 0.054 mmol) and the reaction was stirred for 16 hours. DOWEX 50WX8 (50-100 mesh) ion exchange resin was added until the pH < 7, and the reaction was filtered and concentrated. Following lyophilization, 12 mg of off-white powder was recovered in quantitative yield.

**$^1$H NMR** (400 MHz, *MeOD*) $\delta_{ppm}$ 4.21 (1H, ddd, *J* = 9.4, 5.3, 3.9 Hz), 4.04 (1H, t, *J* = 2.4 Hz), 3.98 (1H, dd, *J* = 8.8, 5.5 Hz), 3.88-3.74 (3H, m), 3.69 (1H, dd, *J* = 13.8, 10.2 Hz), 3.65 (1H, dd, *J* = 9.0, 3.5 Hz), 3.38 (1H, dd, *J* = 13.6, 3.4 Hz); **$^{13}$C NMR** (400 MHz, *MeOD*) $\delta_{ppm}$ 74.9, 73.6, 71.4, 69.1, 68.8, 61.3, 47.7. **ESI-MS** *m/z* calcd for $C_7H_{13}N_3O_5$ $[M + K]^+$: 258.05. Found: 258.09.

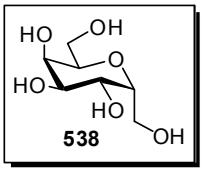
**2-(α-D-galactopyranosyl)ethylazide (537)**




Acetylated azide **420** (100 mg, 0.250 mmol) was dissolved in 10 mL of 0.1 M sodium methoxide in methanol. The reaction was stirred for 16 hours, and quenched with Dowex-50X resin ion exchange resin until the pH <7. Following filtration, the solvent was removed and the residue was lyophilized to provide 58 mg of deprotected azide **537** in quantitative yield as a white powder.

**$^1$H NMR** (400 MHz, *CDCl$_3$*) $\delta_{ppm}$ 4.06 (1H, ddd, *J* = 10.7, 5.3, 4.0 Hz), 3.93-3.88 (2H, m), 3.78 (1H, dd, *J* = 12.5, 8.3 Hz), 3.70-3.61 (3H, m), 3.48-3.37 (2H, m), 2.02-1.79 (2H, m); **$^{13}$C NMR** (100 MHz, *CDCl$_3$*) $\delta_{ppm}$ 74.4, 73.3, 72.0, 70.3, 70.1, 62.4, 49.5, 25.8.

**α-D-galactopyranosyl-methanol (538)**

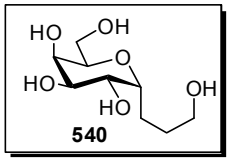



Diacetonide **436** (31 mg, 0.11 mmol), contaminated with Triphenylphosphine oxide (67 mg, 0.24 mmol) was dissolved in 60 % acetic acid and warmed to 80 ºC for 16 hours. Solvent was removed under reduced pressure, and the crude product was purified by preparatory TLC (3:1:1:1, ethyl acetate: water: acetonitrile: methanol) and lyophilization provided 16 mg of **538** as a white powder in 74 % yield.

**$^1$H NMR** (400 MHz, *D$_2$O*) $\delta_{ppm}$ 4.13 (1H, ddd, *J* = 9.6, 6.0, 3.3 Hz), 4.02 (1H, dd, *J* = 9.7, 6.0 Hz), 3.99 (1H, dd, *J* = 3.3, 1.9 Hz), 3.95 (1H, dd, *J* = 12.6, 9.9 Hz), 3.90 (1H, ddd, *J* = 7.4, 4.5,

2.0 Hz), 3.82-3.68 (4H, m); **$^{13}$C NMR** (101 MHz, $D_2O$) $\delta_{ppm}$ 75.9, 72.4, 69.9, 68.7, 67.6, 60.8, 56.2. **ESI-MS** *m/z* calcd for $C_7H_{14}O_6$ $[M + Na]^+$: 217.20. Found 217.19. Rf = 0.40 (3:1:1:1, ethyl acetate: water: acetonitrile: methanol)

**3-(α-D-galactopyranosyl)-propanol (540)**

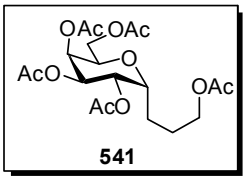


**540**

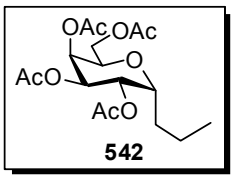
Acetylated derivative **541** (35 mg, 0.081 mmol) was dissolved in 0.1 M sodium methoxide in methanol (3 mL) and the reaction was stirred for 3 hours at ambient temperature. The reaction was quenched with Dowex-50X ion exchange resin until the pH <7. After filtration, the methanol was removed and the crude product was partitioned between water and DCM, and the aqueous phase was washed three times with DCM. The solution was lyophilized to provide 17.5 mg of polyol **540** as a white powder in 97 % yield.

**$^1$H NMR** (400 MHz, $D_2O$) $\delta_{ppm}$ 4.06-3.99 (1H, m), 3.96 (1H, dd, *J* = 9.8, 6.1 Hz), 3.94 (1H, dd, *J* = 3.6, 1.2 Hz), 3.78 (1H, dd, *J* = 9.8, 3.5 Hz), 3.75 (1H, m), 3.70 (1H, d, *J* = 6.3 Hz), 3.69 (1H, d, *J* = 5.2 Hz), 3.63 (2H, t, *J* = 6.2, 6.2 Hz), 1.79-1.46 (4H, m); **$^{13}$C NMR** (75 MHz, $D_2O$) $\delta_{ppm}$ 75.3, 71.5, 69.6, 69.1, 68.3, 61.4, 61.1, 27.5, 20.0. **ESI-MS** *m/z* calcd for $C_9H_{18}O_6$ $[M + H]^+$: 223.25; $[M + Na]^+$: 245.23. Found 223.25, 245.24.

**1-acetoxy-3-(2,3,4,6-Tetra-*O*-acetyl-α-D-galactopyranosyl)propane (541)** and **2,3,4,6-Tetra-*O*-acetyl-propyl-α-D-galactopyranose (542)**



**541**



**542**

Allyl sugar **313** (54 mg, 0.14 mmol) was dissolved in THF (1 mL) in a flask under an argon atmosphere. The flask was cooled to 0 ºC and borane THF complex (500 µL, 0.5 mmol, 1.0 M in THF) was added dropwise and the reaction was allowed to warm to ambient temperature. The reaction was stirred for 2.5 hours, and water (150 µL) was added and the reaction was concentrated. The reaction was resuspended in methanol (1 mL) and solid sodium hydroxide (14 mg, 0.32 mmol) and hydrogen peroxide (33 % in water, 22 µL, 0.2 mmol) were added and the reaction was warmed to 70 ºC for 12 hours. The reaction was then concentrated to dryness and pyridine (1 mL), acetic anhydride (1 mL) and DMAP (1 crystal) were added and the reaction was stirred at ambient temperature for 4

hours. The solution was diluted with ethyl acetate and washed twice with water before being dried and concentrated in the usual manner. The crude product was purified through flash chromatography (6:4, hexanes: ethyl acetate) to provide 40 mg of **541** as a white solid (66 % yield) and 4 mg of a more hydrophobic compound as a white solid, identified as the fully reduced 2,3,4,6-Tetra-*O*-acetyl-propyl-α-D-galactopyranose (**542**).

Characterization data for **541**

**$^{1}$H NMR** (400 MHz, *$CDCl_3$*) $\delta_{ppm}$ 5.39 (1H, dd, *J* = 3.2, 2.5 Hz), 5.24 (1H, dd, *J* = 9.3, 5.0 Hz), 5.17 (1H, dd, *J* = 9.3, 3.3 Hz), 4.23 (1H, dd, *J* = 11.1, 7.2 Hz), 4.21-4.16 (1H, m), 4.10-3.99 (4H, m), 2.11 (3H, s), 2.06 (3H, s), 2.04 (3H, s), 2.03 (3H, s), 2.01 (3H, s), 1.81-1.68 (2H, m), 1.68-1.58 (1H, m), 1.55-1.44 (1H, m); **$^{13}$C NMR** (75 MHz, *$D_2O$*) $\delta_{ppm}$ 171.0, 170.5, 170.0, 169.9, 169.8, 71.7, 68.3, 68.1, 67.9, 67.5, 63.8, 61.4, 24.6, 20.9, 20.74, 20.67, 20.64, 20.61. **ESI-MS** *m/z* calcd for $C_{19}H_{28}O_{11}$ $[M + NH_4]^+$: 450.45; $[M + Na]^+$: 455.41. Found 450.39, 455.35. **Rf** = 0.17 (1:1 hexanes: ethyl acetate).

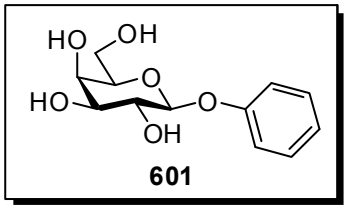
Characterization data for **542** Consistent with previously obtained data.[54]

**$^{1}$H NMR** (500 MHz, *$CDCl_3$*) $\delta_{ppm}$ 5.41 (1H, dd, *J* = 3.1, 2.6 Hz), 5.27 (1H, dd, *J* = 9.5, 5.2 Hz), 5.20 (1H, dd, *J* = 9.5, 3.3 Hz), 4.24 (1H, dd, *J* = 7.7, 3.8 Hz), 4.21 (1H, dd, *J* = 4.5, 4.5 Hz), 4.08 (1H, dd, *J* = 11.3, 5.4 Hz), 4.04 (1H, ddd, *J* = 7.6, 5.6, 2.3 Hz), 2.13 (3H, s), 2.08 (3H, s), 2.06 (3H, s), 2.03 (3H, s), 1.75-1.65 (1H, m), 1.52-1.28 (3H, m), 0.95 (3H, t, *J* = 7.2, 7.2 Hz); **$^{13}$C NMR** (126 MHz, *$D_2O$*) $\delta_{ppm}$ 170.5, 170.1, 170.0, 169.9, 72.0, 68.5, 68.0, 67.9, 67.7, 61.6, 27.6, 20.8, 20.73, 20.72, 20.68, 18.5, 13.8. **ESI-MS** *m/z* calcd for $C_{17}H_{26}O_9$ $[M + Na]^+$: 397.15. Found 397.21. **Rf** = 0.42 (1:1, hexanes: ethyl acetate).

## Experimental Protocols for Chapter 6

**General protocol for the synthesis of substituted Phenyl-β-D-galactopyranoside derivatives.** β-D-galactose pentacetate was dissolved in anhydrous DCM under argon in the presence of freshly activated powdered 4 Å molecular sieves and stirred for five minutes. To this solution were added the appropriate phenol and $BF_3{\cdot}OEt_2$. The resulting mixture was stirred under argon for 18 hrs. The reaction was quenched by the addition of sodium hydrogen carbonate. The solution was filtered through celite and the phases were separated and the aqueous phase was re-extracted twice with DCM. The combined organic phases were washed with brine then dried and concentrated in the usual fashion.[a] This crude product was then dissolved in 0.1 M sodium methoxide in methanol and stirred for 3h. Unless otherwise stated, the solution was concentrated under reduced pressure recrystallized from methanol and ether to provide the product.

**Phenyl-β-D-galactopyranoside (601)**



**601**

β-D-galactose pentacetate (1g, 2.56 mmol) in anhydrous DCM (10 ml) was treated with recrystallized phenol (265.4 mg, 2.82 mmol) and $BF_3{\cdot}OEt_2$ (0.46 ml, 3.84 mmol) according to the general protocol described above. Flash chromatography of the crude tetra-acetate (1:1 EtOAc: hexane) to afforded the acetylated intermediate as a white solid (695.34 mg, 64 %). 100mg of the crude product deprotected and recrystallized as above to afford **601** as a yellowish-white crystalline solid (39 mg, 64 %; 41 % over two steps). Proton spectrum is consistent with that obtained in the literature.[55]

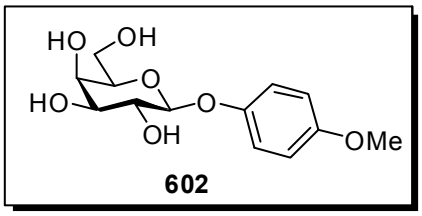
**$^1$H NMR** (500 MHz, *$D_2O$*) $\delta_{ppm}$ 7.40-7.35 (2H, m), 7.15-7.09 (3H, m), 5.05 (1H, d, *J* = 7.4 Hz), 4.80 (1H, m)[b] 3.98 (1H, dd, *J* = 3.2, 0.8 Hz), 3.85 (1H, ddd, *J* = 6.6, 5.6, 0.9 Hz), 3.78 (1H, dd, *J* = 9.9, 7.4 Hz), 3.75 (1H, dd, *J* = 5.3, 3.4 Hz), 3.74 (1H, dd, *J* = 10.0, 3.4 Hz); **$^{13}$C NMR** (126

[a] In some cases this crude product was purified at this stage, or not depending on the purity of the above reaction. In some cases only a small proportion of the recovered acetylated compound was carried through the remainder of the protocol. These deviations from the protocol are described explicitly when relevant.

[b] Buried underneath water peak. Identified by COSY.

MHz, $D_2O$) $\delta_{ppm}$ 156.6, 129.8, 123.1, 116.4, 100.6, 75.3, 72.5, 70.5, 68.4, 60.6. **ESI-MS** *m/z* calcd for $C_{12}H_{16}O_6$ [M + Na]$^+$: 279.08. Found 279.08.

**4-Methoxyphenyl-β-D-galactopyranoside (602)**

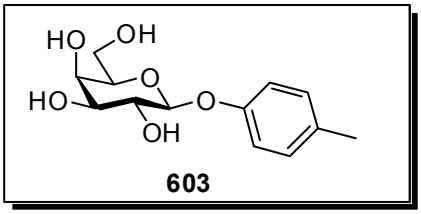


**602**

β-D-galactose pentacetate (500 mg, 1.28 mmol) in anhydrous DCM (5 ml) was treated with 4-methoxyphenol (175.04 mg, 1.41 mmol) and boron $BF_3{\cdot}OEt_2$ (270.1 mg, 1.92 mmol) under the general conditions described above to afford **603** as a white crystalline solid (301 mg, 82%). All spectra are consistent with published data.[56]

**$^1$H NMR** (400 MHz, $D_2O$) $\delta_{ppm}$ 7.12 (2H, d, *J* = 9.1 Hz), 6.97 (2H, d, *J* = 9.1 Hz), 4.94 (1H, d, *J* = 6.8 Hz), 3.98 (1H, d, *J* = 2.18 Hz), 3.80-3.75 (8H, m); **$^{13}$C NMR** (126 MHz, $D_2O$) $\delta_{ppm}$ 154.6, 151.0, 118.1, 115.0, 101.7, 75.4, 72.6, 70.6, 68.5, 60.7, 55.8. **ESI-MS** *m/z* calcd for $C_{13}H_{18}O_7$ [M + Na]$^+$: 309.09. Found 309.10.

**4-Methylphenyl-β-D-galactopyranoside (603**)

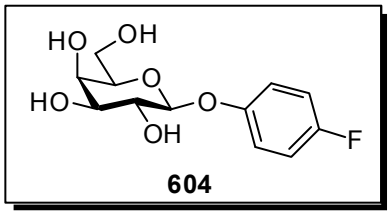


**603**

β-D-galactose pentacetate (1 g, 2.56 mmol) in anhydrous DCM (10 ml) was treated with 4-methylphenol (305 mg, 2.82 mmol) and $BF_3{\cdot}OEt_2$ (0.46ml, 3.84 mmol) under the general conditions described above to afford the crude acetate as a white crystalline solid (819.3 mg, 73%). 100 mg of the crude product was then deprotected and recrystallized as above to provide 42 mg of **603** as a yellowish-white solid (66 %; 48 % over the two steps).

**$^1$H NMR** (500 MHz, $D_2O$) $\delta_{ppm}$ 7.16 (2H, d, *J* = 8.7 Hz), 7.00 (2H, d, *J* = 8.5 Hz), 4.96 (1H, d, *J* = 7.2 Hz), 3.96 (1H, dd, *J* = 3.1, 0.8 Hz), 3.82 (1H, ddd, *J* = 6.4, 5.6, 0.8 Hz), 3.70 (4H, m), 2.26 (1H, s); **$^{13}$C NMR** (126 MHz, $D_2O$) $\delta_{ppm}$ 154.4, 133.0, 130.1, 116.4, 101.0, 75.3, 72.5, 70.49, 70.48, 68.4, 60.7. **ESI-MS** *m/z* calcd for $C_{13}H_{18}O_6$ [M + Na]$^+$: 270.10. Found 293.11.

**4-Fluorophenyl-β-D-galactopyranoside (604)**

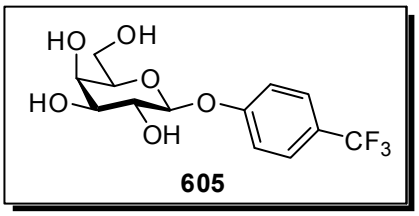


**604**

β-D-galactose pentacetate (200 mg, 0.256 mmol) in anhydrous DCM (2 ml) was treated with 3,5-dimehtylphenol (172 mg, 1.53 mmol) and $BF_3{\cdot}OEt_2$ (100 µl, 0.76 mmol) under the general conditions described above with a 22 hour reaction time. The crude acetate was purified using preparatory TLC (7:3 hexane: ethyl acetate) then deprotected and recrystallized as described above to afford 105 mg of **604** as a white crystalline solid (75 %). Spectral data matches published data.[57]

**$^1$H NMR** (500 MHz, $D_2O$) $\delta_{ppm}$ 7.15-7.02 (4H, m), 4.94 (1H, d, $J$ = 7.6 Hz), 3.97 (1H, d, $J$ = 3.3 Hz), 3.87-3.72 (4H, m), 3.73 (1H, dd, $J$ = 10.0, 3.3 Hz); **$^{13}$C NMR** (126 MHz, $D_2O$) $\delta_{ppm}$ 158.8 (q, $J_{C\text{-}F}$ = 238 Hz), 153.2 (d, $J_{C\text{-}F}$ = 2.3 Hz), 118.5 (d, $J_{C\text{-}F}$ = 8.46 Hz), 116.5 (d, $J_{C\text{-}F}$ = 23.44 Hz, C), 101.9, 75.8, 72.9, 71.0, 68.9, 61.1. **ESI-MS** *m/z* calcd for $C_{12}H_{15}FO_6$ $[M + Na]^+$: 297.07. Found 297.08.

**4-(Trifluoromethyl)phenyl-β-D-galactopyranoside (605)**

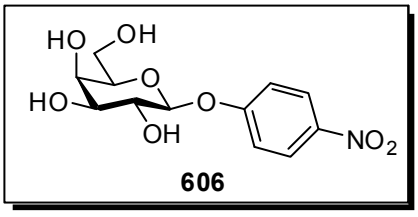


**605**

β-D-galactose pentacetate (100 mg, 0.256 mmol) in anhydrous DCM (1 ml) was treated with 4-(trifluoromethyl)phenol (46 mg, 0.28 mmol) and $BF_3{\cdot}OEt_2$ (50 µl, 0.38 mmol) under the general conditions described above with a 22 hr reaction time. The crude acetate was purified using flash chromatography (6: 4 hexane: ethyl acetate) then deprotected and recrystallized as above to afford 13 mg of **605** as a white crystalline solid in 19 % yield.

**$^1$H NMR** (500 MHz, $D_2O$) $\delta_{ppm}$ 7.75 (2H, d, $J$ = 8.4 Hz), 7.30 (2H, d, $J$ = 8.5 Hz), 5.19 (1H, d, $J$ = 7.8 Hz), 4.06 (1H, d, $J$ = 2.7 Hz), 3.95 (1H, dd, $J$ = 6.1, 5.6 Hz), 3.89 (1H, dd, $J$ = 9.0, 8.5 Hz), 3.85-3.80 (3H, m); **$^{13}$C NMR** (126 MHz, $D_2O$) $\delta_{ppm}$ 159.1, 127. 17, 127.14, 127.11, 116.3, 100.1, 75.4, 72.4, 70.4, 68.3, 60.6. **ESI-MS** *m/z* calcd for $C_{13}H_{15}F_3O_6$ $[M + Na]^+$: 347.07. Found 347.07.

**4-Nitrophenyl-β-D-galactopyranoside (606)**



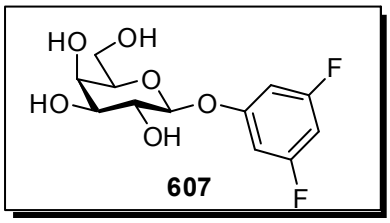
**606**

β-D-galactose pentacetate (100 mg, 0.256 mmol) in anhydrous DCM (1 ml) was treated with 4-nitrophenol (42 mg, 0.28 mmol) and $BF_3{\cdot}OEt_2$ (50 µl, 0.38 mmol) under

the general conditions described above with a 23 hr reaction time. The crude acetate was purified using preparatory TLC (1:1 hexane: ethyl acetate) then deprotected and recrystallized as above to afford 15 mg of **606** as a white crystalline solid (19 %). Spectrum is consistent with published data.[58]

**$^1$H NMR** (500 MHz, *$D_2O$*) $\delta_{ppm}$ 8.24 (2H, d, *J* = 9.2 Hz), 7.22 (2H, d, *J* = 9.3 Hz), 5.18 (1H, d, *J* = 7.6 Hz), 3.99 (1H, d, *J* = 3.0 Hz), 3.91 (1H, dd, *J* = 6.0, 5.9 Hz), 3.83 (1H, dd, *J* = 9.9, 7.6 Hz), 3.78-3.74 (3H, m); **$^{13}$C NMR** (126 MHz, *$D_2O$*) $\delta_{ppm}$ 161.8, 142.5, 126.1, 116.4, 100.0, 75.6, 72.4, 70.3, 68.4, 60.7. **ESI-MS** *m/z* calcd for $C_{12}H_{15}NO_8$ $[M + H]^+$: 302.09. Found 302.09.

**3,5-difluorophenyl-β-D-galactopyranoside (607)**

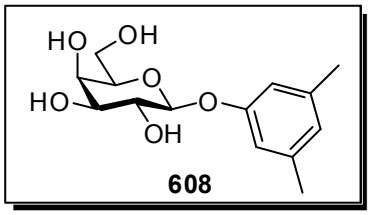


**607**

β-D-galactose pentacetate (100mg, 0.256 mmol) in anhydrous DCM (1 ml) was treated with 3,5-difluorophenol (37mg, 0.282 mmol) $BF_3{\cdot}OEt_2$ (50 µl, 0.38 mmol) under the general conditions described above with a 22 hr reaction time. The crude acetate was purified by preparatory TLC (6: 4 hexane: ethyl acetate) then deprotected and recrystallized as above to afford 16.3 mg of **607** as a white crystalline solid (22 %).

**$^1$H NMR** (500 MHz, *$D_2O$*) $\delta_{ppm}$ 6.74 (2H, dd, *J* = 8.6, 1.9 Hz), 6.67 (1H, tt, *J* = 9.3, 2.0 Hz), 5.04 (1H, d, *J* = 7.3 Hz), 3.99 (1H, d, *J* = 2.9 Hz), 3.87 (1H, dd, *J* = 6.1, 6.1 Hz), 3.81-3.73 (4H, m); **$^{13}$C NMR** (126 MHz, *$D_2O$*) $\delta_{ppm}$ 163.2 (dd, $J_{C\text{-}F}$ = 244.8, 15.9 Hz), 158.2 (t, $J_{C\text{-}F}$ = 14.0 Hz), 100.4, 100.2 (d, $J_{C\text{-}F}$ = 21.9 Hz), 100.2 (d, $J_{C\text{-}F}$ = 21.8 Hz), 98.3 (t, $J_{C\text{-}F}$ = 26.1 Hz), 75.4, 72.4, 70.2, 68.3, 60.5. **ESI-MS** *m/z* calcd for $C_{12}H_{12}F_2O_6$ $[M + Na]^+$: 315.07. Found 315.07.

**3,5-dimethylphenyl-β-D-galactopyranoside (608)**

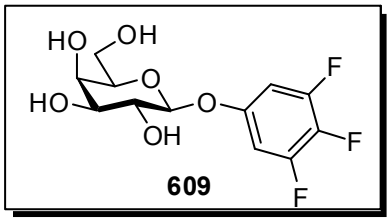


**608**

β-D-galactose pentacetate (100mg, 0.256 mmol) in anhydrous DCM (1 ml) was treated with 3,5-dimethylphenol (34 mg, 0.282 mmol) and $BF_3{\cdot}OEt_2$ (50 µl, 0.38 mmol) according to the general protocol described above. The crude product was purified by preparatory TLC (6:4 hexane: ethyl acetate) and then deprotected and crystallized to afford 21 mg of **608** as a white crystalline solid (29 %).

**$^{1}$H NMR** (400 MHz, *$D_2O$*) $\delta_{ppm}$ 6.84 (1H, bs), 6.80 (2H, bs), 5.02 (1H, d, *J* = 7.2 Hz), 4.00 (1H, d, *J* = 2.6 Hz), 3.84 (1H, d, *J* = 6.4 Hz), 3.81-3.75 (4H, m), 2.29 (6H, s); **$^{13}$C NMR** (126 MHz, *$D_2O$* ) $\delta_{ppm}$ 156.7, 140.3, 124.4, 113.9, 100.6, 75.3, 72.5, 70.5, 68.4, 60.6, 20.3. **ESI-MS** *m*/*z* calcd for $C_{14}H_{20}O_6$ $[M + Na]^+$: 307.12. Found 307.13.

**3,4,5-Trifluorophenyl-β-D-galactopyranoside (609)**



**609**

β-D-galactose pentacetate (100 mg, 0.256 mmol) in anhydrous DCM (1 ml) was treated with 3,4,5-dimethylphenol (42 mg, 0.28 mmol) and $BF_3{\cdot}OEt_2$ (50 µl, 0.38 mmol) according to the general protocol described above with a 22 hr reaction time. The crude acetate was purified using preparatory TLC (1:1 hexane: ethyl acetate) and deprotected and recrystallized as described above to afford 15.6 mg of **609** as a white crystalline solid (20 %) as a 5:2 (β:α) mixture of anomers. Characterization data is provided for the β-anomer with the α-anomer in brackets.

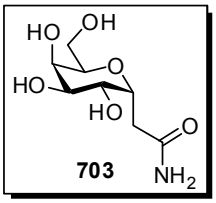
**$^{1}$H NMR** (500 MHz, *$D_2O$*) $\delta_{ppm}$ 6.97-6.84 (2H, m) [6.97-6.84 2H, m], [5.59 (1H, d, *J* = 3.8 Hz)], 4.97 (1H, d, *J* = 7.3 Hz), 4.03-3.93 (1H, m) [4.03-3.93 (2H, m)], 3.98 (1H, dd, *J* = 2.9, 0.7 Hz), 3.85 (1H, ddd, *J* = 6.4, 5.9, 0.7 Hz), 3.80-3.72 (2H, m) [3.80-3.72 (4H, m)], 3.69 (1H, dd, *J* = 6.1, 4.9 Hz); **$^{13}$C NMR** (126 MHz, *$D_2O$*) $\delta_{ppm}$ 150.9 (ddd, $J_{C\text{-}F}$ = 247.4, 10.8, 5.8 Hz) [*ibid*], 151.33 (d, $J_{C\text{-}F}$ = 5 Hz) [*not determined*], 135.7 (dd, $J_{C\text{-}F}$ = 256.1, 13.6 Hz) [*ibid*], 101.57 (d, $J_{C\text{-}F}$ = 19.1 Hz) [102.09 (d, $J_{C\text{-}F}$ = 18.9 Hz)], 101.53 (d, $J_{C\text{-}F}$ = 18.7 Hz) [102.05 (d, $J_{C\text{-}F}$ = 18.8 Hz)], 100.9, [97.7], 75.4 [71.9], 72.3 [69.2], 70.2 [69.0], 68.2 [67.8], 60.5 [60.9]. **ESI-MS** *m*/*z* calcd for $C_{12}H_{13}F_3O_6$ $[M + Na]^+$: 336.06. Found 333.06.

## Experimental Protocols for Chapter 7

**General Protocol for the preparation of 2-(galactopyranosyl)ethylamide derivatives.**

CDI (0.95 eq.) or HCTU (0.95 eq.) and carboxylic acid **315** (1 eq.) were dissolved in DCM or DMF (0.13 M) into a flame dried round-bottom flask under an argon atmosphere containing activated powdered 4 Å molecular sieves and stirred for 30 minutes. DIPEA (2-3 eq.) and the appropriate amine were injected and the flask was sealed under argon and allowed to stir until TLC indicated completion of the reaction (16-72 hours). The reaction mixture was diluted by a factor of 2 with ethyl acetate and filtered through a celite pad, which was then washed twice with ethyl acetate, to remove the sieves. The reaction mixture was then washed sequentially with 10 % HCl, saturated sodium bicarbonate and brine. The organic phase was dried with magnesium sulfate, filtered through a glass wool plug, and concentrated under reduced pressure. The crude product was resuspended in DCM and purified through flash chromatography to provide the title compounds.

**2-(α-D-galactopyranosyl)ethylamide (703)**



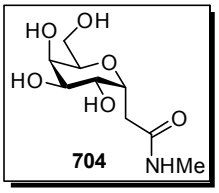
**703**

A mixture of *E*- and *Z*-*N*-(1-propenyl)-2-(2,3,4,6-tetra-*O*-acetyl-α-D-galactopyranosyl)ethylamide (**713** and **714**) (10 mg, 0.023 mmol) were dissolved in 0.1 M NaOMe in methanol (5 mL) and stirred for 3 hours. Solvent was removed under reduced pressure and the crude deprotected product was redissolved in water. DOWEX 50WX8 (50-100 mesh) ion exchange resin was added and the reaction stirred for one hour, to isomerize the enamide to the imide, and then diluted with 4 M HCl and warmed to 40 ºC at 700 mbar. The reaction mixture was neutralized with 10 % sodium hydroxide to pH = 9 and filtered through a sintered glass frit. Solvent was removed *in vacuo* and the crude product was redissolved in minimum boiling methanol. The supernatant was decanted, concentrated and the process repeated on this crude product.[a] The recovered product from the supernatant was lyophilized to provide 2.1 mg of the title compound as a white powder (41 % yield). Spectral data is consistent with the literature.[59]

[a] The precipitate also showed product (as the salt), but contaminated with several organic impurities.

**$^1$H NMR** (500 MHz, $D_2O$) $\delta_{ppm}$ 4.50 (1H, dd, $J$ = 6.8, 5.7 Hz), 3.94 (1H, t, $J$ = 3.0, 3.0 Hz), 3.82-3.77 (2H, m), 3.67 (1H, dd, $J$ = 12.1, 8.5 Hz), 3.61-3.48 (2H, m), 2.75 (1H, dd, $J$ = 18.3, 7.3 Hz), 2.59 (1H, dd, $J$ = 18.4, 5.2 Hz); **$^{13}$C NMR** (126 MHz, $D_2O$) $\delta_{ppm}$ 178.3, 82.9, 75.3, 70.6, 69.4, 67.8, 59.6, 32.9. **ESI-MS** *m/z* calcd for $C_8H_{15}NO_6$ $[M + H]^+$: 222.10; $[M + Na]^+$: 244.08. Found: 222.16, 244.21.

**_N_-Methyl-2-(α-D-galactopyranosyl)ethylamide (704)**

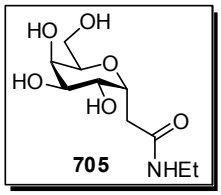


**704**

Using general conditions, 100 mg (0.26 mmol) of carboxylic acid **315**, 42 mg of CDI (0.25 mmol), 19 mg of methylamine hydrochloride (0.28 mmol) and 50 µL of DIPEA, (0.29 mmol), were stirred for 20 hours; following standard work-up, the crude product was directly subjected to deacetylation by the addition of 10 mL of 0.1 M NaOMe in MeOH. The reaction mixture was stirred for 18 hours, at which point it was neutralized with amberlite IR-120 resin beads to pH = 6. The beads were then filtered off and the solvent removed *in vacuo*. The crude product was purified by preparatory TLC (3:1:1:1 EtOAc: MeOH: $CH_3CN$: $H_2O$). Removing the solvent under reduced pressure yielded the title compound as a white powder (40 mg, 65%).

**$^1$H NMR** (500 MHz, *MeOD*) $\delta_{ppm}$ 4.38 (1H, dt, $J$ = 5.0, 13.0 Hz), 3.92 (1H, dd, $J$ = 3.5, 4.0 Hz), 3.88-3.83 (2H, m), 3.79-3.75 (1H, m), 3.67-3.60 (2H, m), 2.70 (3H, s), 2.58 (1H, dd, $J$ = 13, 19 Hz), 2.45 (1H, dd, $J$ = 4.5, 19 Hz); **$^{13}$C NMR** (126 MHz, *MeOD*) $\delta_{ppm}$ 174.9, 75.1, 72.2, 72.1, 70.2, 69.6, 61.7, 34.4, 26.4. **ESI-MS** *m/z* calcd for $C_9H_{15}NO_6$ $[M + H]^+$: 236.11; $[M + Na]^+$: 258.10; . Found: 236.11, 258.09.

**_N_-Ethyl-2-(α-D-galactopyranosyl)ethylamide (705)**



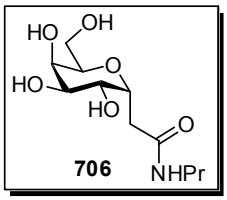
**705**

Using general conditions, 50 mg (0.13 mmol) of carboxylic acid **315**, 64 mg of HCTU (0.16 mmol), 53 mg of ethylamine hydrochloride (0.65 mmol) and 230 µL of DIPEA, (1.3 mmol), were stirred for 20 hours; following standard work-up, the crude product was directly subjected to deacetylation by the addition of 10 mL of 0.1 M NaOMe in MeOH. The reaction mixture was stirred for 18 hours, at which point it was neutralized with amberlite IR-120 resin beads to pH = 6. The beads were then filtered off and the solvent removed *in vacuo*. The crude product was purified by preparatory TLC (3:1:1:1

EtOAc: MeOH: $CH_3CN$: $H_2O$). Removing the solvent under reduced pressure yielded the title compound as a white powder (6.5 mg, 20%).

**$^1$H NMR** (500 MHz, *MeOD*) $\delta_{ppm}$ 4.39 (1H, dt, *J* = 4.0, 10.5 Hz), 3.93 (1H, dd, *J* = 3.0, 3.5 Hz), 3.88-3.84 (2H, m), 3.79 (1H, ddd, J=11.0, 4.5, 3.0 Hz), 3.66-3.62 (2H, m), 3.20 (2H, q, *J* = 7.5 Hz), 2.58 (1H, dd, *J* = 15.0, 10.5 Hz), 2.44 (1H, dd, *J* = 15.0, 3.5 Hz), 1.11 (3H, t, *J* = 7.0 Hz); **$^{13}$C NMR** (126 MHz, *MeOD*) $\delta_{ppm}$ 174.0, 75.0, 72.4, 72.1, 70.2, 69.6, 61.7, 35.4, 34.5, 14.8. **ESI-MS** *m/z* calcd for $C_{10}H_{17}NO_6$ $[M + H]^+$: 250.13; $[M + Na]^+$: 272.11. Found 250.12, 272.02.

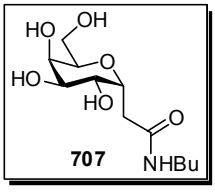
**_N_-Propyl-2-(α-D-galactopyranosyl)ethylamide (706)**




Using general conditions, 100 mg (0.26 mmol) of carboxylic acid **315**, 124 mg of HCTU (0.31 mmol), 170 µL of propylamine (2.08 mmol) and 90 µL of DIPEA, (0.52 mmol), were stirred for 20 hours; following standard work-up, the crude product was directly subjected to deacetylation by the addition of 10 mL of 0.1 M NaOMe in MeOH. The reaction mixture was stirred for 18 hours, at which point it was neutralized with amberlite IR-120 resin beads to pH = 6. The beads were then filtered off and the solvent removed *in vacuo*. The crude product was purified by preparatory TLC (7:1:1:1 EtOAc: MeOH: $CH_3CN$: $H_2O$). Removing the solvent under reduced pressure yielded the title compound as a white powder (51 mg, 45 % yield).

**$^1$H NMR** (300 MHz, *MeOD*) $\delta_{ppm}$ 7.98 (1H, t, *J* = 5.6 Hz), 4.41 (1H, ddd, *J* = 10.4, 4.8, 4.1 Hz), 3.95 (1H, t, *J* = 3.0, 3.0 Hz), 3.92-3.75 (3H, m), 3.69-3.61 (2H, m), 3.19-3.10 (2H, m), 2.62 (1H, dd, *J* = 15.2, 10.4 Hz), 2.47 (1H, dd, *J* = 15.2, 3.8 Hz), 1.53 (2H, quintet, *J* = 7.3 Hz), 0.93 (t, *J* = 7.4, 7.4 Hz, 1H); **$^{13}$C NMR** (75 MHz, *MeOD*) $\delta_{ppm}$ 174.2, 75.0, 72.4, 72.1, 70.2, 69.6, 61.7, 42.3, 34.5, 23.6, 11.8. **ESI-MS** *m/z* calcd for $C_{11}H_{19}NO_6$ $[M + H]^+$: 264.29. Found: 264.23.

**_N_-Butyl-2-(α-D-galactopyranosyl)ethylamide (707)**

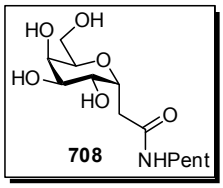



Butyl derivative **710** (35 mg) was dissolved in 20 mL of 0.1 M NaOMe in methanol and stirred for four hours. Dowex-50X resin was added and the solution was stirred an additional five minutes before the resin was removed by filtration and washed with water and methanol successively. Solvent was removed in vacuo and the compound was purified through flash chromatography (6: 1: 1: 1, ethyl acetate: water:

methanol: acetonitrile), concentrated and lyophilized to yield 18 mg of **707** as a white powder (82 % yield).

**$^1$H NMR** (400 MHz, $D_2O$) $\delta_{ppm}$ 4.47 (1H, ddd, $J$ = 10.6, 5.9, 4.3 Hz), 4.01 (1H, dd, $J$ = 9.9, 6.1 Hz), 3.98 (1H, dd, $J$ = 3.3, 1.5 Hz), 3.81 (1H, dt, $J$ = 6.1, 1.4 Hz), 3.73 (1H, dd, $J$ = 9.9, 3.3 Hz), 3.67 (1H, d, $J$ = 6.2 Hz), 3.67 (1H, d, $J$ = 5.8 Hz), 3.26-3.11 (2H, m), 2.66 (1H, dd, $J$ = 14.9, 10.9 Hz), 2.56 (1H, dd, $J$ = 15.0, 4.2 Hz), 1.47 (2H, tt, $J$ = 7.8, 7.2 Hz), 1.31 (2H, qt, $J$ = 7.3, 7.2 Hz), 0.87 (3H, t, $J$ = 7.3 Hz); **$^{13}$C NMR** (101 MHz, $D_2O$) $\delta_{ppm}$ 173.4, 73.0, 72.3, 69.6, 68.7, 67.5, 60.7, 39.2, 32.3, 30.4, 19.4, 12.9. **ESI-MS** *m/z* calcd for $C_{13}H_{25}N_1O_6$ $[M+H]^+$: 278.16. Found: 278.18.

### *N*-Pentyl-2-(α-D-galactopyranosyl)ethylamide (708)

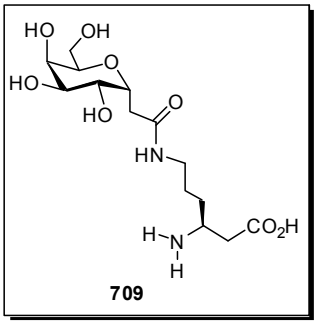


**708**

Acetylated pentyl derivative **711** (72 mg) was dissolved in 10 mL of 0.1 M NaOMe in methanol and stirred for four hours. Dowex-50X resin was added and the solution was stirred an additional five minutes before the resin was removed by filtration and washed with water and methanol successively. The filtrate was concnetrated, resuspended in water and lyophilized to provide 40 mg of the title compound as a white solid (87 % yield).

**$^1$H NMR** (400 MHz, $D_2O$) $\delta_{ppm}$ 4.47 (1H, ddd, $J$ = 10.7, 5.9, 4.3 Hz), 4.01 (1H, dd, $J$ = 9.9, 6.1 Hz), 3.98 (1H, dd, $J$ = 3.2, 1.4 Hz), 3.81 (1H, dt, $J$ = 6.0, 1.2 Hz), 3.73 (1H, dd, $J$ = 10.0, 3.4 Hz), 3.67 (1H, d, $J$ = 6.5 Hz), 3.67 (1H, d, $J$ = 5.7 Hz), 3.25-3.08 (2H, m), 2.65 (1H, dd, $J$ = 15.0, 11.0 Hz), 2.55 (1H, dd, $J$ = 15.0, 4.2 Hz), 1.49 (2H, tt, $J$ = 7.2, 7.0 Hz), 1.35-1.22 (4H, m), 0.85 (3H, t, $J$ = 7.0 Hz); **$^{13}$C NMR** (101 MHz, $D_2O$) $\delta_{ppm}$ 173.4, 73.0, 72.3, 69.6, 68.7, 67.5, 60.7, 39.5, 32.3, 28.3, 28.0, 21.7, 13.2. **ESI-MS** *m/z* calcd for $C_{13}H_{25}N_1O_6$ $[M + H]^+$: 292.18; $[M + Na]^+$: 314.16; $[M + K]^+$: 330.13. Found: 292.21, 314.18, 330.17.

### *N*-[(4*S*)-4-amino-5-carboxypentyl)-2-(α-D-galactopyranosyl)ethylamide hydrochloride (709)



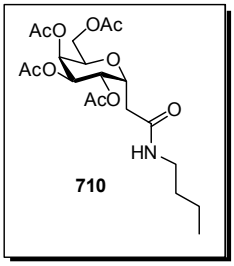
**709**

Acetylated building block **321** (50 mg, 0.068 mmol), prepared according to new conditions was suspended in 2 mL of water and 2 mL of methanol. Piperidine (500 µL, 5.05 mmol) was added and the

mixture was allowed to stir for 10 minutes. 1 mL of 6 N NaOH was added and the mixture was allowed to stir for an additional two hours. The reaction mixture was washed with twice with ether and concentrated. The residue was redissolved in TFA, filtered through a sub-micron filter and diluted with diethyl ether until the mixture became cloudy. The resulting solids were recovered by filtration, redissolved in water and extracted three times with chloroform. 10 % HCl (3 mL) was added and the reaction allowed to stir for 20 minutes before being concentrated to dryness, resuspended in pure water and lyophilized to yield 13 mg of the title compound as a white solid in 50 % yield.

**$^1$H NMR** (400 MHz, *$D_2O$*) $\delta_{ppm}$ 4.48 (1H, q ddd, *J* = 10.5, 5.9, 4.7 Hz), 4.02 (1H, dd, *J* = 9.9, 6.0 Hz), 3.98 ( 1 H, dd, *J* = 3.0, 1.6 Hz), 3.90 (1H, t, *J* = 6.2 Hz), 3.82 (1H, bt, *J* = 5.7 Hz), 3.74 (1H, dd, *J* = 10.0, 3.4 Hz), 3.69 (1H, d, *J* = 6.8 Hz), 3.69 (1H, d, *J* = 5.2 Hz), 3.25 (2H, t, *J* = 6.8, 6.8 Hz), 3.04 (2H, t, *J* = 7.5 Hz), 2.67 (1H, dd, *J* = 15.0, 10.6 Hz), 2.59 (1H, dd, *J* = 15.0, 4.4 Hz), 2.01-1.83 (2H, m), 1.72-1.52 (2H, m); **$^{13}$C NMR** (101 MHz, *$D_2O$*) $\delta_{ppm}$ 173.6, 173.3, 73.0, 72.6, 69.6, 68.8, 67.6, 60.9, 53.6, 38.8, 32.4, 27.5, 27.2, 22.5. **ESI-MS** *m/z* calcd for $C_{13}H_{24}N_2O_8$ $[M + H]^+$: 337.16. Found: 337.22.

**_N_-Butyl-2-(2,3,4,6-tetra-_O_-acetyl-α-D-galactopyranosyl)ethylamide (710)**



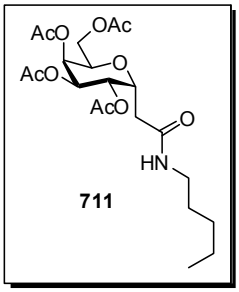
**710**

Using general conditions, 100 mg (0.26 mmol) of carboxylic acid **315**, 100 mg (0.24 mmol) of HCTU, 90 µL (0.50 mmol) of DIPEA, and 51 µL (0.52 mmol) of butylamine were stirred in 2 mL of DCM for 16 hours. Following standard work-up, 140 mg of crude yellow oil was recovered that was purified by flash chromatography (9:1 dichloromethane: methanol) to yield 110 mg of the title compound as a slightly yellow, thick oil (95 % yield).

**$^1$H NMR** (400 MHz, *$CDCl_3$*) $\delta_{ppm}$ 6.22 (1H, t, *J* = 5.4 Hz), 5.42 (1H, t, *J* = 2.8 Hz), 5.28 (1H, dd, *J* = 8.6, 4.7 Hz), 5.17 (1H, dd, *J* = 8.6, 3.3 Hz), 4.68 (1H, td, *J* = 9.3, 4.4 Hz), 4.26-4.15 (3H, m), 3.39-3.14 (2H, m), 2.58 (1H, dd, *J* = 15.5, 9.6 Hz), 2.43 (1H, dd, *J* = 15.5, 4.2 Hz), 2.13 (3H, s), 2.08 (3H, s), 2.06 (3H, s), 2.05 (3H, s), 1.56-1.44 (2H, m), 1.40-1.30 (2H, m), 0.93 (3H, t, *J* = 7.3 Hz); **$^{13}$C NMR** (101 MHz, *$CDCl_3$*) $\delta_{ppm}$ 170.4, 169.9, 169.7, 169.5, 169.0, 69.3, 68.8,

67.8, 67.7, 66.9, 61.2, 39.2, 34.3, 31.5, 20.60, 20.60, 20.59, 20.53, 19.9, 13.6. **ESI-MS** *m/z* calcd for $C_{20}H_{31}N_1O_{10}$ $[M + Na]^+$: 468.19. Found: 468.19.

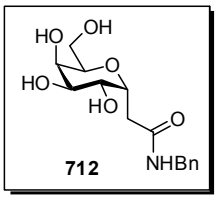
***N*-Pentyl-2-(2,3,4,6-tetra-*O*-acetyl-α-D-galactopyranosyl)ethylamide (711)**




Using the general conditions, 200 mg (0.51 mmol) of carboxylic acid **315**, 202 mg (0.48 mmol) of HCTU, 174 µL (1.0 mmol) of DIPEA, and 115 µL (1.0 mmol) of pentylamine were stirred in 4 mL of DCM for 16 hours. Following standard work-up, 220 mg of crude yellow oil was recovered that was purified by flash chromatography (4: 6 hexanes: ethyl acetate) to yield 172 mg of the title compound as a slightly yellow, thick oil (73 % yield).

**$^1$H NMR** (400 MHz, *CDCl$_3$*) $\delta_{ppm}$ 6.23 (1H, t, *J* = 5.5 Hz), 5.42 (1H, t, *J* = 2.9 Hz), 5.27 (1H, dd, *J* = 8.6, 4.7 Hz), 5.17 (1H, dd, *J* = 8.6, 3.3 Hz), 4.68 (1H, td, *J* = 9.2, 4.4, Hz), 4.31-4.08 (3H, m), 3.33-3.15 (2H, m), 2.58 (1H, dd, *J* = 15.5, 9.6 Hz), 2.43 (1H, dd, *J* = 15.5, 4.2 Hz), 2.13 (3H, s), 2.08 (3H, s), 2.06 (3H, s), 2.05 (3H, s), 1.51 (2H, q, *J* = 6.9 Hz), 1.39-1.22 (4H, m), 0.90 (3H, t, *J* = 6.9 Hz); **$^{13}$C NMR** (101 MHz, *CDCl$_3$*) $\delta_{ppm}$ 170.5, 169.9, 169.7, 169.5, 169.0, 69.4, 68.8, 67.9, 67.7, 66.9, 61.2, 39.6, 34.4, 29.2, 29.0, 22.3, 20.7, 20.7, 20.7, 20.6, 13.9. **ESI-MS** *m/z* calcd for $C_{21}H_{33}N_1O_{10}$ $[M + H]^+$: 460.20; $[M + Na]^+$: 482.18. Found: 460.26, 482.26.

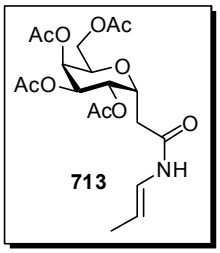
***N*-Benzyl-2-(α-D-galactopyranosyl)ethylamide (712)**

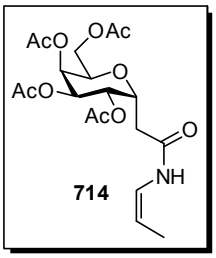



Benzyl amide derivative **757** (180 mg) was treated with 10 mL of 0.1 M sodium methoxide in methanol for 3 hours when TLC (9: 1 DCM: methanol) indicated completion of the reaction. The reaction mixture was neutralized with DOWEX 50WX8 (50-100 mesh) ion exchange resin and filtered through a scintered glass funnel. Methanol was removed under reduced pressure to yield 111 mg of the title compound as a white solid (95 % yield).

**$^1$H NMR** (500 MHz, *MeOD*) $\delta_{ppm}$ 7.42-7.26 (5H, m), 4.49 (1H, dt, *J* = 10.5, 4.7 Hz), 4.40 (1H, d, *J* = 15.1 Hz), 4.32 (1H, d, *J* = 15.1 Hz), 4.00 (1H, dd, *J* = 9.9, 6.1 Hz), 3.94 (1H, dd, *J* = 3.0, 1.4 Hz), 3.77 (1H, t, *J* = 5.6 Hz), 3.71 (1H, dd, *J* = 9.9, 3.3 Hz), 3.63-3.53 (2H, m), 2.70 (1H, dd, *J* = 15.0, 10.9 Hz), 2.60 (1H, dd, *J* = 15.1, 4.1 Hz); **$^{13}$C NMR** (126 MHz, *MeOD*) $\delta_{ppm}$ 174.4,

138.9, 129.7, 128.5, 128.4, 74.0, 73.4, 70.7, 69.7, 68.6, 61.6, 42.7, 33.3, 22.8. **ESI-MS** *m/z* calcd for $C_{15}H_{21}NO_6$ $[M + H]^+$: 312.14; $[M + Na]^+$: 334.13. Found: 312.30, 334.28.




***Z*-*N*-(1-propenyl)-2-(2,3,4,6-tetra-*O*-acetyl-α-D-galactopyranosyl)ethylamide (713)** and ***E*-*N*-(1-propenyl)-2-(2,3,4,6-tetra-*O*-acetyl-α-D-galactopyranosyl)ethylamide (714)**

Allyl amide **744** 75 mg (0.175 mmol) was dissolved in 400μL of dry toluene under an argon atmosphere equipped with a water-cooled condenser. Immediately, 3.4 mg (0.0036 mmol, 2 mol %) of Ruthenium catalyst Z was added and the system was equipped with a balloon. The reaction was heated to 80 ºC for 3 hours. The reaction was cooled to 0 ºC and filtered through celite and washed with ethyl acetate. Solvent was removed *in vacuo*. NMR showed a 1: 7: 15 (starting material: *cis*: *trans*) mixture of the three compounds. The crude product was purified through preparatory TLC (6: 4, hexanes: ethyl acetate) using multiple elutions. The top fraction provided 30 mg of *trans* isomer **713** (40% yield, characterized by J coupling of olefinic protons) and the bottom fraction provided 16 mg of *cis* isomer **714** (21% yield) both as clear oils. The middle fraction provided 22 mg of mixed *cis* and *trans* enamides (29% yield).

Characterization data for **713**

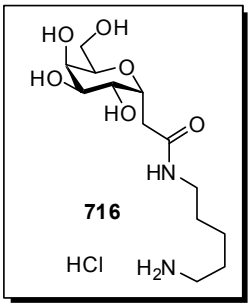
**$^1$H NMR** (400 MHz, *$CDCl_3$*) $\delta_{ppm}$ 7.65 (1H, d, *J* = 10.3 Hz), 6.74 (1H, qdd, *J* = 13.7, 10.5, 1.6 Hz), 5.42 (1H, dd, *J* = 3.2, 3.2 Hz), 5.26 (1H, dd, *J* = 8.4, 4.6 Hz), 5.22-5.14 (2H, m), 4.66 (1H, ddd, *J* = 9.7, 4.2, 4.2 Hz), 4.28 (1H, dd, *J* = 12.7, 9.3 Hz), 4.21-4.15 (2H, m), 2.59 (1H, dd, *J* = 15.7, 9.7 Hz), 2.44 (1H, dd, *J* = 15.8, 4.0 Hz), 2.12 (3H, s), 2.07 (3H, s), 2.05 (3H, s), 2.04 (3H, s), 1.67 (3H, dd, *J* = 6.7, 1.7 Hz); **$^{13}$C NMR** (101 MHz, *$CDCl_3$*) $\delta_{ppm}$ 170.7, 169.9, 169.8, 169.6, 166.2, 123.0, 108.6, 69.8, 68.6, 68.0, 67.7, 66.9, 61.4, 34.4, 20.8, 20.75, 20.74, 20.68, 14.8. **ESI-MS** *m/z* calcd for $C_{19}H_{27}N_1O_{10}$ $[M + H]^+$: 430.17; $[M + Na]^+$: 452.15; $[M + K]^+$: 468.12. Found: 430.23, 542.22, 468.20. **Rf** = 0.5 (8:2, ethyl acetate: hexanes).

Characterization data for **714**

**$^1$H NMR** (400 MHz, *$CDCl_3$*) $\delta_{ppm}$ 7.71 (1H, d, *J* = 10.3 Hz), 6.73 (1H, qdd, *J* = 10.6, 8.8, 1.7 Hz), 5.43 (1H, dd, *J* = 3.1, 3.1 Hz), 5.27 (1H, dd, *J* = 8.4, 4.6 Hz), 5.17 (1H, dd, *J* = 8.4, 3.3

Hz), 4.83 (1H, dqd, *J* = 8.8, 7.2, 0.6 Hz), 4.71 (1H, ddd, *J* = 9.1, 4.3, 4.3 Hz), 4.31-4.06 (3H, m), 2.66 (1H, dd, *J* = 15.9, 9.6 Hz), 2.51 (1H, dd, *J* = 15.9, 4.1 Hz), 2.12 (3H, s), 2.08 (3H, s), 2.05 (3H, s), 2.02 (3H, s), 1.62 (3H, dd, *J* = 7.1, 1.8 Hz); **$^{13}$C NMR** (101 MHz, *$CDCl_3$*) $\delta_{ppm}$ 170.7, 169.9, 169.8, 169.6, 166.5, 121.8, 106.0, 69.8, 68.6, 67.9, 67.6, 66.9, 61.3, 34.3, 20.76, 20.72, 20.67, 20.63, 11.0. **ESI MS** calcd for $C_{19}H_{27}N_1O_{10}$ $[M + H]^+$: 430.17; $[M + Na]^+$: 452.15; $[M + K]^+$: 468.12. Found: 430.22, 542.22, 468.22. **Rf** = 0.5 (8:2, ethyl acetate: hexanes).

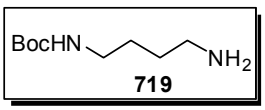
### *N*-(5-aminopentyl)-2-(α-D-galactopyranosyl)ethylamide hydrochloride (716)




Galactoside **723**, (20 mg, 0.035 mmol) was dissolved in 0.1 M sodium methoxide in methanol (10 mL) and stirred for four hours at room temperature. Amberlite 150 resin was added to pH = 3, and removed by filtration. The filtrate was concentrated under reduced pressure and the brown residue was redissolved in 1 mL of trifluoroacetic acid upon which was layered 15 mL of diethyl ether and sealed and stored at -20 ºC for 12 hours. The off white powder was collected through filtration and was washed with ether. The solid was resuspended in 20 mL of 50% HCl and stirred for 1 hour at room temperature and then concentrated *in vacuo*. The resulting off-white gel was resuspended in pure water and lyophilized to provide 11 mg of **716** (94% yield).

**$^1$H NMR** (400 MHz, *$D_2O$*) $\delta_{ppm}$ 4.44 (1H, ddd, *J* = 10.6, 5.8, 4.4 Hz), 3.98 (1H, dd, *J* = 9.9, 6.1 Hz), 3.94 (1H, dd, *J* = 3.3, 1.4 Hz), 3.78 (1H, dt, *J* = 6.0, 1.2 Hz), 3.70 (1H, dd, *J* = 9.9, 3.4 Hz), 3.64 (2H, d, *J* = 6.1 Hz), 3.24-3.09 (2H, m), 2.94 (2H, t, *J* = 7.6 Hz), 2.63 (1H, dd, *J* = 15.0, 10.8 Hz), 2.53 (1H, dd, *J* = 15.0, 4.2 Hz), 1.63 (2H, p, *J* = 7.6 Hz), 1.50 (2H, m), 1.39-1.29 (2H, m); **$^{13}$C NMR** (101 MHz, *$D_2O$*) $\delta_{ppm}$ 173.5, 73.0, 72.4, 69.6, 68.7, 67.5, 60.8, 39.3, 39.1, 32.3, 27.8, 26.3, 22.9. **ESI-MS** *m/z* calcd for $C_{13}H_{26}N_2O_6$ $[M + H]^+$: 307.19; $[M + Na]^+$: 329.17. Found: 307.19, 329.18.

### *tert*-Butyl-4-aminobutylcarbamate (719)

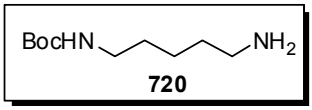



Prepared accoridng to the protocol of West.[60] Putrescine (**717)** (3.35 g, 38.0 mmol) was dissolved in anhydrous chloroform under a

nitrogen atmosphere with stirring. Di-*tert*-butyldicarbonate (1.59 g, 9.5 mmol), predissolved in 15 mL of chloroform, was added by syringe pump over 4 hours. The reaction was stirred over 14 hours when TLC showed consumption of starting material. The reaction mixture was diluted with 100 mL of DCM and then washed twice with saturated sodium bicarbonate. The organic phase was then dried with $MgSO_4$, filtered through a glass wool plug and concentrated under reduced pressure to provide 1.50 g of the title compound as an off-white solid (84 % yield). Spectral data is consistent with the literature.[60]

**$^1$H NMR** (400 MHz, *$CDCl_3$*) $\delta_{ppm}$ 4.71 (4.57) (1H, bs), 3.23-3.03 (2H, m), 2.81-2.65 (2H, m), 1.46-1.38 (4H, m), 1.60-1.47 (9H, m); **$^{13}$C NMR** (101 MHz, *$CDCl_3$*) $\delta_{ppm}$ 79.1, 41.6, 40.4, 28.4, 28.4, 28.4, 28.4, 27.4. **ESI-MS** *m/z* calcd for $C_9H_{20}N_2O_2$ $[M + H]^+$: 189.15; $[2M + K]^+$: 415.26. Found: 189.23, 415.34. **Rf** = 0.10 (9:1, DCM: methanol)

***tert*-Butyl (5-aminopentylcarbamate) (720)**



**720**

Cadaverine (**718**) (2.9 mL, 2.5 g, 24 mmol) was dissolved in 13 mL of dry DCM in a flame-dried round-bottomed flask under argon. Di-*tert*-butyldicarbonate (900 mg, 4.1 mmol), predissolved in 6.5 mL of DCM, was added by syringe pump to the cadaverine solution over 4 hours (0.029 mL/min). The reaction was then allowed to stir for 12 hours. The reaction mixture was diluted with DCM, washed twice with saturated $NaHCO_3$, and once with brine. It was then dried with anhydrous $MgSO_4$, filtered and concentrated to yield 703 mg of the title compound as a white solid in 84 % yield. Characterization data is consistent with the literature.[61]

**$^1$H NMR** (300 MHz, *$CDCl_3$*) $\delta_{ppm}$ 4.62 (1H, bs), 3.12 (2H, dd, *J* = 12.8, 6.6 Hz), 2.69 (2H, t, *J* = 6.8 Hz), 1.55-1.41 (4H, m), 1.44 (9H, s), 1.42-1.30 (4H, m); **$^{13}$C NMR** (101 MHz, *$CDCl_3$*) $\delta_{ppm}$ 156.0, 79.0, 41.8, 40.3, 29.8, 29.6, 28.4, 23.8. **ESI-MS** *m/z* calcd for $C_{10}H_{22}N_2O_2$ $[M + H]^+$: 203.18; $[M + Na]^+$: 225.16. Found: 203.16, 225.16. **Rf** = 0.3 (9:1, methanol: chloroform, 1 drop $NEt_3$).

***tert*-Butyl (pentane-1,5-diyldicarbamate) 721**



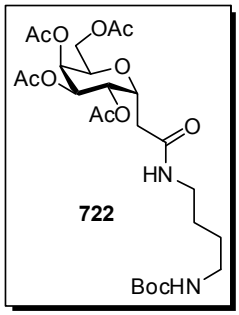
**721**

Cadaverine (**718**) (2.9 mL, 2.5 g, 24 mmol) was dissolved in 10 mL of dry DCM in a flame-dried round-bottomed flask under

argon. Di-*tert*-butyldicarbonate (1.3 g, 5.9 mmol), predissolved in 6.5 mL of DCM, was added by syringe pump to the cadaverine solution over 1.5 hours. The reaction was then allowed to stir for 12 hours. The reaction mixture was diluted with DCM, washed twice with saturated $NaHCO_3$, and once with brine. It was then dried with anhydrous $MgSO_4$, filtered and concentrated to yield 676 mg of the title compound as a white solid in 76 % yield. Characterization data is consistent with the literature.[62]

**$^1$H NMR** (400 MHz, *$CDCl_3$*) $\delta_{ppm}$ 4.85 (2H, bs), 3.11 (4H, dd, *J* = 12.2, 5.9 Hz), 1.55-1.45 (4H, p, *J* = 7.7 Hz), 1.46-1.41 (18H, s), 1.39-1.29 (2H, m); **$^{13}$C NMR** (101 MHz, *$CDCl_3$*) $\delta_{ppm}$ 156.0, 79.0, 40.3, 29.6, 28.3, 23.8. **ESI-MS** *m/z* calcd for $C_{15}H_{30}N_2O_4$ $[M + H]^+$: 303.23; $[M + Na]^+$: 325.21. Found: 303.23, 325.2.

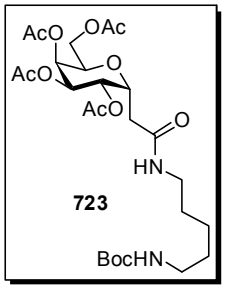
**_N_-[(4-*tert*-butoxycarbonylamino)butyl]-2-(2,3,4,6-tetra-_O_-acetyl-α-D-galactopyranosyl) ethylamide (722)**




Under general conditions, 100 mg (0.26 mmol) of carboxylic acid **315**, 56 mg (0.34 mmol) of CDI, 60 µL (0.34 mmol) of DIPEA, and **719** (150 mg, 0.80 mmol) were stirred in 2 mL of DCM for 18 hours. Following standard work-up, the recovered residue was purified by flash chromatography (1:1, ethyl acetate: hexanes) to yield 106 mg (0.19 mmol) of the title compound as a clear thick gel that solidifies upon extended standing (73 % yield).

**$^1$H NMR** (400 MHz, *$CDCl_3$*) $\delta_{ppm}$ 6.59 (1H, bs), 5.41 (1H, t, *J* = 2.9 Hz), 5.29 (1H, dd, *J* = 8.7, 4.8 Hz), 5.17 (1H, dd, *J* = 8.7, 3.3 Hz), 4.85 (1H, bs), 4.70 (1H, dt, *J* = 9.3, 4.6 Hz), 4.28-4.13 (3H, m), 3.34-3.20 (2H, m), 3.17-3.09 (2H, m), 2.60 (1H, dd, *J* = 15.3, 9.6 Hz), 2.44 (1H, dd, *J* = 15.3, 4.5 Hz), 2.13 (3H, s), 2.07 (3H, s), 2.05 (6H, s), 1.56-1.50 (4H, m), 1.44 (9H, s); **$^{13}$C NMR** (101 MHz, *$CDCl_3$*) $\delta_{ppm}$ 170.4, 169.9, 169.7, 169.5, 169.2, 156.1, 79.0, 69.0, 69.0, 67.7, 67.7, 67.0, 61.1, 39.7, 39.1, 34.2, 28.2, 27.2, 26.3, 20.55, 20.55, 20.55, 20.48. **ESI-MS** *m/z* calcd for $C_{25}H_{40}N_2O_{12}$ $[M + H]^+$: 561.27; $[M + Na]^+$: 583.25. Found: 561.27, 583.25.

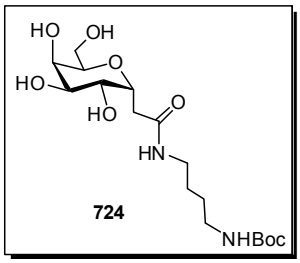
**_N_-[(5-*tert*-butoxycarbonylamino)pentyl]-2-(2,3,4,6-tetra-_O_-acetyl-α-D-galactopyranosyl) ethylamide (723)**



Under general conditions, 400 mg (1.04 mmol) of carboxylic acid **315**, 413 mg (1.00 mmol) of HCTU, 240 μL (1.36 mmol) of DIPEA, and 405 mg (2.00 mmol) of **720** were stirred in 8 mL of DCM for 18 hours. Following standard work-up, the recovered residue was purified by flash chromatography (9:1, DCM: methanol) to yield 302 mg (0.52 mmol) of the title compound as a white solid (50 % yield).[a]

**$^1$H NMR** (400 MHz, *$CDCl_3$*) $\delta_{ppm}$ 6.48 (1H, t, *J* = 5.3 Hz), 5.33 (1H, t, *J* = 3.1 Hz), 5.19 (1H, dd, *J* = 8.6, 4.7 Hz), 5.10 (1H, dd, *J* = 8.7, 3.2 Hz), 4.78 (1H, t, *J* = 5.9 Hz), 4.61 (1H, dt, *J* = 9.2, 4.6 Hz), 4.20 (1H, dd, *J* = 11.0, 7.3 Hz), 4.13 (1H, ddd, *J* = 7.0, 4.3, 3.1 Hz), 4.05 (1H, dd, *J* = 11.1, 4.6 Hz), 3.23-3.08 (2H, m), 3.01 (2H, dd, *J* = 12.5, 6.2 Hz), 2.52 (1H, dd, *J* = 15.3, 9.5 Hz), 2.37 (1H, dd, *J* = 15.2, 4.4 Hz), 2.04 (3H, s), 1.99 (3H, s), 1.97 (3H, s), 1.96 (3H, s), 1.51-1.38 (4H, m), 1.35 (9H, s), 1.30-1.21 (2H, m); **$^{13}$C NMR** (101 MHz, *$CDCl_3$*) $\delta_{ppm}$ 170.7, 170.0, 169.9, 169.7, 169.5, 156.2, 79.0, 69.3, 68.9, 67.9, 67.8, 67.1, 61.2, 40.2, 39.3, 34.4, 29.6, 29.0, 28.4, 23.8, 20.69, 20.65, 20.65, 26.59. **ESI-MS** *m/z* calcd for $C_{10}H_{22}N_2O_{10}$ $[M + H]^+$: 575.28; $[M + Na]^+$: 597.26. Found: 575.28, 597.22.

**N-[(4-*tert*-butoxycarbonylamino)butyl]-2-(α-D-galactopyranosyl)ethylamide (724)**




Acetylated derivative **722** (160 mg, 0.29 mmol) was dissolved in 20 mL of 0.1 M NaOMe in methanol and stirred for 12 hours. Dowex-50X resin was added and the solution was stirred an additional ten minutes before the resin was removed by filtration and washed with methanol. The filtrate was concentrated, resuspended in water and lyophilized to yield 108 mg (0.274 mmol) of the title compound as a yellow gel (96 % yield).

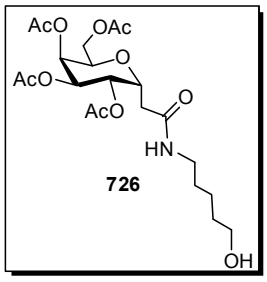
**$^1$H NMR** (500 MHz, *$D_2O$*)[b] $\delta_{ppm}$ 4.44 (1H, ddd, *J* = 10.6, 5.9, 4.4 Hz), 3.98 (1H, dd, *J* = 9.9, 6.1 Hz), 3.95 (1H, dd, *J* = 3.2, 1.2 Hz), 3.78 (1H, t, *J* = 6.0 Hz), 3.70 (1H, dd, *J* = 9.9, 3.3 Hz), 3.64 (1H, d, *J* = 6.6 Hz), 3.64 (1H, d, *J* = 5.5 Hz), 3.21-3.12 (2H, m), 3.06-3.00 (2H, m), 2.63 (1H, dd, *J* = 14.9, 11.0 Hz), 2.53 (1H, dd, *J* = 15.0, 4.1 Hz), 1.52-1.41 (4H, m), 1.28 (9H, s); **$^{13}$C**

[a] Impure fractions were difficult to sepearate from tetramethyl urea and were kept seperately and are not included in the purified reaction yield.

[b] With a presaturation protocol at the frequency of the water peak (4.79 ppm).

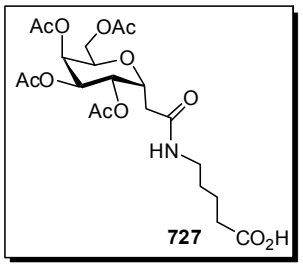
**NMR** (101 MHz, $D_2O$) $\delta_{ppm}$ 173.5, 158.3, 80.8, 72.9, 72.4, 69.6, 68.7, 67.5, 60.7, 39.6, 39.1, 32.3, 27.7, 26.4, 25.6. **ESI-MS** *m/z* calcd for $C_{17}H_{32}N_2O_8$ $[M + H]^+$: 393.22; $[M + Na]^+$: 415.21; $[M + K]^+$: 431.18. Found: 393.24, 415.21, 431.18.

### *N*-(5-hydroxypentyl)-2-(2,3,4,6-tetra-*O*-acetyl-α-D-galactopyranosyl)ethylamide (726)




Under general conditions, 300 mg (0.77 mmol) of carboxylic acid **315**, 302 mg (0.74 mmol) of HCTU, 270 µL (1.53 mmol) of DIPEA, and 159 mg (1.54 mmol) of 5-aminopentanol (**725)** were stirred in 6 mL of DMF for 18 hours. Following standard work-up, the recovered residue was purified by flash column chromatography (100% ethyl acetate to 5 % methanol in 95 % ethyl acetate) to yield 295 mg (0.62 mmol) of the title compound as a thick clear gel (81 % yield). **$^1$H NMR** (500 MHz, *CDCl$_3$*) $\delta_{ppm}$ 6.24 (1H, t, *J* = 5.4 Hz), 5.42 (1H, t, *J* = 3.0 Hz), 5.27 (1H, dd, *J* = 8.5, 4.7 Hz), 5.16 (1H, dd, *J* = 8.6, 3.3 Hz), 4.67 (1H, td, *J* = 9.3, 4.4 Hz), 4.27 (1H, dd, *J* = 10.1, 6.2 Hz), 4.21-4.13 (2H, m), 3.65 (2H, t, *J* = 6.3 Hz), 3.33-3.20 (2H, m), 2.57 (1, dd, *J* = 15.5, 9.7 Hz), 2.42 (1H, dd, *J* = 15.5, 4.2 Hz), 2.13 (3H, s), 2.08 (3H, s), 2.06 (3H, s), 2.05 (3H, s), 1.62-1.51 (4H, m), 1.45-1.37 (2H, m); **$^{13}$C NMR** (101 MHz, *CDCl$_3$*) $\delta_{ppm}$ 170.6, 170.0, 169.8, 169.6, 169.3, 69.3, 68.9, 67.9, 67.7, 66.9, 62.3, 61.2, 39.4, 34.4, 32.0, 29.2, 23.0, 20.69, 20.67, 20.67, 20.59. **ESI-MS** *m/z* calcd for $C_{24}H_{39}NO_{11}$ $[M + H]^+$: 476.21; $[M + Na]^+$: 498.20. Found: 476.22, 498.21. **Rf** = 0.46 (9:1, ethyl acetate: methanol).

### *N*-(4-carboxybutyl)-2-(2,3,4,6-tetra-*O*-acetyl-α-D-galactopyranosyl)ethylamide (727)

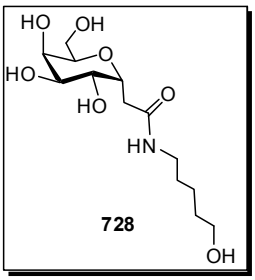



Alcohol derivative **726** (160 mg, 0.34 mmol) was dissolved in 4.8 mL of acetone and cooled to 0 ºC. Jones reagent (500 µL, 1.0 mmol, 2.0 M) was added and the reaction was allowed to warm to ambient temperature and stirred for 3 hours when TLC showed consumption of the starting material. Isopropanol was added dropwise (0.51 mmol, 40 µL) upon whcih the solution turned deep green. The reaction mixture was diluted with 70 mL of DCM. The reactin mixture was washed three times with brine. The organic phase was dried with $MgSO_4$, filtered through a glass-wool plug and concetrated under

reduced pressure. 200 mg of black oil was recovered and purified by dry vacuum chromatography (100 % DCM to 75 % DCM, 25 % methanol in 2.5 % increments) to yield 30 mg (0.061 mmol) of a white solid in 18 % yield.

**$^1$H NMR** (500 MHz, *MeOD*) $\delta_{ppm}$ 5.41 (1H, t, *J* = 2.6 Hz), 5.27 (1H, dd, *J* = 9.5, 4.8 Hz), 5.23 (1H, dd, *J* = 9.5, 3.0 Hz), 4.67 (1H, td, *J* = 9.3, 5.0 Hz), 4.24 (1H, dt, *J* = 6.3, 2.1 Hz), 4.19-4.09 (2H, m), 3.26-3.15 (2H, m), 2.66 (1H, dd, *J* = 14.8, 9.3 Hz), 2.51 (1H, dd, *J* = 14.7, 5.1 Hz), 2.32 (2H, t, *J* = 7.2 Hz), 2.12 (3H, s), 2.05 (3H, s), 2.02 (3H, s), 2.00 (3H, s), 1.67-1.60 (2H, m), 1.55 (2H, m); **$^{13}$C NMR** (126 MHz, *MeOD*) $\delta_{ppm}$ 177.2, 172.19, 172.16, 171.9, 171.5, 171.3, 71.2, 70.1, 69.3, 69.0, 68.9, 62.5, 40.2, 39.9, 34.5, 29.8, 23.4, 20.74, 20.68, 20.67, 20.58. **ESI-MS** *m*/*z* calcd for $C_{21}H_{31}NO_{12}$ $[M + H]^+$: 490.19; $[M + Na]^+$: 512.17. Found: 490.30, 512.28.

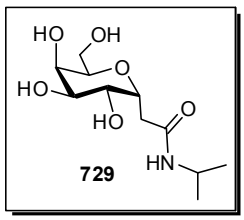
**N-(5-hydroxypentyl)-2-(α-D-galactopyranosyl)ethylamide (728)**




Alcohol **726** (20 mg, 0.042 mmol) was dissolved in 5 mL of 0.1 M NaOMe in methanol and stirred for 18 hours. DOWEX 50WX8 (50-100 mesh) ion exchange resin was added and stirred for 20 minutes. Following filtration, the filtrate was concentrated under reduced pressure. The crude product was redissolved in methanol and purified by preperatory TLC (4: 1: 1: 1, ethyl acetate: water: methanol: acetonitrile). The pure product was resuspended in water and lyophilized to yield 9.3 mg (0.030 mmol) of the title compound as a white powder (72 % yield).

**$^1$H NMR** (400 MHz, $D_2O$) $\delta_{ppm}$ 4.47 (1H, ddd, *J* = 10.6, 5.8, 4.1 Hz), 4.01 (1H, dd, *J* = 9.9, 6.0 Hz), 3.98 (1H, dd, *J* = 3.3, 1.5 Hz), 3.81 (1H, dt, *J* = 6.2, 6.2, 1.2 Hz), 3.73 (1H, dd, *J* = 9.9, 3.4 Hz), 3.67 (1H, d, *J* = 6.5 Hz), 3.67 (1H, d, *J* = 5.7 Hz), 3.58 (2H, t, *J* = 6.6, 6.6 Hz), 3.25-3.13 (2H, m), 2.66 (1H, dd, *J* = 15.0, 10.8 Hz), 2.56 (1H, dd, *J* = 15.0, 4.2 Hz), 1.59-1.47 (4H, m), 1.39-1.29 (2H, m); **$^{13}$C NMR** (101 MHz, $D_2O$) $\delta_{ppm}$ 173.4, 73.0, 72.4, 69.6, 68.7, 67.5, 61.6, 60.7, 39.4, 32.3, 30.9, 28.1, 22.4. **ESI-MS** *m*/*z* calcd for $C_{13}H_{25}NO_7$ $[M + H]^+$: 308.17; $[M + Na]^+$: 330.15. Found: 308.24, 330.22.

***N*-(*iso*-propyl)-2-(α-D-galactopyranosyl)ethylamide (729)**

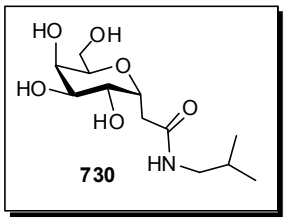



*Iso*-propyl derivative **738** (30 mg, 0.070 mmol) was dissolved in 10 mL of 0.1 M NaOMe in methanol and stirred for four hours. Dowex-50X

resin was added and the solution was stirred an additional five minutes before the resin was removed by filtration and washed with methanol. The filtrate was concentrated and the recovered residue was resuspended in water and lyophilized to yield 17 mg (0.067 mmol) of the title compound as a white solid (95 % yield).

**$^1$H NMR** (400 MHz, $D_2O$) $\delta_{ppm}$ 4.47 (1H, ddd, $J$ = 10.6, 5.9, 4.4 Hz), 4.01 (1H, dd, $J$ = 10.0, 6.1 Hz), 3.97 (1H, dd, $J$ = 3.3, 1.5 Hz), 3.96-3.88 (1H, m), 3.80 (1H, dt, $J$ = 6.6, 1.3 Hz), 3.73 (1H, dd, $J$ = 10.0, 3.3 Hz), 3.68 (1H, d, $J$ = 6.6 Hz), 3.67 (1H, d, $J$ = 5.6 Hz), 2.62 (1H, dd, $J$ = 14.9, 10.8 Hz), 2.53 (1H, dd, $J$ = 14.9, 4.3 Hz), 1.12 (6H, d, $J$ = 6.6 Hz); **$^{13}$C NMR** (101 MHz, $D_2O$) $\delta_{ppm}$ 174.8, 75.6, 74.9, 72.2, 71.3, 70.1, 63.3, 44.3, 34.9, 23.9, 23.8. **ESI-MS** *m/z* calcd for $C_{11}H_{21}NO_6$ $[M + H]^+$: 264.14; $[M + Na]^+$: 286.13; $[M + K]^+$: 302.10. Found: 264.28, 286.26, 302.30.

**N-(2-methylpropyl)-2-(α-D-galactopyranosyl)ethylamide (730)**

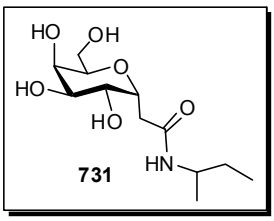


**730**

Isobutyl derivative **739** (20 mg, 0.045 mmol) was dissolved in 5 mL of 0.1 M NaOMe in methanol and stirred for four hours. Dowex-50X resin was added and the solution was stirred an additional five minutes before the resin was removed by filtration and washed with methanol. The filtrate was concentrated and the recovered residue was resuspended in water and lyophilized to yield 11 mg (0.042 mmol) of the title compound as a white solid (93 % yield).

**$^1$H NMR** (400 MHz, $D_2O$) $\delta_{ppm}$ 4.49 (1H, ddd, $J$ = 10.6, 5.9, 4.3 Hz), 4.02 (1H, dd, $J$ = 10.0, 6.1 Hz), 3.99 (1H, dd, $J$ = 3.4, 1.6 Hz), 3.83 (1H, ddd, $J$ = 6.2, 6.1, 1.4 Hz), 3.74 (1H, dd, $J$ = 9.9, 3.3 Hz), 3.68 (2H, dd, $J$ = 6.1, 1.2 Hz), 3.04 (1H, dd, $J$ = 13.2, 6.8 Hz), 2.99 (1H, dd, $J$ = 13.2, 6.8 Hz), 2.69 (1H, dd, $J$ = 15.0, 10.8 Hz), 2.59 (1H, dd, $J$ = 15.0, 4.2 Hz), 1.76 (1H, tsept, $J$ = 6.8 Hz), 0.88 (6H, d, $J$ = 6.7 Hz); **$^{13}$C NMR** (101 MHz, $D_2O$) $\delta_{ppm}$ 173.5, 73.0, 72.3, 69.6, 68.7, 67.6, 60.6, 49.9, 32.3, 27.8, 19.29, 19.28. **ESI-MS** *m/z* calcd for $C_{21}H_{33}NO_{10}$ $[M + H]^+$: 278.16; $[M + Na]^+$: 300.14. Found: 278.11, 300.10.

***N*-(1-methylpropyl)-2-(α-D-galactopyranosyl)ethylamide (731)**



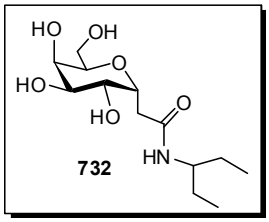
**731**

*Sec*-butyl derivative **740** (23 mg, 0.052 mmol) was dissolved in 5 mL of 0.1 M NaOMe in methanol and stirred for four hours. Dowex-50X resin

was added and the solution was stirred an additional five minutes before the resin was removed by filtration and washed with methanol. The filtrate was concentrated, and the residue was purified by preperatory TLC (6: 1: 1: 1, ethyl acetate: water: methanol: acetonitrile), resuspended in water and lyophilized to yield 12 mg of the title compound, a mixture of diastreomers, as a white solid (84 % yield). Characterization is provide for major diastereomer (minor diastereomer is in parentheses).

**$^1$H NMR** (400 MHz, *$D_2O$*) $\delta_{ppm}$ 4.49 (ddd, *J* = 10.6, 5.8, 4.4 Hz, 1H), 4.03 (1H, dd, *J* = 9.9, 6.1 Hz), 4.01-3.98 (1H, m), 3.83 (1H, ddd, *J* = 6.9, 4.2, 1.3 Hz), 3.82-3.73 (1H, m), 3.74 (1H, dd, *J* = 9.9, 3.4 Hz), 3.68 (2H, bd, *J* = 6.4 Hz), 2.65 (1H, dd, *J* = 14.9, 10.8 Hz), 2.57 (1H, dd, *J* = 15.0, 4.3 Hz), 1.55-1.35 (2H, m), 1.10 (3H, d, *J* = 6.6 Hz), 0.86 (3H, dt, *J* = 7.5, 2.9 Hz); **$^{13}$C NMR** (101 MHz, *$D_2O$*) $\delta_{ppm}$ 172.7, 73.0, 72.2 (72.4), 69.6 (69.7), 68.6 (68.7), 67.5 (67.6), 60.5 (60.7), 47.33 (47.34), 32.3 (32.4), 28.7, 19.3 (19.5), 9.8 (9.7). **ESI-MS** *m/z* calcd for $C_{21}H_{33}NO_{10}$ $[M + H]^+$: 278.16; $[M + Na]^+$: 300.14; $[M + K]^+$: 316.12. Found: 278.18, 300.16, 316.14.

***N*-(1-ethylpropyl)-2-(α-D-galactopyranosyl)ethylamide (732)**

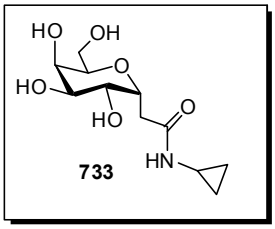


**732**

Ethylpropyl derivative **741** (55 mg, 0.12 mmol) was dissolved in 5 mL of 0.1 M NaOMe in methanol and stirred for four hours. Dowex-50X resin was added and the solution was stirred an additional five minutes before the resin was removed by filtration and washed with methanol. The filtrate was concentrated, and recrystallized from methanol and ether. The recovered precipitate was resuspended in water and lyophilized to yield 30 mg (0.10 mmol) of the title compound as a white solid (86 % yield).

**$^1$H NMR** (400 MHz, *$D_2O$*) $\delta_{ppm}$ 4.36 (1H, ddd, *J* = 10.5, 5.8, 4.4 Hz), 3.89 (1H, dd, *J* =10.1, 6.2 Hz), 3.87 (1H, dd, *J* = 3.4, 1.6 Hz), 3.69 (1H, dt, *J* = 6.2, 1.4 Hz), 3.61 (1H, dd, *J* = 9.9, 3.3 Hz), 3.55 (2H, d, *J* = 6.2 Hz), 3.48 (1H, tt, *J* = 9.0, 4.8 Hz), 2.55 (1H, dd, *J* = 15.0, 10.6 Hz), 2.47 (1H, dd, *J* = 15.1, 4.3 Hz), 1.50-1.34 (2H, m), 1.29-1.17 (2H, m), 0.72 (3H, t, *J* = 7.4 Hz), 0.71 (3H, t, *J* = 7.4 Hz); **$^{13}$C NMR** (101 MHz, *$D_2O$*) $\delta_{ppm}$ 173.3, 73.0, 72.2, 69.65, 68.59, 67.5, 60.4, 53.2, 32.3, 26.9, 26.8, 9.73, 9.66. **ESI-MS** *m/z* calcd for $C_{13}H_{25}NO_6$ $[M + H]^+$: 292.18; $[M + Na]^+$: 314.16; $[M + K]^+$: 330.13. Found: 292.17, 314.14, 330.13.

**N-Cyclopropyl-2-(α-D-galactopyranosyl)ethylamide (733)**

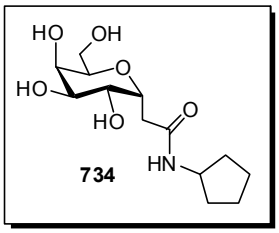


733

Cyclopropyl derivative **742** (70 mg, 0.16 mmol) was dissolved in 10 mL of 0.1 M NaOMe in methanol and stirred for four hours. Dowex-50X resin was added and the solution was stirred an additional five minutes before the resin was removed by filtration and washed with methanol. The filtrate was concentrated, resuspended in water and lyophilized to yield 35 mg (0.13 mmol) of the title compound as a white solid (84 % yield).

**$^1$H NMR** (400 MHz, $D_2O$) $\delta_{ppm}$ 4.47 (1H, ddd, $J$ = 10.5, 5.6, 4.8 Hz), 4.01 (1H, dd, $J$ = 9.9, 6.1 Hz), 3.97 (1H, dd, $J$ = 3.2, 1.3 Hz), 3.78 (1H, ddd, $J$ = 6.7, 5.2, 1.2 Hz), 3.73 (1H, dd, $J$ = 9.9, 3.4 Hz), 3.68 (1H, d, $J$ = 6.7 Hz), 3.67 (1H, d, $J$ = 5.3 Hz), 2.67-2.50 (3H, m), 0.78-0.70 (2H, m), 0.56-0.49 (2H, m); **$^{13}$C NMR** (101 MHz, $D_2O$) $\delta_{ppm}$ 175.4, 72.9, 72.5, 69.6, 68.8, 67.5, 60.8, 32.1, 22.0, 5.5, 5.2. **ESI-MS** *m/z* calcd for $C_{11}H_{19}NO_6$ $[M + H]^+$: 262.13; $[M + Na]^+$: 284.11. Found: 262.13, 284.26.

***N*-Cyclopentyl-2-(α-D-galactopyranosyl)ethylamide (734)**

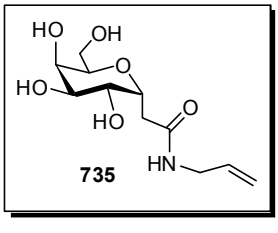


734

Cyclopentyl derivative **743** (85 mg, 0.19 mmol) was dissolved in 15 mL of 0.1 M NaOMe in methanol and stirred for four hours. Dowex-50X resin was added and the solution was stirred an additional five minutes before the resin was removed by filtration and washed with methanol. The filtrate was concentrated, resuspended in water and lyophilized to yield 51 mg (0.18 mmol) of the title compound as a white solid (93 % yield).

**$^1$H NMR** (400 MHz, $D_2O$) $\delta_{ppm}$ 4.48 (1H, dt, $J$ = 10.1, 4.6 Hz), 4.12-3.96 (3H, m), 3.81 (1H, t, $J$ = 6.0 Hz), 3.74 (1H, dd, $J$ = 10.1, 3.2 Hz), 3.68 (2H, d, $J$ = 6.1 Hz), 2.64 (1H, dd, $J$ = 14.7, 11.0 Hz), 2.54 (1H, dd, $J$ = 14.9, 4.1 Hz), 1.90 (2H, ddd, $J$ = 12.8, 6.4, 6.4 Hz), 1.73-1.51 (4H, m), 1.45 (2H, ddd, $J$ = 12.9, 6.3, 6.3 Hz); **$^{13}$C NMR** (101 MHz, $D_2O$) $\delta_{ppm}$ 172.9, 73.1, 72.4, 69.6, 68.8, 67.5, 60.8, 51.5, 32.3, 32.2, 32.0, 32.0, 23.4. **ESI-MS** *m/z* calcd for $C_{13}H_{23}NO_6$ $[M + H]^+$: 290.16; $[M + Na]^+$: 312.14. Found: 290.16, 312.12.

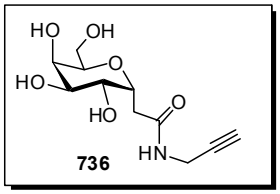
***N*-Allyl-2-(α-D-galactopyranosyl)ethylamide (735)**



735

Allyl derivative **744** (120 mg, 0.20 mmol) was dissolved in 15 mL of 0.1 M NaOMe in methanol to which was added 5 mL of DCM and stirred for four hours. Dowex-50X resin was added and the solution was stirred an additional five minutes before the resin was removed by filtration and washed with methanol. The filtrate was concentrated, and purified by dry vacuum chromatography (100 % ethyl acetate to 60 % ethyl acetate in methanol in 5 % steps) to yield 60 mg (0.14 mmol) of the title compound a white solid following lyophilization (71 % yield). **$^1$H NMR** (400 MHz, *$D_2O$*)[a] $\delta_{ppm}$ 5.86 (1H, ddt, *J* = 17.3, 10.4, 5.1 Hz), 5.20 (1H, ddd, *J* = 17.3, 3.1, 1.6 Hz), 5.15 (1H, ddd, *J* = 10.4, 2.9, 1.5 Hz), 4.51 (1H, ddd, *J* = 10.5, 5.8, 4.3 Hz), 4.03 (1H, dd, *J* = 9.9, 6.1 Hz), 3.99 (1H, dd, *J* = 3.3, 1.5 Hz), 3.87-3.79 (3H, m), 3.76 (1H, dd, *J* = 9.9, 3.4 Hz), 3.70 (2H, dd, *J* = 6.0, 4.3 Hz), 2.72 (1H, dd, *J* = 15.0, 10.8 Hz), 2.63 (1H, dd, *J* = 15.1, 4.2 Hz); **$^{13}$C NMR** (101 MHz, *$D_2O$*) $\delta_{ppm}$ 173.6, 133.4, 115.7, 72.9, 72.5, 69.6, 68.7, 67.6, 60.8, 41.7, 32.3. **ESI-MS** *m/z* calcd for $C_{11}H_{20}NO_6$ $[M + H]^+$: 262.13; $[M + Na]^+$: 284.11. Found: 262.11, 284.08.

***N*- Propargyl-2-(α-D-galactopyranosyl)ethylamide**



**736**

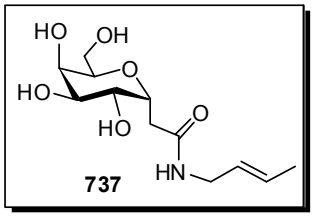
Propargyl derivative **745** (100 mg, 0.23 mmol) was treated with 20 mL of 0.1 M sodium methoxide in methanol for 12 hours. The reaction mixture was neutralized with DOWEX 50WX8 (50-100 mesh) ion exchange resin, filtered through a sintered glass funnel, and the resin was washed sequentially with methanol and water. Solvent was then removed under reduced pressure, and the resulting residue was purified through dry vacuum chromatography (100% ethyl acetate to 60% ethyl acetate in methanol by 5% increments) to yield 48 mg (0.18 mmol) of the title compound as a white solid (81 % yield).

**$^1$H NMR** (500 MHz, *$D_2O$*) $\delta_{ppm}$ 4.37 (1H, ddd, *J* = 10.6, 5.8, 4.4 Hz), 3.89 (1H, dd, *J* = 9.9, 6.1 Hz), 3.85 (1H, dd, *J* = 3.3, 1.4 Hz), 3.84 (1H, dd, *J* = 5.2, 2.6 Hz), 3.68 (1H, *J* = 6.4, 4.9, 1.1 Hz), 3.61 (1H, dd, *J* = 9.9, 3.4 Hz), 3.55 (1H, dd, *J* = 18.1, 7.1 Hz), 3.55 (1H, ddd, *J* = 18.0, 10.7, 4.3 Hz), 2.56 (1H, dd, *J* = 15.0, 10.9 Hz), 2.47 (1H, dd, *J* = 15.1, 4.3 Hz), 2.44 (1H, t, *J* = 2.6 Hz); **$^{13}$C NMR** (101 MHz, *$CDCl_3$*) $\delta_{ppm}$ 173.5, 79.5, 72.9, 72.4, 71.7, 69.6, 68.7, 67.5, 60.7,

[a] With a presaturation protocol at the frequency of the water peak (4.79 ppm).

32.2, 28.8. **ESI-MS** *m/z* calcd for $C_{11}H_{17}NO_6$ $[M + H]^+$: 260.11; $[M + Na]^+$: 282.09. Found: 260.10, 282.06.

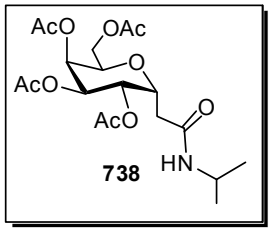
***E*-*N*-(2-butenyl)-2-(α-D-galactopyranosyl)ethylamide (737)**



737

Crotyl derivative **748** (100 mg, 0.22 mmol) was dissolved in 10 mL of 0.1 M NaOMe in methanol and stirred for four hours. Dowex-50X resin was added and the solution was stirred an additional five minutes before the resin was removed by filtration and washed with methanol. The filtrate was concentrated, and purified by preparatory TLC (6:1:1:1, ethyl acetate: water: methanol: acetonitrile) to yield 50 mg of off yellow gel. This gel was redissolved in minimum methanol and ether was added until the solution became cloudy and allowed to stand for 16 hours at -20 ºC. The resulting white precipitate was collected by filtration, resuspended in water and lyophilized to provide 28 mg (0.10 mmol) of the title compound a white solid (46 % yield). **$^1$H NMR** (400 MHz, *$D_2O$*) $\delta_{ppm}$ 5.67 (1H, tqd, *J* = 15.4, 6.6, 1.5 Hz), 5.47 (1H, dddt, *J* = 10.5, 7.2, 5.6, 1.4 Hz), 4.48 (1H, ddd, *J* = 10.6, 5.9, 4.2 Hz), 4.02 (1H, dd, *J* = 9.9, 6.1 Hz), 3.98 (1H, dd, *J* = 3.3, 1.5 Hz), 3.81 (1H, ddd, *J* = 6.7, 5.2, 1.3 Hz), 3.68 (2H, dd, *J* = 6.0, 3.6 Hz), 3.78-3.65 (3H, m), 2.68 (1H, dd, *J* = 14.9, 11.0 Hz), 2.58 (1H, dd, *J* = 15.0, 4.2 Hz), 1.65 (3H, ddd, *J* = 6.4, 2.8, 1.3 Hz); **$^{13}$C NMR** (75 MHz, *$D_2O$*) $\delta_{ppm}$ 173.2, 128.5, 125.6, 72.9, 72.4, 69.6, 68.7, 67.5, 60.7, 41.1, 32.2, 16.8. **ESI-MS** *m/z* calcd for $C_{12}H_{21}NO_6$ $[M + H]^+$: 276.15; $[M + Na]^+$: 298.13. Found: 276.17, 298.15.

***N*-( *iso*-propyl)-2-(2,3,4,6-tetra-*O*-acetyl-α-D-galactopyranosyl)ethylamide (738)**

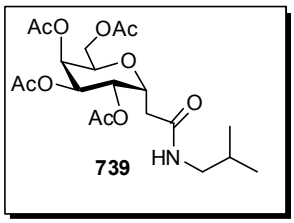


738

Under general conditions, 100 mg (0.26 mmol) of carboxylic acid **315**, 100 mg (0.25 mmol) of HCTU, 90 µL (0.50 mmol) of DIPEA, and 60 µL (0.73 mmol) of *iso*-propylamine were stirred in 2 mL of DCM for 18 hours. Following standard work-up, the recovered residue was purified preparatory TLC (6: 3: 1, acetone: toluene: methanol) to yield 100 mg (0.23 mmol) of the title compound as a clear thick oil (89 % yield). **$^1$H NMR** (400 MHz, *$CDCl_3$*) $\delta_{ppm}$ 6.04 (1H, d, *J* = 7.7 Hz), 5.43-5.40 (1H, m), 5.28 (1H, dd, *J* = 8.6, 4.8 Hz), 5.17 (1H, dd, *J* = 8.6, 3.3 Hz), 4.69 (1H, dt, *J* = 9.2, 4.5 Hz), 4.27-4.16 (3H, m),

4.07 (1H, septd, *J* = 7.7, 6.6 Hz), 2.56 (1H, dd, *J* = 15.3, 9.5 Hz), 2.41 (1H, dd, *J* = 15.3, 4.3 Hz), 2.13 (3H, s), 2.08 (3H, s), 2.06 (3H, s), 2.05 (3H, s), 1.16 (6H, d, *J* = 6.6 Hz); **$^{13}$C NMR** (101 MHz, *CDCl$_3$*) $\delta_{ppm}$ 170.4, 169.8, 169.7, 169.4, 168.2, 69.3, 68.9, 67.8, 67.7, 66.9, 61.1, 41.3, 34.5, 22.6, 22.5, 20.60, 20.56, 20.56, 20.49.

***N*-(2-methylpropyl)-2-(2,3,4,6-tetra-*O*-acetyl-α-D-galactopyranosyl)ethylamide (739)**

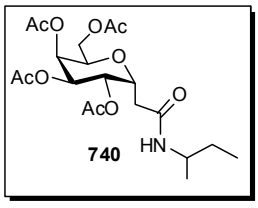


**739**

Under general conditions, 58 mg (0.15 mmol) of carboxylic acid **315**, 32 mg (0.20 mmol) of CDI, 34 µL (0.19 mmol) of DIPEA, and 44 µL (0.44 mmol) of *iso*-butylamine were stirred in 1 mL of DCM for 18 hours. Following standard work-up, the recovered residue was purified preparatory TLC (6:3:1, acetone: toluene: methanol) to yield 60 mg (0.13 mmol) of the title compound as a clear thick oil (90 % yield). Characterization is only provided for the major rotamer.

**$^{1}$H NMR** (400 MHz, *CDCl$_3$*) $\delta_{ppm}$ 6.22 (1H, t, *J* = 5.6 Hz), 5.42 (1H, t, *J* = 2.8 Hz), 5.28 (1H, dd, *J* = 8.6, 4.7 Hz), 5.17 (1H, dd, *J* = 8.6, 3.3 Hz), 4.69 (1H, td, *J* = 9.2, 4.3, 4.3 Hz), 4.25-4.15 (3H, m), 3.21-2.96 (2H, m), 2.59 (1H, dd, *J* = 15.5, 9.6 Hz), 2.44 (1H, dd, *J* = 15.5, 4.1 Hz), 2.13 (3H, s), 2.08 (3H, s), 2.05 (3H, s), 2.05 (3H, s), 1.78 (1H, tsept *J* = 6.6, 4.1 Hz), 0.92 (6H, d, *J* = 6.7 Hz); **ESI-MS** *m*/*z* calcd for $C_{20}H_{31}NO_{10}$ $[M + H]^+$: 446.21. Found: 446.24.

***N*-(1-methylpropyl)-2-(2,3,4,6-tetra-*O*-acetyl-α-D-galactopyranosyl)ethylamide (740)**



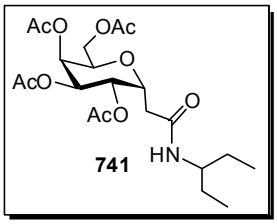
**740**

Under general conditions, 100 mg (0.26 mmol) of carboxylic acid **315**, 56 mg (0.34 mmol) of CDI, 60 µL (0.34 mmol) of DIPEA, and 79 µL (0.79 mmol) of racemic *sec*-butylamine were stirred in 2 mL of DCM for 18 hours. Following standard work-up, the recovered residue was purified preparatory TLC (6:3:1, acetone: toluene: methanol) to yield 100 mg (0.22 mmol) of the title compound, as a mixture of diastereomers, as a clear thick oil (86 % yield). Characterization is provided for major diastereomer (minor diastereomer is in parentheses).

**$^{1}$H NMR** (400 MHz, *CDCl$_3$*) $\delta_{ppm}$ 5.93 (1H, dd, *J* = 8.1, 3.0 Hz), 5.43-5.40 (1H, m), 5.28 (1H, ddd, *J* = 8.2, 4.5, 3.5 Hz), 5.17 (1H, ddd, *J* = 8.6, 2.9, 2.9 Hz), 4.69 (1H, dddd, *J* = 7.1, 4.3, 4.3, 2.8 Hz), 4.24-4.16 (3H, m), 3.91 (1H, tsext., *J* = 6.6, 1.7 Hz), 2.57 (1H, dd, *J* = 15.3, 9.6 Hz),

2.42 (1H, ddd, *J* = 15.4, 4.2, 0.7 Hz), 2.13 (3H, s), 2.08 (3H, s), 2.05 (3H, s), 2.05 (3H, s), 1.47 (1H, p, *J* = 7.3 Hz), 1.13 (3H, d, *J* = 6.6 Hz), 0.91 (3H, t, *J* = 7.4 Hz); **$^{13}$C NMR** (101 MHz, *CDCl$_3$*) $\delta_{ppm}$ 170.4, 169.8, 169.65 (169.67), 169.43 (169.46), 168.37 (168.40), 69.33 (69.36), 68.92 (68.83), 67.83 (67.93), 67.7, 66.91 (66.87), 61.1 (61.0), 46.5 (46.6), 34.57 (34.62), 29.5 (29.4), 20.61, 20.59 (20.58), 20.50, 20.21 (20.23), 10.25 (10.21). **ESI-MS** *m*/*z* calcd for $C_{20}H_{31}NO_{10}$ $[M + H]^+$: 446.21; $[M + Na]^+$: 468.19. Found: 446.25, 468.22.

**_N_-(1-ethylpropyl)-2-(2,3,4,6-tetra-_O_-acetyl-α-D-galactopyranosyl)ethylamide (741)**

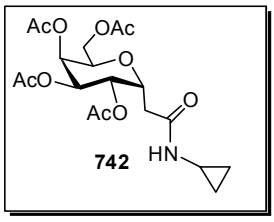


**741**

Under general conditions, 50 mg (0.13 mmol) of carboxylic acid **315**, 27 mg (0.17 mmol) of CDI, 30 µL (0.17 mmol) of DIPEA, and 45 µL (0.38 mmol) of 1-ethylpropylamine were stirred in 1 mL of DCM for 18 hours. Following standard work-up, the recovered residue was purified by gradient flash chromatography (100% hexanes to 100 % ethyl acetate in 10% increments) to yield 55 mg (0.12 mmol) of the title compound as a clear thick oil (92 % yield).

**$^1$H NMR** (400 MHz, *CDCl$_3$*) $\delta_{ppm}$ 5.70 (1H, d, *J* = 8.9 Hz), 5.42 (1H, dt, *J* = 2.8, 1.3 Hz), 5.27 (1H, dd, *J* = 8.4, 4.6 Hz), 5.16 (1H, dd, *J* = 8.4, 3.3 Hz), 4.69 (1H, td, *J* = 8.8, 4.2 Hz), 4.24-4.19 (2H, m), 3.85-3.73 (1H, m), 3.56-3.45 (1H, m), 2.56 (1H, dd, *J* = 15.3, 9.8 Hz), 2.43 (1H, dd, *J* = 15.3, 4.0 Hz), 2.12 (3H, s), 2.09 (3H, s), 2.05 (3H, s), 2.05 (3H, s), 1.62-1.47 (2H, m), 1.43-1.30 (2H, m), 0.90 (6H, dt, *J* = 7.4, 2.4 Hz); **$^{13}$C NMR** (101 MHz, *CDCl$_3$*) $\delta_{ppm}$ 170.5, 169.9, 169.7, 169.5, 168.8, 69.54, 68.9, 68.0, 67.8, 66.8, 61.0, 52.1, 34.8, 27.34, 27.31, 20.70, 20.68, 20.66, 20.60, 10.20, 10.16. **ESI-MS** *m*/*z* calcd for $C_{21}H_{33}NO_{10}$ $[M + H]^+$: 460.22; $[M + Na]^+$: 482.20; $[M + K]^+$: 498.17. Found: 460.34, 482.34, 498.34.

**_N_-Cyclopropyl-2-(2,3,4,6-tetra-_O_-acetyl-α-D-galactopyranosyl)ethylamide (742)**



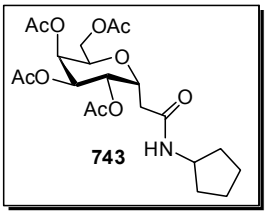
**742**

Under general conditions, 79 mg (0.20 mmol) of carboxylic acid **315**, 42 mg (0.26 mmol) of CDI, 45 µL (0.26 mmol) of DIPEA, and 42 µL (0.60 mmol) of cyclopropylamine were stirred in 2 mL of DCM for 18 hours. Following standard work-up, the recovered residue was purified by gradient flash chromatography (100% hexanes to 100 % ethyl acetate in

10% increments) to yield 70 mg (0.16 mmol) of the title compound as a clear thick oil (82 % yield).

**$^1$H NMR** (400 MHz, *CDCl$_3$*) $\delta_{ppm}$ 6.39 (1H, d, *J* = 1.8 Hz), 5.41 (1H, t, *J* = 3.1 Hz), 5.26 (1H, dd, *J* = 8.5, 4.7 Hz), 5.15 (1H, dd, *J* = 8.5, 3.3 Hz), 4.65 (1H, td, *J* = 9.3, 4.3 Hz), 4.27-4.15 (3H, m), 2.71 (1H, dtt, *J* = 7.1, 3.7, 3.7 Hz), 2.56 (1H, dd, *J* = 15.6, 9.8 Hz), 2.39 (1H, dd, *J* = 15.6, 4.1 Hz), 2.12 (3H, s), 2.09 (3H, s), 2.08 (3H, s), 2.05 (3H, s), 0.80-0.75 (2H, m), 0.53-0.49 (2H, m); **$^{13}$C NMR** (101 MHz, *CDCl$_3$*) $\delta_{ppm}$ 170.6, 170.5, 169.9, 169.7, 169.5, 69.4, 68.6, 67.9, 67.6, 66.9, 61.3, 34.2, 22.5, 20.7, 20.6, 20.6, 20.6, 6.6, 6.4. **ESI-MS** *m*/*z* calcd for $C_{19}H_{27}NO_6$ $[M + H]^+$: 430.17; $[M + Na]^+$: 452.15. Found: 430.31, 452.30.

### *N*-Cyclopentyl-2-(2,3,4,6-tetra-*O*-acetyl-α-D-galactopyranosyl)ethylamide (743)

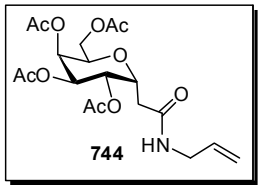


743

Under general conditions, 100 mg (0.26 mmol) of carboxylic acid **315**, 56 mg (0.34 mmol) of CDI, 60 µL (0.34 mmol) of DIPEA, and 78 µL (0.79 mmol) of cyclopentylamine were stirred in 2 mL of DCM for 18 hours. Following standard work-up, the recovered residue was purified by gradient flash chromatography (100% hexanes to 100 % ethyl acetate in 10% increments) to yield 90 mg (0.20 mmol) of the title compound as a clear thick oil (76 % yield).

**$^1$H NMR** (400 MHz, *CDCl$_3$*) $\delta_{ppm}$ 6.30 (1H, d, *J* = 7.3 Hz), 5.41 (1H, dt, *J* = 2.9, 1.4 Hz), 5.28 (1H, dd, *J* = 8.8, 4.8 Hz), 5.17 (1H, dd, *J* = 8.8, 3.3 Hz), 4.77 (1H, d, *J* = 7.2 Hz), 4.70 (1H, td, *J* = 9.4, 4.7 Hz), 4.25-4.14 (3H, m), 2.57 (1H, dd, *J* = 15.3, 9.4 Hz), 2.43 (1H, dd, *J* = 15.3, 4.6 Hz), 2.13 (3H, s), 2.07 (3H, s), 2.05 (3H, s), 2.04 (3H, s), 2.02-1.88 (2H, m), 1.73-1.50 (4H, m), 1.47-1.30 (2H, m); **$^{13}$C NMR** (101 MHz, *CDCl$_3$*) $\delta_{ppm}$ 170.45, 169.9, 169.7, 169.5, 168.7, 69.2, 69.0, 67.74, 67.71, 67.0, 61.2, 51.8, 33.4, 32.9, 32.8, 23.6, 23.5, 20.58, 20.56, 20.56, 20.49.

### *N*-Allyl-2-(2,3,4,6-tetra-*O*-acetyl-α-D-galactopyranosyl)ethylamide (744)

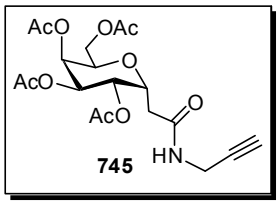


744

Using general conditions, 300 mg (0.75 mmol) of carboxylic acid **315**, 300 mg (0.72 mmol) of HCTU, 270 µL (1.5 mmol) of DIPEA, and 120 µL (1.6 mmol) of allylamine were stirred in 4 mL of DMF for 72 hours. Following standard work-up the crude yellow oil was recovered and

purified by flash chromatography (3: 7 hexanes: ethyl acetate) to yield 260 mg (0.61 mmol) of the title compound as a thick clear oil (81 % yield).
**$^1$H NMR** (400 MHz, *CDCl$_3$*) $\delta_{ppm}$ 6.60 (1H, t, *J* = 5.7, 5.7 Hz), 5.76 (1H, tdd, *J* = 17.1, 10.5, 5.4 Hz), 5.34 (1H, t, *J* = 3.1 Hz), 5.20 (1H, dd, *J* = 8.6, 4.7 Hz), 5.10 (1H, ddd, *J* = 17.0, 1.5, 3.0 Hz), 5.09 (1H, dd, *J* = 8.7, 3.2 Hz) 5.05 (1H, ddd, *J* = 10.3, 2.7, 1.3 Hz), 4.64 (1H, td, *J* = 9.3, 4.4 Hz), 4.24-4.12 (2H, m), 4.05 (1H, dd, *J* = 10.7, 3.6 Hz) 3.86-3.75 (2H, m), 2.59 (1H, dd, *J* = 15.4, 9.7 Hz), 2.42 (1H, dd, *J* = 15.4, 4.3 Hz), 2.05 (3H, s), 2.00 (3H, s), 1.97 (3H, s), 1.97 (3H, s); **$^{13}$C NMR** (101 MHz, *CDCl$_3$*) $\delta_{ppm}$ 170.7, 169.93, 169.92, 169.74, 169.50, 133.8, 115.9, 69.4, 68.5, 67.9, 67.6, 66.9, 61.1, 41.7, 32.3, 20.6, 20.51, 20.50, 20.4. **ESI-MS** *m*/*z* calcd for $C_{19}H_{27}N_1O_{10}$ $[M + H]^+$: 430.17; $[M + Na]^+$: 452.15; $[M + K]^+$: 468.13. Found: 430.30, 452.29, 468.29. **Rf** = 0.32 (7:3, ethyl acetate: hexanes).

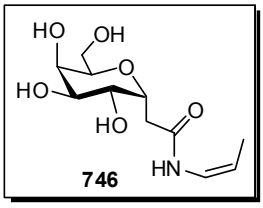
**_N_-Propargyl-2-(2,3,4,6-tetra-_O_-acetyl-α-D-galactopyranosyl)ethylamide (745)**



**745**

Under general conditions, 90 mg (0.23 mmol) of carboxylic acid **315**, 49 mg (0.30 mmol) of CDI, 53 µL (0.3 mmol) of DIPEA, and 44 µL (0.69 mmol) of propargylamine were stirred in 2 mL of DMF for 18 hours. Following standard work-up, 200 mg of crude brown oil was recovered that was purified by gradient flash chromatography (100% hexanes to 100 % ethyl acetate in 10% steps) to yield 80 mg of the title compound as a clear thick oil (81 % yield).
**$^1$H NMR** (400 MHz, *CDCl$_3$*) $\delta_{ppm}$ 6.36 (1H, t, *J* = 5.2 Hz), 5.43 (1H, t, *J* = 3.2 Hz), 5.26 (1H, dd, *J* = 8.3, 4.6 Hz), 5.16 (1H, dd, *J* = 8.3, 3.2 Hz), 4.66 (1H, dt, *J* = 9.5, 4.2 Hz), 4.30 (1H, dd, *J* = 12.9, 9.4 Hz), 4.23-4.16 (2H, m), 4.06 (2H, ddd, *J* = 5.4, 3.4, 2.7 Hz), 2.60 (1H, dd, *J* = 15.9, 9.8 Hz), 2.45 (1H, dd, *J* = 15.8, 3.8 Hz), 2.23 (1H, t, *J* = 2.5 Hz), 2.12 (3H, s), 2.10 (3H, s), 2.09 (3H, s), 2.06 (3H, s); **$^{13}$C NMR** (101 MHz, *CDCl$_3$*) $\delta_{ppm}$ 170.4, 169.9, 169.7, 169.6, 168.9, 71.8, 69.8, 68.4, 68.0, 67.7, 66.8, 61.2, 34.3, 29.2, 20.4, 20.3, 20.26, 20.26. **ESI-MS** *m*/*z* calcd for $C_{19}H_{25}NO_{10}$ $[M + H]^+$: 428.16; $[M + Na]^+$: 450.14. Found: 428.16, 450.13. **Rf** = 0.77 (9:1, ethyl acetate: methanol).

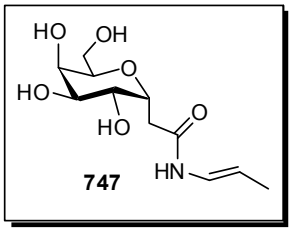
**_Z_-_N_-(1-propenyl)-2-(α-D-galactopyranosyl)ethylamide (746)**



**746**

Enamine **713** (10 mg, 0.233 mmol) was treated with 10 mL of a 0.1 M sodium methoxide in methanol with vigorous stirring for 2 hours. The solution was diluted with 20 mL of water and solvent was removed *in vacuo*. The solution was resuspended in a further 20 mL of water and again solvent was removed *in vacuo*. The solution was resuspended in methanol and filtered through a 20 μm filter. The filtrate was less basic than the original solution by pH test. Solvent was removed and the filtration process was repeated. The product was resuspended in water and lyophilized to give 5 mg of the title compound as white crystals in 82% yield.
**$^1$H NMR** (400 MHz, $D_2O$) $\delta_{ppm}$ 6.49 (1H, qd, $J$ = 8.7, 1.7 Hz), 5.05 (1H, qd, $J$ = 8.8, 7.2 Hz), 4.52 (1H, ddd, $J$ = 10.5, 5.9, 4.5 Hz), 4.03 (1H, dd, $J$ = 9.9, 6.0 Hz), 3.99 (1H, dd, $J$ = 3.4, 1.5 Hz), 3.86 (1H, ddd, $J$ = 6.7, 5.1, 1.3 Hz), 3.75 (1H, dd, $J$ = 9.9, 3.3 Hz), 3.68 (2H, dd, $J$ = 6.0, 3.8 Hz), 3.66-3.57 (m, 1H), 2.80 (1H, dd, $J$ = 15.1, 10.5 Hz), 2.68 (1H, dd, $J$ = 15.0, 4.3 Hz), 1.63 (3H, dd, $J$ = 7.1, 1.7 Hz); **$^{13}$C NMR** (101 MHz, $D_2O$) $\delta_{ppm}$ 171.7, 120.7, 111.0, 72.7, 69.7, 69.6, 68.8, 67.6, 60.8, 32.2, 10.5. **ESI-MS** *m*/*z* calcd for $C_{11}H_{19}N_1O_6$ $[M + Na]^+$: 284.11. Found: 284.26.

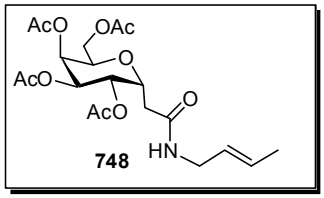
***E*-*N*-(1-propenyl)-2-(α-D-galactopyranosyl)ethylamide (747)**



**747**

Enamine **714** (6 mg, 0.014 mmol) was treated with 10 mL of a 0.1 M sodium methoxide in methanol with vigorous stirring for 2 hours. The solution was diluted with 20 mL of water and solvent was removed *in vacuo*. The solution was resuspended in a further 20 mL of water and again solvent was removed *in vacuo*. The solution was resuspended in methanol and filtered through a 20 μm filter. The filtrate was less basic than the original solution by pH test. Solvent was removed and the filtration process was repeated. The product was resuspended in water and lyophilized to give 2.8 mg of the title compound as white crystals in 77% yield.
**$^1$H NMR** (500 MHz, $D_2O$) $\delta_{ppm}$ 6.57 (1H, qd, $J$ = 14.1, 1.5 Hz), 5.38 (1H, qd, $J$ = 14.1, 6.8 Hz), 4.47 (1H, ddd, $J$ = 10.5, 6.0, 4.7 Hz), 4.00 (1H, dd, $J$ = 9.9, 6.0 Hz), 3.96 (1H, dd, $J$ = 3.3, 1.5 Hz), 3.68-3.63 (1H, m), 3.72 (1H, dd, $J$ = 9.9, 3.3 Hz), 3.65 (2H, ddd, $J$ = 4.2, 4.2, 1.6 Hz), 2.66 (1H, dd, $J$ = 15.0, 10.6 Hz), 2.59 (1H, dd, $J$ = 15.0, 4.5 Hz), 1.63 (3H, dd, $J$ = 6.8, 1.5 Hz); **$^{13}$C NMR** (126 MHz, $D_2O$) $\delta_{ppm}$ 170.5, 121.9, 112.2, 72.5, 69.65, 69.62, 68.7, 67.5, 60.7, 32.2, 14.1. **ESI-MS** *m*/*z* calcd for $C_{11}H_{19}N_1O_6$ $[M + Na]^+$: 284.11. Found: 284.25.

***E*-*N*-(2-butenyl)-2-(2,3,4,6-tetra-*O*-acetyl-α-D-galactopyranosyl)ethylamide (748)**

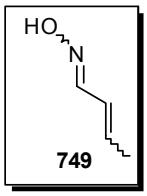


748

Under general conditions, 200 mg (0.51 mmol) of carboxylic acid **315**, 200 mg (0.48 mmol) of HCTU, 180 µL (1 mmol) of DIPEA, and 400 µL (5 mmol) of crotyl amine were stirred in 4 mL of DMF for 18 hours. Following standard work-up, 250 mg of crude brown oil was recovered that was purified by flash chromatography (6: 4 ethyl acetate: hexanes, Rf= 0.16) to yield 160 mg of the title compound as a clear thick oil (71 % yield).

**$^1$H NMR** (400 MHz, *CDCl$_3$*) $\delta_{ppm}$ 6.35 (1H, t, *J* = 5.4 Hz), 5.63 (1H, tqd, *J* = 15.4, 6.3, 1.3 Hz), 5.46 (1H, dddt, *J* = 12.0, 7.6, 6.0, 1.6 Hz), 5.42 (1H, t, *J* = 2.6 Hz), 5.29 (1H, dd, *J* = 8.8, 4.8 Hz, 1H), 5.17 (1H, dd, *J* = 8.8, 3.3 Hz, 1H), 4.71 (1H, td, *J* = 9.4, 4.6 Hz), 4.27-4.14 (3H, m), 3.81 (1H, td, *J* = 6.3, 0.7 Hz), 2.62 (1H, dd, *J* = 15.5, 9.6 Hz), 2.46 (1H, dd, *J* = 15.5, 4.4 Hz), 2.13 (3H, s), 2.07 (3H, s), 2.05 (3H, s), 2.04 (3H, s), 1.68 (3H, ddd, *J* = 6.3, 2.7, 1.3 Hz); **$^{13}$C NMR** (101 MHz, *CDCl$_3$*) $\delta_{ppm}$ 170.5, 170.0, 169.8, 169.6, 169.0, 128.1, 126.7, 69.3, 69.0, 67.9, 67.8, 67.1, 61.4, 41.4, 34.3, 20.68, 20.68, 20.66, 20.61, 17.6. **ESI-MS** *m*/*z* calcd for $C_{20}H_{29}NO_{10}$ $[M + H]^+$: 444.19; $[M + Na]^+$: 466.17. Found: 444.28, 466.26. **Rf** = 0.16 (6:4, ethyl acetate: hexanes).

**Crotylhydroxylamine (749)**

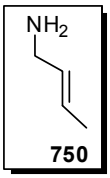


749

Freshly distilled crotonaldehyde[63] (1.7 g, 24 mmol), hydroxylamine hydrochloride (1.8 g, 27 mmol) and sodium acetate (5.9 g, 72 mmol) were dissolved in 45 mL of anhydrous methanol in a flame-dried round-bottomed flask under a nitrogen atmosphere. The mixture was stirred for 12 hours and quenched with 30 mL of saturated sodium bicarbonate. The reaction mixture was extracted thrice with DCM and the combined organic phases were dried with $MgSO_4$, filtered through a glass-wool plug and concentrated under reduced pressure to yield 2.0 g (23.4 mmol) of the title compound as a thick yellow oil (98 %). Characteriztion data is consistent with the literature, only major isomer (E,E) is provided.[64]

**$^1$H NMR** (400 MHz, *CDCl$_3$*) $\delta_{ppm}$ 7.71 (1H, d, *J* = 9.6 Hz), 6.26-5.92 (2H, m), 2.03 (3H, s); **$^{13}$C NMR** (101 MHz, *CDCl$_3$*) $\delta_{ppm}$ 151.4, 137.2, 125.0, 21.4. **EI-MS** *m*/*z* calcd for $C_4H_7NO$ $[M]^+$: 85.05. Found: 85.05.

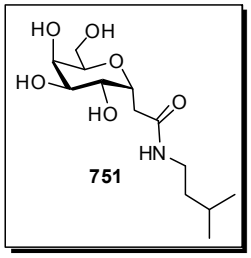
**Crotyl amine (750)**




Crotylhydroxylamine **749** (10.6 g, 125 mmol), was dissolved in 200 mL of THF and cooled to 0 ºC under an argon atmosphere. $LiAlH_4$ (7.1 g, 190 mmol) was added portionwise 1 g at a time and the reaction was allowed to stir vigorously for 12 hours. 7.1 mL of water was added dropwise, followed by a dropwise addition of 14 mL of 10% NaOH and finally 21 mL of water. The reaction mixtures was filtred through a celite plug and washed with water. The reaction mixture was acidified to pH <2 with 4 M HCl, and washed thrice with ether. The aqueous phase was then made alkaline with 6 N NaOH to pH >12 and extracted four times with diethyl ether. The combined organic phases were dried with $MgSO_4$ and filtered through a cotton plug and was fractionally distilled using an oil bath and a Vigreaux column to remove the ether fraction, and the fraction condensing at 90 ºC was collected. This fraction was redistilled under the same conditions, and the fractions condensing from 84-86 ºC were collected yielding 2.4 g (34 mmol) of the title compound as a yellow liquid (STENCH) in 27 % yield. The amine was stored under argon in a sealed ampule until required and the boiling point matched that previously published.[65]

**$^1$H NMR** (400 MHz, *$CDCl_3$*) $\delta_{ppm}$ 5.59-5.54 (2H, m), 3.25-3.21 (2H, m), 1.68 (3H, ddd, *J* = 3.2, 2.5, 1.2 Hz); **$^{13}$C NMR** (101 MHz, *$CDCl_3$*) $\delta_{ppm}$ 132.4, 124.9, 44.0, 17.5.

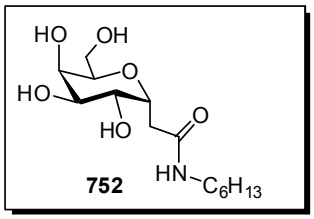
***N*-(3-methylbutyl)-2-(α-D-galactopyranosyl)ethylamide (751)**




Isoamyl derivative **761** (120 mg, 0.26 mmol) was dissolved in 15 mL of 0.1 M NaOMe in methanol and stirred for four hours. Dowex-50X resin was added and the solution was stirred an additional five minutes before the resin was removed by filtration and washed with methanol. The filtrate was concentrated, and recrystallized from methanol and ether. The recovered precipitate was resuspended in water and lyophilized to yield 60 mg (0.21 mmol) of the title compound as a white solid (80 % yield).

**$^1$H NMR** (400 MHz, $D_2O$) $\delta_{ppm}$ 4.47 (1H, ddd, $J$ = 10.6, 5.9, 4.2 Hz), 4.02 (1H, dd, $J$ = 9.9, 6.1 Hz), 3.98 (1H, dd, $J$ = 3.3, 1.5 Hz), 3.81 (1H, dt, $J$ = 6.1, 1.4 Hz), 3.74 (1H, dd, $J$ = 10.0, 3.4 Hz), 3.68 (2H, d, $J$ = 5.7 Hz), 3.21 (2H, m), 2.66 (1H, dd, $J$ = 15.0, 11.0 Hz), 2.56 (1H, dd, $J$ = 15.0, 4.2 Hz), 1.59 (1H, m), 1.39 (2H, q, $J$ = 7.2 Hz), 0.88 (6H, d, $J$ = 6.6 Hz); **$^{13}$C NMR** (101 MHz, $D_2O$) $\delta_{ppm}$ 173.3, 73.0, 72.3, 69.6, 68.7, 67.5, 60.7, 37.8, 37.2, 32.3, 25.0, 21.6. **ESI-MS** $m/z$ calcd for $C_{13}H_{25}NO_6$ $[M + H]^+$: 292.18; $[M + Na]^+$: 314.16. Found: 292.19, 314.16.

***N*-Hexyl-2-(α-D-galactopyranosyl)ethylamide (752)**

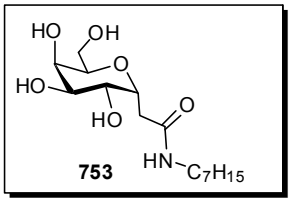


**752**

Hexyl derivative **762** (75 mg, 0.16 mmol) was dissolved in 15 mL of 0.1 M NaOMe in methanol and stirred for four hours. Dowex-50X resin was added and the solution was stirred an additional five minutes before the resin was removed by filtration and washed with water and methanol successively. The filtrate was concentrated, and further purifed by preperatory TLC (6: 1: 1: 1, ethyl acetate: water: methanol: acetonitrile), resuspended in water and lyophilized to provide 38 mg (0.12 mmol) of the title compound as a white solid (78 % yield).

**$^1$H NMR** (400 MHz, $D_2O$) $\delta_{ppm}$ 4.47 (1H, m), 4.01 (1H, dd, $J$ = 9.9, 6.1 Hz), 3.98 (1H, dd, $J$ = 3.3, 1.4 Hz), 3.80 (1H, dt, $J$ = 6.2, 1.3 Hz), 3.73 (1H, dd, $J$ = 9.9, 3.4 Hz), 3.70-3.64 (2H, m), 3.26-3.07 (2H, m), 2.65 (1H, dd, $J$ = 14.9, 11.0 Hz), 2.55 (1H, dd, $J$ = 15.0, 4.1 Hz), 1.48 (2H, q, $J$ = 7.3 Hz), 1.35-1.18 (6H, m), 0.84 (3H, t, $J$ = 6.9 Hz); **$^{13}$C NMR** (101 MHz, $D_2O$) $\delta_{ppm}$ 173.3, 73.0, 72.3, 69.6, 68.7, 67.5, 60.6, 39.5, 32.3, 30.7, 28.3, 25.7, 21.9, 13.3. **ESI-MS** $m/z$ calcd for $C_{14}H_{27}N_1O_6$ $[M + H]^+$: 306.19; $[M + Na]^+$: 328.17; $[M + K]^+$: 344.15. Found: 306.20, 328.18, 344.15.

***N*-Heptyl-2-(α-D-galactopyranosyl)ethylamide (753)**



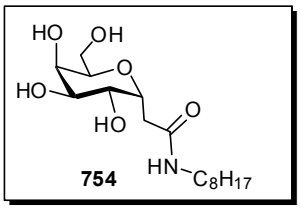
**753**

Heptyl derivative **763** (110 mg, 0.23 mmol) was dissolved in 16 mL of 0.1 M NaOMe in methanol and stirred for 12 hours. Dowex-50X resin was added and the solution was stirred an additional five minutes before the resin was removed by filtration and washed with water and methanol successively. The filtrate was concentrated, and dissolved in methanol. Diethyl ether

was added until the solution became cloudy and was left to stand for 2 hours at -20 ºC. The solid was collected by filtration, resuspended in water and lyophilized to provide 57 mg (0.18 mmol) of the title compound as a white solid (78 % yield).

**$^{1}$H NMR** (300 MHz, *MeOD*) $\delta_{ppm}$ 4.40 (1H, td, *J* = 9.1, 4.0 Hz), 3.94 (1H, t, *J* = 2.9 Hz), 3.90-3.75 (3H, m), 3.68-3.59 (2H, m), 3.16 (2H, t, *J* = 7.1 Hz), 2.60 (1H, dd, *J* = 15.3, 10.4 Hz), 2.46 (1H, dd, *J* = 15.1, 3.9 Hz), 1.49 (2H, p, *J* = 6.5 Hz), 1.37-1.23 (8H, m), 0.89 (3H, t, *J* = 6.6 Hz); **$^{13}$C NMR** (126 MHz, *MeOD*) $\delta_{ppm}$ 174.2, 75.0, 72.4, 72.1,70.2, 69.6, 61.7, 40.6, 35.5, 33.0, 30.4, 30.2, 28.1, 23.7, 14.5. **ESI-MS** *m/z* calcd for $C_{15}H_{29}N_1O_6$ $[M + Na]^+$: 342.19. Found: 342.20.

**_N_-Octyl-2-(α-D-galactopyranosyl)ethylamide (754)**

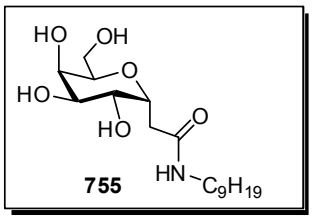


**754**

Octyl derivative **764** (82 mg, 0.16 mmol) was dissolved in 15 mL of 0.1 M NaOMe in methanol and stirred for four hours. Dowex-50X resin was added and the solution was stirred an additional five minutes before the resin was removed by filtration and washed with water and methanol successively. The filtrate was concentrated, and further purifed by preperatory TLC (6: 1: 1: 1, ethyl acetate: water: methanol: acetonitrile), resuspended in water and lyophilized to provide 36 mg (0.10 mmol) of the title compound as a white solid (70 % yield).

$^{1}$H **NMR** (400 MHz, *MeOD*) $\delta_{ppm}$ 4.34-4.20 (m, 1H), 3.86-3.76 (m, 1H), 3.80-3.76 (m, 1H), 3.62 (t, *J* = 6.0, 6.0 Hz, 1H), 3.58-3.43 (m, 1H), 3.04-2.92 (m, 1H), 2.46 (dd, *J* = 15.0, 10.9 Hz, 1H), 2.34 (dd, *J* = 14.9, 3.8 Hz, 1H), 1.39-1.24 (m, 1H), 1.20-1.00 (m, 1H), 0.68 (t, *J* = 6.6, 6.6 Hz, 1H); **$^{13}$C NMR** (101 MHz, *MeOD*) $\delta_{ppm}$ 174.2, 73.8, 73.6, 71.0, 69.7, 68.9, 61.6, 40.6, 33.4, 32.3, 29.65, 29.63, 29.58, 27.3, 23.2, 14.4. **ESI-MS** *m/z* calcd for $C_{13}H_{25}N_1O_6$ $[M + H]^+$: 334.22; $[M + Na]^+$: 356.41; $[M + K]^+$: 372.52. Found: 334.21, 356.19, 372.18.

**_N_-Nonyl-2-(α-D-galactopyranosyl)ethylamide (755)**



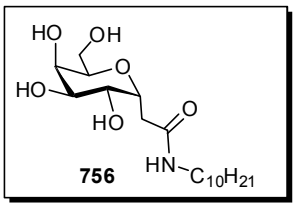
**755**

Nonyl derivative **765** (50 mg, 0.10 mmol) was dissolved in 10 mL of 0.1 M NaOMe in methanol and stirred for four hours. Dowex-50X resin was added and the solution was stirred an additional five minutes before the resin was removed by filtration and washed with water and methanol successively. The filtrate was concentrated, and dissolved in methanol. Diethyl ether

was added until the solution became cloudy and was left to stand for 2 hours at -20 ºC. The solid was collected by filtration, resuspended in water and lyophilized to provide 25 mg (0.072 mmol) of the title compound as a white solid (72 % yield).

**$^1$H NMR** (400 MHz, *MeOD*) $\delta_{ppm}$ 4.40 (1H, td, *J* = 9.1, 4.0 Hz), 3.94 (1H, t, *J* = 3.0 Hz), 3.90-3.75 (3H, m), 3.65 (1H, dd, *J* = 9.5, 3.7 Hz), 3.63 (1H, dd, *J* = 6.7, 3.8 Hz), 3.16 (2H, t, *J* = 7.2, 7.2 Hz), 2.60 (1H, dd, *J* = 15.2, 10.5 Hz), 2.46 (1H, dd, *J* = 15.2, 3.7 Hz), 1.49 (2H, p, *J* = 7.0 Hz), 1.37-1.24 (12H, m), 0.89 (3H, t, *J* = 6.9 Hz); **$^{13}$C NMR** (101 MHz, *MeOD*) $\delta_{ppm}$ 174.1, 74.9, 72.4, 72.1, 70.2, 69.6, 61.7, 40.6, 34.5, 33.1, 30.7, 30.5, 30.5, 30.4, 28.1, 23.8, 14.5. **ESI-MS** *m*/*z* calcd for $C_{17}H_{33}N_1O_6$ $[M + H]^+$: 348.24; $[M + Na]^+$: 370.22. Found: 348.26, 370.24.

### *N*-Decyl-2-(α-D-galactopyranosyl)ethylamide (756)

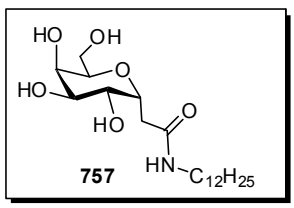


**756**

Decyl derivative **766** (20 mg, 0.037 mmol) was dissolved in 15 mL of 0.1 M NaOMe in methanol and stirred for four hours. Dowex-50X resin was added and the solution was stirred an additional five minutes before the resin was removed by filtration and washed with water and methanol successively. The filtrate was concentrated, and further purifed by preperatory TLC (8:1:1:1, ethyl acetate: water: methanol: acetonitrile), resuspended in water and lyophilized to provide 9 mg (0.025 mmol) of the title compound as a white solid (68 % yield).

**$^1$H NMR** (400 MHz, *MeOD*) $\delta_{ppm}$ 4.41 (1H, ddd, *J* = 8.9, 4.2, 4.2 Hz), 3.95 (1H, t, *J* = 3.0, Hz), 3.88 (1H, dd, *J* = 8.1, 4.9 Hz), 3.86 (1H, dd, *J* = 11.0, 7.8 Hz), 3.79 (1H, m), 3.66 (1H, dd, *J* = 10.8, 4.5 Hz), 3.63 (1H, dd, *J* = 8.1, 3.2 Hz), 3.17 (2H, t, *J* = 7.1, 7.1 Hz,), 2.60 (1H, dd, *J* = 15.2, 10.5 Hz), 2.46 (1H, dd, *J* = 15.2, 3.7 Hz), 1.50 (2H, m), 1.39-1.23 (14H, m), 0.90 (3H, t, *J* = 6.8 Hz). **$^{13}$C NMR** (101 MHz, *MeOD*) $\delta_{ppm}$ 174.1, 75.0, 72.4, 72.1, 70.2, 69.6, 61.7, 40.6, 34.5, 33.1, 30.8, 30.5, 30.4, 28.1, 23.8, 14.5. **ESI-MS** *m*/*z* calcd for $C_{13}H_{25}N_1O_6$ $[M + H]^+$: 362.25; $[M + Na]^+$: 384.24. Found: 362.26, 384.22. **Rf** = 0.26 (12:1:1:1, ethyl acetate: water :acetonitrile: methanol).

### *N*-Dodecyl-2-(α-D-galactopyranosyl)ethylamide (757)



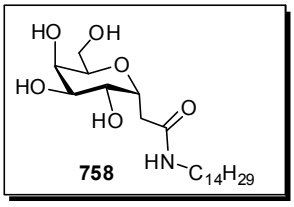
**757**

Dodecyl derivative **767** (25 mg, 0.044 mmol) was dissolved in 15 mL of 0.1 M NaOMe in methanol and stirred for four hours. Dowex-

50X resin was added and the solution was stirred an additional five minutes before the resin was removed by filtration and washed with water and methanol successively. The filtrate was concentrated, and further purifed by preperatory TLC (8:1:1:1, ethyl acetate: water: methanol: acetonitrile), resuspended in water and lyophilized to provide 14 mg (0.036 mmol) of the title compound as a white solid (81 % yield).

**$^1$H NMR** (400 MHz, *MeOD*) $\delta_{ppm}$ 4.41 (1H, dt, *J* = 8.9, 4.1, Hz), 3.95 (1H, t, *J* = 3.0 Hz), 3.88 (1H, dd, *J* = 8.1, 4.9 Hz), 3.86 (1H, dd, *J* = 11.0, 7.8 Hz), 3.79 (1H, m), 3.66 (1H, dd, *J* = 10.8, 4.5 Hz), 3.63 (1H, dd, *J* = 8.1, 3.2 Hz), 3.17 (2H, t, *J* = 7.0 Hz), 2.61 (1H, dd, *J* = 15.2, 10.5 Hz), 2.47 (1H, dd, *J* = 15.2, 3.7 Hz), 1.56-1.43 (2H, m), 1.37-1.25 (m, 18H), 0.90 (3H, t, *J* = 6.9 Hz); **$^{13}$C NMR** (101 MHz, *MeOD*) $\delta_{ppm}$ 174.1, 74.9, 72.5, 72.1, 70.2, 69.6, 61.7, 40.6, 35.5, 33.1, 30.8, 30.8, 30.8, 30.8, 30.53, 30.52, 30.4, 28.1, 23.8, 14.5. **ESI-MS** *m/z* calcd for $C_{20}H_{39}NO_6$ $[M + H]^+$: 390.29; $[M + Na]^+$: 412.27. Found: 390.30, 412.27. **Rf** = 0.3 (12:1:1:1, ethyl acetate: water: acetonitrile: methanol).

***N*-Tetradecyl-2-(α-D-galactopyranosyl)ethylamide (758)**

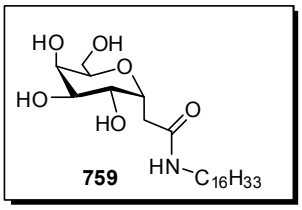


**758**

Tetradecyl derivative **768** (110 mg, 0.19 mmol) was dissolved in 15 mL of 0.1 M NaOMe in methanol to which was added 5 mL of DCM and stirred for four hours. Dowex-50X resin was added and the solution was stirred an additional five minutes before the resin was removed by filtration and washed with methanol. The filtrate was concentrated, and purified by dry vacuum chromatography (100 % ethyl acetate to 60 % ethyl acetate in methanol in 5 % steps) to yield 45 mg of the title compound a white solid following drying *in vacuo* (56 % yield).

**$^1$H NMR** (500 MHz, *CDCl$_3$/MeOD*) $\delta_{ppm}$ 4.42 (1H, td, *J* = 9.4, 4.8 Hz), 3.97 (1H, t, *J* = 3.0 Hz), 3.91 (1H, dd, *J* = 8.4, 5.1 Hz), 3.89 (1H, dd, *J* = 11.5, 7.2 Hz), 3.78 (1H, ddd, *J* = 7.1, 3.7, 3.0), 3.69 (1H, dd, *J* = 11.6, 4.1 Hz), 3.64 (1H, dd, *J* = 8.4, 3.4 Hz), 3.25-3.12 (2H, m), 2.61-2.47 (2H, m), 1.56-1.44 (2H, m), 1.36-1.21 (22H, m), 0.88 (3H, t, *J* = 6.8, 6.8 Hz); **$^{13}$C NMR** (126 MHz, *CDCl$_3$/MeOD*) $\delta_{ppm}$ 173.5, 74.3, 71.9, 71.6, 69.8, 69.2, 61.6, 40.4, 34.2, 32.6, 30.32, 30.31, 30.30, 30.28, 30.25, 30.23, 30.02, 30.00, 29.97, 27.7, 23.3, 14.4. **ESI-MS** *m/z* calcd for $C_{13}H_{25}N_1O_6$ $[M + H]^+$: 418.32; $[M + Na]^+$: 440.30; $[M + K]^+$: 456.27. Found: 418.49, 440.47, 456.46. **Rf** = 0.50 (2:8 methanol: ethyl acetate).

***N*-Hexadecyl-2-(α-D-galactopyranosyl)ethylamide (759)**

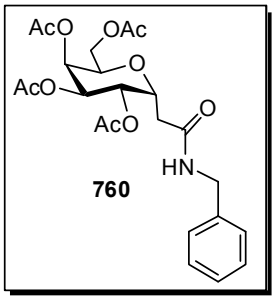


**759**

Hexadecyl derivative **769** (120 mg, 0.20 mmol) was dissolved in 15 mL of 0.1 M NaOMe in methanol to which was added 5 mL of DCM and stirred for four hours. Dowex-50X resin was added and the solution was stirred an additional five minutes before the resin was removed by filtration and washed with methanol. The filtrate was concentrated, and purified by dry vacuum chromatography (100 % ethyl acetate to 60 % ethyl acetate in methanol in 5 % steps) to yield 60 mg (0.14 mmol) of the title compound a white solid following drying *in vacuo* (71 % yield).

**$^1$H NMR** (400 MHz, *$CDCl_3$/MeOD*) $\delta_{ppm}$ 4.43 (1H, ddd, *J* = 9.4, 9.2, 4.7 Hz), 3.97 (1H, t, *J* = 2.9 Hz), 3.95-3.85 (2H, m), 3.80 (1H, ddd, *J* = 7.1, 3.7, 3.1 Hz), 3.70 (1H, dd, *J* = 11.4, 4.0 Hz), 3.64 (1H, dd, *J* = 8.5, 3.4 Hz), 3.25-3.12 (2H, m), 2.63-2.48 (2H, m), 1.50 (2H, t, *J* = 6.9), 1.35-1.21 (26H, m), 0.89 (3H, t, *J* = 6.8 Hz); **$^{13}$C NMR** (101 MHz, *$CDCl_3$/MeOD*) $\delta_{ppm}$ 173.4, 73.9, 71.9, 71.3, 69.4, 69.1, 61.4, 40.2, 33.7, 32.5, 30.28, 30.28, 30.28, 30.26, 30.24, 30.20, 30.1, 30.0, 29.8, 29.7, 27.6, 23.3, 14.4. **ESI-MS** *m*/*z* calcd for $C_{13}H_{25}N_1O_6$ $[M + H]^+$: 446.35; $[M + Na]^+$: 468.33; $[M + K]^+$: 484.30. Found: 446.53, 468.51, 484.50. **Rf** = 0.52 (2:8, methanol: ethyl acetate).

***N*-Benzyl-2-(2,3,4,6-tetra-*O*-acetyl-α-D-galactopyranosyl)ethylamide (760)**



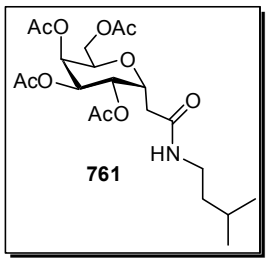
**760**

Under general conditions, 205 mg (0.54 mmol) of carboxylic acid **315**, 200 mg (0.48 mmol) of HCTU, 200 µL (1.1 mmol) of DIPEA, and 150 µL (1.63 mmol) of benzylamine were stirred in 4 mL of DMF for 64 hours. Following standard work-up, 300 mg of crude yellow oil was recovered that was purified by flash chromatography (6: 4 ethyl acetate: hexanes) to yield 215 mg of the title compound as a clear thick oil (83 % yield).

**$^1$H NMR** (300 MHz, *$D_2O$*) $\delta_{ppm}$ 7.40-7.12 (5H, m), 6.59 (1H, t, *J* = 5.6 Hz), 5.37 (1H, t, *J* = 2.7 Hz), 5.24 (1H, dd, *J* = 8.5, 4.7 Hz), 5.13 (1H, dd, *J* = 8.6, 3.2 Hz), 4.68 (1H, dt, *J* = 9.3, 4.4, Hz), 4.45-4.34 (3H, m), 4.18-4.06 (3H, m), 2.60 (1H, dd, *J* = 15.5, 9.6 Hz), 2.44 (1H, dd, *J* = 15.5, 4.2 Hz), 2.07 (3H, s), 2.01 (3H, m), 2.00 (3H, s), 1.86 (3H, s); **$^{13}$C NMR** (75 MHz,

*$D_2O$*) $\delta_{ppm}$ 170.4, 169.9, 169.7, 169.5, 169.2, 138.0, 128.65, 128.60, 127.7, 27.66, 127.4, 69.4, 68.8, 67.9, 67.7, 66.9, 61.1, 43.6, 38.5, 34.4, 23.1, 20.64, 20.61, 20.56, 20.46. **ESI-MS** *m/z* calcd for $C_{23}H_{29}NO_{10}$ $[M + H]^+$: 480.19; $[M + Na]^+$: 502.17. Found: 480.38, 502.38. **Rf** =0.32 (6:4 ethyl acetate: hexanes).

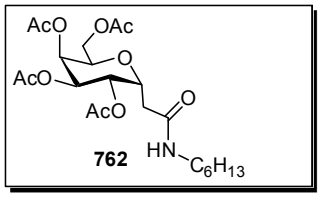
### *N*-(3-methylbutyl)-2-(2,3,4,6-tetra-*O*-acetyl-α-D-galactopyranosyl)ethylamide (761)




Under general conditions, 150 mg (0.38 mmol) of carboxylic acid **315**, 81 mg (0.5 mmol) of CDI, 87 µL (0.5 mmol) of DIPEA, and 134 µL (1.15 mmol) of 4-methylpentylamine were stirred in 3 mL of DCM for 18 hours. Following standard work-up, the recovered residue was purified by gradient flash chromatography (100% hexanes to 100 % ethyl acetate in 10% increments) to yield 140 mg (0.30 mmol) of the title compound as a clear thick oil (80 % yield).

**$^1$H NMR** (400 MHz, *$CDCl_3$*) $\delta_{ppm}$ 6.28 (1H, t, *J* = 5.3 Hz), 5.42 (1H, m), 5.29 (1H, dd, *J* = 8.7, 4.8 Hz), 5.17 (1H, dd, *J* = 8.7, 3.3 Hz), 4.69 (1H, td, *J* = 9.3, 4.5 Hz), 4.26-4.15 (3H, m), 3.27 (2H, m), 2.59 (1H, dd, *J* = 15.5, 9.6 Hz), 2.44 (1H, dd, *J* = 15.5, 4.3 Hz), 2.13 (3H, s), 2.08 (3H, s), 2.06 (3H, s), 2.05 (3H, s), 1.62 (3H, dseptd, *J* = 6.7, 6.6, 3.0 Hz), 1.40 (1H, dd, *J* = 14.7, 7.3 Hz), 0.92 (1H, d, *J* = 6.7 Hz). **ESI-MS** *m/z* calcd for $C_{21}H_{33}NO_{10}$ $[M + H]^+$: 460.22; $[M + Na]^+$: 482.20; $[M + Na]^+$: 498.17. Found: 460.21, 482.21, 498.22.

### *N*-Hexyl-2-(2,3,4,6-tetra-*O*-acetyl-α-D-galactopyranosyl)ethylamide (762)

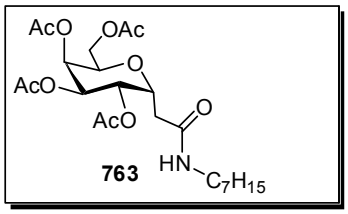



Using general conditions, 100 mg (0.26 mmol) of carboxylic acid **315**, 100 mg (0.24 mmol) of HCTU, 60 µL (0.33 mmol) of DIPEA, and 100 µL (0.77 mmol) of hexylamine were stirred in 2 mL of DCM for 16 hours. Following standard work-up, 120 mg of crude yellow oil was recovered that was purified by flash chromatography (1: 1 hexanes: ethyl acetate) to yield 80 mg of the title compound as a clear, thick oil (65% yield).

**$^1$H NMR** (400 MHz, *$CDCl_3$*) $\delta_{ppm}$ 6.28 (1H, t, *J* = 5.3, Hz), 5.42 (1H, t, *J* = 2.6 Hz), 5.28 (1H, dd, *J* = 8.7, 4.8 Hz), 5.17 (1H, dd, *J* = 8. 7, 3.2 Hz), 4.69 (1H, dt, *J* = 9.2, 4.4 Hz, 1H), 4.27-4.15 (3H, m), 3.32-3.15 (2H, m), 2.59 (1H, dd, *J* = 15.48, 9.58 Hz), 2.44 (1H, dd, *J* = 15.47, 4.25

Hz), 2.13 (3H, s), 2.08 (3H, s), 2.06 (3H, s), 2.05 (3H, s), 1.50 (2H, q, *J* = 7.0 Hz), 1.39-1.21 (6H, m), 0.88 (3H, t, *J* = 6.62 Hz); **$^{13}$C NMR** (101 MHz, *CDCl$_3$*) $\delta_{ppm}$ 170.4, 169.9, 169.7, 169.5, 169.0, 69.3, 68.9, 67.8, 67.7, 66.9, 61.2, 39.6, 34.3, 31.3, 29.4, 26.5, 22.4, 20.6, 20.5, 13.9. **ESI-MS** *m*/*z* calcd for $C_{22}H_{35}N_1O_{10}$ $[M + H]^+$: 474.23; $[M + Na]^+$: 496.21. Found: 474.28, 496.26.

**_N_-Heptyl-2-(2,3,4,6-tetra-_O_-acetyl-α-D-galactopyranosyl)ethylamide (763)**

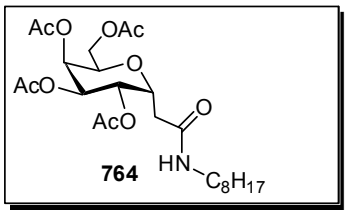


**763**

Using general conditions, 145 mg (0.37 mmol) of carboxylic acid **315**, 146 mg (0.35 mmol) of HCTU, 130 µL (0.74 mmol) of DIPEA, and 111 µL (0.74 mmol) of heptylamine were stirred in 3 mL of DMF for 48 hours. Following standard work-up, 173 mg of crude yellow oil was recovered that was purified by flash chromatography (1: 1 hexanes: ethyl acetate) to yield 150 mg of the title compound as a clear, thick oil (83% yield).

**$^1$H NMR** (400 MHz, *CDCl$_3$*) $\delta_{ppm}$ 6.35 (1H, t, *J* = 5.6 Hz), 5.42 (1H, t, *J* = 3.0 Hz), 5.28 (1H, dd, *J* = 8.6, 4.7 Hz), 5.18 (1H, dd, *J* = 8.7, 3.3 Hz), 4.69 (1H, dt, *J* = 9.1, 4.5 Hz), 4.30-4.07 (3H, m), 3.30-3.16 (2H, m), 2.60 (1H, dd, *J* = 15.4, 9.5 Hz), 2.44 (1H, dd, *J* = 15.4, 4.4 Hz), 2.13 (3H, s), 2.08 (3H, s), 2.06 (3H, s), 2.05 (3H, s), 1.50 (2H, q, *J* = 6.8 Hz), 1.36-1.18 (8H, m), 0.88 (3H, t, *J* = 6.9 Hz); **$^{13}$C NMR** (101 MHz, *CDCl$_3$*) $\delta_{ppm}$ 170.5, 169.9, 169.8, 169.5, 169.2, 69.2, 28.7, 27.8, 27.6, 66.9, 61.2 39.5, 34.2, 31.5, 29.4, 28.8, 26.7, 22.4, 20.5, 20.4, 13.8. **Rf**= 0.77 (9: 1, DCM: methanol).

***N*-Octyl-2-(2,3,4,6-tetra-*O*-acetyl-α-D-galactopyranosyl)ethylamide (764)**



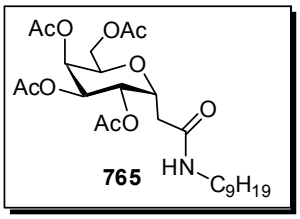
**764**

Using general conditions, 100 mg (0.26 mmol) of carboxylic acid **315**, 100 mg (0.24 mmol) of HCTU, 60 µL (0.33 mmol) of DIPEA, and 130 µL (0.78 mmol) of octylamine were stirred in 2 mL of DCM for 16 hours. Following standard work-up, 100 mg of crude brown oil was recovered that was purified by flash chromatography (1: 1 hexanes: ethyl acetate) to yield 55 mg of the title compound as a clear, thick oil (43% yield).

**$^1$H NMR** (400 MHz, *CDCl$_3$*) $\delta_{ppm}$ 6.18 (1H, t, *J* = 5.4, Hz), 5.42 (1H, t, *J* = 3.0 Hz), 5.28 (1H, dd, *J* = 8.6, 4.7 Hz), 5.16 (1H, dd, *J* = 8.6, 3.3 Hz), 4.68 (1H, dt, *J* = 9.3, 4.4 Hz), 4.27-4.15 (3H,

m), 3.30-3.16 (2H, m), 2.57 (1H, dd, *J* = 15.5, 9.6 Hz), 2.43 (1H, dd, *J* = 15.5, 4.2 Hz), 2.13 (3H, s), 2.08 (3H, s), 2.05 (6H, s), 1.50 (2H, p, *J* = 6.7 Hz), 1.33-1.23 (10H, m), 0.88 (1H, t, *J* = 6.9 Hz); **$^{13}$C NMR** (101 MHz, *CDCl$_3$*) $\delta_{ppm}$ 170.4, 169.9, 169.7, 169.5, 169.1, 69.4, 68.9, 67.9, 67.7, 66.9, 61.2, 39.6, 34.4, 31.7, 29.53, 29.50, 29.17, 29.12, 26.9, 22.5, 20.65, 20.65, 20.65, 20.57, 14.0. **Rf** = 0.35 (2: 8, hexanes: ethyl acetate).

### *N*-Nonyl-2-(2,3,4,6-tetra-*O*-acetyl-α-D-galactopyranosyl)ethylamide (765)

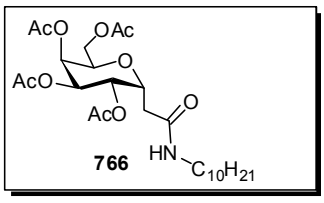


765

Using general conditions, 100 mg (0.26 mmol) of carboxylic acid **315**, 100 mg (0.24 mmol) of HCTU, 90 µL (0.50 mmol) of DIPEA, and 140 µL (0.78 mmol) of nonylamine were stirred in 1 mL of DMF for 36 hours. Following standard work-up, the crude brown oil was recovered that was purified by dry vacuum chromatography (100 % hexanes to 50 % ethyl acetate in hexanes in 5 % steps) to yield 105 mg of the title compound as a clear, thick oil (85 % yield).

**$^{1}$H NMR** (400 MHz, *CDCl$_3$*) $\delta_{ppm}$ 6.25 (1H, t, *J* = 5.4, Hz), 5.42 (1H, t, *J* = 3.0 Hz), 5.28 (1H, dd, *J* = 8.6, 4.7 Hz), 5.16 (1H, dd, *J* = 8.6, 3.3 Hz), 4.68 (1H, dt, *J* = 9.3, 4.4 Hz), 4.27-4.15 (3H, m), 3.30-3.16 (2H, m), 2.57 (1H, dd, *J* = 15.5, 9.6 Hz), 2.43 (1H, dd, *J* = 15.5, 4.2 Hz), 2.13 (3H, s), 2.08 (3H, s), 2.05 (6H, s), 1.50 (2H, p, *J* = 6.7 Hz), 1.33-1.23 (12H, m), 0.88 (1H, t, *J* = 6.9 Hz); **$^{13}$C NMR** (101 MHz, *CDCl$_3$*) $\delta_{ppm}$ 170.4, 169.9, 169.8, 169.5, 169.1, 69.4, 68.9, 67.9, 67.7, 66.9, 61.2, 39.6, 34.4, 31.7, 29.56, 29.35, 29.20, 29.15, 26.9, 22.5, 20.65, 20.65, 20.65, 20.60, 14.0. **ESI-MS** *m/z* calcd for $C_{25}H_{41}N_1O_{10}$ $[M + H]^+$: 516.28; $[M + Na]^+$: 538.26. Found: 516.31, 538.29. **Rf** = 0.39 (2: 8, hexanes: ethyl acetate).

### *N*-Decyl-2-(2,3,4,6-tetra-*O*-acetyl-α-D-galactopyranosyl)ethylamide (766)

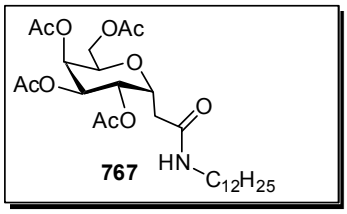


766

Using general conditions, 100 mg (0.26 mmol) of carboxylic acid **315**, 100 mg (0.24 mmol) of HCTU, 60 µL (0.5 mmol) of DIPEA, and 154 µL (0.76 mmol) of decylamine were stirred in 2 mL of DCM for 18 hours. Following standard work-up, 200 mg of crude clear oil was recovered that was purified by flash chromatography (6:4 hexanes: ethyl acetate) to yield 121 mg of the title compound as an amorphous white solid (73 % yield).

**$^1$H NMR** (400 MHz, *CDCl$_3$*) $\delta_{ppm}$ 6.24 (1H, bs), 5.42 (1H, dd, *J* = 2.9 Hz), 5.28 (1H, dd, *J* = 8.6, 4.8 Hz), 5.16 (1H, dd, *J* = 8.6, 3.3 Hz), 4.68 (1H, dt, *J* = 9.3, 4.4 Hz), 4.27-4.14 (3H, m), 3.22 (1H, dt, *J* = 7.2, 6.1 Hz), 2.57 (1H, dd, *J* = 15.5, 9.6 Hz), 2.43 (1H, dd, *J* = 15.5, 4.3 Hz), 2.12 (3H, s), 2.07 (3H, s), 2.05 (3H, s), 2.05 (3H, s), 1.49 (2H, q, *J* = 7.3 Hz), 1.36-1.19 (14H, m), 0.88 (3H, t, *J* = 6.8 Hz); **$^{13}$C NMR** (101 MHz, *CDCl$_3$*) $\delta_{ppm}$ 170.0, 169.9, 169.7, 169.4, 169.0, 69.2, 69.0, 67.8, 67.7, 67.0, 61.2, 34.2, 31.8, 29.49, 29.46, 29.43, 29.42, 29.20, 29.28, 26.8, 22.5, 20.9, 20.6, 20.6, 20.5, 14.0. **ESI-MS** *m/z* calcd for $C_{26}H_{43}NO_{10}$ $[M + H]^+$: 530.30; $[M + Na]^+$: 552.28. Found: 530.46, 552.44.

### *N*-Dodecyl-2-(2,3,4,6-tetra-*O*-acetyl-α-D-galactopyranosyl)ethylamide (767)

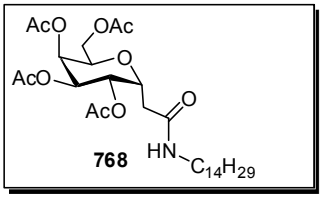


**767**

Using general conditions, 100 mg (0.26 mmol) of carboxylic acid **315**, 100 mg (0.24 mmol) of HCTU, 60 µL (0.5 mmol) of DIPEA, and 142 mg (0.77 mmol) of dodecylamine were stirred in 2 mL of DCM for 16 hours. Following standard work-up, 100 mg of crude brown oil was recovered that was purified by flash chromatography (1: 1 hexanes: ethyl acetate) to yield 80 mg of the title compound as a white amorphous solid (55% yield).

**$^1$H NMR** (400 MHz, *CDCl$_3$*) $\delta_{ppm}$ 6.15 (1H, s, *J* = 5.4 Hz), 5.39 (1H, t, *J* = 2.8 Hz), 5.25 (1H, dd, *J* = 8.6, 4.7 Hz), 5.13 (1H, dd, *J* = 8.6, 3.3 Hz), 4.65 (1H, dt, *J* = 9.3, 4.6 Hz), 4.23-4.11 (3H, m), 3.25-3.14 (2H, m), 2.54 (1H, dd, *J* = 15.5, 9.6 Hz), 2.40 (1H, dd, *J* = 15.5, 4.2 Hz), 2.10 (3H, s), 2.05 (3H, s), 2.03 (3H, s), 2.02 (3H, s), 1.45 (2H, p, *J* = 6.7 Hz), 1.33-1.17 (18H, m), 0.85 (3H, t, *J* = 6.8 Hz); **$^{13}$C NMR** (101 MHz, *CDCl$_3$*) $\delta_{ppm}$ 170.4, 169.9, 169.7, 169.5, 169.0, 69.4, 68.9, 67.9, 67.7, 66.9, 61.2, 39.7, 34.4, 31.8, 29.58, 29.56, 29.54, 29.52, 29.49, 29.28, 29.25, 26.9, 22.6, 20.7, 20.6, 14.0. **Rf** = 0.26 (6: 4 hexanes:ethyl acetate).

### *N*-Tetradecyl-2-(2,3,4,6-tetra-*O*-acetyl-α-D-galactopyranosyl)ethylamide (768)

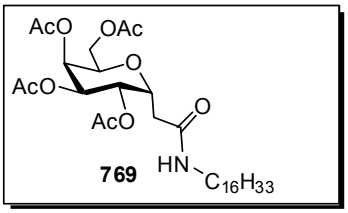


**768**

Using general conditions, 200 mg (0.51 mmol) of carboxylic acid **315**, 200 mg (0.48 mmol) of HCTU, 178 µL (1 mmol) of DIPEA, and 243 mg (1.5 mmol) of tetradecylamine (92% technical grade) were stirred in 4 mL of DCM for 48 hours. Following standard work-up,

440 mg crude white solid was recovered that was purified by flash chromatography (6: 4 hexanes: ethyl acetate) to yield 202 mg of the title compound as a white solid (68 % yield). **$^1$H NMR** (500 MHz, *CDCl$_3$*) $\delta_{ppm}$ 6.44 (1H, t, *J* = 5.6 Hz), 5.41 (1H, t, *J* = 2.9 Hz), 5.29 (1H, dd, *J* = 8.7, 4.8 Hz), 5.17 (1H, dd, *J* = 8.7, 3.3 Hz), 4.70 (1H, ddd, *J* = 9.3, 4.5 Hz), 4.27-4.13 (3H, m), 2.60 (1H, dd, *J* = 15.4, 9.7 Hz), 2.44 (1H, dd, *J* = 15.4, 4.3 Hz), 2.12 (3H, s), 2.07 (3H, s), 2.05 (3H, s), 2.04 (3H, s), 1.49 (2H, bt, *J* = 6.3 Hz), 1.28 (2H, q, *J* = 6.1 Hz), 1.27-1.23 (22 H, m), 0.88 (3H, t, *J* = 6.9, Hz); **$^{13}$C NMR** (101 MHz, *CDCl$_3$*) $\delta_{ppm}$ 170.5, 170.0, 169.9, 169.8, 169.6, 169.1, 69.5, 68.8, 68.0, 67.8, 66.9, 61.2, 29.66, 29.64, 29.62, 29.57, 29.56, 29.52, 29.32, 29.28, 26.9, 23.3, 22.7, 20.7, 14.1. **ESI-MS** *m/z* calcd for $C_{30}H_{51}NO_{10}$ $[M + H]^+$: 586.36; $[M + Na]^+$: 608.34. Found: 586.48, 608.47. **Rf** = 0.34 (6:4 hexanes: ethyl acetate).

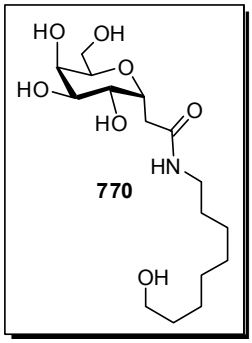
***N*-Hexadecyl-2-(2,3,4,6-tetra-*O*-acetyl-α-D-galactopyranosyl)ethylamide (769)**



**769**

Using general conditions, 200 mg (0.51 mmol) of carboxylic acid **315**, 200 mg (0.48 mmol) of HCTU, 178 µL (1.5 mmol) of DIPEA, and 281 mg (1.5 mmol) of hexadecylamine were stirred in 4 mL of DCM for 48 hours. Following standard work-up, 440 mg crude white solid was recovered that was purified by flash chromatography (6: 4 hexanes: ethyl acetate) to yield 220 mg of the title compound as a white solid (72% yield). **$^1$H NMR** (500 MHz, *CDCl$_3$*) $\delta_{ppm}$ 6.44 (1H, t, *J* = 5.4, Hz), 5.33 (1H, dd, *J* = 2.6, 2.6 Hz), 5.20 (1H, dd, *J* = 8.8, 4.9 Hz), 5.09 (1H, dd, *J* = 8.8, 3.2 Hz), 4.62 (1H, td, *J* = 9.2, 4.5, 4.5 Hz,), 4.16-4.05 (3H, m), 2.53 (1H, dd, *J* = 15.4, 9.6 Hz), 2.37 (1H, dd, *J* = 15.4, 4.3 Hz), 2.04 (3H, s), 1.98 (3H, s), 1.96 (3H, s), 1.95 (3H, s), 1.40 (2H, bt, *J* = 6.0 Hz), 1.19 (2H, q, *J* = 6.1 Hz),1.19-1.15 (24H, bs), 0.79 (3H, t, *J* = 6.9 Hz); **$^{13}$C NMR** (101 MHz, *CDCl$_3$*) $\delta_{ppm}$ 170.5, 169.9, 169.8, 169.5, 169.0, 69.5, 68.8, 68.0, 67.8, 66.9, 60.2, 39.7, 34.5, 31.9, 29.7, 29.6, 29.55, 29.53, 29.33, 29.28, 26.9, 23.3, 22.7, 20.7, 20.7, 20.7, 20.6, 14.1. **ESI-MS** *m/z* calcd for $C_{32}H_{55}NO_{10}$ $[M + H]^+$: 614.39; $[M + Na]^+$: 636.37; $[M + K]^+$: 652.35. Found: 614.46, 636.46, 652.45. **Rf** = 0.32 (6:4, hexanes: ethyl acetate).

***N*-(8-hydroxyoctyl)-2-(α-D-galactopyranosyl)ethylamide (770)**

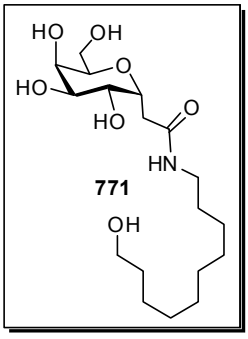


**770**

Octanol derivative **780** (100 mg, 0.19 mmol) was dissolved in 20 mL of 0.1 M NaOMe in methanol and stirred for six hours. The reaction was quenched with 60% acetic acid to pH = 5 and the reaction mixture was concentrated under reduced pressure. The filtrate was concentrated and redissolved in water and passed through an SPE cartridge. The water rinsings were discarded and the compound was eluted with methanol, concentrated, and resuspended in minumum methanol. Diethyl ether was added until the solution became cloudy and the solution was left to stand for 5 hours and the resulting precipitate was resuspended in water and lyophilized to yield 59 mg (0.17 mmol) of the title compound as a white solid (92 % yield).

**$^1$H NMR** (400 MHz, *MeOD*) $\delta_{ppm}$ 4.41 (1H, td, *J* = 10.3, 4.2 Hz), 3.95 (1H, t, *J* = 2.9 Hz), 3.91-3.82 (2H, m), 3.79 (1H, m), 3.66 (1H, dd, *J* = 10.6, 3.9 Hz), 3.64 (1H, dd, *J* = 8.2, 3.4 Hz), 3.53 (2H, t, *J* = 6.6 Hz), 3.17 (1H, t, *J* = 7.1 Hz), 2.61 (1H, dd, *J* = 15.2, 10.5 Hz), 2.47 (1H, dd, *J* = 15.1, 3.7 Hz), 1.59-1.44 (4H, m), 1.41-1.27 (8H, m); **$^{13}$C NMR** (101 MHz, *MeOD*) $\delta_{ppm}$ 174.1, 74.9, 72.6, 72.1, 70.2, 69.7, 63.0, 61.8, 40.6, 34.4, 33.7, 30.5, 30.5, 30.4, 28.0, 26.9. **ESI-MS** *m*/*z* calcd for $C_{16}H_{31}NO_7$ $[M + Na]^+$: 372.20. Found: 372.30.

***N*-(10-hydroxydecyl)-2-(α-D-galactopyranosyl)ethylamide (771)**

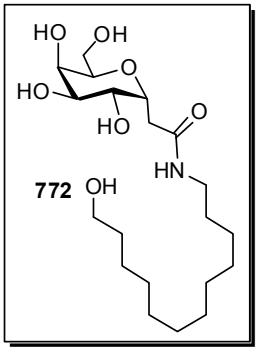



Decanol derivative **781** (100 mg, 0.19 mmol) was dissolved in 20 mL of 0.1 M NaOMe in methanol and stirred for six hours. The reaction was quenched with 60% acetic acid to pH = 5 and the reaction mixture was concentrated under reduced pressure. The filtrate was concentrated and redissolved in water and passed through an SPE cartridge. The water rinsings were discarded and the compound was eluted with methanol, concentrated, and resuspended in minumum methanol. Diethyl ether was added until the solution became cloudy and the solution was left to stand for 5 hours and the resulting precipitate was filtered and dried *in vacuo* to yield 61 mg (0.16 mmol) of the title compound as a white solid (84 % yield).

**$^1$H NMR** (400 MHz, *MeOD*) $\delta_{ppm}$ 4.40 (1H, td, *J* = 10.5, 4.2 Hz), 3.95 (1H, t, *J* = 3.0 Hz), 3.90-3.83 (2H, m), 3.79 (1H, ddd, *J* = 7.4, 4.0, 2.9 Hz), 3.69-3.61 (2H, m), 3.53 (2H, t, *J* = 6.6 Hz), 3.17 (2H, t, *J* = 7.1 Hz), 2.60 (1H, dd, *J* = 15.1, 10.5 Hz), 2.46 (1H, dd, *J* = 15.2, 3.7 Hz), 1.56-1.45 (4 H, m), 1.41-1.26 (12H, m); **$^{13}$C NMR** (101 MHz, *MeOD*) $\delta_{ppm}$ 174.1, 75.0, 72.4, 72.1,

70.2, 69.6, 63.1, 61.7, 40.6, 34.5, 33.7, 30.74, 30.67, 30.63, 30.48, 30.43, 30.42, 30.42, 28.06, 26.99. **ESI-MS** *m/z* calcd for $C_{18}H_{35}NO_7$ $[M + H]^+$: 378.25; $[M + Na]^+$: 400.23. Found: 378.38, 400.36.

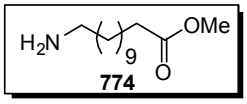
**_N_-(12-hydroxydodecyl)-2-(α-D-galactopyranosyl)ethylamide (772)**




Dodecanol derivative **782** (100 mg, 0.17 mmol) was dissolved in 20 mL of 0.1 M NaOMe in methanol and stirred for six hours. The reaction was quenched with 60% acetic acid to pH = 5 and the reaction mixture was concentrated under reduced pressure. The filtrate was concentrated and redissolved in water and passed through an SPE cartridge. The water rinsings were discarded and the compound was eluted with methanol, concentrated, and resuspended in minumum methanol. Diethyl ether was added until the solution became cloudy and the solution was left to stand for 5 hours and the resulting precipitate was filtered and dried *in vacuo* to yield 64 mg (0.158 mmol) of the title compound as a white solid (93 % yield).

**$^1$H NMR** (400 MHz, *MeOD*) $\delta_{ppm}$ 4.40 (1H, td, *J* = 8.8, 4.1 Hz), 3.95 (1H, t, *J* = 3.0 Hz), 3.90-3.82 (2H, m), 3.79 (1H, ddd, *J* = 7.4, 4.0, 2.9), 3.69-3.61 (2H, m), 3.53 (2H, t, *J* = 6.6 Hz), 3.17 (2H, t, *J* = 7.1 Hz), 2.60 (1H, dd, *J* = 15.1, 10.5 Hz), 2.46 (1H, dd, *J* = 15.2, 3.7 Hz), 1.57-1.45 (4H, m), 1.39-1.25 (16H, m); **$^{13}$C NMR** (101 MHz, *MeOD*) $\delta_{ppm}$ 170.5, 75.0, 72.4, 72.1, 70.2, 69.6, 63.1, 61.7, 40.6, 34.5, 33.8, 30.8, 30.76, 30.76, 30.73, 30.66, 30.5, 30.4, 28.1, 27.0. **ESI-MS** *m/z* calcd for $C_{20}H_{39}NO_7$ $[M + H]^+$: 406.28; $[M+ Na]^+$: 428.27. Found: 406.42, 428.40.

**Methyl-12-amino-dodecanoate (774)**

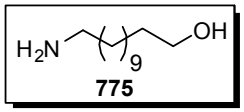



Derivative **774** was obtained according to modified protocol of Usuki.[66] In a flame-dried round-bottomed flask under an argon atmosphere, 2 g of 12-aminododecanoic acid (**773**) (9.2 mmol) was suspended in 15 mL of methanol and cooled to 0 ºC. Thionyl chloride (2.1 mL, 29.4 mmol) was added and the reaction was slowly warmed to ambient temperature over 1 hour and then warmed to 50 ºC and stirred for 2 hours when the suspension had fully dissolved, and then the reaction was allowed to cool to ambient temperature. The reaction was then quenched with 6 N NaOH, and stored at -20 ºC for 12 hours. Methanol was then removed under reduced pressure and the residue was re-suspended in ethyl

acetate and water and following extraction, the organic phase was dried with $MgSO_4$ and filtered through a glass-wool plug and concentrated under reduced pressure to provide a quantitative yield of 2.1 g of the title compound as an off-white powder. Spectral data is consistent with literature.[66]

**$^1$H NMR** (400 MHz, *$CDCl_3$*) $\delta_{ppm}$ 3.67 (3H, s), 2.72 (2H, t, *J* = 7.5 Hz), 2.30 (2H, t, *J* = 7.6 Hz), 1.62 (2H, p, *J* = 7.5 Hz), 1.49(2H, p, *J* = 7.4 Hz), 1.36-1.23 (14H, m); **$^{13}$C NMR** (101 MHz, *$CDCl_3$*) $\delta_{ppm}$ 174.3, 51.4, 41.8, 34.1, 32.6, 29.6, 29.5, 29.4, 29.2, 29.1, 26.9, 24.9. **ESI MS** calcd for $C_{13}H_{27}N_1O_2$ $[M + H]^+$: 230.21. Found: 230.26.

**12-amino-1-dodecanol (775)**

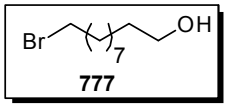


**775**

Methyl-12-amino-dodecanoate (**774**) (2.4 g, 10.5 mmol) was dissolved in 35 mL of anhydrous THF under an argon atmosphere with stirring. Simultaneously, 608 mg of lithium aluminum hydride (16 mmol) was suspended, with vigorous stirring, in 5 mL of anhydrous THF in a separate flask under an argon atmosphere. Both flasks were cooled to 0 ºC, and the ester was cannulated into the slurry, and the originating flask was washed with an additional 5 mL of THF. The reaction was allowed to warm to 40 ºC with stirring for 18 hours and then cooled to 0 ºC. The reaction was quenched through the dropwise addition of 1 mL of water, followed by 2 mL of 10% NaOH, and finally 4 mL of water. The reaction mixture was diluted with ethyl acetate, and filtered through a celite pad. The solvent was removed under reduced to yield 2.06 g the product as an off white solid (quantitative). Spectral data is consistent with literature.[66]

**$^1$H NMR** (400 MHz, *$CDCl_3$*) $\delta_{ppm}$ 3.62 (2H, t, *J* = 6.6 Hz), 2.67 (1H, t, *J* =7.4 Hz), 1.68-1.37 (6H, m), 1.37-1.22 (14H, m); **$^{13}$C NMR** (101 MHz, *$CDCl_3$*) $\delta_{ppm}$ 62.9, 42.2, 33.8, 32.8, 29.54, 29.52, 29.51, 29.54, 29.38, 29.37, 26.9, 25.7. **ESI-MS** *m*/*z* calcd for $C_{12}H_{27}N_1O_1$ $[M + H]^+$: 202.22. Found 202.23.

**10-bromo-1-decanol (777)**



**777**

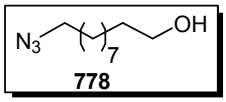
10-bromodecanoic acid (**776**) (2.00 g, 7.96 mmol) was dissolved in anhydrous THF (12 mL) and cooled to 0 ºC. $BH_3$·THF (11.2 mL, 11.2 mmol, 1.0 M in THF) was added dropwise to the reaction mixture and the ice bath was removed

and the reaction allowed to warm to room temperature with stirring for 6 hours at which time TLC indicated completion of the reaction. Saturated sodium bicarbonate (10 mL) was added dropwise and the reaction was extracted thrice with ethyl acetate. The combined organic phases were washed with brine then dried with anhydrous $MgSO_4$, filtered through a glass wool plug and concentrated under reduced pressure to provide the title alcohol (1.81 g, 7.6 mmol) in 96 % yield. Spectral data is consistent with the literature.[67]

**$^1$H NMR** (400 MHz, *$CDCl_3$*) $\delta_{ppm}$ 3.56 (2H, t, *J* = 6.7 Hz), 3.36 (2H, t, *J* = 6.9 Hz), 2.20 (1H, bs), 1.80 (2H, p, *J* = 7.4), 1.51 (2H, p, *J* = 7.5 Hz), 1.43-1.33 (2H, m), 1.33-1.20 (10H, m); **$^{13}$C NMR** (101 MHz, *$CDCl_3$*) $\delta_{ppm}$ 63.0, 34.0, 32.8, 32.7, 29.4, 29.3, 29.3, 28.7, 28.1, 25.7. **ESI-MS** *m*/*z* calcd for $C_{10}H_{21}O_1Br$ $[M + H]^+$: 237.09, 239.09. Found 237.14, 239.18.

**10-azido-1-decanol (778)**

Sodium azide (1.65 g, 25.4 mmol) and 10-bromodecanol (**777**) (2 g, 8.4 mmol) were suspended in 2 mL of DMF and 2 mL of HMPA with stirring. The reaction was allowed to stir for 18 hours and then diluted with water and diethyl ether. The phases were separated and the organic phase was washed twice with water and once with brine before being dried with anhydrous $MgSO_4$ and filtered. Solvent was removed under reduced pressure to provide 1.53 g (7.7 mmol) of 10-azidodecanol as an off-white powder in 91 % yield. Spectral data is consistent with the literature.[67]

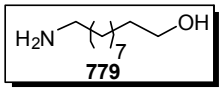


**778**

**$^1$H NMR** (400 MHz, *$CDCl_3$*) $\delta_{ppm}$ 3.59 (2H, t, *J* = 6.7 Hz), 3.22 (2H, t, *J* = 7.0 Hz), 1.80 (1H, bs), 1.61-1.49 (4H, m), 1.39-1.25 (12H, m); **$^{13}$C NMR** (101 MHz, *$CDCl_3$*) $\delta_{ppm}$ 62.8, 51.4, 32.7, 29.4, 29.30, 29.29, 29.0, 28.7, 26.6, 25.6. **ESI-MS** *m*/*z* calcd for $C_{10}H_{21}O_1N_3$ $[M + NH_4]^+$: 217.20. Found 217.10.

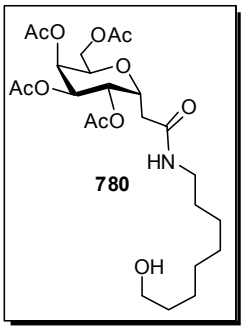
**10-amino-1-decanol (779)**

Nitrogen gas was bubbled through a solution of 673 mg of 10-azido-1-decanol (**778**) (3.37 mmol) dissolved in 20 mL of methanol. Palladium on carbon (80 mg) was added and hydrogen gas was then bubbled through the solution for twenty minutes and was then replaced by a Hydrogen-filled balloon. The reaction was allowed to stir for



**779**

6 hours when TLC showed completion of the reaction. The reaction mixture was filtered through a celite pad and methanol was removed under reduced pressure to provide 573 mg of the title amine as a yellow powder (98 % yield). Spectral data is consistent with the literature.[67]
**$^1$H NMR** (400 MHz, *$CDCl_3$/MeOD*) $\delta_{ppm}$ 3.64 (2H, t, *J* = 6.6 Hz), 2.68 (2H, t, *J* = 6.2 Hz), 1.56 (2H, t, *J* = 6.8 Hz), 1.48-1.38 (2H, m), 1.38-1.19 (12H, m); **$^{13}$C NMR** (101 MHz, *$CDCl_3$/MeOD*) $\delta_{ppm}$ 62.6, 41.8, 33.2, 32.8, 29.80, 29.77, 29.70, 29.66, 27.1, 26.0. **ESI-MS** *m/z* calcd for $C_{10}H_{23}NO$ $[M + H]^+$: 174.19. Found: 174.21.

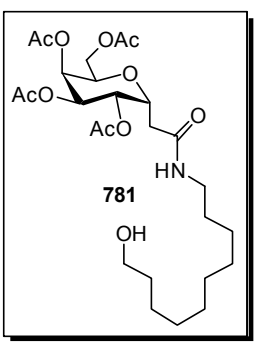



***N*-(8-hydroxyoctyl)-2-(2,3,4,6-tetra-*O*-acetyl-α-D-galactopyranosyl)ethylamide (780)**

Under general conditions, 200 mg (0.52 mmol) of carboxylic acid **315**, 200 mg (0.51 mmol) of HCTU, 270 µL (1.53 mmol) of DIPEA, and 145 mg (1.0 mmol) of 8-aminooctanol were stirred in 4 mL of DCM for 18 hours. Following standard work-up, the recovered residue was purified by dry vacuum chromatography (100% dichloromethane to 20 % methanol in 80% dichloromethane) to yield 220 mg (0.43 mmol) of the title compound as an amorphous white solid (83 % yield).
**$^1$H NMR** (400 MHz, *$CDCl_3$*) $\delta_{ppm}$ 6.09 (1H, t, *J* = 5.9, Hz), 5.42 (1H, t, *J* = 3.1, Hz), 5.26 (1H, dd, *J* = 8.5, 4.7 Hz), 5.16 (1H, dd, *J* = 8.5, 3.3 Hz), 4.66 (1H, td, *J* = 9.3, 4.3 Hz), 4.25 (1H, dd, *J* = 12.6, 8.9 Hz), 4.20-4.14 (2H, m), 3.64 (2H, t, *J* = 6.6 Hz), 3.25 (2H, m), 2.56 ( 1 H, dd, *J* = 15.6, 9.7 Hz), 2.42 ( 1 H, dd, *J* = 15.6, 4.1 Hz), 2.37-2.29 (1H, bs), 2.13 (3H, s), 2.08 (3H, s), 2.06 (3H, s), 2.05 (3H, s), 1.61-1.46 (4H, m), 1.40-1.25 (8H, m); **$^{13}$C NMR** (101 MHz, *$CDCl_3$*) $\delta_{ppm}$ 170.6, 170.0, 169.8, 169.6, 169.3, 69.5, 68.9, 68.0, 67.8, 66.9, 63.0, 61.3, 39.7, 34.4, 32.7, 29.6, 29.2, 29.2, 26.8, 25.6, 20.8. **ESI-MS** *m/z* calcd for $C_{24}H_{39}NO_{11}$ $[M + H]^+$: 518.26; $[M + Na]^+$: 540.24. Found: 518.37, 540.39. **Rf**= 0.25 (8:2, DCM: methanol).

***N*-(10-hydroxydecyl)-2-(2,3,4,6-tetra-*O*-acetyl-α-D-galactopyranosyl)ethylamide (781)**

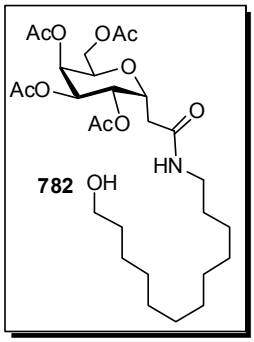
Under general conditions, 200 mg (0.52 mmol) of carboxylic acid **315**, 200 mg (0.51 mmol) of HCTU, 270 µL (1.53 mmol) of DIPEA, and 200 mg (1.1 mmol) of 10-aminodecanol were stirred in 4 mL of DCM for 18 hours. Following standard work-up, the recovered residue was purified by



dry vacuum chromatography (100% hexanes to 100 % ethyl acetate in 10 % increments and through a second gradient from 100 % ethyl acetate to 15 % methanol in 85% ethylacetate in 5 % increments) to yield 230 mg (0.42 mmol) of the title compound as an amorphous white solid (81 % yield).

**$^1$H NMR** (400 MHz, *CDCl$_3$*) $\delta_{ppm}$ 6.06 (1H, t, *J* = 5.4 Hz), 5.42 (1H, t, *J* = 3.1 Hz), 5.27 (1H, dd, *J* = 8.5, 4.7 Hz), 5.16 (1H, dd, *J* = 8.5, 3.3 Hz), 4.67 (1H, td, *J* = 9.2, 4.3 Hz), 4.28-4.14 (3H, m), 3.64 (2H, t, *J* = 6.6 Hz), 3.34-3.14 (2H, m), 2.55 (1H, dd, *J* = 15.6, 9.7 Hz), 2.42 (1H, dd, *J* = 15.6, 4.1 Hz), 2.13 (3H, s), 2.08 (3H, s), 2.06 (3H, s), 2.05 (3H, s), 1.64-1.43 (5H, m), 1.40-1.22 (12H, m); **$^{13}$C NMR** (101 MHz, *CDCl$_3$*) $\delta_{ppm}$ 170.5, 169.9, 169.8, 169.6, 169.0, 69.5, 68.8, 68.0, 67.7, 66.9, 63.0, 61.2, 39.6, 34.4, 32.7, 29.5, 29.4, 29.32, 29.28, 29.1, 26.8, 25.6, 20.71, 20.70, 20.70, 20.6. **ESI-MS** *m*/*z* calcd for $C_{26}H_{43}NO_{11}$ $[M + H]^+$: 545.28; $[M + Na]^+$: 568.27. Found: 546.40, 568.42.

***N*-(12-hydroxydodecyl)-2-(2,3,4,6-tetra-*O*-acetyl-α-D-galactopyranosyl)ethylamide (782)**

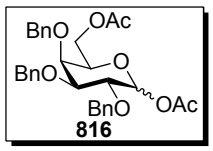



Under general conditions, 200 mg (0.52 mmol) of carboxylic acid **315**, 200 mg (0.51 mmol) of HCTU, 270 µL (1.53 mmol) of DIPEA, and 200 mg (1.0 mmol) of 12-aminododecanol were stirred in 4 mL of DCM for 18 hours. Following standard work-up, the recovered residue was purified by dry vacuum chromatography (100% hexanes to 100 % ethyl acetate in 10 % increments and through a second gradient from 100 % ethyl acetate to 15 % methanol in 85% ethyl acetate in 5 % increments) to yield 210 mg (0.37 mmol) of the title compound as an amorphous white solid (72 % yield).

**$^1$H NMR** (400 MHz, *CDCl$_3$*) $\delta_{ppm}$ 6.45 (1H, t, *J* = 5.6 Hz), 5.41 (1H, t, *J* = 3.0 Hz), 5.28 (1H, dd, *J* = 8.7, 4.8 Hz), 5.17 (1H, dd, *J* = 8.8, 3.3 Hz), 4.69 (1H, td, *J* = 9.6, 4.6, Hz), 4.30-4.11 (3 H, m), 3.62 (2 H, t, *J* = 6.7 Hz), 3.29-3.15 (2H, m), 2.60 (1H, dd, *J* = 15.3, 9.5 Hz), 2.44 (1H, dd, *J* = 15.4, 4.4 Hz), 2.35 (1H, bs) 2.13 (3H, s), 2.07 (3H, s), 2.06 (3H, s), 2.05 (3H, s), 1.60-1.43 (4H, m), 1.38-1.23 (16H, m); **$^{13}$C NMR** (101 MHz, *CDCl$_3$*) $\delta_{ppm}$ 170.0, 169.6, 169.4, 169.1, 169.0, 69.2, 68.4, 67.5, 67.2, 67.0, 62.0, 61.3 39.1, 33.6, 32.3, 29.1, 29.04, 29.04, 29.04, 29.0, 28.8, 28.6, 26.5, 25.4, 20.19, 20.19, 20.19, 20.12. **ESI-MS** *m*/*z* calcd for $C_{28}H_{47}NO_{11}$ $[M + H]^+$: 574.32; $[M + Na]^+$: 596.30. Found: 574.46, 596.48.

## Experimental Protocols for Chapter 8

**1,6-di-O-Acetyl-2,3,4-tri-O-benzyl-α-D-galactopyranose** and **1,6-di-O-Acetyl-2,3,4-tri-O-benzyl-β-D-galactopyranose (816)**



816

Prepared according to the protocol of Madaj and co-workers.[72] Tetrabenzyl galactose derivative **819** (8.2 g, 14.8 mmol) was dissolved in a mixture of acetic acid (39 mL), acetic anhydride (39 mL) and cooled to 0 ºC. Sulphuric acid (1.5 mL) was then added dropwise, and the reaction was stirred for 1 hour at room temperature and diluted with water (100 mL). The reaction mixture was extracted twice with ethyl acetate and the combined organics were washed with 1 M sodium bicarbonate and brine successively. The organic phase was dried and concentrated in the usual fashion and was purified using flash chromatography (7: 3 hexanes: ethyl acetate) to provide 5.15 g of the title compound as a thick, clear oil in 65 % yield as a mixture of anomers (4:1 β:α). Spectral data is consistent with the literature.[72]

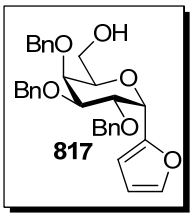
Characterization for the β-isomer

**$^1$H NMR** (400 MHz, *CDCl$_3$*) $\delta_{ppm}$ 7.46-7.23 (20H, m), 6.41 (1H, d, *J* = 3.7 Hz), 5.00 (1H, d, *J* = 11.4 Hz), 4.89 (1H, d, *J* = 11.7 Hz), 4.78 (1H, d, *J* = 11.9 Hz), 4.76 (1H, d, *J* = 10.1 Hz), 4.72-4.70 (1H, m), 4.64 (1H, d, *J* = 11.4 Hz), 4.20 (1H, dd, *J* = 9.9, 3.7 Hz), 4.13 (1H, d, *J* = 6.7 Hz), 4.09 (1H, d, *J* = 5.8 Hz), 4.03 (1H, dd, *J* = 6.8, 0.9 Hz), 3.94 (1H, dd, *J* = 2.6, 0.9 Hz), 3.91 (1H, dd, *J* = 9.9, 2.7 Hz), 2.13 (3H, s), 1.99 (3H, s); **$^{13}$C NMR** (101 MHz, *CDCl$_3$*) $\delta_{ppm}$ 170.5, 169.4, 138.4, 138.0, 137.9, 128.4, 128.3, 128.0, 127.82, 127.76, 127.6, 127.4, 90.6, 78.6, 75.3, 74.7, 74.2, 73.40, 73.38, 70.8, 63.0, 21.1, 20.8. **ESI-MS** *m/z* calcd for $C_{32}H_{36}O_7$ $[M + NH_4]^+$: 552.3; $[M + Na]^+$: 557.21. Found 552.5, 557.5. **Rf** = 0.31 (7:3 hexanes: ethyl acetate).

Characterization data for the α-isomer (partial)

**$^1$H NMR** (400 MHz, *CDCl$_3$*) $\delta_{ppm}$ 5.59 (1H, d, *J* = 8.0 Hz), 4.99 (1H, d, *J* = 11.6 Hz), 4.85 (1H, d, *J* = 11.4 Hz), 4.77 (1H, d, *J* = 11.9 Hz), 4.76 (1H, d, *J* = 10.1 Hz), 3.84 (1H, dd, *J* = 2.7, 0.8 Hz), 3.69 (1H, ddd, *J* = 6.7, 5.8, 0.9 Hz), 3.64 (1H, dd, *J* = 9.7, 2.8 Hz), 2.05 (3H, s), 1.97 (3H, s). **ESI-MS** *m/z* calcd for $C_{32}H_{36}O_7$ $[M + NH_4]^+$: 552.3; $[M + Na]^+$: 557.21. Found 552.5, 557.5. **Rf** = 0.31 (7:3 hexanes: ethyl acetate).

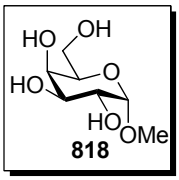
**2-(2,3,4-Tri-*O*-benzyl-α-D-galactopyranosyl)furan (817)**



**817**

Acetate **820** (450 mg, 0.83 mmol) was dissolved in 0.1 M sodium methoxide in methanol (20 mL) and stirred at ambient temperature under a nitrogen atmosphere for 2 hours. The reaction was quenched with Amberlite 120 ion-exchange resin, and the filtrate was concentrated under reduced pressure to provide 415 mg of the title compound as a white solid in quantitative yield. **$^1$H NMR** (400 MHz, *$CDCl_3$*) $\delta_{ppm}$ 7.41-7.18 (20H, m), 6.45 (1H, ddd, *J* = 3.2, 0.7, 0.7 Hz), 6.34 (1H, dd, *J* = 3.3, 1.8 Hz), 5.20 (1H, d, *J* = 5.2 Hz), 4.87 (1H, d, *J* = 11.7 Hz), 4.81 (1H, d, *J* = 11.9 Hz), 4.76 (1H, d, *J* = 11.9 Hz), 4.64 (1H, d, *J* = 11.7 Hz), 4.58 (2H, s), 4.24 (1H, dd, *J* = 8.5, 5.2 Hz), 4.07 (1H, dd, *J* = 8.6, 3.0 Hz), 3.97 (1H, dd, *J* = 2.8, 2.8 Hz), 3.85 (1H, dd, *J* = 11.4, 7.1 Hz), 3.73 (1H, ddd, *J* = 7.1, 4.6, 2.6 Hz), 3.55 (1H, dd, *J* = 11.4, 4.7 Hz); **$^{13}$C NMR** (101 MHz, *$CDCl_3$*) $\delta_{ppm}$ 151.2, 142.4, 138.5, 138.22, 138.19, 128.53, 128.48, 128.45, 128.35, 128.0, 127.9, 127.8, 127.7, 110.3, 110.2, 77.9, 76.3, 74.27, 74.25, 73.8, 73.4, 73.2, 69.3, 61.7. **ESI-MS** *m/z* calcd for $C_{31}H_{32}O_6$ $[M + Na]^+$: 523.21; $[M + K]^+$: 539.18. Found 523.5, 539.5. **Rf** = 0.51 (7:3 hexanes: ethyl acetate).

**α-D-methylgalactopyranose (818)**

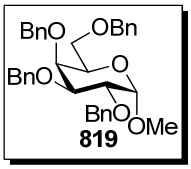


**818**

Galactose (35.0 g, 194 mmol) was dissolved in anhydrous methanol (350 mL) along with 35 g of Amberlite 120 ion-exchange resin. The flask was equipped with a water-cooled condenser and flushed with argon. The methanolic solution was heated to reflux, with stirring, for 48 hours. Following cooling, the reaction was filtered through a celite pad and purified through a silica plug (20 % methanol in DCM) to remove unreacted galactose. Solvent was removed in vacuo, and the residue was crystallized from 2-propanol according to the protocol of Moradei and co-workers.[73] The resulting crystals were washed with methanol (0 ºC) and dried *in vacuo* to provide 22.6 g of the product as a white solid in 60 % yield. Spectral data is consistent with the literature.[74]
**$^1$H NMR** (300 MHz, *$D_2O$*) $\delta_{ppm}$ 4.83 (1H, d, *J* = 2.4 Hz), 3.95 (1H, m), 3.89 (1H, dd, *J* = 6.2, 6.2 Hz), 3.81 (1H, d, *J* = 1.6 Hz), 3.80 (1H, d, *J* = 2.8 Hz), 3.74 (1H, d, *J* = 6.5 Hz), 3.73 (1H, d, *J* = 5.8 Hz), 3.40 (3H, s); **$^{13}$C NMR** (101 MHz, *$D_2O$*) $\delta_{ppm}$ 108.1, 82.9, 80.7, 76.6, 70.9, 62.7, 54.9.

**ESI-MS** *m/z* calcd for $C_7H_{14}O_6$ $[M + Na]^+$: 217.07; $[2M + Na]^+$: 411.15. Found 217.08, 411.22. **Rf** = 0.12 (15 % methanol in DCM)

**2,3,4,6-Tetra-*O*-benzyl-α-D-methylgalactopyranose (819)**

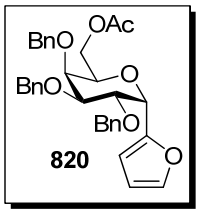


**819**

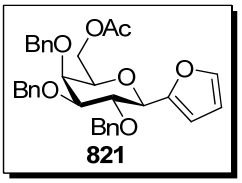
Methyl galactose **818** (6.22 g, 32 mmol) and tetrabutylammonium iodide (25 mg, 0.068 mmol) was dissolved in anhydrous DMF (60 mL), cooled to 0 ºC and cannulated into a suspension of sodium hydride (95 %, 5.38 g, 224 mmol) in anhydrous DMF (60 mL) at 0 ºC. The flask containing the reagent was washed with an additional 20 mL, and the reaction was allowed to stir at 0 ºC for 1 hour. Benzyl bromide (26.5 mL, 38.1 g, 224 mmol) was added dropwise and reaction was stirred for an additional 12 hours. The reaction was diluted with ethyl acetate and water and the two phases were partitioned. The aqueous phase was extracted thrice with ethyl acetate and the combined organic phases were washed with brine before being dried and concentrated in the usual fashion to provide the crude product hat was immeidatly purified by flash chromatography (9:1 hexanes: ethyl acetate) to provide 14.9 g of tetrabenzyl **819** as a thick, clear oil in 84 % yield. Spectral data is consistent with the literature.[75]

**$^1$H NMR** (400 MHz, *CDCl$_3$*) $\delta_{ppm}$ 7.42-7.22 (20H, m), 4.94 (1H, d, *J* = 11.5 Hz), 4.85 (1H, d, *J* = 11.8 Hz), 4.83 (1H, d, *J* = 12.1 Hz), 4.73 (1H, d, *J* = 11.8 Hz), 4.69 (1H, d, *J* = 8.5 Hz), 4.68 (1H, d, *J* = 7.1 Hz), 4.57 (1H, d, *J* = 11.5 Hz), 4.48 (1H, d, *J* = 11.8 Hz), 4.39 (1H, d, *J* = 11.8 Hz), 4.03 (1H, ddd, *J* = 11.0, 3.6, 1.2 Hz), 3.95-3.87 (3H, m), 3.55-3.50 (2H, m), 3.37 (3H, s); **$^{13}$C NMR** (101 MHz, *CDCl$_3$*) $\delta_{ppm}$ 138.8, 138.6, 138.5, 138.0, 128.35, 128.35, 128.30, 128.22, 128.18, 128.07, 127.73, 127.6, 127.65, 127.53, 127.26, 98.8, 79.1, 76.4, 75.2, 74.7, 73.55, 73.46, 73.3, 69.2, 69.1, 55.3. **ESI-MS** *m/z* calcd for $C_{35}H_{38}O_6$ $[M + NH_4]^+$: 572.30; $[M + Na]^+$: 577.26. Found 572.35, 577.31. **Rf** = 0.26 (9:1, hexanes: ethyl acetate)

**2-(6-*O*-Acetyl-2,3,4-tri-*O*-benzyl-α-D-galactopyranosyl)furan (820)** and **2-(6-*O*-Acetyl-2,3,4-tri-*O*-benzyl-β-D-galactopyranosyl)furan (821)**



**820**



**821**

Diacetate **816** (2.2 g, 4.11 mmol) was dissolved in anhydrous nitromethane (35 mL) over freshly activated powdered 4 Å molecular sieves

and stirred for 1 hour. The flask was cooled to -50 ºC[a] and freshly distilled furan (1.5 mL, 1.4 g, 20.6 mmol) was added and the mixture was stirred for an additional 30 minutes at -50 ºC before the reaction was activated through the addition of TMS-OTf (1.75 mL, 2.0 g, 9.04 mmol). The reaction was maintained at -50 ºC for 1 hour before being warmed to -30 ºC for 3 hours. Triethylamine (2 mL) was added and the reaction was allowed to warm to ambient temperature. After being diluted with ethyl acetate, the reaction was filtered through a celite pad, and the filtrate was washed successively with 10 % HCl, saturated sodium bicarbonate, and brine. The organic phase was dried and concentrated in the usual fashion to provide 2.3 g of a crude brown oil that was purified through flash chromatography (10 % to 30 % ethyl acetate in hexanes) to provide 1.003 g of α-anomer **820** in the first fraction as a clear thick gel, (45 % yield) and 446 mg of β-anomer **821** in the second fraction as a clear thick oil (20 % yield).

Characterization data for **820**

**$^{1}$H NMR** (400 MHz, *$CDCl_3$*) $\delta_{ppm}$ 7.39 (1H, dd, *J* = 1.8, 0.8 Hz), 7.38-7.24 (13H, m), 7.20-7.15 (2H, m), 6.42 (1H, td, *J* = 3.2, 0.7, 0.7 Hz), 6.35 (1H, dd, *J* = 3.3, 1.8 Hz), 5.16 (1H, d, *J* = 4.6 Hz), 4.81 (1H, d, *J* = 11.7 Hz), 4.75 (2H, s), 4.63 (1H, d, *J* = 11.7 Hz), 4.55-4.47 (2H, m), 4.43 (1H, dd, *J* = 11.9, 8.2 Hz), 4.18 (1H, dd, *J* = 11.9, 4.2 Hz), 4.13 (1H, dd, *J* = 7.2, 4.7 Hz), 4.03-3.93 (3H, m), 1.97 (3H, s). **ESI-MS** *m/z* calcd for $C_{33}H_{34}O_7$ $[M + Na]^+$: 565.19; $[M + K]^+$: 581.16. Found 565.2, 581.2. **Rf** = 0.74 (6:4, hexanes: ethyl acetate).

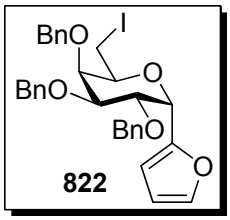
Characterization data for **821**

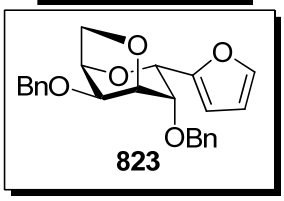
**$^{1}$H NMR** (400 MHz, *$CDCl_3$*) $\delta_{ppm}$ 7.45 (1H, dd, *J* = 1.8, 0.7 Hz), 7.42-7.28 (10H, m), 7.24-7.21 (3H, m), 7.05-7.01 (2H, m), 6.46 (1H, dd, *J* = 3.3, 0.8 Hz), 6.40 (1H, dd, *J* = 3.3, 1.8 Hz), 5.04 (1H, d, *J* = 11.8 Hz), 4.83 (1H, d, *J* = 11.9 Hz), 4.79 (1H, d, *J* = 11.8 Hz), 4.73 (1H, d, *J* = 11.8 Hz), 4.60 (1H, d, *J* = 10.3 Hz), 4.34-4.26 (2H, m), 4.18 (1H, dd, *J* = 11.3, 6.7 Hz), 4.12 (1H, d, *J* = 10.4 Hz), 4.10 (1H, dd, *J* = 11.4, 5.6 Hz), 3.90 (1H, dd, *J* = 2.7, 0.9 Hz), 3.69-3.63 (2H, m), 1.96 (3H, s); **$^{13}$C NMR** (101 MHz, *$CDCl_3$*) $\delta_{ppm}$ 170.6, 151.2, 142.6, 138.4, 138.3, 138.0, 128.5, 128.4, 128.30, 128.25, 128.21,127.71, 127.66, 127.52, 110.5, 110.0, 84.2, 77.7, 76.4, 75.3, 75.1,

[a] This temperature was obtained using a mixture of ethylene glycol and ethanol: from reference 76. Jensen, C. M.; Lee, D. W., *J. Chem. Ed.* **2000,** *77* (5), 629-630.

74.2, 73.5, 73.1, 63.7, 20.9. **ESI-MS** *m/z* calcd for $C_{33}H_{34}O_7$ $[M + NH_4]^+$: 560.26. Found 560.34. **Rf** = 0.58 (6:4, hexanes: ethyl acetate).

**2-(2,3,4-Tri-*O*-benzyl-6-iodo-α-D-galactopyranosyl)furan (822)** and **2,4-Di-*O*-benzyl-3,6-anhydro-α-D-galactopyranose (823)**




Alcohol **817** (97 mg, 0.19 mmol) was dissolved in anhydrous toluene under argon. To this solution were added imidazole (40 mg, 0.58 mmol), triphenylphosphine (74 mg, 0.28 mmol) and iodine (54 mg, 0.21 mmol) and the solution was heated to 70 ºC for 1 hour. The reaction was cooled to ambient temperature and quenched with sodium thiosulfate, diluted with ethyl acetate, and washed with brine. The organic phase was dried and concentrated in the usual fashion, and the residue purified by flash chromatography (9: 1 hexanes: ethyl acetate) to provide 6 mg of iodide **822** as a white solid in 5 % yield. In addition, 58 mg of anhydrosugar **823** was also recovered (78 % yield).

Characterization data for **822**

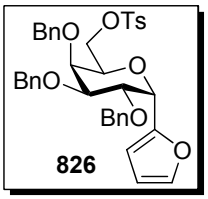
$^1$H **NMR** (300 MHz, *CDCl$_3$*) $\delta_{ppm}$ 7.42 (1H, dd, *J* = 1.7, 0.7 Hz), 7.38-7.24 (13H, m), 7.22-7.16 (2H, m), 6.48-6.44 (1H, dd, *J* = 3.3, 0.6 Hz), 6.36 (1H, dd, *J* = 3.2, 1.8 Hz), 5.08 (1H, d, *J* = 5.0 Hz), 4.93 (1H, d, *J* = 11.3 Hz), 4.81 (1H, d, *J* = 11.9 Hz), 4.76 (1H, d, *J* = 11.9 Hz), 4.64 (1H, d, *J* = 11.3 Hz), 4.55 (2H, bs), 4.20 (1H, dd, *J* = 7.9, 4.5 Hz), 4.17 (1H, d, *J* = 2.8 Hz), 4.07 (1H, dd, *J* = 8.3, 2.9 Hz), 3.87 (1H, ddd, *J* = 7.1, 7.0, 2.2 Hz), 3.41 (1H, dd, *J* = 10.1, 7.4 Hz), 3.32 (1H, dd, *J* = 10.2, 7.0 Hz); **$^{13}$C NMR** (101 MHz, *CDCl$_3$*) $\delta_{ppm}$ 151.1, 142.3, 138.5, 138.3, 138.2, 128.5, 128.3, 128.2, 127.8, 127.7, 127.6, 78.2, 75.9, 74.92, 74.87, 74.3, 73.4, 73.2, 69.0, 3.6. **ESI-MS** *m/z* calcd for $C_{31}H_{31}O_5I$ $[M + Na]^+$: 633.11; $[M + NH_4]^+$: 628.15. Found 633.3, 628.4. **Rf** = 0.62 (2:1, hexanes: ethyl acetate).

Characterization data for **823**

**$^1$H NMR** (300 MHz, *CDCl$_3$*) $\delta_{ppm}$ 7.41 (1H, dd, *J* = 1.4, 1.1 Hz), 7.36-7.25 (8H, m), 7.14-7.09 (2H, m), 6.39-6.36 (2H, m), 4.98 (1H, d, *J* = 2.8 Hz), 4.62 (1H, d, *J* = 12.1 Hz), 4.57 (1H, d, *J* = 12.0 Hz), 4.48-4.44 (2H, m), 4.42 (1H, d, *J* = 5.5 Hz), 4.25-4.07 (4H, m), 3.82 (1H, dd, *J* = 5.5, 2.8 Hz); **$^{13}$C NMR** (101 MHz, *CDCl$_3$*) $\delta_{ppm}$ 150.8, 141.9, 137.9, 137.8, 128.5, 128.4, 127.9, 127.8, 127.7, 110.6, 108.2, 78.8, 78.21, 78.18, 77.0, 73.0, 71.2, 69.2, 69.1. **ESI-MS** *m/z* calcd for

$C_{24}H_{24}O_5$ $[M + H]^+$: 393.2; $[M + Na]^+$: 415.2. Found 393.4, 415.4. **Rf** = 0.76 (2:1, hexanes: ethyl acetate).

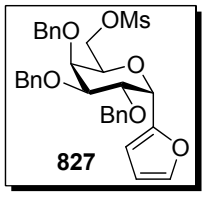
**2-(2,3,4-Tri-*O*-benzyl-6-*O*-toluenesulfonyl-α-D-galactopyranosyl)furan (826)**




Alcohol **817** (24.9 mg, 0.050 mmol) was dissolved in pyridine (200 µL) at 0 ºC. Toluenesulfonyl chloride (15 mg, 0.08 mmol) was added and the reaction stirred for 5 hours. The reaction was diluted with ethyl acetate, and washed with 10 % HCl, saturated sodium bicarbonate and brine successively. The organic fraction was dried and concentrated in the usual fashion. The resulting crude product was purified by flash chromatography (9:1 hexanes: ethyl acetate) to provide 15.2 mg of the tosylate, **826**, as a white solid in 53 % yield.

**$^1$H NMR** (400 MHz, *CDCl$_3$*) $\delta_{ppm}$ 7.68 (2H, d, *J* = 8.3 Hz), 7.37 (1H, dd, *J* = 1.7, 0.9 Hz), 7.35-7.21 (12H, m), 7.31 (2H, d, *J* = 8.2 Hz), 7.18-7.14 (2H, m), 7.12-7.08 (2H, m), 6.36 (1H, dd, *J* = 3.3, 1.8 Hz), 6.34 (1H, dd, *J* = 3.3, 0.7 Hz), 4.80 (1H, d, *J* = 3.6 Hz), 4.67 (1H, d, *J* = 11.7 Hz), 4.68 (1H, d, *J* = 11.5 Hz), 4.63 (1H, d, *J* = 11.9 Hz), 4.48 (1H, d, *J* = 11.5 Hz), 4.44-4.32 (3H, m), 4.21 (1H, dd, *J* = 11.0, 4.3 Hz), 4.09 (1H, ddd, *J* = 7.6, 4.1, 4.1 Hz), 4.01 (1H, dd, *J* = 4.0, 2.7 Hz), 3.94 (1H, dd, *J* = 6.9, 3.6 Hz), 3.90 (1H, dd, *J* = 7.0, 2.5 Hz), 2.38 (3H, s); **$^{13}$C NMR** (101 MHz, *CDCl$_3$*) $\delta_{ppm}$ 151.0, 144.6, 141.9, 138.2, 137.91, 137.87, 132.8, 129.7, 128.41, 128.38, 128.29, 127.96, 127.91, 127.84, 127.81, 127.7, 127.6, 110.3, 109.3, 76.0, 75.9, 73.4, 73.3, 73.13, 73.08, 72.2, 67.6, 67.2, 21.6. **ESI-MS** *m/z* calcd for $C_{38}H_{38}O_8S$ $[M + H]^+$: 655.24. Found 655.32. **Rf** = 0.46 (7:3, hexanes: ethyl acetate).

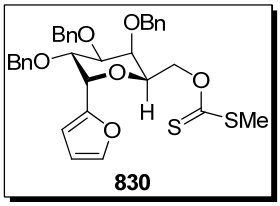
**2-(2,3,4-Tri-*O*-benzyl-6-*O*-methanesulfonyl-α-D-galactopyranosyl)furan (827)**




Alcohol **817** (28.3 mg, 0.056 mmol) was dissolved in pyridine (200 µL) at 0 ºC. Methanesulfonyl chloride (7 µL, 10 mg, 0.08 mmol) was added and the reaction stirred for 3 hours. The reaction was diluted with ethyl acetate, and washed with 10 % HCl, saturated sodium bicarbonate and brine successively. The organic fraction was dried and concentrated in the usual fashion. The resulting crude product was purified by flash chromatography (9:1, hexanes: ethyl acetate) to provide 22 mg of the mesylate as a white solid in 68 % yield.

**$^1$H NMR** (400 MHz, *$CDCl_3$*) $\delta_{ppm}$ 7.39 (1H, dd, *J* = 1.8, 0.8 Hz), 7.38-7.26 (13H, m), 7.15-7.12 (2H, m), 6.41 (1H, dd, *J* = 3.2, 0.7 Hz), 6.35 (1H, dd, *J* = 3.3, 1.8 Hz), 5.14 (1H, d, *J* = 3.8 Hz), 4.78 (1H, dd, *J* = 8.5, 12.0 Hz), 4.72 (1H, d, *J* = 11.8 Hz), 4.70 (2H, s), 4.56 (1H, d, *J* = 11.7 Hz), 4.47 (1H, d, *J* = 11.9 Hz), 4.39 (1H, d, *J* = 11.9 Hz), 4.29 (1H, dd, *J* = 12.1, 3.0 Hz), 4.15 (1H, ddd, *J* = 7.7, 3.3, 3.3 Hz), 4.04 (1H, dd, *J* = 4.1, 2.9 Hz), 4.01 (1H, dd, *J* = 6.8, 3.8 Hz), 3.95 (1H, dd, *J* = 6.9, 2.8 Hz), 2.95 (3H, s); **$^{13}$C NMR** (101 MHz, *$CDCl_3$*) $\delta_{ppm}$ 150.8, 142.2, 138.0, 137.8, 137.7, 128.49, 128.46, 128.40, 128.34, 128.1, 128.0, 127.88, 127.83, 127.81, 127.71, 127.65, 110.3, 109.5, 76.0, 75.7, 73.4, 73.3, 73.2, 73.05, 73.00, 68.1, 67.5, 37.9. **ESI-MS** *m*/*z* calcd for $C_{32}H_{34}O_8S$ $[M + H]^+$: 579.20. Found 579.32. **Rf** = 0.51 (7:3, hexanes: ethyl acetate).

**2-(2,3,4-Tri-*O*-benzyl-6-*O*-methylxanthyl-α-D-galactopyranosyl)furan (830)**

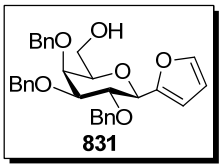


**830**

Alcohol **817** (121 mg, 0.224 mmol) was dissolved in anhydrous THF (24 mL) under argon. The solution was cooled to 0 ºC, and sodium hydride (54 mg, 2.24 mmol) was added and the reaction was stirred for 2 hours at 0 ºC. Carbon disulfide (900 µL, 1.1 g, 14.8 mmol) was added and the reaction was stirred for an additional 1.5 hours at the same temperature before being finally quenched with methyl iodide (450 µL, 1.0 g, 7.2 mmol). The ice bath was then removed and the reaction stirred an additional 12 hours. The reaction was then diluted with ether and water, and the two phases were separated. The organic phase was washed with brine, and dried and concentrated in the usual fashion. The crude product was purified by flash chromatography to yield 42 mg of the desired xanthate as a white powder in 32 % yield.

**$^1$H NMR** (300 MHz, *$C_6D_6$*) $\delta_{ppm}$ 7.20-7.15 (14H, m), 6.43 (2H, dd, *J* = 3.3, 0.7 Hz), 6.35 (1H, dd, *J* = 3.3, 1.8 Hz), 5.16 (1H, d, *J* = 4.4 Hz), 4.95 (1H, dd, *J* = 11.6, 7.7 Hz), 4.80 (1H, d, *J* = 11.7 Hz), 4.76 (2H, s), 4.71 (1H, dd, *J* = 11.8, 4.5 Hz), 4.63 (1H, d, *J* = 11.7 Hz), 4.50 (2H, s), 4.17 (1H, m), 4.13 (1H, dd, *J* = 7.1, 4.6 Hz), 4.03 (1H, dd, *J* = 11.6, 2.9 Hz), 4.05-4.02 (1H, m), 2.49 (3H, s); **$^{13}$C NMR** (101 MHz, *$CDCl_3$*) $\delta_{ppm}$ 213.1, 142.1, 128.5, 128.4, 128.3, 128.2, 127.9, 127.8, 127.74, 127.70, 127.66, 110.3, 109.8, 80.1, 77.2, 76.3, 73.9, 73.5, 73.1, 71.9, 71.2, 65.6, 19.0. **ESI-MS** *m*/*z* calcd for $C_{33}H_{34}O_6S_2$ $[M + H]^+$: 591.19. Found 591.25

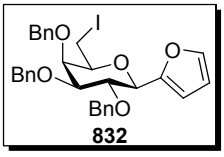
**2-(2,3,4-Tri-*O*-benzyl-β-D-galactopyranosyl)furan (831)**



**831**

Acetate **821** (638 mg, 1.18 mmol) was dissolved in 0.1 M sodium methoxide in methanol (5 mL) and stirred for 15 hours. The reaction was quenched with Amberlite 120 ion-exchange resin, and the reaction was filtered through a sintered glass funnel. The solvent was removed, and the residue recrystallized from methanol and ether to provide 526 mg of the product in 89 % yield. **$^1$H NMR** (400 MHz, *CDCl$_3$*) $\delta_{ppm}$ 7.44 (1H, dd, *J* = 1.7, 0.7 Hz), 7.41-7.27 (10H, m), 7.23-7.20 (3H, m), 7.04-7.00 (2H, m), 6.43 (1H, dd, *J* = 3.3, 0.8 Hz), 6.38 (1H, dd, *J* = 3.2, 1.8 Hz), 5.00 (1H, d, *J* = 11.9 Hz), 4.81 (1H, d, *J* = 11.9 Hz), 4.77 (1H, d, *J* = 11.8 Hz), 4.72 (1H, d, *J* = 11.9 Hz), 4.61 (1H, d, *J* = 10.3 Hz), 4.29 (2H, m), 4.11 (1H, d, *J* = 10.3 Hz), 3.88 (1H, dd, *J* = 3.0, 0.6 Hz), 3.78 (1H, ddd, *J* = 10.4, 6.2, 3.1 Hz), 3.65 (1H, ddd, *J* = 8.1, 2.8, 1.1 Hz), 3.49 (1H, m), 3.47-3.40 (1H, m); **$^{13}$C NMR** (101 MHz, *CDCl$_3$*) $\delta_{ppm}$ 151.3, 142.6, 138.3, 138.0, 128.6, 128.55, 128.48, 128.44, 128.24, 128.16, 127.9, 127.7, 127.64, 127.58, 110.5, 110.0, 84.2, 79.0, 77.8, 75.3, 75.0, 74.1, 73.5, 73.1, 62.4. **ESI-MS** *m/z* calcd for $C_{31}H_{32}O_6$ $[M + H]^+$: 501.23; $[M + NH_4]^+$: 518.25; $[M + Na]^+$: 523.21. Found 501.30, 518.33, 523.29. **Rf** = 0.29 (6:4, hexanes: ethyl acetate).

**2-(2,3,4-Tri-*O*-benzyl-6-iodo-β-D-galactopyranosyl)furan (832)**



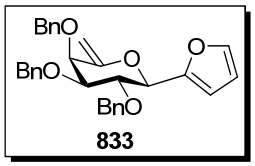
**832**

Alcohol **831** (44 mg, 0.087 mmol) was dissolved in anhydrous toluene under argon. To this solution were added imidazole (18 mg, 0.26 mmol), triphenylphosphine (34 mg, 0.13 mmol) and iodine (25 mg, 0.10 mmol) and the solution was heated to 70 ºC for 1 hour. The reaction was cooled to ambient temperature and quenched with sodium thiosulfate, diluted with ethyl acetate, and washed with brine. The organic phase was dried and concentrated in the usual fashion, and the residue purified by flash chromatography (9: 1 hexanes: ethyl acetate) to provide 37 mg of iodide **832** as a white solid in 70 % yield.

**$^1$H NMR** (400 MHz, *CDCl$_3$*) $\delta_{ppm}$ 7.47-7.28 (11H, m), 7.24-7.21 (3H, m), 7.05-7.01 (2H, m), 6.44 (1H, dd, *J* = 3.3, 0.8 Hz), 6.39 (1H, dd, *J* = 3.2, 1.8 Hz), 5.13 (1H, d, *J* = 11.4 Hz), 4.82 (2H, s), 4.75 (1H, d, *J* = 11.4 Hz), 4.61 (1H, d, *J* = 10.4 Hz), 4.31 (1H, d, *J* = 7.5 Hz), 4.28 (1H, d, *J* = 5.0 Hz), 4.26 (1H, dd, *J* = 2.8, 0.9 Hz), 4.14 (1H, d, *J* = 10.4 Hz), 3.69-3.64 (2H, m), 3.33 (1H, dd, *J* = 9.6, 8.8 Hz), 3.24 (1H, dd, *J* = 9.7, 5.3 Hz); **$^{13}$C NMR** (101 MHz, *CDCl$_3$*) $\delta_{ppm}$

151.1, 142.7, 138.5, 138.3, 138.0, 128.5, 128.38, 128.5, 128.2, 128.20, 127.75, 127.75, 127.69, 127.55, 110.5, 110.1, 84.5, 79.4, 75.15, 75.05, 75.03, 74.1, 73.1, 2.8. **ESI-MS** *m/z* calcd for $C_{31}H_{31}O_5I$ $[M + Na]^+$: 633.11; $[M + K]^+$: 649.08. Found 633.4, 649.3. **Rf** = 0.32 (7:3, hexanes: ethyl acetate).

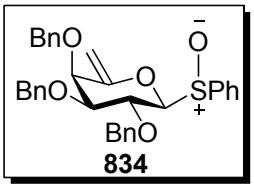
**2-(2,3,4-Tri-*O*-benzyl-β-D-arabino-hex-5-enopyranosyl)furan (833)**



**833**

Iodide **832** (60 mg, 0.10 mmol) was dissolved in anhydrous DMF (2 mL) under argon. Sodium hydride (95 %, 24 mg, 1.0 mmol) was added and the reaction was stirred for 1 hour at 70 ºC. The reaction was cooled to 0 ºC and quenched with methanol (5 mL). The solvent was removed and the residue was portioned between DCM and water. The aqueous phase was extracted three times with DCM, and the combined organic phases were washed with brine before being dried and concentrated in the usual manner. The crude product was purified by preparatory TLC to provide 41 mg of the product as a thick clear oil that solidified upon extended standing in 84 % yield. **$^1$H NMR** (400 MHz, *$CDCl_3$*) $\delta_{ppm}$ 7.50-7.18 (14H, m), 7.08-7.03 (2H, m), 6.50 (1H, d, *J* = 3.1 Hz), 6.42 (1H, dd, *J* = 3.0, 1.8 Hz), 4.86 (1H, s), 4.82 (1H, d, *J* = 12.6 Hz), 4.73 (1H, d, *J* = 10.5 Hz), 4.64 (1H, d, *J* = 11.9 Hz), 4.60 (1H, d, *J* = 11.9 Hz), 4.52-4.40 (4H, m), 4.18 (1H, d, *J* = 10.5 Hz), 4.11 (1H, d, *J* = 3.2 Hz), 3.68 (1H, dd, *J* = 8.9, 3.2 Hz); **$^{13}$C NMR** (101 MHz, *$CDCl_3$*) $\delta_{ppm}$ 154.6, 151.0, 142.9, 138.2, 138.1, 137.9, 128.3, 128.2, 128.0, 127.65, 127.63, 127.59, 110.6, 110.2, 10.6, 81.0, 76.6, 75.7, 75.1, 73.6, 71.7, 69.2. **ESI-MS** *m/z* calcd for $C_{31}H_{30}O_5$ $[M + Na]^+$: 505.20. Found 505.4. **Rf** = 0.67 (7:3, hexanes: ethyl acetate).

**2,3,4-Tri-*O*-benzyl-phenylsulfinyl-β-D-arabino-hex-5-enopyranose (834)**



**834**

Reaction was carried out using the protocol of Chen.[77] Silica (200 mg, E. Merck 60 (230-400 mesh)) was wetted with water (100 µL,100 mg) under argon, and the silica was vigorously stirred until it formed a free flowing powder. Magnesium monoperoxyphtalate (MMPP, 24 mg, 0.048 mmol) was added and blended with the silica. DCM was then added (1 mL) and the reaction was cooled to 0 ºC. At this temperature, sulphide **835** (50 mg, 0.095 mmol) dissolved in DCM (100 µL) was added and the reaction was stirred for 2 hours. The mixture was then diluted with DCM and filtered through a sintered glass frit and concentrated. The crude reaction mixture was purified

using flash chromatography (8:2 hexanes: ethyl acetate) to provide both diastereomers of the sulfoxide (configuration at sulfur not determined) as thick, clear oils in 86 % combined yield. The first fraction contained 36 mg of **834a** (70 % yield), and the second fraction contained 8 mg of **834b** (16 % yield).

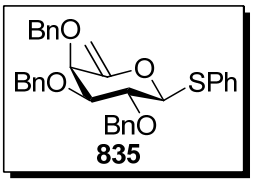
Characterization data for **834a**

**$^1$H NMR** (400 MHz, *CDCl$_3$*) $\delta_{ppm}$ 7.64-7.60 (2H, m), 7.51-7.27 (16H, m), 7.16-7.12 (2H, m), 4.83-4.80 (1H, m), 4.80 (1H, d, *J* = 10.3 Hz), 4.69 (1H, d, *J* = 11.8 Hz), 4.54 (1H, d, *J* = 12.2 Hz), 4.52 (1H, bs), 4.50 (1H, d, *J* = 11.0 Hz), 4.46 (1H, d, *J* = 12.4 Hz), 4.36 (1H, d, *J* = 5.3 Hz), 4.36 (1H, d, *J* = 11.0 Hz), 4.15 (1H, d, *J* = 2.7 Hz), 4.03 (1H, dd, *J* = 7.4, 5.3 Hz), 3.74 (1H, dd, *J* = 7.4, 2.8 Hz); **$^{13}$C NMR** (101 MHz, *CDCl$_3$*) $\delta_{ppm}$ 153.2, 140.9, 137.7, 137.6, 137.4, 131.4, 129.1, 128.43, 128.42, 128.39, 128.05, 127.99, 127.91, 12.86, 127.83, 127.79, 125.8, 99.4, 98.1, 79.1, 73.8, 73.6, 73.1, 72.2, 70.3. **ESI-MS** *m*/*z* calcd for $C_{33}H_{32}O_5S$ $[M + H]^+$: 541.2; $[M + Na]^+$: 563.2. Found 541.2, 563.4.

Characterization data for **834b**

**$^1$H NMR** (400 MHz, *CDCl$_3$*) $\delta_{ppm}$ 7.77-7.71 (2H, m), 7.54-7.51 (3H, m), 7.41-7.23 (15H, m), 4.77 (1H, d, *J* = 12.5 Hz), 4.73 (1H, bs), 4.69 (1H, d, *J* = 11.6 Hz), 4.67 (1H, d, *J* = 11.9 Hz), 4.64 (1H, d, *J* = 12.1 Hz), 4.64 (1H, bs), 4.57 (1H, d, *J* = 12.4 Hz), 4.57-4.54 (2H, m), 4.43 (1H, d, *J* = 12.3 Hz), 4.25-4.21 (1H, m), 3.88 (1H, dd, *J* = 6.2, 2.8 Hz); **$^{13}$C NMR** (101 MHz, *CDCl$_3$*) $\delta_{ppm}$ 153.6, 143.2, 137.7, 137.6, 137.4, 131.4, 128.97, 128.94, 128.6, 128.44, 128.41, 128.39, 128.33, 127.91, 127.89, 127.87, 17.72, 127.69, 127.63, 125.1, 96.3, 95.8, 75.9, 73.2, 72.6, 72.5, 72.1, 70.8. **ESI-MS** *m*/*z* calcd for $C_{33}H_{32}O_5S$ $[M + H]^+$: 541.2; $[M + Na]^+$: 563.2. Found 541.3, 563.4.

***S*-(2,3,4-Tri-*O*-benzyl-β-arabino-hex-5-enopyranosyl) thiophenol (835)**



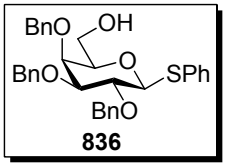
**835**

Mesylate **841** (2.5 g, 4.0 mmol) was dissolved in anhydrous DMF (90 mL). Sodium hydride (1.92 g, 80 mmol) was added portionwise to the reaction (10 mmol/10 minutes) and after addition was complete, the reaction was heated to 70 ºC. The reaction was stirred for 3 hours, cooled to ambient temperature, and quenched with water. The reaction was then partitioned between DCM and water, and the organic phase was washed successively with 10 % HCl, saturated sodium

bicarbonate and brine prior to being dried and concentrated in the usual fashion. The crude product was purified by flash chromatography (5 to 15 % ethyl acetate in hexanes) to provide 1.66 g of the enol ether **835** as a white powder in 79 % yield.

**$^1$H NMR** (400 MHz, *CDCl$_3$*) $\delta_{ppm}$ 7.59-7.54 (2H, m), 7.40-7.23 (18H, m), 4.96-4.91 (1H, d, *J* = 7.6 Hz), 4.89-4.88 (1H, d, *J* = 0.6 Hz), 4.75 (1H, bs), 4.74 (1H, d, *J* = 12.4 Hz), 4.61 (2H, bs), 4.52 (1H, bs), 4.44 (1H, d, *J* = 12.5 Hz), 4.08 (1H, d, *J* = 7.6 Hz), 4.07 (1H, d, *J* = 12.2 Hz), 3.67 (1H, dd, *J* = 8.1, 3.1 Hz); $^{13}$C NMR (101 MHz, *CDCl$_3$*) $\delta_{ppm}$ 131.7, 128.9, 128.4, 128.3, 128.1, 128.0, 127.81, 127.78, 127.69, 127.66, 127.4, 100.1, 88.4, 79.9, 76.9, 74.9, 73.3,72.0, 69.7. ESI-MS *m*/*z* calcd for $C_{33}H_{32}O_4S$ $[M + H]^+$: 525.2; $[M + Na]^+$: 547.2. Found 525.5, 547.5.

### *S*-(2,3,4-tri-*O*-benzyl-β-D-galactopyranosyl) thiophenol (836)

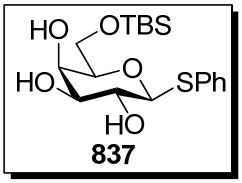


**836**

TBDMS protected **839** (200 mg, 0.153 mmol) was dissolved in acetonitrile (3 mL). Hydrofluoric acid (40 % in water, 150 µL) was added, and the reaction was stirred at ambient temperature for 2 hours. The reaction was diluted with saturated sodium bicarbonate and chloroform. The two phases were separated and the organic phase was washed with brine, then dried and concentrated in the usual fashion. The crude product was purified through flash chromatography (7: 3 hexanes: ethyl acetate) to provide 126 mg of the product as a thick clear oil. Characterization data is consistent with the literature.[78]

**$^1$H NMR** (500 MHz, *CDCl$_3$*) $\delta_{ppm}$ 7.58-7.53 (2H, m), 7.42-7.27 (15H, m), 7.25-7.21 (3H, m), 4.98 (1H, d, *J* = 11.7 Hz), 4.83 (1H, d, *J* = 10.2 Hz), 4.80-4.74 (3H, m), 4.66 (1H, d, *J* = 9.7 Hz), 4.64 (1H, d, *J* = 11.7 Hz), 3.95 (1H, dd, *J* = 9.4, 9.4 Hz), 3.86-3.85 (1H, m), 3.84 (1H, dd, *J* = 10.6, 6.4 Hz), 3.62 (1H, dd, *J* = 9.2, 2.8 Hz), 3.51 (1H, dd, *J* = 11.3, 5.1 Hz), 3.45 (1H, dd, *J* = 6.8, 5.3 Hz); **$^{13}$C NMR** (101 MHz, *CDCl$_3$*) $\delta_{ppm}$ 138.3, 138.2, 138.1, 133.9, 131.6, 128.9, 28.5, 128.4, 128.35, 128.32, 128.21, 127.86, 127.82 127.79, 127.65, 127.21, 87.7, 84.3, 78.8, 77.5, 75.7, 74.2, 73.3, 73.1, 62.3. **ESI-MS** *m*/*z* calcd for $C_{33}H_{34}O_5S$ $[M + Na]^+$: 565.2; $[M + NH_4]^+$: 560.24. Found 565.4, 560.4.

### *S*-[6-(*tert*-butyldimethylsiloxy)-β-D-galactopyranosyl] thiophenol (837)

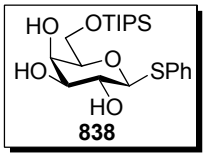


**837**

Deprotected sugar **529** (1.0 g, 3.7 mmol) was dissolved in anhydrous DMF (4 mL) under argon. Tetrabutyldimethylsilylchloride (613 mg, 4.1 mmol), a crystal of 4-(dimethylamino)pyridine (DMAP) and imidazole (554 mg, 8.2 mmol) was stirred for 12 hours. The solvent was diluted with ethyl acetate and washed with 10 % HCl, saturated sodium bicarbonate and brine. The combined organic layers were dried and concentrated in the usual fashion to provide crude product as an oil. The crude product was purified by flash chromatography (75 % ethyl acetate in hexanes) to provide 1.10 g of the title compound as a white solid in 77 % yield. Spectral data is consistent with the literature.[79]

**$^1$H NMR** (400 MHz, *MeOD*) $\delta_{ppm}$ 7.55-7.49 (2H, m), 7.31-7.17 (3H, m), 4.59 (1H, d, *J* = 9.7 Hz), 3.89 (1H, dd, *J* = 3.3, 0.8 Hz), 3.83 (1H, d, *J* = 2.1 Hz), 3.81 (1H, d, *J* = 0.9 Hz), 3.61 (1H, dd, *J* = 9.4, 9.4 Hz), 3.56 (1H, ddd, *J* = 6.3, 5.4, 0.9 Hz), 3.49 (1H, dd, *J* = 9.2, 3.3 Hz), 0.90 (9H, s), 0.08 (3H, s), 0.06 (3H, s); **$^{13}$C NMR** (101 MHz, *MeOD*) $\delta_{ppm}$ 136.3, 131.8, 129.9, 127.9, 90.2, 80.7, 76.3, 71.0, 70.4, 64.1, 26.5, 19.2, -5.0, -5.2. **ESI-MS** *m/z* calcd for $C_{18}H_{30}O_5SSi$ $[M + H]^+$: 387.17; $[M + Na]^+$: 409.15. Found 387.28, 409.24. **Rf** = 0.25 (3:1, ethyl acetate: hexanes).

***S*-[6-(triisopropylsiloxy)-β-D-galactopyranosyl] thiophenol (838)**

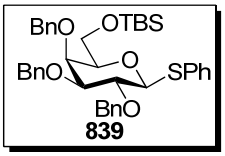


**838**

Deprotected sugar **529** (116 mg, 0.43 mmol) was dissolved in anhydrous DMF (400 µL) under argon. Triisopropylsilylchloride (100 µL, 90 mg, 0.47 mmol) and imidazole (65 mg, 0.95 mmol) was stirred for 12 hours. The solvent was diluted with ethyl acetate and washed with 10 % HCl, saturated sodium bicarbonate and brine. The combined organic layers were dried and concentrated in the usual fashion to provide crude product as an oil. The crude product was purified by flash chromatography (75 % ethyl acetate in hexanes) to provide 126 mg of the title compound as a white solid in 68 % yield.

**$^1$H NMR** (400 MHz, *MeOD*) $\delta_{ppm}$ 7.56-7.51 (2H, m), 7.30-7.19 (3H, m), 4.61 (1H, d, *J* = 9.7 Hz), 3.94-3.90 (3H, m), 3.61 (1H, dd, *J* = 10.9, 8.0 Hz), 3.61 (1H, dd, *J* = 5.7, 1.0 Hz), 3.50 (1H, dd, *J* = 9.1, 3.3 Hz), 1.15-1.05 (21H, m); **$^{13}$C NMR** (101 MHz, *MeOD*) $\delta_{ppm}$ 136.4, 131.9, 129.9, 127.9, 90.4, 81.0, 76.5, 71.1, 70.6, 64.6, 18.5, 18.2, 13.2. **ESI-MS** *m/z* calcd for $C_{21}H_{36}O_5SSi$ $[M + Na]^+$: 451.19. Found 451.3. **Rf** =0.31 (8:2, ethyl acetate: hexanes).

***S*-[2,3,4-Tri-*O*-benzyl-6-(*tert*-butyldimethylsiloxy)-β-D-galactopyranosyl] thiophenol (839)**

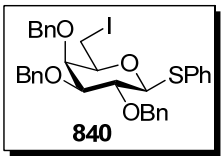


**839**

TBDMS-protected **837** (100 mg, 0.26 mmol) was dissolved in anhydrous DMF (1 mL) and was cannulated into a suspension of sodium hydride (96 mg, 1.04 mmol) in anhydrous DMF (2 mL) at 0 ºC. The mixture was stirred for 30 minutes at 0 ºC before benzyl bromide (473 µL, 680 mg, 1.04 mmol) was added dropwise, the ice bath removed, and the reaction stirred for an additional 12 hours. At this point the reaction was diluted with water and partitioned with ethyl acetate. The organic phase was washed with 10 % HCl, saturated sodium bicarbonate and brine successively. The organic phase was dried and concentrated in the usual fashion. The cude product was purified using flash chromatography (9:1, hexanes: ethyl acetate) providing 304 mg of the product as a thick oil in 93 % yield. Spectral data is consistent with the literature.[80]

**$^{1}$H NMR** (400 MHz, *$CDCl_3$*) $\delta_{ppm}$ 7.60-7.54 (2H, m), 7.41-7.27 (15H, m), 7.22-7.16 (3H, m), 4.99 (1H, d, *J* = 11.4 Hz), 4.80-4.71 (4H, m), 4.66 (1H, d, *J* = 6.2 Hz), 4.63 (1H, d, *J* = 9.6 Hz), 3.97-3.92 (2H, m), 3.77 (1H, dd, *J* = 10.0, 6.2 Hz), 3.73 (1H, dd, *J* = 10.0, 7.6 Hz), 3.61 (1H, dd, *J* = 9.2, 2.8 Hz), 3.45 (1H, m), 0.88 (9H, s), 0.03 (6H, s); **$^{13}$C NMR** (101 MHz, *$CDCl_3$*) $\delta_{ppm}$ 138.9, 138.4, 138.3, 137.8, 134.3, 131.6, 131.3, 128.9, 128.8, 128.5, 128.43, 128.40, 128.32, 128.30, 128.21, 128.1, 127.9, 127.72, 127.67, 127.62, 127.59, 127.3, 126.9, 87.7, 74.2, 78.9, 75.6, 74.5, 73.5, 72.8, 69.5, 61.5, 25.9, 18.2, -5.4, -5.5. **ESI-MS** *m/z* calcd for $C_{39}H_{48}O_5SSi$ $[M]^+$: 656.30; $[M + Na]^+$: 679.29. Found 656.5, 679.5.

***S*-[2,3,4-Tri-*O*-benzyl-6-Iodo-β-D-galactopyranosyl] thiophenol (840)**

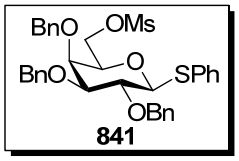


**840**

Thiophenyl derivative **839** (430 mg, 0.80 mmol) was dissolved in anhydrous toluene (7.2 mL) along with imidazole (163 mg, 2.4 mmol), iodine (244 mg, 0.96 mmol) and triphenylphosphine (315 mg, 1.2 mmol). The reaction was equipped with an air-cooled condenser and an argon-filled balloon and heated to 70 ºC for 1 hour. The reaction was then cooled to ambient temperature, quenched with sodium thiosulfate and diluted with ethyl acetate before being washed extensively with brine. The organic phase was dried and cocnetrated in the usual manner, and the crude product was purified by flash chromatography (9: 1 hexanes: ethyl acetate) to provide 62 mg of primary iodide **840** in 12 % yield.

**$^1$H NMR** (400 MHz, *CDCl$_3$*) $\delta_{ppm}$ 7.63-7.56 (2H, m), 7.42-7.19 (18H, m), 5.07 (1H, d, *J* = 11.3 Hz), 4.82 (1H, d, *J* = 10.3 Hz), 4.77 (2H, s), 4.75 (1H, d, *J* = 10.3 Hz), 4.67 (1H, d, *J* = 11.3 Hz), 4.63 (1H, d, *J* = 9.7 Hz), 4.13 (1H, dd, *J* = 2.7, 0.6 Hz), 3.91 (1H, dd, *J* = 9.5, 9.5 Hz), 3.59 (1H, dd, *J* = 9.3, 2.7 Hz), 3.57 (1H, ddd, *J* = 7.3, 6.7, 0.5 Hz), 3.31 (1H, dd, *J* = 9.9, 6.1 Hz), 3.26 (1H, dd, *J* = 9.9, 7.7 Hz); **$^{13}$C NMR** (101 MHz, *CDCl$_3$*) $\delta_{ppm}$ 138.3, 138.1, 138.0, 133.8, 131.8, 128.8, 128.44, 128.37, 128.33, 128.28, 128.26, 128.0, 127.76, 127.73, 127.6, 127.5, 127.3, 87.8, 84.2, 79.0, 76.9, 75.6, 74.8, 74.1, 73.1, 2.7. **ESI-MS** *m*/*z* calcd for $C_{33}H_{33}O_4IS$ $[M + Na]^+$: 675.10. Found 675.3. **Rf** = 0.42 (7:3, hexanes: ethyl acetate).

**_S_-[2,3,4-Tri-_O_-benzyl-6-_O_-methanesulfonyl-β-D-galactopyranosyl] thiophenol (841)**

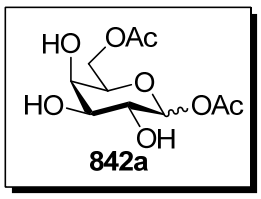


**841**

Tribenzylated **836** (284 mg, 0.52 mmol) was dissolved in pyridine (1.1 mL) and cooled to – 20 ºC. Methanesulfonyl chloride (61 µL, 0.78 mmol) was added and the reaction stirred for 4 hours. Once complete, the reaction was warmed to ambient temperature and partitioned between water and DCM. The aqueous phase was extracted three times with DCM, and the combined organics were washed successively with saturated copper (II) sulphate, 10 % HCl and brine. Following drying and concentration, the organic phase was purified through flash chromatography (8:2 to 7:3 hexanes: ethyl acetate) to provide 230 mg of the title compound as a white solid in 72 % yield.

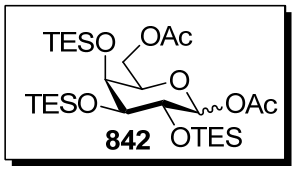
**$^1$H NMR** (400 MHz, *CDCl$_3$*) $\delta_{ppm}$ 7.55-7.50 (2H, m), 7.41-7.29 (15H, m), 7.25-7.22 (3H, m), 5.02 (1H, d, *J* = 11.5 Hz), 4.82 (1H, d, *J* = 10.3 Hz), 4.81-4.74 (3H, m), 4.69 (1H, d, *J* = 9.6 Hz), 4.62 (1H, d, *J* = 11.5 Hz), 4.40 (1H, dd, *J* = 10.9, 7.3 Hz), 4.08 (1H, dd, *J* = 10.9, 4.8 Hz), 3.94 (1H, t, *J* = 9.4, 9.4 Hz), 3.88 (1H, dd, *J* = 2.7, 0.9 Hz), 3.69 (1H, ddd, *J* = 7.4, 4.9, 0.8 Hz), 3.63 (1H, dd, *J* = 9.2, 2.7 Hz), 2.87 (3H, s); **$^{13}$C NMR** (101 MHz, *CDCl$_3$*) $\delta_{ppm}$ 138.05, 137.97, 137.90, 133.7, 131.4, 128.9, 128.5, 128.44, 128.38, 128.30, 128.16, 127.91, 127.85, 127.66, 127.3, 87.7, 83.8, 77.2, 77.1, 76.0, 75.7, 74.4, 73.3, 73.1, 68.9, 37.4. **ESI-MS** *m*/*z* calcd for $C_{34}H_{36}O_7S_2$ $[M + NH_4]^+$: 638.2; $[M + Na]^+$: 643.2. Found 638.4, 643.5.

**1,6-Di-O-acetyl-2,3,4-tri-O-triethylsilyl-D-galactopyranose (842)**



**842a**

Tribenzyl **869** (2.2 g, 4.1 mmol) was dissolved in 36 mL of methanol and 4 mL of acetic acid. Nitrogen was then bubbled through the solvent followed by the addition of charcoal-supported palladium (260 mg). Hydrogen was bubbled through the reaction for 1 hour, and the reaction was sealed under a hydrogen atmosphere. The reaction was then stirred for 48 hours at ambient temperature. The reaction mixture was then filtered through a celite pad, and the solvent was removed under reduced pressure. The crude product was purified through dry vacuum chromatography (100 % hexanes to 50 % ethyl acetate to hexanes in 5 % increments) to provide 376 mg of triol **842a** as a mixture of anomers in 35 % yield.



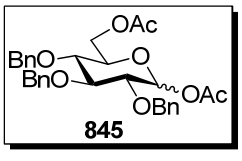
**842**

**$^1$H NMR** (400 MHz, *MeOD*) $\delta_{ppm}$ 6.09 (1H, d, *J* = 3.9 Hz), 4.22-4.13 (2H, m), 4.05 (1H, m), 3.93-3.88 (2H, m), 3.76 (1H, dd, *J* = 10.2, 3.3 Hz), 2.08 (3H, s), 2.01 (3H, s); **$^{13}$C NMR** (101 MHz, *MeOD*) $\delta_{ppm}$ (Minor anomer in parentheses) 171.3 (170.34), 170.31 (170.1), 92.4 (94.6), 70.6, 69.7, 69.1, 67.3, 63.4, (73.5, 73.2, 69.7, 68.7, 63.3), 19.6 (19.6), 19.4 (19.4). **ESI-MS** *m*/*z* calcd for $C_{10}H_{16}O_8$ $[M + Na]^+$: 287.1; $[2M + Na]^+$: 551.15. Found 287.5, 551.4. **Rf** = 0.52 (8:2, hexanes: ethyl acetate).

Triol **842a** (100 mg, 0.38 mmol) was dissolved in anhydrous DMF (4 mL) along with imidazole (817 mg, 12 mmol) and triethylsilylchloride (1.0 mL, 904 mg, 6 mmol). The reaction mixture was heated to 70 ºC and stirred for 12 hours. After the reaction was cooled, the reaction was diluted with ethyl acetate and water and the two phases were partitioned. The organic phase was washed with saturated sodium bicarbonate and brine successively before being dried and concentrated in the usual fashion. The crude product was purified by flash chromatography (5 to 10 % ethyl acetate in hexanes) to provide 136 mg of **842** as an amorphous white solid in 59 %.

**$^1$H NMR** (400 MHz, *$CDCl_3$*) $\delta_{ppm}$ 6.14 (1H, d, *J* = 3.4 Hz), 4.17 (1H, dd, *J* = 11.3, 7.2 Hz), 4.11 (1H, dd, *J* = 11.1, 5.8 Hz), 4.09 (1H, dd, *J* = 9.4, 3.4 Hz), 3.97 (1H, ddd, *J* = 6.7, 5.4, 1.0 Hz), 3.93 (1H, m), 3.89 (1H, dd, *J* = 9.4, 2.4 Hz), 2.07 (3H, s), 2.06 (3H, s), 1.03-0.91 (27H, m), 0.72-0.58 (18H, m); **$^{13}$C NMR** (101 MHz, *$CDCl_3$*) $\delta_{ppm}$ 170.7, 169.5, 92.7, 72., 71.8, 71.5, 68.4, 63.3, 21.0, 20.9, 7.1, 6.9, 6.8, 5.3, 5.1, 4.8. **ESI-MS** *m*/*z* calcd for $C_{28}H_{58}O_8Si$ $[M + Na]^+$: 629.33; $[M + K]^+$: 645.30. Found 629.19, 645.12.

**1,6-Di-*O*-acetyl-2,3,4-tri-*O*-benzyl-α-D-glucopyranose (845)**



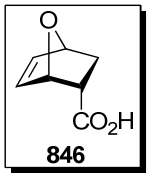
**845**

Prepared according to the protocol of Madaj and co-workers.[72] 2,3,4,6-Tetra-*O*-benzyl-α-D-methylglucopyranose[72] (5.98 g, 10.8 mmol) was dissolved in a mixture of acetic acid (35 mL), acetic anhydride (35 mL) and cooled to 0 ºC. Sulphuric acid (1.5 mL) was then added dropwise, and the reaction was stirred for 1 hour at room temperature and diluted with water (100 mL). The reaction mixture was extracted twice with ethyl acetate and the combined organics were washed with 1 M sodium bicarbonate and brine successively. The organic phase was dried and concentrated in the usual fashion and was purified using flash chromatography (8: 2 hexanes: ethyl acetate) to provide 3.25 g of the title compound as a thick, clear oil in 61 % yield as a mixture of anomers (12:1, α:β).

Characterization is provided for the α-anomer only and is consistent with the literature.[72]

**$^1$H NMR** (400 MHz, *$CDCl_3$*) $\delta_{ppm}$ 7.37-7.27 (15H, m), 6.32 (1H, d, *J* = 3.5 Hz), 5.00 (1H, d, *J* = 10.8 Hz), 4.89 (1H, d, *J* = 10.7 Hz), 4.83 (1H, d, *J* = 10.8 Hz), 4.71 (1H, d, *J* = 11.4 Hz), 4.64 (1H, d, *J* = 11.4 Hz), 4.57 (1H, d, *J* = 10.7 Hz), 4.29 (1H, dd, *J* = 12.2, 3.9 Hz), 4.24 (1H, dd, *J* = 12.1, 2.2 Hz), 3.98 (1H, dd, *J* = 9.3, 9.3 Hz), 3.93 (1H, ddd, *J* = 10.1, 3.6, 2.3 Hz), 3.67 (1H, dd, *J* = 9.6, 3.5 Hz), 3.57 (1H, dd, *J* = 9.9, 9.2 Hz), 2.16 (3H, s), 2.03 (3H, s); **$^{13}$C NMR** (101 MHz, *$CDCl_3$*) $\delta_{ppm}$ 170.6, 169.3, 138.4, 137.6, 137.4, 128.53, 128.50, 128.45, 128.18, 128.0, 128.05, 128.02, 127.88, 127.75, 89.6, 81.6, 78.8, 76.6, 75.7, 75.3, 73.2, 71.0, 62.6, 21.0, 20.8. **ESI-MS** *m/z* calcd for $C_{31}H_{34}O_8$ $[M + Na]^+$: 557.21. Found 557.40. Rf = 0.29 (7:3, hexanes: ethyl acetate).

**(±)-7-endo-Oxabicyclo-[2.2.1]-hept-5-ene-2-carboxylic acid (846)**



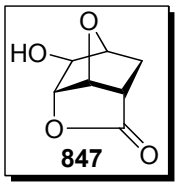
**846**

This compound was prepared according to a modified protocol of that proposed by Tomoya: a 100 mL flame-dried round bottomed flask equipped with a magnetic stir-bar was charged with freshly distilled furan (60.0 mL, 56.2 g, 825 mmol) and acrylic acid (15.0 mL,15.8 g, 219 mmol).[68] The reaction flask was sealed, cooled to -5 ºC, fitted with an outlet, and $BH_3$·THF (2.3 mL, 1.0 M in THF) was added dropwise. The outlet was removed, and the flask was completely isolated and allowed to stir for 48 hours. The resulting white precipitate was collected by filtration and washed with ice-cold diethyl ether, and

dried *in vacuo* to provide 16.9 g of the title compound (55 % yield).[a] Spectral data is consistent with the literature.[69]

**$^1$H NMR** (300 MHz, *$CDCl_3$*) $\delta_{ppm}$ 6.47 (1H, dd, *J* = 5.8, 1.6 Hz), 6.31 (1H, dd, *J* = 5.8, 1.4 Hz), 5.22-5.18 (1H, ddd, *J* = 4.7, 1.4, 0.6 Hz), 5.05 (1H, dd, *J* = 4.6, 1.6, 0.6 Hz), 3.18 (1H, ddd, *J* = 8.8, 4.7, 3.9 Hz), 2.13 (1H, ddd, *J* = 11.4, 9.3, 4.7 Hz), 1.57 (1H, dd, *J* = 11.5, 3.8 Hz); **$^{13}$C NMR** (101 MHz, *$CDCl_3$*) $\delta_{ppm}$ 172.2, 137.3, 132.7, 79.1, 78.7, 42.7, 28.5. **ESI-MS** *m*/*z* calcd for $C_7H_8O_3$ $[M + Na]^+$: 163.04. Found: 163.06.

**(±)-2-exo-hydroxy-4,8-dioxatricyclo[4.2.1.O$^{3,7}$]nonan-5-one (847)**



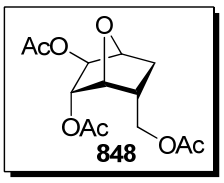

This compound was prepared according to a modified protocol of that outlined by Ogawa.[70] Bicyclic carboxylic acid **846** (25 g, 178 mmol) was dissolved in a mixture of formic acid (48 mL) and 30 % hydrogen peroxide (55 mL). The reaction flask was equipped with a water cooled condenser and the reaction was heated to 70 ºC open to the atmosphere for 35 minutes. The reaction was cooled to ambient temperature and the solvents were removed under reduced pressure to provide 28 g of the product as a white powder in quantitative yield. CAUTION: This reaction should not be run on larger than 30 g scale as an exotherm results under these scales stimulating a vigorous retro-Diels-Alder reaction that results in the unfortunate complete loss of product and a redecorated fume-hood. This occurred both times the reaction was attempted in larger batches. Spectral data is consistent with the partial listing in the literature.[70]

**$^1$H NMR** (400 MHz, *MeOD*) $\delta_{ppm}$ 5.35 (1H, dd, *J* = 4.9, 4.9 Hz), 4.50 (1H, ddd, *J* = 5.4, 1.2, 0.8 Hz), 4.44 (1H, ddd, *J* = 5.0, 1.4, 0.8 Hz), 3.80 (1H, bs), 2.66 (1H, dddd, *J* = 11.3, 4.8, 1.8, 0.7 Hz), 2.15 (1H, ddd, *J* = 13.3, 11.3, 5.3 Hz), 1.91 (1H, dd, *J* = 13.4, 1.9 Hz); **$^{13}$C NMR** (101 MHz, *$CDCl_3$*) $\delta_{ppm}$ 179.4, 87.0, 84.0, 82.0, 78.2, 40.2, 34.3. **ESI-MS** *m*/*z* calcd for $C_7H_8O_4$ $[M + NH_4]^+$: 174.18. Found: 174.3.

**(±)-2-exo-3-endo-diacetoxy-5-endo-acetoxymethyl-7-oxabicyclo[2.2.1]heptane (848)**

---

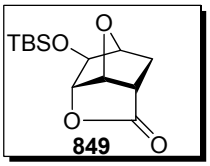
[a] Additional crops of crystals could be obtained by cocentrating the mother liquor and recrystallizing from isopropanol and ethyl acetate.




The following protocol was carried out in 3 parallel reactions as a modification to that outlined by Ogawa. [70] A flame dried round bottomed flask purged with argon was charged with THF (50 mL). The flask was cooled to 0 ºC, and $LiAlH_4$ (2.0 g, 52.7 mmol) was added portionwise, 0.5 g at a time, with stirring to produce a slurry. Simultaneously, in a second flask under argon, hydroxyl lactone **847** (8.0 g, 51.3 mmol) was dissolved in 160 mL of THF. This solution was then cannulated slowly into the $LiAlH_4$ suspension and the reaction was allowed to warm to ambient temperature and stir for 1.5 hours. The reaction was then returned to 0 ºC, and water (40.0 mL) was added dropwise. The reaction was then neutralized with 4 M HCl to pH < 6, and the solution was concentrated to dryness. The crude triol was then treated with pyridine (160 mL) and acetic anhydride (160 mL) along with a catalytic amount of DMAP for 4 hours. Solvent was removed and the residue was partitioned between ethyl acetate and 10 % HCl, and the organic phase was washed successively with saturated sodium bicarbonate and brine, dried, filtered and concentrated to provide 10.1 g of the title compound as a clear syrup (69 % yield). Spectral data is consistent with partial listing in the literature.[69]

**$^1$H NMR** (400 MHz, *$CDCl_3$*) $\delta_{ppm}$ 5.08 (1H, dddd, *J* = 4.9, 2.3, 1.3, 1.3 Hz), 4.71 (1H, d, *J* = 2.5 Hz), 4.68 (1H, t, *J* = 4.8, 4.8 Hz), 4.49 (1H, d, *J* = 6.3 Hz), 4.37 (1H, dd, *J* = 11.1, 7.9 Hz), 4.21 (1H, dd, *J* = 11.0, 9.2 Hz), 2.68-2.55 (1H, m), 2.21 (1H, ddd, *J* = 12.5, 11.7, 6.6 Hz), 2.11 (3H, s), 2.07 (3H, s), 2.04 (3H, s), 1.34 (1H, dd, *J* = 12.8, 6.0 Hz); **$^{13}$C NMR** (101 MHz, *$CDCl_3$*) $\delta_{ppm}$ 170.4, 170.3, 169.6, 81.8, 80.6, 80.2, 76.3, 63.7, 39.8, 30.2, 20.6, 20.4, 20.2. **ESI-MS** *m*/*z* calcd for $C_{13}H_{18}O_7$ $[M + H]^+$: 287.1. Found: 287.1.

**(±)-2-exo-(*tert*-Butyldimethylsilyloxy)-4,8-dioxatricyclo[4.2.1.O$^{3,7}$]nonan-5-one (849)**



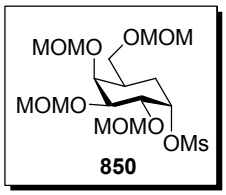

Alcohol **847** (5.0 g, 32 mmol) and TBSCl (10.0 g, 66 mmol) along with DMAP (40 mg, 0.3 mmol) were dissolved in a solution of DCM (200 mL) and pyridine (200 mL). The reaction was then heated to 80 ºC for 8 hours. At this point the reaction was cooled and volatiles were removed under reduced pressure. The crude product was partitioned between water and ethyl acetate, and the aqueous layer was extracted twice with fresh ethyl acetate. The combined organic layers were dried, filtered and concentrated in the usual fashion to provide 7.3 g of crude product. This material was purified through flash

chromatography (15 % ethyl acetate in hexanes) to provide 7.2 g of the title compound as an amorphous white solid in 84 % yield.

**$^1$H NMR** (400 MHz, *$CDCl_3$*) $\delta_{ppm}$ 5.27 (1H, dd, *J* = 4.9, 4.9 Hz), 4.43 (1H, ddd, *J* = 5.3, 1.3, 0.8 Hz), 4.40 (1H, ddd, *J* = 5.0, 1.4, 0.9 Hz), 3.80 (1H, s), 2.64 (1H, dddd, *J* = 11.3, 4.8, 1.8, 0.8 Hz), 2.13 (1H, ddd, *J* = 13.4, 11.3, 5.3 Hz), 1.87 (1H, dd, *J* = 13.4, 1.8 Hz), 0.86 (9H, s), 0.08 (6H, s); **$^{13}$C NMR** (100 MHz, *$CDCl_3$*) $\delta_{ppm}$ 176.8, 86.0, 82.8, 80.4, 78.3, 38.7, 33.4, 25.6, 18.0, -4.9, -4.9. **ESI-MS** *m/z* calcd for $C_{13}H_{22}O_4Si$ $[M + H]^+$: 271.14. Found 271.16. **Rf** = 0.83 (7:3, ethyl acetate: hexanes).

**5a-carba-1-*O*-mesyl-2,3,4,6-tetra-*O*-methoxymethyl-α-galactopyranose (850)**

Prepared according to a modified version of the protocol of Ogawa.[82]

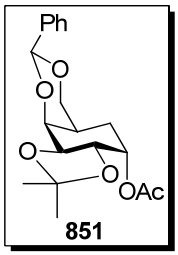


**850**

Deprotected carbasugar **858** (443 mg, 1.7 mmol) was dissolved in anhydrous DCM (10 mL) under an argon atmosphere with stirring. Methylchloromethyl ether (1.03 mL, 101 g, 13.6 mmol) was added followed by diisopropylethylamine (2.6 g, 3.5 mL, 20.4 mmol), and the reaction was heated to 42 ºC for 14 hours. After cooling, the reaction mixture was diluted with chloroform (150 mL) and extracted with 5 % HCl, saturated $NaHCO_3$ and brine successively. The organic phase was dried, filtered and concentrated to provide 600 mg of crude product that was further purified by flash chromatography (3:1, hexanes: ethyl acetate) to yield 330 mg of the title product as a clear, thick oil (48 % yield) over 4 steps. Spectral data is consistent with the literature.[82]

**$^1$H NMR** (400 MHz, *$CDCl_3$*) $\delta_{ppm}$ 5.06 (1H, dd, *J* = 6.4, 3.3 Hz), 4.74 (2H, dd, *J* = 7.9, 6.6 Hz), 4.72-4.56 (4H, m), 4.55 (2H, s), 4.07 (1H, bs), 3.99 (1H, dd, *J* = 10.3, 3.0 Hz), 3.79 (1H, dd, *J* = 10.3, 2.4 Hz), 3.36 (3H, s), 3.34 (3H, s), 3.33 (3H, s), 3.30 (3H, s), 3.06 (3H, s), 2.17-2.10 (1H, m), 1.85 (1H, ddd, *J* = 14.4, 3.3, 3.3 Hz), 1.69 (1H, ddd, *J* = 14.5, 12.9, 1.8 Hz); **$^{13}$C NMR** (101 MHz, *$CDCl_3$*) $\delta_{ppm}$ 97.4, 96.6, 96.5, 95.7, 77.7, 75.9, 74.1, 68.0, 67.6, 55.7, 55.6, 55.5, 55.2, 38.7, 35.3, 28.1. **ESI-MS** *m/z* calcd for $C_{16}H_{32}O_{11}S$ $[M + H]^+$: 433.18; $[M + Na]^+$: 455.16. Found: 433.23, 455.21. **Rf** = 0.35 (2:1, hexanes: acetone)

**1-*O*-Acetyl-4,6-*O*-benzylidene-2,3-*O*-isopropylidene-5a-carba-α-galactopyranose (851)**

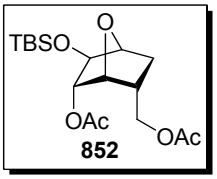


**851**

Prepared according to a modified version of the protocol of Ogawa.[82] In a flame dried round bottomed flask equipped with a stir bar and charged with argon, benzylidene **855** (1.61 g, 6.0 mmol) was dissolved in anhydrous DMF (30 mL, 0.2M). The flask was cooled to 0 ºC with stirring. To this solution was added 2-methoxypropene (2.87 mL, 2.16 g, 30.0 mmol) and *p*-TsOH·$H_2O$ (200 mg, 1.2 mmol). The reaction mixture was stirred for 30 minutes and neutralized with triethylamine (1 mL). The solution was concentrated to dryness and treated with 6 mL of acetic anhydride, 15 mL of pyridine and a crystal of DMAP for 5 hours. Solvent was removed under reduced pressure and the crude product was purified by flash chromatography (10: 1 to 5: 1 hexanes: ethyl acetate) to provide 570 mg of the title product as white crystals (30 % yield).[a]

**$^1$H NMR** (300 MHz, *$CDCl_3$*) $\delta_{ppm}$ 7.47-7.21 (5H, m), 5.57 (1H, ddd, *J* = 7.5, 7.4, 4.6 Hz), 5.55 (1H, s), 4.57 (1H, dd, *J* = 2.4, 2.4 Hz), 4.19 (1H, dd, *J* = 7.6, 2.7 Hz), 4.15 (1H, dd, *J* = 9.3, 2.6 Hz), 4.00 (1H, dd, *J* = 9.8, 2.6 Hz), 3.98 ( 1 H, dd, *J* = 11.4, 1.1 Hz), 2.36 ( 1 H, ddd, *J* = 15.1, 12.5, 2.8 Hz), 2.09 (3H, s), 1.89 (1H, m), 1.84-1.74 (1H, m), 1.45 (3H, s), 1.43 (3H, s); **$^{13}$C NMR** (75 MHz, *$CDCl_3$*) $\delta_{ppm}$ 170.0, 137.9, 128.8, 128.0, 126.0, 110.0, 100.9, 74.9, 73.9, 73.2, 70.3, 68.1, 30.5, 28.3, 26.6, 26.5, 21.0. **ESI-MS** *m*/*z* calcd for $C_{19}H_{24}O_6$ $[M + H]^+$: 344.04; $[M + Na]^+$: 366.02; $[M + K]^+$: 381.99. Found 344.28, 366.14, 382.31.

**(±)-3-endo-Acetoxy-5-endo-acetoxymethyl-2-exo-(*tert*-butyldimethylsilyloxy)-7-oxabicyclo[2.2.1]heptane (852)**



**852**

Bicyclic lactone **849** (6.5 g, 24 mmol) was dissolved in anhydrous THF (57 mL) under an argon atmosphere in a flame dried round-bottomed flask. This solution was cannulated into a second flask under argon containing a stirring solution of 95 % lithium aluminum hydride in THF (912 mg, 23 mmol, 23 mL of THF) at 0 ºC. The reaction was stirred for 1 hour at ambient temperature before 900 mL of water, followed by 1.8 mL of 10 % sodium hydroxide and finally by 2.7 mL of water. The reaction was stirred for

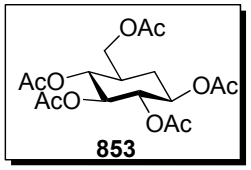
---

[a] Mixed fractions containing the product and its isomer, 3-*O*-acetyl-4,6-*O*-benzylidene-1,2-*O*-isopropylidene-5a-carba-α-galactopyranose, accounted for a further 1.2 g of material accounting for a further 63 % yield in an approximately 1:1 mixture of isomers.

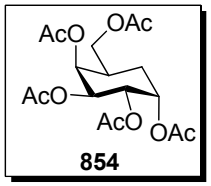
an additional 10 minutes and then filtered through a celite pad. The filtrate was acidified to pH =5 with 10 % HCl, and was concentrated to dryness, and then resuspended in pyridine (45 mL) and acetic anhydride (45 mL) along with catalytic DMAP and allowed to stir for 12 hours. Solvent was removed under reduced pressure and the crude product was purified by flash chromatography (9:1 hexanes: acetone) to provide 8.2 g of the title compound as a white solid (95 % yield).

**$^1$H NMR** (300 MHz, *$CDCl_3$*) $\delta_{ppm}$ 4.89-4.84 (1H, m), 4.64 (1H, dd, *J* = 4.8, 4.8 Hz), 4.34 (1H, dd, *J* = 11.0, 8.1 Hz), 4.29 (1H, d, *J* = 6.4 Hz), 4.10 (1H, dd, *J* = 10.7, 9.4 Hz), 3.83 (1H, dd, *J* = 2.3, 0.4 Hz), 2.62-2.47 (1H, m), 2.13 ( 1 H, dd, *J* = 12.1, 6.2 Hz), 2.03 (3H, s), 2.02 (3H, s), 1.15 (1H, dd, *J* = 12.6, 5.9 Hz), 0.87 (9H, s), 0.05 (3H, s), 0.04 (3H, s); **$^{13}$C NMR** (75 MHz, *$CDCl_3$*) $\delta_{ppm}$ 170.8, 170.0, 85.6, 84.6, 79.8,76.5, 64.2, 40.0, 30.7, 25.7, 22.1, 20.7, 20.6, -4.8, -4.9. **ESI-MS** *m/z* calcd for $C_{17}H_{30}O_6Si$ $[M + H]^+$: 359.19. Found 359.24. **Rf** = 0.23 (9:1, hexanes: acetone).

**1,2,3,4,6-Penta-*O*-acetyl-5a-carba-β-glucopyranose (853)** and **1,2,3,4,6-penta-*O*-acetyl-5a-carba-α-galactopyranose (854)**



**853**



**854**

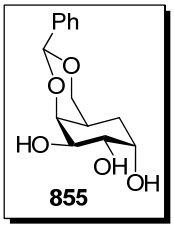
Prepared according to a modified version of the protocol of Ogawa.[82] Bicyclic **852** (8.2 g, 23 mmol) was dissolved in a solution acetic acid (20 mL), acetic anhydride (11.6 mL) and sulphuric acid (1.3 mL). The tube was sealed, and the mixture was heated, with stirring, at 85 ºC for 48 hours. The reaction was removed from heat and allowed to cool before being poured into 50 mL of water at 0 ºC, and the solution was neutralized to pH >7 through the portion-wise addition of solid sodium bicarbonate. The aqueous phase was then extracted thrice with ethyl acetate and the combined organic layers were washed with saturated bicarbonate, and brine successively before being dried, filtered and concentrated in the usual manner. This provided 7.3 g of crude material that was then purified through flash chromatography ( 9:1 hexanes: acetone) to provide 4.02 g of galactose derivative **854** in the first fraction (45 % yield) as a white solid and 2.78 g of glucose derivative **853** (31 % yield) in the second fraction as a thick oil that solidified upon extended standing. Spectral data is consistent with the literature.[82] Characterization data for **853**

**$^1$H NMR** (300 MHz, *CDCl$_3$*) $\delta_{ppm}$ 5.14 (2H, m), 5.05 (1H, dd, *J* = 10.0, 10.0 Hz), 4.97 (1H, ddd, *J* = 11.8, 9.3, 4.7 Hz), 4.10 (1H, dd, *J* = 11.4, 5.1 Hz), 3.97 (1H, dd, *J* = 11.4, 3.2 Hz), 2.20 (1H, ddd, *J* = 12.9, 4.6, 3.8 Hz), 2.15-2.08 (2H, m), 2.06 (3H, s), 2.03 (6H, s), 2.01 (3H, s), 1.99 (3H, s), 1.60 (1H, ddd, *J* = 12.7, 12.7, 12.6 Hz); **$^{13}$C NMR** (101 MHz, *CDCl$_3$*) $\delta_{ppm}$ 170.0, 169.4, 169.3, 169.2, 72.7, 72.3, 70.3, 70.0, 62.4, 35.8, 28.8, 20.3, 20.2, 20.04, 20.02, 19.96. **ESI-MS** *m*/*z* calcd for $C_{21}H_{22}O_3$ $[M + Na]^+$: 411.13. Found 411.21.

Characterization data for **854**

**$^1$H NMR** (300 MHz, *CDCl$_3$*) $\delta_{ppm}$ 5.56 (1H, dd, *J* = 2.4, 2.4 Hz), 5.50 (1H, ddd, *J* = 3.1, 2.9, 2.9 Hz), 5.21 (1H, dd, *J* = 16.0, 2.6 Hz), 5.17 (1H, dd, *J* = 16.0, 2.7 Hz), 3.95 (1H, dd, *J* = 11.1, 9.2 Hz), 3.87 (1H, dd, *J* = 11.1, 6.0 Hz), 2.46 (1H, m), 2.10 (3H, s), 2.10 (3H, s), 2.03 (3H, s), 1.99 (3H, s), 1.98 (3H, s), 1.77(1H, dd, *J* = 2.6, 1.4 Hz), 1.74 (1H, *pseudo*-d, *J* = 3.0 Hz); **$^{13}$C NMR** (101 MHz, *CDCl$_3$*) $\delta_{ppm}$ 170.1, 169.7, 169.5, 169.4, 69.1, 68.9, 67.75, 67.73, 62.4, 32.7, 26.1, 20.5, 20.2. **ESI-MS** *m*/*z* calcd for $C_{17}H_{24}O_{10}$ $[M + NH_4]^+$: 406.17; $[M + Na]^+$: 411.13; $[M + K]^+$: 427.10. Found 406.20, 411.16, 427.15.

### 4,6-*O*-Benzylidene-5a-carba-α-galactopyranose (855)



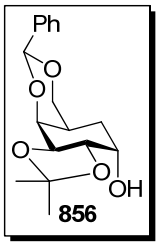
**855**

Prepared according to a modified version of the protocol of Ogawa.[82] 5a-carba-α-galactopyranose (**232**, 2.5 g,13.9 mmol) was dissolved in 20 mL of anhydrous DMF under an argon atmosphere along with α, α-dimethoxytoluene (2.5 mL, 16.8 mmol) and *p*-TsOH (400 mg, 2.35 mmol). The reaction was heated to 50 ºC for three hours and neutralized with triethylamine (4 mL) prior to concentration. The crude product was then immeidatly purified by flash chromatography (19:1, chloroform: methanol) to yield 1.65 g of product as white crystals in 54 % yield. Spectral data is consistent with the literature.[82]

**$^1$H NMR** (400 MHz, *D$_2$O*) $\delta_{ppm}$ 7.58-7.44 (5H, m), 5.65 (1H, s), 4.37 (1H, ddd, *J* = 3.2, 1.7, 1.7 Hz), 4.24 (1H, dd, *J* = 11.7, 2.7 Hz), 4.21 (1H, dd, *J* = 6.0, 2.8 Hz), 3.95 (1H, dd, *J* = 11.6, 1.1 Hz), 3.90 (1H, dd, *J* = 10.3, 3.3 Hz), 3.84 (1H, dd, *J* = 10.4, 2.9 Hz), 2.33 (1H, ddd, *J* = 14.4, 13.5, 2.5 Hz), 2.03-1.96 (1H, m), 1.78 (1H, dddd, *J* = 14.4, 4.5, 3.5, 1.2 Hz); **$^{13}$C NMR** (101 MHz, *D$_2$O*) $\delta_{ppm}$ 137.4, 129.8, 128.7, 126.3, 101.8, 78.5, 70.9, 70.4, 69.8, 69.7, 46.7, 29.0**. ESI-**

**MS** *m/z* calcd for $C_{14}H_{18}O_5$ $[M + Na]^+$: 289.10. Found: 289.15. **Rf** = 0.54 (9:1, ethyl acetate: methanol).

**4,6-*O*-Benzylidene-2,3-*O*-isopropylidene-5a-carba-α-galactopyranose (856)**

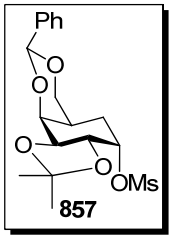


**856**

Prepared according to a modified version of the protocol of Ogawa.[82] Acetate **851** (570 mg, 1.7 mmol) was dissolved in 0.1 M sodium methoxide in methanol (10 mL) and stirred for two hours. The reaction was neutralized with pre-rinsed Amberlite IR120 Ion exchange resin, hydrogen form and stirred for an additional five minutes. The resin was removed by filtration and the reaction was concentrated under reduced pressure and dried *in vacuo* to produce 534 mg of **851** in quantitative yield as white powder. The product was sufficiently pure to be used directly in subsequent steps. Spectral data is consistent with the literature.[82]

**$^1$H NMR** (300 MHz, *$CDCl_3$*) $\delta_{ppm}$ 7.55-7.31 (5H, m), 5.55 (1H, s), 4.55 (1H, dd, *J* = 2.4, 2.4 Hz), 4.46 (1H, dd, *J* = 5.2, 2.7 Hz), 4.18 (1H, dd, *J* = 11.6, 2.7 Hz), 4.13 (1H, dd, *J* = 10.0, 2.2 Hz), 4.06 (1H, dd, *J* = 9.9, 2.3 Hz), 4.00 (1H, dd, *J* = 11.6, 1.0 Hz), 2.36 (1H, bs), 1.96-1.81 (2H, m), 1.47 (6H, s). **ESI-MS** *m/z* calcd for $C_{17}H_{22}O_5$ $[M + H]^+$: 307.15; $[M + Na]^+$: 329.14; $[M + K]^+$: 345.11. Found: 307.20, 329.19, 345.18.

**4,6-*O*-Benzylidene-2,3-*O*-isopropylidene-1-*O*-methanesulfonyl-5a-carba-α-galactopyranose (857)**

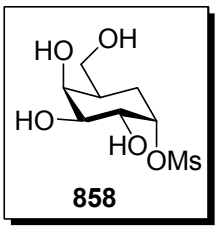


**857**

Prepared according to a modified version of the protocol of Ogawa.[82] Carbasugar **856** (530 mg, 1.7 mmol) was dissolved in pyridine (10 mL) in an argon-charged flask and then cooled to 0 ºC. Methanesulfonylchloride (394 μL, 5.1 mmol) was added and the reaction was stirred for 14 hours at ambient temperature. Methanol (1 mL) was added and the reaction stirred for an additional hour and solvent was removed under reduced pressure. The crude product was partitioned between ethyl acetate and water and the organic phase was washed with brine, then dried, filtered and concentrated to produce the product as a film in quantitative yield (670 mg), sufficiently pure to be used without any further purification. Spectral data is consistent with the literature.[82]

**$^1$H NMR** (300 MHz, *$CDCl_3$*) $\delta_{ppm}$ 7.53-7.29 (5H, m), 5.56 (1H, s), 5.29 (1H, dd, *J* = 5.0, 2.5 Hz), 4.60-4.56 (1H, m), 4.21-4.14 (2H, m), 4.01 (1H, dd, *J* = 11.8, 0.8 Hz), 3.99 (1H, dd, *J* = 10.1, 2.5 Hz), 3.10 (3H, s), 2.45 (1H, ddd, *J* = 15.1, 12.5, 2.4 Hz), 2.14-2.06 (1H, m), 1.98-1.85 (1H, m), 1.45 (6H, s); **$^{13}$C NMR** (75 MHz, *$CDCl_3$*) $\delta_{ppm}$ 137.8, 128.9, 128.1, 126.0, 110.6, 100.9, 77.2, 74.8, 73.7, 72.8, 70.1, 38.6, 30.2, 29.9, 26.6. **ESI-MS** *m/z* calcd for $C_{18}H_{24}O_7S$ $[M + H]^+$: 385.14; $[M + Na]^+$: 407.11; $[M + K]^+$: 423.10. Found: 385.18, 407.17, 423.14.

**1-*O*-Methanesulfonyl-5a-carba-α-galactopyranose (858)**

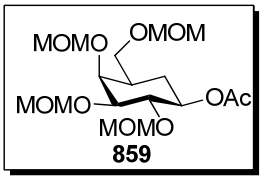


**858**

Prepared according to a modified version of the protocol of Ogawa.[82] Mesylate **857** (670 mg, 1.7 mmol) was dissolved in 60 % acetic acid (3 mL) and heated to 65 ºC for 5 hours. The reaction was allowed to cool to ambient temperature and the solvent was removed under reduced pressure to provide the crude product as an off white solid in quantitative yield (443 mg). No further purification was necessary.

**$^1$H NMR** (500 MHz, *$D_2O$*) $\delta_{ppm}$ 4.89 (1H, dd, *J* = 5.0, 3.1 Hz), 3.95 (1H, bs), 3.72 (1H, dd, *J* = 10.3, 3.1 Hz), 3.55 (1H, dd, *J* = 10.3, 3.0 Hz), 3.49 (1H, dd, *J* = 10.9, 7.8 Hz), 3.36 (1H, dd, *J* = 11.0, 6.4 Hz), 3.14-3.07 (1H, m), 3.06 (3H, s), 1.98 (1H, m), 1.78 (1H, td, *J* = 15.1, 3.2 Hz), 1.56 (1H, ddd, *J* = 14.8, 13.4, 1.4 Hz); **$^{13}$C NMR** (101 MHz, *$D_2O$*) $\delta_{ppm}$ 82.5, 71.0, 69.3, 68.9, 62.0, 37.4, 36.2, 26.4. **ESI-MS** *m/z* calcd for $C_8H_{16}O_7S$ $[M + H]^+$: 257.07; $[M + Na]^+$: 279.05. Found: 257.16, 279.14.

**1-*O*-Acetyl-2,3,4,6-tetra-*O*-(methoxymethyl)-5a-carba-β-galactopyranose (859)**



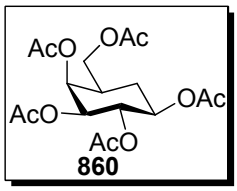
**859**

Prepared according to a modified version of the protocol of Ogawa.[82] Mesylate **850** (300 mg, 0.69 mmol) was dissolved in anhydrous DMF (5 mL) under an argon atmosphere in a sealed tube. Potassium acetate (1.3 g, 13.8 mmol) was added and the reaction was sealed and heated to 100 ºC for 48 hours. Following cooling to ambient temperature, the reaction mixture was diluted with ethyl acetate (40 mL) and extracted repeatedly with brine. The organic phase was dried, filtered, concentrated and residual solvent was removed *in vacuo*. The crude product was then purified by

flash chromatography (9: 1 hexanes: acetone) to provide 170 mg of the product as a thick, clear syrup in 62 % yield.[a]

**$^1$H NMR** (400 MHz, *CDCl$_3$*) $\delta_{ppm}$ 4.79 (1H, d, *J* = 6.7 Hz), 4.76 (1 H, d, *J* = 6.6 Hz), 4.71 (1H, d, *J* = 6.8 Hz), 4.65 (1H, d, *J* = 6.7 Hz), 4.64 (1H, d, *J* = 6.4 Hz), 4.63 (1H, d, *J* = 6.3 Hz), 4.54 (2H, bs), 4.03-4.01 (1H, m), 3.90 (1H, dd, *J* = 9.6, 9.6 Hz), 3.46 (1H, dd, *J* = 9.8, 2.4 Hz), 3.44 (1H, dd, *J* = 9.4, 8.2 Hz), 3.35 (3H, s), 3.34 (3H, s), 3.33 (3H, s), 3.29 (3H, s), 2.02 (3H, s), 1.83-1.71 (2H, m), 1.47 (1H, ddd, *J* = 13.2, 11.5, 11.5 Hz); **$^{13}$C NMR** (101 MHz, *CDCl$_3$*) $\delta_{ppm}$ 170.3, 98.9, 97.4, 96.5, 95.7, 79.5, 78.0, 73.5, 73.4, 67.8, 55.74, 55.71, 55.63, 55.28, 37.02, 27.17, 21.21. **ESI-MS** *m*/*z* calcd for $C_{17}H_{32}O_{10}$ $[M + Na]^+$: 419.42; $[M + K]^+$: 435.40. Found: 419.40, 435.40.

**5a-carba-1,2,3,4,6-penta-*O*-acetyl-β-galactopyranose (860)**



**860**

Protected carbasugar **859** (100 mg 0.25 mmol), was dissolved in 4 M HCl and warmed to 65 ºC for four hours. Following cooling, the solvent was removed under reduced pressure to yield 46 mg of the deprotected carbasugar as a white powder in quantitative yield (> 95 % purity). This powder was redissolved in doubly distilled water and extracted four times with chloroform. The aqueous phase was reconcentrated, suspended in 4 mL of pyridine, 4 mL of acetic anhydride and a catalytic amount of DMAP and allowed to stir for 8 hours. Solvent was removed in vacuo, and the residue was dissolved in dichloromethane and washed with 10 % HCl, saturated sodium hydrogen carbonate and brine successively. The organic phase was then dried, filtered and concentrated and dried *in vacuo* to provide 91 mg of the peracetylated compound in 93 % yield as a white solid.

**$^1$H NMR** (400 MHz, *CDCl$_3$*) $\delta_{ppm}$ 5.47 (1H, dd, *J* = 2.5, 2.5 Hz), 5.38 (1H, dd, *J* = 10.1, 10.1 Hz), 4.91 (1H, ddd, *J* = 11.7, 9.8, 5.1 Hz), 4.88 (1H, dd, *J* = 10.4, 3.0 Hz), 3.98 (1H, dd, *J* = 11.1, 8.8 Hz), 3.86 (1H, dd, *J* = 11.1, 6.1 Hz), 2.22-2.14 (1H, m), 2.12 (3H, s), 2.03 (3H, s), 2.02 (3H, s), 2.01 (3H, s), 1.97 (3H, s), 1.63 (1H, ddd, *J* = 12.9, 12.9, 12.9 Hz); **$^{13}$C NMR** (101 MHz,

[a] A further 110 mg of partially deprotected beta-anomeric compounds were recovered from the flash column; crude NMR of the reaciton mixture indicated that some protecting groups were lost during the displacement of the mesylate.

*CDCl₃*) $\delta_{ppm}$ 170.7, 170.1, 170.0, 169.9, 72.0, 71.3, 70.8, 67.5, 62.7, 34.7, 27.1, 20.9, 20.7, 20.7, 20.6. **ESI-MS** *m/z* calcd for $C_{17}H_{24}O_{10}$ $[M + Na]^+$: 411.13; $[M + NH_4]^+$: 406.17; $[M + K]^+$: 427.10. Found 406.22, 411.17, 427.16.


1. Pedersen, D. S.; Rosenbohm, C., *Synthesis* **2001**, 2431-2434.

2. Sreerama, N.; Woody, R. W., *Anal. Biochem.* **2000,** *287* (2), 252-260.

3. Tam, R. Y.; Rowley, C. N.; Petrov, I.; Zhang, T.; Afagh, N. A.; Woo, T. K.; Ben, R. N., *J. Am. Chem. Soc.* **2009,** *131*, 15745-15753.

4. Chakrabartty, A.; Hew, C. L., *Eur. J. Biochem.* **1991,** *202*, 1057-1063.

5. Knight, C. A.; Hallet, J.; DeVries, A. L., *Cryobiology* **1988,** *25*, 55-60.

6. Jackman, J.; Noestheden, M.; Moffat, D.; Pezacki, J. P.; Findlay, S.; Ben, R. N., *Biochem. Biophys. Res. Commun.* **2007,** *354*, 340-344.

7. Chan, W. C.; White, P. D., Basic procedures. In *Fmoc Solid Phase Peptide Synthesis: A Practical Approach*, Chan, W. C.; White, P. D., Eds. Oxford Univesity Press: Oxford, 2000; pp 41-76.

8. Pavia, A. A.; Rocheville, J.-M.; Ung, S. N., *Carb. Res.* **1980,** *79*, 79-89.

9. Czechura, P.; Tam, R. Y.; Dimitrijevic, E.; Murphy, A. V.; Ben, R. N., *J. Am. Chem. Soc.* **2008,** *130*, 2928-2929.

10. Bock, K.; Fernandez Bolanos Guzman, J.; Ogawa, S., *Carb. Res.* **1988,** *174* (0), 354-359.

11. Berthold, H. J.; Franke, S.; Thiem, J.; Schotten, T., *J. Org. Chem.* **2010,** *75* (11), 3859-3862.

12. Pontén, F.; Magnusson, G., *J. Org. Chem.* **1996,** *61* (21), 7463-7466.

13. Larionov, O. V.; de Meijere, A., *Org. Lett.* **2004,** *6* (13), 2153-2156.

14. Arndt, F., *Org. Syn.* **1935,** *15*, 3.

15. Abele, S.; Guichard, G.; Seebach, D., *Helv. Chim. Acta* **1998,** *81* (12), 2141-2156.

16. Oppolzer, W.; Lienard, P., *Helv. Chim. Acta* **1992,** *75* (8), 2572-2582.

17. Ibatullin, F. M.; Selivanov, S. I., *Tetrahedron Lett.* **2002,** *43*, 9577-9580.

18. Szilágyi, L.; Györgydeák, Z. A., *Carb. Res.* **1985,** *143*, 21.

19. Comfort, D. A.; Bobrov, K. S.; Ivanen, D. R.; Shabalin, K. A.; Harris, J. M.; Kulminskaya, A. A.; Brumer, H.; Kelly, R. M., *Biochemistry* **2007,** *46*, 3319.

20. Podlipnik, C.; Velter, I.; La Ferla, B.; Macou, G.; Belvisi, L.; Nicotra, F.; Bernardi, A., *Carb. Res.* **2007,** *342*, 1651-1660.

21. Ajaj, K. A.; Hennig, L.; Findeisen, M.; Giesa, S.; Müller, D.; Welzel, P., *Tetrahedron* **2002,** *58*, 8439-8451.

22. Aldhoun, M.; Massi, A.; Dondoni, A., *J. Org. Chem.* **2008,** *73* (24), 9565-9575.

23. Patman, R.; Juárez-Ruiz, J. M.; Roy, R., *Org. Lett.* **2006,** *8*, 2691-2694.

24. Francisco, C. G.; Herrera, A. J.; Suárez, E., *J. Org. Chem.* **2002,** *67* (21), 7439-7445.

25. Le Chevalier Isaad, A.; Barbetti, F.; Rovero, P.; D'Ursi, A. M.; Chelli, M.; Chorev, M.; Papini, A. M., *Eur. J. Org. Chem.* **2008,** *2008* (31), 5308-5314.

26. Zhang, M. M.; Tsou, L. K.; Charron, G.; Raghavan, A. S.; Hang, H. C., *PNAS.* **2010,** *107* (19), 8627-8632.

27. Link, A. J.; Vink, M. K. S.; Tirrell, D. A., *J. Am. Chem. Soc.* **2004,** *126* (34), 10598-10602.

28. Liu, S.; Ben, R. N., *Org. Lett.* **2005,** *7* (12), 2385-2388.

29. Nyffeler, P. T.; Liang, C.-H.; Koeller, K. M.; Wong, C.-H., *J. Am. Chem. Soc.* **2002,** *124*, 10773-10778.

30. Boyle, P. H.; Davis, A. P.; Dempsey, K. J.; Hosken, G. D., *Tetrahedron: Assym.* **1995,** *6* (11), 2819-2828.

31. Jamieson, A. G.; Boutard, N.; Beauregard, K.; Bodas, M. S.; Ong, H.; Quiniou, C.; Chemtob, S.; Lubell, W. D., *J. Am. Chem. Soc.* **2009,** *131* (22), 7917-7927.

32. Tanasova, M.; Yang, Q.; Olmsted, C. C.; Vasileiou, C.; Li, X.; Anyika, M.; Borhan, B., *Eur. J. Org. Chem.* **2009,** *2009* (25), 4242-4253.

33. Xiao, Y.; Lee, K.; Liu, P., *Org. Lett.* **2008,** *10* (24), 5521-5524.

34. McLaughlin, M.; Mohareb, R. M.; Rapoport, H., *J. Org. Chem.* **2003,** *68* (1), 50-54.

35. Hlaváček, J.; Pícha, J.; Vaněk, V.; Jiráček, J.; Slaninová, J.; Fučík, V.; Buděšínský, M.; Gilner, D.; Holz, R., *Amino Acids* **2010,** *38* (4), 1155-1164.

36. AIST, In *AIST: Integrated spectral database system of organic compounds*.

37. Pietruszka, J.; Witt, A., *Synthesis* **2006,** (24), 4266-4268.

38. Pollex, A.; Hiersemann, M., *Org. Lett.* **2005,** *7* (25), 5705-5708.

39. Katritzky, A.; Widyan, K.; Gyanda, K., *Synthesis* **2008,** *2008* (EFirst), 1201,1204.

40. Tam, R. Y. Studies into the structural features of *C*-linked antifreeze glycoprotein analogues responsible for ice-recrystallization inhibition activity. PhD. Thesis, University of Ottawa, Ottawa, 2010.

41. Logue, M. W.; Teng, K., *J. Org. Chem.* **1982,** *47* (13), 2549-2553.

42. Meana, I.; Albéniz, A. C.; Espinet, P., *Adv. Synth. Cat.* **2010,** *352* (17), 2887-2891.

43. Jobron, L.; Leteux, C.; Veyrières, A.; Beau, J.-M., *J. Carb. Chem.* **1994,** *13* (3), 507-512.

44. Steinmann, A.; Thimm, J.; Matwiejuk, M.; Thiem, J., *Macromol.* **2010,** *43* (8), 3606-3612.

45. Branderhorst, H. M.; Liskamp, R. M. J.; Pieters, R. J., *Tetrahedron* **2007,** *63* (20), 4290-4296.

46. Lee, R. T.; Lee, Y. C., *Carb. Res.* **1994,** *251* (0), 69-79.

47. Janczuk, A. J.; Zhang, W.; Andreana, P. R.; Warrick, J.; Wang, P. G., *Carb. Res.* **2002,** *337* (14), 1247-1259.

48. Busse, H.; Hakoda, M.; Stanley, M.; Streicher, H., *J. Carb. Chem.* **2007,** *26* (3), 159-194.

49. Agnihotri, G.; Misra, A. K., *Tetrahedron Lett.* **2005,** *46* (47), 8113-8116.

50. Chernyak, A. Y.; Levinsky, A. B.; Dmitriev, B. A.; Kochetkov, N. K., *Carb. Res.* **1984,** *128*, 269-282.

51. Lin, Y. A.; Chalker, J. M.; Davis, B. G., *J. Am. Chem. Soc.* **2010,** *132* (47), 16805-16811.

52. Beaton, S. A.; Huestis, M. P.; Sadeghi-Khomami, A.; Thomas, N. R.; Jakeman, D. L., *Chem. Commun.* **2009,** (2), 238-240.

53. Ohlsson, J.; Magnusson, G., *Carb. Res.* **2000,** *329* (1), 49-55.

54. Chaytor, J. L. Examining the role of carbohydrate hydration and structure in preventing ice-recrystallization. PhD. Thesis, University of Ottawa, Ottawa, 2010.

55. Rye, C. S.; Withers, S. G., *J. Am. Chem. Soc.* **2002,** *124* (33), 9756-9767.

56. Zhao, G.-L.; Yu, Z.-Y.; Li, Y.; Pang, L.-N.; Wang, J.-W., *Chin. J. Chem.* **2008,** *26* (1), 158-164.

57. Yu, J.; Otten, P.; Ma, Z.; Cui, W.; Liu, L.; Mason, R. P., *Bioconjugate Chem.* **2004,** *15* (6), 1334-1341.

58. Mori, T.; Fujita, S.; Okahata, Y., *Carb. Res.* **1997,** *298* (1-2), 65-73.

59. Xian, M.; Fatima, Z.; Zhang, W.; Fang, J.; Li, H.; Pei, D.; Loo, J.; Stevenson, T.; Wang, P. G., *J. Comb. Chem.* **2003,** *6* (1), 126-134.

60. West, C. W.; Estiarte, M. A.; Rich, D. H., *Org. Lett.* **2001,** *3* (8), 1205-1208.

61. Gardner, R. A.; Ghobrial, G.; Naser, S. A.; Phanstiel, *J. Med. Chem* **2004,** *47* (20), 4933-4940.

62. Yoshimi, Y.; Itou, T.; Hatanaka, M., *Chem. Commun.* **2007,** (48), 5244-5246.

63. Armarego, W. L. F.; Chai, C. L. L., *Purification of laboratory chemicals*. 6 ed.; Butterworth-Heinemann: New York, 2009.

64. Wolkowski, Z. W.; Vauthier, E.; Gonbeau, B.; Sauvaitre, H.; Musso, J. A., *Tetrahedron Lett.* **1972,** *13* (7), 565-568.

65. Curtin, D. Y.; Gerber, S. M., *J. Am. Chem. Soc.* **1952,** *74* (16), 4052-4056.

66. Usuki, Y.; Matsumoto, K.; Inoue, T.; Yoshioka, K.; Iio, H.; Tanaka, T., *Bioorg. Med. Chem. Lett.* **2006,** *16* (6), 1553-1556.

67. Yamakoshi, H.; Ohori, H.; Kudo, C.; Sato, A.; Kanoh, N.; Ishioka, C.; Shibata, H.; Iwabuchi, Y., *Bioorg. Med. Chem.* **2010,** *18* (3), 1083-1092.

68. Tomoya, K.; Katsuji, U.; Smimizu, K.; Shiro, T. Process for preparation of 7-oxobicyclo[2.2.1]hept-5-ene-2caboxylic acid derivatives. 2003.

69. Suami, T.; Ogawa, S.; Nakamoto, K.; Kasahara, I., *Carb. Res.* **1977,** *58* (1), 240-244.

70. Ogawa, S.; Iwasawa, Y.; Nose, T.; Suami, T.; Ohba, S.; Ito, M.; Saito, Y., *J. Chem. Soc. Perkin. Trans. I* **1985**, 903-906.

71. Ogawa, S.; Kasahara, I.; Suami, T., *Bulletin of the chemical society of Japan* **1979,** *52* (1), 118-123.

72. Madaj, J.; Jankowska, M.; Wisniewski, A., *Carb. Res.* **2004,** *339* (7), 1293-1300.

73. Moradei, O.; du Mortier, C.; Cirelli, A. F.; Thiem, J., *J. Carb. Chem.* **1995,** *14* (4-5), 525-532.

74. Parikka, K.; Tenkanen, M., *Carb. Res.* **2009,** *344* (1), 14-20.

75. Fletcher, S.; Jorgensen, M. R.; Miller, A. D., *Org. Lett.* **2004,** *6* (23), 4245-4248.

76. Jensen, C. M.; Lee, D. W., *J. Chem. Ed.* **2000,** *77* (5), 629-630.

77. Chen, M.-Y.; Patkar, L. N.; Lin, C.-C., *J. Org. Chem* **2004,** *69*, 2884-2887.

78. Ren, C.-T.; Tsai, Y.-H.; Yang, Y.-L.; Wu, S.-H., *J. Org. Chem.* **2007,** *72* (14), 5427-5430.

79. Keliris, A.; Ziegler, T.; Mishra, R.; Pohmann, R.; Sauer, M. G.; Ugurbil, K.; Engelmann, J., *Bioorg. Med. Chem.* **2011,** *19* (8), 2529-2540.

80. Jin, Y.; Hada, N.; Oka, J.; Kanie, O.; Daikoku, S.; Kanie, Y.; Yamada, H.; Takeda, T., *Chem. Pharm. Bull.* **2006,** *54* (4), 485-492.

81. Ogawa, S.; Maruyama, A.; Odagiri, T.; Yuasa, H.; Hashimoto, H., *Eur. J. Org. Chem.* **2001,** (5), 967-974.

82. Ogawa, S.; Aoyama, H.; Sato, T., *Carb. Res.* **2002,** *337* (21-23), 1979-1992.

# Claims to Original Research

1) Synthesis and IRI analysis of mixed α/β-amino acid containing glycopeptides (**201-206**).
2) Development of conditions appropriate for the application of CuAAC conditions to Wang resin-supported peptides; the application of this methodology to the synthesis of triazole-containing glycopeptides (**209**-**211**, **213-221**), and the IRI analysis of these glycopetides.
3) Investigation into the effect of disaccharide regio- and stereochemistry on IRI activity through the synthesis and IRI analysis of various 1-1 and a 1-3 linked galactosyl-galactose derivatives.
4) Investigation into the effect of modifying the electronics of the anomeric oxygen on IRI activity through the preparation of anomerically aryl-substituted galactose derivatives and the analysis thereof.
5) Investigation into the IRI activity of truncated analogues of **118** through the synthesis of a variety of functionalized derivatives and, especially, the re-discovery of the potent IRI activity of hydrogelators to demonstrate the feasibility of small molecule inhibitors of ice recrystallization.
6) Investigations into applying known approaches towards the synthesis of carbasugar-containing glycopeptide **231** and the preparation and IRI analysis of carbasugars **232**-**234**, for the determination of the role of the endocyclic oxygen to IRI activity.

# Publications (Published and submitted as of submission of thesis)

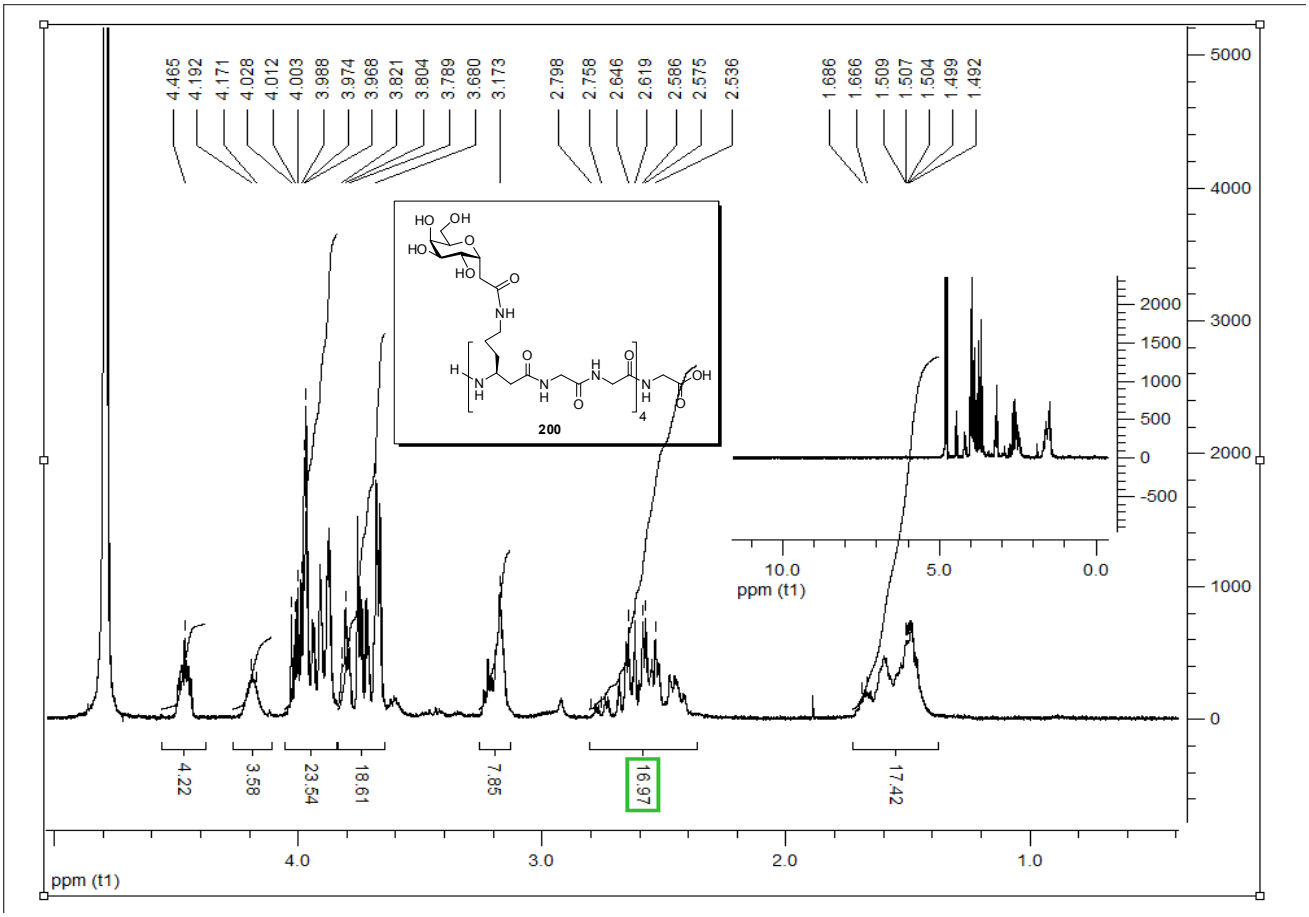
1. Capicciotti, C. J.; **Trant, J. F**.; Leclère, M.; Ben, R. N. "Synthesis of C-Linked Triazole-Containing AFGP Analogues and Their Ability to Inhibit Ice Recrystallization." *Bioconjugate Chemistry* **2011,** *22* (4), 605-616.

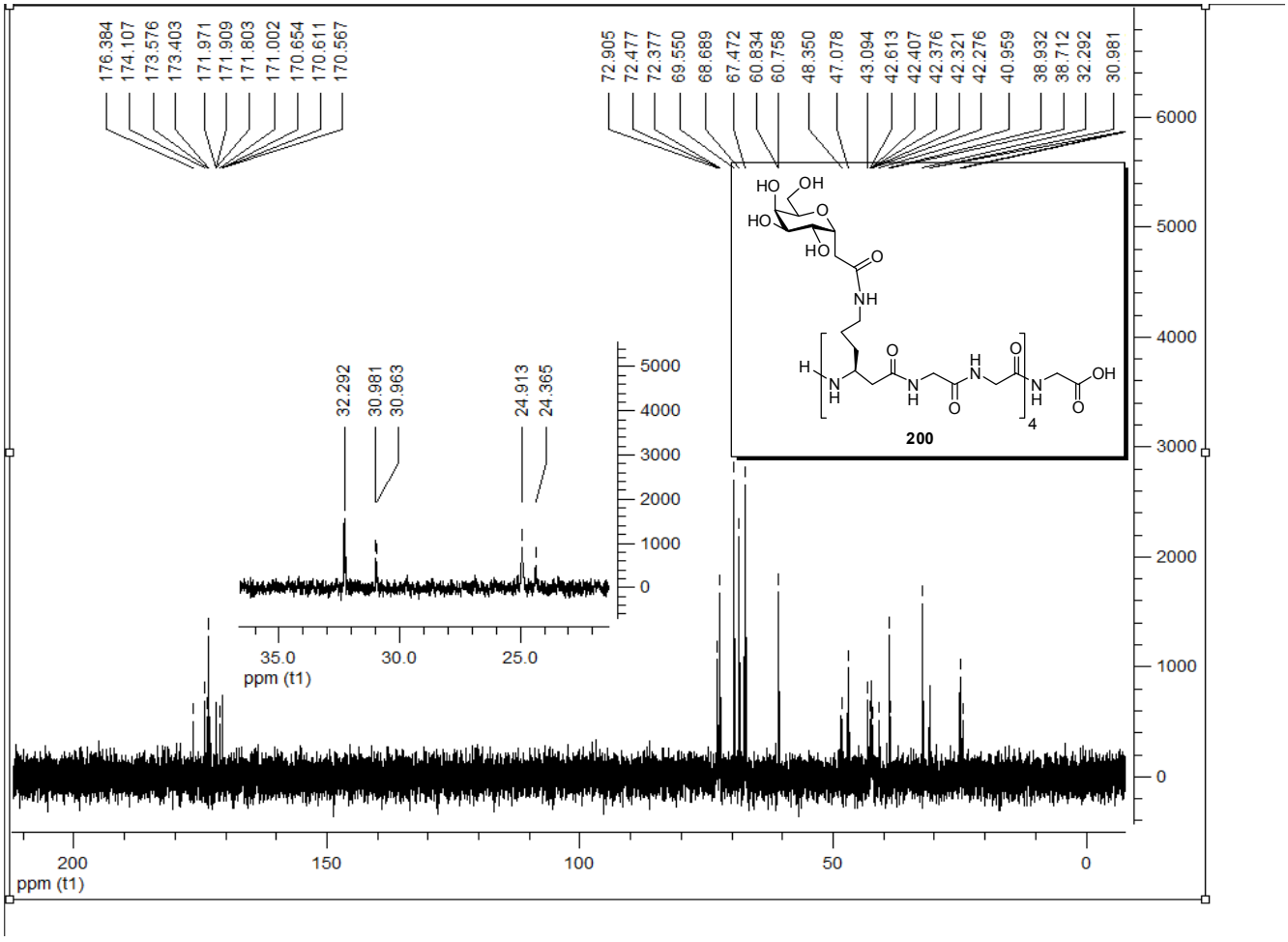
2. Balcerzak, A. K.; Ferreira, S.S.; **Trant, J.F.**; Ben, R.N. “Structurally Diverse Disaccharide Analogs of Antifreeze Glycoproteins and Their Ability to Inhibit Ice Recrystallization.” *Bioorganic and Medicinal Chemistry Letters* **2012**, *22* (4), 1719-1721.

# Supplementary Spectral Data

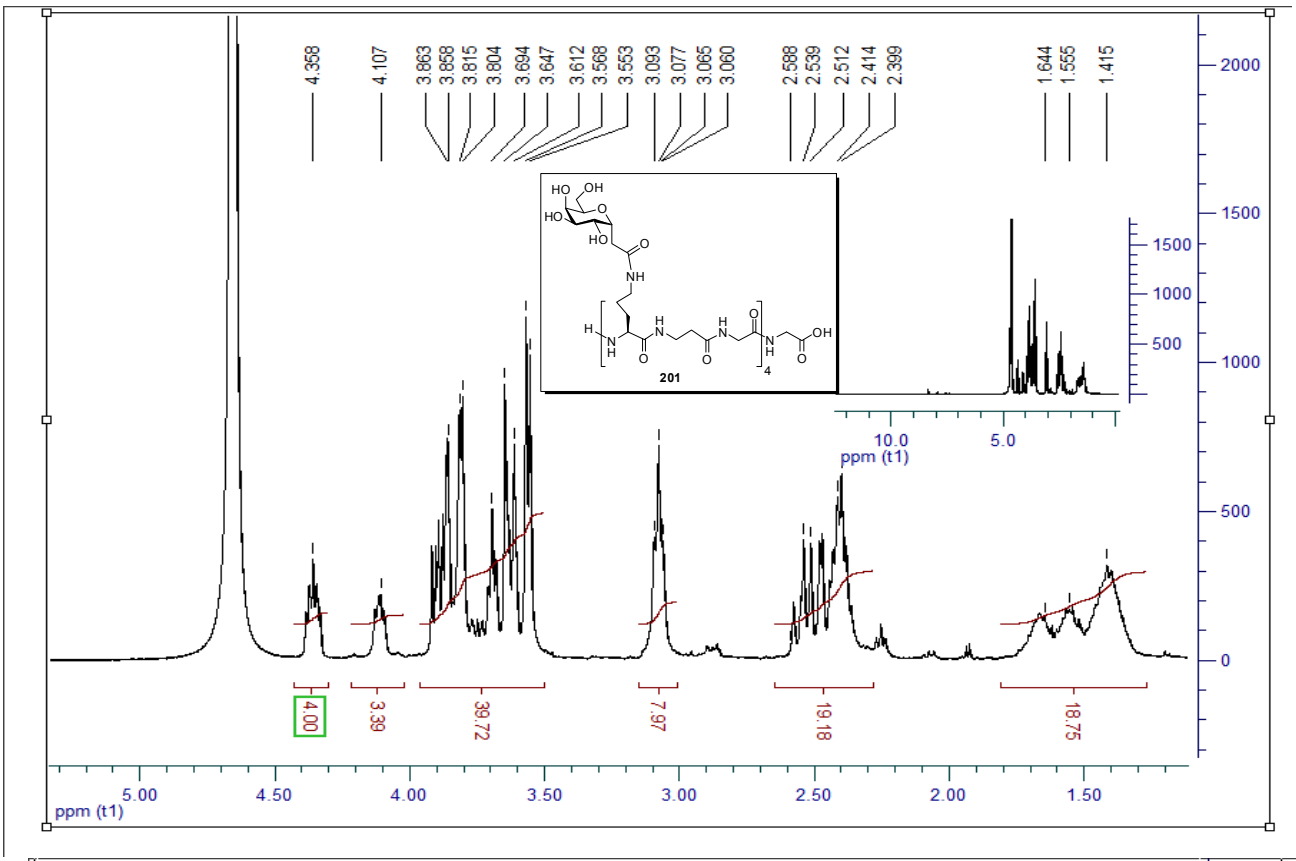
$^{1}H$ and $^{13}C$ spectra are provided for previously unpublished compounds, published compounds with poor or no available spectral data, and key compounds; all other compounds have references to the published spectra provided in the experimental section above.

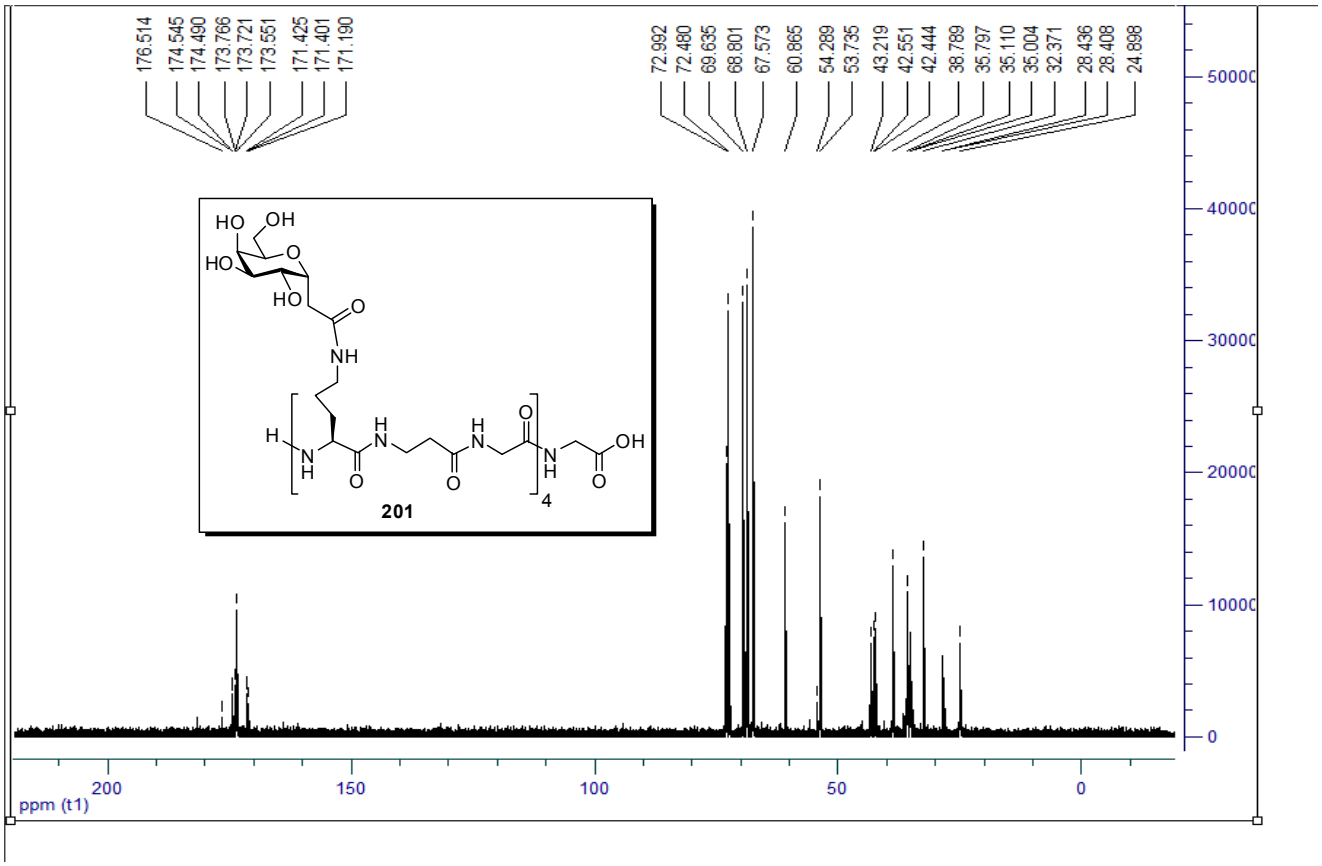
488a

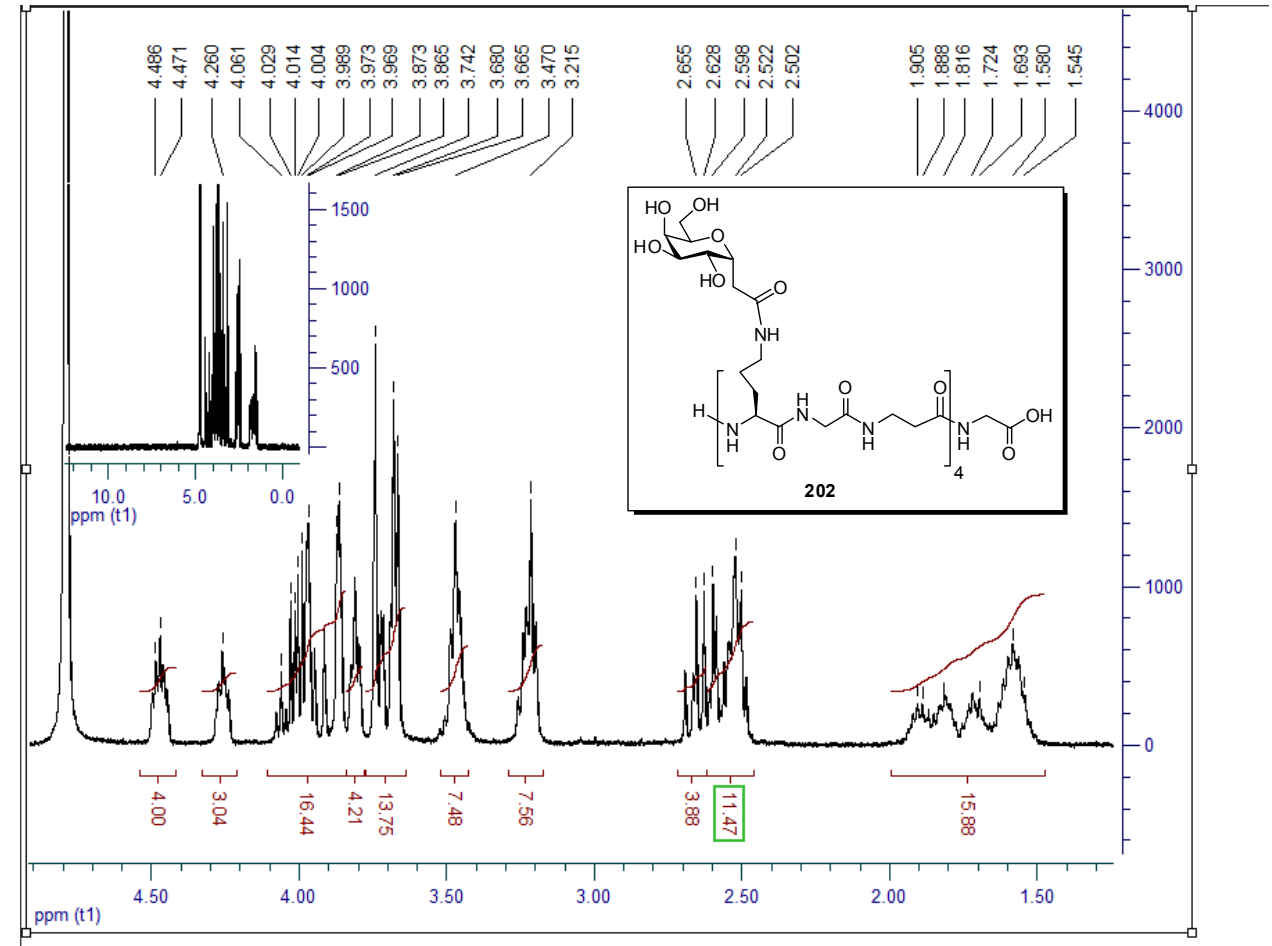

4.465
4.192
4.171
4.028
4.012
4.003
3.988
3.974
3.968
3.821
3.804
3.789
3.680
3.173
2.798
2.758
2.646
2.619
2.586
2.575
2.536
1.686
1.666
1.509
1.507
1.504
1.499
1.492
200
4.22
3.58
23.54
18.61
7.85
16.97
17.42
ppm (t1)

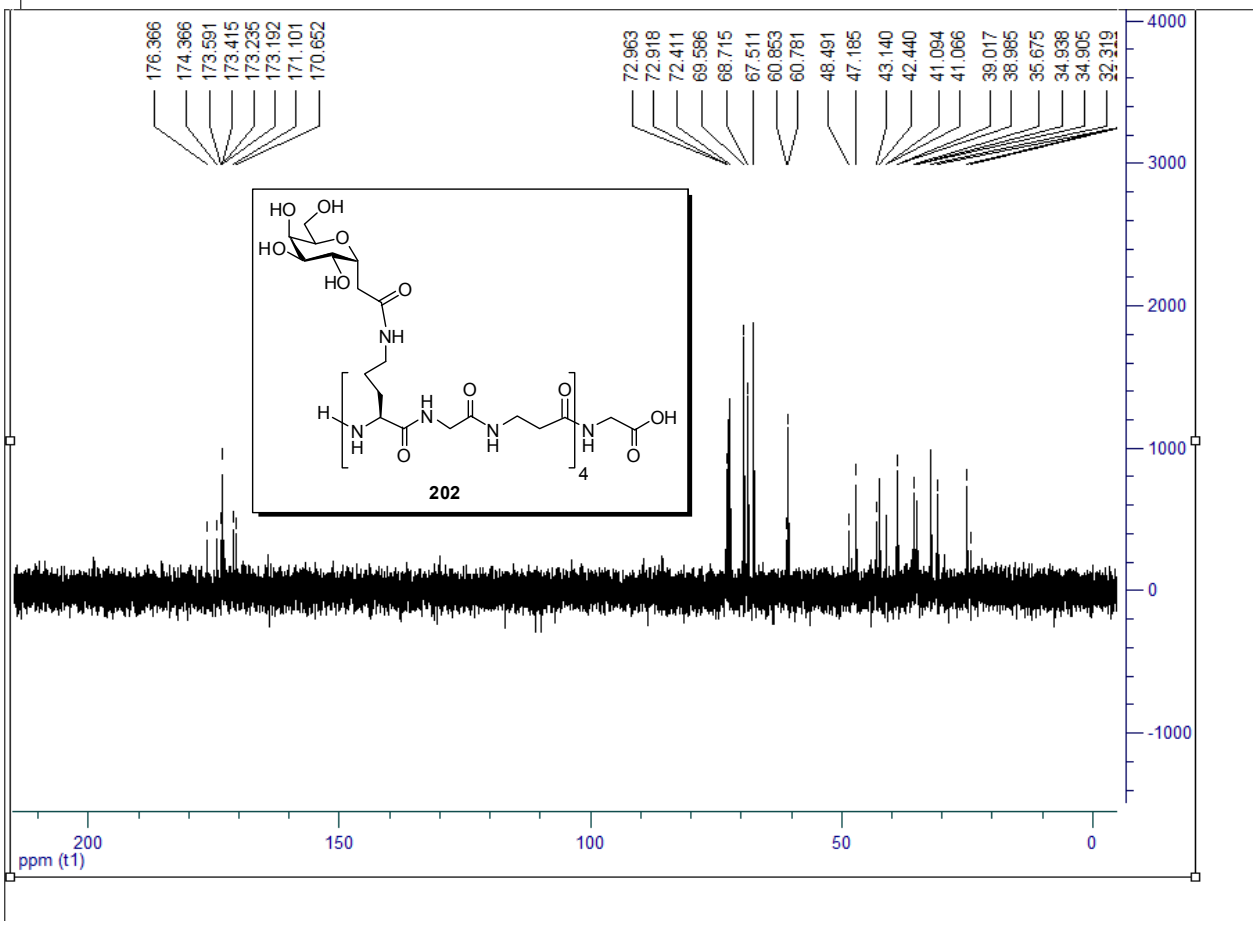

176.384
174.107
173.576
173.403
171.971
171.909
171.803
171.002
170.654
170.611
170.567
72.905
72.477
72.377
69.550
68.689
67.472
60.834
60.758
48.350
47.078
43.094
42.613
42.407
42.376
42.321
42.276
40.959
38.932
38.712
32.292
30.981
32.292
30.981
30.963
24.913
24.365
200
ppm (t1)

488b

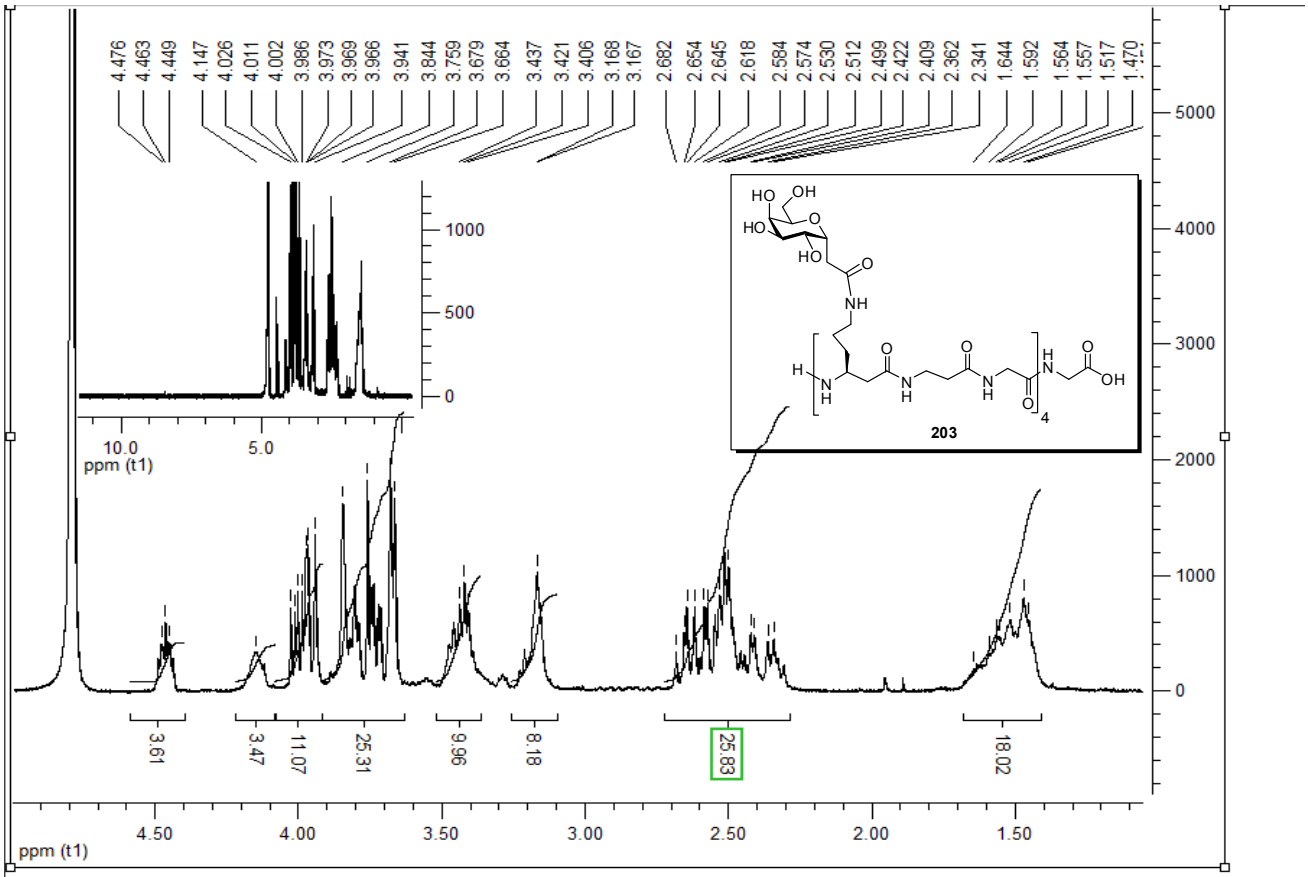

4.358
4.107
3.863
3.858
3.815
3.804
3.694
3.647
3.612
3.568
3.553
3.093
3.077
3.065
3.060
2.588
2.539
2.512
2.414
2.399
1.644
1.555
1.415
201
4.00
3.39
39.72
7.97
19.18
18.75
ppm (t1)

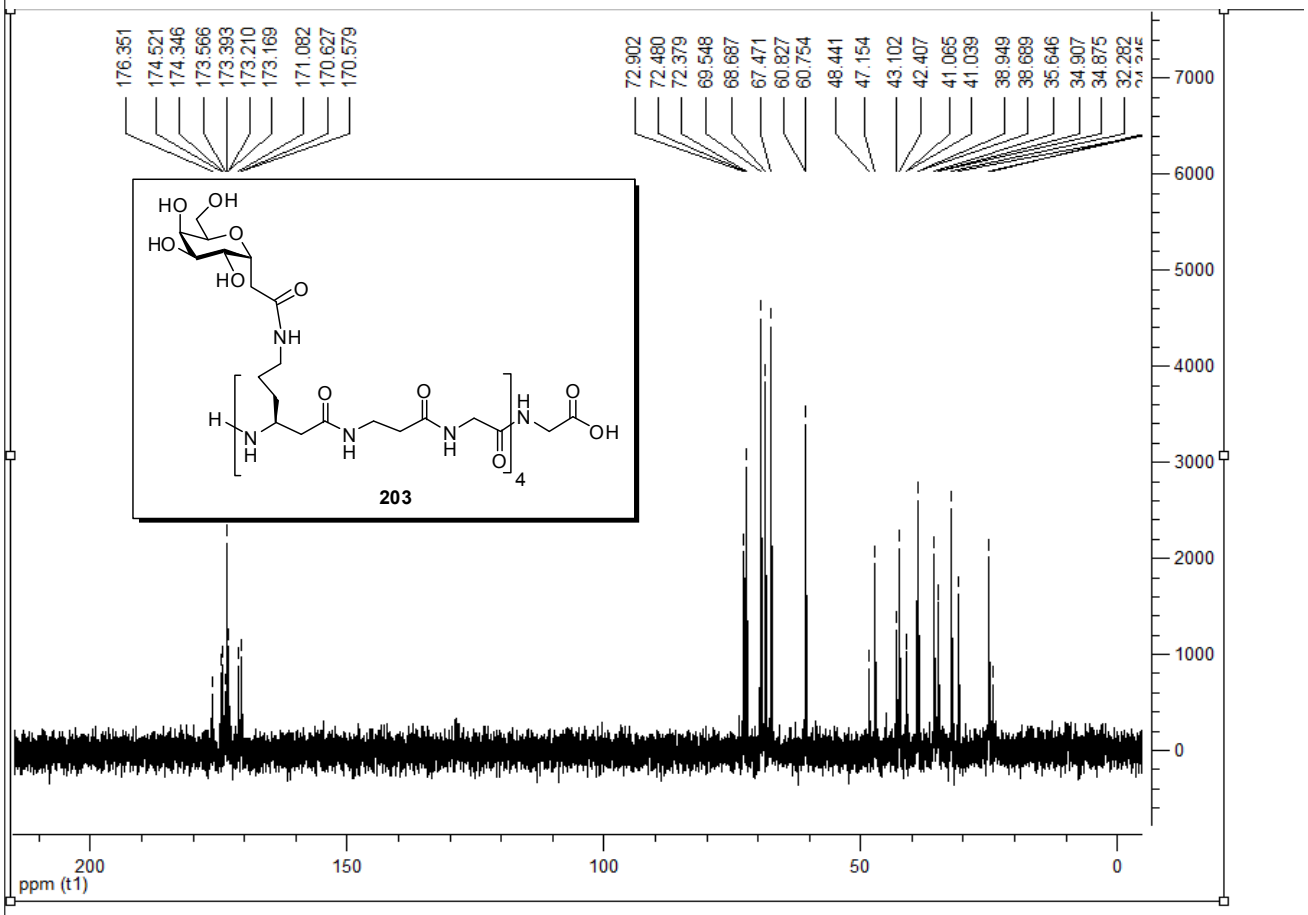

176.514
174.545
174.490
173.766
173.721
173.551
171.425
171.401
171.190
72.992
72.480
69.635
68.801
67.573
60.865
54.289
53.735
43.219
42.551
42.444
38.789
35.797
35.110
35.004
32.371
28.436
28.408
24.898
201
ppm (t1)


4.486
4.471
4.260
4.061
4.029
4.014
4.004
3.989
3.973
3.969
3.873
3.865
3.742
3.680
3.665
3.470
3.215
2.655
2.628
2.598
2.522
2.502
1.905
1.888
1.816
1.724
1.693
1.580
1.545
HO
OH
O
HO
HO
O
NH
H
N
H
O
N
H
O
O
N
H
O
N
H
O
OH
4
202
ppm (t1)
4.00
3.04
19.44
4.21
13.75
7.48
7.55
3.88
11.47
15.88
4.50
4.00
3.50
3.00
2.50
2.00
1.50

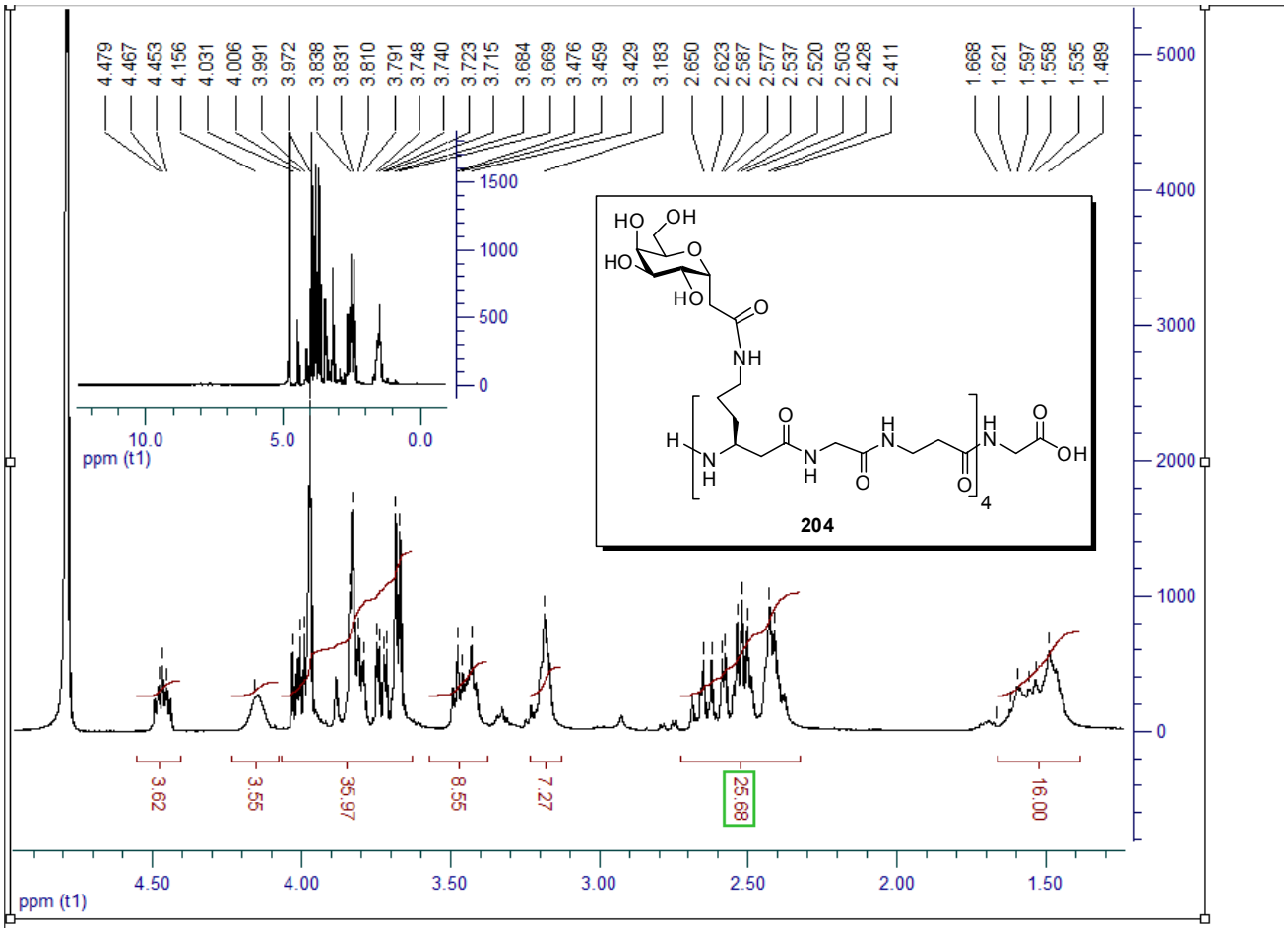

176.366
174.366
173.591
173.415
173.235
173.192
171.101
170.652
72.963
72.918
72.411
69.586
68.715
67.511
60.853
60.781
48.491
47.185
43.140
42.440
41.094
41.066
39.017
38.985
35.675
34.938
34.905
32.319
HO
OH
O
HO
HO
O
NH
H
N
H
O
N
H
O
O
N
H
O
N
H
O
OH
4
202
ppm (t1)
200
150
100
50
0

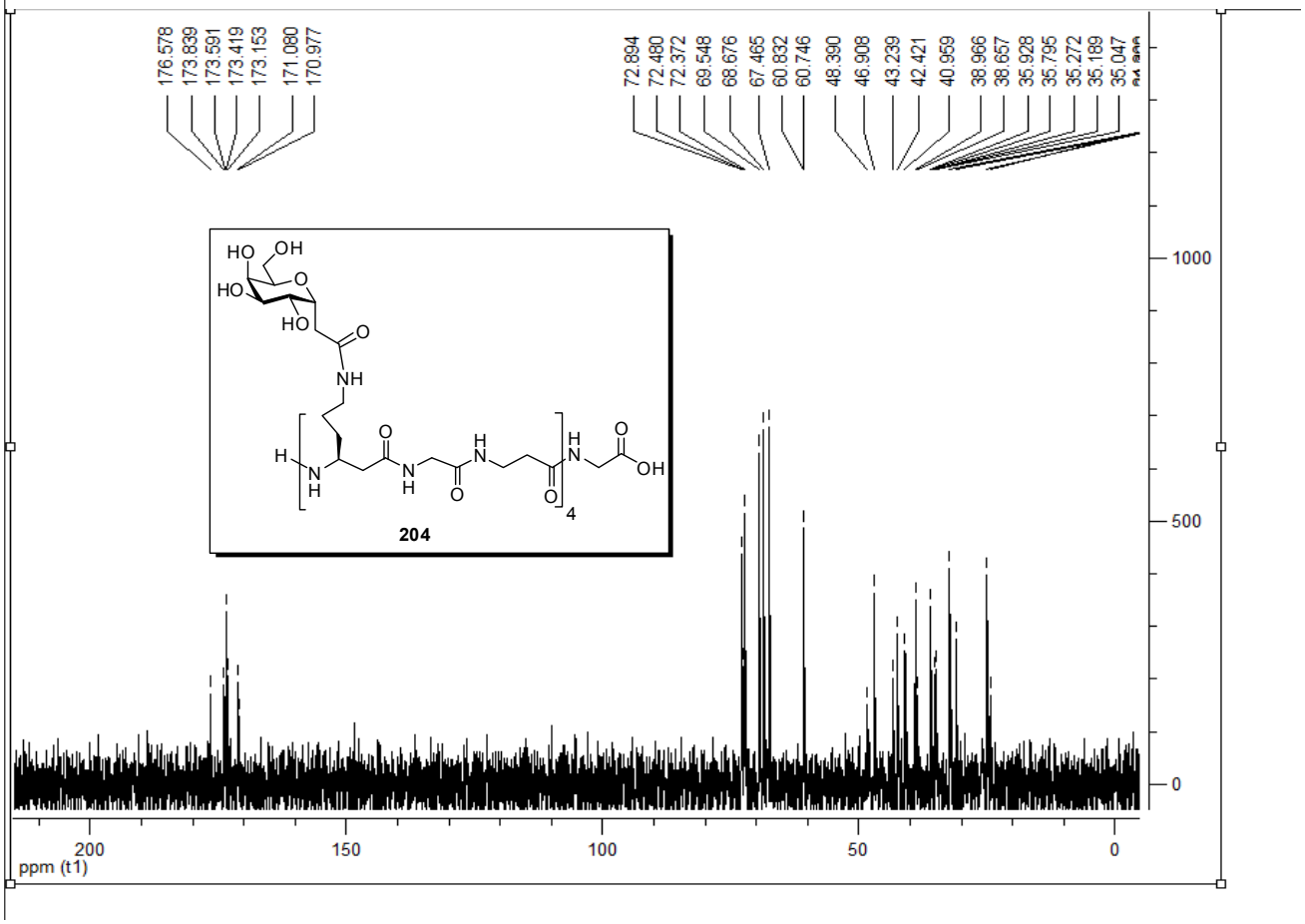
488d


4.476
4.463
4.449
4.147
4.026
4.011
4.002
3.986
3.973
3.969
3.966
3.941
3.844
3.759
3.679
3.664
3.437
3.421
3.406
3.168
3.167
2.682
2.654
2.645
2.618
2.584
2.574
2.530
2.512
2.499
2.422
2.409
2.362
2.341
1.644
1.592
1.564
1.557
1.517
1.470
10.0
5.0
ppm (t1)
203
3.61
3.47
11.07
25.31
9.96
8.18
25.83
18.02
4.50
4.00
3.50
3.00
2.50
2.00
1.50
ppm (t1)

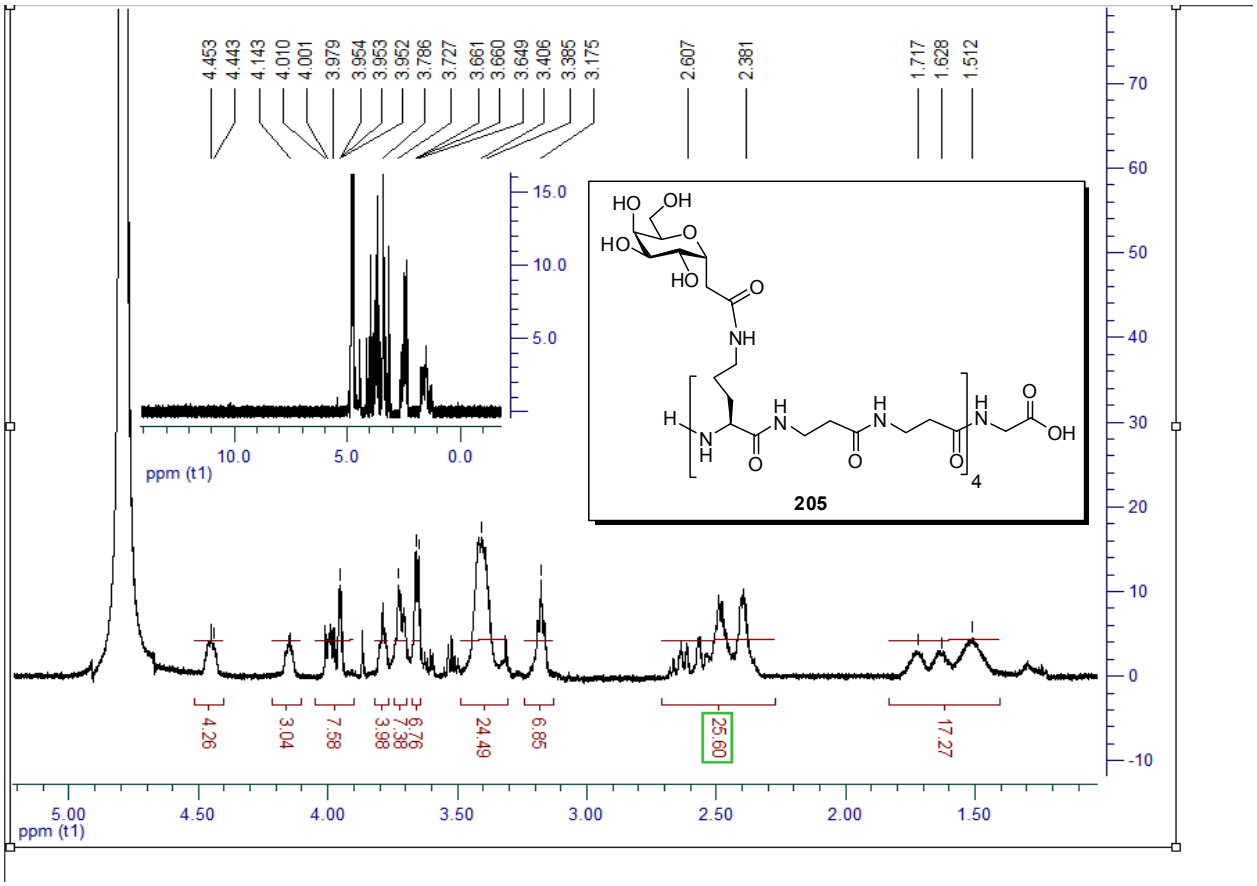

176.351
174.521
174.346
173.566
173.393
173.210
173.169
171.082
170.627
170.579
72.902
72.480
72.379
69.548
68.687
67.471
60.827
60.754
48.441
47.154
43.102
42.407
41.065
41.039
38.949
38.689
35.646
34.907
34.875
32.282
203
200
150
100
50
0
ppm (t1)

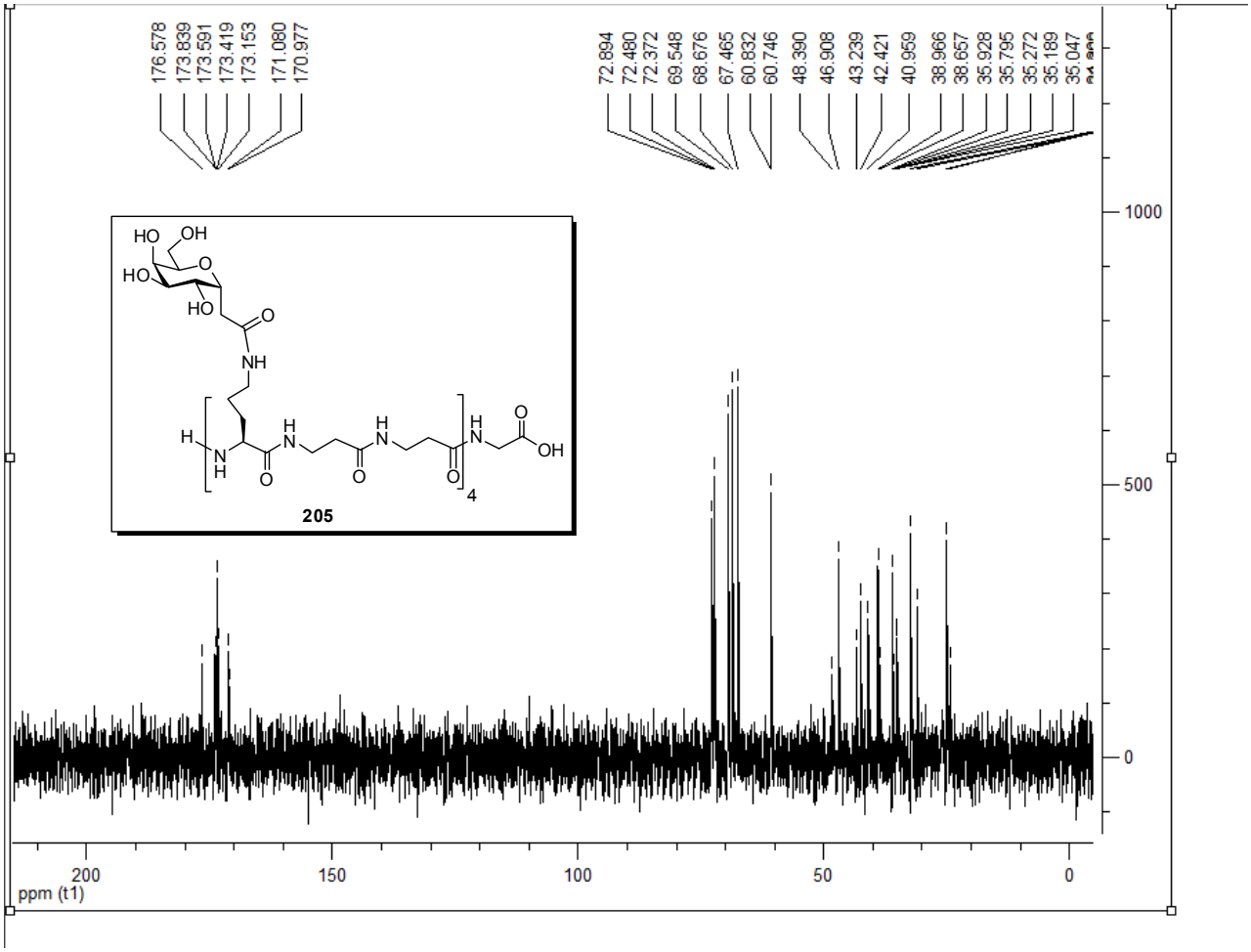
488e


4.479
4.467
4.453
4.156
4.031
4.006
3.991
3.972
3.838
3.831
3.810
3.791
3.748
3.740
3.723
3.715
3.684
3.669
3.476
3.459
3.429
3.183
2.650
2.623
2.587
2.577
2.537
2.520
2.503
2.428
2.411
1.668
1.621
1.597
1.558
1.535
1.489
ppm (t1)
3.62
3.55
36.97
8.55
7.27
25.68
16.00
4.50
4.00
3.50
3.00
2.50
2.00
1.50
204

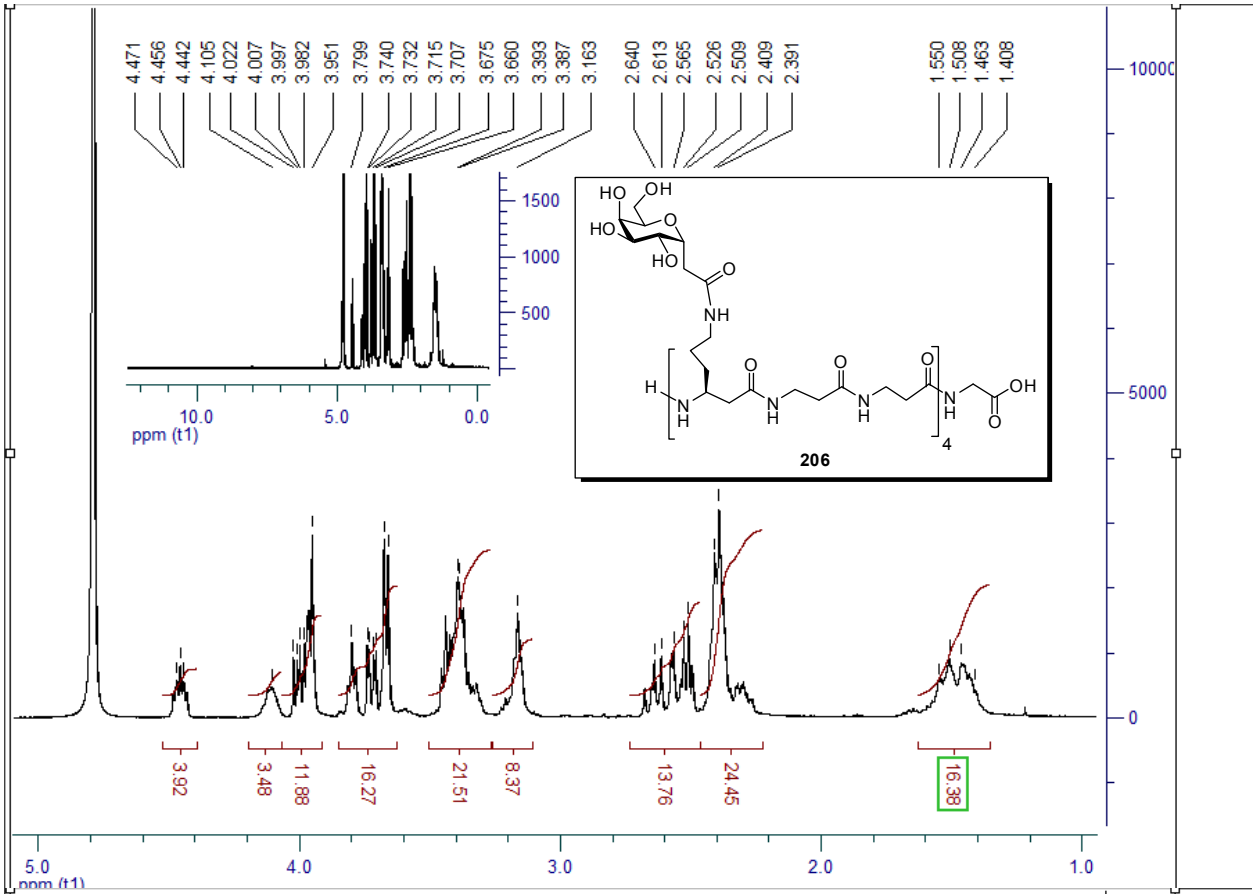

176.578
173.839
173.591
173.419
173.153
171.080
170.977
72.894
72.480
72.372
69.548
68.676
67.465
60.832
60.746
48.390
46.908
43.239
42.421
40.959
38.966
38.657
35.928
35.795
35.272
35.189
35.047
ppm (t1)
200
150
100
50
0
204

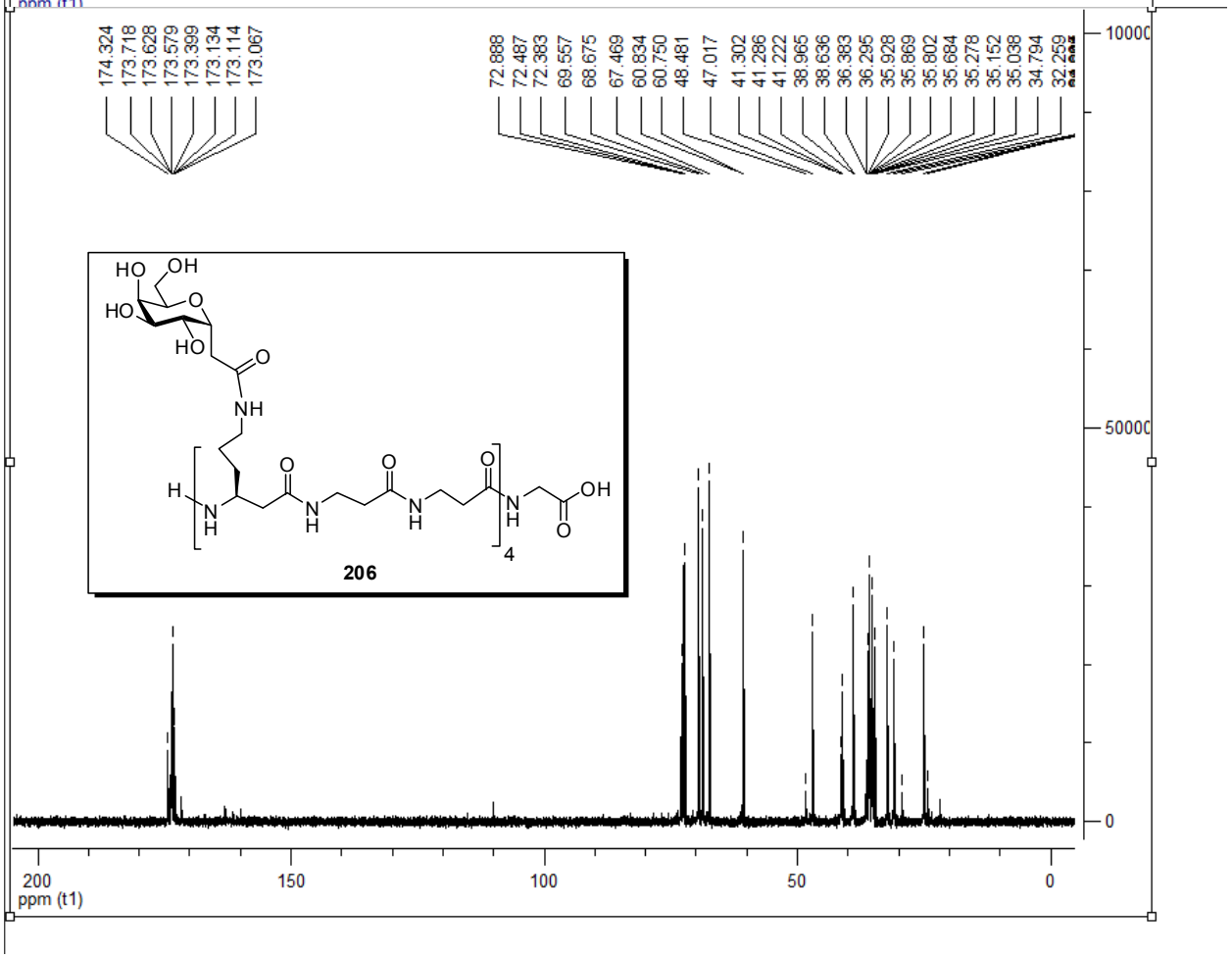
488f


4.453
4.443
4.143
4.010
4.001
3.979
3.954
3.953
3.952
3.786
3.727
3.661
3.660
3.649
3.406
3.385
3.175
2.607
2.381
1.717
1.628
1.512
205
ppm (t1)
4.26
3.04
7.58
3.98
3.88
7.76
2.49
6.86
25.60
17.27

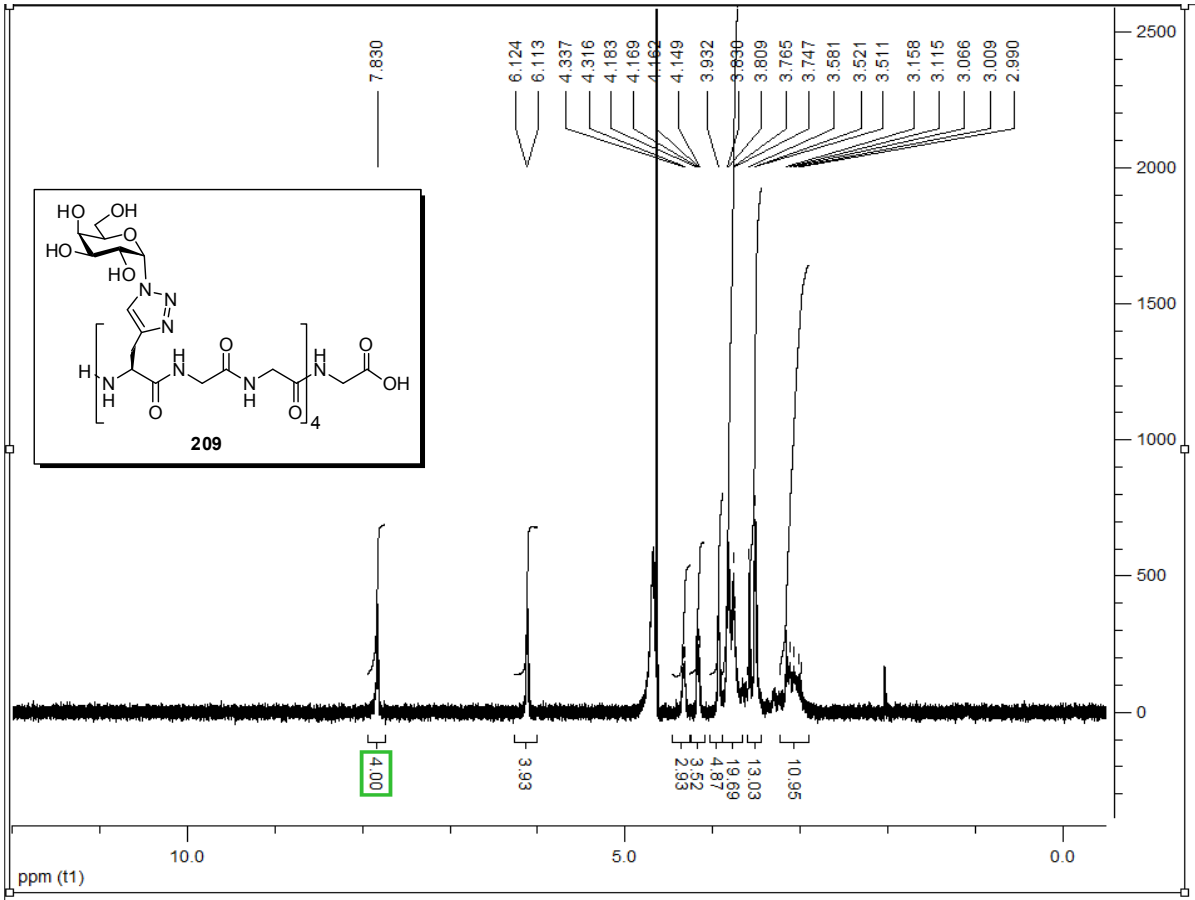

176.578
173.839
173.591
173.419
173.153
171.080
170.977
72.894
72.480
72.372
69.548
68.676
67.465
60.832
60.746
48.390
46.908
43.239
42.421
40.959
38.966
38.657
35.928
35.795
35.272
35.189
35.047
205
ppm (t1)

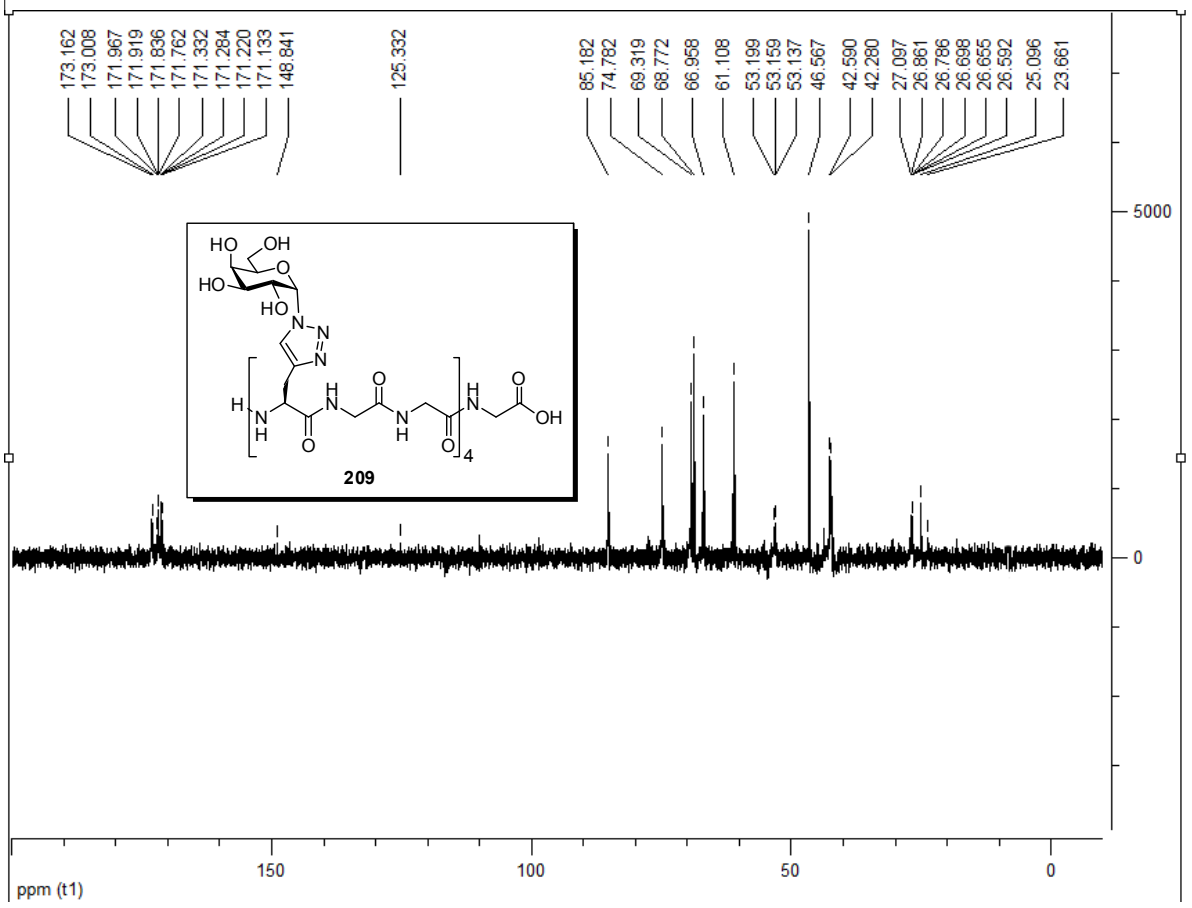
488g


4.471
4.456
4.442
4.105
4.022
4.007
3.997
3.982
3.951
3.799
3.740
3.732
3.715
3.707
3.675
3.660
3.393
3.387
3.163
2.640
2.613
2.565
2.526
2.509
2.409
2.391
1.550
1.508
1.463
1.408
ppm (t1)
206
3.92
3.48
11.88
16.27
21.51
8.37
13.76
24.45
16.38
ppm (t1)

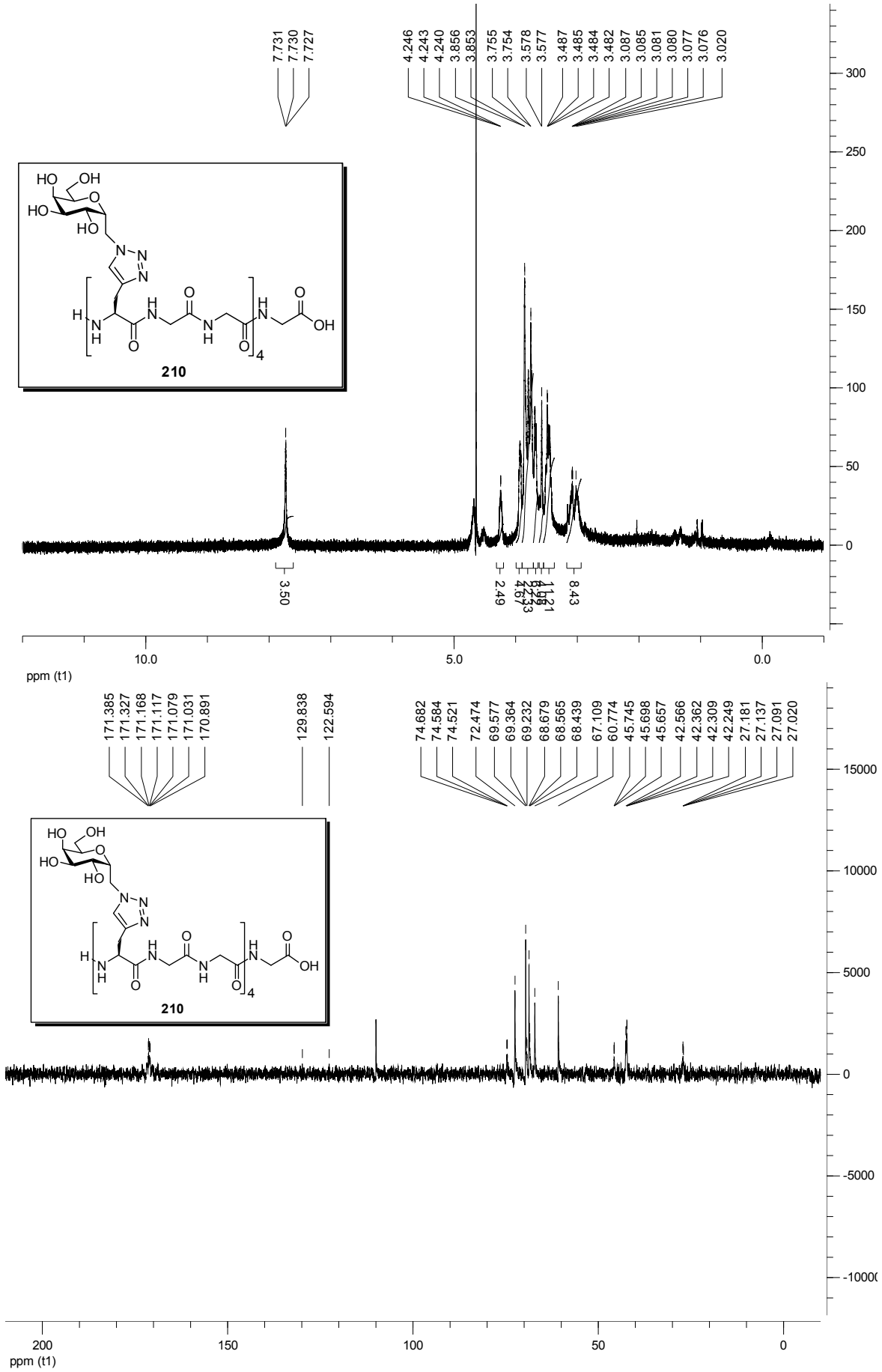

174.324
173.718
173.628
173.579
173.399
173.134
173.114
173.067
72.888
72.487
72.383
69.557
68.675
67.469
60.834
60.750
48.481
47.017
41.302
41.286
41.222
38.965
38.636
38.383
36.295
35.928
35.869
35.802
35.684
35.278
35.152
35.038
34.794
32.259
206
ppm (t1)

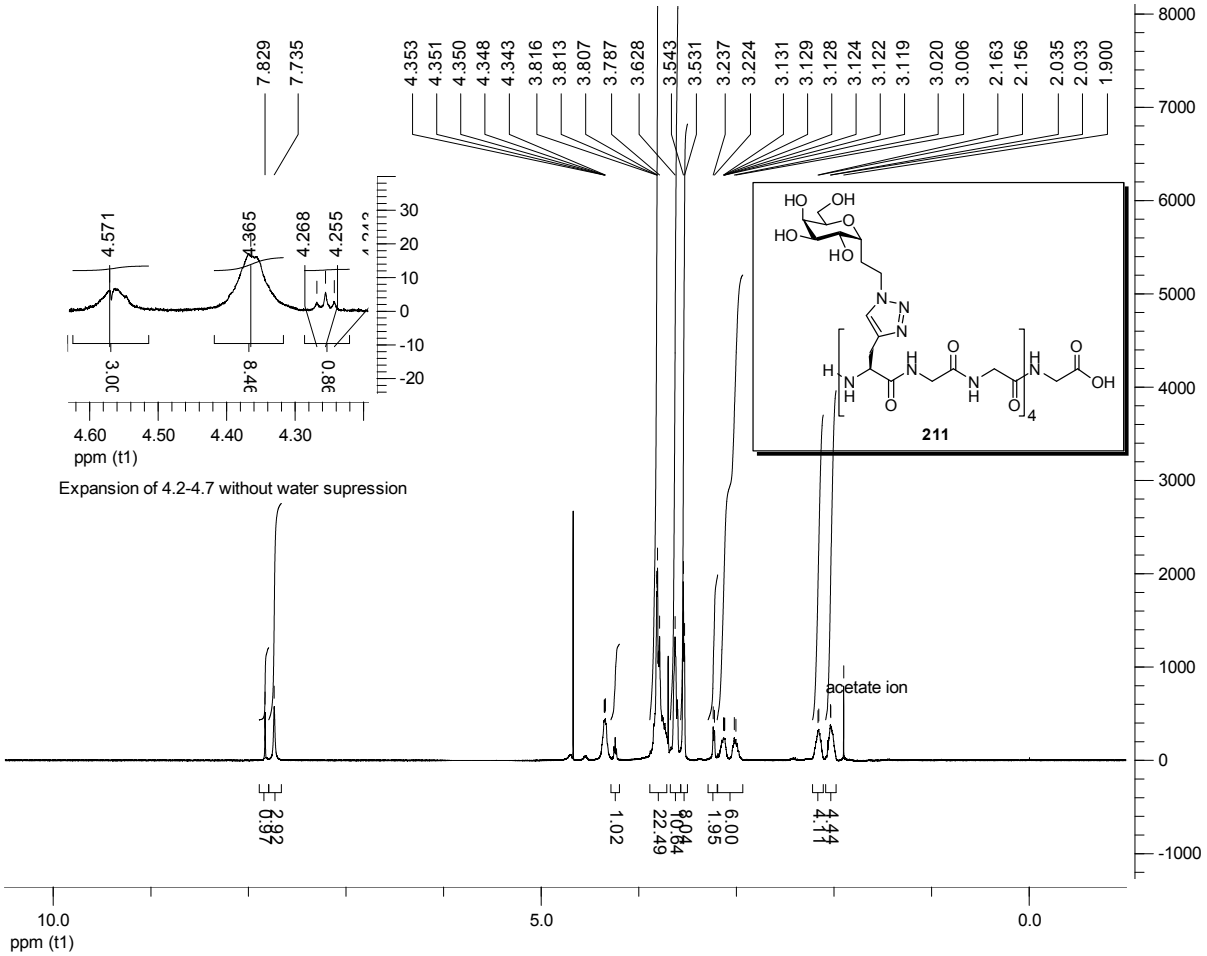
488i

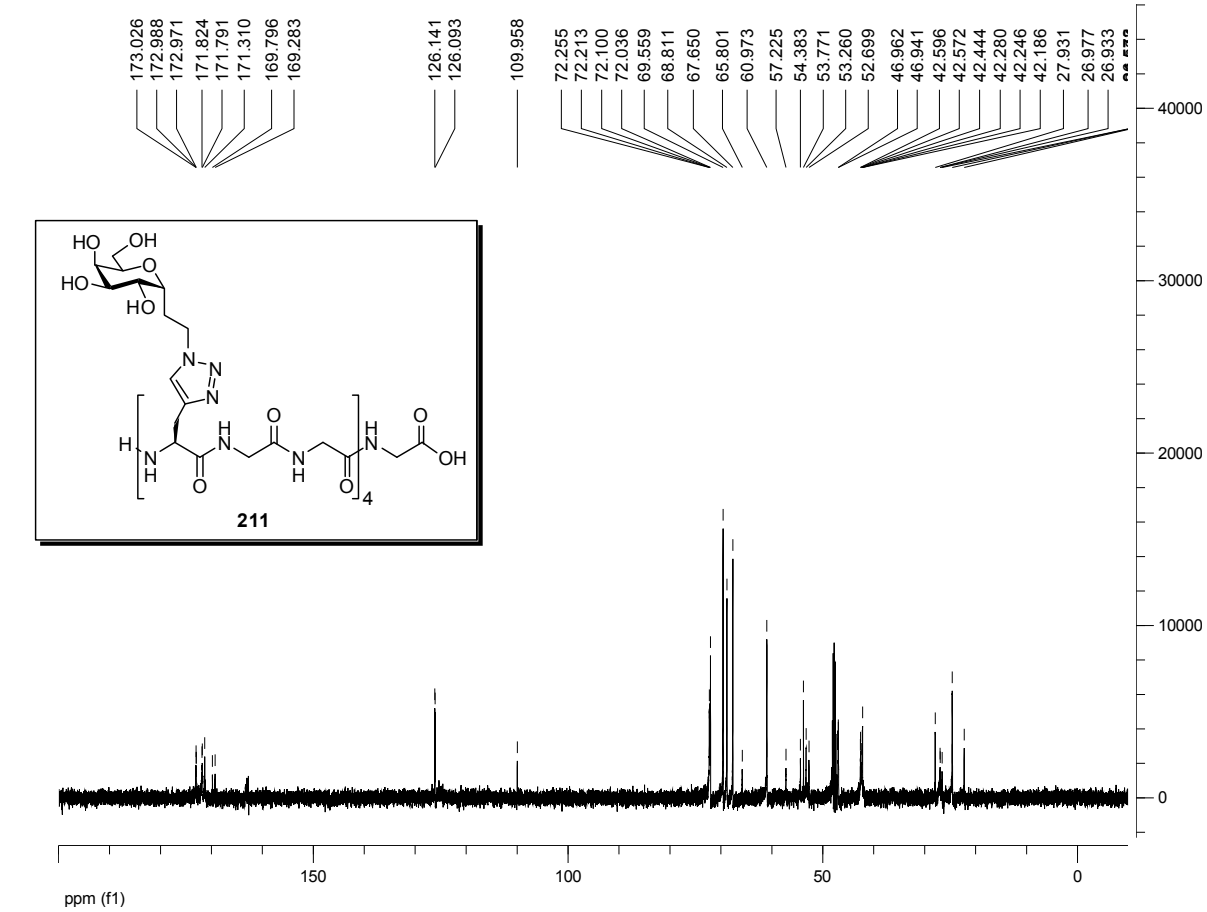

7.830
6.124
6.113
4.337
4.316
4.183
4.169
4.162
4.149
3.932
3.830
3.809
3.765
3.747
3.581
3.521
3.511
3.158
3.115
3.066
3.009
2.990
209
4.00
3.93
2.93
2.52
4.87
19.69
13.03
10.95
ppm (t1)

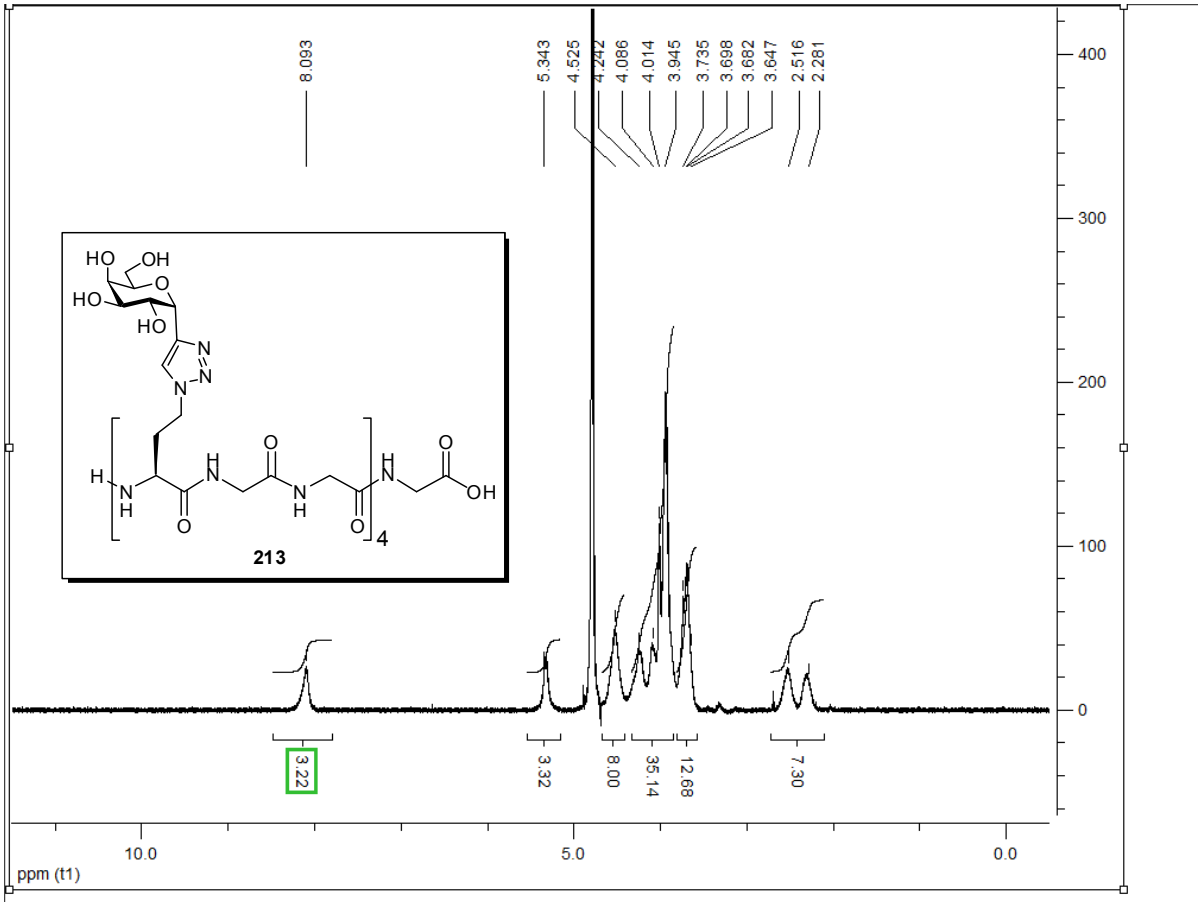

173.162
173.008
171.967
171.919
171.836
171.762
171.332
171.284
171.220
171.133
148.841
125.332
85.182
74.782
69.319
68.772
66.958
61.108
53.199
53.159
53.137
46.567
42.590
42.280
27.097
26.861
26.786
26.698
26.655
26.592
25.096
23.661
209
ppm (t1)

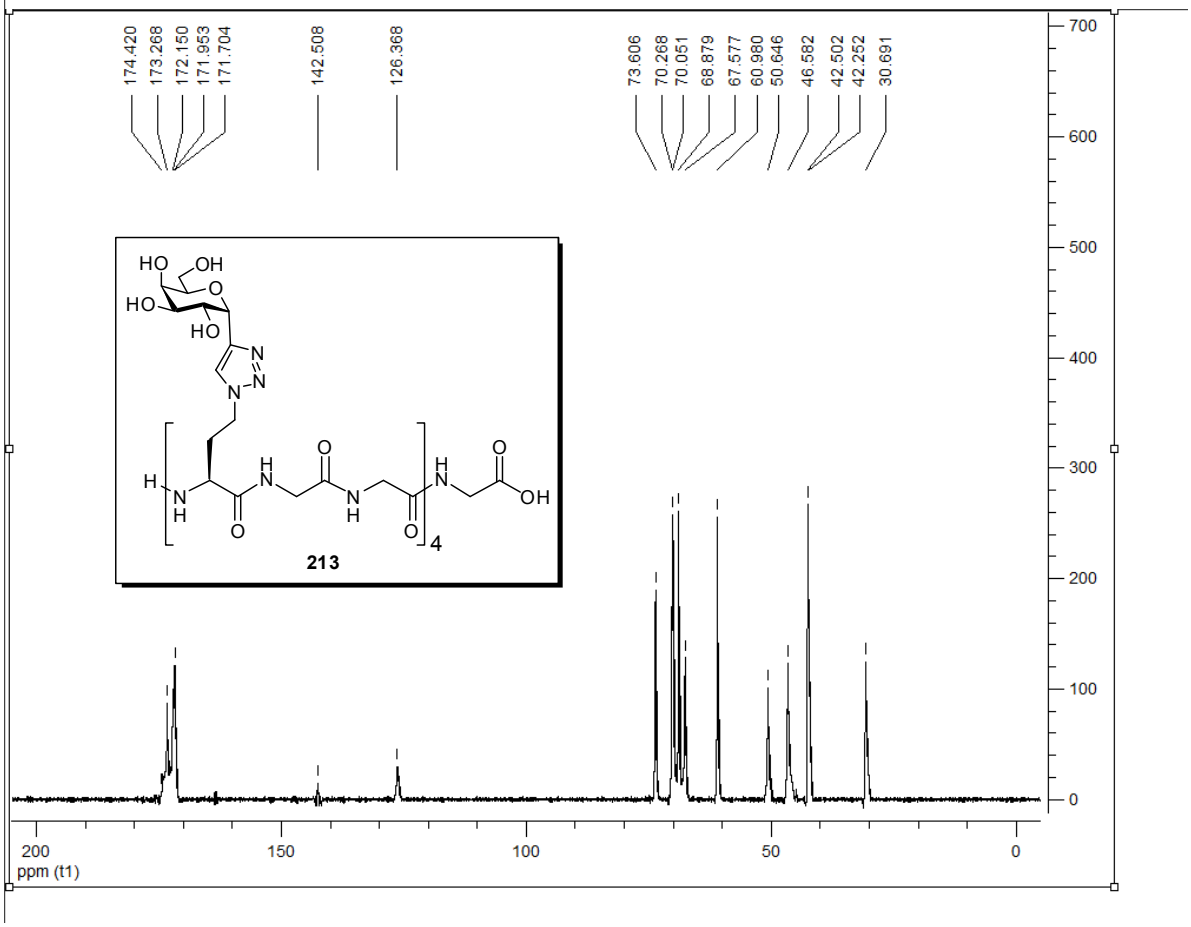
488j

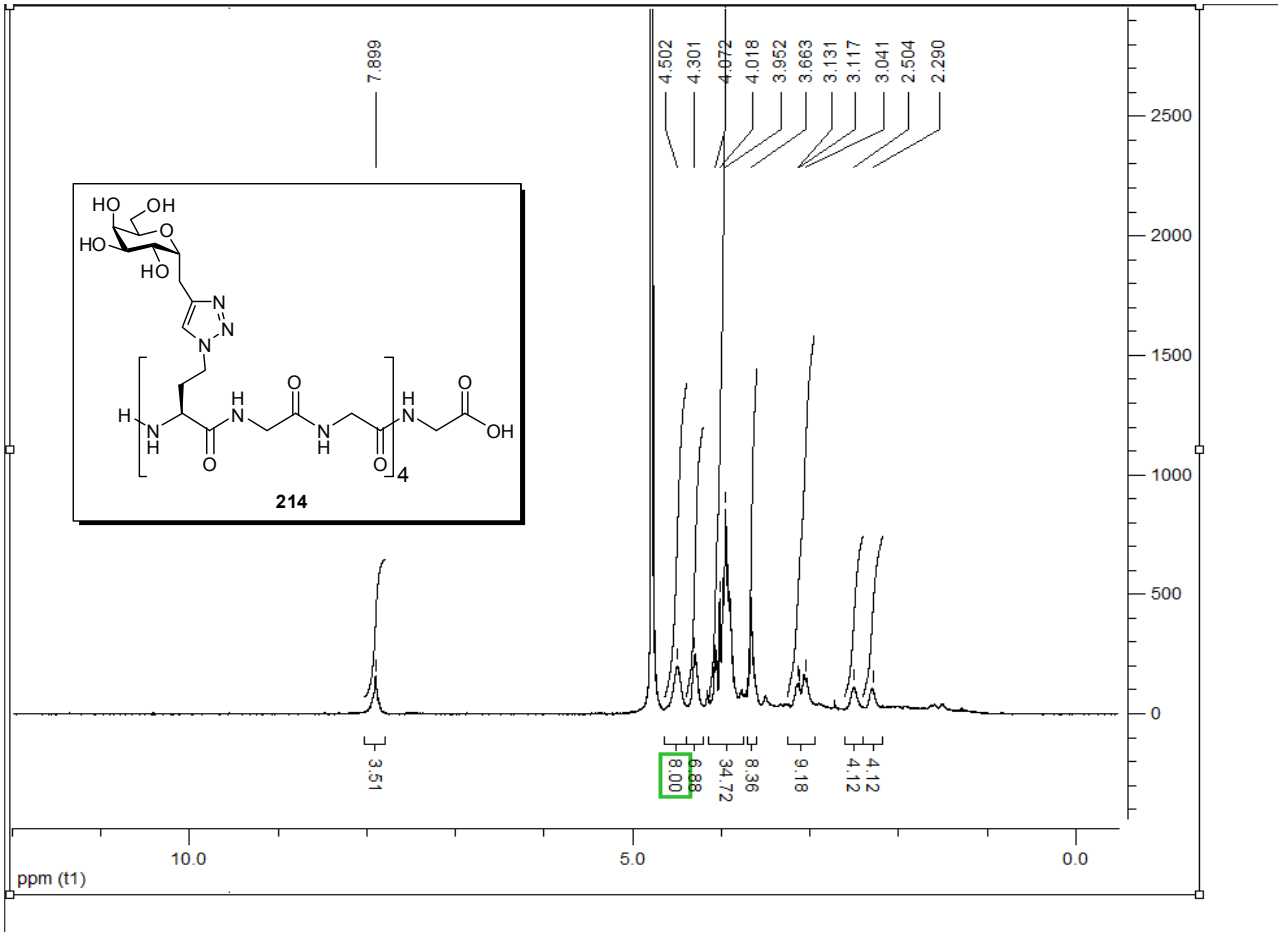

7.731
7.730
7.727
4.246
4.243
4.240
3.856
3.853
3.755
3.754
3.578
3.577
3.487
3.485
3.484
3.482
3.087
3.085
3.081
3.080
3.077
3.076
3.020
210
3.50
2.49
8.43
ppm (t1)
171.385
171.327
171.168
171.117
171.079
171.031
170.891
129.838
122.594
74.682
74.584
74.521
72.474
69.577
69.364
69.232
68.679
68.565
68.439
67.109
60.774
45.745
45.698
45.657
42.566
42.362
42.309
42.249
27.181
27.137
27.091
27.020
210
ppm (t1)

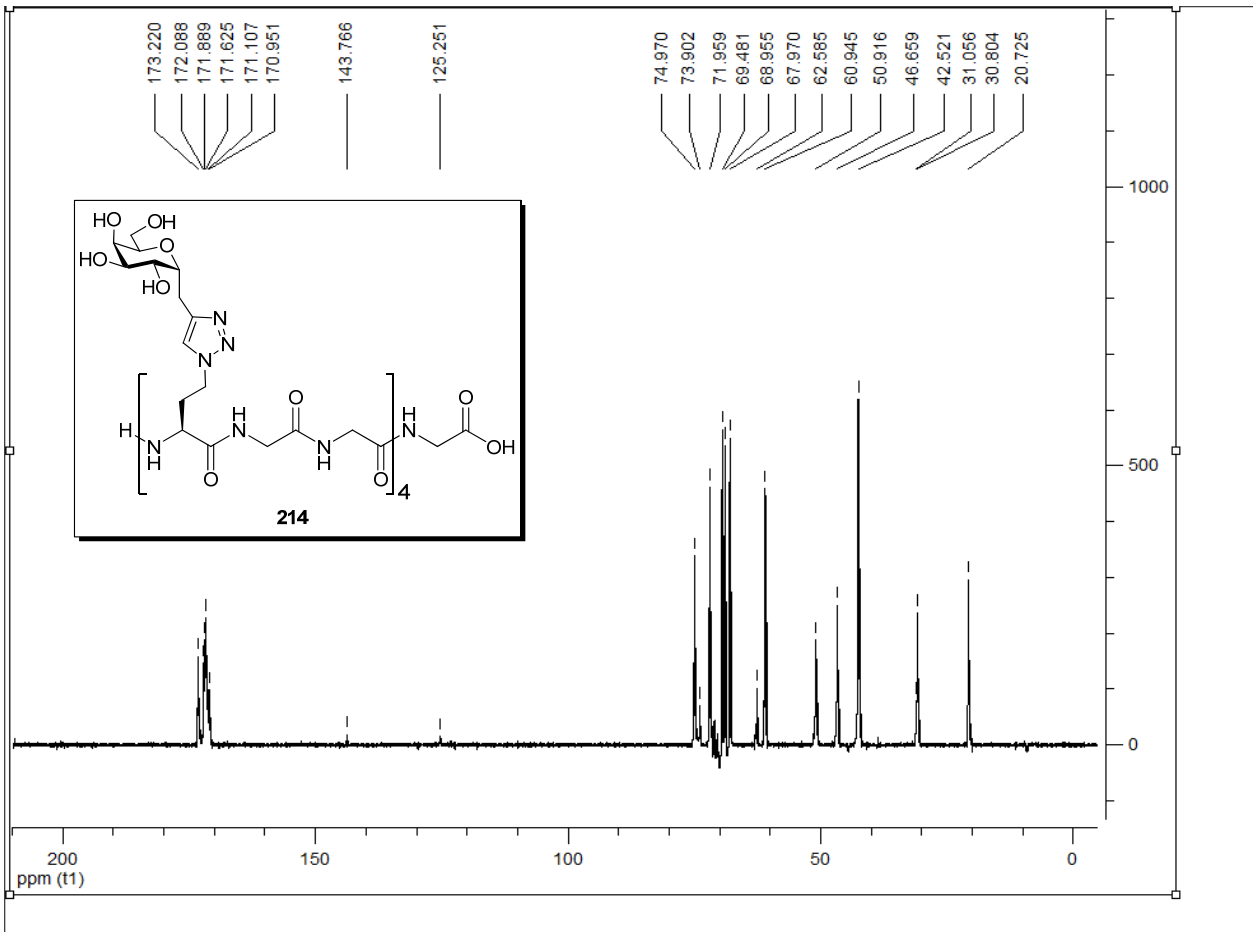

7.829
7.735
4.353
4.351
4.350
4.348
4.343
3.816
3.813
3.807
3.787
3.628
3.543
3.531
3.237
3.224
3.131
3.129
3.128
3.124
3.122
3.119
3.020
3.006
2.163
2.156
2.035
2.033
1.900
4.571
4.365
4.268
4.255
3.00
8.46
0.86
4.60
4.50
4.40
4.30
ppm (t1)
Expansion of 4.2-4.7 without water supression
HO
OH
O
HO
HO
N
N
N
H
N
H
O
H
N
O
H
N
O
OH
4
211
acetate ion
2.87
1.02
2.49
8.04
1.95
6.00
4.11
10.0
5.0
0.0
ppm (t1)

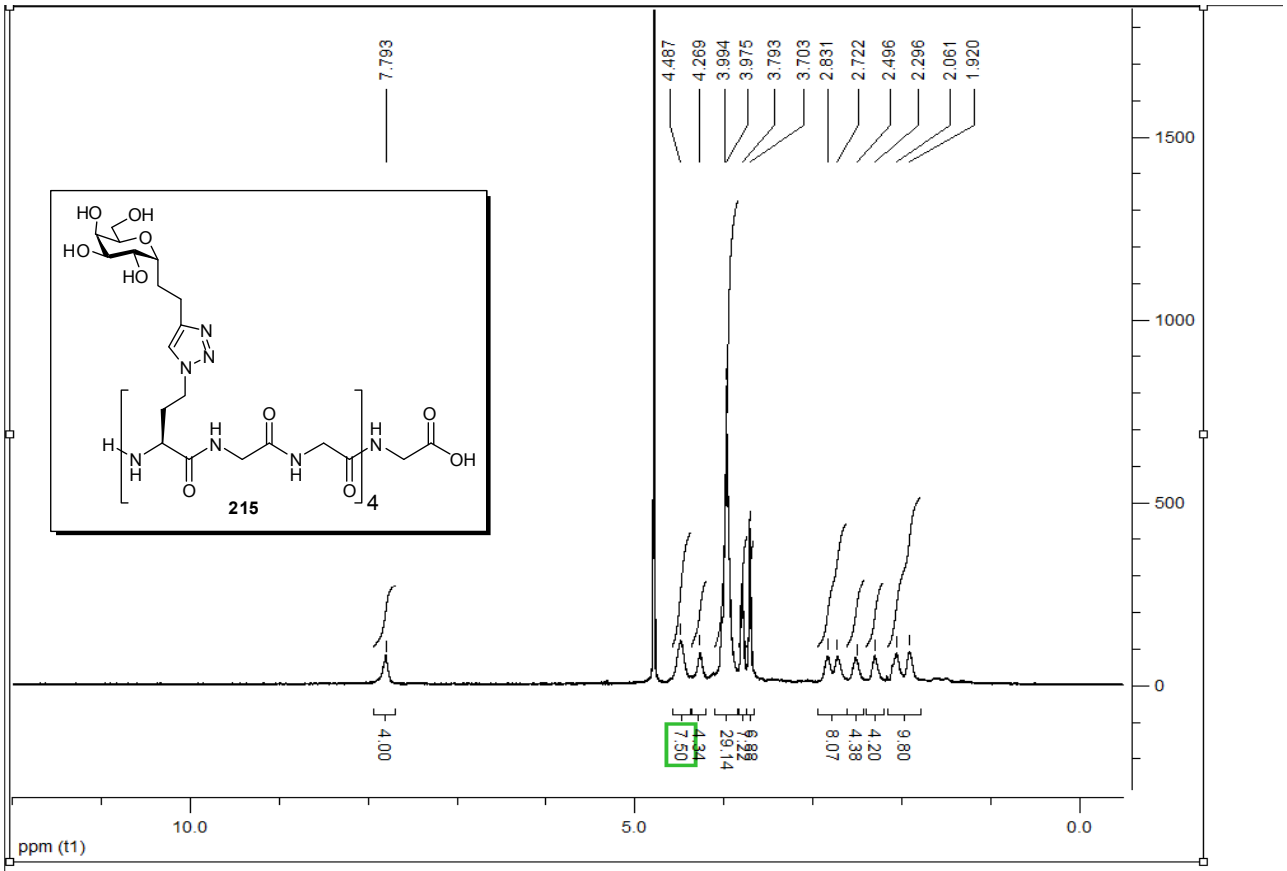

173.026
172.988
172.971
171.824
171.791
171.310
169.796
169.283
126.141
126.093
109.958
72.255
72.213
72.100
72.036
69.559
68.811
67.650
65.801
60.973
57.225
54.383
53.771
53.260
52.699
46.962
46.941
42.596
42.572
42.444
42.280
42.246
42.186
27.931
26.977
26.933
HO
OH
O
HO
HO
N
N
N
H
N
H
O
H
N
O
H
N
O
OH
4
211
150
100
50
0
ppm (f1)

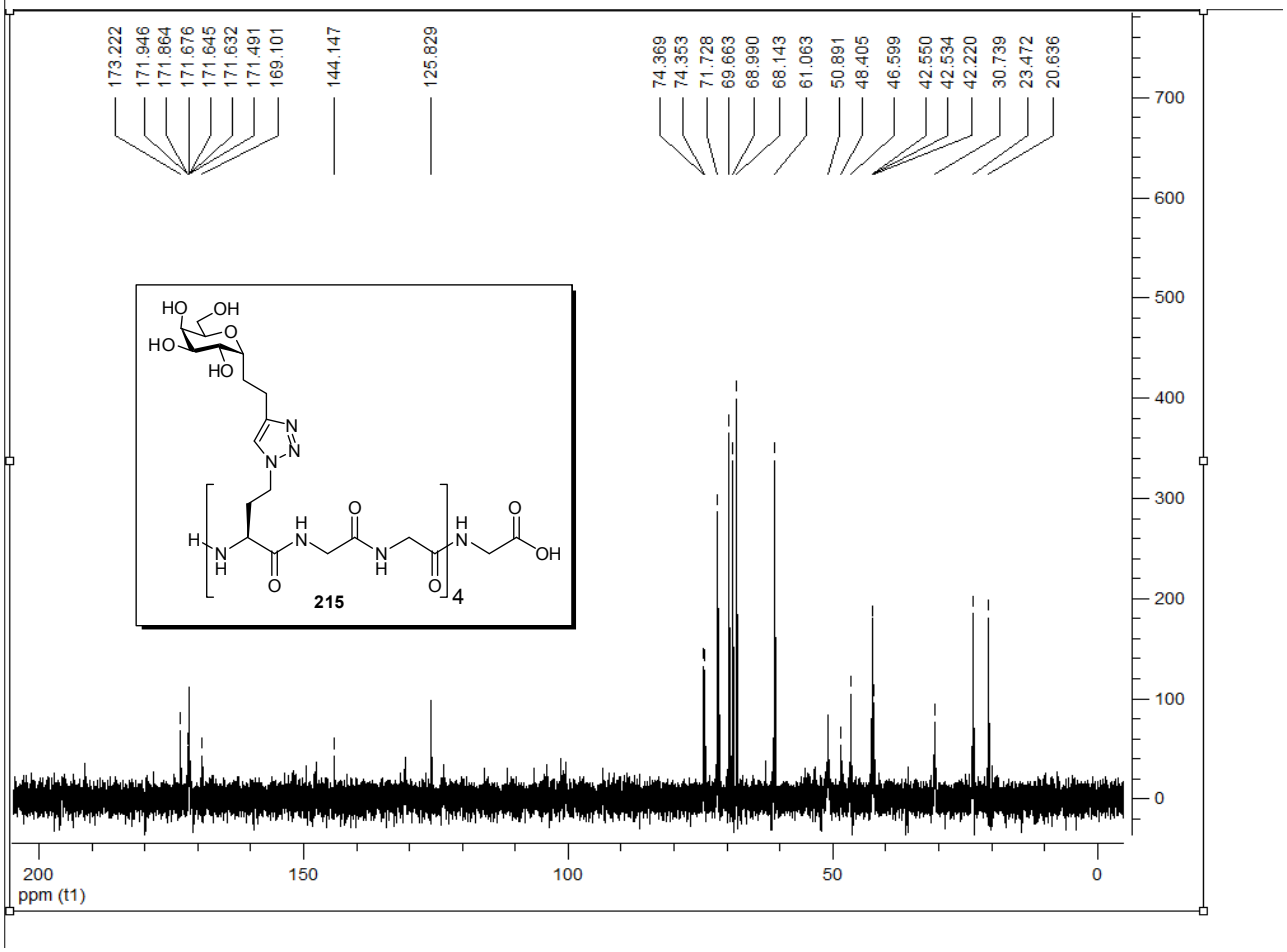

8.093
5.343
4.525
4.242
4.086
4.014
3.945
3.735
3.698
3.682
3.647
2.516
2.281
213
3.22
3.32
8.00
35.14
12.88
7.30
ppm (t1)

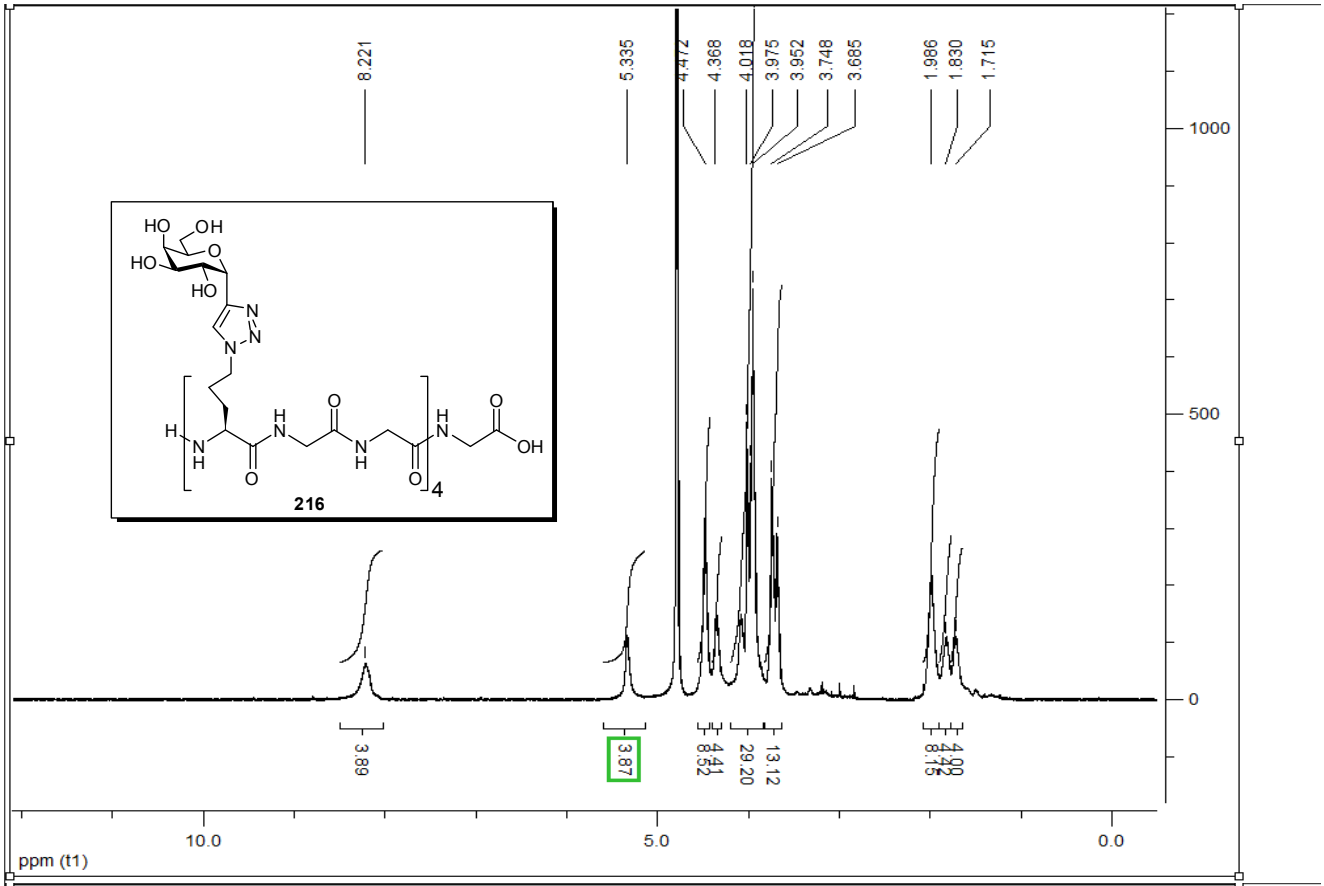

174.420
173.268
172.150
171.953
171.704
142.508
126.368
73.606
70.268
70.051
68.879
67.577
60.980
50.646
46.582
42.502
42.252
30.691
213
ppm (t1)

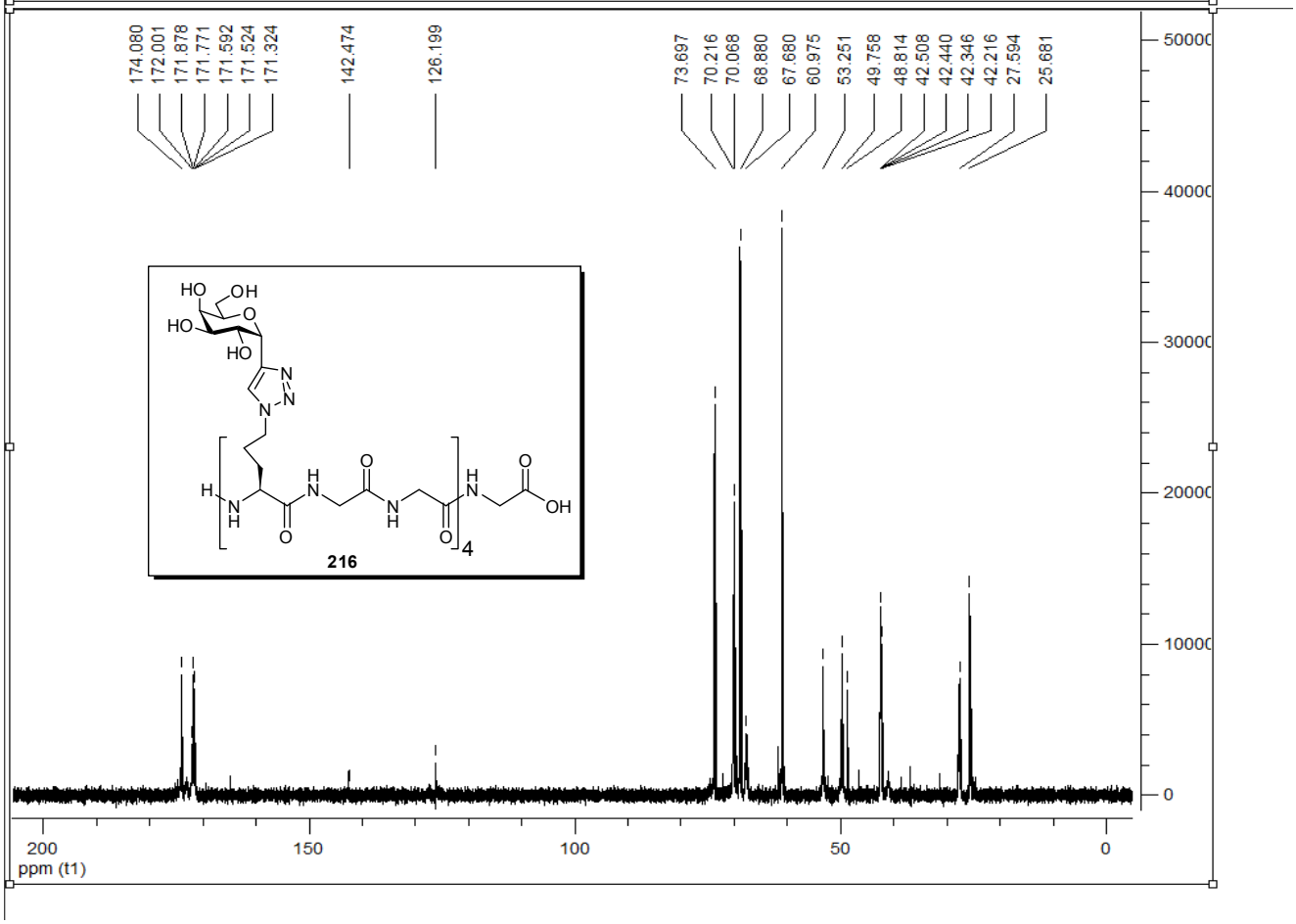

7.899
4.502
4.301
4.072
4.018
3.952
3.663
3.131
3.117
3.041
2.504
2.290
214
3.51
8.00
6.88
34.72
8.36
9.18
4.12
4.12
ppm (t1)

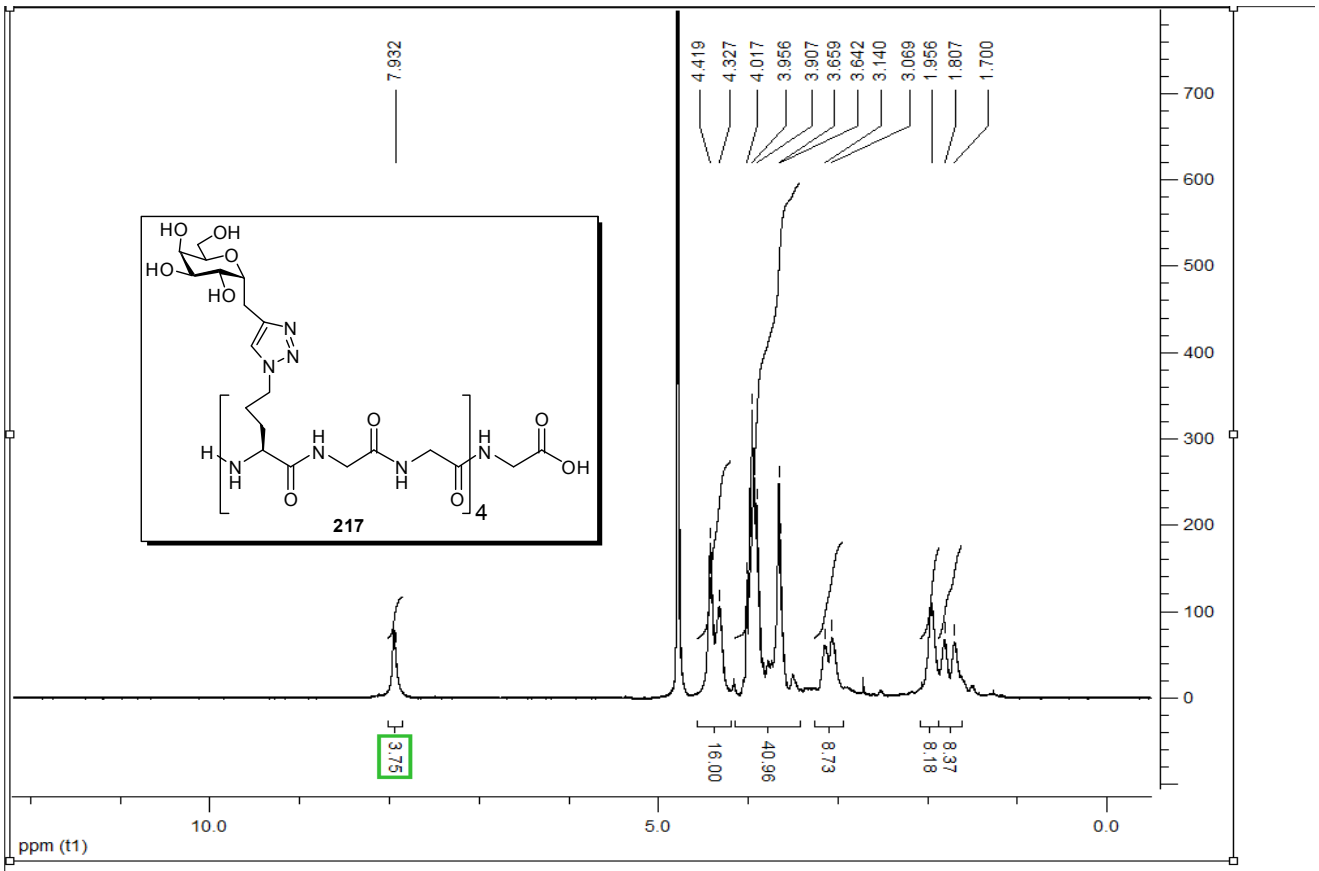

173.220
172.088
171.889
171.625
171.107
170.951
143.766
125.251
74.970
73.902
71.959
69.481
68.955
67.970
62.585
60.945
50.916
46.659
42.521
31.056
30.804
20.725
214
ppm (t1)

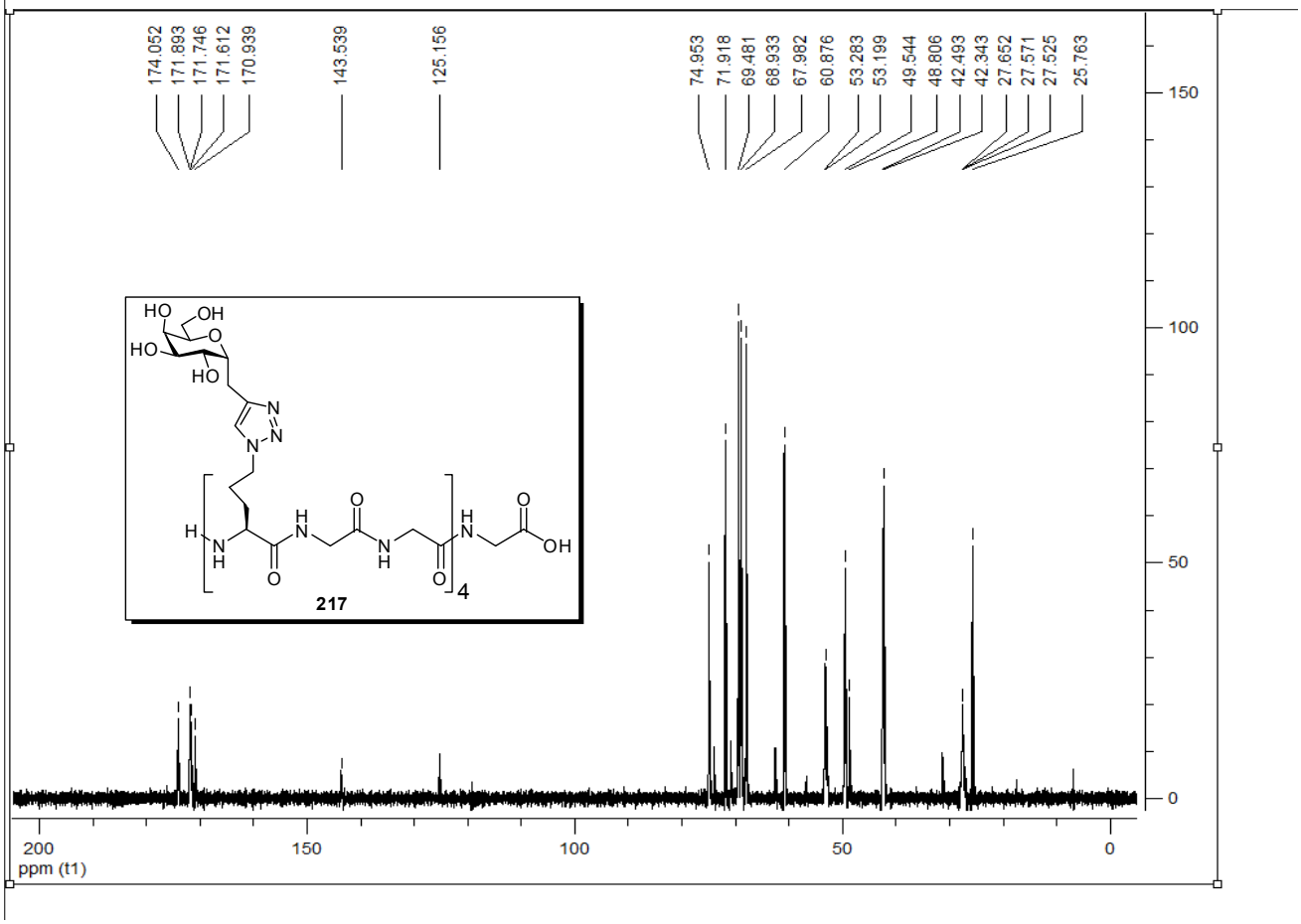

7.793
4.487
4.269
3.994
3.975
3.793
3.703
2.831
2.722
2.496
2.296
2.061
1.920
215
4.00
7.50
4.34
2.91
8.07
4.38
4.20
9.80
ppm (t1)

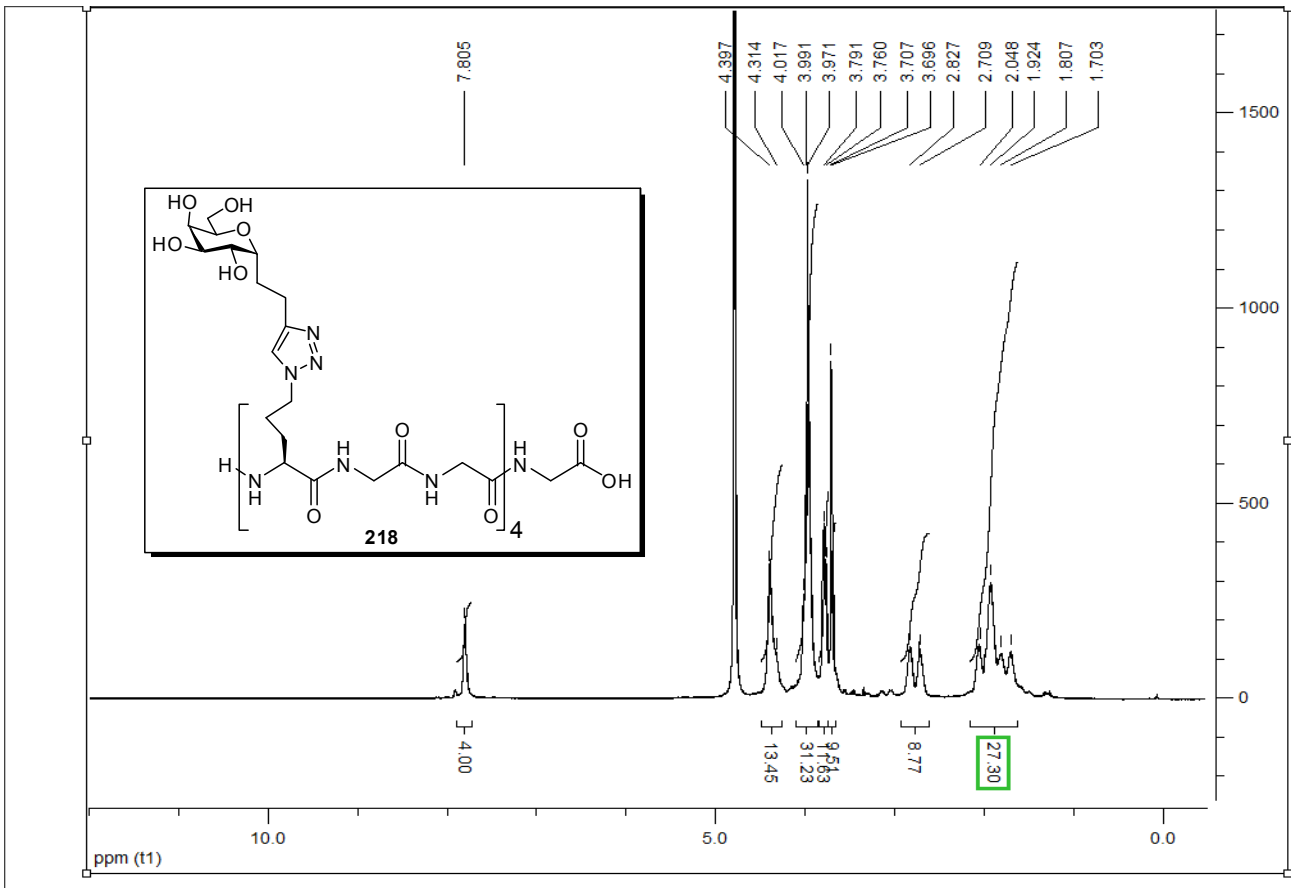

173.222
171.946
171.864
171.676
171.645
171.632
171.491
169.101
144.147
125.829
74.369
74.353
71.728
69.663
68.990
68.143
61.063
50.891
48.405
46.599
42.550
42.534
42.220
30.739
23.472
20.636
215
ppm (t1)

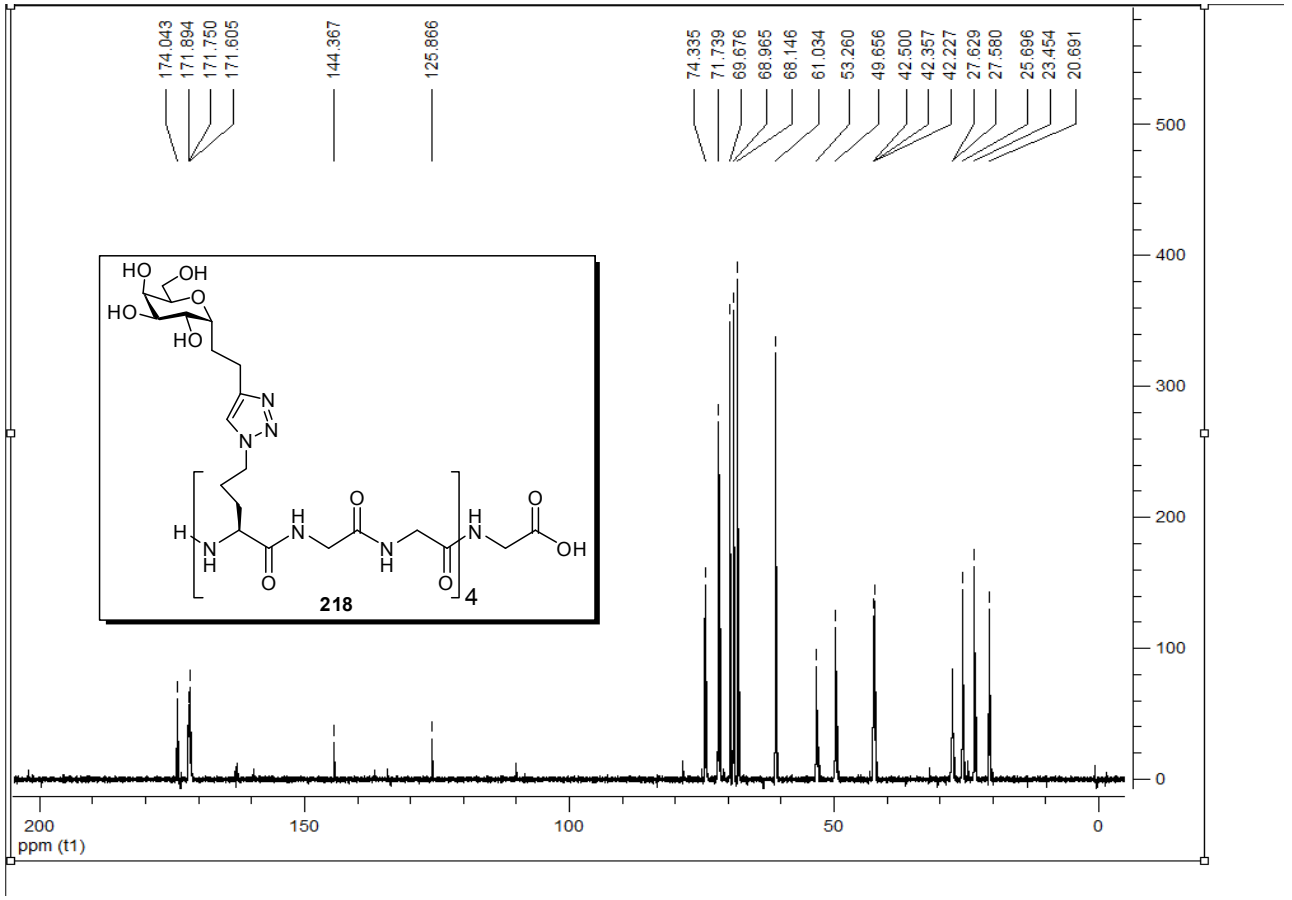

8.221
5.335
4.472
4.368
4.018
3.975
3.952
3.748
3.685
1.986
1.830
1.715
216
3.89
3.87
8.52
8.41
2.92
2.20
1.31
8.18
4.22
4.00
10.0
5.0
0.0
ppm (t1)

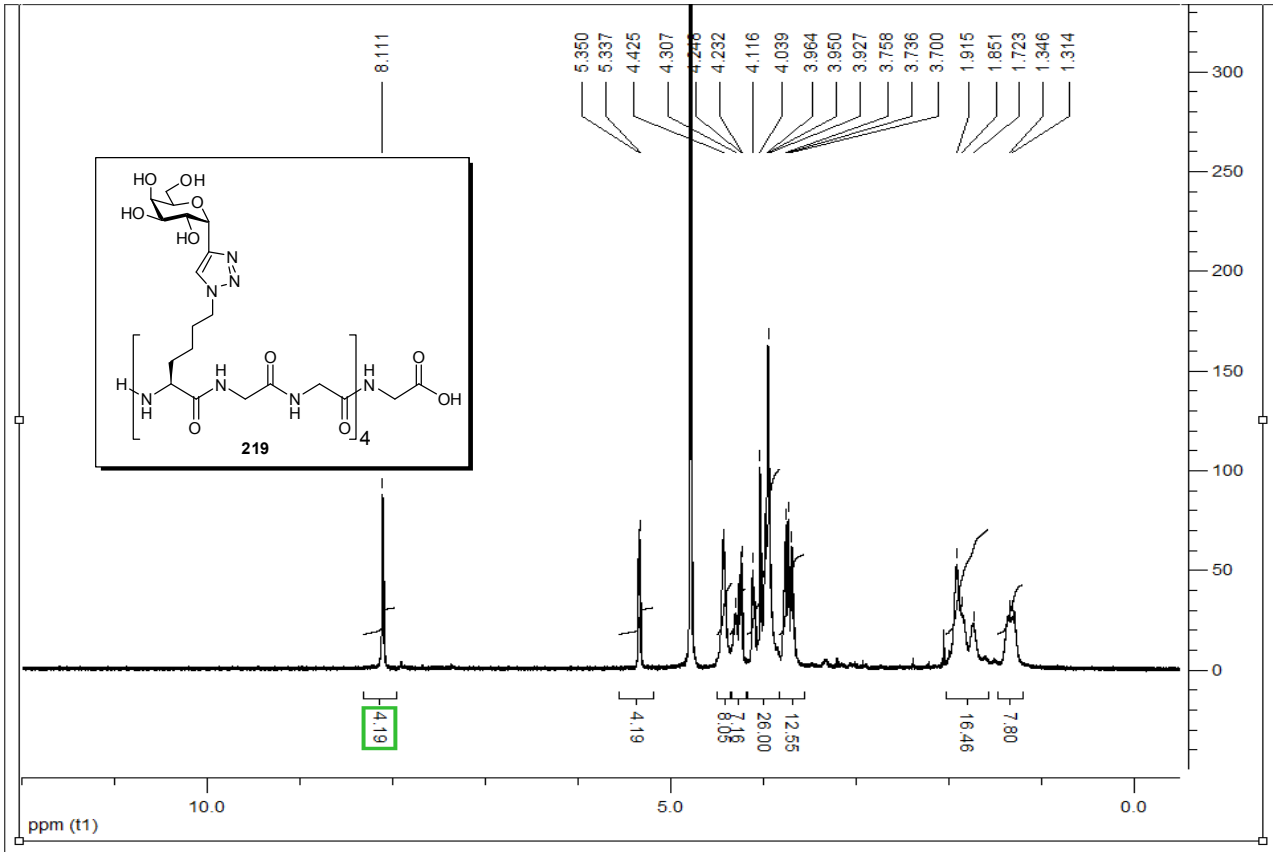

174.080
172.001
171.878
171.771
171.592
171.524
171.324
142.474
126.199
73.697
70.216
70.068
68.880
67.680
60.975
53.251
49.758
48.814
42.508
42.440
42.346
42.216
27.594
25.681
216
200
150
100
50
0
ppm (t1)

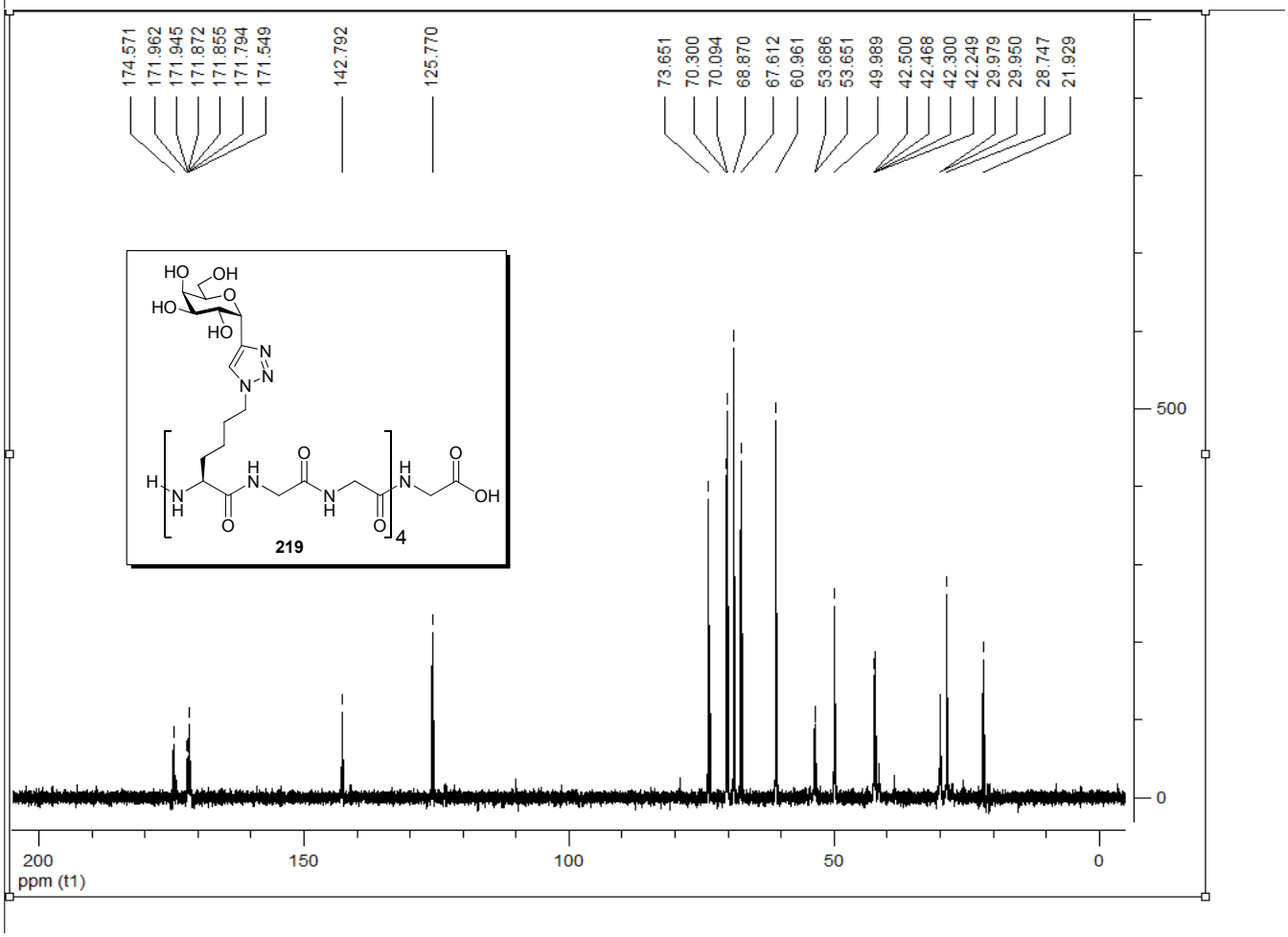

7.932
4.419
4.327
4.017
3.956
3.907
3.659
3.642
3.140
3.069
1.956
1.807
1.700
217
3.75
16.00
40.96
8.73
8.18
8.37
ppm (t1)

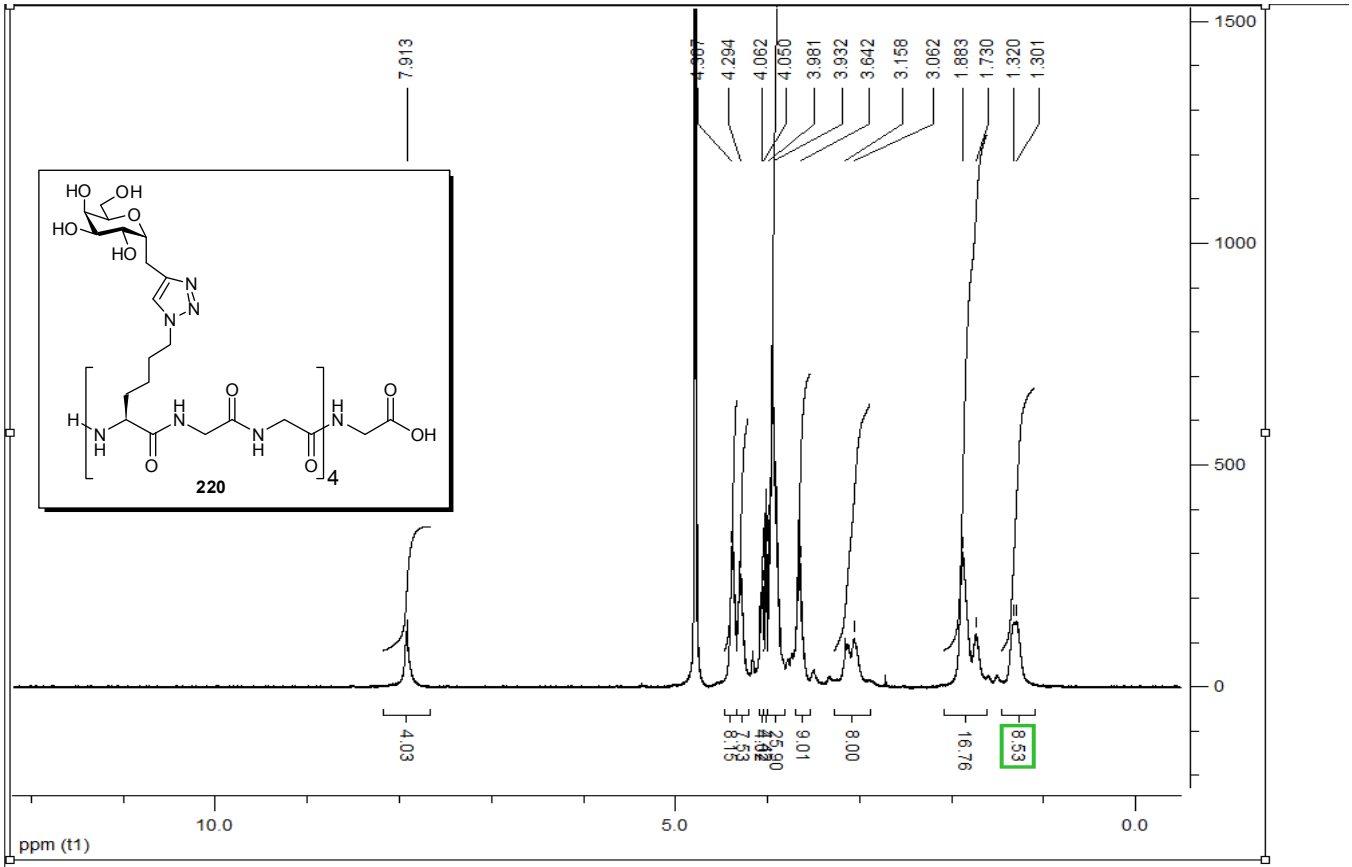

174.052
171.893
171.746
171.612
170.939
143.539
125.156
74.953
71.918
69.481
68.933
67.982
60.876
53.283
53.199
49.544
48.806
42.493
42.343
27.652
27.571
27.525
25.763
217
ppm (t1)

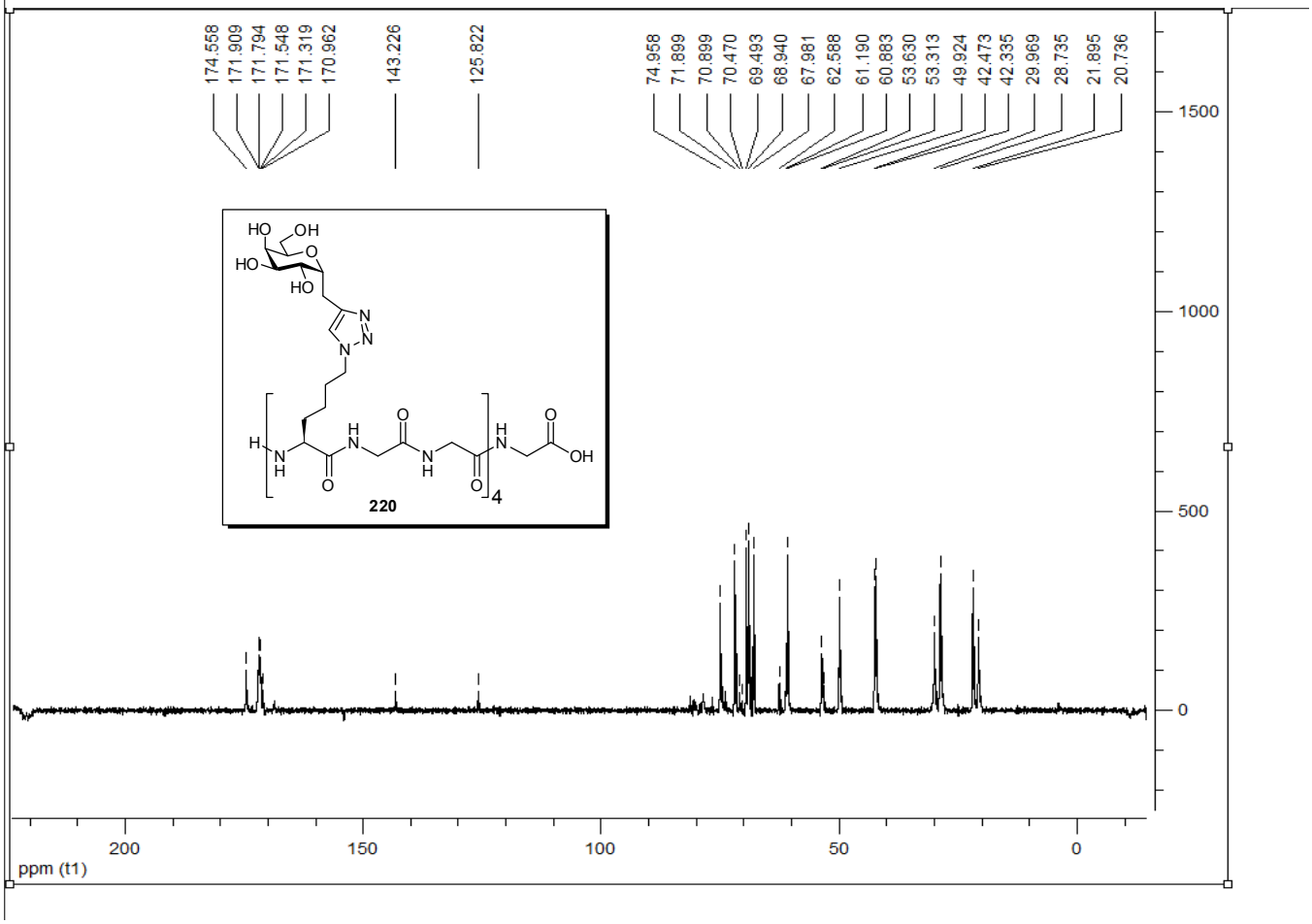

7.805
4.397
4.314
4.017
3.991
3.971
3.791
3.760
3.707
3.696
2.827
2.709
2.048
1.924
1.807
1.703
4.00
13.45
13.23
9.513
9.263
8.77
27.30
1500
1000
500
0
10.0
5.0
0.0
ppm (t1)
218
4

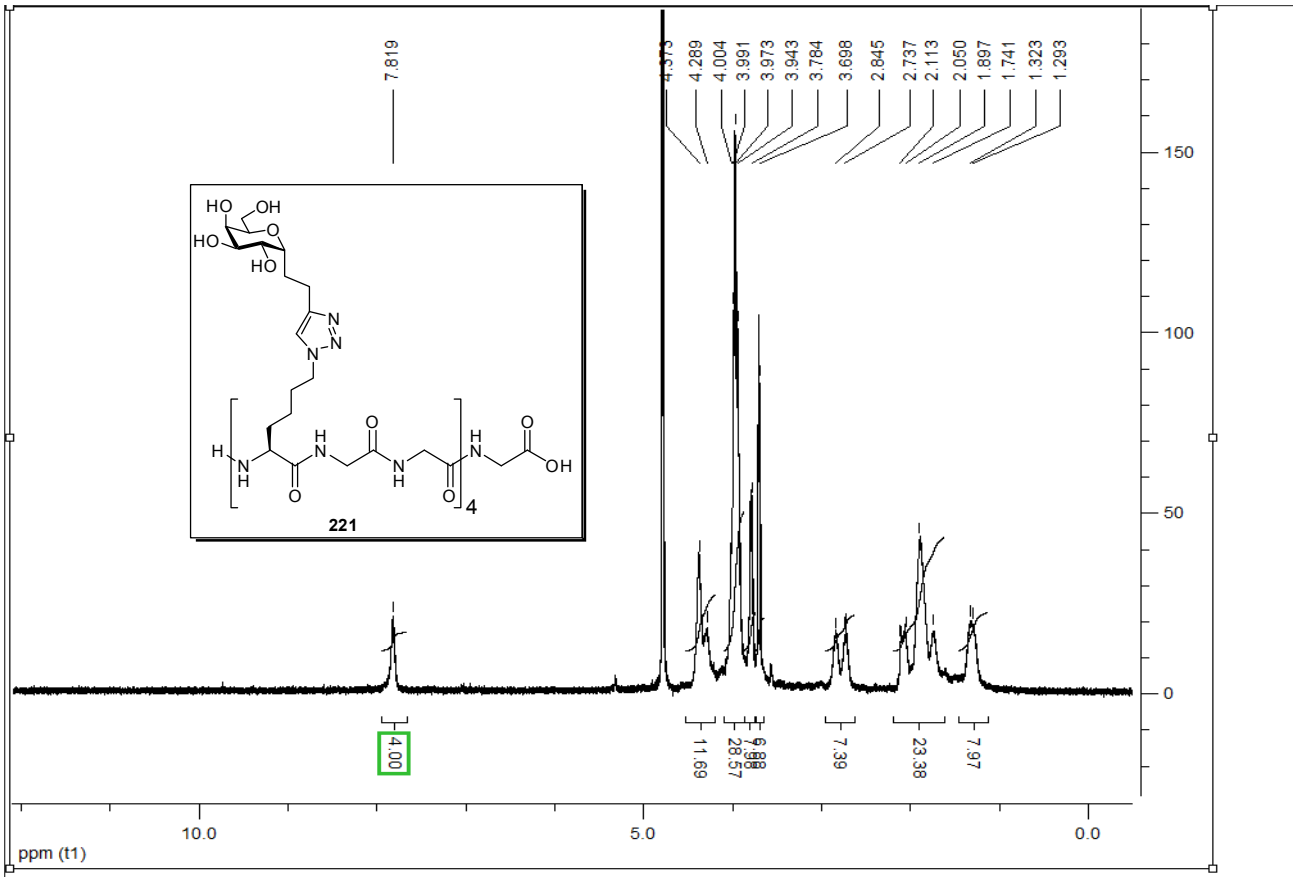

174.043
171.894
171.750
171.605
144.367
125.866
74.335
71.739
69.676
68.965
68.146
61.034
53.260
49.656
42.500
42.357
42.227
27.629
27.580
25.696
23.454
20.691
500
400
300
200
100
0
200
150
100
50
0
ppm (t1)
218
4

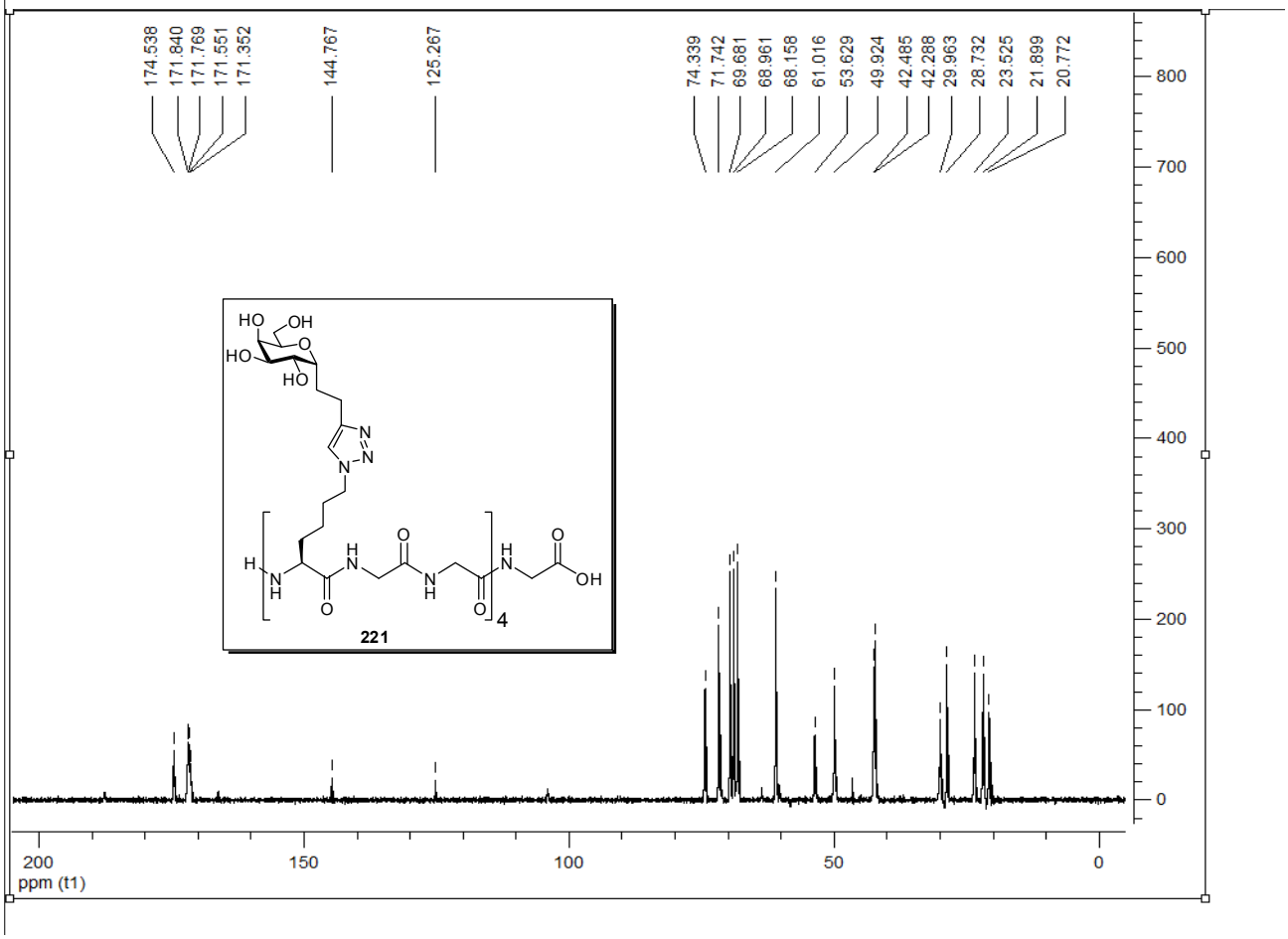

8.111
5.350
5.337
4.425
4.307
4.248
4.232
4.116
4.039
3.964
3.950
3.927
3.758
3.736
3.700
1.915
1.851
1.723
1.346
1.314
219
4.19
4.19
8.05
7.15
26.00
12.55
16.46
7.80
ppm (t1)

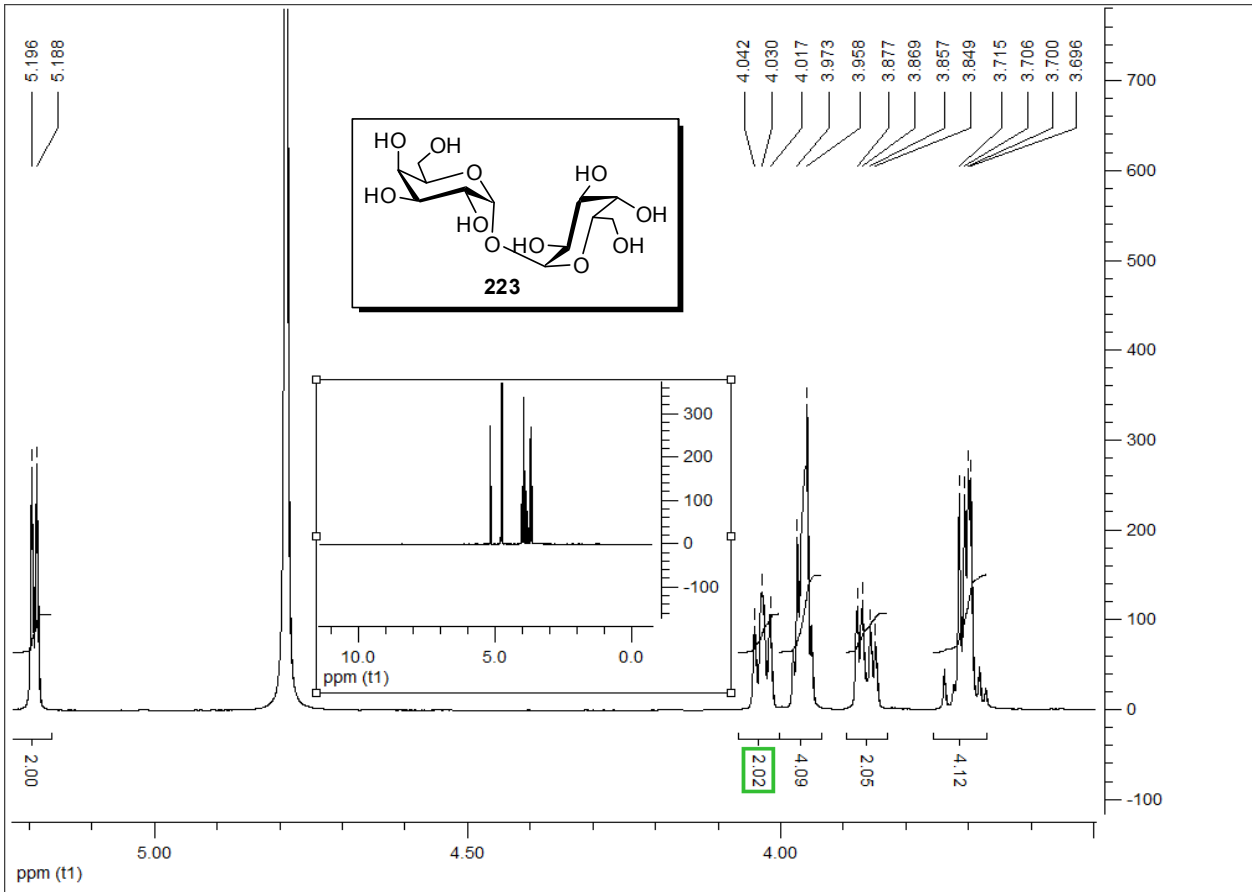

174.571
171.962
171.945
171.872
171.855
171.794
171.549
142.792
125.770
73.651
70.300
70.094
68.870
67.612
60.961
53.686
53.651
49.989
42.500
42.468
42.300
42.249
29.979
29.950
28.747
21.929
219
ppm (t1)

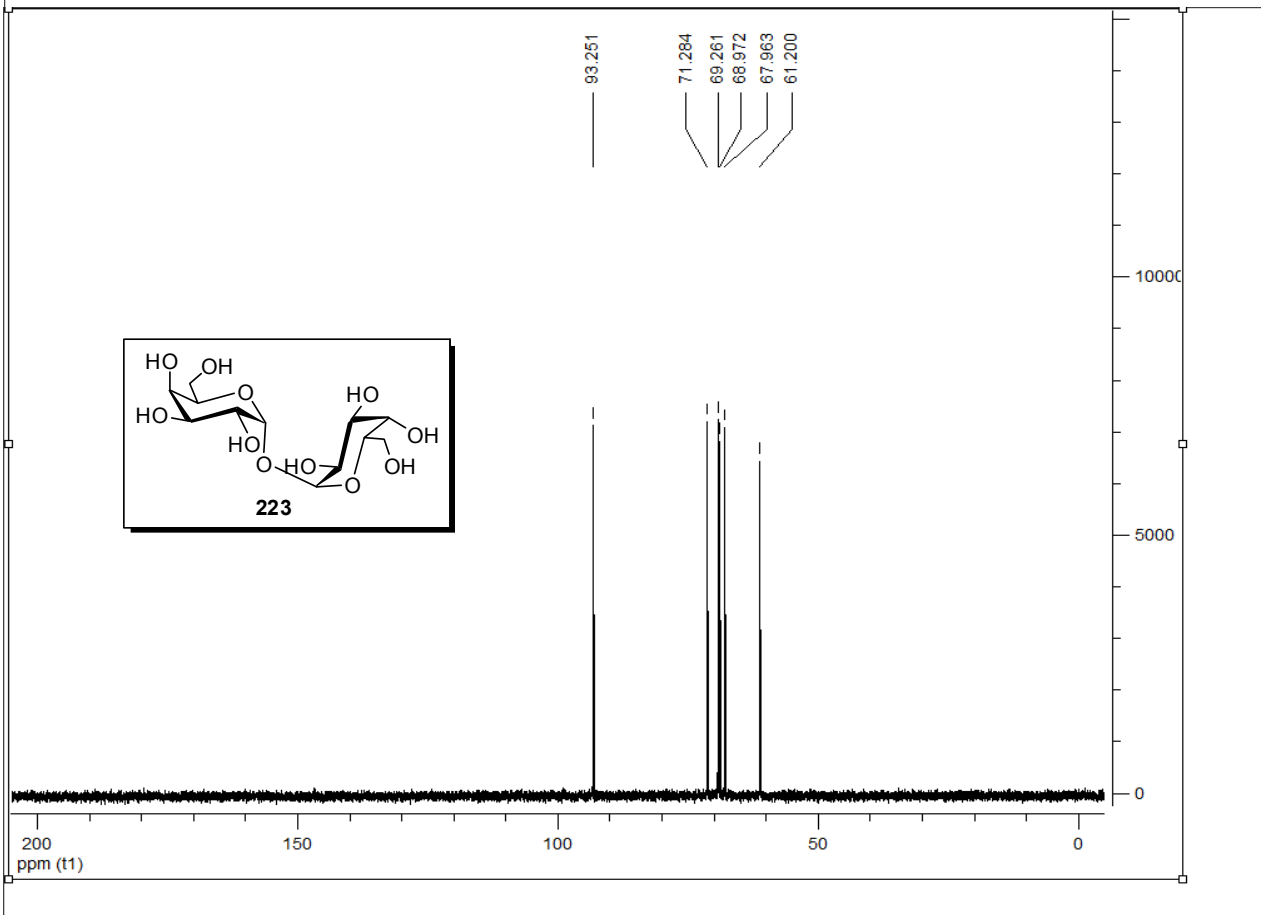

7.913
4.367
4.294
4.062
4.050
3.981
3.932
3.642
3.158
3.062
1.883
1.730
1.320
1.301
220
4.03
9.01
8.00
16.76
8.53
1500
1000
500
0
10.0
5.0
0.0
ppm (t1)

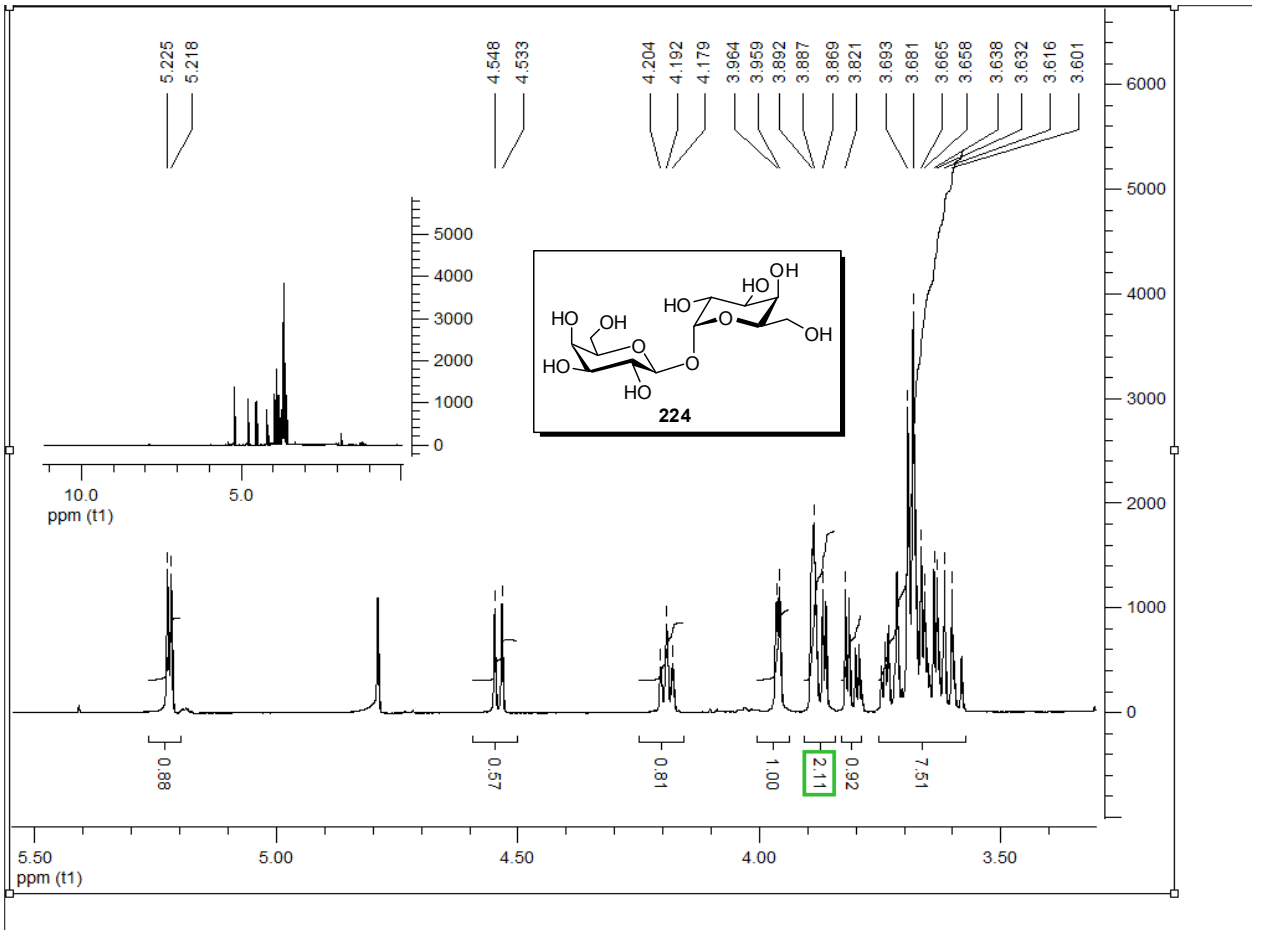

174.558
171.909
171.794
171.548
171.319
170.962
143.226
125.822
74.958
71.899
70.899
70.470
69.493
68.940
67.981
62.588
61.190
60.883
53.630
53.313
49.924
42.473
42.335
29.969
28.735
21.895
20.736
220
1500
1000
500
0
200
150
100
50
0
ppm (t1)

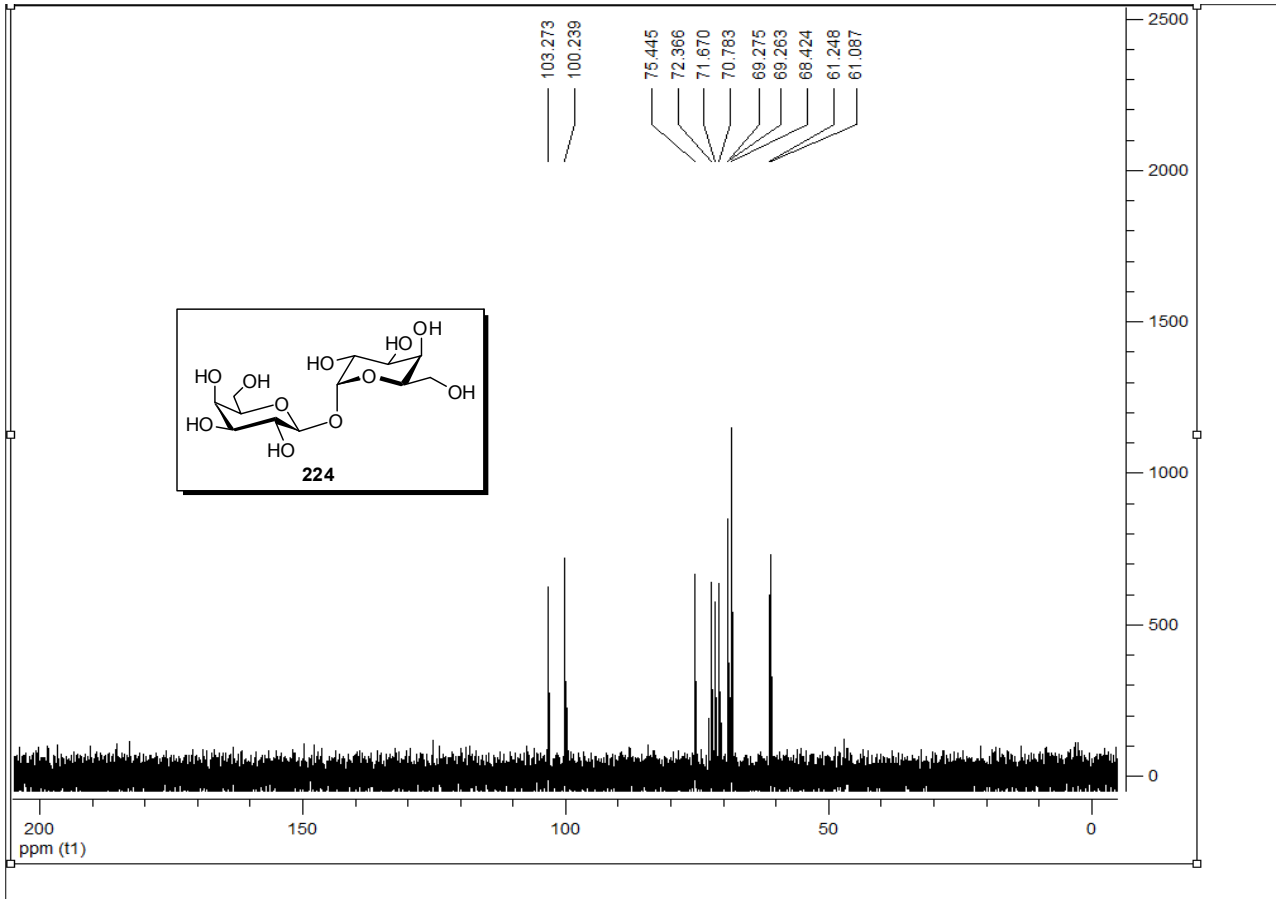

7.819
4.373
4.289
4.004
3.991
3.973
3.943
3.784
3.698
2.845
2.737
2.113
2.050
1.897
1.741
1.323
1.293
HO
OH
HO
O
HO
N
N
N
H
N
H
O
H
N
O
N
H
O
H
N
OH
O
4
221
4.00
11.69
28.57
7.39
23.38
7.97
150
100
50
0
10.0
5.0
0.0
ppm (t1)

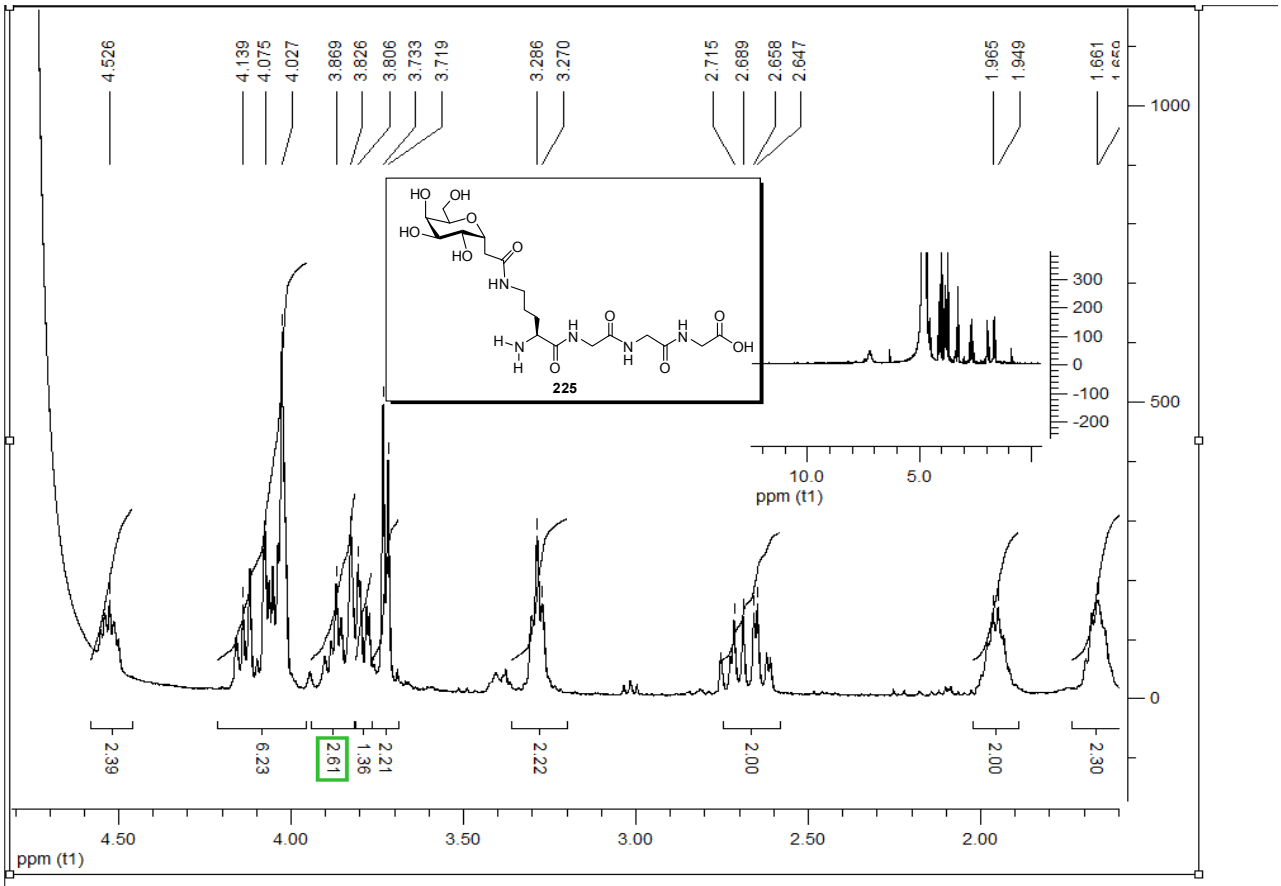

174.538
171.840
171.769
171.551
171.352
144.767
125.267
74.339
71.742
69.681
68.961
68.158
61.016
53.629
49.924
42.485
42.288
29.963
28.732
23.525
21.899
20.772
HO
OH
HO
O
HO
N
N
N
H
N
H
O
H
N
O
N
H
O
H
N
OH
O
4
221
800
700
600
500
400
300
200
100
0
200
150
100
50
0
ppm (t1)

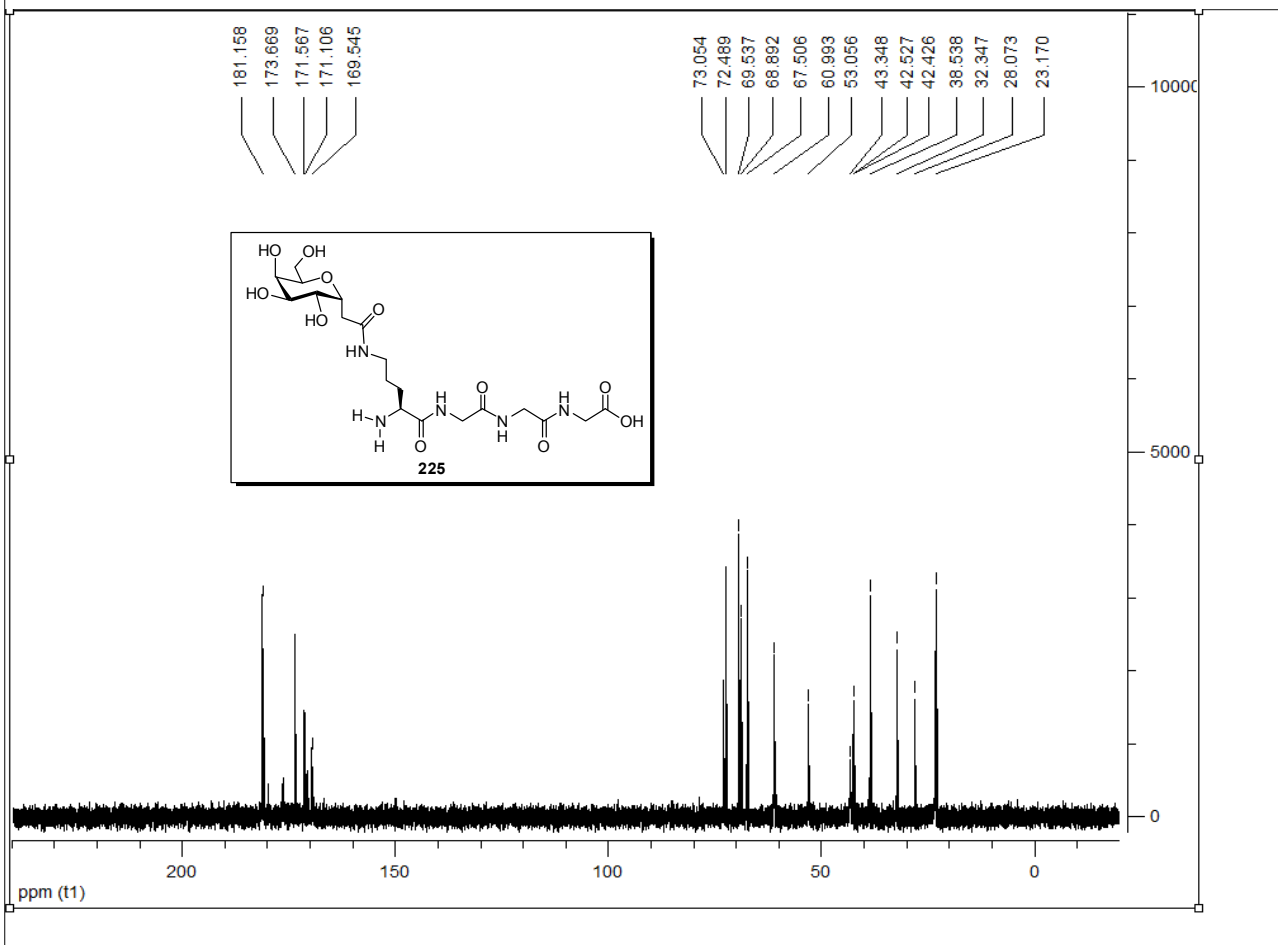

5.196
5.188
4.042
4.030
4.017
3.973
3.958
3.877
3.869
3.857
3.849
3.715
3.706
3.700
3.696
223
2.00
2.02
4.09
2.05
4.12
ppm (t1)
5.00
4.50
4.00

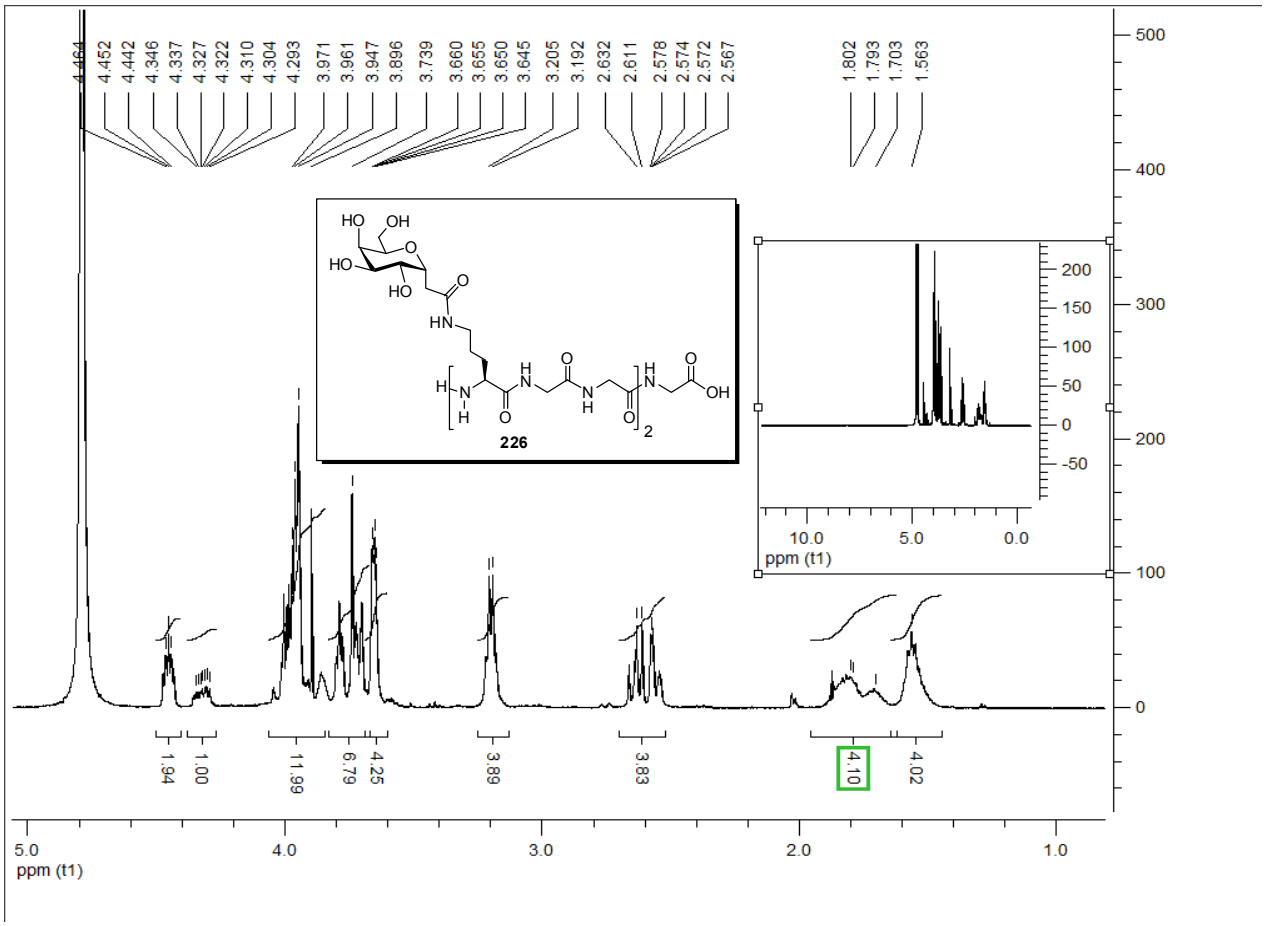

93.251
71.284
69.261
68.972
67.963
61.200
223
ppm (t1)
200
150
100
50
0

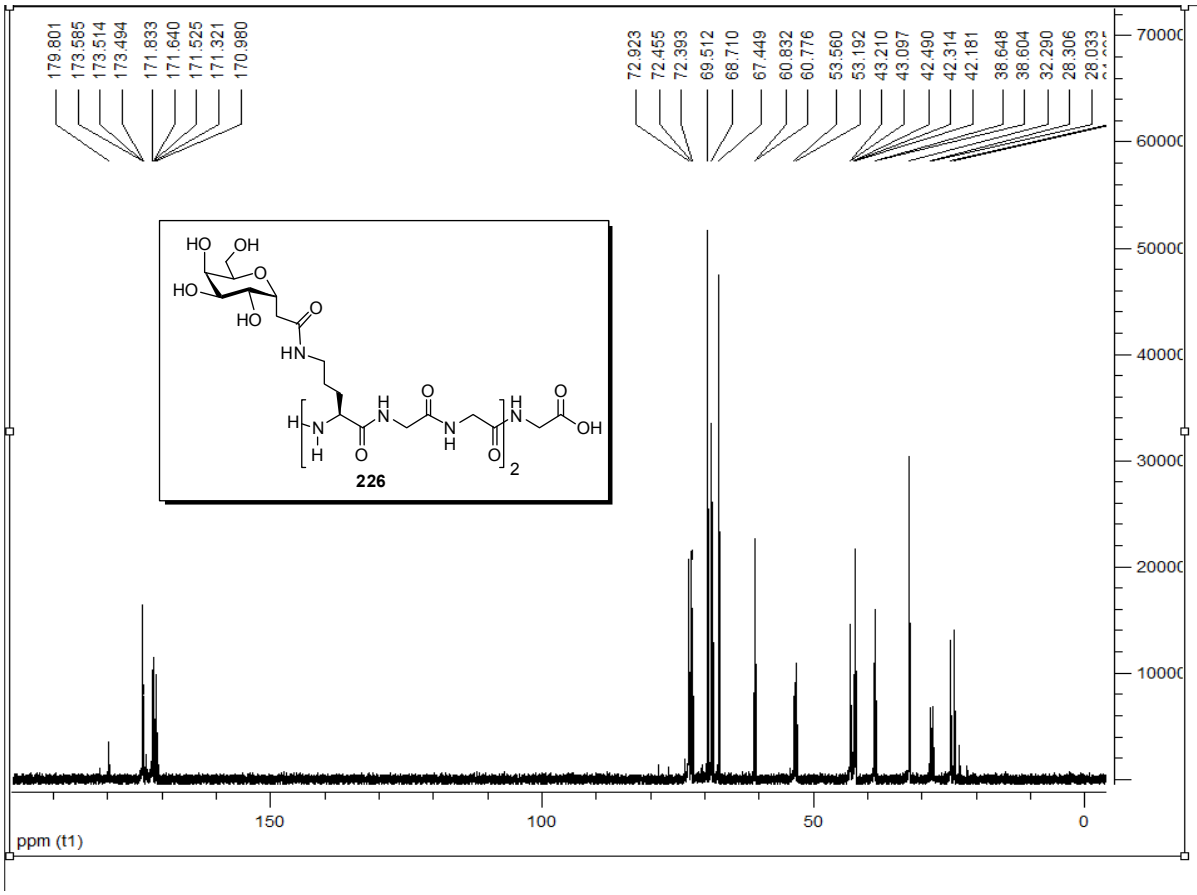

5.225
5.218
4.548
4.533
4.204
4.192
4.179
3.964
3.959
3.892
3.887
3.869
3.821
3.693
3.681
3.665
3.658
3.638
3.632
3.616
3.601
224
10.0
5.0
ppm (t1)
0.88
0.57
0.81
1.00
2.11
0.92
7.51
5.50
5.00
4.50
4.00
3.50
ppm (t1)

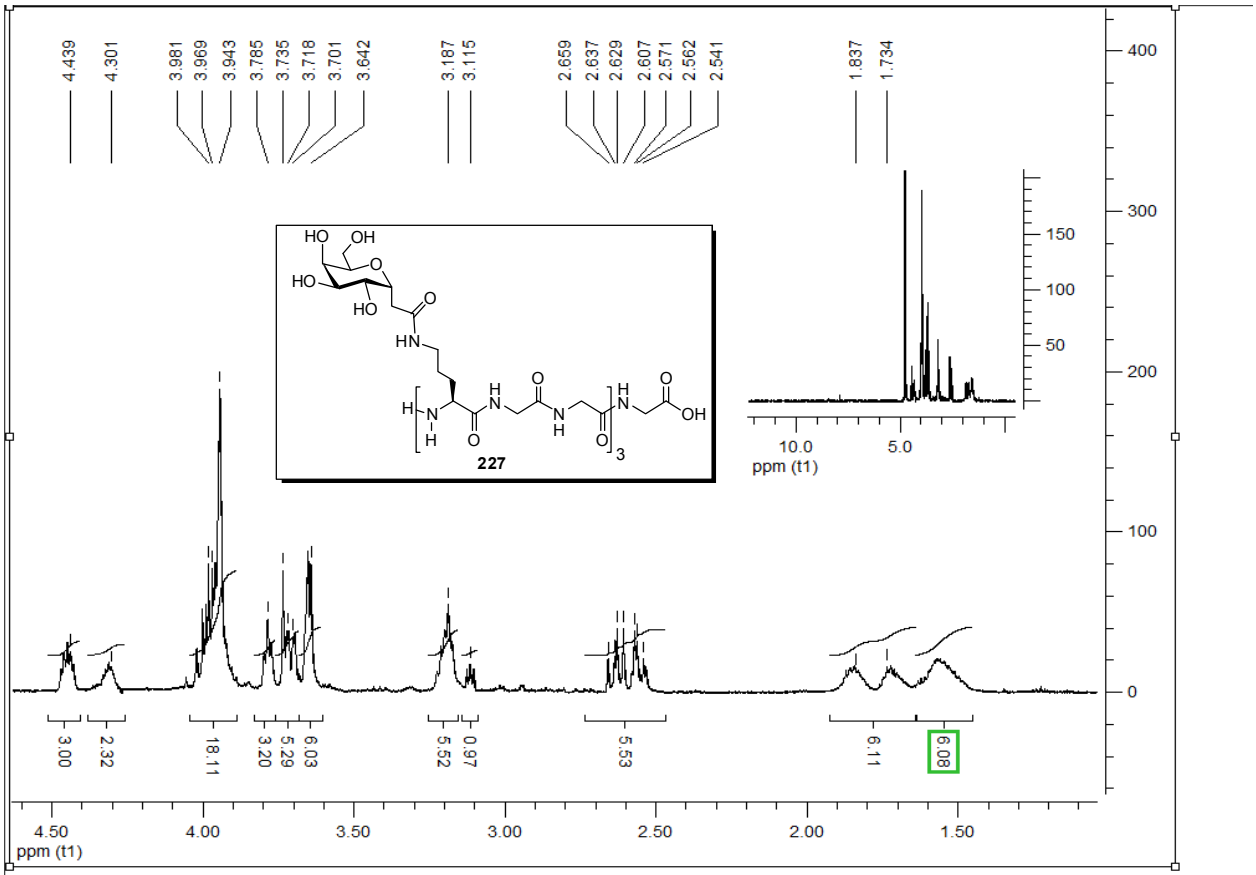

103.273
100.239
75.445
72.366
71.670
70.783
69.275
69.263
68.424
61.248
61.087
224
200
150
100
50
0
ppm (t1)

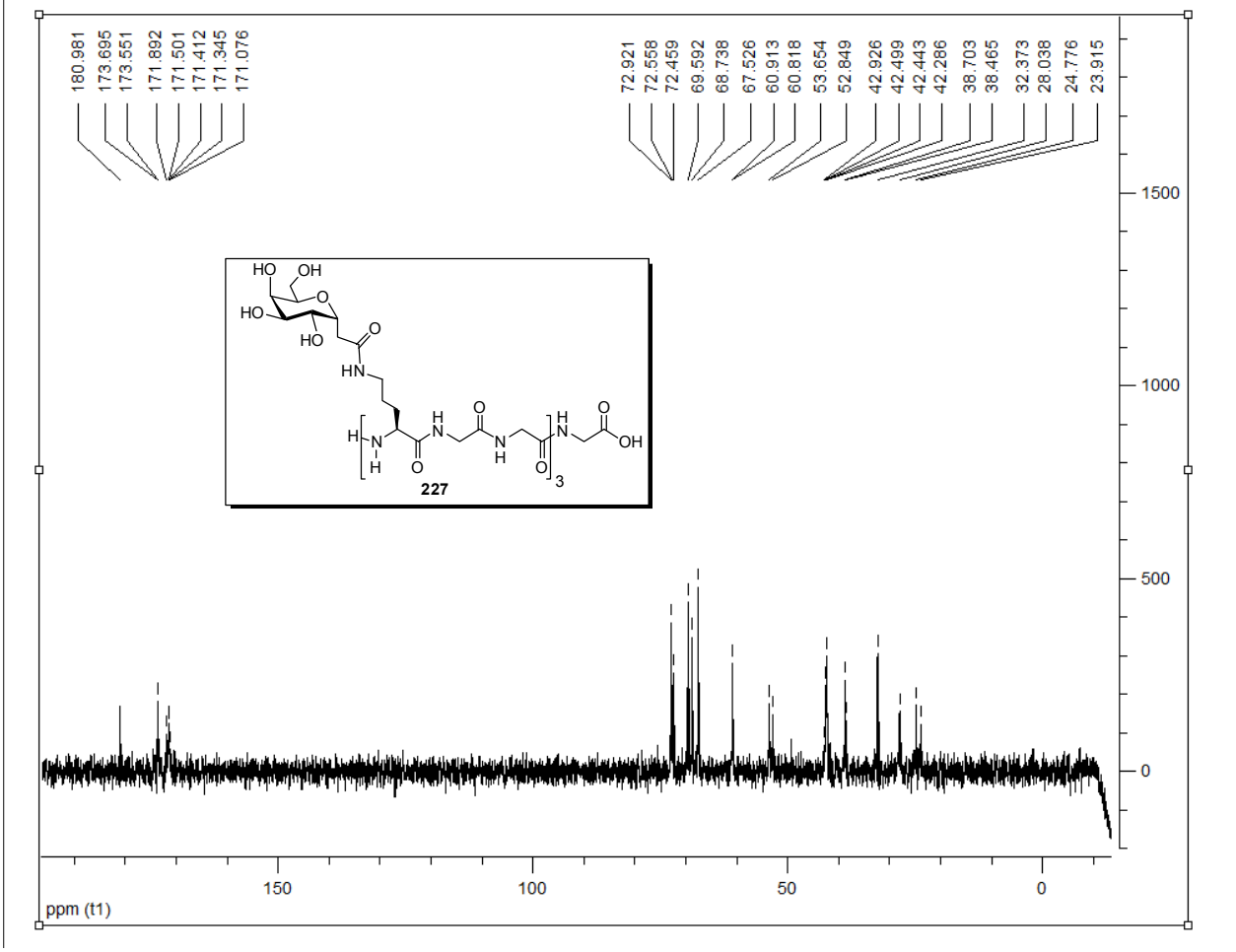

4.526
4.139
4.075
4.027
3.869
3.826
3.806
3.733
3.719
3.286
3.270
2.715
2.689
2.658
2.647
1.965
1.949
1.661
HO
OH
HO
HO
O
HN
H
N
H
O
N
H
O
N
H
O
OH
225
1000
500
0
300
200
100
0
-100
-200
10.0
5.0
ppm (t1)
2.39
9.23
2.91
1.36
2.21
2.22
2.00
2.00
2.30
4.50
4.00
3.50
3.00
2.50
2.00
ppm (t1)

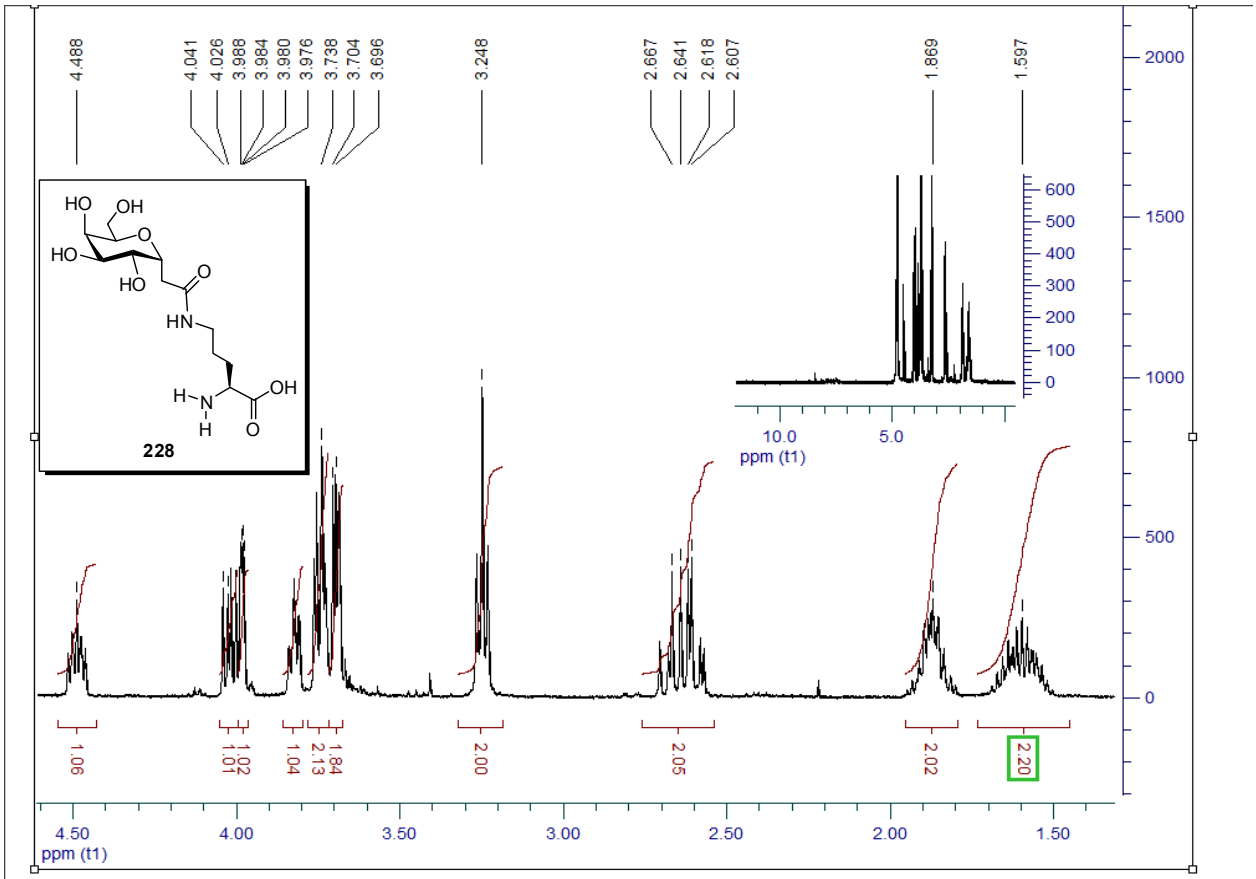

181.158
173.669
171.567
171.106
169.545
73.054
72.489
69.537
68.892
67.506
60.993
53.056
43.348
42.527
42.426
38.538
32.347
28.073
23.170
HO
OH
HO
HO
O
HN
H
N
H
O
N
H
O
N
H
O
OH
225
10000
5000
0
200
150
100
50
0
ppm (t1)

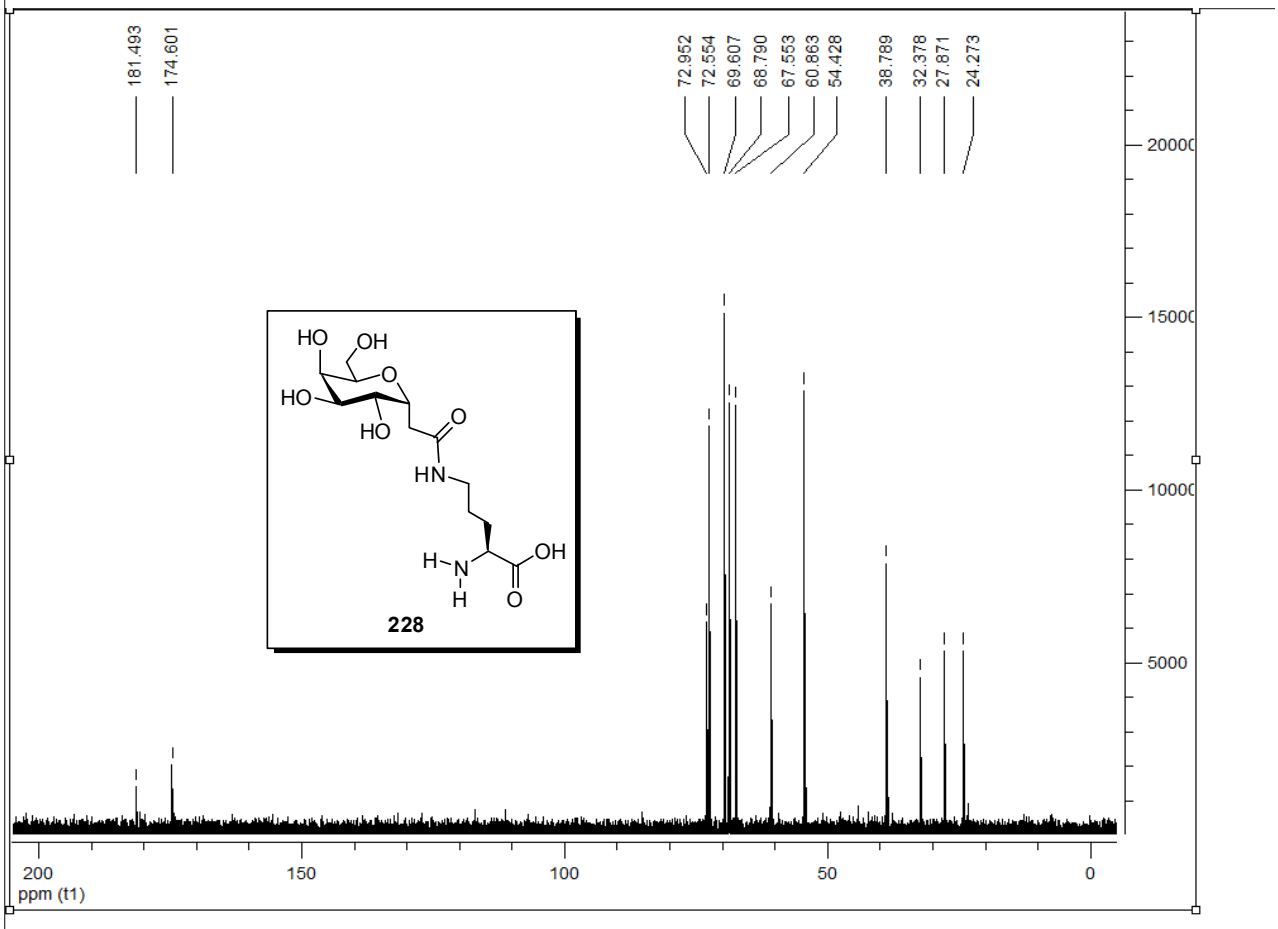

4.464
4.452
4.442
4.346
4.337
4.327
4.322
4.310
4.304
4.293
3.971
3.961
3.947
3.896
3.739
3.660
3.655
3.650
3.645
3.205
3.192
2.632
2.611
2.578
2.574
2.572
2.567
1.802
1.793
1.703
1.563
226
ppm (t1)
1.94
1.00
11.99
9.79
4.25
3.89
3.83
4.10
4.02

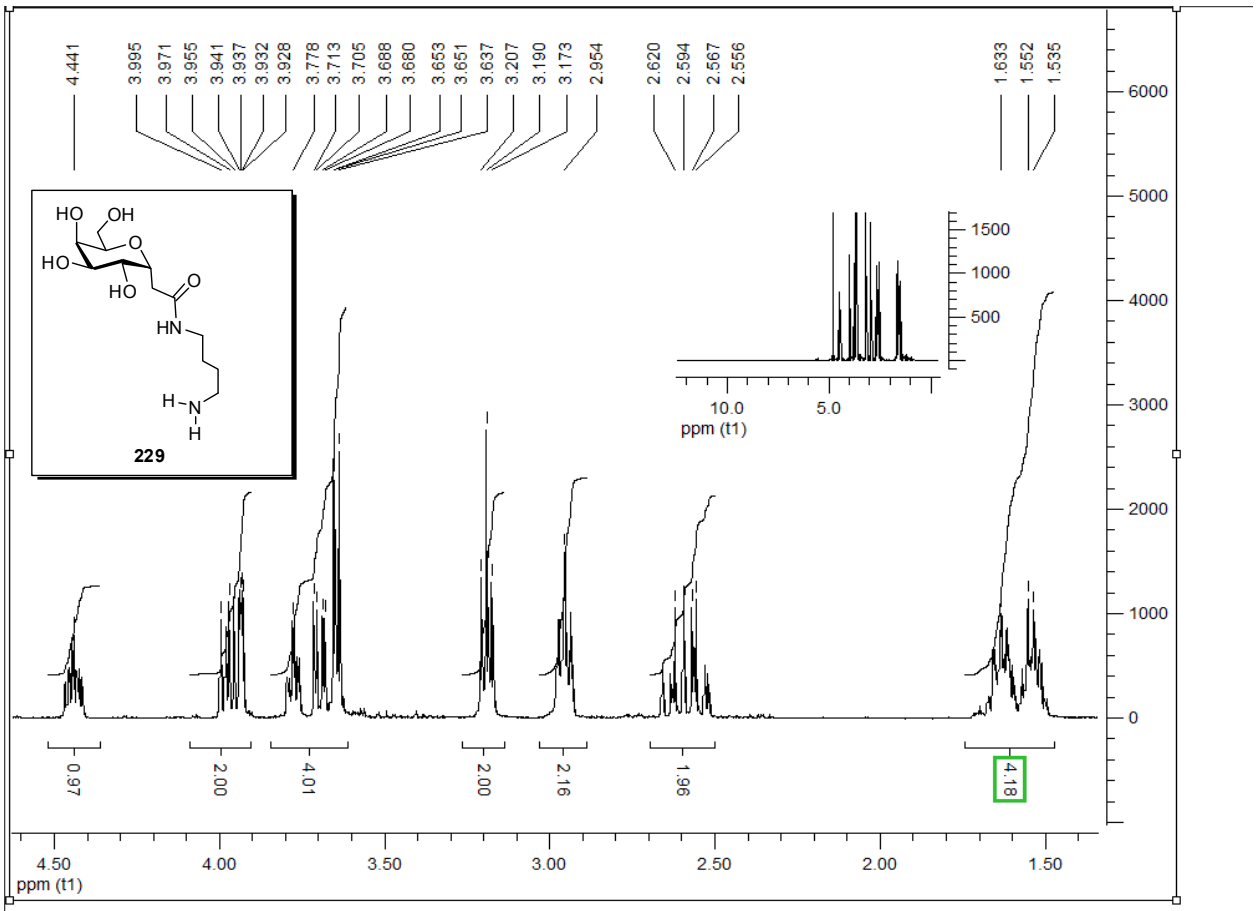

179.801
173.585
173.514
173.494
171.833
171.640
171.525
171.321
170.980
72.923
72.455
72.393
69.512
68.710
67.449
60.832
60.776
53.560
53.192
43.210
43.097
42.490
42.314
42.181
38.648
38.604
32.290
28.306
28.033
226
ppm (t1)

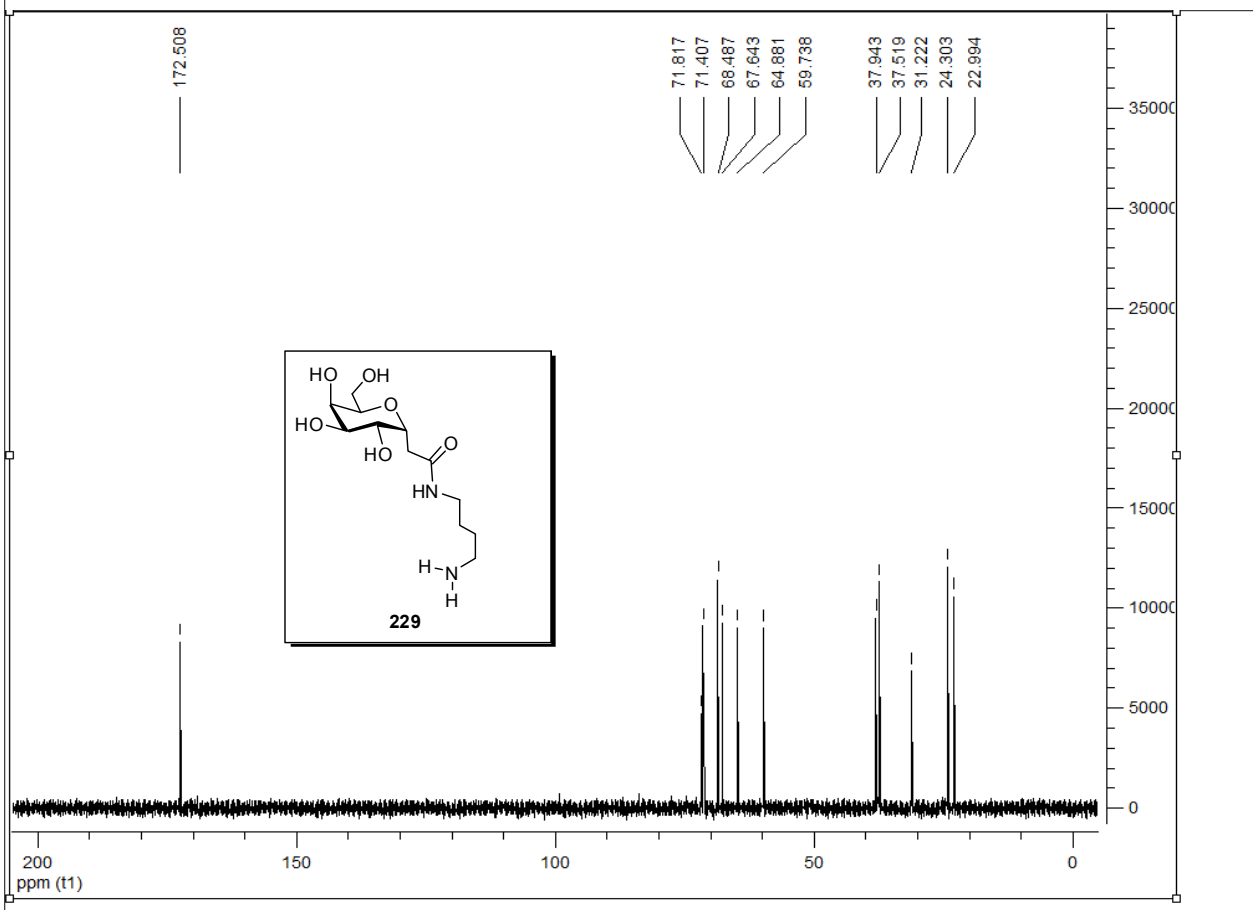

4.439
4.301
3.981
3.969
3.943
3.785
3.735
3.718
3.701
3.642
3.187
3.115
2.659
2.637
2.629
2.607
2.571
2.562
2.541
1.837
1.734
227
ppm (t1)
3.00
2.32
18.11
3.20
5.29
6.03
5.52
0.97
5.53
6.11
6.08
ppm (t1)

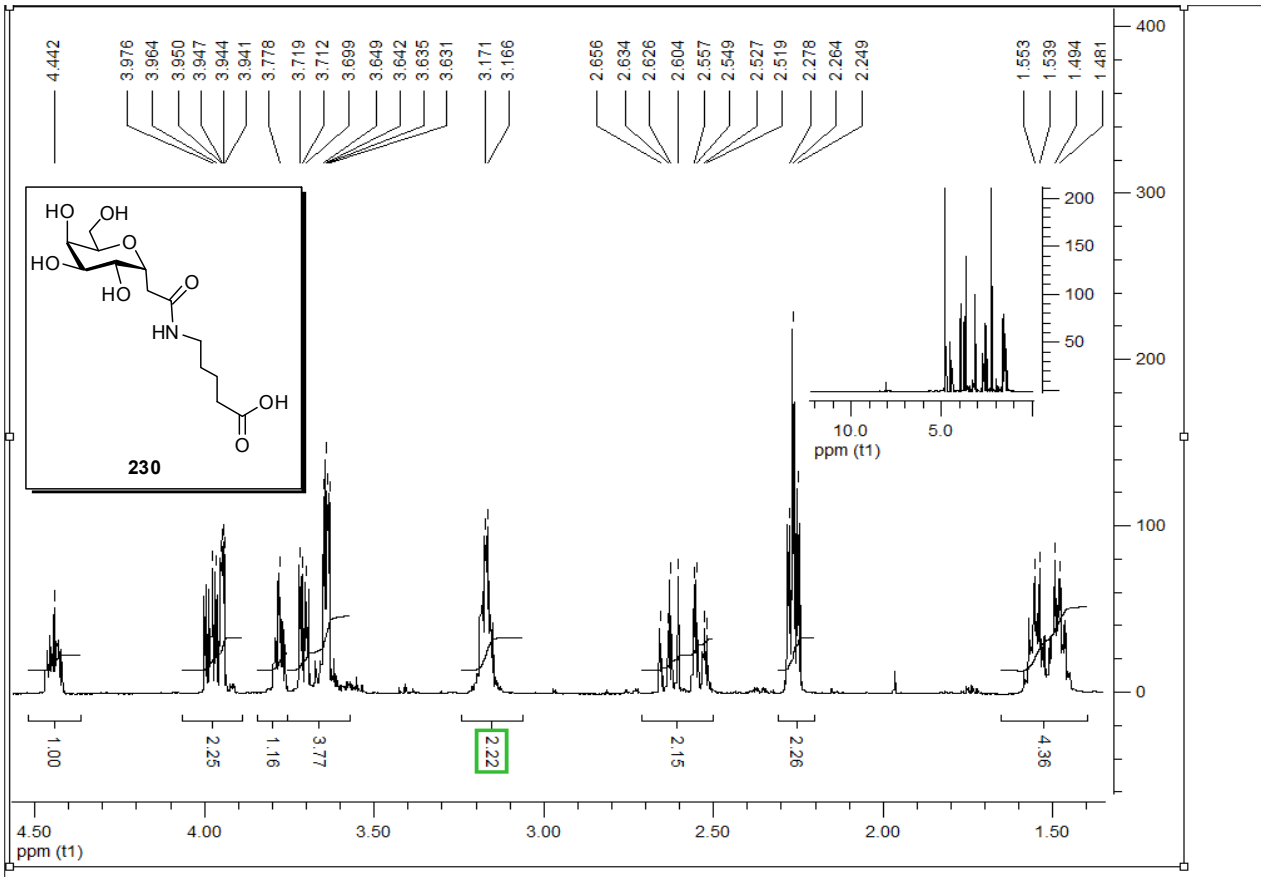

180.981
173.695
173.551
171.892
171.501
171.412
171.345
171.076
72.921
72.558
72.459
69.592
68.738
67.526
60.913
60.818
53.654
52.849
42.926
42.499
42.443
42.286
38.703
38.465
32.373
28.038
24.776
23.915
227
ppm (t1)

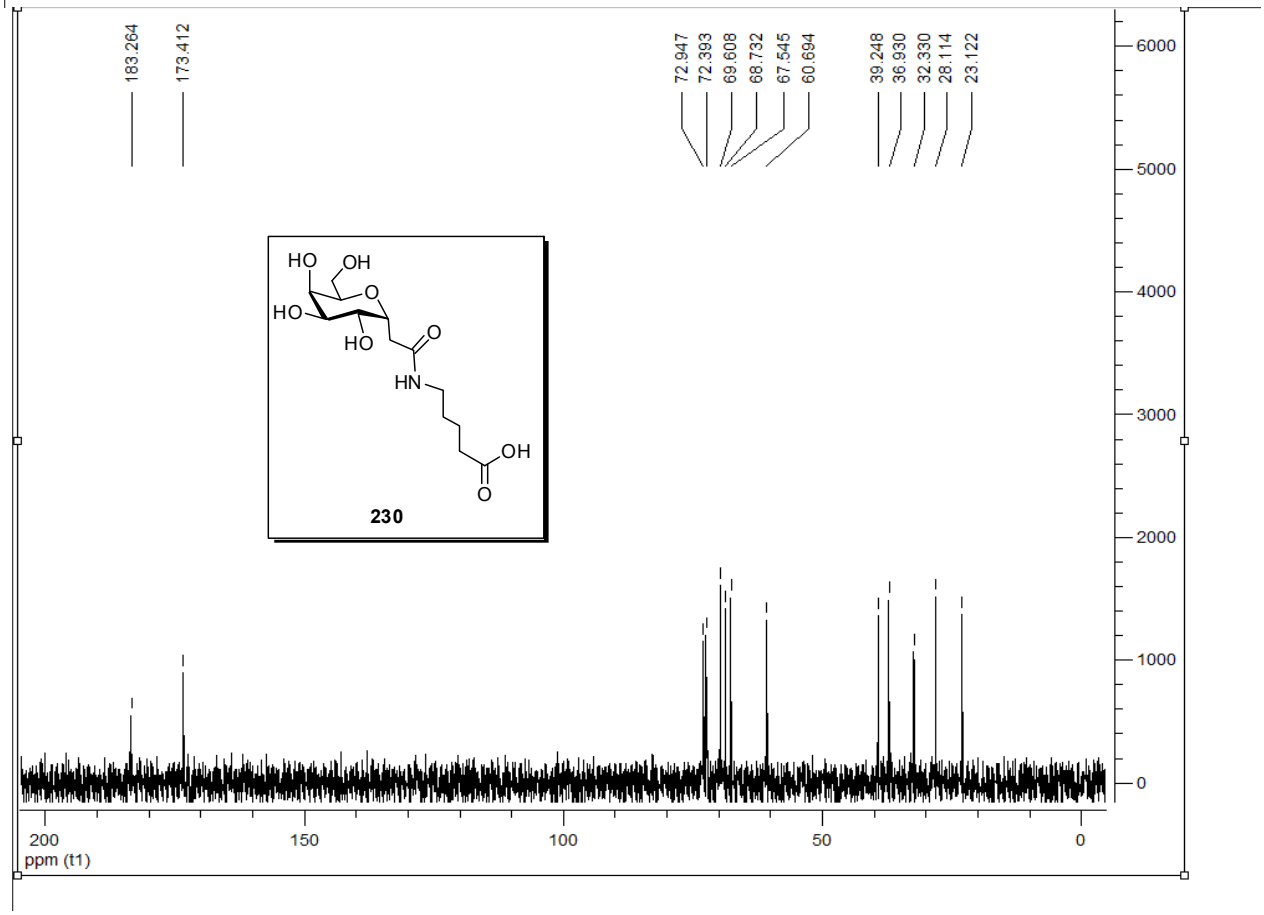

4.488
4.041
4.026
3.988
3.984
3.980
3.976
3.738
3.704
3.696
3.248
2.667
2.641
2.618
2.607
1.869
1.597
HO
OH
O
HO
HO
O
HN
H
N
H
OH
O
228
10.0
5.0
ppm (t1)
4.50
4.00
3.50
3.00
2.50
2.00
1.50
ppm (t1)
1.06
1.01
1.02
1.04
2.13
1.84
2.00
2.05
2.02
2.20

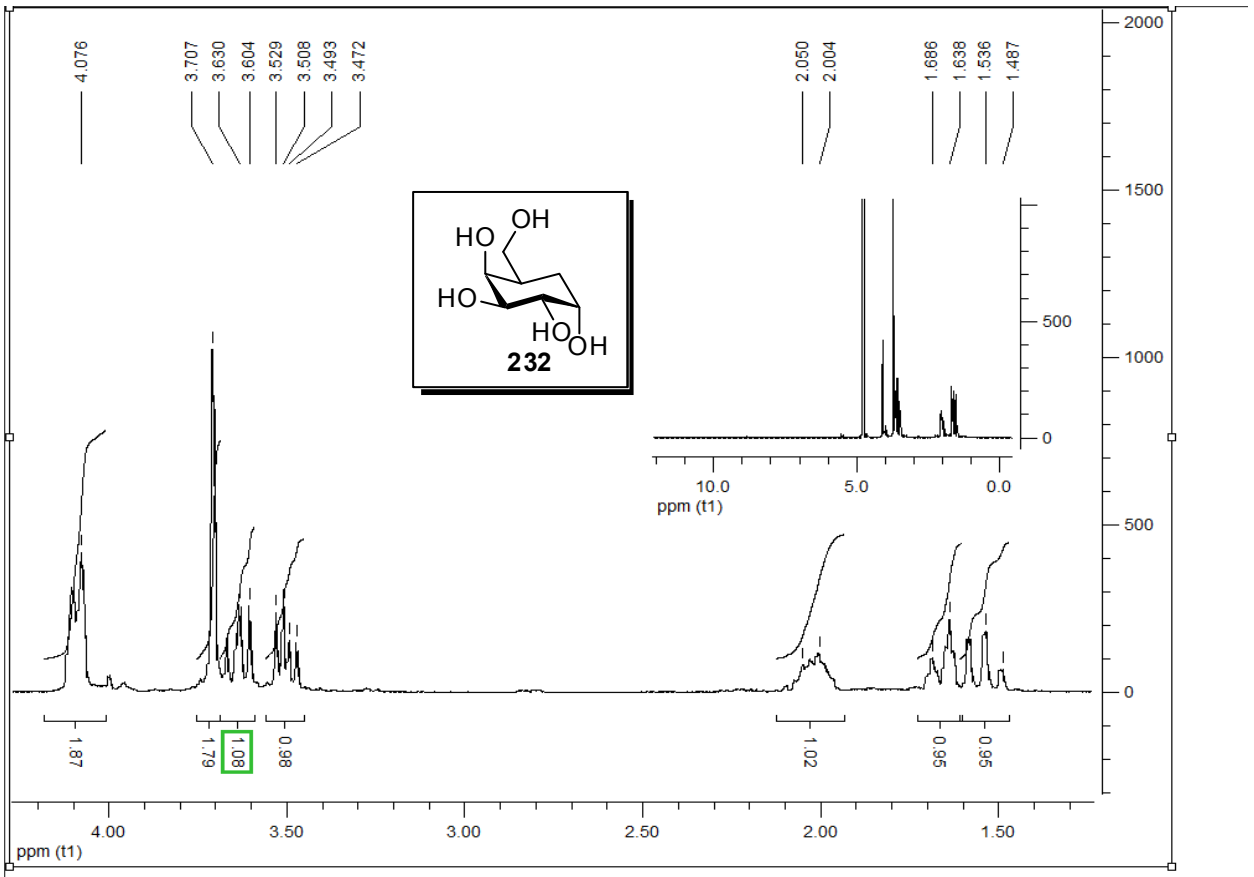

181.493
174.601
72.952
72.554
69.607
68.790
67.553
60.863
54.428
38.789
32.378
27.871
24.273
HO
OH
O
HO
HO
O
HN
H
N
H
OH
O
228
200
150
100
50
0
ppm (t1)

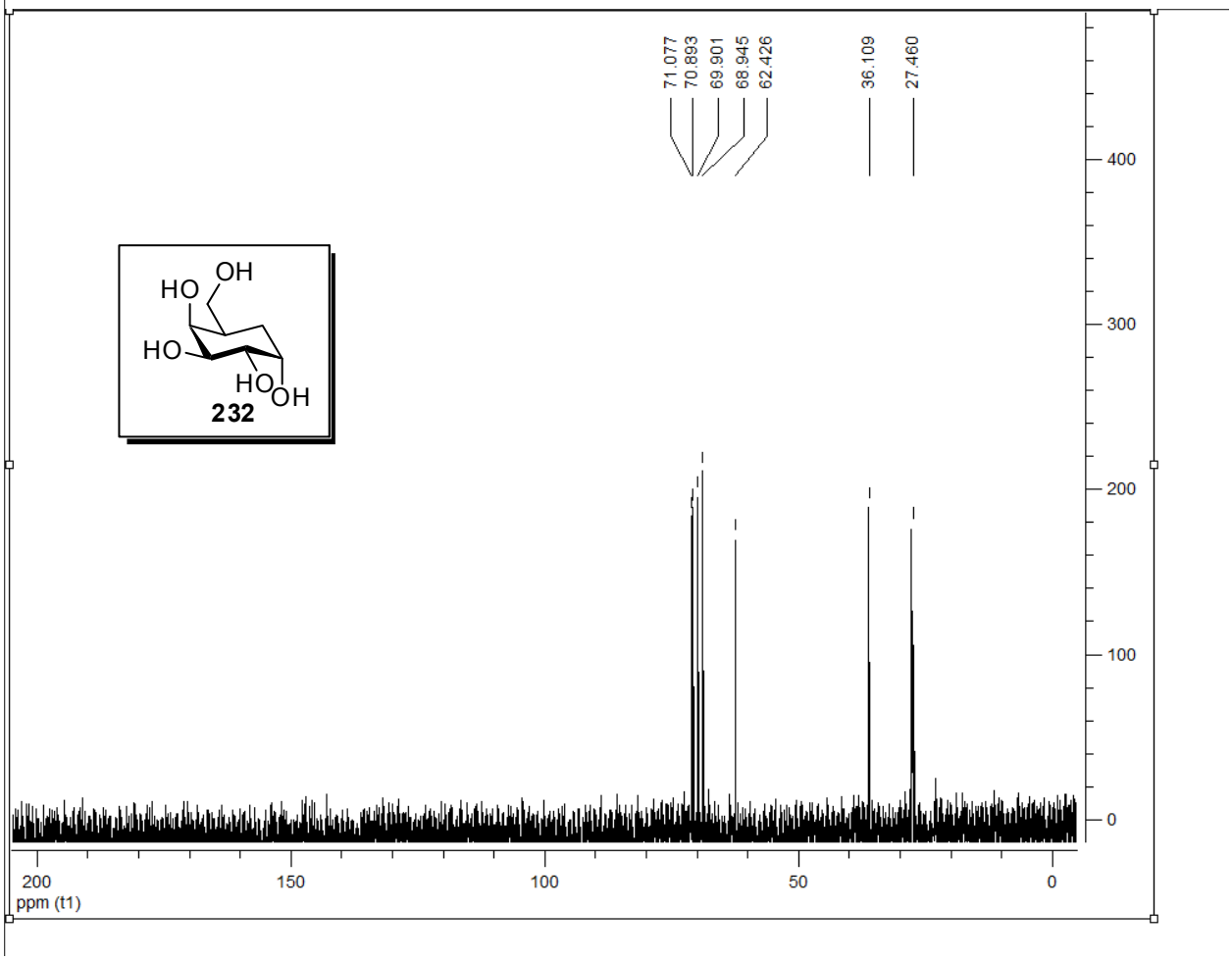

4.441
3.995
3.971
3.955
3.941
3.937
3.932
3.928
3.778
3.713
3.705
3.688
3.680
3.653
3.651
3.637
3.207
3.190
3.173
2.954
2.620
2.594
2.567
2.556
1.633
1.552
1.535
HO
OH
O
HO
HO
O
HN
H
N
H
229
0.97
2.00
4.01
2.00
2.16
1.96
4.18
4.50
4.00
3.50
3.00
2.50
2.00
1.50
ppm (t1)
10.0
5.0
ppm (t1)

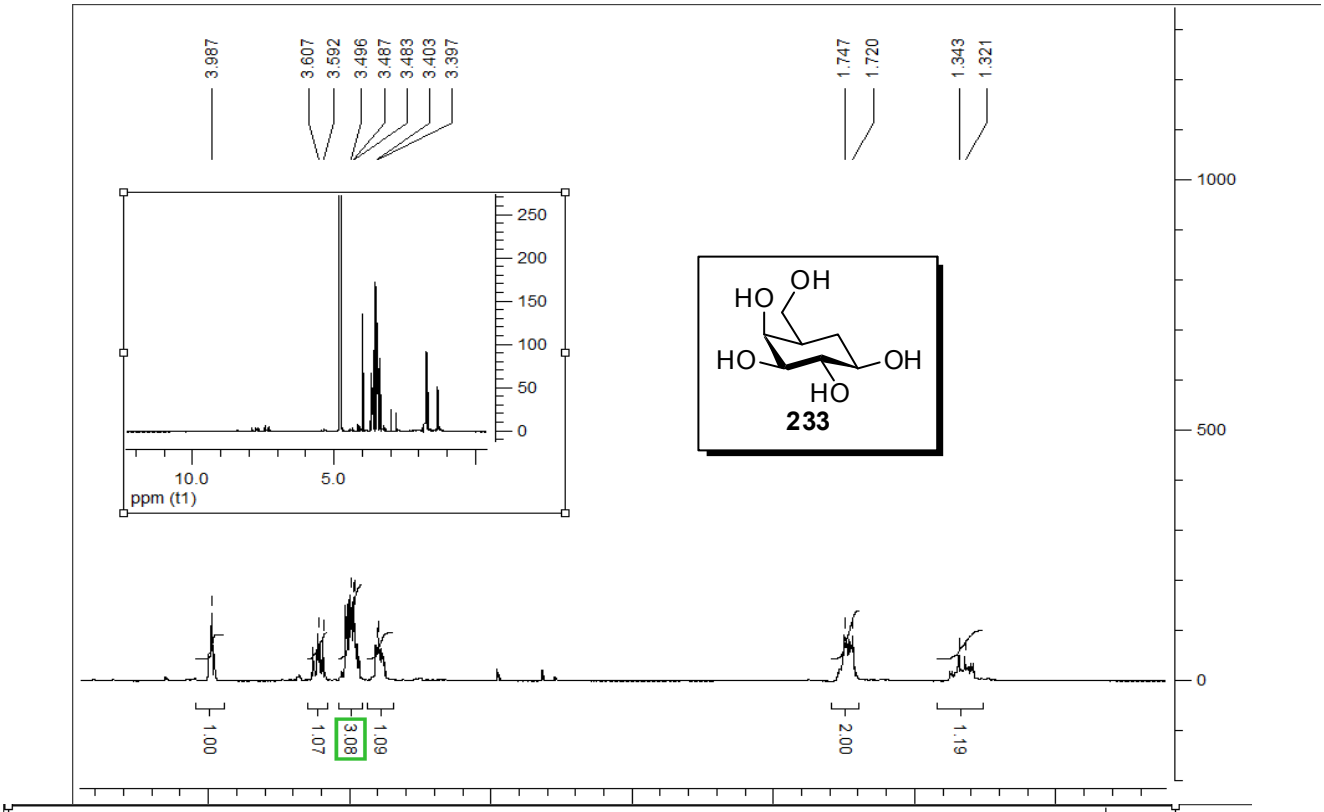

172.508
71.817
71.407
68.487
67.643
64.881
59.738
37.943
37.519
31.222
24.303
22.994
HO
OH
O
HO
HO
O
HN
H
N
H
229
200
150
100
50
0
ppm (t1)

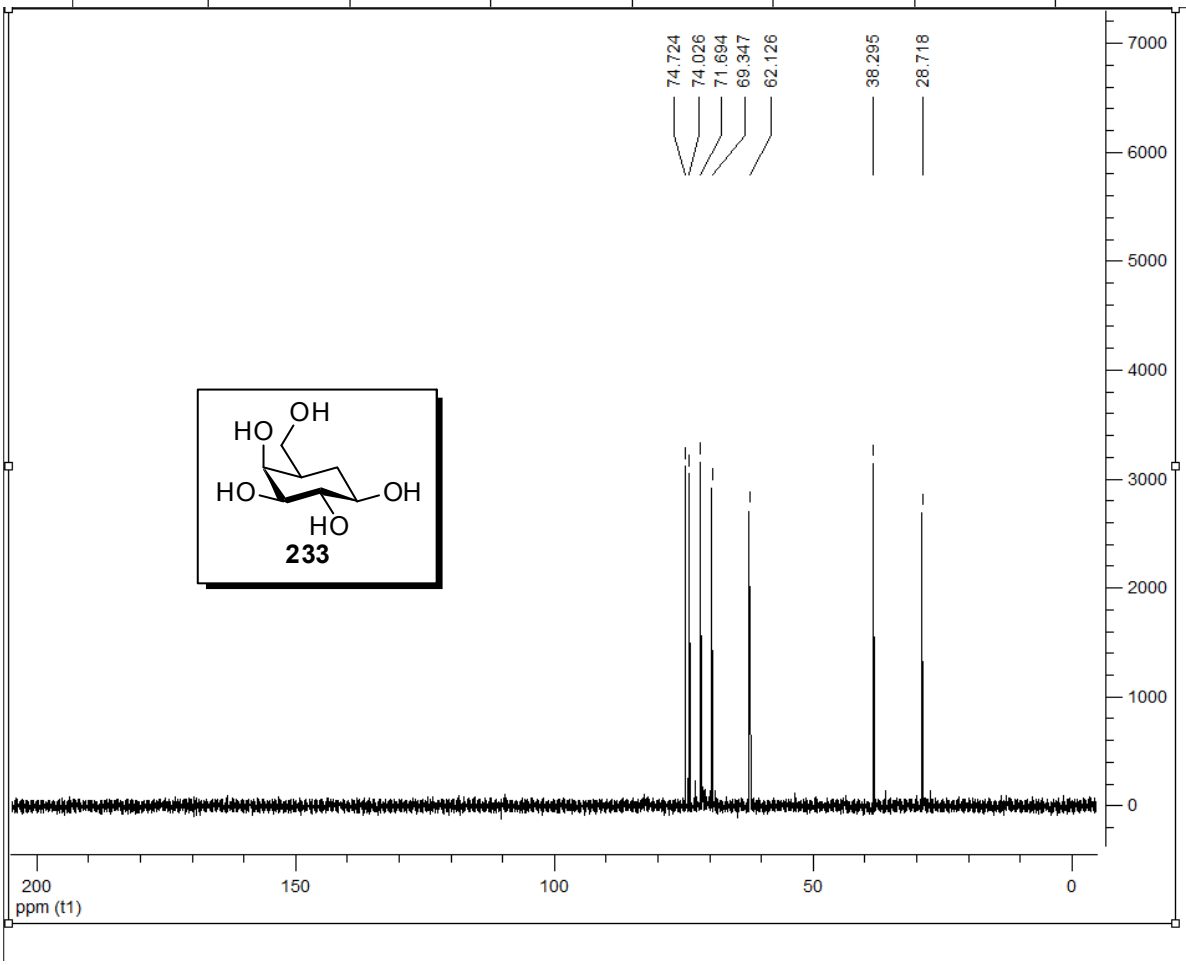

4.442
3.976
3.964
3.950
3.947
3.944
3.941
3.778
3.719
3.712
3.699
3.649
3.642
3.635
3.631
3.171
3.166
2.656
2.634
2.626
2.604
2.557
2.549
2.527
2.519
2.278
2.264
2.249
1.553
1.539
1.494
1.481
HO
OH
HO
HO
O
HN
OH
O
230
ppm (t1)
1.00
2.25
1.16
3.77
2.22
2.15
2.26
4.36

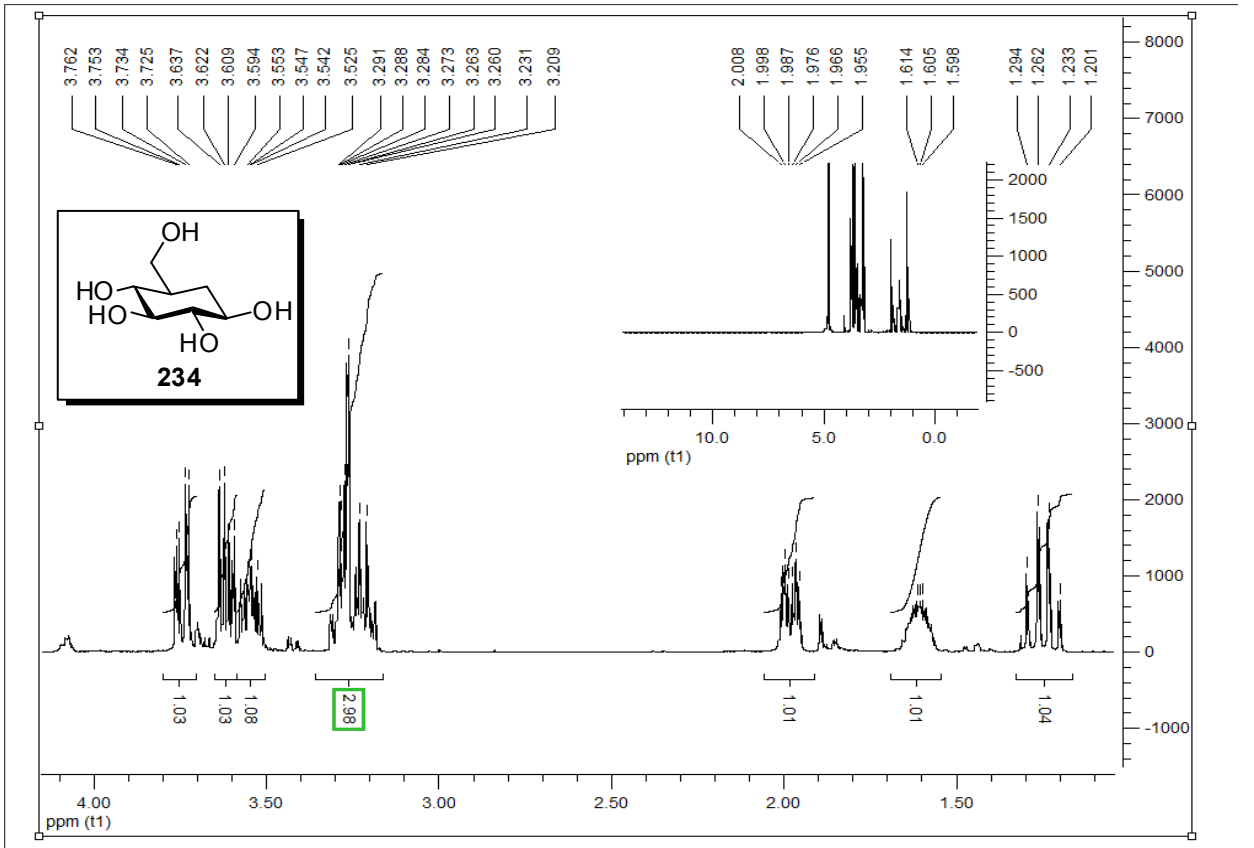

183.264
173.412
72.947
72.393
69.608
68.732
67.545
60.694
39.248
36.930
32.330
28.114
23.122
HO
OH
HO
HO
O
HN
OH
O
230
ppm (t1)

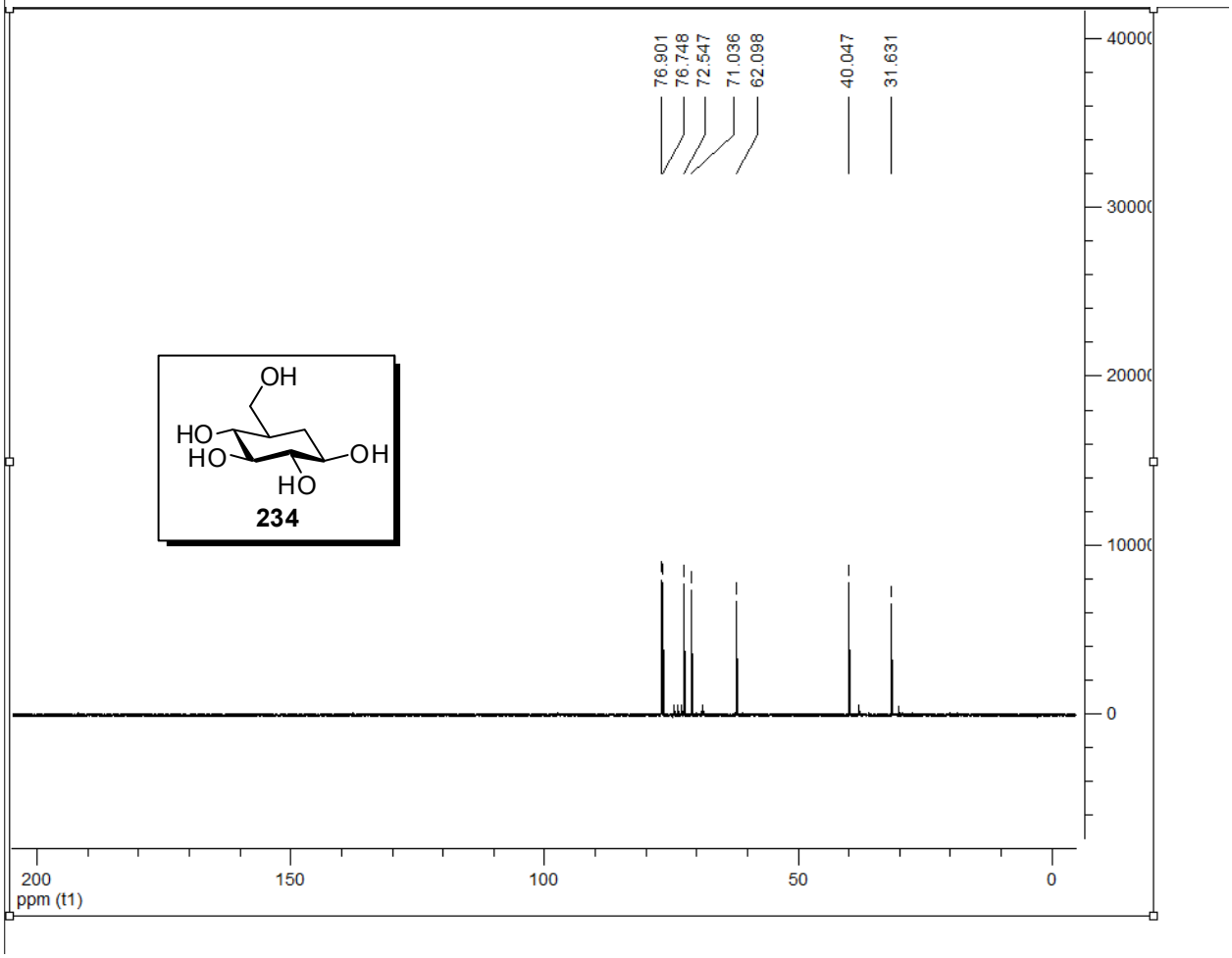

4.076
3.707
3.630
3.604
3.529
3.508
3.493
3.472
2.050
2.004
1.686
1.638
1.536
1.487
HO
OH
HO
HO
OH
232
ppm (t1)
1.87
1.79
1.08
0.98
1.02
0.96
0.95
ppm (t1)

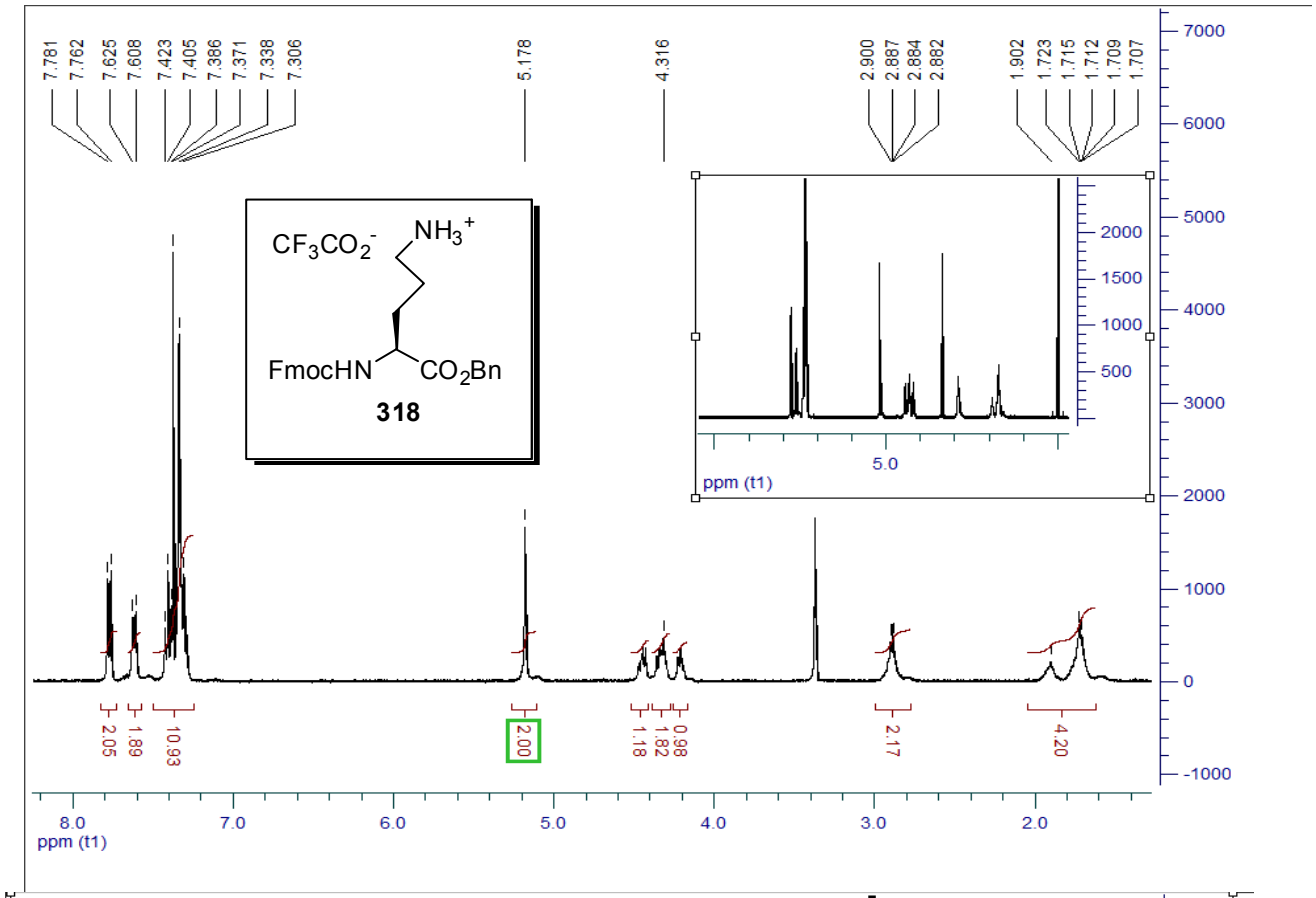

71.077
70.893
69.901
68.945
62.426
36.109
27.460
HO
OH
HO
HO
OH
232
ppm (t1)

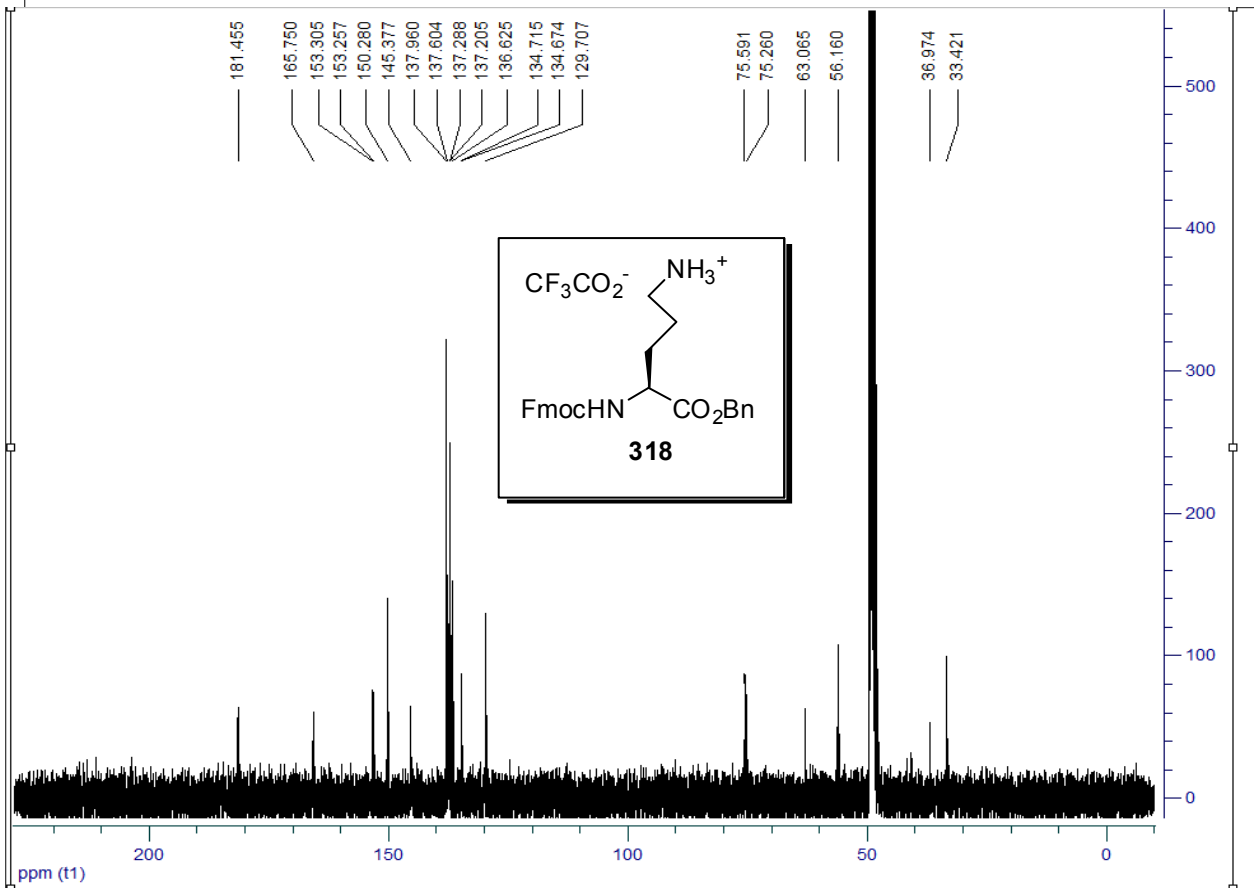

3.987
3.607
3.592
3.496
3.487
3.483
3.403
3.397
1.747
1.720
1.343
1.321
1000
500
0
250
200
150
100
50
0
10.0
5.0
ppm (t1)
HO
OH
HO
OH
HO
233
1.00
1.07
3.08
1.09
2.00
1.19

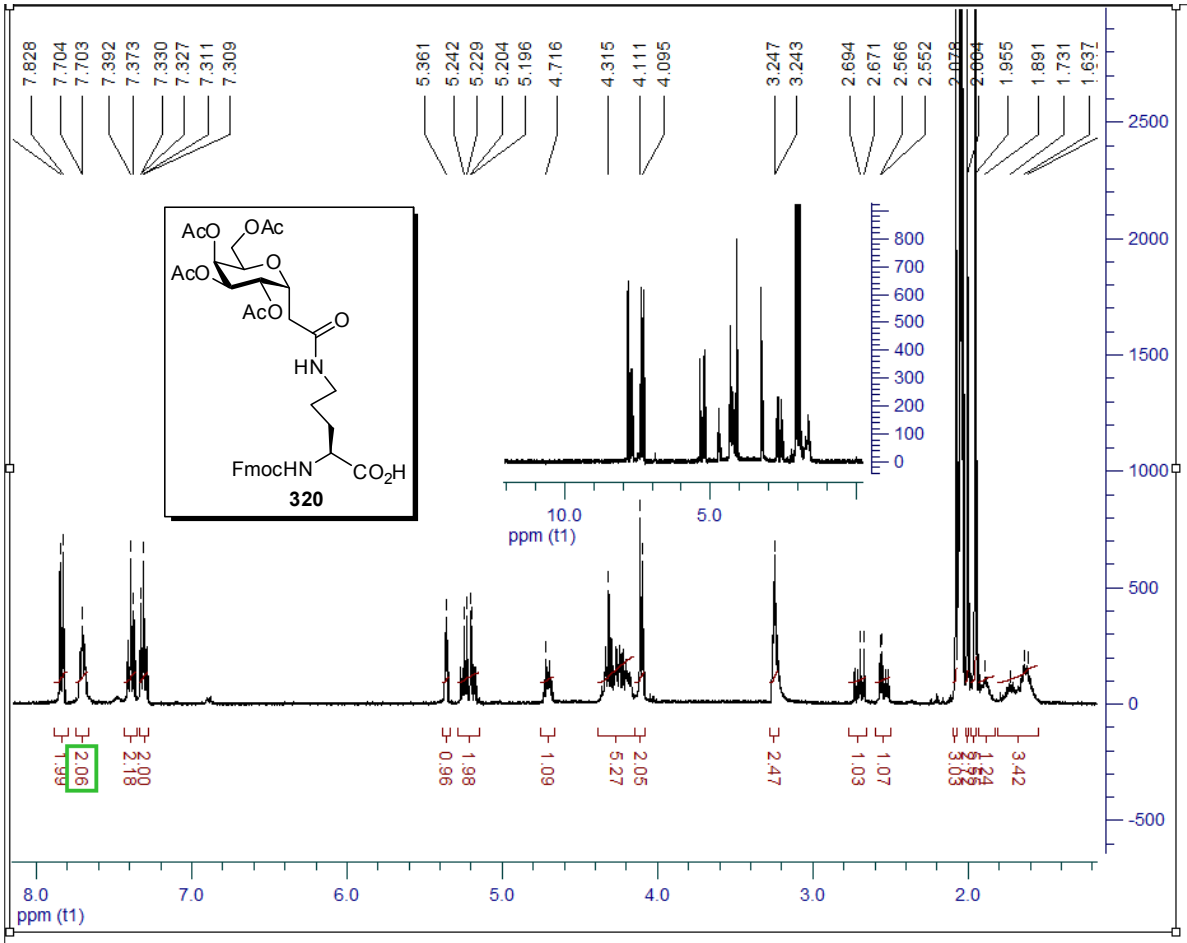

74.724
74.026
71.694
69.347
62.126
38.295
28.718
7000
6000
5000
4000
3000
2000
1000
0
HO
OH
HO
OH
HO
233
200
150
100
50
0
ppm (t1)

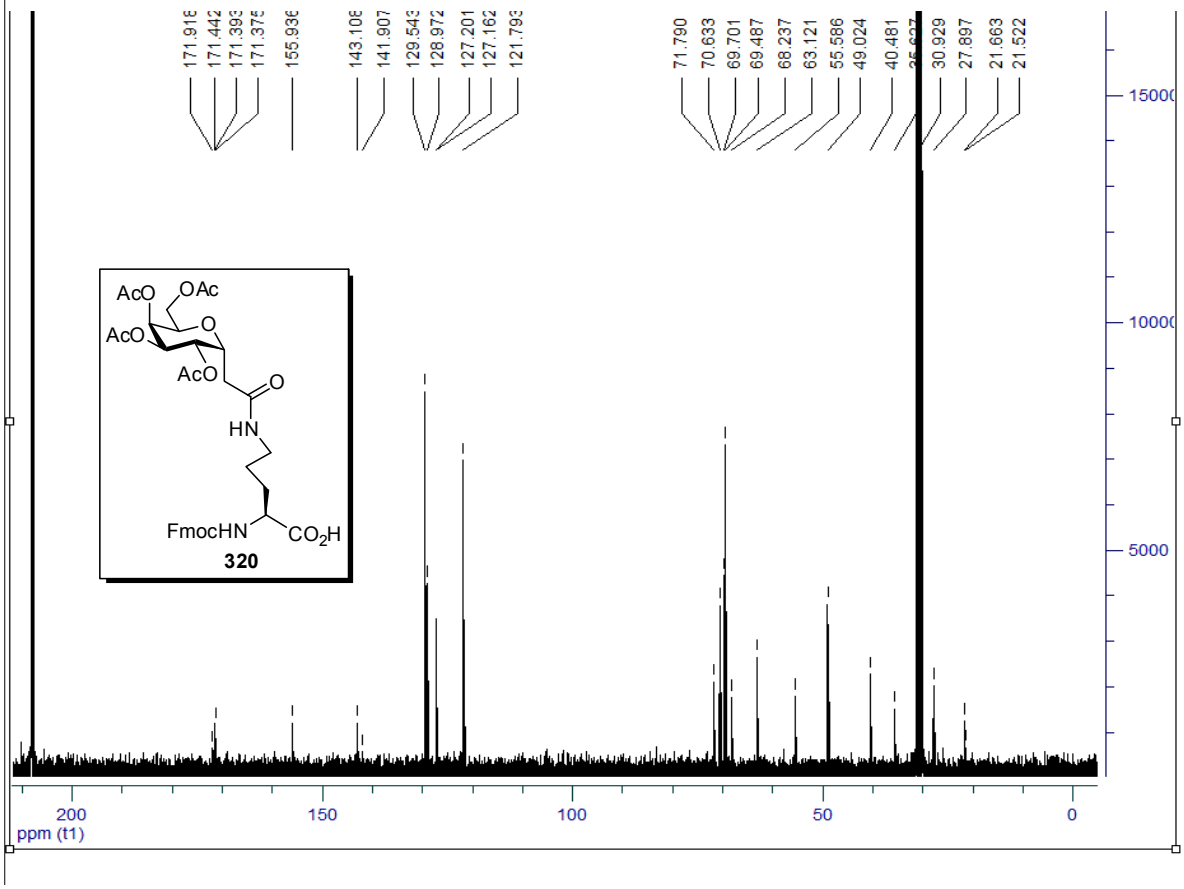

3.762
3.753
3.734
3.725
3.637
3.622
3.609
3.594
3.553
3.547
3.542
3.525
3.291
3.288
3.284
3.273
3.263
3.260
3.231
3.209
2.008
1.998
1.987
1.976
1.966
1.955
1.614
1.605
1.598
1.294
1.262
1.233
1.201
OH
HO
HO
OH
HO
234
ppm (t1)
1.03
1.03
1.08
2.86
1.01
1.01
1.04
ppm (t1)

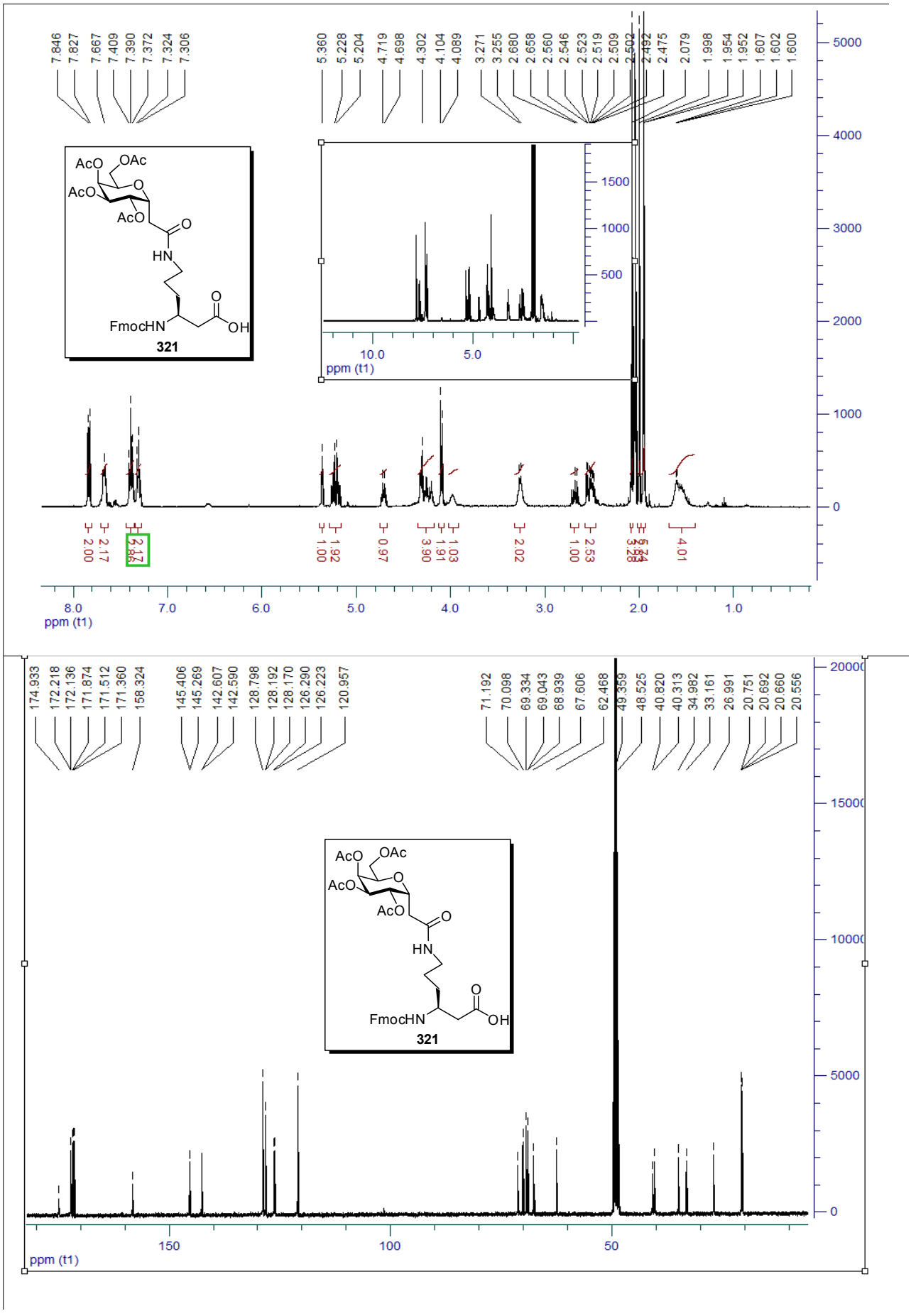

76.901
76.748
72.547
71.036
62.098
40.047
31.631
OH
HO
HO
OH
HO
234
ppm (t1)


7.781
7.762
7.625
7.608
7.423
7.405
7.386
7.371
7.338
7.306
5.178
4.316
2.900
2.887
2.884
2.882
1.902
1.723
1.715
1.712
1.709
1.707
CF3CO2-
NH3+
FmocHN
CO2Bn
318
ppm (t1)
2.05
1.89
10.93
2.00
1.18
2.82
0.98
2.17
4.20
8.0
7.0
6.0
5.0
4.0
3.0
2.0

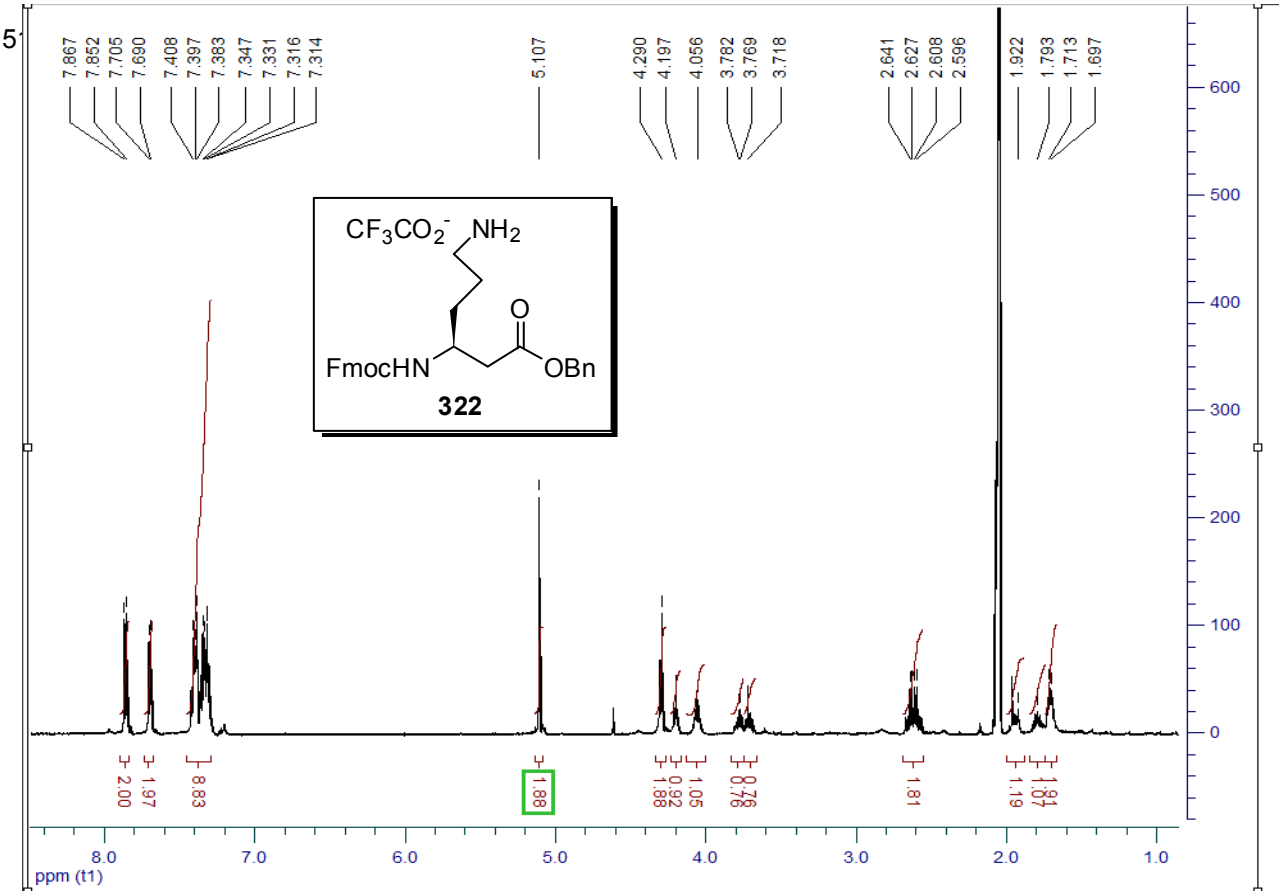

181.455
165.750
153.305
153.257
150.280
145.377
137.960
137.604
137.288
137.205
136.625
134.715
134.674
129.707
75.591
75.260
63.065
56.160
36.974
33.421
CF3CO2-
NH3+
FmocHN
CO2Bn
318
ppm (t1)
200
150
100
50
0

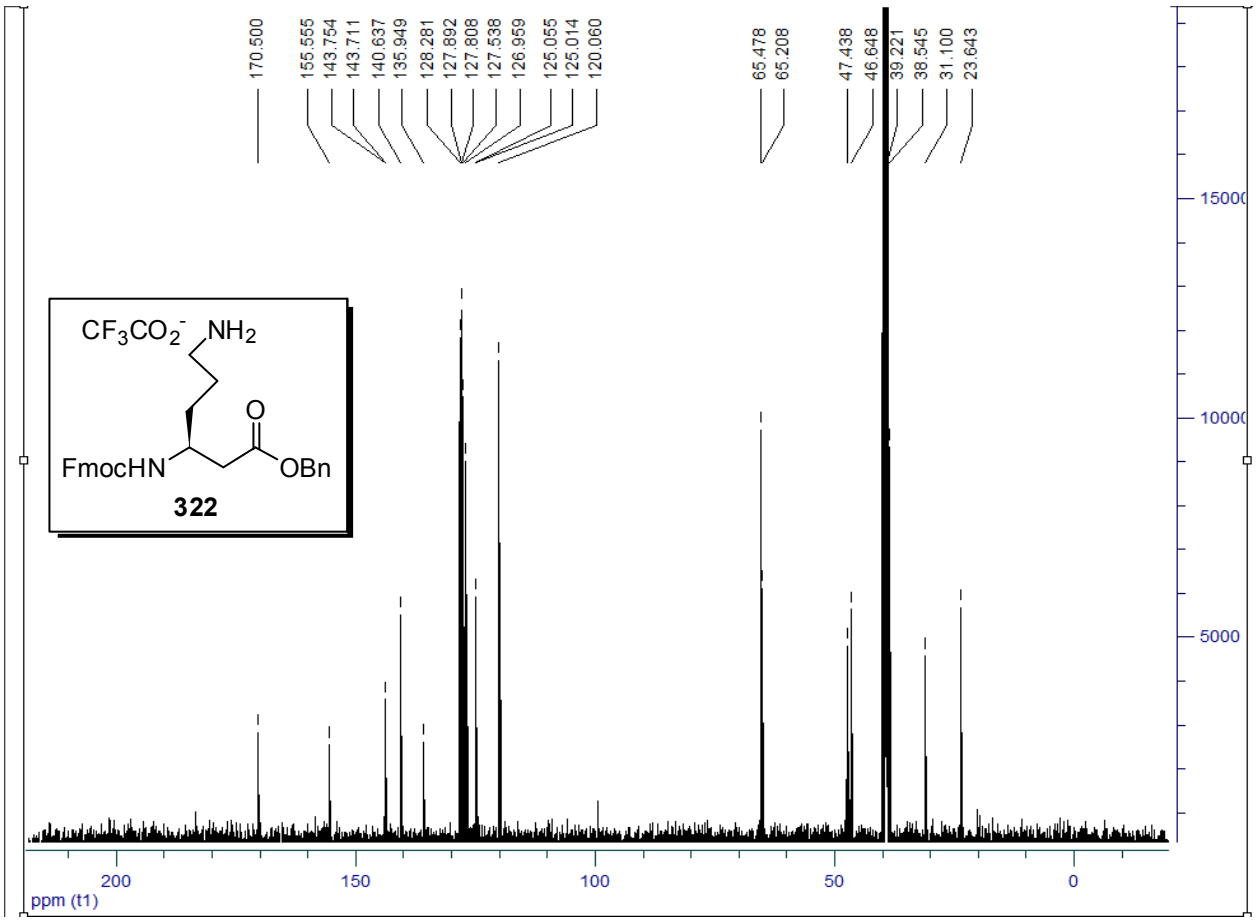

7.828
7.704
7.703
7.392
7.373
7.330
7.327
7.311
7.309
5.361
5.242
5.229
5.204
5.196
4.716
4.315
4.111
4.095
3.247
3.243
2.694
2.671
2.566
2.552
2.078
2.064
1.955
1.891
1.731
1.637
AcO
OAc
AcO
AcO
O
HN
FmocHN
CO2H
320
ppm (t1)
8.0
7.0
6.0
5.0
4.0
3.0
2.0

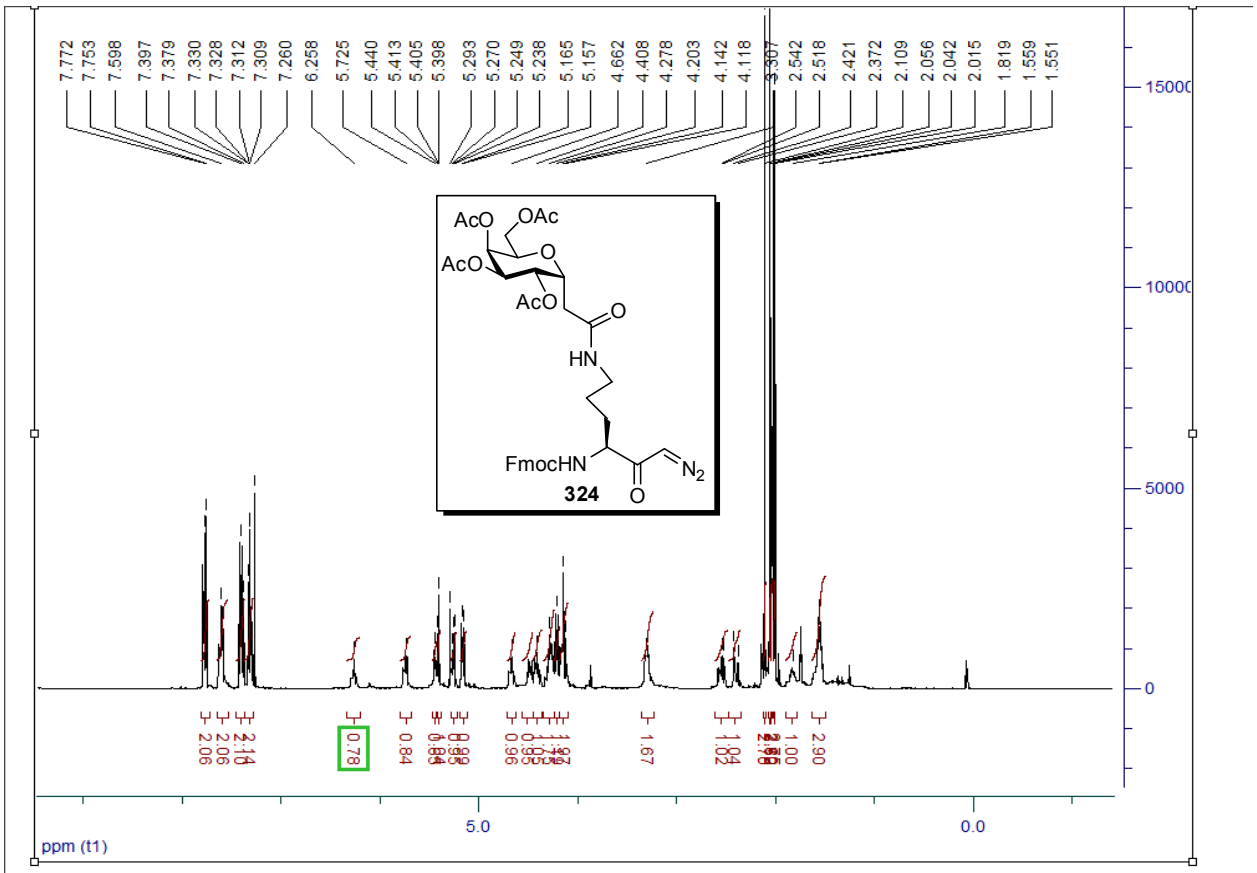

171.918
171.442
171.393
171.375
155.936
143.108
141.907
129.543
128.972
127.201
127.162
121.793
71.790
70.633
69.701
69.487
68.237
63.121
55.586
49.024
40.481
30.929
27.897
21.663
21.522
AcO
OAc
AcO
AcO
O
HN
FmocHN
CO2H
320
ppm (t1)
200
150
100
50
0

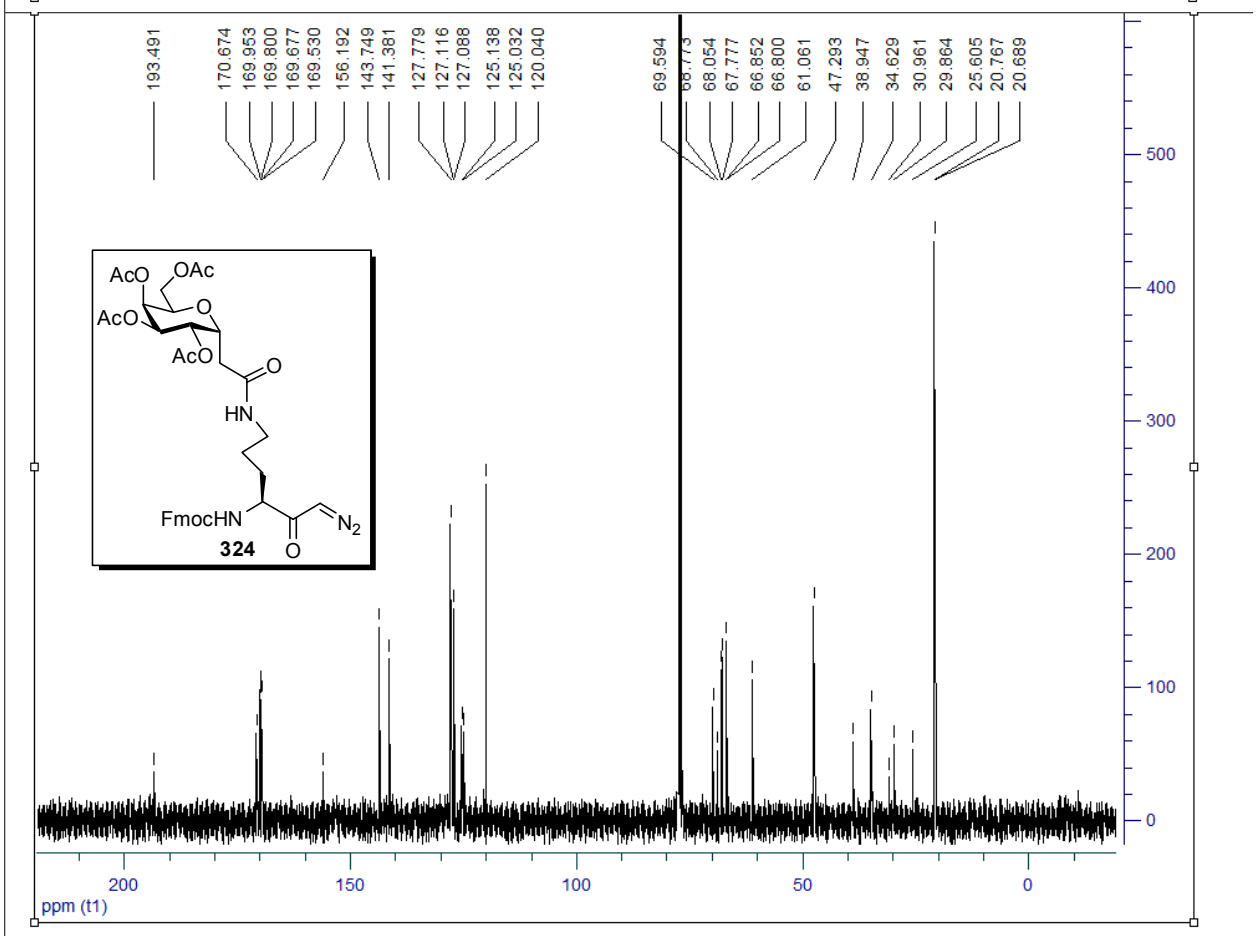

7.846
7.827
7.667
7.409
7.390
7.372
7.324
7.306
5.360
5.228
5.204
4.719
4.698
4.302
4.104
4.089
3.271
3.255
2.680
2.658
2.560
2.546
2.523
2.519
2.509
2.502
2.492
2.475
2.079
1.998
1.954
1.952
1.607
1.602
1.600
AcO
OAc
AcO
AcO
O
HN
FmocHN
OH
321
ppm (t1)
2.00
2.17
2.27
1.00
1.82
0.97
3.90
1.91
1.03
2.02
1.00
2.53
4.01
ppm (t1)
174.933
172.218
172.136
171.874
171.512
171.360
158.324
145.406
145.269
142.607
142.590
128.798
128.192
128.170
126.290
126.223
120.957
71.192
70.098
69.334
69.043
68.939
67.606
62.468
49.359
48.525
40.820
40.313
34.982
33.161
26.991
20.751
20.692
20.660
20.556
AcO
OAc
AcO
AcO
O
HN
FmocHN
OH
321
ppm (t1)

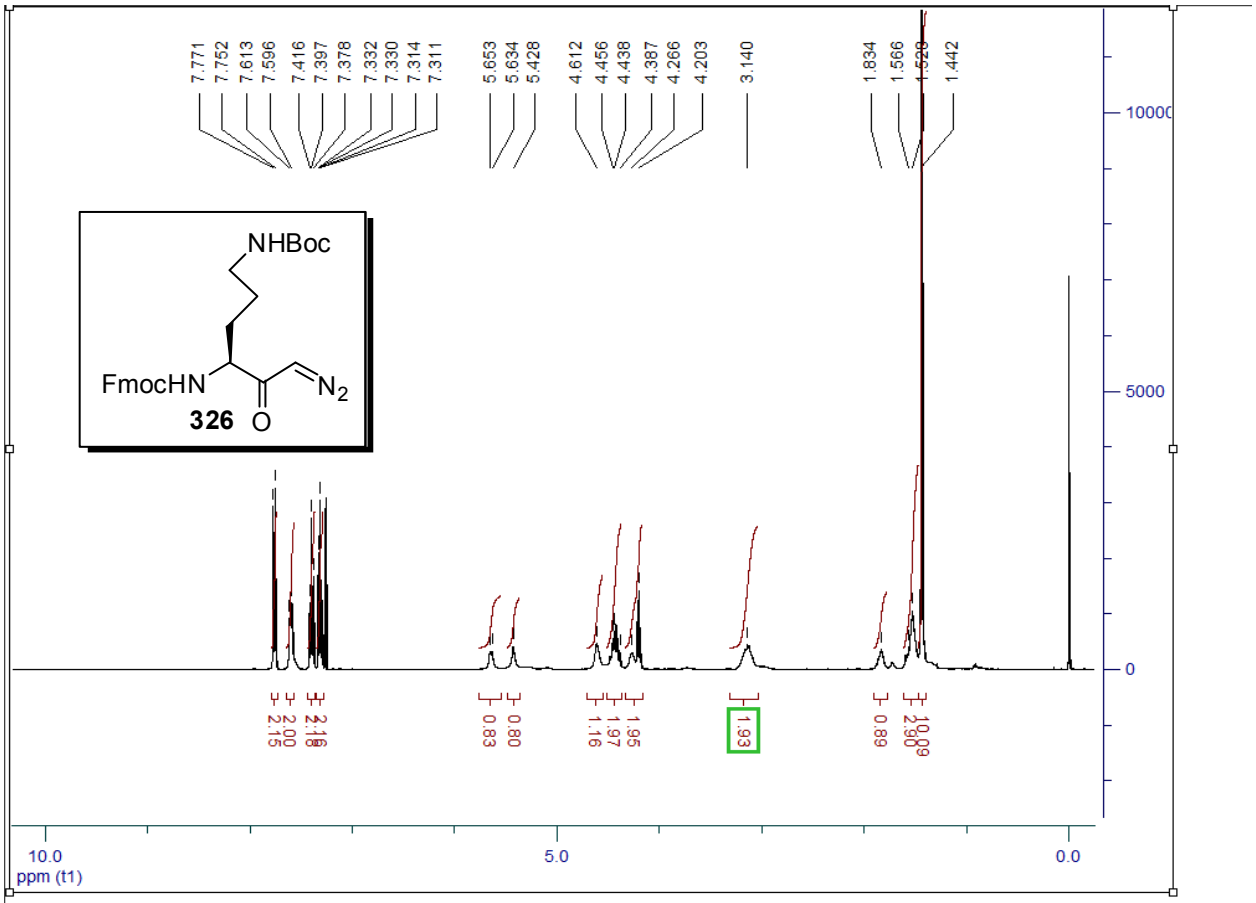
5

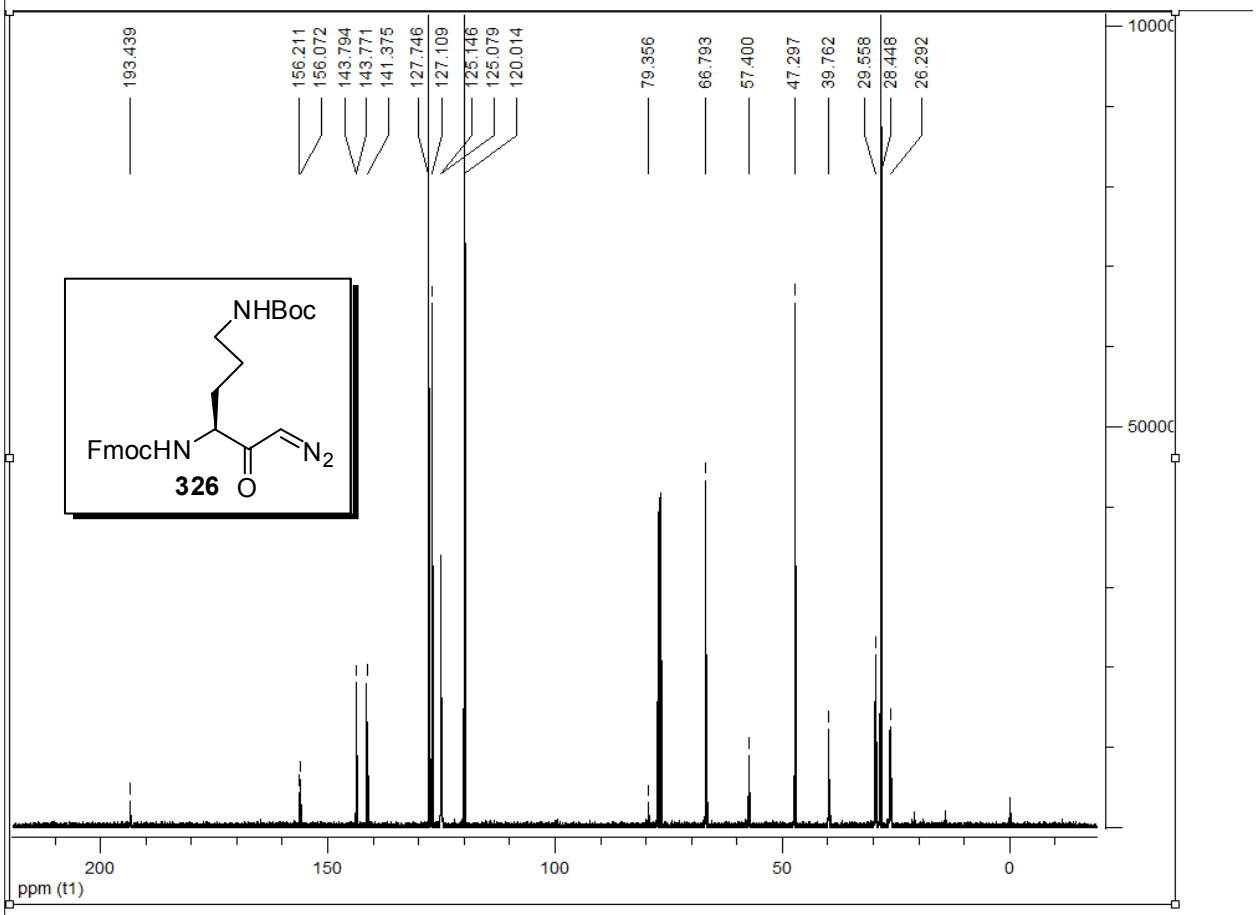

7.867
7.852
7.705
7.690
7.408
7.397
7.383
7.347
7.331
7.316
7.314
5.107
4.290
4.197
4.056
3.782
3.769
3.718
2.641
2.627
2.608
2.596
1.922
1.793
1.713
1.697
CF3CO2- NH2
FmocHN
O
OBn
322
2.00
1.97
8.83
1.88
0.92
1.05
0.78
0.76
1.81
1.19
1.07
1.84
ppm (t1)

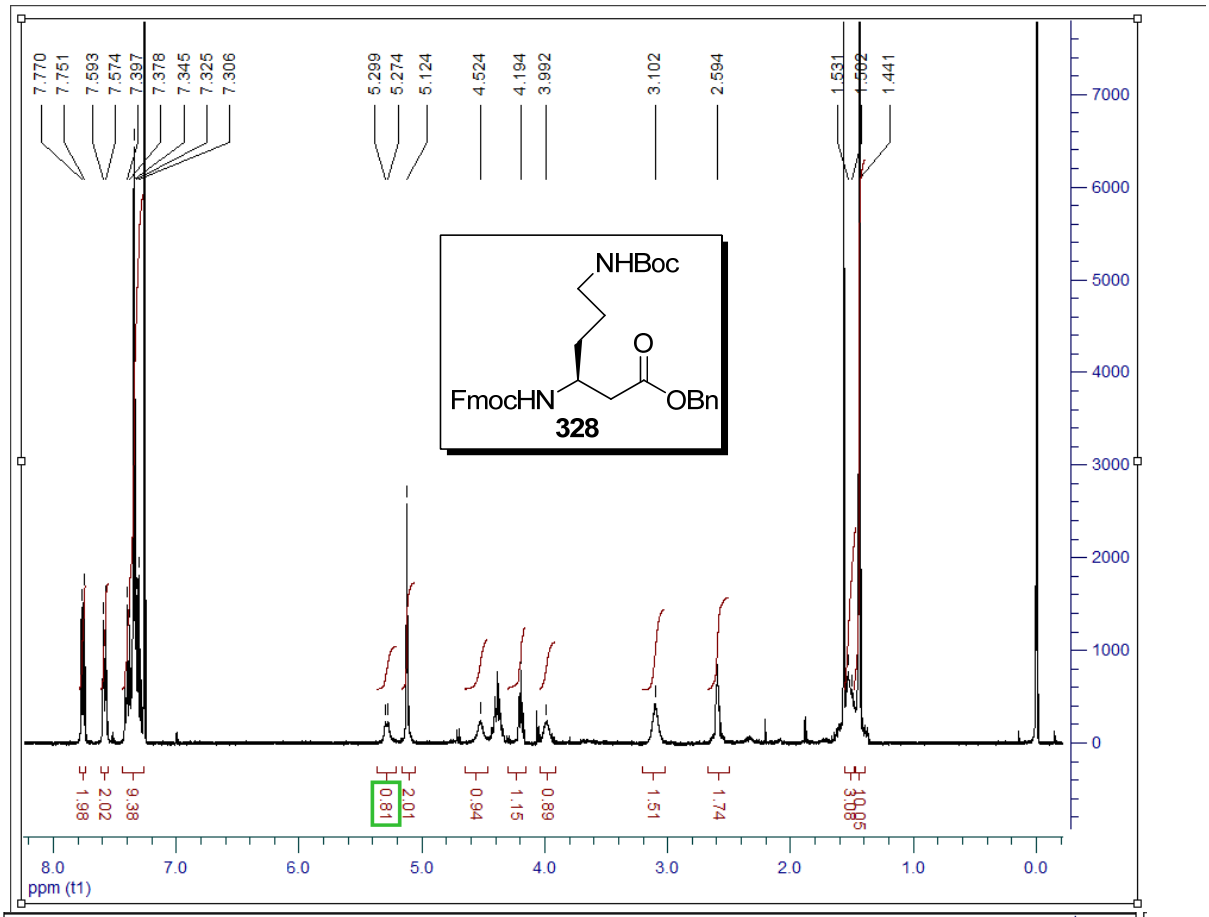

170.500
155.555
143.754
143.711
140.637
135.949
128.281
127.892
127.808
127.538
126.959
125.055
125.014
120.060
65.478
65.208
47.438
46.648
39.221
38.545
31.100
23.643
CF3CO2- NH2
FmocHN
O
OBn
322
ppm (t1)

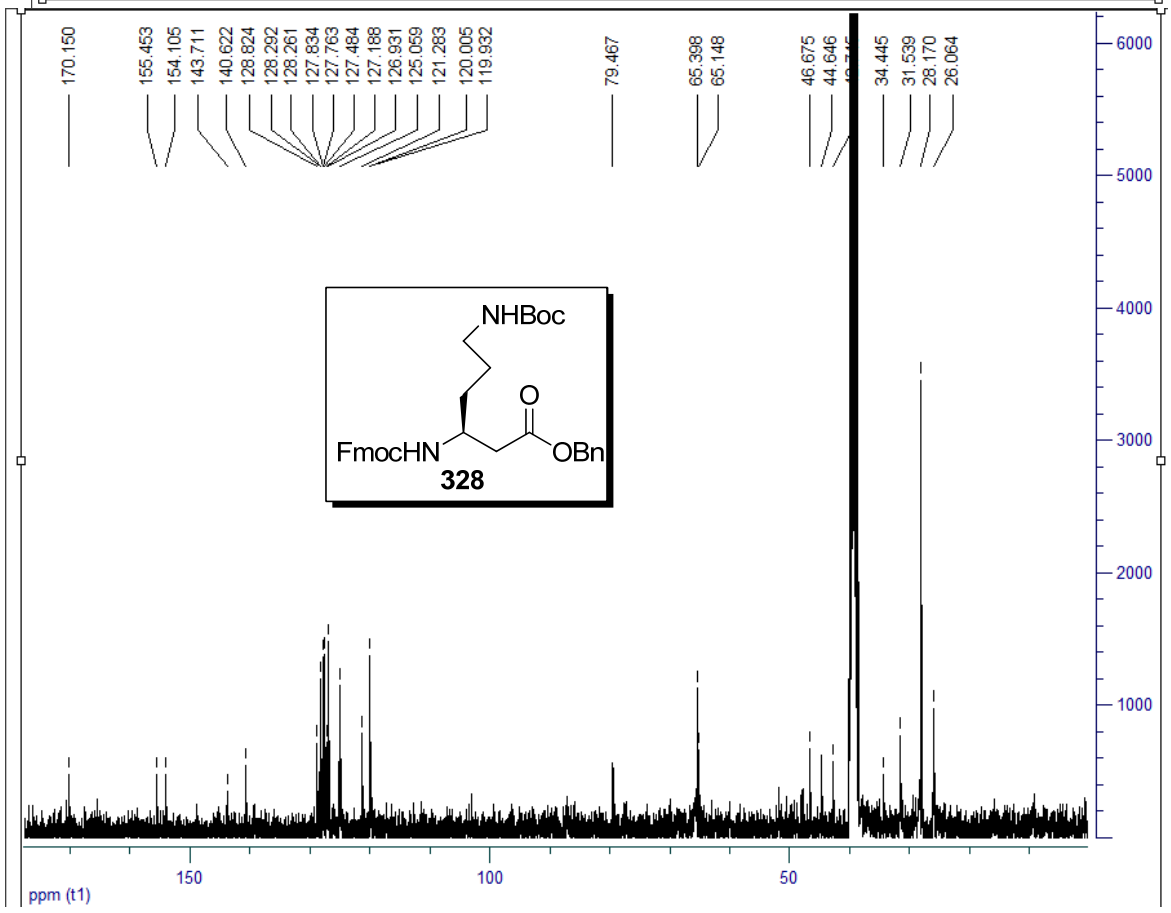

7.772
7.753
7.598
7.397
7.379
7.330
7.328
7.312
7.309
7.260
6.258
5.725
5.440
5.413
5.405
5.398
5.293
5.270
5.249
5.238
5.165
5.157
4.662
4.408
4.278
4.203
4.142
4.118
3.387
2.542
2.518
2.421
2.372
2.109
2.056
2.042
2.015
1.819
1.559
1.551
AcO
OAc
AcO
AcO
O
HN
FmocHN
N2
O
324
15000
10000
5000
0
2.06
2.06
2.14
0.78
0.84
0.96
1.67
1.02
1.00
2.90
5.0
0.0
ppm (t1)

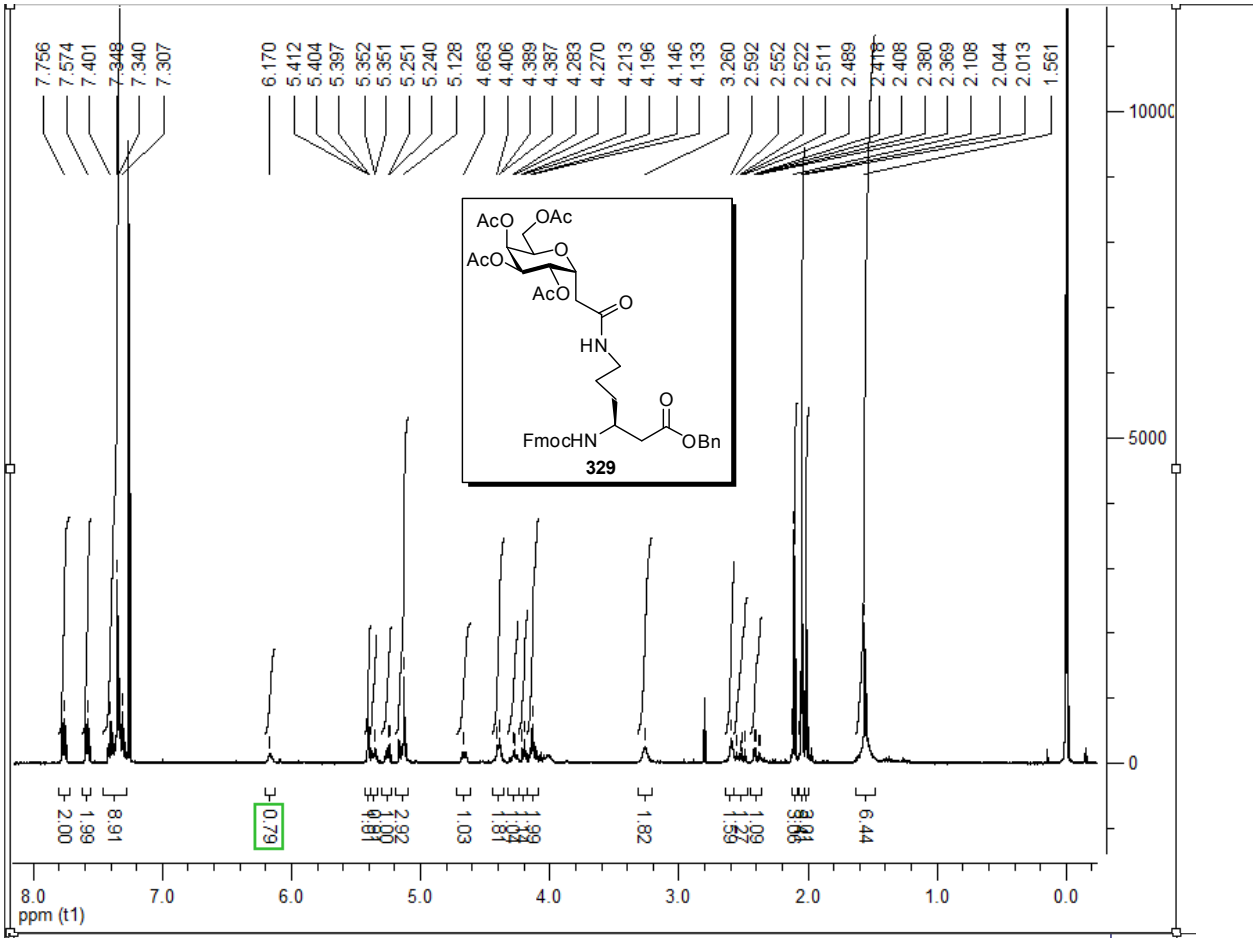

193.491
170.674
169.953
169.800
169.677
169.530
156.192
143.749
141.381
127.779
127.116
127.088
125.138
125.032
120.040
69.594
68.773
68.054
67.777
66.852
66.800
61.061
47.293
38.947
34.629
30.961
29.864
25.605
20.767
20.689
AcO
OAc
AcO
AcO
O
HN
FmocHN
N2
O
324
500
400
300
200
100
0
200
150
100
50
0
ppm (t1)

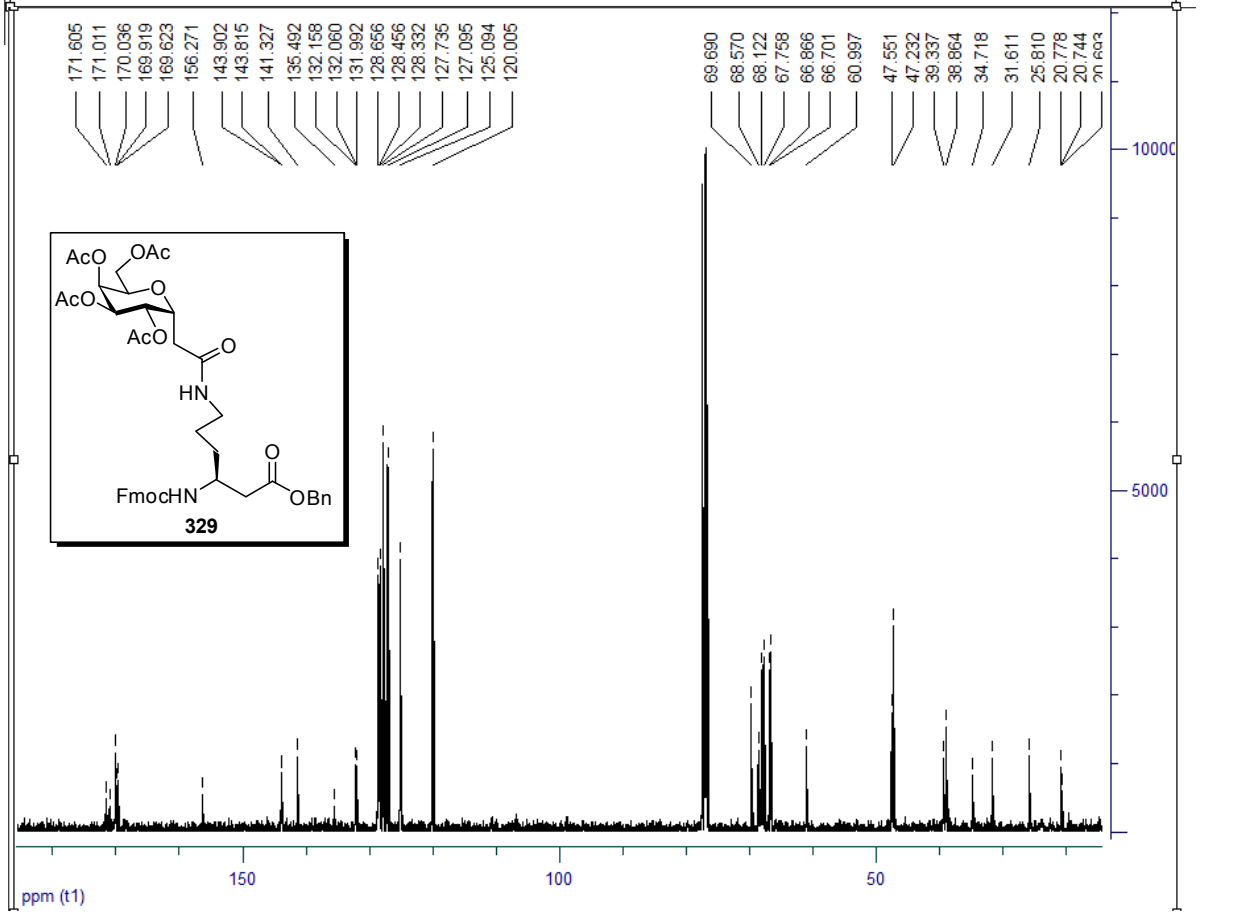

7.771
7.752
7.613
7.596
7.416
7.397
7.378
7.332
7.330
7.314
7.311
5.653
5.634
5.428
4.612
4.456
4.438
4.387
4.266
4.203
3.140
1.834
1.566
1.529
1.442
NHBoc
FmocHN
N2
326
O
10000
5000
0
2.15
2.00
2.18
0.83
0.80
1.96
1.97
1.16
1.93
0.89
2.00
10.0
5.0
0.0
ppm (t1)

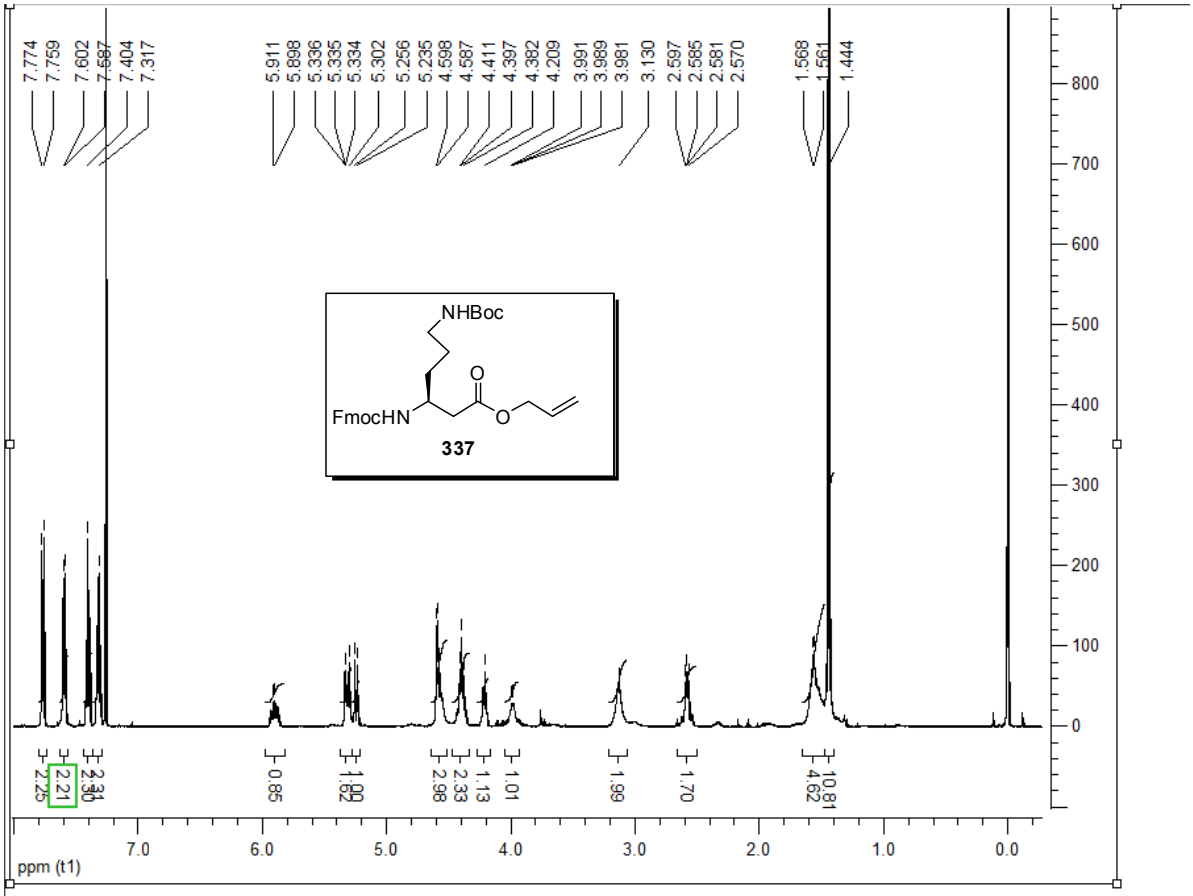

193.439
156.211
156.072
143.794
143.771
141.375
127.746
127.109
125.146
125.079
120.014
79.356
66.793
57.400
47.297
39.762
29.558
28.448
26.292
NHBoc
FmocHN
N2
326
O
10000
50000
200
150
100
50
0
ppm (t1)

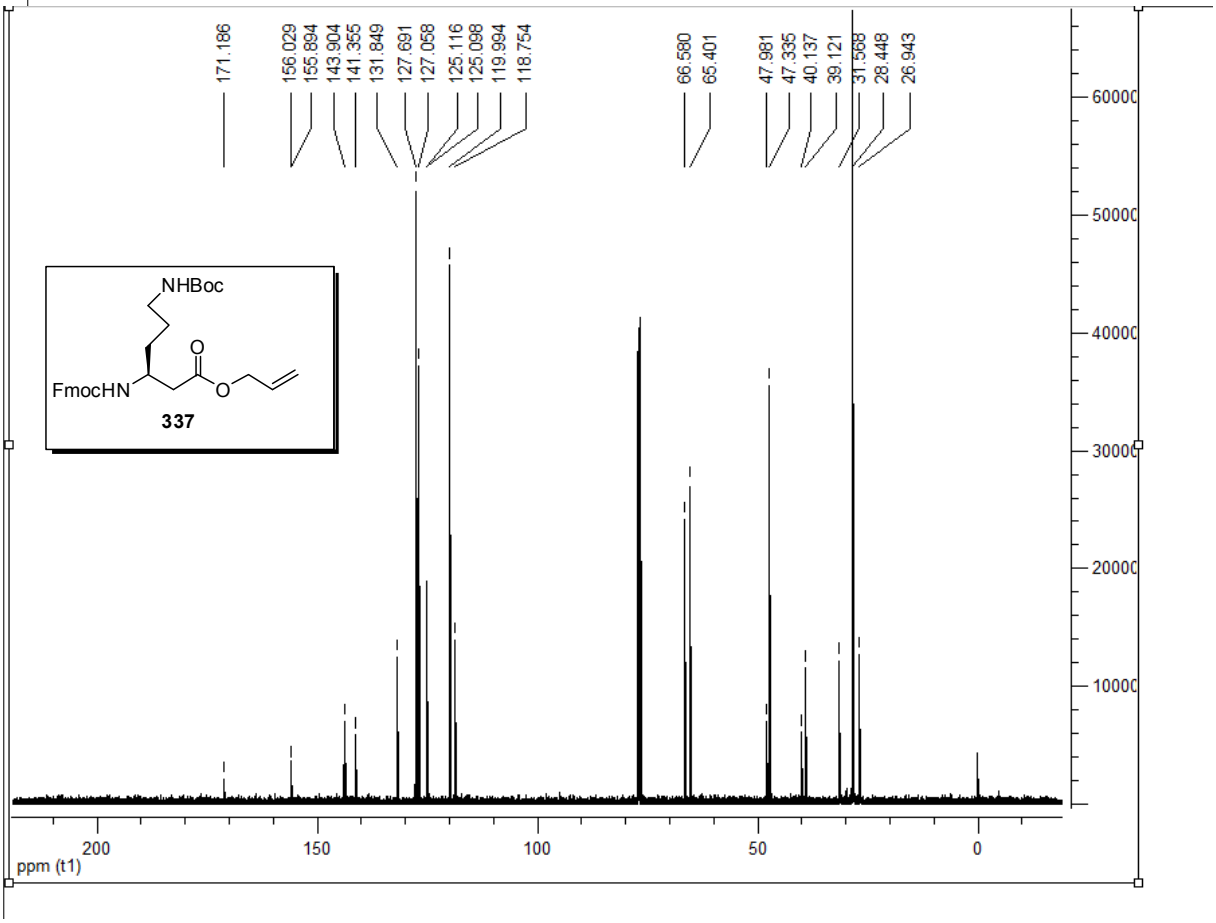

7.770
7.751
7.593
7.574
7.397
7.378
7.345
7.325
7.306
5.299
5.274
5.124
4.524
4.194
3.992
3.102
2.594
1.531
1.502
1.441
NHBoc
O
FmocHN
OBn
328
1.98
2.02
9.38
0.81
2.01
0.94
1.15
0.89
1.51
1.74
10.05
3.80
8.0
7.0
6.0
5.0
4.0
3.0
2.0
1.0
0.0
ppm (t1)

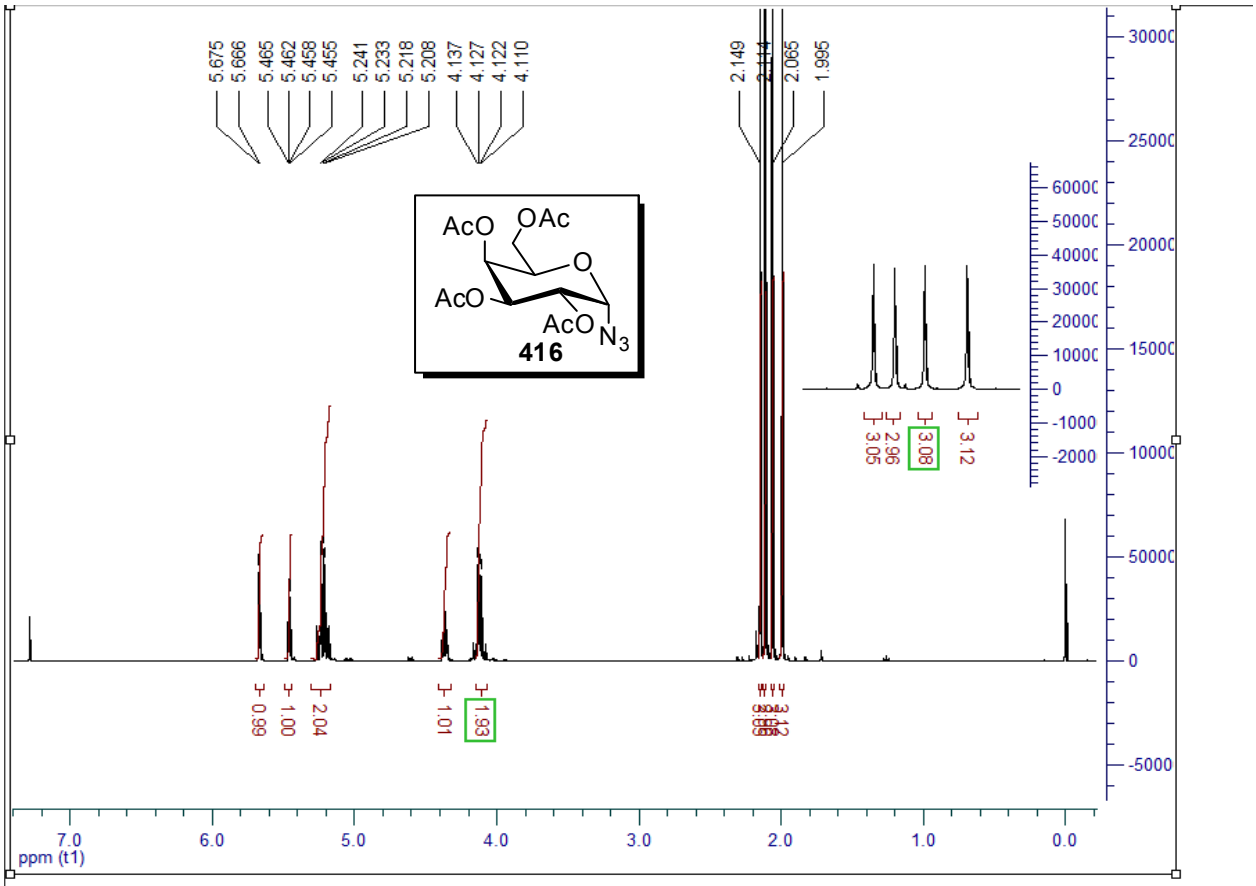

170.150
155.453
154.105
143.711
140.622
128.824
128.292
128.261
127.834
127.763
127.484
127.188
126.931
125.059
121.283
120.005
119.932
79.467
65.398
65.148
46.675
44.646
34.445
31.539
28.170
26.064
NHBoc
O
FmocHN
OBn
328
150
100
50
ppm (t1)

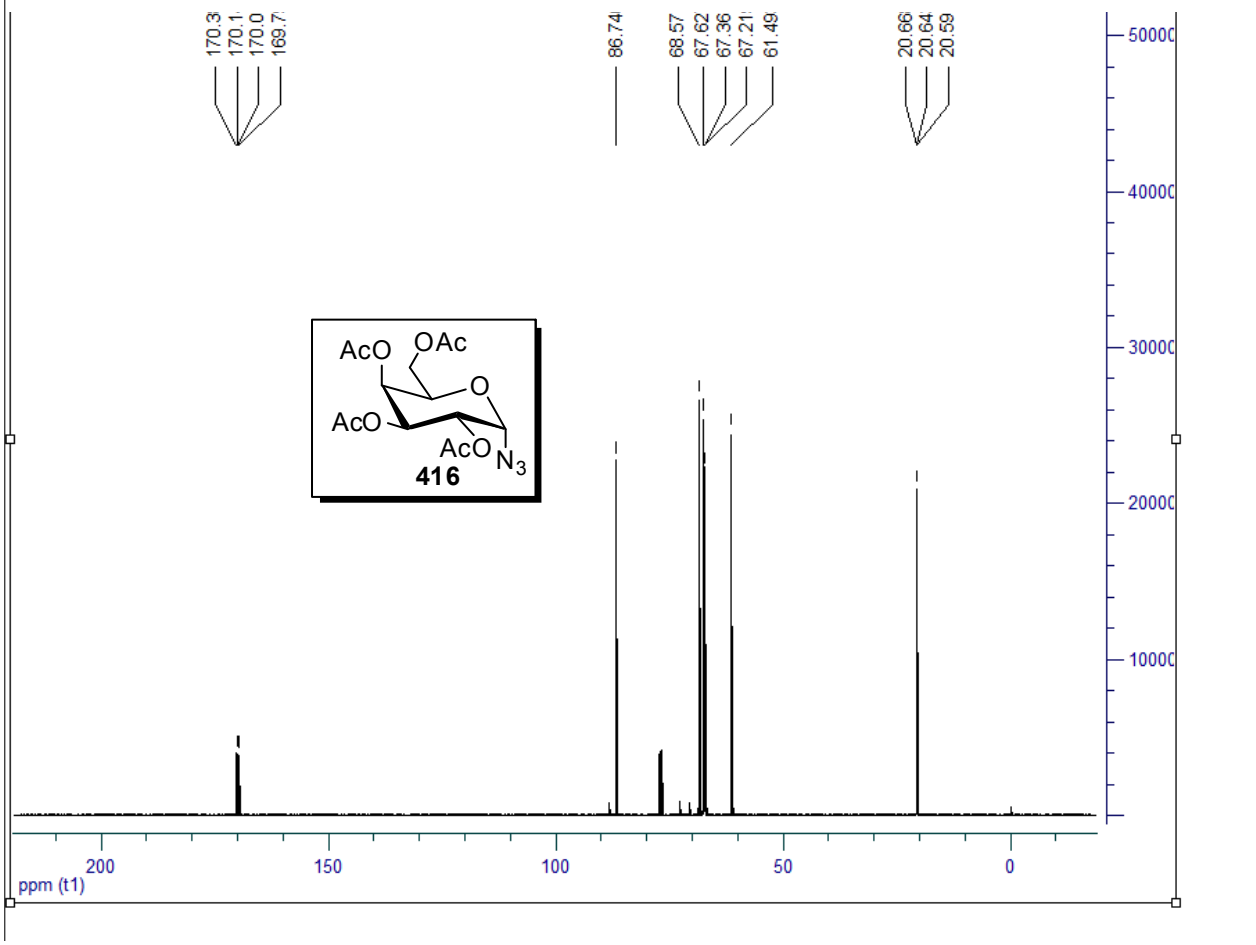

7.756
7.574
7.401
7.348
7.340
7.307
6.170
5.412
5.404
5.397
5.352
5.351
5.251
5.240
5.128
4.663
4.406
4.389
4.387
4.283
4.270
4.213
4.196
4.146
4.133
3.260
2.592
2.552
2.522
2.511
2.489
2.418
2.408
2.380
2.369
2.108
2.044
2.013
1.561
AcO
OAc
AcO
AcO
O
O
HN
FmocHN
O
OBn
329
10000
5000
0
2.00
1.99
8.91
0.79
2.92
1.03
1.87
1.82
1.59
1.09
6.44
8.0
7.0
6.0
5.0
4.0
3.0
2.0
1.0
0.0
ppm (t1)

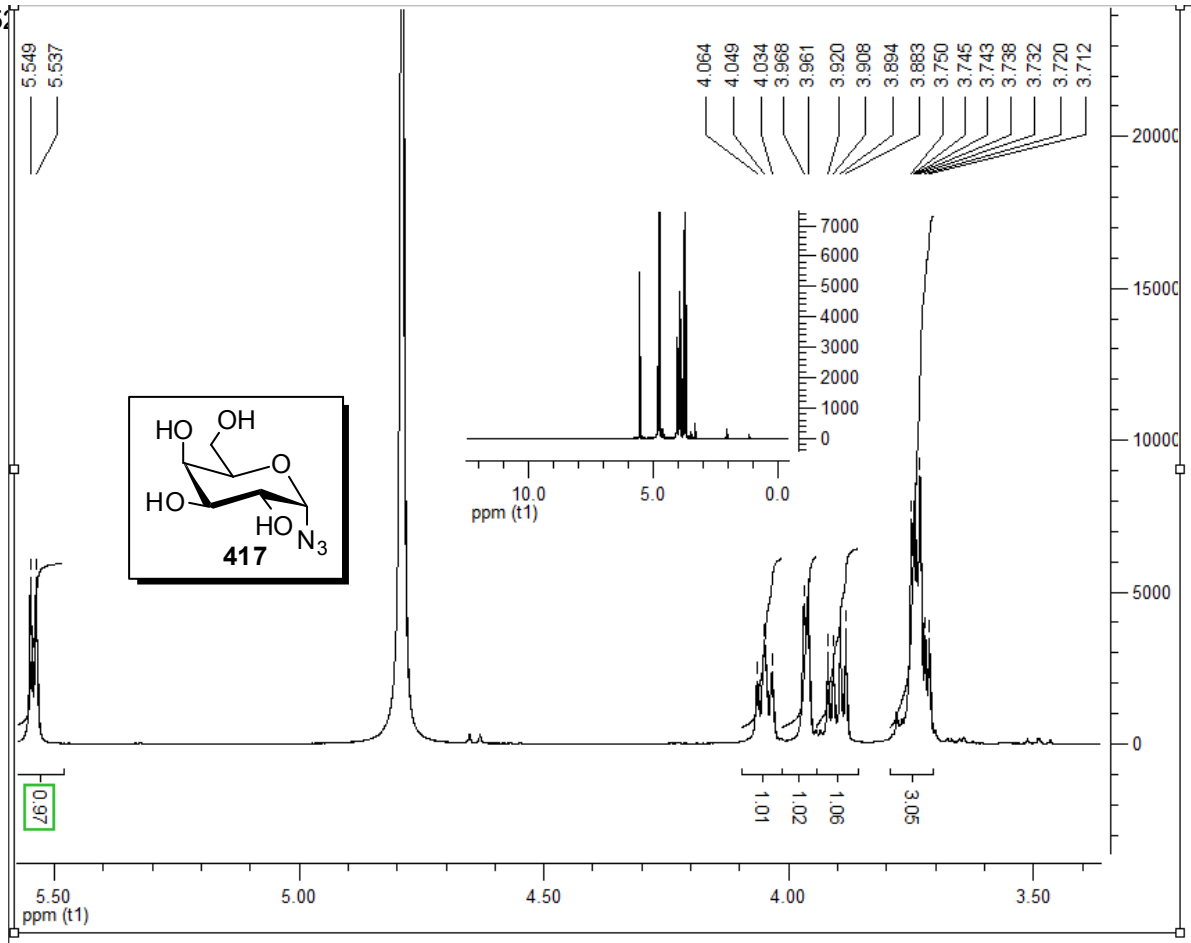

171.605
171.011
170.036
169.919
169.623
156.271
143.902
143.815
141.327
135.492
132.158
132.060
131.992
128.656
128.456
128.332
127.735
127.095
125.094
120.005
69.690
68.570
68.122
67.758
66.866
66.701
60.997
47.551
47.232
39.337
38.864
34.718
31.611
25.810
20.778
20.744
AcO
OAc
AcO
AcO
O
O
HN
FmocHN
O
OBn
329
10000
5000
150
100
50
ppm (t1)

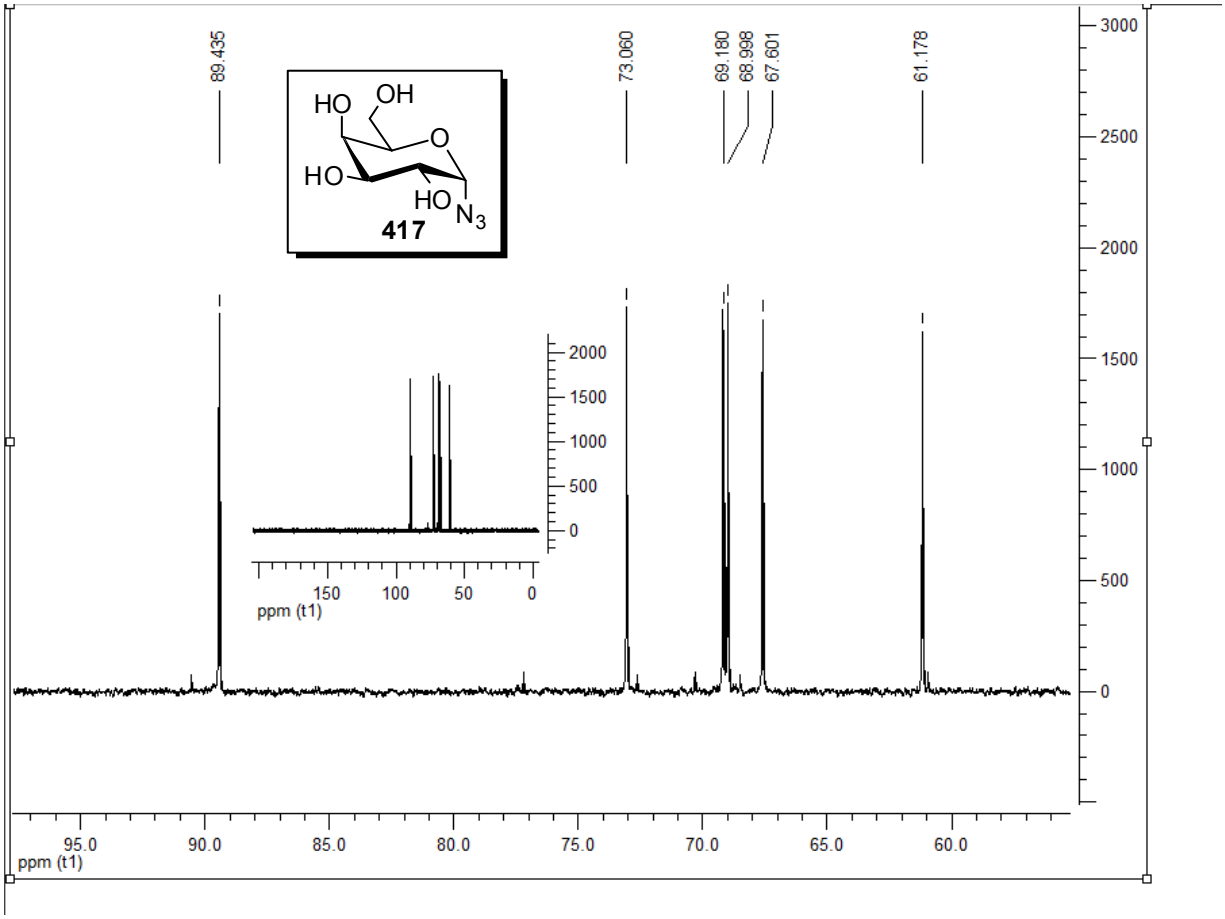

7.774
7.759
7.602
7.587
7.404
7.317
5.911
5.898
5.336
5.335
5.334
5.302
5.256
5.235
4.598
4.587
4.411
4.397
4.382
4.209
3.991
3.989
3.981
3.130
2.597
2.585
2.581
2.570
1.568
1.561
1.444
NHBoc
FmocHN
O
O
337
2.25
2.21
2.30
2.31
0.85
1.82
1.00
2.98
2.33
1.13
1.01
1.99
1.70
4.92
10.81
ppm (t1)

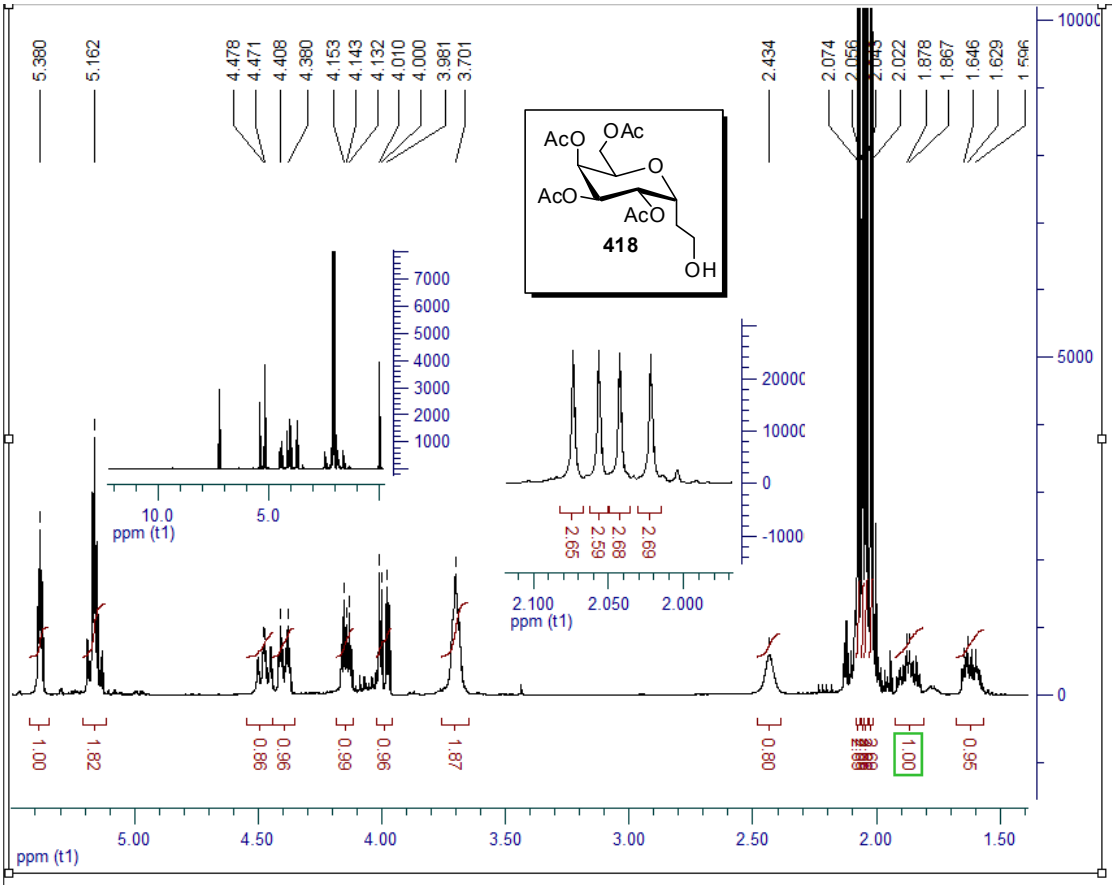

171.186
156.029
155.894
143.904
141.355
131.849
127.691
127.058
125.116
125.098
119.994
118.754
66.580
65.401
47.981
47.335
40.137
39.121
31.588
28.448
26.943
NHBoc
FmocHN
O
O
337
ppm (t1)

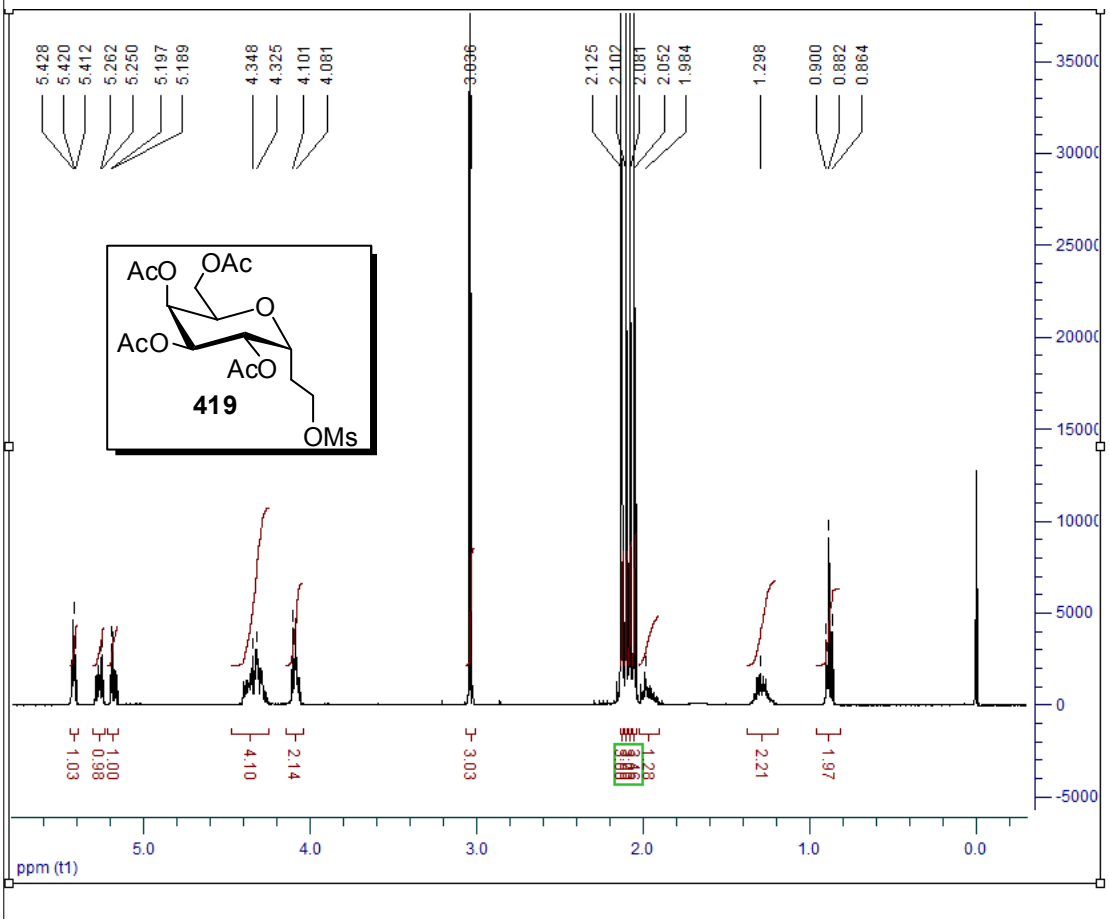

5.675
5.666
5.465
5.462
5.458
5.455
5.241
5.233
5.218
5.208
4.137
4.127
4.122
4.110
2.149
2.114
2.065
1.995
AcO
OAc
O
AcO
AcO
N3
416
3.05
2.96
3.08
3.12
0.99
1.00
2.04
1.01
1.93
ppm (t1)

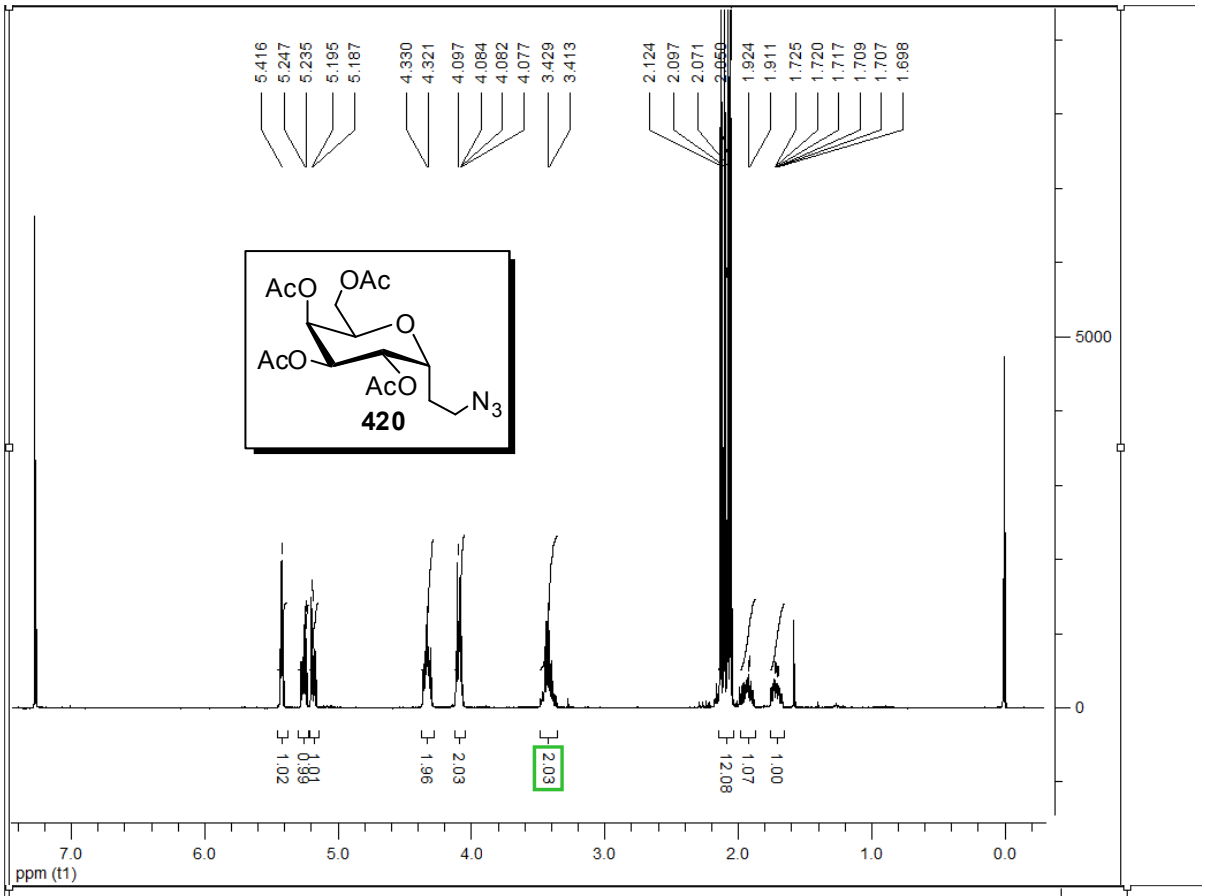

170.3
170.1
170.0
86.74
68.57
67.62
67.36
67.21
61.49
20.66
20.64
20.59
AcO
OAc
O
AcO
AcO
N3
416
ppm (t1)

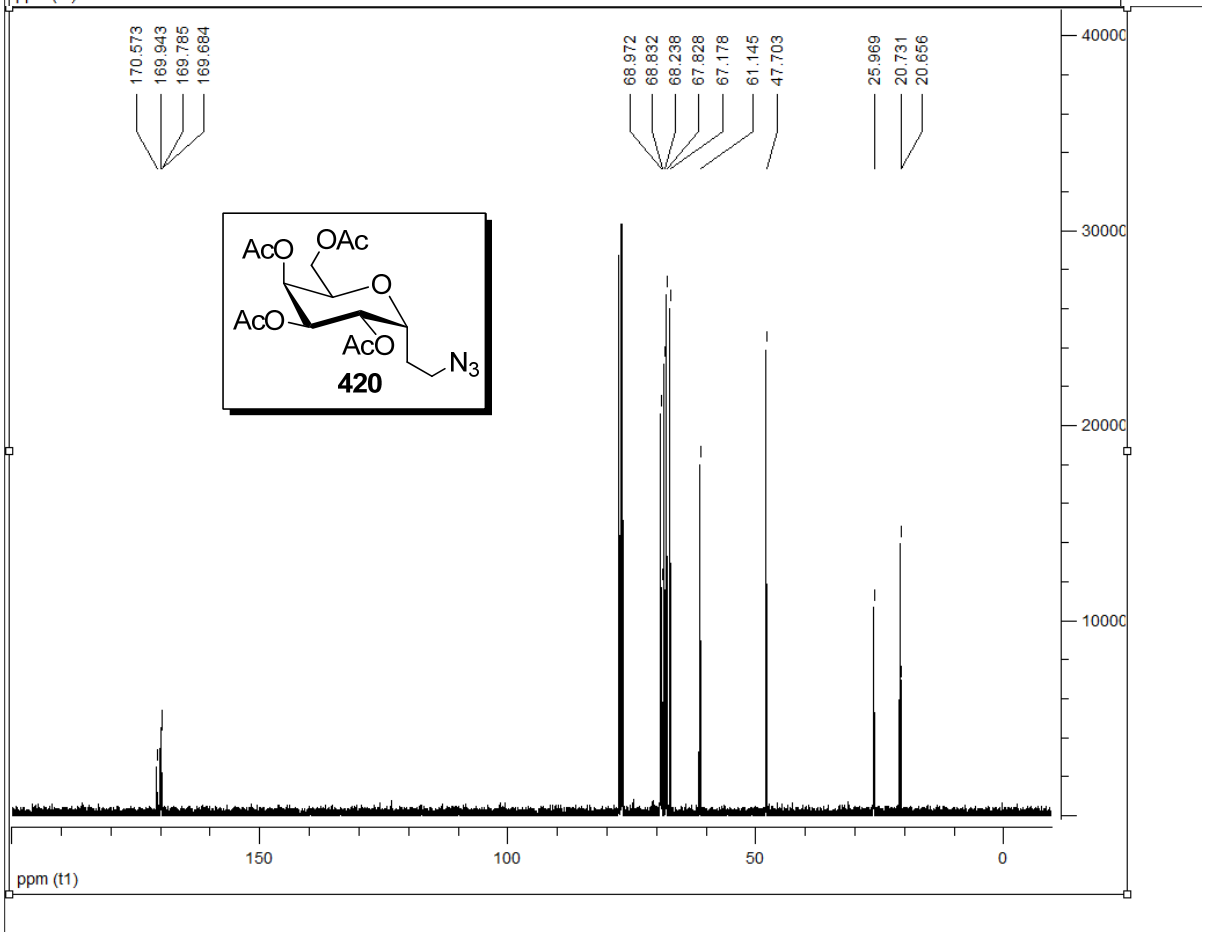

5.549
5.537
4.064
4.049
4.034
3.968
3.961
3.920
3.908
3.894
3.883
3.750
3.745
3.743
3.738
3.732
3.720
3.712
HO
OH
O
HO
HO
N3
417
0.97
1.01
1.02
1.06
3.06
ppm (t1)

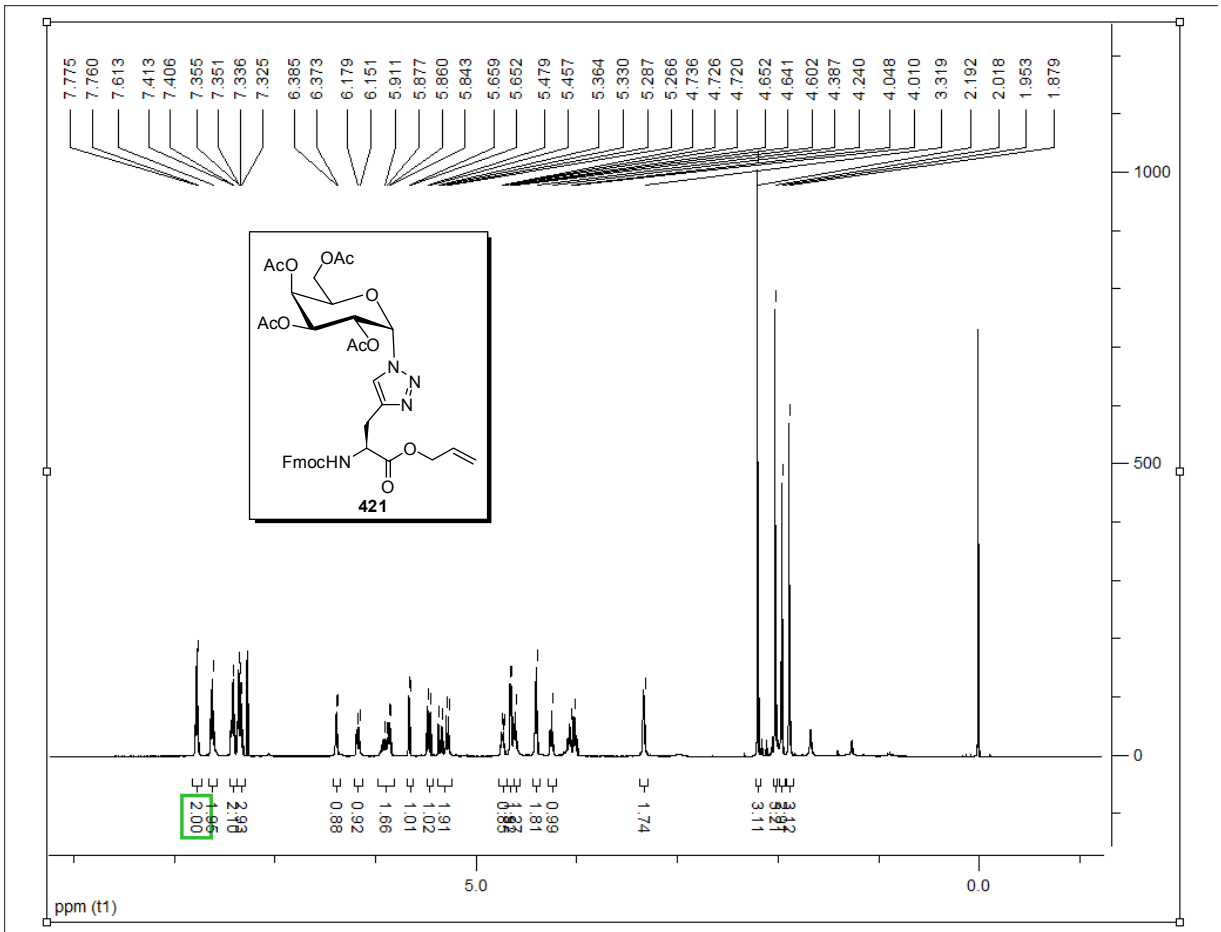

89.435
73.060
69.180
68.998
67.601
61.178
HO
OH
O
HO
HO
N3
417
ppm (t1)

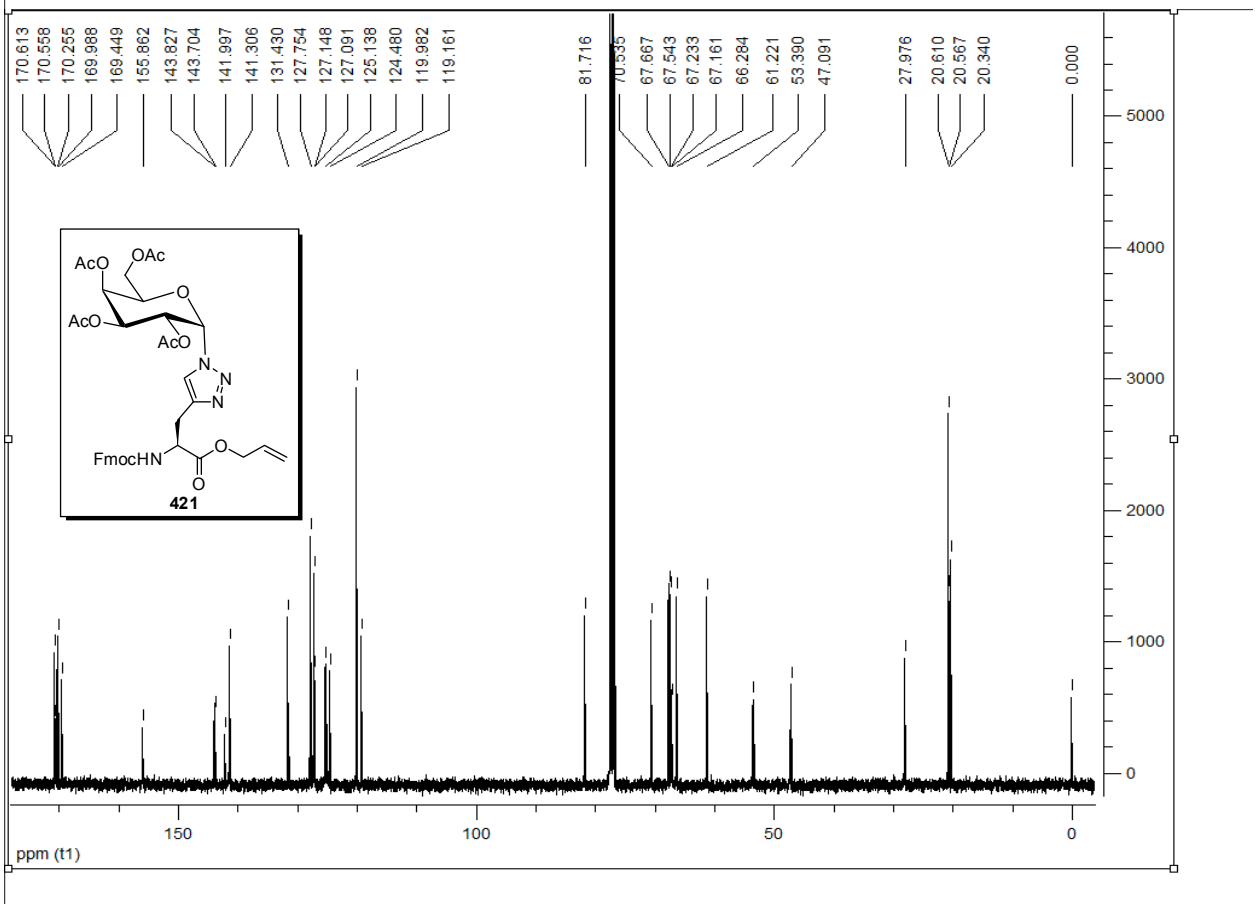

5.380
5.162
4.478
4.471
4.408
4.380
4.153
4.143
4.132
4.010
4.000
3.981
3.701
2.434
2.074
2.056
2.043
2.022
1.878
1.867
1.646
1.629
1.596
AcO
OAc
O
AcO
AcO
418
OH
ppm (t1)
1.00
1.82
0.86
0.96
0.99
0.96
1.87
0.80
1.00
0.95
5.00
4.50
4.00
3.50
3.00
2.50
2.00
1.50

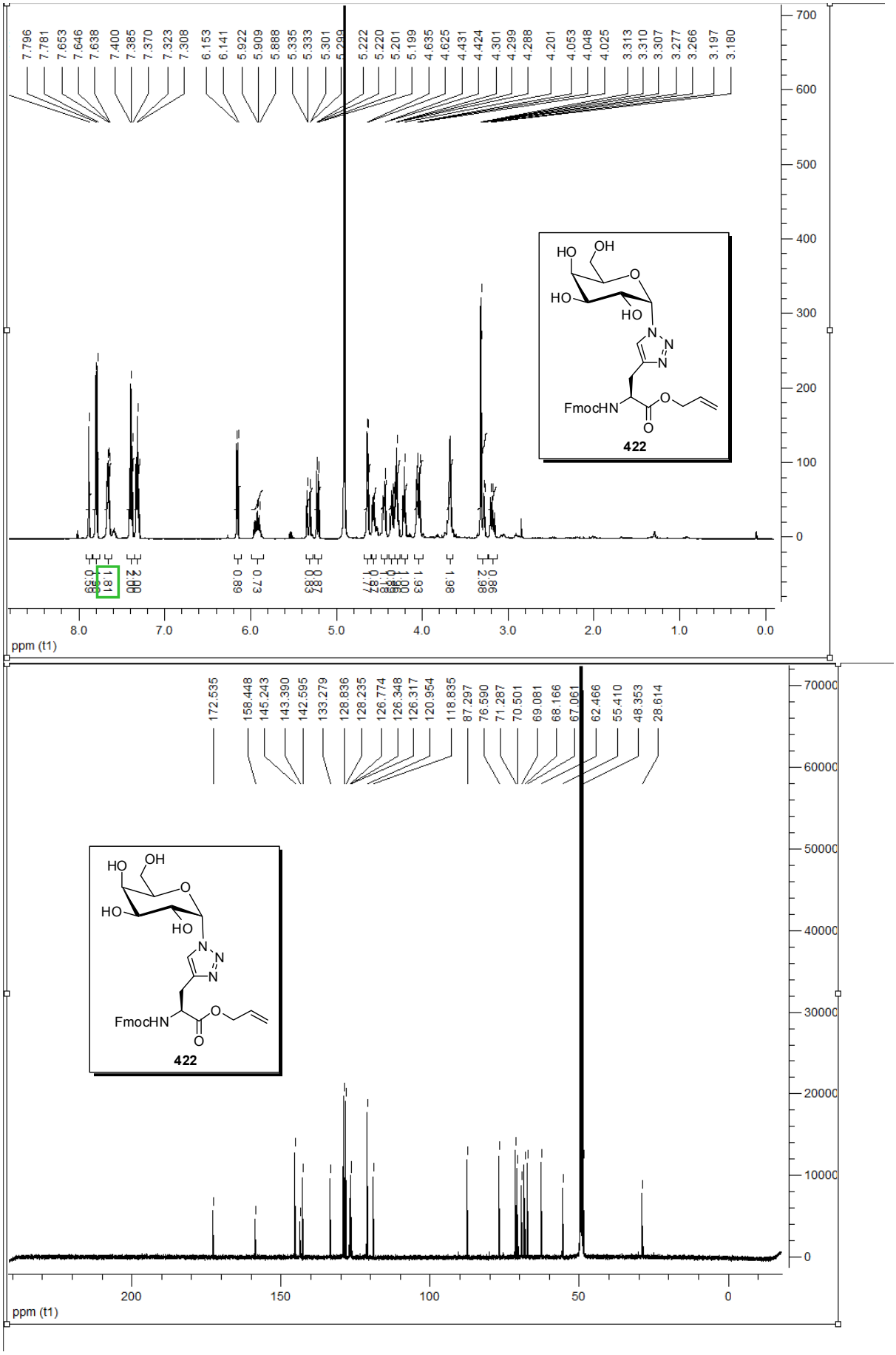

5.428
5.420
5.412
5.262
5.250
5.197
5.189
4.348
4.325
4.101
4.081
3.036
2.125
2.102
2.081
2.052
1.984
1.298
0.900
0.882
0.864
AcO
OAc
O
AcO
AcO
419
OMs
1.03
1.00
0.98
4.10
2.14
3.03
1.28
2.21
1.97
ppm (t1)
5.0
4.0
3.0
2.0
1.0
0.0

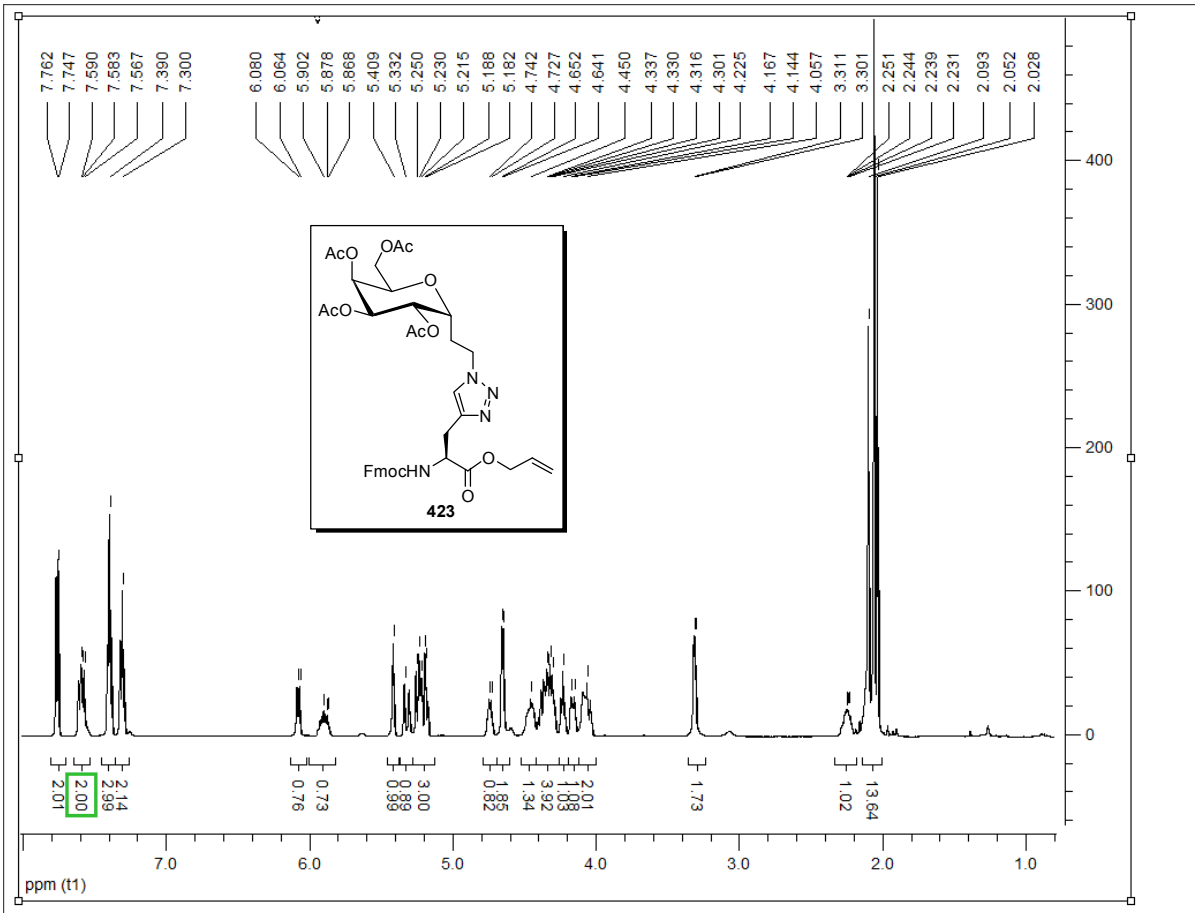

5.416
5.247
5.235
5.195
5.187
4.330
4.321
4.097
4.084
4.082
4.077
3.429
3.413
2.124
2.097
2.071
2.059
1.924
1.911
1.725
1.720
1.717
1.709
1.707
1.698
AcO
OAc
O
AcO
AcO
N3
420
1.02
0.99
1.01
1.96
2.03
2.03
12.08
1.07
1.00
5000
0
7.0
6.0
5.0
4.0
3.0
2.0
1.0
0.0
ppm (t1)

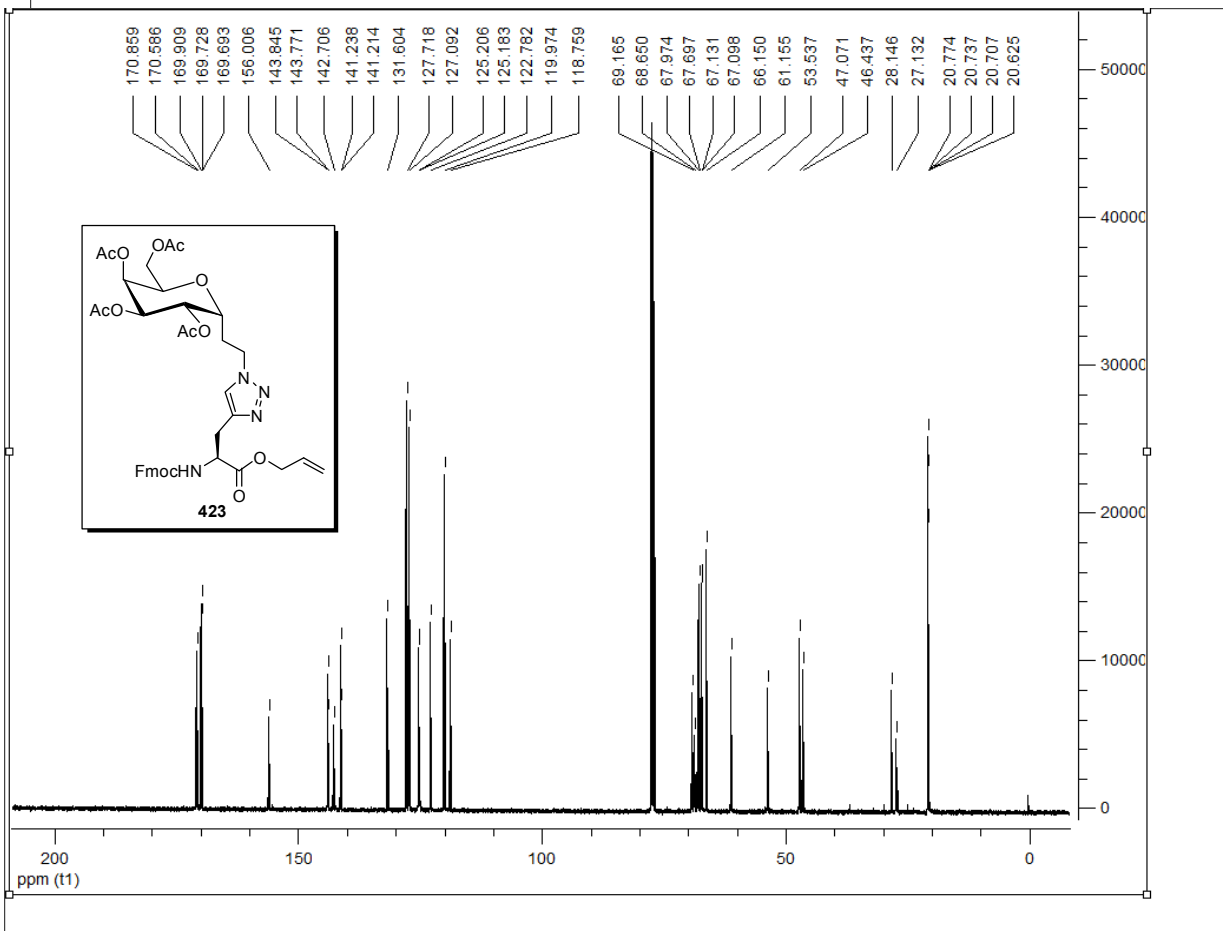

170.573
169.943
169.785
169.684
68.972
68.832
68.238
67.828
67.178
61.145
47.703
25.969
20.731
20.656
AcO
OAc
O
AcO
AcO
N3
420
40000
30000
20000
10000
150
100
50
0
ppm (t1)

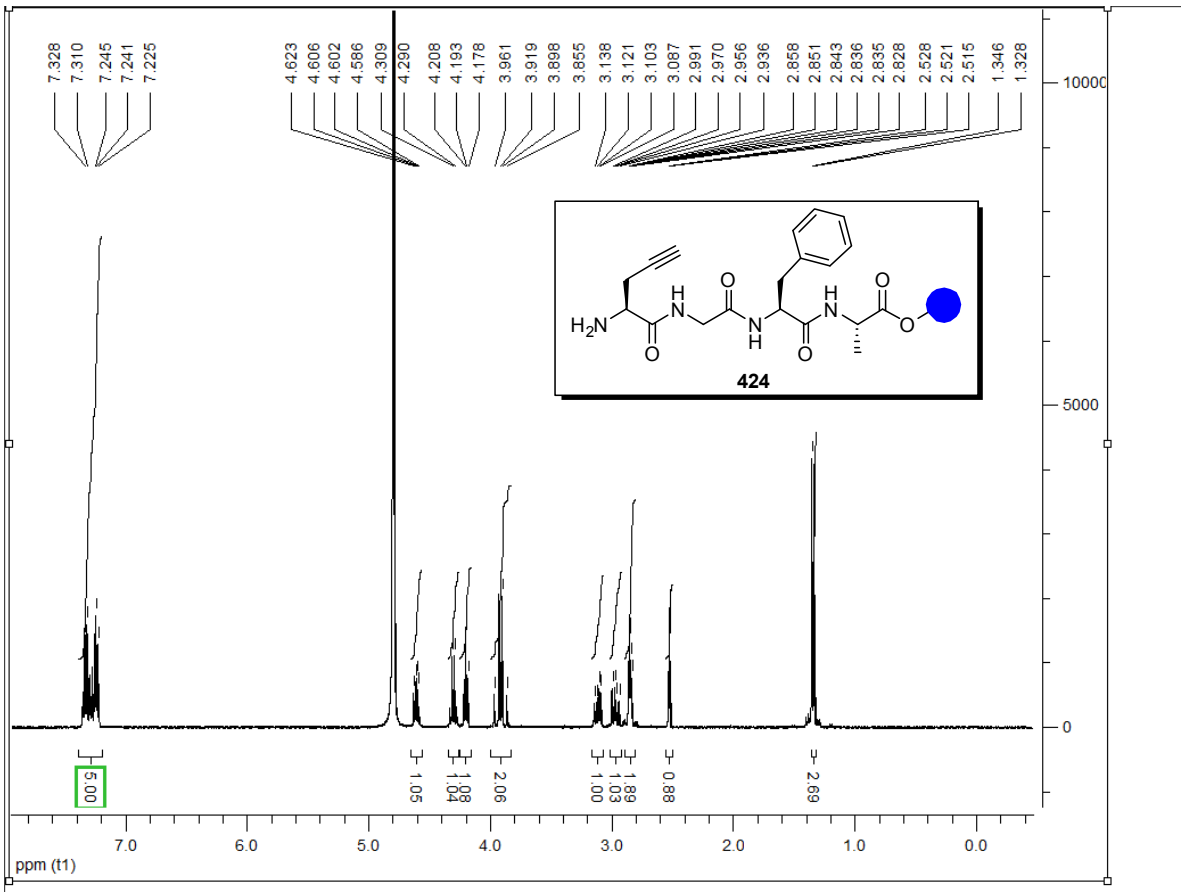

7.775
7.760
7.613
7.413
7.406
7.355
7.351
7.336
7.325
6.385
6.373
6.179
6.151
5.911
5.877
5.860
5.843
5.659
5.652
5.479
5.457
5.364
5.330
5.287
5.266
4.736
4.726
4.720
4.652
4.641
4.602
4.387
4.240
4.048
4.010
3.319
2.192
2.018
1.953
1.879
AcO
OAc
AcO
AcO
FmocHN
421
1000
500
0
2.00
0.88
0.92
1.66
1.01
1.02
1.91
0.98
1.81
0.99
1.74
3.11
5.0
0.0
ppm (t1)

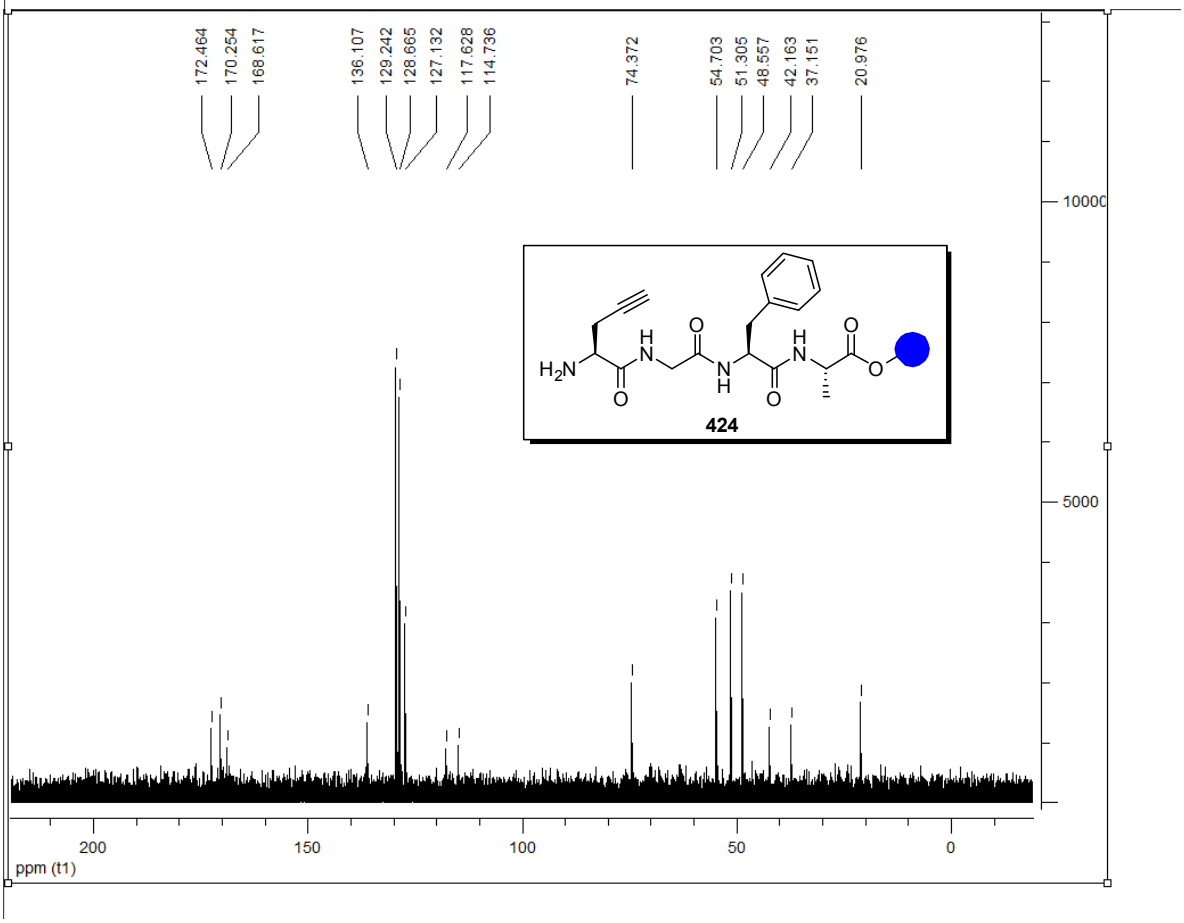

170.613
170.558
170.255
169.988
169.449
155.862
143.827
143.704
141.997
141.306
131.430
127.754
127.148
127.091
125.138
124.480
119.982
119.161
81.716
70.535
67.667
67.543
67.233
67.161
66.284
61.221
53.390
47.091
27.976
20.610
20.567
20.340
0.000
AcO
OAc
AcO
AcO
FmocHN
421
5000
4000
3000
2000
1000
0
150
100
50
0
ppm (t1)

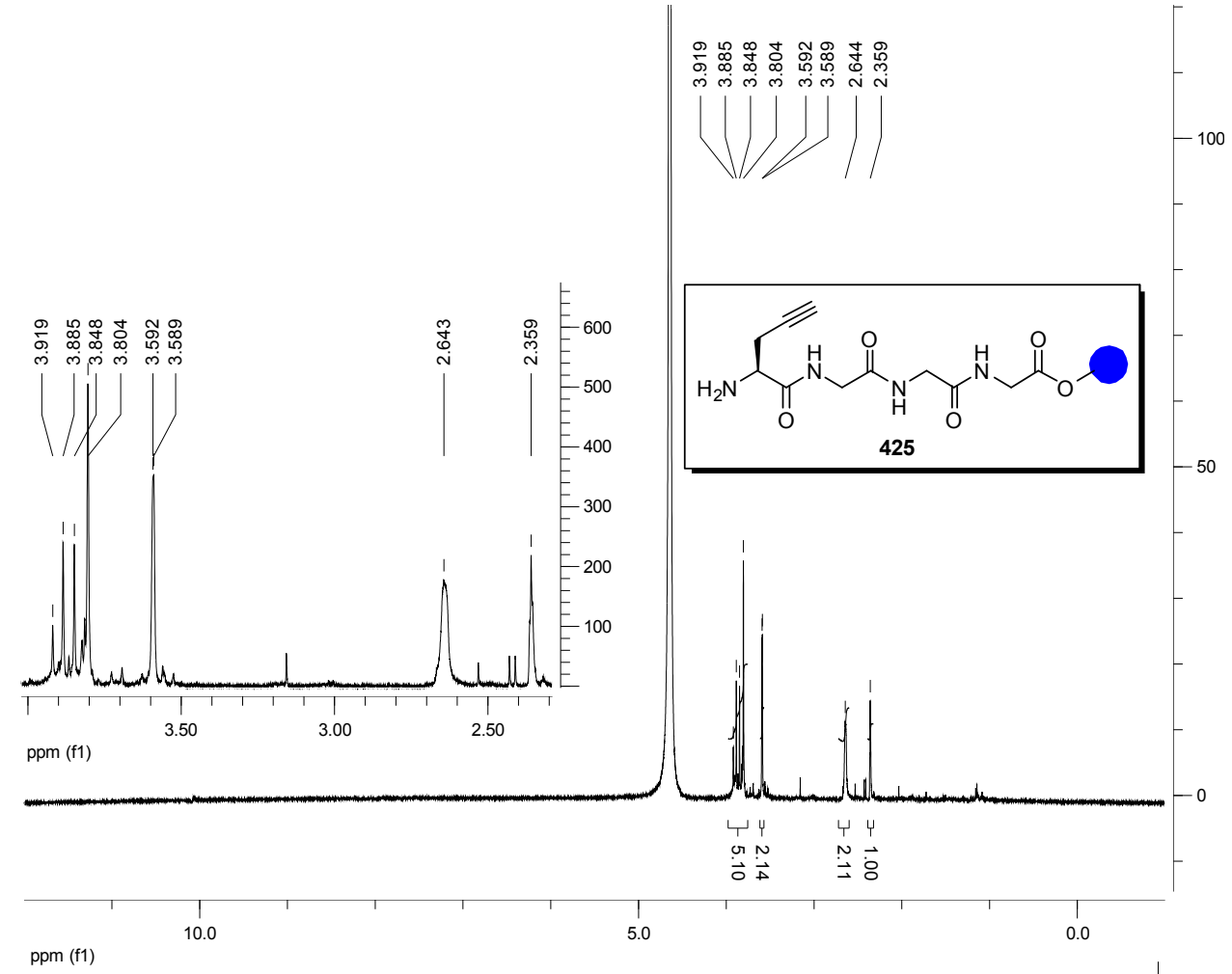

7.796
7.781
7.653
7.646
7.638
7.400
7.385
7.370
7.323
7.308
6.153
6.141
5.922
5.909
5.888
5.335
5.333
5.301
5.299
5.222
5.220
5.201
5.199
4.635
4.625
4.431
4.424
4.301
4.299
4.288
4.201
4.053
4.048
4.025
3.313
3.310
3.307
3.277
3.266
3.197
3.180
HO
OH
O
HO
HO
N
N
N
FmocHN
O
O
O
422
ppm (t1)
172.535
158.448
145.243
143.390
142.595
133.279
128.836
128.235
126.774
126.348
126.317
120.954
118.835
87.297
76.590
71.287
70.501
69.081
68.166
67.061
62.466
55.410
48.353
28.614
ppm (t1)

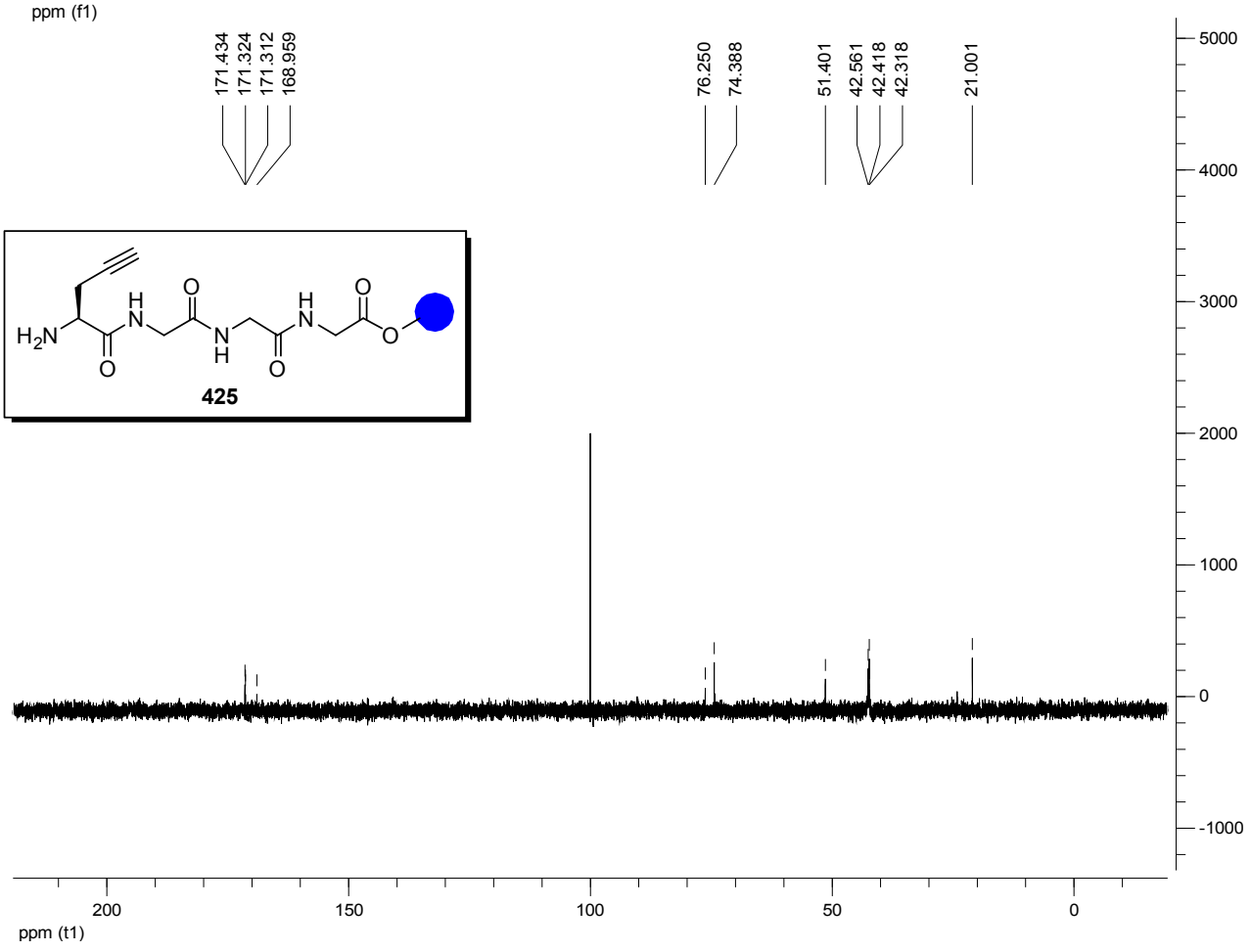

7.762
7.747
7.590
7.583
7.567
7.390
7.300
6.080
6.064
5.902
5.878
5.868
5.409
5.332
5.250
5.230
5.215
5.188
5.182
4.742
4.727
4.652
4.641
4.450
4.337
4.330
4.316
4.301
4.225
4.167
4.144
4.057
3.311
3.301
2.251
2.244
2.239
2.231
2.093
2.052
2.028
AcO
OAc
AcO
AcO
FmocHN
423
2.01
2.00
2.99
2.14
0.76
0.73
0.90
0.89
3.00
0.82
1.85
1.34
2.92
3.08
1.08
2.01
1.73
1.02
13.64
ppm (t1)

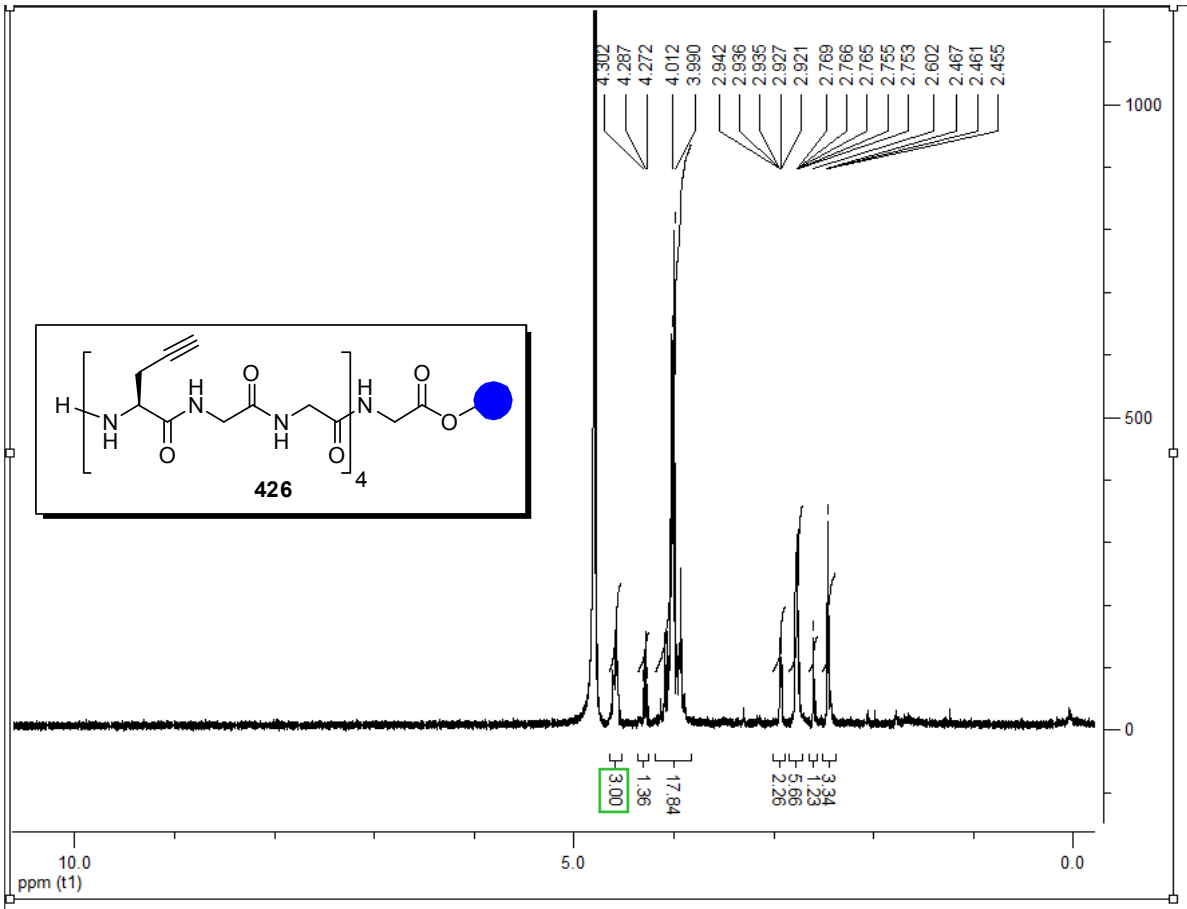

170.859
170.586
169.909
169.728
169.693
156.006
143.845
143.771
142.706
141.238
141.214
131.604
127.718
127.092
125.206
125.183
122.782
119.974
118.759
69.165
68.650
67.974
67.697
67.131
67.098
66.150
61.155
53.537
47.071
46.437
28.146
27.132
20.774
20.737
20.707
20.625
AcO
OAc
AcO
AcO
FmocHN
423
ppm (t1)

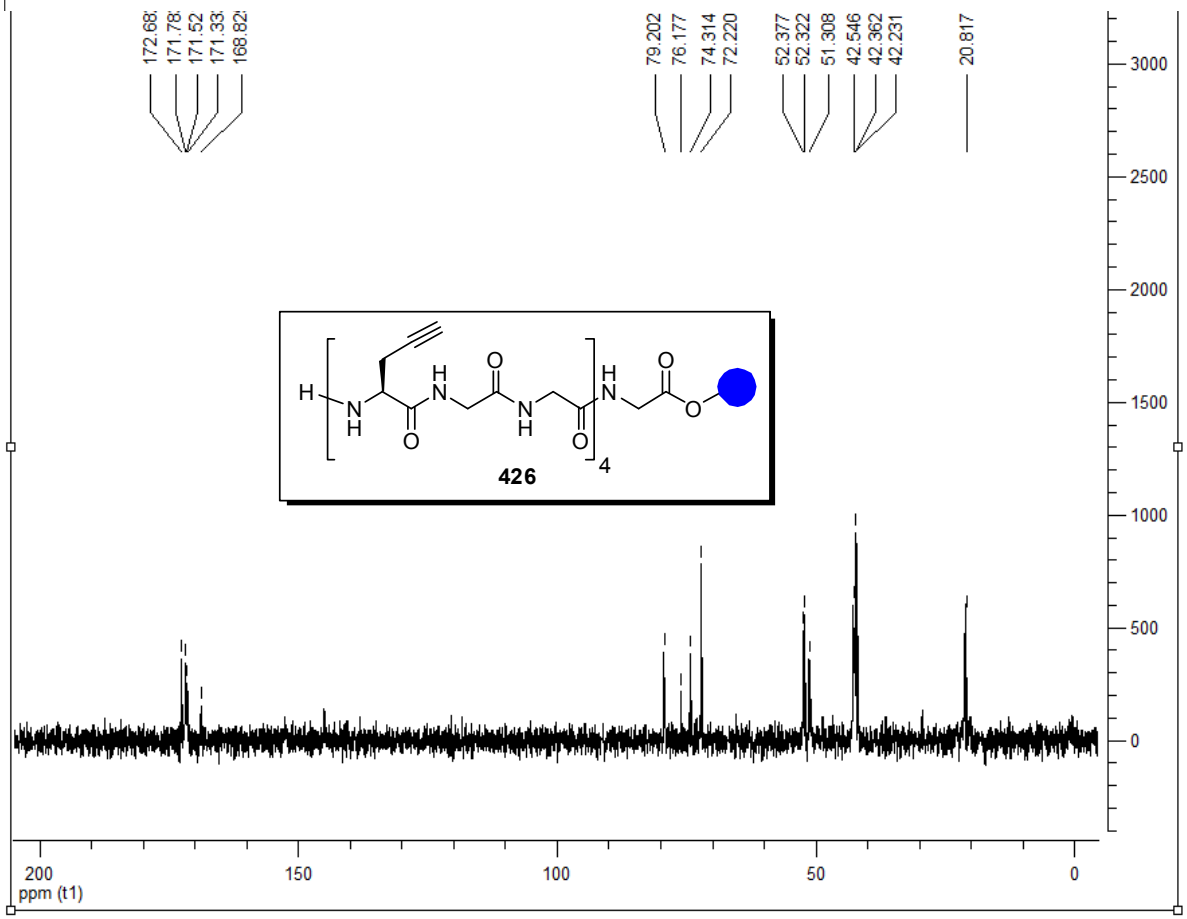

7.328
7.310
7.245
7.241
7.225
4.623
4.606
4.602
4.586
4.309
4.290
4.208
4.193
4.178
3.961
3.919
3.898
3.855
3.138
3.121
3.103
3.087
2.991
2.970
2.956
2.936
2.858
2.851
2.843
2.836
2.835
2.828
2.528
2.521
2.515
1.346
1.328
424
5.00
1.05
1.04
1.08
2.06
1.00
1.03
1.89
0.88
2.69
ppm (t1)

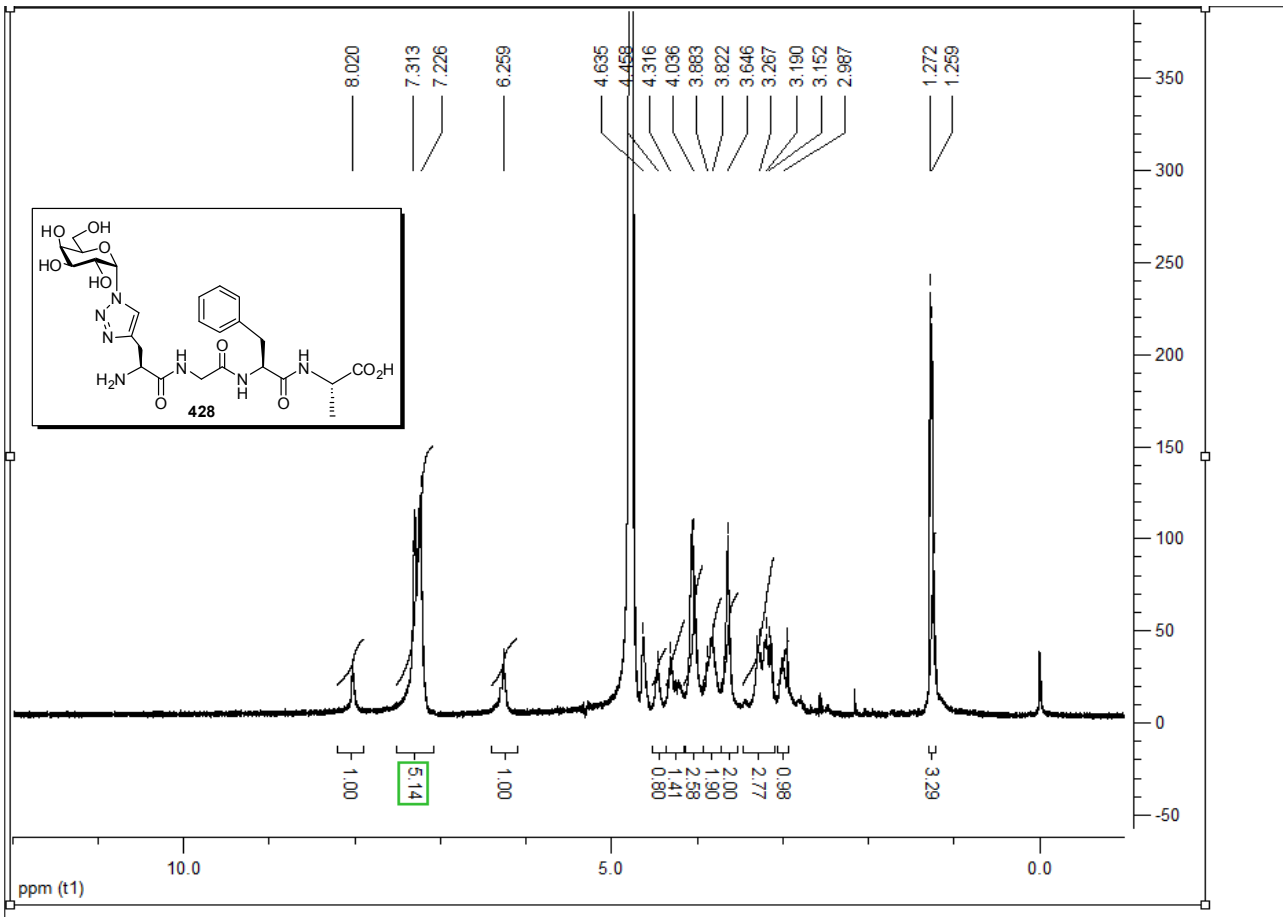

172.464
170.254
168.617
136.107
129.242
128.665
127.132
117.628
114.736
74.372
54.703
51.305
48.557
42.163
37.151
20.976
424
ppm (t1)

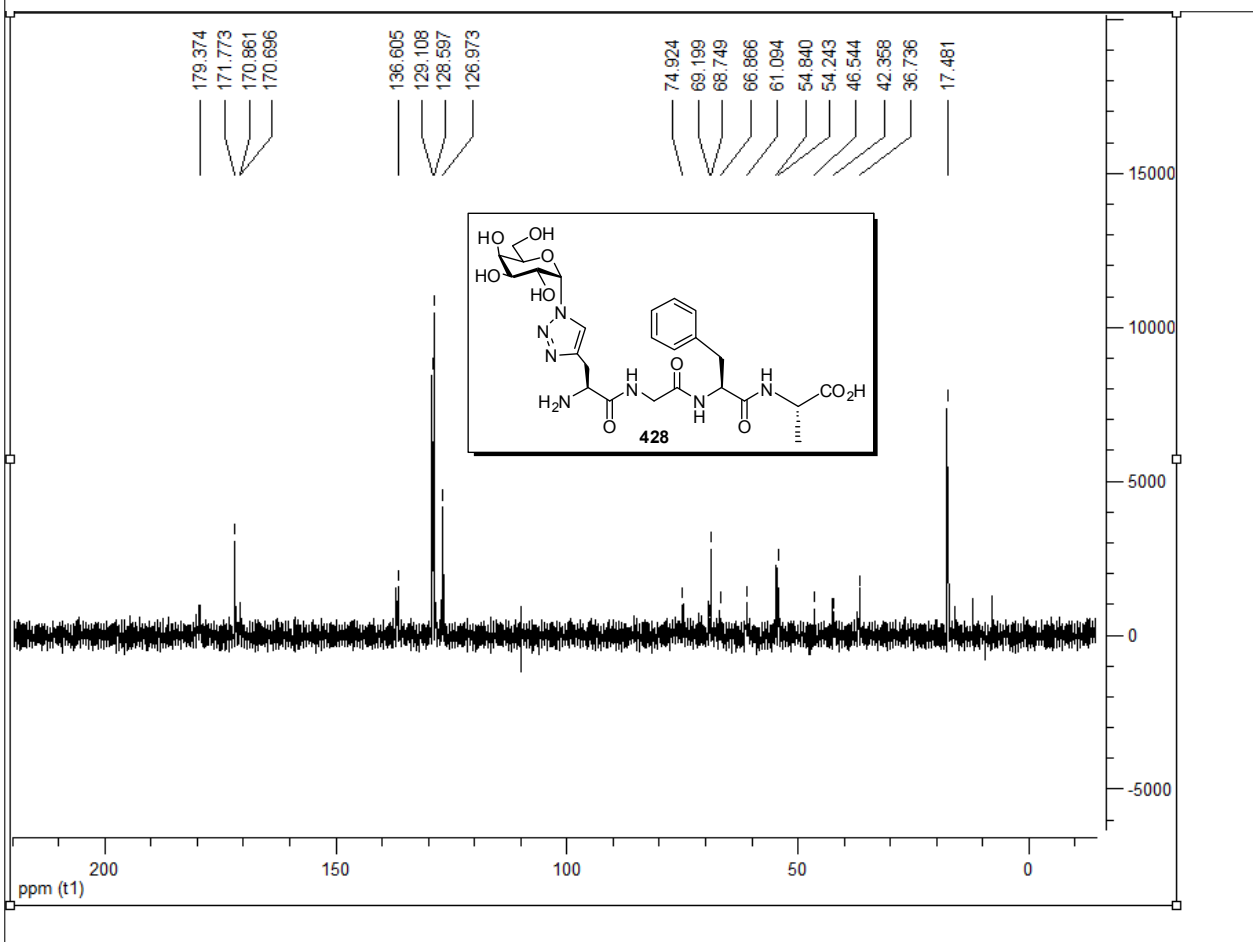

3.919
3.885
3.848
3.804
3.592
3.589
2.644
2.359
2.643
2.359
425
5.10
2.14
2.11
1.00
ppm (f1)

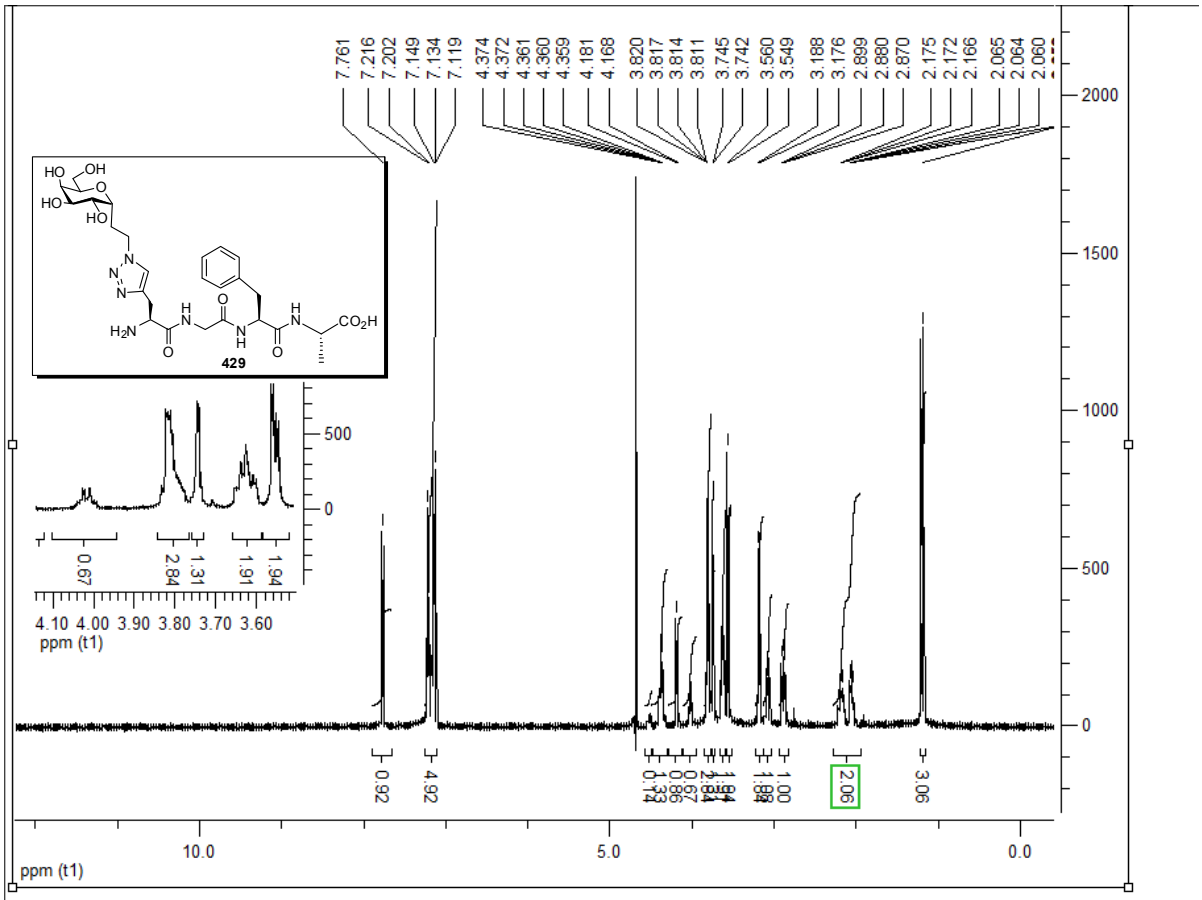

171.434
171.324
171.312
168.959
76.250
74.388
51.401
42.561
42.418
42.318
21.001
425
ppm (t1)

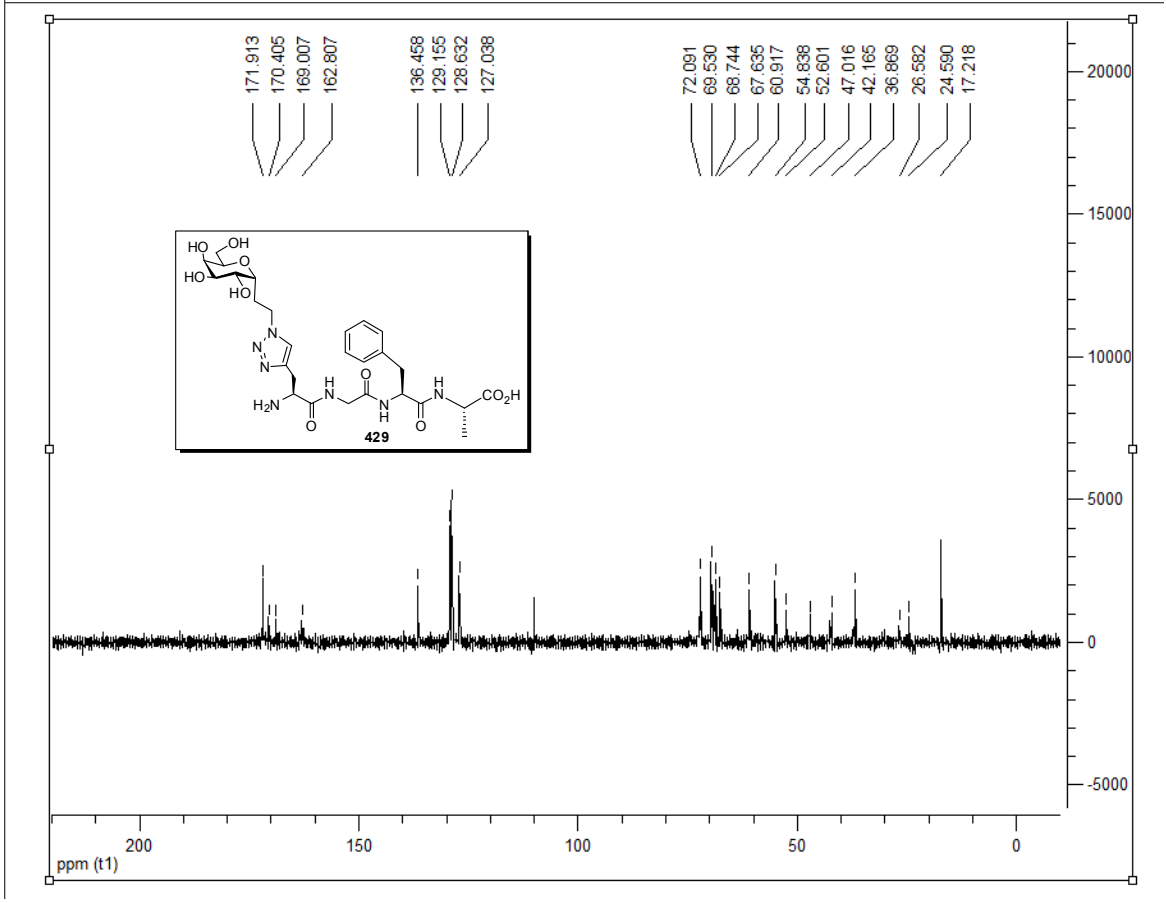

4.302
4.287
4.272
4.012
3.990
2.942
2.936
2.935
2.927
2.921
2.769
2.766
2.765
2.755
2.753
2.602
2.467
2.461
2.455
3.00
1.36
17.84
2.26
5.66
2.23
3.34
1000
500
0
10.0
5.0
0.0
ppm (t1)
426

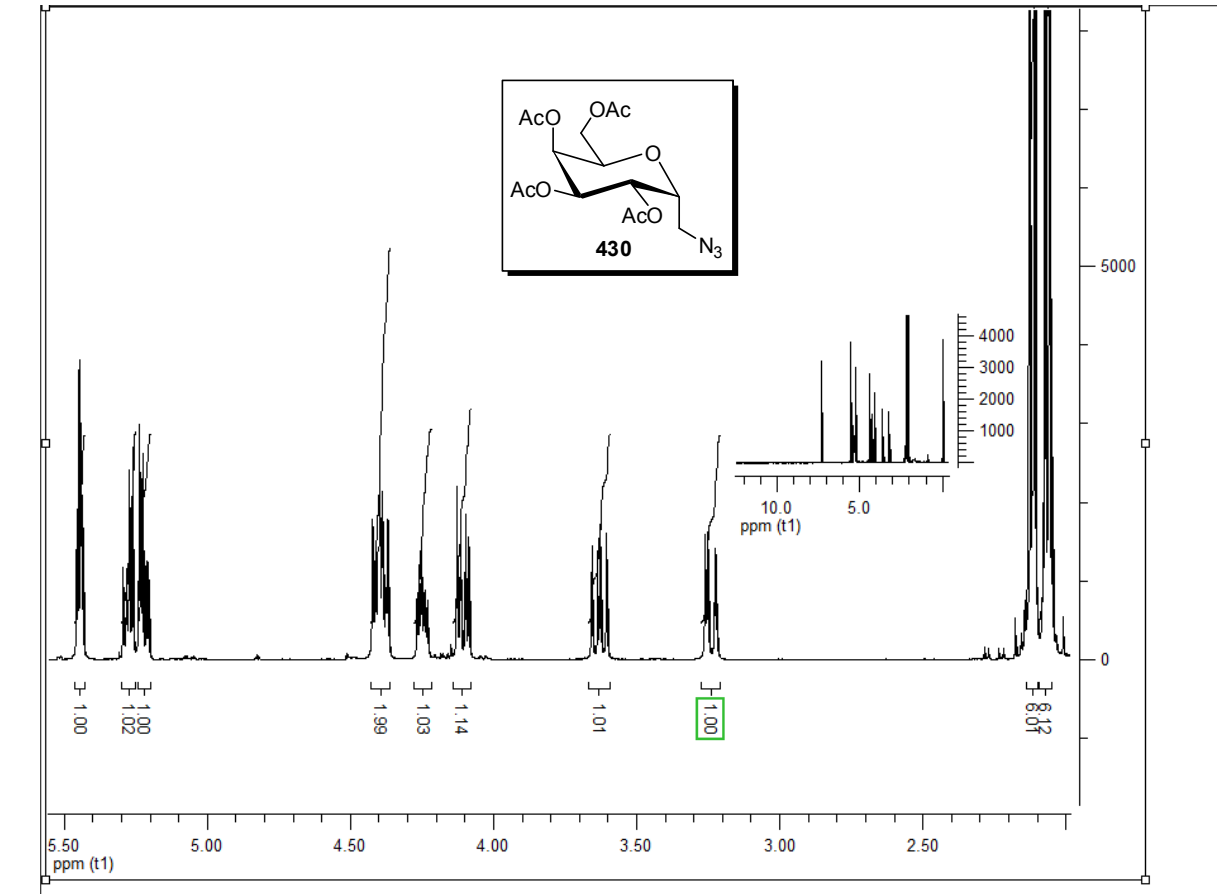

172.68
171.78
171.52
171.33
168.82
79.202
76.177
74.314
72.220
52.377
52.322
51.308
42.546
42.362
42.231
20.817
3000
2500
2000
1500
1000
500
0
200
150
100
50
0
ppm (t1)
426

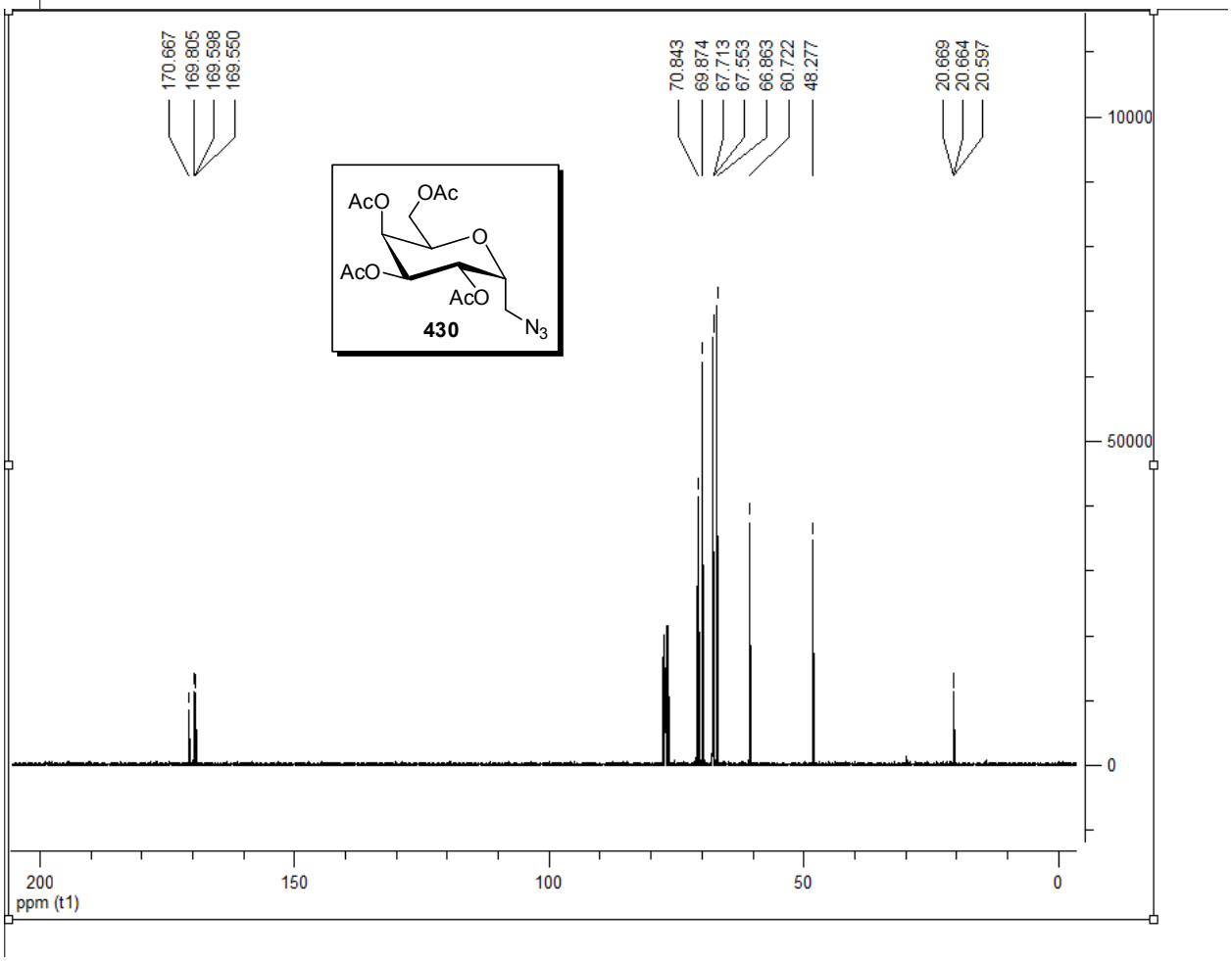

8.020
7.313
7.226
6.259
4.635
4.458
4.316
4.036
3.883
3.822
3.646
3.267
3.190
3.152
2.987
1.272
1.259
428
1.00
5.14
1.00
0.80
1.41
2.58
2.00
1.90
2.77
0.98
3.29
ppm (t1)

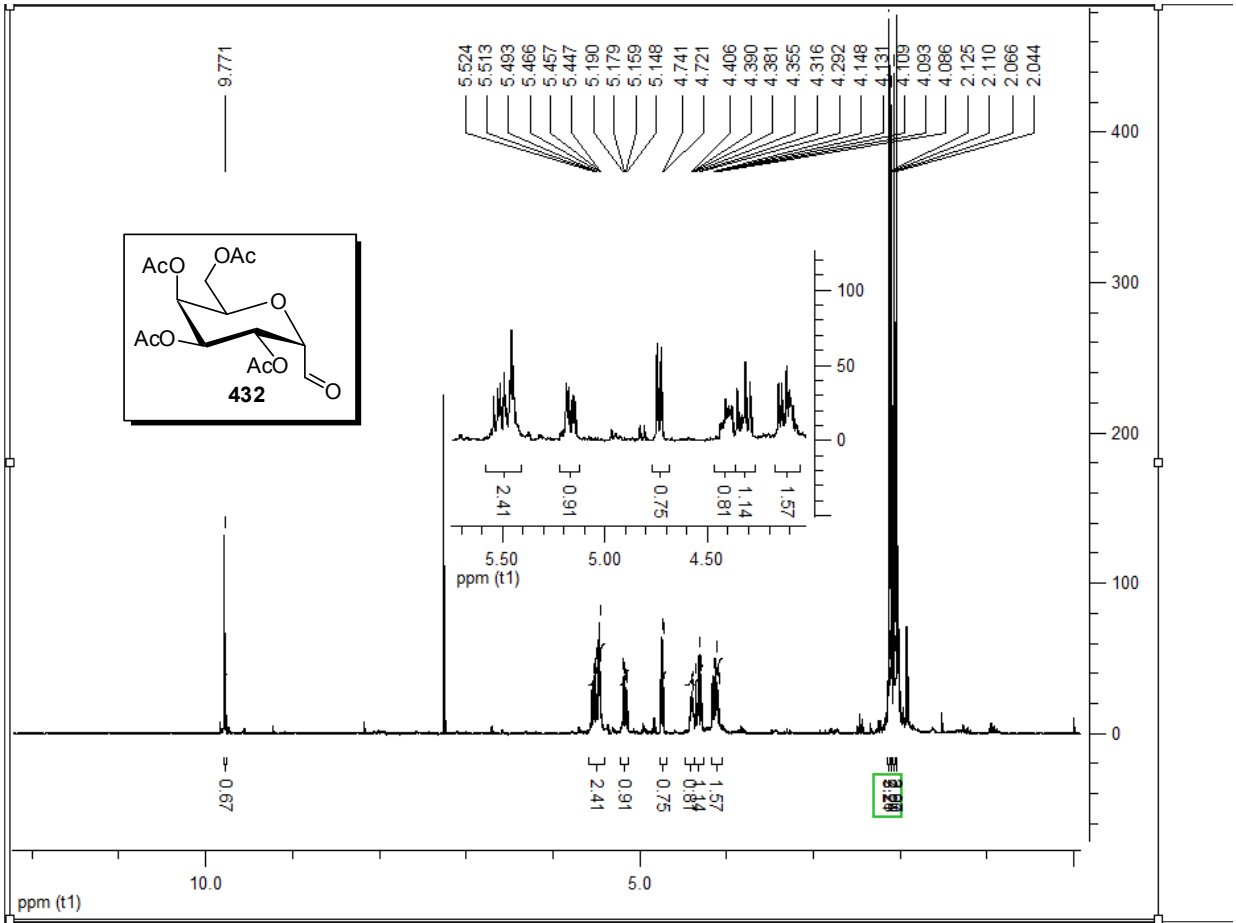

179.374
171.773
170.861
170.696
136.605
129.108
128.597
126.973
74.924
69.199
68.749
66.866
61.094
54.840
54.243
46.544
42.358
36.736
17.481
428
ppm (t1)

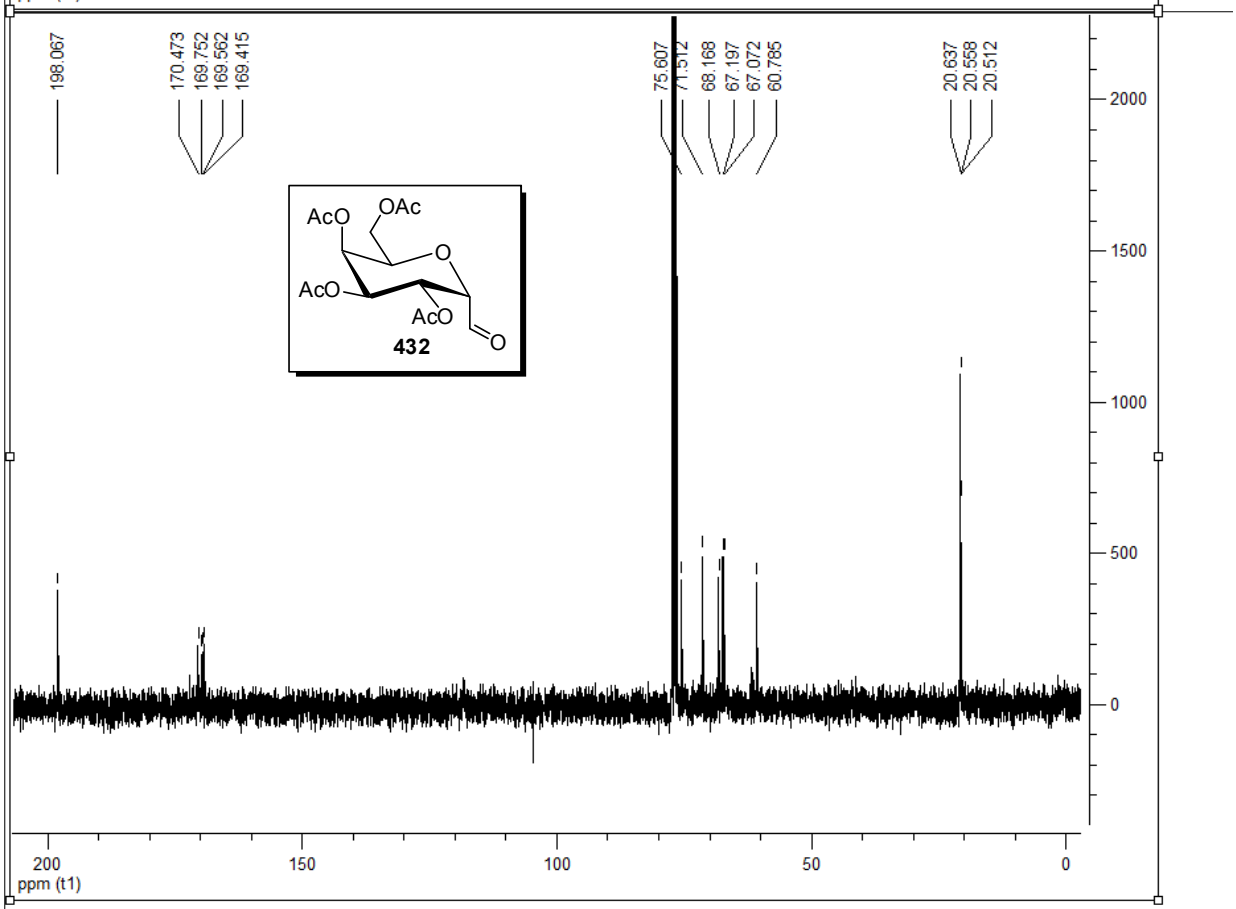

7.761
7.216
7.202
7.149
7.134
7.119
4.374
4.372
4.361
4.360
4.359
4.181
4.168
3.820
3.817
3.814
3.811
3.745
3.742
3.560
3.549
3.188
3.176
2.899
2.880
2.870
2.175
2.172
2.166
2.065
2.064
2.060
429
0.67
2.84
1.31
1.91
1.94
4.10 4.00 3.90 3.80 3.70 3.60
ppm (t1)
0.92
4.92
2.06
3.06
10.0
5.0
0.0
ppm (t1)

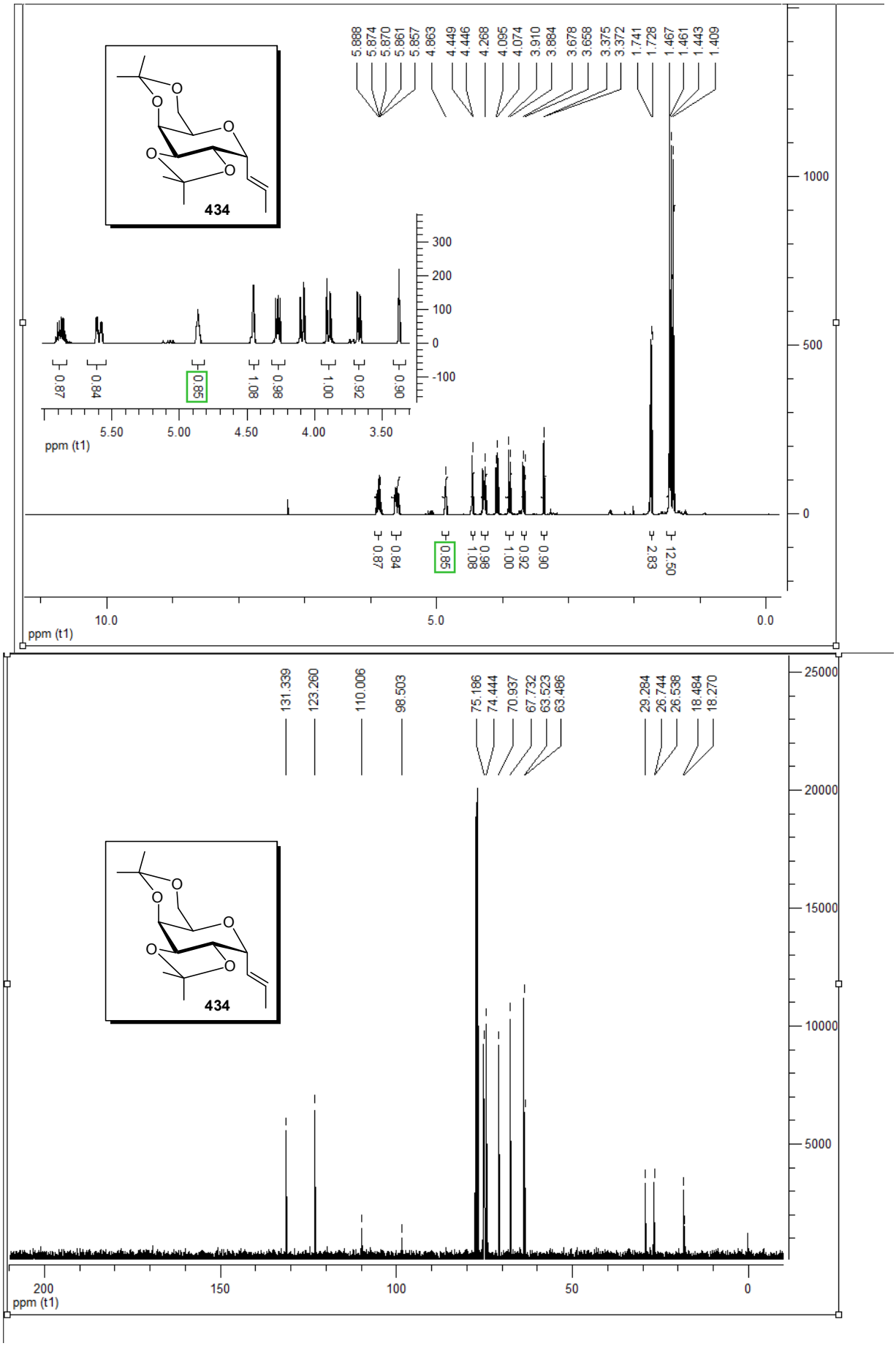

171.913
170.405
169.007
162.807
136.458
129.155
128.632
127.038
72.091
69.530
68.744
67.635
60.917
54.838
52.601
47.016
42.165
36.869
26.582
24.590
17.218
429
200
150
100
50
0
ppm (t1)

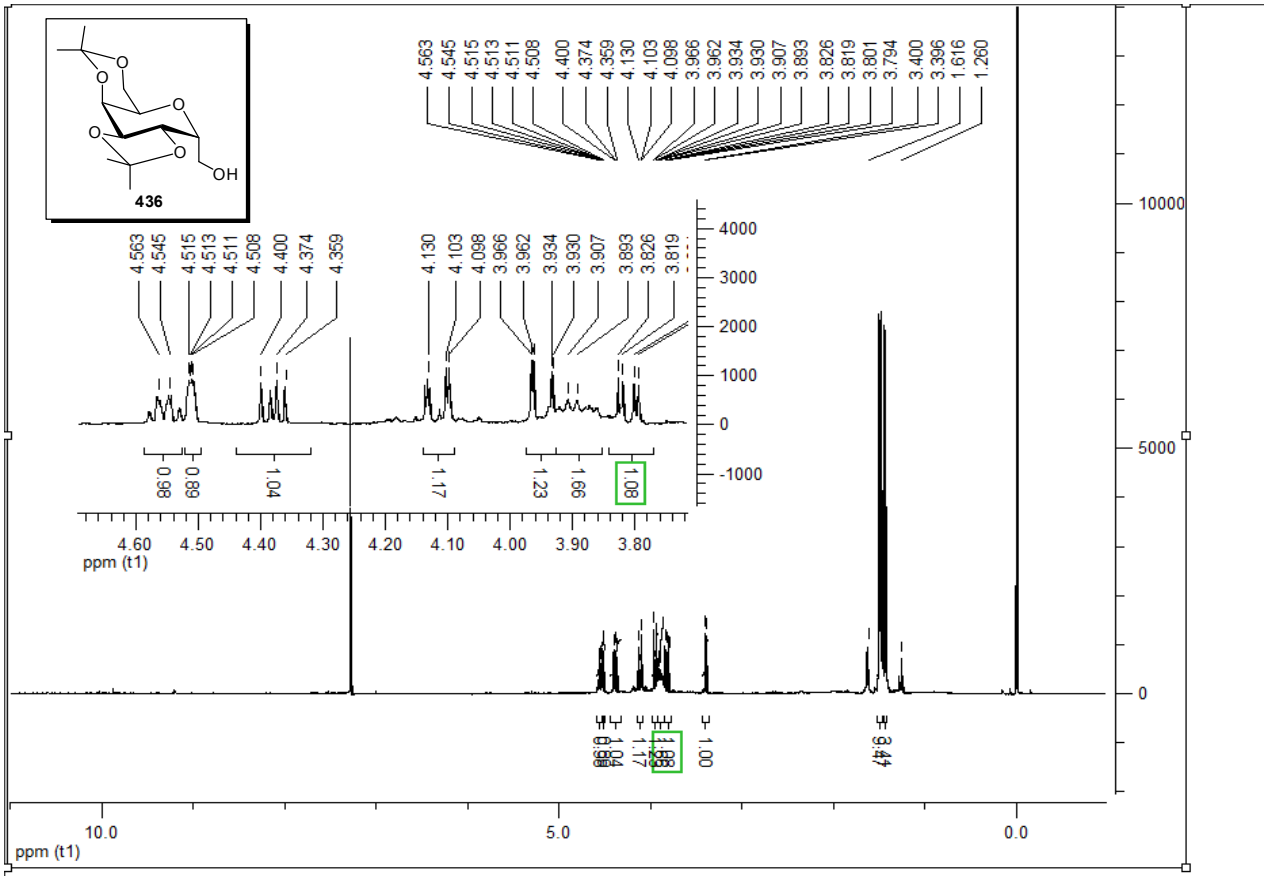

AcO
OAc
O
AcO
AcO
N3
430
5000
0
4000
3000
2000
1000
10.0
5.0
ppm (t1)
1.00
1.00
1.02
1.99
1.03
1.14
1.01
1.00
6.12
6.07
5.50
5.00
4.50
4.00
3.50
3.00
2.50
ppm (t1)

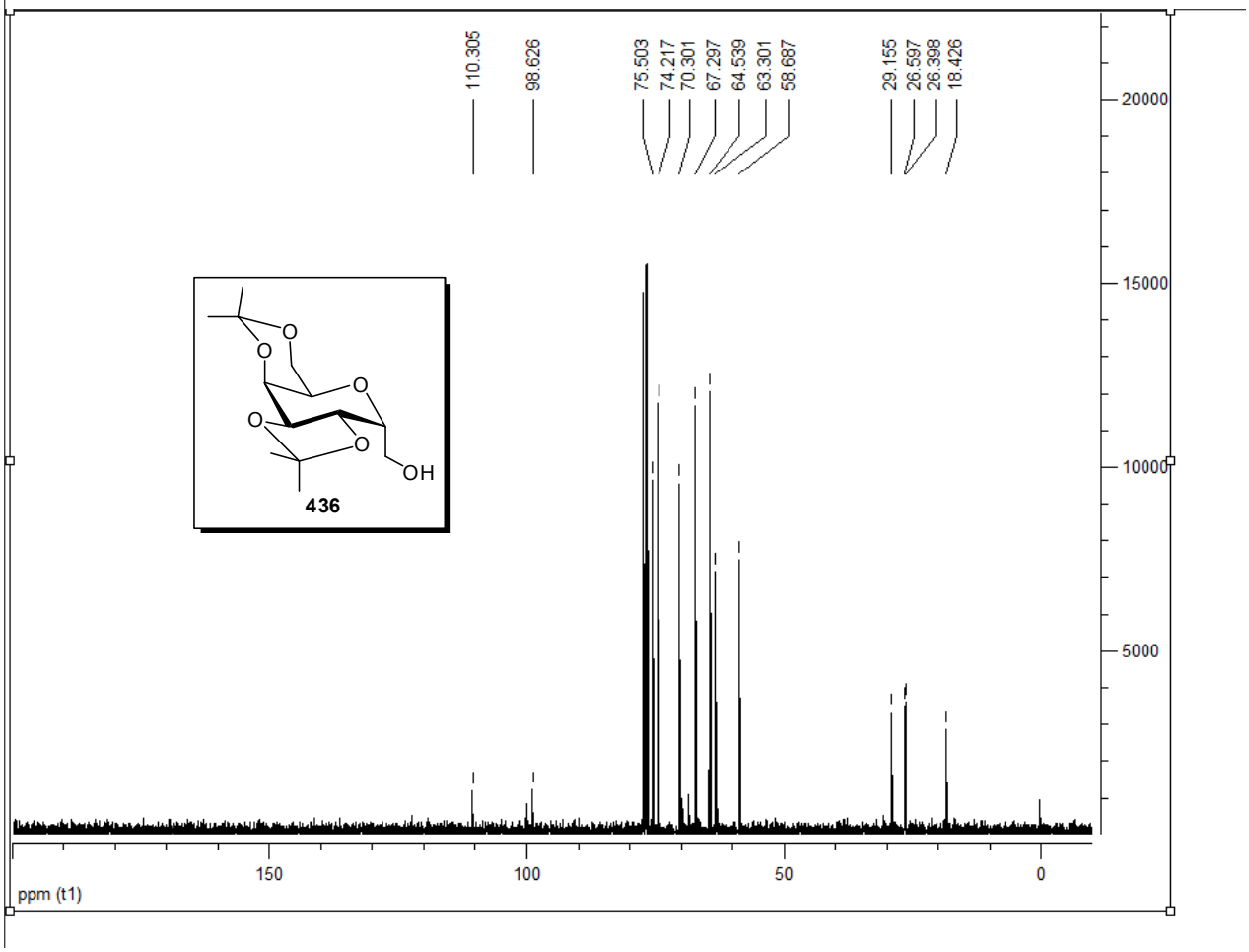

170.667
169.805
169.598
169.550
70.843
69.874
67.713
67.553
66.863
60.722
48.277
20.669
20.664
20.597
AcO
OAc
O
AcO
AcO
N3
430
10000
50000
0
200
150
100
50
0
ppm (t1)

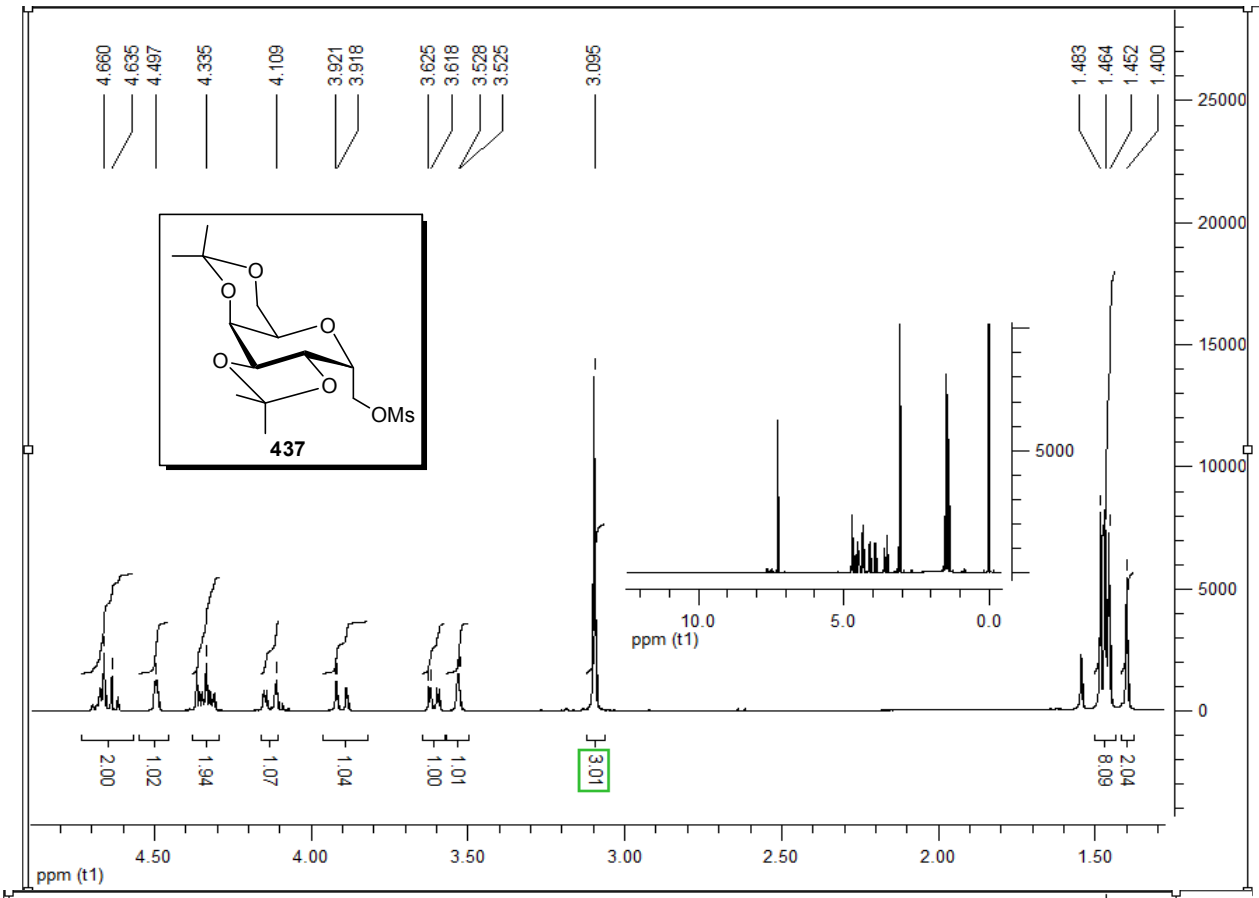

9.771
5.524
5.513
5.493
5.466
5.457
5.447
5.190
5.179
5.159
5.148
4.741
4.721
4.406
4.390
4.381
4.355
4.316
4.292
4.148
4.131
4.109
4.093
4.086
2.125
2.110
2.066
2.044
AcO
OAc
AcO
AcO
O
O
432
2.41
0.91
0.75
0.81
1.14
1.57
0.67
5.50
5.00
4.50
ppm (t1)
10.0
5.0
ppm (t1)

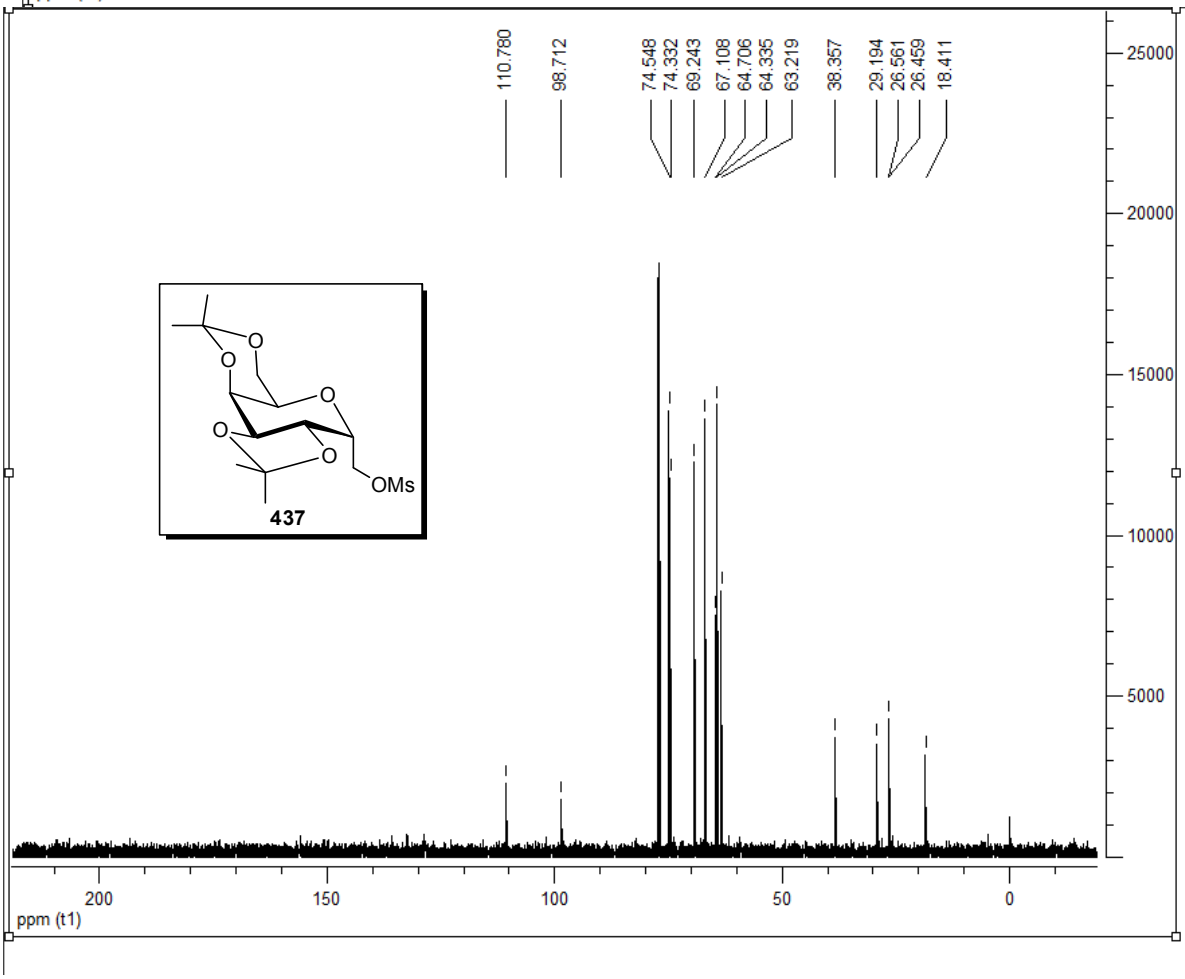

198.067
170.473
169.752
169.562
169.415
75.607
71.512
68.168
67.197
67.072
60.785
20.637
20.558
20.512
AcO
OAc
AcO
AcO
O
O
432
200
150
100
50
0
ppm (t1)

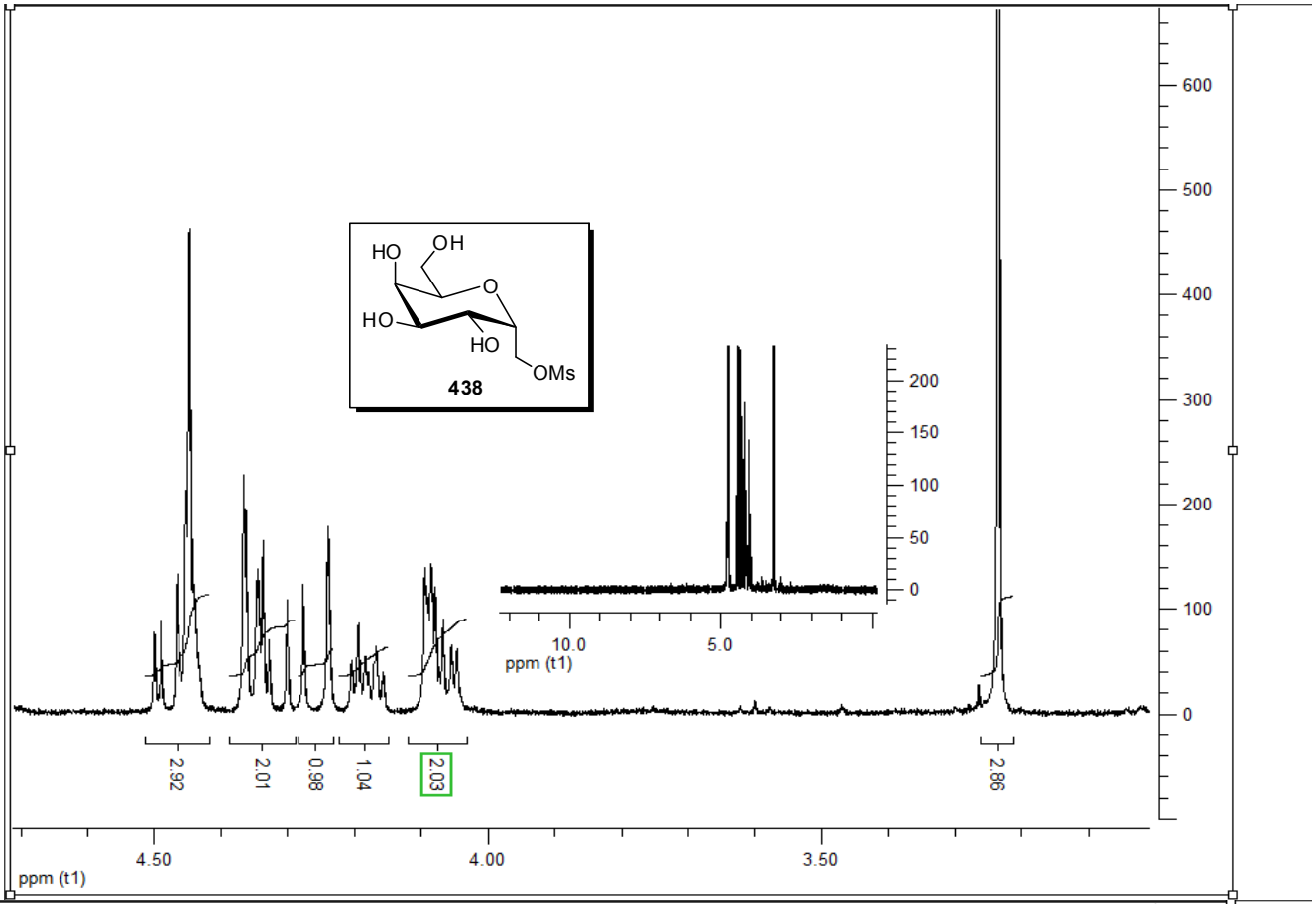

434
5.888
5.874
5.870
5.861
5.857
4.863
4.449
4.446
4.268
4.095
4.074
3.910
3.884
3.678
3.658
3.375
3.372
1.741
1.728
1.467
1.461
1.443
1.409
0.87
0.84
0.85
1.08
0.98
1.00
0.92
0.90
2.83
12.50
ppm (t1)
131.339
123.260
110.006
98.503
75.186
74.444
70.937
67.732
63.523
63.486
29.284
26.744
26.538
18.484
18.270
ppm (t1)

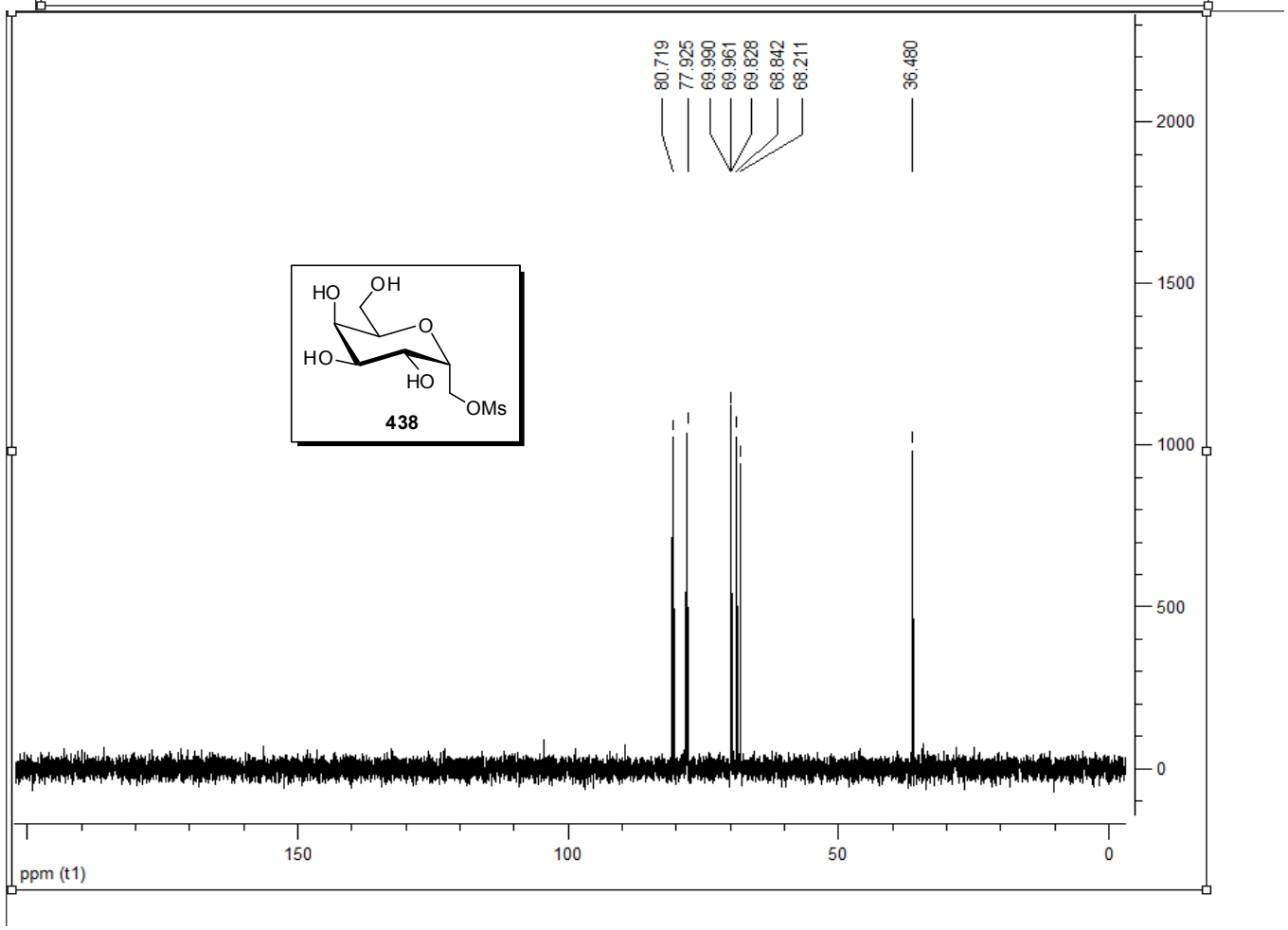

436
4.563
4.545
4.515
4.513
4.511
4.508
4.400
4.374
4.359
4.130
4.103
4.098
3.966
3.962
3.934
3.930
3.907
3.893
3.826
3.819
3.801
3.794
3.400
3.396
1.616
1.260
0.98
0.89
1.04
1.17
1.23
1.66
1.08
1.00
9.47
ppm (t1)

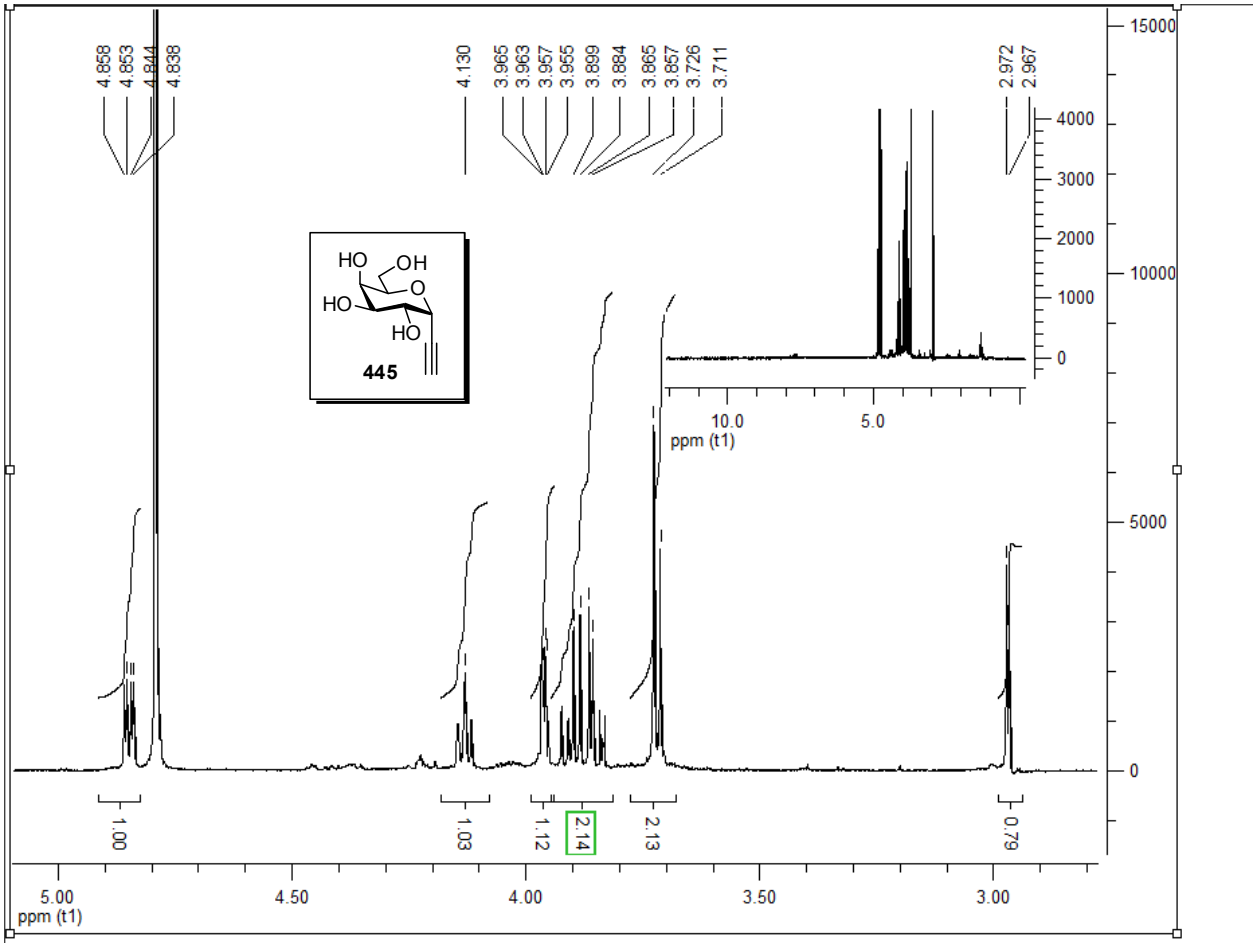

436
110.305
98.626
75.503
74.217
70.301
67.297
64.539
63.301
58.687
29.155
26.597
26.398
18.426
ppm (t1)

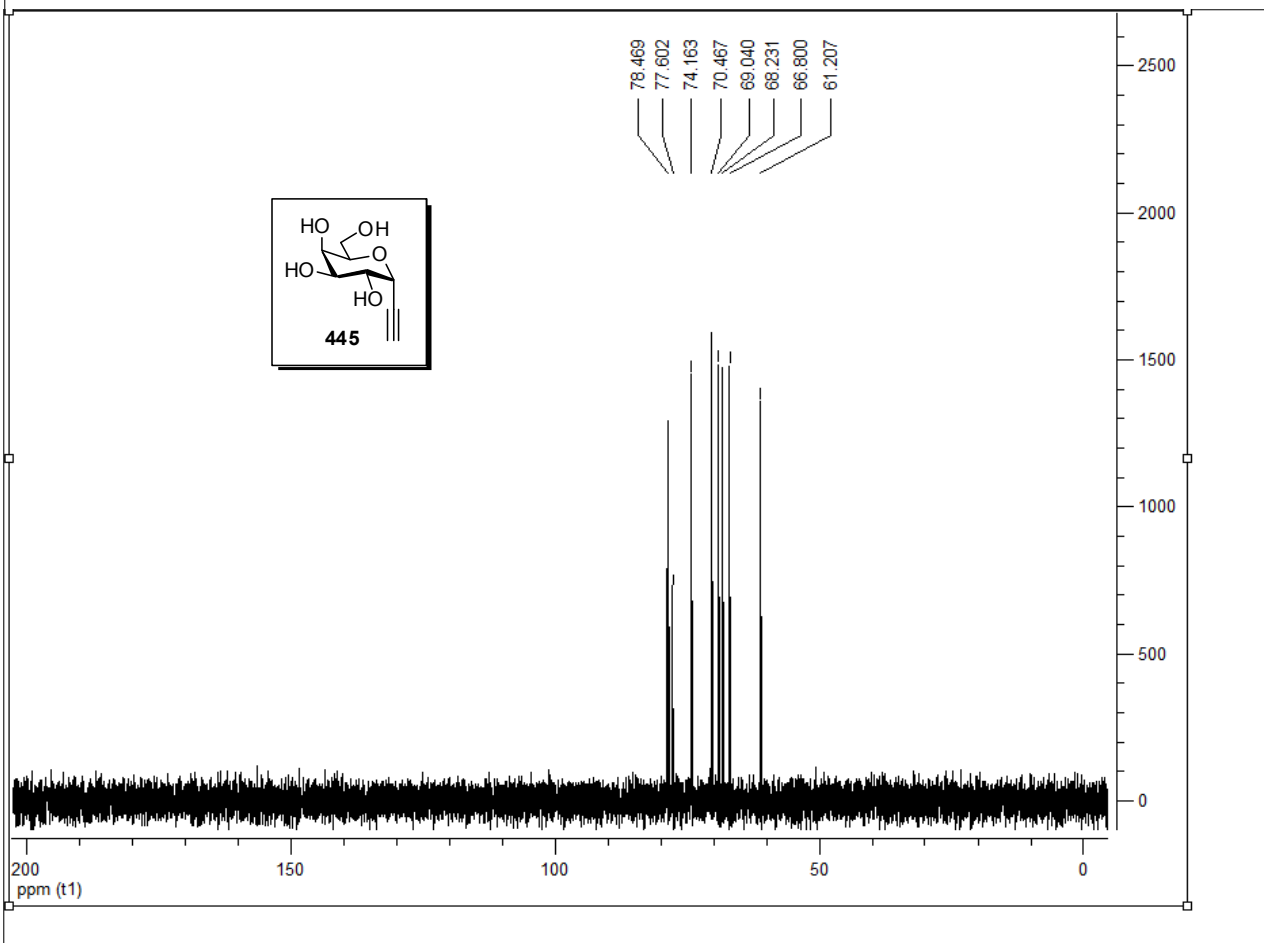

4.660
4.635
4.497
4.335
4.109
3.921
3.918
3.625
3.618
3.528
3.525
3.095
1.483
1.464
1.452
1.400
OMs
437
ppm (t1)
2.00
1.02
1.94
1.07
1.04
1.00
1.01
3.01
8.09
2.04

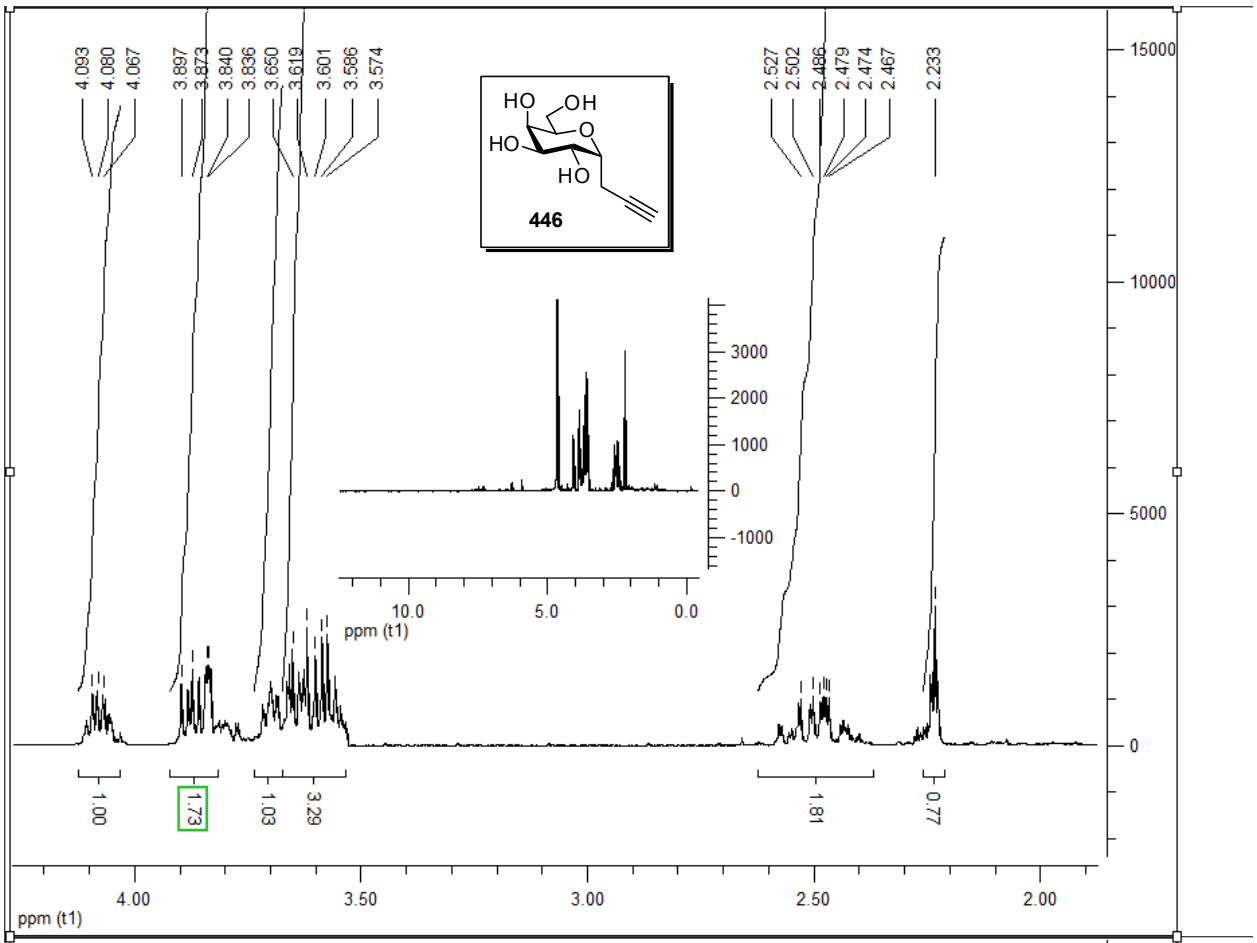

110.780
98.712
74.548
74.332
69.243
67.108
64.706
64.335
63.219
38.357
29.194
26.561
26.459
18.411
OMs
437
ppm (t1)

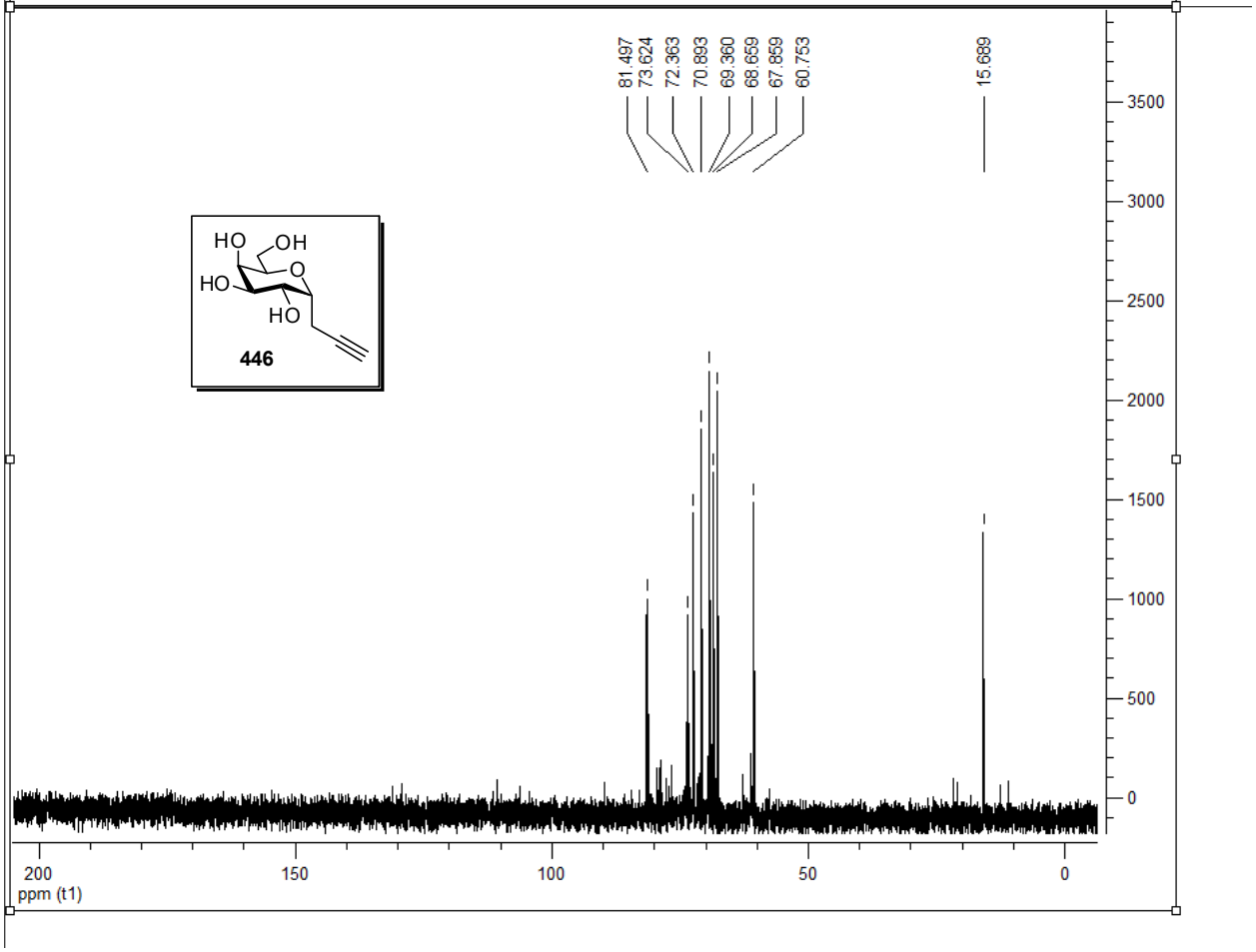

HO
OH
O
HO
HO
OMs
438
2.92
2.01
0.98
1.04
2.03
2.86
4.50
4.00
3.50
ppm (t1)
10.0
5.0
ppm (t1)

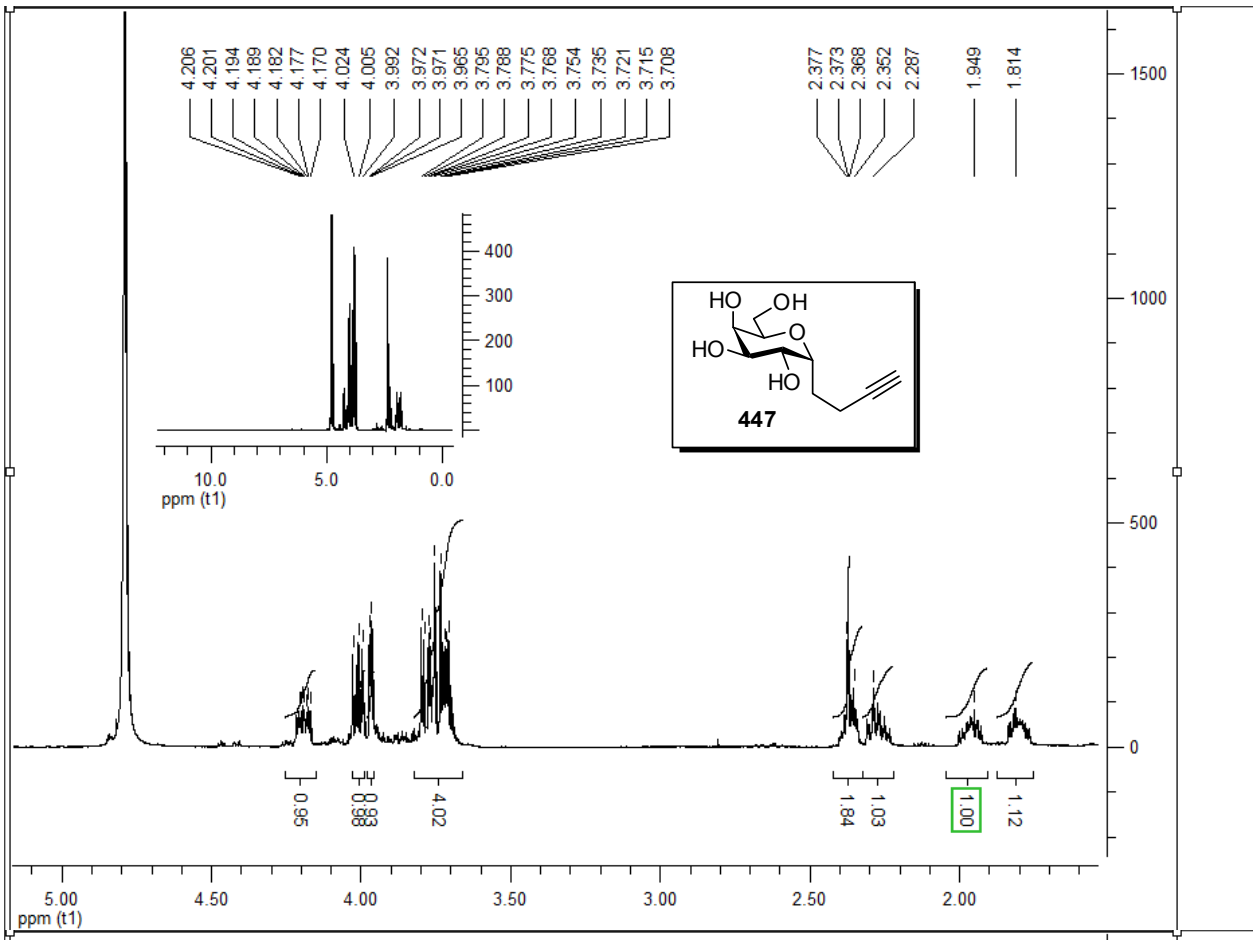

80.719
77.925
69.990
69.961
69.828
68.842
68.211
36.480
HO
OH
O
HO
HO
OMs
438
150
100
50
0
ppm (t1)

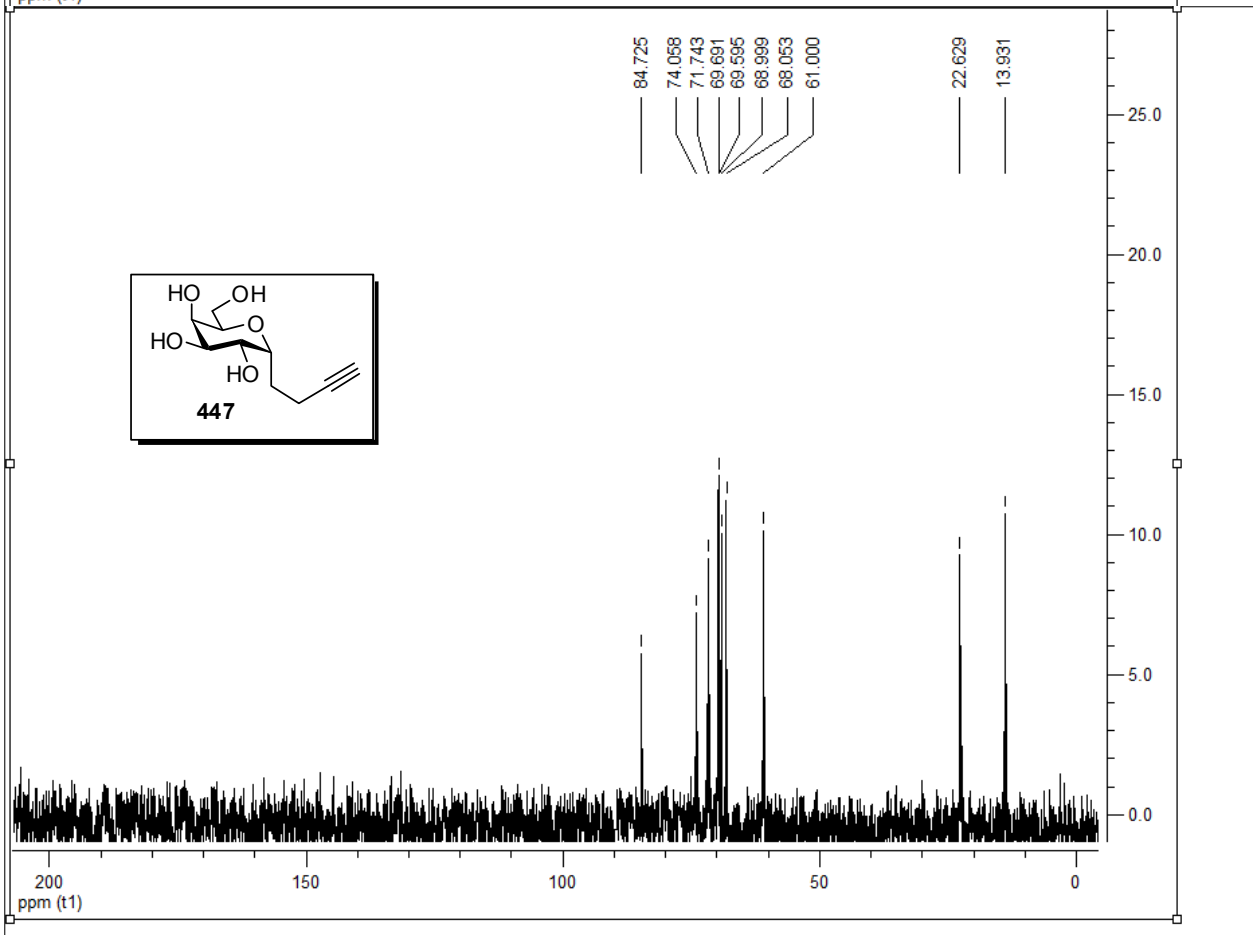

4.858
4.853
4.844
4.838
4.130
3.965
3.963
3.957
3.955
3.899
3.884
3.865
3.857
3.726
3.711
2.972
2.967
HO
OH
O
HO
HO
445
10.0
5.0
ppm (t1)
15000
10000
5000
0
4000
3000
2000
1000
1.00
1.03
1.12
2.14
2.13
0.79
5.00
4.50
4.00
3.50
3.00
ppm (t1)

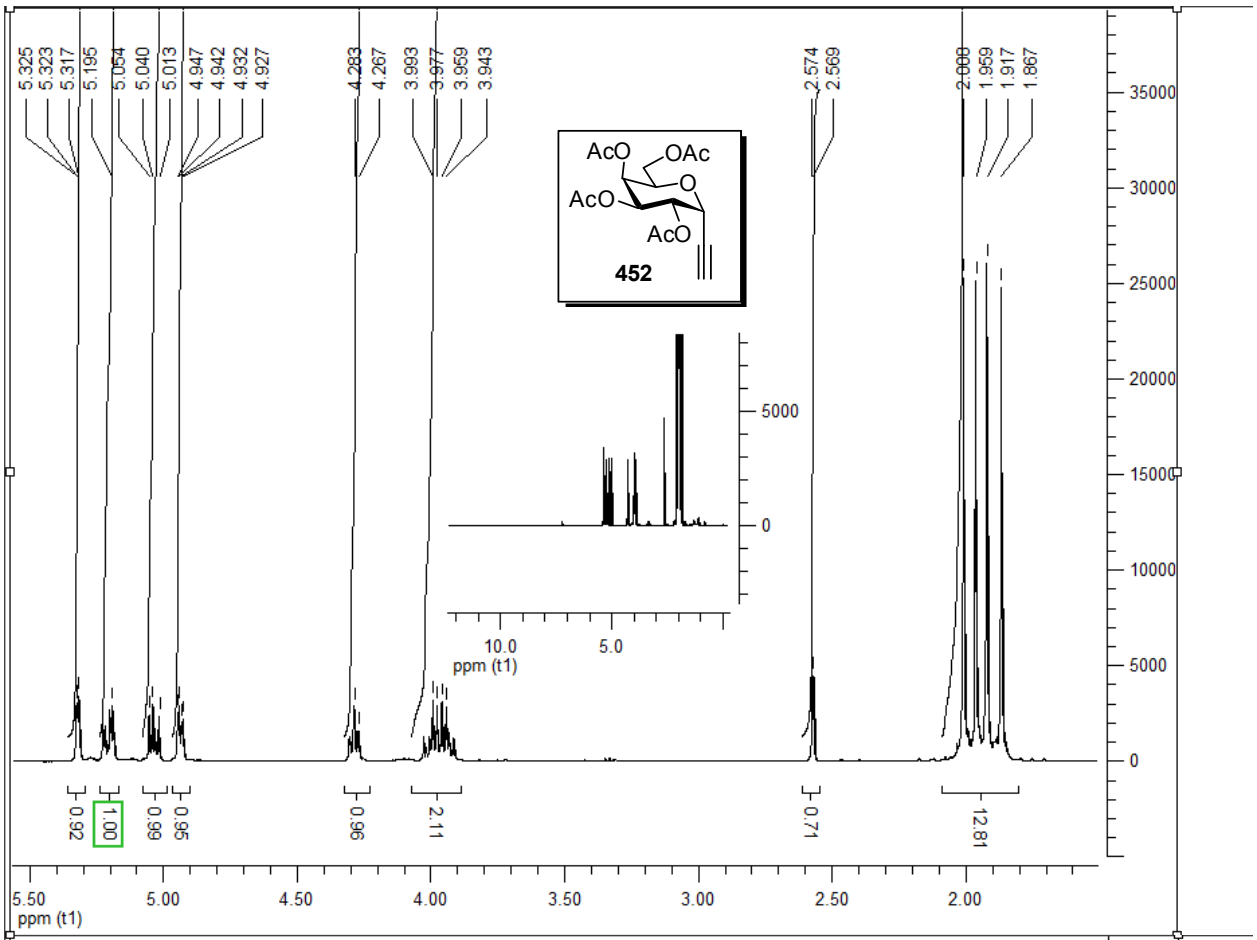

78.469
77.602
74.163
70.467
69.040
68.231
66.800
61.207
HO
OH
O
HO
HO
445
2500
2000
1500
1000
500
0
200
150
100
50
0
ppm (t1)

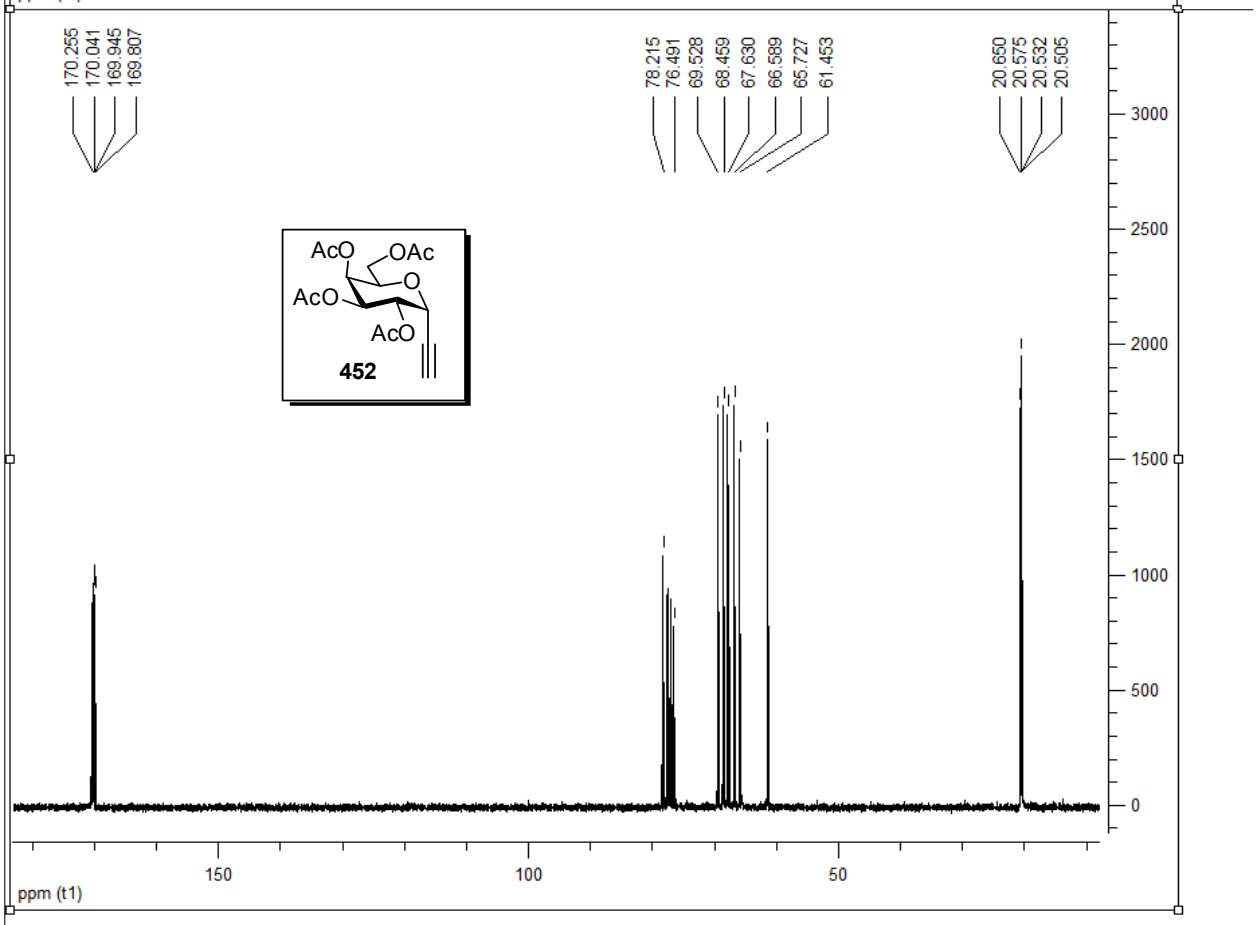

4.093
4.080
4.067
3.897
3.873
3.840
3.836
3.650
3.619
3.601
3.586
3.574
2.527
2.502
2.486
2.479
2.474
2.467
2.233
HO
OH
O
HO
HO
446
1.00
1.73
1.03
3.29
1.81
0.77
ppm (t1)

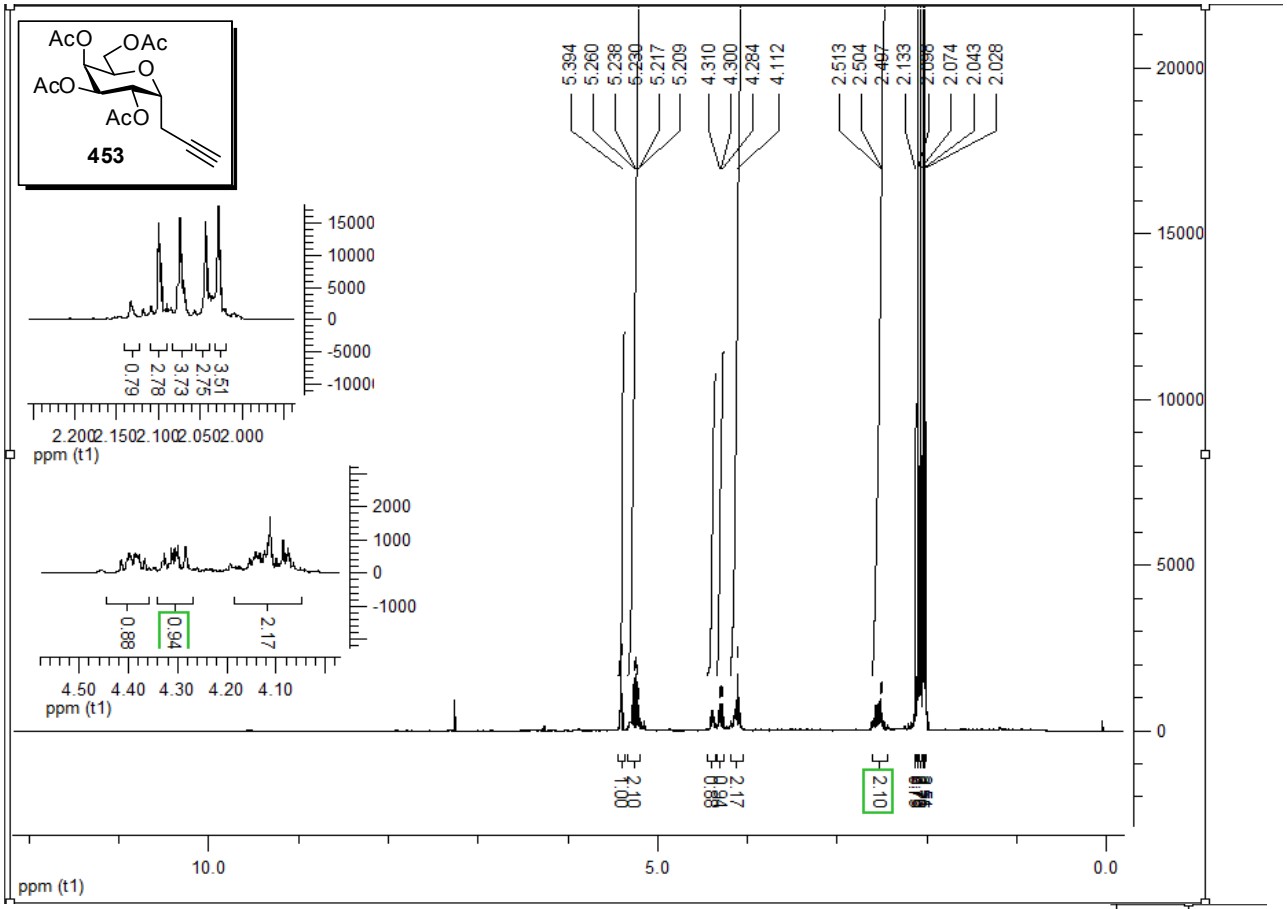

81.497
73.624
72.363
70.893
69.360
68.659
67.859
60.753
15.689
HO
OH
O
HO
HO
446
ppm (t1)

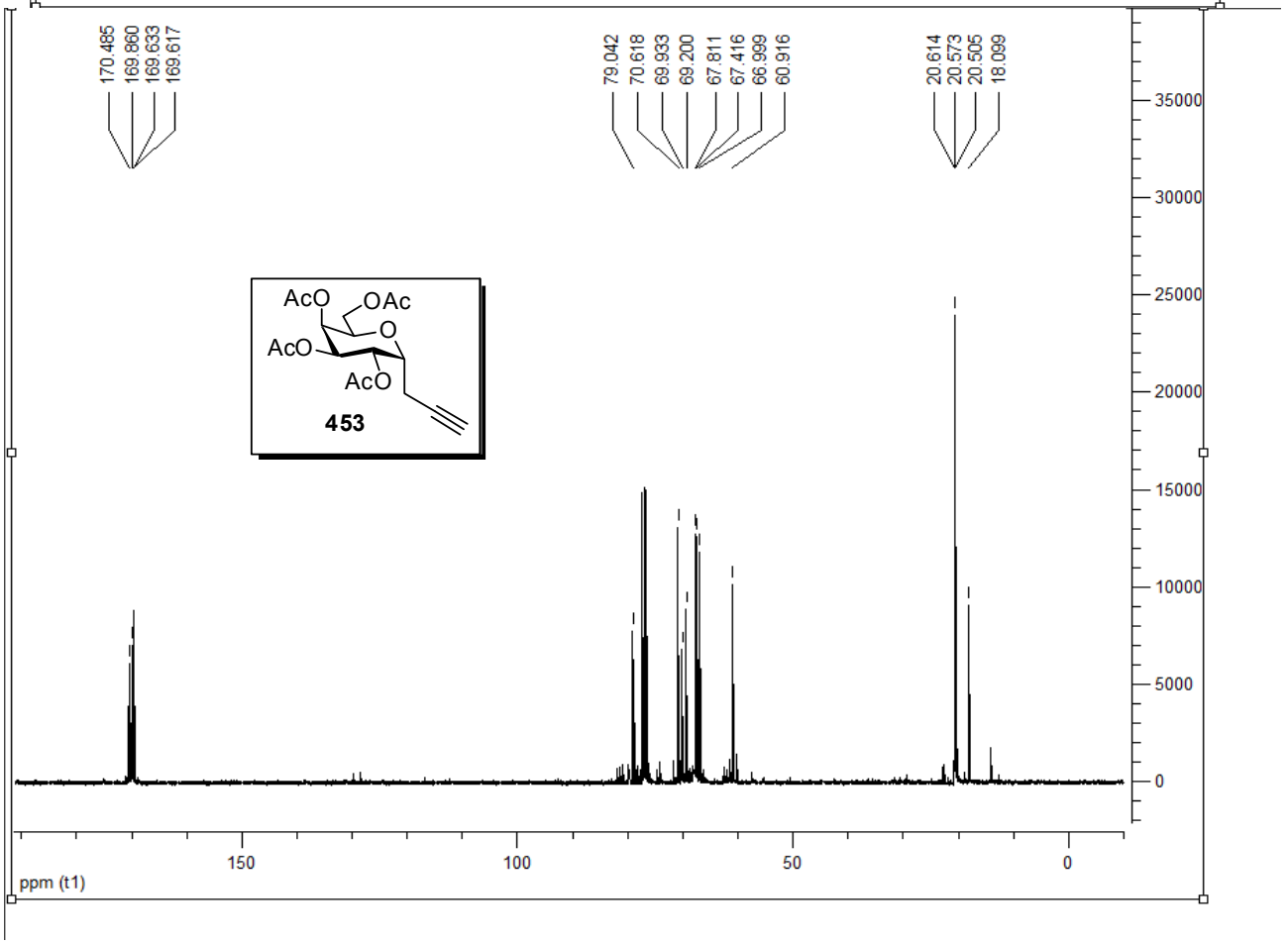

4.206
4.201
4.194
4.189
4.182
4.177
4.170
4.024
4.005
3.992
3.972
3.971
3.965
3.795
3.788
3.775
3.768
3.754
3.735
3.721
3.715
3.708
2.377
2.373
2.368
2.352
2.287
1.949
1.814
HO
OH
O
HO
HO
447
ppm (t1)
0.96
0.88
0.88
4.02
1.84
1.03
1.00
1.12
5.00
4.50
4.00
3.50
3.00
2.50
2.00
ppm (t1)

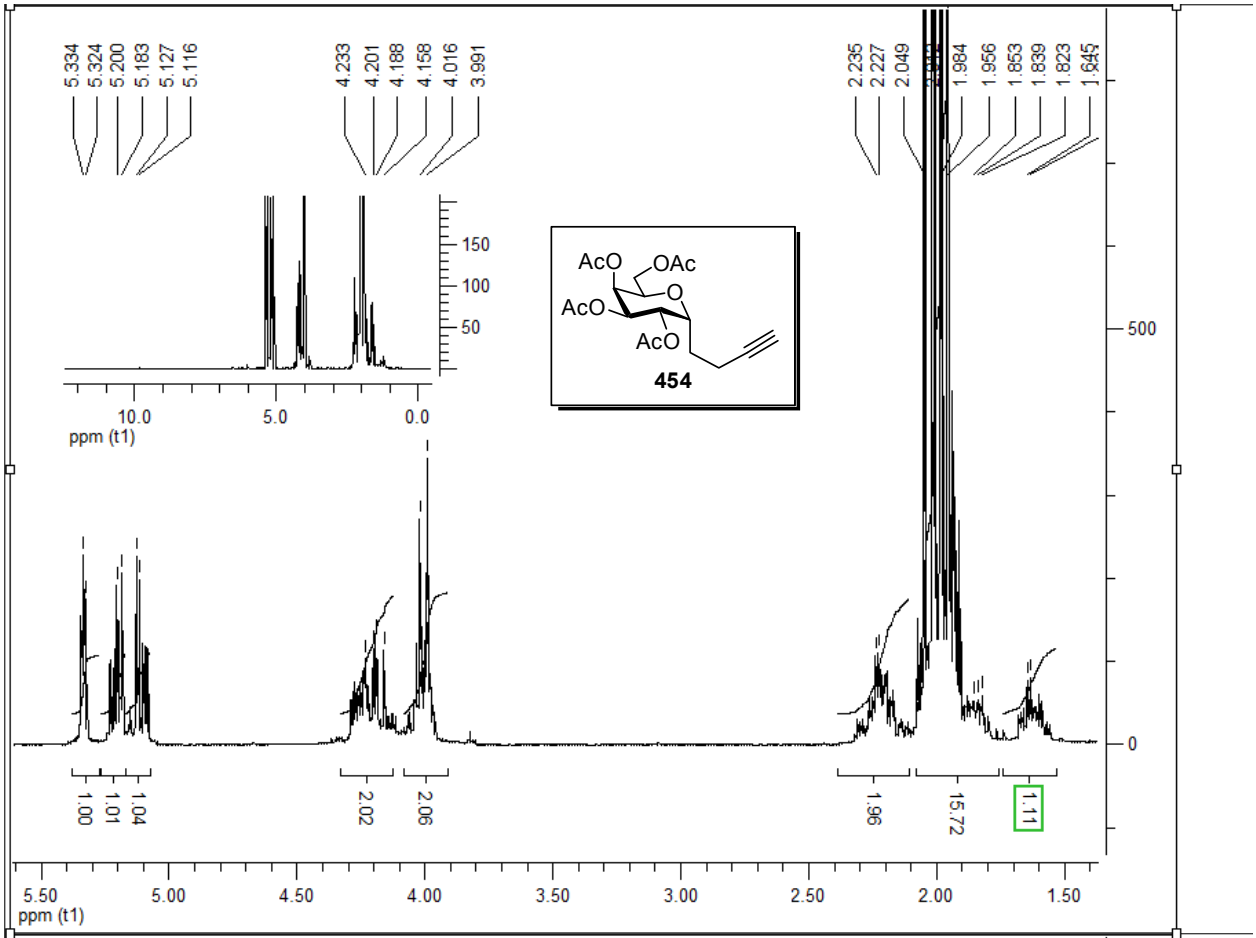

84.725
74.058
71.743
69.691
69.595
68.999
68.053
61.000
22.629
13.931
HO
OH
O
HO
HO
447
200
150
100
50
0
ppm (t1)

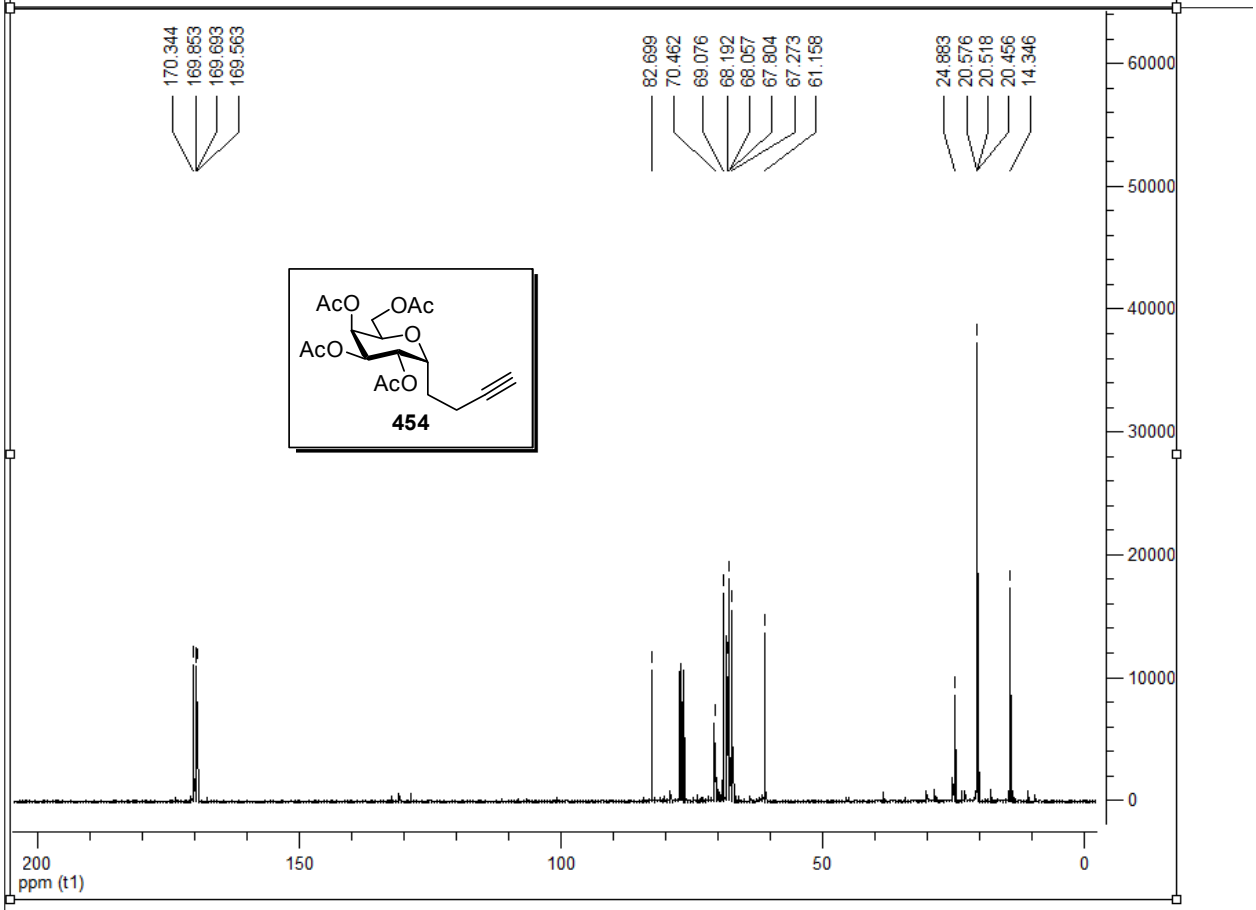

5.325
5.323
5.317
5.195
5.054
5.040
5.013
4.947
4.942
4.932
4.927
4.283
4.267
3.993
3.977
3.959
3.943
2.574
2.569
2.000
1.959
1.917
1.867
AcO
OAc
AcO
O
AcO
452
0.92
1.00
0.99
0.96
0.96
2.11
0.71
12.81
ppm (t1)

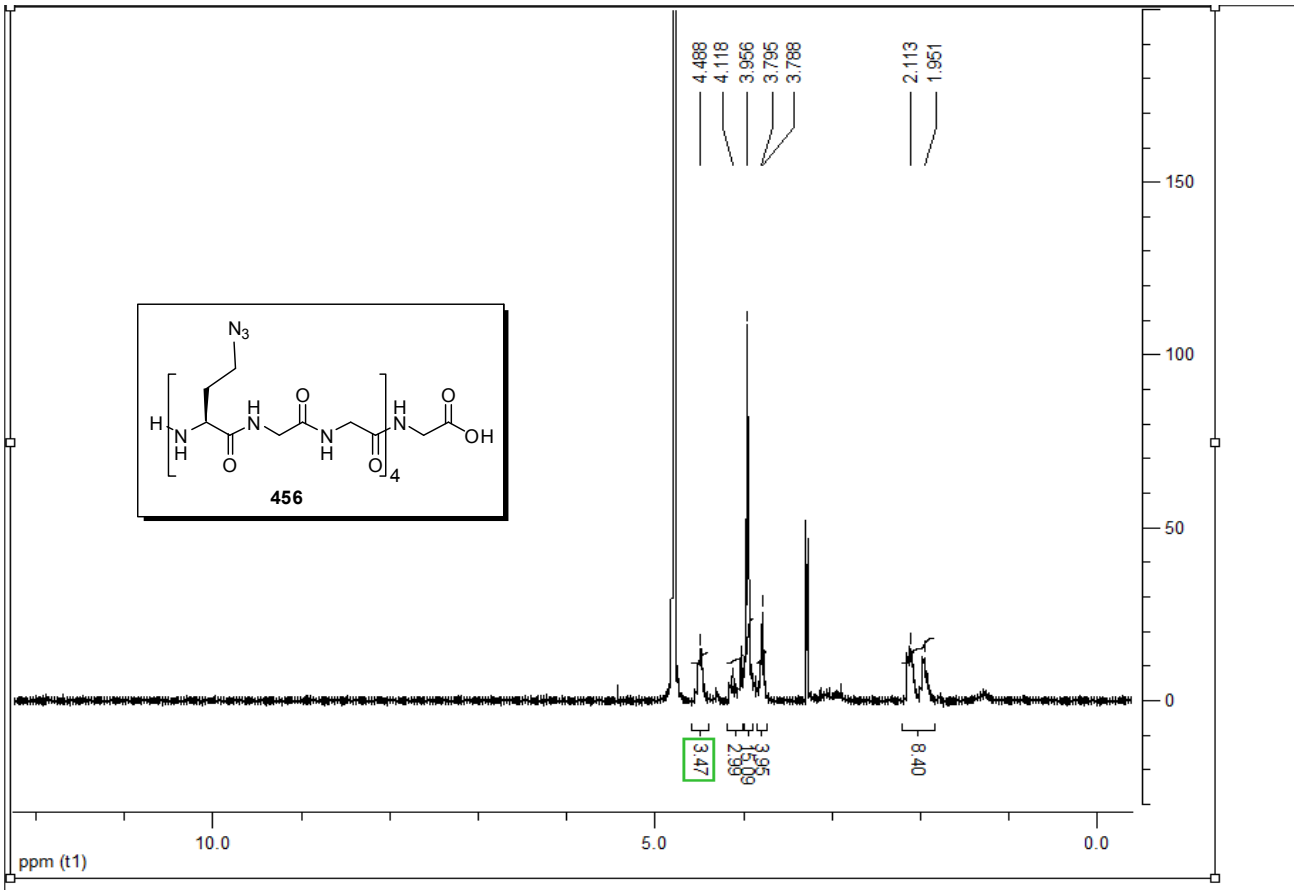

170.255
170.041
169.945
169.807
78.215
76.491
69.528
68.459
67.630
66.589
65.727
61.453
20.650
20.575
20.532
20.505
AcO
OAc
AcO
O
AcO
452
ppm (t1)

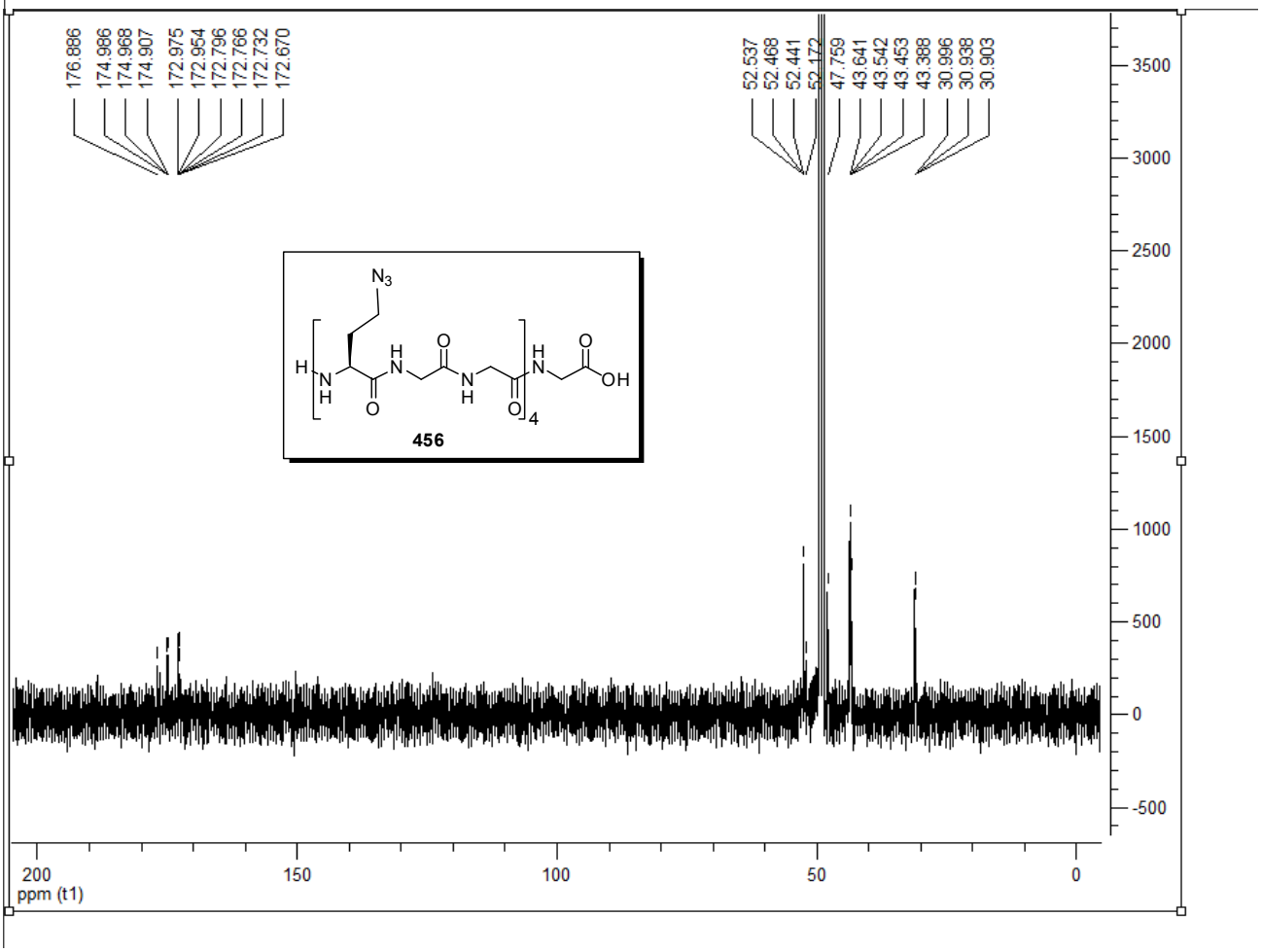

AcO
OAc
O
AcO
AcO
453
5.394
5.260
5.238
5.230
5.217
5.209
4.310
4.300
4.284
4.112
2.513
2.504
2.497
2.133
2.074
2.043
2.028
ppm (t1)
10.0
5.0
0.0

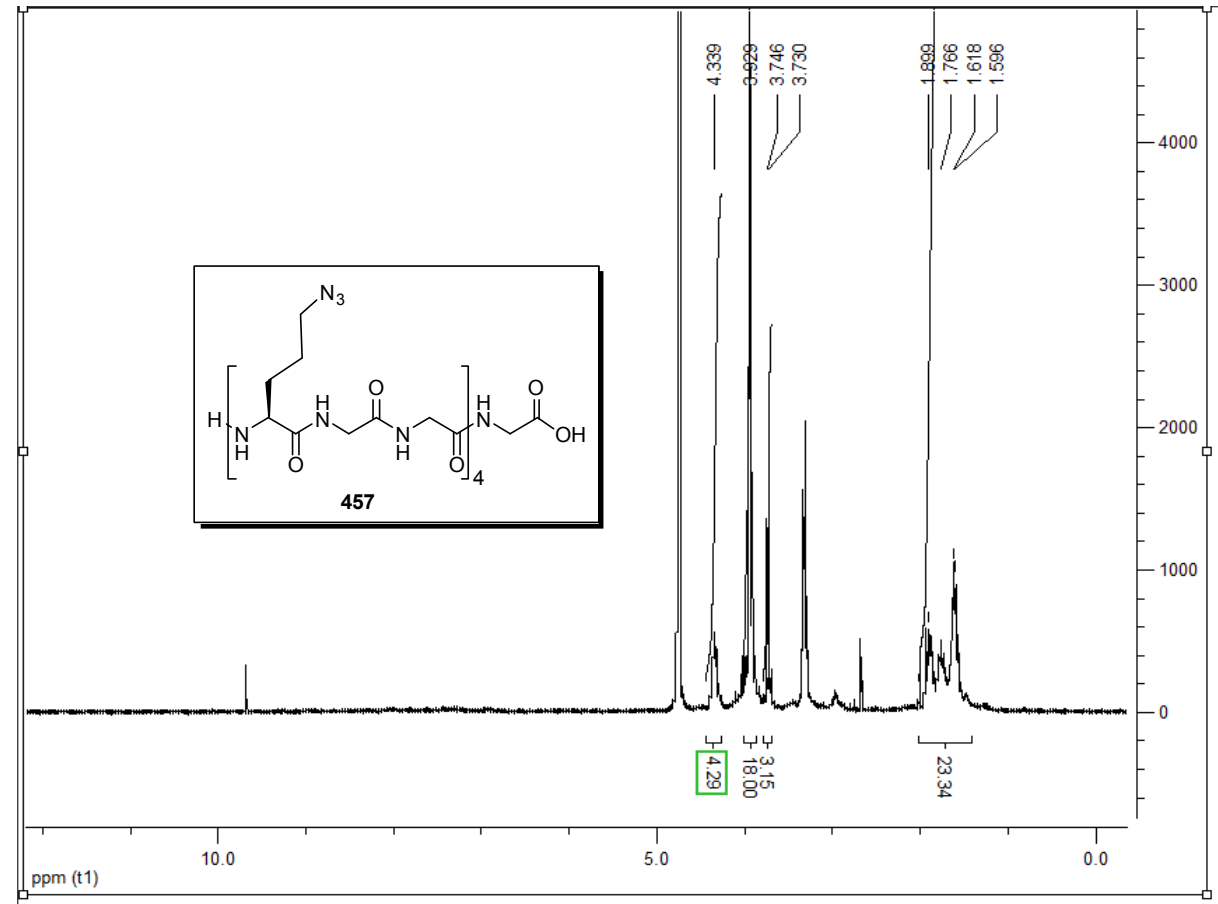

170.485
169.860
169.633
169.617
79.042
70.618
69.933
69.200
67.811
67.416
66.999
60.916
20.614
20.573
20.505
18.099
AcO
OAc
O
AcO
AcO
453
ppm (t1)
150
100
50
0

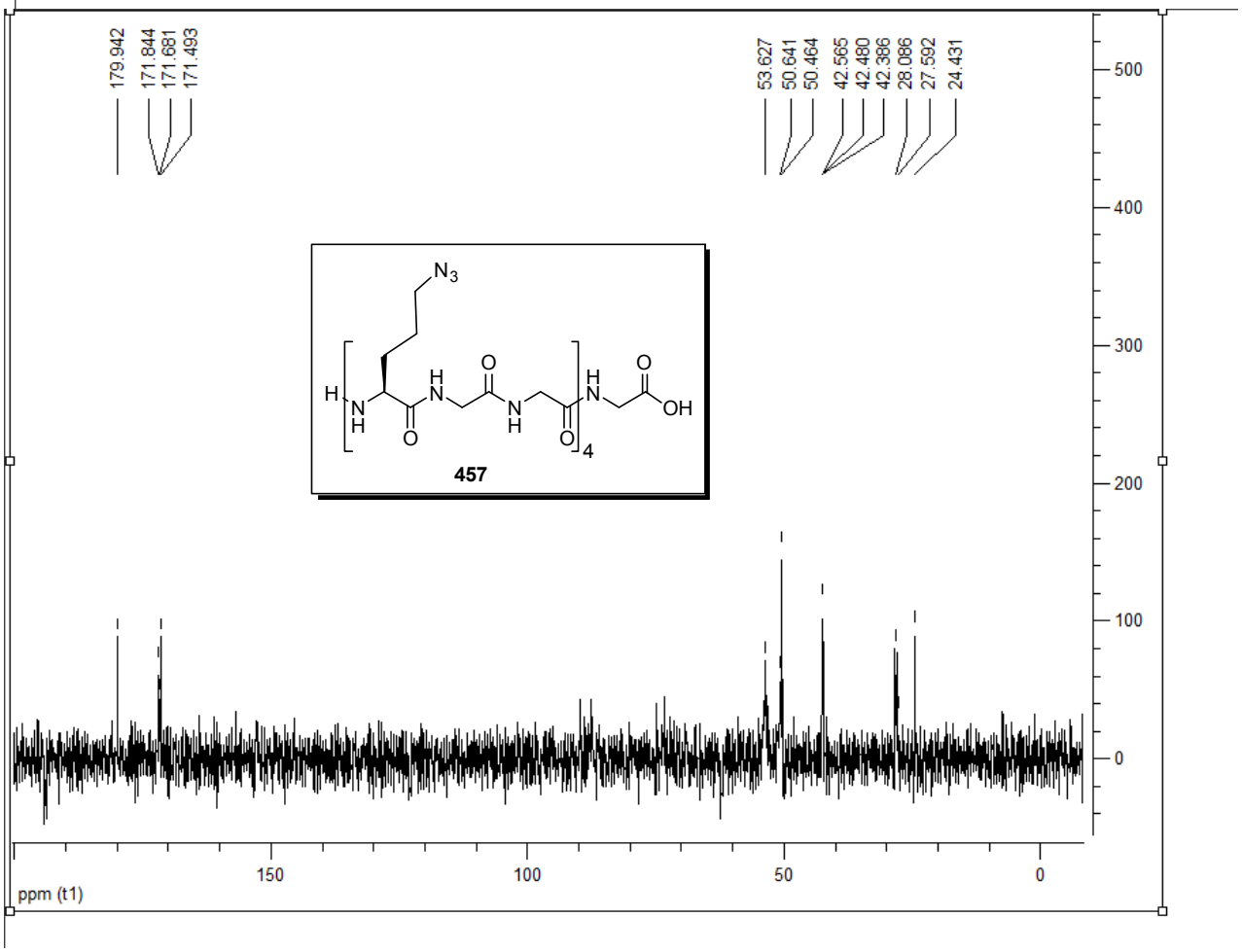

5.334
5.324
5.200
5.183
5.127
5.116
4.233
4.201
4.188
4.158
4.016
3.991
2.235
2.227
2.049
1.984
1.956
1.853
1.839
1.823
1.645
AcO
OAc
AcO
AcO
O
454
ppm (t1)
1.00
1.01
1.04
2.02
2.06
1.96
15.72
1.11

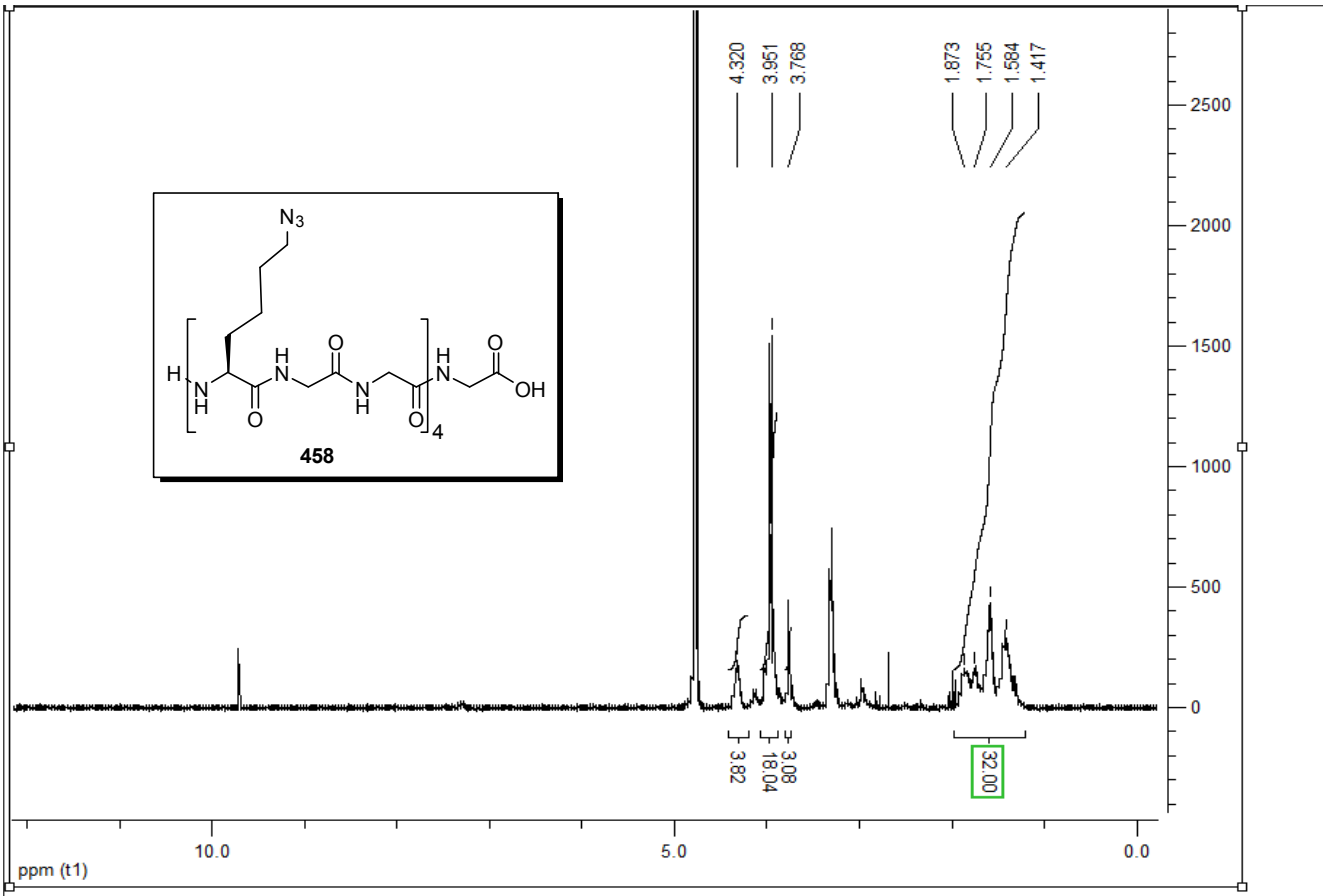

170.344
169.853
169.693
169.563
82.699
70.462
69.076
68.192
68.057
67.804
67.273
61.158
24.883
20.576
20.518
20.456
14.346
AcO
OAc
AcO
AcO
O
454
ppm (t1)

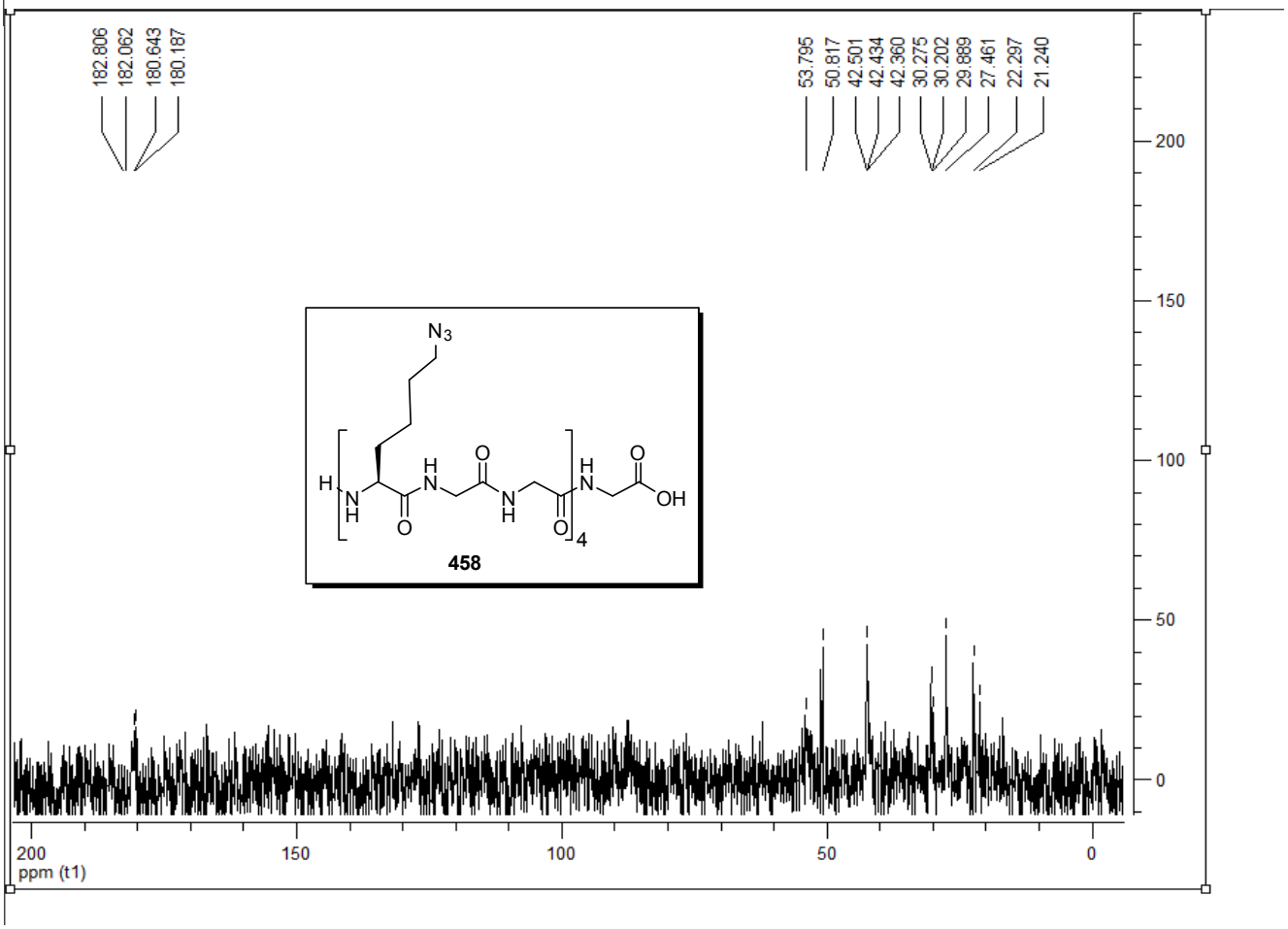

4.488
4.118
3.956
3.795
3.788
2.113
1.951
150
100
50
0
3.47
2.98
3.95
8.40
10.0
5.0
0.0
ppm (t1)
N3
H
N
H
O
H
N
O
H
N
O
OH
O
4
456

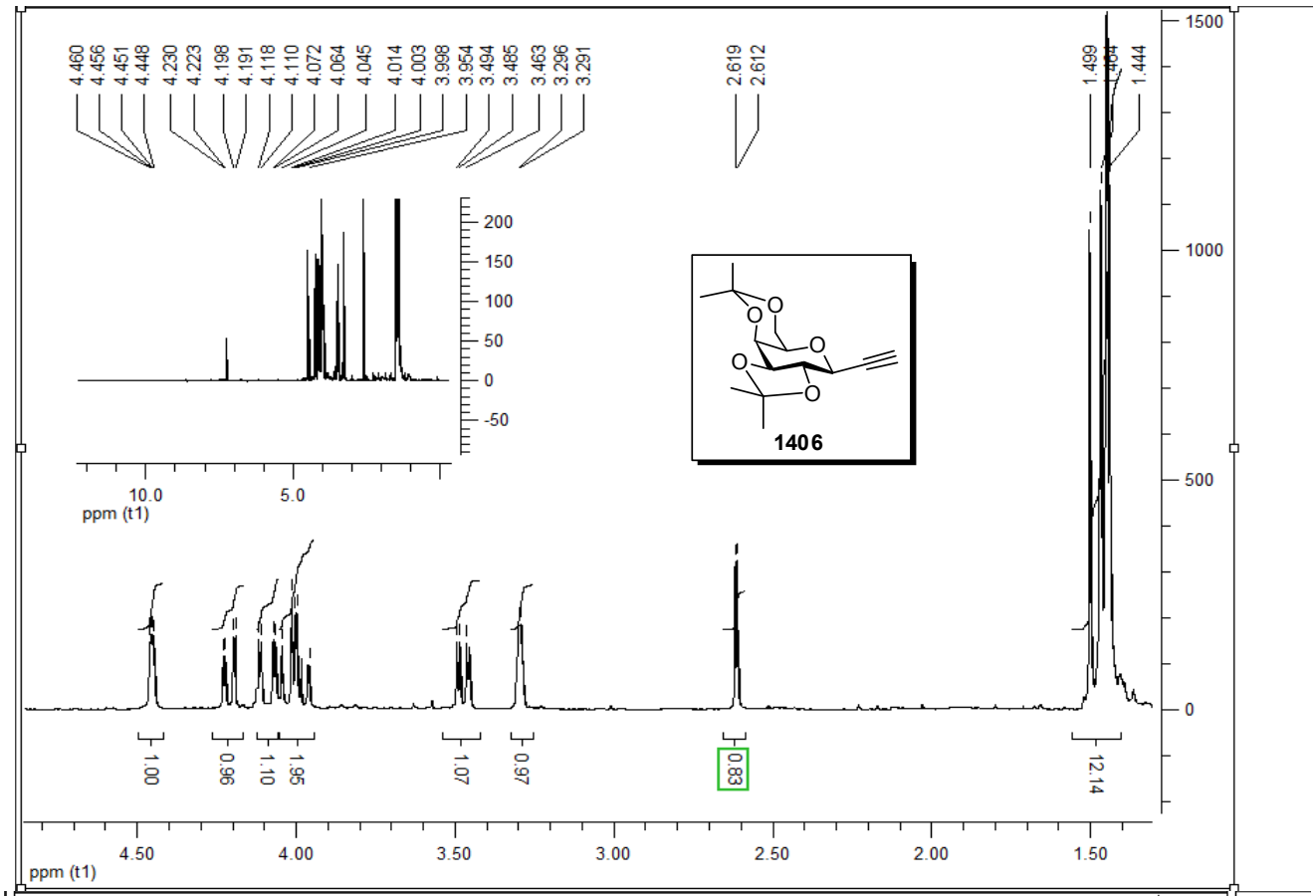

176.886
174.986
174.968
174.907
172.975
172.954
172.796
172.766
172.732
172.670
52.537
52.468
52.441
52.172
47.759
43.641
43.542
43.453
43.388
30.996
30.938
30.903
3500
3000
2500
2000
1500
1000
500
0
-500
200
150
100
50
0
ppm (t1)
N3
H
N
H
O
H
N
O
H
N
O
OH
O
4
456

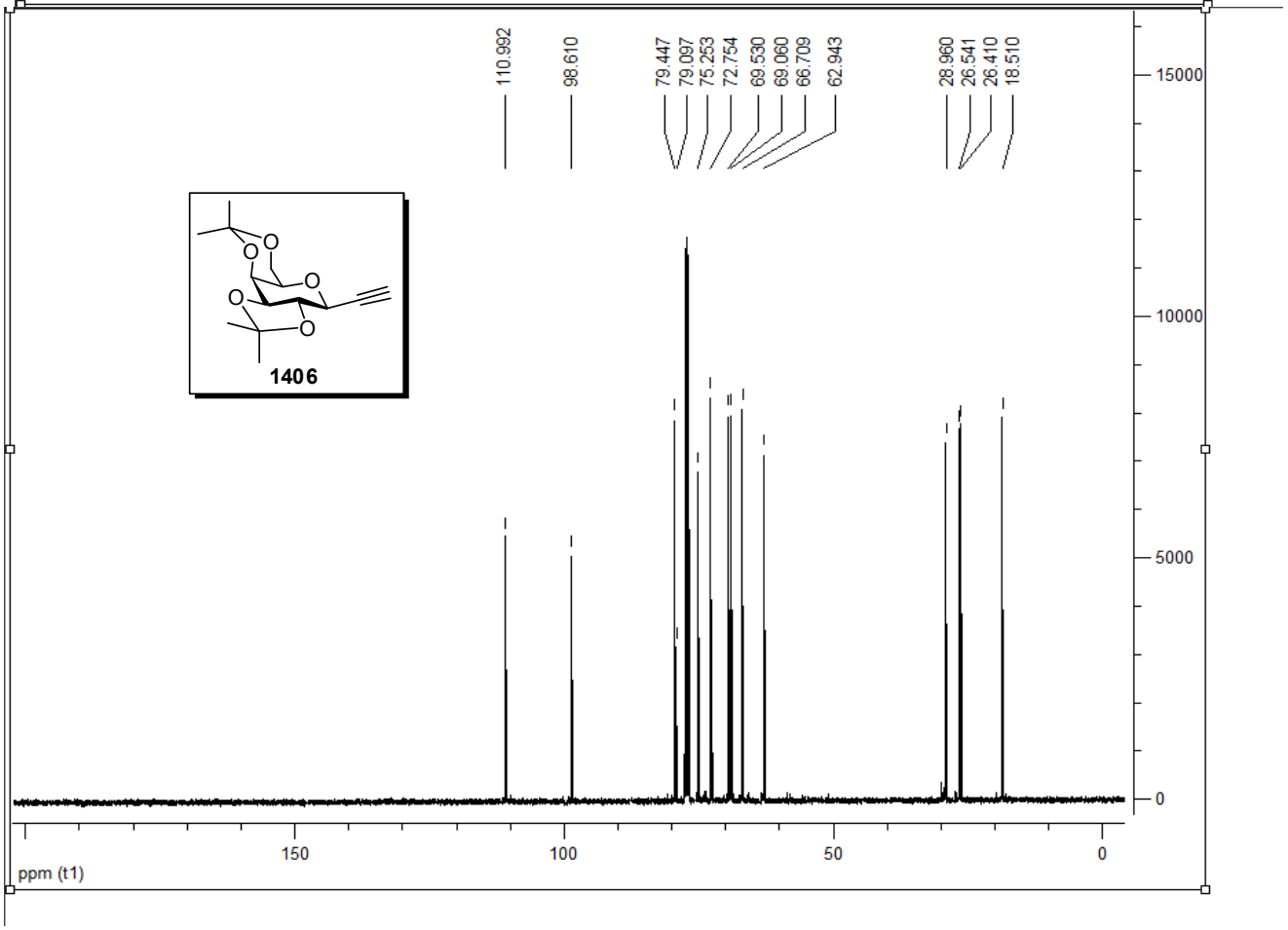

4.339
3.929
3.746
3.730
1.899
1.766
1.618
1.596
4.29
18.00
3.15
23.34
457
ppm (t1)

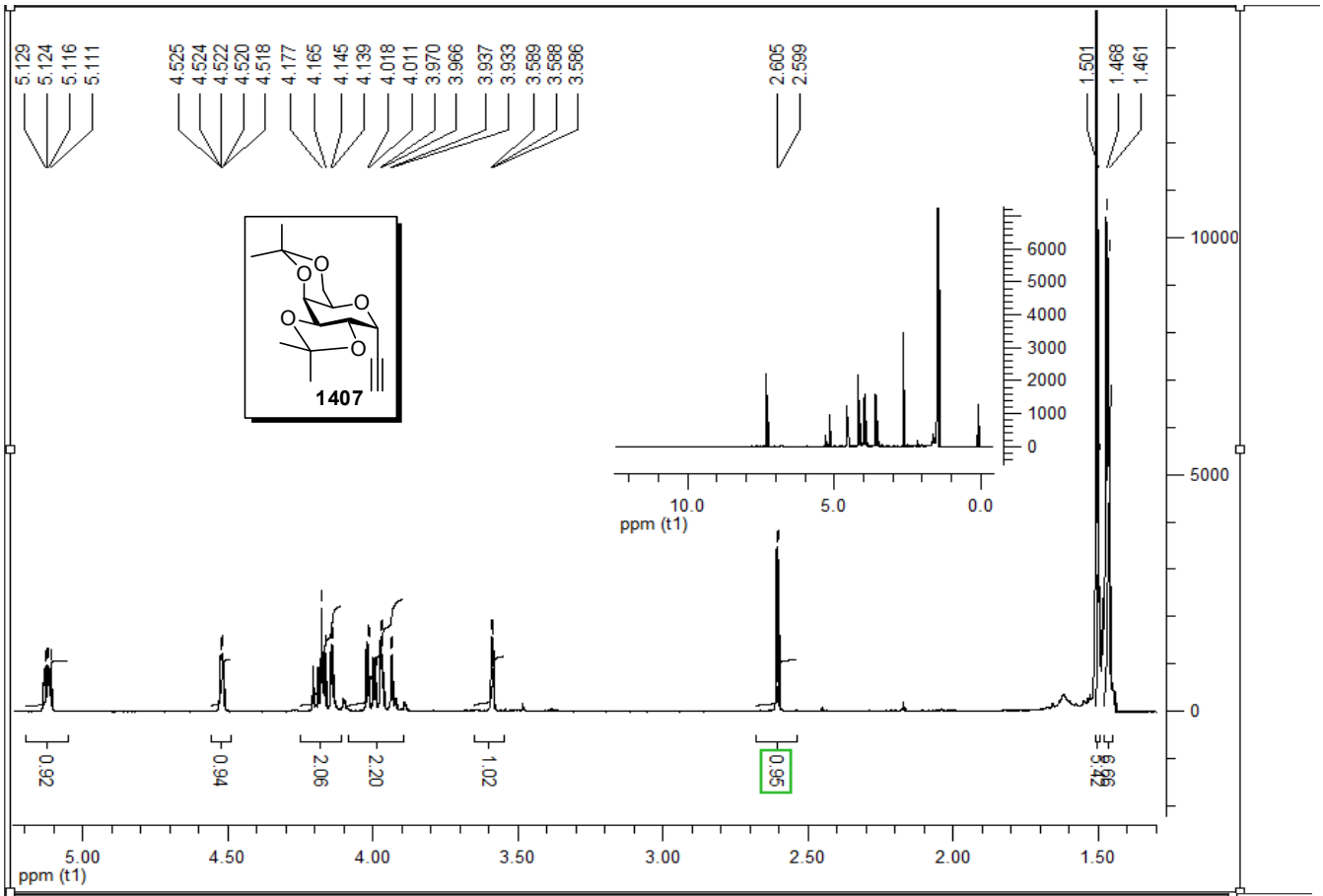

179.942
171.844
171.681
171.493
53.627
50.641
50.464
42.565
42.480
42.386
28.086
27.592
24.431
457
ppm (t1)

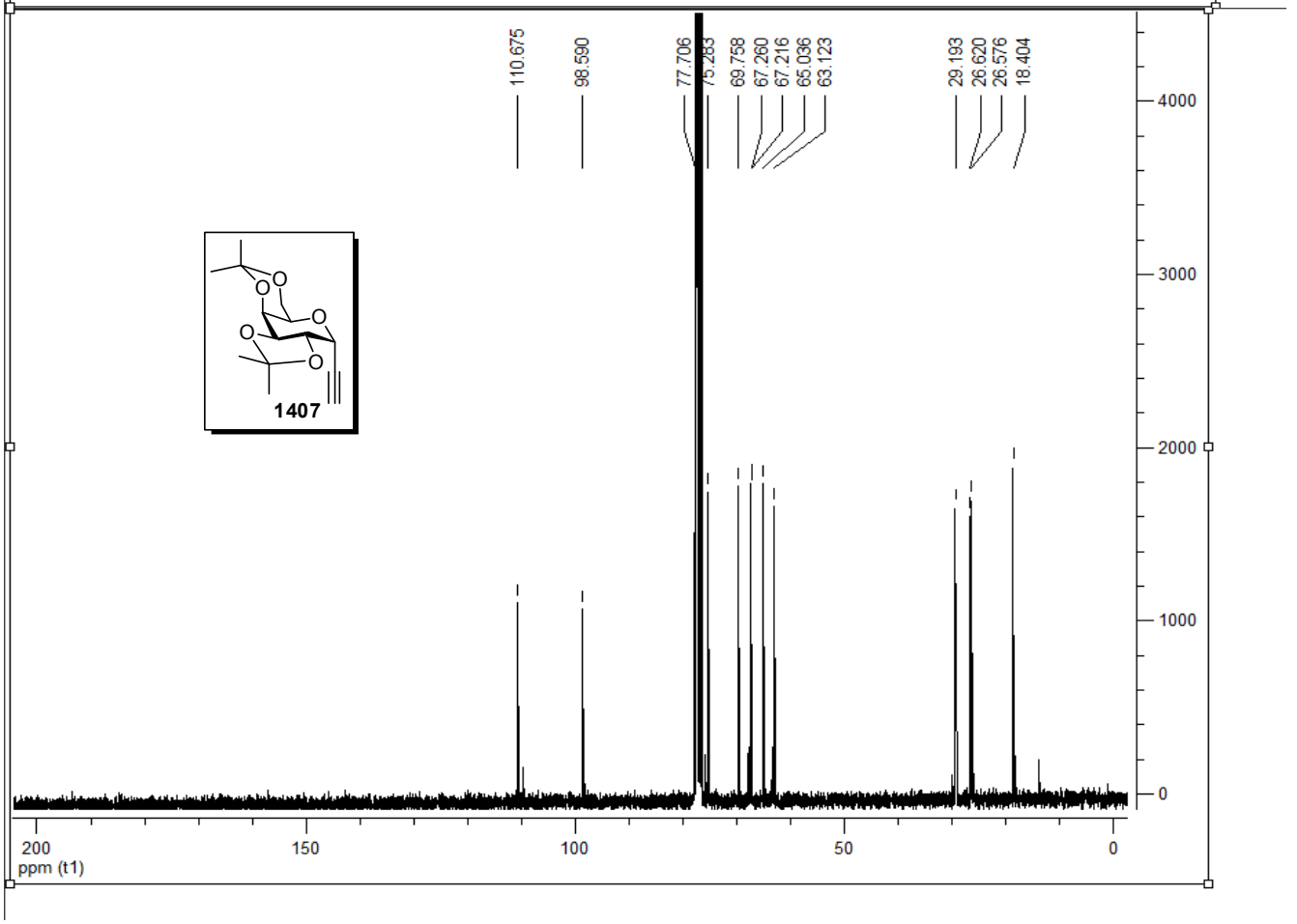

4.320
3.951
3.768
1.873
1.755
1.584
1.417
3.82
18.04
3.08
32.00
2500
2000
1500
1000
500
0
10.0
5.0
0.0
ppm (t1)
N3
H
N
H
O
H
N
O
H
N
O
OH
O
4
458

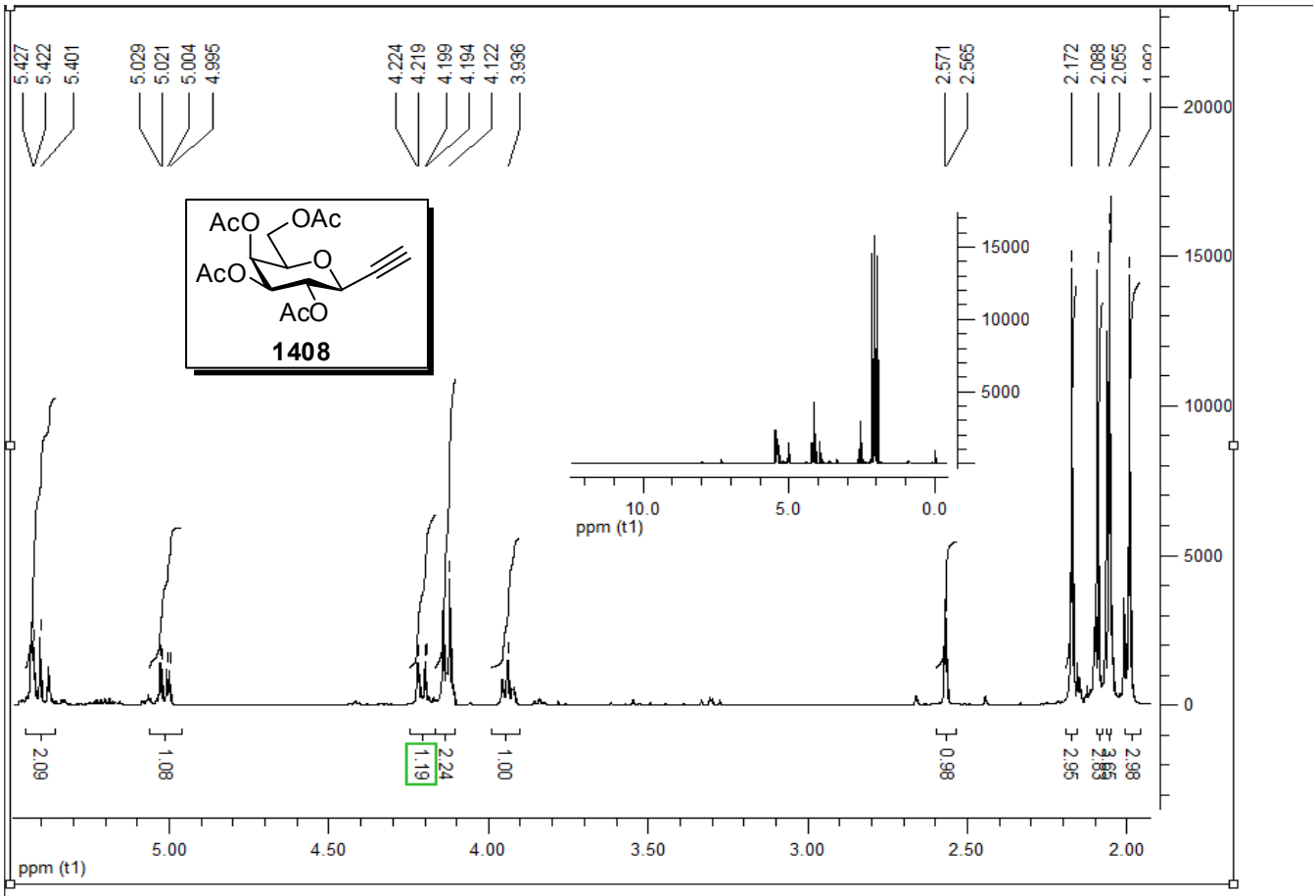

182.806
182.062
180.643
180.187
53.795
50.817
42.501
42.434
42.360
30.275
30.202
29.889
27.461
22.297
21.240
200
150
100
50
0
200
150
100
50
0
ppm (t1)
N3
H
N
H
O
H
N
O
H
N
O
OH
O
4
458

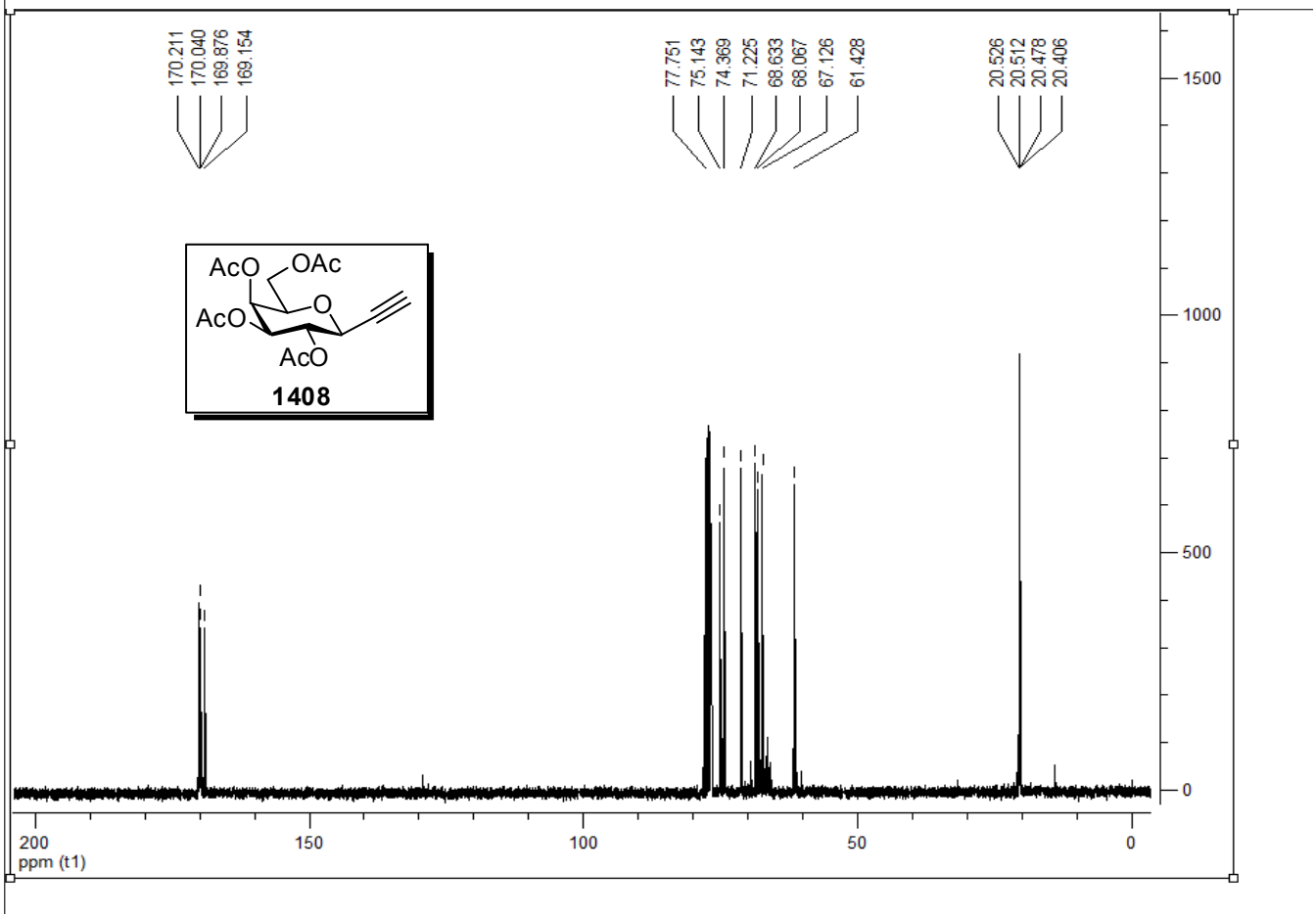

4.460
4.456
4.451
4.448
4.230
4.223
4.198
4.191
4.118
4.110
4.072
4.064
4.045
4.014
4.003
3.998
3.954
3.494
3.485
3.463
3.296
3.291
2.619
2.612
1.499
1.444
1406
ppm (t1)
1.00
0.96
1.10
1.95
1.07
0.97
0.83
12.14

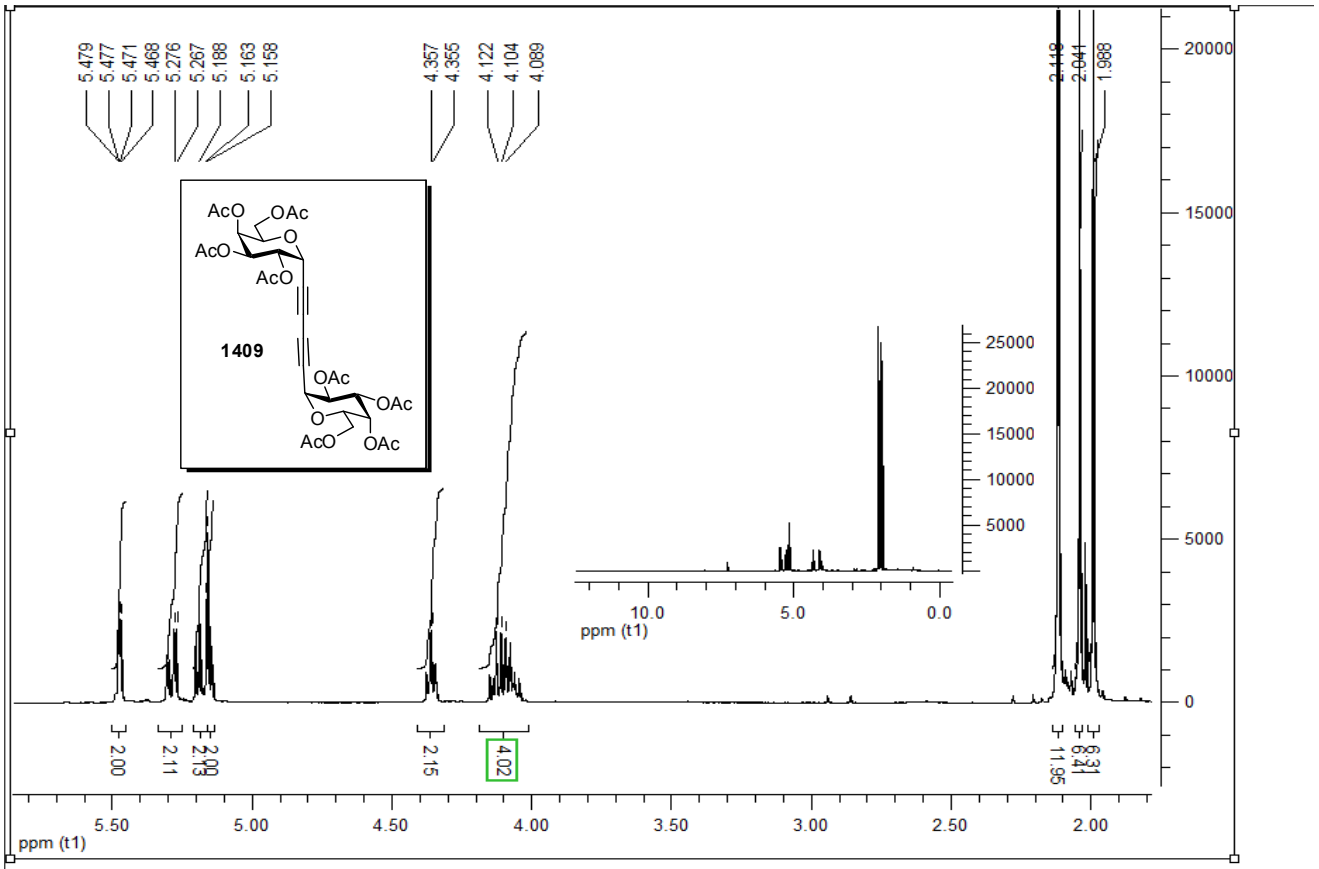

110.992
98.610
79.447
79.097
75.253
72.754
69.530
69.060
66.709
62.943
28.960
26.541
26.410
18.510
1406
ppm (t1)

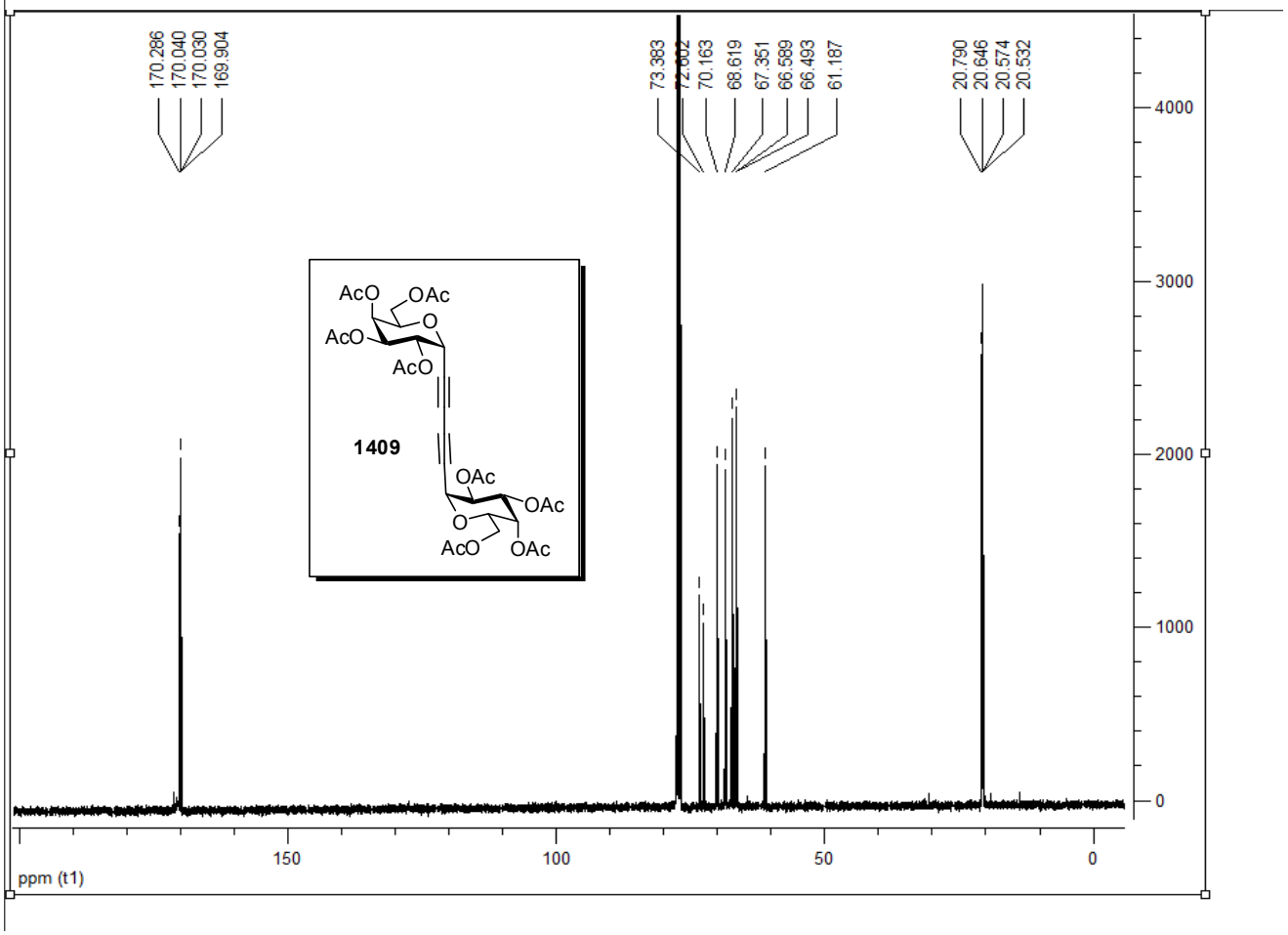

5.129
5.124
5.116
5.111
4.525
4.524
4.522
4.520
4.518
4.177
4.165
4.145
4.139
4.018
4.011
3.970
3.966
3.937
3.933
3.589
3.588
3.586
2.605
2.599
1.501
1.468
1.461
1407
ppm (t1)
0.92
0.94
2.06
2.20
1.02
0.95
5.00
4.50
4.00
3.50
3.00
2.50
2.00
1.50

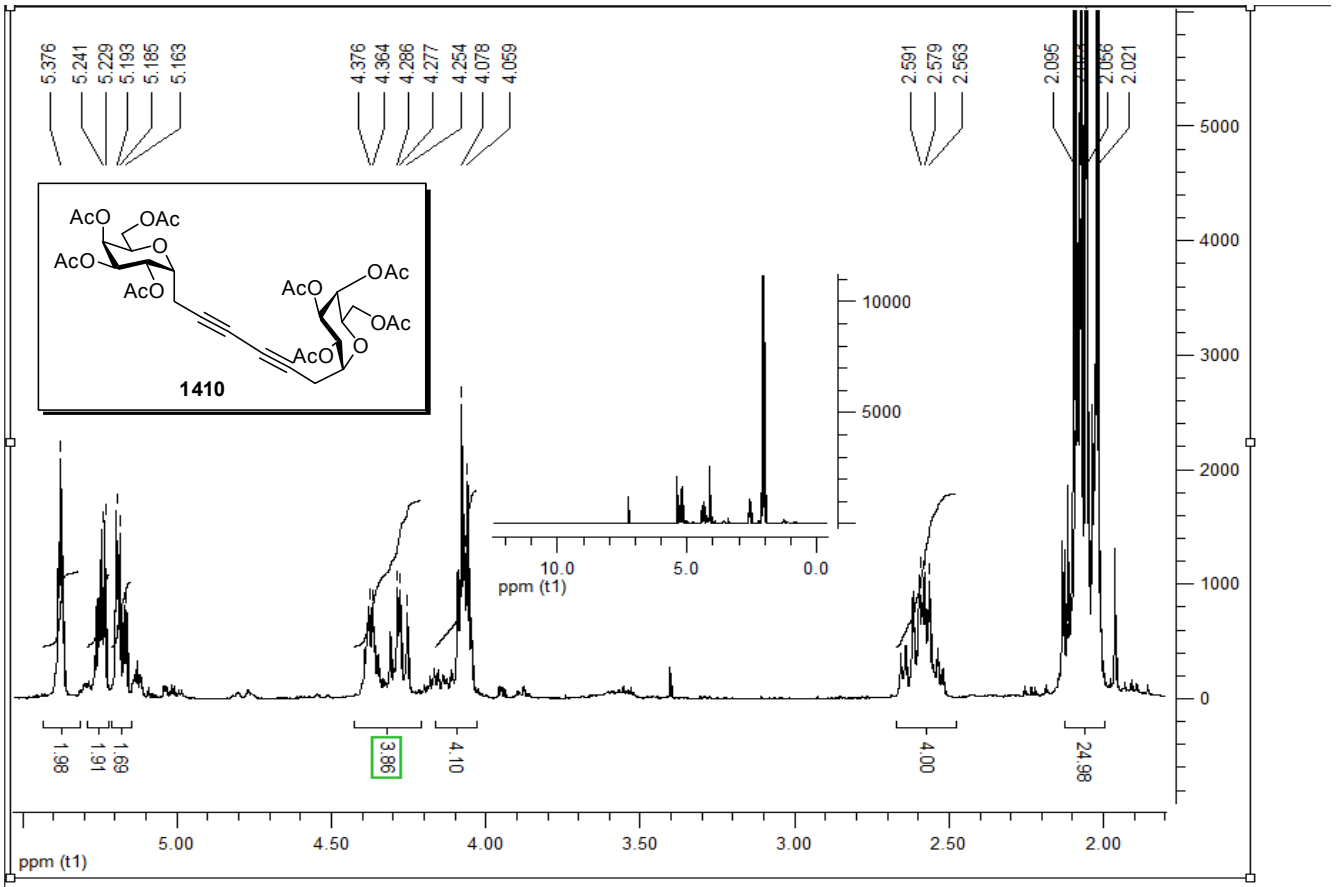

110.675
98.590
77.706
75.283
69.758
67.260
67.216
65.036
63.123
29.193
26.620
26.576
18.404
1407
200
150
100
50
0
ppm (t1)

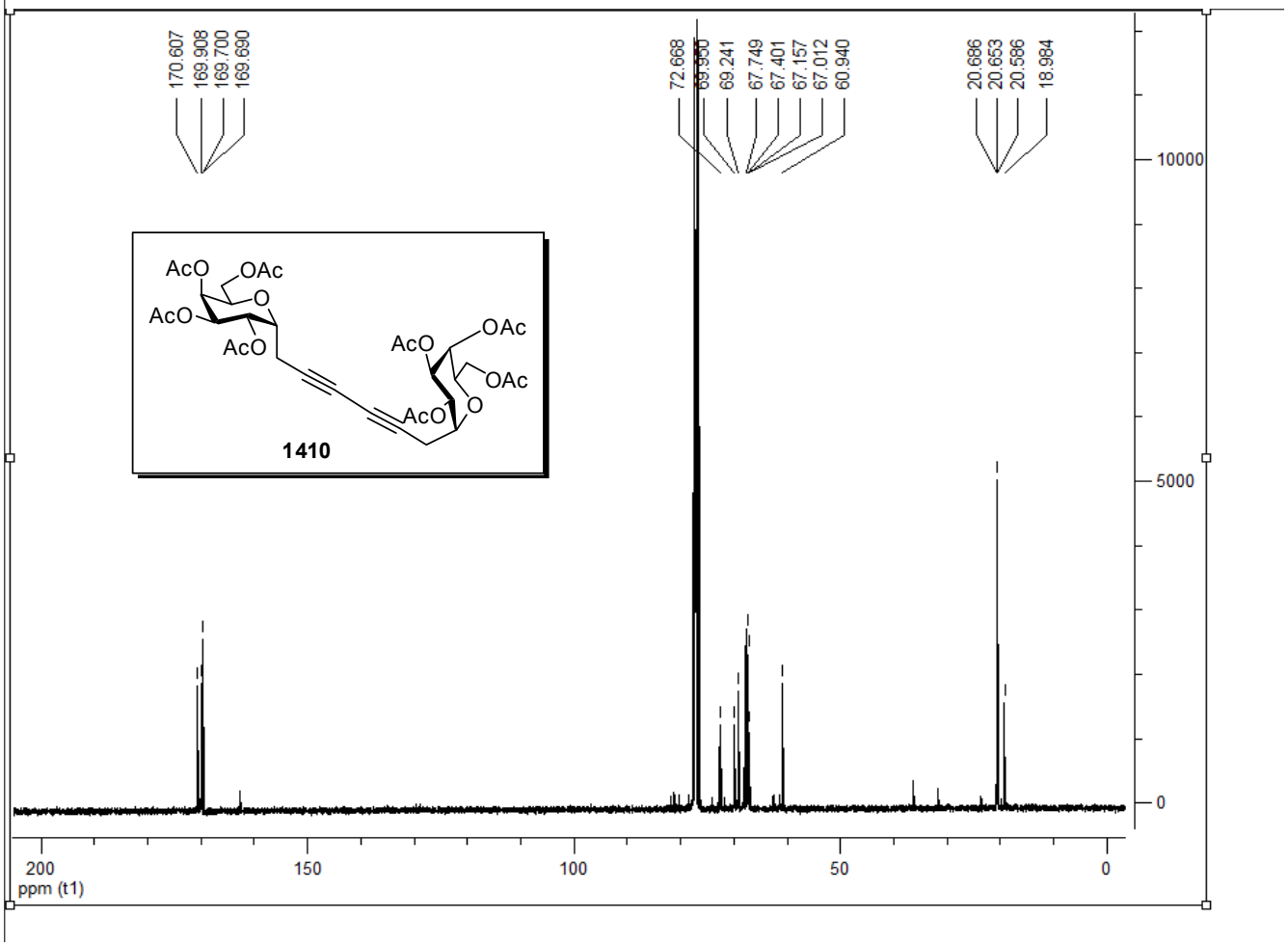

5.427
5.422
5.401
5.029
5.021
5.004
4.995
4.224
4.219
4.199
4.194
4.122
3.936
2.571
2.565
2.172
2.088
2.055
AcO
OAc
AcO
O
AcO
1408
ppm (t1)
2.09
1.08
1.19
2.24
1.00
0.98
2.95
2.98
ppm (t1)

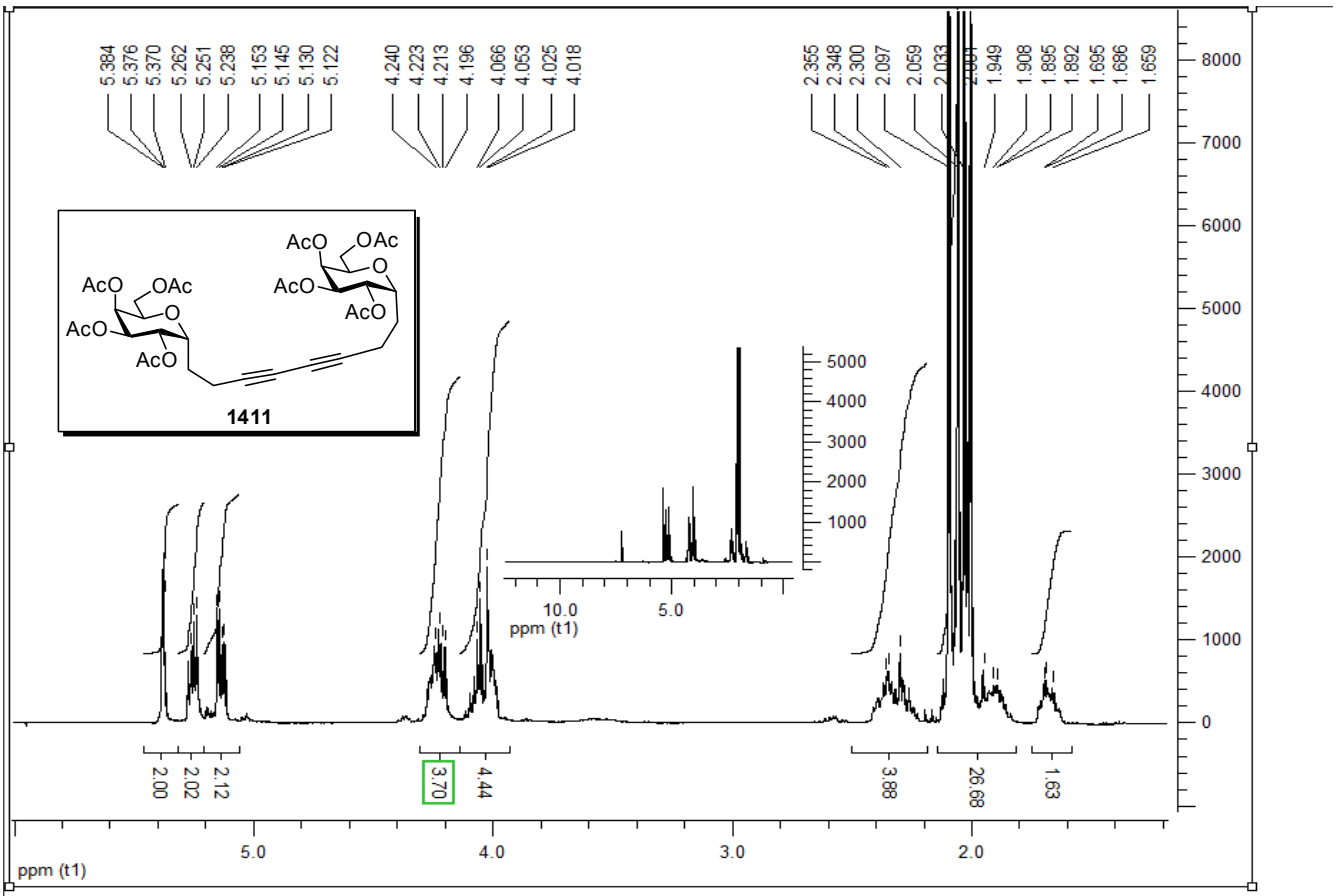

170.211
170.040
169.876
169.154
77.751
75.143
74.369
71.225
68.633
68.067
67.126
61.428
20.526
20.512
20.478
20.406
AcO
OAc
AcO
O
AcO
1408
ppm (t1)

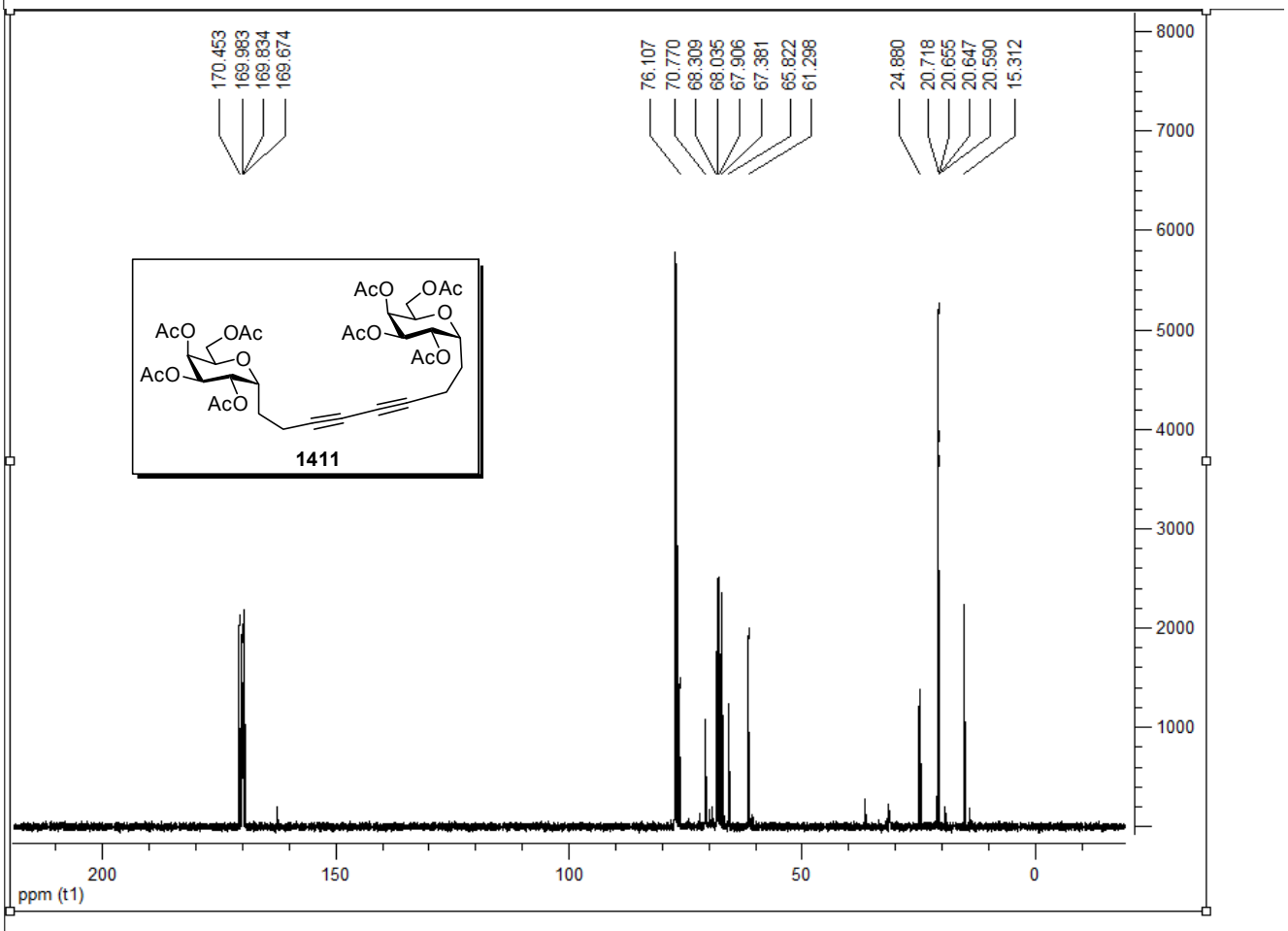

5.479
5.477
5.471
5.468
5.276
5.267
5.188
5.163
5.158
4.357
4.355
4.122
4.104
4.089
2.119
2.041
1.988
AcO
OAc
AcO
AcO
1409
OAc
OAc
AcO
OAc
2.00
2.11
2.13
2.15
4.02
11.95
ppm (t1)

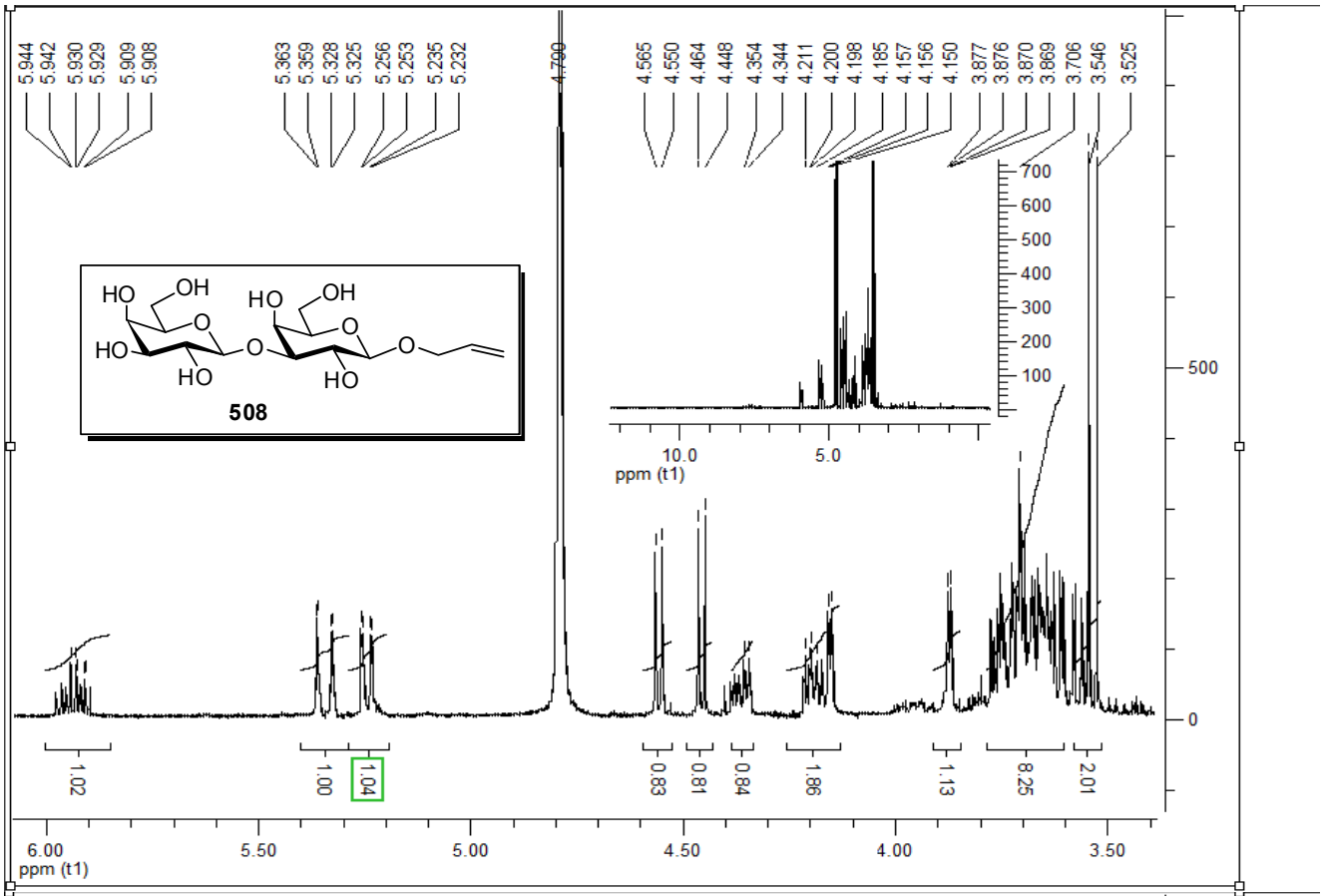

170.286
170.040
170.030
169.904
73.383
72.602
70.163
68.619
67.351
66.589
66.493
61.187
20.790
20.646
20.574
20.532
AcO
OAc
AcO
AcO
1409
OAc
OAc
AcO
OAc
ppm (t1)

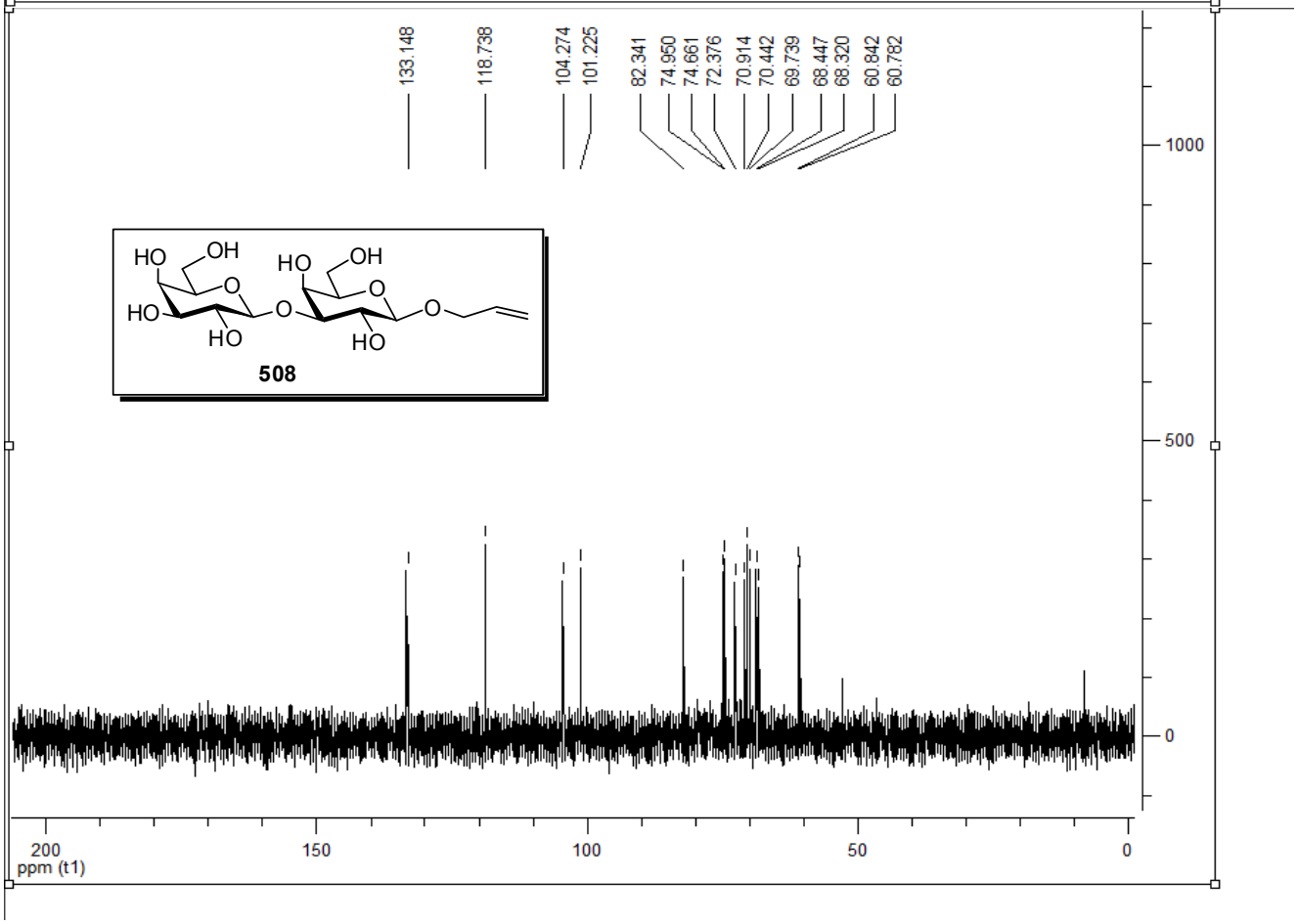

5.376
5.241
5.229
5.193
5.185
5.163
4.376
4.364
4.286
4.277
4.254
4.078
4.059
2.591
2.579
2.563
2.095
2.056
2.021
AcO
OAc
AcO
AcO
AcO
OAc
OAc
AcO
1410
10000
5000
10.0
5.0
0.0
ppm (t1)
5000
4000
3000
2000
1000
0
1.98
1.91
1.69
3.86
4.10
4.00
24.98
5.00
4.50
4.00
3.50
3.00
2.50
2.00
ppm (t1)

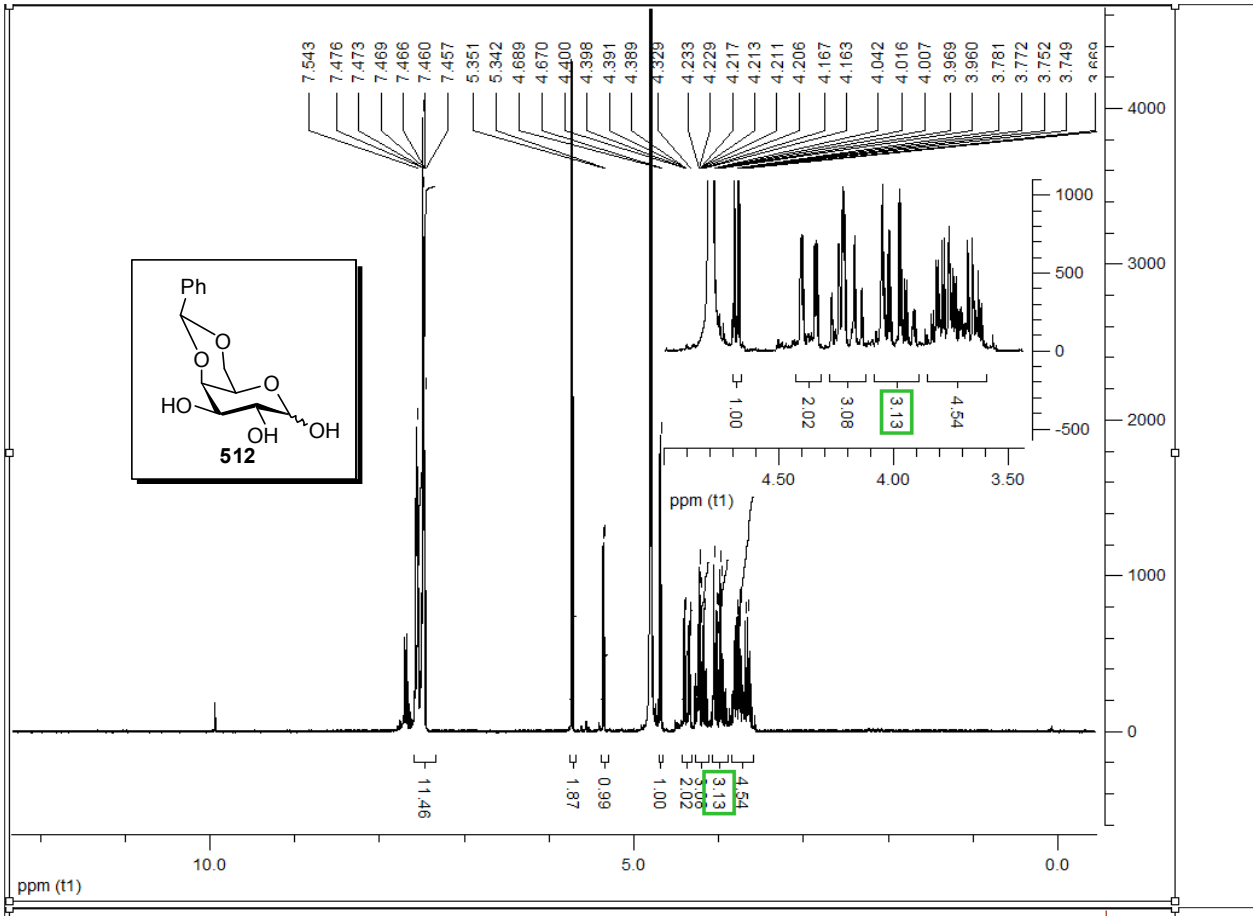

170.607
169.908
169.700
169.690
72.668
69.900
69.241
67.749
67.401
67.157
67.012
60.940
20.686
20.653
20.586
18.984
AcO
OAc
AcO
AcO
AcO
OAc
OAc
AcO
1410
10000
5000
0
200
150
100
50
0
ppm (t1)

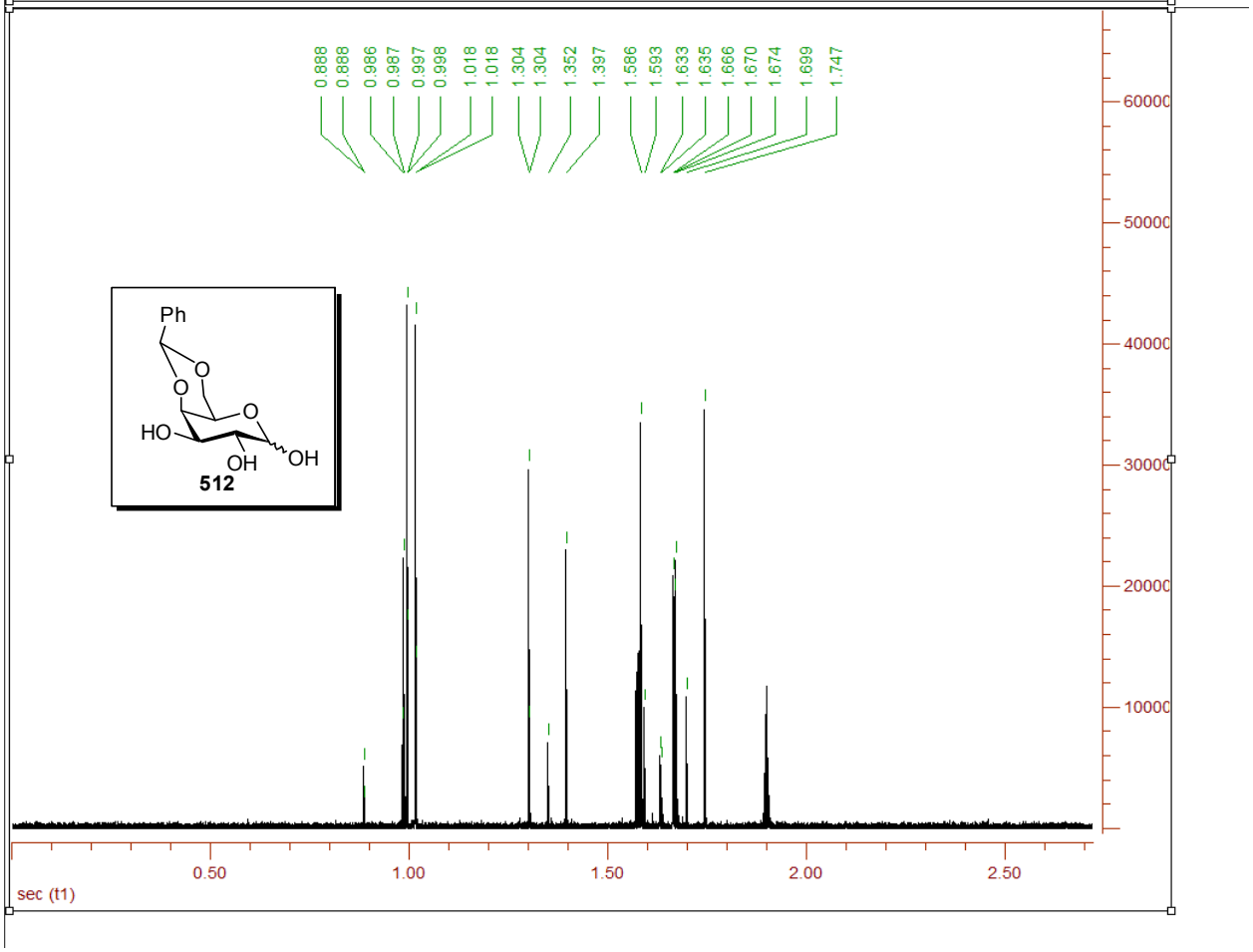

5.384
5.376
5.370
5.262
5.251
5.238
5.153
5.145
5.130
5.122
4.240
4.223
4.213
4.196
4.066
4.053
4.025
4.018
2.355
2.348
2.300
2.097
2.059
2.033
1.949
1.908
1.895
1.892
1.695
1.686
1.659
AcO
OAc
O
AcO
AcO
AcO
OAc
O
AcO
AcO
1411
2.00
2.02
2.12
3.70
4.44
3.88
26.68
1.63
ppm (t1)
5.0
4.0
3.0
2.0
10.0
5.0
ppm (t1)

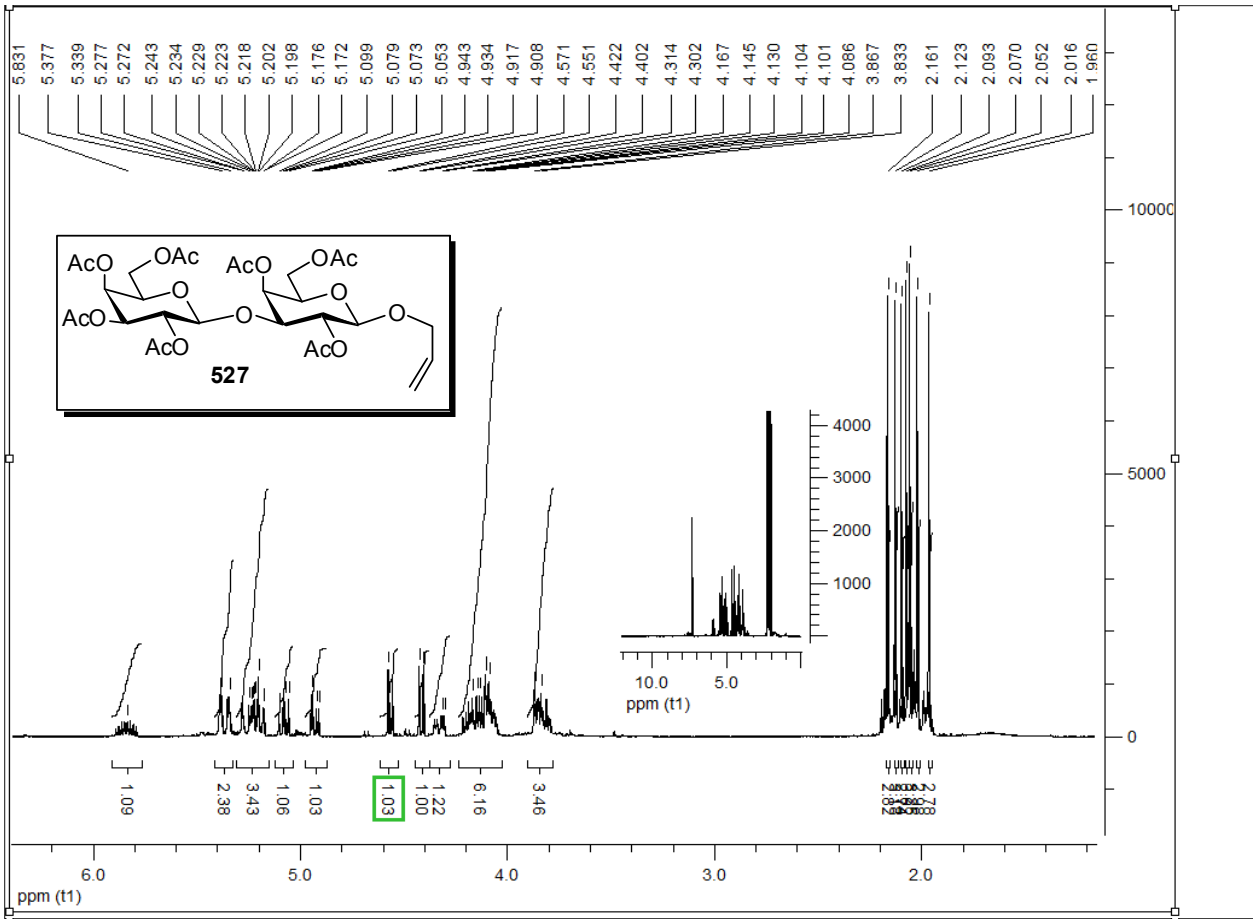

170.453
169.983
169.834
169.674
76.107
70.770
68.309
68.035
67.906
67.381
65.822
61.298
24.880
20.718
20.655
20.647
20.590
15.312
AcO
OAc
O
AcO
AcO
AcO
OAc
O
AcO
AcO
1411
200
150
100
50
0
ppm (t1)

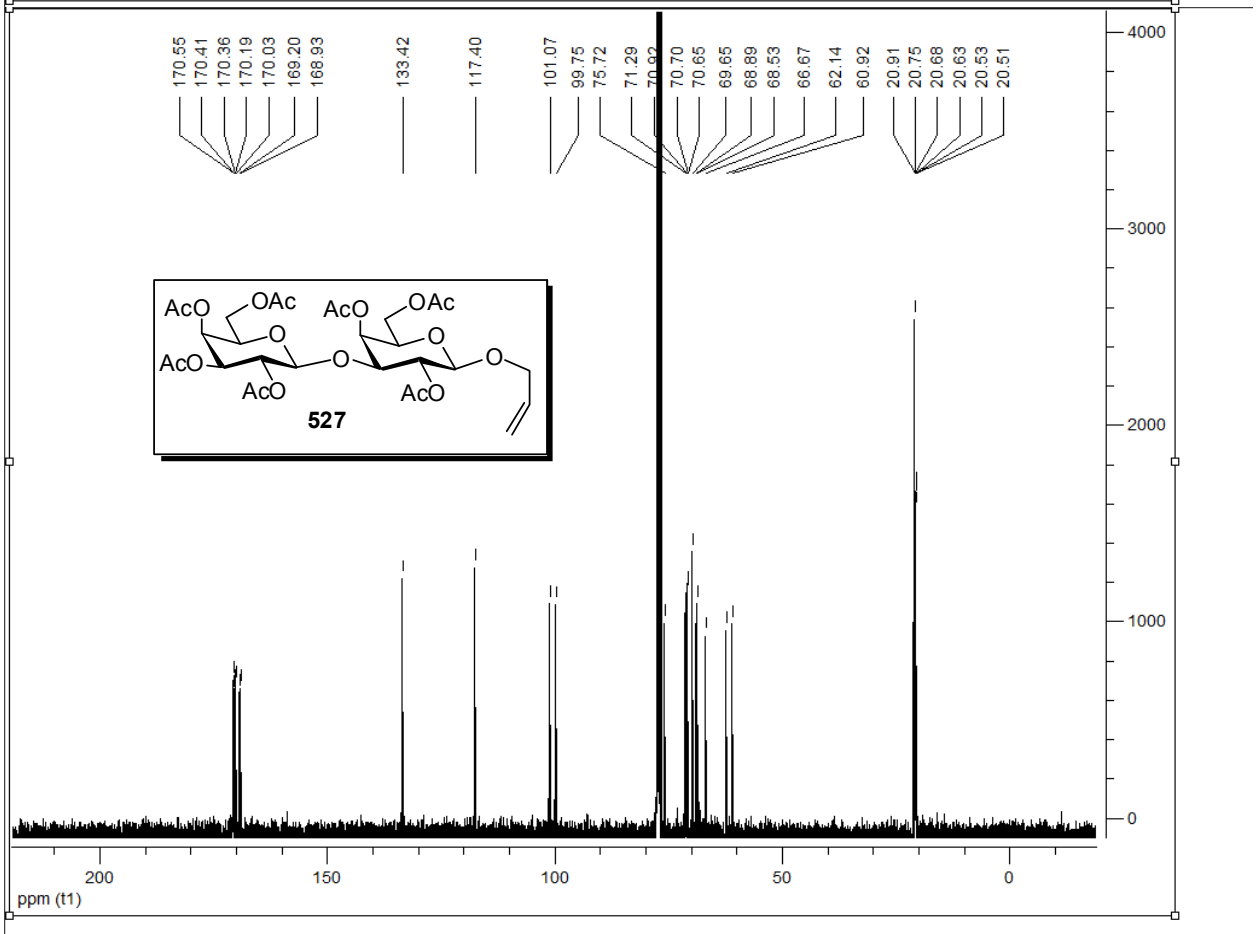

5.944
5.942
5.930
5.929
5.909
5.908
5.363
5.359
5.328
5.325
5.256
5.253
5.235
5.232
4.799
4.565
4.550
4.464
4.448
4.354
4.344
4.211
4.200
4.198
4.185
4.157
4.156
4.150
3.877
3.876
3.870
3.869
3.706
3.546
3.525
HO
OH
HO
OH
HO
O
O
O
HO
HO
HO
508
10.0
5.0
ppm (t1)
1.02
1.00
1.04
0.83
0.81
0.84
1.86
1.13
8.25
2.01
6.00
5.50
5.00
4.50
4.00
3.50
ppm (t1)
500
0

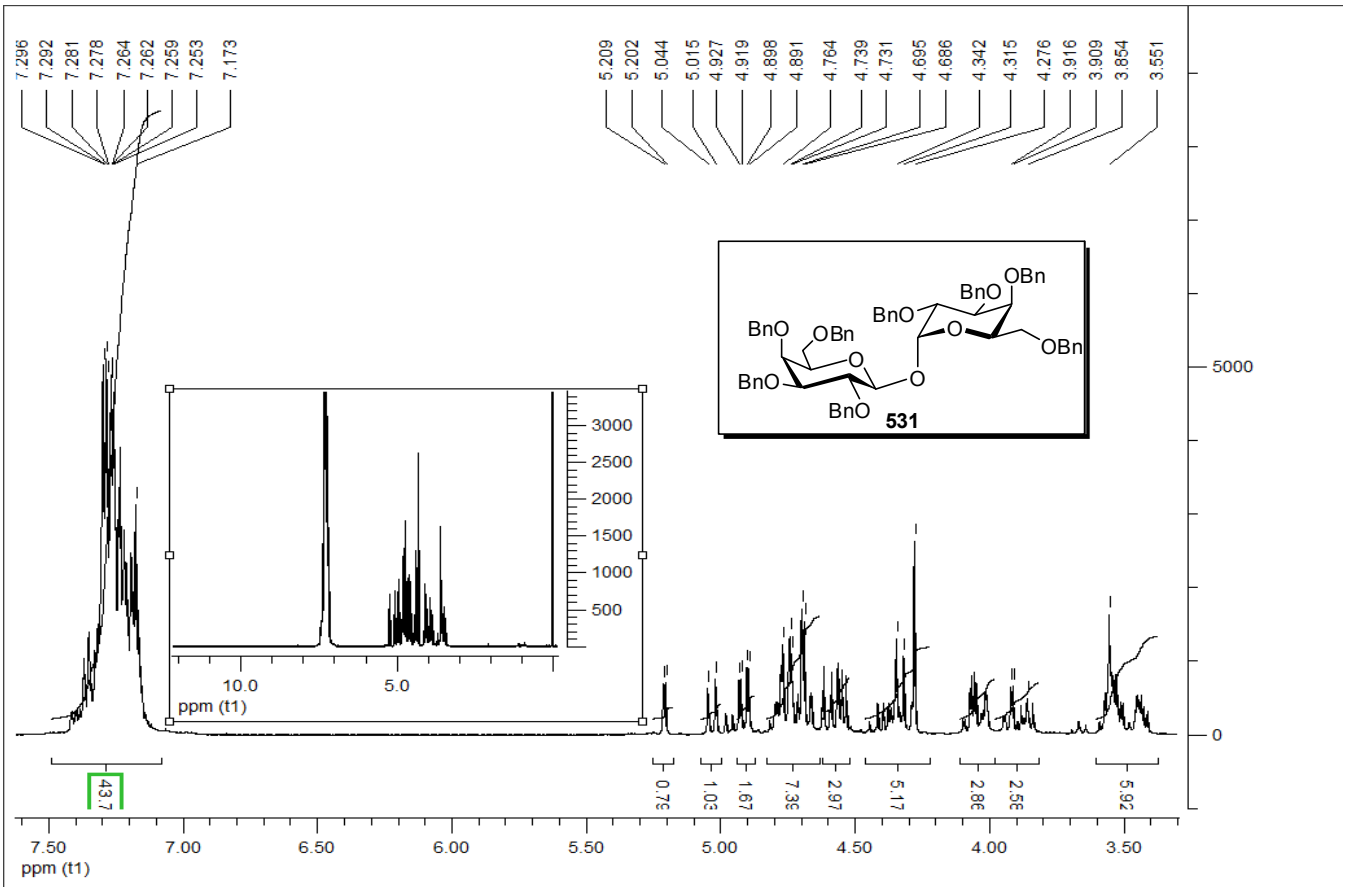

133.148
118.738
104.274
101.225
82.341
74.950
74.661
72.376
70.914
70.442
69.739
68.447
68.320
60.842
60.782
HO
OH
HO
OH
HO
O
O
O
HO
HO
HO
508
1000
500
0
200
150
100
50
0
ppm (t1)

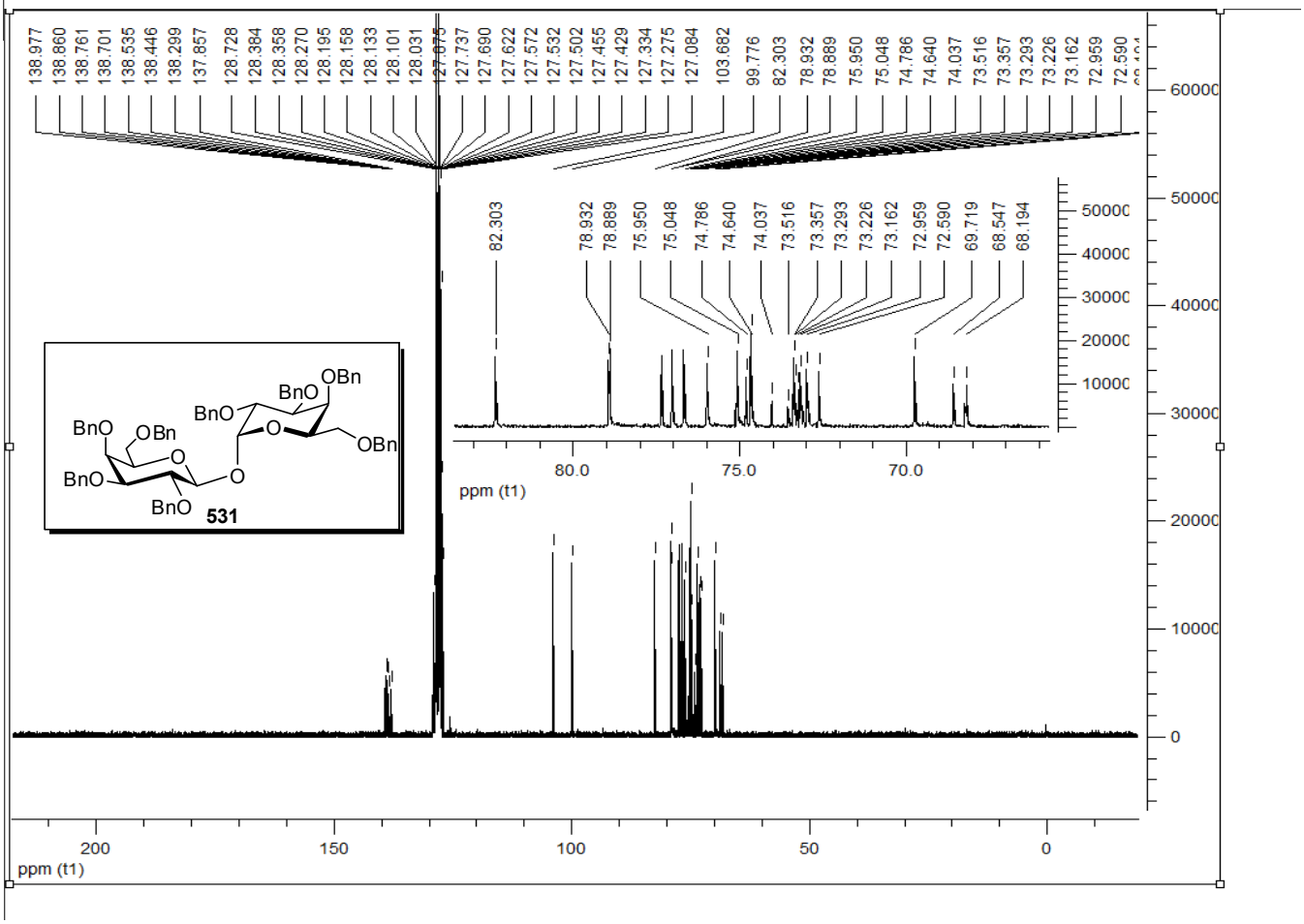

7.543
7.476
7.473
7.469
7.466
7.460
7.457
5.351
5.342
4.689
4.670
4.400
4.398
4.391
4.389
4.329
4.233
4.229
4.217
4.213
4.211
4.206
4.167
4.163
4.042
4.016
4.007
3.969
3.960
3.781
3.772
3.752
3.749
Ph
O
O
O
HO
OH
OH
512
11.46
1.87
0.99
1.00
2.02
3.08
3.13
4.54
ppm (t1)
10.0
5.0
0.0
4000
3000
2000
1000
0
1000
500
0
-500
4.50
4.00
3.50

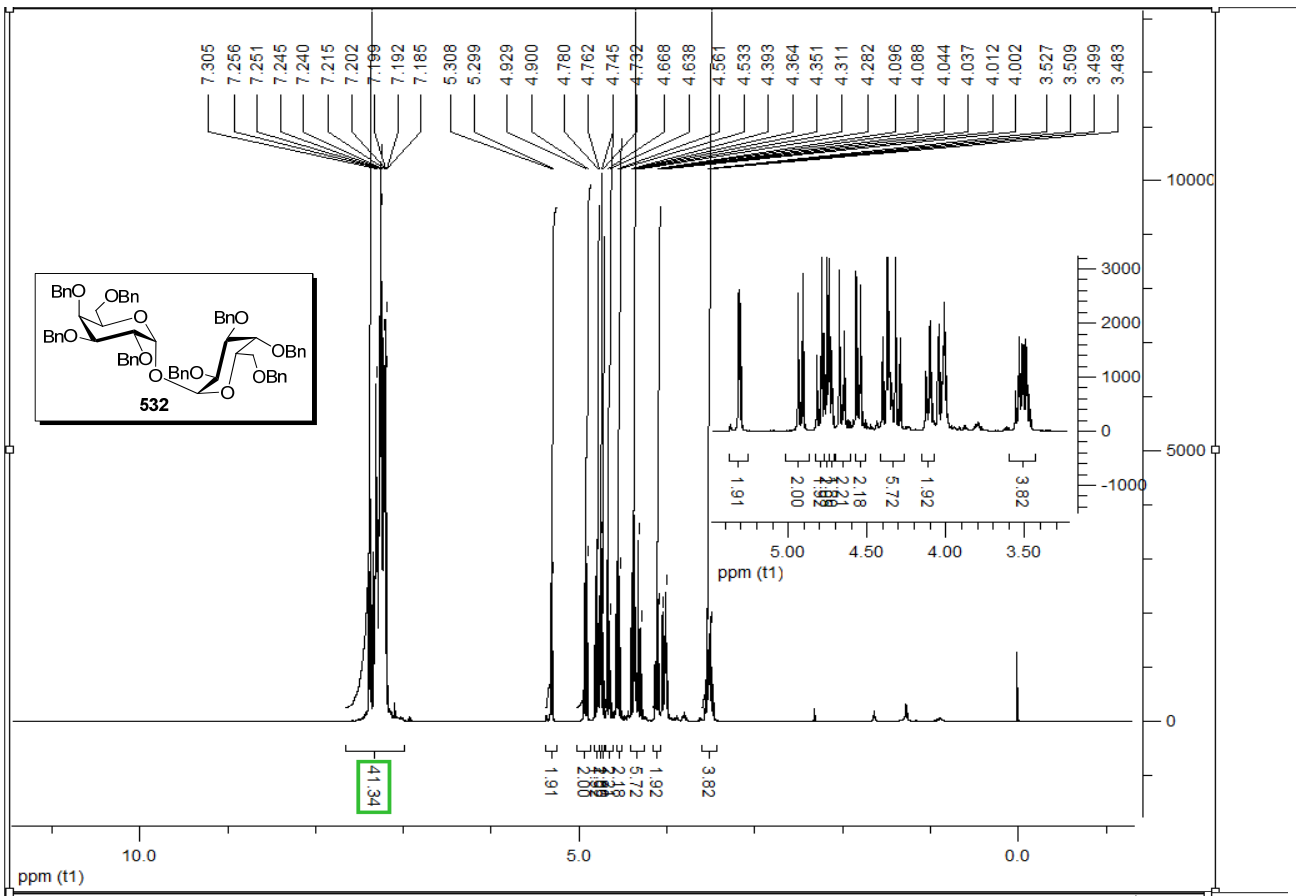

0.888
0.888
0.986
0.987
0.997
0.998
1.018
1.018
1.304
1.304
1.352
1.397
1.586
1.593
1.633
1.635
1.666
1.670
1.674
1.699
1.747
Ph
O
O
O
HO
OH
OH
512
sec (t1)
0.50
1.00
1.50
2.00
2.50
60000
50000
40000
30000
20000
10000

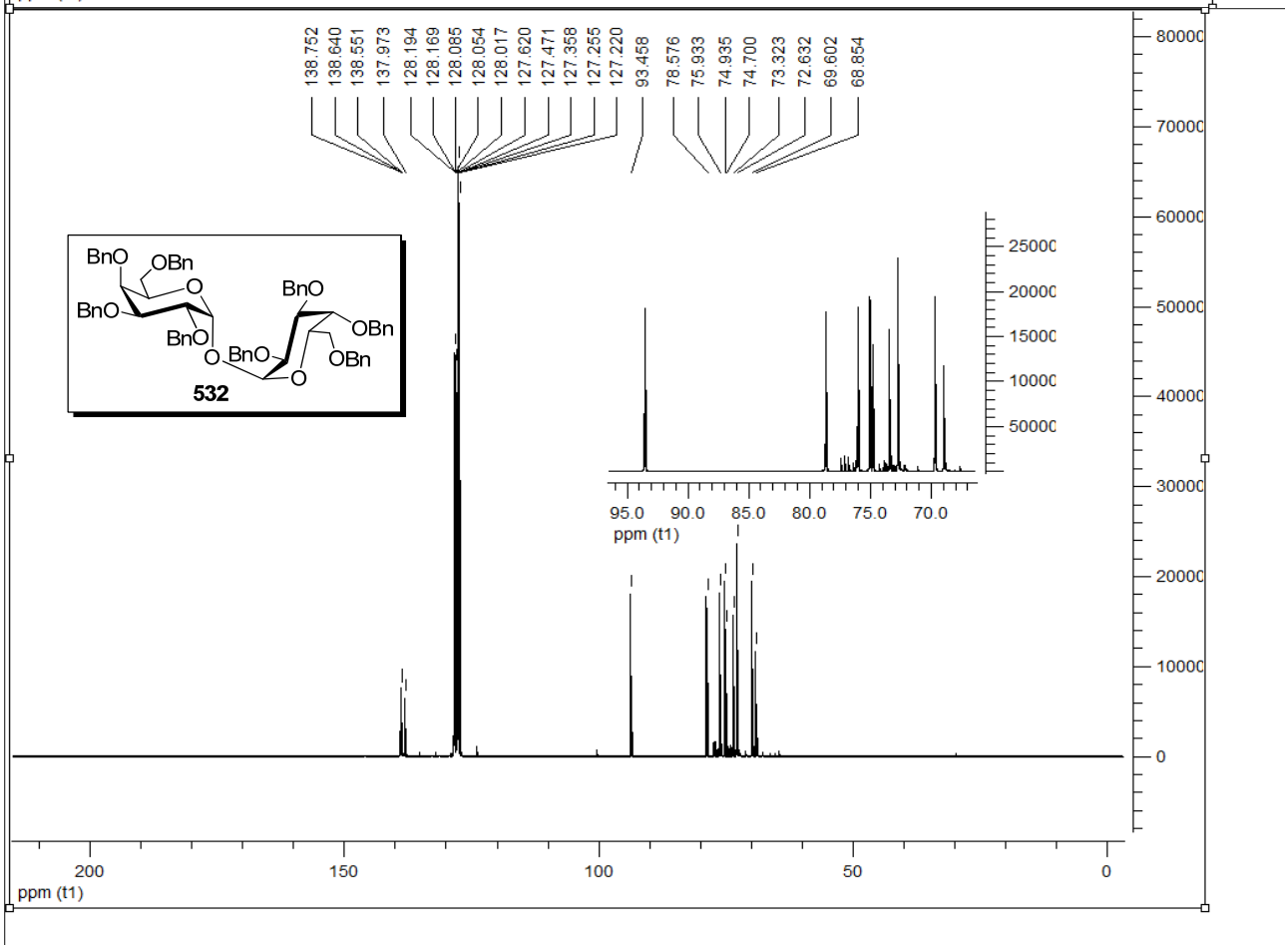

5.831
5.377
5.339
5.277
5.272
5.243
5.234
5.229
5.223
5.218
5.202
5.198
5.176
5.172
5.099
5.079
5.073
5.053
4.943
4.934
4.917
4.908
4.571
4.551
4.422
4.402
4.314
4.302
4.167
4.145
4.130
4.104
4.101
4.086
3.867
3.833
2.161
2.123
2.093
2.070
2.052
2.016
1.960
AcO
OAc
AcO
OAc
AcO
AcO
AcO
AcO
O
O
O
O
527
10000
5000
0
4000
3000
2000
1000
10.0
5.0
ppm (t1)
1.09
2.38
3.43
1.06
1.03
1.03
1.00
1.22
6.16
3.46
6.0
5.0
4.0
3.0
2.0
ppm (t1)

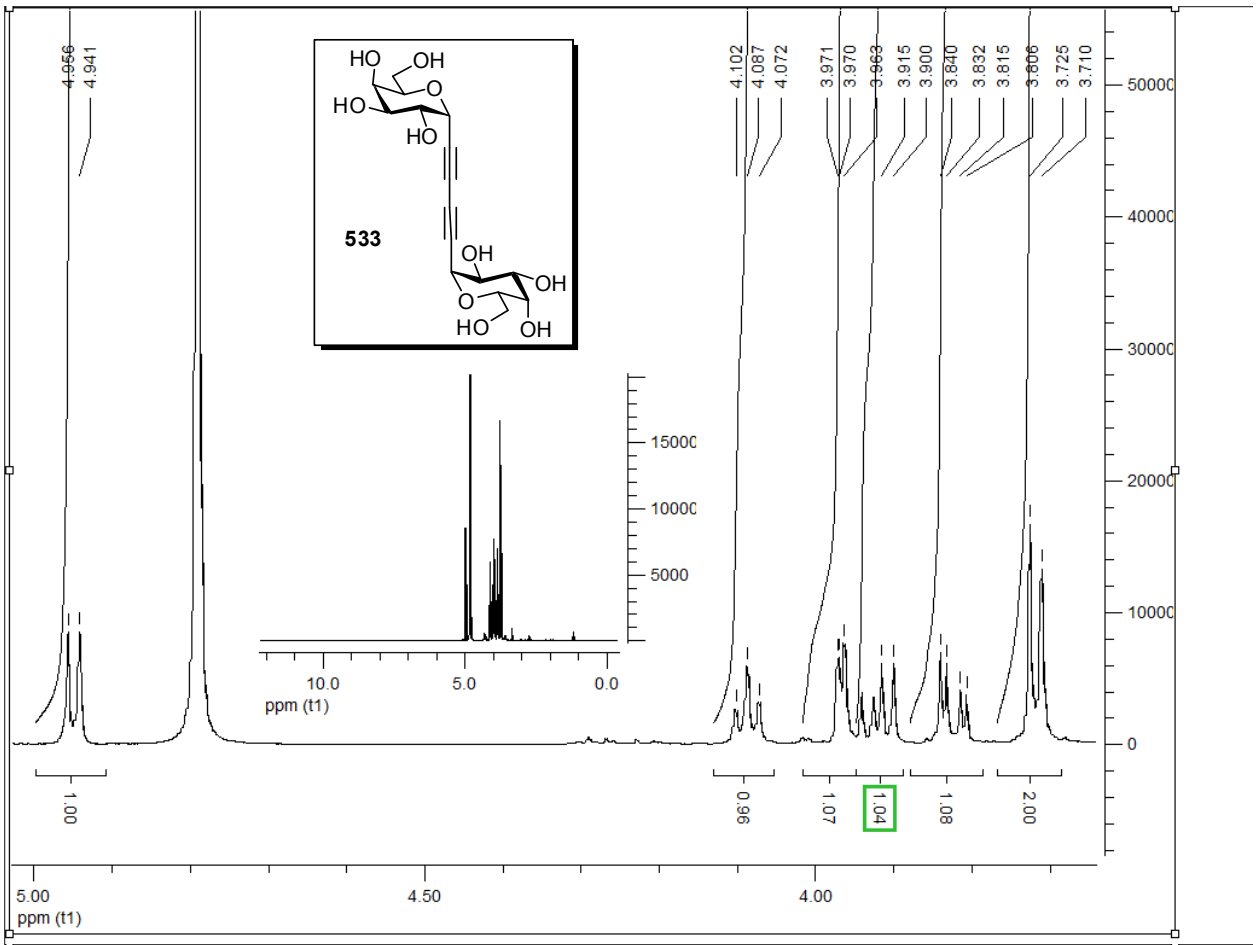

170.55
170.41
170.36
170.19
170.03
169.20
168.93
133.42
117.40
101.07
99.75
75.72
71.29
70.92
70.70
70.65
69.65
68.89
68.53
66.67
62.14
60.92
20.91
20.75
20.68
20.63
20.53
20.51
AcO
OAc
AcO
OAc
AcO
AcO
AcO
AcO
O
O
O
O
527
4000
3000
2000
1000
0
200
150
100
50
0
ppm (t1)

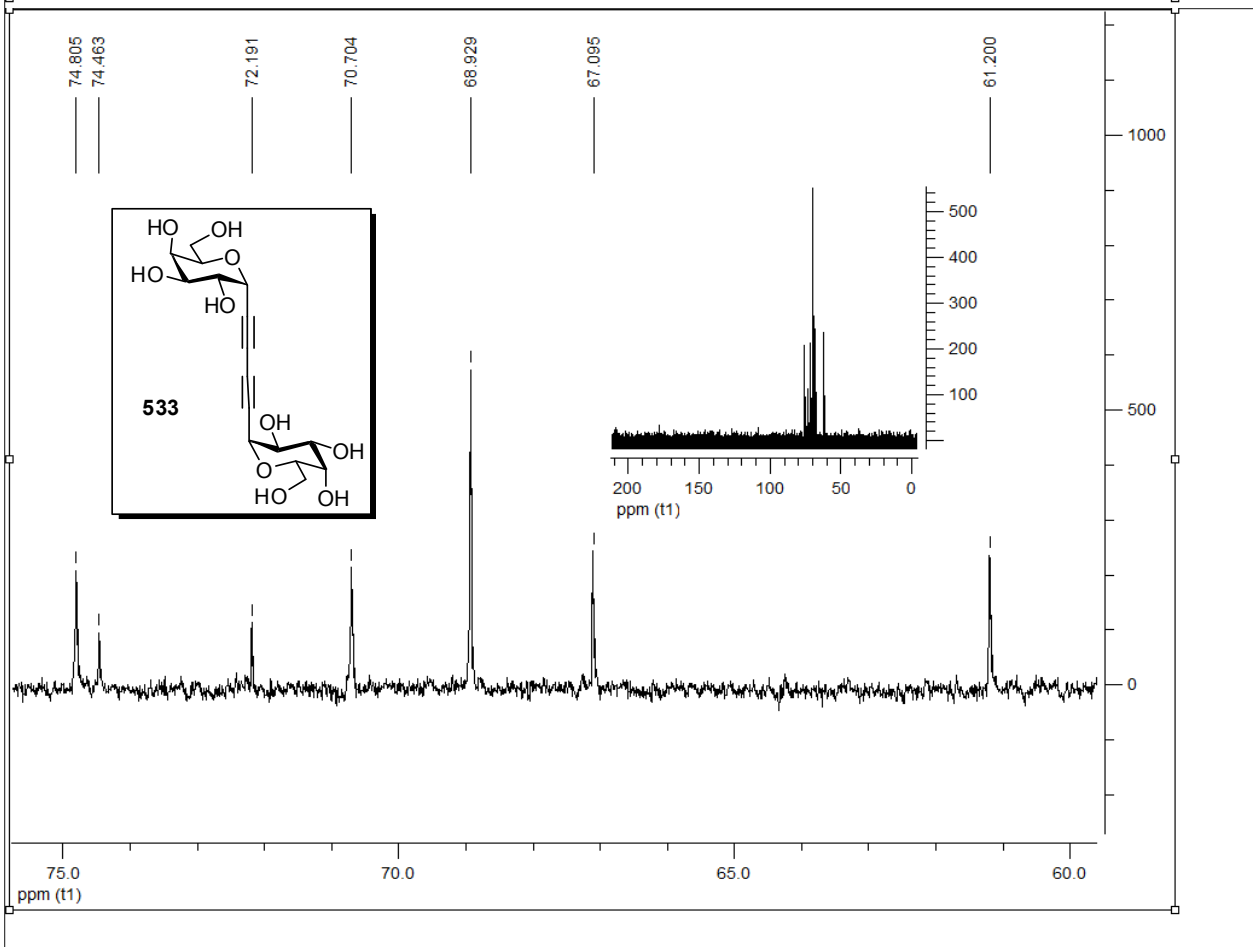

7.296
7.292
7.281
7.278
7.264
7.262
7.259
7.253
7.173
5.209
5.202
5.044
5.015
4.927
4.919
4.898
4.891
4.764
4.739
4.731
4.695
4.686
4.342
4.315
4.276
3.916
3.909
3.854
3.551
BnO
OBn
BnO
OBn
BnO
BnO
BnO
O
O
531
ppm (t1)
ppm (t1)

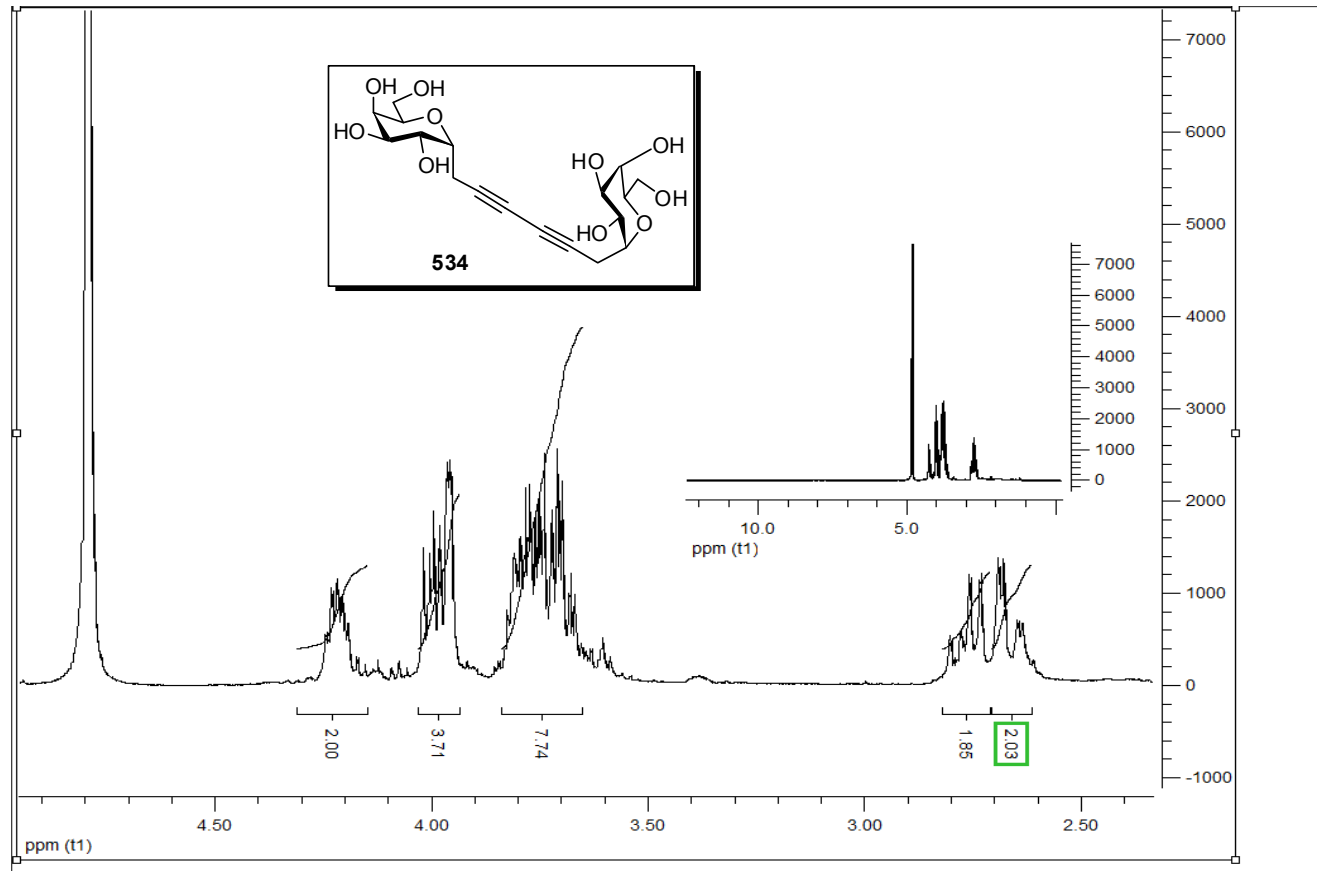

138.977
138.860
138.761
138.701
138.535
138.446
138.299
137.857
128.728
128.384
128.358
128.270
128.195
128.158
128.133
128.101
128.031
127.737
127.690
127.622
127.572
127.532
127.502
127.455
127.429
127.334
127.275
127.084
103.682
99.776
82.303
78.932
78.889
75.950
75.048
74.786
74.640
74.037
73.516
73.357
73.293
73.226
73.162
72.959
72.590
69.719
68.547
68.194
BnO
OBn
BnO
OBn
BnO
BnO
BnO
O
O
531
ppm (t1)
ppm (t1)

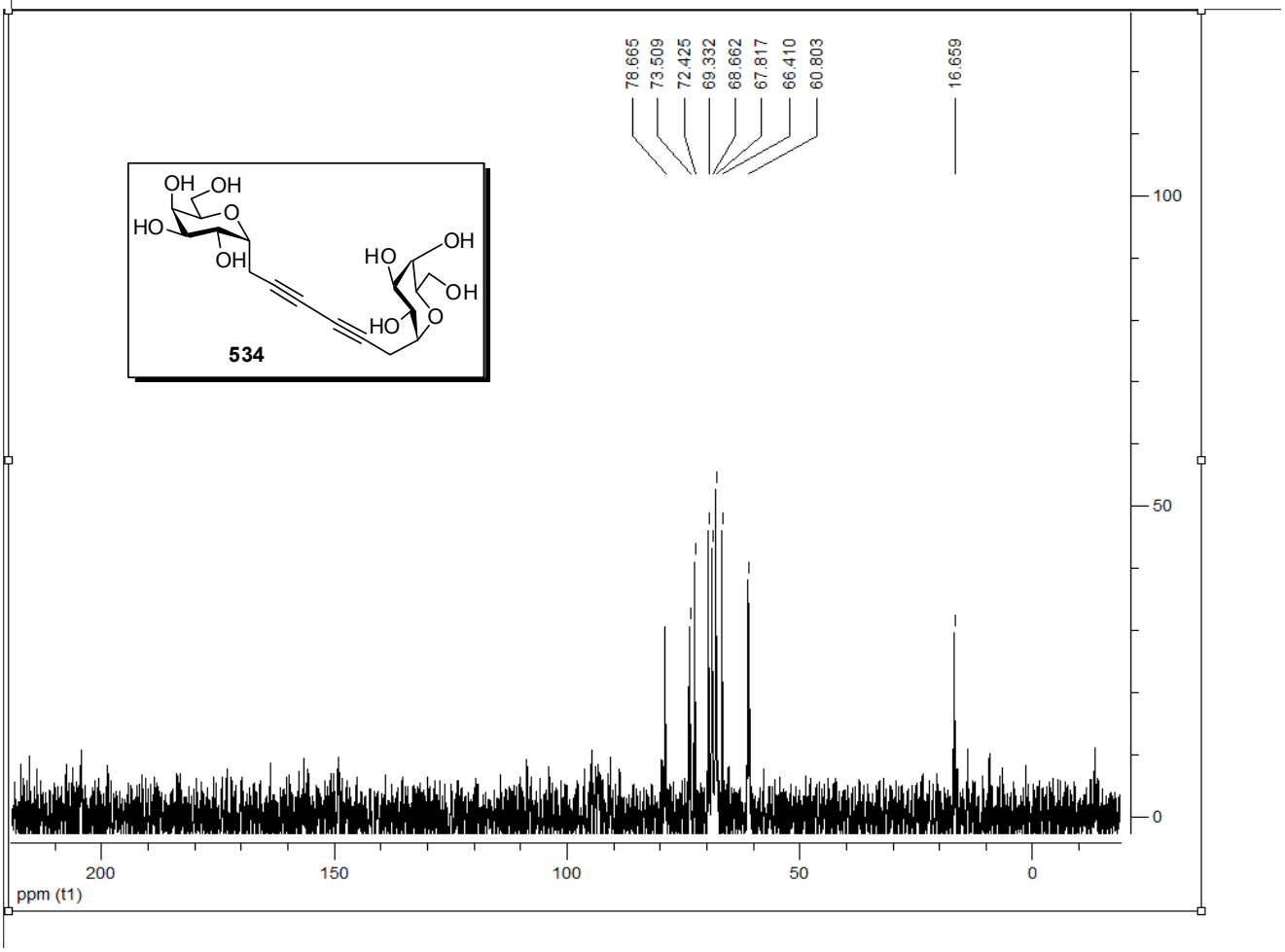

7.305
7.256
7.251
7.245
7.240
7.215
7.202
7.199
7.192
7.185
5.308
5.299
4.929
4.900
4.780
4.762
4.745
4.732
4.668
4.638
4.561
4.533
4.393
4.364
4.351
4.311
4.282
4.096
4.088
4.044
4.037
4.012
4.002
3.527
3.509
3.499
3.483
BnO
OBn
532
4.34
1.91
2.00
2.18
5.72
1.92
3.82
ppm (t1)

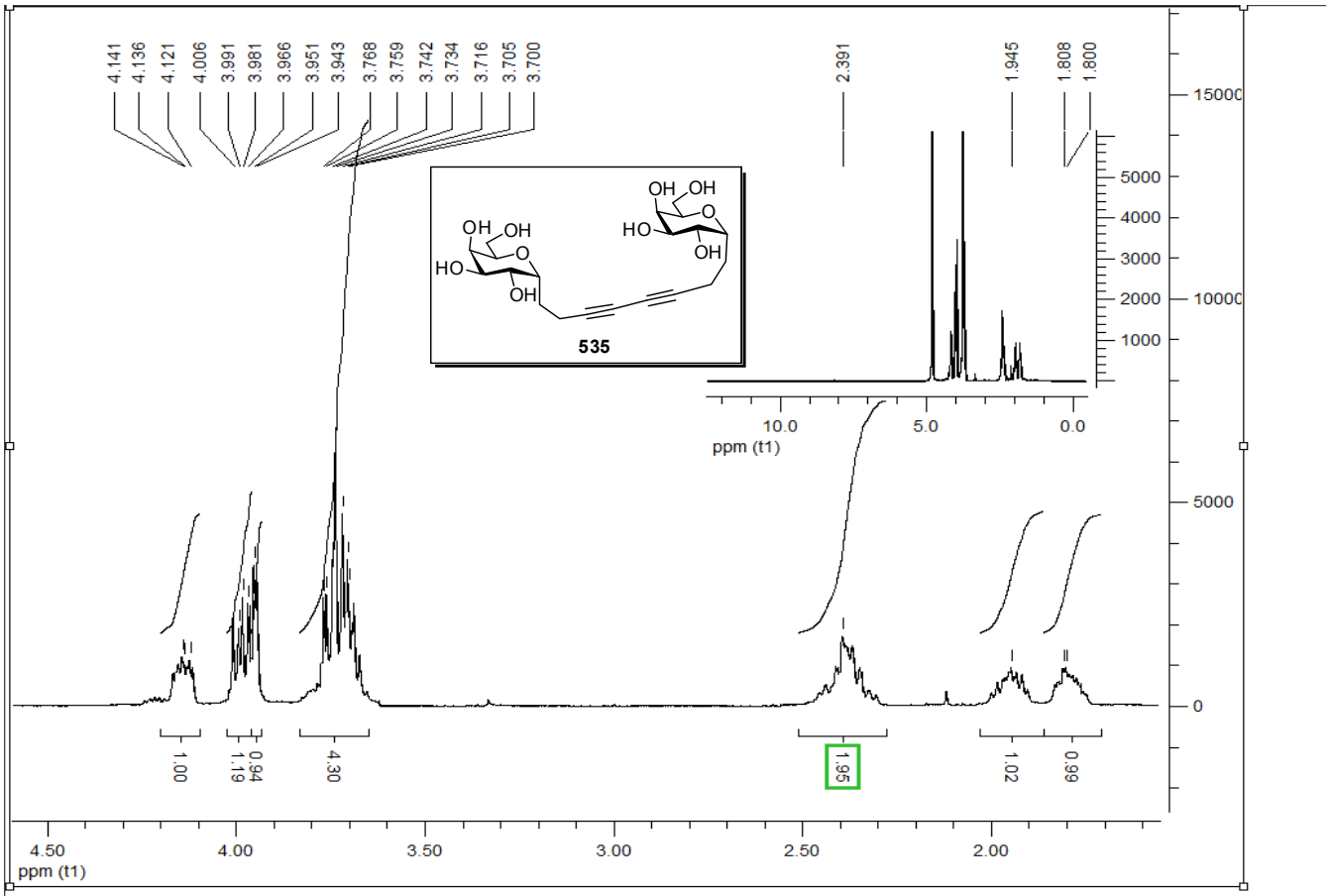

138.752
138.640
138.551
137.973
128.194
128.169
128.085
128.054
128.017
127.620
127.471
127.358
127.255
127.220
93.458
78.576
75.933
74.935
74.700
73.323
72.632
69.602
68.854
BnO
OBn
532
ppm (t1)

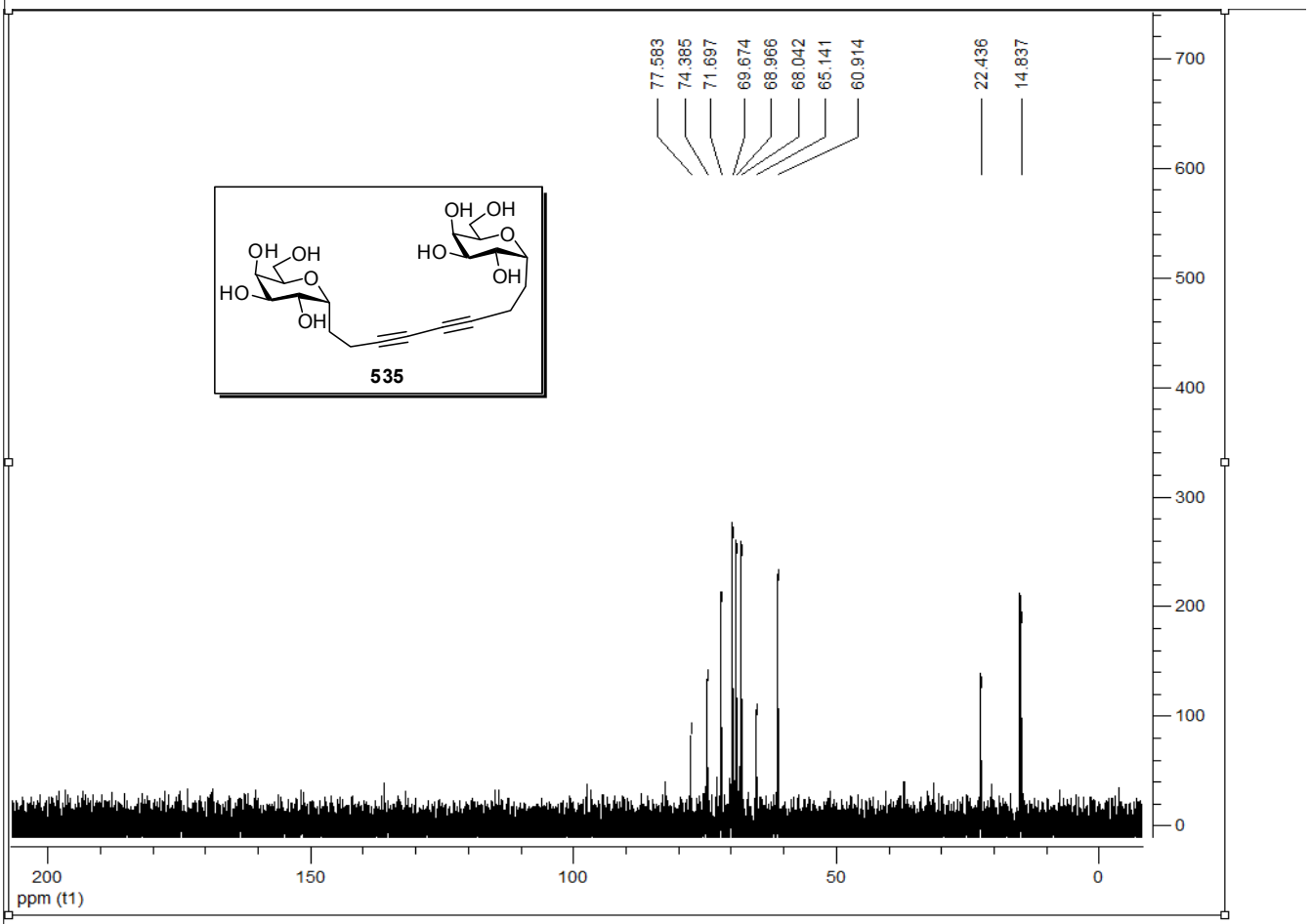

4.956
4.941
4.102
4.087
4.072
3.971
3.970
3.963
3.915
3.900
3.840
3.832
3.815
3.806
3.725
3.710
HO
OH
O
HO
HO
533
OH
OH
O
HO
OH
50000
40000
30000
20000
10000
0
15000
10000
5000
10.0
5.0
0.0
ppm (t1)
1.00
0.96
1.07
1.04
1.08
2.00
5.00
4.50
4.00
ppm (t1)

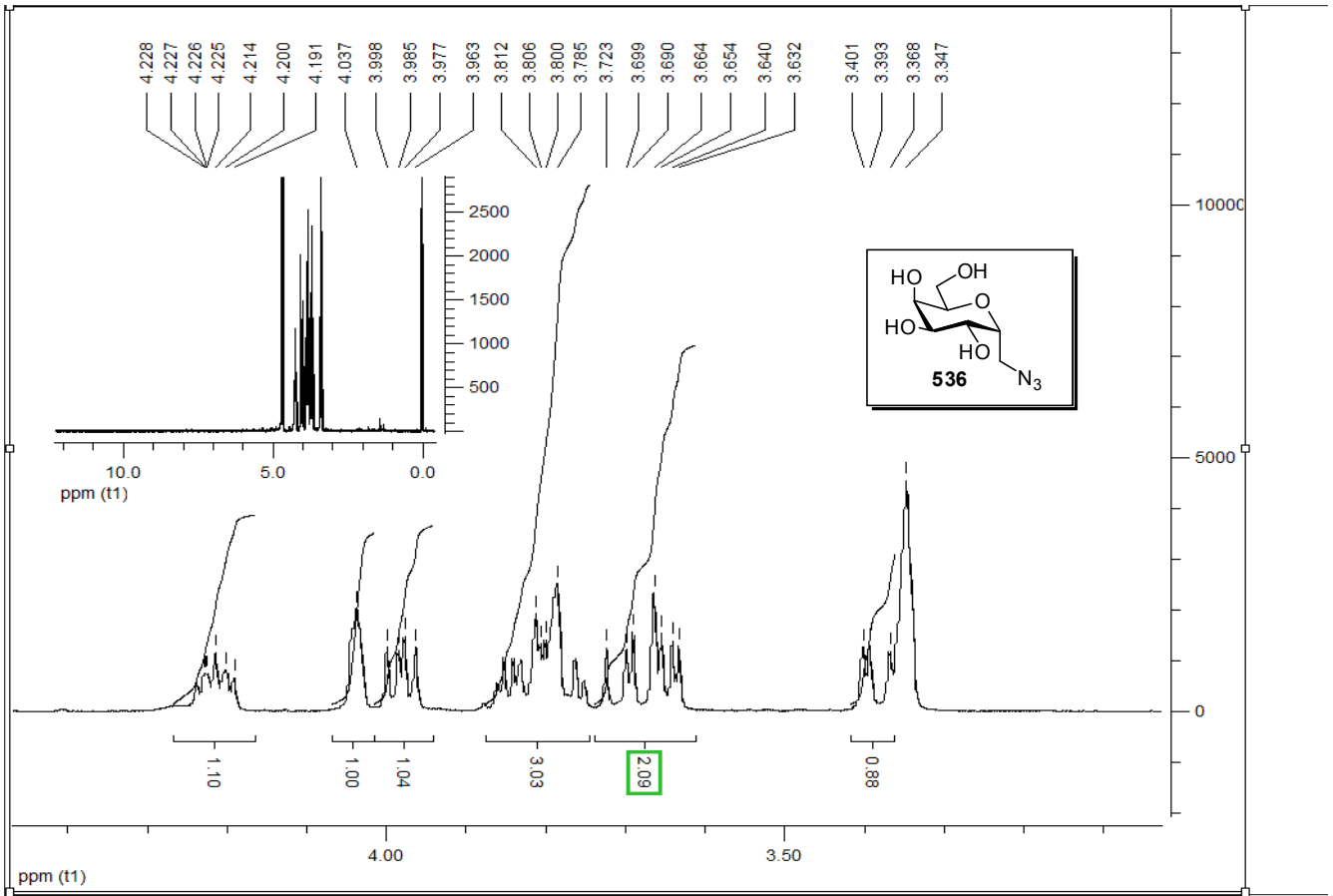

74.805
74.463
72.191
70.704
68.929
67.095
61.200
HO
OH
O
HO
HO
533
OH
OH
O
HO
OH
1000
500
0
500
400
300
200
100
200
150
100
50
0
ppm (t1)
75.0
70.0
65.0
60.0
ppm (t1)

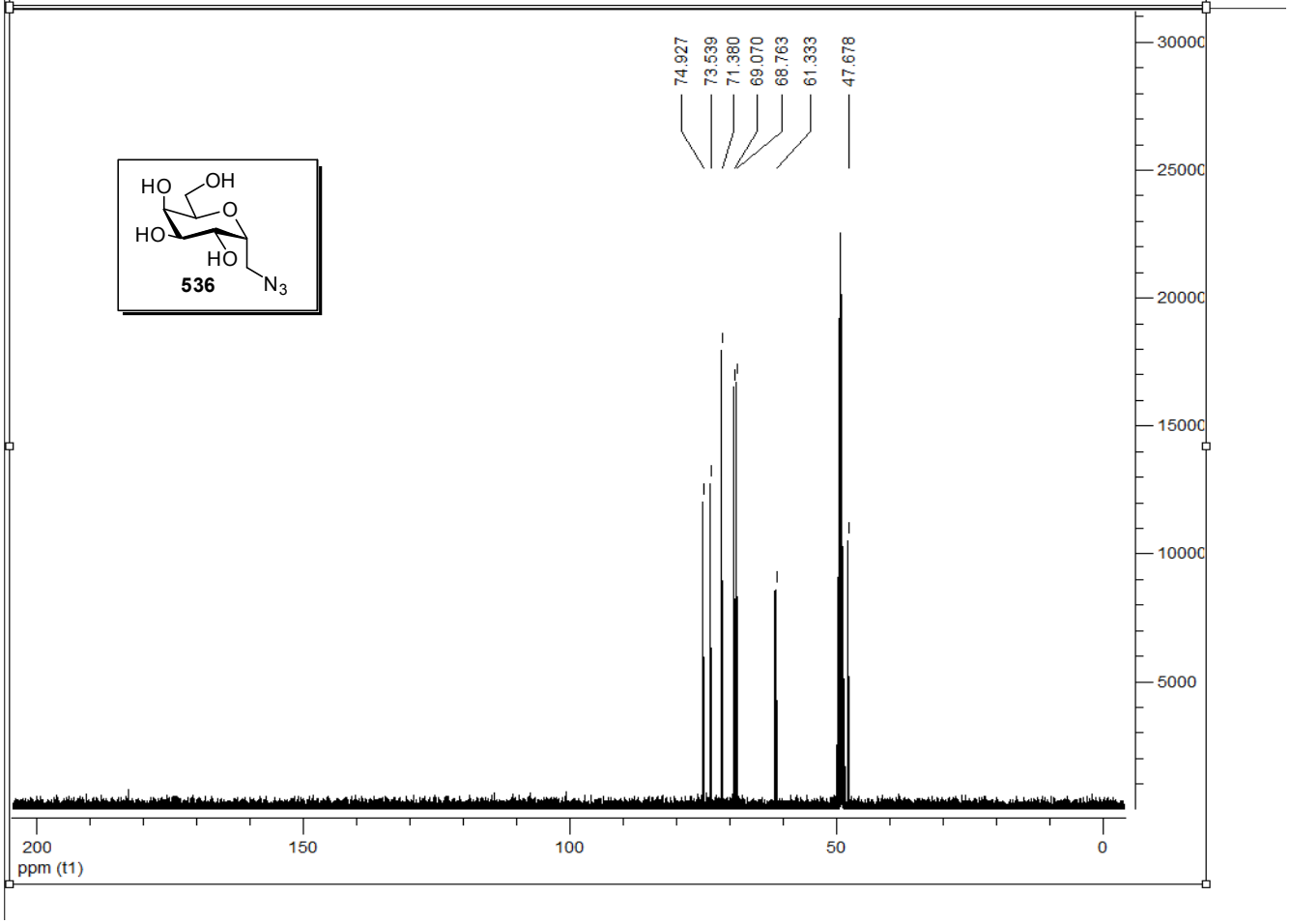

534
2.00
3.71
7.74
1.85
2.03
ppm (t1)

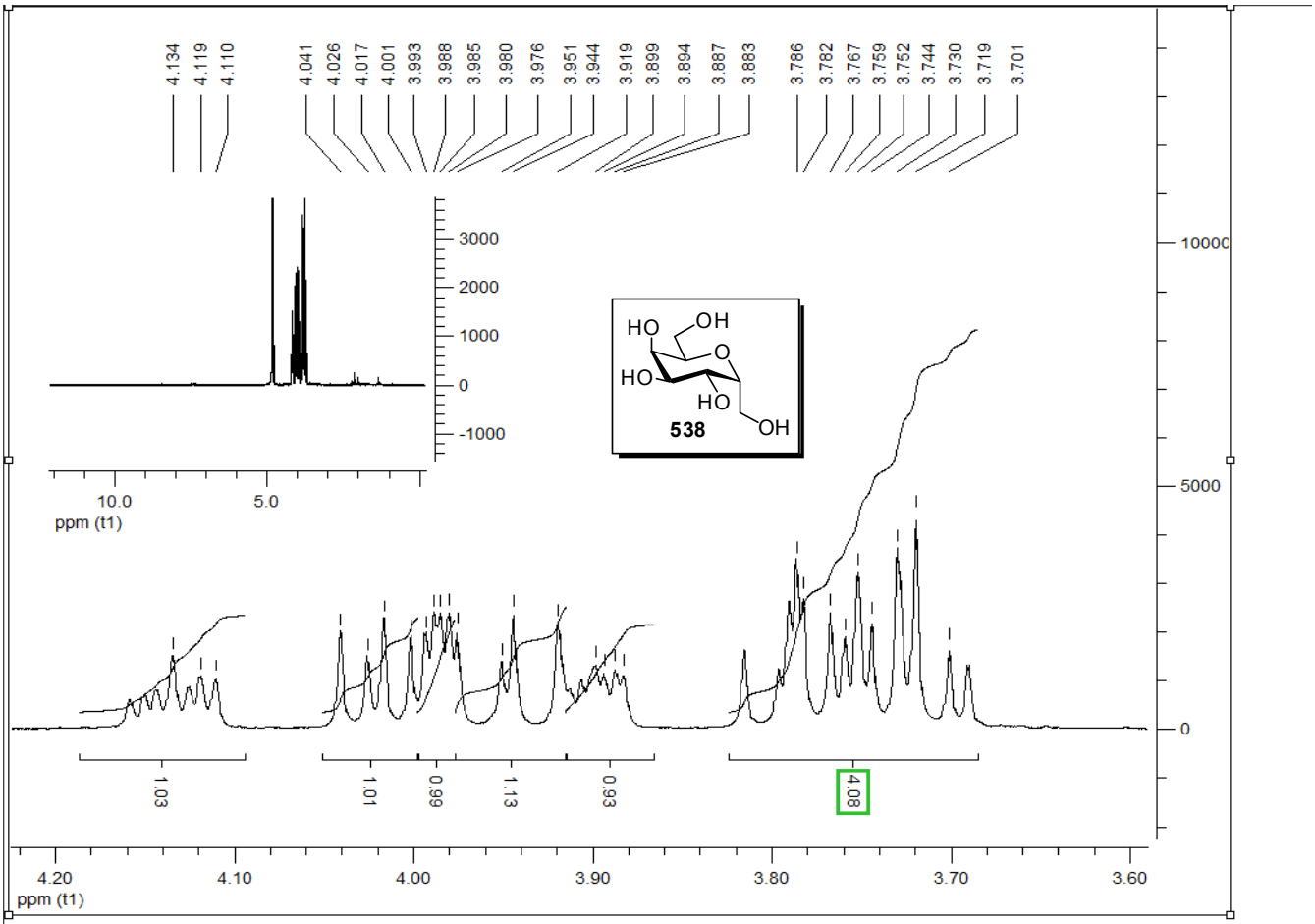

78.665
73.509
72.425
69.332
68.662
67.817
66.410
60.803
16.659
534
ppm (t1)

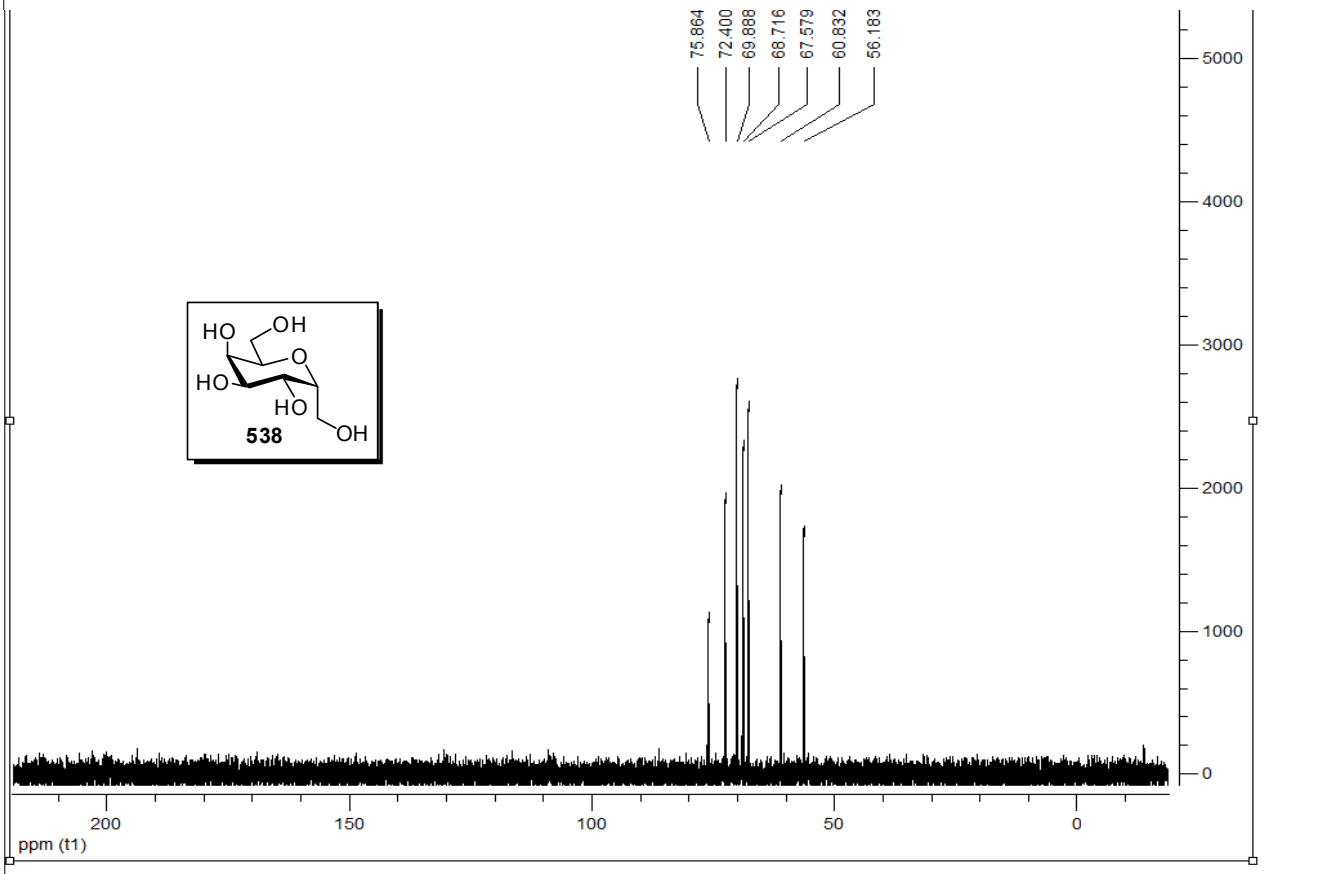

4.141
4.136
4.121
4.006
3.991
3.981
3.966
3.951
3.943
3.768
3.759
3.742
3.734
3.716
3.705
3.700
2.391
1.945
1.808
1.800
OH
OH
O
HO
OH
535
15000
10000
5000
0
5000
4000
3000
2000
1000
10.0
5.0
0.0
ppm (t1)
1.00
1.16
0.94
4.30
1.95
1.02
0.99
4.50
4.00
3.50
3.00
2.50
2.00
ppm (t1)

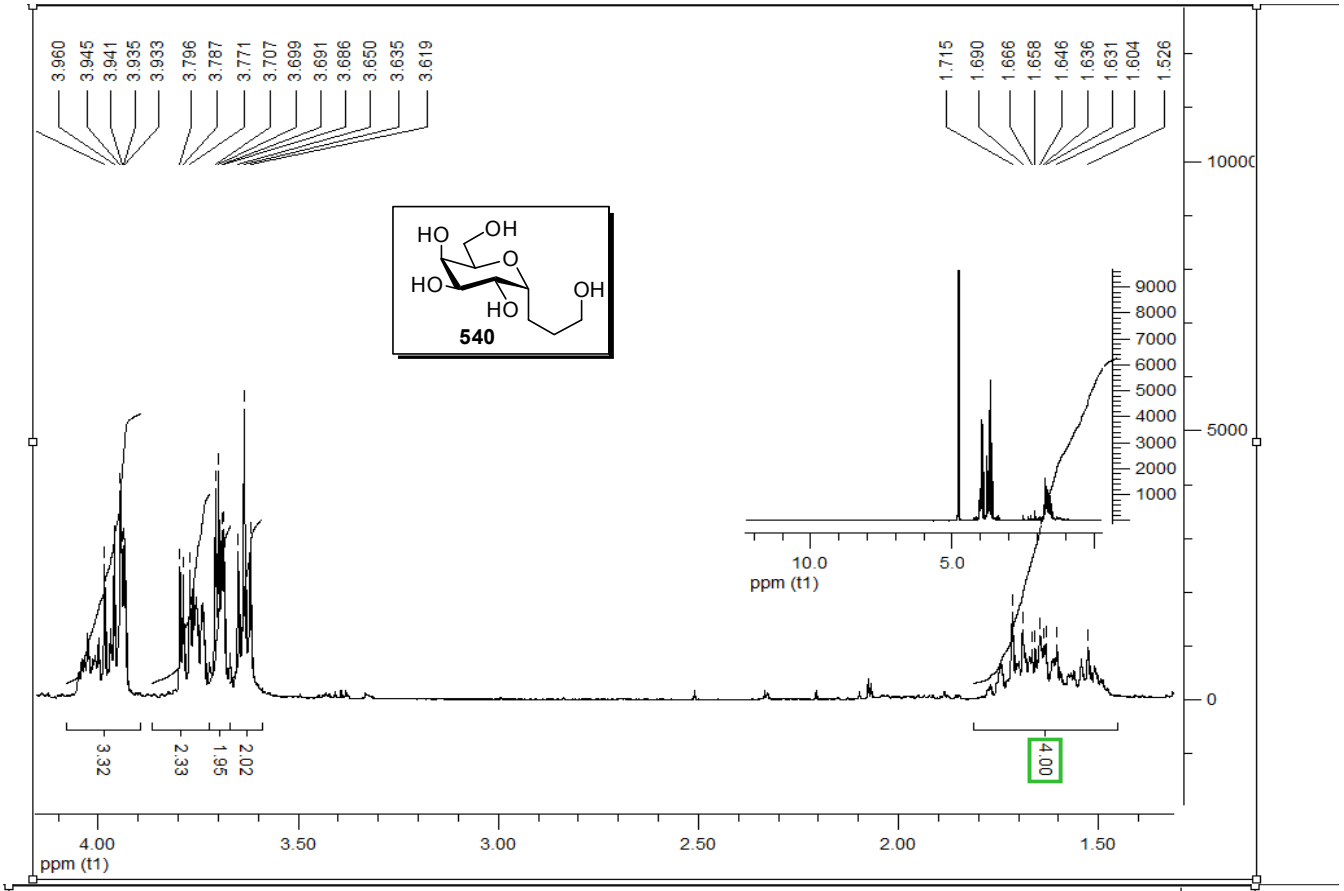

77.583
74.385
71.697
69.674
68.966
68.042
65.141
60.914
22.436
14.837
OH
OH
O
HO
OH
535
700
600
500
400
300
200
100
0
200
150
100
50
0
ppm (t1)

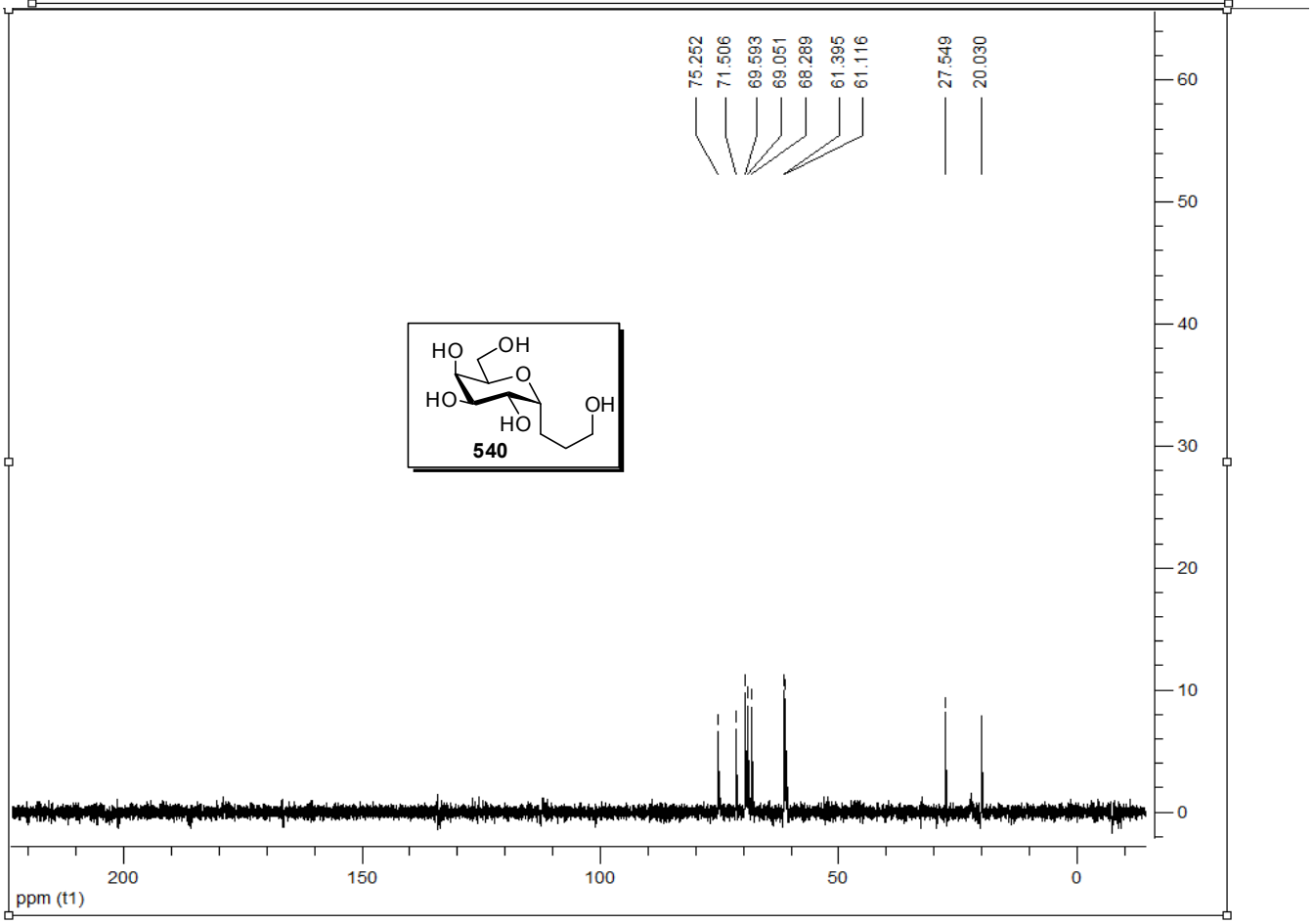

4.228
4.227
4.226
4.225
4.214
4.200
4.191
4.037
3.998
3.985
3.977
3.963
3.812
3.806
3.800
3.785
3.723
3.699
3.690
3.664
3.654
3.640
3.632
3.401
3.393
3.368
3.347
HO
OH
O
HO
HO
N3
536
ppm (t1)
1.10
1.00
1.04
3.03
2.09
0.88
4.00
3.50

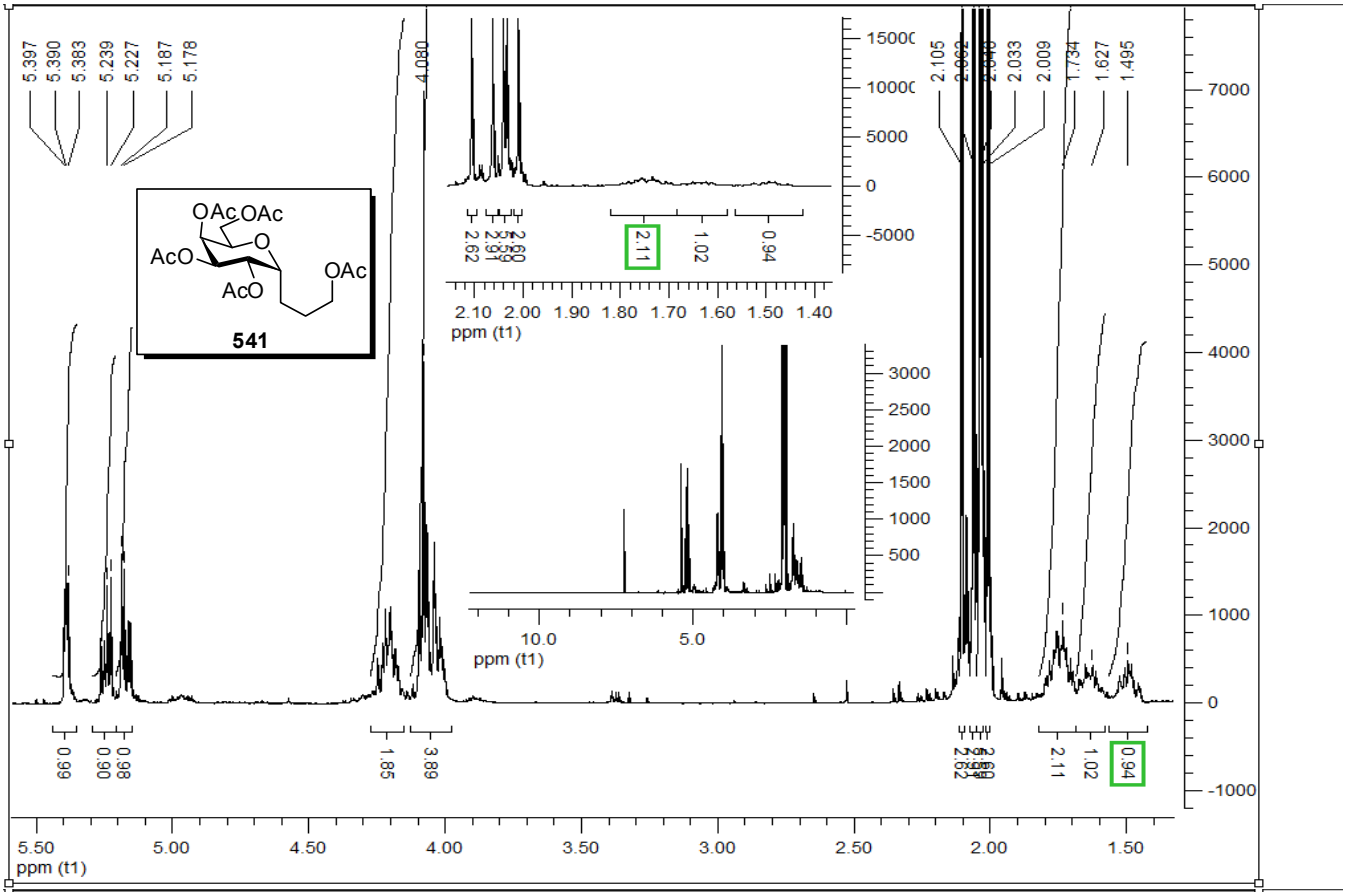

74.927
73.539
71.380
69.070
68.763
61.333
47.678
HO
OH
O
HO
HO
N3
536
200
150
100
50
0
ppm (t1)

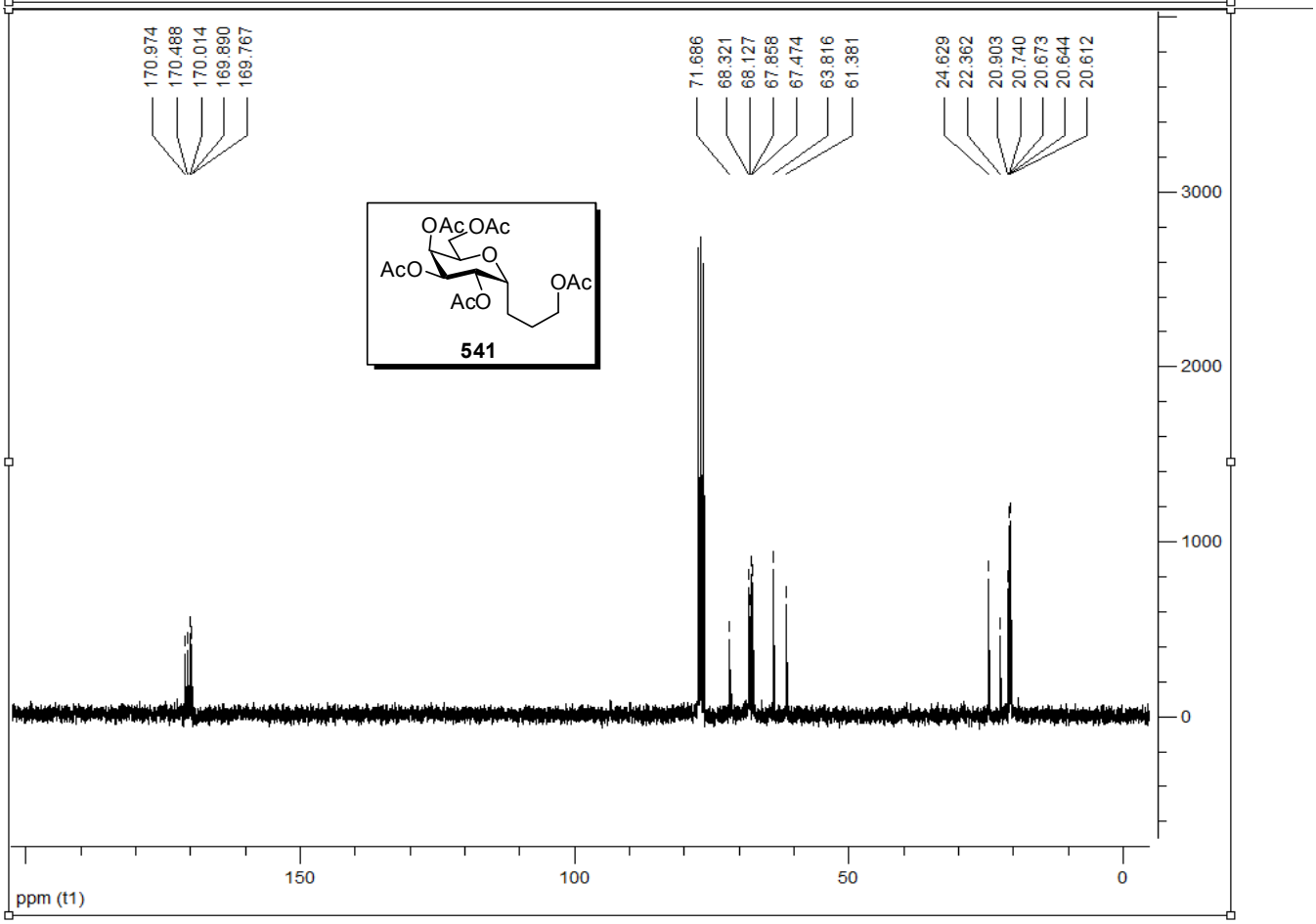

4.134
4.119
4.110
4.041
4.026
4.017
4.001
3.993
3.988
3.985
3.980
3.976
3.951
3.944
3.919
3.899
3.894
3.887
3.883
3.786
3.782
3.767
3.759
3.752
3.744
3.730
3.719
3.701
HO
OH
O
HO
HO
OH
538
ppm (t1)
1.03
1.01
0.99
1.13
0.93
4.08
ppm (t1)

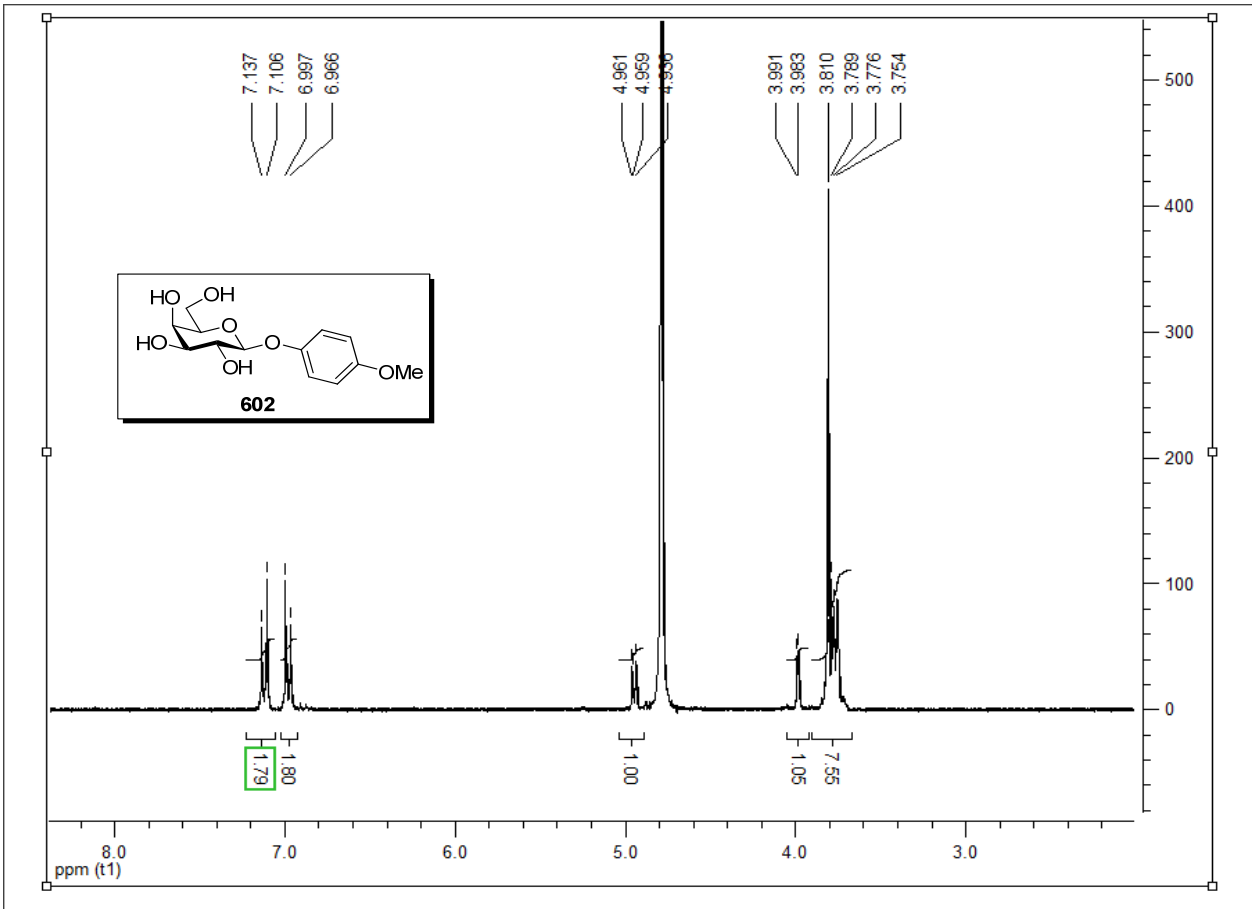

75.864
72.400
69.888
68.716
67.579
60.832
56.183
HO
OH
O
HO
HO
OH
538
ppm (t1)

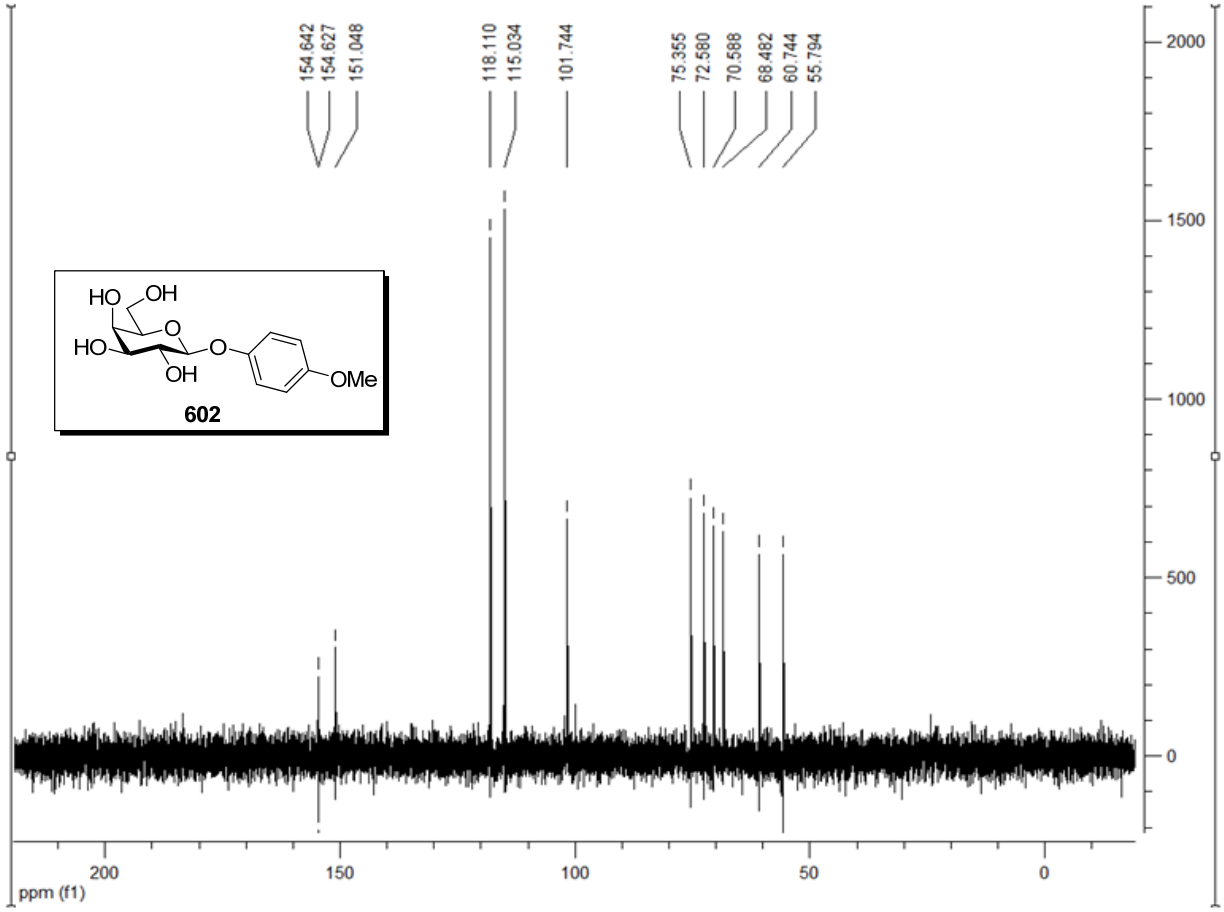

3.960
3.945
3.941
3.935
3.933
3.796
3.787
3.771
3.707
3.699
3.691
3.686
3.650
3.635
3.619
1.715
1.690
1.666
1.658
1.646
1.636
1.631
1.604
1.526
HO
OH
O
HO
OH
HO
540
10000
5000
0
9000
8000
7000
6000
5000
4000
3000
2000
1000
10.0
5.0
ppm (t1)
3.32
2.33
1.95
2.02
4.00
4.00
3.50
3.00
2.50
2.00
1.50
ppm (t1)

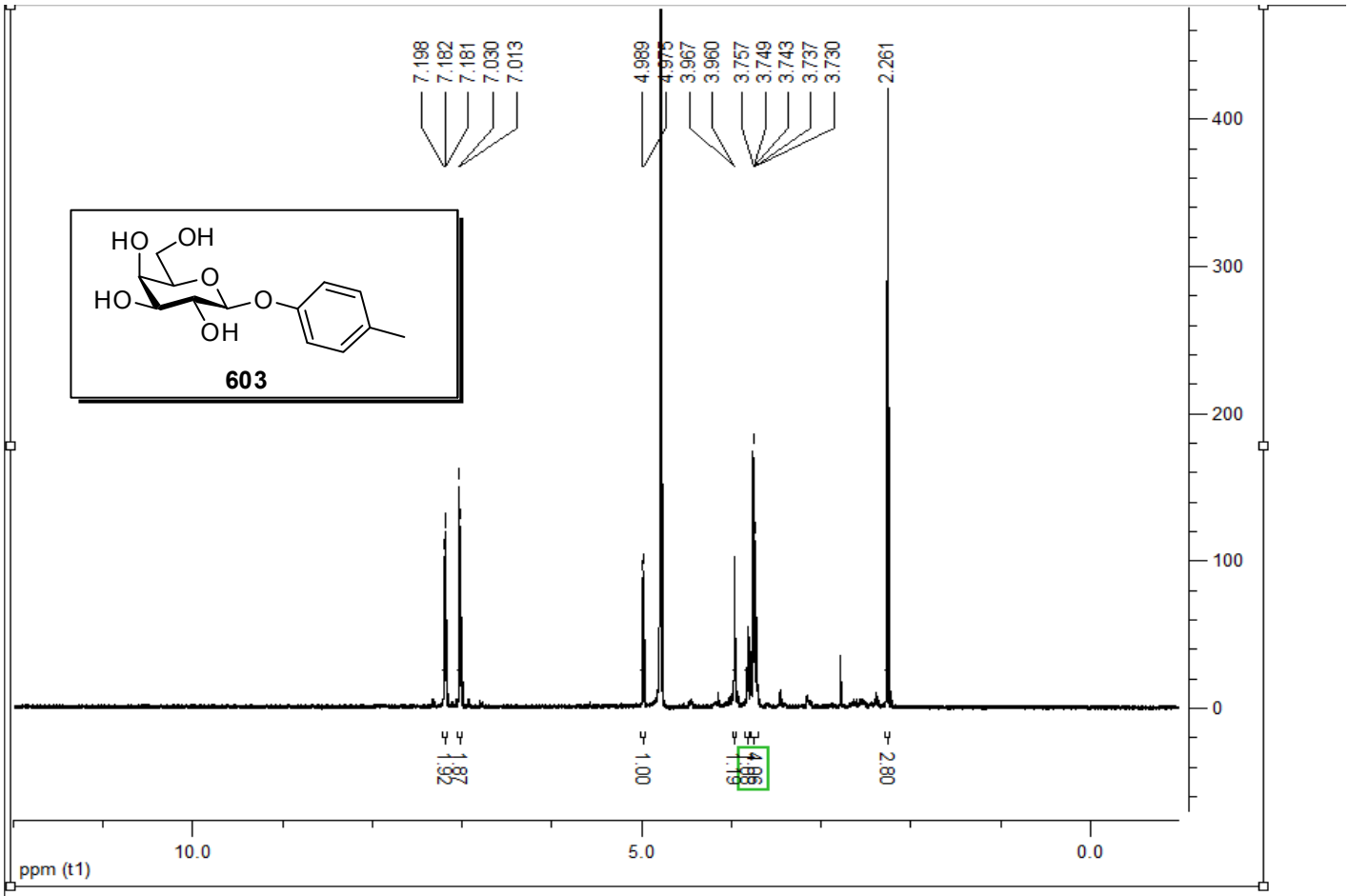

75.252
71.506
69.593
69.051
68.289
61.395
61.116
27.549
20.030
HO
OH
O
HO
OH
HO
540
60
50
40
30
20
10
0
200
150
100
50
0
ppm (t1)

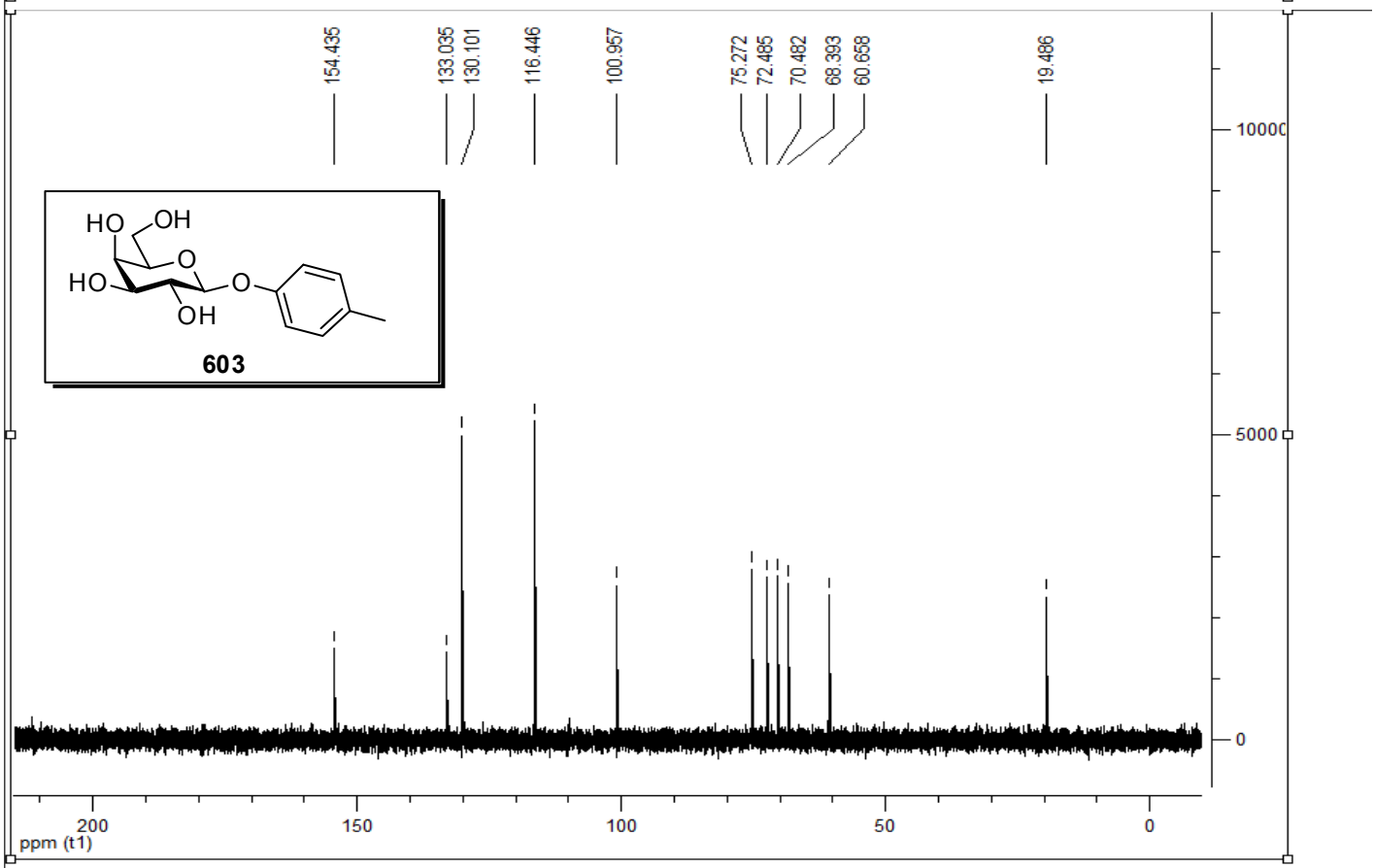

5.397
5.390
5.383
5.239
5.227
5.187
5.178
4.080
2.105
2.033
2.009
1.734
1.627
1.495
OAc OAc
AcO
O
AcO
OAc
541
2.11
1.02
0.94
ppm (t1)
10.0
5.0
0.99
0.90
0.98
1.85
3.89
2.11
1.02
0.94
5.50
5.00
4.50
4.00
3.50
3.00
2.50
2.00
1.50
ppm (t1)

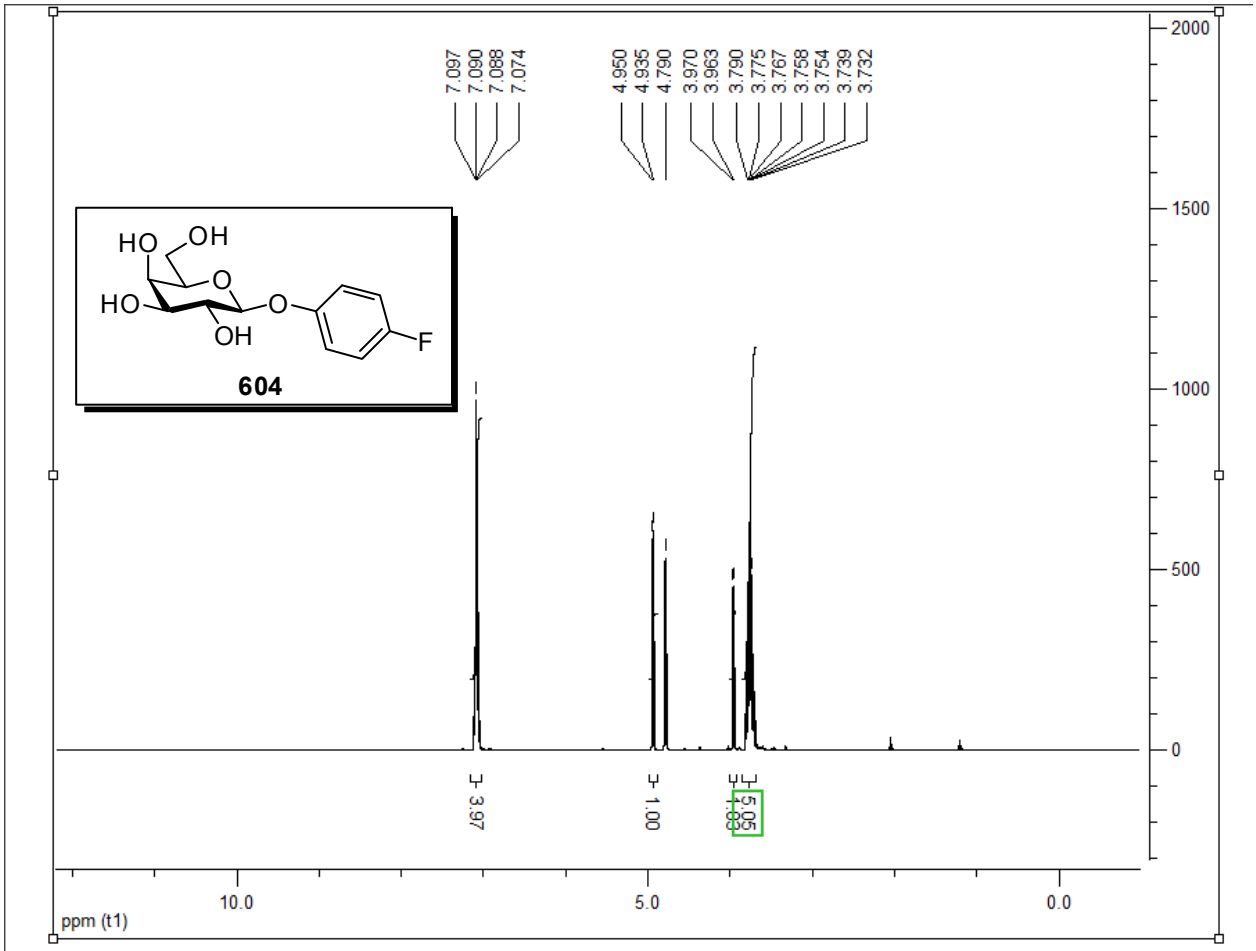

170.974
170.488
170.014
169.890
169.767
71.686
68.321
68.127
67.858
67.474
63.816
61.381
24.629
22.362
20.903
20.740
20.673
20.644
20.612
OAc OAc
AcO
O
AcO
OAc
541
150
100
50
0
ppm (t1)

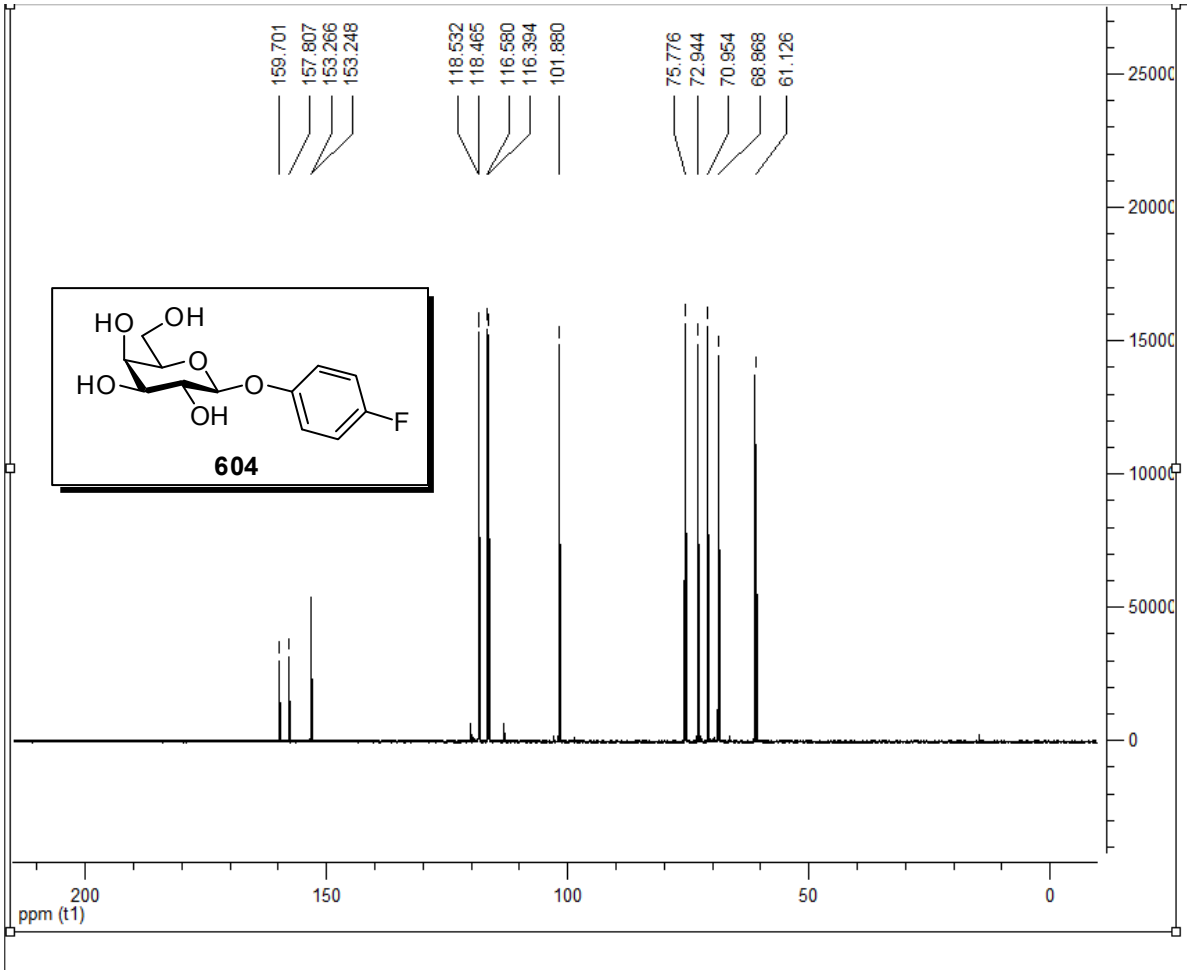

7.137
7.106
6.997
6.966
4.961
4.959
4.956
3.991
3.983
3.810
3.789
3.776
3.754
HO
OH
O
HO
O
OH
OMe
602
1.79
1.80
1.00
1.06
7.56
ppm (t1)

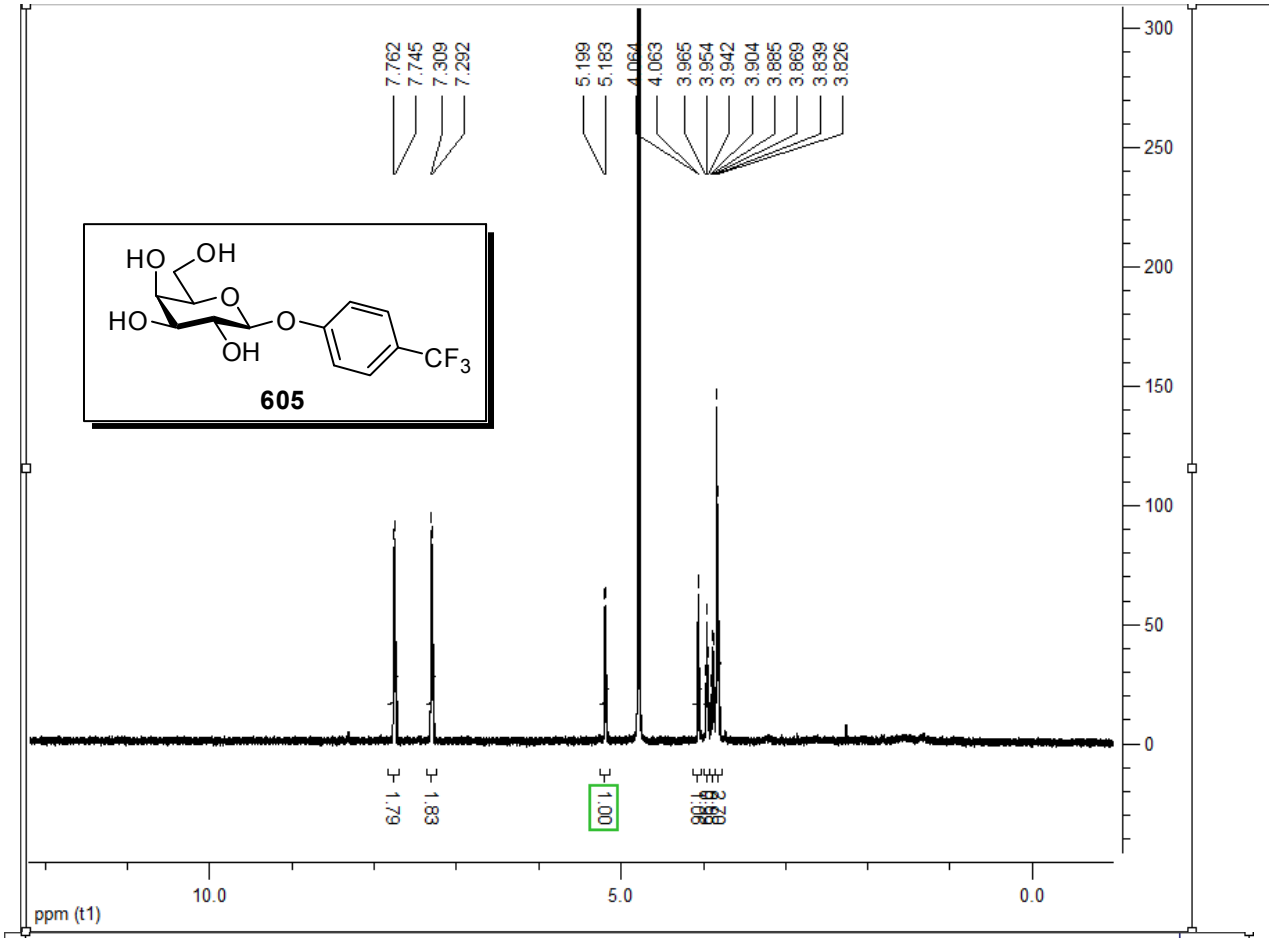

154.642
154.627
151.048
118.110
115.034
101.744
75.355
72.580
70.588
68.482
60.744
55.794
HO
OH
O
HO
O
OH
OMe
602
ppm (f1)

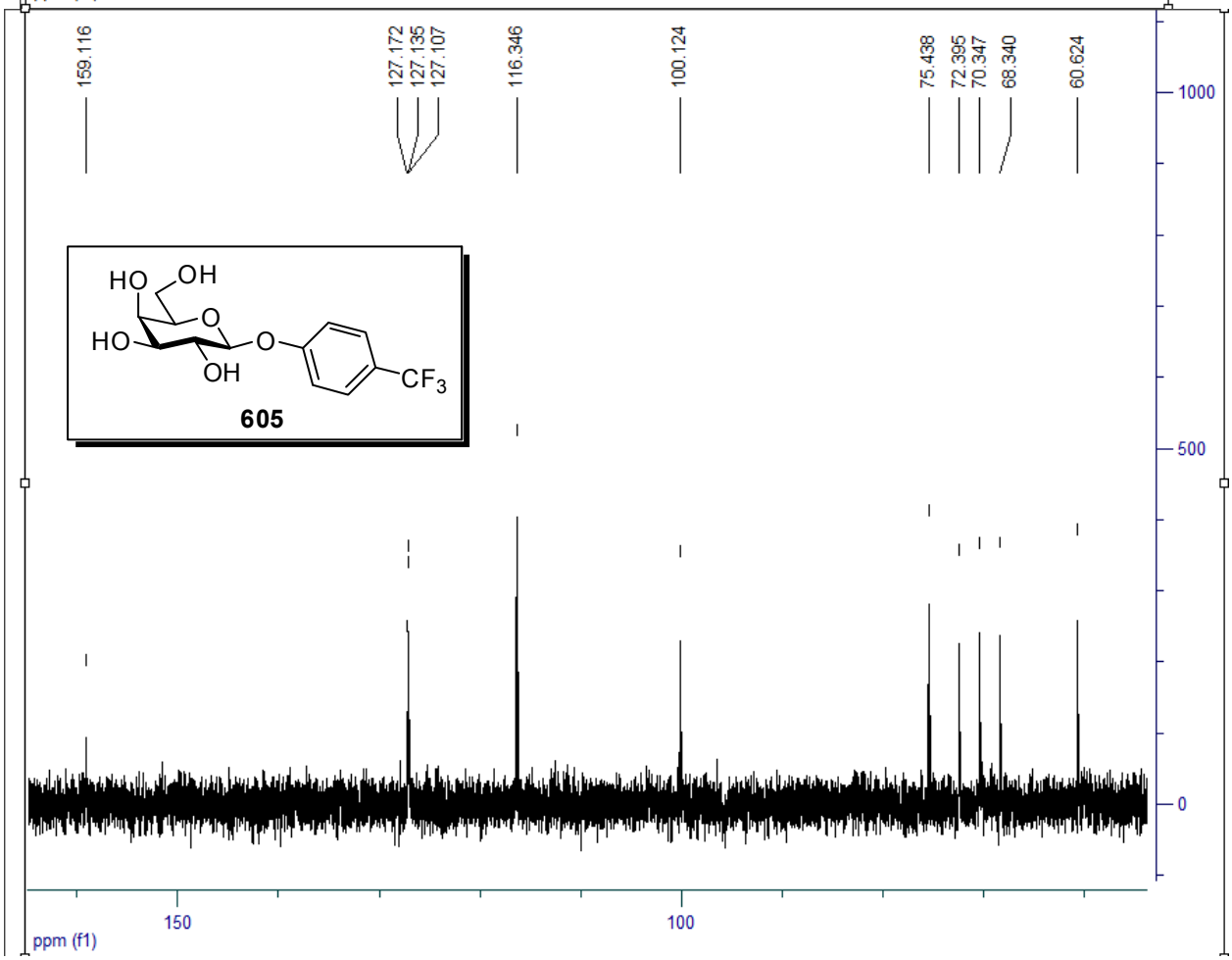

7.198
7.182
7.181
7.030
7.013
4.989
4.975
3.967
3.960
3.757
3.749
3.743
3.737
3.730
2.261
HO
OH
O
HO
O
OH
603
400
300
200
100
0
1.92
2.81
1.00
4.08
2.80
10.0
5.0
0.0
ppm (t1)

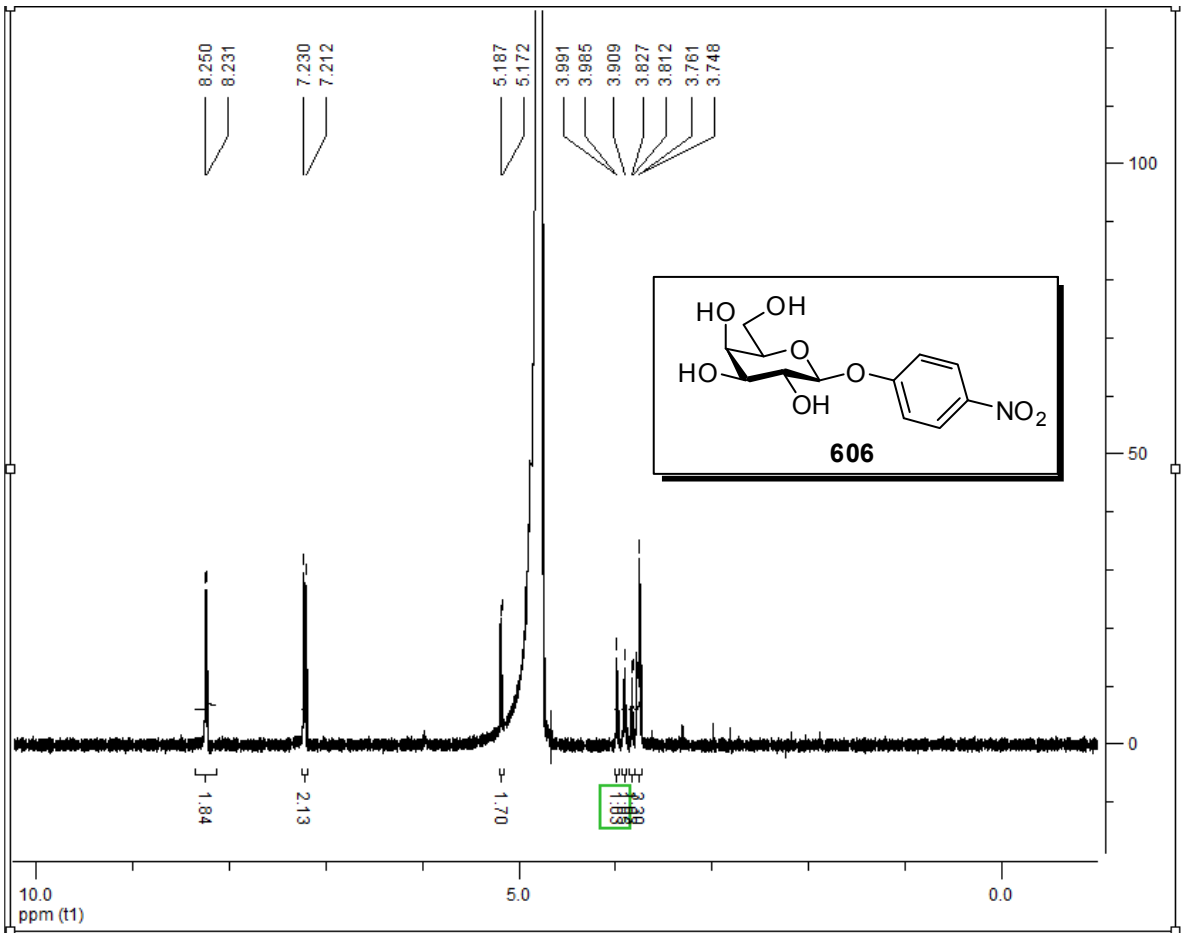

154.435
133.035
130.101
116.446
100.957
75.272
72.485
70.482
68.393
60.658
19.486
HO
OH
O
HO
O
OH
603
10000
5000
0
200
150
100
50
0
ppm (t1)

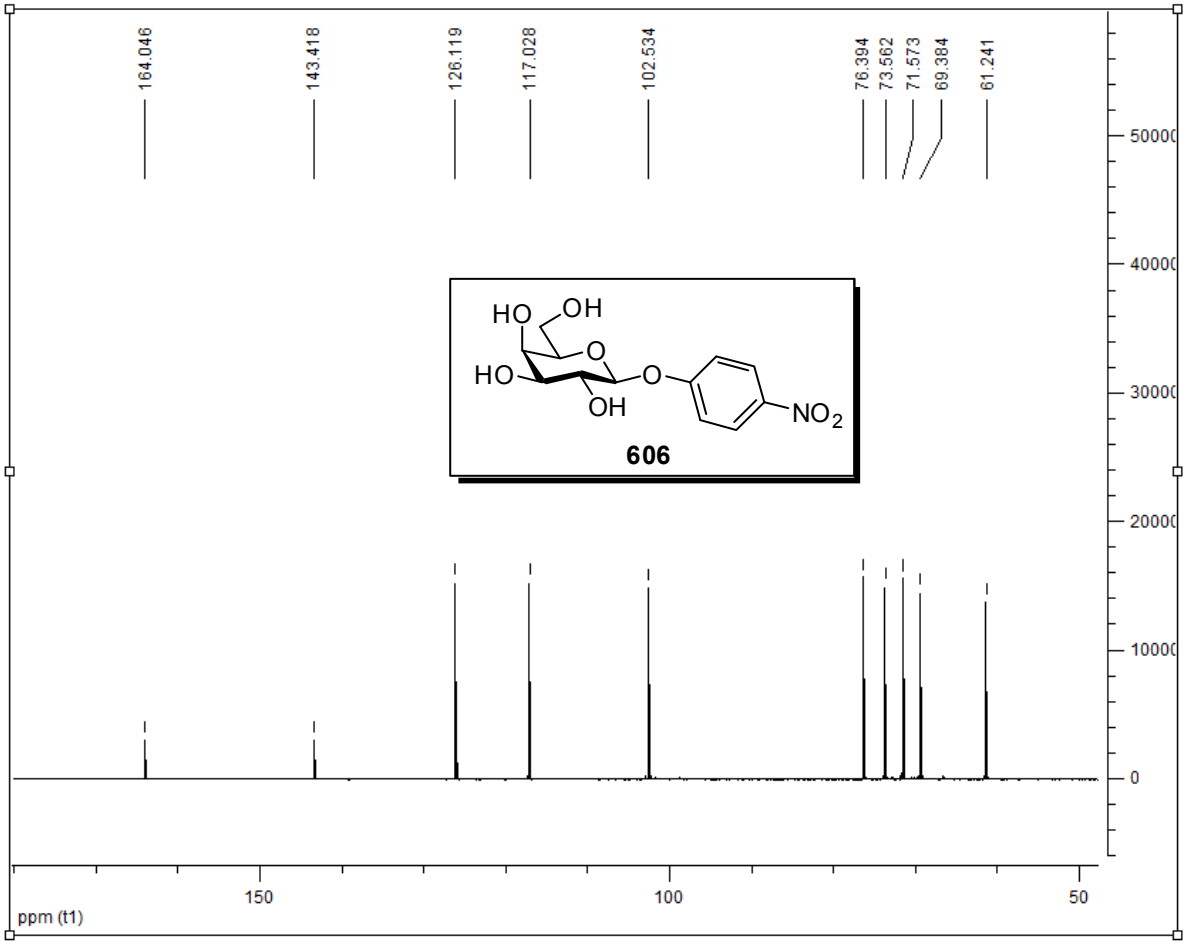

7.097
7.090
7.088
7.074
4.950
4.935
4.790
3.970
3.963
3.790
3.775
3.767
3.758
3.754
3.739
3.732
HO
OH
O
HO
O
OH
F
604
3.97
1.00
6.06
2000
1500
1000
500
0
10.0
5.0
0.0
ppm (t1)

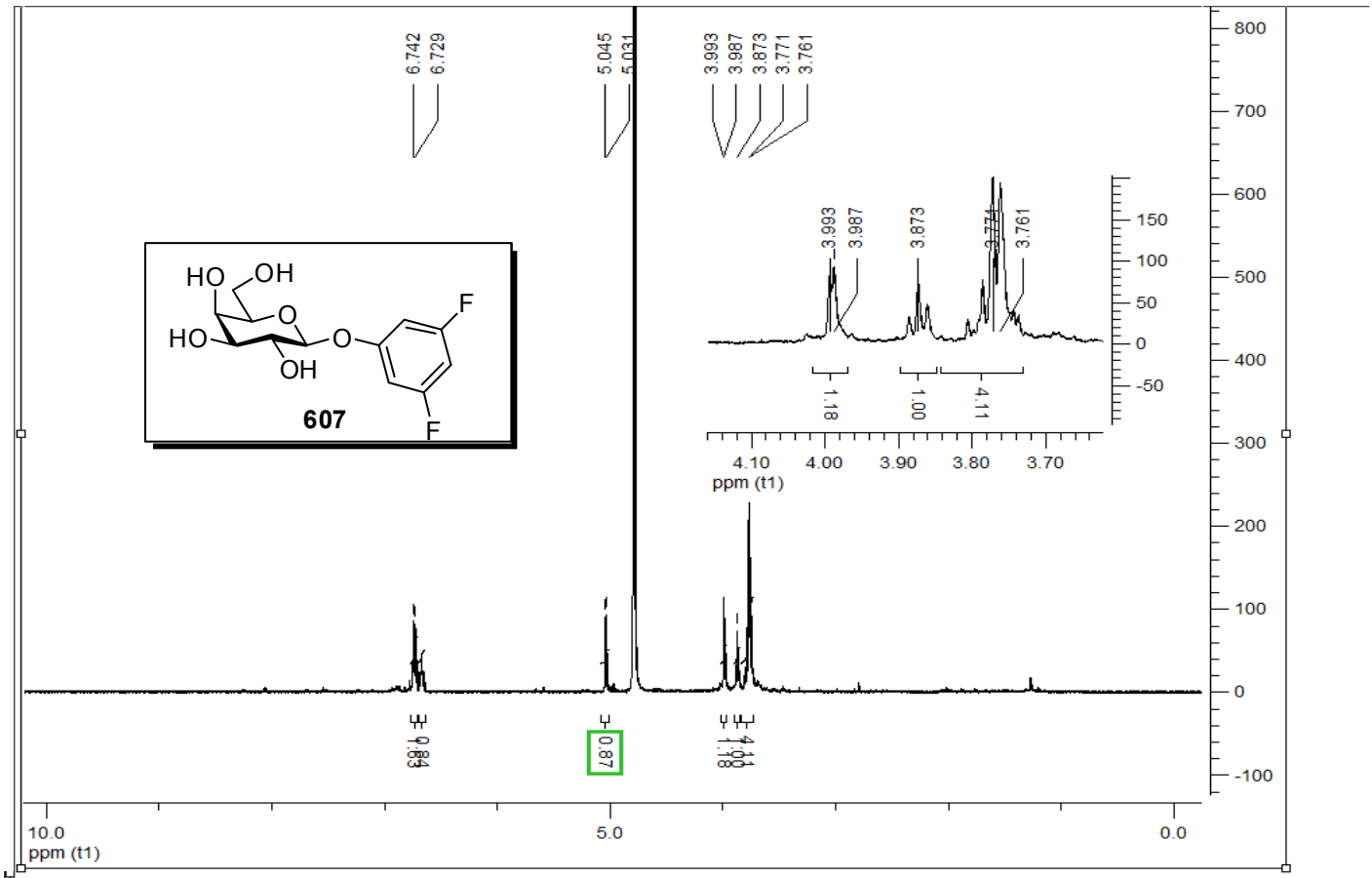

159.701
157.807
153.266
153.248
118.532
118.465
116.580
116.394
101.880
75.776
72.944
70.954
68.868
61.126
HO
OH
O
HO
O
OH
F
604
25000
20000
15000
10000
50000
0
200
150
100
50
0
ppm (t1)

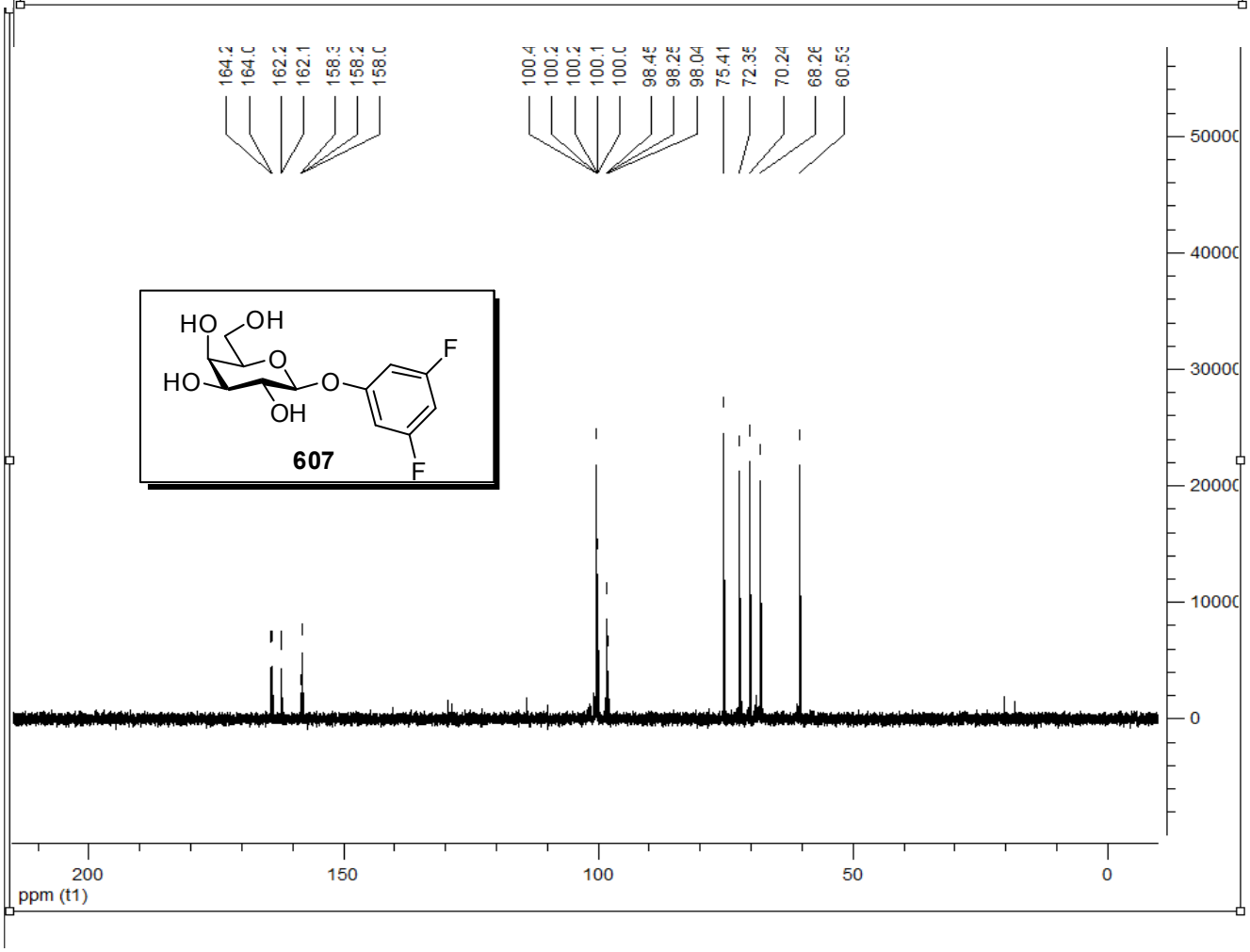

7.762
7.745
7.309
7.292
5.199
5.183
4.064
4.063
3.965
3.954
3.942
3.904
3.885
3.869
3.839
3.826
HO
OH
O
HO
O
OH
CF3
605
300
250
200
150
100
50
0
1.79
1.83
1.00
10.0
5.0
0.0
ppm (t1)

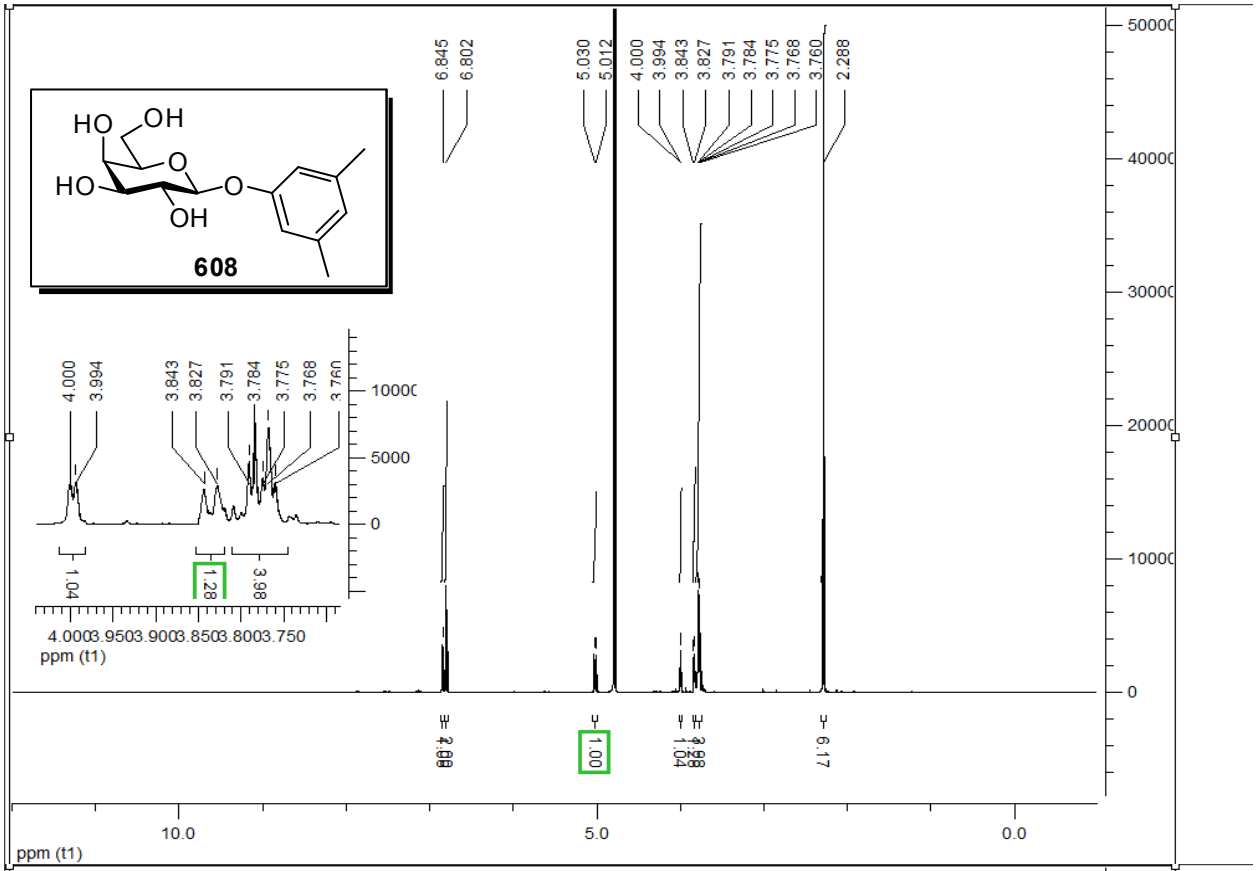

159.116
127.172
127.135
127.107
116.346
100.124
75.438
72.395
70.347
68.340
60.624
HO
OH
O
HO
O
OH
CF3
605
1000
500
0
150
100
ppm (f1)

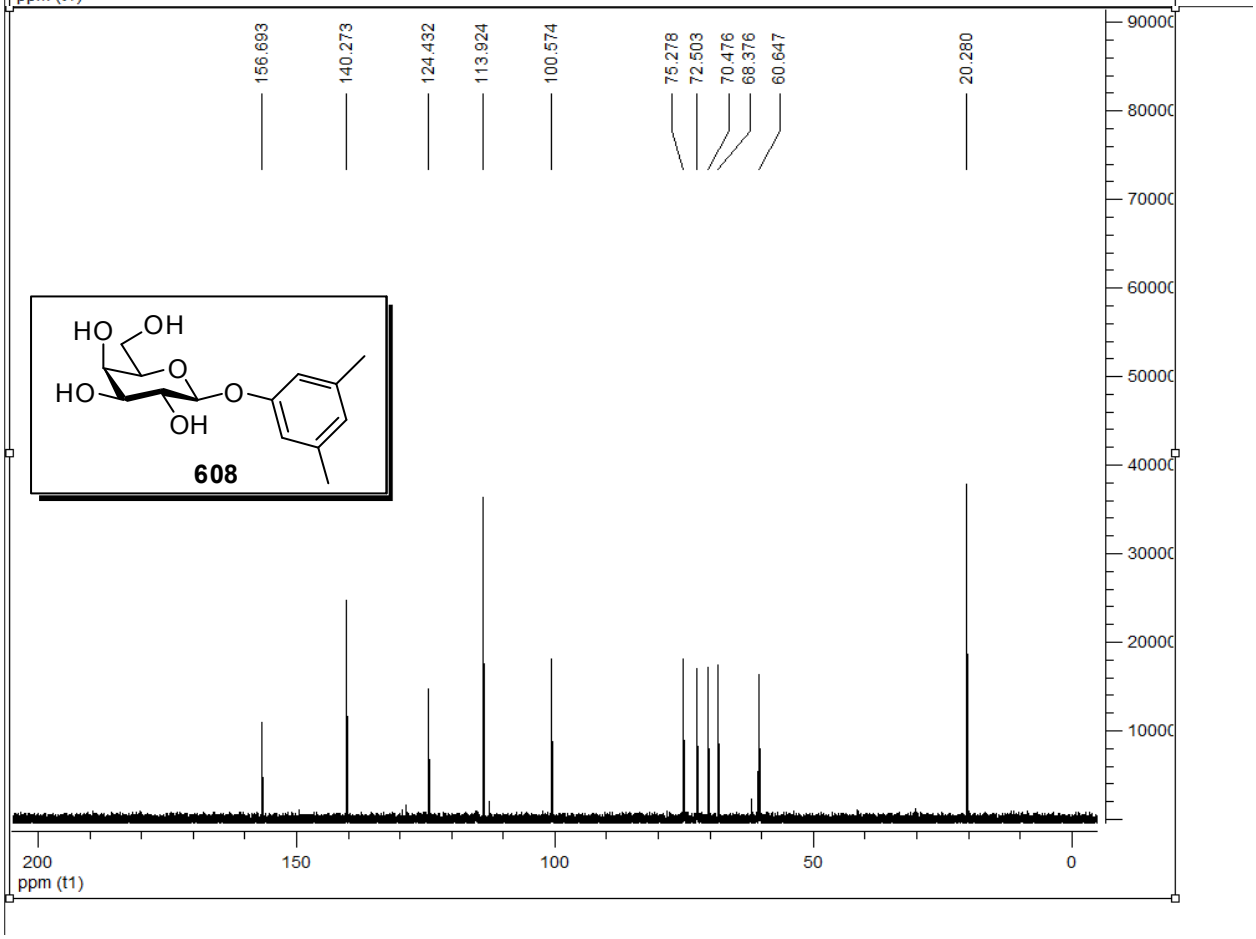

8.250
8.231
7.230
7.212
5.187
5.172
3.991
3.985
3.909
3.827
3.812
3.761
3.748
HO
OH
O
HO
O
OH
NO2
606
1.84
2.13
1.70
2.30
100
50
0
10.0
5.0
0.0
ppm (t1)

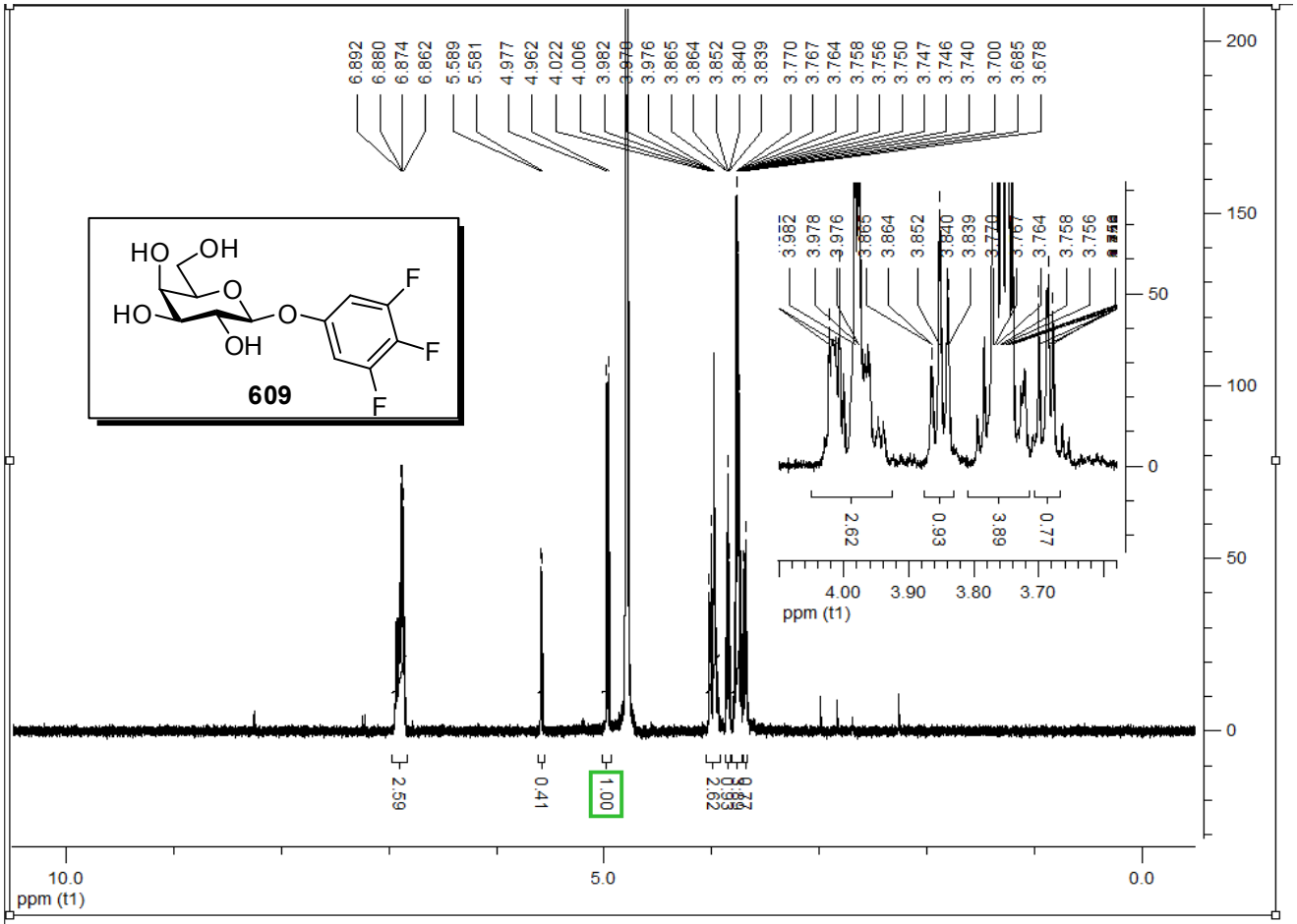

164.046
143.418
126.119
117.028
102.534
76.394
73.562
71.573
69.384
61.241
HO
OH
O
HO
O
OH
NO2
606
50000
40000
30000
20000
10000
0
150
100
50
ppm (t1)

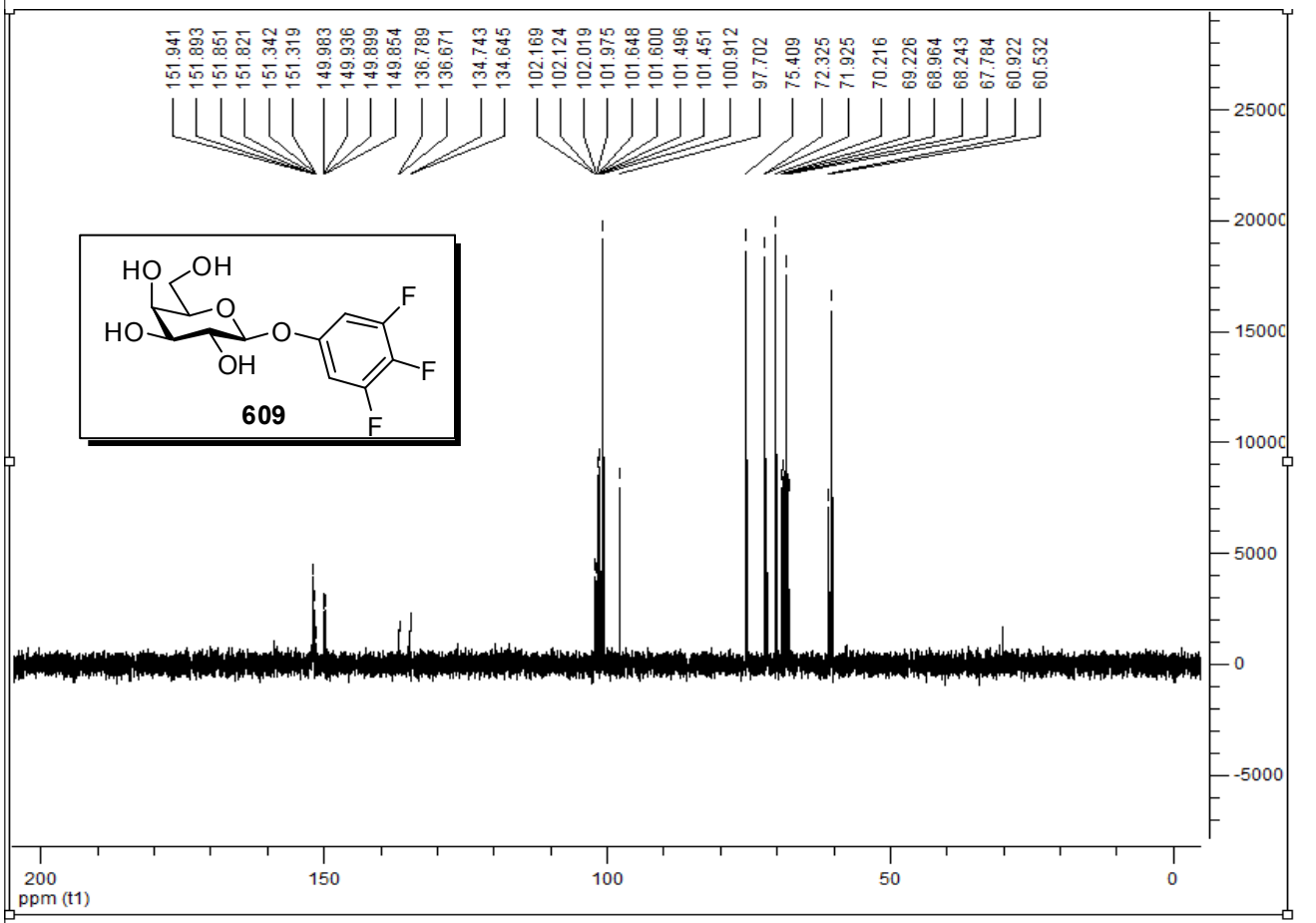

6.742
6.729
5.045
5.031
3.993
3.987
3.873
3.771
3.761
HO
OH
HO
O
OH
O
F
F
607
4.10
4.00
3.90
3.80
3.70
ppm (t1)
1.18
1.00
4.11
0.87
10.0
5.0
0.0
ppm (t1)

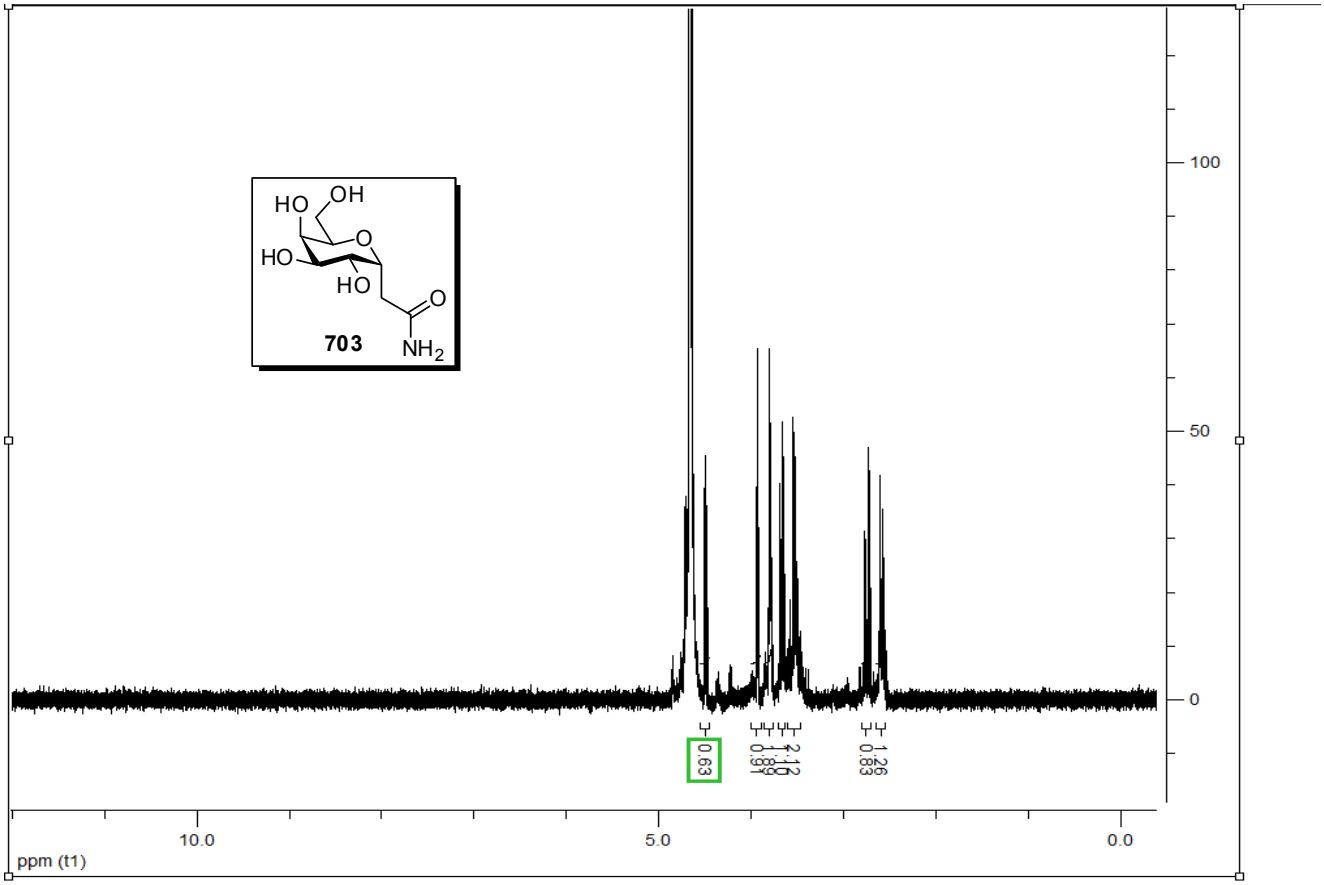

HO
OH
HO
O
OH
O
F
F
607
200
150
100
50
0
ppm (t1)

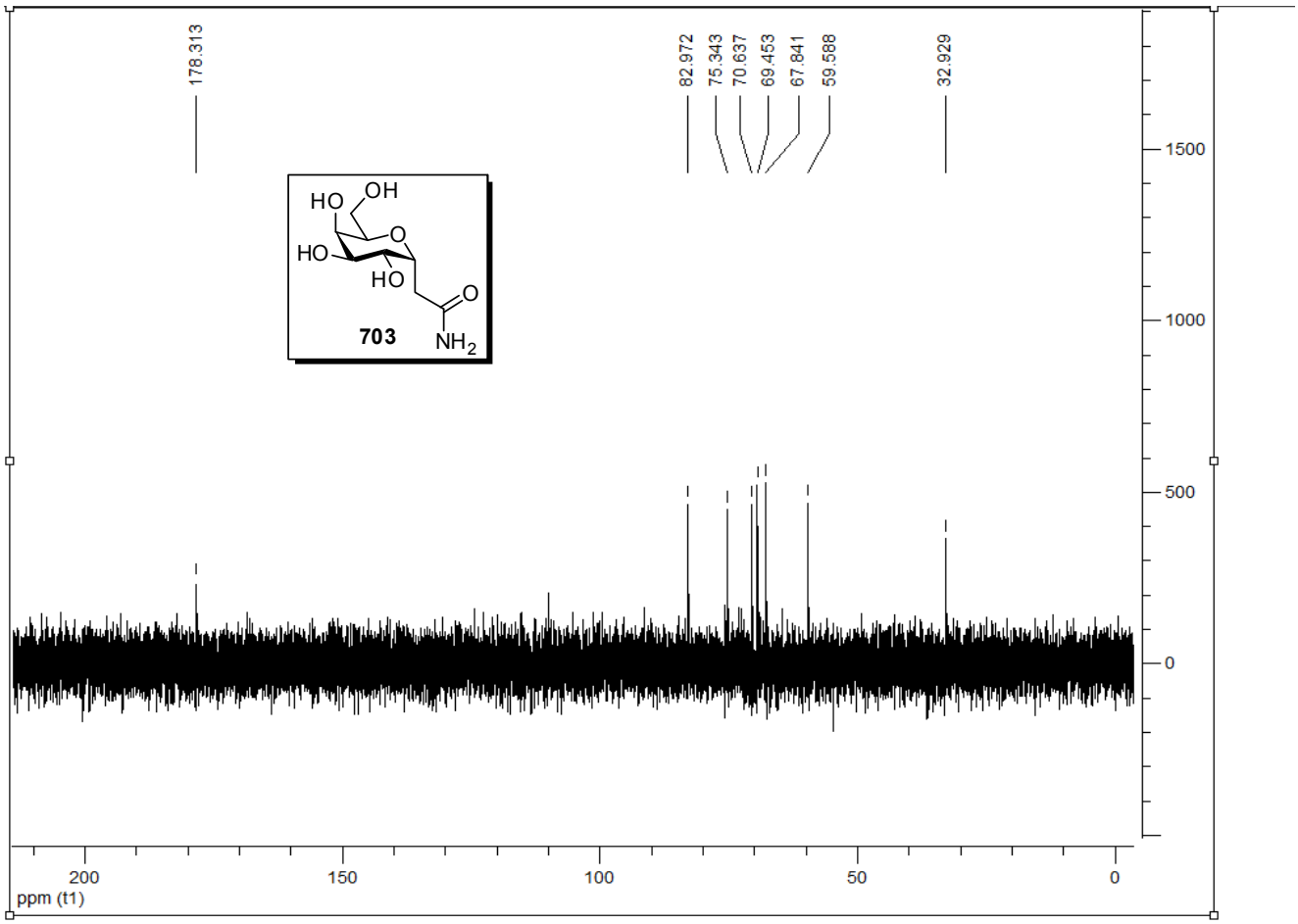

HO
OH
O
HO
O
OH
608
6.845
6.802
5.030
5.012
4.000
3.994
3.843
3.827
3.791
3.784
3.775
3.768
3.760
2.288
1.04
1.28
3.98
1.00
6.17
ppm (t1)

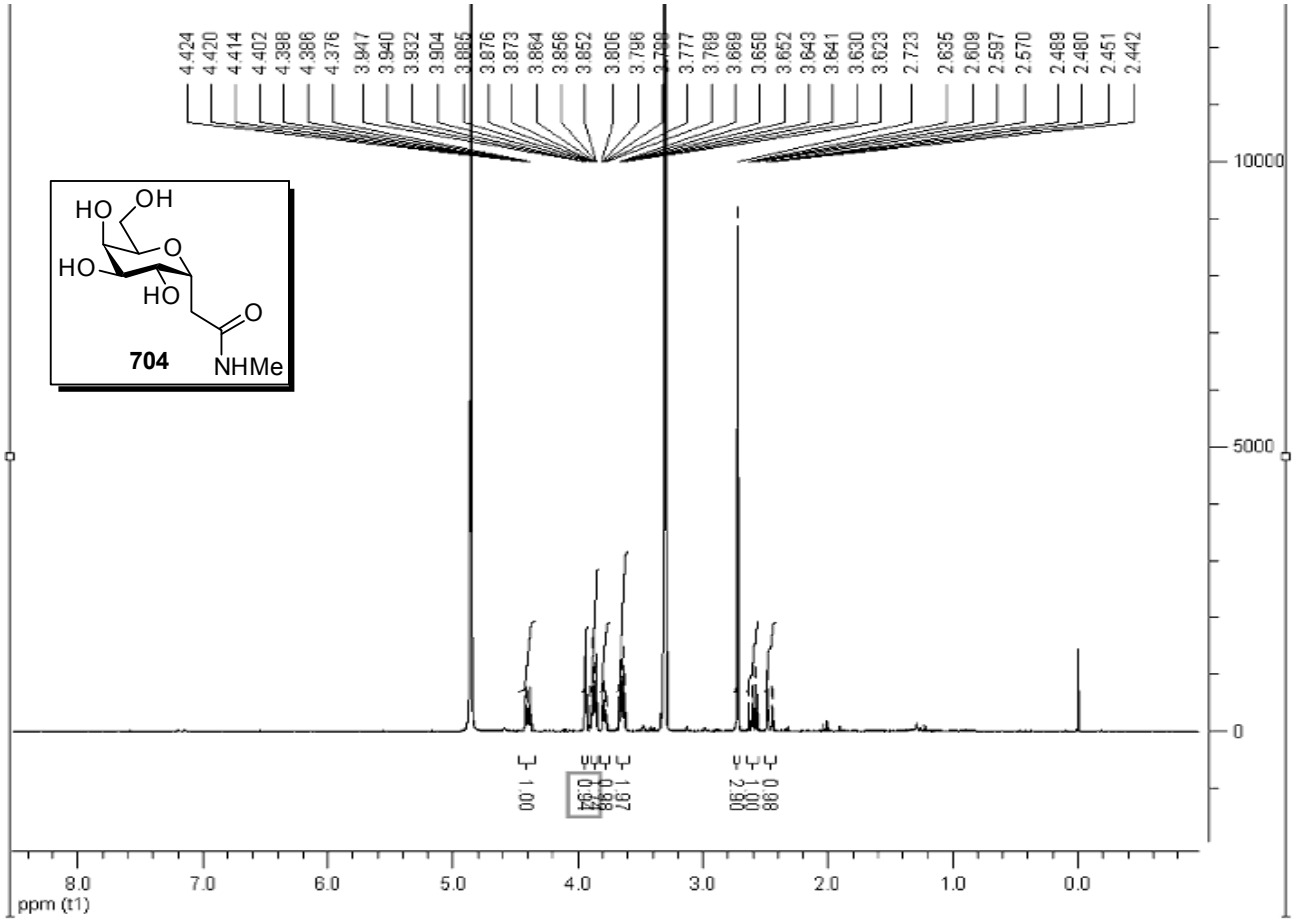

156.693
140.273
124.432
113.924
100.574
75.278
72.503
70.476
68.376
60.647
20.280
HO
OH
O
HO
O
OH
608
ppm (t1)

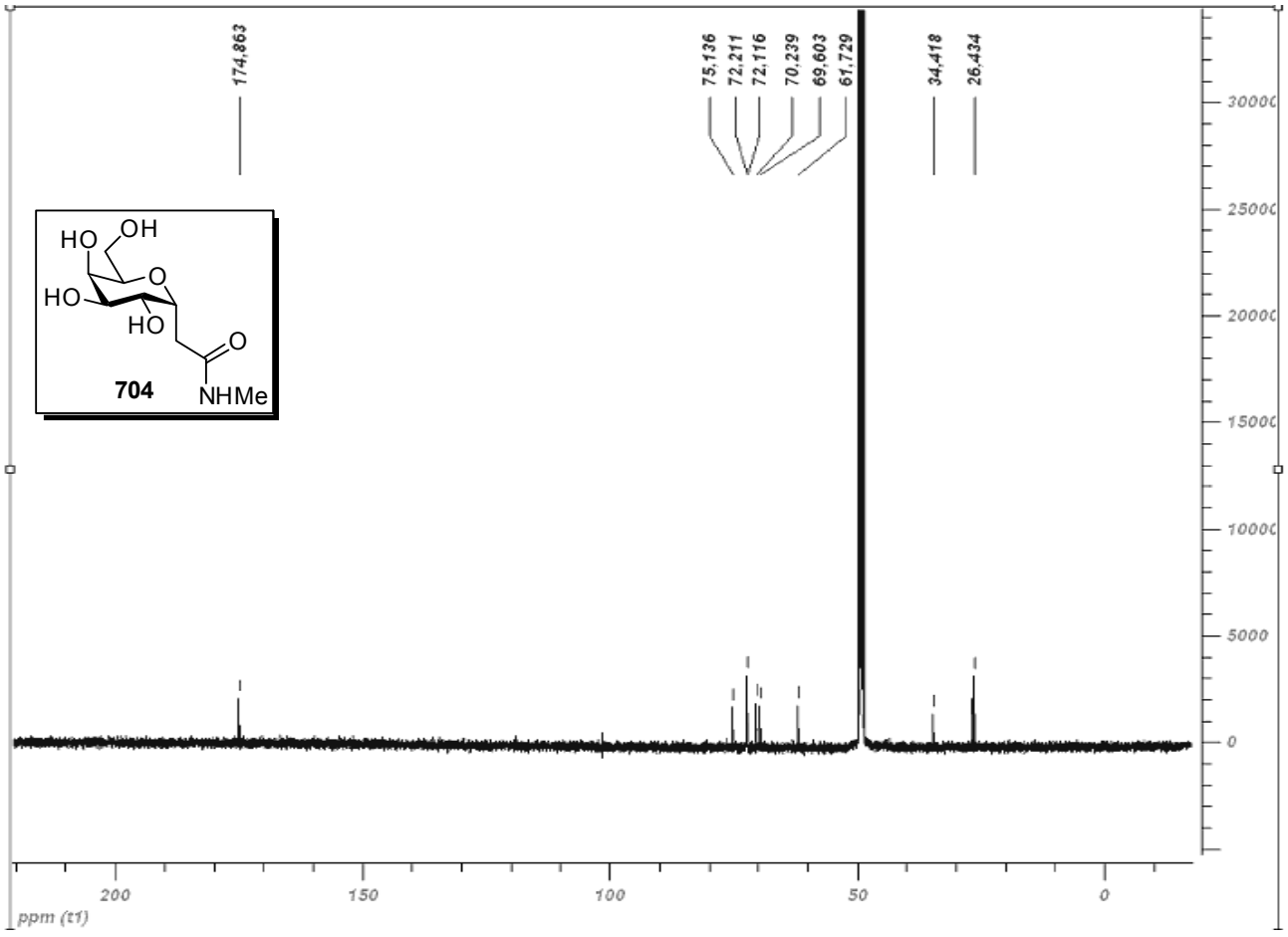

6.892
6.880
6.874
6.862
5.589
5.581
4.977
4.962
4.022
4.006
3.982
3.976
3.865
3.864
3.852
3.840
3.839
3.770
3.767
3.764
3.758
3.756
3.750
3.747
3.746
3.740
3.700
3.685
3.678
HO
OH
O
HO
O
OH
F
F
F
609
2.62
0.93
3.89
0.77
4.00
3.90
3.80
3.70
ppm (t1)
2.59
0.41
1.00
2.62
10.0
5.0
0.0
ppm (t1)

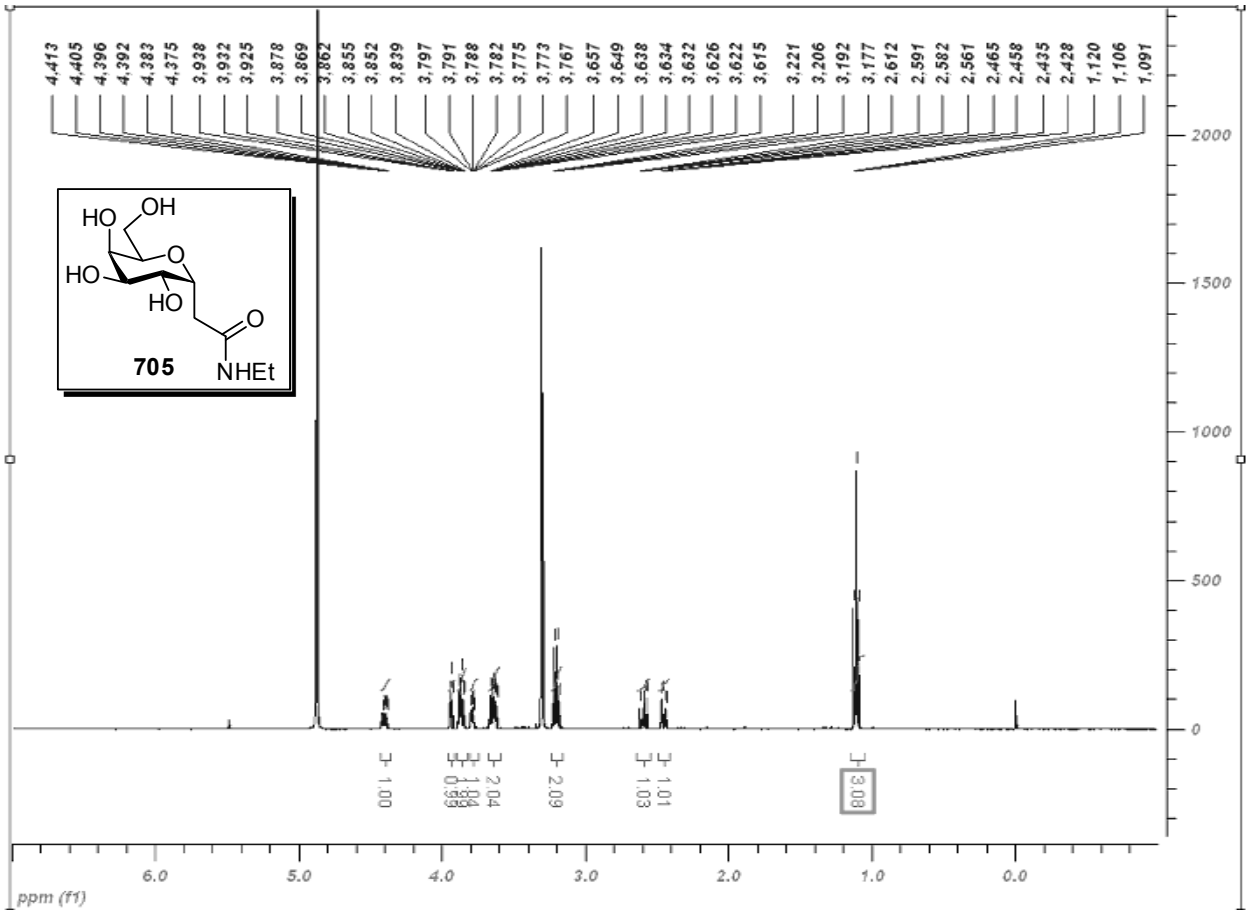

151.941
151.893
151.851
151.821
151.342
151.319
149.983
149.936
149.899
149.854
136.789
136.671
134.743
134.645
102.169
102.124
102.019
101.975
101.648
101.600
101.496
101.451
100.912
97.702
75.409
72.325
71.925
70.216
69.226
68.964
68.243
67.784
60.922
60.532
HO
OH
O
HO
O
OH
F
F
F
609
200
150
100
50
0
ppm (t1)

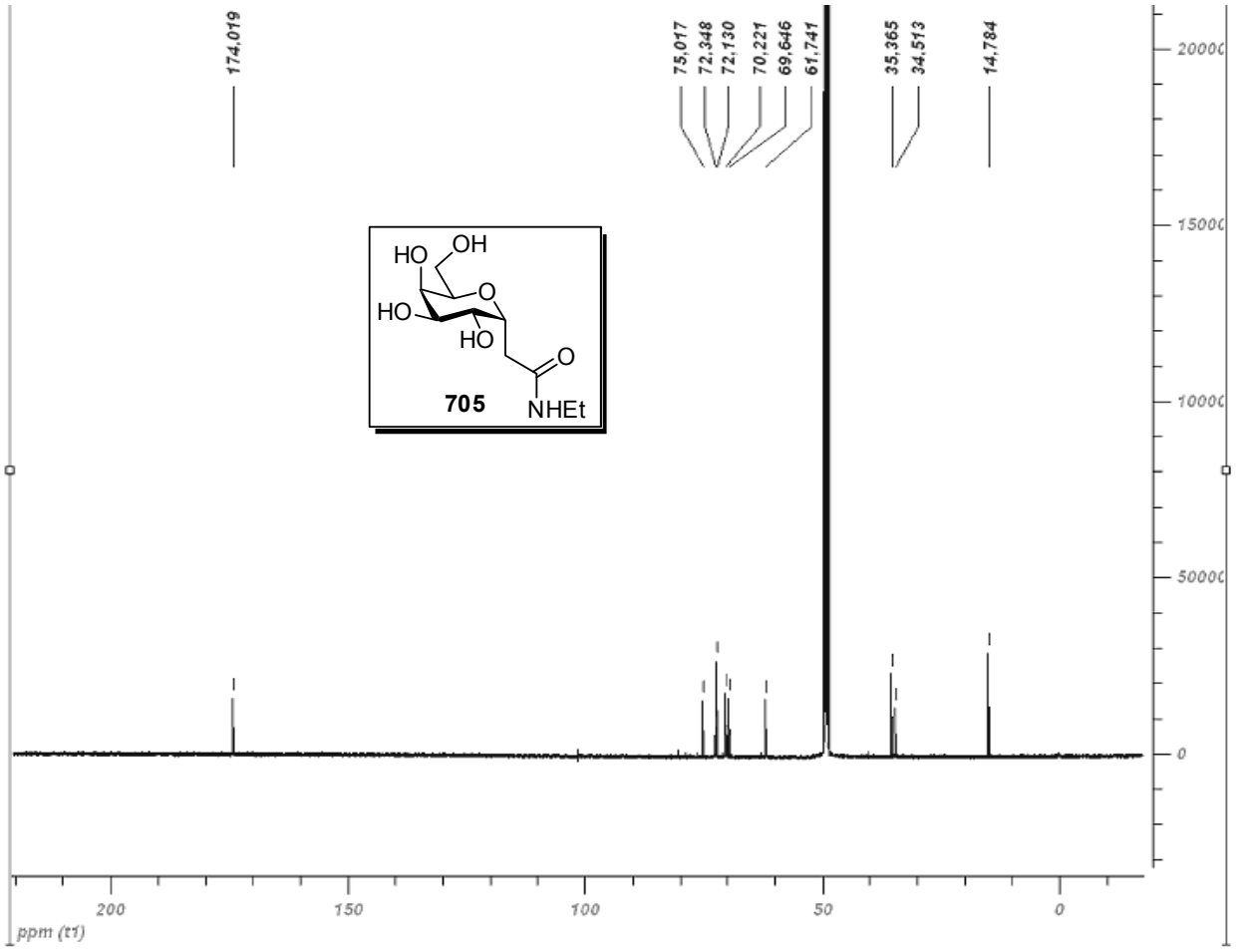

HO
OH
O
HO
HO
O
NH2
703
100
50
0
0.63
1.97
1.89
2.12
1.00
1.26
0.83
10.0
5.0
0.0
ppm (t1)

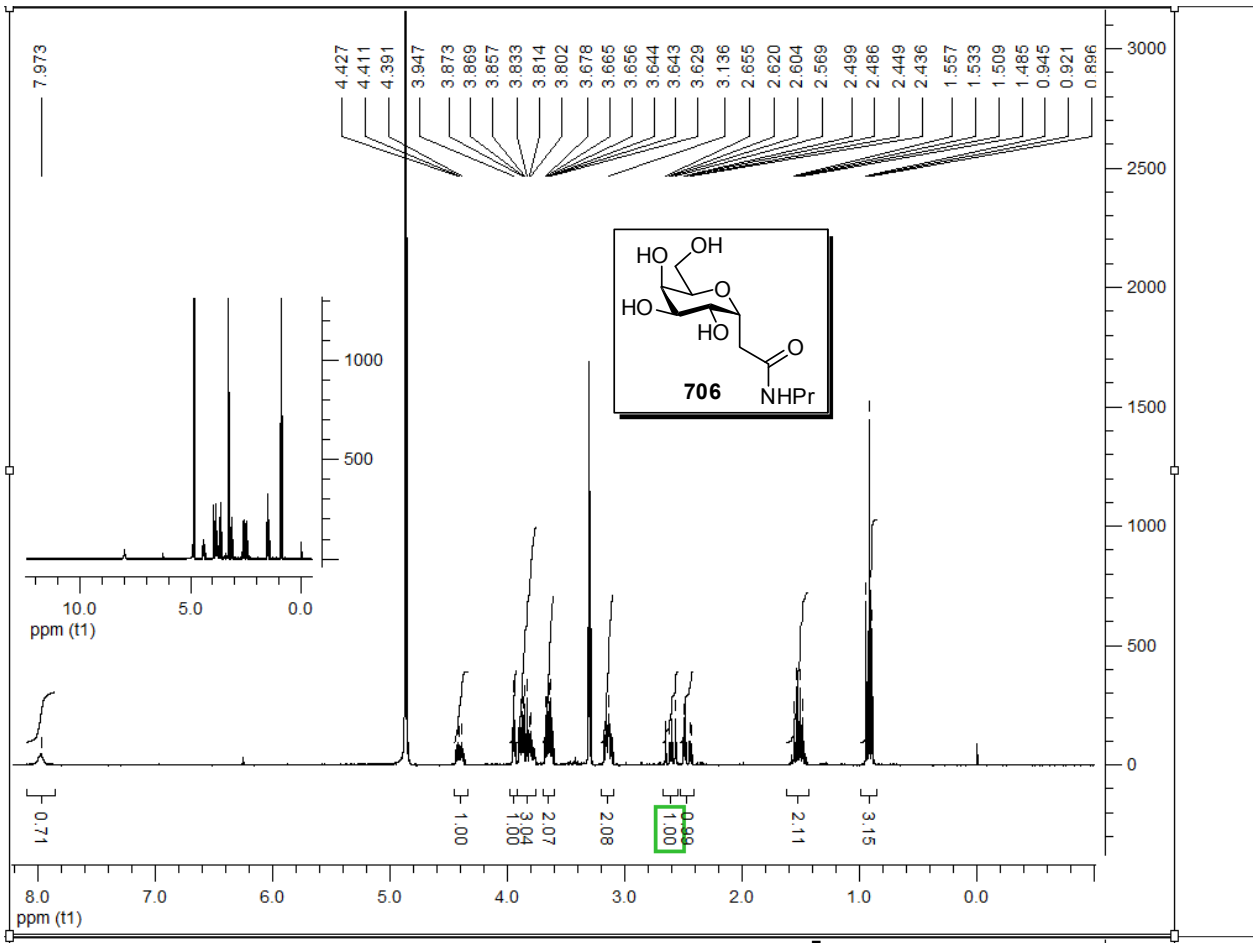

178.313
82.972
75.343
70.637
69.453
67.841
59.588
32.929
HO
OH
O
HO
HO
O
NH2
703
1500
1000
500
0
200
150
100
50
0
ppm (t1)

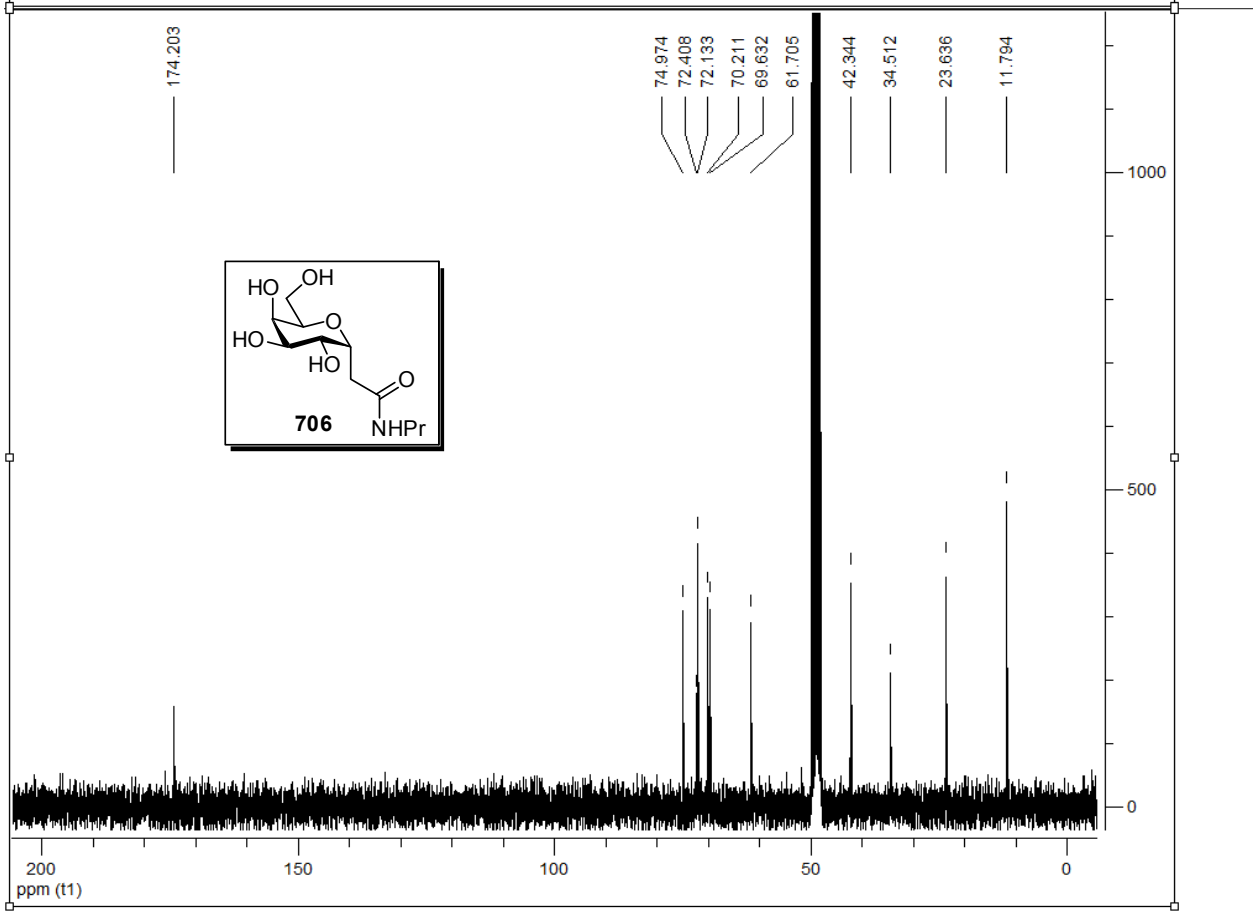

4.424
4.420
4.414
4.402
4.398
4.386
4.376
3.947
3.940
3.932
3.904
3.885
3.876
3.873
3.864
3.856
3.852
3.806
3.796
3.777
3.769
3.669
3.650
3.652
3.643
3.641
3.630
3.623
2.723
2.635
2.609
2.597
2.570
2.489
2.480
2.451
2.442
HO
OH
O
HO
HO
O
NHMe
704
10000
5000
0
1.00
0.94
0.98
1.07
2.90
1.00
0.98
8.0
7.0
6.0
5.0
4.0
3.0
2.0
1.0
0.0
ppm (t1)

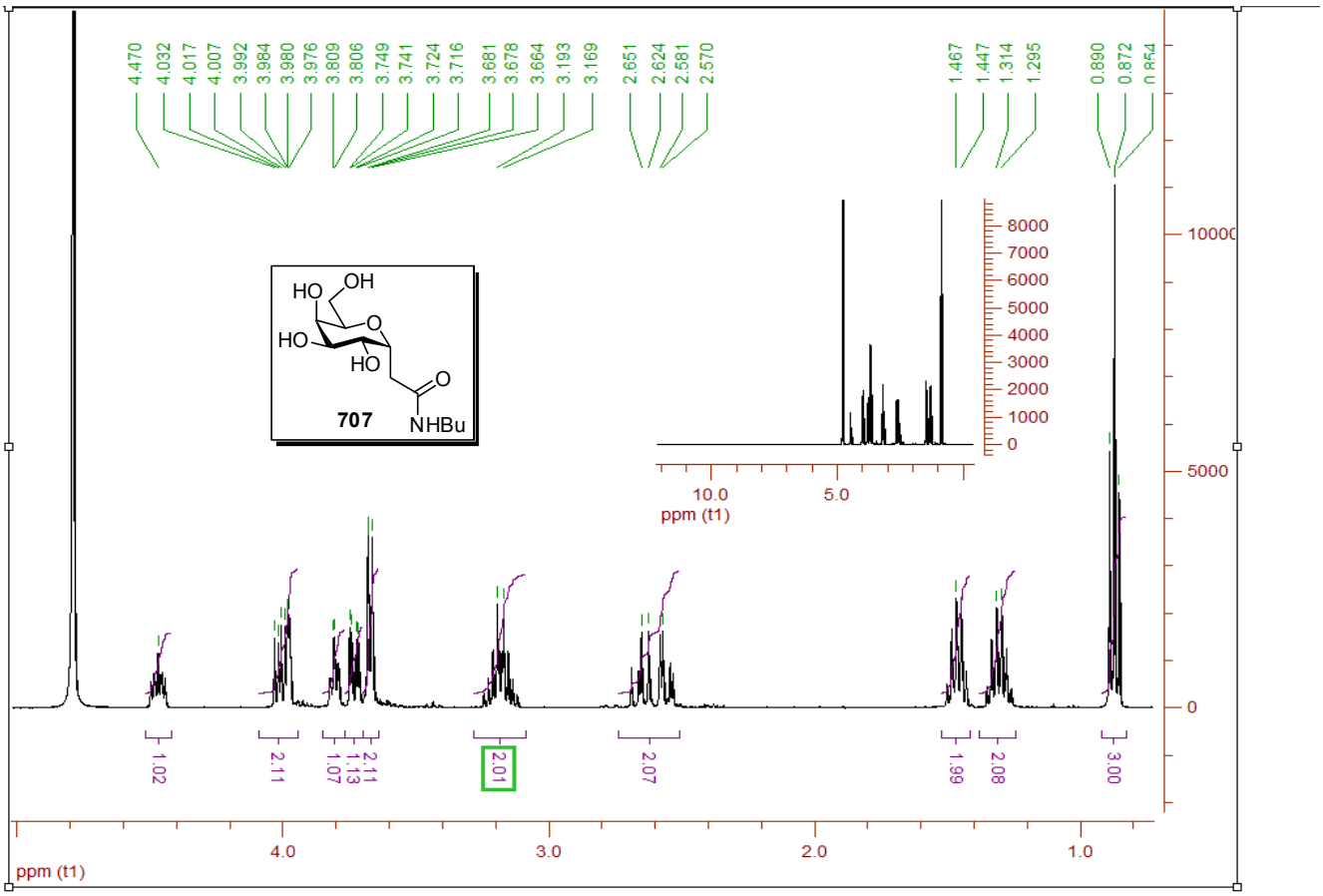

174,863
75,136
72,211
72,116
70,239
69,603
61,729
34,418
26,434
HO
OH
O
HO
HO
O
NHMe
704
30000
25000
20000
15000
10000
5000
0
200
150
100
50
0
ppm (t1)

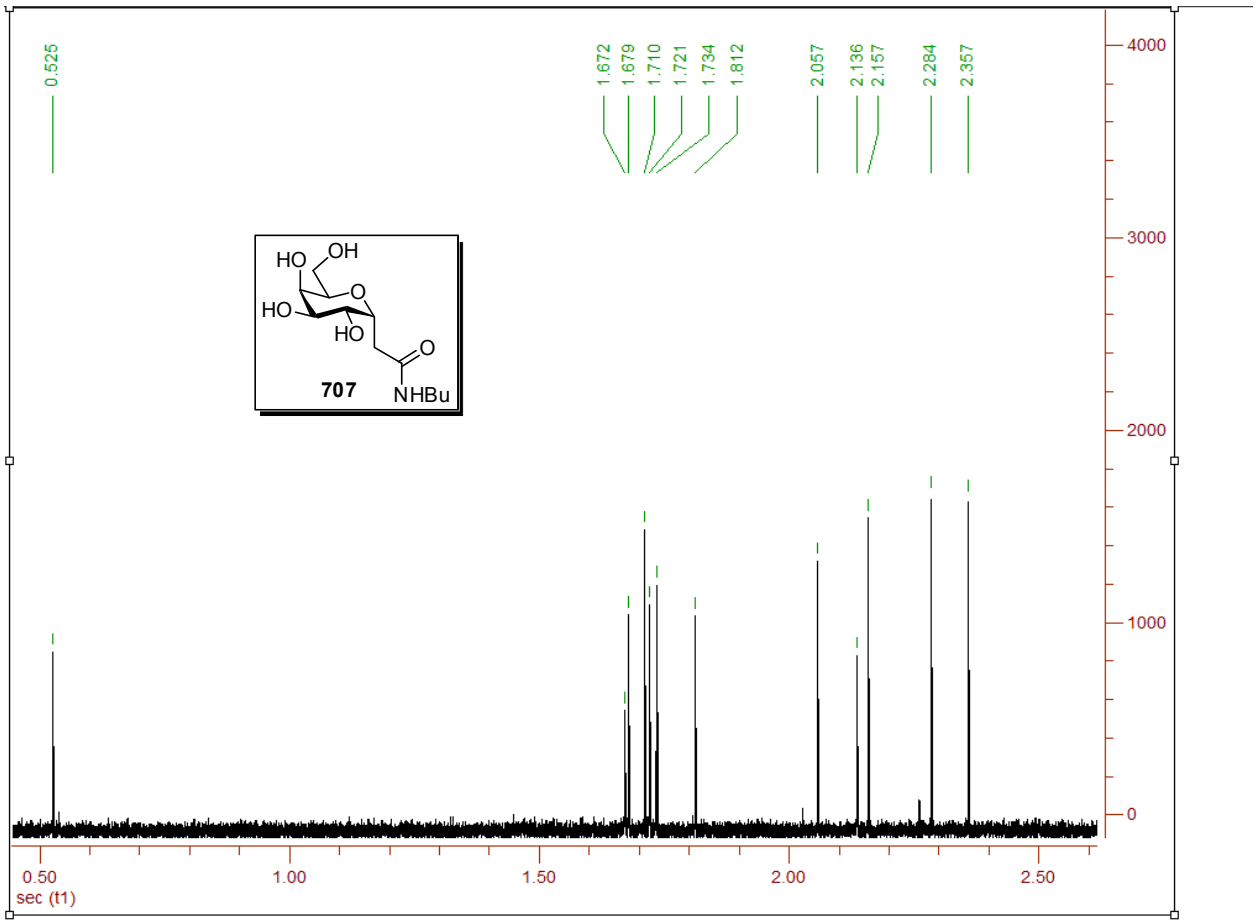

4.413
4.405
4.396
4.392
4.383
4.375
3.938
3.932
3.925
3.878
3.869
3.862
3.855
3.852
3.839
3.797
3.791
3.788
3.782
3.775
3.773
3.767
3.657
3.649
3.638
3.634
3.632
3.626
3.622
3.615
3.221
3.206
3.192
3.177
2.612
2.591
2.582
2.561
2.465
2.458
2.435
2.428
1.120
1.106
1.091
HO
OH
O
HO
HO
O
NHEt
705
1.00
0.99
1.00
2.04
2.09
1.03
1.01
3.08
6.0
5.0
4.0
3.0
2.0
1.0
0.0
ppm (f1)

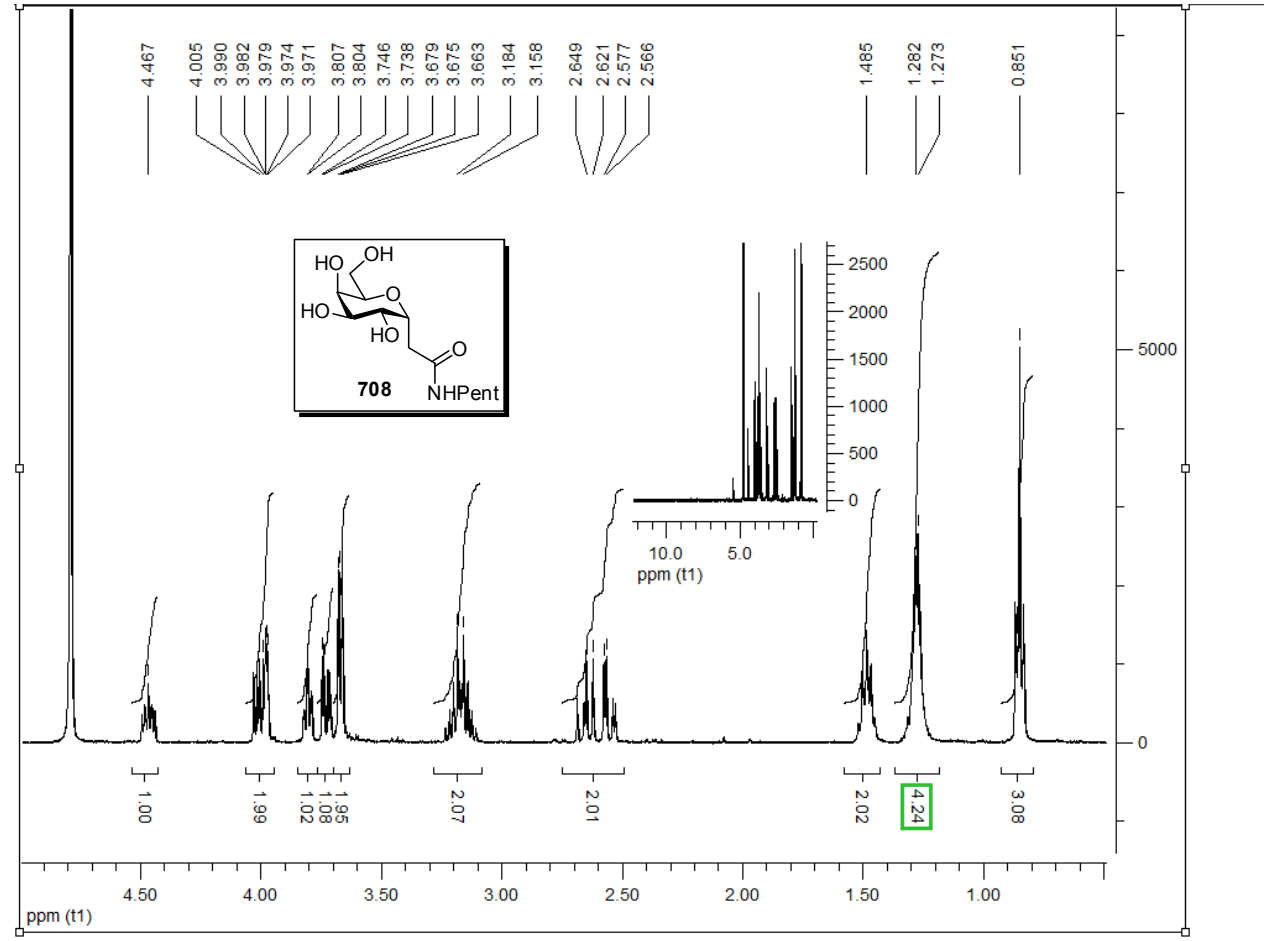

174.019
75.017
72.348
72.130
70.221
69.646
61.741
35.365
34.513
14.784
HO
OH
O
HO
HO
O
NHEt
705
200
150
100
50
0
ppm (t1)

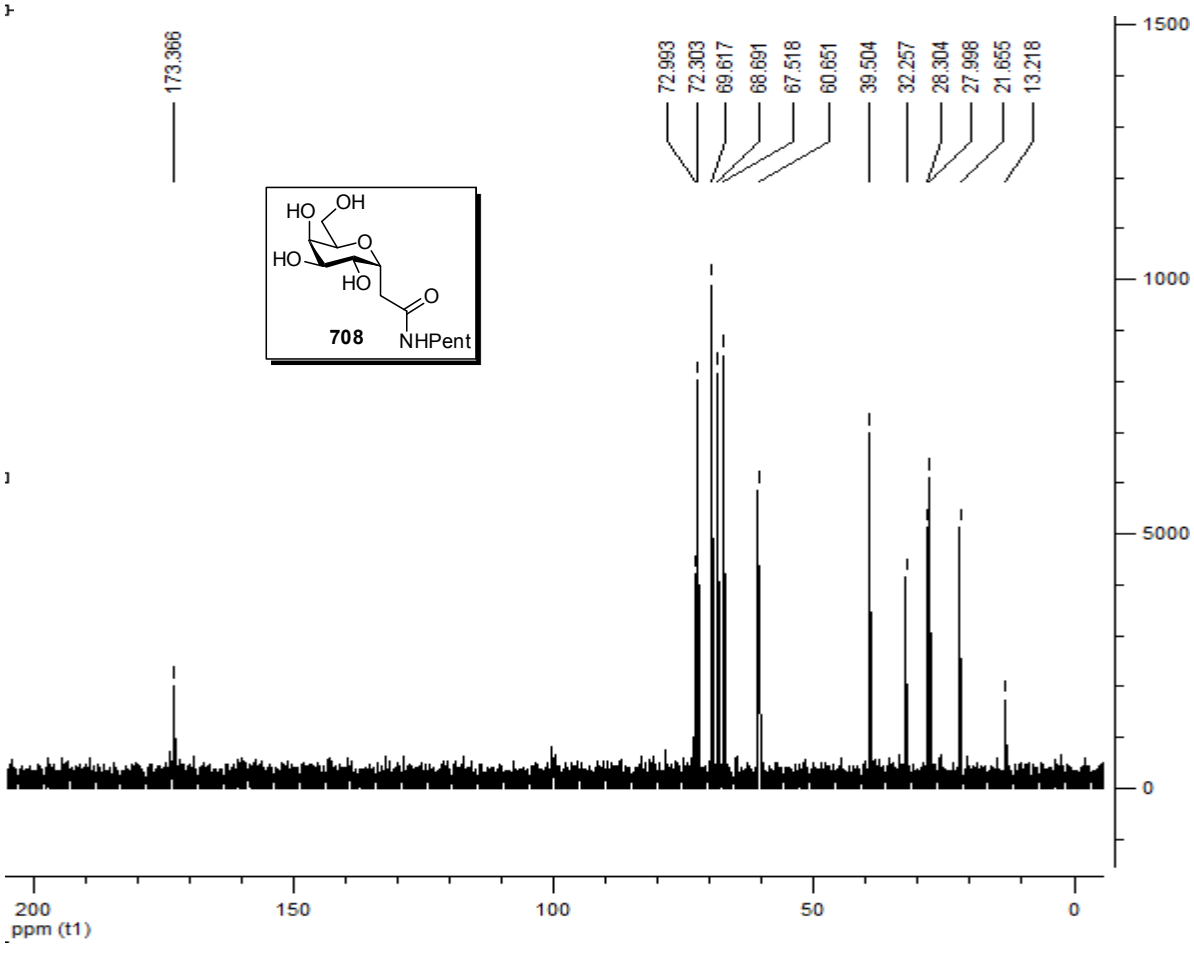

7.973
4.427
4.411
4.391
3.947
3.873
3.869
3.857
3.833
3.814
3.802
3.678
3.665
3.656
3.644
3.643
3.629
3.136
2.655
2.620
2.604
2.569
2.499
2.486
2.449
2.436
1.557
1.533
1.509
1.485
0.945
0.921
0.896
HO
OH
O
HO
HO
O
706
NHPr
ppm (t1)
0.71
1.00
3.04
1.00
2.07
2.08
1.00
0.98
2.11
3.15
ppm (t1)

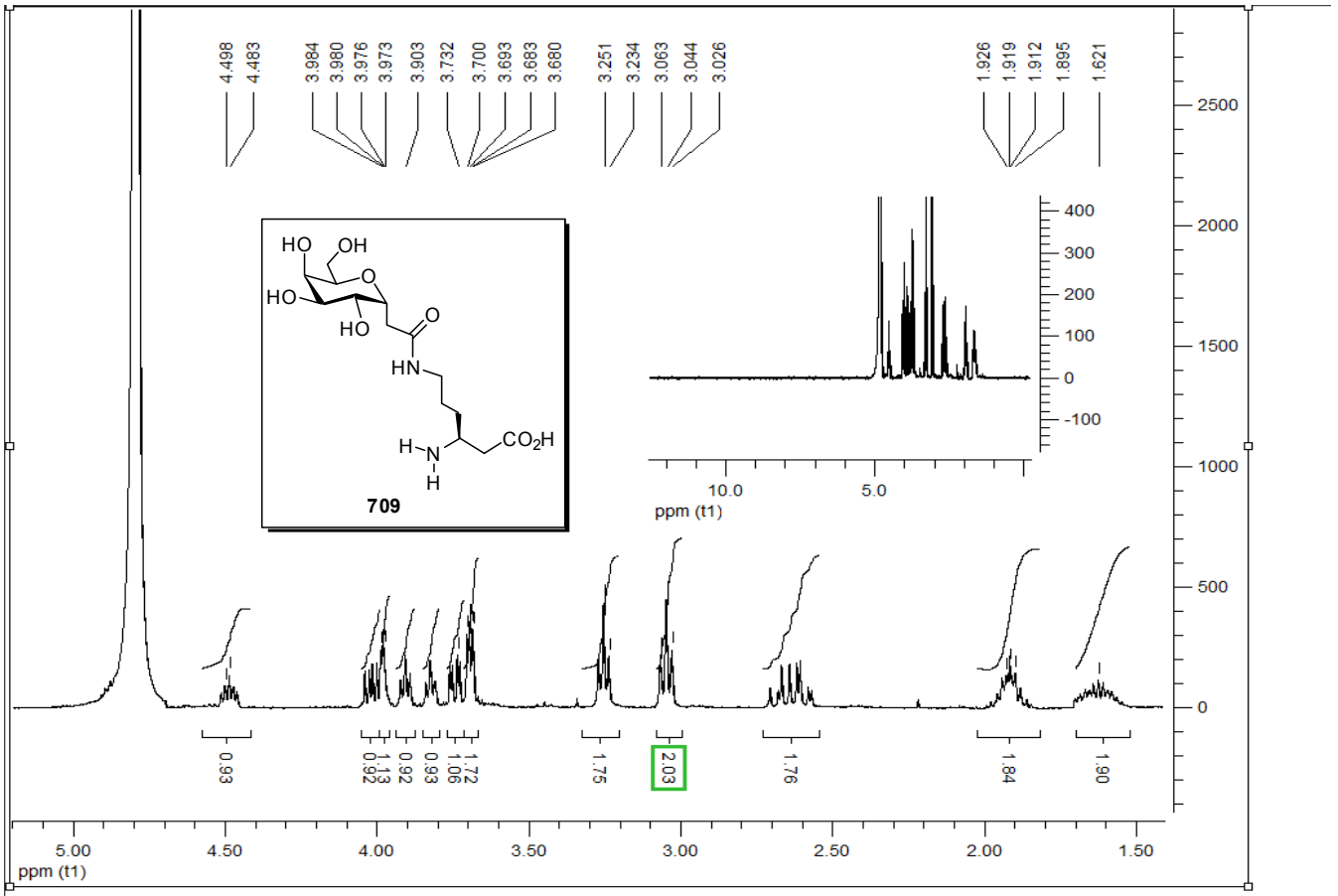

174.203
74.974
72.408
72.133
70.211
69.632
61.705
42.344
34.512
23.636
11.794
HO
OH
O
HO
HO
O
706
NHPr
ppm (t1)

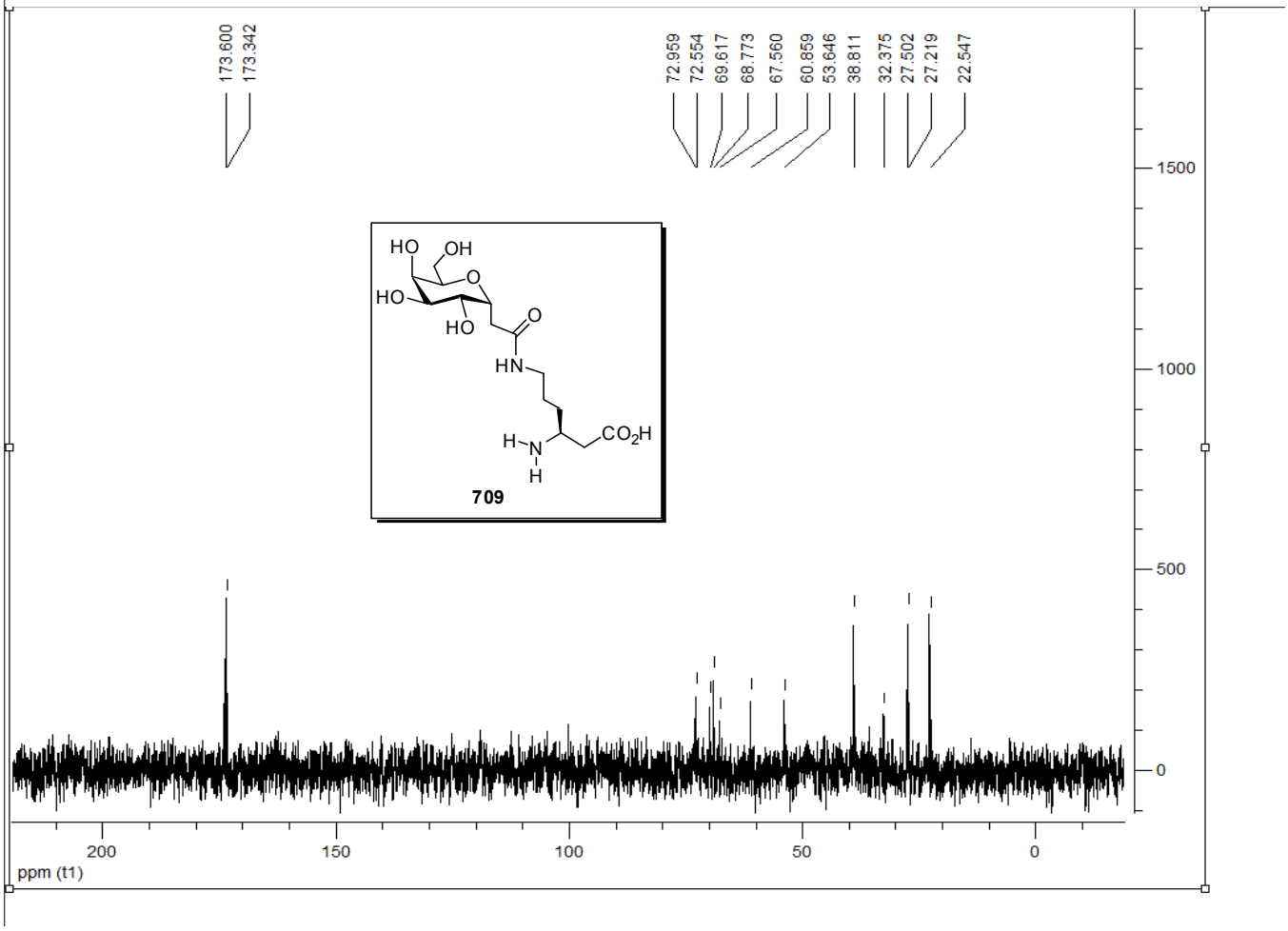

4.470
4.032
4.017
4.007
3.992
3.984
3.980
3.976
3.809
3.806
3.749
3.741
3.724
3.716
3.681
3.678
3.664
3.193
3.169
2.651
2.624
2.581
2.570
1.467
1.447
1.314
1.295
0.890
0.872
HO
OH
HO
O
HO
O
NHBu
707
ppm (t1)
1.02
2.11
1.07
1.13
2.11
2.01
2.07
1.69
2.08
3.00

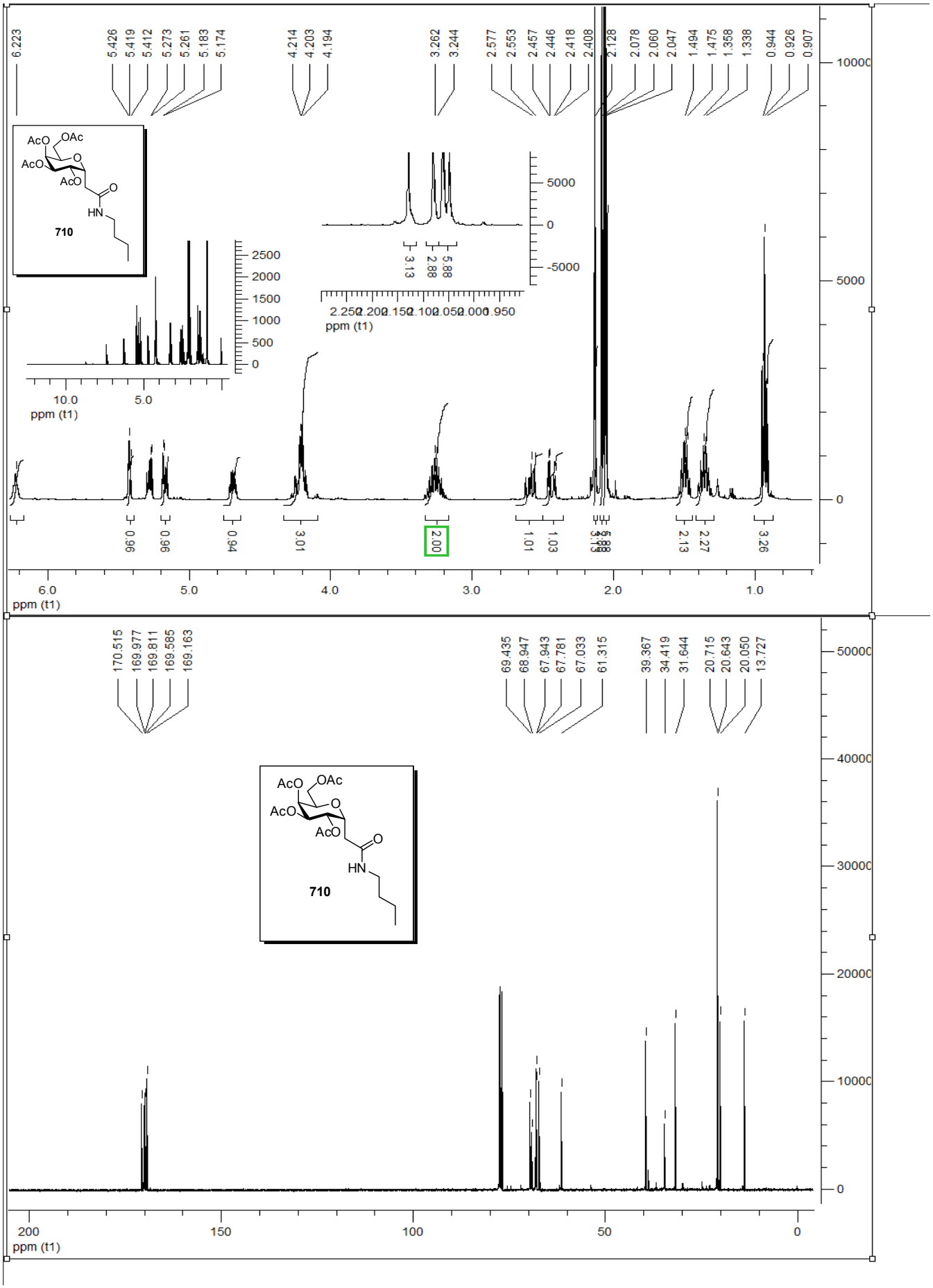

0.525
1.672
1.679
1.710
1.721
1.734
1.812
2.057
2.136
2.157
2.284
2.357
HO
OH
HO
O
HO
O
NHBu
707
sec (t1)

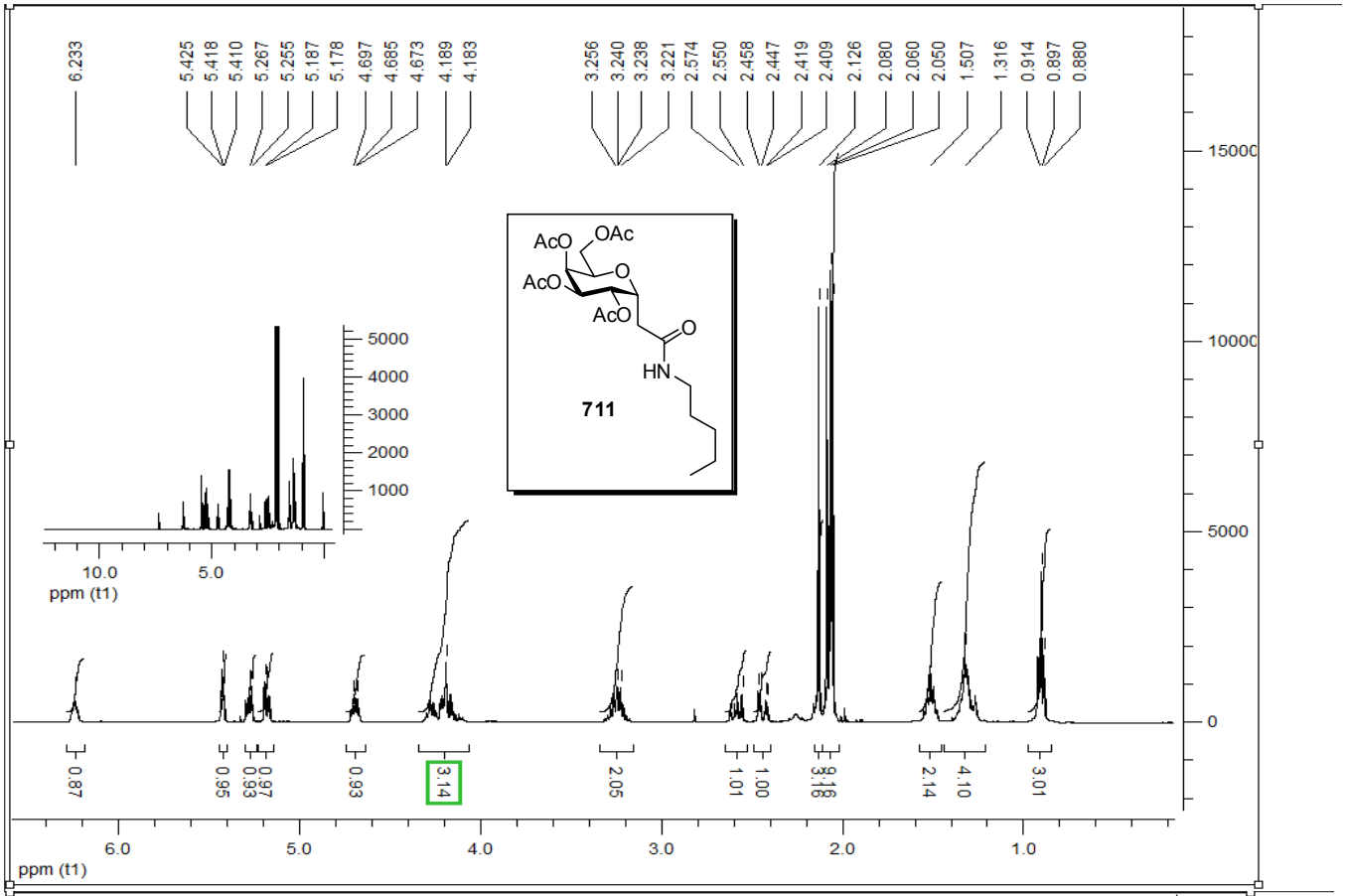

4.467
4.005
3.990
3.982
3.979
3.974
3.971
3.807
3.804
3.746
3.738
3.679
3.675
3.663
3.184
3.158
2.649
2.621
2.577
2.566
1.485
1.282
1.273
0.851
HO
OH
O
HO
HO
O
NHPent
708
2500
2000
1500
1000
500
0
10.0
5.0
ppm (t1)
5000
0
1.00
1.69
1.02
1.08
1.95
2.07
2.01
2.02
4.24
3.08
4.50
4.00
3.50
3.00
2.50
2.00
1.50
1.00
ppm (t1)

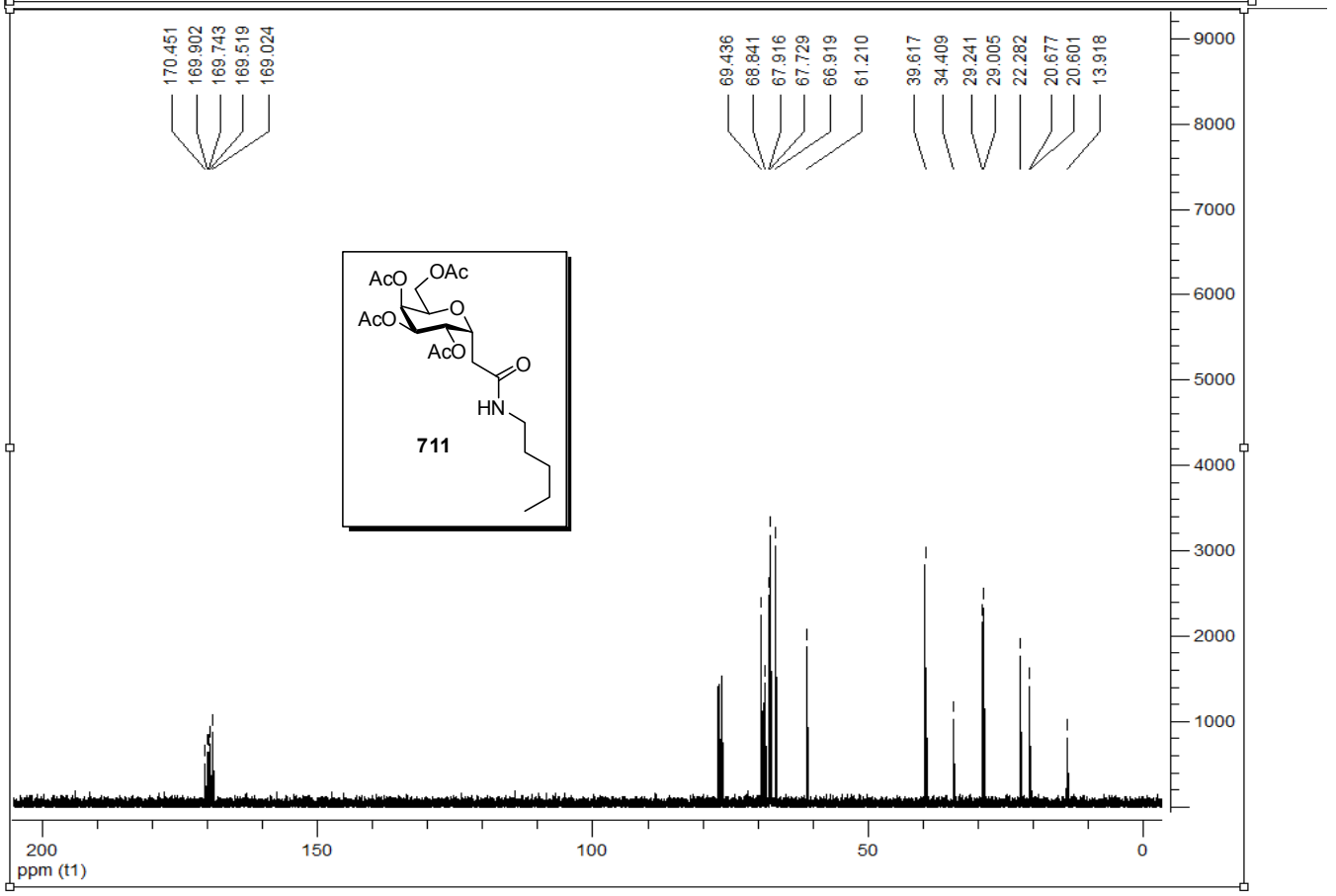

173.366
72.993
72.303
69.617
68.691
67.518
60.651
39.504
32.257
28.304
27.998
21.655
13.218
HO
OH
O
HO
HO
O
NHPent
708
1500
1000
5000
0
200
150
100
50
0
ppm (t1)

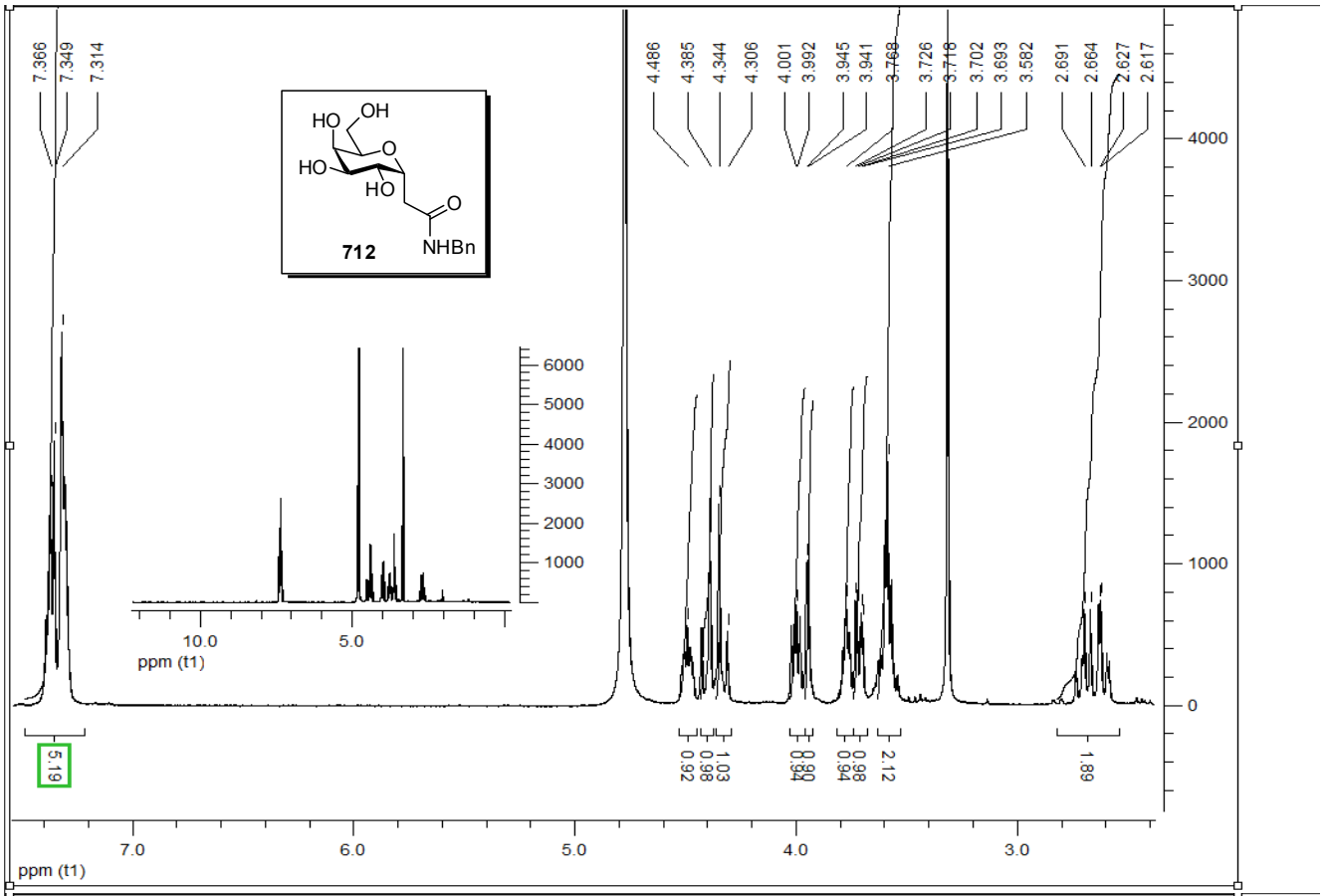

4.498
4.483
3.984
3.980
3.976
3.973
3.903
3.732
3.700
3.693
3.683
3.680
3.251
3.234
3.063
3.044
3.026
1.926
1.919
1.912
1.895
1.621
HO
OH
HO
HO
O
HN
H
N
CO2H
709
ppm (t1)
0.93
1.13
0.92
0.92
0.93
1.06
1.72
1.75
2.03
1.76
1.84
1.90
5.00
4.50
4.00
3.50
3.00
2.50
2.00
1.50

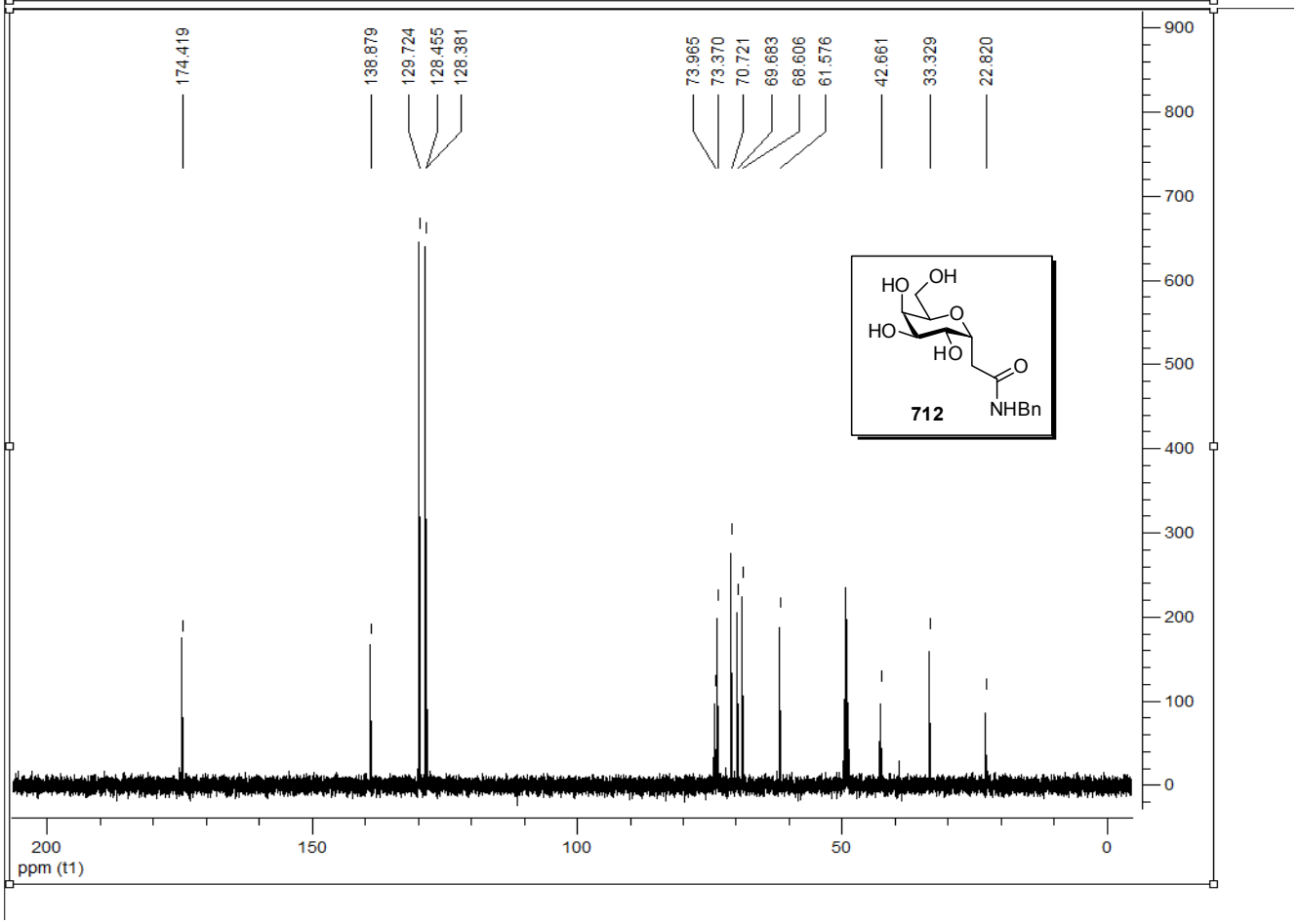

173.600
173.342
72.959
72.554
69.617
68.773
67.560
60.859
53.646
38.811
32.375
27.502
27.219
22.547
HO
OH
HO
HO
O
HN
H
N
CO2H
709
ppm (t1)
200
150
100
50
0

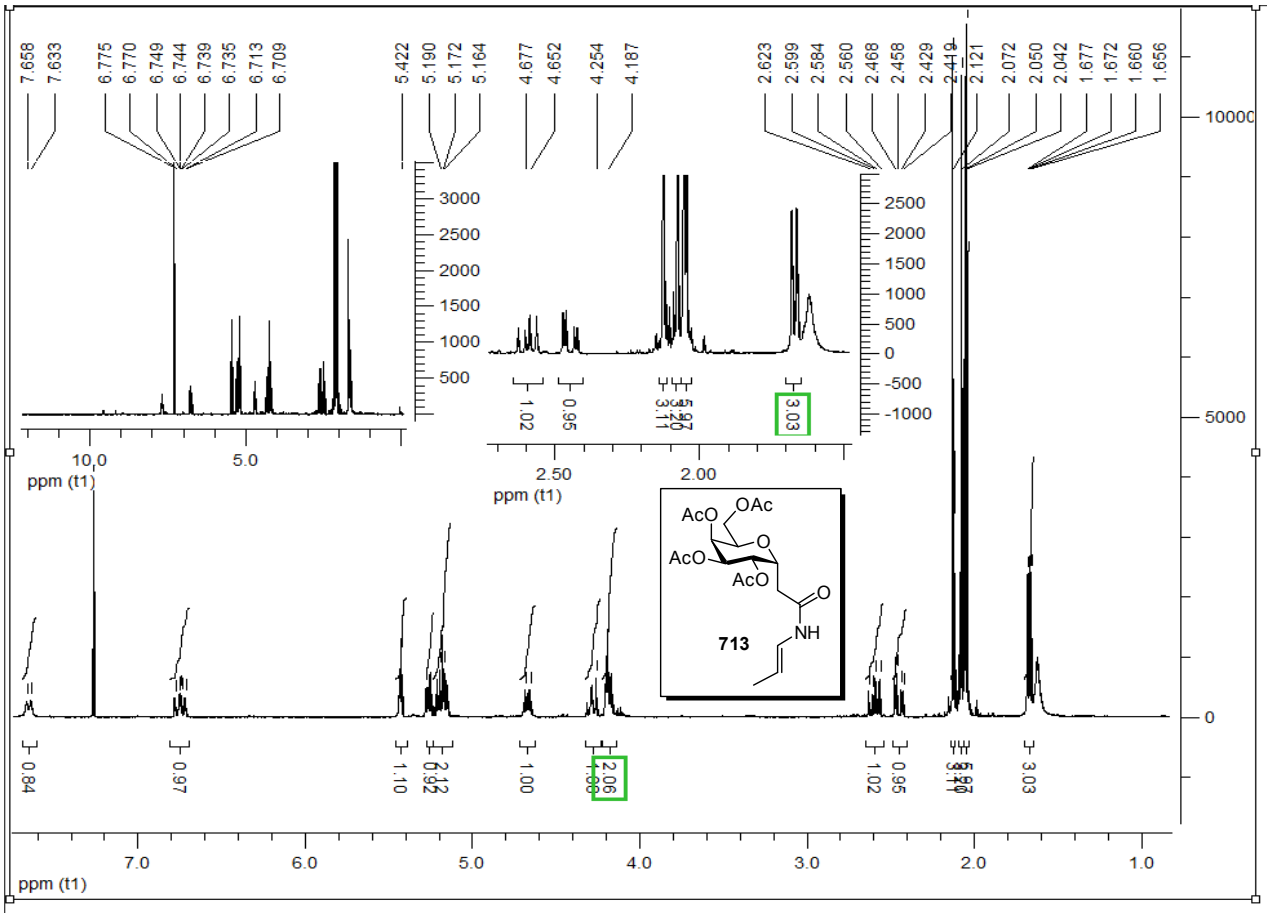

710
ppm (t1)
710
ppm (t1)

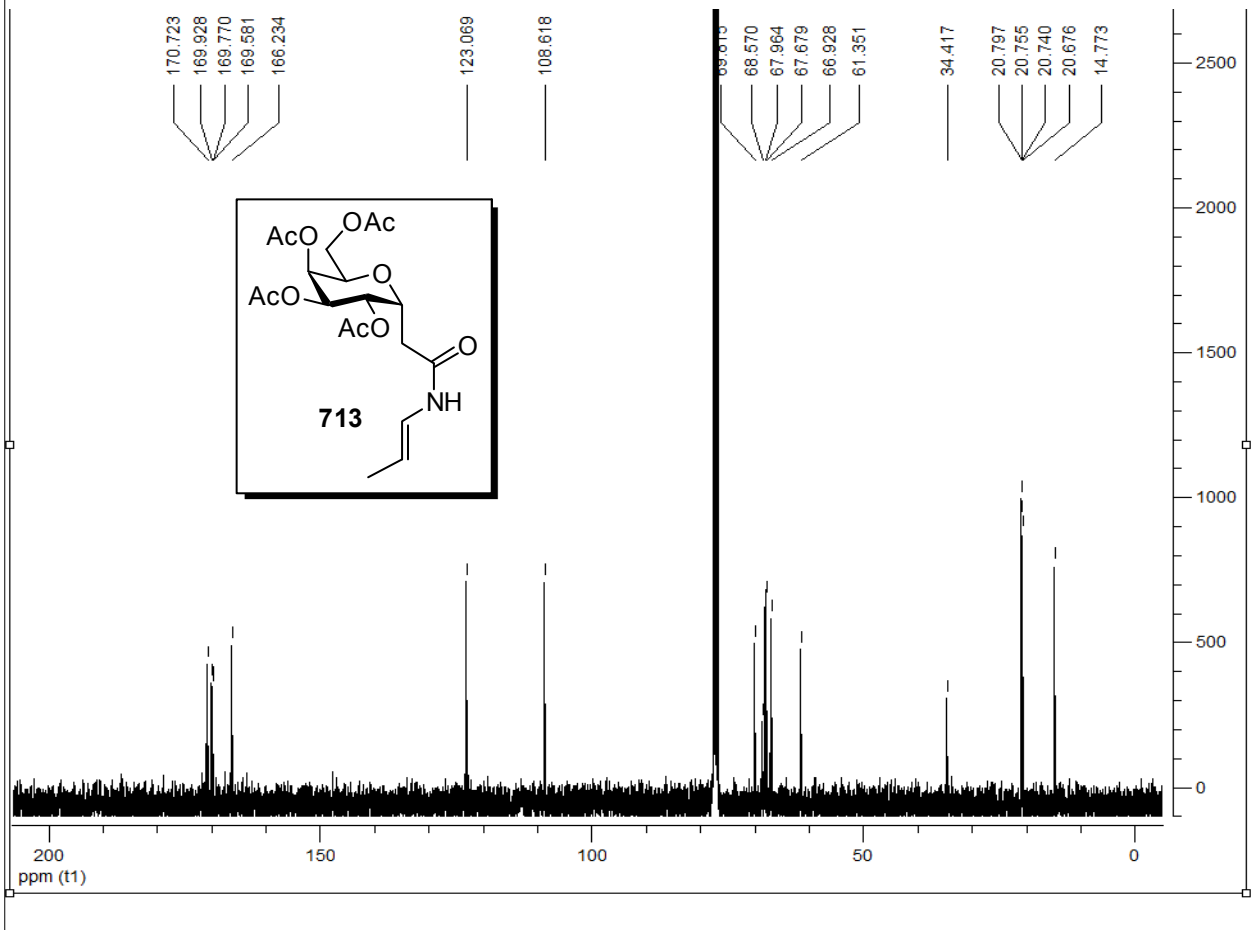

6.233
5.425
5.418
5.410
5.267
5.255
5.187
5.178
4.697
4.685
4.673
4.189
4.183
3.256
3.240
3.238
3.221
2.574
2.550
2.458
2.447
2.419
2.409
2.126
2.080
2.060
2.050
1.507
1.316
0.914
0.897
0.880
AcO
OAc
AcO
AcO
O
HN
O
711
ppm (t1)
0.87
0.96
0.93
0.87
0.93
3.14
2.05
1.01
1.00
3.18
2.14
4.10
3.01

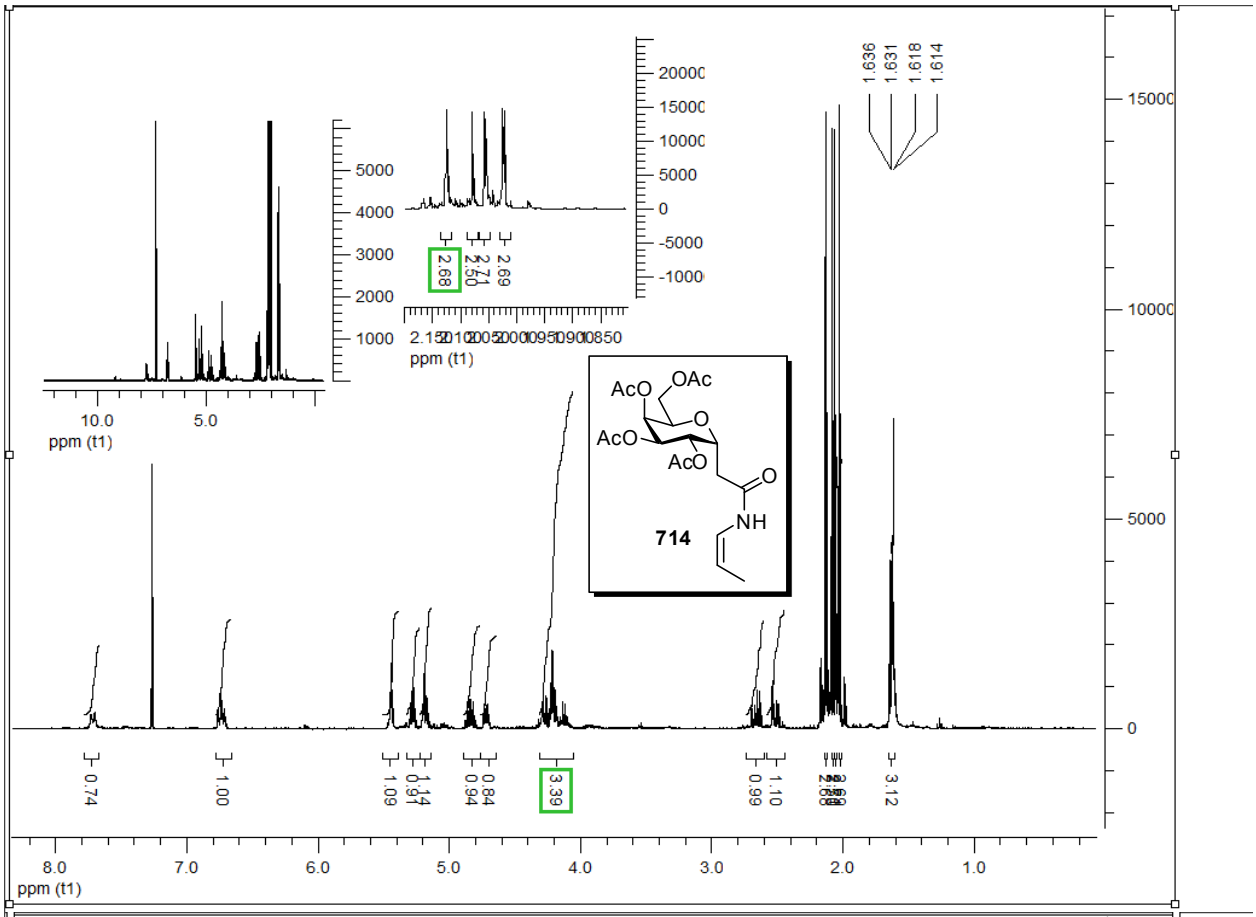

170.451
169.902
169.743
169.519
169.024
69.436
68.841
67.916
67.729
66.919
61.210
39.617
34.409
29.241
29.005
22.282
20.677
20.601
13.918
AcO
OAc
AcO
AcO
O
HN
O
711
ppm (t1)

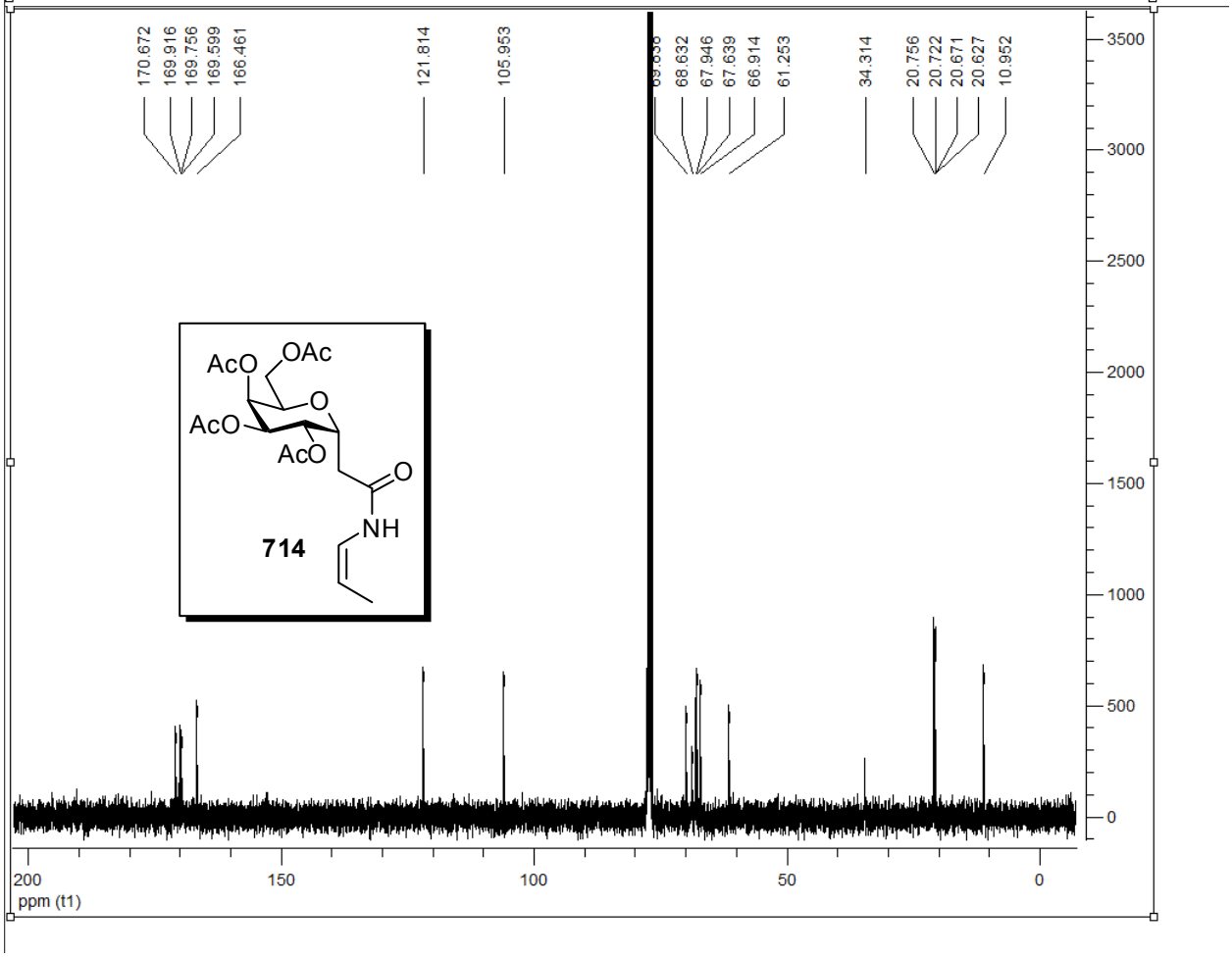

7.366
7.349
7.314
4.486
4.385
4.344
4.306
4.001
3.992
3.945
3.941
3.768
3.726
3.718
3.702
3.693
3.582
2.691
2.664
2.627
2.617
712
NHBn
ppm (t1)
5.19
0.92
0.98
1.03
0.98
0.94
2.12
1.89

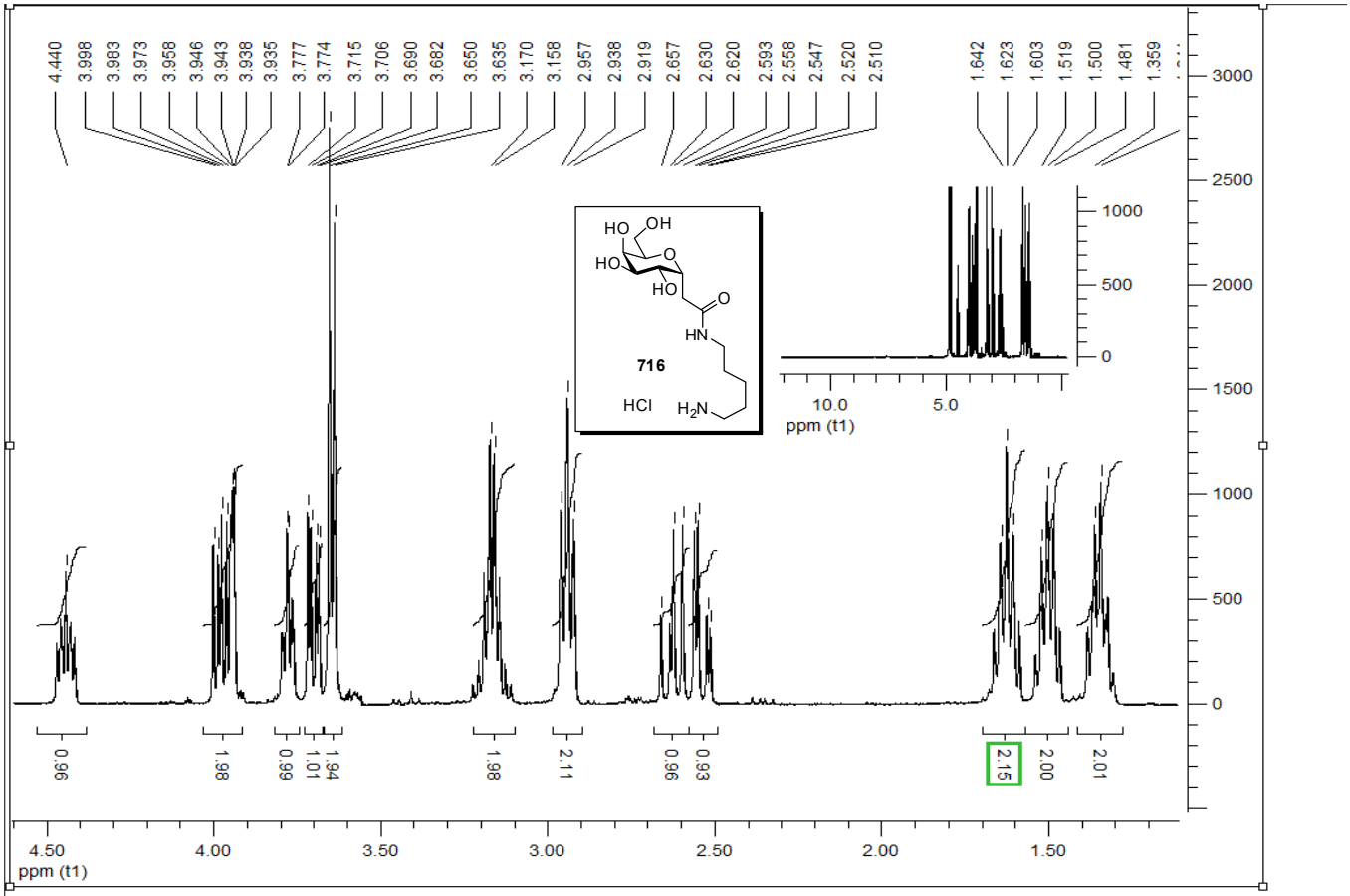

174.419
138.879
129.724
128.455
128.381
73.965
73.370
70.721
69.683
68.606
61.576
42.661
33.329
22.820
712
NHBn
ppm (t1)

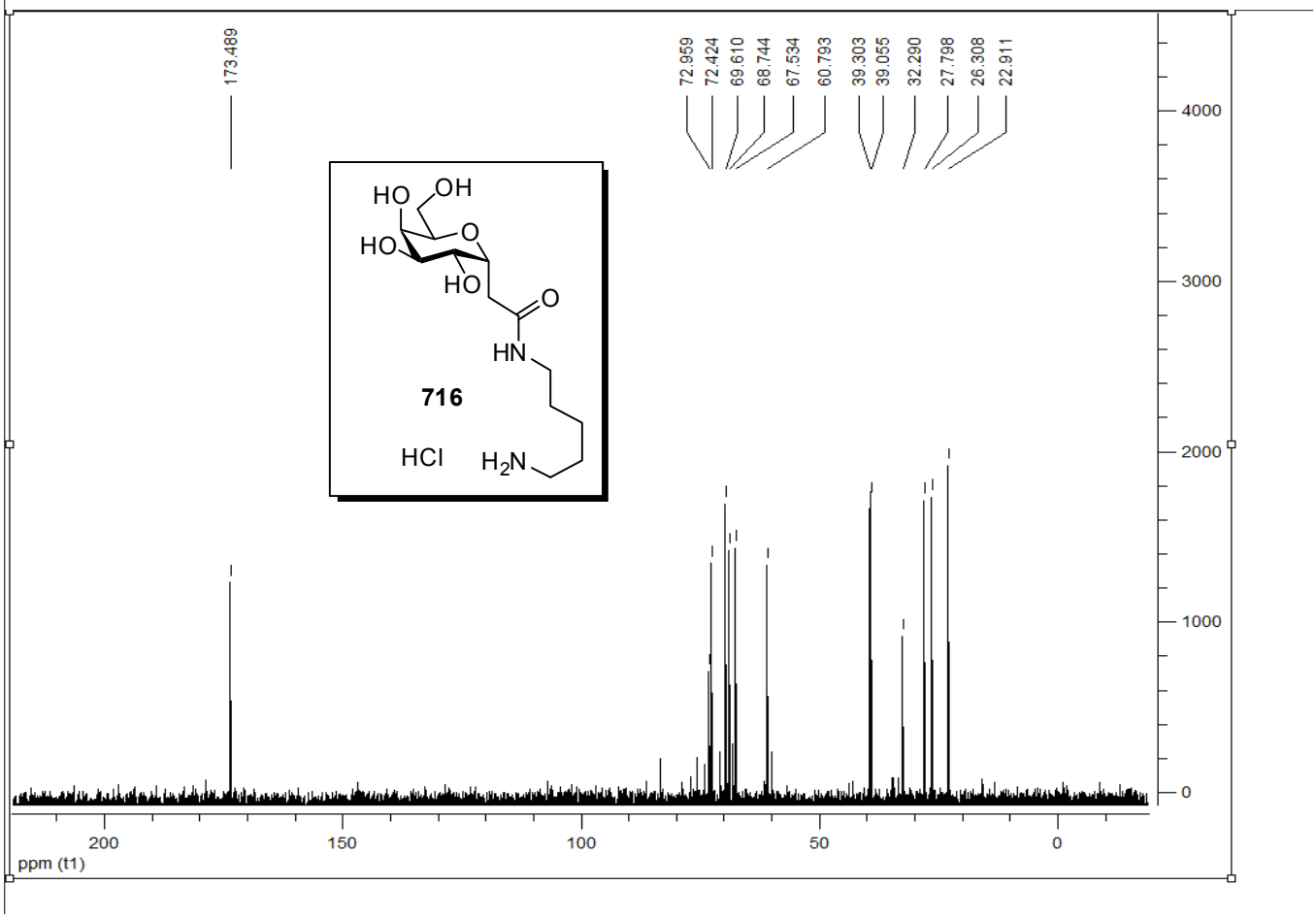

7.658
7.633
6.775
6.770
6.749
6.744
6.739
6.735
6.713
6.709
5.422
5.190
5.172
5.164
4.677
4.652
4.254
4.187
2.623
2.599
2.584
2.560
2.468
2.458
2.429
2.419
2.121
2.072
2.050
2.042
1.677
1.672
1.660
1.656
ppm (t1)
AcO
OAc
AcO
AcO
O
NH
O
713
0.84
0.97
1.10
2.12
1.00
2.06
1.02
0.95
3.11
3.03

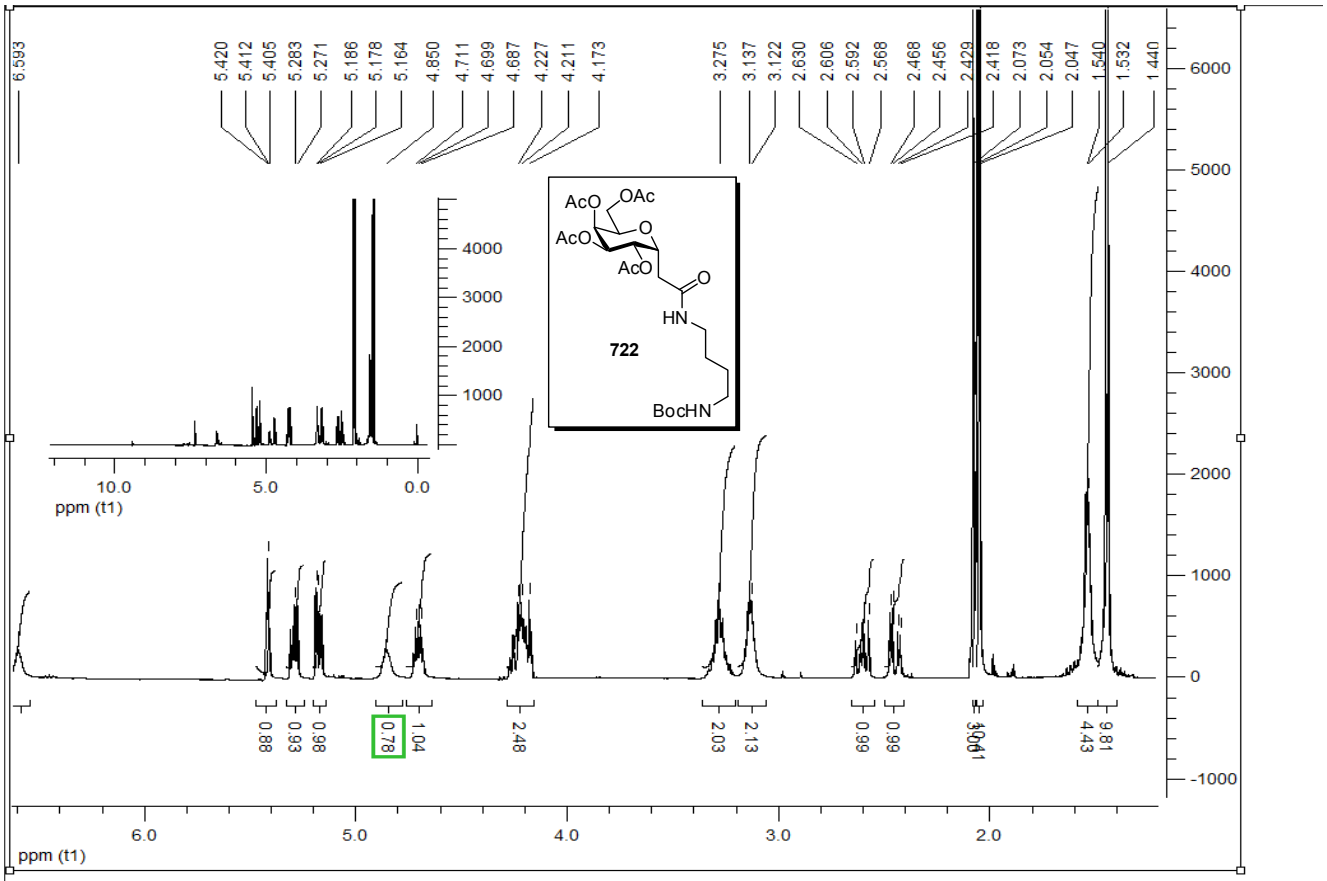

170.723
169.928
169.770
169.581
166.234
123.069
108.618
68.570
67.964
67.679
66.928
61.351
34.417
20.797
20.755
20.740
20.676
14.773
ppm (t1)
AcO
OAc
AcO
AcO
O
NH
O
713

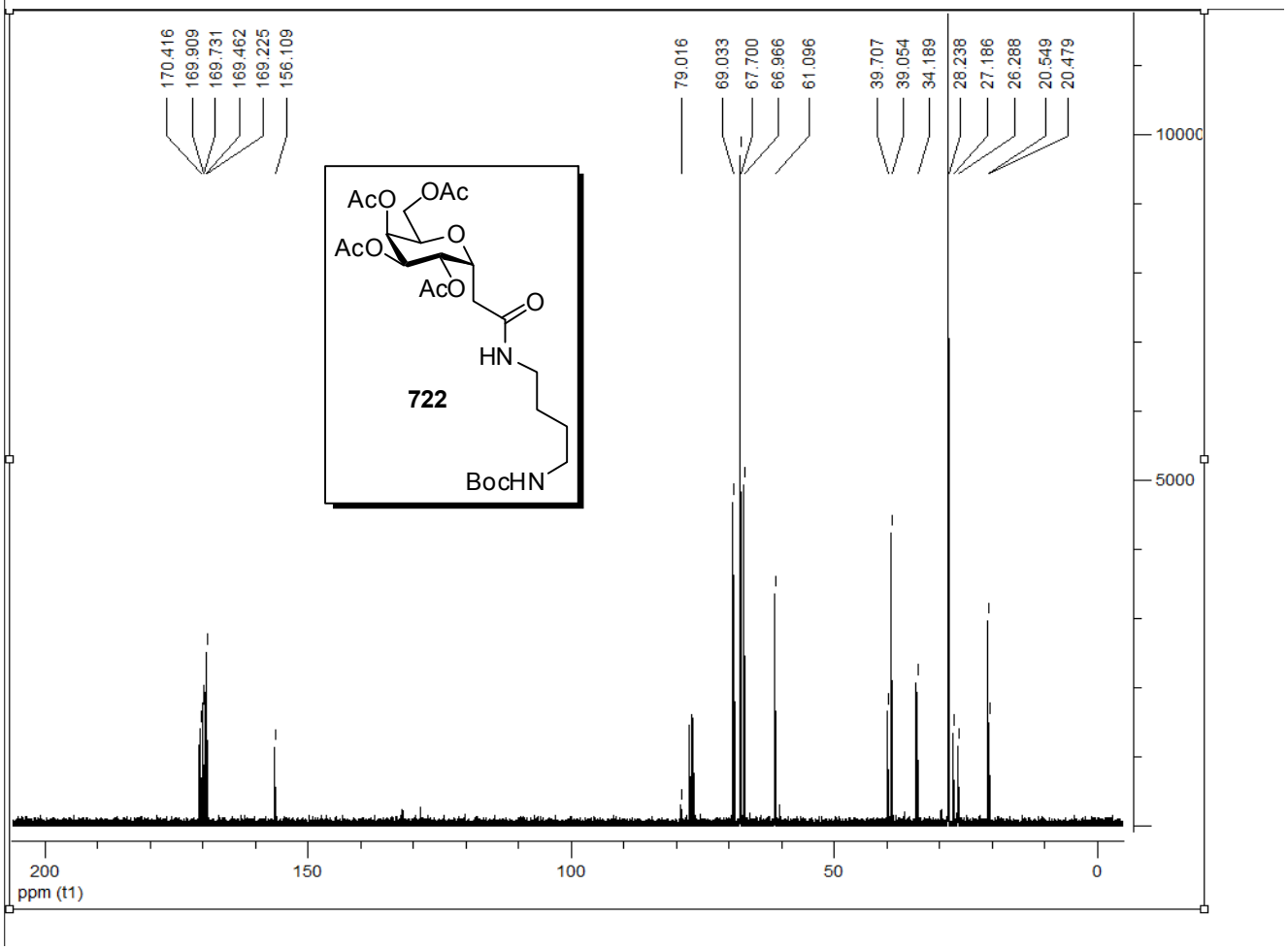

1.636
1.631
1.618
1.614
AcO
OAc
AcO
AcO
O
NH
714
0.74
1.00
1.09
0.91
1.14
0.84
0.94
3.39
0.99
1.10
3.12
ppm (t1)

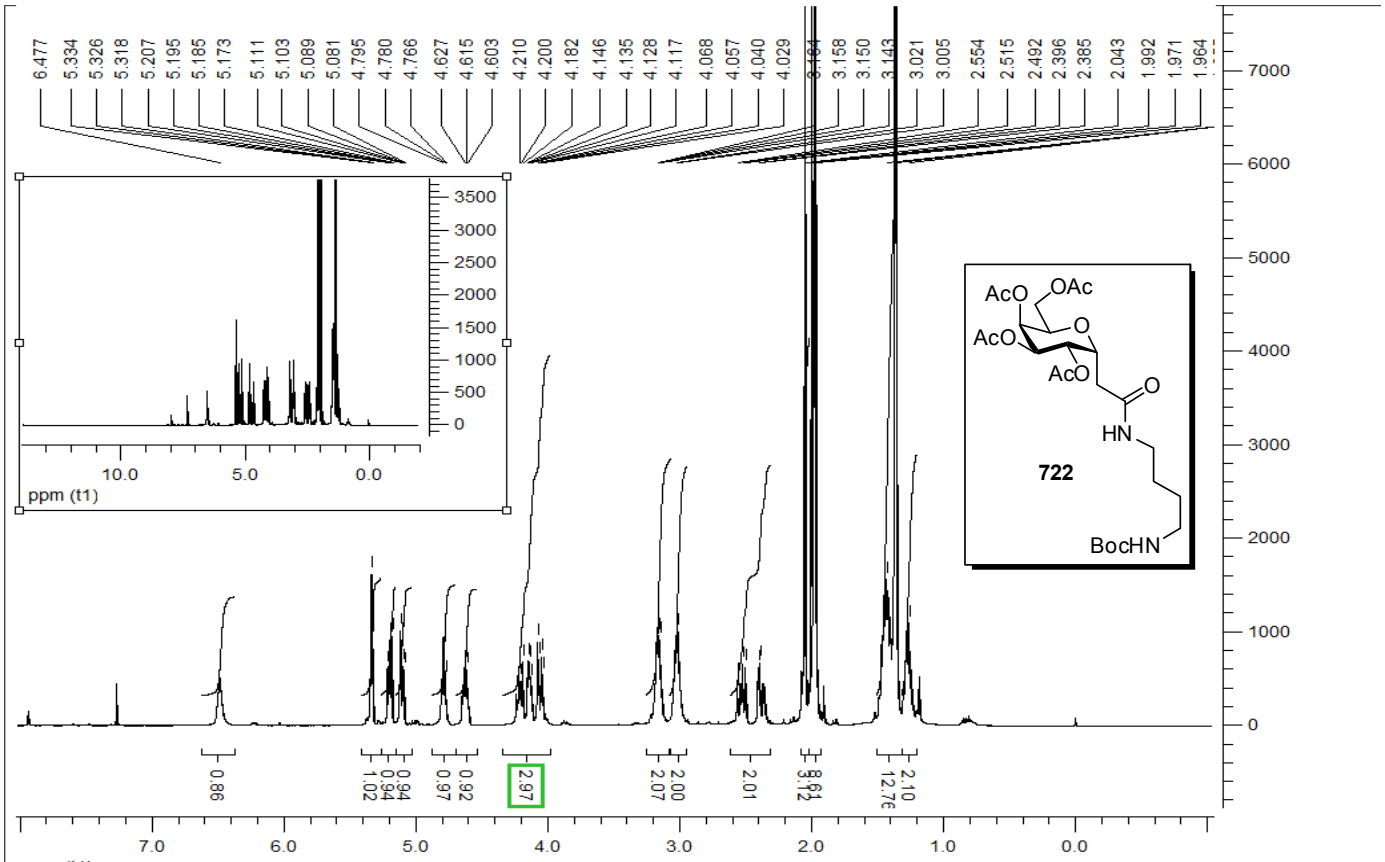

170.672
169.916
169.756
169.599
166.461
121.814
105.953
68.632
67.946
67.639
66.914
61.253
34.314
20.756
20.722
20.671
20.627
10.952
AcO
OAc
AcO
AcO
O
NH
714
ppm (t1)

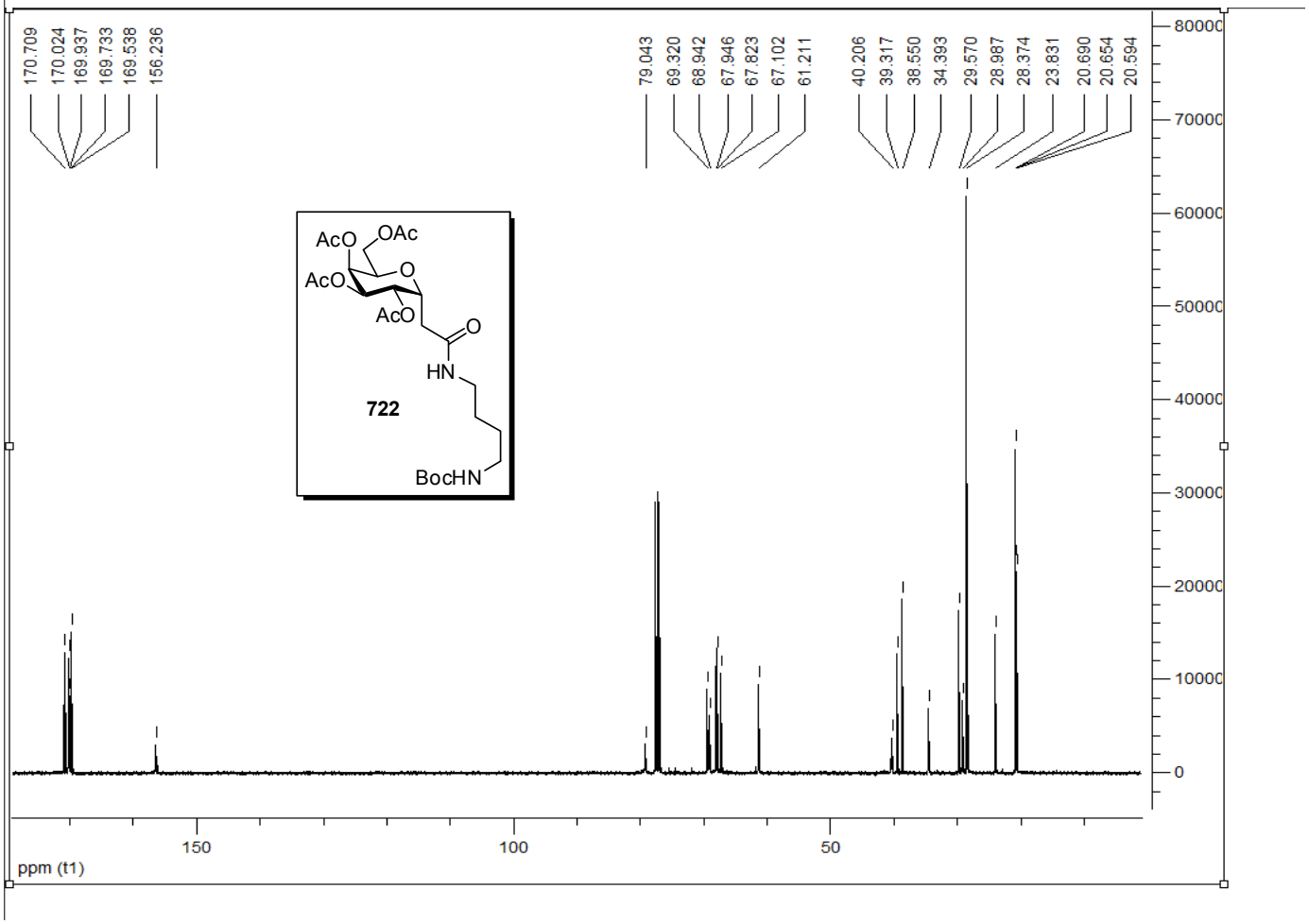

4.440
3.998
3.983
3.973
3.958
3.946
3.943
3.938
3.935
3.777
3.774
3.715
3.706
3.690
3.682
3.650
3.635
3.170
3.158
2.957
2.938
2.919
2.657
2.630
2.620
2.593
2.558
2.547
2.520
2.510
1.642
1.623
1.603
1.519
1.500
1.481
1.359
HO
OH
O
HO
HO
O
HN
716
HCl
H2N
10.0
5.0
ppm (t1)
0.96
1.98
0.99
1.01
1.64
1.98
2.11
0.96
0.93
2.15
2.00
2.01
4.50
4.00
3.50
3.00
2.50
2.00
1.50
ppm (t1)

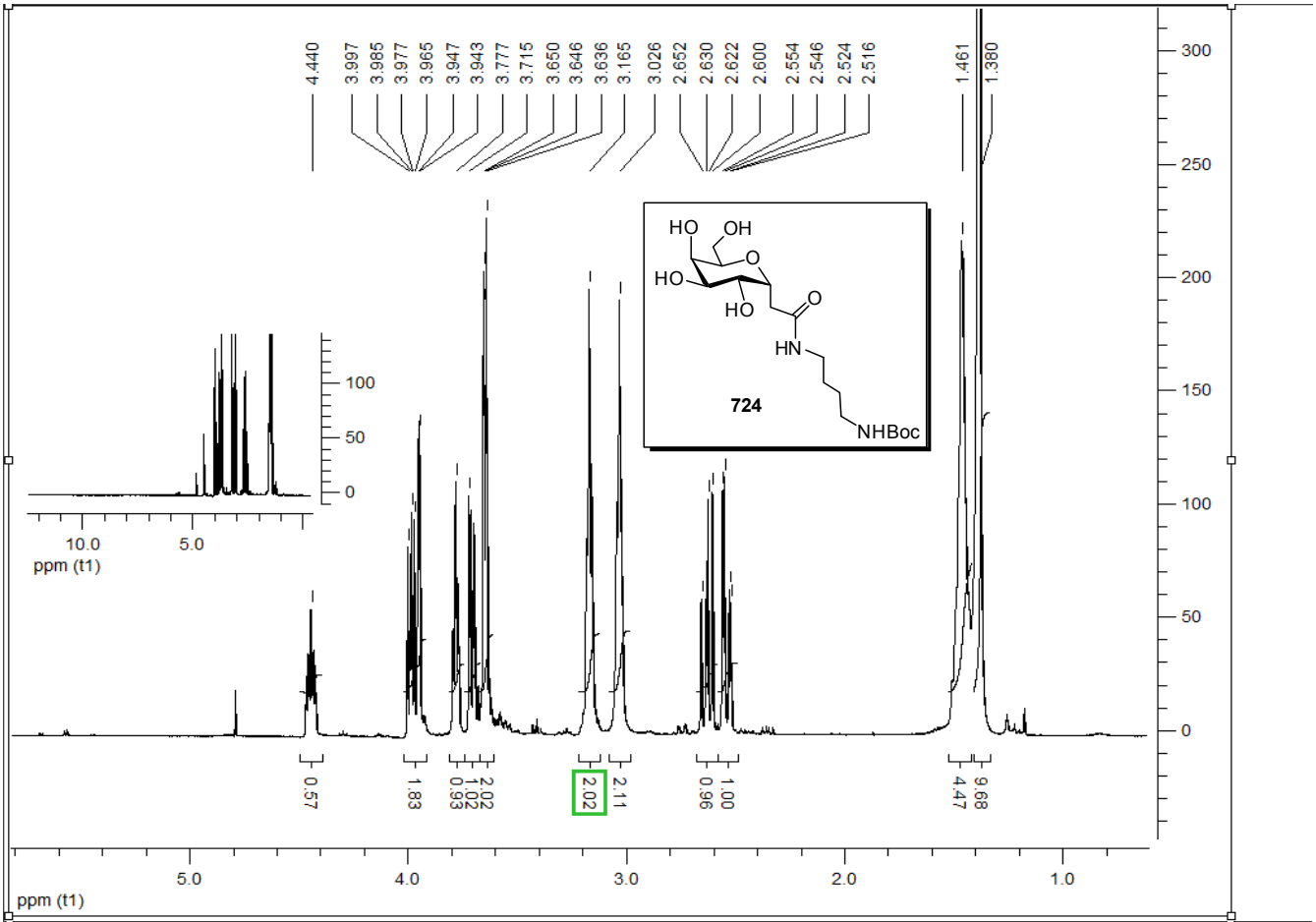

173.489
72.959
72.424
69.610
68.744
67.534
60.793
39.303
39.055
32.290
27.798
26.308
22.911
HO
OH
O
HO
HO
O
HN
716
HCl
H2N
200
150
100
50
0
ppm (t1)

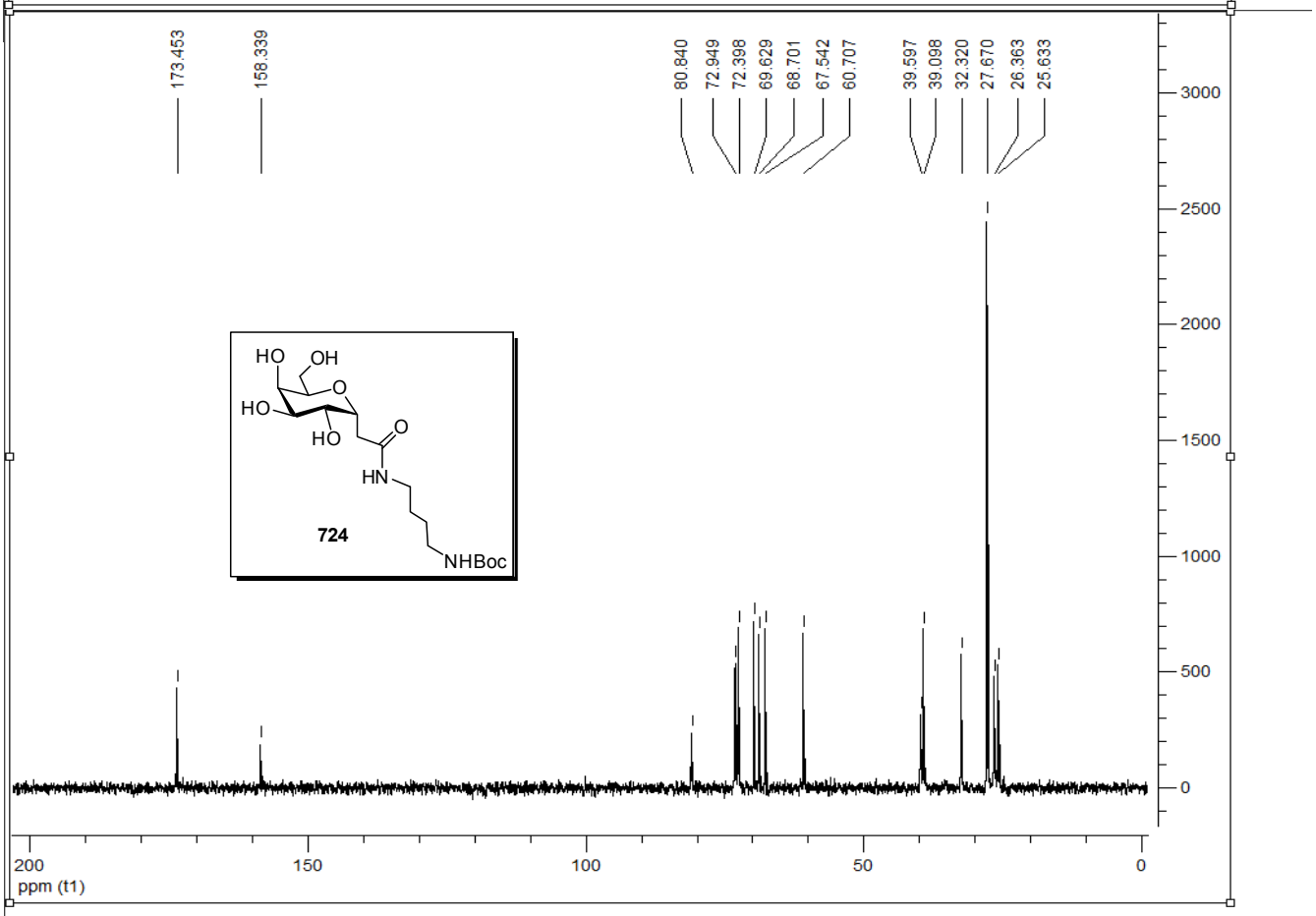

6.593
5.420
5.412
5.405
5.283
5.271
5.186
5.178
5.164
4.850
4.711
4.699
4.687
4.227
4.211
4.173
3.275
3.137
3.122
2.630
2.606
2.592
2.568
2.468
2.456
2.429
2.418
2.073
2.054
2.047
1.540
1.532
1.440
AcO
OAc
AcO
AcO
O
O
HN
722
BocHN
ppm (t1)
0.88
0.93
0.98
0.78
1.04
2.48
2.03
2.13
0.99
0.99
30.41
4.43
9.81

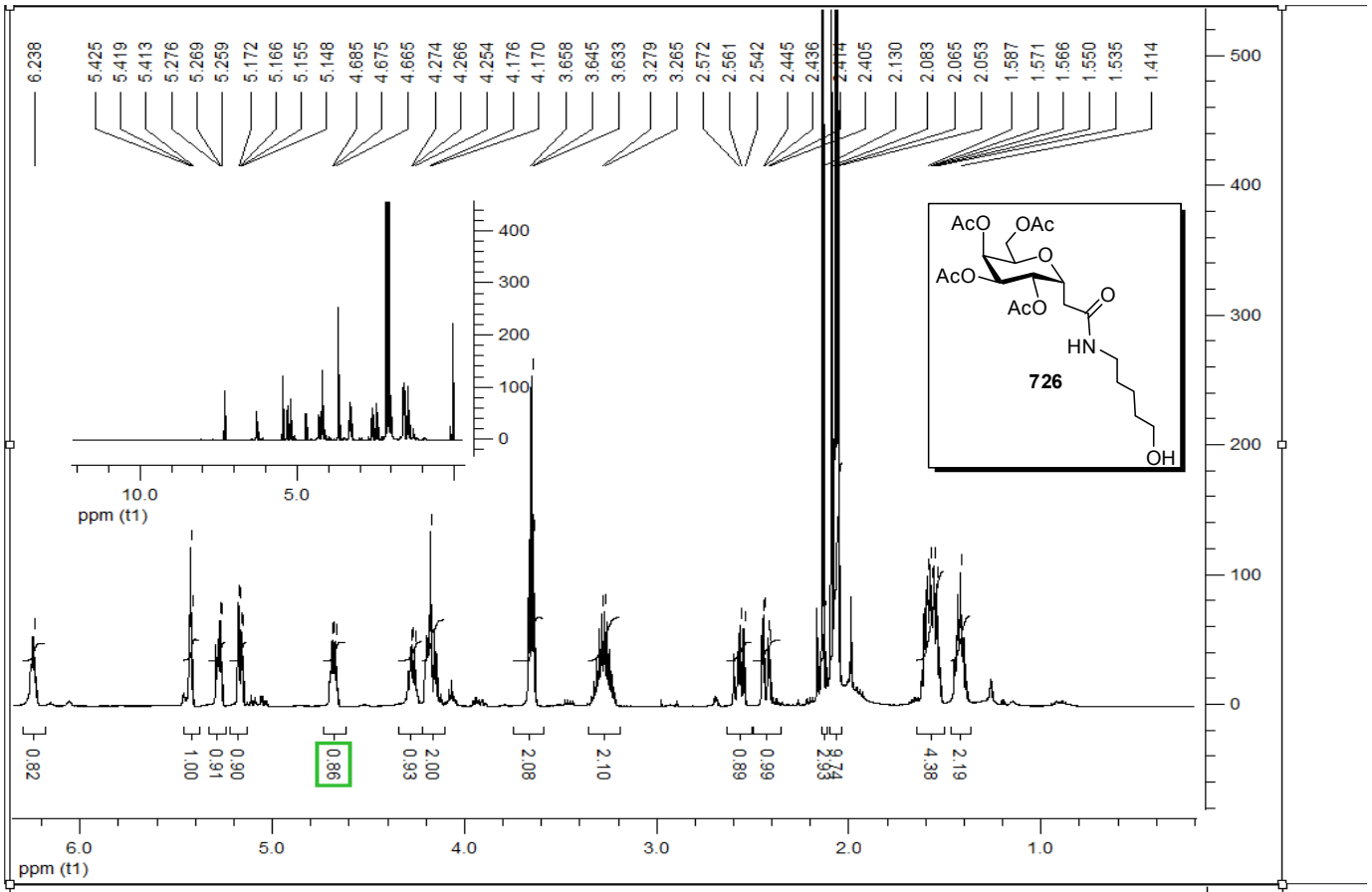

170.416
169.909
169.731
169.462
169.225
156.109
79.016
69.033
67.700
66.966
61.096
39.707
39.054
34.189
28.238
27.186
26.288
20.549
20.479
AcO
OAc
AcO
AcO
O
O
HN
722
BocHN
ppm (t1)

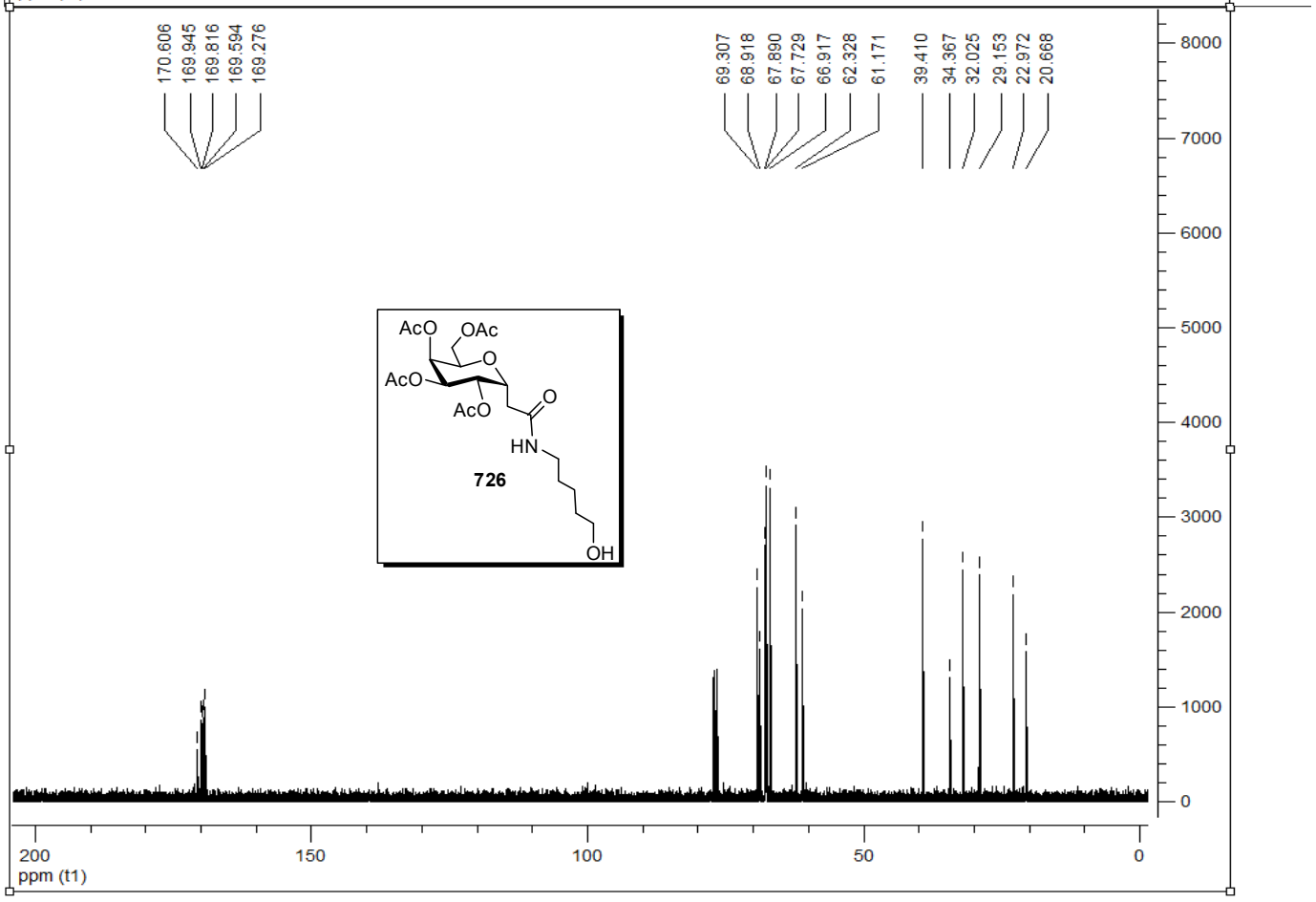

6.477
5.334
5.326
5.318
5.207
5.195
5.185
5.173
5.111
5.103
5.089
5.081
4.795
4.780
4.766
4.627
4.615
4.603
4.210
4.200
4.182
4.146
4.135
4.128
4.117
4.068
4.057
4.040
4.029
3.158
3.150
3.143
3.021
3.005
2.554
2.515
2.492
2.396
2.385
2.043
1.992
1.971
1.964
ppm (t1)
AcO
OAc
AcO
AcO
O
HN
O
722
BocHN
0.86
1.02
0.94
0.84
0.97
0.92
2.97
2.07
2.00
2.01
3.17
8.91
2.10
12.76
ppm (t1)

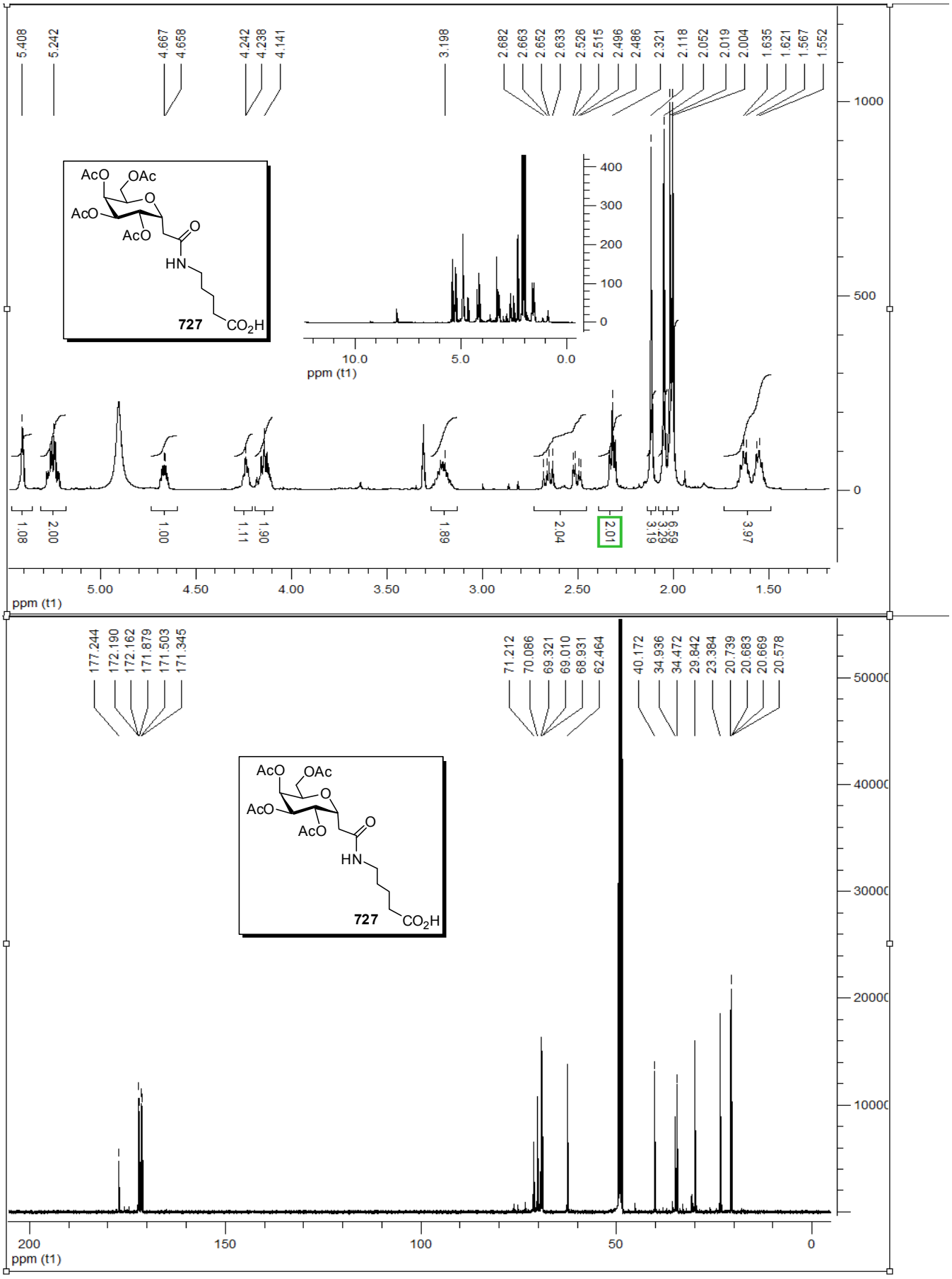

170.709
170.024
169.937
169.733
169.538
156.236
79.043
69.320
68.942
67.946
67.823
67.102
61.211
40.206
39.317
38.550
34.393
29.570
28.987
28.374
23.831
20.690
20.654
20.594
AcO
OAc
AcO
O
AcO
HN
O
722
BocHN
ppm (t1)

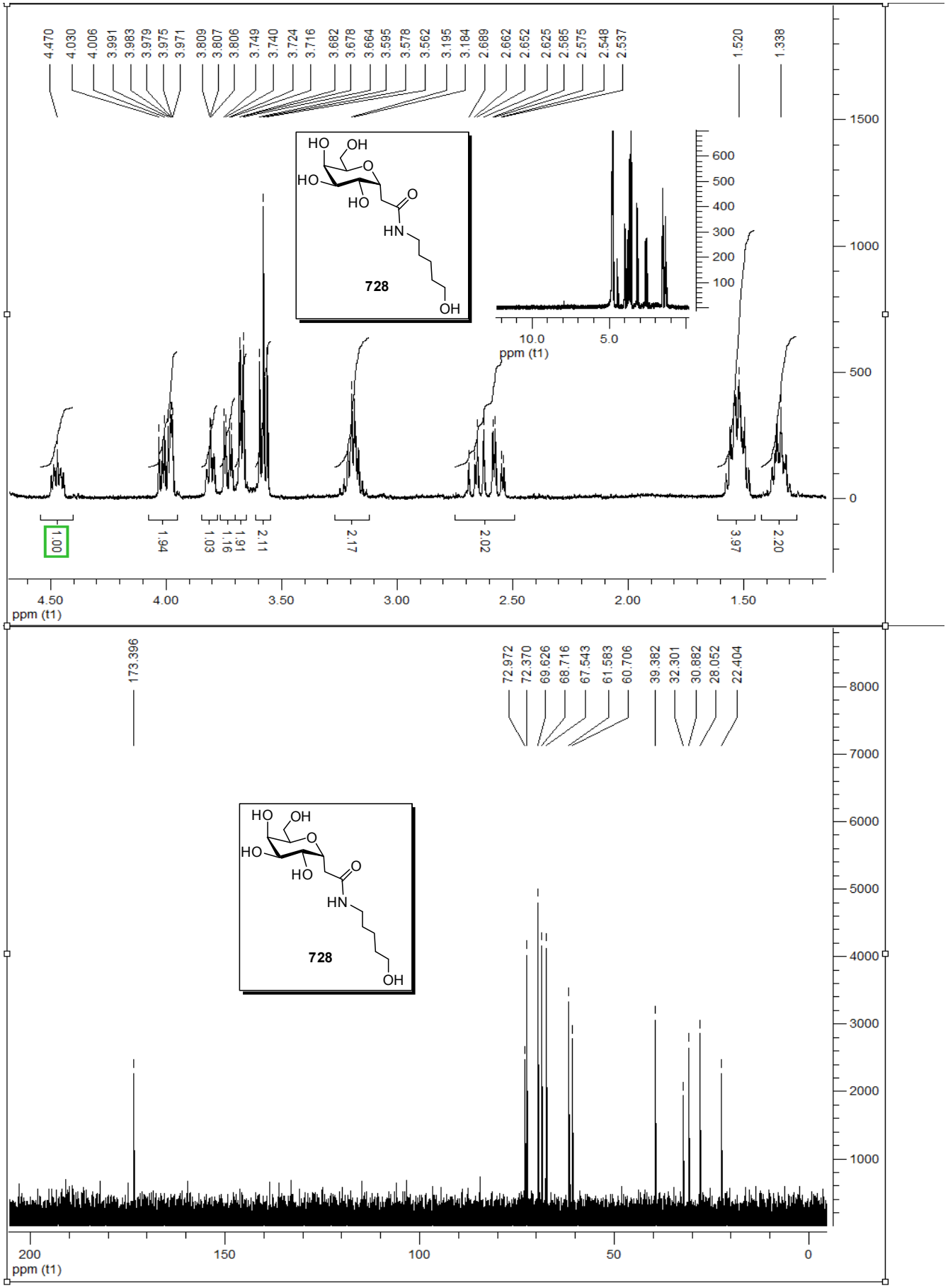

4.440
3.997
3.985
3.977
3.965
3.947
3.943
3.777
3.715
3.650
3.646
3.636
3.165
3.026
2.652
2.630
2.622
2.600
2.554
2.546
2.524
2.516
1.461
1.380
HO
OH
O
HO
HO
O
HN
NHBoc
724
ppm (t1)
0.57
1.83
0.93
1.02
2.02
2.11
0.96
1.00
4.47
9.68

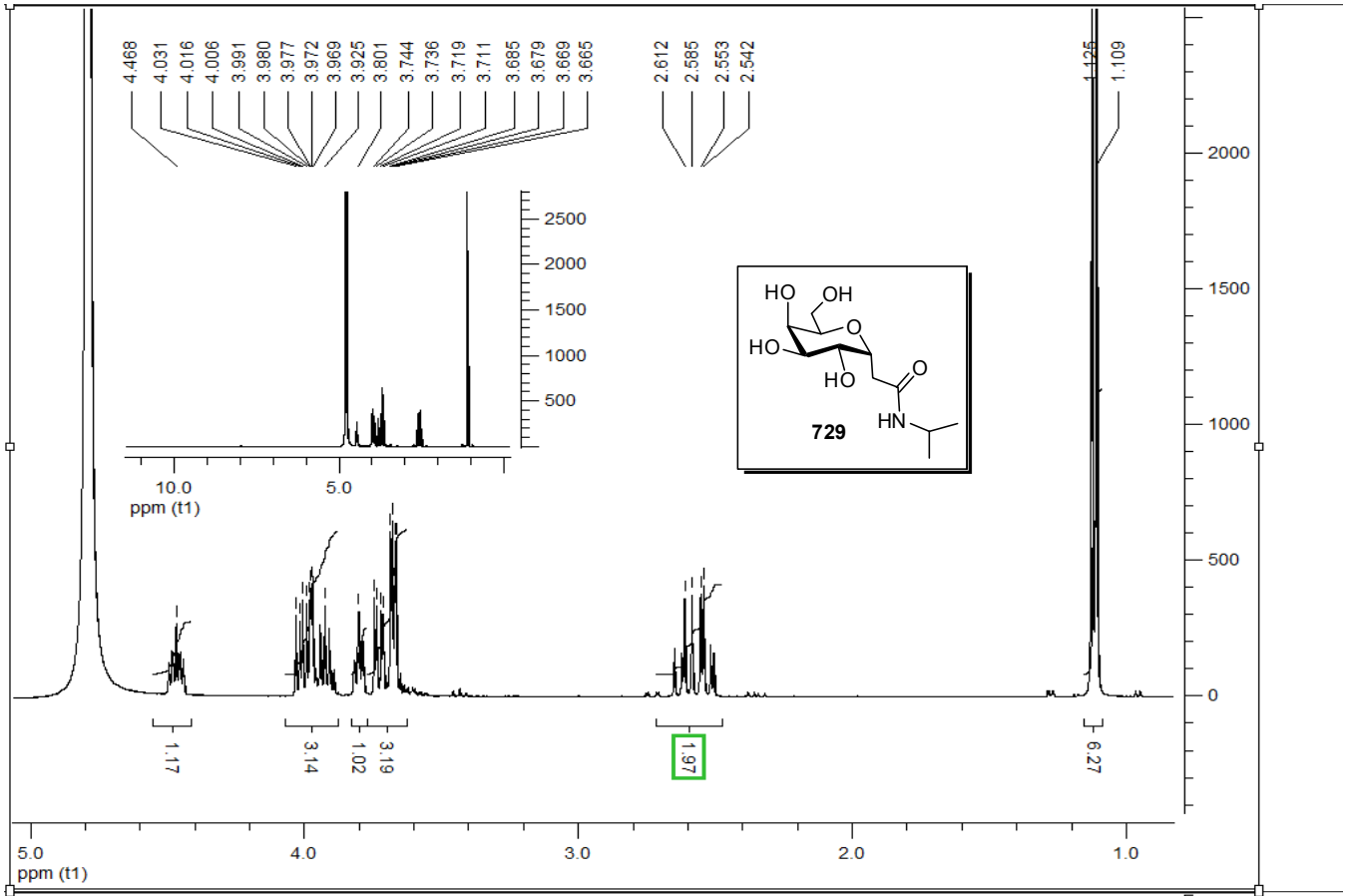

173.453
158.339
80.840
72.949
72.398
69.629
68.701
67.542
60.707
39.597
39.098
32.320
27.670
26.363
25.633
HO
OH
O
HO
HO
O
HN
NHBoc
724
ppm (t1)

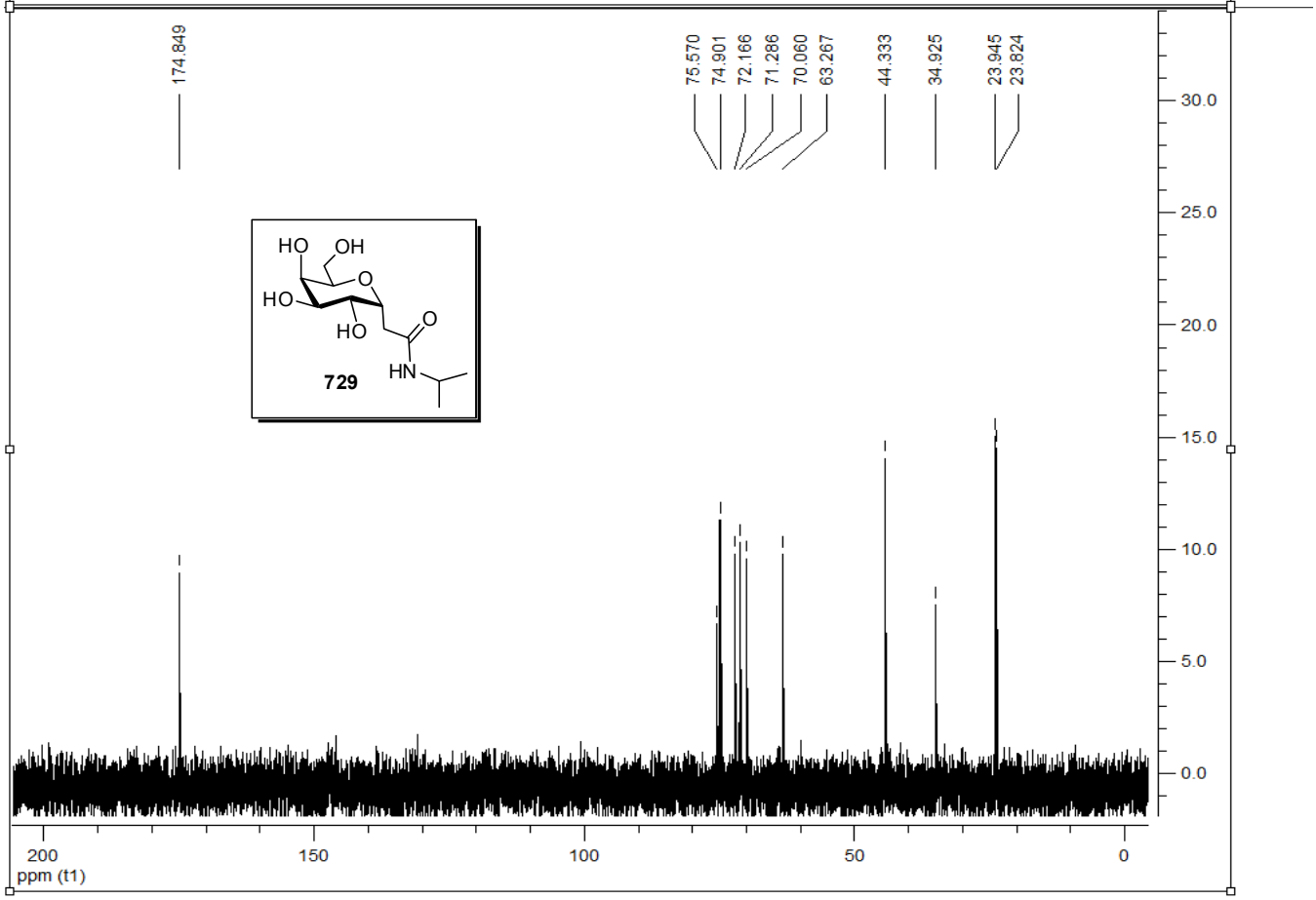

6.238
5.425
5.419
5.413
5.276
5.269
5.259
5.172
5.166
5.155
5.148
4.685
4.675
4.665
4.274
4.266
4.254
4.176
4.170
3.658
3.645
3.633
3.279
3.265
2.572
2.561
2.542
2.445
2.436
2.414
2.405
2.130
2.083
2.065
2.053
1.587
1.571
1.566
1.550
1.535
1.414
AcO
OAc
AcO
AcO
HN
726
OH
ppm (t1)
0.82
1.00
0.91
0.90
0.86
0.93
2.00
2.08
2.10
0.89
0.99
7.93
8.74
4.38
2.19

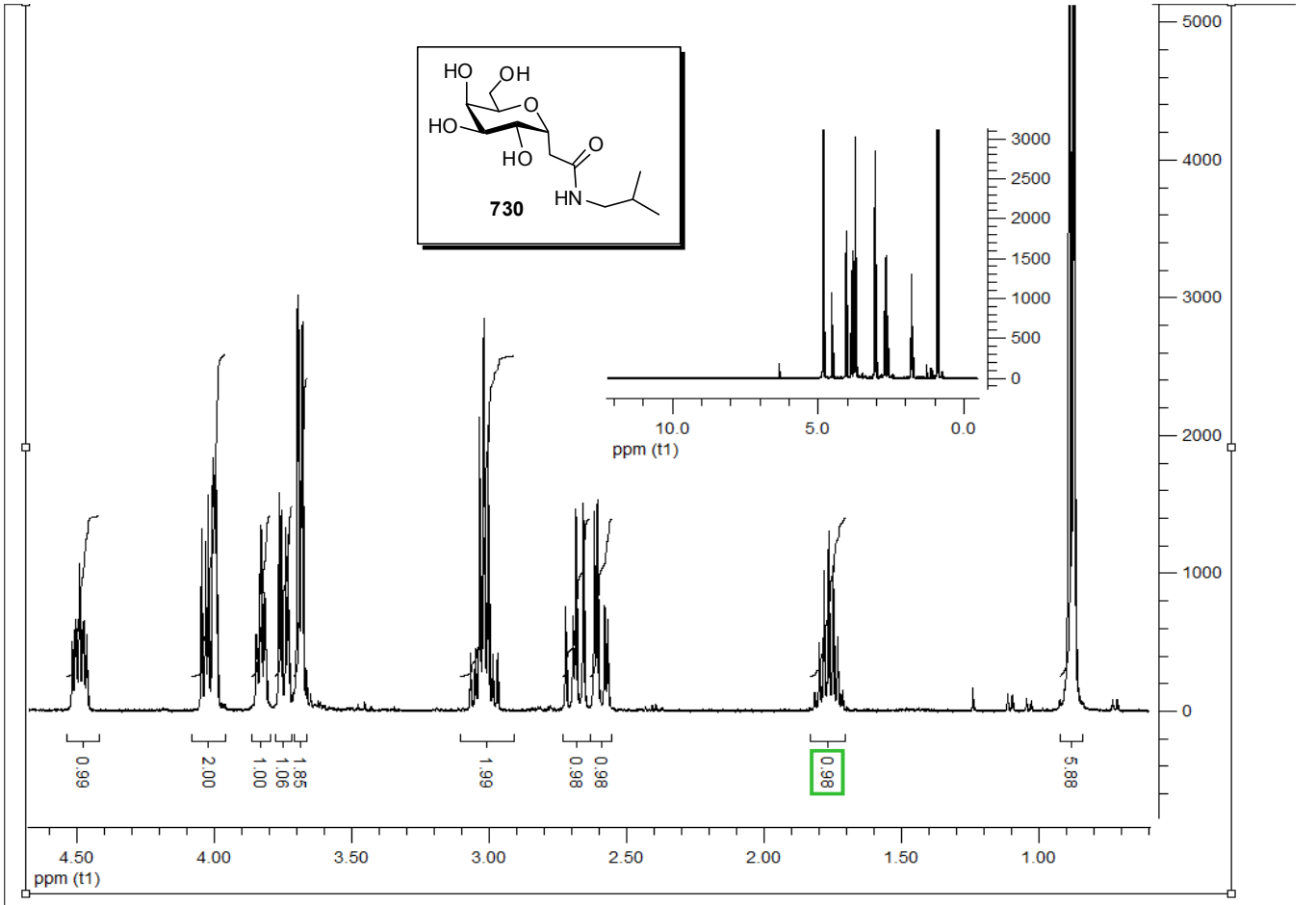

170.606
169.945
169.816
169.594
169.276
69.307
68.918
67.890
67.729
66.917
62.328
61.171
39.410
34.367
32.025
29.153
22.972
20.668
AcO
OAc
AcO
AcO
HN
726
OH
ppm (t1)

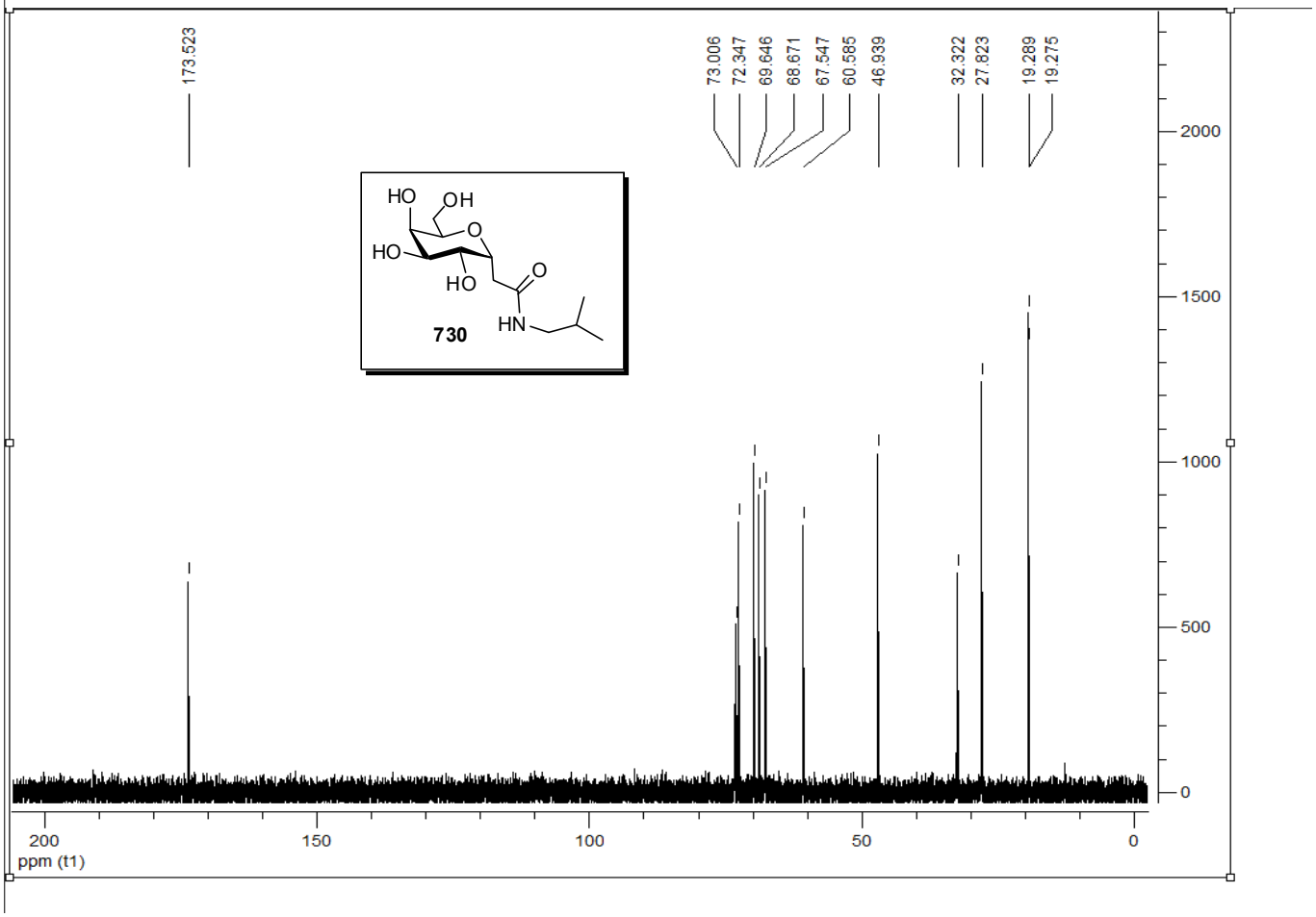

5.408
5.242
4.667
4.658
4.242
4.238
4.141
3.198
2.682
2.663
2.652
2.633
2.526
2.515
2.496
2.486
2.321
2.118
2.052
2.019
2.004
1.635
1.621
1.567
1.552
AcO
OAc
AcO
AcO
O
HN
O
727
CO2H
ppm (t1)
1.08
2.00
1.00
1.11
1.90
1.89
2.04
2.01
3.19
3.29
3.59
3.97
177.244
172.190
172.162
171.879
171.503
171.345
71.212
70.086
69.321
69.010
68.931
62.464
40.172
34.936
34.472
29.842
23.384
20.739
20.683
20.669
20.578

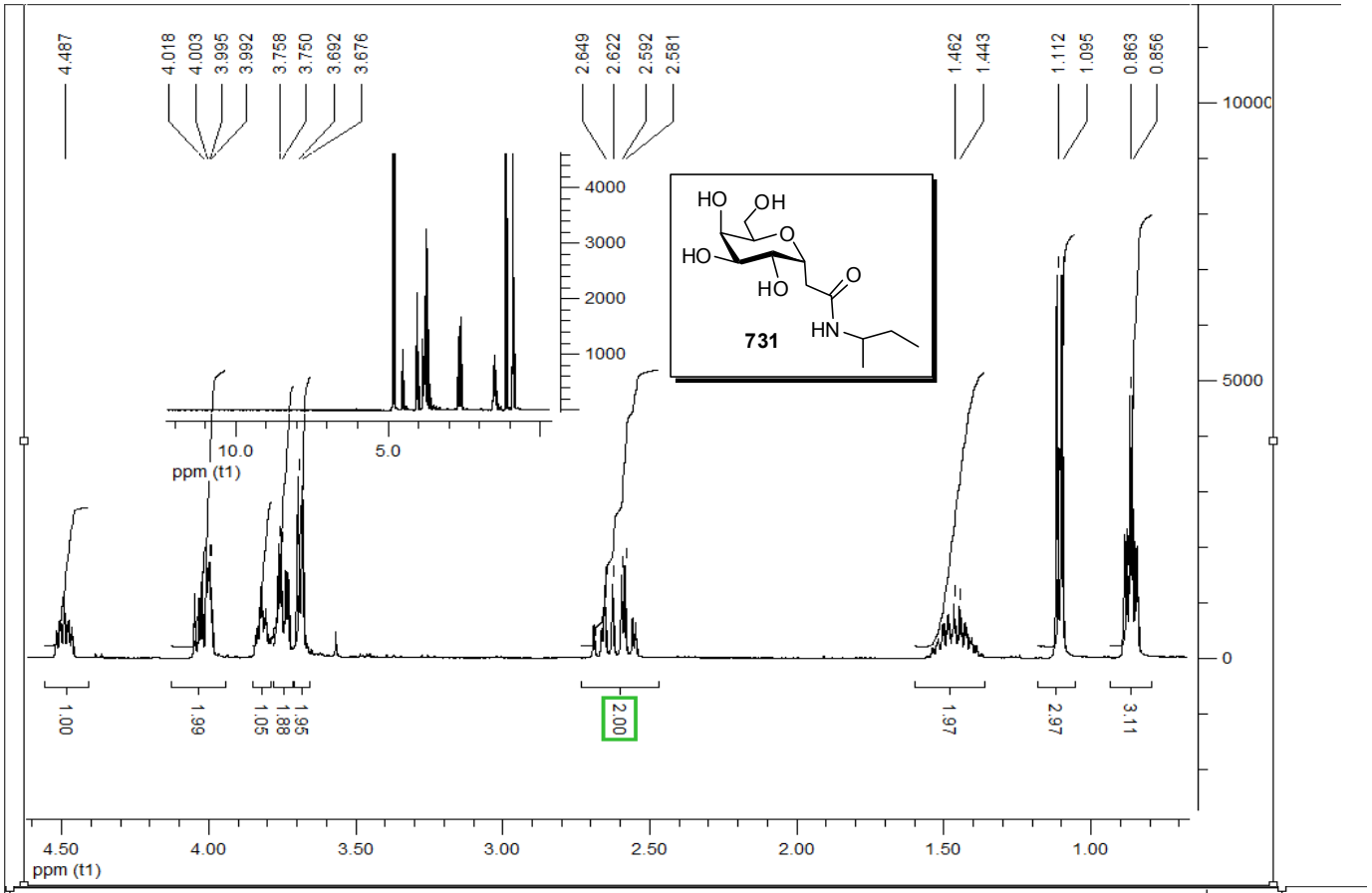

4.470
4.030
4.006
3.991
3.983
3.979
3.975
3.971
3.809
3.807
3.806
3.749
3.740
3.724
3.716
3.682
3.678
3.664
3.595
3.578
3.562
3.195
3.184
2.689
2.662
2.652
2.625
2.585
2.575
2.548
2.537
1.520
1.338
HO
OH
O
HO
HO
O
HN
OH
728
ppm (t1)
1.00
1.94
1.03
1.16
1.91
2.11
2.17
2.02
3.97
2.20
4.50
4.00
3.50
3.00
2.50
2.00
1.50
ppm (t1)
173.396
72.972
72.370
69.626
68.716
67.543
61.583
60.706
39.382
32.301
30.882
28.052
22.404
728
200
150
100
50
0
ppm (t1)

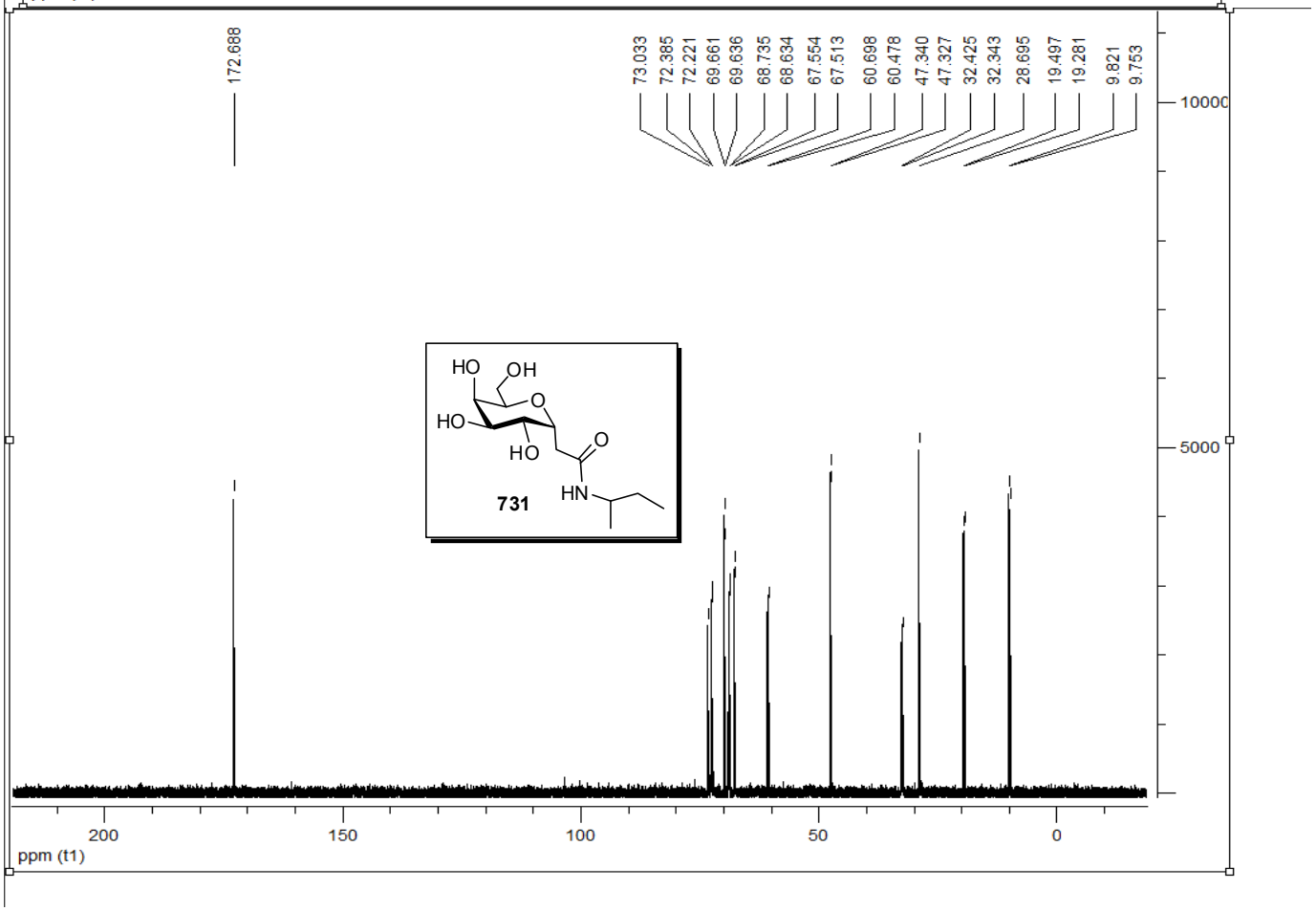

4.468
4.031
4.016
4.006
3.991
3.980
3.977
3.972
3.969
3.925
3.801
3.744
3.736
3.719
3.711
3.685
3.679
3.669
3.665
2.612
2.585
2.553
2.542
1.125
1.109
HO
OH
O
HO
HO
O
HN
729
10.0
ppm (t1)
5.0
1.17
3.14
1.02
3.19
1.97
6.27
5.0
4.0
3.0
2.0
1.0
ppm (t1)

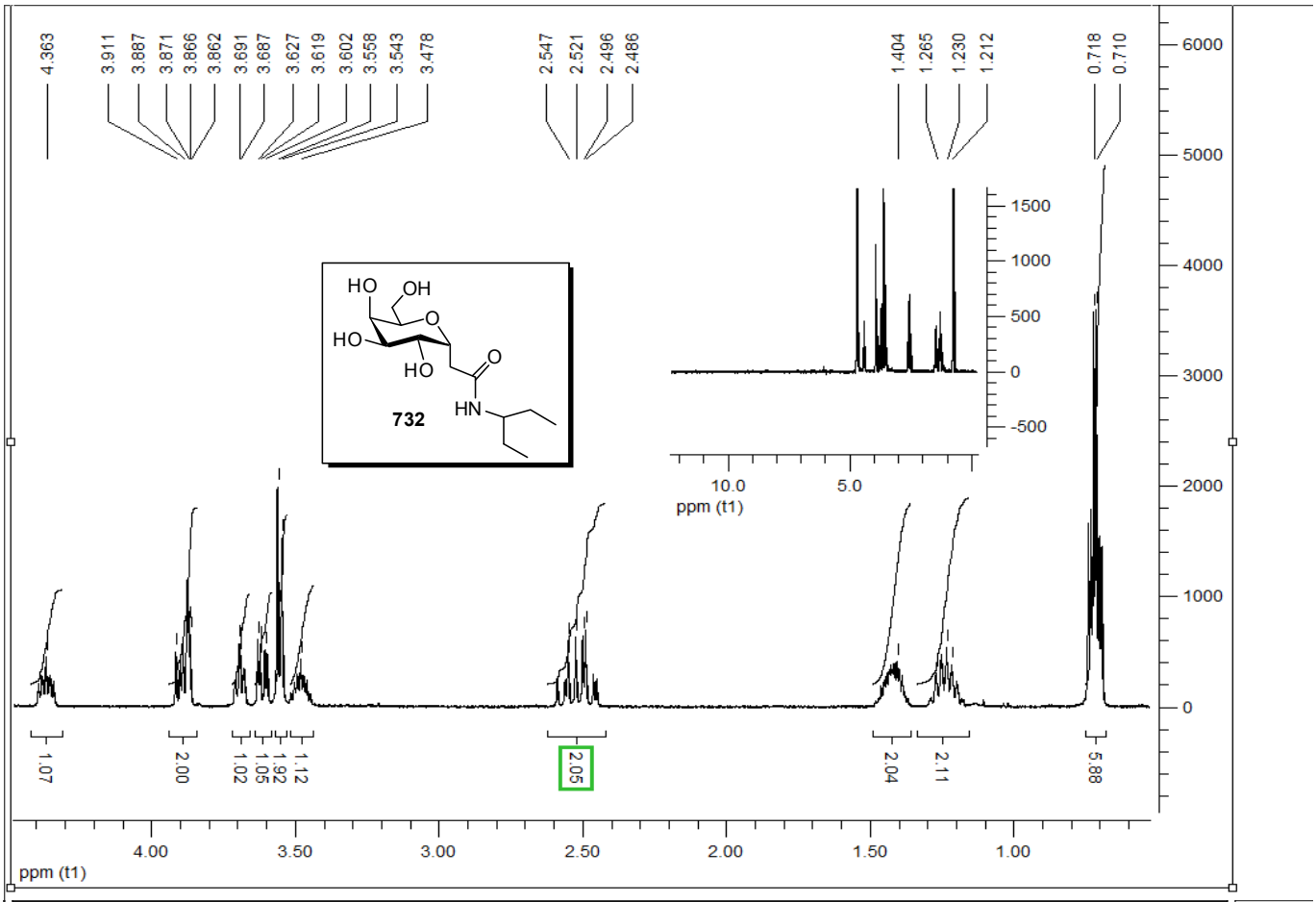

174.849
75.570
74.901
72.166
71.286
70.060
63.267
44.333
34.925
23.945
23.824
HO
OH
O
HO
HO
O
HN
729
200
150
100
50
0
ppm (t1)

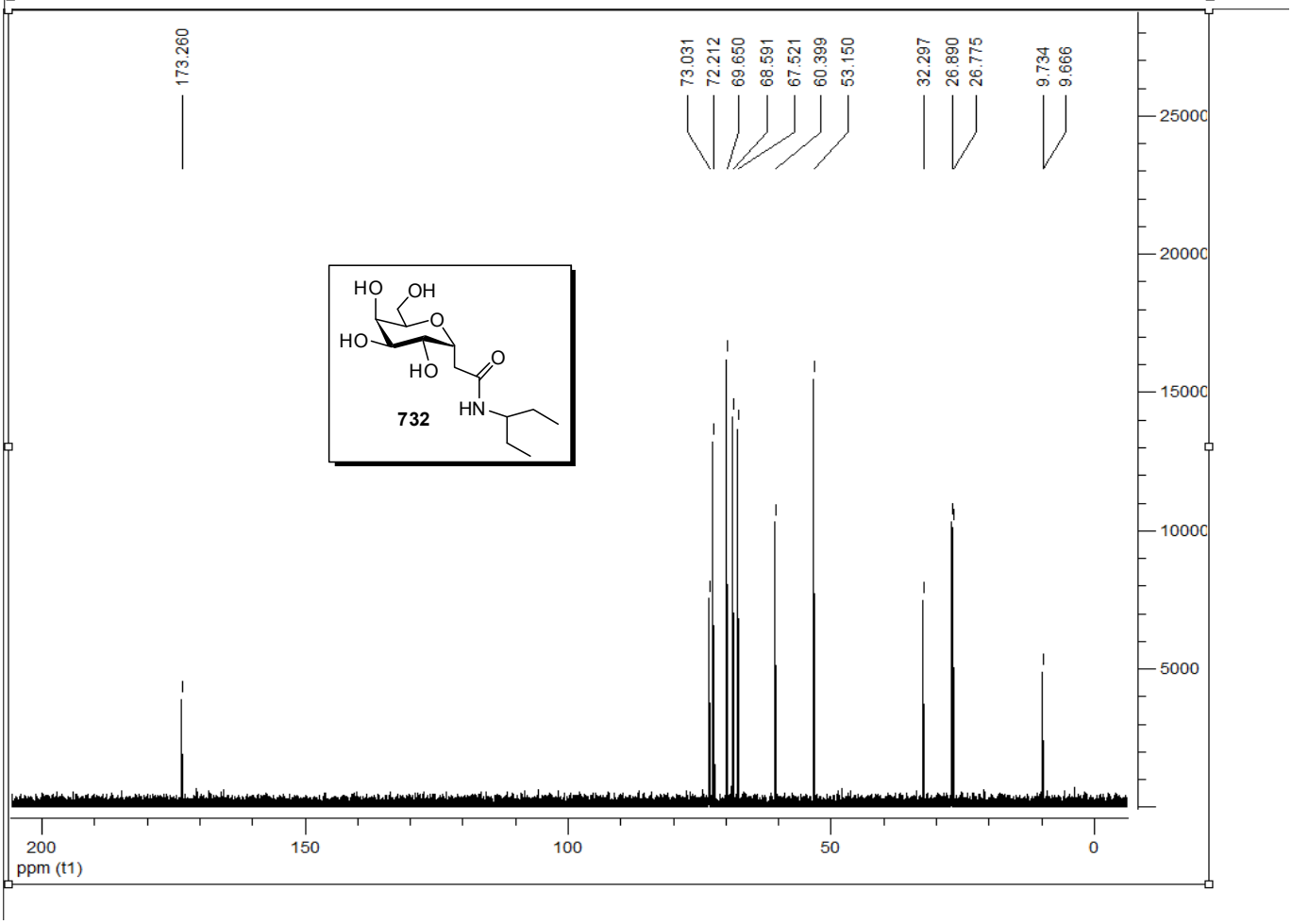

HO
OH
O
HO
HO
O
HN
730
5000
4000
3000
2000
1000
0
3000
2500
2000
1500
1000
500
0
10.0
5.0
0.0
ppm (t1)
0.99
2.00
1.00
1.06
1.85
1.99
0.98
0.98
0.98
5.88
4.50
4.00
3.50
3.00
2.50
2.00
1.50
1.00
ppm (t1)

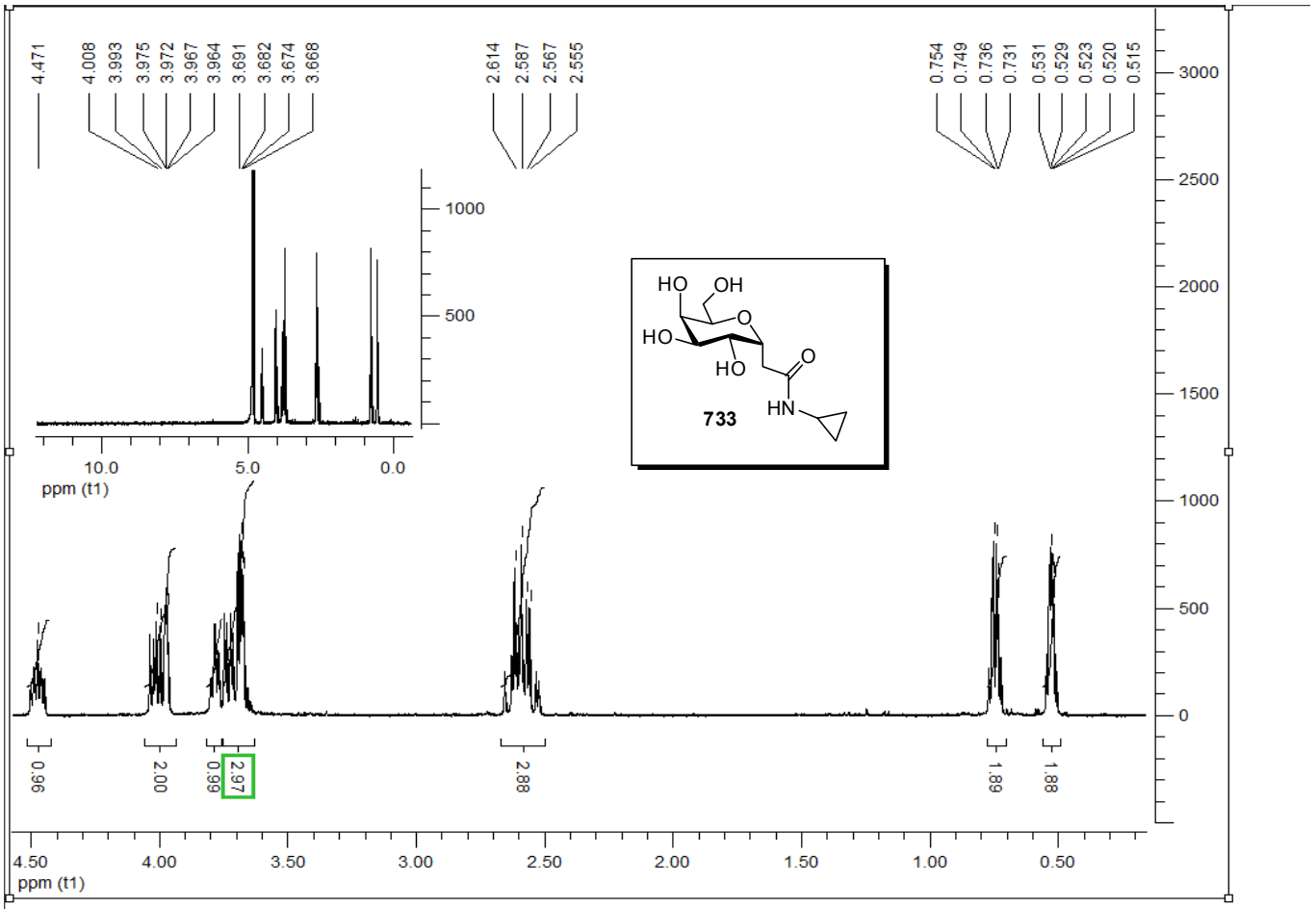

173.523
73.006
72.347
69.646
68.671
67.547
60.585
46.939
32.322
27.823
19.289
19.275
HO
OH
O
HO
HO
O
HN
730
2000
1500
1000
500
0
200
150
100
50
0
ppm (t1)

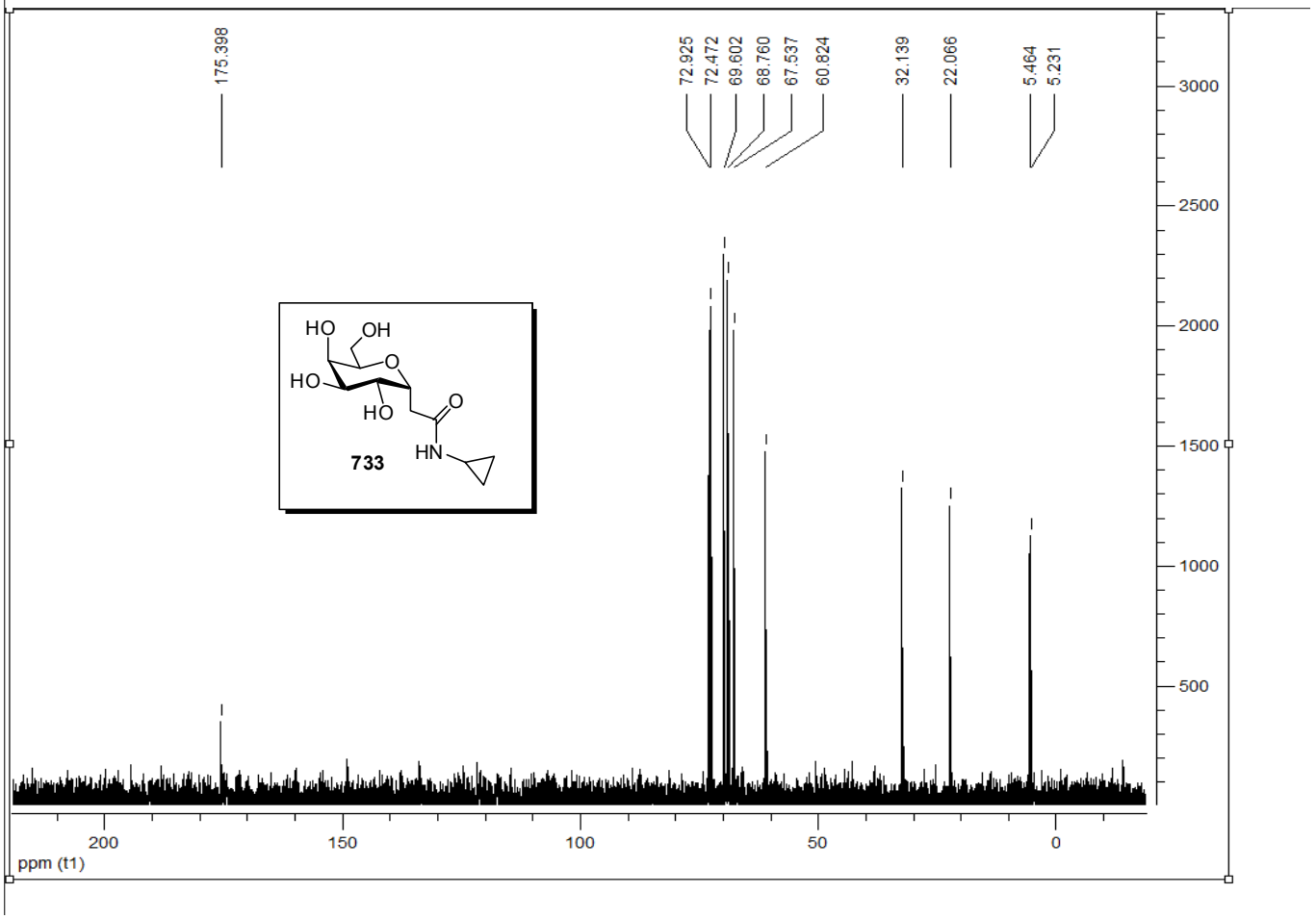

4.487
4.018
4.003
3.995
3.992
3.758
3.750
3.692
3.676
2.649
2.622
2.592
2.581
1.462
1.443
1.112
1.095
0.863
0.856
HO
OH
O
HO
HO
O
HN
731
ppm (t1)
1.00
1.99
1.05
1.88
1.95
2.00
1.97
2.97
3.11

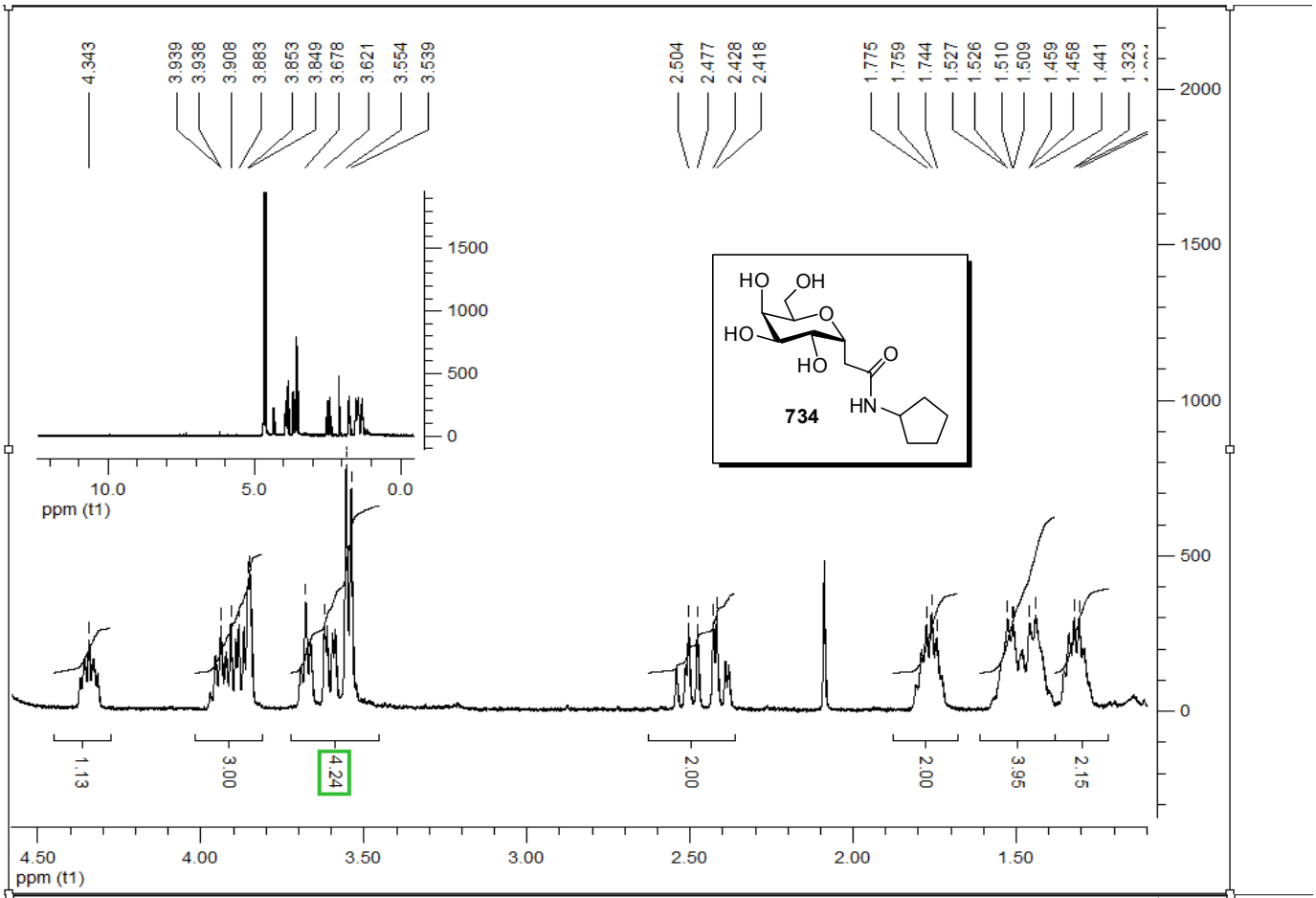

172.688
73.033
72.385
72.221
69.661
69.636
68.735
68.634
67.554
67.513
60.698
60.478
47.340
47.327
32.425
32.343
28.695
19.497
19.281
9.821
9.753
HO
OH
O
HO
HO
O
HN
731
ppm (t1)

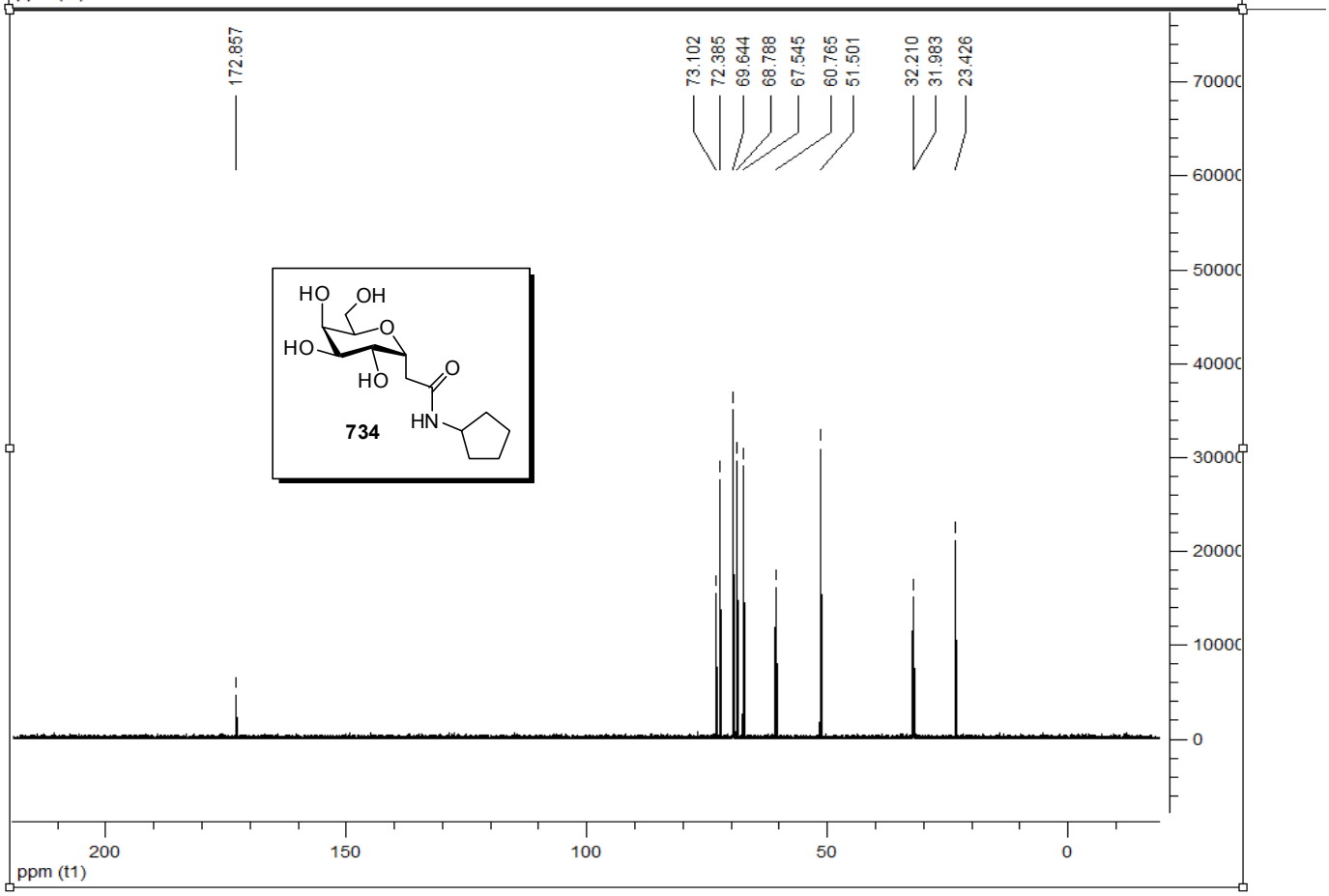

4.363
3.911
3.887
3.871
3.866
3.862
3.691
3.687
3.627
3.619
3.602
3.558
3.543
3.478
2.547
2.521
2.496
2.486
1.404
1.265
1.230
1.212
0.718
0.710
HO
OH
O
HO
HO
O
HN
732
ppm (t1)
1.07
2.00
1.02
1.05
1.92
1.12
2.05
2.04
2.11
5.88
4.00
3.50
3.00
2.50
2.00
1.50
1.00

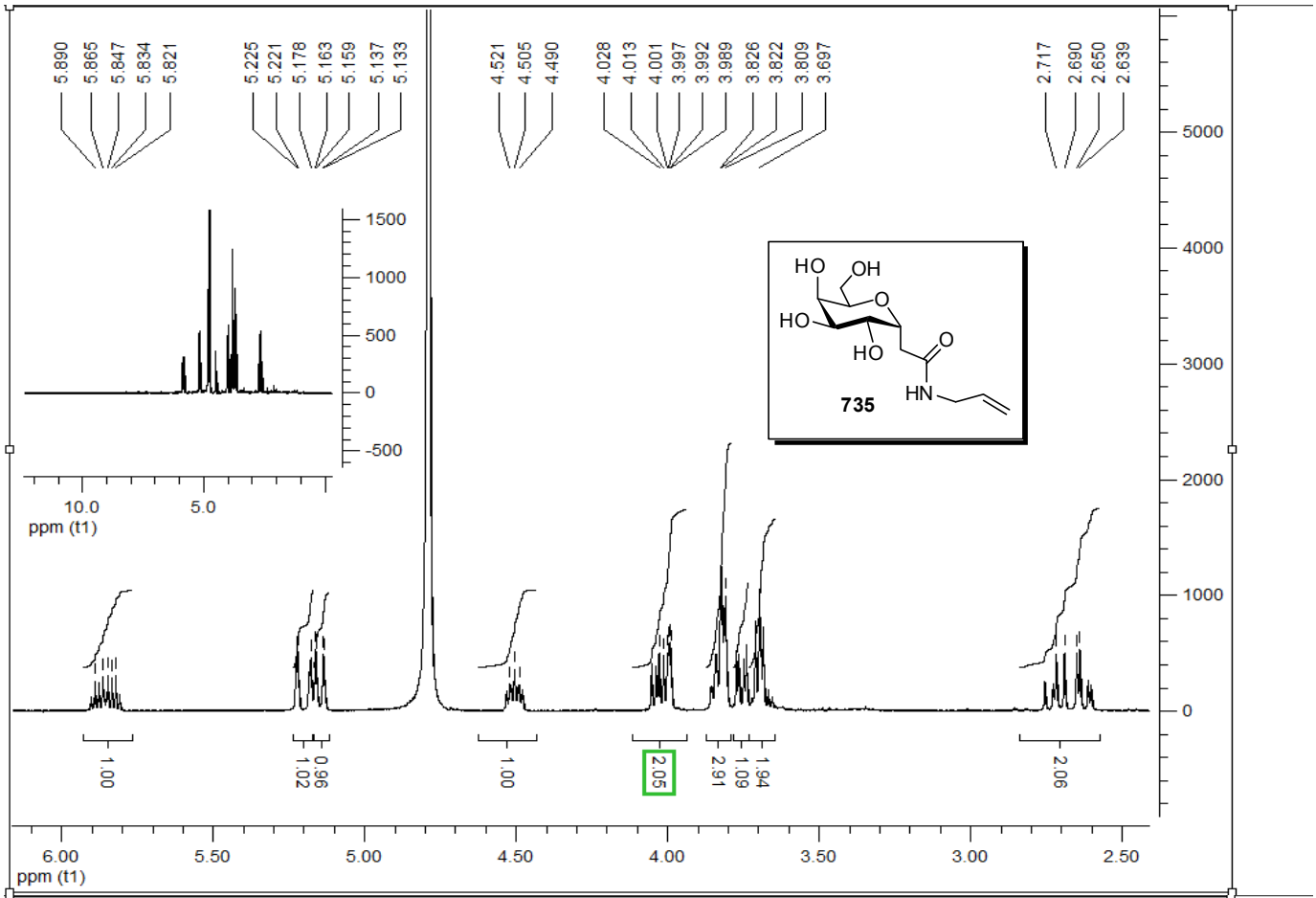

173.260
73.031
72.212
69.650
68.591
67.521
60.399
53.150
32.297
26.890
26.775
9.734
9.666
HO
OH
O
HO
HO
O
HN
732
ppm (t1)
200
150
100
50
0

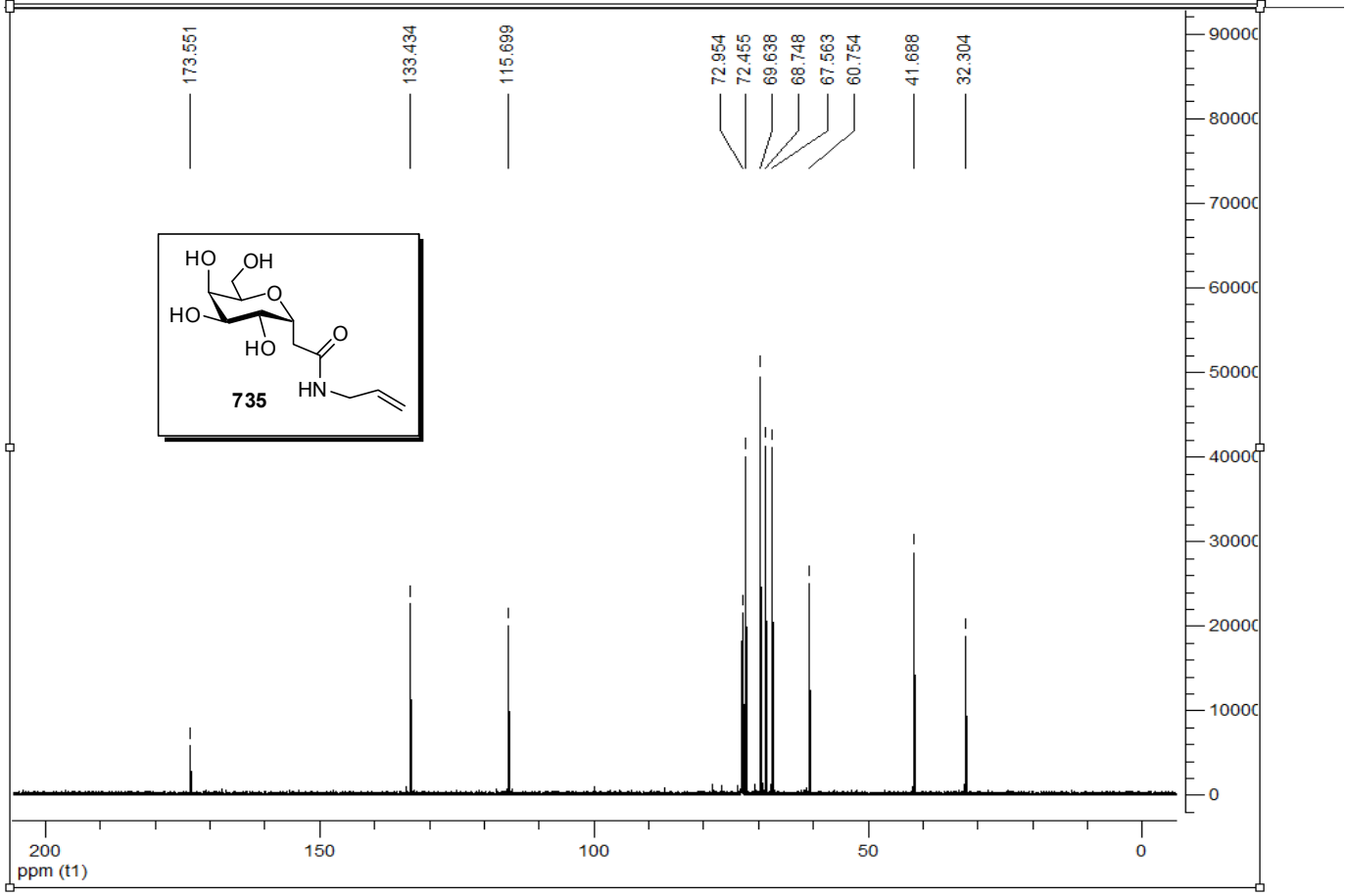

4.471
4.008
3.993
3.975
3.972
3.967
3.964
3.691
3.682
3.674
3.668
2.614
2.587
2.567
2.555
0.754
0.749
0.736
0.731
0.531
0.529
0.523
0.520
0.515
HO
OH
O
HO
HO
O
HN
733
ppm (t1)
0.96
2.00
0.99
2.97
2.88
1.89
1.88

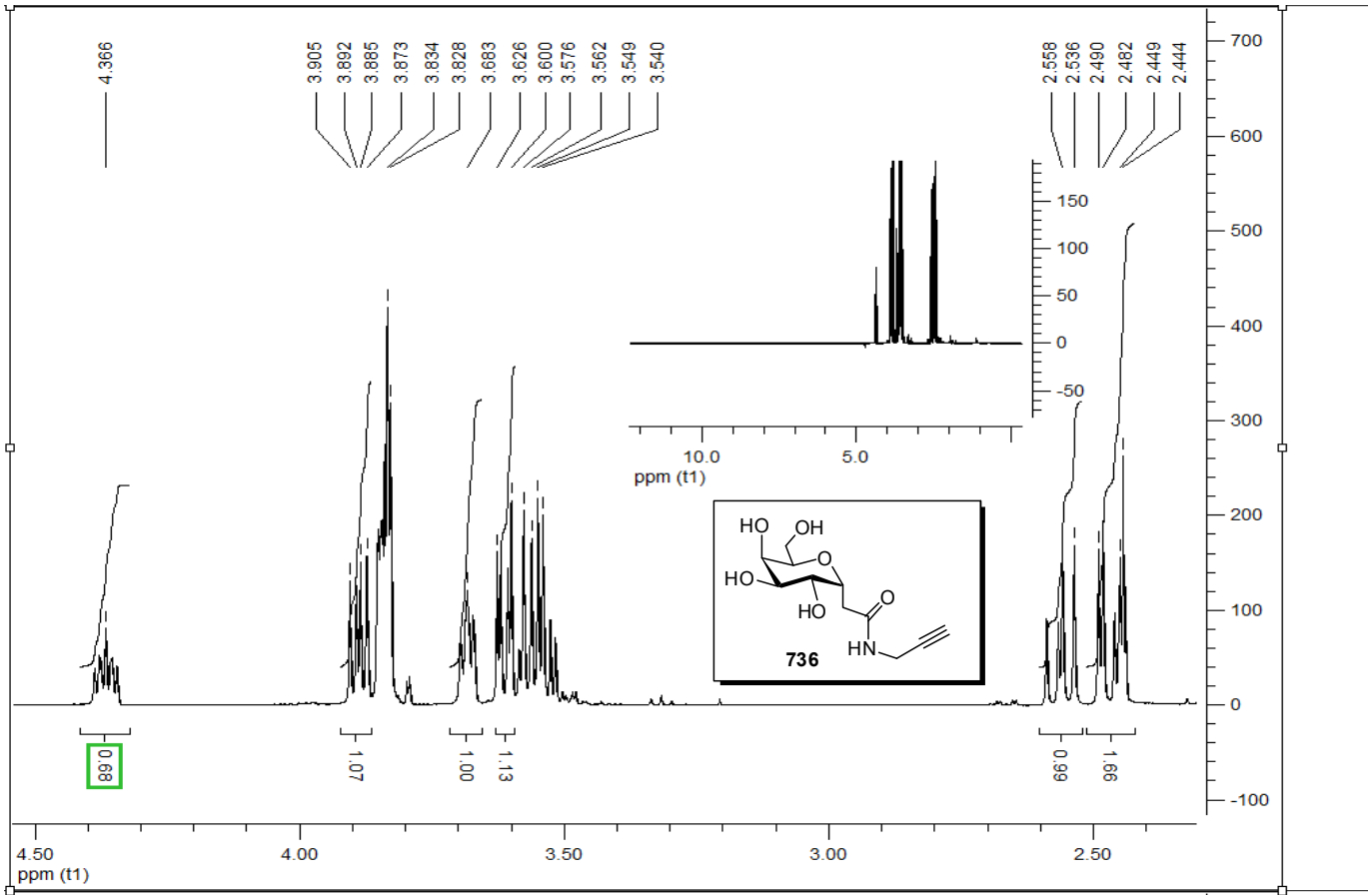

175.398
72.925
72.472
69.602
68.760
67.537
60.824
32.139
22.066
5.464
5.231
HO
OH
O
HO
HO
O
HN
733
ppm (t1)

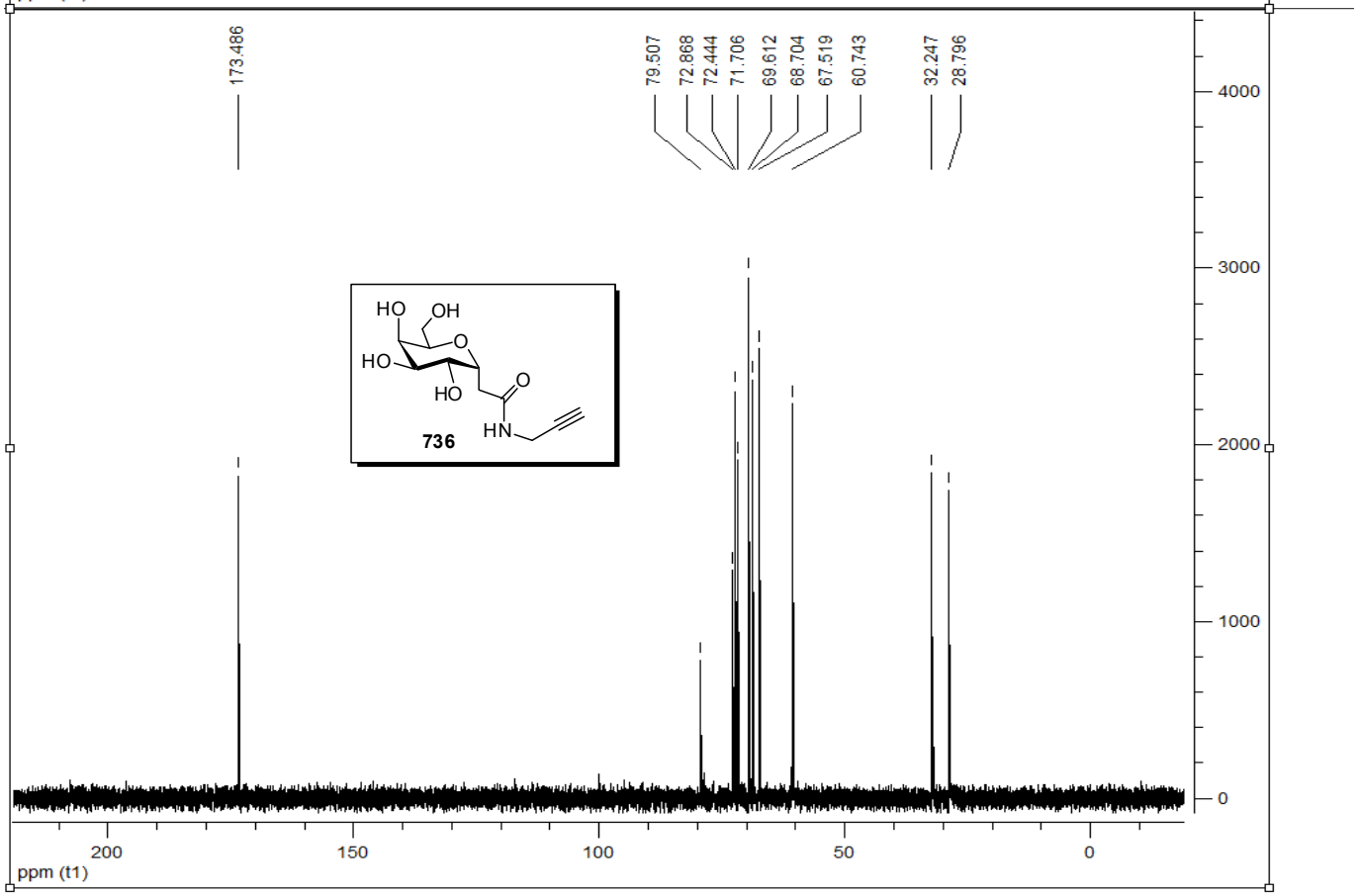

4.343
3.939
3.938
3.908
3.883
3.853
3.849
3.678
3.621
3.554
3.539
2.504
2.477
2.428
2.418
1.775
1.759
1.744
1.527
1.526
1.510
1.509
1.459
1.458
1.441
1.323
HO
OH
O
HO
HO
O
HN
734
ppm (t1)
1.13
3.00
4.24
2.00
2.00
3.96
2.15
4.50
4.00
3.50
3.00
2.50
2.00
1.50

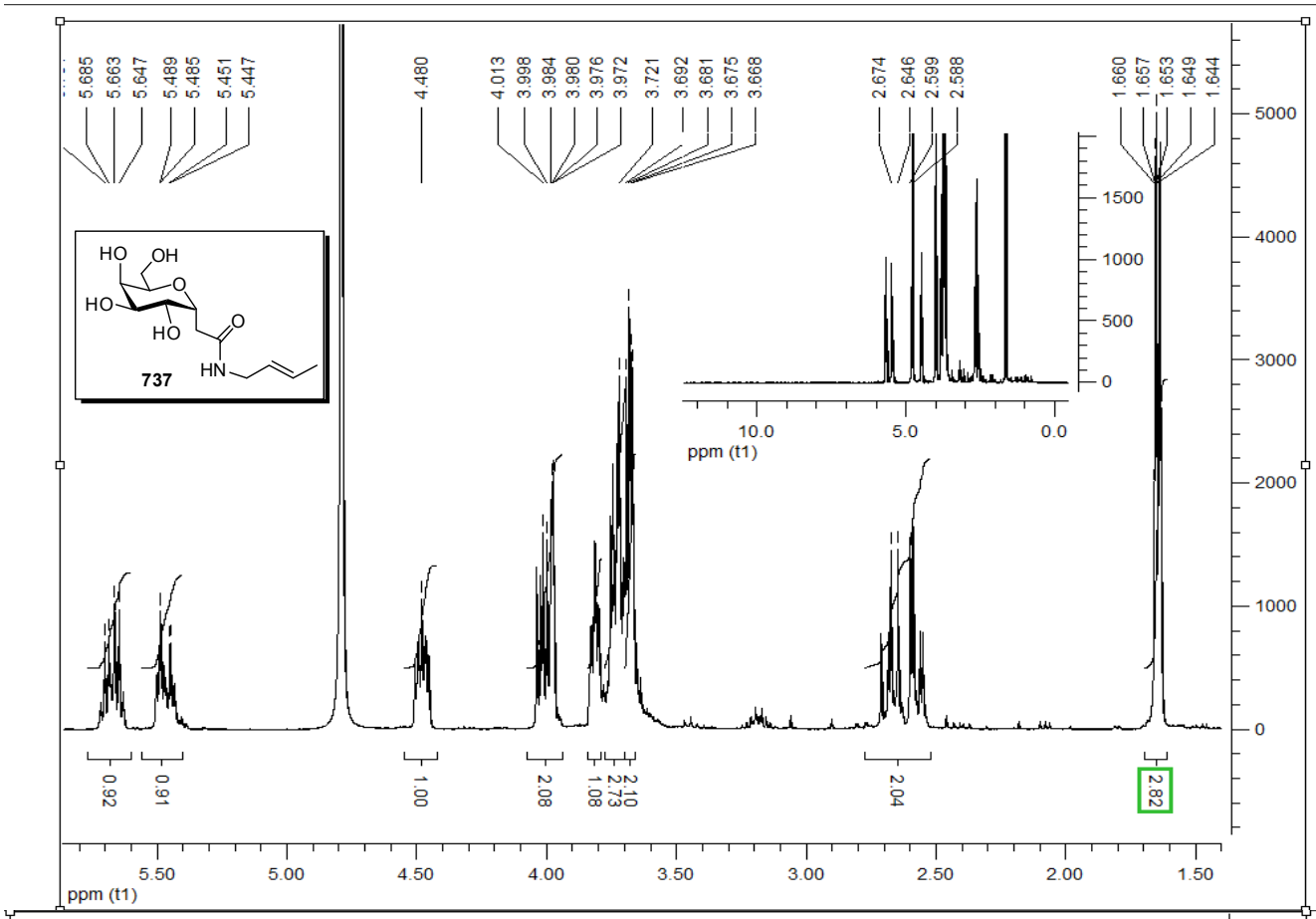

172.857
73.102
72.385
69.644
68.788
67.545
60.765
51.501
32.210
31.983
23.426
HO
OH
O
HO
HO
O
HN
734
200
150
100
50
0
ppm (t1)

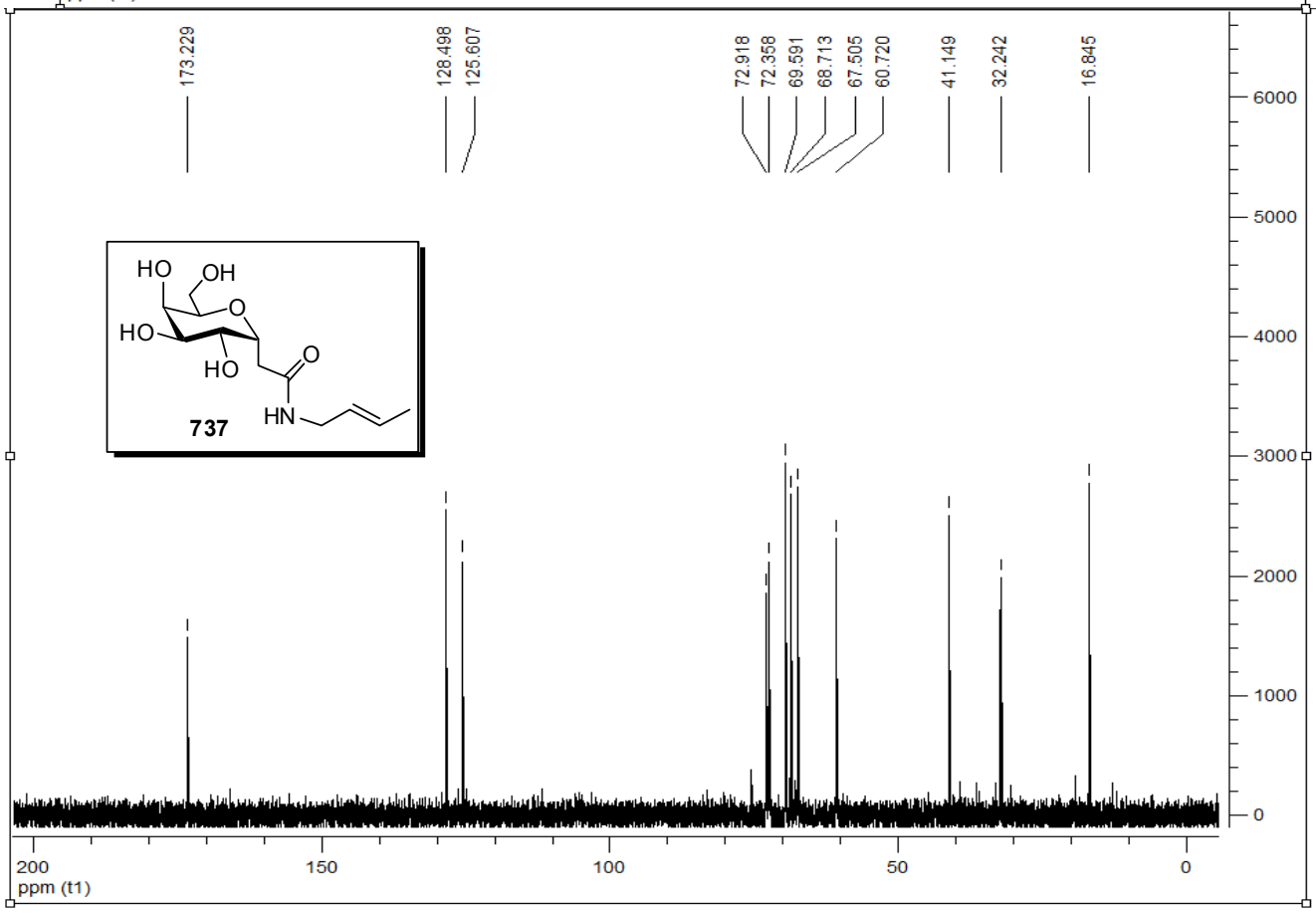

5.890
5.865
5.847
5.834
5.821
5.225
5.221
5.178
5.163
5.159
5.137
5.133
4.521
4.505
4.490
4.028
4.013
4.001
3.997
3.992
3.989
3.826
3.822
3.809
3.697
2.717
2.690
2.650
2.639
HO
OH
HO
HO
O
O
HN
735
ppm (t1)
1.00
1.02
0.96
1.00
2.05
2.11
1.09
1.94
2.06

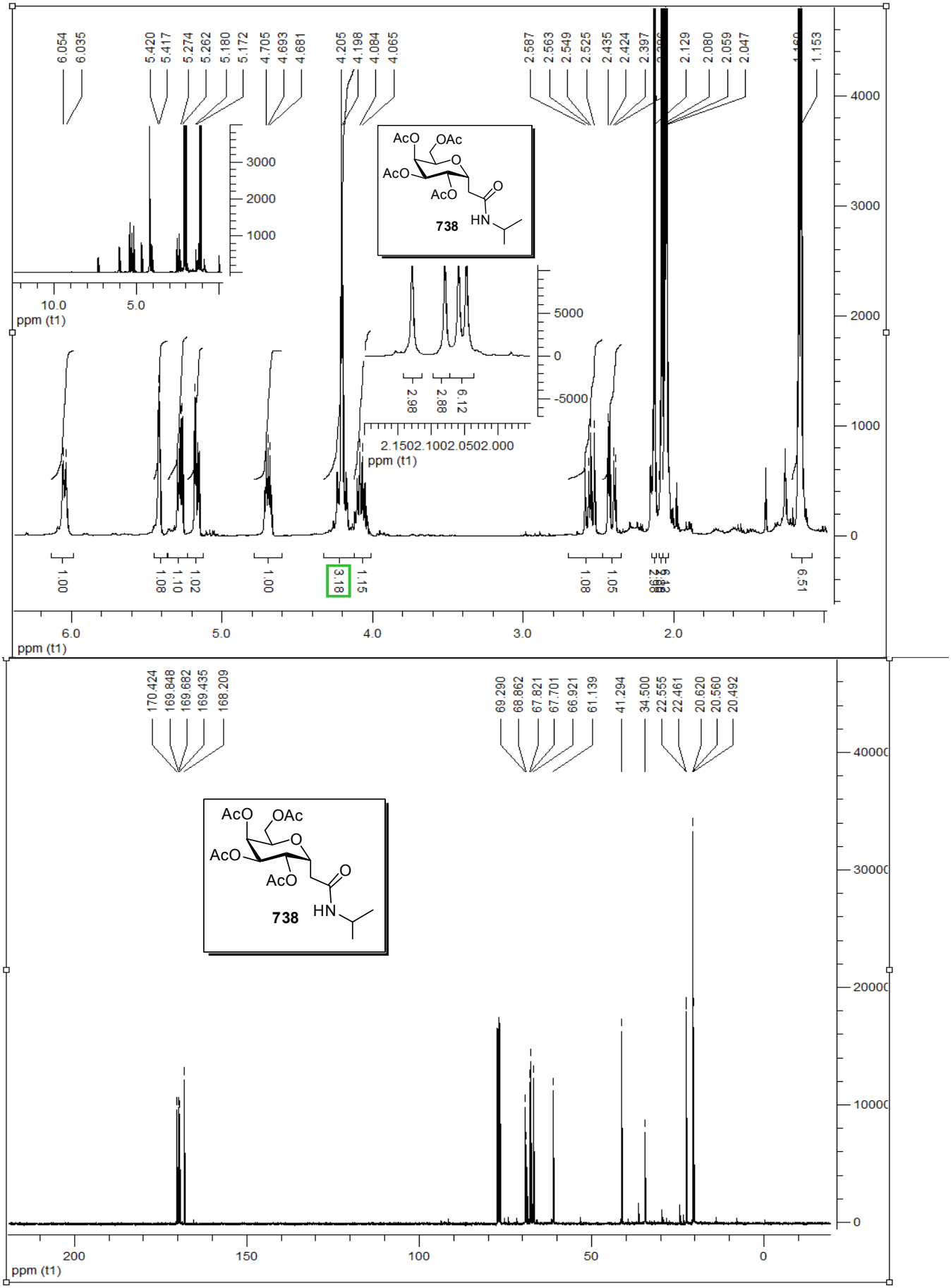

173.551
133.434
115.699
72.954
72.455
69.638
68.748
67.563
60.754
41.688
32.304
HO
OH
HO
HO
O
O
HN
735
ppm (t1)


4.366
3.905
3.892
3.885
3.873
3.834
3.828
3.683
3.626
3.600
3.576
3.562
3.549
3.540
2.558
2.536
2.490
2.482
2.449
2.444
0.68
1.07
1.00
1.13
0.99
1.66
ppm (t1)
HO
OH
O
HO
HO
O
HN
736

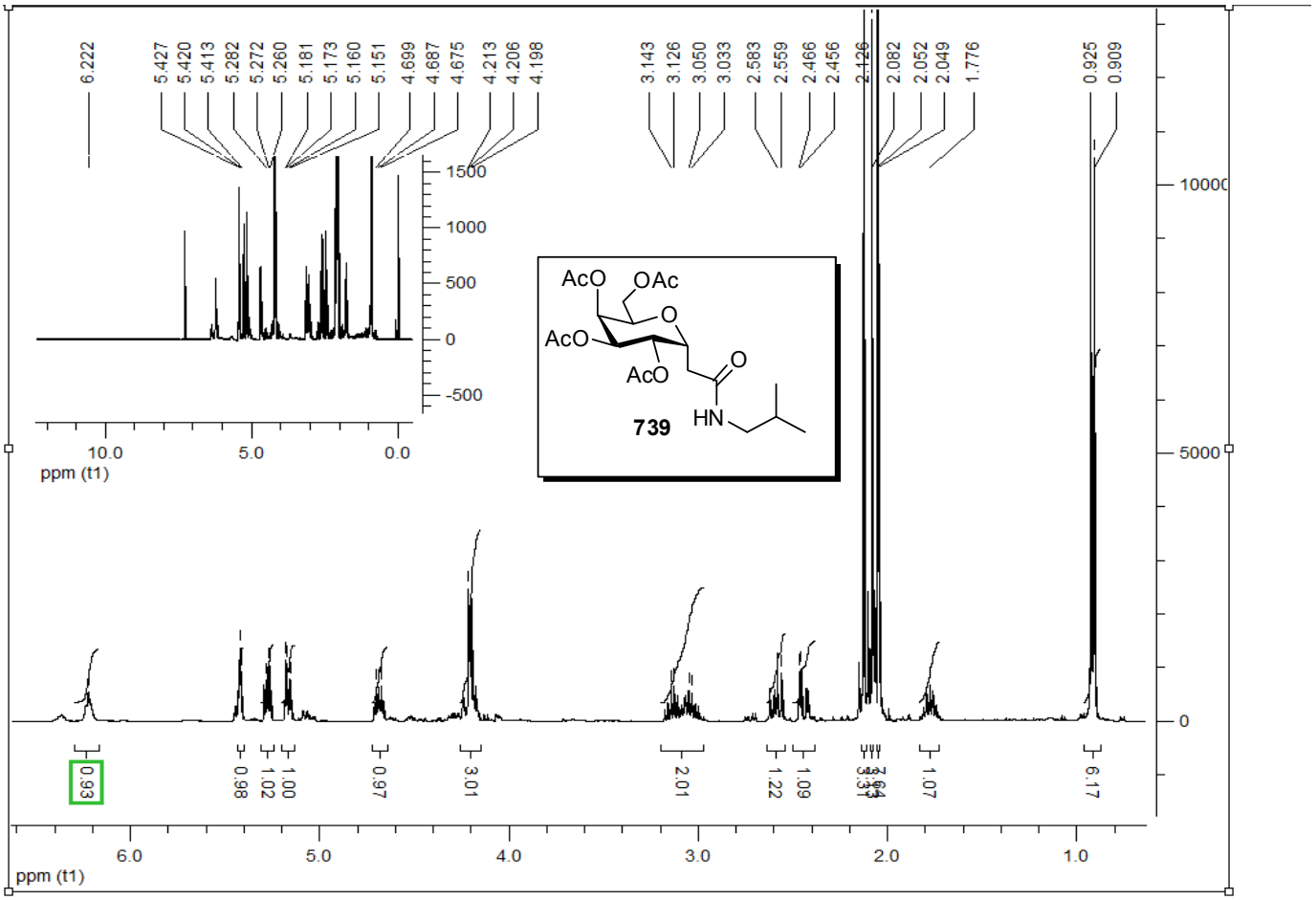

173.486
79.507
72.868
72.444
71.706
69.612
68.704
67.519
60.743
32.247
28.796
ppm (t1)
HO
OH
O
HO
HO
O
HN
736

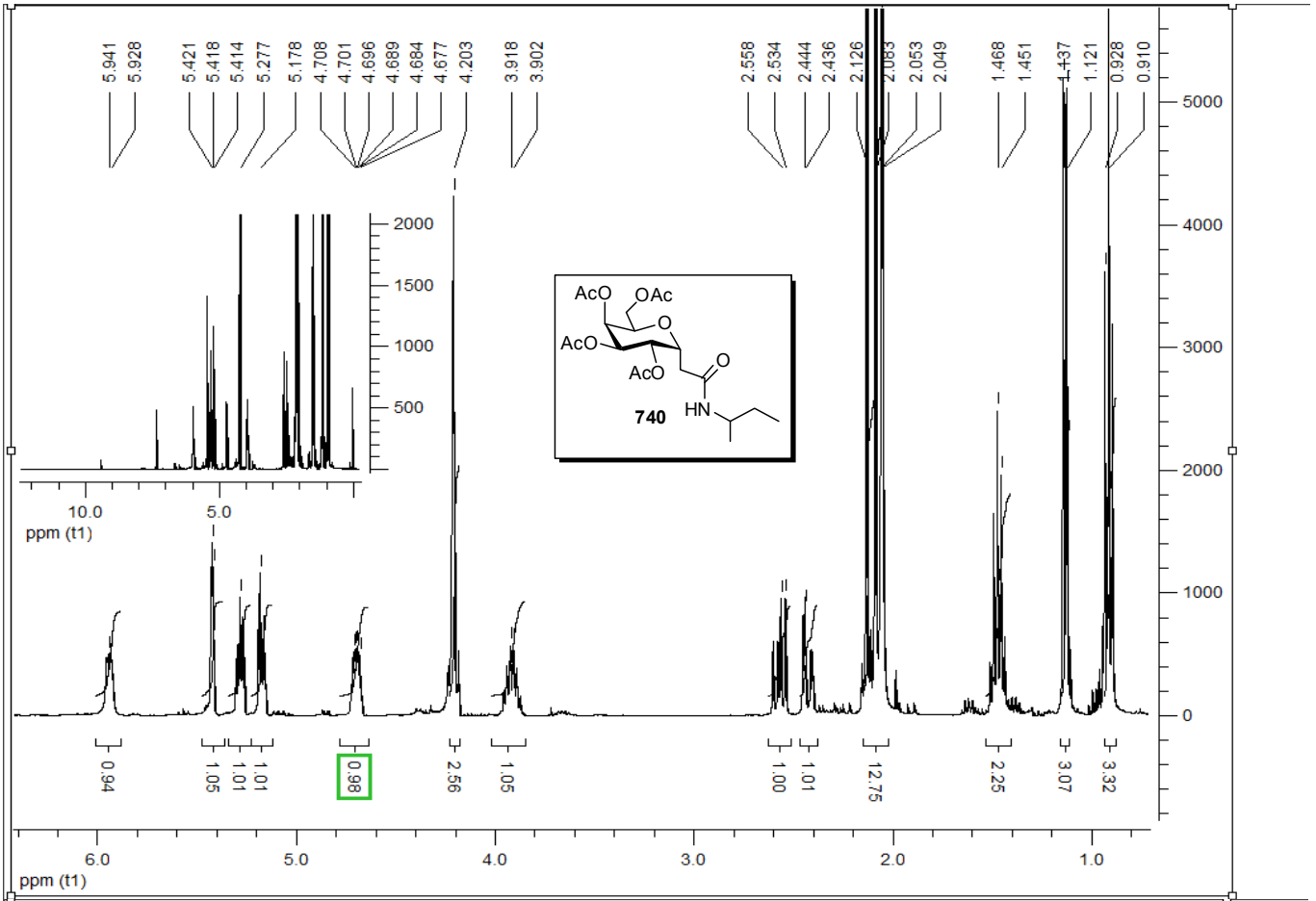

5.685
5.663
5.647
5.489
5.485
5.451
5.447
4.480
4.013
3.998
3.984
3.980
3.976
3.972
3.721
3.692
3.681
3.675
3.668
2.674
2.646
2.599
2.588
1.660
1.657
1.653
1.649
1.644
HO
OH
HO
HO
O
O
HN
737
ppm (t1)
0.92
0.91
1.00
2.08
1.08
2.73
2.10
2.04
2.82
5.50
5.00
4.50
4.00
3.50
3.00
2.50
2.00
1.50

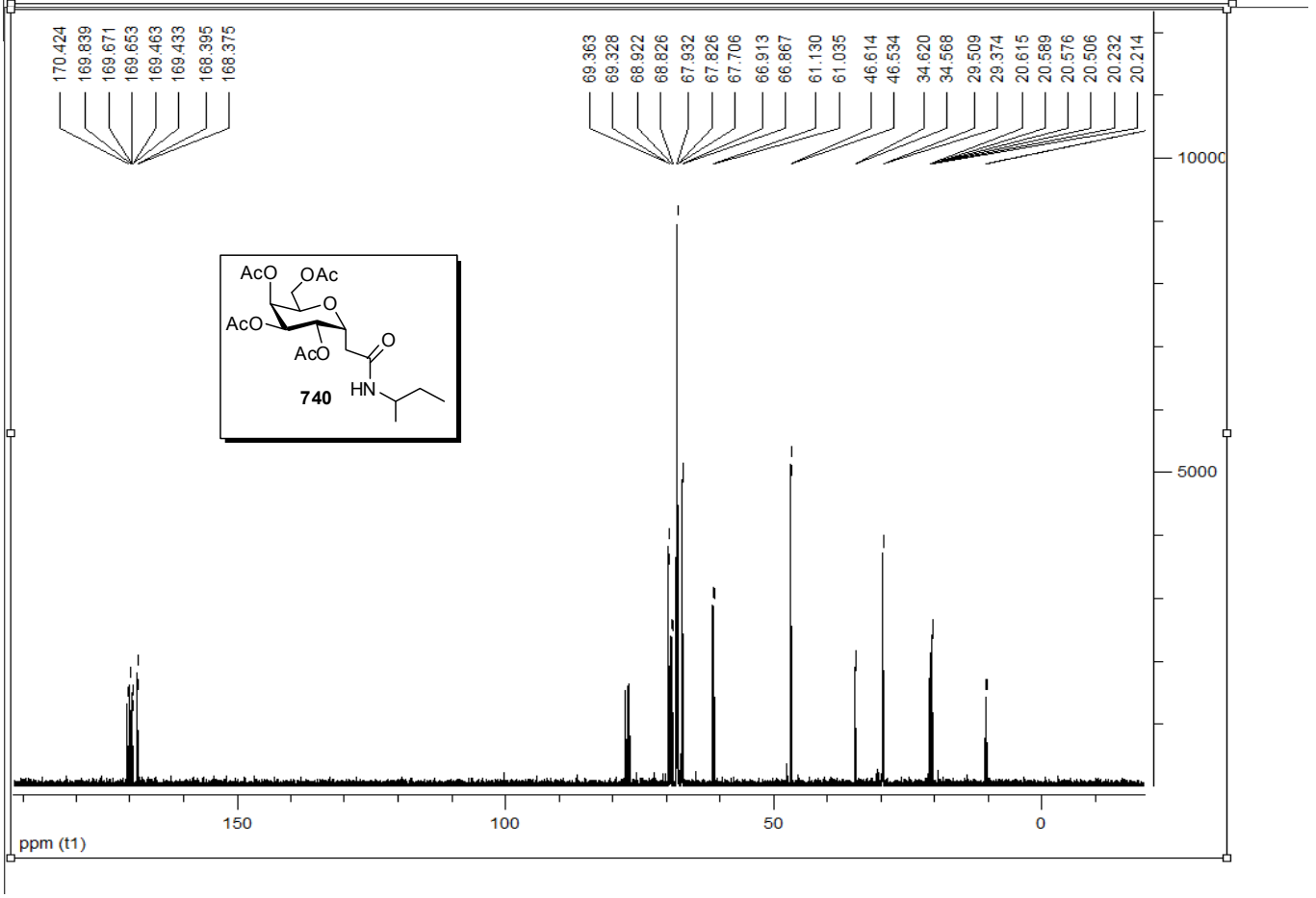

173.229
128.498
125.607
72.918
72.358
69.591
68.713
67.505
60.720
41.149
32.242
16.845
HO
OH
HO
HO
O
O
HN
737
200
150
100
50
0
ppm (t1)

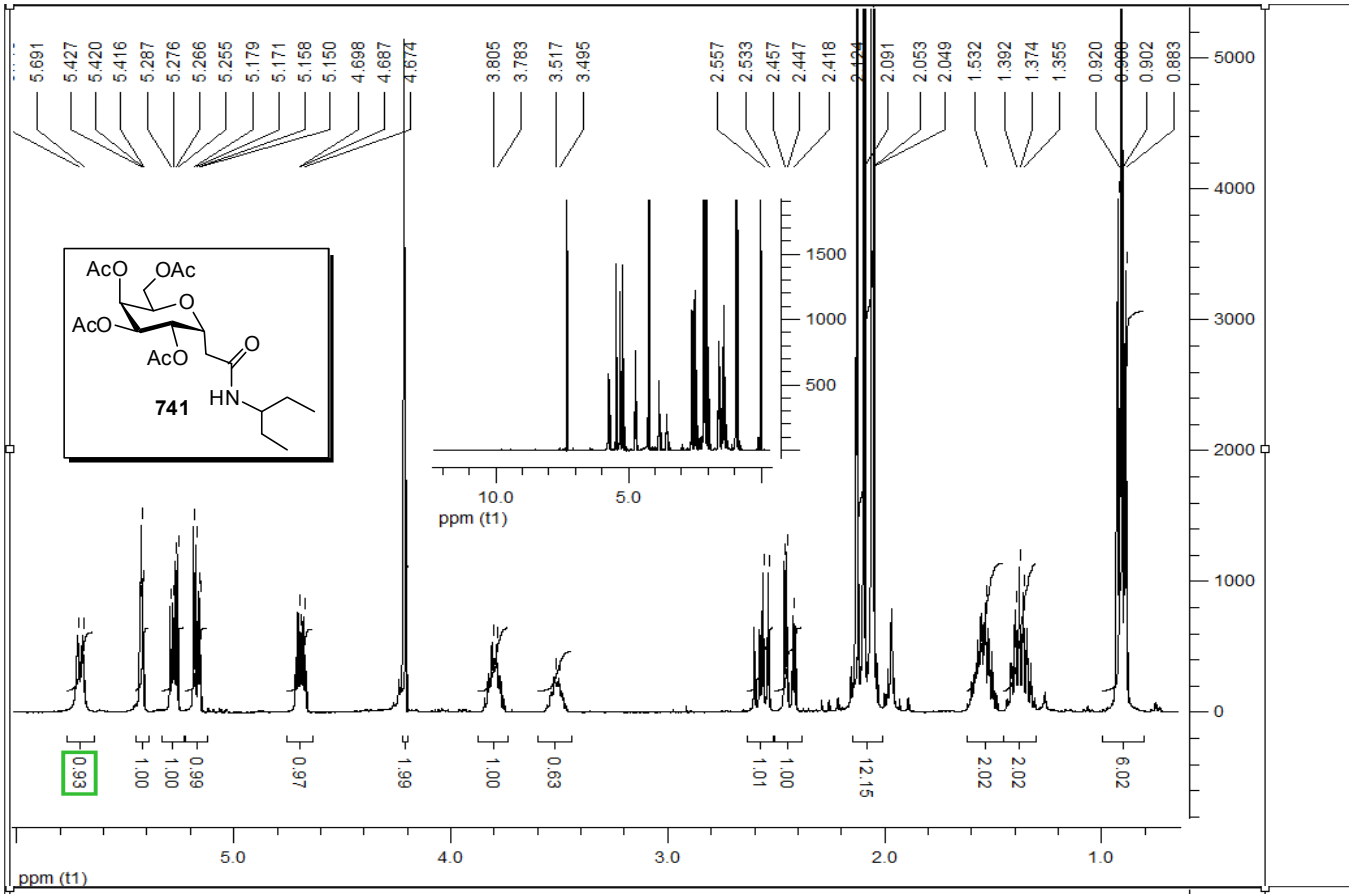

738
ppm (t1)
738
ppm (t1)

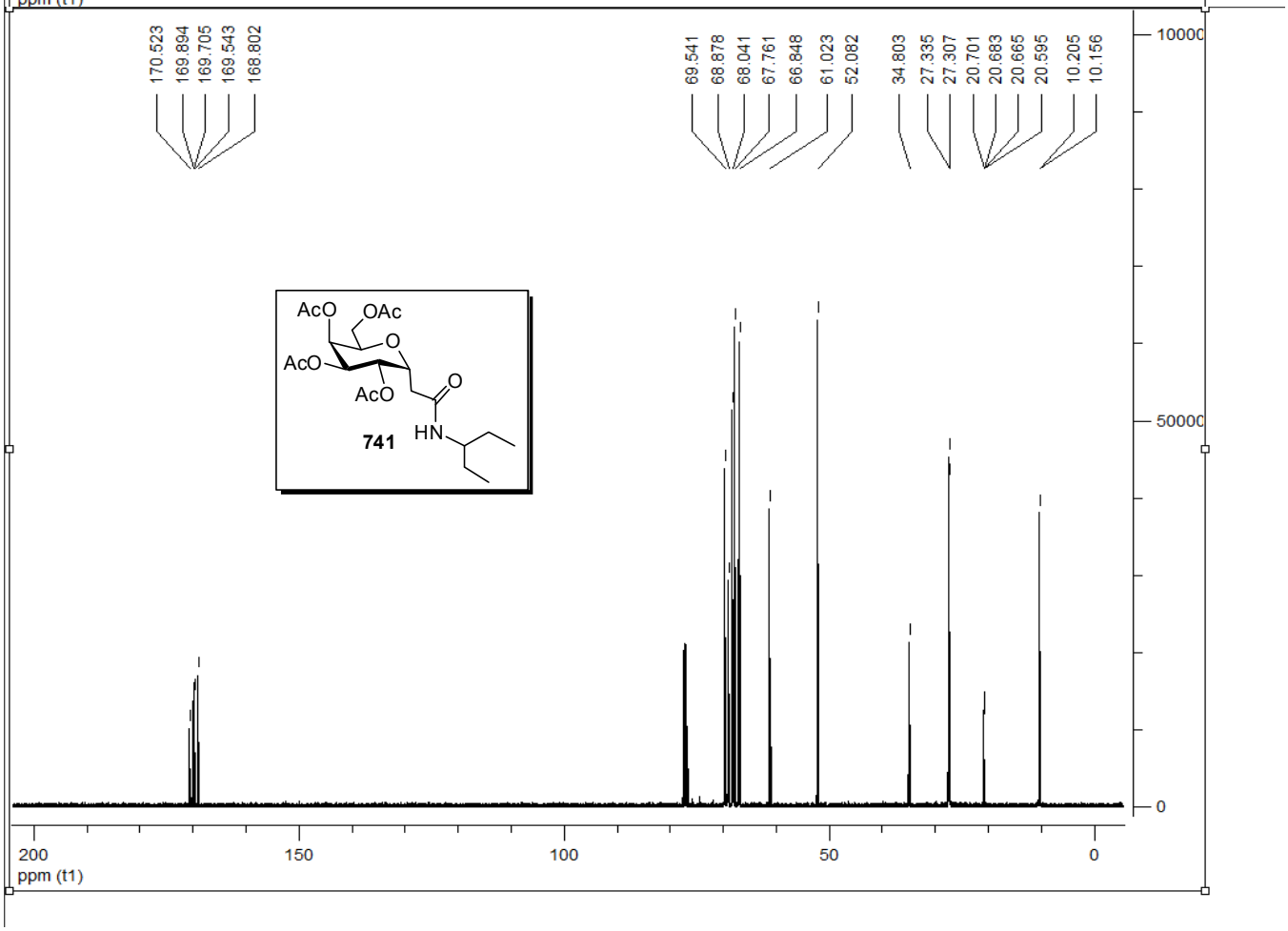
601

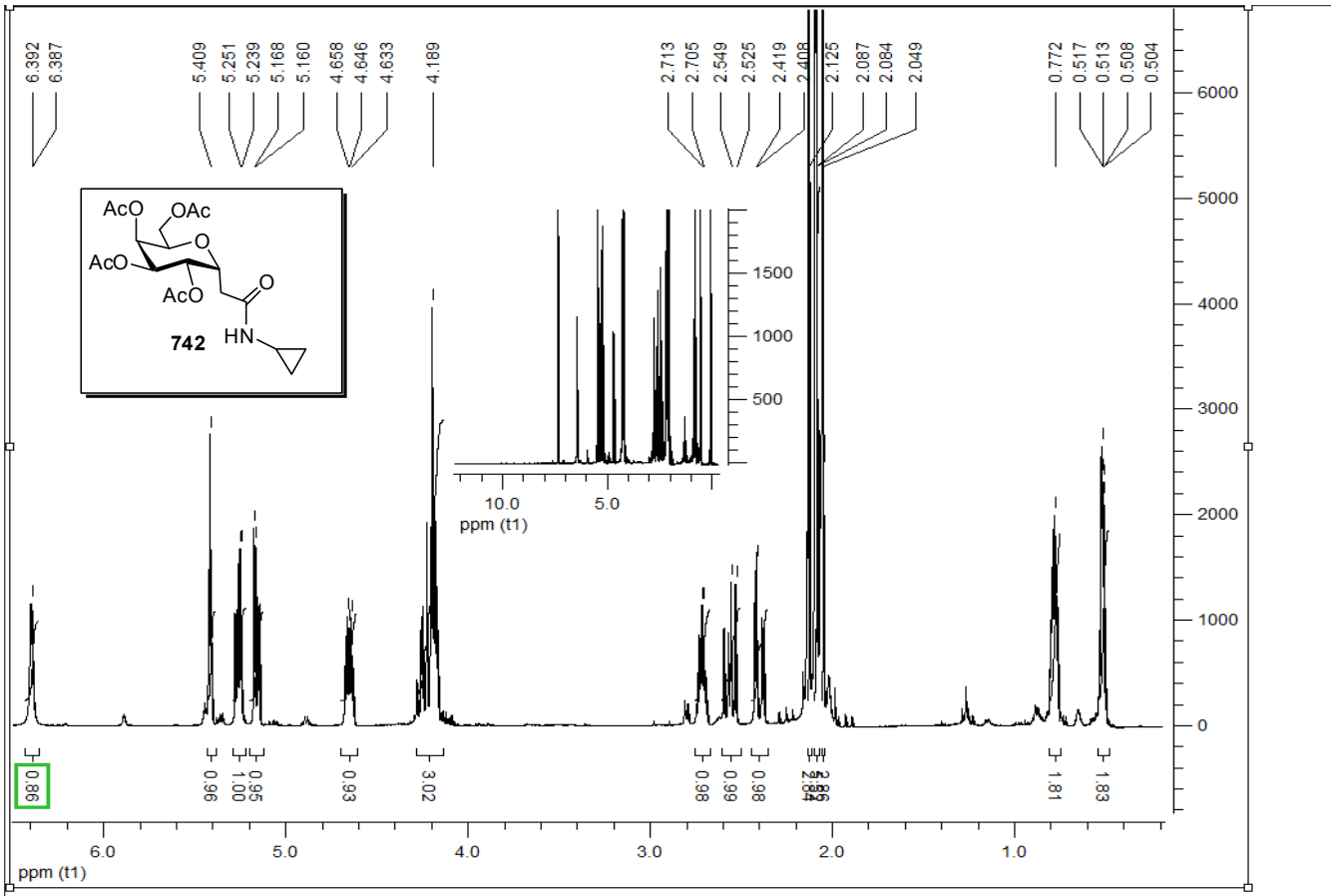

6.222
5.427
5.420
5.413
5.282
5.272
5.260
5.181
5.173
5.160
5.151
4.699
4.687
4.675
4.213
4.206
4.198
3.143
3.126
3.050
3.033
2.583
2.559
2.466
2.456
2.126
2.082
2.052
2.049
1.776
0.925
0.909
AcO
OAc
O
AcO
AcO
O
HN
739
ppm (t1)
ppm (t1)
0.93
0.98
1.02
1.00
0.97
3.01
2.01
1.22
1.09
1.07
6.17

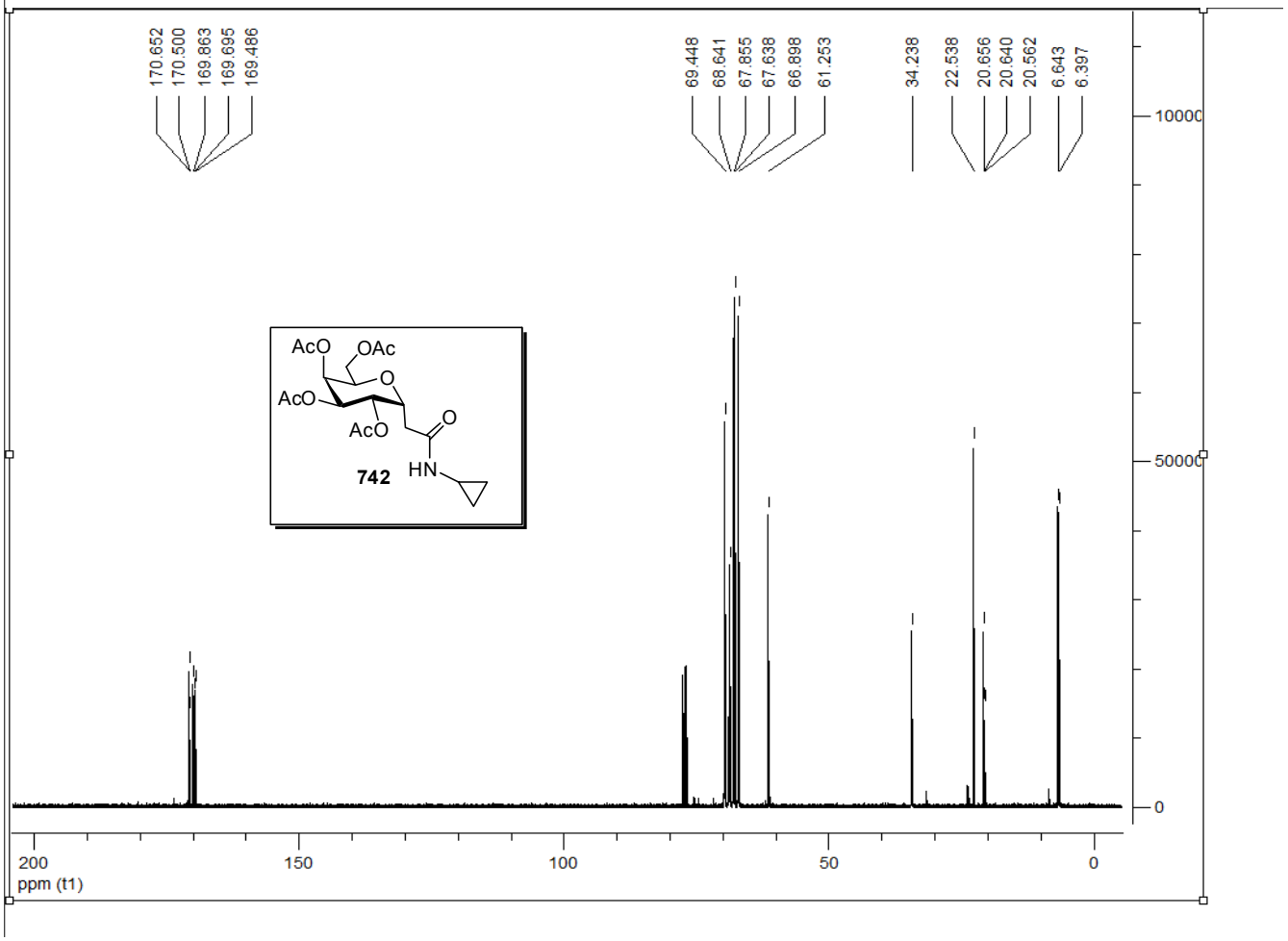

5.941
5.928
5.421
5.418
5.414
5.277
5.178
4.708
4.701
4.696
4.689
4.684
4.677
4.203
3.918
3.902
2.558
2.534
2.444
2.436
2.126
2.083
2.053
2.049
1.468
1.451
1.437
1.121
0.928
0.910
AcO
OAc
AcO
AcO
O
HN
740
ppm (t1)
0.94
1.05
1.01
1.01
0.98
2.56
1.95
1.00
1.01
12.75
2.25
3.07
3.32

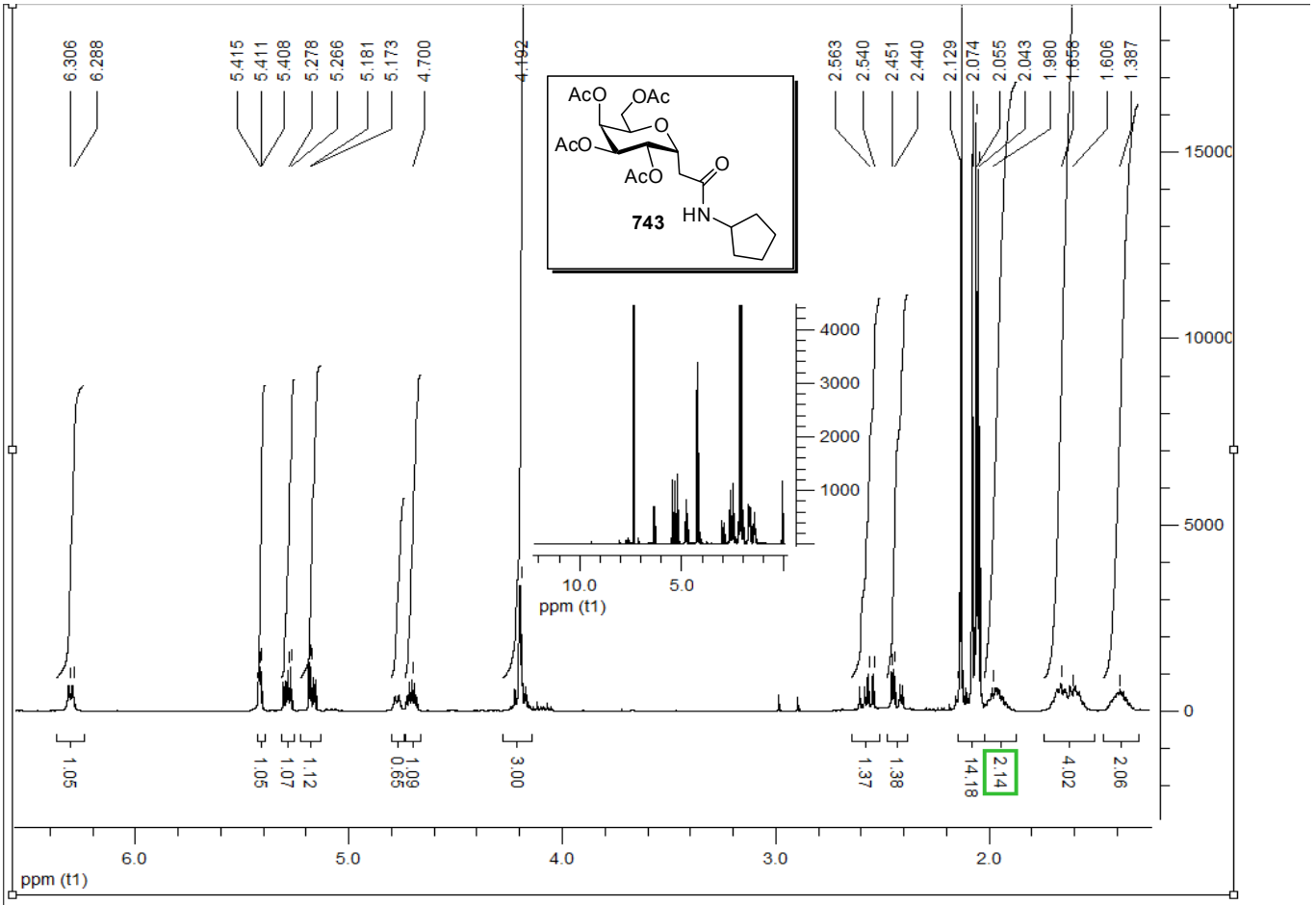

170.424
169.839
169.671
169.653
169.463
169.433
168.395
168.375
69.363
69.328
68.922
68.826
67.932
67.826
67.706
66.913
66.867
61.130
61.035
46.614
46.534
34.620
34.568
29.509
29.374
20.615
20.589
20.576
20.506
20.232
20.214
AcO
OAc
AcO
AcO
O
HN
740
ppm (t1)

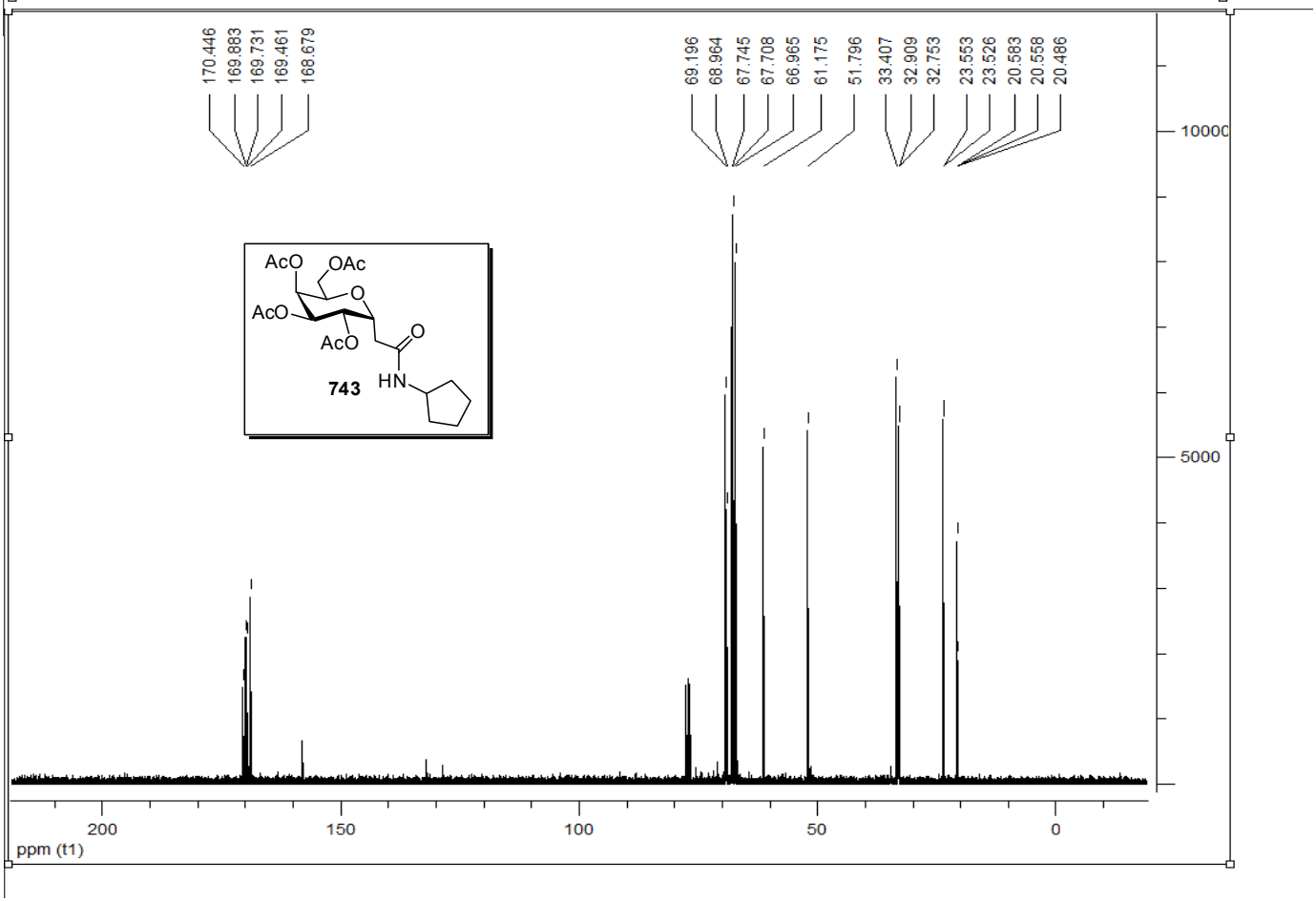

5.691
5.427
5.420
5.416
5.287
5.276
5.266
5.255
5.179
5.171
5.158
5.150
4.698
4.687
4.674
3.805
3.783
3.517
3.495
2.557
2.533
2.457
2.447
2.418
2.124
2.091
2.053
2.049
1.532
1.392
1.374
1.355
0.920
0.908
0.902
0.883
AcO
OAc
AcO
AcO
O
O
HN
741
ppm (t1)
0.93
1.00
0.99
0.97
1.99
1.00
0.63
1.01
1.00
12.15
2.02
2.02
6.02
ppm (t1)

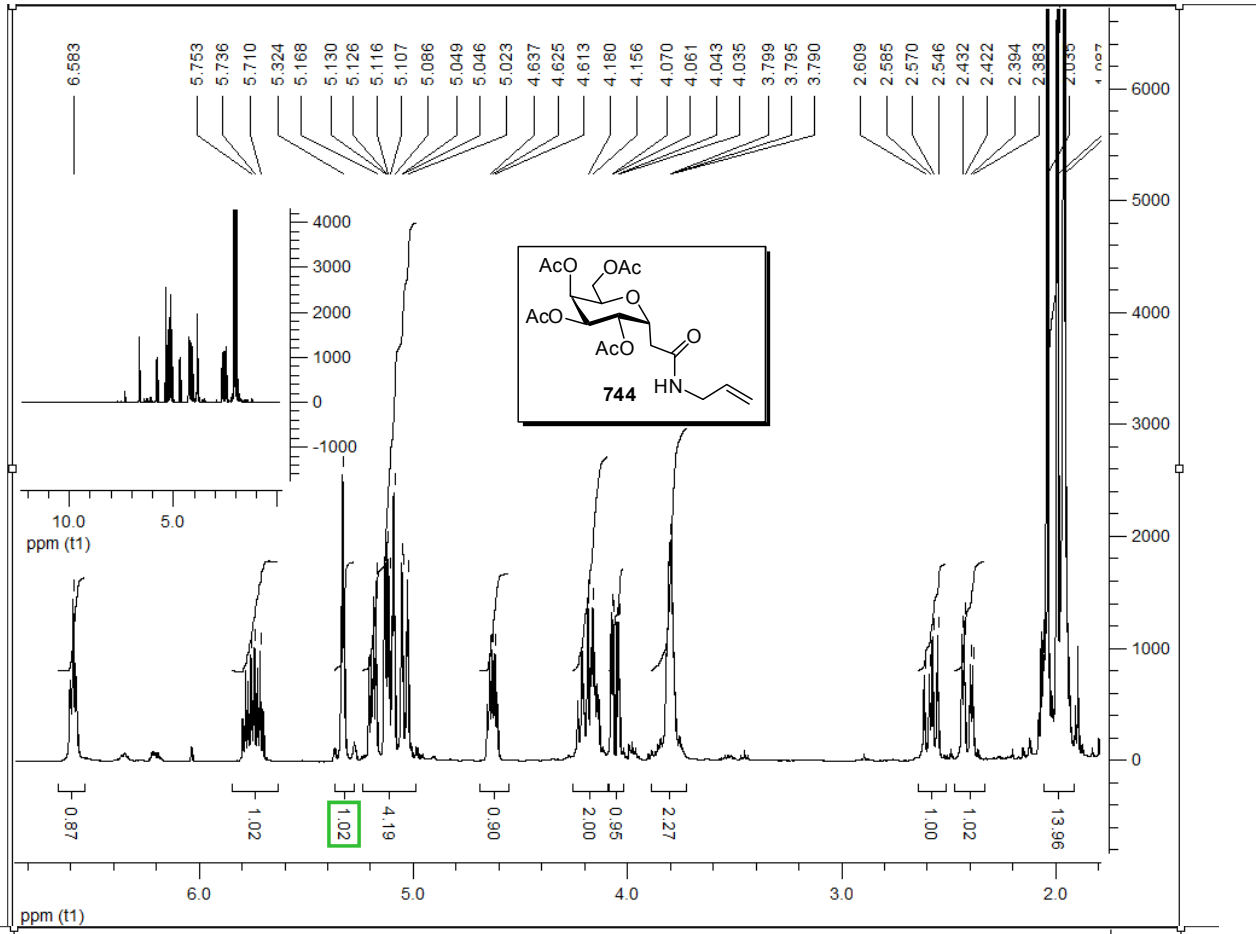

170.523
169.894
169.705
169.543
168.802
69.541
68.878
68.041
67.761
66.848
61.023
52.082
34.803
27.335
27.307
20.701
20.683
20.665
20.595
10.205
10.156
AcO
OAc
AcO
AcO
O
O
HN
741
ppm (t1)

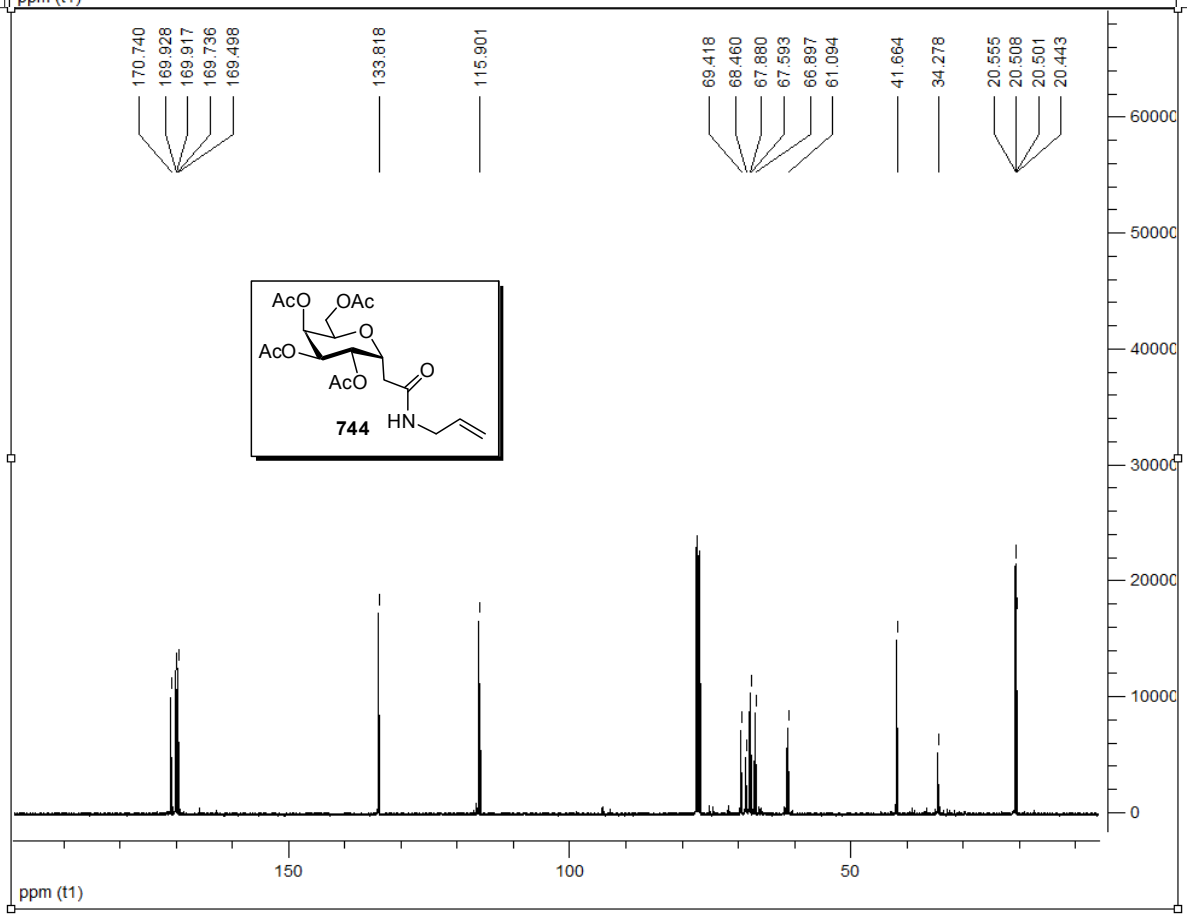

6.392
6.387
5.409
5.251
5.239
5.168
5.160
4.658
4.646
4.633
4.189
2.713
2.705
2.549
2.525
2.419
2.408
2.125
2.087
2.084
2.049
0.772
0.517
0.513
0.508
0.504
AcO
OAc
AcO
AcO
O
O
HN
742
ppm (t1)
0.86
0.96
1.00
0.95
0.93
3.02
0.98
0.99
0.98
1.81
1.83

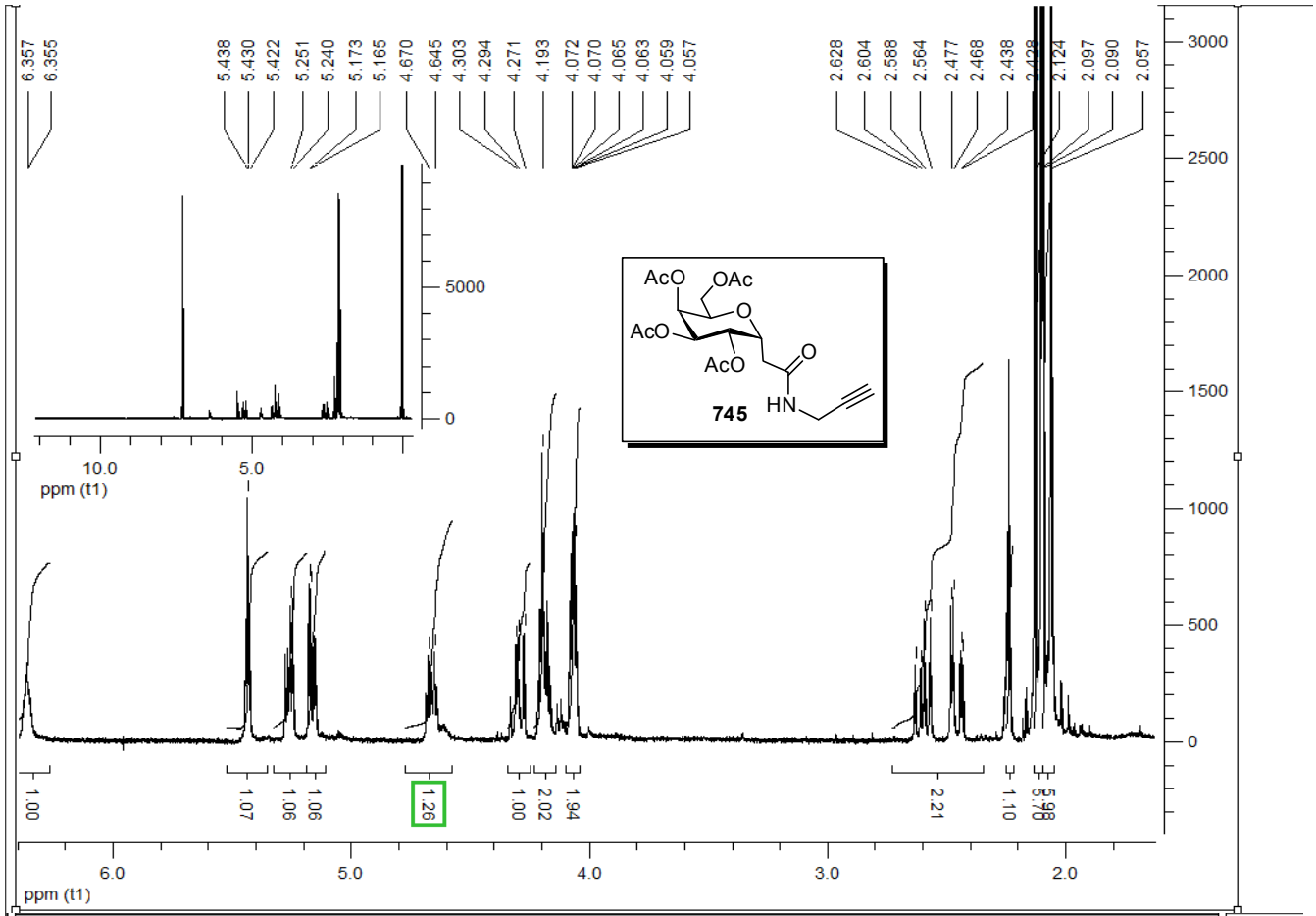

170.652
170.500
169.863
169.695
169.486
69.448
68.641
67.855
67.638
66.898
61.253
34.238
22.538
20.656
20.640
20.562
6.643
6.397
AcO
OAc
AcO
AcO
O
O
HN
742
ppm (t1)

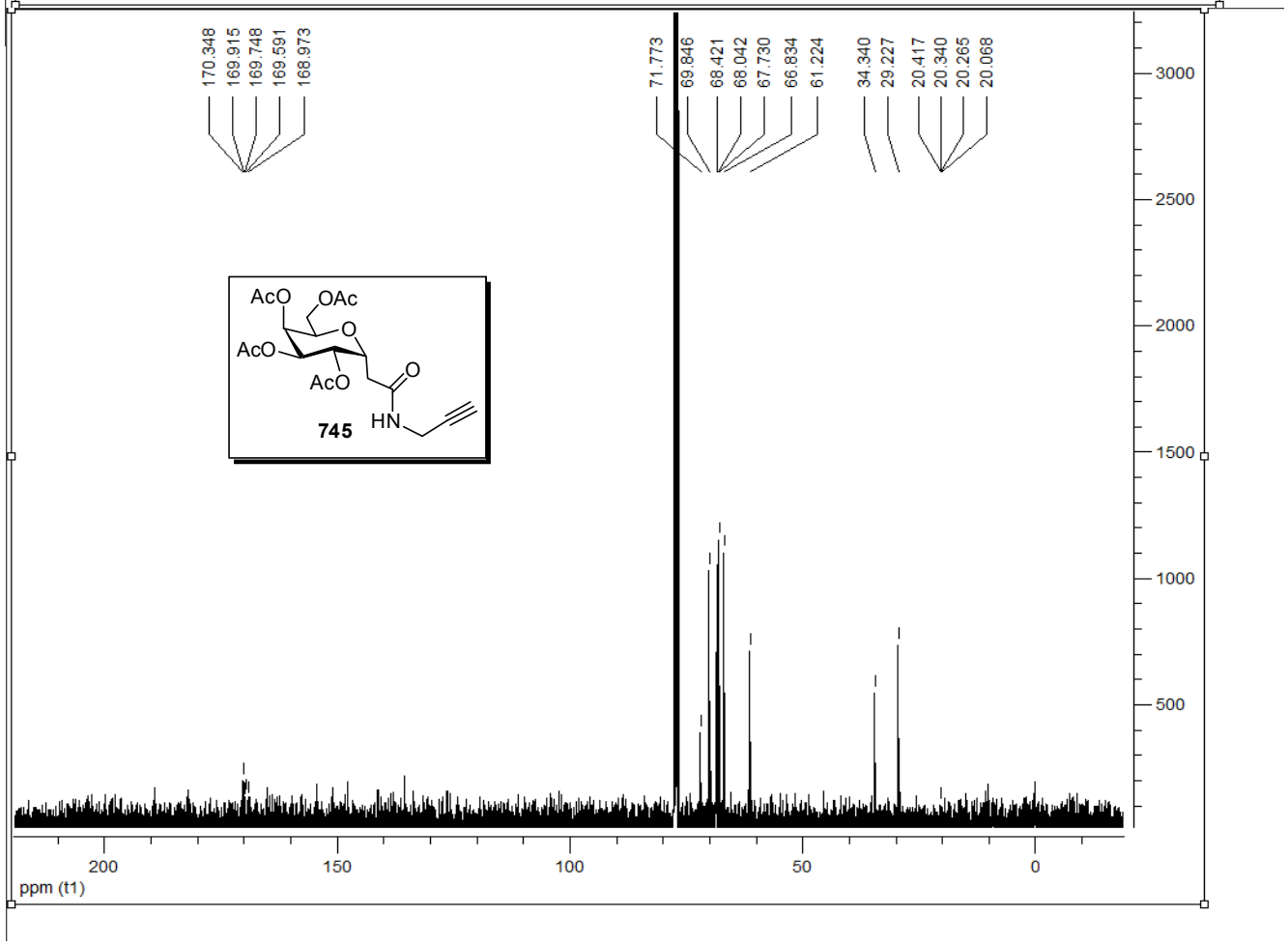

6.306
6.288
5.415
5.411
5.408
5.278
5.266
5.181
5.173
4.700
4.192
2.563
2.540
2.451
2.440
2.129
2.074
2.055
2.043
1.980
1.658
1.606
1.387
AcO
OAc
AcO
AcO
O
HN
743
ppm (t1)
1.05
1.05
1.07
1.12
1.09
0.65
3.00
1.37
1.38
14.18
2.14
4.02
2.09
ppm (t1)

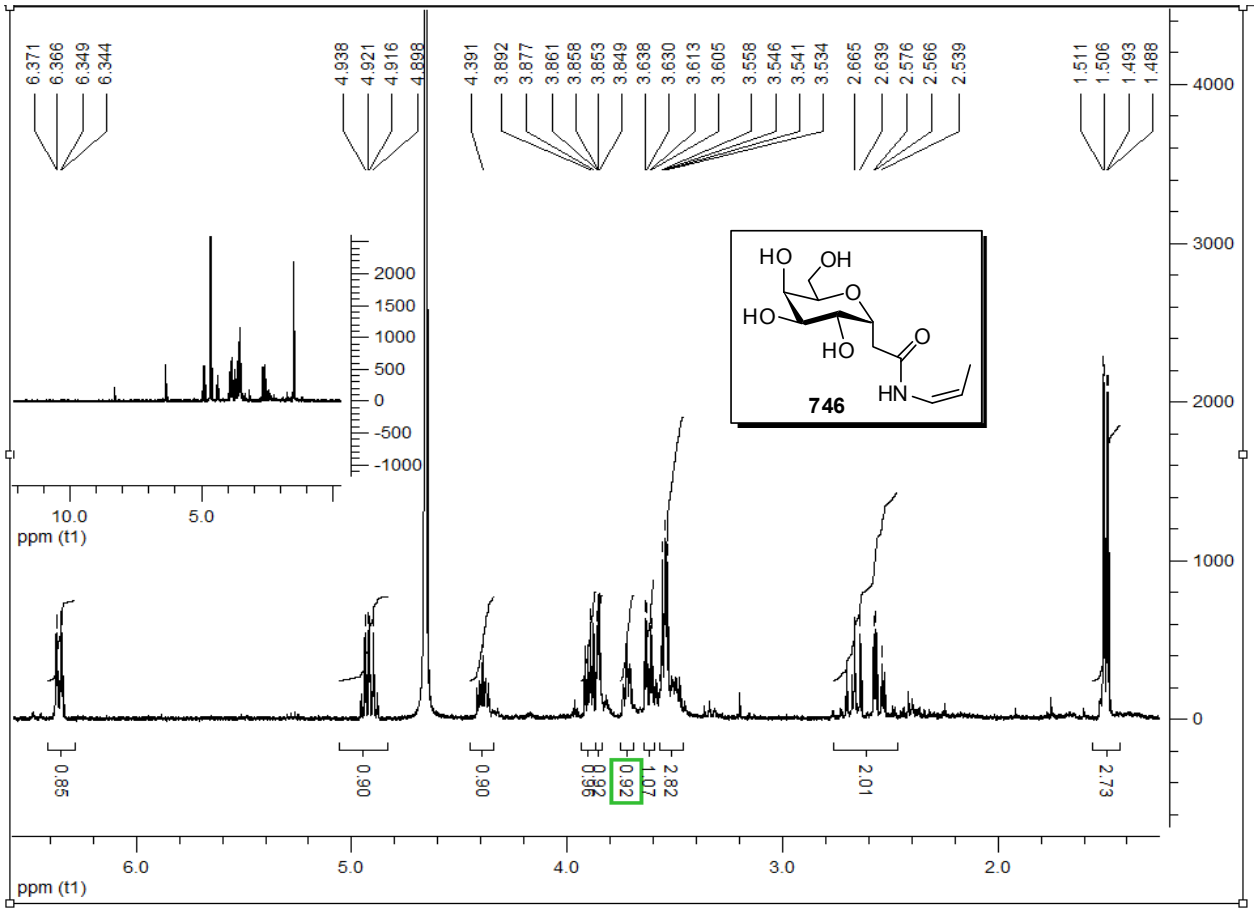

170.446
169.883
169.731
169.461
168.679
69.196
68.964
67.745
67.708
66.965
61.175
51.796
33.407
32.909
32.753
23.553
23.526
20.583
20.558
20.486
AcO
OAc
AcO
AcO
O
HN
743
ppm (t1)

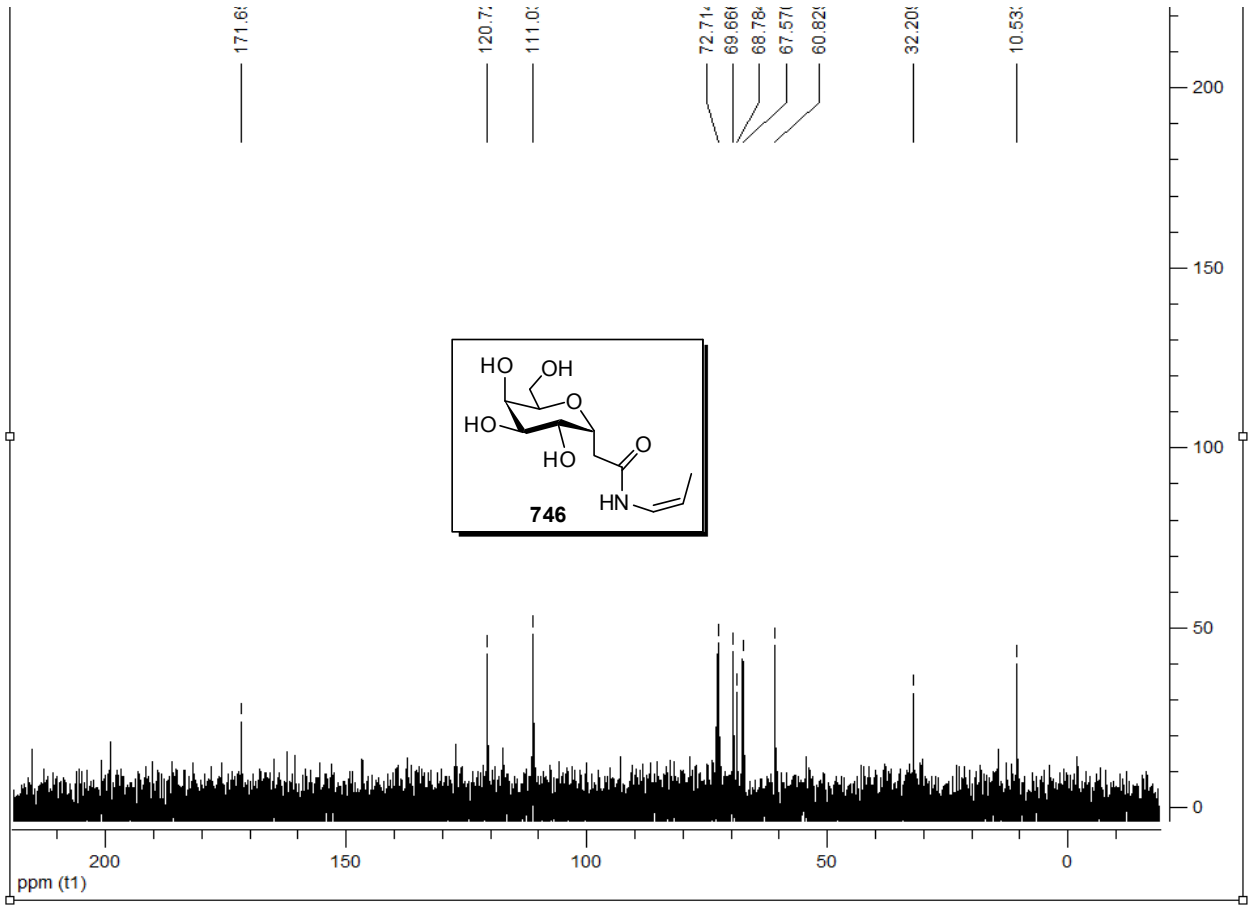

6.583
5.753
5.736
5.710
5.324
5.168
5.130
5.126
5.116
5.107
5.086
5.049
5.046
5.023
4.637
4.625
4.613
4.180
4.156
4.070
4.061
4.043
4.035
3.799
3.795
3.790
2.609
2.585
2.570
2.546
2.432
2.422
2.394
2.383
2.035
AcO
OAc
AcO
AcO
O
O
HN
744
ppm (t1)
0.87
1.02
1.02
4.19
0.90
2.00
0.95
2.27
1.00
1.02
13.96
ppm (t1)

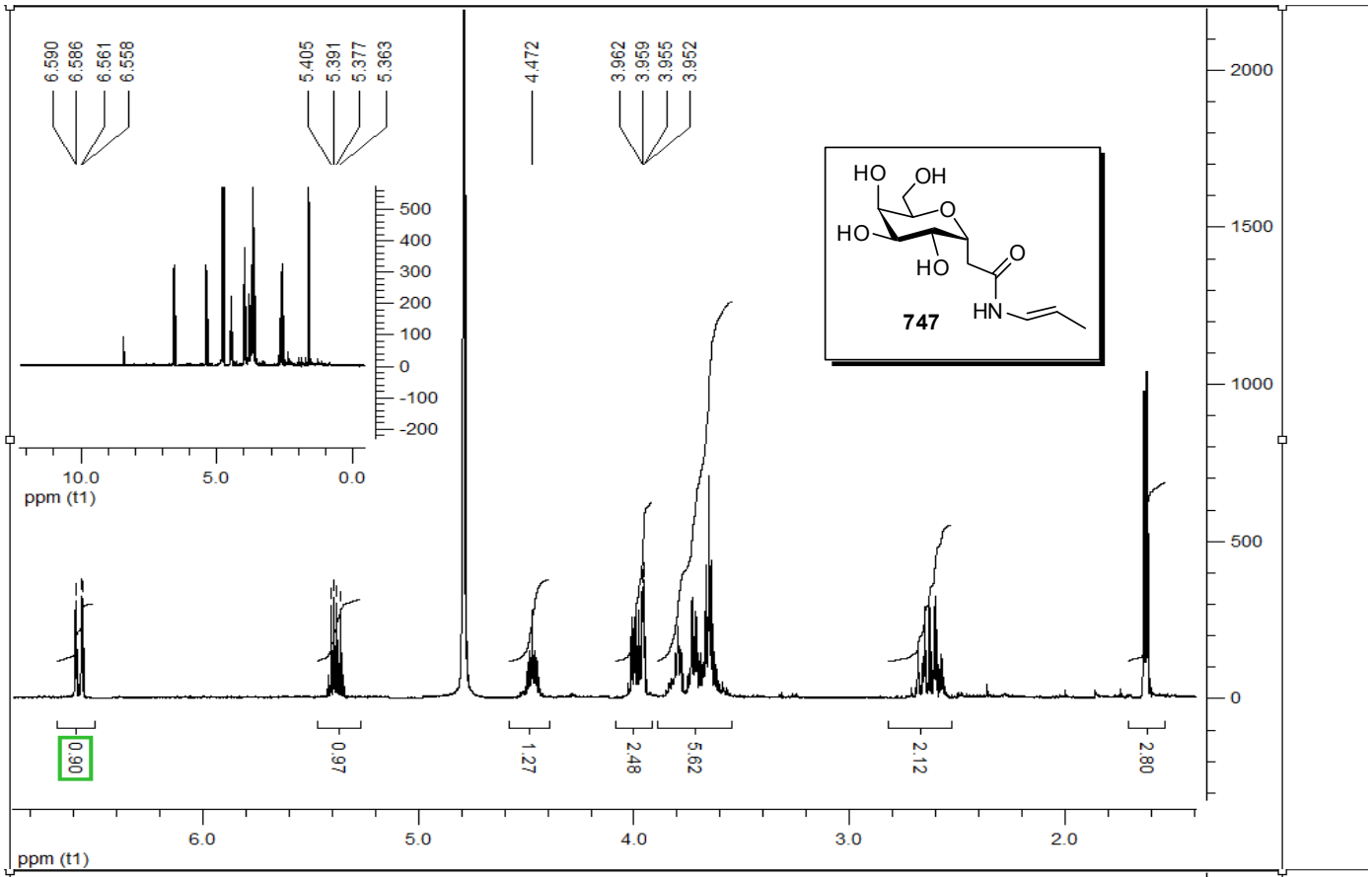

170.740
169.928
169.917
169.736
169.498
133.818
115.901
69.418
68.460
67.880
67.593
66.897
61.094
41.664
34.278
20.555
20.508
20.501
20.443
AcO
OAc
AcO
AcO
O
O
HN
744
ppm (t1)

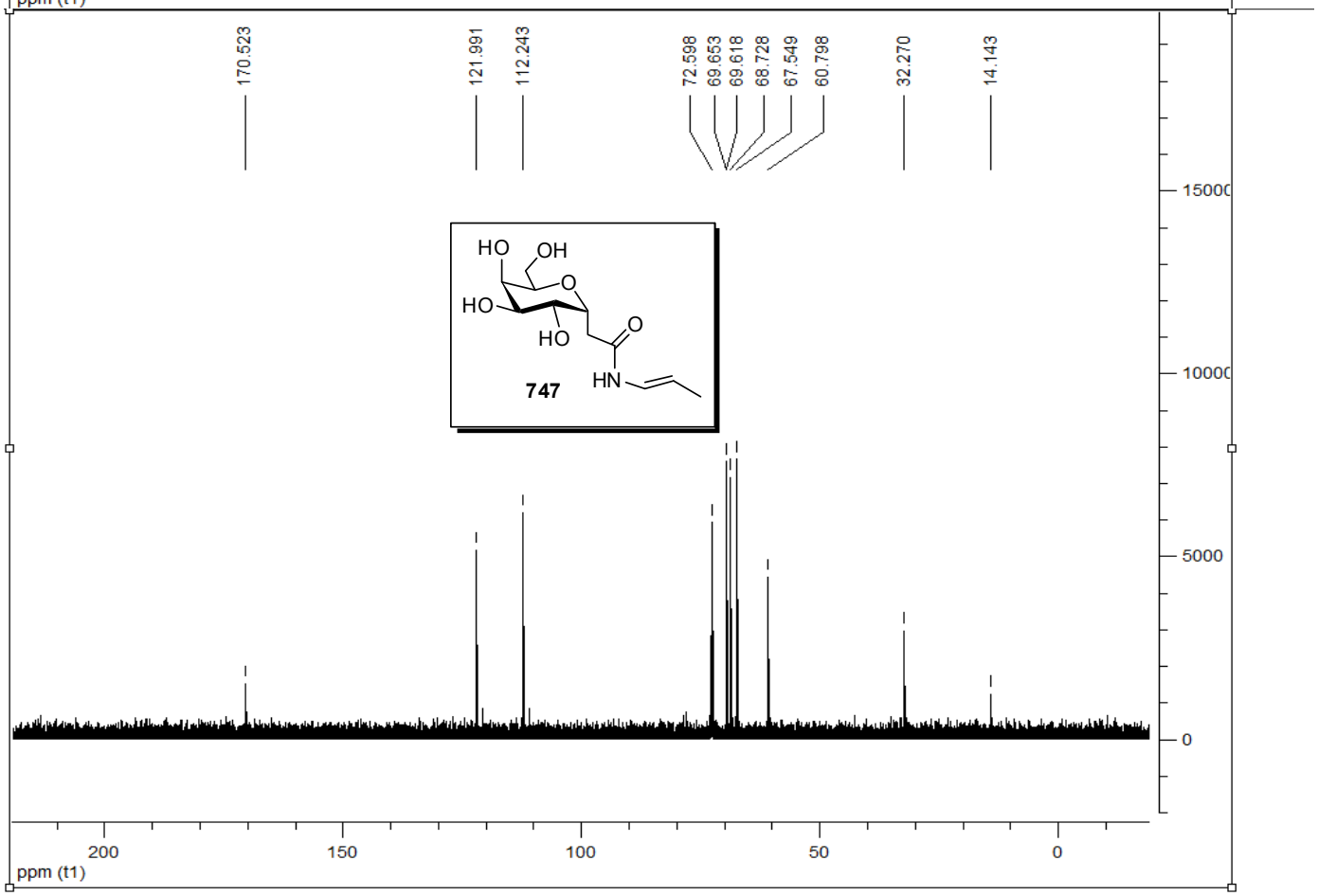

6.357
6.355
5.438
5.430
5.422
5.251
5.240
5.173
5.165
4.670
4.645
4.303
4.294
4.271
4.193
4.072
4.070
4.065
4.063
4.059
4.057
2.628
2.604
2.588
2.564
2.477
2.468
2.438
2.124
2.097
2.090
2.057
AcO
OAc
AcO
AcO
O
HN
745
ppm (t1)
1.00
1.07
1.06
1.06
1.26
1.00
2.02
1.94
2.21
1.10
5.98
5.78

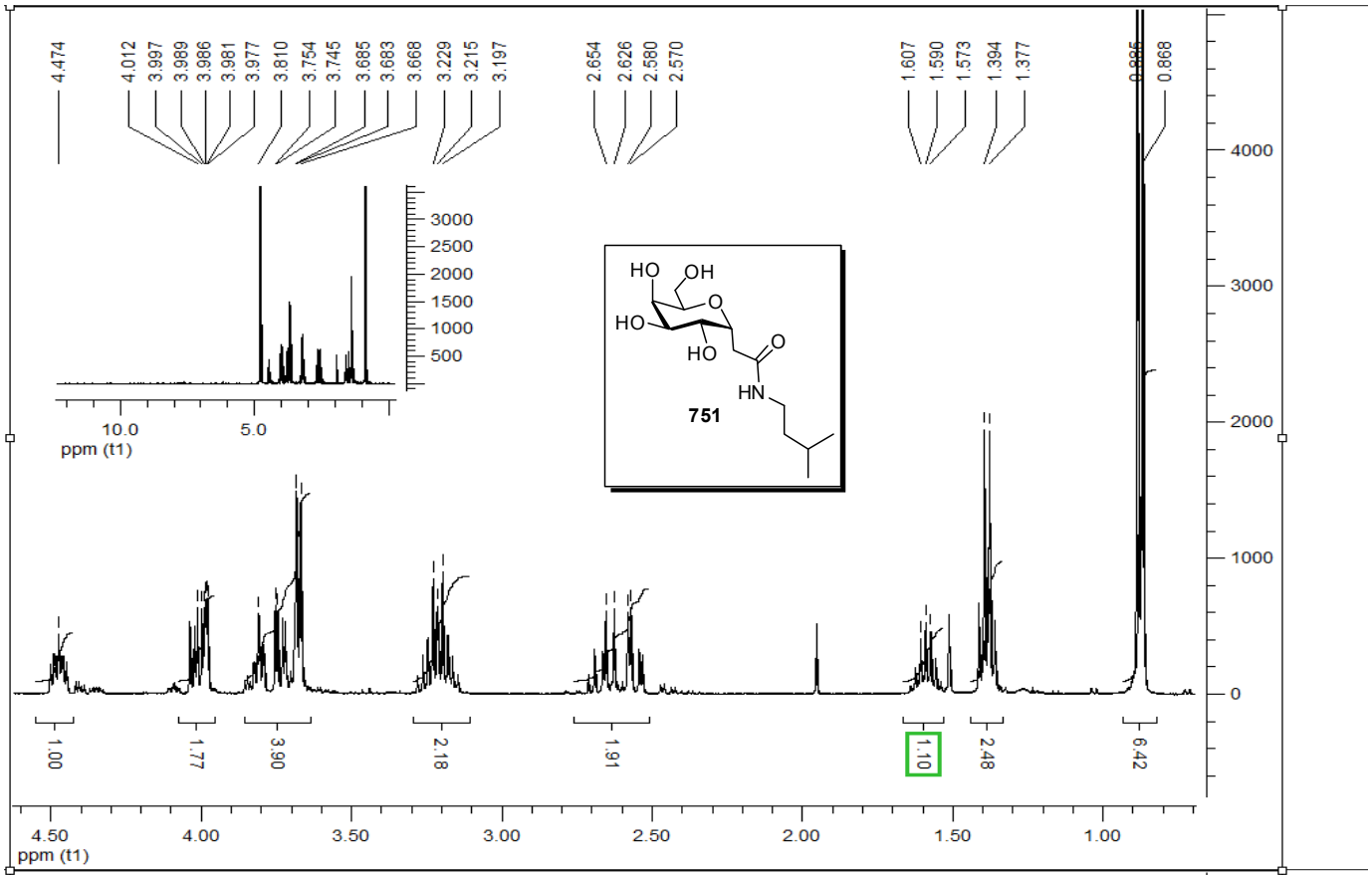

170.348
169.915
169.748
169.591
168.973
71.773
69.846
68.421
68.042
67.730
66.834
61.224
34.340
29.227
20.417
20.340
20.265
20.068
AcO
OAc
AcO
AcO
O
HN
745
ppm (t1)

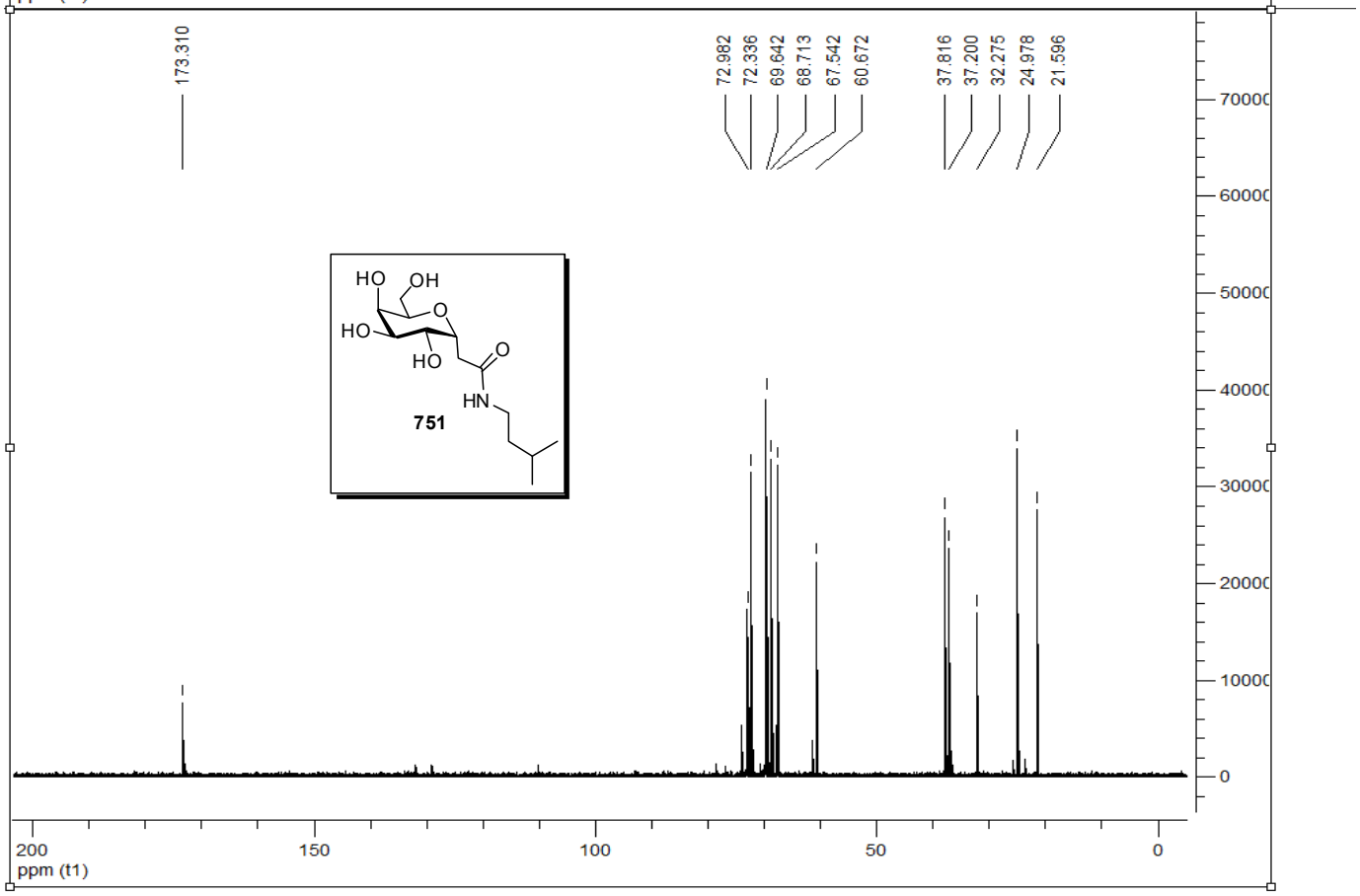

6.371
6.366
6.349
6.344
4.938
4.921
4.916
4.898
4.391
3.892
3.877
3.861
3.858
3.853
3.849
3.638
3.630
3.613
3.605
3.558
3.546
3.541
3.534
2.665
2.639
2.576
2.566
2.539
1.511
1.506
1.493
1.488
HO
OH
O
HO
HO
O
HN
746
ppm (t1)
0.85
0.90
0.90
0.96
0.92
1.07
2.82
2.01
2.73

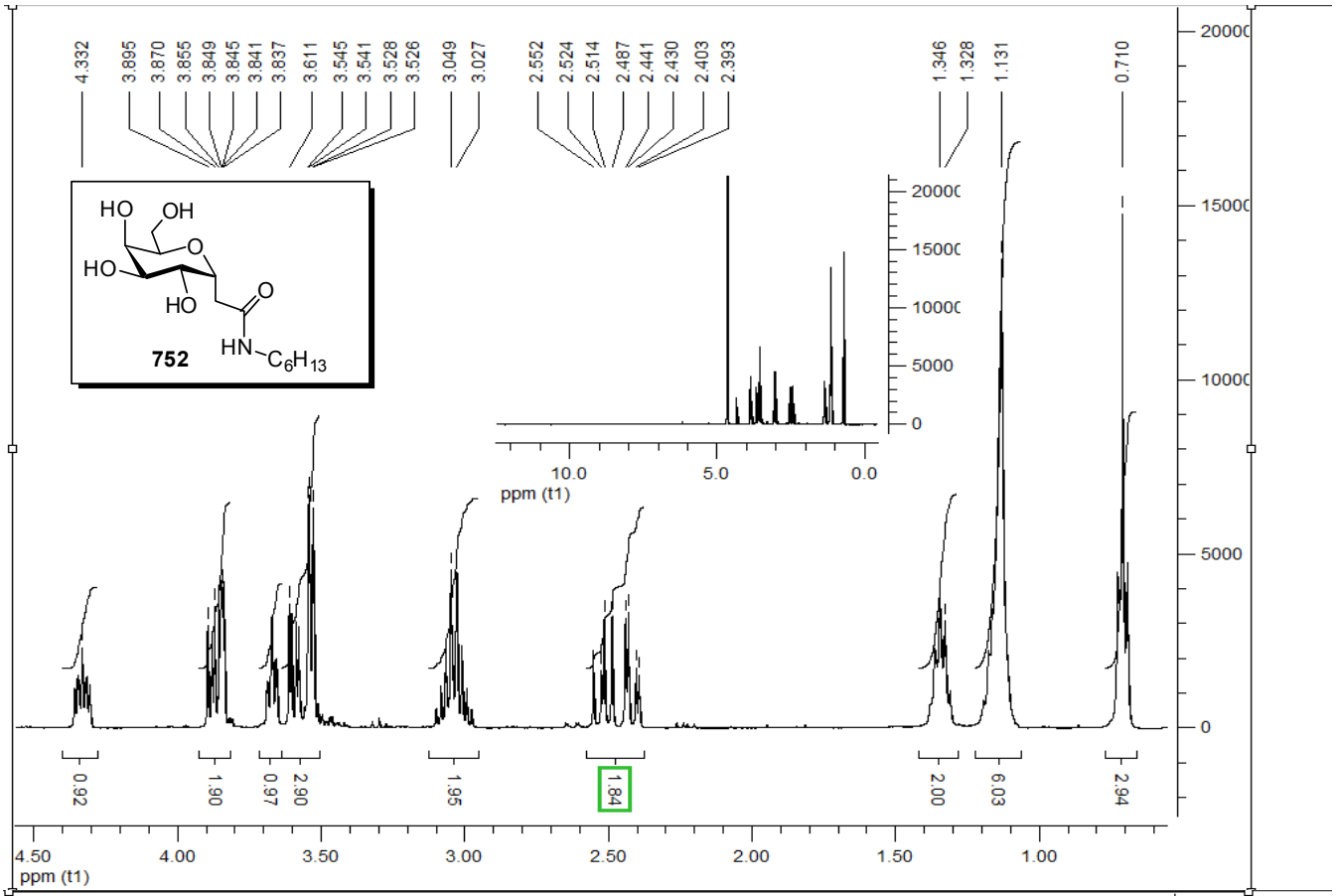

171.6
120.7
111.0
72.71
69.66
68.78
67.57
60.82
32.20
10.53
HO
OH
O
HO
HO
O
HN
746
ppm (t1)

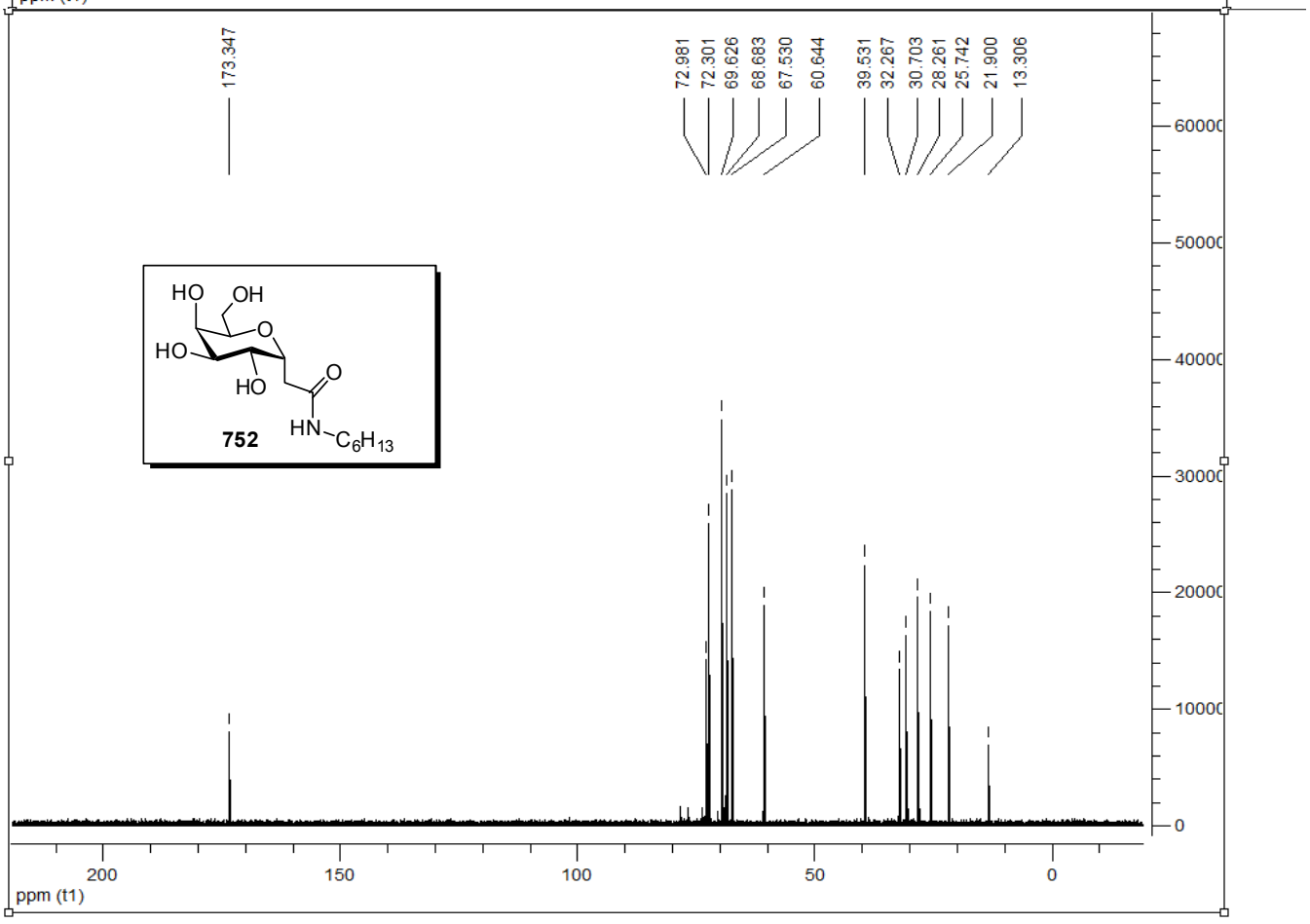

6.590
6.586
6.561
6.558
5.405
5.391
5.377
5.363
4.472
3.962
3.959
3.955
3.952
HO
OH
O
HO
HO
O
HN
747
ppm (t1)
0.90
0.97
1.27
2.48
5.92
2.12
2.80
ppm (t1)

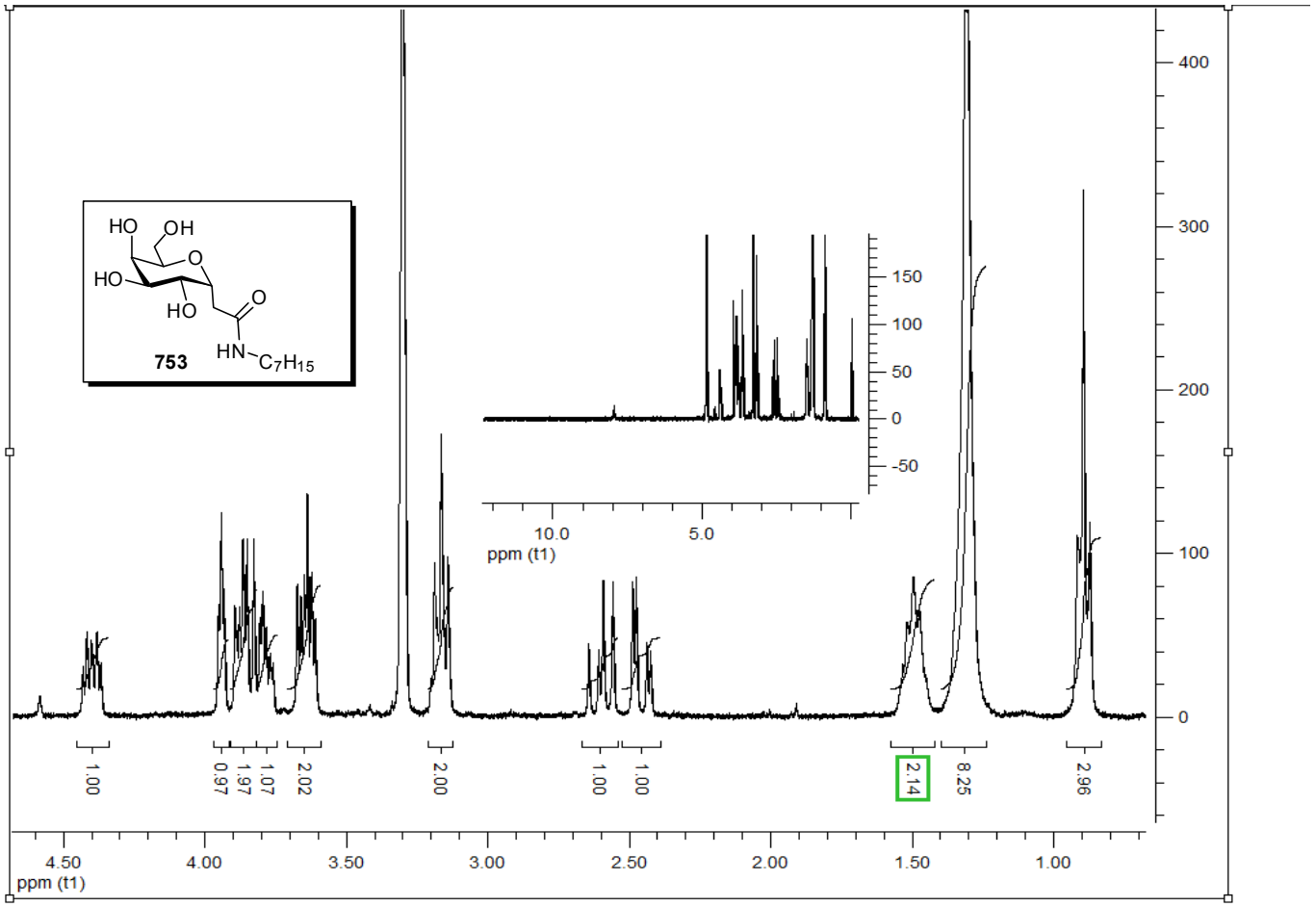

170.523
121.991
112.243
72.598
69.653
69.618
68.728
67.549
60.798
32.270
14.143
HO
OH
O
HO
HO
O
HN
747
ppm (t1)

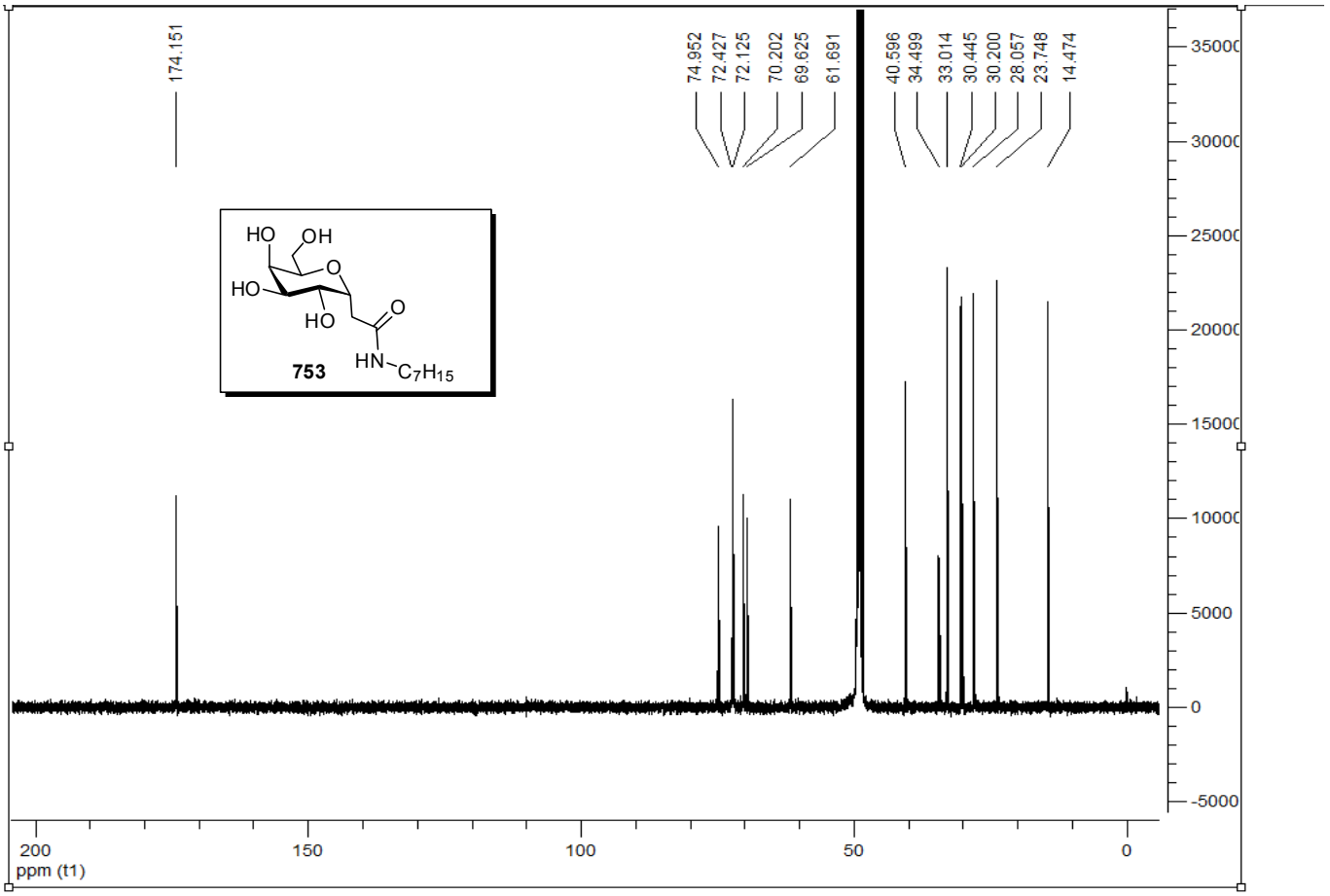

4.474
4.012
3.997
3.989
3.986
3.981
3.977
3.810
3.754
3.745
3.685
3.683
3.668
3.229
3.215
3.197
2.654
2.626
2.580
2.570
1.607
1.590
1.573
1.394
1.377
0.885
0.868
HO
OH
O
HO
HO
O
HN
751
ppm (t1)
1.00
1.77
3.90
2.18
1.91
1.10
2.48
6.42

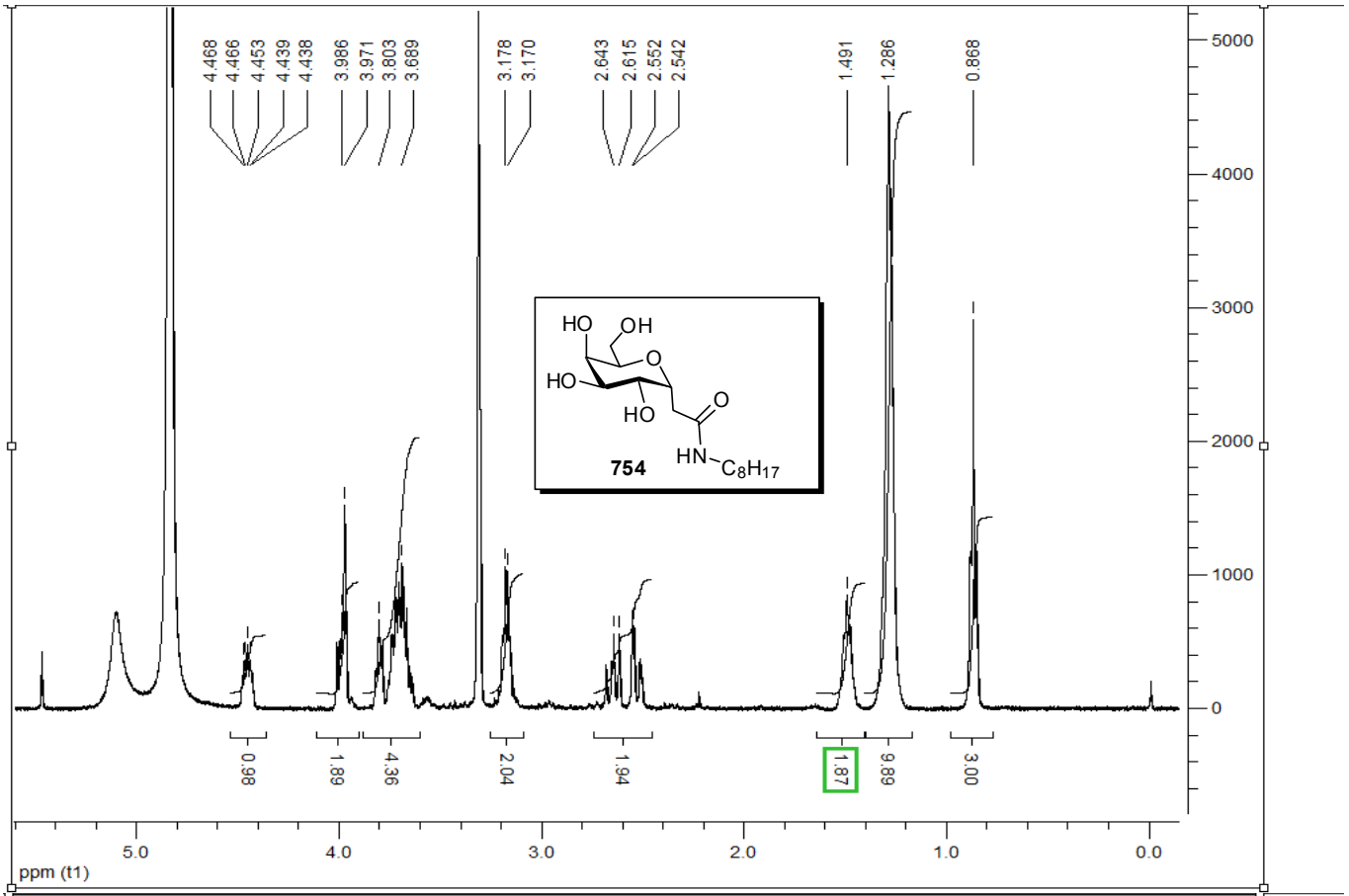

173.310
72.982
72.336
69.642
68.713
67.542
60.672
37.816
37.200
32.275
24.978
21.596
HO
OH
O
HO
HO
O
HN
751
ppm (t1)

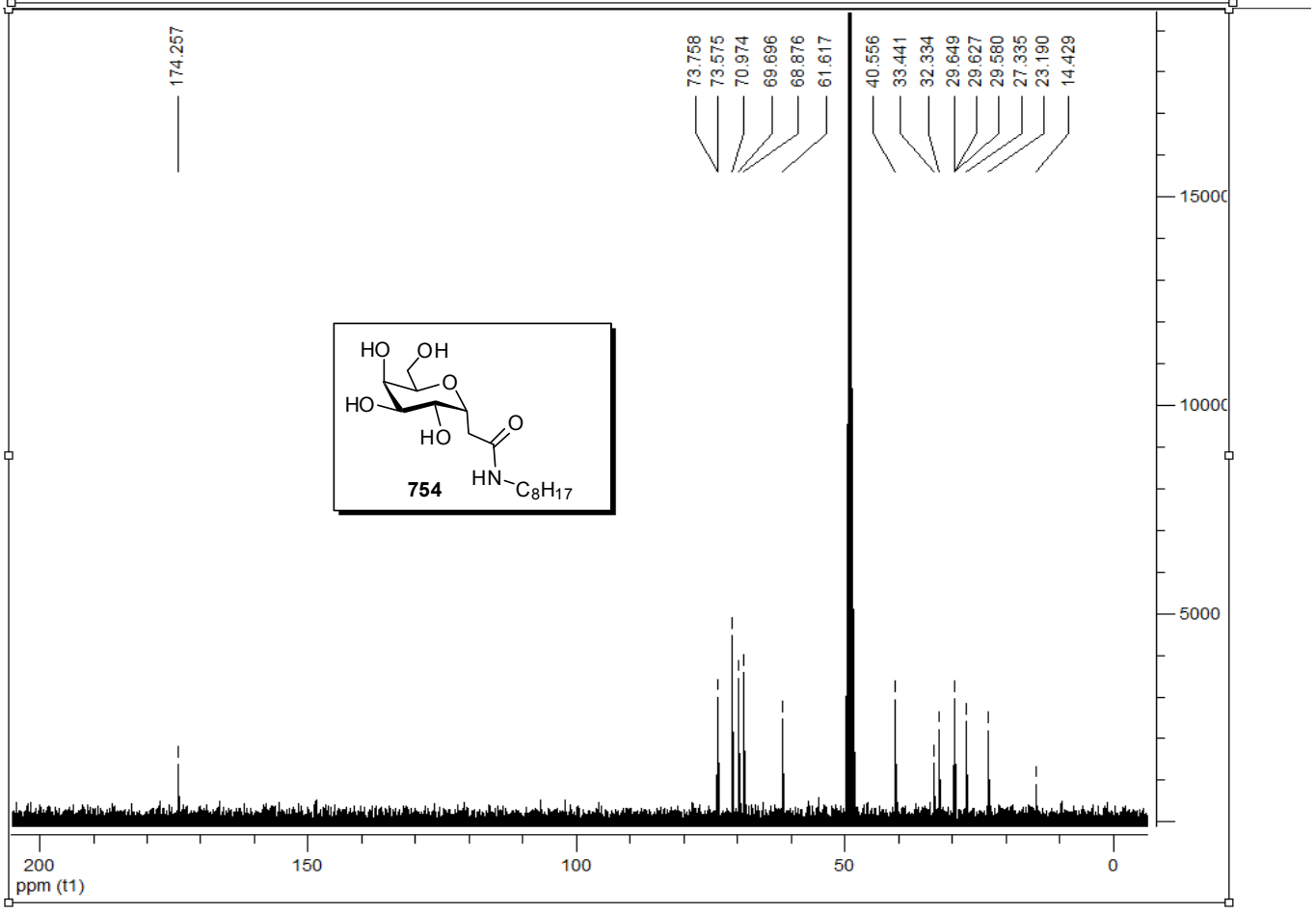

4.332
3.895
3.870
3.855
3.849
3.845
3.841
3.837
3.611
3.545
3.541
3.528
3.526
3.049
3.027
2.552
2.524
2.514
2.487
2.441
2.430
2.403
2.393
1.346
1.328
1.131
0.710
HO
OH
O
HO
HO
O
HN
C6H13
752
ppm (t1)
0.92
1.90
0.97
2.90
1.95
1.84
2.00
6.03
2.94

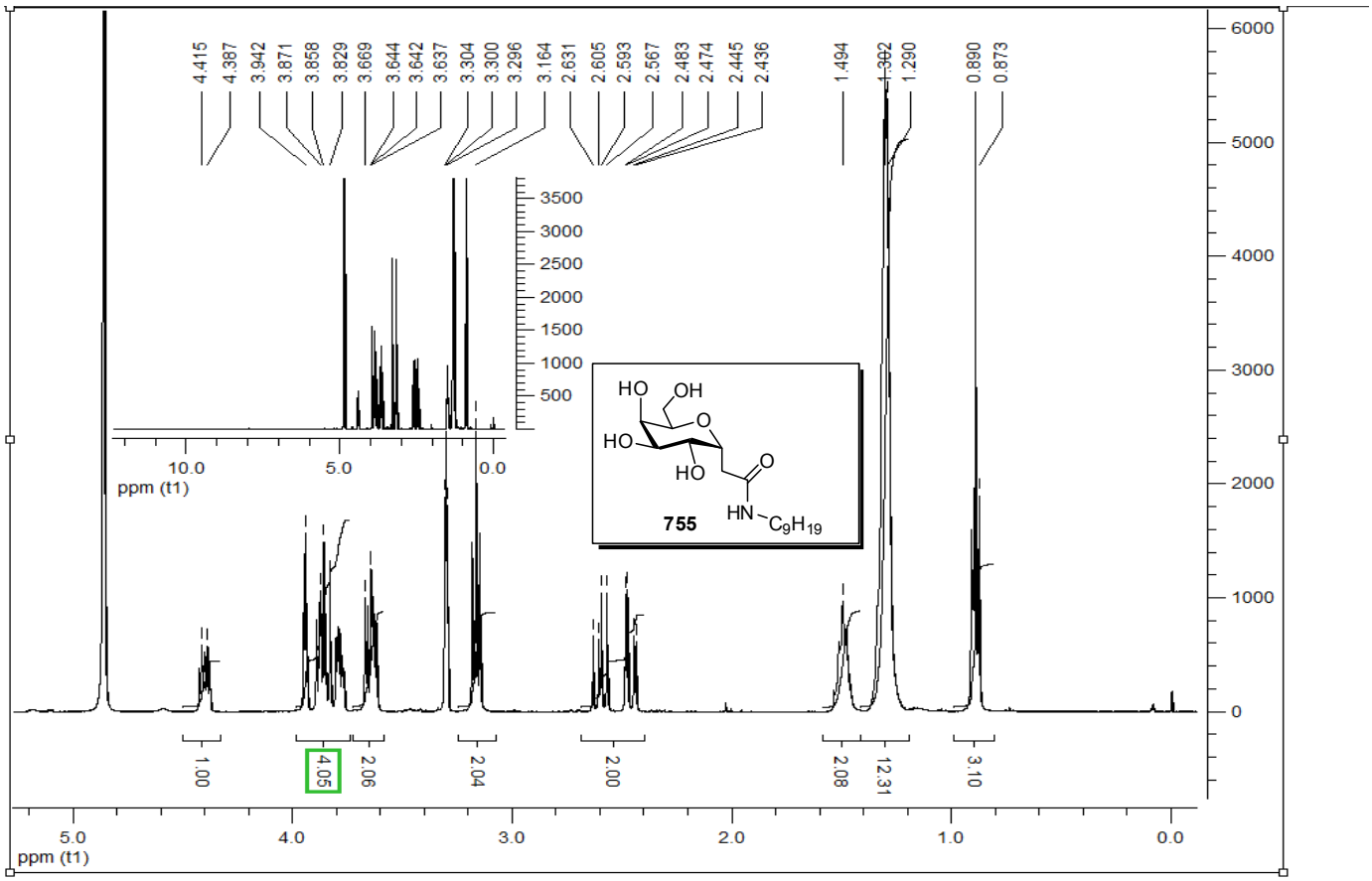

173.347
72.981
72.301
69.626
68.683
67.530
60.644
39.531
32.267
30.703
28.261
25.742
21.900
13.306
HO
OH
O
HO
HO
O
HN
C6H13
752
ppm (t1)

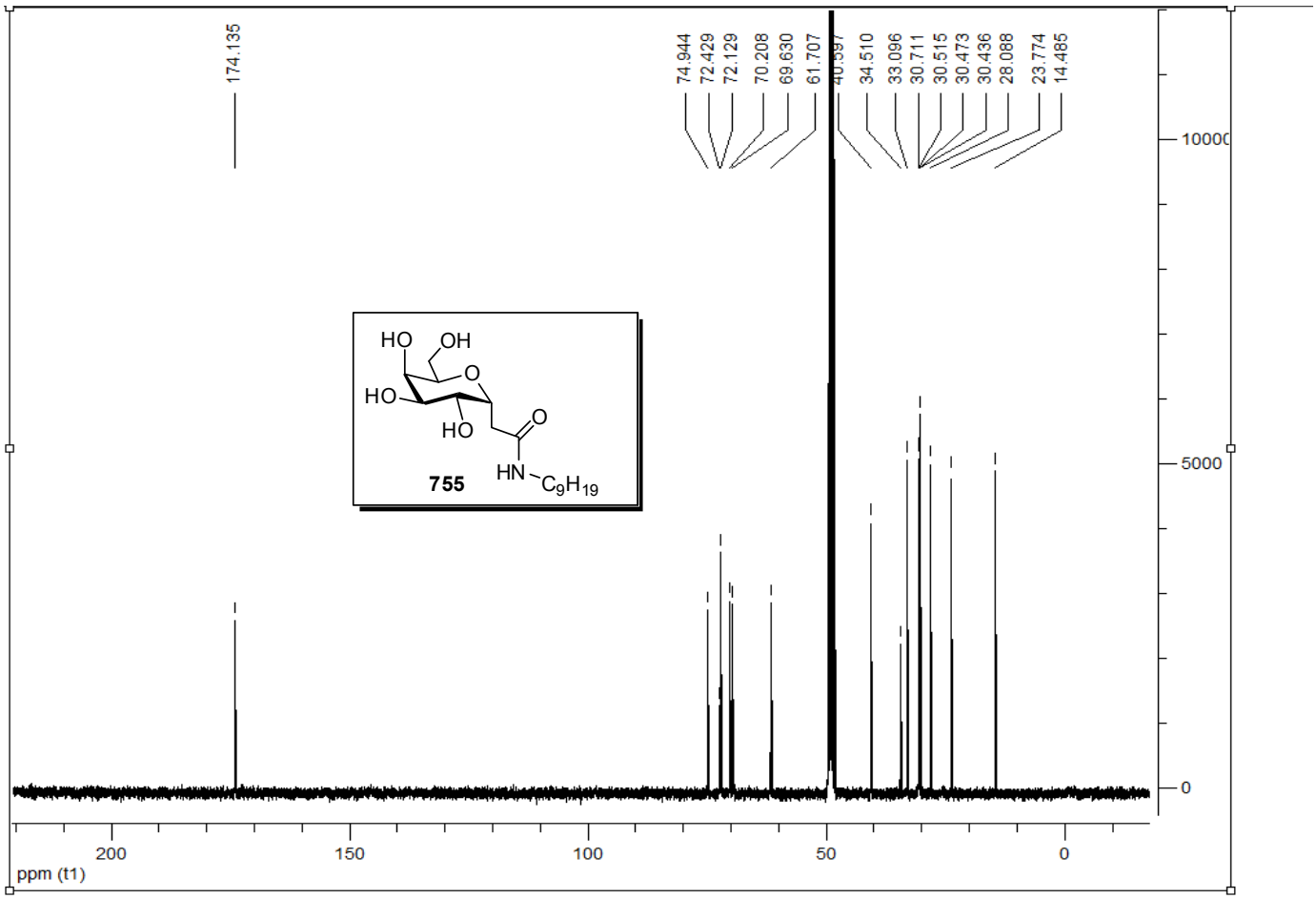

HO
OH
HO
HO
O
O
HN
C7H15
753
ppm (t1)
1.00
0.97
1.97
1.07
2.02
2.00
1.00
1.00
2.14
8.25
2.96

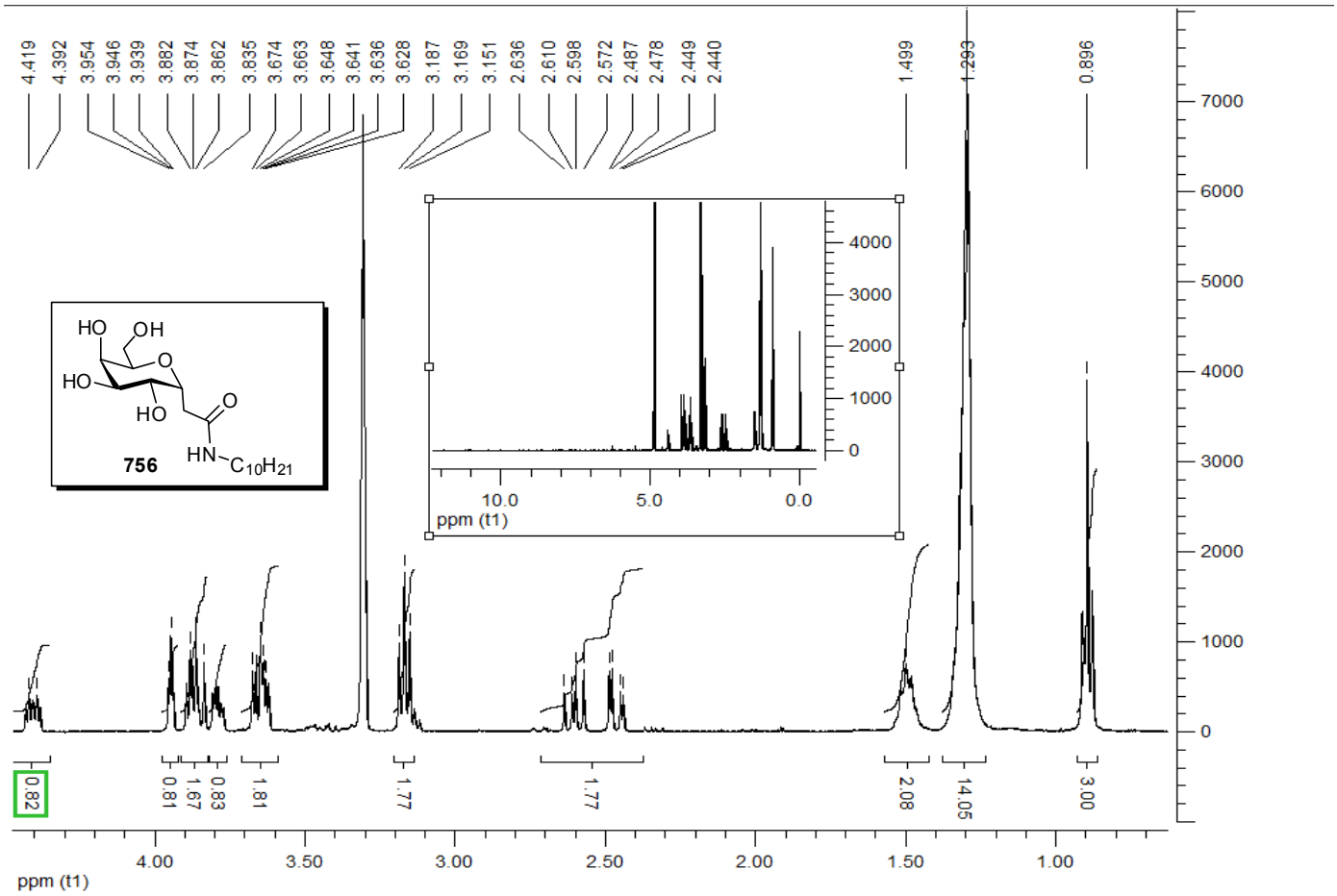

174.151
74.952
72.427
72.125
70.202
69.625
61.691
40.596
34.499
33.014
30.445
30.200
28.057
23.748
14.474
HO
OH
HO
HO
O
O
HN
C7H15
753
ppm (t1)

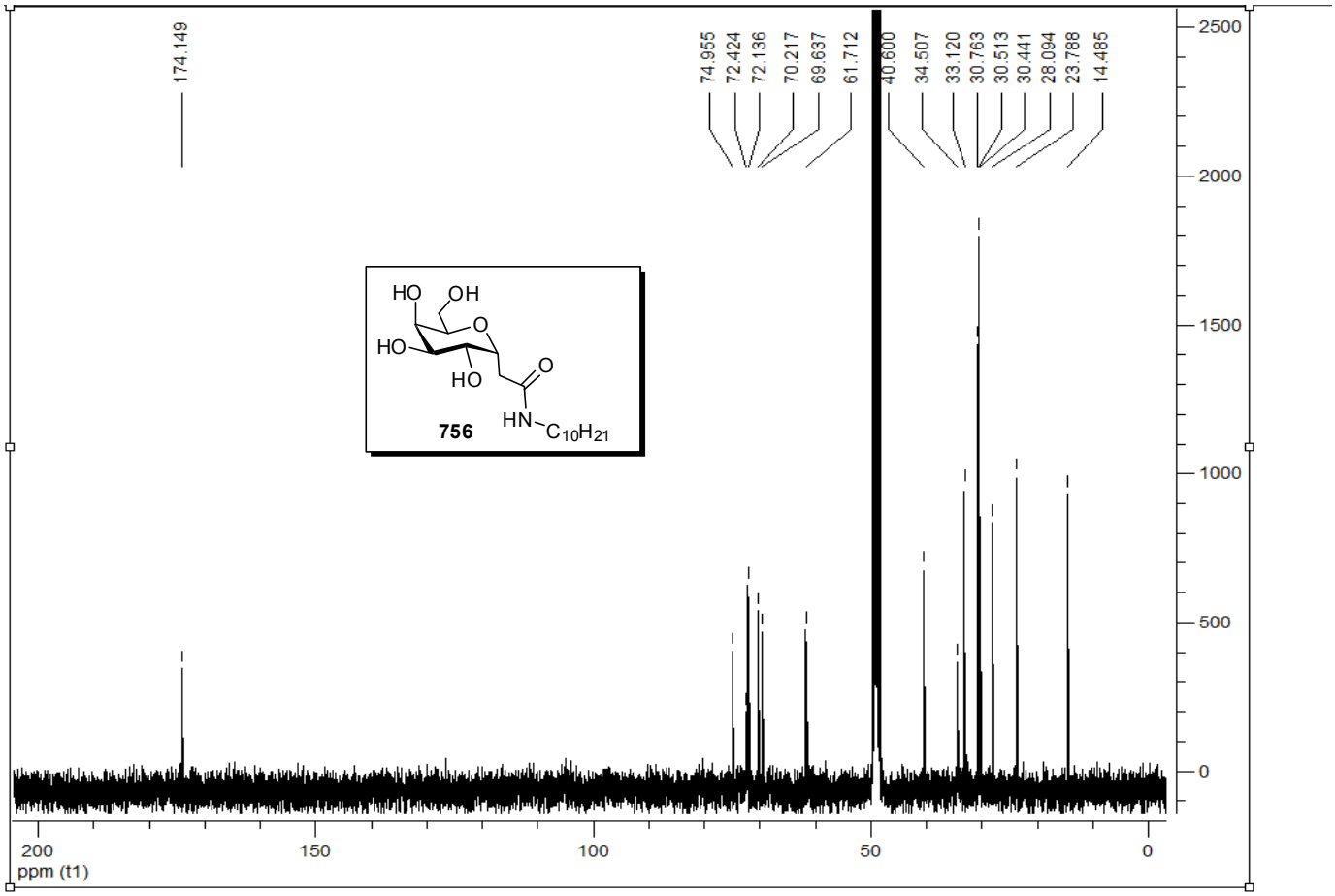

4.468
4.466
4.453
4.439
4.438
3.986
3.971
3.803
3.689
3.178
3.170
2.643
2.615
2.552
2.542
1.491
1.286
0.868
HO
OH
O
HO
HO
O
HN
C8H17
754
0.98
1.89
4.36
2.04
1.94
1.87
9.89
3.00
5.0
4.0
3.0
2.0
1.0
0.0
ppm (t1)
5000
4000
3000
2000
1000
0

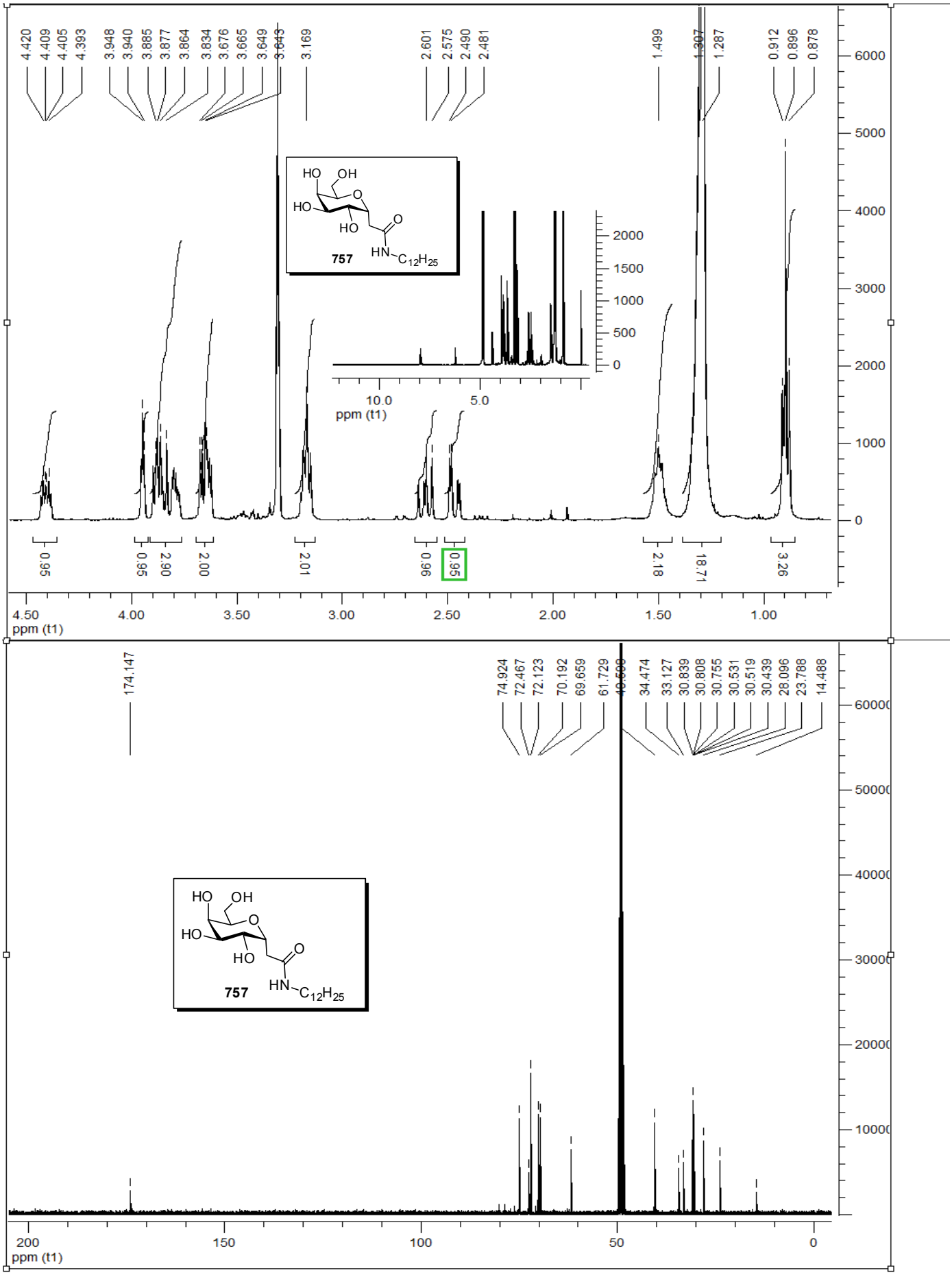

174.257
73.758
73.575
70.974
69.696
68.876
61.617
40.556
33.441
32.334
29.649
29.627
29.580
27.335
23.190
14.429
HO
OH
O
HO
HO
O
HN
C8H17
754
200
150
100
50
0
ppm (t1)
15000
10000
5000

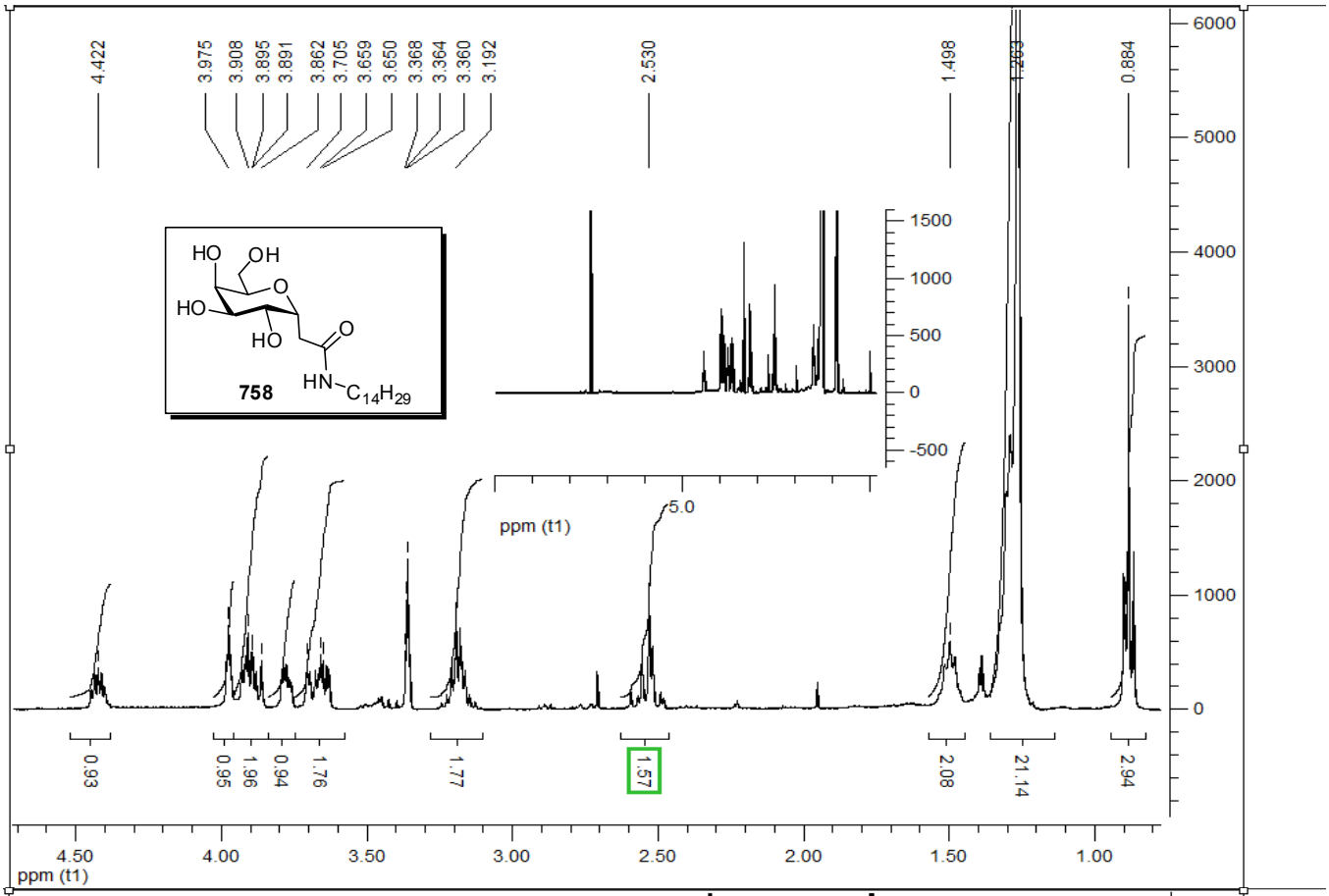

4.415
4.387
3.942
3.871
3.858
3.829
3.669
3.644
3.642
3.637
3.304
3.300
3.296
3.164
2.631
2.605
2.593
2.567
2.483
2.474
2.445
2.436
1.494
1.302
1.290
0.890
0.873
ppm (t1)
HO
OH
O
HO
HO
O
HN
$C_9H_{19}$
755
1.00
4.05
2.06
2.04
2.00
2.08
12.31
3.10
ppm (t1)

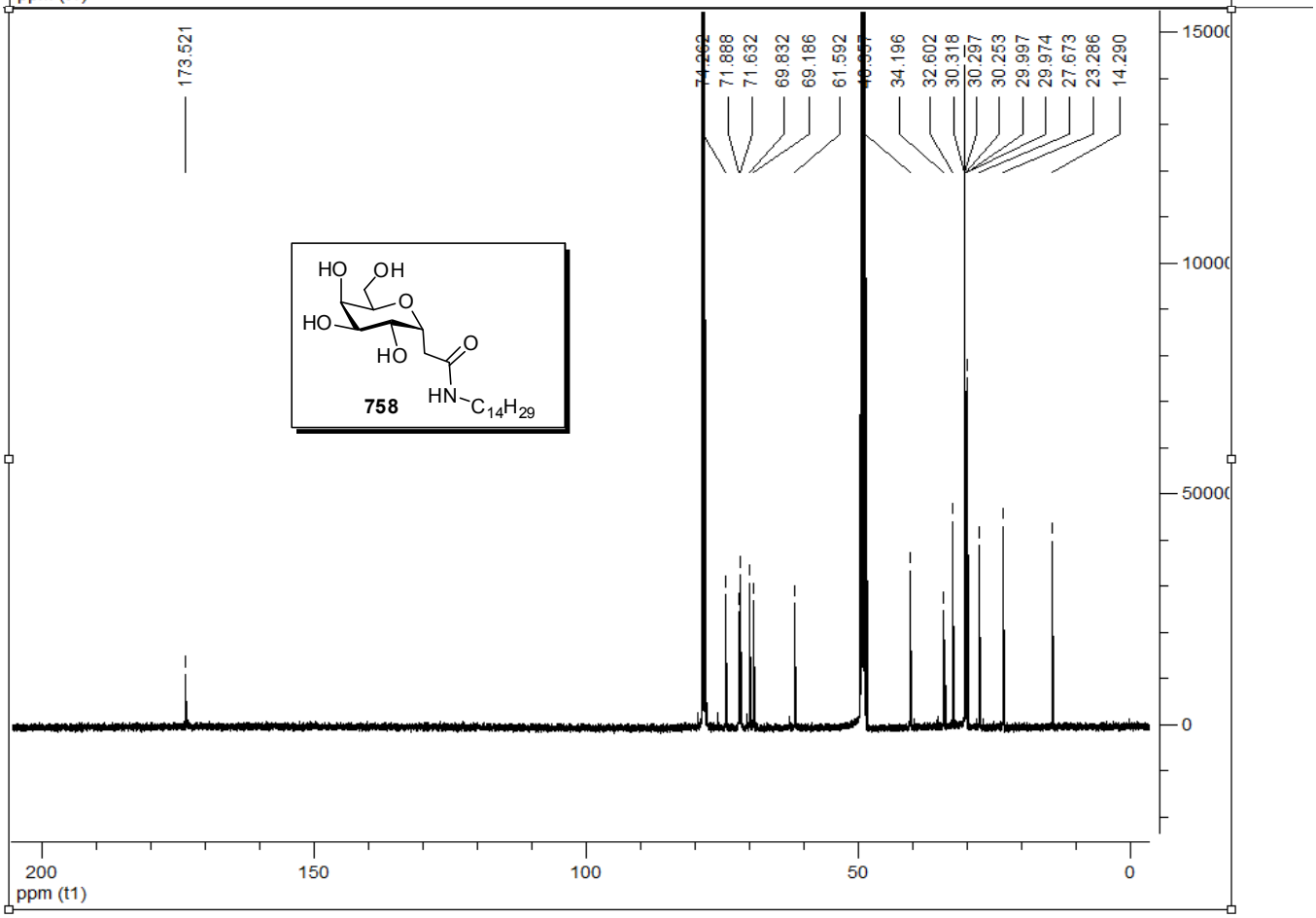

174.135
74.944
72.429
72.129
70.208
69.630
61.707
34.510
33.096
30.711
30.515
30.473
30.436
28.088
23.774
14.485
HO
OH
O
HO
HO
O
HN
$C_9H_{19}$
755
ppm (t1)

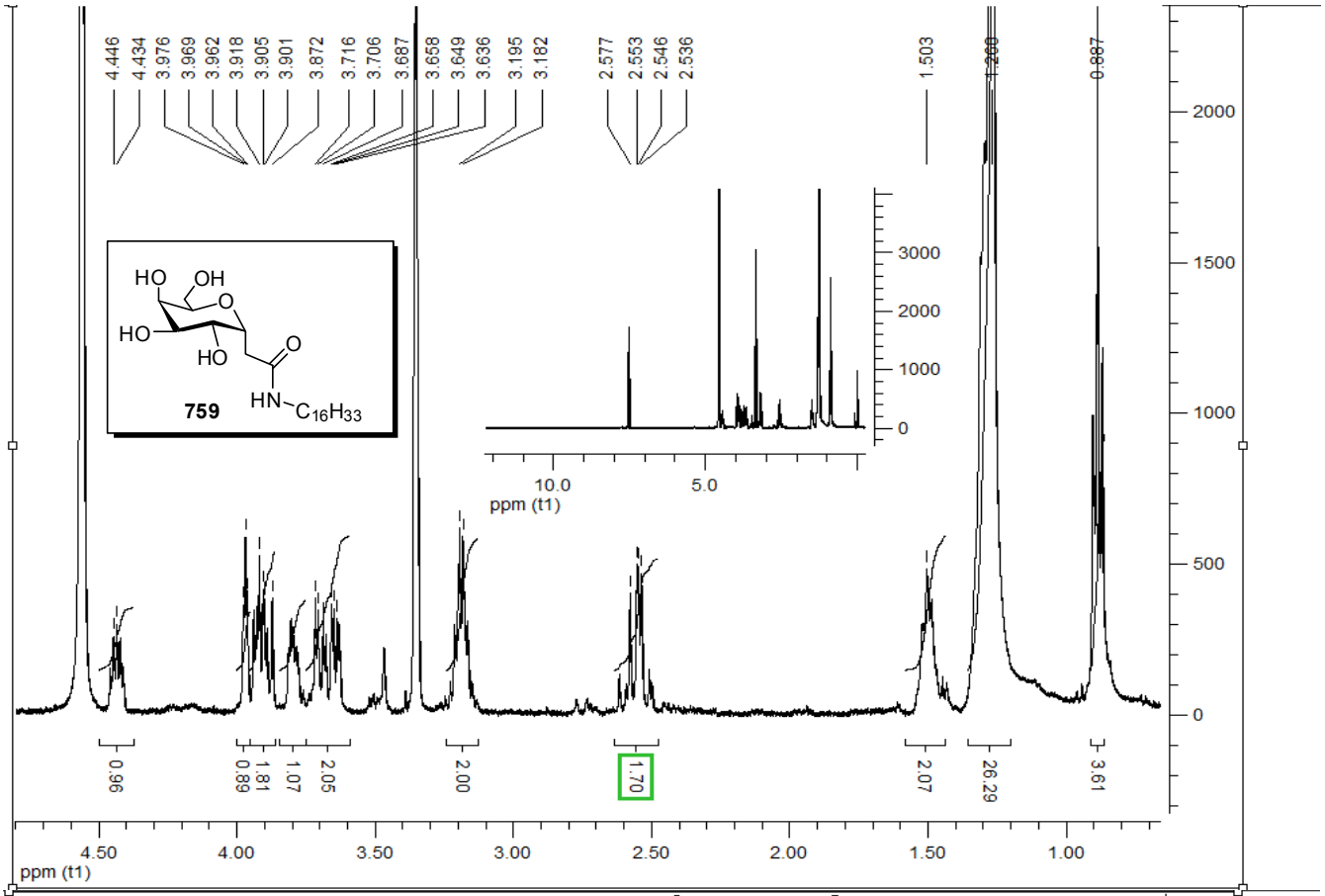

4.419
4.392
3.954
3.946
3.939
3.882
3.874
3.862
3.835
3.674
3.663
3.648
3.641
3.636
3.628
3.187
3.169
3.151
2.636
2.610
2.598
2.572
2.487
2.478
2.449
2.440
1.499
1.293
0.896
HO
OH
O
HO
HO
O
HN
C10H21
756
ppm (t1)
0.82
0.81
1.67
0.83
1.81
1.77
1.77
2.08
14.05
3.00
ppm (t1)

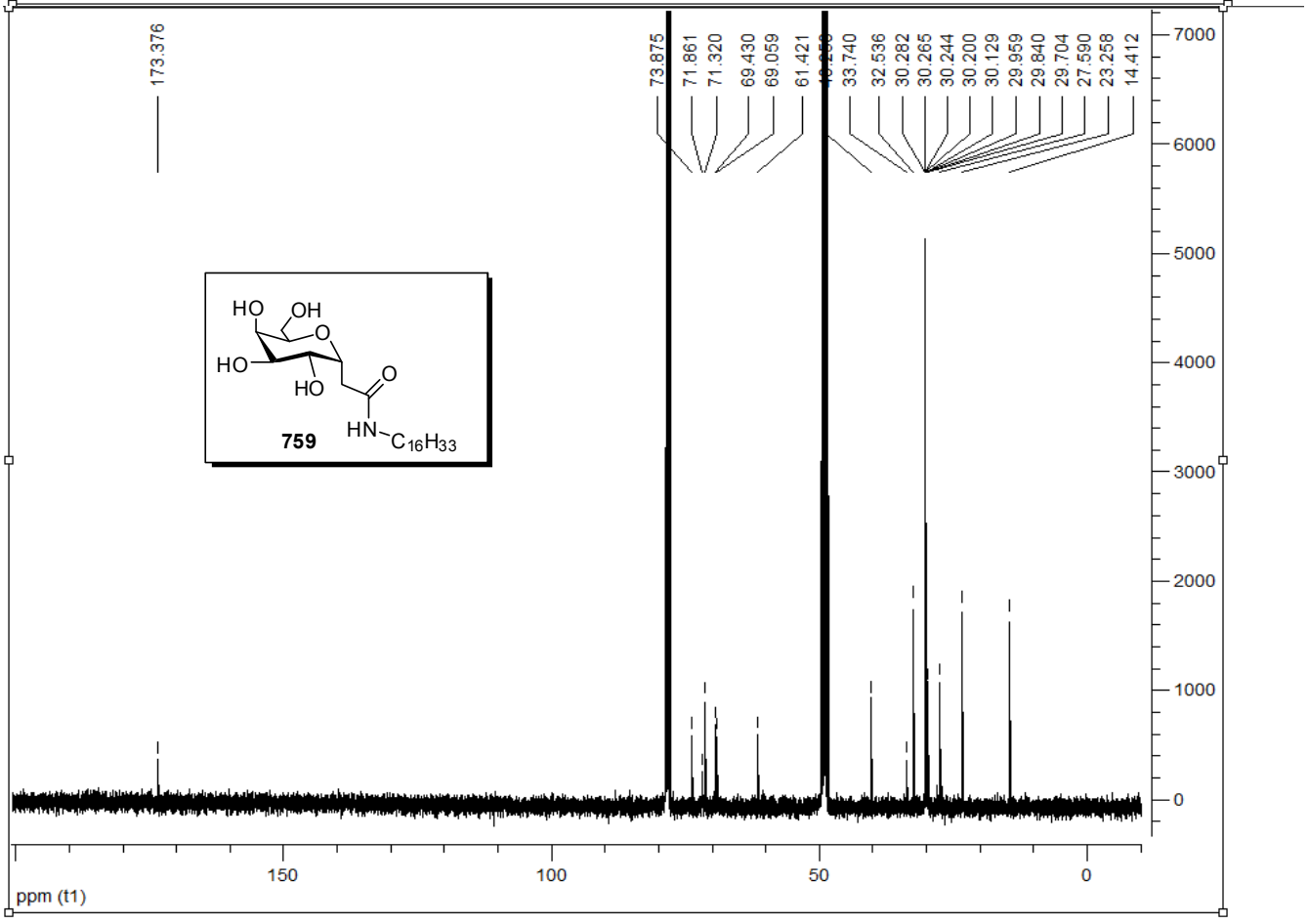

174.149
74.955
72.424
72.136
70.217
69.637
61.712
40.600
34.507
33.120
30.763
30.513
30.441
28.094
23.788
14.485
HO
OH
O
HO
HO
O
HN
C10H21
756
ppm (t1)

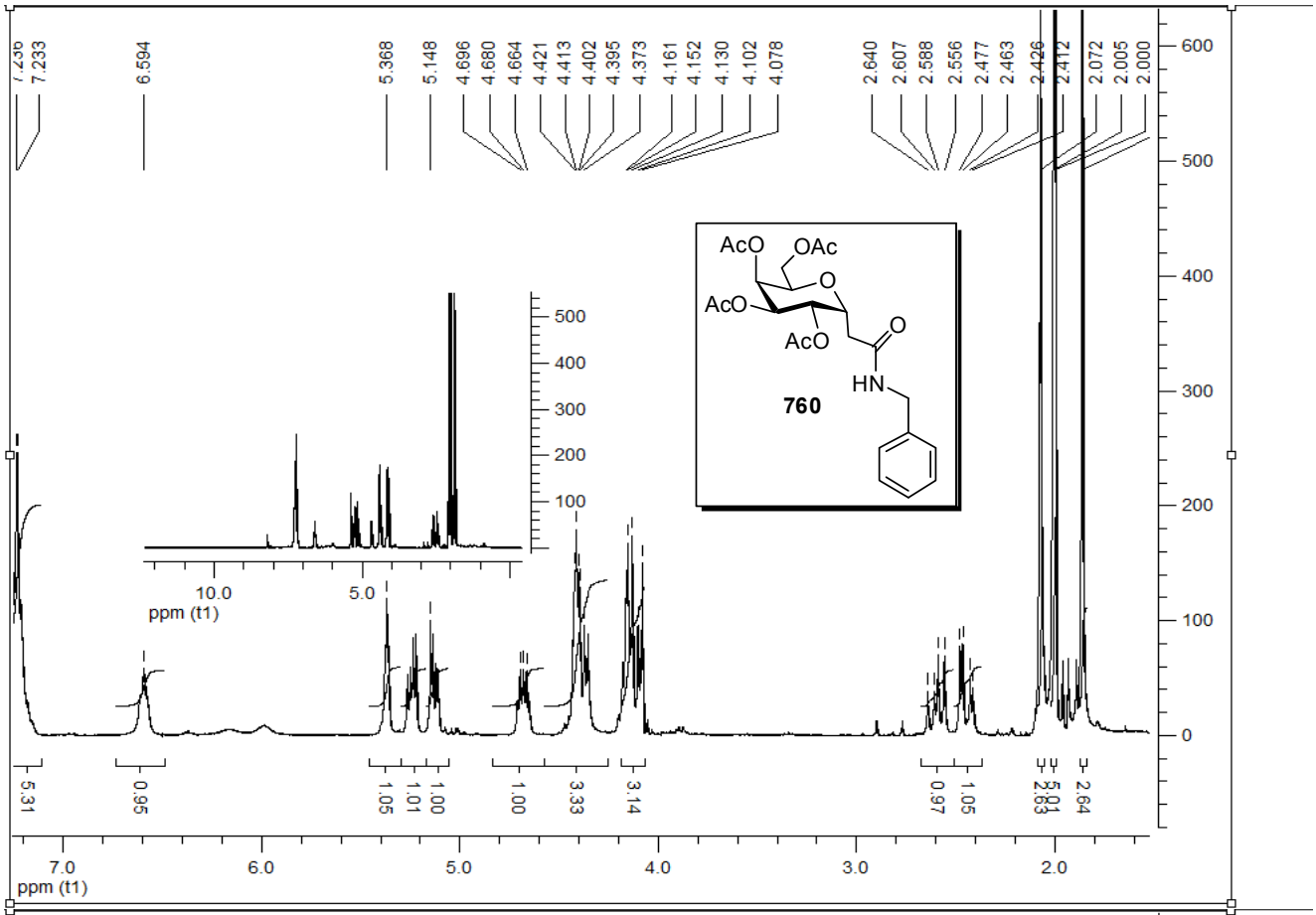

4.420
4.409
4.405
4.393
3.948
3.940
3.885
3.877
3.864
3.834
3.676
3.665
3.649
3.643
3.169
2.601
2.575
2.490
2.481
1.499
1.307
1.287
0.912
0.896
0.878
HO
OH
O
HO
HO
O
HN
C12H25
757
10.0
5.0
ppm (t1)
0.95
0.95
2.90
2.00
2.01
0.96
0.95
2.18
18.71
3.26
4.50
4.00
3.50
3.00
2.50
2.00
1.50
1.00
ppm (t1)
174.147
74.924
72.467
72.123
70.192
69.659
61.729
49.690
34.474
33.127
30.839
30.808
30.755
30.531
30.519
30.439
28.096
23.788
14.488
HO
OH
O
HO
HO
O
HN
C12H25
757
200
150
100
50
0
ppm (t1)

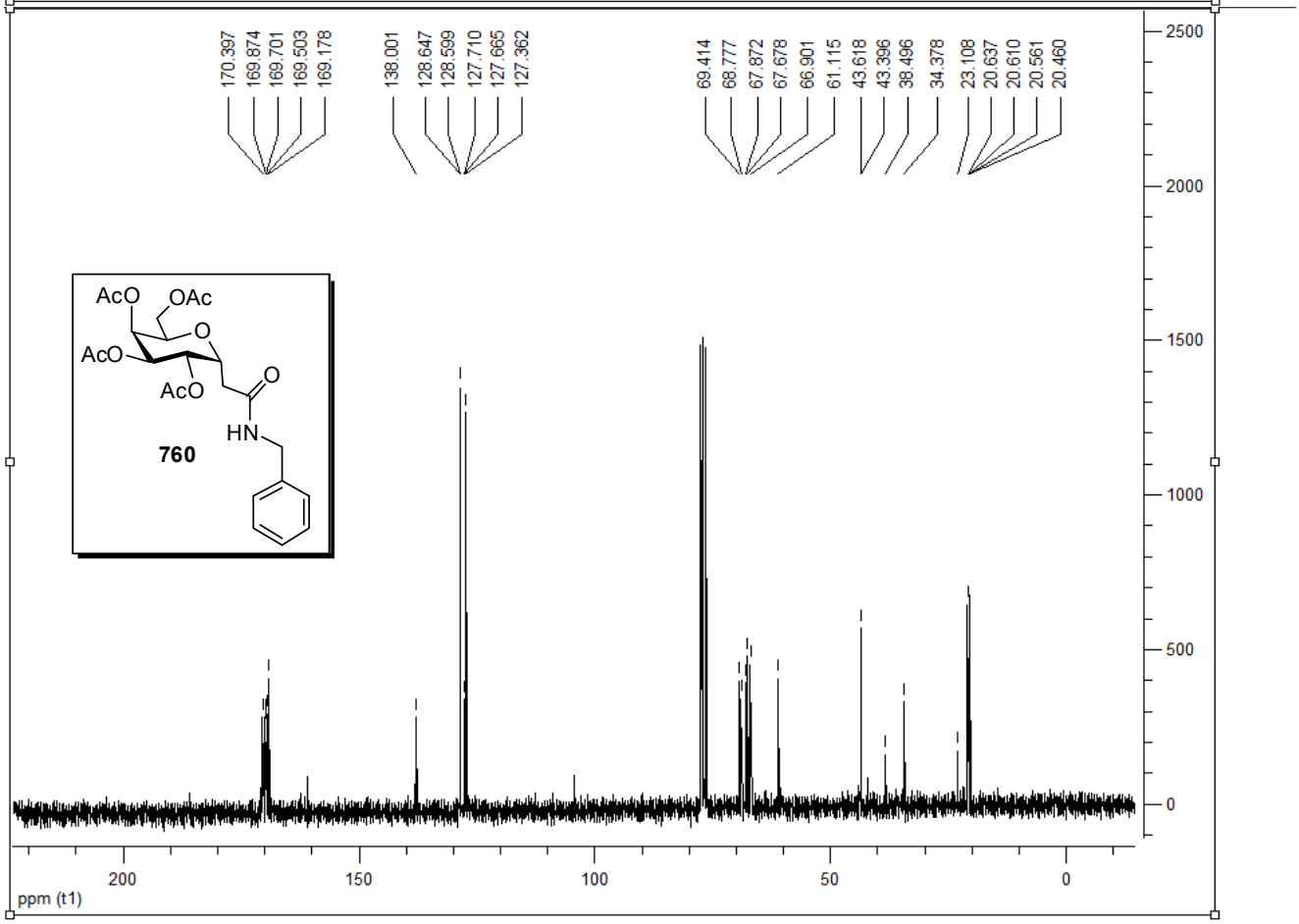

4.422
3.975
3.908
3.895
3.891
3.862
3.705
3.659
3.650
3.368
3.364
3.360
3.192
2.530
1.498
1.263
0.884
HO
OH
O
HO
HO
O
HN
C14H29
758
ppm (t1)
5.0
0.93
0.95
1.96
0.94
1.76
1.77
1.57
2.08
21.14
2.94
4.50
4.00
3.50
3.00
2.50
2.00
1.50
1.00
ppm (t1)

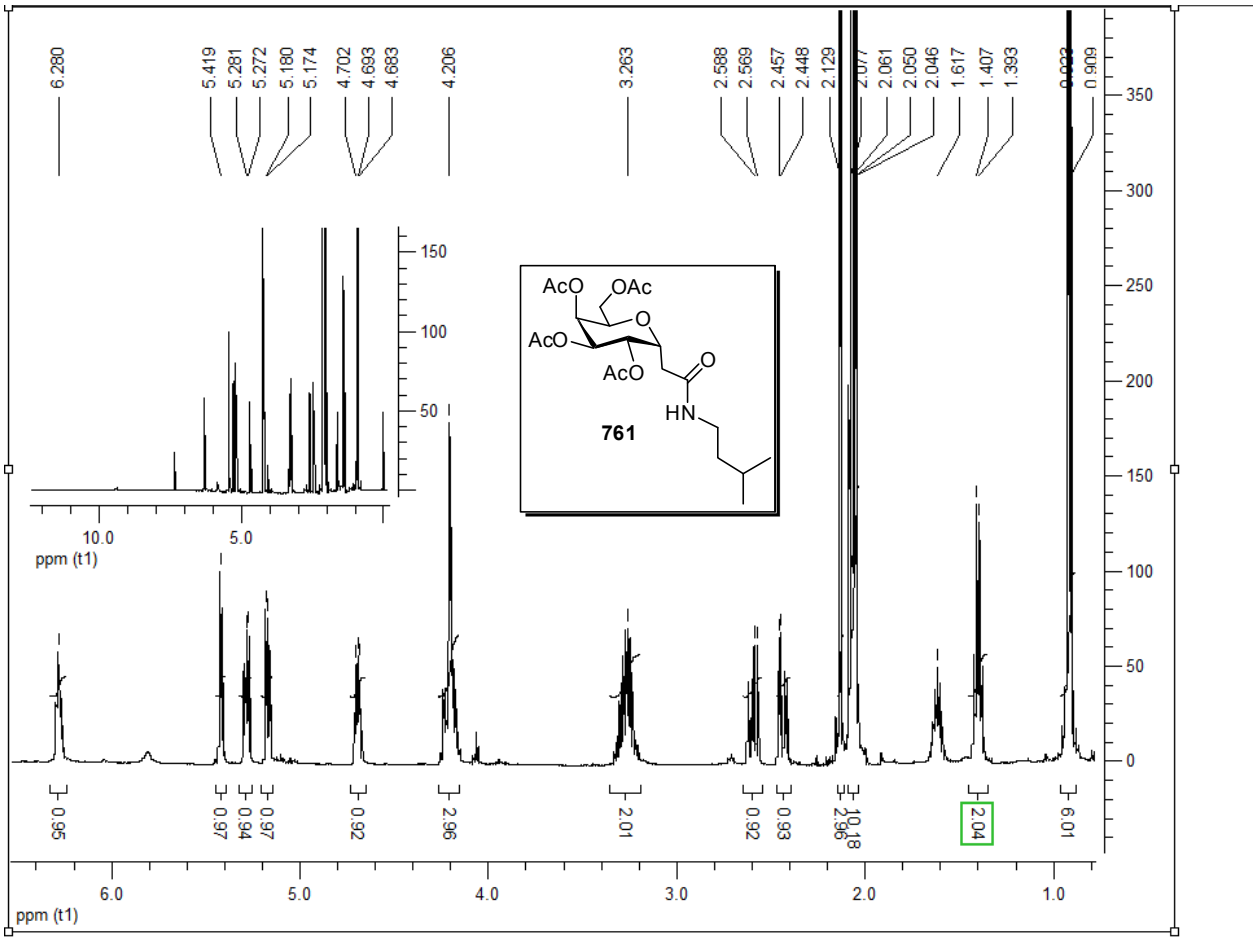

173.521
74.202
71.888
71.632
69.832
69.186
61.592
34.196
32.602
30.318
30.297
30.253
29.997
29.974
27.673
23.286
14.290
HO
OH
O
HO
HO
O
HN
C14H29
758
200
150
100
50
0
ppm (t1)

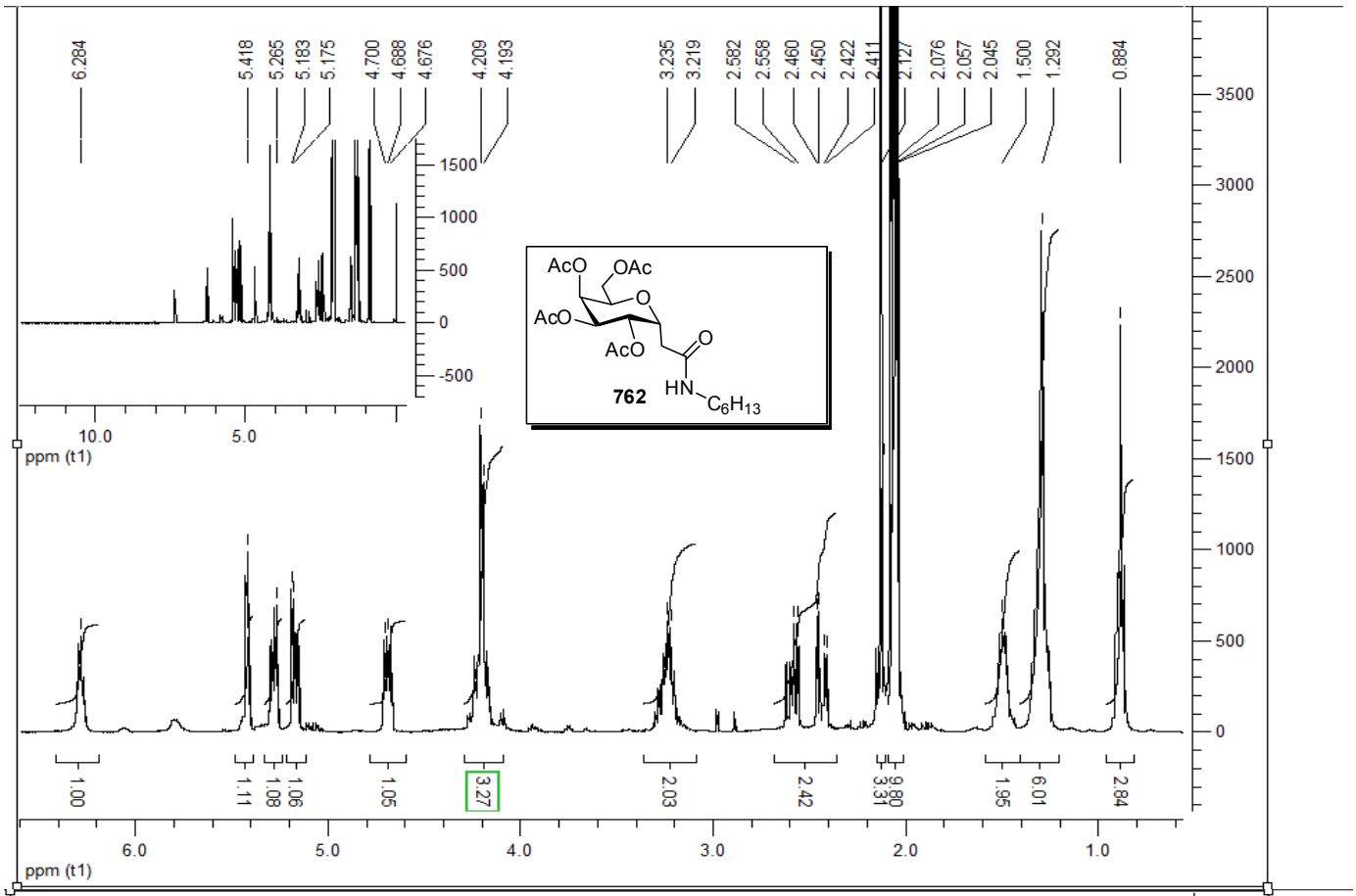

4.446
4.434
3.976
3.969
3.962
3.918
3.905
3.901
3.872
3.716
3.706
3.687
3.658
3.649
3.636
3.195
3.182
2.577
2.553
2.546
2.536
1.503
1.260
0.887
HO
OH
O
HO
HO
O
HN
C16H33
759
ppm (t1)
0.96
0.89
1.81
1.07
2.05
2.00
1.70
2.07
26.29
3.61
ppm (t1)

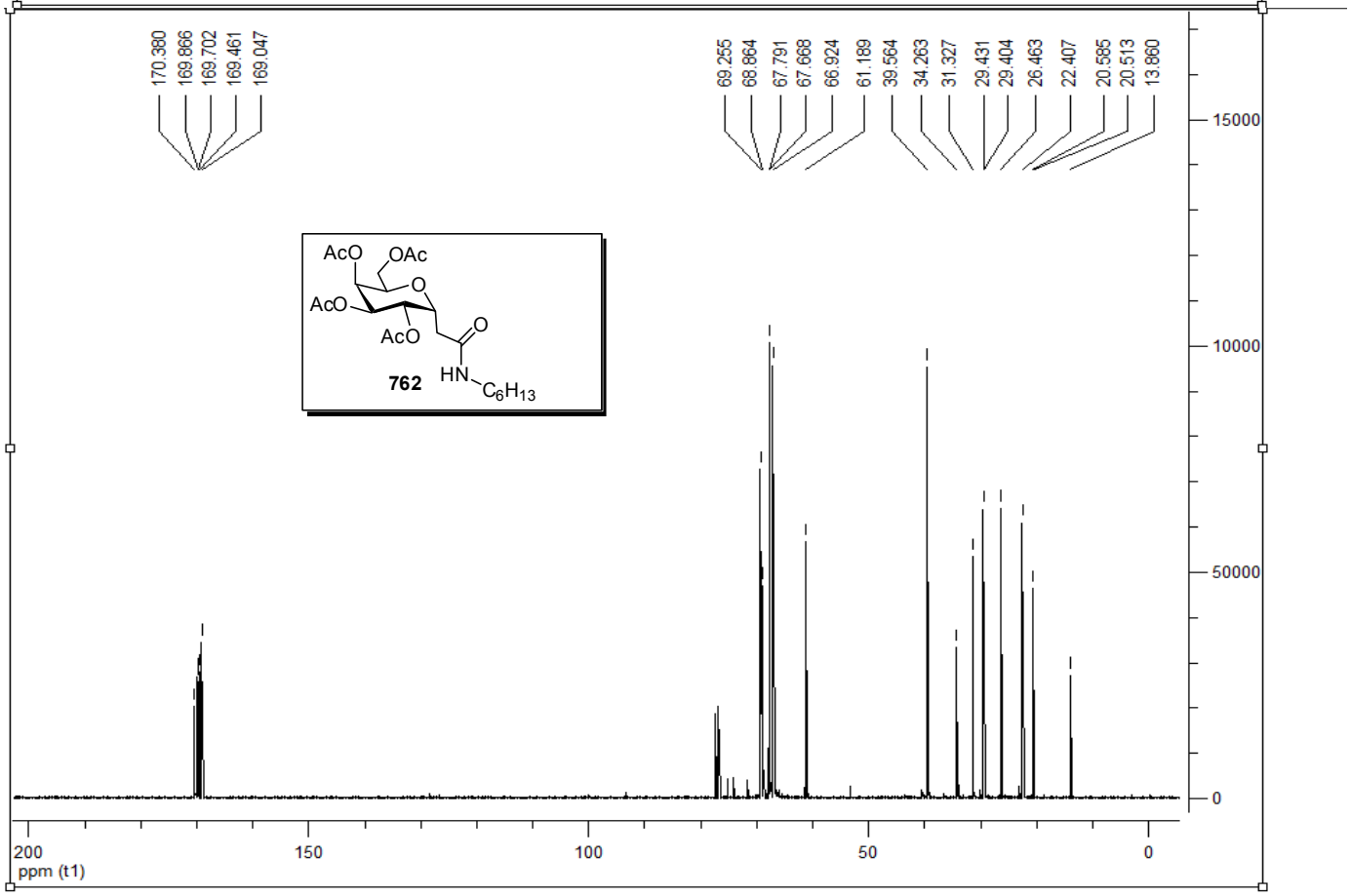

173.376
73.875
71.861
71.320
69.430
69.059
61.421
33.740
32.536
30.282
30.265
30.244
30.200
30.129
29.959
29.840
29.704
27.590
23.258
14.412
HO
OH
O
HO
HO
O
HN
C16H33
759
ppm (t1)

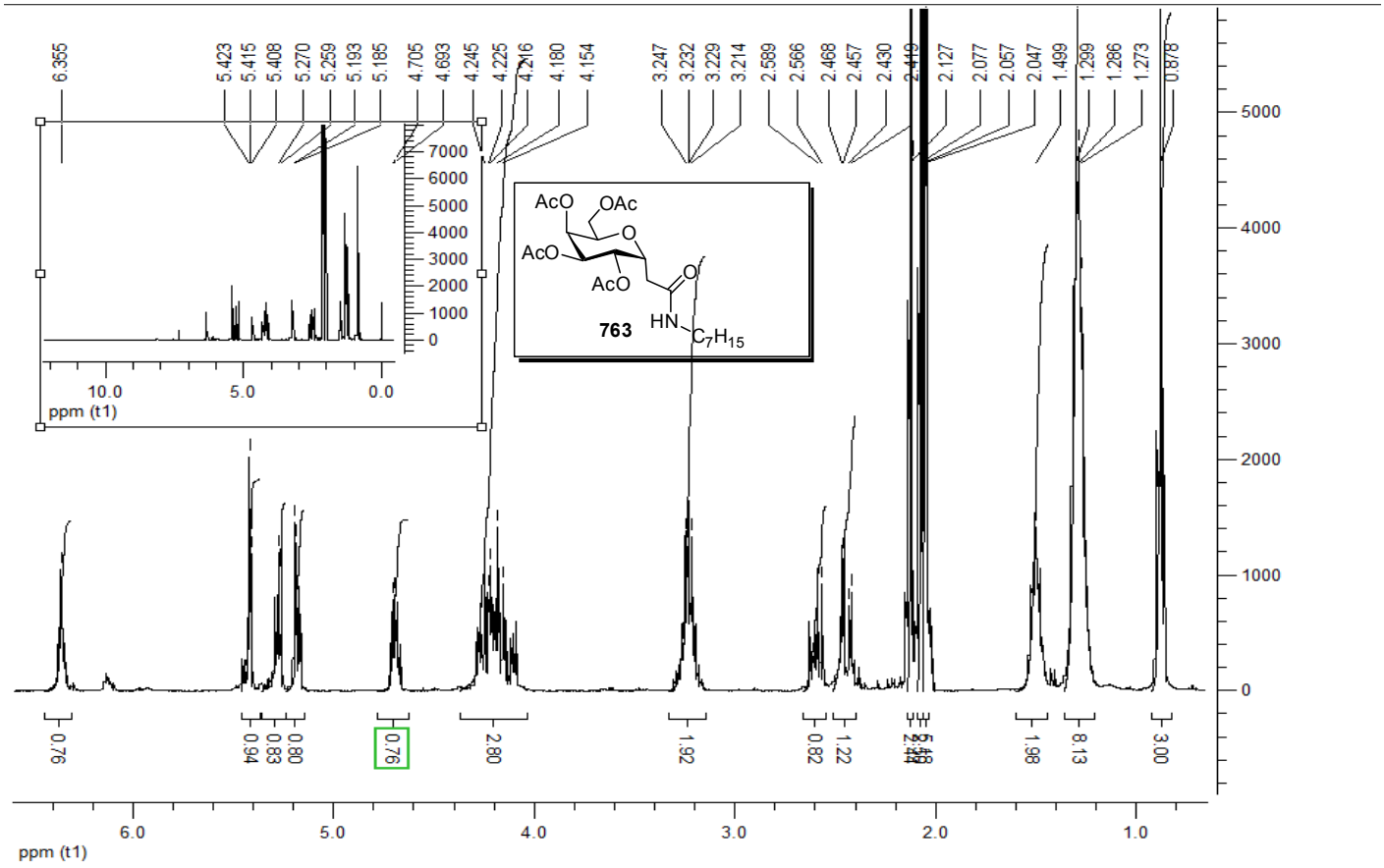

7.233
6.594
5.368
5.148
4.696
4.680
4.664
4.421
4.413
4.402
4.395
4.373
4.161
4.152
4.130
4.102
4.078
2.640
2.607
2.588
2.556
2.477
2.463
2.426
2.412
2.072
2.005
2.000
AcO
OAc
AcO
AcO
O
HN
760
ppm (t1)
5.31
0.95
1.05
1.01
1.00
1.00
3.33
3.14
0.97
1.05
5.01
2.94

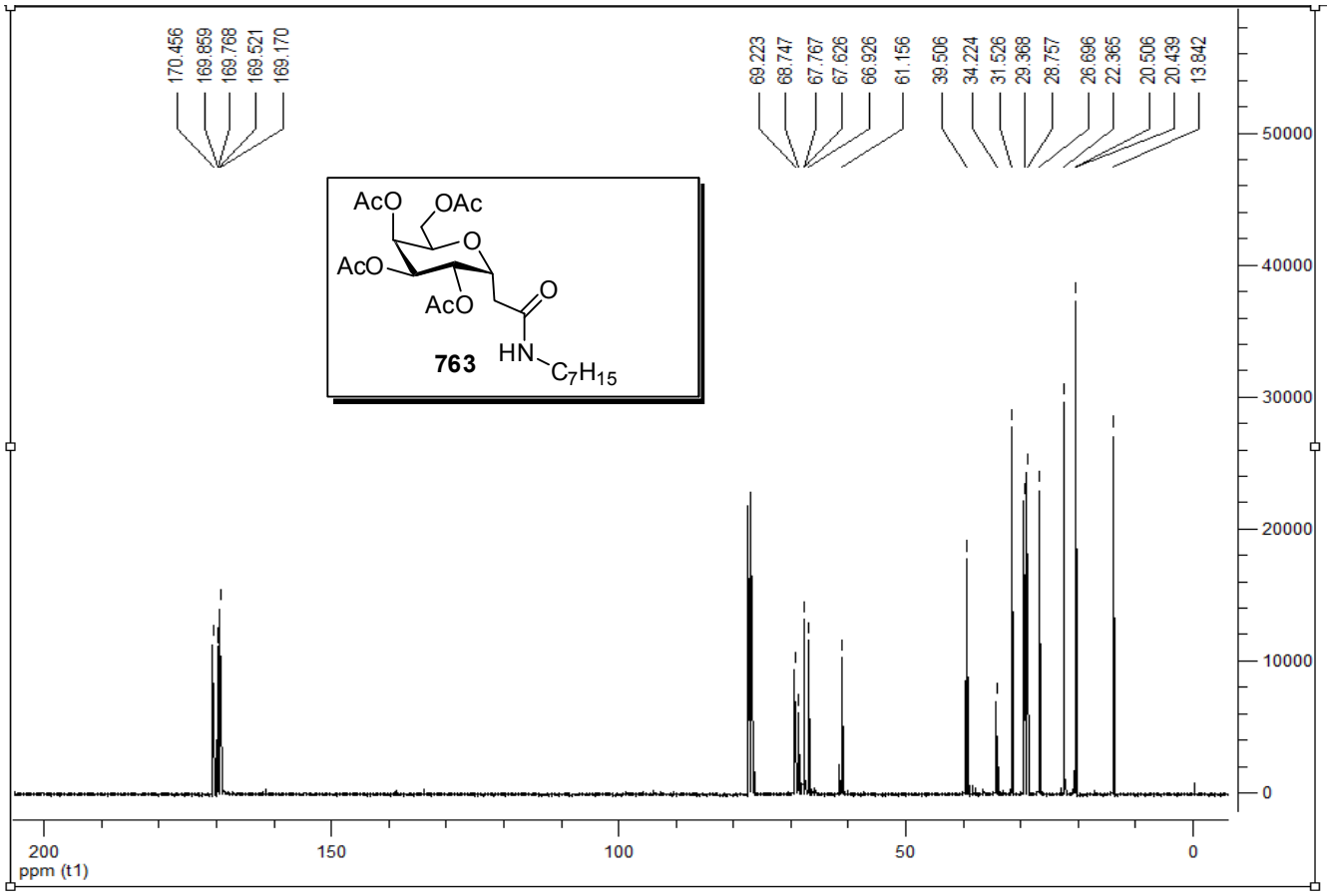

170.397
169.874
169.701
169.503
169.178
138.001
128.647
128.599
127.710
127.665
127.362
69.414
68.777
67.872
67.678
66.901
61.115
43.618
43.396
38.496
34.378
23.108
20.637
20.610
20.561
20.460
AcO
OAc
AcO
AcO
O
HN
760
ppm (t1)

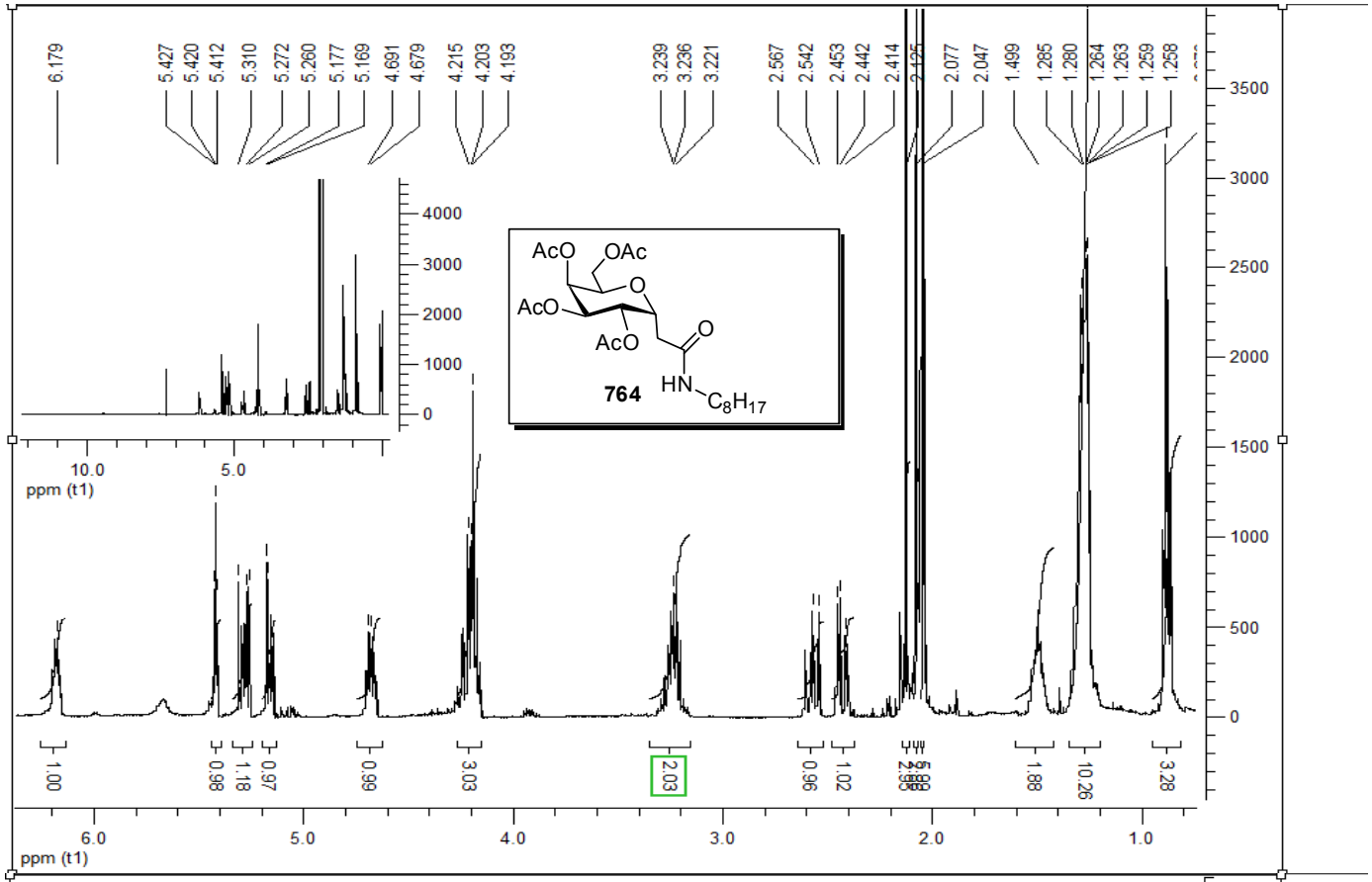

6.280
5.419
5.281
5.272
5.180
5.174
4.702
4.693
4.683
4.206
3.263
2.588
2.569
2.457
2.448
2.129
2.077
2.061
2.050
2.046
1.617
1.407
1.393
0.909
AcO
OAc
O
AcO
AcO
O
HN
761
ppm (t1)
0.95
0.97
0.94
0.87
0.92
2.96
2.01
0.92
0.93
10.18
2.04
6.01

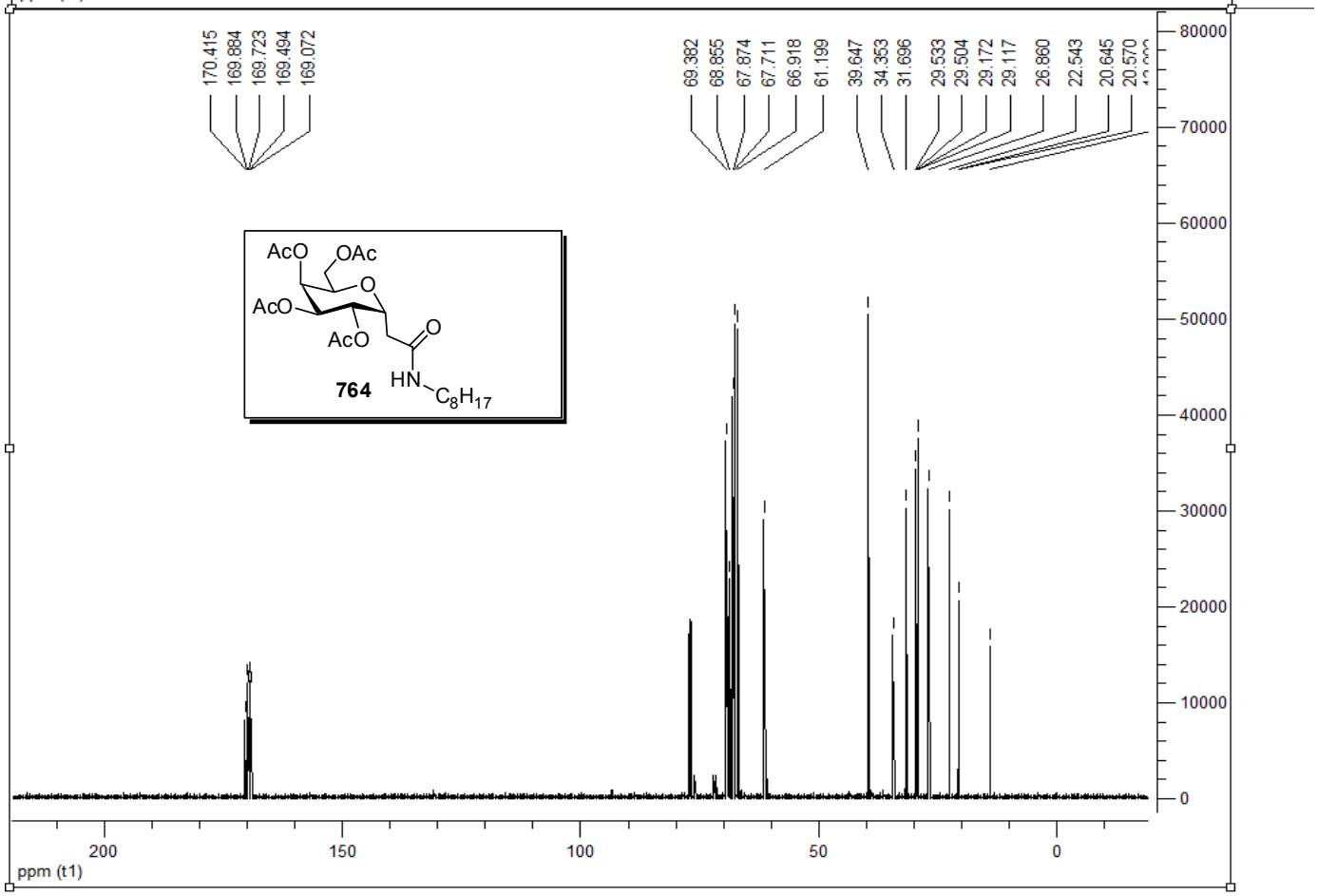

6.284
5.418
5.265
5.183
5.175
4.700
4.688
4.676
4.209
4.193
3.235
3.219
2.582
2.558
2.460
2.450
2.422
2.411
2.127
2.076
2.057
2.045
1.500
1.292
0.884
AcO
OAc
AcO
AcO
O
HN
C6H13
762
ppm (t1)
1.00
1.11
1.08
1.09
1.05
3.27
2.03
2.42
3.80
3.31
1.95
6.01
2.84

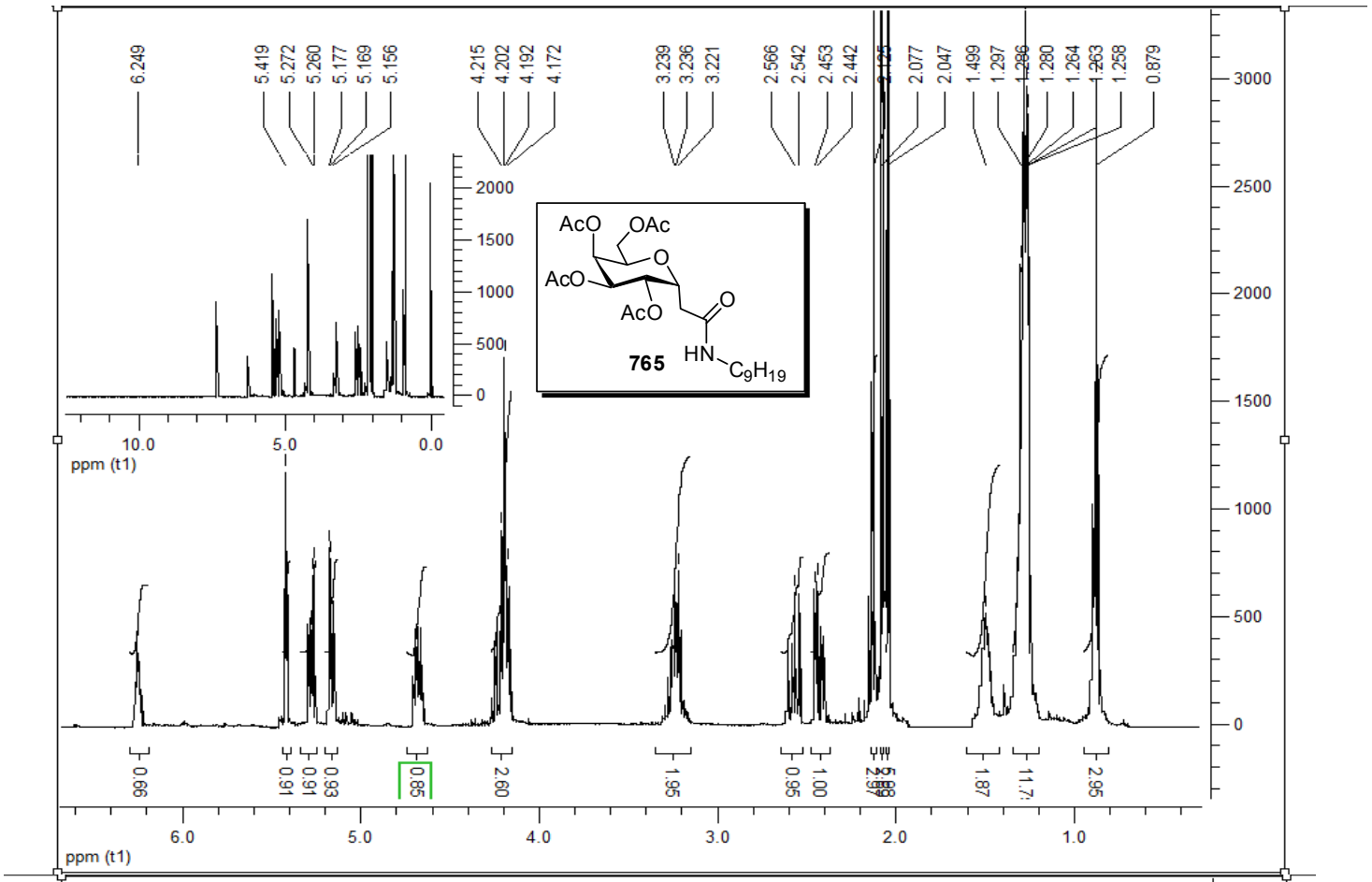

170.380
169.866
169.702
169.461
169.047
69.255
68.864
67.791
67.668
66.924
61.189
39.564
34.263
31.327
29.431
29.404
26.463
22.407
20.585
20.513
13.860
AcO
OAc
AcO
AcO
O
HN
C6H13
762
ppm (t1)

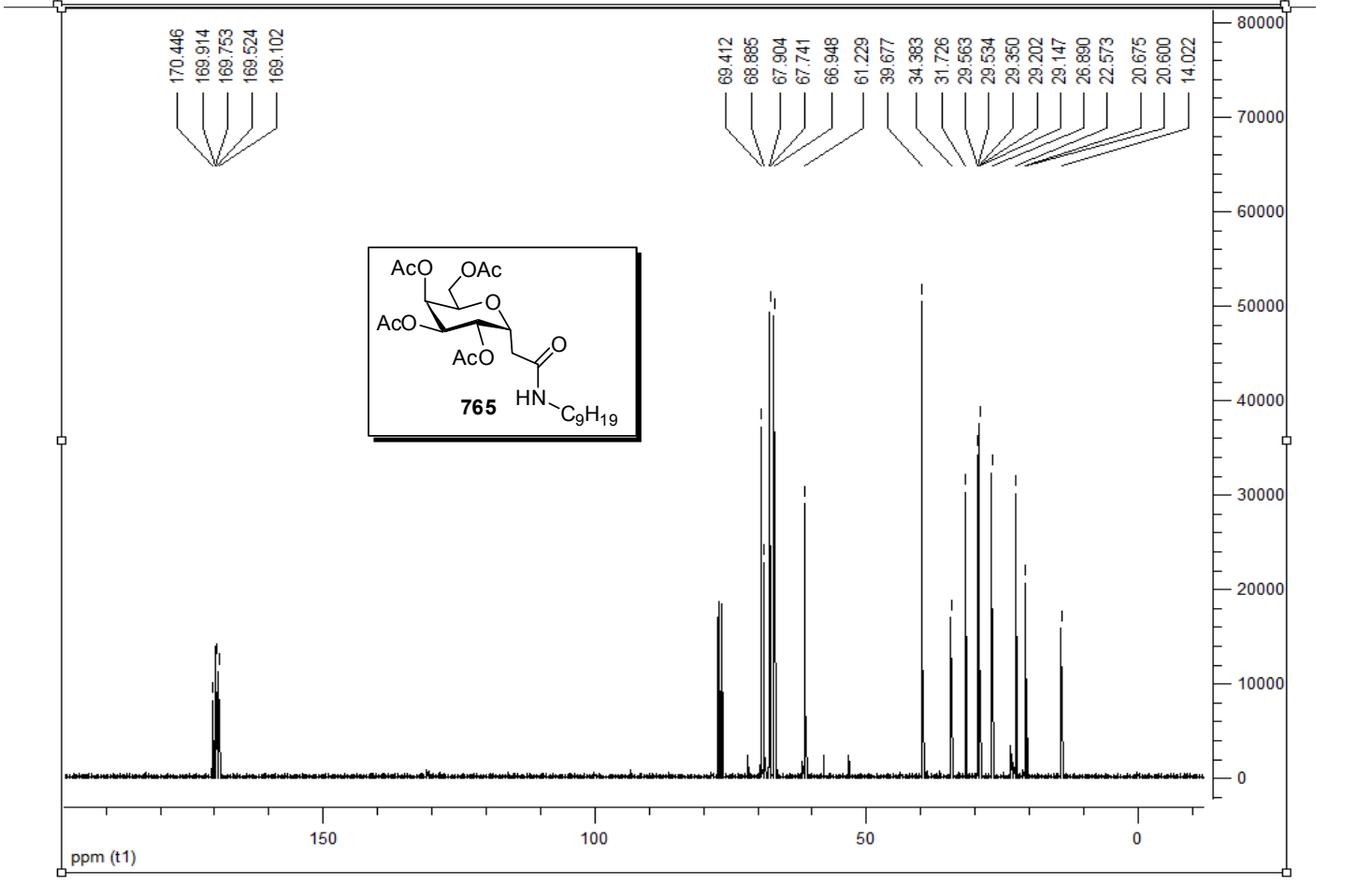

6.355
5.423
5.415
5.408
5.270
5.259
5.193
5.185
4.705
4.693
4.245
4.225
4.216
4.180
4.154
3.247
3.232
3.229
3.214
2.589
2.566
2.468
2.457
2.430
2.127
2.077
2.057
2.047
1.499
1.299
1.286
1.273
0.878
AcO
OAc
AcO
AcO
O
HN
C7H15
763
ppm (t1)
0.76
0.94
0.83
0.80
0.76
2.80
1.92
0.82
1.22
1.98
8.13
3.00
ppm (t1)

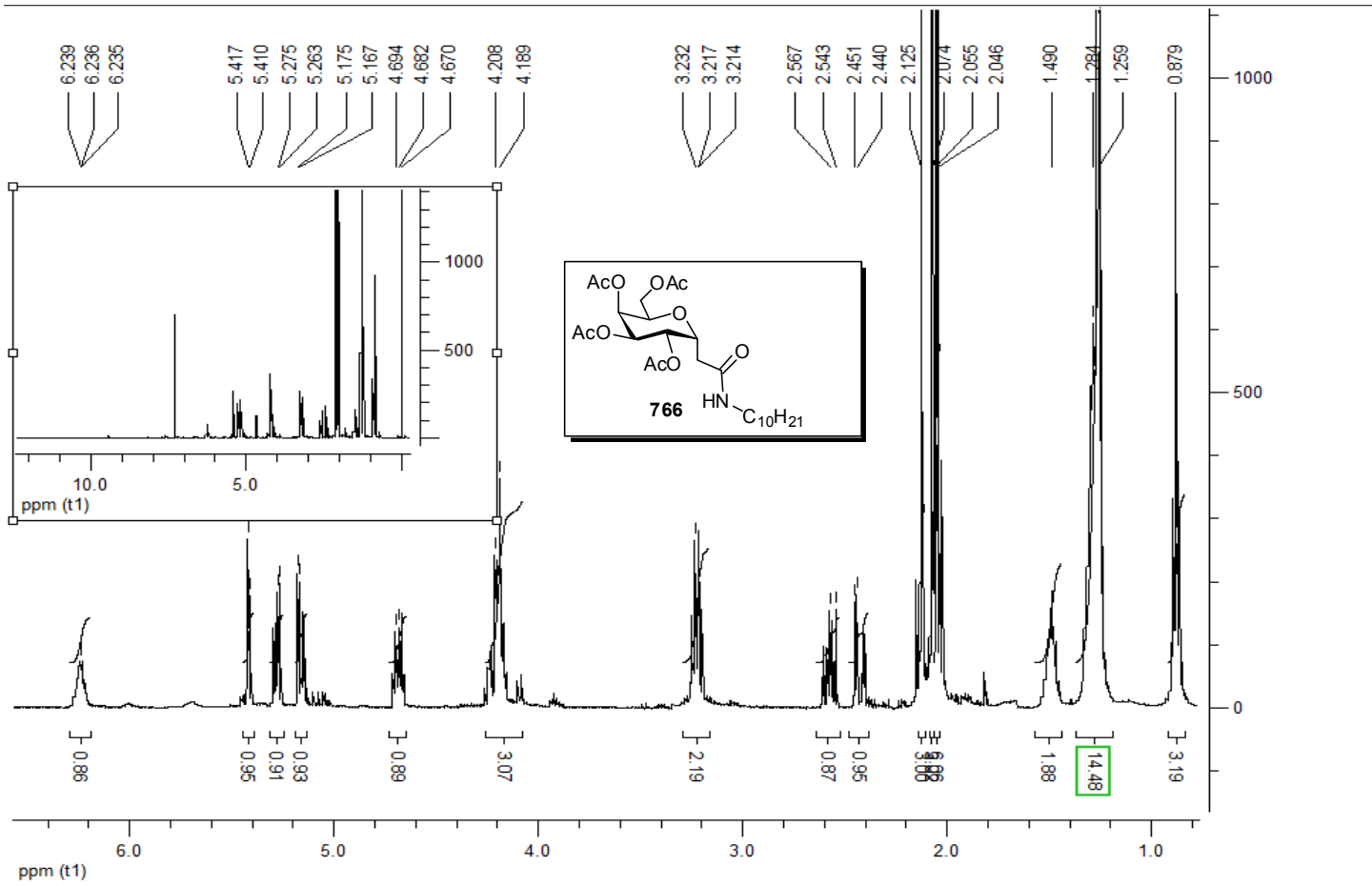

170.456
169.859
169.768
169.521
169.170
69.223
68.747
67.767
67.626
66.926
61.156
39.506
34.224
31.526
29.368
28.757
26.696
22.365
20.506
20.439
13.842
AcO
OAc
AcO
AcO
O
HN
C7H15
763
ppm (t1)

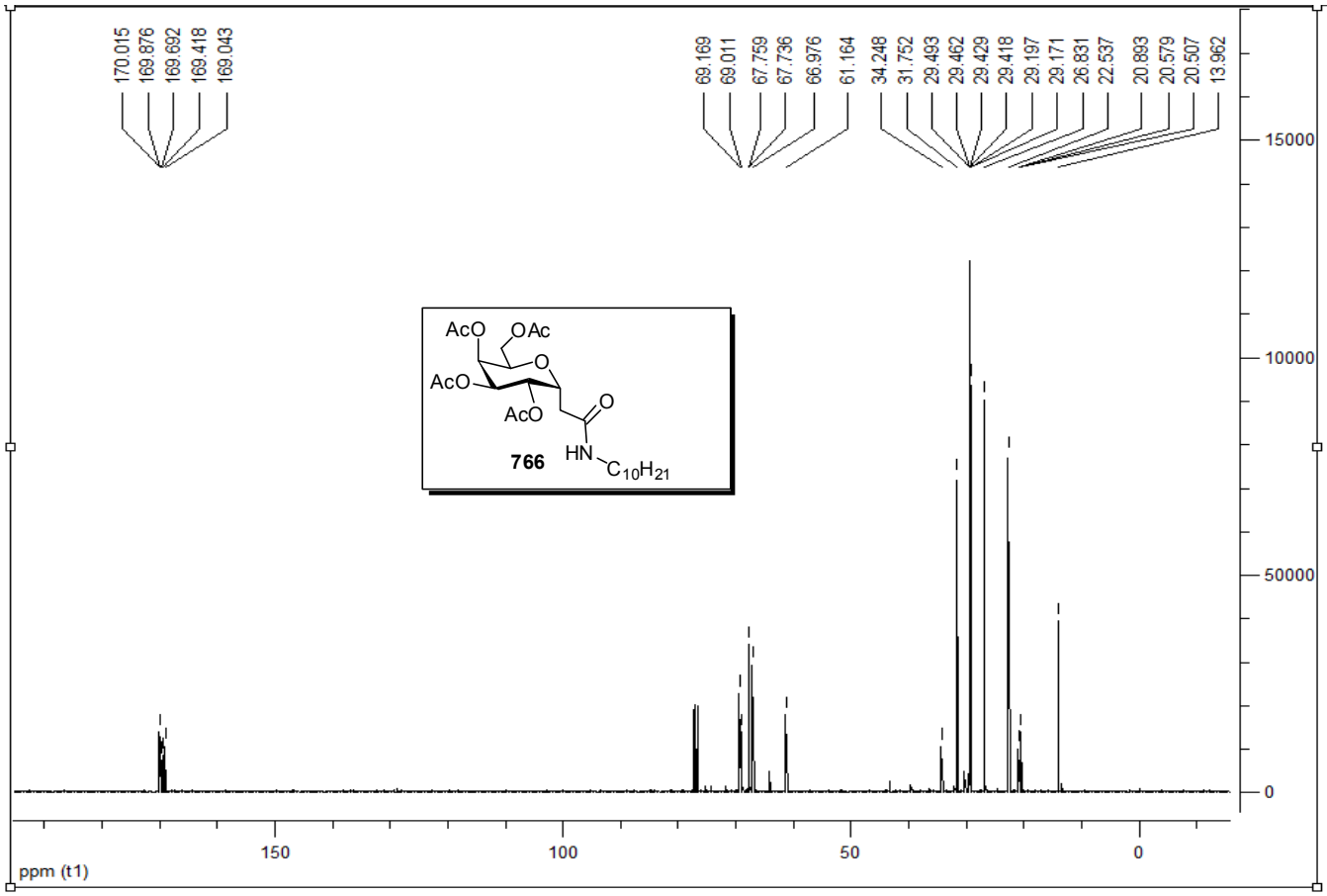

6.179
5.427
5.420
5.412
5.310
5.272
5.260
5.177
5.169
4.691
4.679
4.215
4.203
4.193
3.239
3.236
3.221
2.567
2.542
2.453
2.442
2.414
2.077
2.047
1.499
1.285
1.280
1.264
1.263
1.259
1.258
AcO
OAc
AcO
AcO
O
O
HN
C8H17
764
ppm (t1)
1.00
0.98
1.18
0.97
0.99
3.03
2.03
0.96
1.02
1.88
10.26
3.28

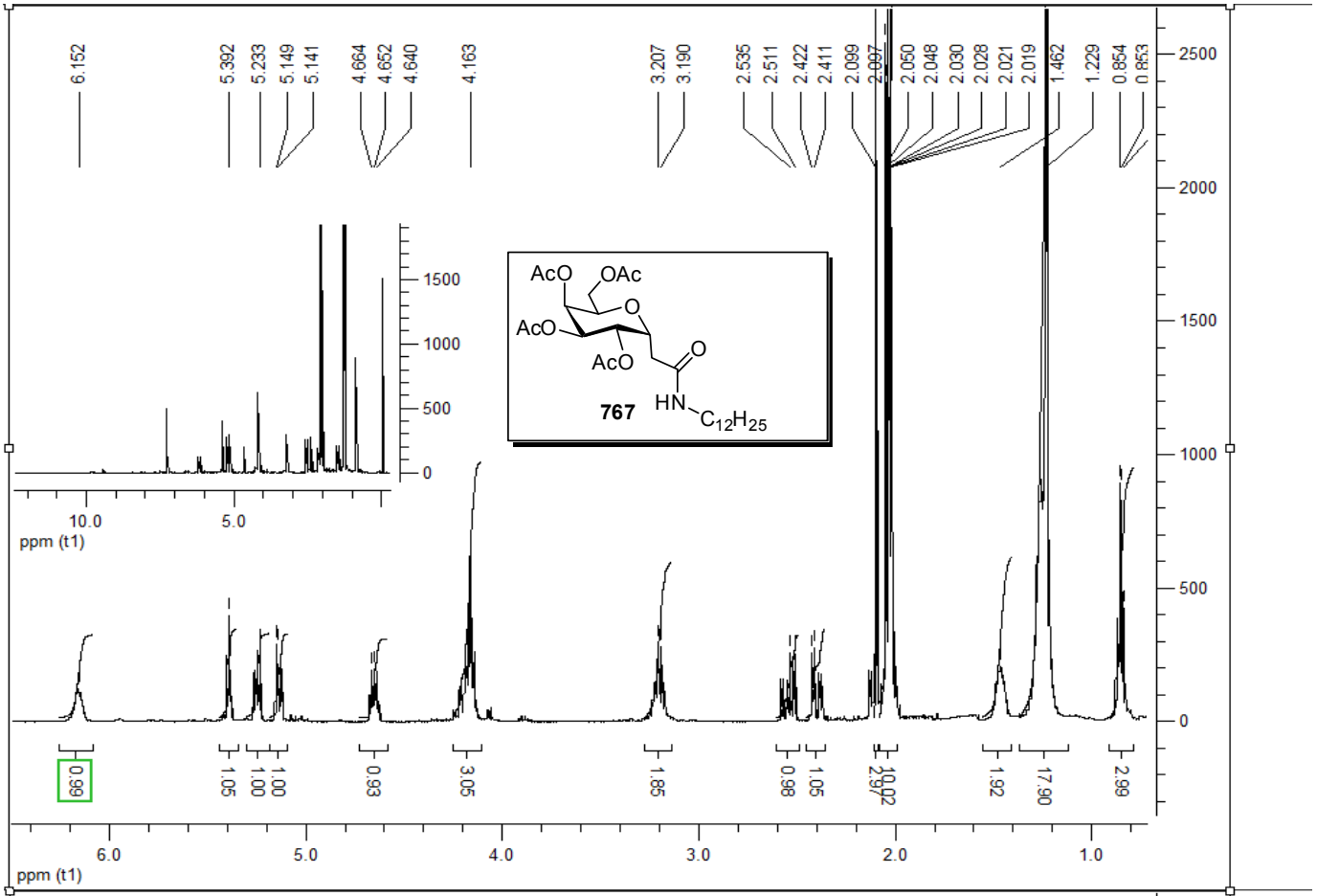

170.415
169.884
169.723
169.494
169.072
69.382
68.855
67.874
67.711
66.918
61.199
39.647
34.353
31.696
29.533
29.504
29.172
29.117
26.860
22.543
20.645
20.570
AcO
OAc
AcO
AcO
O
O
HN
C8H17
764
ppm (t1)

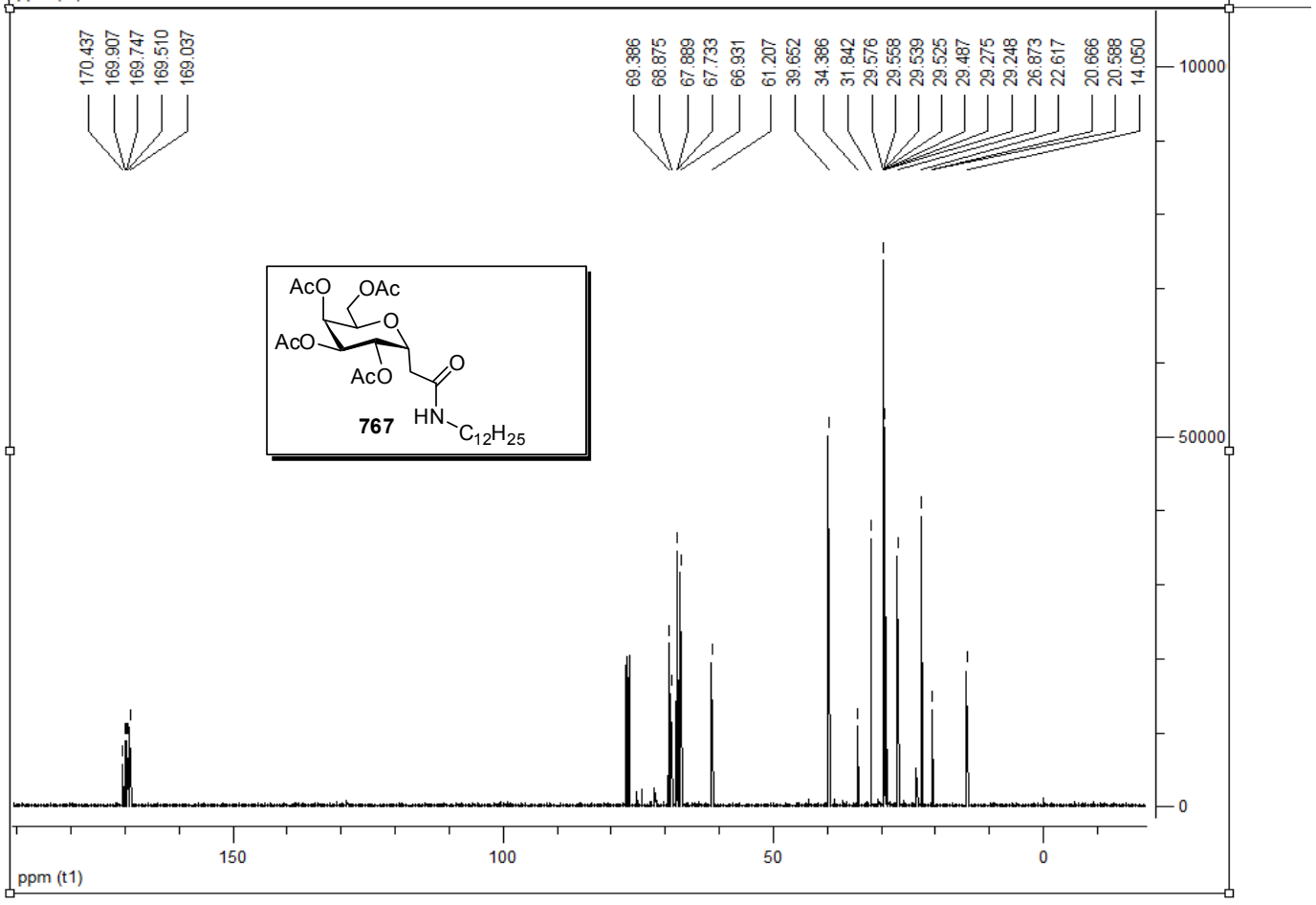

6.249
5.419
5.272
5.260
5.177
5.169
5.156
4.215
4.202
4.192
4.172
3.239
3.236
3.221
2.566
2.542
2.453
2.442
2.077
2.047
1.499
1.297
1.280
1.264
1.258
0.879
AcO
OAc
AcO
AcO
O
O
HN
C9H19
765
ppm (t1)
0.66
0.91
0.91
0.89
0.85
2.60
1.96
0.96
1.00
1.87
2.96

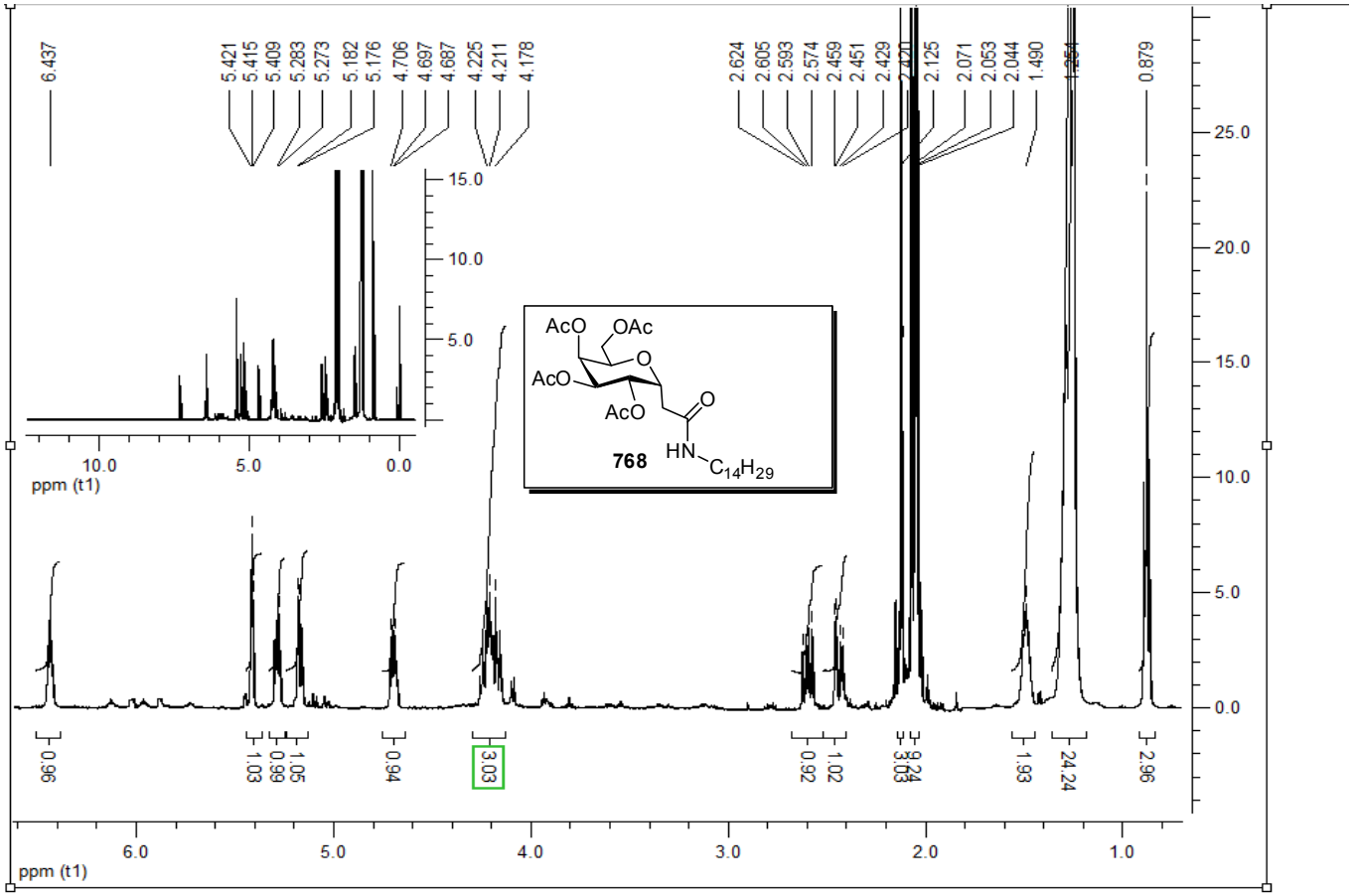

170.446
169.914
169.753
169.524
169.102
69.412
68.885
67.904
67.741
66.948
61.229
39.677
34.383
31.726
29.563
29.534
29.350
29.202
29.147
26.890
22.573
20.675
20.600
14.022
AcO
OAc
AcO
AcO
O
O
HN
C9H19
765
ppm (t1)

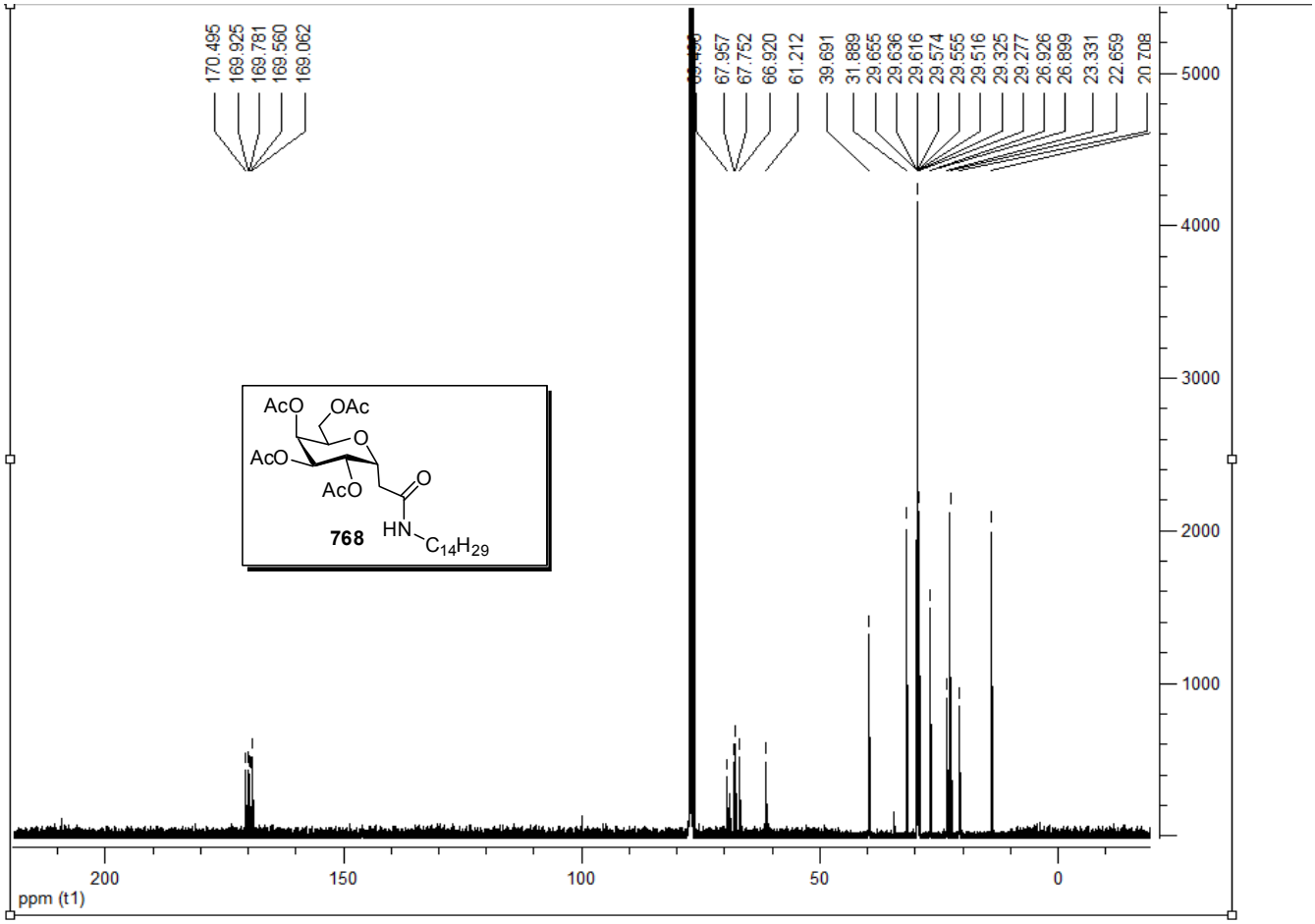

6.239
6.236
6.235
5.417
5.410
5.275
5.263
5.175
5.167
4.694
4.682
4.670
4.208
4.189
3.232
3.217
3.214
2.567
2.543
2.451
2.440
2.125
2.074
2.055
2.046
1.490
1.284
1.259
0.879
AcO
OAc
AcO
AcO
O
HN
C10H21
766
ppm (t1)
0.86
0.95
0.91
0.93
0.89
3.07
2.19
0.87
0.95
1.88
14.48
3.19

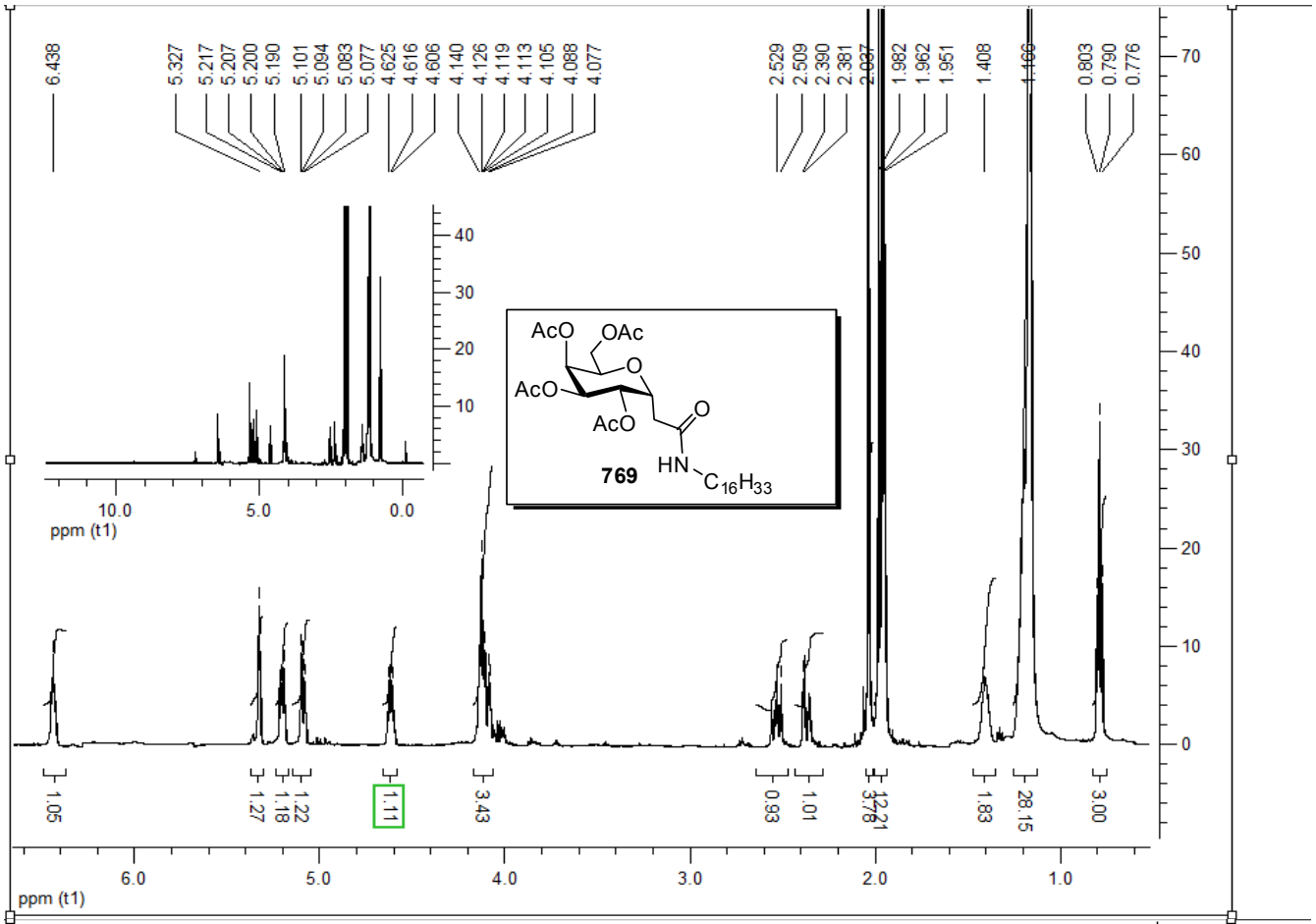

170.015
169.876
169.692
169.418
169.043
69.169
69.011
67.759
67.736
66.976
61.164
34.248
31.752
29.493
29.462
29.429
29.418
29.197
29.171
26.831
22.537
20.893
20.579
20.507
13.962
AcO
OAc
AcO
AcO
O
HN
C10H21
766
ppm (t1)

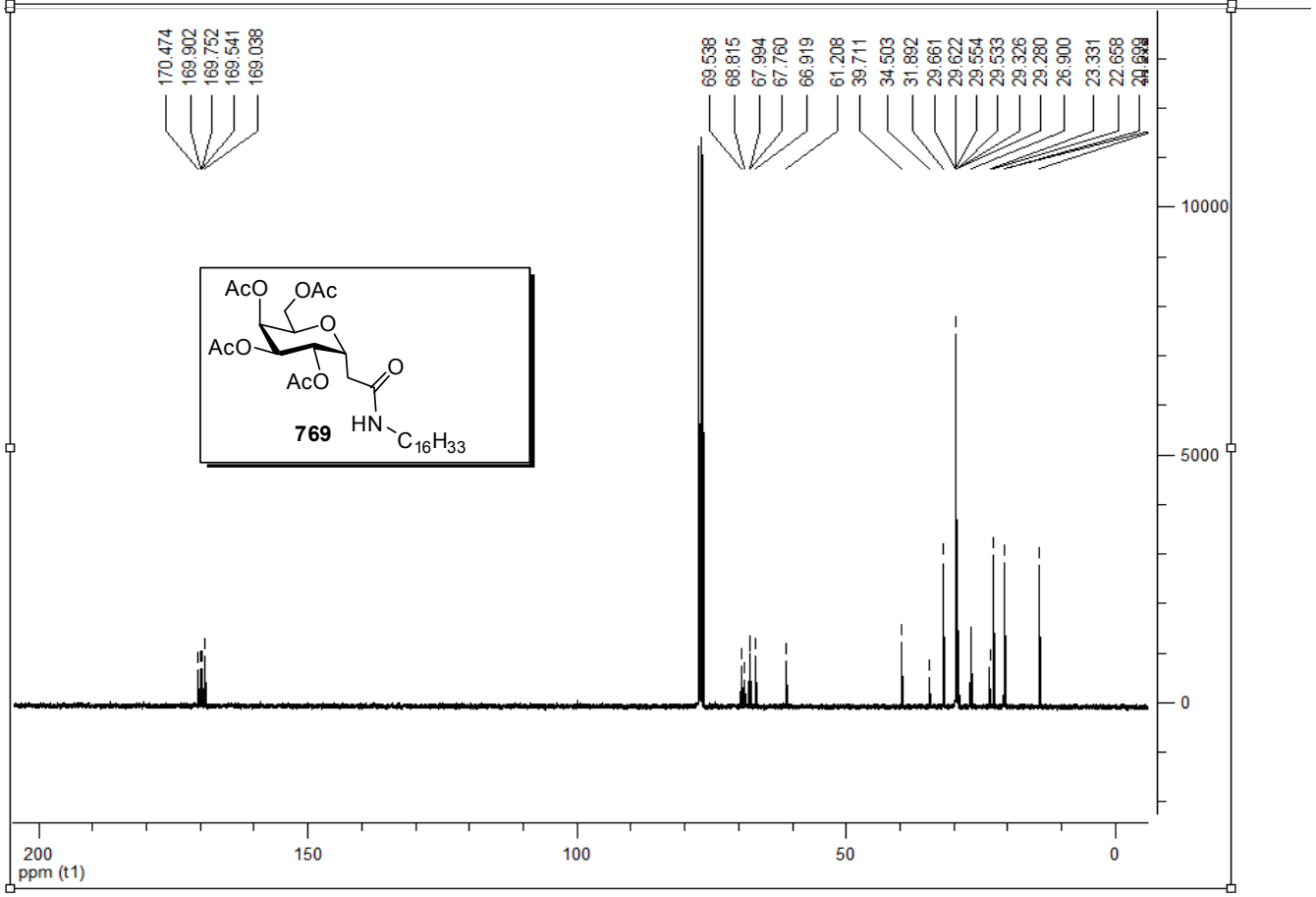

6.152
5.392
5.233
5.149
5.141
4.664
4.652
4.640
4.163
3.207
3.190
2.535
2.511
2.422
2.411
2.099
2.097
2.050
2.048
2.030
2.028
2.021
2.019
1.462
1.229
0.854
0.853
AcO
OAc
AcO
AcO
O
O
HN
C12H25
767
0.99
1.06
1.00
1.00
0.93
3.06
1.86
0.98
1.06
2.97
1.92
17.90
2.99
ppm (t1)

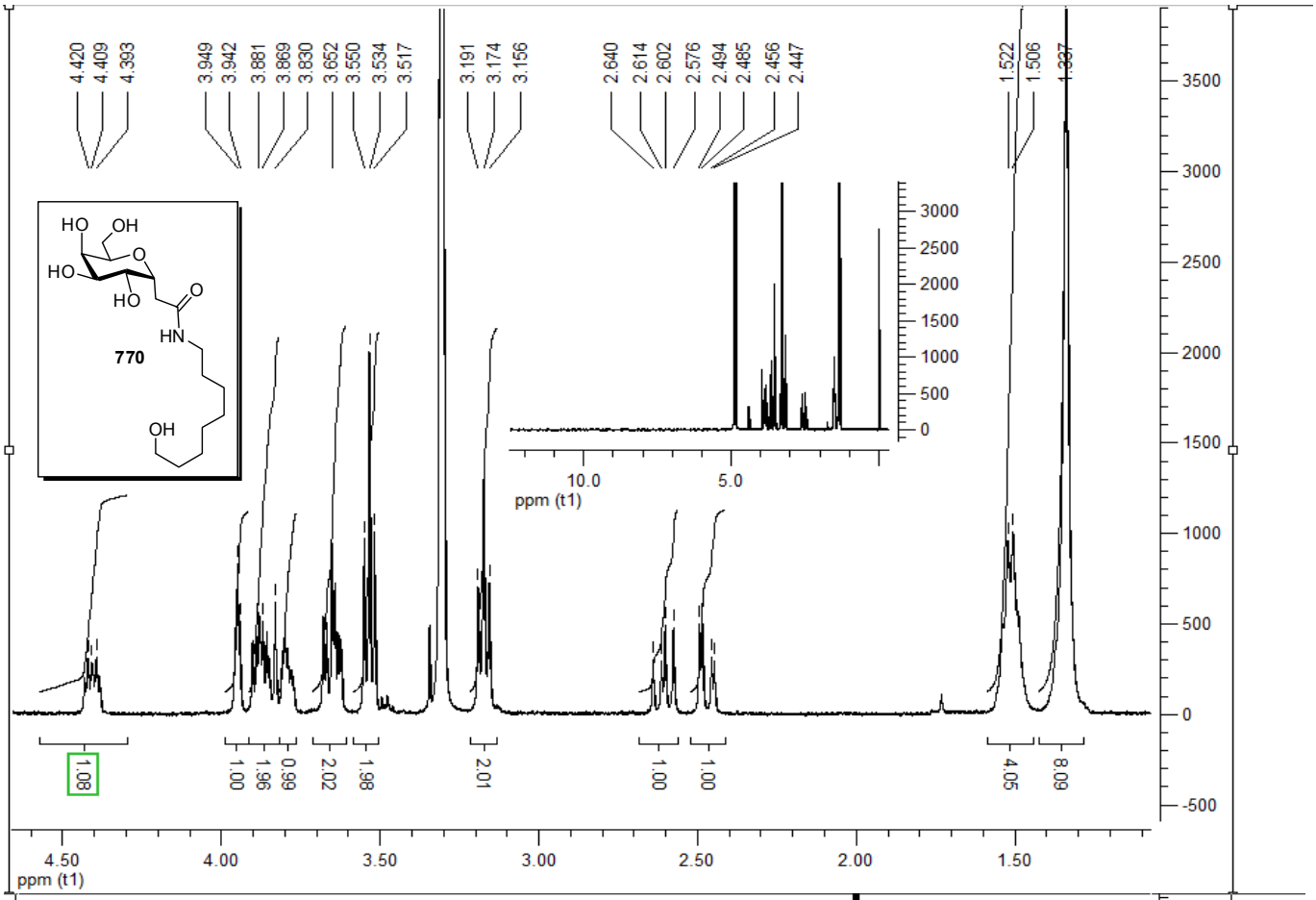

170.437
169.907
169.747
169.510
169.037
69.386
68.875
67.889
67.733
66.931
61.207
39.652
34.386
31.842
29.576
29.558
29.539
29.525
29.487
29.275
29.248
26.873
22.617
20.666
20.588
14.050
AcO
OAc
AcO
AcO
O
O
HN
C12H25
767
ppm (t1)

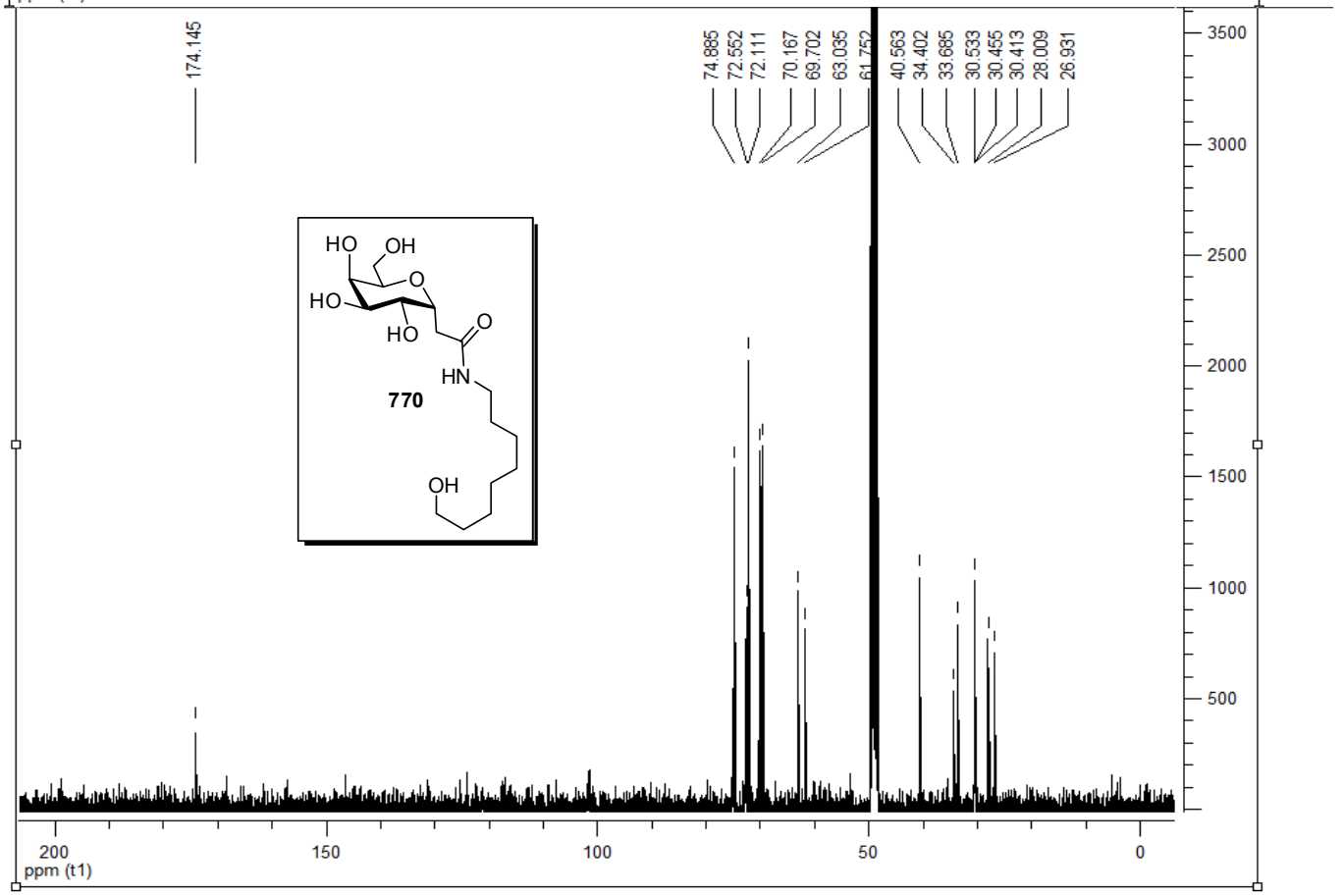

6.437
5.421
5.415
5.409
5.283
5.273
5.182
5.176
4.706
4.697
4.687
4.225
4.211
4.178
2.624
2.605
2.593
2.574
2.459
2.451
2.429
2.420
2.125
2.071
2.053
2.044
1.490
1.264
0.879
AcO
OAc
AcO
AcO
O
O
HN
C14H29
768
ppm (t1)
0.96
1.03
0.99
1.05
0.94
3.03
0.92
1.02
8.24
1.93
24.24
2.96

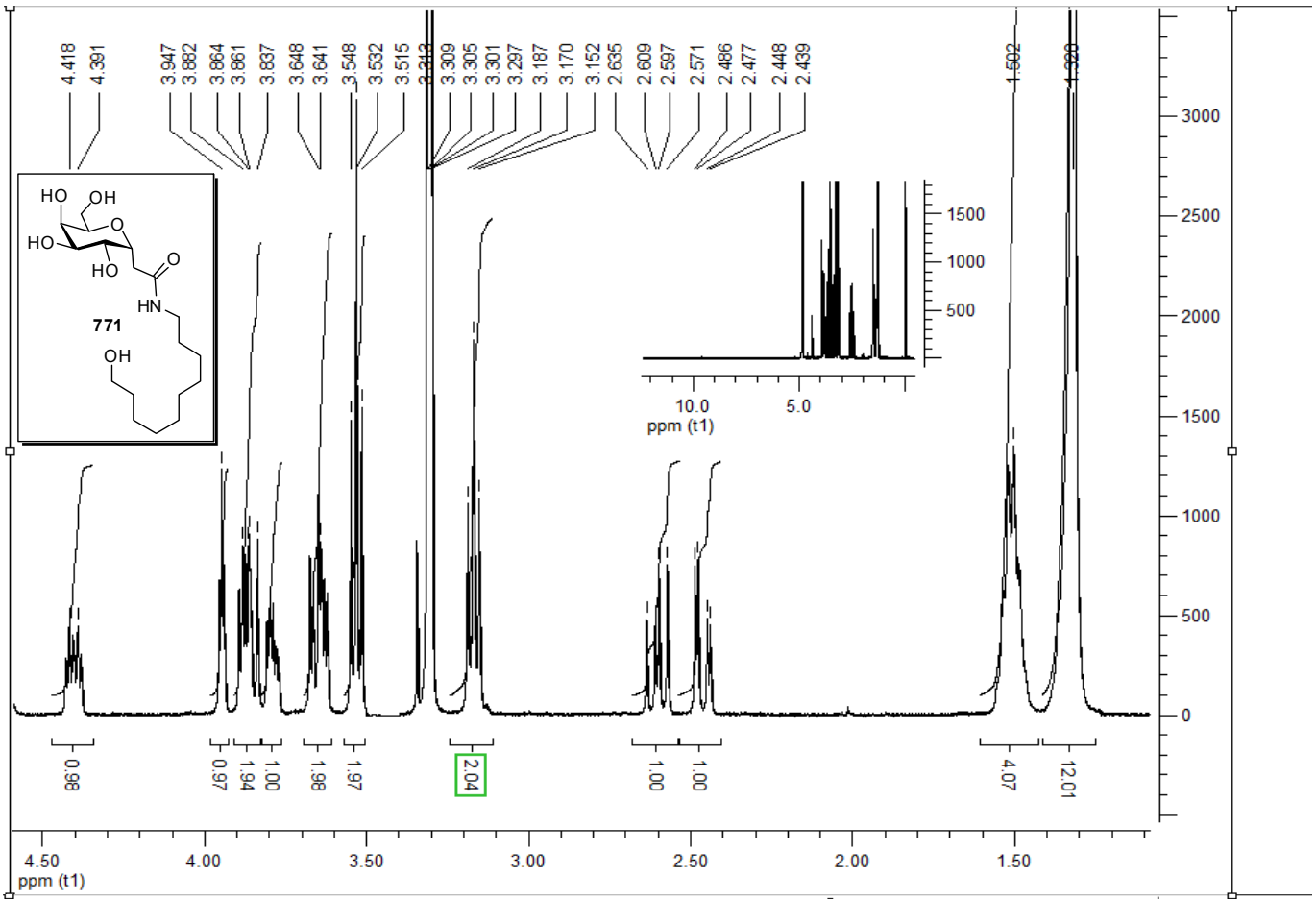

170.495
169.925
169.781
169.560
169.062
77.480
67.957
67.752
66.920
61.212
39.691
31.889
29.655
29.636
29.616
29.574
29.555
29.516
29.325
29.277
26.926
26.899
23.331
22.659
20.708
AcO
OAc
AcO
AcO
O
O
HN
C14H29
768
ppm (t1)

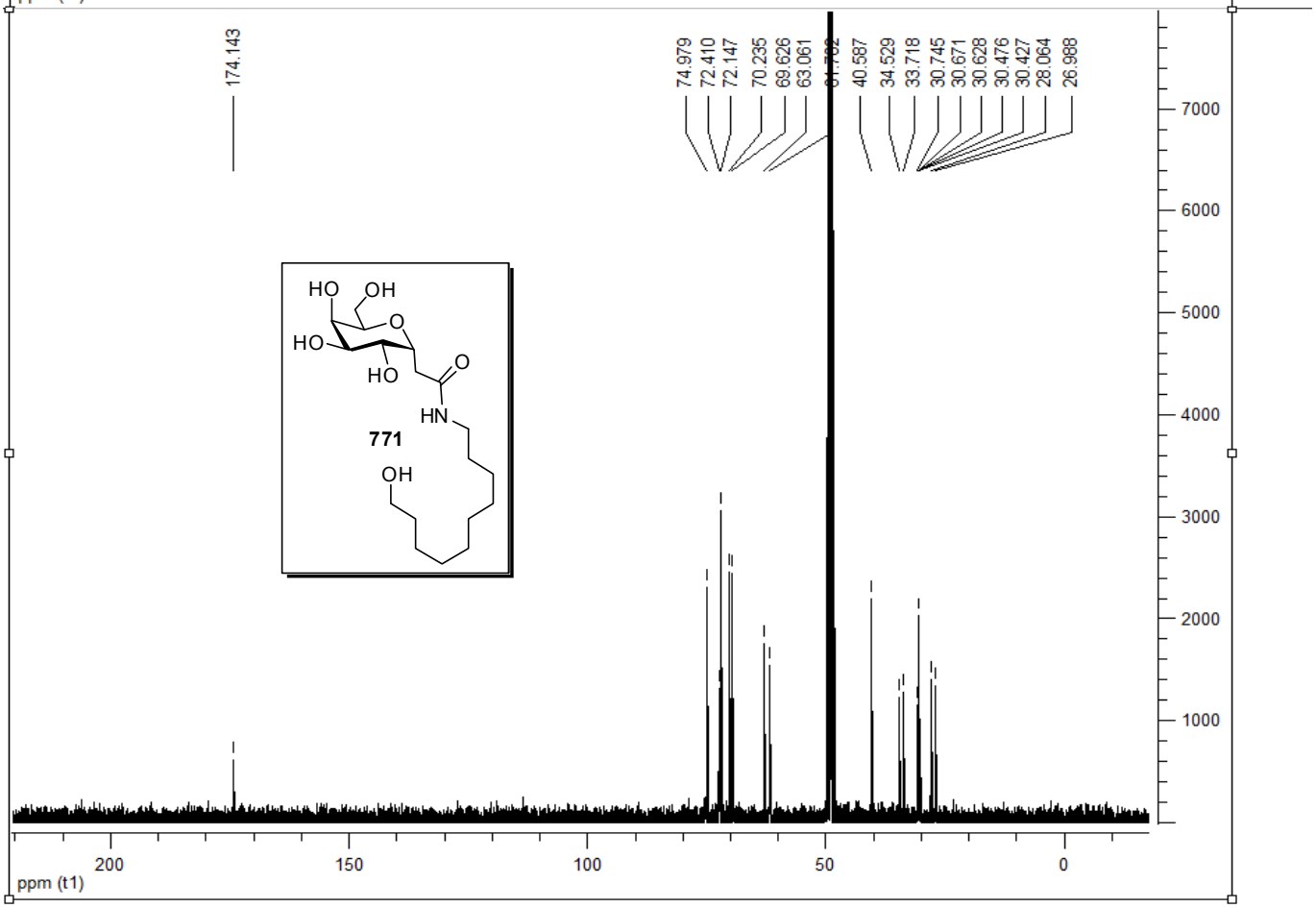

6.438
5.327
5.217
5.207
5.200
5.190
5.101
5.094
5.083
5.077
4.625
4.616
4.606
4.140
4.126
4.119
4.113
4.105
4.088
4.077
2.529
2.509
2.390
2.381
2.037
1.982
1.962
1.951
1.408
1.166
0.803
0.790
0.776
AcO
OAc
AcO
AcO
HN
C16H33
769
ppm (t1)
1.05
1.27
1.18
1.22
1.11
3.43
0.93
1.01
3.78
1.83
28.15
3.00

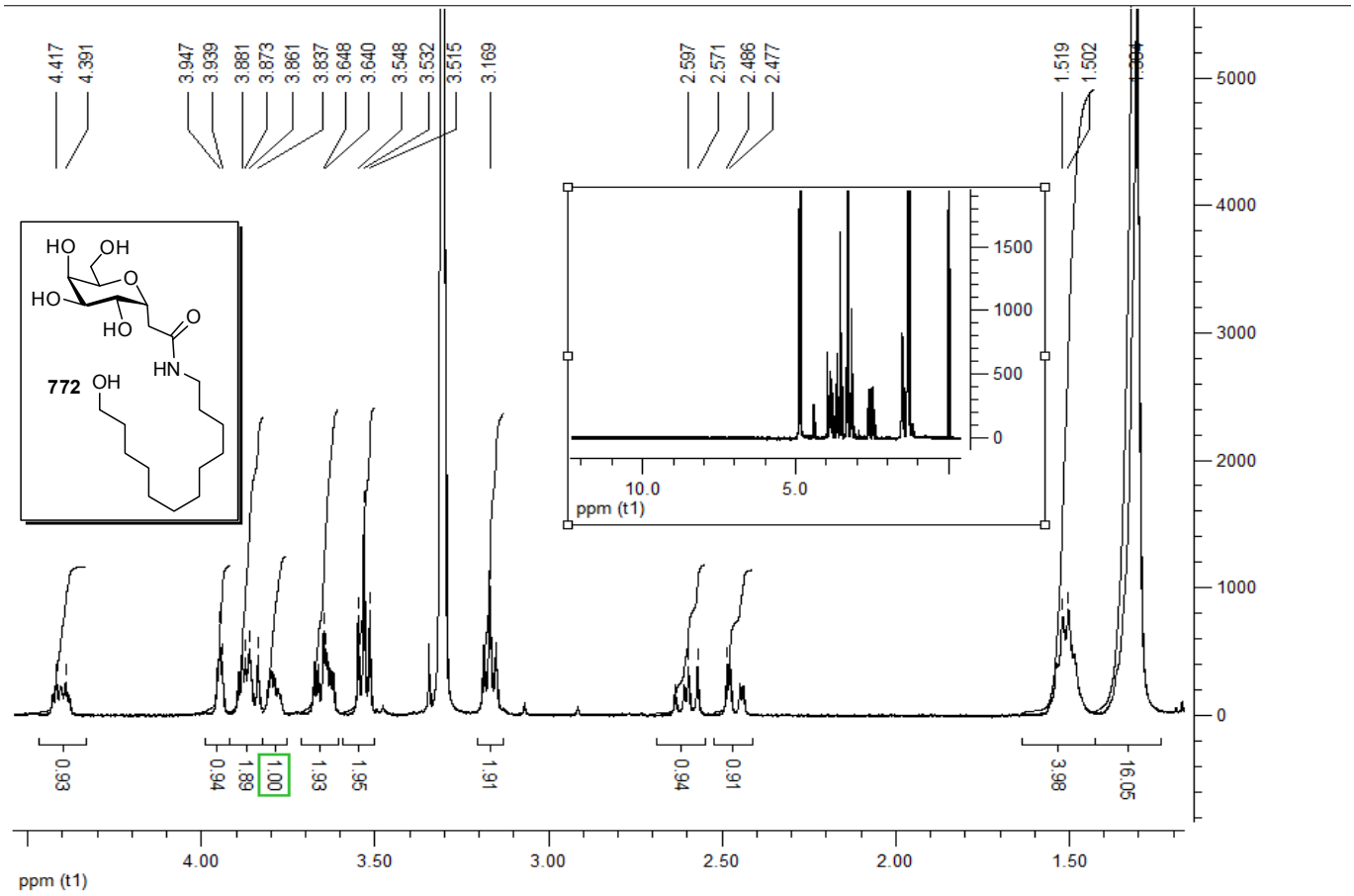

170.474
169.902
169.752
169.541
169.038
69.538
68.815
67.994
67.760
66.919
61.208
39.711
34.503
31.892
29.661
29.622
29.554
29.533
29.326
29.280
26.900
23.331
22.658
AcO
OAc
AcO
AcO
HN
C16H33
769
ppm (t1)

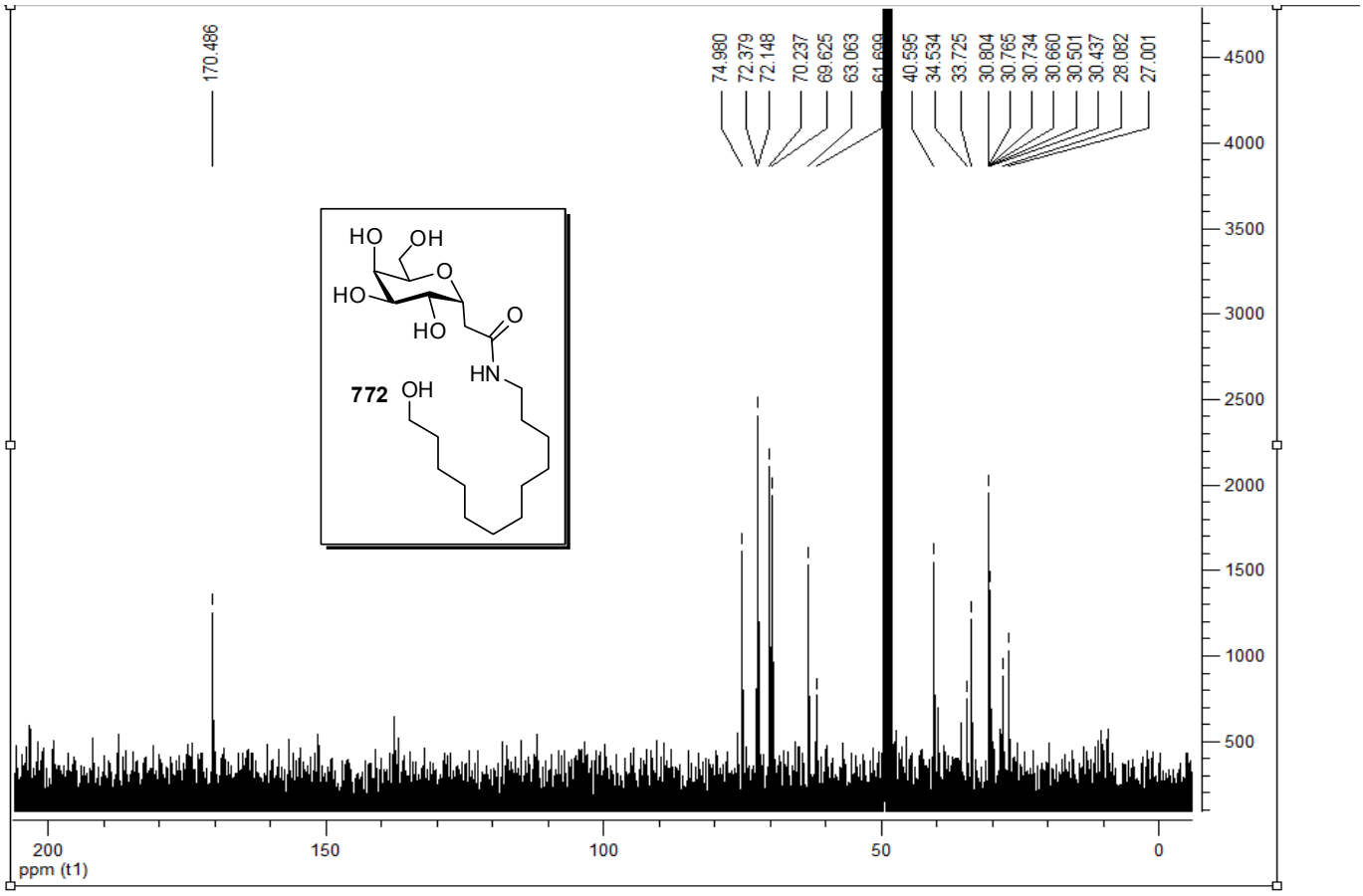

4.420
4.409
4.393
3.949
3.942
3.881
3.869
3.830
3.652
3.550
3.534
3.517
3.191
3.174
3.156
2.640
2.614
2.602
2.576
2.494
2.485
2.456
2.447
1.522
1.506
1.337
HO
OH
HO
HO
O
HN
OH
770
ppm (t1)
1.08
1.00
1.96
0.99
2.02
1.98
2.01
1.00
1.00
4.06
8.09
4.50
4.00
3.50
3.00
2.50
2.00
1.50

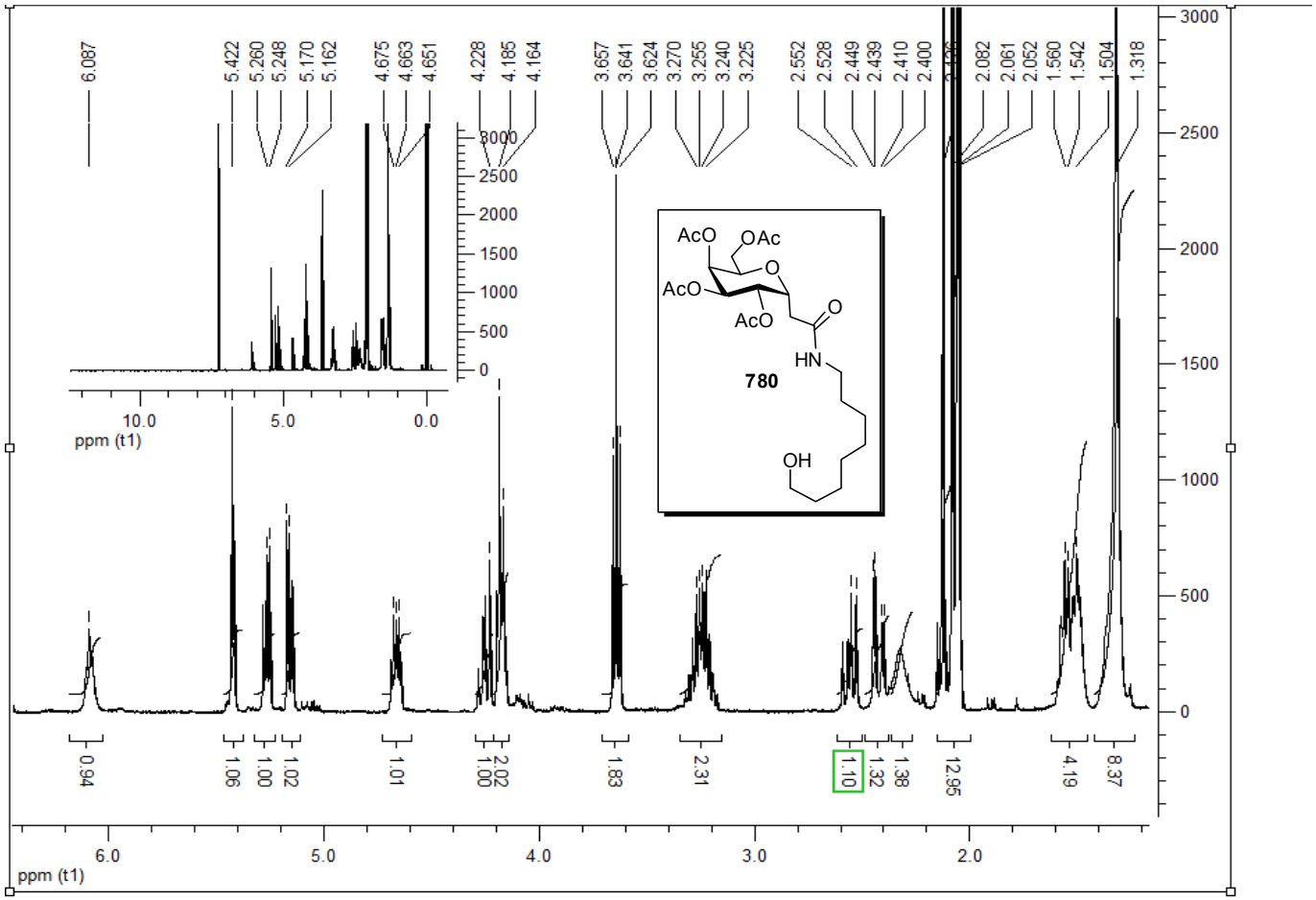

174.145
74.885
72.552
72.111
70.167
69.702
63.035
61.752
40.563
34.402
33.685
30.533
30.455
30.413
28.009
26.931
HO
OH
HO
HO
O
HN
OH
770
ppm (t1)
200
150
100
50
0

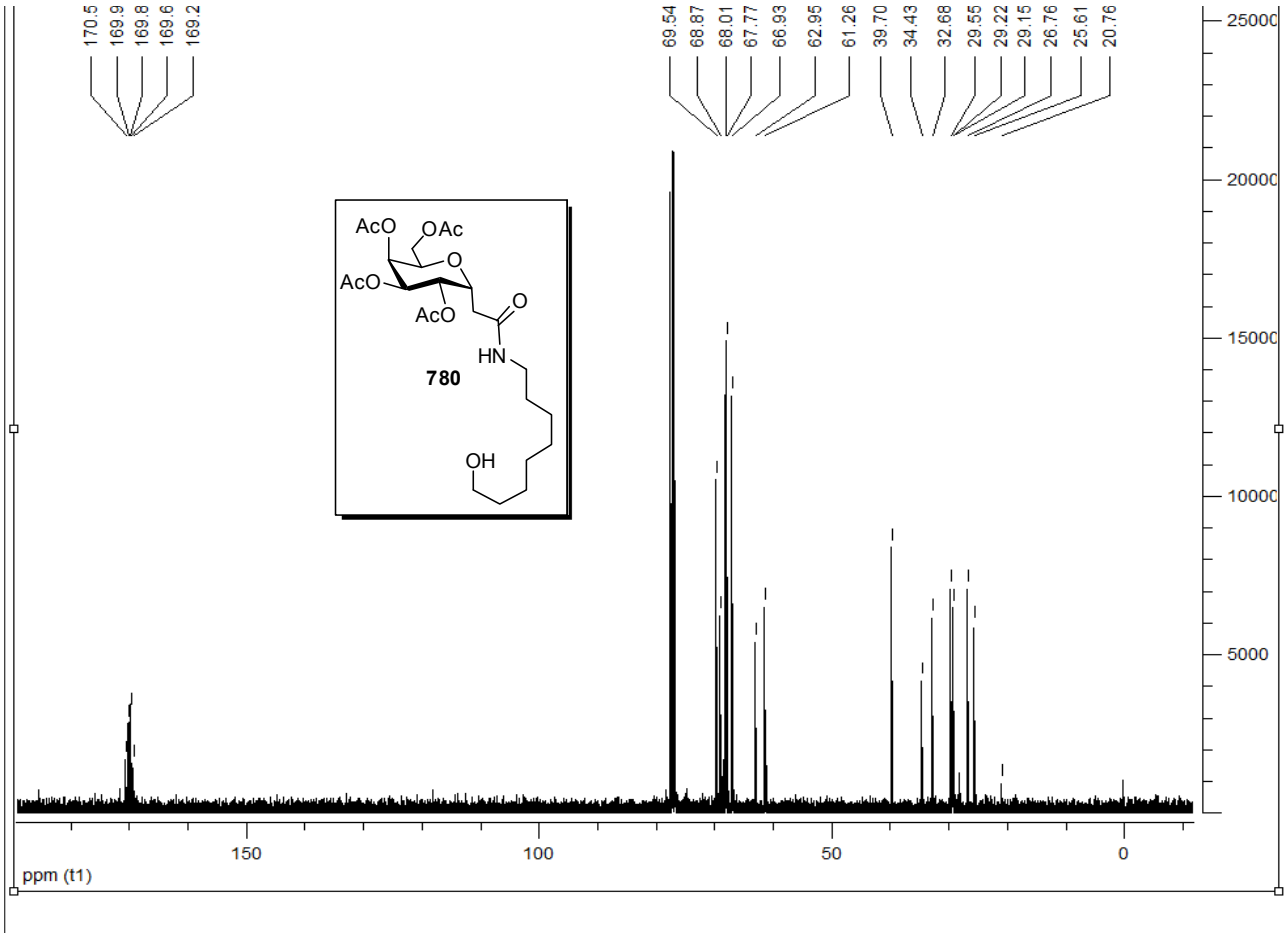

4.418
4.391
3.947
3.882
3.864
3.861
3.837
3.648
3.641
3.548
3.532
3.515
3.309
3.305
3.301
3.297
3.187
3.170
3.152
2.635
2.609
2.597
2.571
2.486
2.477
2.448
2.439
1.502
1.390
HO
OH
HO
HO
O
O
HN
771
OH
0.98
0.97
1.94
1.00
1.98
1.97
2.04
1.00
1.00
4.07
12.01
4.50
4.00
3.50
3.00
2.50
2.00
1.50
ppm (t1)
10.0
5.0
ppm (t1)

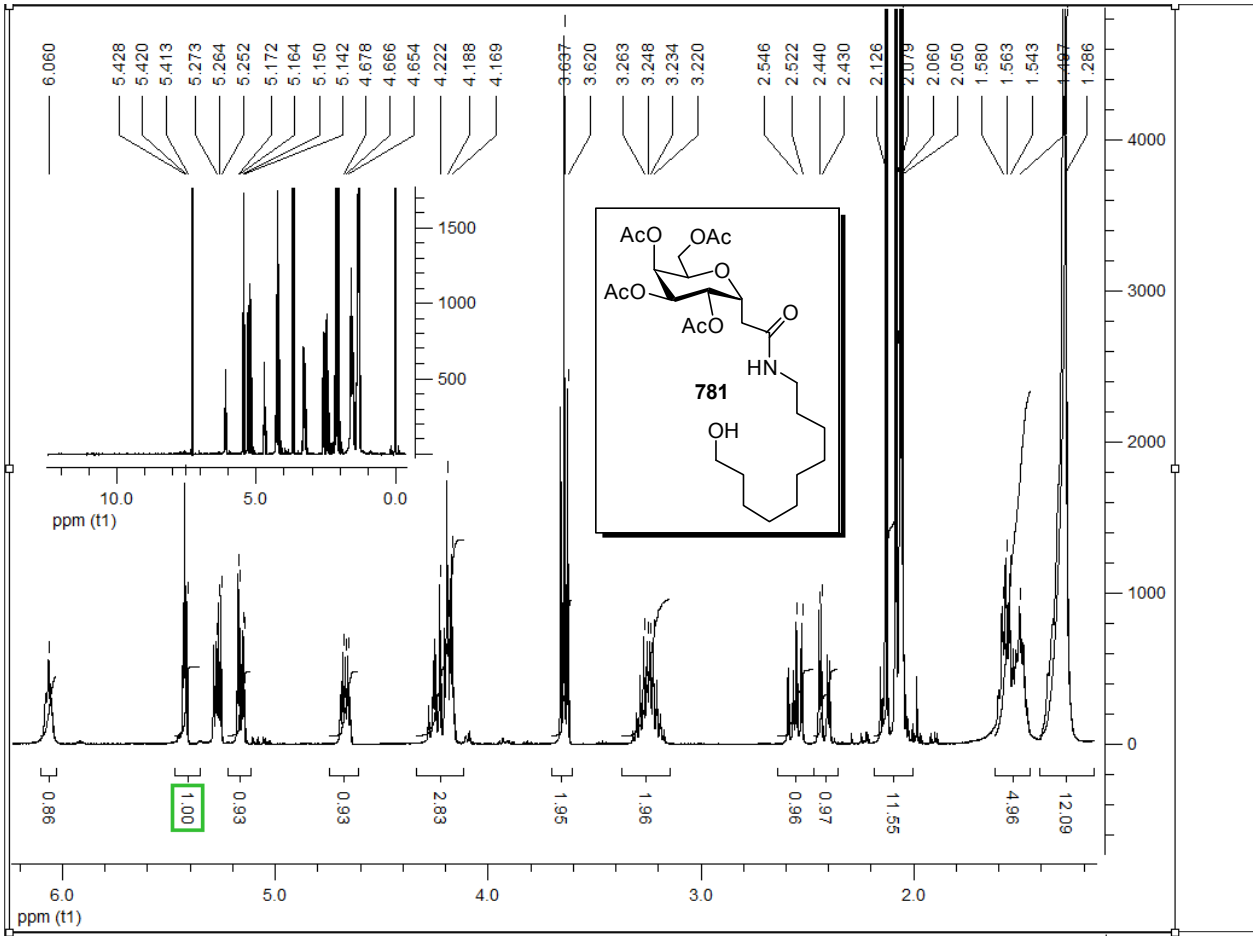

174.143
74.979
72.410
72.147
70.235
69.626
63.061
40.587
34.529
33.718
30.745
30.671
30.628
30.476
30.427
28.064
26.988
HO
OH
HO
HO
O
O
HN
771
OH
200
150
100
50
0
ppm (t1)

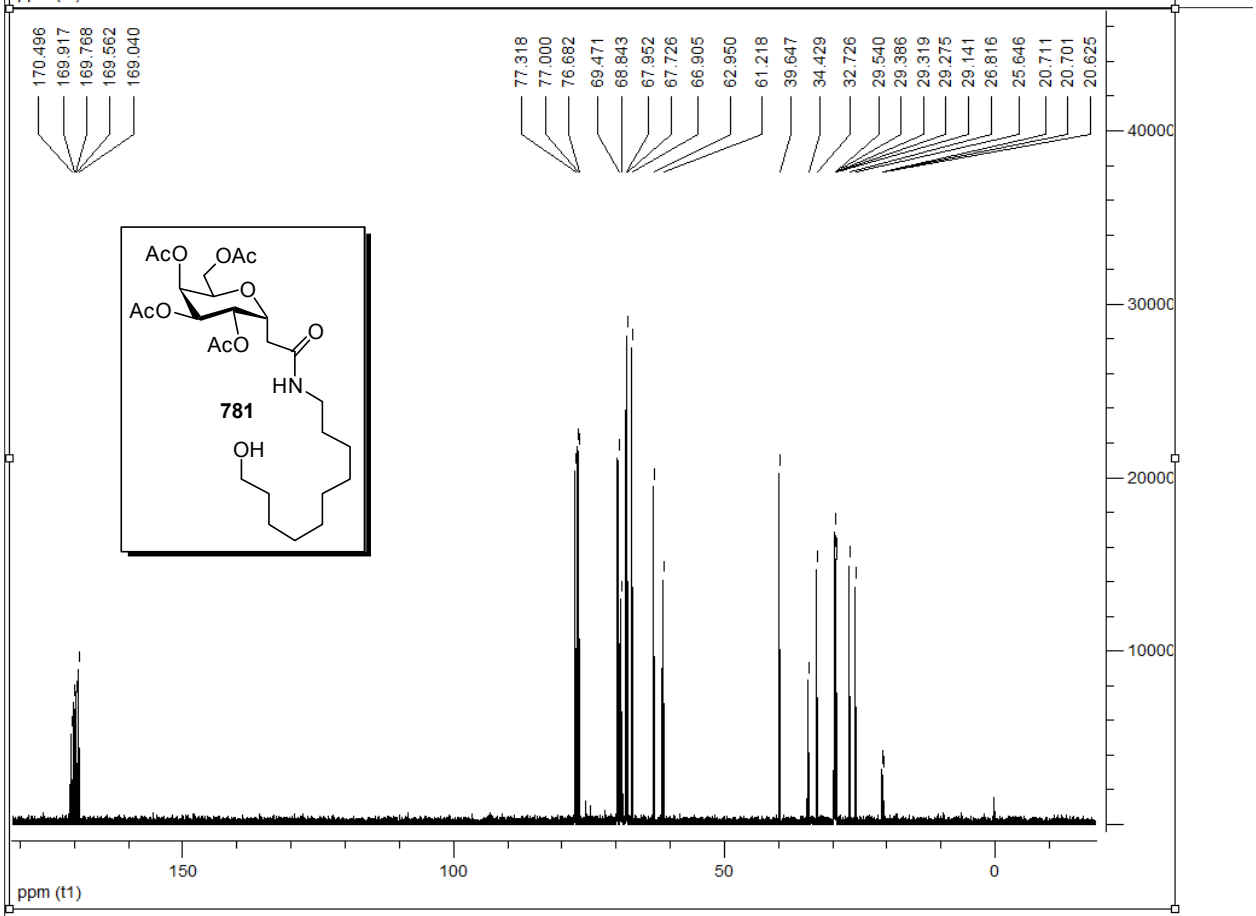

4.417
4.391
3.947
3.939
3.881
3.873
3.861
3.837
3.648
3.640
3.548
3.532
3.515
3.169
2.597
2.571
2.486
2.477
1.519
1.502
HO
OH
HO
O
HO
O
HN
772
OH
1500
1000
500
0
10.0
5.0
ppm (t1)
5000
4000
3000
2000
1000
0
0.93
0.94
1.89
1.00
1.93
1.96
1.91
0.94
0.91
3.98
16.05
4.00
3.50
3.00
2.50
2.00
1.50
ppm (t1)

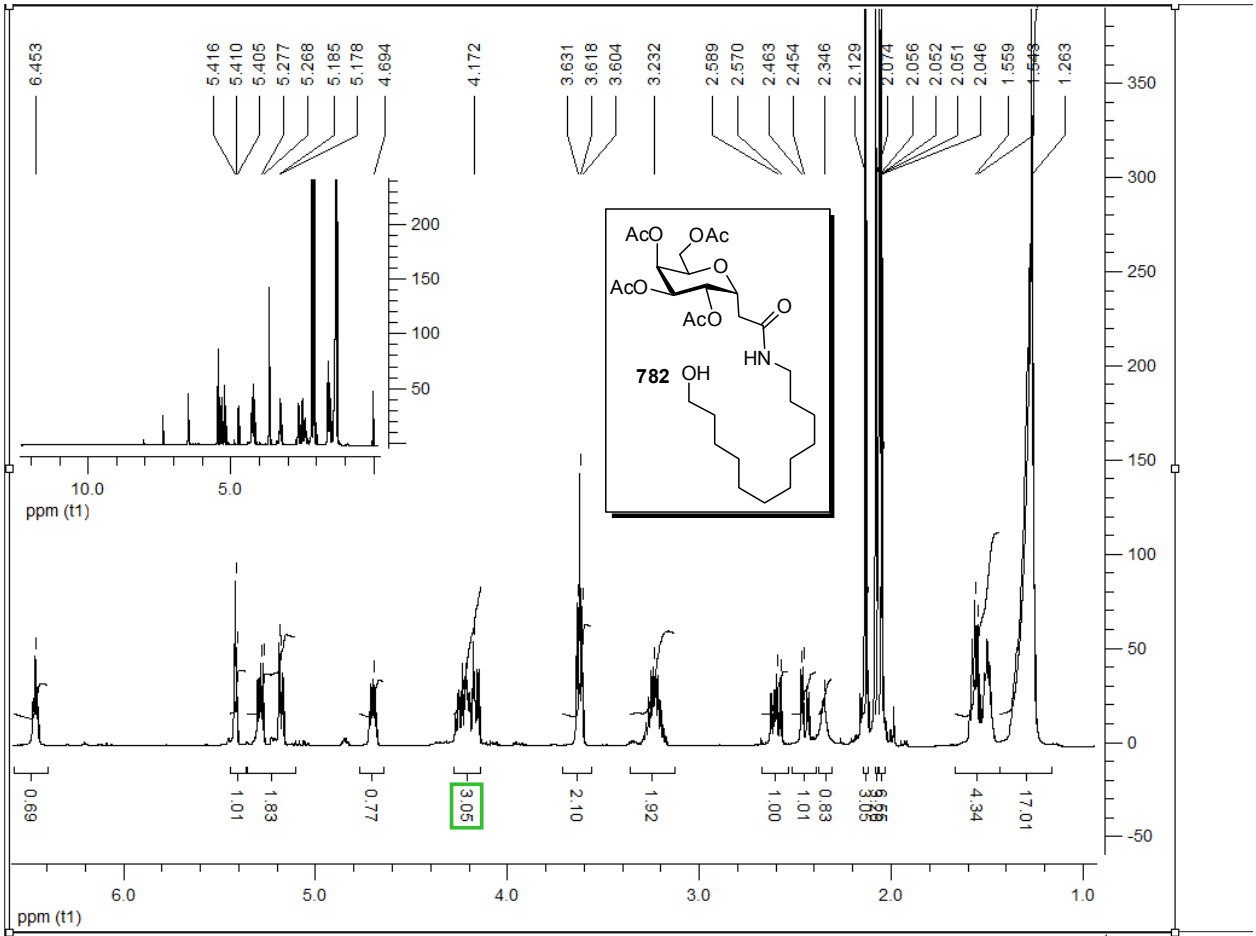

170.486
74.980
72.379
72.148
70.237
69.625
63.063
40.595
34.534
33.725
30.804
30.765
30.734
30.660
30.501
30.437
28.082
27.001
HO
OH
HO
O
HO
O
HN
772
OH
4500
4000
3500
3000
2500
2000
1500
1000
500
200
150
100
50
0
ppm (t1)

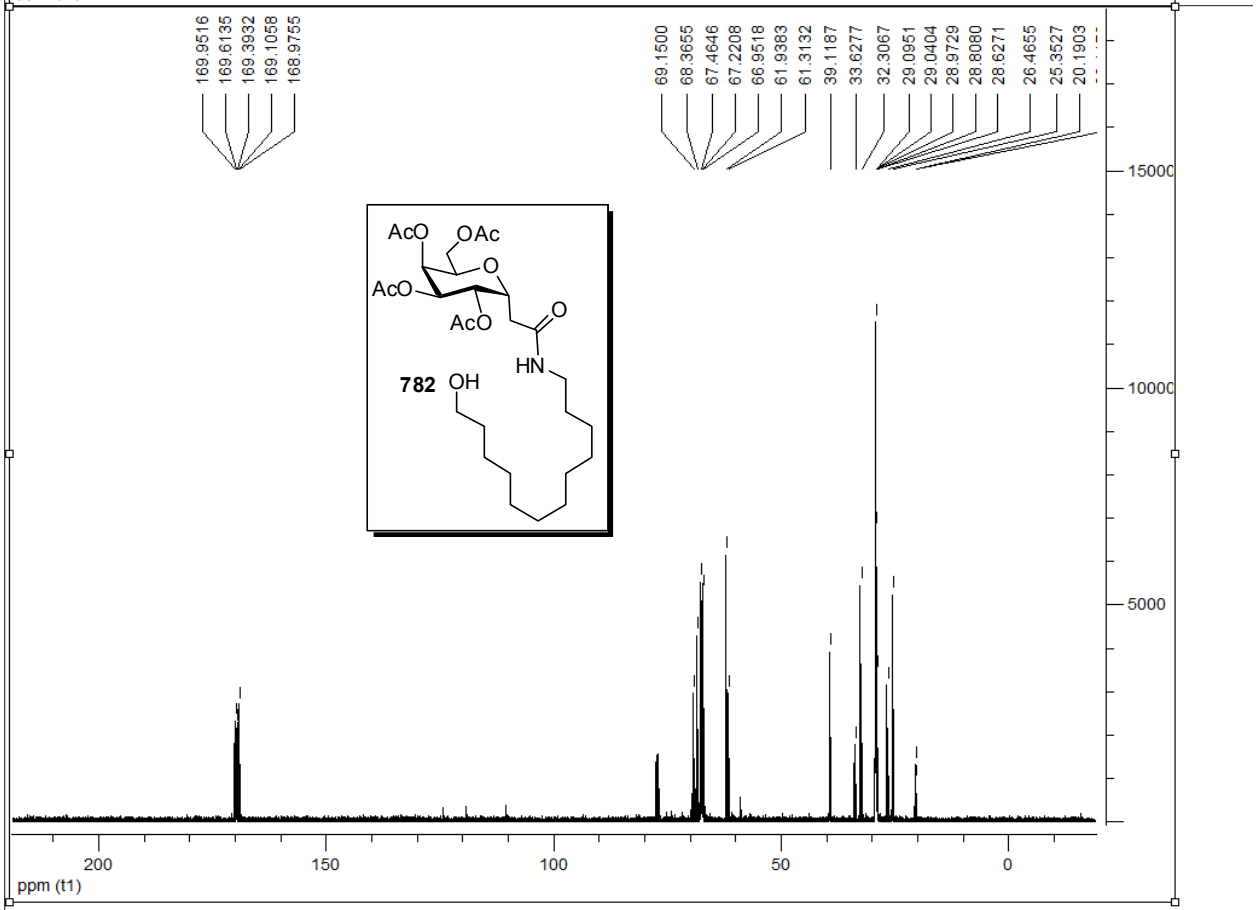

6.087
5.422
5.260
5.248
5.170
5.162
4.675
4.663
4.651
4.228
4.185
4.164
3.657
3.641
3.624
3.270
3.255
3.240
3.225
2.552
2.528
2.449
2.439
2.410
2.400
2.082
2.061
2.052
1.560
1.542
1.504
1.318
AcO
OAc
AcO
AcO
O
HN
780
OH
ppm (t1)
0.94
1.06
1.00
1.02
1.01
2.02
1.83
2.31
1.10
1.32
1.38
12.95
4.19
8.37

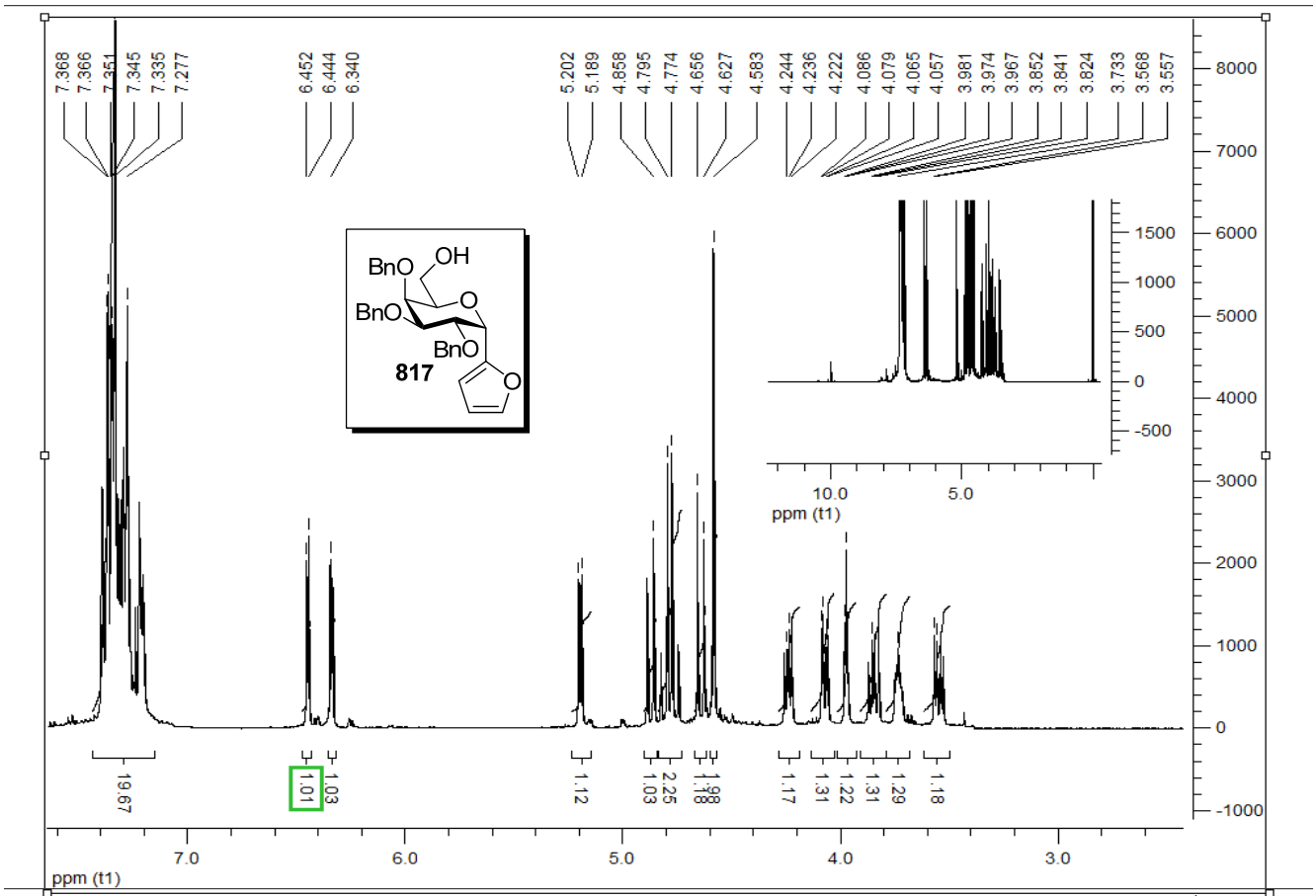

170.5
169.9
169.8
169.6
169.2
69.54
68.87
68.01
67.77
66.93
62.95
61.26
39.70
34.43
32.68
29.55
29.22
29.15
26.76
25.61
20.76
AcO
OAc
AcO
AcO
O
HN
780
OH
ppm (t1)

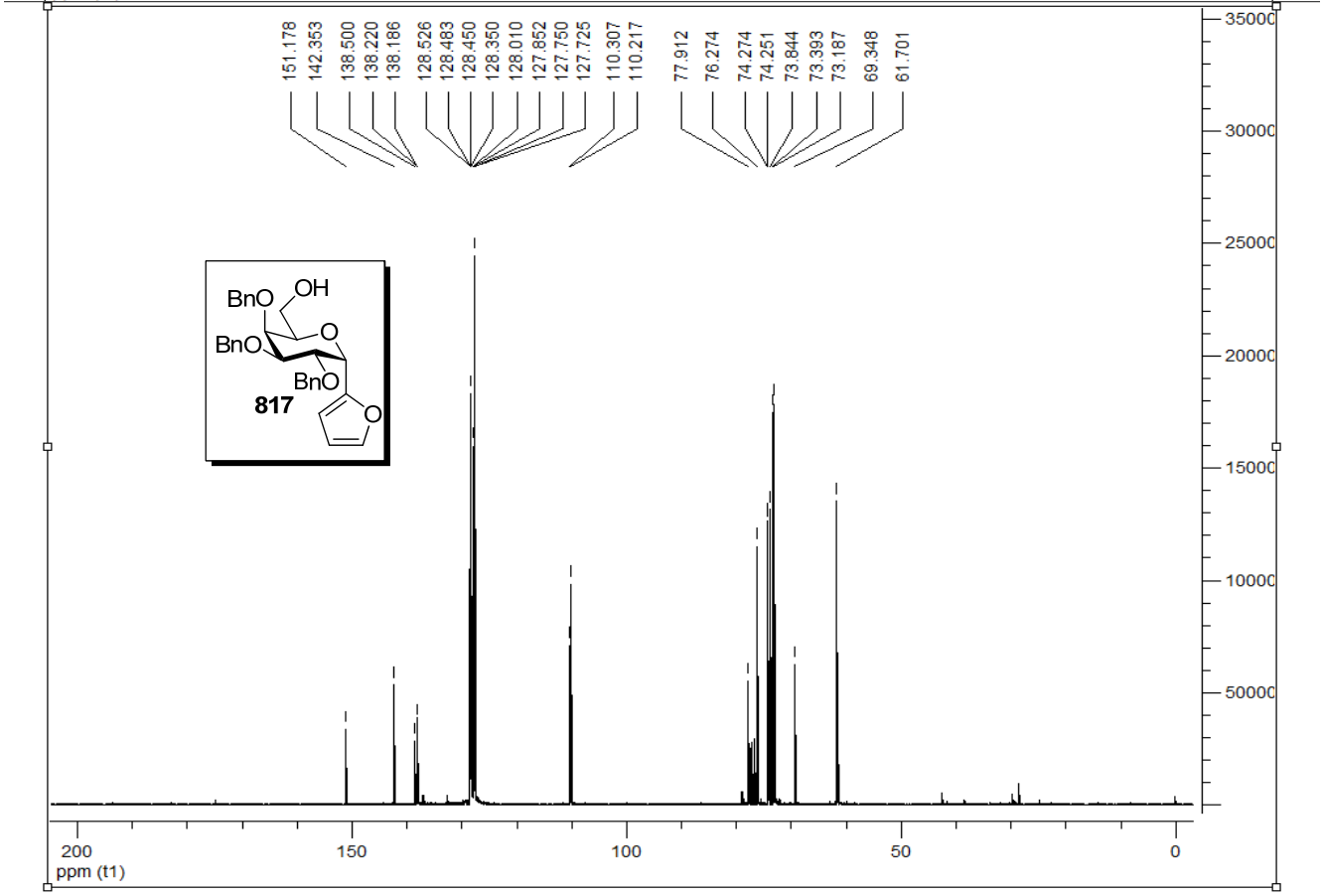

6.060
5.428
5.420
5.413
5.273
5.264
5.252
5.172
5.164
5.150
5.142
4.678
4.666
4.654
4.222
4.188
4.169
3.637
3.620
3.263
3.248
3.234
3.220
2.546
2.522
2.440
2.430
2.126
2.079
2.060
2.050
1.580
1.563
1.543
1.497
1.286
AcO
OAc
AcO
AcO
O
HN
781
OH
ppm (t1)
0.86
1.00
0.93
0.93
2.83
1.95
1.96
0.96
0.97
11.55
4.96
12.09

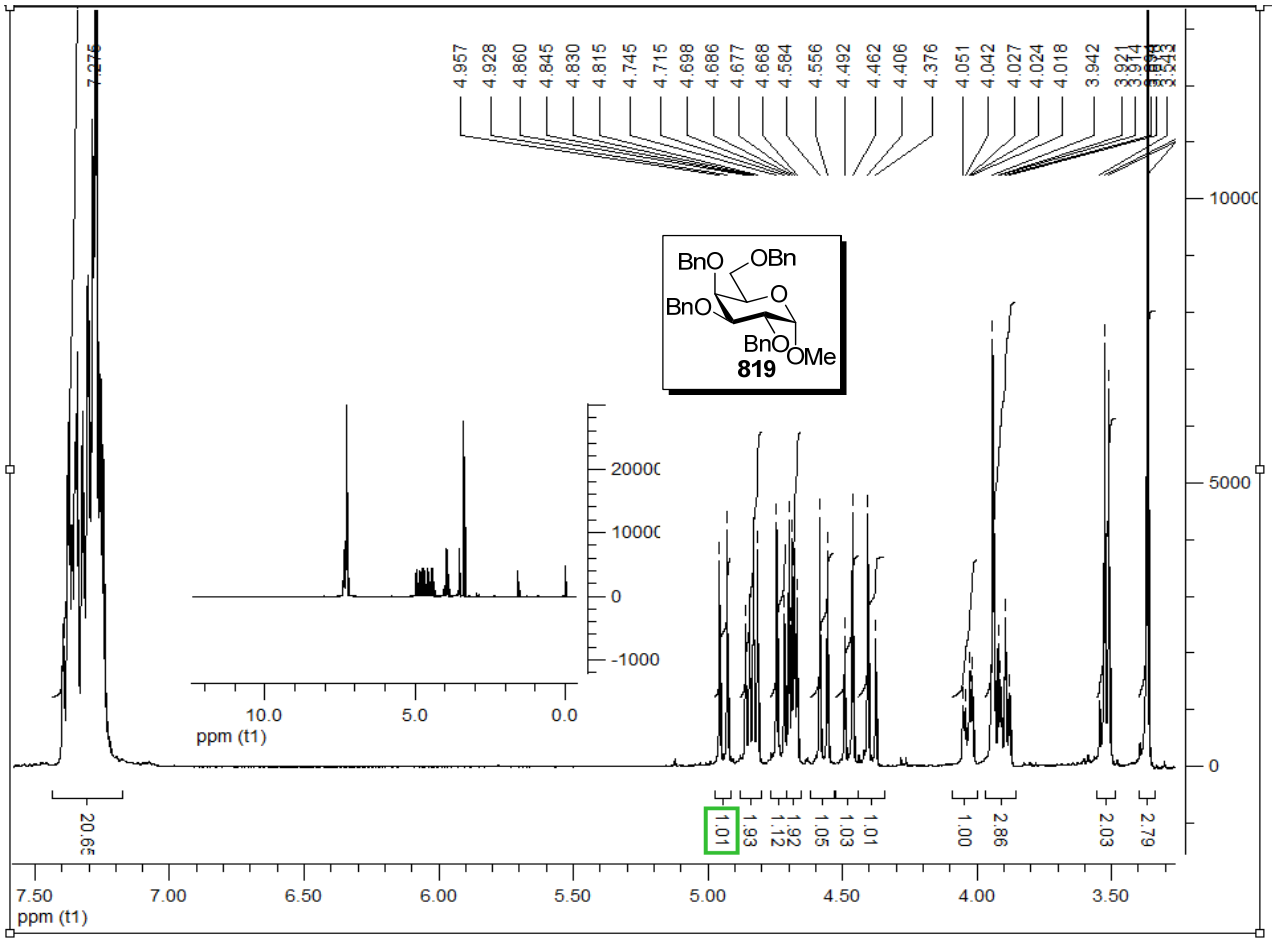

170.496
169.917
169.768
169.562
169.040
77.318
77.000
76.682
69.471
68.843
67.952
67.726
66.905
62.950
61.218
39.647
34.429
32.726
29.540
29.386
29.319
29.275
29.141
26.816
25.646
20.711
20.701
20.625
AcO
OAc
AcO
AcO
O
HN
781
OH
ppm (t1)

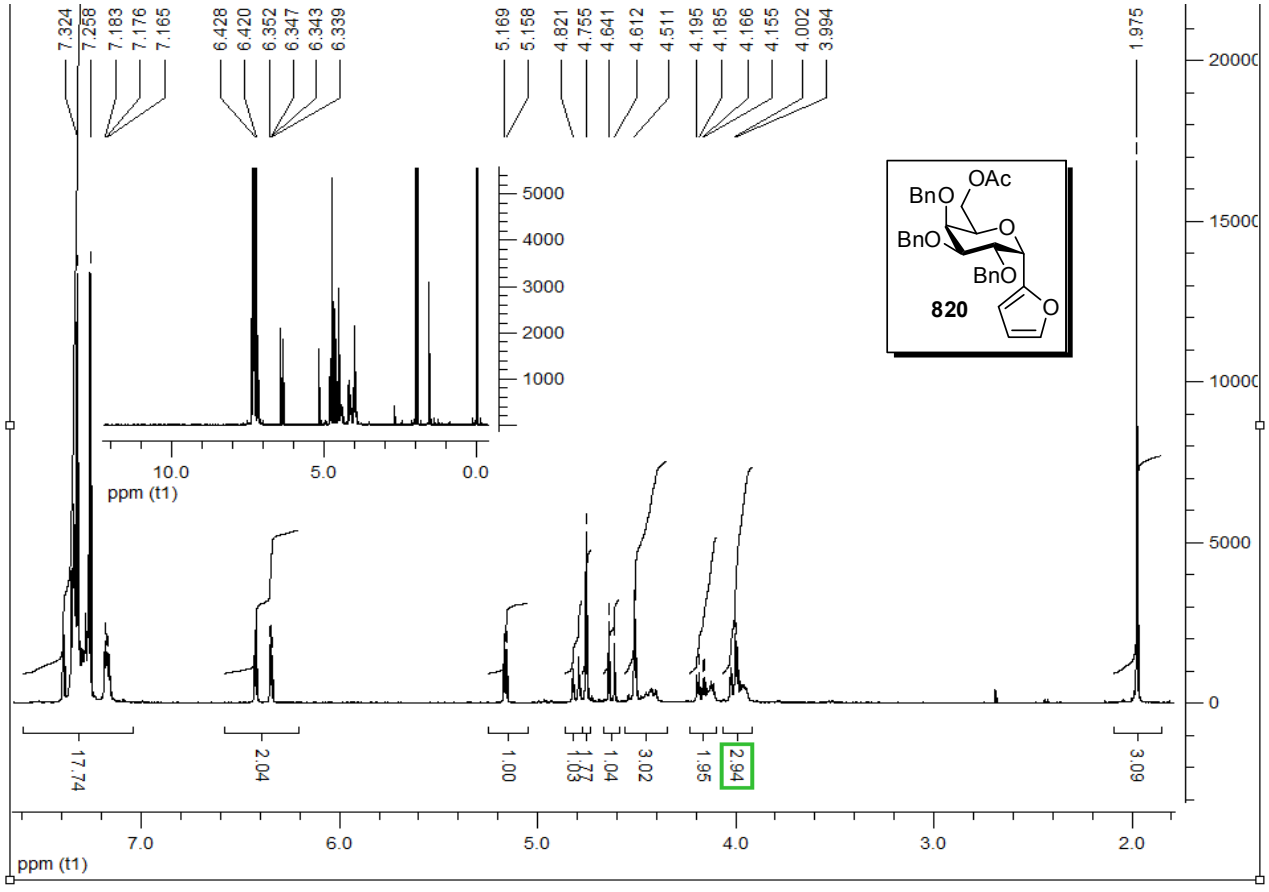

6.453
5.416
5.410
5.405
5.277
5.268
5.185
5.178
4.694
4.172
3.631
3.618
3.604
3.232
2.589
2.570
2.463
2.454
2.346
2.129
2.074
2.056
2.052
2.051
2.046
1.559
1.543
1.263
AcO
OAc
AcO
AcO
O
HN
782
OH
ppm (t1)
0.69
1.01
1.83
0.77
3.05
2.10
1.92
1.00
1.01
0.83
4.34
17.01

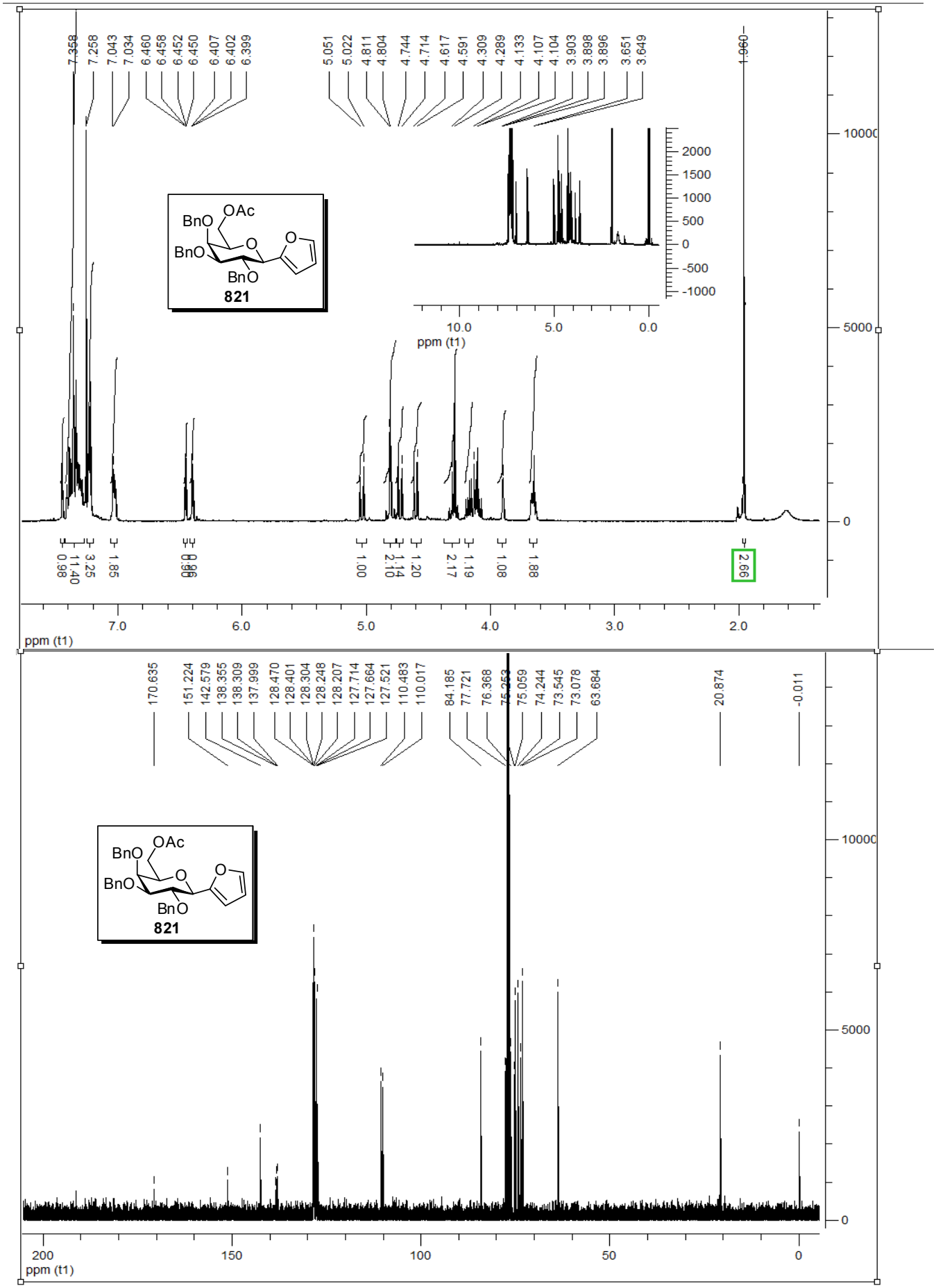

169.9516
169.6135
169.3932
169.1058
168.9755
69.1500
68.3655
67.4646
67.2208
66.9518
61.9383
61.3132
39.1187
33.6277
32.3067
29.0951
29.0404
28.9729
28.8080
28.6271
26.4655
25.3527
20.1903
AcO
OAc
AcO
AcO
O
HN
782
OH
ppm (t1)

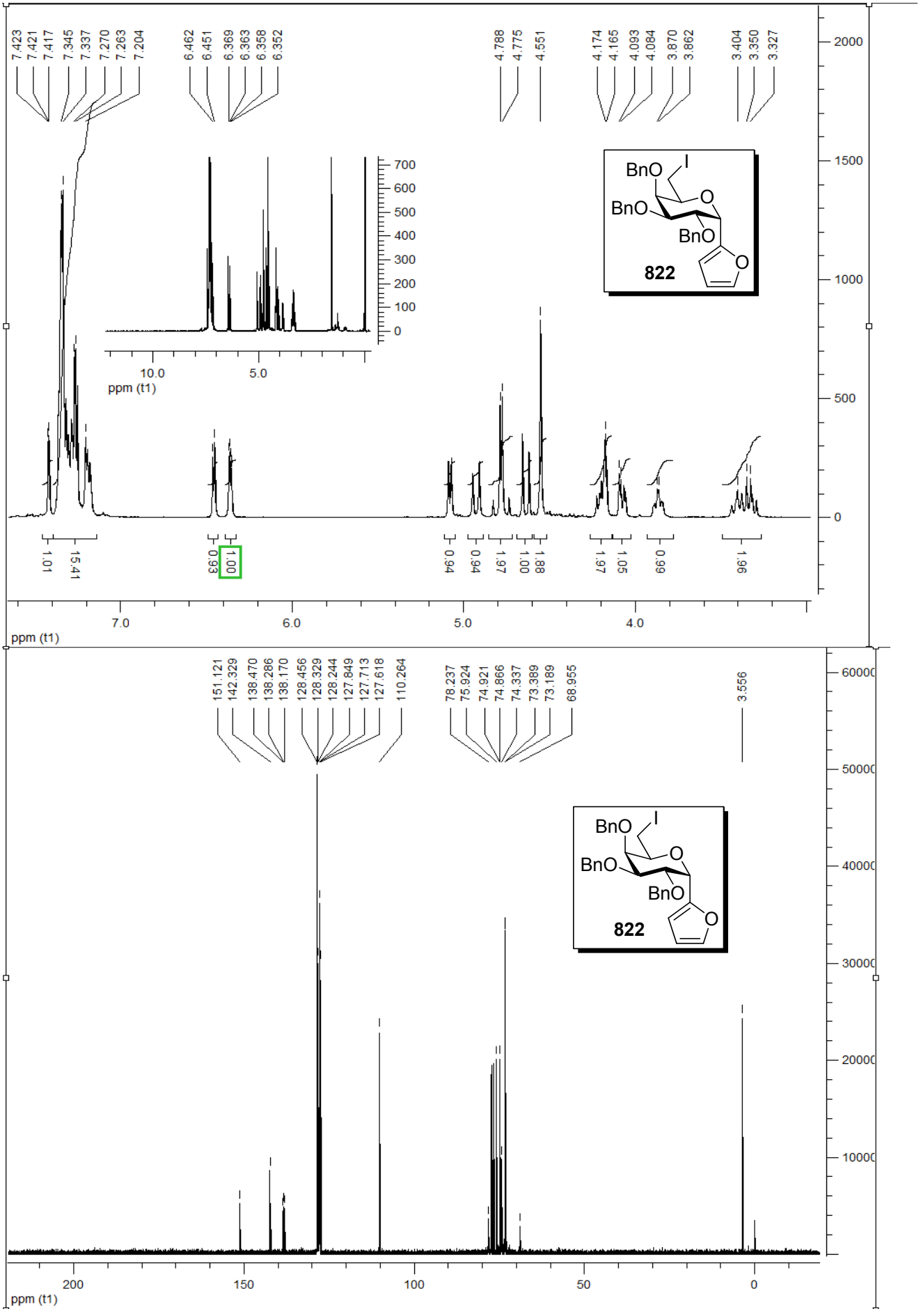

7.368
7.366
7.351
7.345
7.335
7.277
6.452
6.444
6.340
5.202
5.189
4.858
4.795
4.774
4.656
4.627
4.583
4.244
4.236
4.222
4.086
4.079
4.065
4.057
3.981
3.974
3.967
3.852
3.841
3.824
3.733
3.568
3.557
BnO
OH
BnO
O
BnO
O
817
19.67
1.01
1.03
1.12
1.03
2.25
1.88
1.17
1.31
1.22
1.31
1.29
1.18
ppm (t1)
ppm (t1)

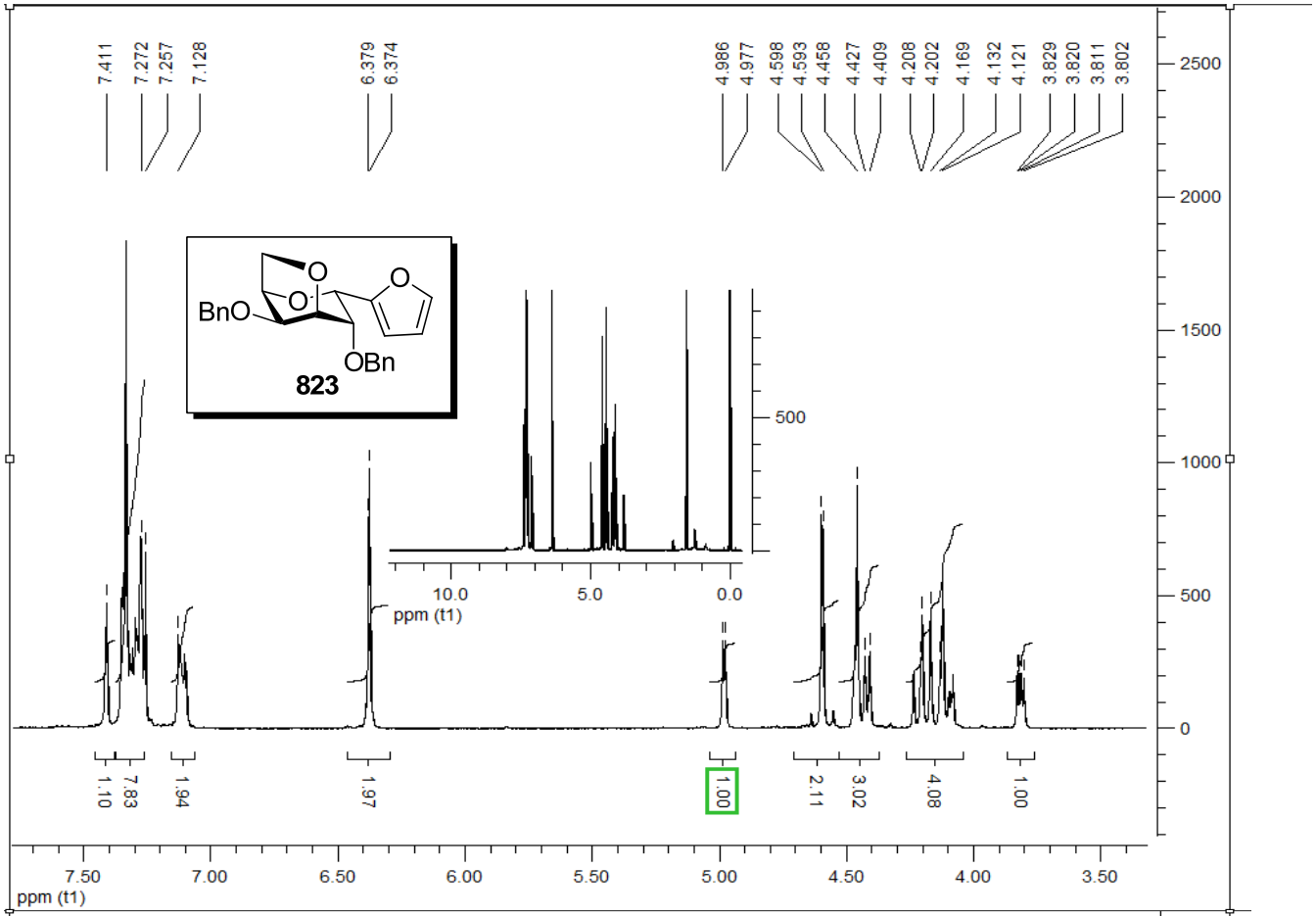

151.178
142.353
138.500
138.220
138.186
128.526
128.483
128.450
128.350
128.010
127.852
127.750
127.725
110.307
110.217
77.912
76.274
74.274
74.251
73.844
73.393
73.187
69.348
61.701
BnO
OH
BnO
O
BnO
O
817
ppm (t1)

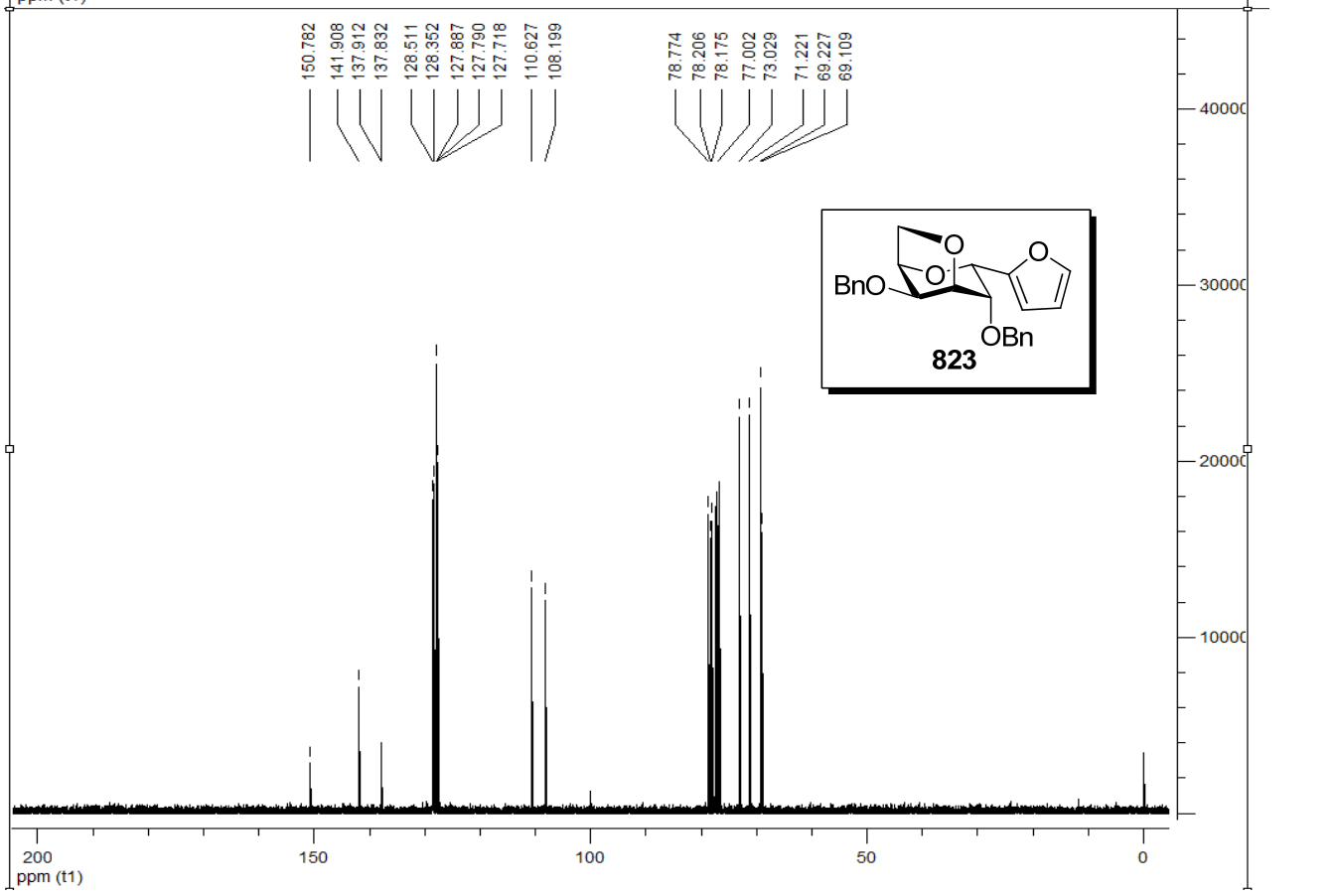

BnO
OBn
O
BnO
BnO
OMe
819
ppm (t1)
7.50
7.00
6.50
6.00
5.50
5.00
4.50
4.00
3.50

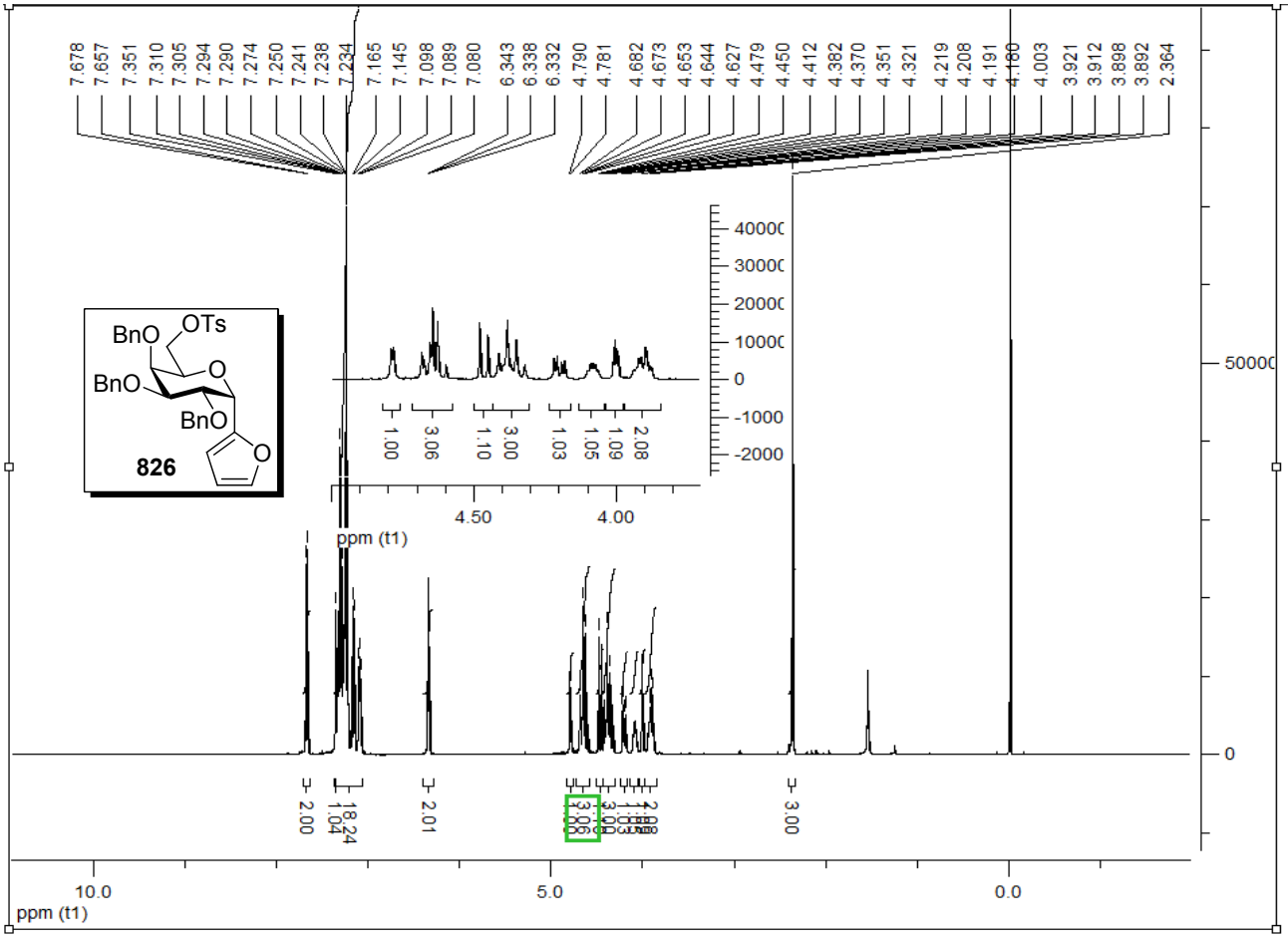

OAc
BnO
O
BnO
BnO
820
O
ppm (t1)
7.0
6.0
5.0
4.0
3.0
2.0

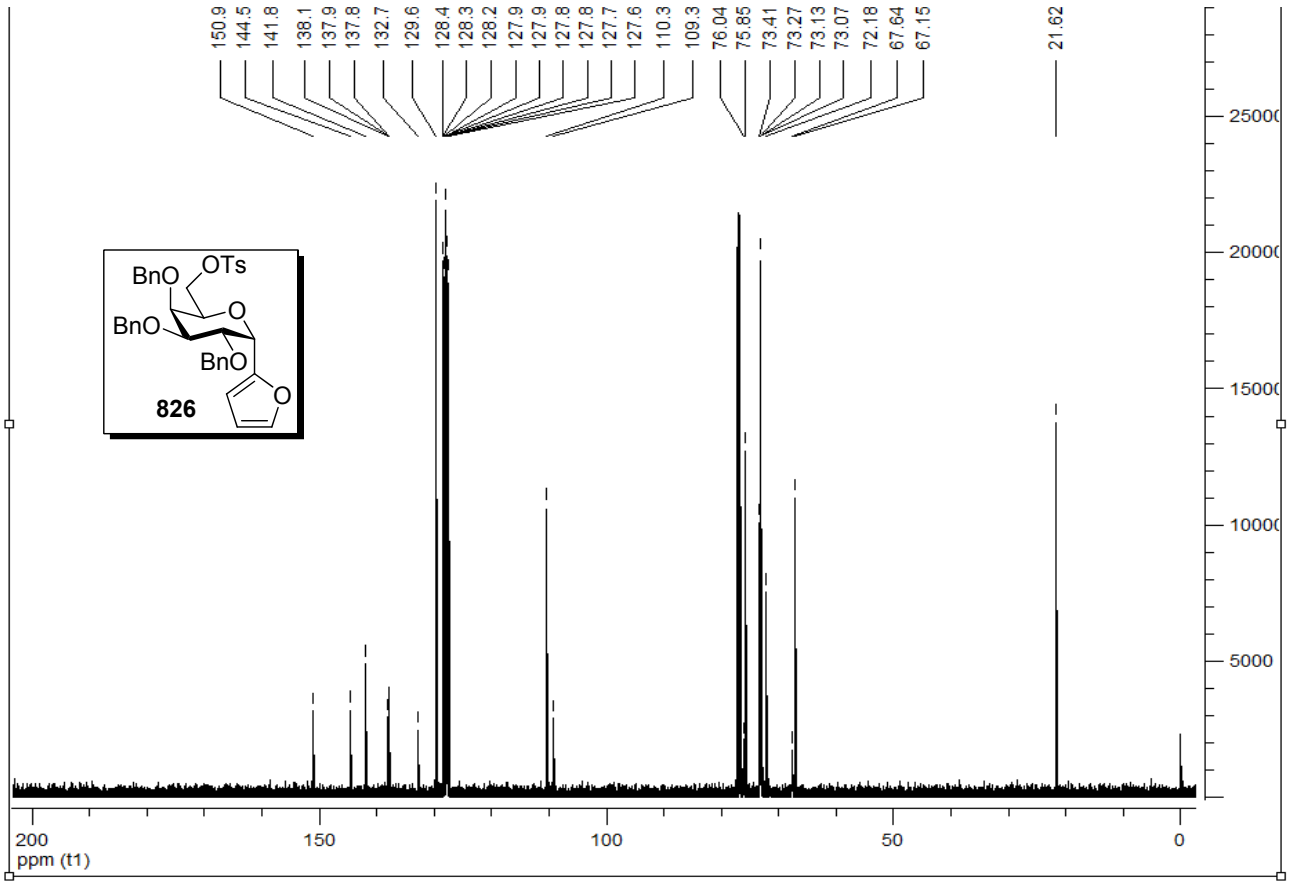

7.358
7.258
7.043
7.034
6.460
6.458
6.452
6.450
6.407
6.402
6.399
5.051
5.022
4.811
4.804
4.744
4.714
4.617
4.591
4.309
4.289
4.133
4.107
4.104
3.903
3.898
3.896
3.651
3.649
1.960
BnO
OAc
BnO
O
O
BnO
821
ppm (t1)
0.98
1.40
3.25
1.85
0.90
0.90
1.00
2.10
1.14
1.20
2.17
1.19
1.08
1.88
2.99
ppm (t1)
170.635
151.224
142.579
138.355
138.309
137.999
128.470
128.401
128.304
128.248
128.207
127.714
127.664
127.521
110.483
110.017
84.185
77.721
76.368
75.253
75.059
74.244
73.545
73.078
63.684
20.874
-0.011
BnO
OAc
BnO
O
O
BnO
821
ppm (t1)

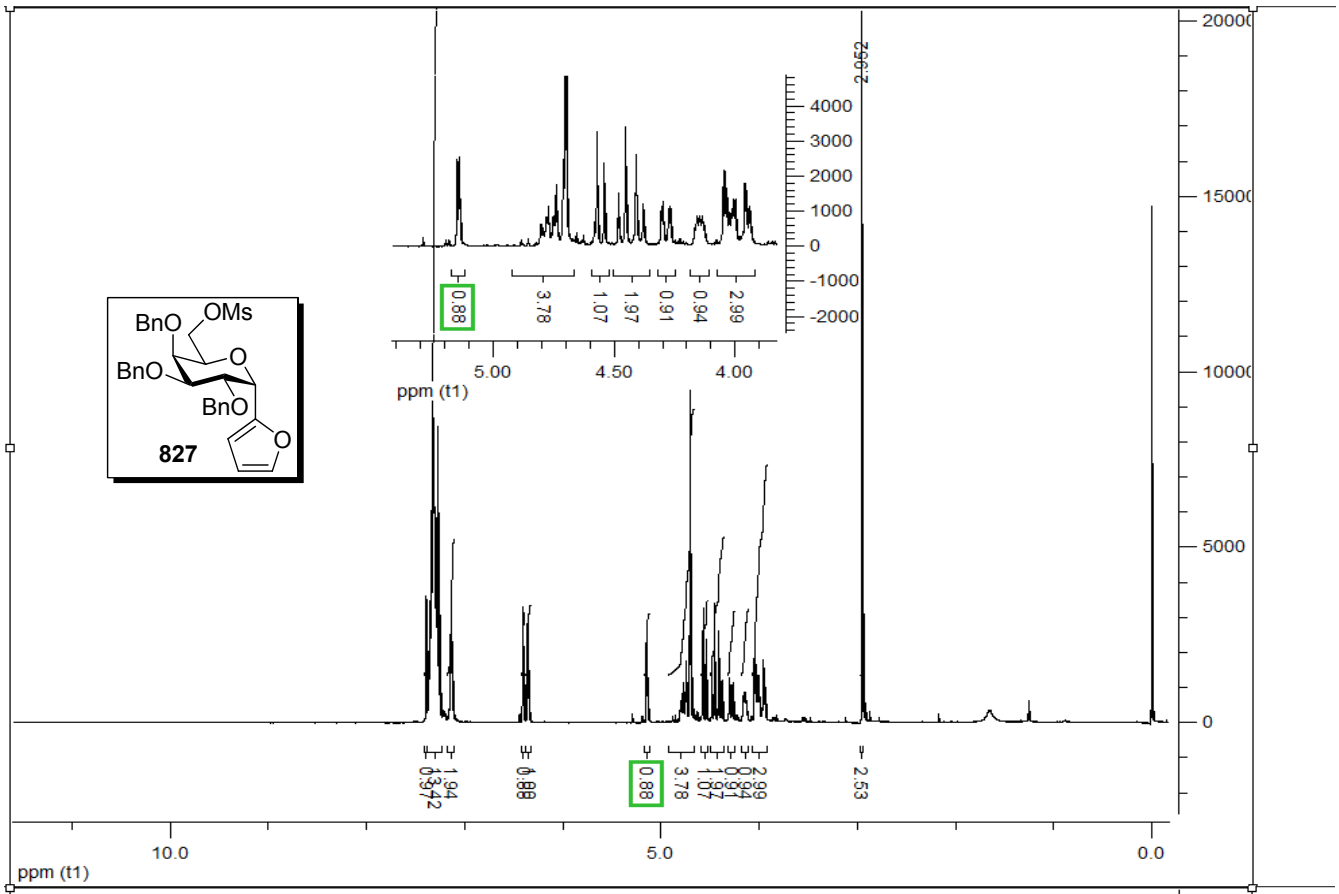

7.423
7.421
7.417
7.345
7.337
7.270
7.263
7.204
6.462
6.451
6.369
6.363
6.358
6.352
4.788
4.775
4.551
4.174
4.165
4.093
4.084
3.870
3.862
3.404
3.350
3.327
BnO
I
O
BnO
BnO
O
822
ppm (t1)
1.01
1.41
0.93
1.00
0.94
0.94
1.87
1.00
1.88
1.97
1.05
0.99
1.96
151.121
142.329
138.470
138.286
138.170
128.456
128.329
128.244
127.849
127.713
127.618
110.264
78.237
75.924
74.921
74.866
74.337
73.389
73.189
68.955
3.556

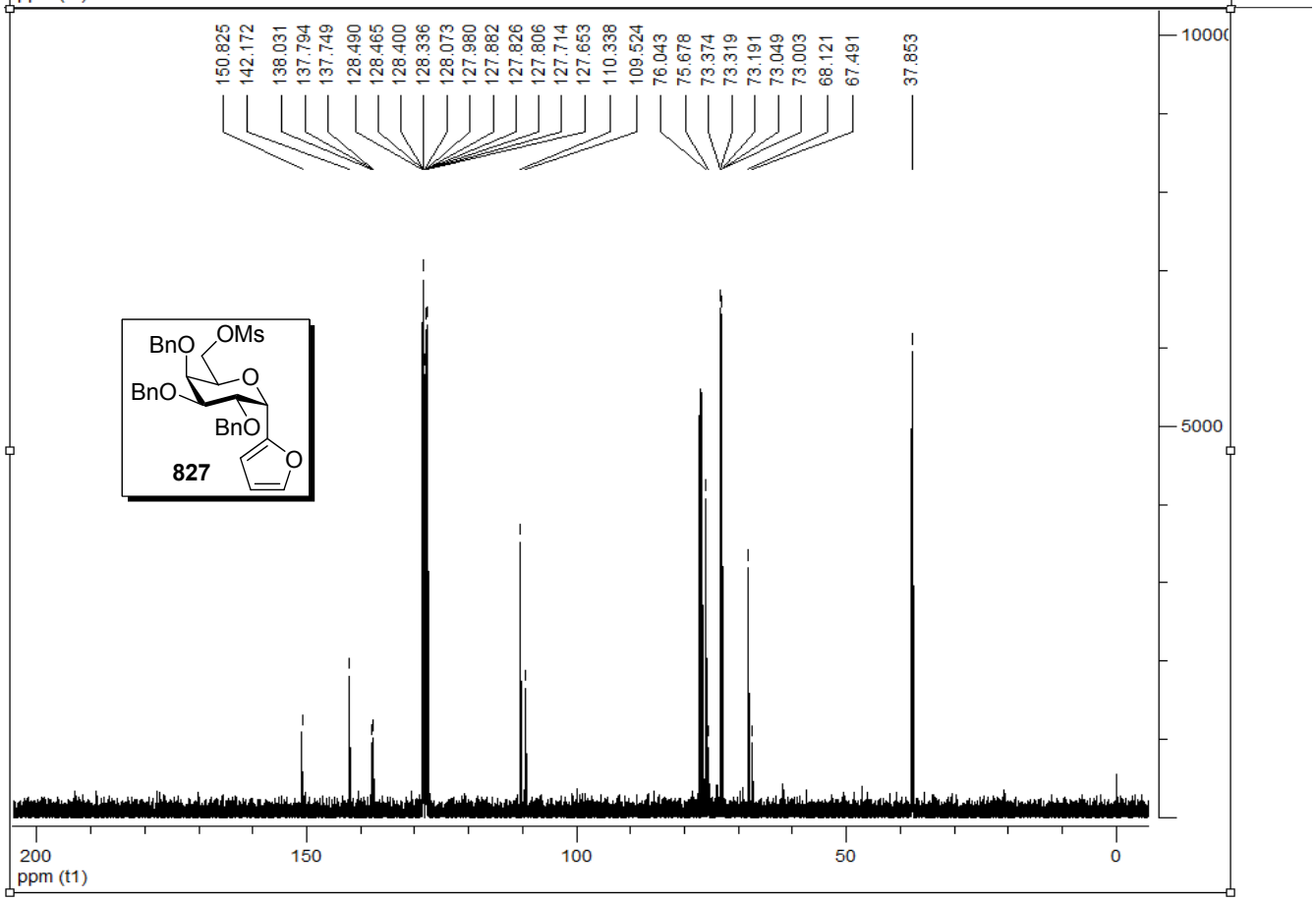

7.411
7.272
7.257
7.128
6.379
6.374
4.986
4.977
4.598
4.593
4.458
4.427
4.409
4.208
4.202
4.169
4.132
4.121
3.829
3.820
3.811
3.802
BnO
OBn
823
ppm (t1)
1.10
7.83
1.94
1.97
1.00
2.11
3.02
4.08
1.00

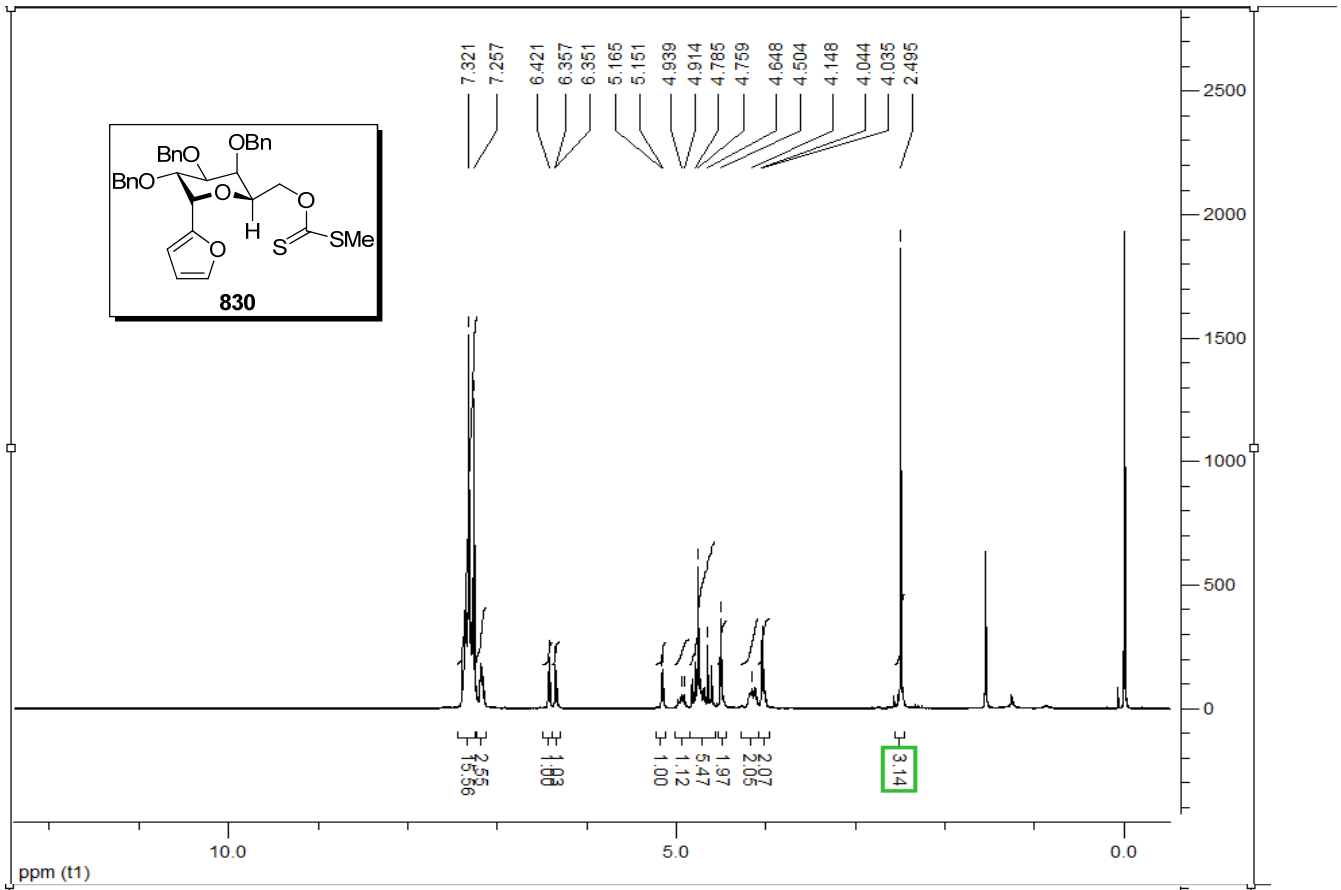

150.782
141.908
137.912
137.832
128.511
128.352
127.887
127.790
127.718
110.627
108.199
78.774
78.206
78.175
77.002
73.029
71.221
69.227
69.109
BnO
OBn
823
ppm (t1)

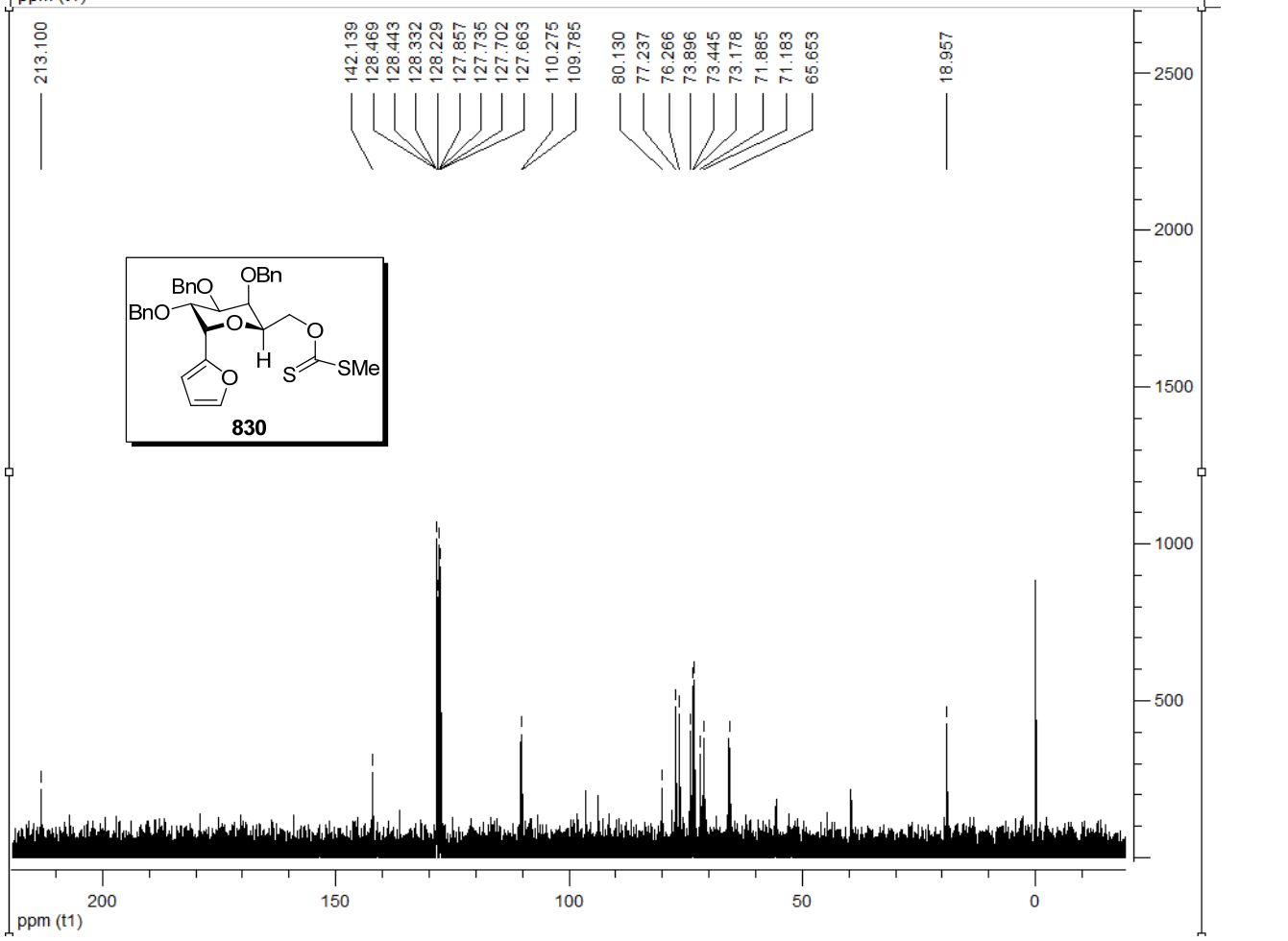

7.678
7.657
7.351
7.310
7.305
7.294
7.290
7.274
7.250
7.241
7.238
7.234
7.165
7.145
7.098
7.089
7.080
6.343
6.338
6.332
4.790
4.781
4.682
4.673
4.653
4.644
4.627
4.479
4.450
4.412
4.382
4.370
4.351
4.321
4.219
4.208
4.191
4.180
4.003
3.921
3.912
3.898
3.892
2.364
BnO
OTs
O
BnO
BnO
O
826
ppm (t1)
10.0
5.0
0.0

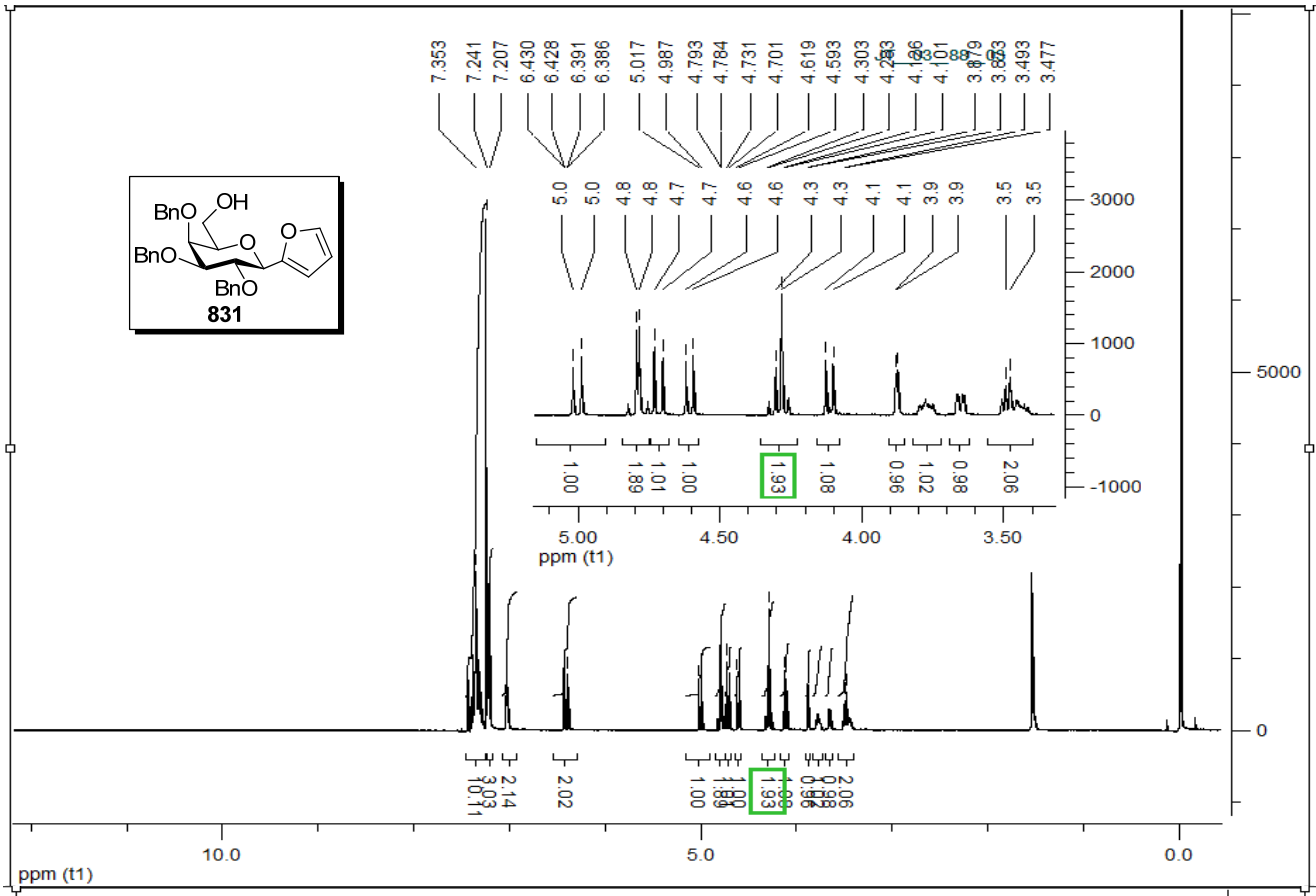

150.9
144.5
141.8
138.1
137.9
137.8
132.7
129.6
128.4
128.3
128.2
127.9
127.9
127.8
127.8
127.7
127.6
110.3
109.3
76.04
75.85
73.41
73.27
73.13
73.07
72.18
67.64
67.15
21.62
BnO
OTs
O
BnO
BnO
O
826
200
150
100
50
0
ppm (t1)

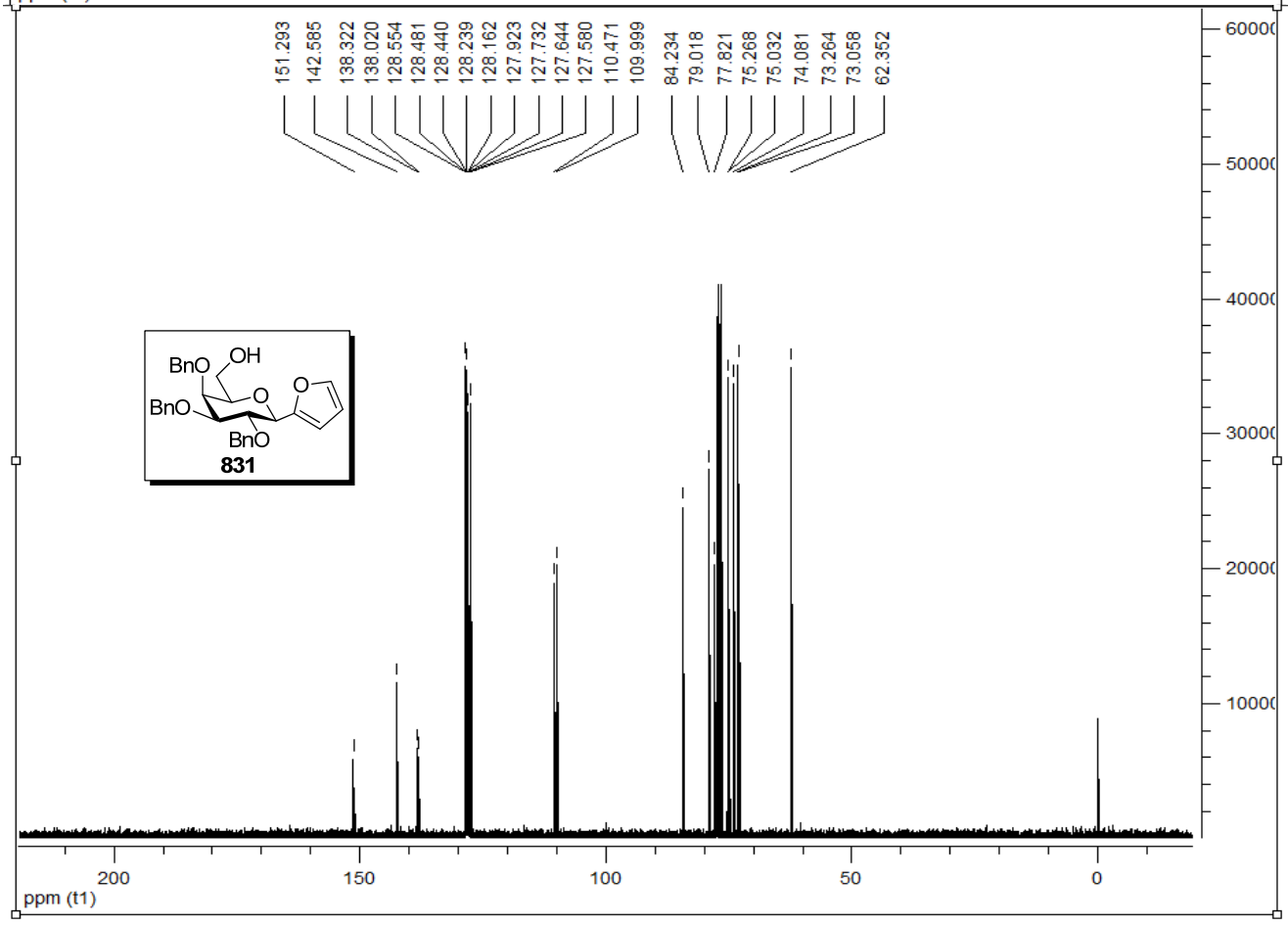

BnO
OMs
BnO
O
BnO
O
827
ppm (t1)
10.0
5.0
0.0
5.00
4.50
4.00

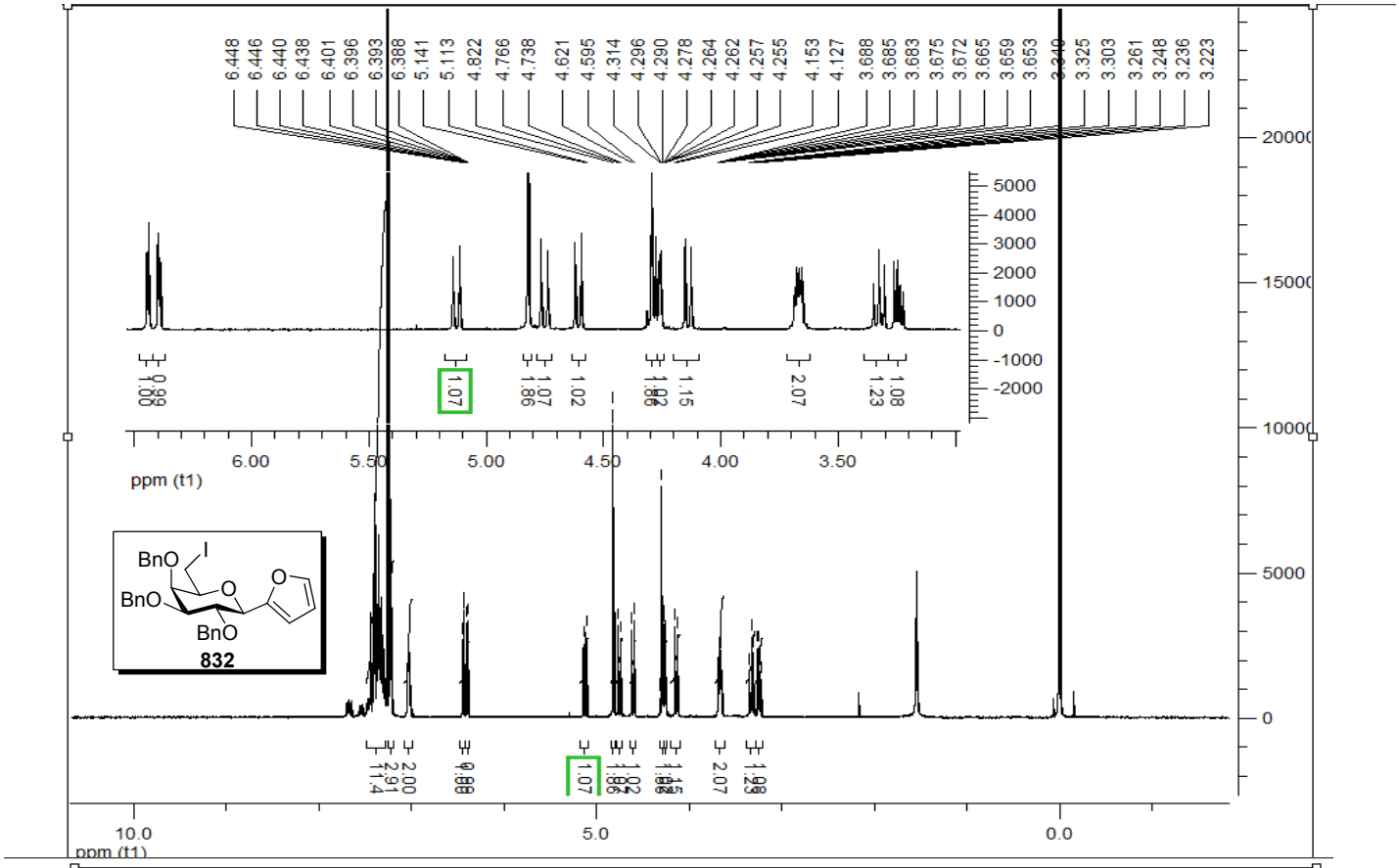

150.825
142.172
138.031
137.794
137.749
128.490
128.465
128.400
128.336
128.073
127.980
127.882
127.826
127.806
127.714
127.653
110.338
109.524
76.043
75.678
73.374
73.319
73.191
73.049
73.003
68.121
67.491
37.853
BnO
OMs
BnO
O
BnO
O
827
200
150
100
50
0
ppm (t1)

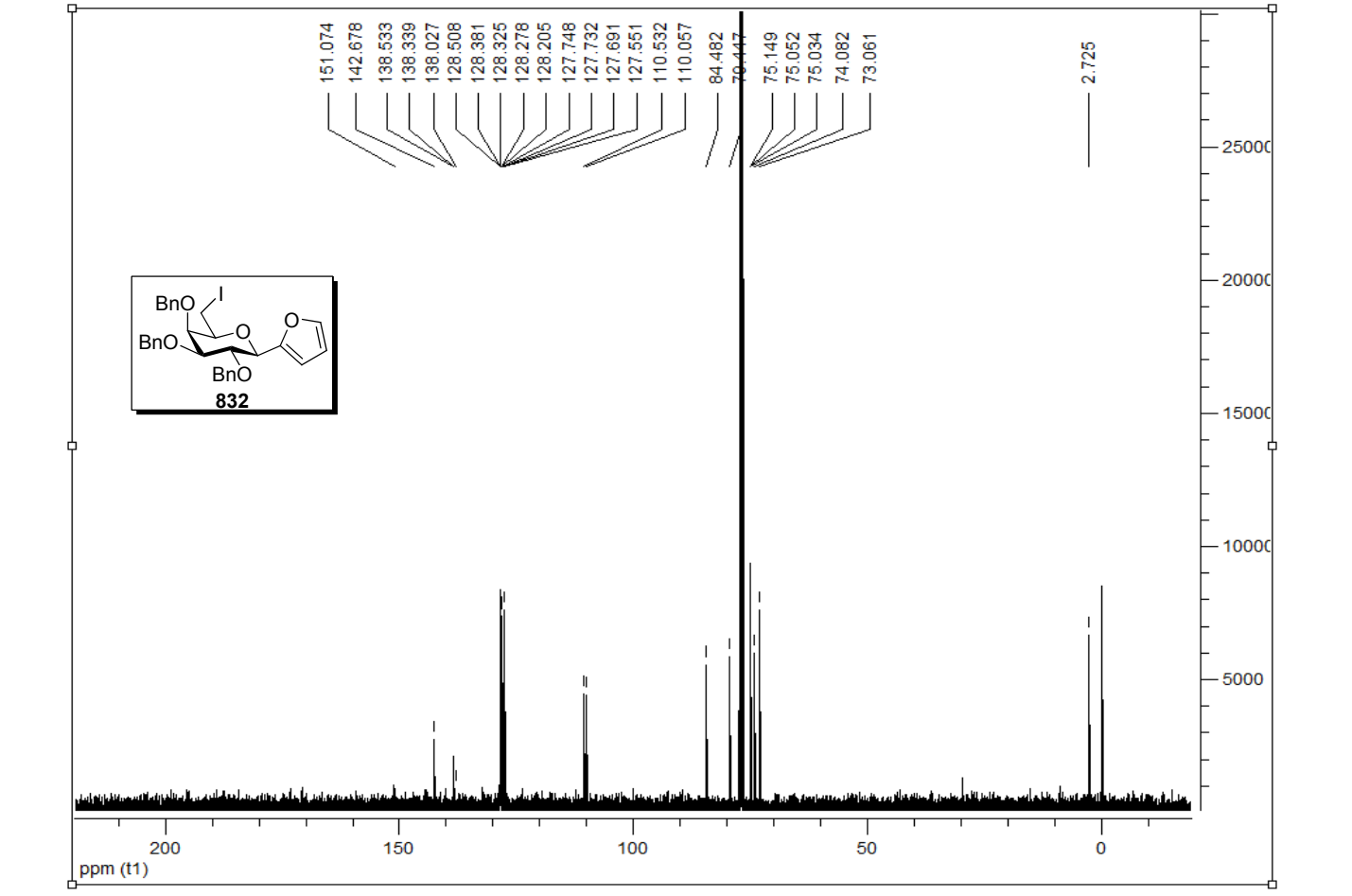

7.321
7.257
6.421
6.357
6.351
5.165
5.151
4.939
4.914
4.785
4.759
4.648
4.504
4.148
4.044
4.035
2.495
BnO
OBn
BnO
O
O
H
S
SMe
O
830
2500
2000
1500
1000
500
0
2.56
2.55
1.00
1.00
1.12
5.47
1.97
2.05
2.07
3.14
10.0
5.0
0.0
ppm (t1)

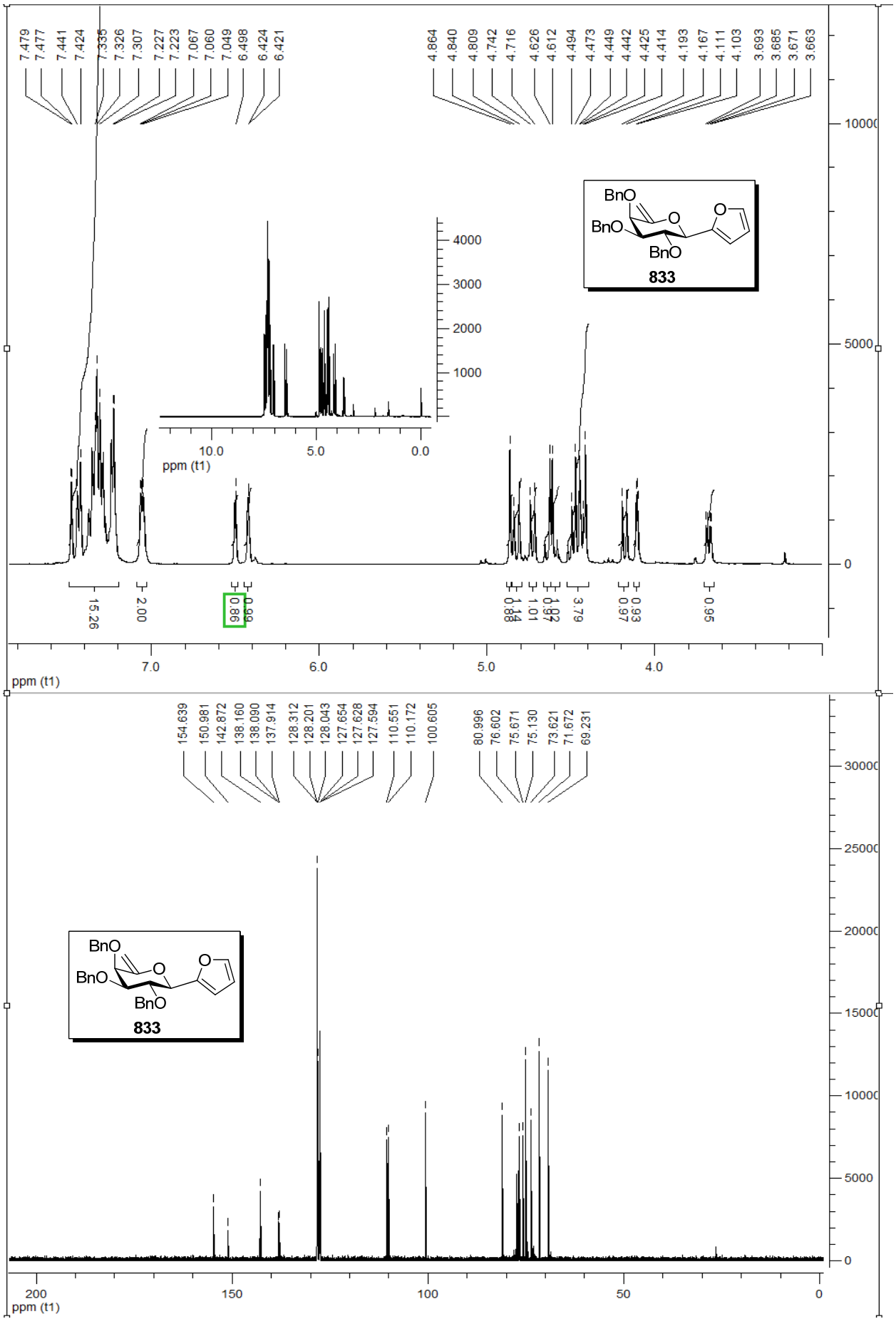

213.100
142.139
128.469
128.443
128.332
128.229
127.857
127.735
127.702
127.663
110.275
109.785
80.130
77.237
76.266
73.896
73.445
73.178
71.885
71.183
65.653
18.957
BnO
OBn
BnO
O
O
H
S
SMe
O
830
2500
2000
1500
1000
500
200
150
100
50
0
ppm (t1)

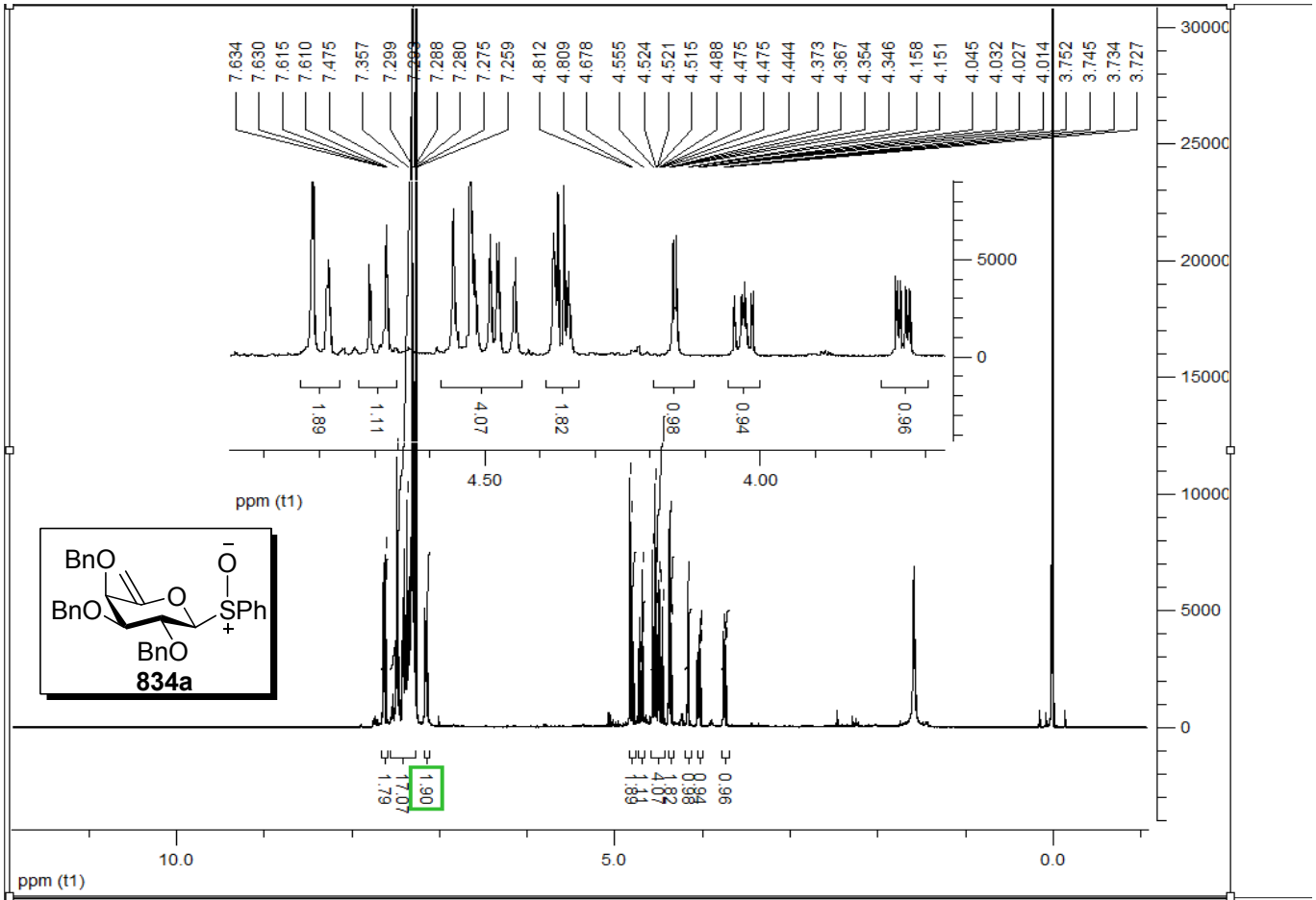

BnO
OH
O
BnO
BnO
831
ppm (t1)

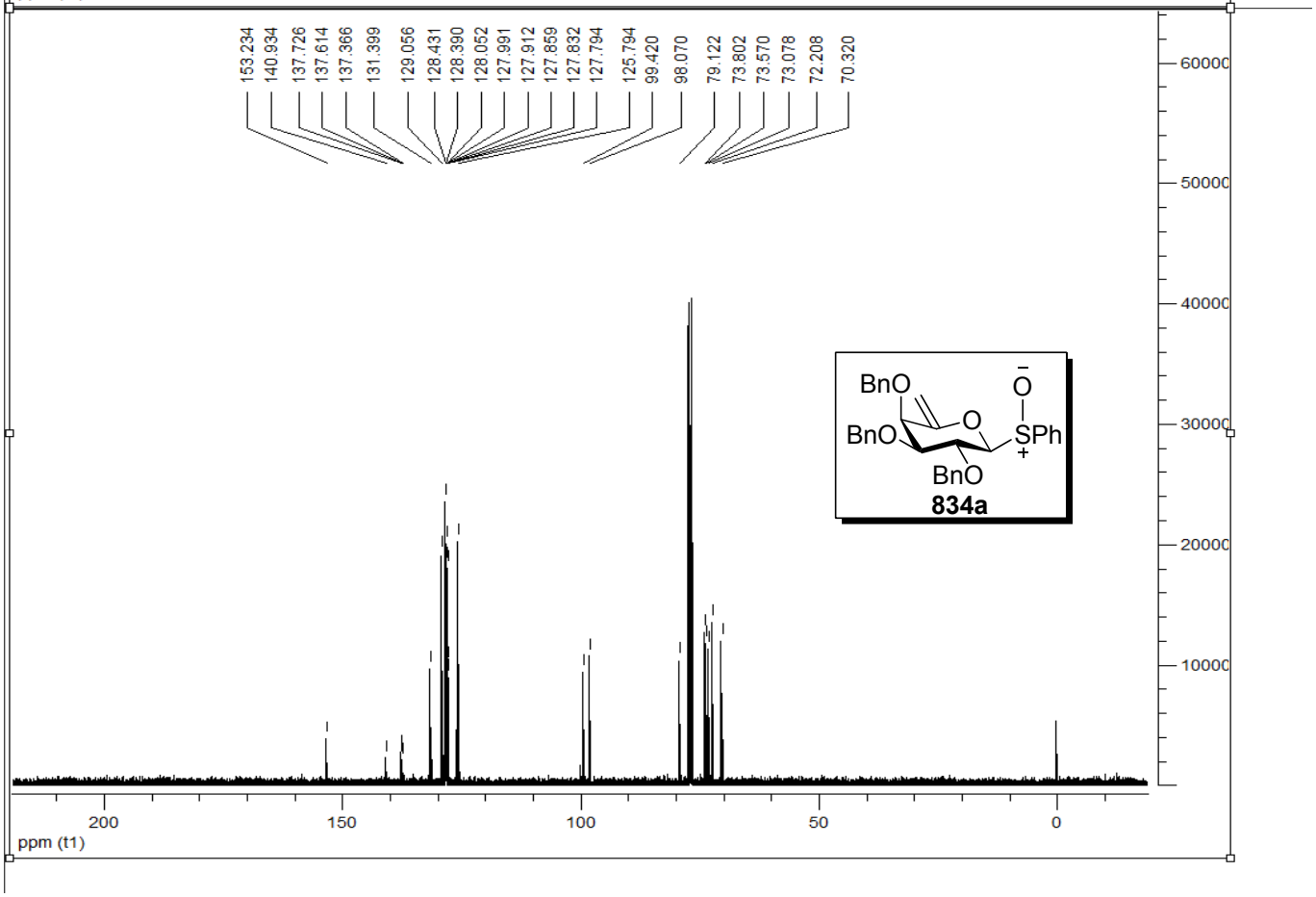

BnO
OH
O
BnO
BnO
831
ppm (t1)

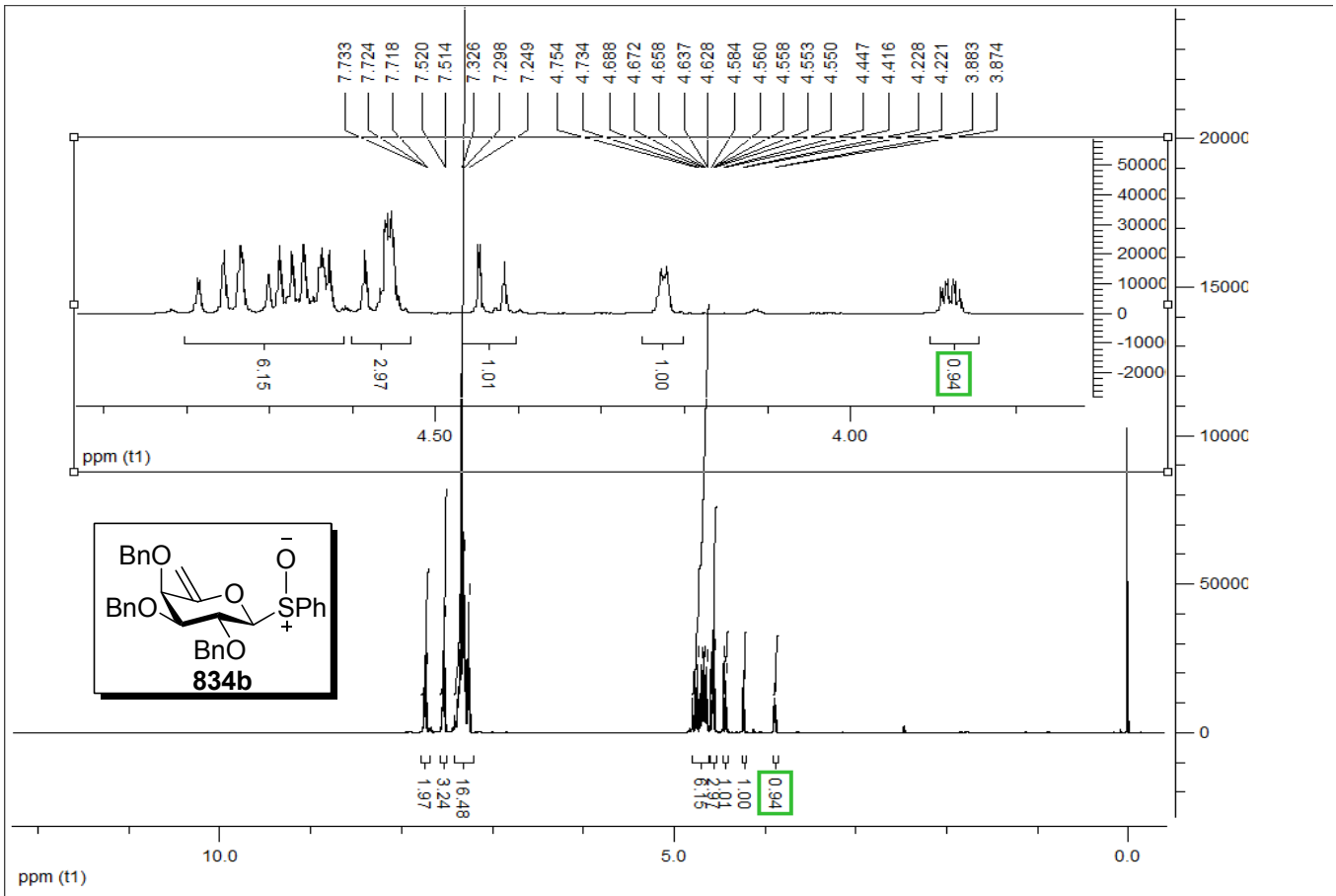

6.448
6.446
6.440
6.438
6.401
6.396
6.393
6.388
5.141
5.113
4.822
4.766
4.738
4.621
4.595
4.314
4.296
4.290
4.278
4.264
4.262
4.257
4.255
4.153
4.127
3.688
3.685
3.683
3.675
3.672
3.665
3.659
3.653
3.325
3.303
3.261
3.248
3.236
3.223
ppm (t1)
BnO
BnO
BnO
O
O
I
832

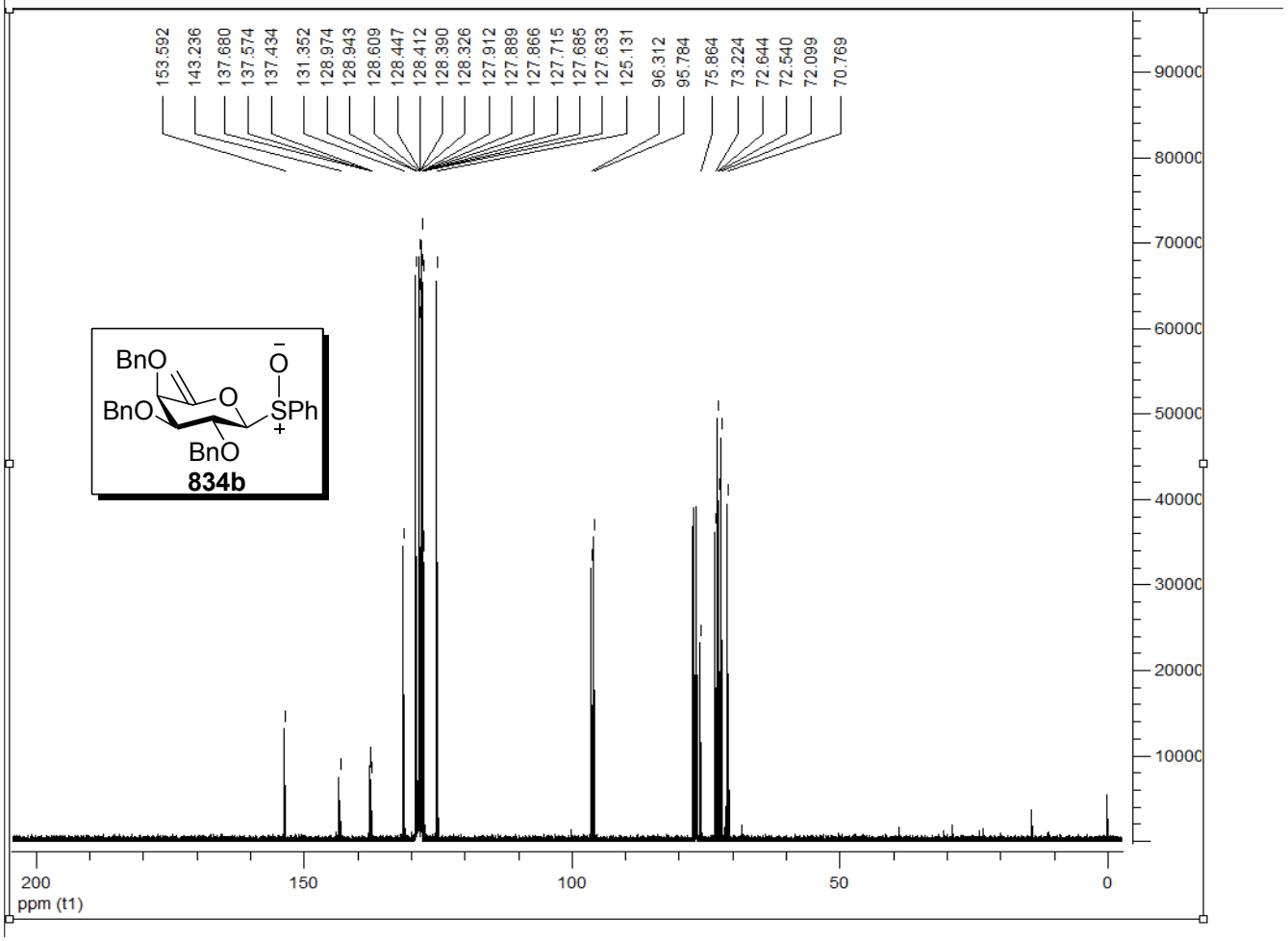

151.074
142.678
138.533
138.339
138.027
128.508
128.381
128.325
128.278
128.205
127.748
127.732
127.691
127.551
110.532
110.057
84.482
79.447
75.149
75.052
75.034
74.082
73.061
2.725
ppm (t1)
BnO
BnO
BnO
O
O
I
832

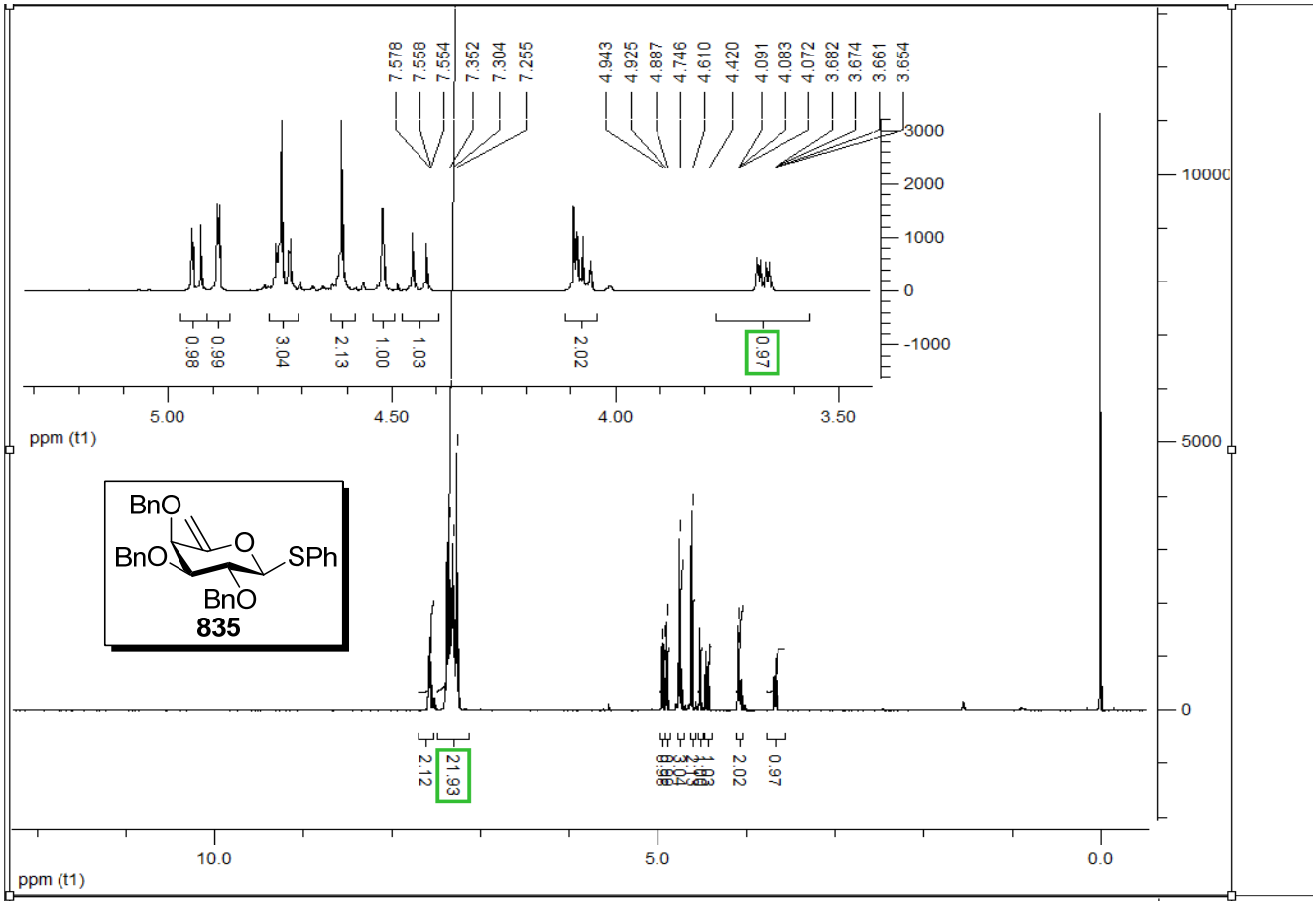

7.479
7.477
7.441
7.424
7.335
7.326
7.307
7.227
7.223
7.067
7.060
7.049
6.498
6.424
6.421
4.864
4.840
4.809
4.742
4.716
4.626
4.612
4.494
4.473
4.449
4.442
4.425
4.414
4.193
4.167
4.111
4.103
3.693
3.685
3.671
3.663
BnO
BnO
BnO
O
O
833
ppm (t1)
15.26
2.00
0.86
0.88
1.14
1.01
2.07
0.97
3.79
0.93
0.97
0.95
ppm (t1)
154.639
150.981
142.872
138.160
138.090
137.914
128.312
128.201
128.043
127.654
127.628
127.594
110.551
110.172
100.605
80.996
76.602
75.671
75.130
73.621
71.672
69.231
BnO
BnO
BnO
O
O
833
ppm (t1)

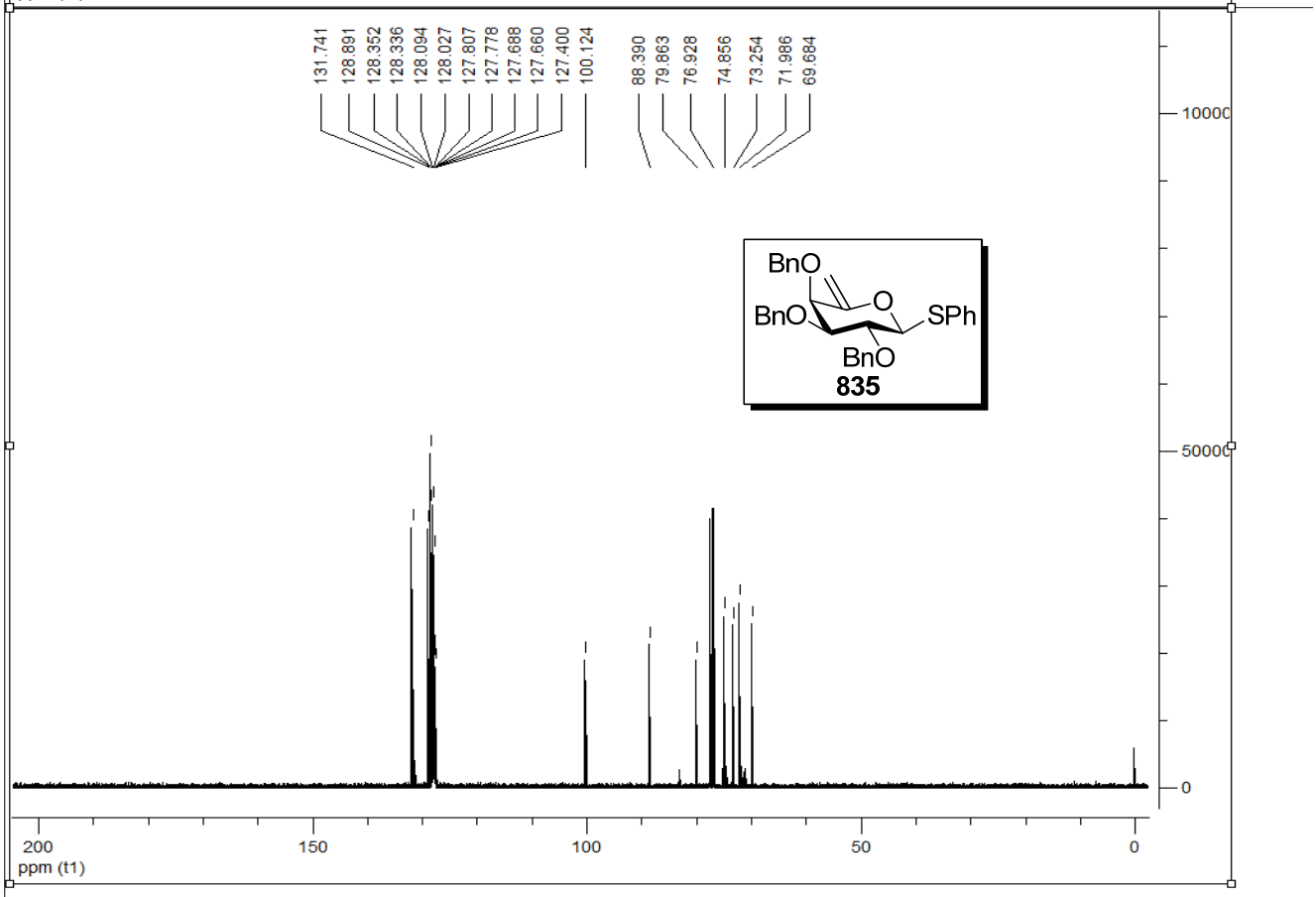

7.634
7.630
7.615
7.610
7.475
7.357
7.299
7.288
7.280
7.275
7.259
4.812
4.809
4.678
4.555
4.524
4.521
4.515
4.488
4.475
4.475
4.444
4.373
4.367
4.354
4.346
4.158
4.151
4.045
4.032
4.027
4.014
3.752
3.745
3.734
3.727
1.89
1.11
4.07
1.82
0.98
0.94
0.96
4.50
4.00
ppm (t1)
1.79
1.07
1.90
1.89
1.11
4.07
2.82
0.98
0.84
0.96
10.0
5.0
0.0
ppm (t1)
BnO
BnO
O
SPh
BnO
834a

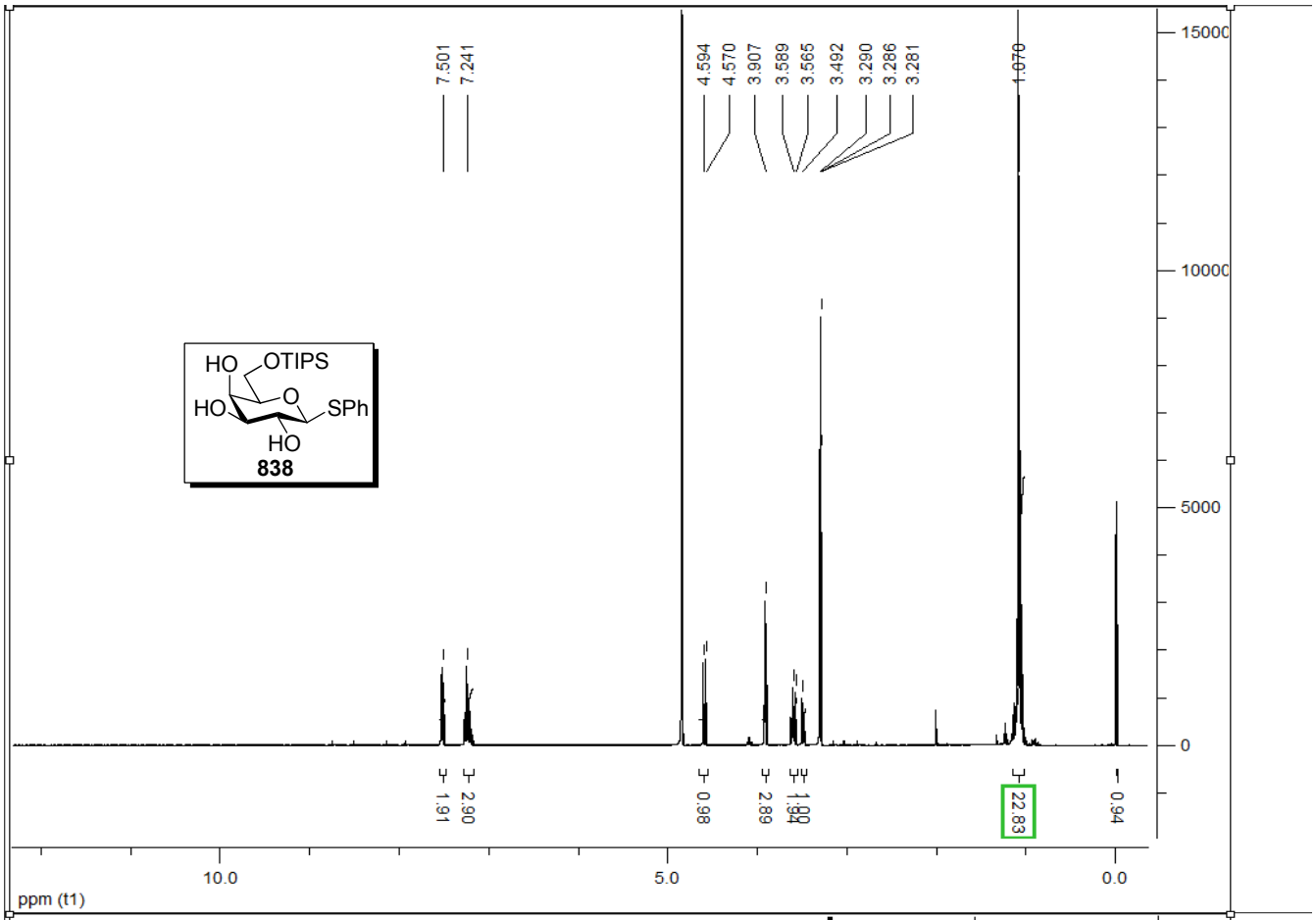

153.234
140.934
137.726
137.614
137.366
131.399
129.056
128.431
128.390
128.052
127.991
127.912
127.859
127.832
127.794
125.794
99.420
98.070
79.122
73.802
73.570
73.078
72.208
70.320
200
150
100
50
0
ppm (t1)
BnO
BnO
O
SPh
BnO
834a

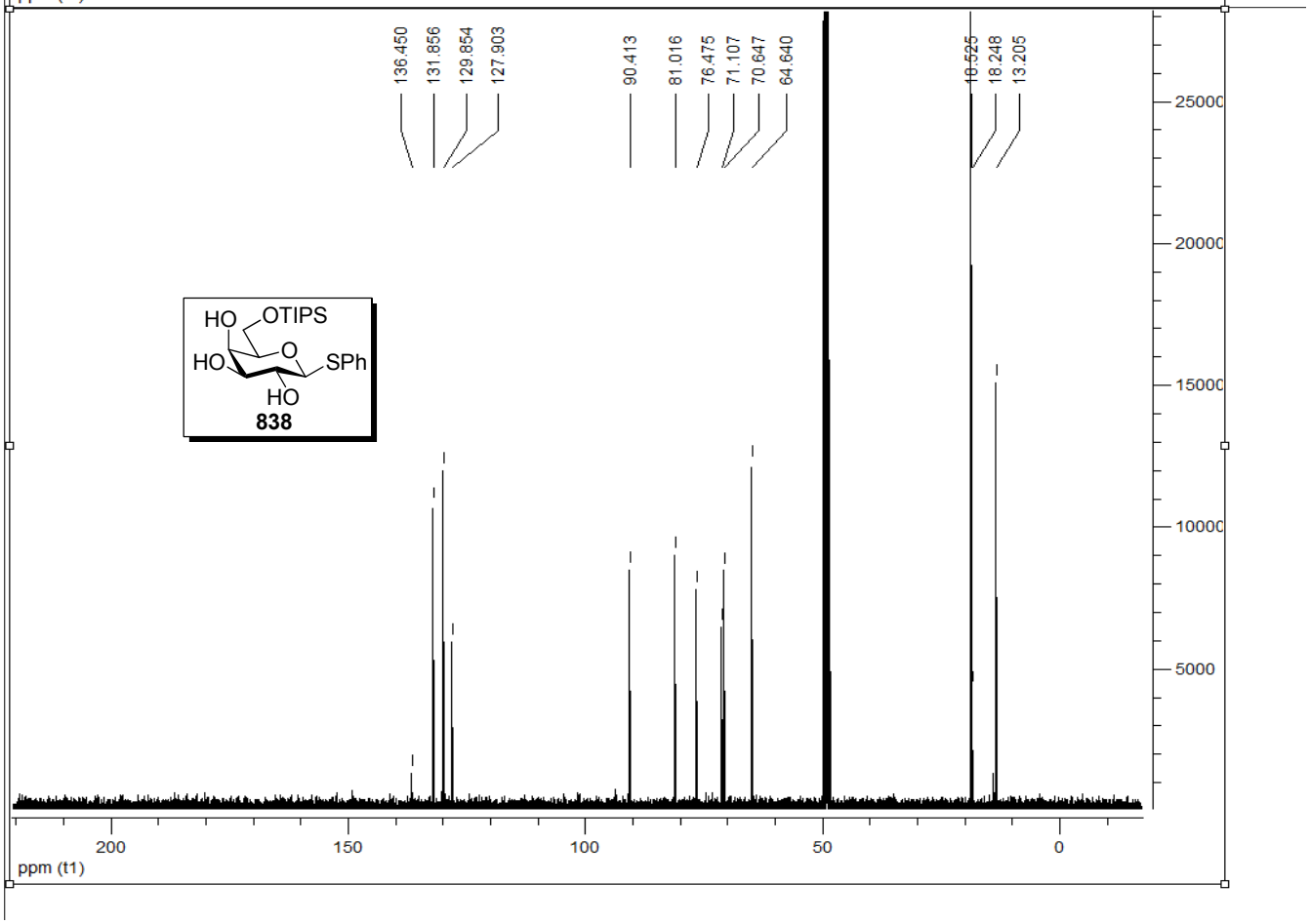

7.733
7.724
7.718
7.520
7.514
7.326
7.298
7.249
4.754
4.734
4.688
4.672
4.658
4.637
4.628
4.584
4.560
4.558
4.553
4.550
4.447
4.416
4.228
4.221
3.883
3.874
6.15
2.97
1.01
1.00
0.94
4.50
4.00
ppm (t1)
BnO
BnO
BnO
O
SPh
834b
1.97
3.24
19.48
6.15
2.97
1.01
1.00
0.94
10.0
5.0
0.0
ppm (t1)

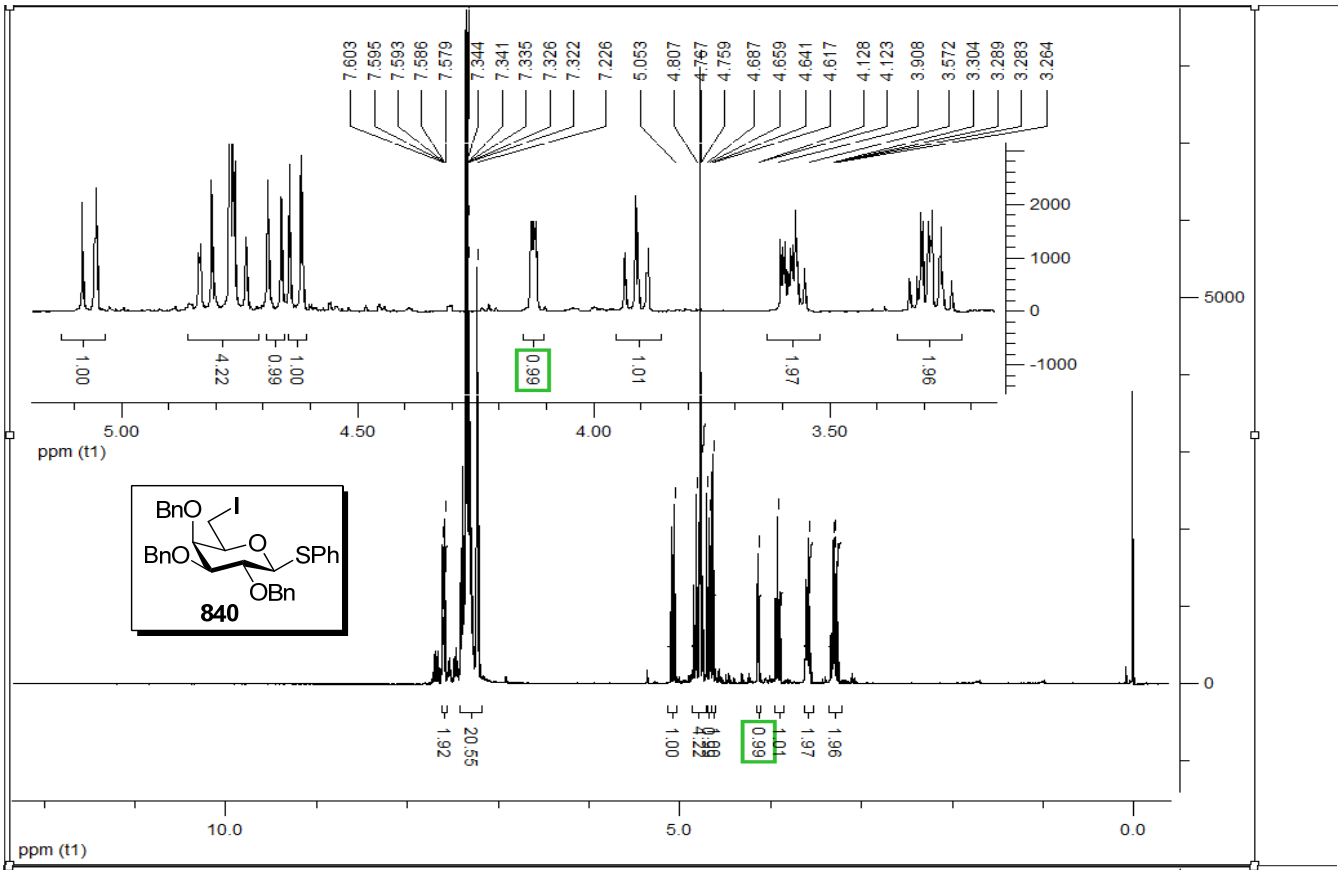

153.592
143.236
137.680
137.574
137.434
131.352
128.974
128.943
128.609
128.447
128.412
128.390
128.326
127.912
127.889
127.866
127.715
127.685
127.633
125.131
96.312
95.784
75.864
73.224
72.644
72.540
72.099
70.769
BnO
BnO
BnO
O
SPh
834b
200
150
100
50
0
ppm (t1)

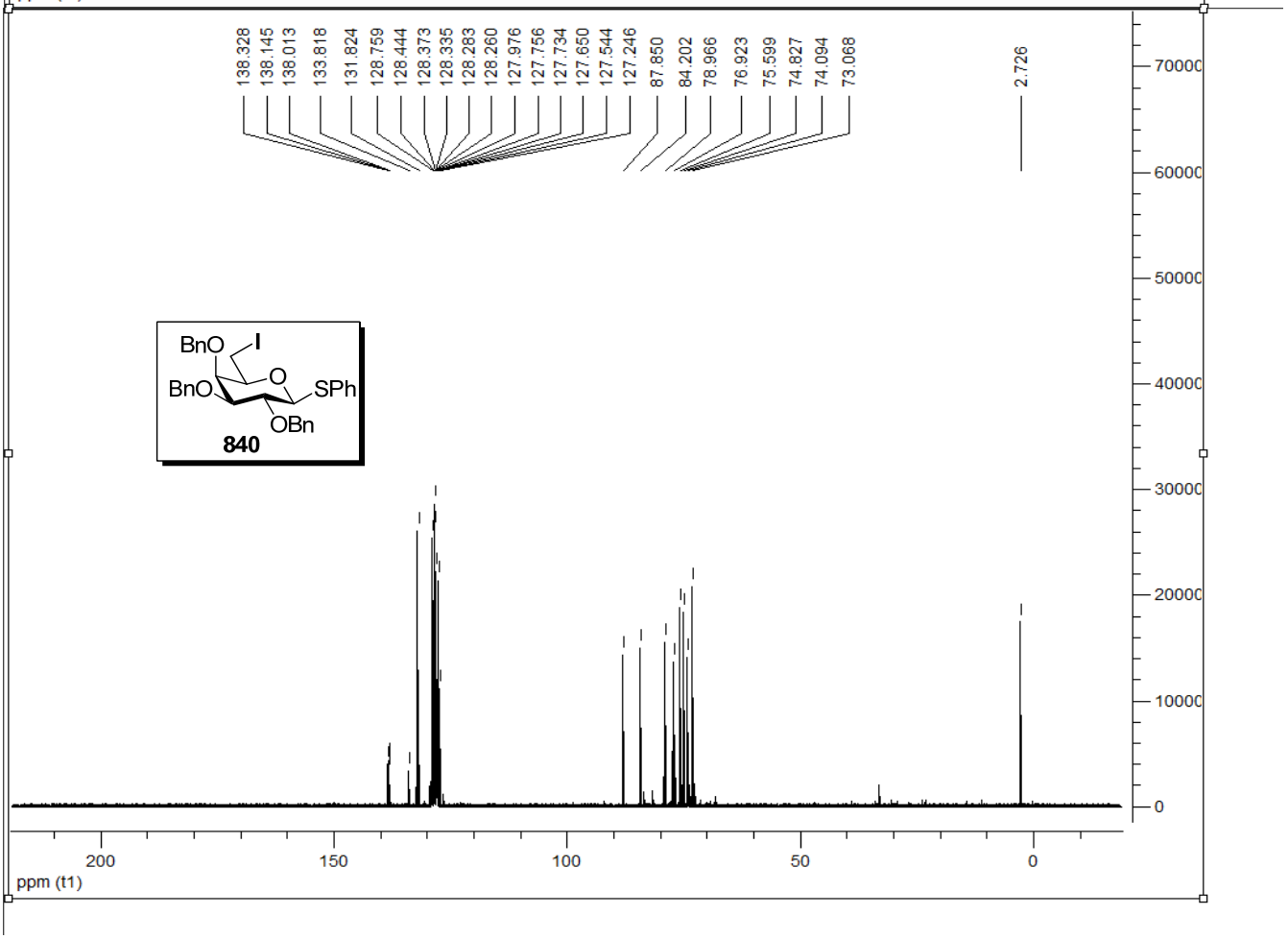

7.578
7.558
7.554
7.352
7.304
7.255
4.943
4.925
4.887
4.746
4.610
4.420
4.091
4.083
4.072
3.682
3.674
3.661
3.654
0.98
0.99
3.04
2.13
1.00
1.03
2.02
0.97
ppm (t1)
BnO
BnO
O
SPh
BnO
835
2.12
21.93
2.02
0.97
ppm (t1)

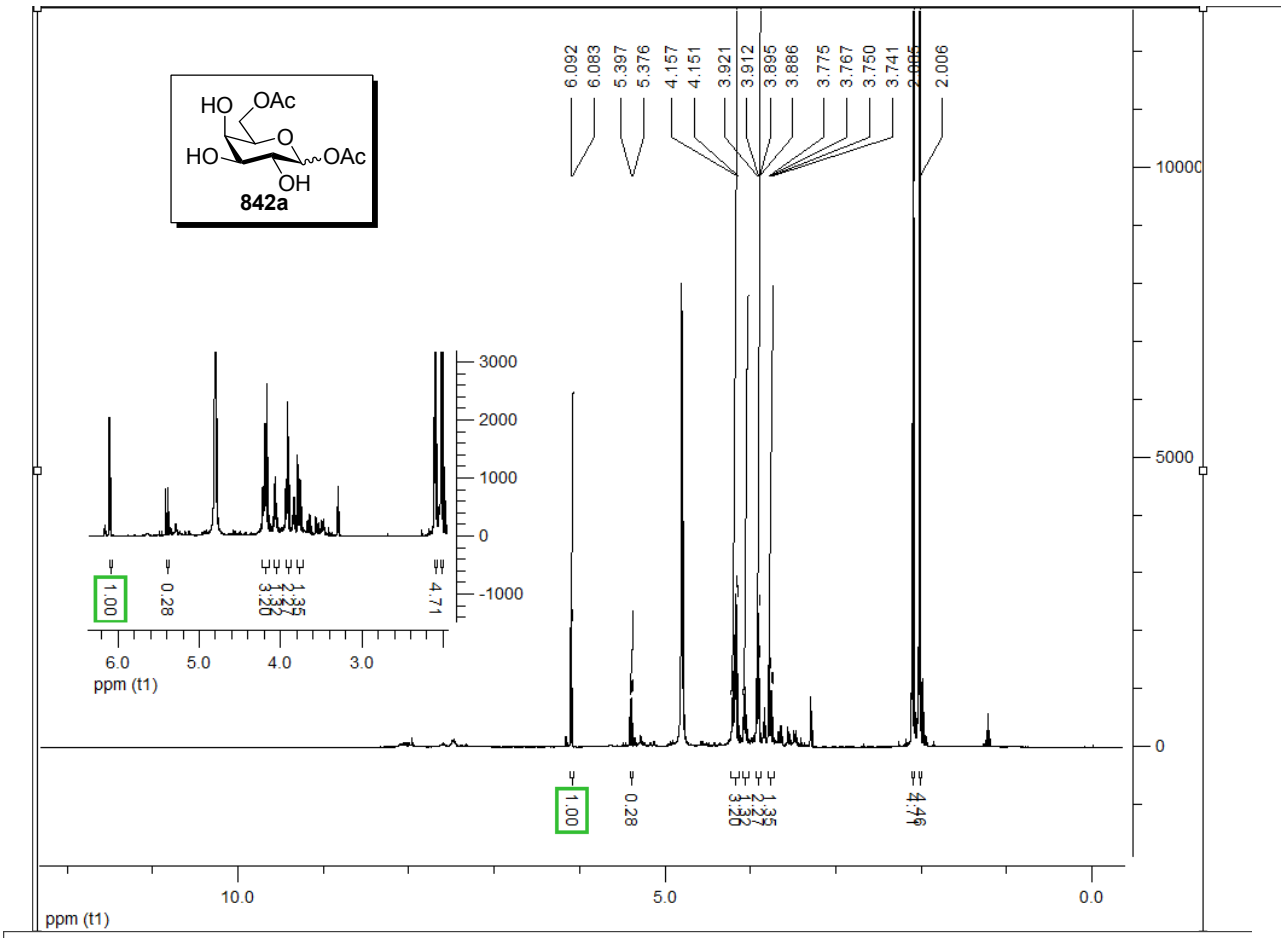

131.741
128.891
128.352
128.336
128.094
128.027
127.807
127.778
127.688
127.660
127.400
100.124
88.390
79.863
76.928
74.856
73.254
71.986
69.684
BnO
BnO
O
SPh
BnO
835
ppm (t1)

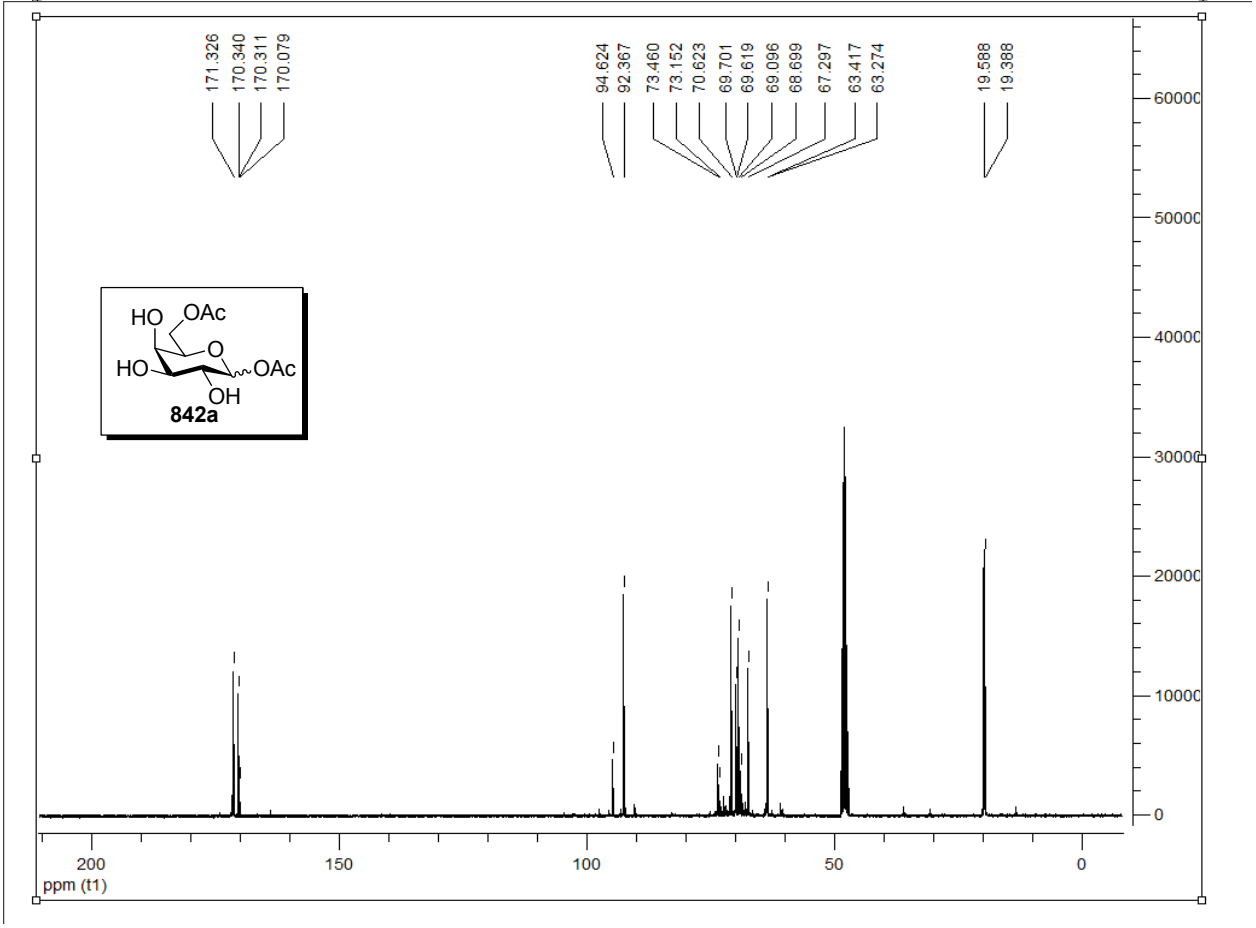

7.501
7.241
4.594
4.570
3.907
3.589
3.565
3.492
3.290
3.286
3.281
1.070
HO
OTIPS
HO
O
SPh
HO
838
1.91
2.90
0.98
2.89
1.94
1.00
22.83
0.94
10.0
5.0
0.0
ppm (t1)

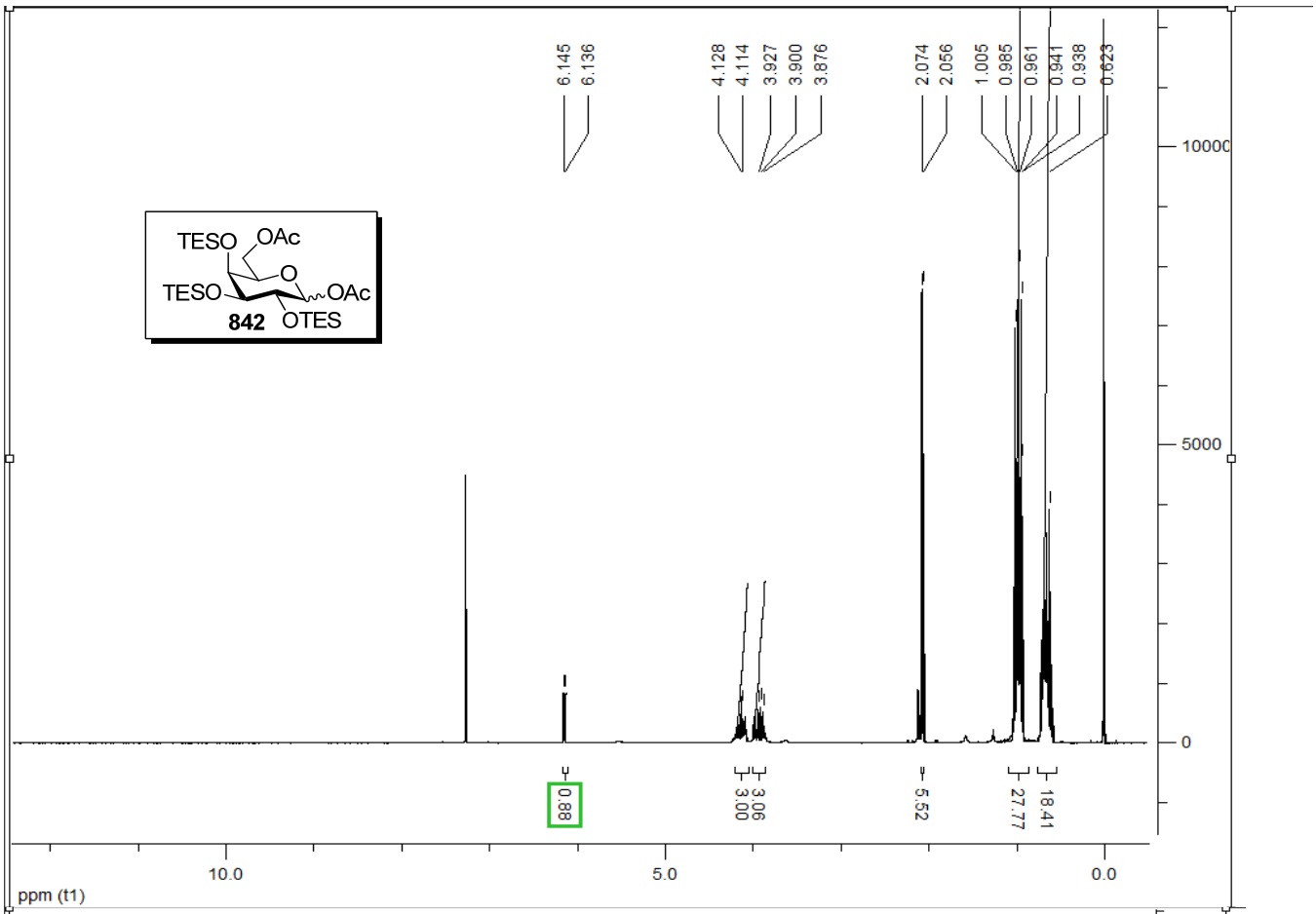

136.450
131.856
129.854
127.903
90.413
81.016
76.475
71.107
70.647
64.640
18.525
18.248
13.205
HO
OTIPS
HO
O
SPh
HO
838
200
150
100
50
0
ppm (t1)

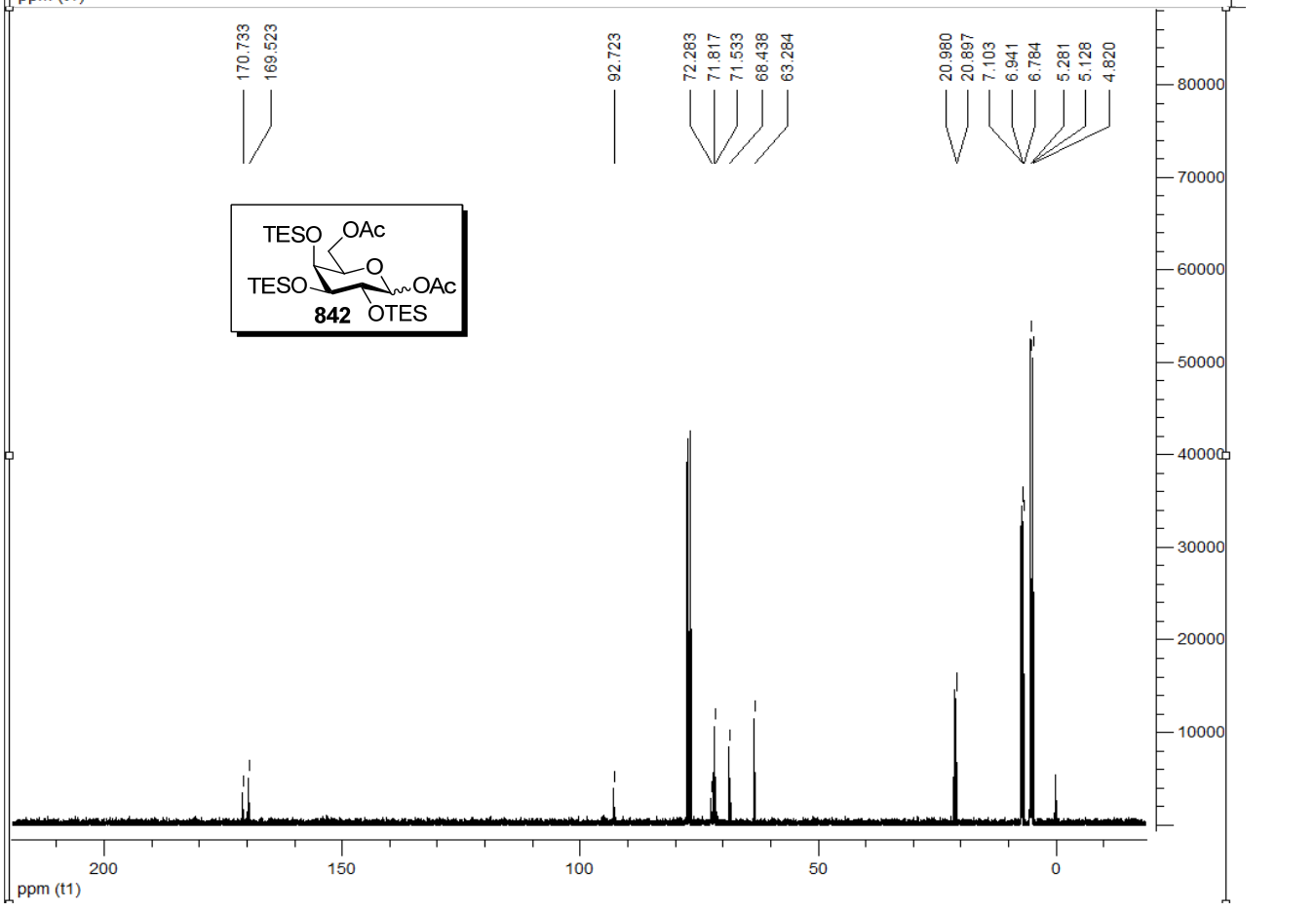

7.603
7.595
7.593
7.586
7.579
7.344
7.341
7.335
7.326
7.322
7.226
5.053
4.807
4.767
4.759
4.687
4.659
4.641
4.617
4.128
4.123
3.908
3.572
3.304
3.289
3.283
3.264
1.00
4.22
0.99
1.00
0.99
1.01
1.97
1.96
ppm (t1)
BnO
I
BnO
O
SPh
OBn
840
1.92
20.55
1.00
0.99
1.01
1.97
1.96
ppm (t1)

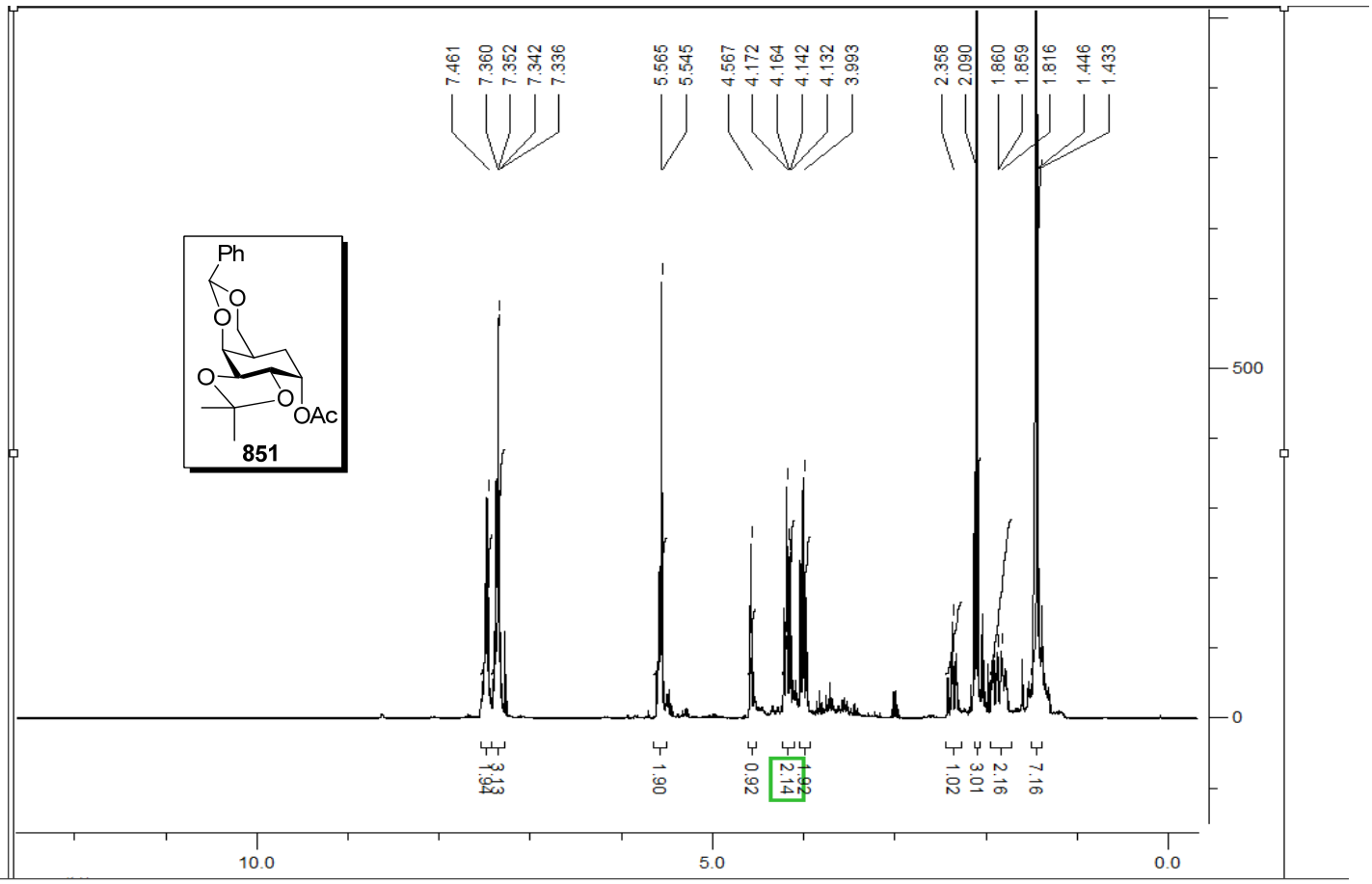

138.328
138.145
138.013
133.818
131.824
128.759
128.444
128.373
128.335
128.283
128.260
127.976
127.756
127.734
127.650
127.544
127.246
87.850
84.202
78.966
76.923
75.599
74.827
74.094
73.068
2.726
BnO
I
BnO
O
SPh
OBn
840
ppm (t1)

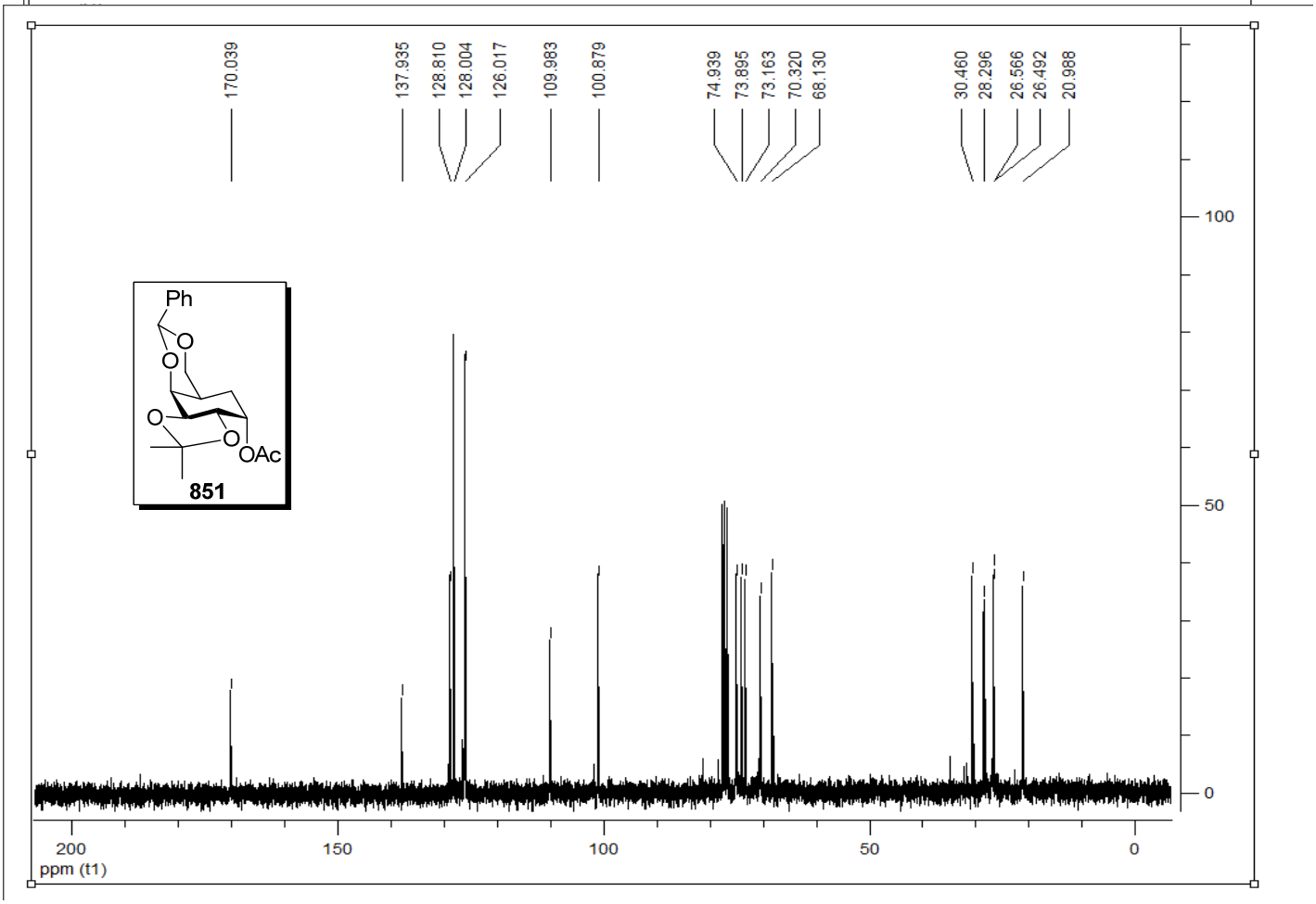

HO
OAc
HO
O
OAc
OH
842a
6.092
6.083
5.397
5.376
4.157
4.151
3.921
3.912
3.895
3.886
3.775
3.767
3.750
3.741
2.006
1.00
0.28
3.20
4.71
ppm (t1)

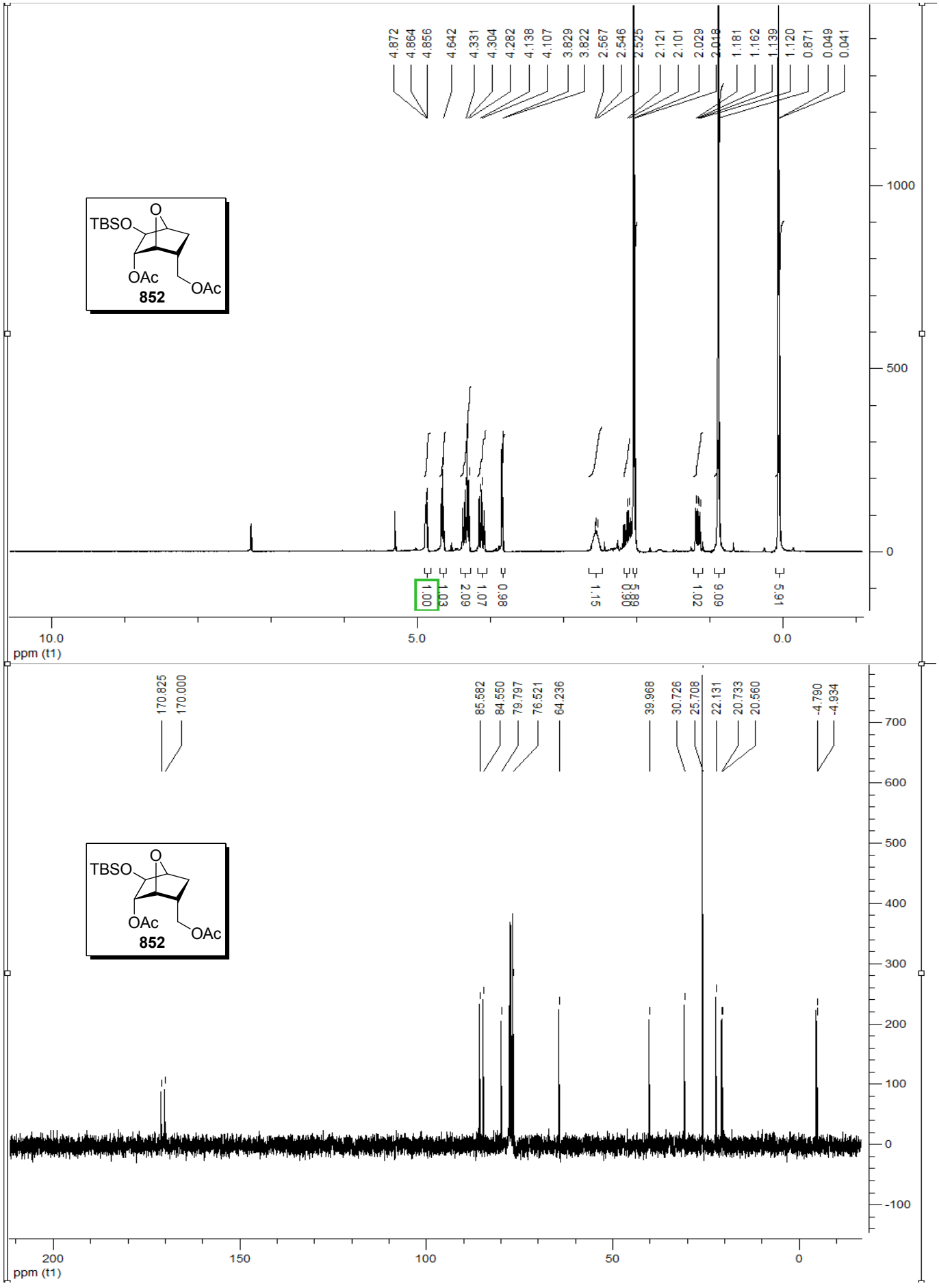

171.326
170.340
170.311
170.079
94.624
92.367
73.460
73.152
70.623
69.701
69.619
69.096
68.699
67.297
63.417
63.274
19.588
19.388
HO
OAc
HO
O
OAc
OH
842a
ppm (t1)

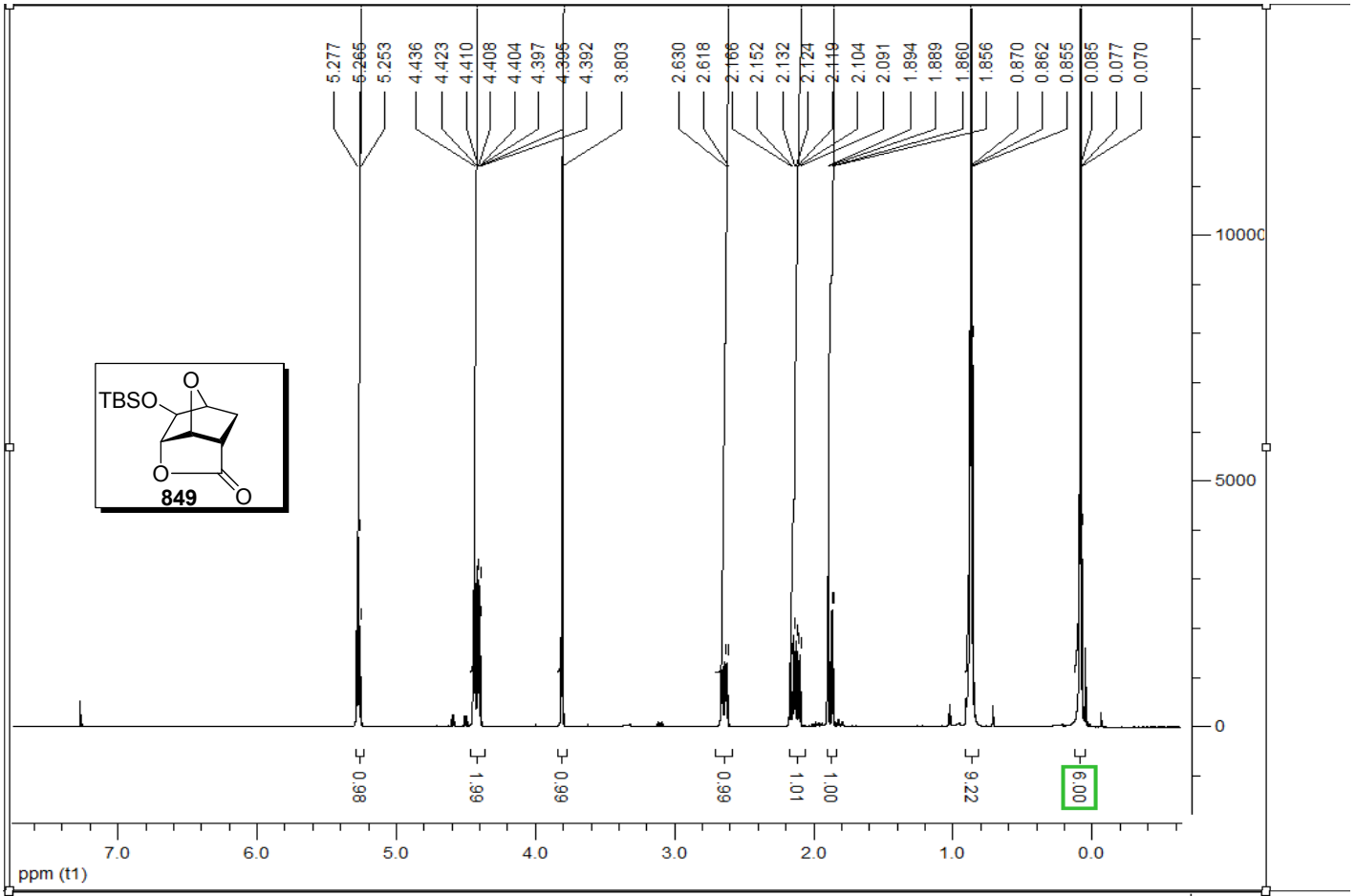

6.145
6.136
4.128
4.114
3.927
3.900
3.876
2.074
2.056
1.005
0.985
0.961
0.941
0.938
0.623
TESO
OAc
O
TESO
OAc
842
OTES
10000
5000
0
0.88
3.06
3.00
5.52
27.77
18.41
10.0
5.0
0.0
ppm (t1)

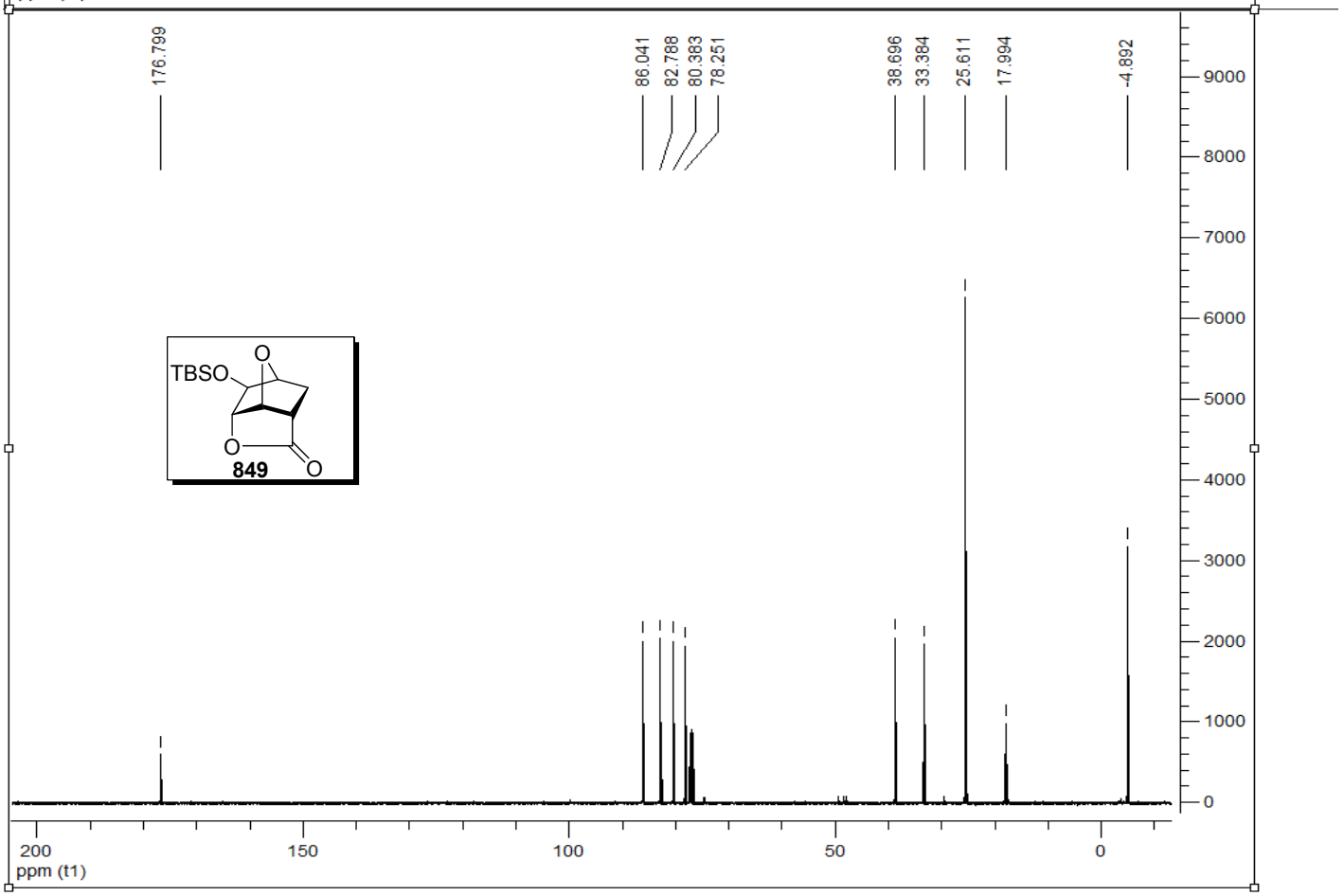

170.733
169.523
92.723
72.283
71.817
71.533
68.438
63.284
20.980
20.897
7.103
6.941
6.784
5.281
5.128
4.820
TESO
OAc
O
TESO
OAc
842
OTES
80000
70000
60000
50000
40000
30000
20000
10000
200
150
100
50
0
ppm (t1)

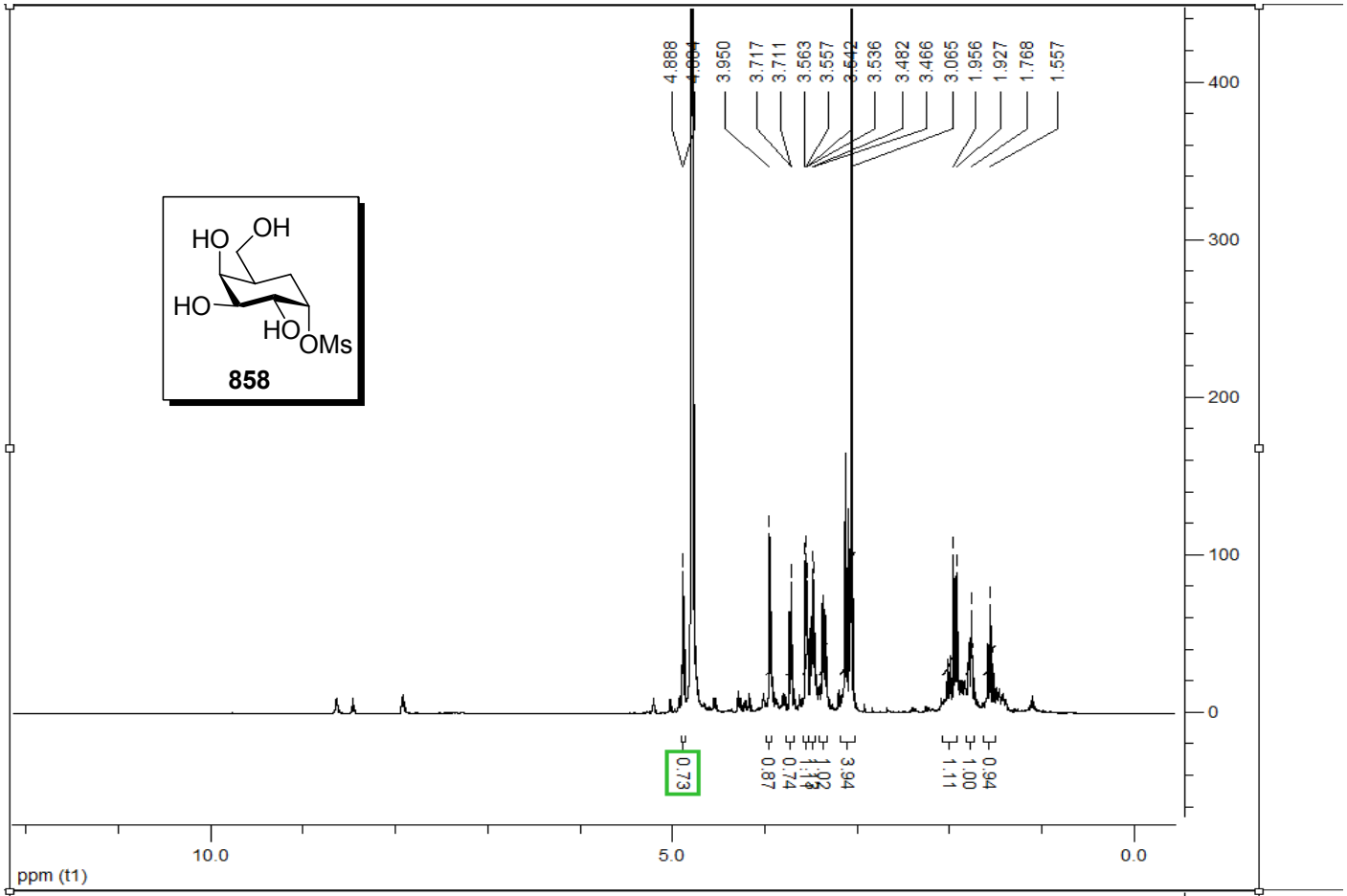

7.461
7.360
7.352
7.342
7.336
5.565
5.545
4.567
4.172
4.164
4.142
4.132
3.993
2.358
2.090
1.860
1.859
1.816
1.446
1.433
Ph
O
O
O
O
OAc
851
3.83
1.90
0.92
2.14
1.92
1.02
3.01
2.16
7.16
500
0
10.0
5.0
0.0

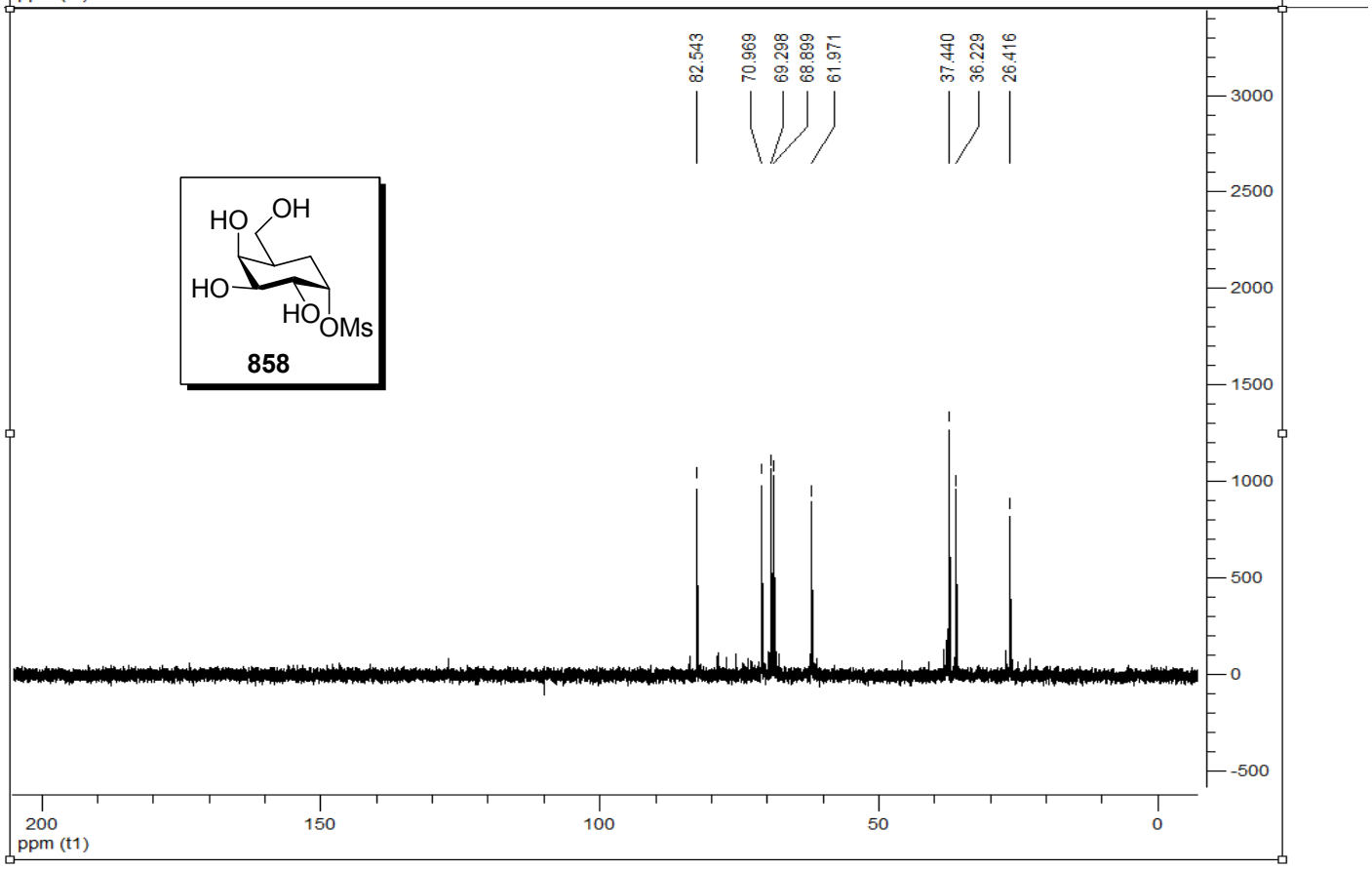

170.039
137.935
128.810
128.004
126.017
109.983
100.879
74.939
73.895
73.163
70.320
68.130
30.460
28.296
26.566
26.492
20.988
Ph
O
O
O
O
OAc
851
100
50
0
200
150
100
50
0
ppm (t1)

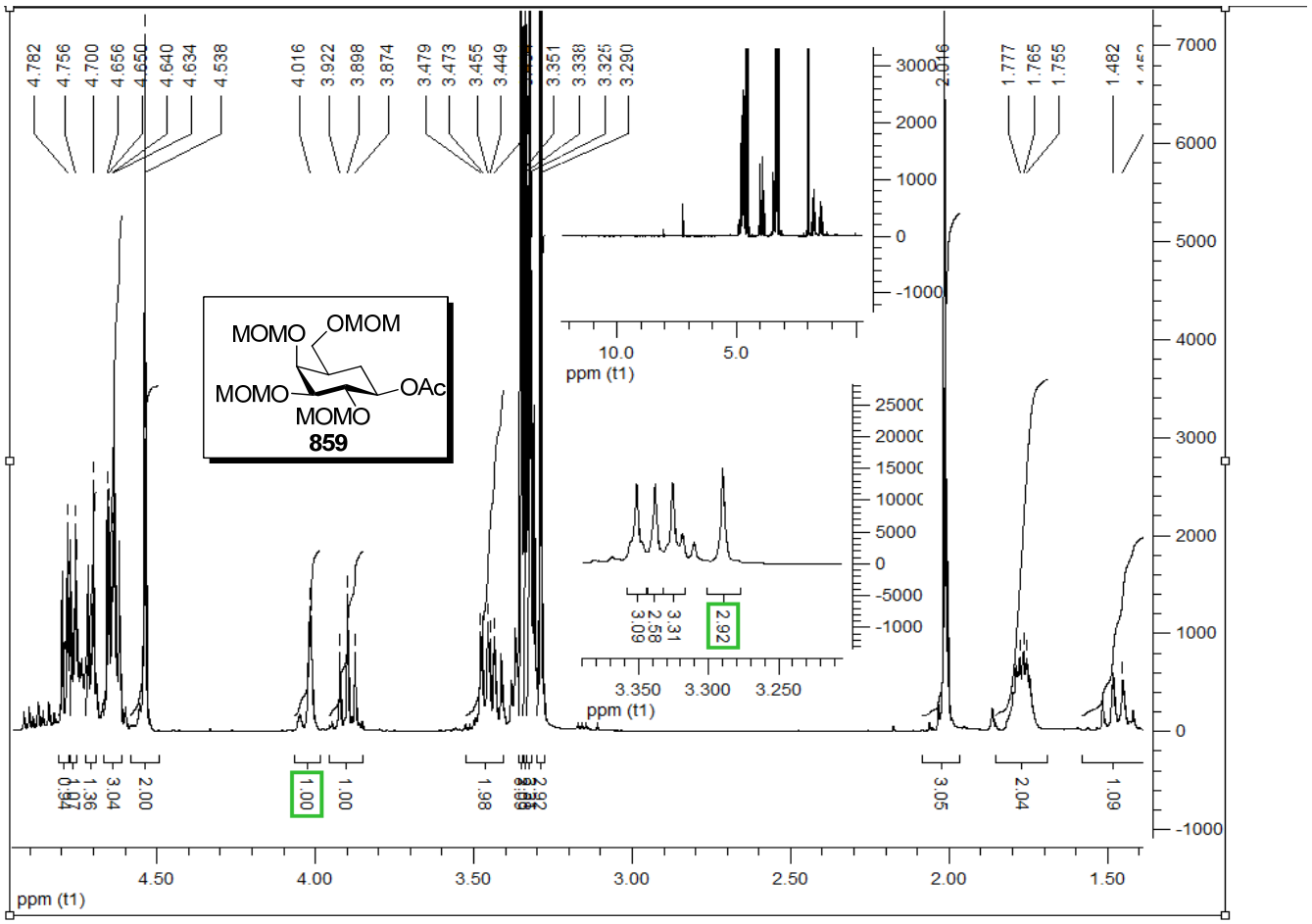

4.872
4.864
4.856
4.642
4.331
4.304
4.282
4.138
4.107
3.829
3.822
2.567
2.546
2.525
2.121
2.101
2.029
2.018
1.181
1.162
1.139
1.120
0.871
0.049
0.041
1.00
1.03
2.09
1.07
0.98
1.15
5.88
5.90
1.02
9.09
5.91
TBSO
O
OAc
OAc
852
10.0
5.0
0.0
ppm (t1)
170.825
170.000
85.582
84.550
79.797
76.521
64.236
39.968
30.726
25.708
22.131
20.733
20.560
-4.790
-4.934
TBSO
O
OAc
OAc
852
200
150
100
50
0
ppm (t1)

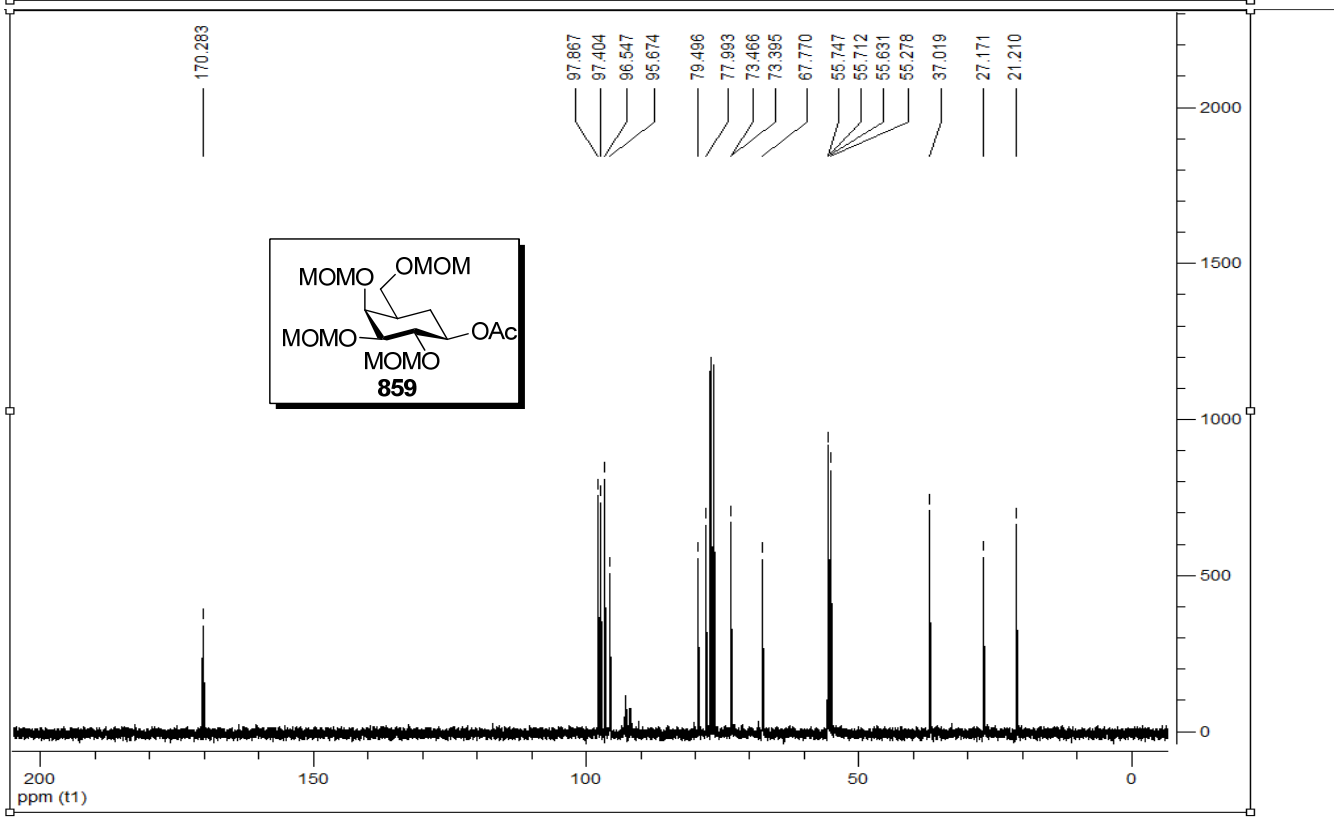

5.277
5.265
5.253
4.436
4.423
4.410
4.408
4.404
4.397
4.395
4.392
3.803
2.630
2.618
2.166
2.152
2.132
2.124
2.119
2.104
2.091
1.894
1.889
1.860
1.856
0.870
0.862
0.855
0.085
0.077
0.070
TBSO
O
O
O
849
0.98
1.99
0.99
0.99
1.01
1.00
9.22
6.00
10000
5000
0
7.0
6.0
5.0
4.0
3.0
2.0
1.0
0.0
ppm (t1)

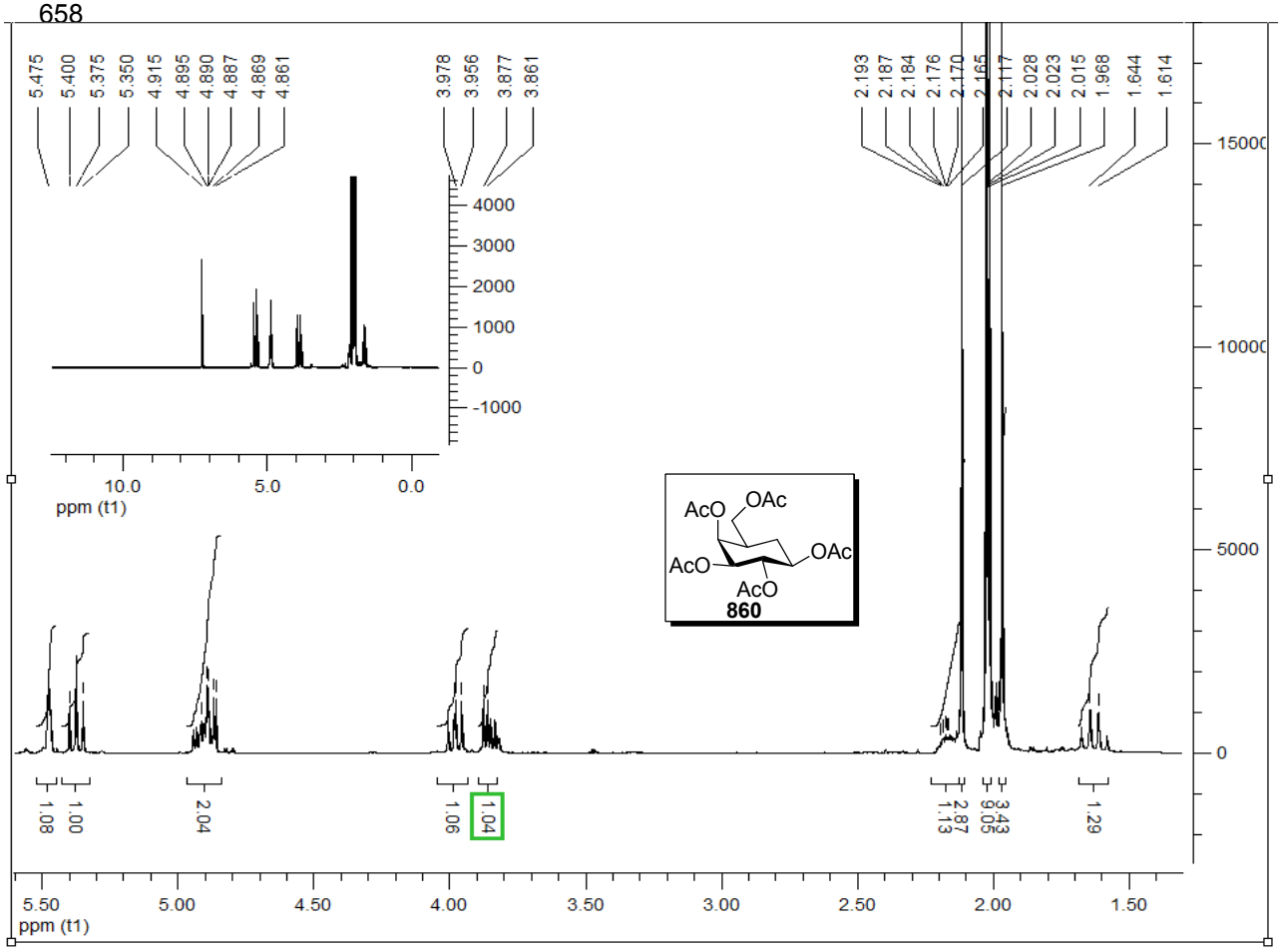

176.799
86.041
82.788
80.383
78.251
38.696
33.384
25.611
17.994
-4.892
TBSO
O
O
O
849
9000
8000
7000
6000
5000
4000
3000
2000
1000
0
200
150
100
50
0
ppm (t1)

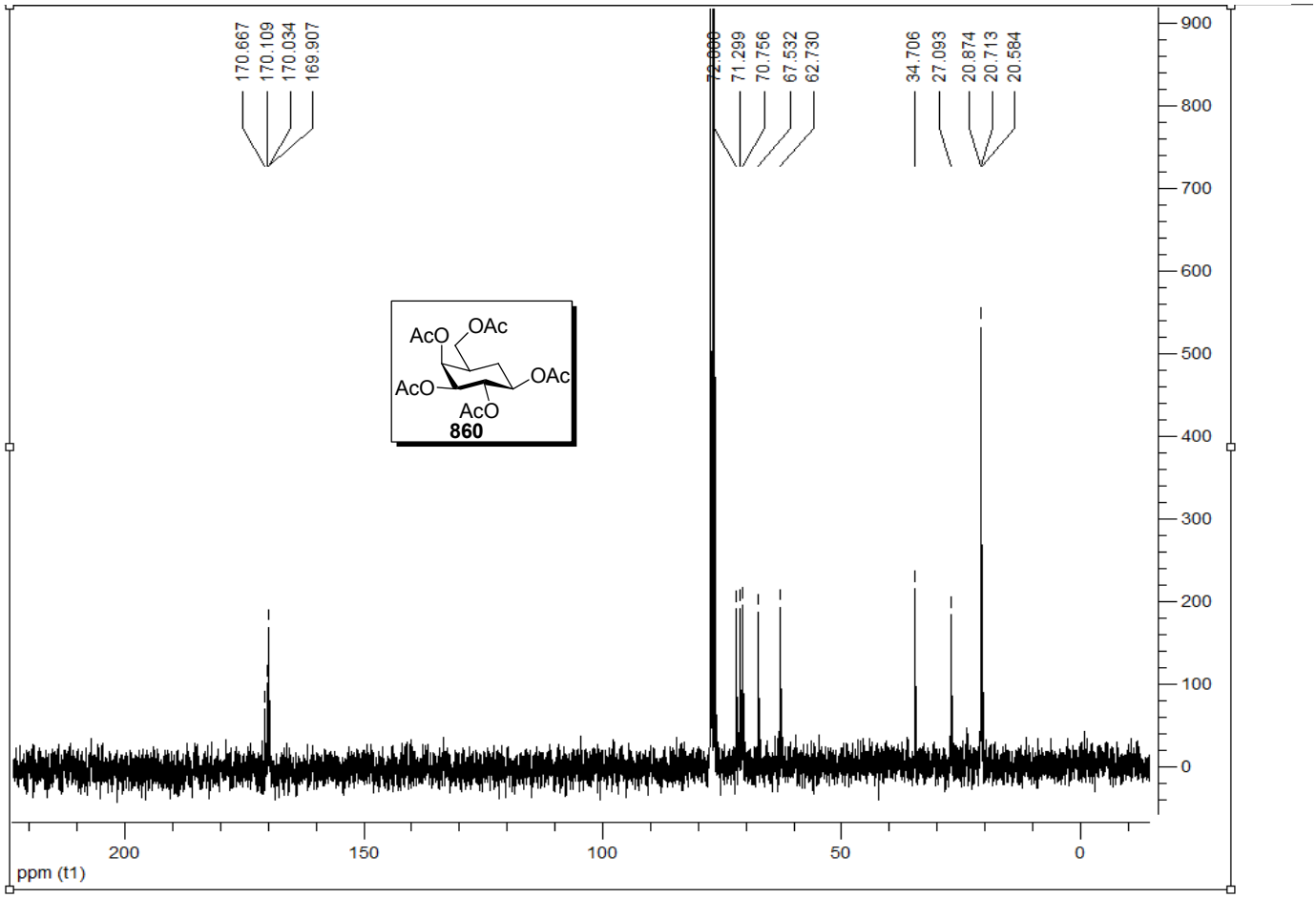

4.888
4.864
3.950
3.717
3.711
3.563
3.557
3.542
3.536
3.482
3.466
3.065
1.956
1.927
1.768
1.557
HO
OH
HO
HO
OMs
858
0.73
0.87
0.74
1.11
1.02
3.94
1.11
1.00
0.94
400
300
200
100
0
10.0
5.0
0.0
ppm (t1)


82.543
70.969
69.298
68.899
61.971
37.440
36.229
26.416
HO
OH
HO
HO
OMs
858
3000
2500
2000
1500
1000
500
0
-500
200
150
100
50
0
ppm (t1)


MOMO
OMOM
MOMO
OAc
MOMO
859
ppm (t1)


MOMO
OMOM
MOMO
OAc
MOMO
859
ppm (t1)


5.475
5.400
5.375
5.350
4.915
4.895
4.890
4.887
4.869
4.861
3.978
3.956
3.877
3.861
2.193
2.187
2.184
2.176
2.170
2.165
2.117
2.028
2.023
2.015
1.968
1.644
1.614
AcO
OAc
AcO
OAc
AcO
860
ppm (t1)
1.08
1.00
2.04
1.06
1.04
1.13
2.87
6.05
3.43
1.29


170.667
170.109
170.034
169.907
72.000
71.299
70.756
67.532
62.730
34.706
27.093
20.874
20.713
20.584
AcO
OAc
AcO
OAc
AcO
860
ppm (t1)